

2014

Biodiversity crisis and recovery during the Triassic-Jurassic greenhouse interval: testing ocean acidification hypotheses

Jacobsen, Nikita Danielle

<http://hdl.handle.net/10026.1/9329>

<http://dx.doi.org/10.24382/3333>

Plymouth University

All content in PEARL is protected by copyright law. Author manuscripts are made available in accordance with publisher policies. Please cite only the published version using the details provided on the item record or document. In the absence of an open licence (e.g. Creative Commons), permissions for further reuse of content should be sought from the publisher or author.

This copy of the thesis has been supplied on condition that anyone who consults it is understood to recognise that its copyright rests with its author and that no quotation from the thesis and no information derived from it may be published without the author's prior consent.

Biodiversity crisis and recovery during the Triassic-
Jurassic greenhouse interval: testing ocean
acidification hypotheses.

By

Nikita Danielle Jacobsen

A thesis submitted to Plymouth University in partial fulfilment for the degree
of

Doctor of Philosophy

School of Geography, Earth and Environmental Sciences

Faculty of Science and Environment

October 2014

Abstract

Nikita Danielle Jacobsen

Biodiversity crisis and recovery during the Triassic-Jurassic greenhouse interval: testing ocean acidification hypotheses.

The Late Rhaetian (Late Triassic) extinction event is characterised by shelled species showing a reduction in size, and thickness, which together with changed mineralogy is thought to be as a result of increased atmospheric $p\text{CO}_2$ levels. Similar morphological changes have been demonstrated for extant species exposed experimentally to high CO_2 leading to the hypothesis that Late Triassic extinctions were linked with global ocean acidification and increased oceanic palaeotemperatures. Consequently, the aim of this present work was to test this ocean acidification hypothesis by investigating morphological changes in selected shelled fossil species across this extinction event, and attempt to correlate them with changes in environmental temperature and $p\text{CO}_2$. The abundance, size, shell thickness and mineralogy was determined for three common species, the bivalves *Liostrea hisingeri* and *Plagiostoma gigantea* and the ostracod *Ogmoconchella aspinata* collected from Triassic and Jurassic rocks from two locations in southwest England. Palaeotemperature was reconstructed from examination of these fossils and from the literature and atmospheric $p\text{CO}_2$ estimated from published accounts.

The shell size of bivalves increased during periods of high $p\text{CO}_2$ and high palaeotemperature at both locations. Ostracod carapace sizes increased at St Audrie's Bay but decreased at Lyme Regis during periods of high $p\text{CO}_2$, while ostracod carapace size decreased during periods of high palaeotemperature at St Audrie's Bay. However, ostracod shell thickness increased and decreased as $p\text{CO}_2$ increased but shows no relationship with palaeotemperature at either location. Laboratory experiments on the effect of elevated $p\text{CO}_2$ and elevated temperature on three modern species of ostracod was carried out. Modern species *Leptocythere* sp. and *L. castanea* subjected to either elevated $p\text{CO}_2$ or elevated temperature showed increased dissolution, however size and thickness did not significantly change. In the same experimental conditions *L. lacertosa* showed increased dissolution however size continued to increase, while thickness was maintained. Comparison of fossil bivalve and ostracod data to modern high $p\text{CO}_2$ and high temperature experiments illustrates some correlations to the modern experiments results indicating high $p\text{CO}_2$ and high palaeotemperature conditions could have been occurring during the Triassic-Jurassic boundary interval. From the evidence presented, combined with an appropriate trigger (CAMP volcanism), it can be concluded that both ocean acidification and palaeotemperature were contributing to the species adaptations identified across the Triassic-Jurassic boundary interval.

Contents

Chapter 1–Introduction	2
1.1 Late Triassic extinction event	2
1.2 Triassic – Jurassic boundary $p\text{CO}_2$ record	6
1.2.2 Tr-J ocean acidification and the fossil record	10
1.2.3 Triassic-Jurassic boundary palaeotemperature curve.....	14
1.3 Modern ocean acidification	17
1.3.2 Modern high CO_2 studies	23
1.4 Effect of warming on extant species	25
1.5 Aim and objectives	27
Chapter 2 – Geological Setting	29
2.1 Introduction	29
2.1.2 Aims and objectives	30
2.2 Field locations	31
2.3 Location lithology	33
2.3.2 Lyme Regis (including Pinhay Bay).....	33
2.3.3 Lyme Regis depositional settings.....	39
2.3.4 St Audrie’s Bay.....	40
2.3.5 St Audrie’s Bay depositional setting	46
2.4 Carbon and oxygen isotope data from the studied sites in southwest England	49
2.5 Correlation of the Tr-J GSSP section to the sections studied here and other key sites including the Newark Basin and East Greenland locations.	55
These can be used as an alternative means of correlating the FO of <i>Psiloceras</i> sp. cf. <i>P. spelae</i> to other marine or terrestrial Tr-J sections to determine the boundary (e.g., ASSP, Newark Basin, southwest England and Astartekloft) (Figure 2.11) (Hesselbo <i>et al.</i> , 2002; Whiteside <i>et al.</i> , 2007; Pálffy <i>et al.</i> , 2007; Korte <i>et al.</i> , 2009; Bonis <i>et al.</i> , 2010b; Deenen <i>et al.</i> , 2010; Ruhl <i>et al.</i> , 2010; Črne <i>et al.</i> , 2011)....	58
2.6 Magnetostratigraphy at St Audrie’s Bay and correlation to the Newark Basin	58
2.7 $p\text{CO}_2$ correlations.....	61
2.8 Further work.....	66
Chapter 3 – Fossil Morphometric Studies	67
3.1 Introduction	67
3.1.2 Aim	67
3.2 Choice of fossil species	68

3.3 Studied Taxa	68
3.4 Materials and methods	71
3.4.2 Digestion and picking of marl samples for ostracods	71
3.4.3 Bivalve morphometrics	73
3.4.4 Ostracod morphometrics	74
3.4.5 Data analysis and presentation	79
3.5 Results	80
3.5.2 Relationships between the number of individuals measured and the minimum, maximum, mean and range of geometric sizes on each bed.....	84
3.5.3 The size variations of <i>L. hisingeri</i> , <i>P. gigantea</i> and <i>O. aspinata</i> through the Lyme Regis and St Audrie's Bay sections	91
3.5.4 <i>L. hisingeri</i>	91
3.5.5 <i>P. gigantea</i>	95
3.5.6 <i>O. aspinata</i>	98
3.6 What do the <i>L. hisingeri</i> , <i>P. gigantea</i> and <i>O. aspinata</i> size changes identified at both locations indicate?	108
3.7 Identification of any significant relationships between the variations in geometric shell size or shell thickness and the different species at each location	115
3.8 Identification of any significant relationships between the geometric shell size or shell thickness of the same species from both Lyme Regis and St Audrie's Bay.	120
3.8.2 <i>L. hisingeri</i>	121
These include the possibility that the environment at St Audrie's Bay is more restricted due to either, less conducive water depths, longer periods of anoxia, adverse higher temperatures or more acidic conditions and therefore not as conductive to these species producing the larger sized shells seen at Lyme Regis (Hallam, 1995, 1997; Hesselbo <i>et al.</i> , 2004; Barras and Twitchett, 2007; Gallois, 2007; Warrington <i>et al.</i> , 2008; Wignall and Bond, 2008; Mander <i>et al.</i> , 2008; Ruhl <i>et al.</i> , 2010).	123
3.8.3 <i>O. aspinata</i>	124
3.9 Summary	131
3.9.2 Further work.....	132
Chapter 4 - Palaeoenvironmental effects on shell size and thickness of bivalves and ostracods across the Triassic-Jurassic boundary interval.	133
4.1 Introduction.....	133
4.2 Aim and objectives	134
4.3 Materials and methods	134
4.3.2 Sampling material for geochemical analysis.....	134

4.3.3 Stable isotope and trace element analyses.....	137
4.3.4 Trace element geochemistry	137
4.3.5 Palaeotemperature estimates	138
4.3.6 Data analysis and presentation	140
4.3.7 Diagenetic versus the primary signal	144
4.4 Relationships between the palaeotemperature curves and the atmospheric $p\text{CO}_2$ curves.	151
4.5 Relationships between the $p\text{CO}_2$ data and the morphometric data.	156
4.5.2 <i>L. hisingeri</i>	156
4.5.3 <i>P. gigantea</i>	160
4.5.4 <i>O. aspinata</i>	161
4.5.5 Implications of relationships identified between $p\text{CO}_2$ and morphometric data.	164
4.6 Relationships between $\delta^{13}\text{C}$ and morphometric data from each species. ...	169
4.6.2 <i>L. hisingeri</i>	169
4.6.3 <i>P. gigantea</i>	171
4.6.4 <i>O. aspinata</i>	172
4.6.5 Implications of relationships identified between $\delta^{13}\text{C}$ and morphometric data.	177
4.7 Relationships between the palaeotemperature data and the morphometric data from each species.....	179
4.7.2 <i>L. hisingeri</i>	179
4.7.3 <i>P. gigantea</i>	182
4.7.4 <i>O. aspinata</i>	183
4.7.5 Implications of relationships identified between palaeotemperature and morphometric data.	186
4.8 How do these Tr-J boundary interval results correlate with other perceived palaeo-ocean acidification or palaeotemperature events?	188
4.9 Summary	190
4.9.2 Further work.....	191
Chapter 5 – Effects of elevated $p\text{CO}_2$ and temperature on three extant ostracod species.	193
5.1 Introduction	193
5.2 Aim and objectives.....	195
5.3 Choice of experimental species	196
5.3.2 <i>Leptocythere</i> sp.....	197
5.3.3 <i>Leptocythere castanea</i> (Sars, 1866)	198

5.3.4 <i>Leptocythere lacertosa</i> (Hirschmann, 1912).....	199
5.4 Materials and methods	200
5.4.2 Animal material	200
5.4.3 Experimental cages	201
5.4.4 Experimental mesocosm set-up	203
5.4.5 Measurement of pH, salinity, oxygen and total alkalinity	206
5.4.6 Experimental protocol	207
5.4.7 Ostracod morphometrics	210
5.4.8 Preparation of resin blocks for carapace thickness measurements	213
5.4.9 Carapace mineralogy.....	217
5.4.10 Data manipulation.....	219
5.5 Results	220
5.5.2 Field collected individuals	220
5.5.3 <i>Leptocythere</i> sp.	220
5.5.4 <i>L. castanea</i>	220
5.5.5 <i>L. lacertosa</i>	221
5.6 Effects of elevated CO ₂ and temperature on survival.....	221
5.6.2 Effect of elevated CO ₂ and temperature on ostracod morphometrics for living individuals.....	224
5.6.3 Effect of elevated CO ₂ and temperature on live ostracod mineralogy. ..	224
5.6.4 Effect of elevated CO ₂ and temperature on carapace condition of live ostracods.	227
5.7 Effect of exposure to elevated CO ₂ and temperature conditions on the carapaces of dead individuals over 21 days and 95 days?	232
5.8 Significant relationships between the variations in geometric carapace size, thickness, average Ca, and Mg and preservation for each species.	243
5.9 Discussion	249
5.9.2 Survival	249
5.9.3 Carapace condition in live individuals	252
5.9.4 Variations in the carapace size of live individuals.....	255
5.9.5 Variations in the carapace thickness of live individuals	259
5.9.6 Variations in the carapace mineralogy of live individuals	260
5.9.7 Carapace preservation when dead	263
5.9.8 Summary	266
5.9.9 Further work.....	267
Chapter 6 – Discussion.....	268
6.1 Introduction.....	268

6.2 Aims and objectives	271
6.3 Comparison of fossil relationships (Chapter 4) with the results from laboratory experiments using living organisms.....	271
6.4 Comparison of fossil relationships (Chapter 4) with the results from laboratory experiments using deceased organisms.....	278
6.5 Summary	281
Chapter 7 - Conclusions.....	283
Appendix 1 – Summary of previously published modern high CO ₂ experiments using bivalves (relates to Chapter 1)	287
Appendix 2 – Summary of previously published modern temperature experiments using bivalves (relates to Chapter 1)	295
Appendix 3 – Previously published data correlated to Lyme Regis and St Audrie's Bay (relates to Chapter 2)	299
A3.1: Previously published isotope data from Lyme Regis and St Audrie's Bay	299
A3.2: Previously published pCO ₂ data correlated to Lyme Regis and St Audrie's Bay.....	305
Appendix 4 – Raw fossil data collected from both locations and the corresponding analysis of the results (relates to Chapter 3)	308
A4.1: Lyme Regis raw fossil data.....	308
A4.1.2: Relationships between the fossil size recorded and the number of individuals measured at Lyme Regis.....	367
A4.1.3: Statistical analysis results for fossil data from Lyme Regis.	382
A4.2: St Audrie's Bay raw fossil data	391
A4.2.2: Relationships between the fossil size recorded and the number of individuals measured at St Audrie's Bay.	457
A4.2.3: Statistical analysis results for fossil data from St Audrie's Bay.....	465
A4.3: Comparisons of fossil data between both locations	470
Appendix 5 – Raw isotope data collected from both locations and the corresponding analysis of the isotope results and pCO ₂ data with the fossil size data (relates to Chapter 4)	478
A5.1: Raw isotope data from both locations	478
A5.2: Raw mineralogical results from both locations	480
A5.3: Tables of the temperature data from Lyme Regis or St Audrie's Bay that corresponds with the available pCO ₂ results.	483
A5.3.2: Linear regression models demonstrating there were no significant relationships between the temperature data from Lyme Regis or St Audrie's Bay and the available corresponding pCO ₂ results.	487
A5.4: Tables of the available pCO ₂ results that corresponds with the Lyme Regis or St Audrie's Bay fossil size data from this study.	490

A5.4.2: Linear regression models indicating no significant relationships between the available $p\text{CO}_2$ results that correspond with the fossil size data from Lyme Regis or St Audrie's Bay	505
A5.5: Tables of the available temperature results that corresponds with the Lyme Regis or St Audrie's Bay fossil size data from this study.	515
A5.5.2: Linear regression models demonstrating there were no significant relationships between the available temperature results that correspond with the Lyme Regis or St Audrie's Bay fossil size data from this study.	526
Appendix 6 – Raw ostracod data and its statistical analysis (relates to Chapter 5)	538
A6.1: TA and ICPOES results collected during the experiment	538
A6.2: <i>Leptocythere</i> sp. raw data sets	540
A6.2.2: <i>Leptocythere</i> sp. analysis of raw data	545
A6.3: <i>L. castanea</i> raw data sets	564
A6.3.2: <i>L. castanea</i> analysis of raw data	571
A6.4: <i>L. lacertosa</i> raw data sets	590
A6.4.2: <i>L. lacertosa</i> analysis of raw data	596
References.....	614

LIST OF FIGURES

Figure 1.1	$p\text{CO}_2$ levels reconstructed for the Tr-J boundary using fossil Ginkgoalean leaves and palaeosol data	8
Figure 1.2	The effects of increased atmospheric carbon dioxide on the ocean chemistry and calcareous organisms	17
Figure 2.1	Location of southwest England during the Early Jurassic	31
Figure 2.2	Locations of Lyme Regis and St Audrie's Bay in southwest England	32
Figure 2.3	An overview of the stratigraphy of southwest England	32
Figure 2.4	Geological map of the coastal section from Pinhay bay to Lyme Regis	35
Figure 2.5	A stratigraphical log of the Lyme Regis section	37
Figure 2.6	Blue Lias Formation between Pinhay Bay and Lyme Regis	38
Figure 2.7	Geological map of St Audrie's Bay	41
Figure 2.8	The Lilstock Formation and Blue Lias Formation at St Audrie's Bay	45
Figure 2.9	A stratigraphical log of the St Audrie's Bay section	48
Figure 2.10a	Published $\delta^{18}\text{O}$ values and the $\delta^{13}\text{C}$ values from St Audrie's Bay correlated to this study St Audrie's Bay log and bed numbers	53
Figure 2.10b	$\delta^{18}\text{O}$ values and the $\delta^{13}\text{C}$ values from Lyme Regis	54
Figure 2.11	Correlation of the Tr-J southwest England sites to Kuhjoch (GSSP), Astartekløft (East Greenland) and	57

	Newark basin	
Figure 2.12	Magnetostratigraphy and the $\delta^{13}\text{C}_{\text{org}}$ curve from St Audrie's Bay correlated with the latest time calibration for the Newark Basin sequence	59
Figure 2.13	Schematic correlation of the Astartekløft plant beds, the Astartekløft sporomorph zonation and the St Audrie's Bay sporomorph biozonations	63
Figure 2.14	The $p\text{CO}_2$ curves from Greenland, Sweden, Larné and the Newark Basin correlated with the St Audrie's Bay and Lyme Regis logs	65
Figure 3.1	Images of studied fossil specimens	71
Figure 3.2	Position of length and width measurements on studied fossil specimens	75
Figure 3.3	Representative bivalve specimens showing the different types of preservation found	76
Figure 3.4	Example of the mould used to produce the ostracod resin blocks	78
Figure 3.5	Examples of several <i>O. aspinata</i> cut from the ventral edge to the dorsal hinge from sample SAB60	78
Figure 3.6	Linear regression models with trend lines showing Lyme Regis <i>P. gigantea</i> geometric sizes on each bed against the corresponding number of individuals measured in each bed	86
Figure 3.7	Linear regression models with trend lines showing <i>L. hisingeri</i> relationships between geometric shell size and the number of individuals measured in each bed, (A-C) Lyme Regis (D-E) St Audrie's Bay	87
Figure 3.8	Linear regression models with trend lines showing <i>O. aspinata</i> relationships between geometric shell size and the number of individuals measured bed by bed, (A-B) Lyme Regis (C-E) St Audrie's Bay	88
Figure 3.9	Linear regression models with trend lines showing <i>O. aspinata</i> relationships between thickness and the number of individuals measured bed by bed, (A-B) Lyme Regis (C-D) St Audrie's Bay	89
Figure 3.10	The geometric shell sizes of <i>L. hisingeri</i> measured on each bed at Lyme Regis and collated into zones and subzones	92
Figure 3.11	The geometric shell sizes of <i>L. hisingeri</i> measured on each bed at St Audrie's Bay and collated into zones and subzones	93
Figure 3.12	The geometric shell sizes of <i>P. gigantea</i> measured on each bed at Lyme Regis and collated into zones and subzones	97
Figure 3.13	The geometric shell sizes of <i>O. aspinata</i> measured on each bed at Lyme Regis and collated into zones and subzones	100
Figure 3.14	The geometric shell sizes of <i>O. aspinata</i> measured on each bed at St Audrie's Bay and collated into zones and subzones	101

Figure 3.15	Relationships between <i>O. aspinata</i> length against width from (A) Lyme Regis, (B) St Audrie's Bay showing variations in the range of carapace sizes found and measured in each bed	102
Figure 3.16	The mean shell thickness of <i>O. aspinata</i> measured on each bed at Lyme Regis and collated into zones and subzones	105
Figure 3.17	The mean shell thickness of <i>O. aspinata</i> measured on each bed at St Audrie's Bay and collated into zones and subzones	106
Figure 3.18	The geometric shell sizes of <i>L. hisingeri</i> , <i>P. gigantea</i> and <i>O. aspinata</i> measured on each bed to highlight any corresponding increasing or decreasing size trends between the three species	116
Figure 3.19	The geometric shell sizes of <i>L. hisingeri</i> and <i>O. aspinata</i> measured on each bed to highlight any corresponding increasing or decreasing size trends between the three species	117
Figure 3.20	Linear regression model showing relationships between Lyme Regis fossil geometric shell size data at subzonal scale	119
Figure 3.21	Linear regression model showing relationships between St Audrie's Bay fossil geometric shell size at subzonal scale	119
Figure 3.22	The geometric shell size data of <i>L. hisingeri</i> measured on each bed at Lyme Regis and St Audrie's Bay	122
Figure 3.23	Linear regression model showing relationships between the <i>L. hisingeri</i> geometric size for each subzone from Lyme Regis and St Audrie's Bay	123
Figure 3.24	Comparison of the geometric mean shell size of <i>L. hisingeri</i> from Lyme Regis and St Audrie's Bay	123
Figure 3.25	The geometric shell size data of <i>O. aspinata</i> measured on each bed at Lyme Regis and St Audrie's Bay	125
Figure 3.26	Linear regression model showing relationships between the <i>O. aspinata</i> 95th percentile maximum geometric size for each subzone from Lyme Regis and St Audrie's Bay	127
Figure 3.27	Comparison of the geometric shell size of <i>O. aspinata</i> in Lyme Regis and St Audrie's Bay	127
Figure 3.28	The shell thickness data of <i>O. aspinata</i> measured on each bed at Lyme Regis and St Audrie's Bay	128
Figure 3.29	Shell thickness of <i>O. aspinata</i> at Lyme Regis and St Audrie's Bay	129
Figure 3.30	Comparison of the shell thickness of <i>O. aspinata</i> in Lyme Regis and St Audrie's Bay	129
Figure 4.1	Cross plots between $\delta^{13}\text{C}$ or $\delta^{18}\text{O}$ and Mn (ppm) or Fe (ppm)	146
Figure 4.2	Cross plots between $\delta^{18}\text{O}$ and $\delta^{13}\text{C}_{\text{carb}}$ bulk rock and fossil samples from (A) Lyme Regis, (B) St Audrie's Bay	148
Figure 4.3	Atmospheric $p\text{CO}_2$ curves from the Newark Basin, Greenland, Sweden and Larné correlated to the Lyme	154

	Regis fossil palaeotemperature curves	
Figure 4.4	Atmospheric $p\text{CO}_2$ curves from the Newark Basin, Greenland, Sweden and Larne correlated to the St Audrie's Bay fossil palaeotemperature curves	155
Figure 4.5	Atmospheric $p\text{CO}_2$ curves correlated to the <i>L. hisingeri</i> data from St Audrie's Bay and Lyme Regis	157
Figure 4.6	Linear regression models showing relationships between the geometric size of <i>L. hisingeri</i> at Lyme Regis (A-E) and the $p\text{CO}_2$ levels	158
Figure 4.7	Atmospheric $p\text{CO}_2$ curves correlated to the Lyme Regis <i>P. gigantea</i> data	159
Figure 4.8	Linear regression models showing relationships between the geometric size of <i>P. gigantea</i> at Lyme Regis (A-C) and the $p\text{CO}_2$ levels	160
Figure 4.9	Atmospheric $p\text{CO}_2$ curves correlated to the Lyme Regis <i>O. aspinata</i> data	162
Figure 4.10	Linear regression models showing relationships between the geometric size of <i>O. aspinata</i> from Lyme Regis or St Audrie's Bay and the $p\text{CO}_2$ levels	163
Figure 4.11	Linear regression models showing relationships between the shell thickness of <i>O. aspinata</i> from Lyme Regis and St Audrie's Bay and the $p\text{CO}_2$ levels	164
Figure 4.12	$\delta^{13}\text{C}$ curve correlated to the Lyme Regis <i>L. hisingeri</i> data	170
Figure 4.13	$\delta^{13}\text{C}$ curve correlated to the St Audrie's Bay <i>L. hisingeri</i> data	171
Figure 4.14	$\delta^{13}\text{C}$ curve correlated to the Lyme Regis <i>P. gigantea</i> data	172
Figure 4.15	Linear regression models showing relationships between the geometric size of <i>O. aspinata</i> from Lyme Regis and the $\delta^{13}\text{C}$ data	173
Figure 4.16	$\delta^{13}\text{C}$ curve correlated to the Lyme Regis <i>L. hisingeri</i> data	174
Figure 4.17	$\delta^{13}\text{C}$ curve correlated to the St Audrie's Bay <i>L. hisingeri</i> data	175
Figure 4.18	Linear regression models showing relationships between the geometric size of <i>O. aspinata</i> from St Audrie's Bay and the $\delta^{13}\text{C}$ data	176
Figure 4.19	Linear regression models showing relationships between the shell thickness of <i>O. aspinata</i> from Lyme Regis and the $\delta^{13}\text{C}$ data	176
Figure 4.20	Linear regression models showing relationships between the shell mineralogy of <i>O. aspinata</i> from Lyme Regis and the $\delta^{13}\text{C}$ data	177
Figure 4.21	Palaeotemperature curve correlated to the Lyme Regis <i>L. hisingeri</i> data	180
Figure 4.22	Palaeotemperature curve correlated to the St Audrie's Bay <i>L. hisingeri</i> data	181
Figure 4.23	Linear regression models showing relationships between the <i>P. gigantea</i> from Lyme Regis and the	182

	palaeotemperature	
Figure 4.24	Palaeotemperature curve correlated to the Lyme Regis <i>P. gigantea</i> data	183
Figure 4.25	Palaeotemperature curve correlated to the Lyme Regis <i>O. aspinata</i> data	184
Figure 4.26	Palaeotemperature curve correlated to the St Audrie's Bay <i>O. aspinata</i> data	185
Figure 4.27	Linear regression models showing relationships between the geometric size of <i>O. aspinata</i> from St Audrie's Bay (A-G) and the palaeotemperature	186
Figure 5.1	<i>Leptocythere</i> sp. images	198
Figure 5.2	<i>Leptocythere castanea</i> images	198
Figure 5.3	<i>Leptocythere lacertosa</i> images	199
Figure 5.4	Components used to construct the cages and a constructed cage.	203
Figure 5.5	Schematic of CO ₂ & Temperature Equilibration System	205
Figure 5.6	SEM image of the recorded measurements for ostracod carapace	211
Figure 5.7	The ostracod preservation scale	212
Figure 5.8	Photographs illustrating how resin blocks were made	214
Figure 5.9	Two different sections through one ostracod valve	216
Figure 5.10	Carapace preservation of the different field collected species	221
Figure 5.11	Survival of (A) <i>Leptocythere</i> sp., (B) <i>L. castanea</i> , (C) <i>L. lacertosa</i> after 21 and 95 days	223
Figure 5.12	<i>L. lacertosa</i> : The box and whisker plot displays the geometric carapace size data (µm) from each treatment	224
Figure 5.13	<i>L. lacertosa</i> : The box and whisker plot displays the live average Mg data (%) in each treatment	226
Figure 5.14	<i>Leptocythere</i> sp.: The box and whisker plot displays the live carapace condition data from each treatment set	227
Figure 5.15	<i>L. castanea</i> : The box and whisker plot displays the live carapace condition data from each treatment	228
Figure 5.16	<i>L. lacertosa</i> : The box and whisker plot displays the live carapace condition data from each treatment	228
Figure 5.17	Images of <i>Leptocythere</i> sp. showing examples of the preservation after 21 days and then 95 days	229
Figure 5.18	Images of <i>L. castanea</i> showing examples of the preservation after 21 days and then 95 days	230
Figure 5.19	Images of <i>L. lacertosa</i> showing examples of the preservation after 21 days and then 95 days	231
Figure 5.20	<i>Leptocythere</i> sp.: The box and whisker plot displays the dead carapace preservation data from each treatment set	232
Figure 5.21	<i>L. castanea</i> : The box and whisker plot displays the dead carapace preservation data from each treatment	233
Figure 5.22	<i>L. lacertosa</i> : The box and whisker plot displays the dead carapace preservation data from each treatment	233
Figure 5.23	<i>Leptocythere</i> sp.: The box and whisker plot illustrates the dead geometric carapace size data (µm) from each	235

	treatment	
Figure 5.24	<i>L. castanea</i> : The box and whisker plot illustrates the dead geometric carapace size data (μm) from each treatment	236
Figure 5.25	<i>L. lacertosa</i> : The box and whisker plot illustrates the dead geometric carapace size data (μm) from each treatment	236
Figure 5.26	<i>L. castanea</i> : The box and whisker plot illustrates the dead mean carapace thickness data (μm) from each treatment set	238
Figure 5.27	<i>Leptocythere</i> sp.: The box and whisker plot illustrates the dead average Mg data (%) from each treatment	239
Figure 5.28	<i>L. castanea</i> : The box and whisker plot illustrates the dead average Mg data (%) from each treatment	240
Figure 5.29	<i>L. lacertosa</i> : The box and whisker plot illustrates the dead average Mg data (%) from each treatment	240
Figure 5.30	<i>Leptocythere</i> sp.: The box and whisker plot illustrates the dead average Ca data (%) from each treatment	242
Figure 5.31	<i>L. castanea</i> : The box and whisker plot illustrates the dead average Ca data (%) from each treatment	242
Figure 5.32	<i>L. lacertosa</i> : The box and whisker plot illustrates the dead average Ca data (%) from each treatment	243
Figure 5.33	<i>Leptocythere</i> sp.: Linear regression models and Spearmans rank results (p-values) from comparing all the different data sets against the relevant preservation rank	245
Figure 5.34	<i>L. lacertosa</i> : Linear regression models and Spearmans rank results (p-values) from comparing all the different data sets against the relevant preservation rank	246
Figure 5.35	<i>L. castanea</i> : Linear regression models and Spearmans rank results (p-values) from comparing all the different data sets against the relevant preservation rank	247
Figure 5.36	<i>Leptocythere</i> sp.: Linear regression models comparing all the data against each other	247
Figure 5.37	<i>L. castanea</i> : Linear regression models comparing all the data against each other	248
Figure 5.38	<i>L. lacertosa</i> : Linear regression models comparing all the data against each other	248
Figure 6.1	Summary diagram showing key changes during Tr-J boundary interval at St Audrie's Bay and Lyme Regis	270

LIST OF TABLES

Table 1.1	A summary of previously published results from modern bivalve increased $p\text{CO}_2$ experiments.	25
Table 1.2	A summary of previously published results from modern bivalve temperature experiments.	26
Table 1.3	Summary of published data showing the responses of different ostracod taxa to increased temperature.	26
Table 2.1	Proposed correlation of ammonite zones for the Early Hettangian.	56
Table 3.1	The type of preservation recorded and the coding used.	74
Table 3.2	Summary of <i>L. hisingeri</i> morphometric data from Lyme Regis and St Audrie's Bay.	81
Table 3.3	Summary of <i>P. gigantea</i> morphometric data from Lyme Regis and St Audrie's Bay.	82
Table 3.4	Summary of <i>O. aspinata</i> morphometric data from Lyme Regis and St Audrie's Bay.	83
Table 3.5	Summary of <i>O. aspinata</i> shell thickness data from Lyme Regis and St Audrie's Bay.	84
Table 3.6	Summary of significant differences found between the numbers of individuals measured and the geometric sizes measured.	85
Table 3.7	Minimum number of individuals needed from each bed or sample to have no significant relationship to the geometric sizes measured.	90
Table 4.1	Number of isotope samples for <i>O. aspinata</i> , <i>L. hisingeri</i> , <i>P. gigantea</i> and bulk rock.	137
Table 4.2	Calibration standards used in the ICP-OES.	138
Table 4.3	Relationships between the geometric size of <i>L. hisingeri</i> and the $p\text{CO}_2$ levels.	158
Table 4.4	Relationships between the geometric size of <i>P. gigantea</i> and the $p\text{CO}_2$ levels.	160
Table 4.5a	Relationships between the geometric size of <i>O. aspinata</i> and the $p\text{CO}_2$ levels.	161
Table 4.5b	Relationships between the shell thickness of <i>O. aspinata</i> and the $p\text{CO}_2$ levels.	161
Table 4.6a	Relationships between the geometric size of <i>O. aspinata</i> and the $\delta^{13}\text{C}$ levels.	173
Table 4.6b	Relationships between the shell thickness of <i>O. aspinata</i> and the $\delta^{13}\text{C}$ levels.	173
Table 4.6c	Relationships between the shell mineralogy of <i>O. aspinata</i> and the $\delta^{13}\text{C}$ levels.	173
Table 4.7	Relationships between the geometric size of <i>P. gigantea</i> and the palaeotemperature.	182
Table 4.8	Relationships between the geometric size of <i>O. aspinata</i> and the palaeotemperature.	184
Table 5.1	Calibration standards for trace element geochemistry.	218
Table 5.2	Ostracod morphometrics data where no statistically	225

	significant differences were found.	
Table 5.3	Ostracod mineralogy data where no statistically significant differences were found.	226
Table 5.4	Ostracod carapace thickness data where no statistically significant differences were found.	237
Table 5.5	Relationships between any two of geometric carapace size, carapace thickness, average Mg and Ca and carapace preservation for live, dead and all the data for each species.	244
Table 6.1	The shell condition of living marine organisms during modern $p\text{CO}_2$ and temperature experiments combined with the morphological results from the Tr-J boundary.	273– 275
Table 6.2	The shell preservation of dead marine organisms during modern $p\text{CO}_2$ and temperature experiments combined with the morphological results from the Tr-J boundary.	279

ACKNOWLEDGEMENTS

Firstly I would like to thank my supervisors: Prof. John Spicer for his continued inspiration, constructive and positive comments as well as significant support and encouragement and Prof. Richard Twitchett for his academic input and chapter corrections. I would like to thank Plymouth University for funding this research because, without this, I would not have been able to complete this work.

Secondly, I would like to thank Prof. Malcolm Hart for his continued support, advice and constructive comments. Further thanks are due to Prof. David Horne for his assistance in the identification of the modern ostracods and the staff of the Natural History Museum who provided assistance in accessing relevant collections. In relation to all my fieldwork I am greatly appreciative and indebted to Phil Martin and Rosalind Beveridge for assisting me, keeping me sane and entertaining me during my fieldwork. I would also like to thank Marie Hawkins, Piero Calosi and Richard Ticehurst for their invaluable technical assistance and patience during the completion of the modern ostracod experiments. I also wish to thank Dr Roy Moate, Peter Bond and Glenn Harper from the Plymouth Electron Microscopy Centre for their invaluable SEM training as well as problem solving and friendship. Further thanks go to the staff of the Plymouth University Geology department for their assistance, friendship and encouragement over the duration of my PhD and I specifically wish to thank both Sharon Healy and Debbie Petherick from the Graduate School plus Prof. Jim Griffiths for listening to me and offering their invaluable help and support over the years.

Finally, I would like to give my warmest thanks to my partner, James Williams who believed in me and without that support I would not have managed to complete this PhD, my parents Ken and Annette Jacobsen and the rest of my family and my partner's family for their continuous support and encouragement which was also vital especially through the hard times. I would also like to thank my friends here and elsewhere, Sam Ilott, Phil Martin, Rosalind Beveridge, Martha Koot and Rob Hall, Tom Dixon, Hannah Pim, Ross Minall, Caroline Davies, Alice Thompson, Jodie Franklin, Hayley Manners, Marie-Emilie Clemence, Helen Hughes and many others for listening, their continued support, keeping me sane and on occasion making me take a break from the work.

AUTHOR'S DECLARATION

At no time during the registration for the degree of Doctor of Philosophy has the author been registered for any other University award without prior agreement of the Graduate Committee. Work submitted for this research degree at the Plymouth University has not formed part of any other degree either at Plymouth University or at another establishment

This study was financed with the aid of a studentship from Plymouth University.

A programme of advanced study was undertaken, which included a range of skills development courses available at Plymouth University, Scanning Electron Microscopy training and a postgraduate course on laboratory-based teaching methods and practice.

Relevant scientific seminars and conferences were regularly attended at which work was often presented; external institutions were visited for consultation purposes and several papers prepared for publication.

Publications:

Jacobsen, N.D., Twitchett, R.J. & Krystyn, L. 2011. Palaeoecological methods for assessing marine ecosystem recovery following the Late Permian mass extinction event. *Palaeogeography, Palaeoclimatology, Palaeoecology*, **308**, 200-212.

Presentation and Conferences Attended:

55th Annual Meeting, Palaeontological Association, Plymouth, UK (December 2011, poster)

The Ostracod Group of The Micropalaeontology Society, Leicester, UK (June 2011)

Progressive Palaeontology, Palaeontological Association, Leicester, UK (May 2011, talk)

54th Annual Meeting, Palaeontological Association, Ghent, Belgium (December 2010)

1st Centre for Research in Earth Sciences conference, Plymouth, UK (November 2010, talk)

53rd Annual Meeting, Palaeontological Association, Birmingham, UK (December 2009)

Word count of main body of thesis: 60,203 words

Signed: Nikita Jacobsen

Date: 02 October 2014

Chapter 1–Introduction

1.1 Late Triassic extinction event

The Late Rhaetian (Late Triassic) extinction event is classed as one of the big five Phanerozoic extinctions (Sepkoski, 1982; Benton, 1999; McGhee *et al.*, 2004; Alroy *et al.*, 2008; Alroy, 2010). Evidence for this extinction event can be seen both in the marine realm and on the continents. It is ranked fourth in rate of overall severity but third in ecological severity (McGhee *et al.*, 2004), with ~80% of all species becoming extinct (Sepkoski, 1996; Hallam and Wignall, 1997). Several different causes have been suggested for this extinction event, but palaeoclimate studies have indicated a significant increase in $p\text{CO}_2$ levels in the atmosphere (McElwain *et al.*, 1999; Tanner *et al.*, 2001; Wignall, 2005; Schaller *et al.*, 2011; Hoenisch *et al.*, 2012) which led to the hypothesis of global ocean acidification and increased temperature in the oceans (Hesselbo *et al.*, 2002; Pálffy *et al.*, 2007; van de Schootbrugge *et al.*, 2007; Korte *et al.*, 2009).

Triassic-Jurassic outcrops can be found around the world, some of the best exposed sections include southwest England (Lyme Regis, St Audrie's Bay), the Northern Calcareous Alps (Italy, Hungary and Austria (Global Stratotype Section and Point of the base Jurassic; GSSP: Von Hillebrandt *et al.*, 2007; International Commission on stratigraphy, 2013)) and North America (British Columbia, Canada and Nevada, USA (Auxiliary Stratotype Section and Point; ASSP: Guex *et al.*, 2004; International Commission on stratigraphy, 2013)). Radiometric ages for the end-Rhaetian have been determined as $\sim 201.3 \pm 0.2\text{Ma}$ and the end-Hettangian as $\sim 199.3 \pm 0.3\text{Ma}$ based on zircon U-Pb

dating (Whiteside *et al.*, 2010; International Commission on stratigraphy, 2013).

Evidence for a marine mass extinction event during the late Rhaetian comes from the fossil record of reef building organisms as well as ammonites, ostracods, foraminifera, bivalves and brachiopods, which show a sudden turnover at this time, loss of reef habitats and a reduction in their geographical distribution (Pálffy, 2005; Kiessling *et al.*, 2007; Tomašových and Siblik, 2007; Wignall and Bond, 2008; Martindale *et al.*, 2012; McRoberts *et al.*, 2012). During this period one of the biggest turnovers in reef ecosystem history took place causing morphologically complex and diverse assemblages to be replaced by morphologically primitive and impoverished assemblages (Pálffy, 2005; Kiessling *et al.*, 2007; Greene *et al.*, 2012).

The timing of the extinction event has been investigated (Pálffy *et al.*, 2000; Warrington *et al.*, 2008; Mander *et al.*, 2008) and in southwest England the event is recorded from the fossil record during the middle of the Lillstock Formation (Upper Rhaetian, 201.3Ma; as shown in Ruhl *et al.*, 2010: Figure 7 p272). Deenen *et al.* (2010) have suggested that, in South west England, the bivalve extinction and a change in dinoflagellate cyst assemblages occurred within the Cotham Member and that a calcification crisis occurred in calcareous nanofossils through the Langport Member. This position correlates with the same extinction event found at other Triassic-Jurassic (Tr-J) locations around the global including the Northern Calcareous Alps (Austria) and North America (Whiteside *et al.*, 2010).

Towards the end of the Triassic, Pangaea began to break up and the Palaeo-Tethys closed (Golonka, 2007). These plate movements resulted in a number of volcanic events including the formation of the Central Atlantic Magmatic Province (CAMP) during a period of extensional tectonics (Golonka, 2007). This volcanic centre generated a 25km thick sequence of magma with a volume of $2 \times 10^6 \text{ km}^3$, forming the CAMP and causing a significant increase in atmospheric CO_2 levels (Tanner *et al.*, 2004; Marzoli *et al.*, 2004; Huynh and Poulsen, 2005; Golonka, 2007; Hesselbo *et al.*, 2004; Deenen *et al.*, 2010; Rampino, 2010; Schaller *et al.*, 2011).

Many of the potential causes of the Tr-J mass extinction event in terrestrial and oceanic realms include; sea-level fluctuation (which does not explain the turnover in the terrestrial realm), bolide impact and long term climate change (both of which could explain the turnover in both terrestrial and oceanic realms; Tanner *et al.*, 2004; McRoberts *et al.*, 2012). Another explanation is high atmospheric CO_2 levels from the formation of CAMP. Using the known CAMP volume and modern volcanic degassing rates, 1900 to 17,454 Gt C (Gt = mass; in thousands) of CO_2 was thought to have been released, whereas the recorded amount of total gases based on volatile content were calculated to range from 1110 to 21,000 Gt C (Bernier and Beerling, 2007). Fossil stomatal characteristics (stomatal index) are used to reconstruct $p\text{CO}_2$ levels over a period of time and provided the evidence that atmospheric CO_2 levels have increased significantly with a 2 to 3 fold rise across the Tr-J boundary (McElwain *et al.*, 1999; Beerling and Bernier, 2002; Huynh and Poulsen, 2005; Steinthorsdottir *et al.*, 2011; Höenisch *et al.*, 2012). Experiments using coupled ocean-atmosphere GCM models concluded that

rising CO₂ would cause a severe enough environmental stress (e.g., ocean acidification and stratification leading to reduced available oxygen, depressed aragonite and calcite saturation state, increased heat stress and extreme seasonal fluctuations) to bring about a biological turnover both on land and in the ocean (Huynh and Poulsen, 2005). Depending on the level of dissolved inorganic carbon (DIC) in the ocean, together with the level of CAMP CO₂ and the length of time it was being injected into the atmosphere, using the GEOCARBIII model it can be determined how quickly and to what level a change in pH impacted the oceans (Hautmann, 2004; Hautmann *et al.*, 2008; Greene *et al.*, 2012). Martindale *et al.*, (2012) suggests that if pCO₂ values were as extreme as suggested a mass extinction could have occurred due to undersaturation of aragonite in moderate to low DIC reservoirs and undersaturation of calcite in low dissolved inorganic carbon reservoirs, causing a short but extreme period of ocean acidification during the late Rhaetian until the mid-Hettangian.

Greene *et al.*, (2012) stated that if 21,000 Gt C was released over a period of 25kyr, a 20kyr period of extreme undersaturation could occur, but if this same mass was released over a 100kyr period, only slight undersaturation would occur over a 5kyr period (Bernier and Beerling, 2007). Schaller *et al.* (2011) indicated that from the Tr-J Newark Basin section each CAMP pulse was followed immediately by an increase in pCO₂ levels which doubled or tripled within 20kyr, suggesting an instantaneous influence on the global carbon cycle (Bernier and Beerling, 2007; Greene *et al.*, 2012). This would explain the coral reef gap and extinction of other calcareous organisms through the late Rhaetian to mid-Hettangian (Martindale *et al.*, 2012).

1.2 Triassic – Jurassic boundary $p\text{CO}_2$ record

To be able to investigate the patterns of marine organism response to global ocean acidification, reconstructions of past atmospheric CO_2 levels are needed (McElwain *et al.*, 1999; Retallack, 2001; Retallack, 2002; Royer, 2006; Bonis *et al.*, 2010; Schaller *et al.*, 2011; Steinthorsdottir *et al.*, 2011). Intervals of geological time that record a period of substantial CO_2 release, a reduction in the CaCO_3 saturation and a reduced level of oceanic pH can be classified as an ocean acidification event (Hönisch *et al.*, 2012). Hönisch *et al.* (2012) report the results of several experiments using an Earth system model. The results indicate that mean ocean surface pH and aragonite saturation become progressively decoupled when the rapid rate of $p\text{CO}_2$ increase occurs over a time scale of 100,000 years or less (Hönisch *et al.*, 2012). Atmospheric $p\text{CO}_2$ records from palaeosols and ginkgoalean leaves indicate that, on average, $p\text{CO}_2$ doubled over a 20ky period. It has been suggested, however, that the CO_2 was not released at a uniform rate but that the increase was the result of several pulses (Kemp *et al.*, 2005; Ruhl *et al.*, 2011; Schaller *et al.*, 2011). The average rate of CO_2 emissions during the whole of the CAMP eruption period would probably not record the levels required for periods of ocean acidification, although some of the individual pulses could have attained the appropriate levels in the 100,000 year time scale for ocean acidification (Hönisch *et al.*, 2012).

McElwain *et al.* (1999), Bonis *et al.* (2010) and Steinthorsdottir *et al.* (2011) reconstructed $p\text{CO}_2$ levels using stomatal characters of fossil ginkgoalean leaves. The fossil leaves came from East Greenland and southern Sweden (McElwain *et al.*, 1999), East Greenland and Larne, Northern Ireland

(Steinhorsdottir *et al.*, 2011) and Wustenwelsberg, Germany (Bonis *et al.*, 2010). This method utilizes an inverse correlation between the stomatal index and atmospheric $p\text{CO}_2$, which is established from measurements of the stomatal index of fossil cuticles divided by the stomatal index of equivalent modern cuticles which produce a stomata ratio (SR) (Royer, 2001). The stomatal ratio (SR) is directly related to past atmospheric CO_2 ratios that are relative to the present day (McElwain *et al.*, 1999; Beerling and Berner, 2002). Two different calibrations using SR have been suggested (Berner, 1994; McElwain and Chaloner, 1995; McElwain, 1998; Beerling and Berner, 2002; Beerling and Royer, 2002), $1\text{SR}=600\text{ppm}$ and $1\text{SR}=450\text{ppm}$, which provide the upper and lower $p\text{CO}_2$ estimates for each section.

Estimates of $p\text{CO}_2$ change from Sweden (McElwain *et al.*, 1999), Greenland (McElwain *et al.*, 1999; Steinhorsdottir *et al.*, 2011) and the Newark Basin (Schaller *et al.*, 2011) show substantial increases in $p\text{CO}_2$ levels across the Tr-J boundary (Figure 1.1; Beerling and Berner, 2002). This indicates that even at different locations, the $p\text{CO}_2$ levels found from stomatal indices are showing a very similar pattern of results (McElwain *et al.*, 1999). The issue with the studies using stomatal frequency is that they are of low resolution and based around small numbers of specimens from multiple locations and as a proxy is thought to underestimate $p\text{CO}_2$ as well as not be as accurate as experimental and sub fossil responses (Royer, 2001; Schaller *et al.*, 2011). A further issue is that in some studies the comparisons between modern and fossil plants were made with two separate but ecologically equivalent sets of species which could affect the $p\text{CO}_2$ reconstructions and CO_2 is not the sole factor determining the stomatal index (McElwain *et al.*, 1999; Royer, 2001).

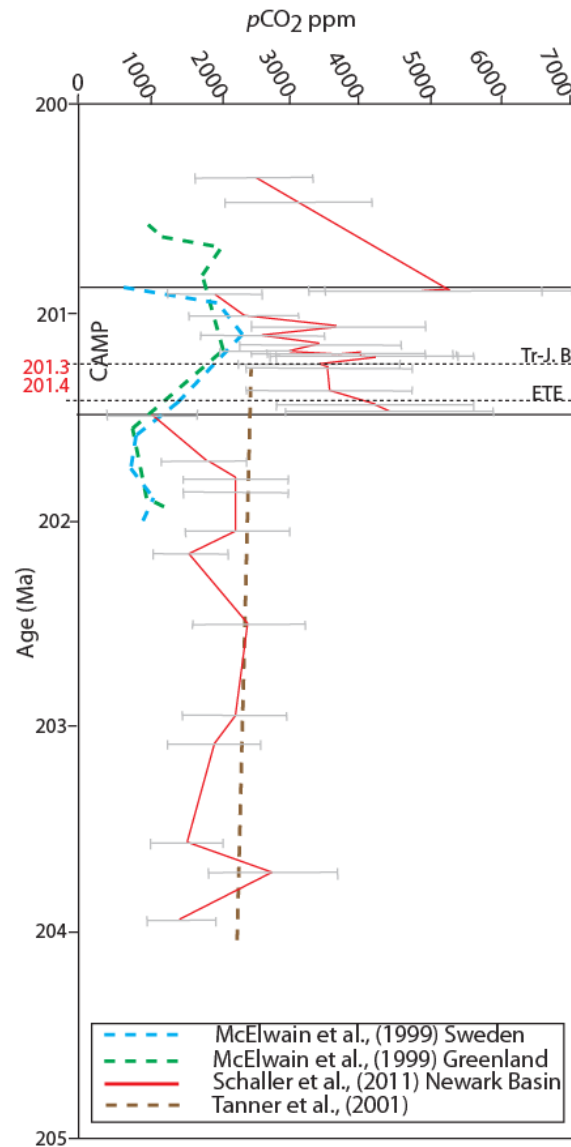


Figure 1.1: $p\text{CO}_2$ levels reconstructed for the Tr-J boundary using fossil ginkgoalean leaves by McElwain *et al.* (1999) (Greenland and Sweden) and palaeosol data by Tanner *et al.* (2001) and Schaller *et al.* (2011) (Newark Basin). Figure modified from Schaller *et al.* (2011). Acronyms: End Triassic Extinction (ETE), Triassic – Jurassic Boundary (Tr-J. B). McElwain *et al.* (1999) data were combined with the Schaller *et al.* (2011) data using the magnetic stratigraphy of Kent and Clemmensen (1996) and Whiteside *et al.* (2010).

Several studies have used pedogenic carbonate nodules from palaeosols to investigate the $p\text{CO}_2$ record from the eastern North American Newark Supergroup (Figure 1.1; Tanner *et al.*, 2001; Schaller *et al.*, 2011). The $p\text{CO}_2$ results from these studies were calculated using the $\delta^{13}\text{C}$ values and a diffusion reaction model (Tanner *et al.*, 2001; Schaller *et al.*, 2011). Tanner *et*

al. (2001) conclude from a very low sampling resolution, that there is an increase in palaeo- $p\text{CO}_2$ across the boundary but that the increase was not significant. Schaller *et al.* (2011) analysed a data set with a significantly higher sampling resolution from throughout the CAMP sequence. Their results produced pre-CAMP values ranging from ~2000ppm to ~4000ppm and post-eruption values peaking at around 6000ppm (Figure 1.1; Schaller *et al.*, 2011). Between each volcanic unit mean $p\text{CO}_2$ values show a decreasing trend, returning to pre-eruption levels after approximately 300kyr (Schaller *et al.*, 2011). These increasing $p\text{CO}_2$ values are thought to be in response to the localised episodes of relatively short magmatic activity occurring in the Newark Basin and the decrease in $p\text{CO}_2$ thought to be due to the weathering of silicates consuming the CO_2 (Schaller *et al.*, 2011). There are several issues with the use of pedogenic carbonate nodules: (1) confirming the preservation; (2) the need to consider changes in the carbon isotopic composition measured from the palaeosol's terrestrial organic matter; and (3) the use of certain assumptions within a diffusion model (e.g., carbon cycle perturbations and assuming constant fractionation by photosynthesis) (Schaller *et al.*, 2011). The issue with using a diffusion model is that the assumptions for that model, and model itself, may be updated or changed in the future (if they have not already) which could change these results.

Overall, the data from each location and method discussed here show a significant rise in $p\text{CO}_2$ levels corresponding with CAMP volcanism and the Tr-J boundary (Figure 1.1; McElwain *et al.*, 1999; Tanner *et al.*, 2001; Beerling and Berner, 2002; Schaller *et al.*, 2011). However, the $p\text{CO}_2$ values vary significantly between the two methods. The palaeosol results record

significantly higher $p\text{CO}_2$ values than the fossil ginkgoalean leaves (which are thought to underestimate $p\text{CO}_2$ levels) from Greenland, Sweden and Larné (Figure 1.1; McElwain *et al.*, 1999; Tanner *et al.*, 2001; Beerling and Berner, 2002; Steinhorsdottir *et al.*, 2011; Schaller *et al.*, 2011).

1.2.2 Tr-J ocean acidification and the fossil record

McElwain *et al.* (1999) was one of the first to suggest that elevated atmospheric $p\text{CO}_2$ levels (partial pressure of CO_2) inferred during the Tr-J mass extinction event were the result of the eruption of the Central Atlantic Magmatic Province (CAMP) and that this caused a massive temperature increase of up to 4°C (Olsen, 1999; McHone, 2000; McElwain *et al.*, 2007). This greenhouse effect has also been indicated to have occurred during other significant periods of increased volcanic CO_2 emissions, for example during the release of CO_2 from the Siberian traps and the Permian-Triassic extinction as well as the increased volcanic CO_2 emissions from the Deccan traps and the Cretaceous-Paleogene boundary (Retallack, 2001; Beerling *et al.*, 2002; Kidder and Worsley, 2003). This is believed to trigger reduced pH causing ocean acidification and a temporary under saturation of aragonite and calcite in seawater leading to a biocalcification crisis (Hautmann, 2004; Galli *et al.*, 2005, 2007). No studies have been found that specifically measure for changes in pH through the Tr-J period possibly due to the fact that it is not actually possible. However, it is possible to infer a reduction in pH because the measured increase in $p\text{CO}_2$ coincided with an interruption in Tr-J carbonate sedimentation at numerous locations which suggests a substantial decrease in seawater pH producing more acidic oceans and inhibiting the precipitation of calcium carbonate (Hautmann *et al.*, 2008).

The biocalcification crisis and ocean acidification (reduced pH) is expected to be expressed in reduced shell growth both in overall size and thickness, increased mortality and shell dissolution (Hautmann, 2004; Galli *et al.*, 2005; Berge *et al.*, 2006; Gazeau *et al.*, 2007; Kurihara *et al.*, 2008; Talmage and Gobler, 2009). Increased $p\text{CO}_2$ is thought to cause dissolution of calcareous skeletons in organisms with little or no physiological buffering, which weakens the skeleton (Berge *et al.*, 2006; Gazeau *et al.*, 2007; Kurihara *et al.*, 2008; Hautmann *et al.*, 2008; Talmage and Gobler, 2009; Greene *et al.*, 2012). Hautmann (2004) predicted extinction rates to be exceptionally high in aragonitic and high magnesium calcite organisms, due to the increased energy costs to produce their shells in acidic conditions, but thought that the skeletons of non-calcareous taxa would cope reasonably well. Further empirical data indicated that taxa with smooth shell exteriors and partly calcitic shell mineralogy were more dominant during times of low or reduced CaCO_3 saturation during a carbonate gap (McRoberts *et al.*, 2012).

Hautmann (2004) also found that some epifaunal bivalve families (Ostreidae, Gryphaeidae, Plicatulidae and Pectinidae) from localities spread throughout the globe (e.g., Kendelbach, New York Canyon and Chilingote) showed minimal detrimental reactions to ocean acidification due to significantly higher proportions of calcite within their shells (Hautmann, 2004). Using the Palaeobiology Database, Kiessling *et al.* (2007) also determined that a significant increase in survival rate was evident in bivalves whose shell material contained a greater calcite concentration over purely aragonitic skeletons. St Audrie's Bay and the South Wales Tr-J locality have also shown a bias in the bivalve fauna towards calcitic taxa specifically throughout

the Pre-planorbis beds, which could either indicate bivalves adapting to the change in water chemistry or post mortem dissolution (Wright *et al.*, 2003; Mander and Twitchett, 2008). It was also noted that extinction rates significantly varied between infaunal and epifaunal bivalves, with infaunal bivalves experiencing the highest extinction rates (McRoberts and Newton, 1995; Kiessling *et al.*, 2007; Greene *et al.*, 2012). However, when the Palaeobiology Database data from bivalve taxa were combined with all the other organisms and analysed no significant selectivity in skeletal mineralogy was identified (Kiessling *et al.*, 2007). This does not support Hautmann (2004) biocalcification hypothesis because it indicates that skeletal mineralogy alone could not be the dominant factor in the extinction rates of marine organisms (Kiessling *et al.*, 2007). Mander and Twitchett (2008) investigated variations in bivalve shell mineralogy and it was discovered that aragonitic taxa made up $\geq 65\%$ of the assemblage, except through the Pre-Planorbis zone (45%).

Megalodontoidea, specifically from the Northern Calcareous Alps, did not change their original aragonite shell composition through the extinction event but drastically reduced their overall shell size (Hallam, 2002; Hautmann, 2004). In Alpine sections, none of the bivalves with the largest geometric shell sizes survived the extinction event and *Gervillea inflata*, *Conchodon* and *Megalodon* showed significantly reduced shell size (Hallam, 2002). Data from St Audrie's Bay and Lavernock Point show that bivalve body size fluctuated before the extinction event and then remained suppressed through the Hettangian (Mander *et al.*, 2008). However, at both these locations, Mander *et al.* (2008) found a distinct, but brief increase in body size within the pooled data through the lower Blue Lias Formation due to a bloom in

Liostrea within the Pre-Planorbis Zone. Shell thickness remained fairly constant throughout both sections, except for a brief temporary increase in thickness in the middle of the Pre-Planorbis zone which corresponds with the brief increase in *Liostrea* body size (Mander *et al.*, 2008). This lack of reduced shell thickness throughout the Tr-J extinction event, however, does not support Hautmann (2004) proposed biocalcification crisis during this period (Mander *et al.*, 2008). In the aftermath of an extinction event it has been commonly found that there is a temporary within-lineage reduction in the body size (dwarfism, stunting) of surviving taxa which has been described as the Lilliput effect (e.g., Urbanek, 1993; Twitchett, 2001, 2006, 2007). This reduction in body size (the Lilliput Effect) has been documented during many extinction events, including the Tr-J, Cretaceous-Palaeogene and Permian-Triassic extinctions (Jablonski and Rump, 1995; Twitchett *et al.*, 2004; Twitchett, 2001, 2006, 2007). If this is the case, it is very important for predictions of future marine environmental changes due to the increase in present day CO₂ levels.

The Tr-J extinction event was followed by a significant reef crisis as the extinction event was thought to be highly selective against hypercalcifying sponges and corals due to high $p\text{CO}_2$ causing the hypothesised ocean acidification (Marzoli *et al.*, 1999, 2004; Kiessling and Simpson, 2011). The hypothesised acidification is believed to have inhibited the coral from maintaining skeletal integrity and hence caused their extinction. Some modern corals are however, able to exist without a skeleton as polyps for short time periods (Fine and Tchernov, 2007; Greene *et al.*, 2012). This suggests that the reef gap during the Tr-J ocean acidification event in the

fossil record is due to their existence as polyps without a skeleton until supersaturated levels returned and they could rebuild their skeletons (Stanley, 2003; Greene *et al.*, 2012; Martindale *et al.*, 2012). Under saturation of sea water is observed to occur at $p\text{CO}_2 = 1200\text{-}1700\mu\text{atm}$ for aragonite and $p\text{CO}_2 = 1900\text{-}2800\mu\text{atm}$ for calcite (Hautmann *et al.*, 2008). Green *et al.* (2012) hypothesised that the significant impact on marine invertebrates (reef ecosystems), found during the Tr-J, could have been caused by ocean acidification and could in turn provide insights and predictions into how modern reef ecosystems would be affected during any future ocean acidification events.

1.2.3 Triassic-Jurassic boundary palaeotemperature curve

Previous studies have investigated changes in palaeotemperature across the Tr-J mass extinction event using $\delta^{18}\text{O}$ measurements from benthic species, mainly using oysters (Korte *et al.*, 2005; Pálffy *et al.*, 2007; van de Schootbrugge *et al.*, 2007; Korte *et al.*, 2009). Palaeotemperature curves are produced from $\delta^{18}\text{O}$ measurements from fossil or bulk rock samples which are attributed to variations in temperature (Pálffy *et al.*, 2007; Korte *et al.*, 2009). However, Korte *et al.* (2009) suggested that an argument could be made for the decreasing oxygen-isotope trend specifically identified leading into the Planorbis Zone was due in part to global or local lowering of seawater $\delta^{18}\text{O}$ rather than increasing temperature. A further factor that could affect $\delta^{18}\text{O}$ values to produce more positive values has been identified as the selective dissolution of shells, which is significant in any ocean-acidified environments (Spero *et al.*, 1998).

Live planktic species of foraminifera have also been investigated in laboratory experiments for their $\delta^{18}\text{O}$ values. Spero *et al.* (1997, 1998) established that the $\delta^{18}\text{O}$ values of planktic foraminifera tests can also be affected by photosynthetic activity from algal symbionts and the carbonate ion concentrations (CO_3^{2-}) of seawater. It was further concluded that the effect of CO_3^{2-} on the planktic foraminifera $\delta^{18}\text{O}$ record varies on a species-specific basis (Spero *et al.*, 1998). During shell calcification planktic foraminifera migrate vertically which complicates the temperature: $\delta^{18}\text{O}$ relationship because the relationship requires an assumption that the shell was calcified in the same environment (Hemleben and Bijma, 1994; Spero *et al.*, 1998). Therefore, it is plausible that if sea level is changing rapidly this could affect any recorded $\delta^{18}\text{O}$ results from the benthic species studied and explain any changes recorded (Hemleben and Bijma, 1994; Spero *et al.*, 1998).

The palaeotemperature equation used was: T ($^{\circ}\text{C}$) = $16.0 - 4.14 (\partial_c - \partial_w) + 0.13 (\partial_c - \partial_w)^2$ (Shackleton and Kennett, 1975; Anderson and Arthur, 1983) and the theoretical seawater $\delta^{18}\text{O}$ value was -1.2‰ . The expressions stand for: ∂_c = calcite oxygen isotope composition and ∂_w = oxygen isotope composition with respect to the Standard Mean Ocean Water that precipitated the calcite. Further assumptions that had to be made for this equation include: the seawater pH which was assumed to be similar to present day values and the theoretical $\delta^{18}\text{O}$ value used (-1.2‰) was estimated from an ice free world with the assumption that there was no local change in the seawater $\delta^{18}\text{O}$ during this interval (Zachos *et al.*, 2001; Korte *et al.*, 2009).

Using this palaeotemperature equation, and the above assumptions, the results correspond to an increase in temperature of between +10°C to +15°C (from 13°C to 28°C) (Pálffy *et al.*, 2007). A temperature increase of between 10°C – 15°C is very high and is also slightly higher than that suggested by van de Schootbrugge *et al.* (2007). The increase that they proposed, 4°C – 8°C, was also greater than the 2°C – 4°C increase that Beerling and Berner (2002) determined from carbon cycle modelling. These variations in temperature range could be due to the different taxonomic groups used in each study and the proposed environment in which they lived (not including the carbon cycle modelling). The quantity of CO₂ emitted into the atmosphere from several volcanic pulses over a prolonged period of time would cause an increase in temperature, although it is difficult to determine, for certain, that the resulting pCO₂ increase would have been enough to produce the temperature ranges recorded in these studies (McElwain *et al.*, 1999). It was also noted that the δ¹⁸O recorded at Csővár follows similar trends to those from other locations (e.g., St Audrie's Bay/Lyme Regis) across the Tr-J boundary (Dickens *et al.*, 1995; Kennett *et al.*, 2000; Hesselbo *et al.*, 2002; Ward *et al.*, 2004; Pálffy *et al.*, 2007). The information gathered in these studies shows an increase in temperature at several different locations including; St Audrie's Bay, Lavernock Point, Lyme Regis, Kennecott Point, Csővár (Ward *et al.*, 2004; Korte *et al.*, 2005; Pálffy *et al.*, 2007; van de Schootbrugge *et al.*, 2007; Korte *et al.*, 2009) so it could be suggested that any changes in the body size of marine organisms could be due to the change in temperature rather than changes in pCO₂ causing ocean acidification.

1.3 Modern ocean acidification

The rate of present day atmospheric CO₂ increase is approximately 100 times faster than any previous changes in atmospheric CO₂ over the past 650,000 years (The Royal Society, 2005). This rate caused CO₂ to increase from 280 ppmv to approximately 390 ppmv over the past 200 years and in the future CO₂ levels are predicted to reach 780 ppmv by the year 2100 (The Royal Society, 2005). Of the total amount of CO₂ released into the present day atmosphere, around one third is absorbed into the oceans to naturally produce a sea water concentration that is in equilibrium with the atmosphere, as part of the carbon cycle (Figure 1.2; The Royal Society, 2005; Doney *et al.*, 2009; InterAcademy Panel on International Issues, 2009). Since 1780, 50% of the anthropogenic CO₂ produced is present in the atmosphere, while the remainder is split between the oceans (30%) and land biosphere (20%; Figure 1.2; The Royal Society, 2005).

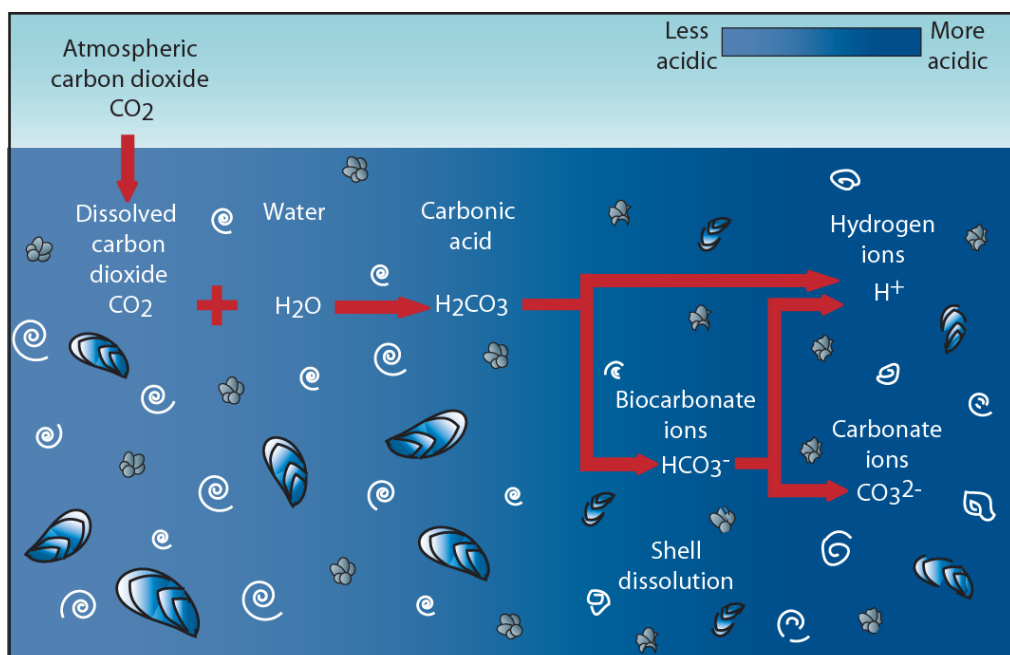


Figure 1.2: The effects of increased atmospheric carbon dioxide on the ocean chemistry and calcareous organisms (Information used to produce this diagram from The Royal Society, 2005).

Once dissolved in the oceans, CO₂ is used in a number of different reactions including photosynthesis and the chemical production of carbonate ions, bicarbonate ions and hydrogen ions which lowers the oceans pH and is damaging some of the ocean's calcareous organisms (Figure 1.2; The Royal Society, 2005; Fabry *et al.*, 2008; InterAcademy Panel on International Issues, 2009). The reaction of some of these ions causes under-saturation of CaCO₃, which decreases the quantity of carbonate ions available for calcium carbonate production (Fabry *et al.*, 2008). Shell formation occurs in seawater where Ω_{arag} and Ω_{cal} is >1.0. At values below 1.0, it has been determined that dissolution of unprotected shells will occur (Fabry *et al.*, 2008). The present day excess atmospheric CO₂ is also resulting in the aragonite/calcite saturation horizons in the world's oceans moving to shallower depths (Guinotte and Fabry, 2008; Fabry *et al.*, 2008). This can cause a reduction in habitable environments which are suitable for calcifying organisms (Guinotte and Fabry, 2008; Fabry *et al.*, 2008). Increases in atmospheric CO₂ can also cause hypercapnic stress, where the resulting rise in $p\text{CO}_2$ causes CO₂ to enter into a marine organism's body fluids and tissues by diffusion. Hypercapnic stress can occur regardless of whether the pH of the enclosing water changes markedly or not. The result can be a number of negative responses in marine organisms, including metabolic depression or reduced protein synthesis which would, in turn, restrict growth and reproduction.

There are many impacts from ocean acidification on calcifying organisms and one is thought to be the development of pitting on the shell surface, leading to shell dissolution (e.g., The Royal Society, 2005; Guinotte and Fabry, 2008; Greene *et al.*, 2012). This can occur while the organism is alive,

if the organism cannot repair its shell, whilst after death shell dissolution in calcifying organisms can be significantly exacerbated (Findlay *et al.*, 2011). Many shelled taxa also show evidence of reduced growth or thinning while alive and in some cases growth stops altogether in living organisms due to a reduced ability to calcify in a decreasing carbonate saturation state (Orr *et al.*, 2005; Fabry *et al.*, 2008; Pelejero *et al.*, 2010; Greene *et al.*, 2012). Some experiments however showed no significant response to increased CO₂ levels, leading to the idea that an organism's ability to regulate pH at the site of calcification controls any response to increased CO₂ levels, but this requires a great deal of energy (Ries *et al.*, 2009; Findlay *et al.*, 2009).

The effects of ocean acidification have been extensively studied using a wide variety of marine species and the results have been reviewed in a number of key papers which have shown high CO₂ affects the ecology, behaviour, morphology and physiology of various marine organisms (Fabry *et al.*, 2008; Kurihara *et al.*, 2008; Doney *et al.*, 2009; Kroeker *et al.*, 2010; Hendriks *et al.*, 2010; Andersson *et al.*, 2011; Greene *et al.*, 2012). These reviews have shown overall that survival, reproduction and calcification significantly decrease, growth and photosynthesis show both an increase and decrease while metabolism increases significantly during high CO₂ (Fabry *et al.*, 2008; Kurihara *et al.*, 2008; Doney *et al.*, 2009; Kroeker *et al.*, 2010; Hendriks *et al.*, 2010; Andersson *et al.*, 2011; Greene *et al.*, 2012).

It is difficult to investigate ocean acidification over geological time scales because of a lack of predicted, preservable responses so is often made from disparate lines of evidence (e.g., causal mechanism, carbonate deposition, rate of extinction and any extinction selectivity). These should be used

together to evaluate whether ocean acidification occurred. However, the geological record does indicate that changes in the marine carbonate system have affected calcifying organisms (Knoll and Fischer, 2011). It was identified that extinctions were exacerbated when several biological challenges occurred at the same time (e.g., combined high $p\text{CO}_2$ and high temperature: Kiessling *et al.*, 2007; Knoll *et al.*, 2007). The majority of ocean acidification indicators involve certain features being absent for instance successions showing an absence of a continuous carbonate deposition due to an inability for the environment to produce carbonate or dissolution of the carbonate produced (Hautmann, 2004, Hautmann *et al.*, 2008). Another indicator is the rate of extinction or any preference to unbuffered organisms as well as trends in shell size and shell thickness (Kiessling *et al.*, 2007; Hautmann *et al.*, 2008).

It is important to use the results from the fossil record combined with physiological insights from extant species as they can help inform how the modern day oceans and marine organisms living within could change in the future (Knoll *et al.*, 1996; Finkel *et al.*, 2005; Knoll *et al.*, 2007; Dahl *et al.*, 2010; Zeebe, 2012). Several studies have used this approach (physiological research) in order to investigate hypoxia, increased palaeotemperature and ocean acidification in the geological record (e.g., Knoll *et al.*, 1996; Finkel *et al.*, 2005; Knoll *et al.*, 2007; Ries *et al.*, 2009; Dahl *et al.*, 2010; Zeebe, 2012). Examples of this method include: (1) Knoll *et al.* (1996, 2007) who investigated the Permian–Triassic extinction using this method to further understand the observed species selectivity and assist in understanding the relative impacts of the various kill mechanisms; (2) Ries *et al.* (2009) who

also utilised results from extant species living in high CO₂ laboratory experiments in order to start generating the quantity of data needed to assist in identifying ocean acidification in the fossil record, and therefore anticipate the effects for future oceans; and (3) Finkel *et al.* (2005) who used this same method to compare the size of diatom frustule with the $\delta^{13}\text{C}$ record during the Cenozoic to assist in the interpretation of palaeoenvironmental indicators.

In order to interpret these shell size and thickness trends, results from modern high CO₂ and high temperature experiments using a variety of different marine species could be used. There are several different limitations of this method of interpreting the marine fossil record: (1) the meaning of any palaeo-trends could change as new data is acquired from modern experiments; (2) limited experimental data available for some of the groups with the greatest fossil records; (3) modern experiments do not look at the evolutionary capacity for species adaptation or acclimation over significantly long time periods (e.g., years or geological time scales); (4) between the various experimental studies the conditions used can vary greatly (Widdicombe and Spicer, 2008; Kiessling and Simpson, 2011; Hönisch *et al.*, 2012; Greene *et al.*, 2012). Even with these limitations the experimental results can be used as a guide to those species found in the fossil record rather than as a direct link (Knoll *et al.*, 2007; Knoll and Fischer, 2011; Greene *et al.*, 2012). Individually these features are not enough to definitively identify ocean acidification but would be if combined with an identifiable significant causal mechanism. Mass volcanism (e.g., the CAMP emplacement during the Tr-J interval) in a sufficiently large enough volume combined with rapid eruptions would be a suitable causal mechanism and

has been identified during several extinction events including the Tr-J (McElwain *et al.*, 1999; Hautmann, 2004; Schaller *et al.*, 2011; Greene *et al.*, 2012). The rapid increase in $p\text{CO}_2$ caused by the CAMP eruptions should have outstripped the buffering capacity of the oceans and in many cases an ability for calcifying species to adapt (McElwain *et al.*, 1999; Hautmann, 2004; Schaller *et al.*, 2011; Knoll and Fischer, 2011; Greene *et al.*, 2012)

From the big five Phanerozoic extinctions it has been suggested that many of them (four out of the five) were partially effected by ocean acidification and or changing seawater temperature, however only three show significant geological evidence of ocean acidification which include mass depletion of biodiversity specifically for unbuffered organisms, shallowing of the carbonate compensation depth and a sharp rise in $p\text{CO}_2$ (Kiessling and Simpson, 2011; Knoll and Fischer, 2011; Greene *et al.*, 2012; Hönisch *et al.*, 2012). These three extinctions include the Permian-Triassic (P-T), the Triassic-Jurassic (Tr-J) and the Paleocene-Eocene (P-E) (Zachos *et al.*, 2003; Knoll *et al.*, 2007; Kiessling and Simpson, 2011; Knoll and Fischer, 2011; Greene *et al.*, 2012). The Tr-J extinction event will be investigated because it has no deep sea record and it shows strong evidence for ocean acidification to have occurred from multiple lines of evidence (e.g., high $p\text{CO}_2$ from mass volcanism, a significant mass extinction with a preference against unbuffered organisms and those that did survive show a preference to smaller thinner shells with poor preservation; e.g., McElwain *et al.*, 1999; Hautmann, 2004; Kiessling and Simpson, 2011; Greene *et al.*, 2012). It is also a particularly well studied interval and comprehensive studies have been done on absolute dating and cyclostratigraphy which will assist in

evaluating the hypothesis. This strong evidence will allow the results from this study to be compared and combined with the results already published in order to help expand the previous knowledge and further determine if this event was dominated by ocean acidification.

1.3.2 Modern high CO₂ studies

Increasing anthropogenic CO₂ levels in the ocean leads to lowered pH from the surface to greater depths (Berge *et al.*, 2006; Ries, 2010). This is thought to have major consequences for shell forming organisms (Berge *et al.*, 2006; Ries, 2010). It is believed that when atmospheric CO₂ reaches 450ppm only ~8% of tropical coral reefs will remain in 'favourable' environments and, if the rise continues to 550ppm, almost all reefs will begin to suffer dissolution (IAP Statement., 2009). Modern studies have tried to test what would happen to live individuals of different taxa under high CO₂ conditions. These experiments investigated a number of effects of increased CO₂ levels, including survival (Talmage and Gobler, 2009), growth (Berge *et al.*, 2006), development (Kurihara *et al.*, 2008) and net calcification (see Appendix 1: Table A1.1; Gazeau *et al.*, 2007). Growth is one of the most common parameters used to investigate levels of stress, as reduced growth is associated with increased stress and thus it may be inferred that the environment is not optimum for that species (Berge *et al.*, 2006). Many different species have been extensively studied including molluscs, tropical corals, echinoderms, foraminifera, coccolithophores and coralline red algae (Doney *et al.*, 2009), but very few studies have been carried out using extant ostracod species. The lack of experimental studies using extant ostracods is mainly because they can be difficult to investigate and identify due to both

their size and ability to survive for long periods outside of their natural habitat. Ostracods are not as economically viable as other marine species (e.g., lobsters, shrimps, crayfish, oysters, mussels etc.) and, almost certainly, regarded as less important. As a result of this, they have largely been overlooked for ocean acidification experiments, even though the fossil ostracod record is very good.

The results of these experimental studies have shown a variable response to changes in $p\text{CO}_2$ between the different taxa and individuals within these taxa (Appendix 1: Table A1.1). Modern experiments in bivalves, specifically those taxonomically equivalent to the Triassic – Jurassic taxa being studied (i.e. mussels and oysters) show a variety of responses to high CO_2 (Table 1.1; e.g., Gazeau *et al.*, 2007; Kurihara *et al.*, 2007; Talmage and Gobler, 2009). The different bivalve taxa in the short term experiments (e.g., 20-30 days) showed some effects of increased $p\text{CO}_2$ to their shells (e.g., Ries *et al.*, 2009; Talmage and Gobler, 2009), however over long time periods (e.g., 44-60 days) there was a more significant reduction in shell growth or no shell growth compared to the results from the short term experiments (e.g., 20-30 days) because of the increased energy cost to maintain their shells (e.g., Berge *et al.*, 2006). Other experiments found that shell size continued to increase in bivalve (*Mytilus galloprovincialis*) individuals but at a slower rate (Michaelidis *et al.*, 2005; Kurihara *et al.*, 2008; Range *et al.*, 2012). Findlay *et al.* (2011) found no change in calcium carbonate in the shells of live individuals of *Mytilus edulis* during high CO_2 . Hiebenthal *et al.*, (2012) found that a combination of high $p\text{CO}_2$ (1,358 μatm) and high temperature (e.g., 20-25°C) significantly hindered shell growth, as $p\text{CO}_2$ alone did not significantly

alter shell growth. The isolated shell of the Antarctic brachiopod *Liothyrella uva* showed significant shell dissolution after 35 days and the exposure of aragonite or calcite prisms by 56 days when subjected to acidic pH conditions (7.4) (McClintock *et al.*, 2009).

Taxon	Development stage	Response to changes in $p\text{CO}_2$	References
<i>Mercenaria mercenaria</i>	Larval and juvenile individuals	Shell dissolution leading to increased mortality; mortality rates varies for different stages and delays in metamorphosis.	Green <i>et al.</i> , 2004; Talmage & Gobler, 2009.
<i>Crassostrea gigas</i>	Juvenile and adults individuals	Increased mortality with increased exposure time and decreased growth rate; declining calcification rates and shell dissolution.	Bamber, 1990; Gazeau <i>et al.</i> , 2007.
<i>Crassostrea virginica</i>	Larval stage	Detrimental to early development especially shell mineralisation and growth.	Kurihara <i>et al.</i> , 2007; Ries <i>et al.</i> , 2009; Talmage & Gobler, 2009.
<i>Ostrea edulis</i>	Newly settled, small (1cm), large (4cm)	Survival improves with size but decreases with exposure time; reduction in growth rate and shell dissolution.	Bamber, 1990.
<i>Mytilus edulis</i>	Juvenile and adults individuals. Alive and dead.	Combined high temperature and high $p\text{CO}_2$ hindered shell growth but $p\text{CO}_2$ alone did not. No effect on a shells breaking force. Increased mortality of larger individuals; reduced shell growth due to the increased energy cost; shell dissolution and calcification rates decline. Several studies found no significant change in calcium carbonate in live individuals but at a cost of reduced health. Dead individuals lost calcium carbonate at $1.5\% \text{ day}^{-1}$	Bamber, 1990; Berge <i>et al.</i> , 2006; Gazeau <i>et al.</i> , 2007; Beesley <i>et al.</i> , 2008; Bibby <i>et al.</i> , 2008; Findlay <i>et al.</i> , 2009; Ries <i>et al.</i> , 2009; Findlay <i>et al.</i> , 2011; Hiebenthal <i>et al.</i> , 2012.
<i>Mytilus galloprovincialis</i>	Embryos, juveniles and adult individuals	Shell weight decreased with pH levels but only for the inorganic component. Growth increased at a slower rate but were overall smaller and delayed shell formation	Michaelidis <i>et al.</i> , 2005; Kurihara <i>et al.</i> , 2008; Range <i>et al.</i> , 2012.

Table 1.1: Summary of the data in Appendix 1; Table A1.1, showing the responses of different bivalve taxa to increased $p\text{CO}_2$.

1.4 Effect of warming on extant species

Temperatures show a rise of 0.6°C over the last century, with an increase of $1.4\text{--}5.8^\circ\text{C}$ predicted for the next century (Petes *et al.*, 2007). This could lead to corresponding increased ocean temperatures, which can affect marine systems and different species (Petes *et al.*, 2007). Many experimental studies have investigated effects of changes in temperature, specifically a

temperature increase, on aspects of the biology of various marine taxa; growth (e.g., Wanamaker *et al.*, 2007), survival (e.g., Rayssac *et al.*, 2010) and development (e.g., Rico-Villa *et al.*, 2009), with growth and survival the most common. In those species that are taxonomically equivalent to the groups in the fossil record described above (see Sect. 1.2.2; mussels, oysters and ostracods), a variety of responses (Tables 1.2 and 1.3) have been recorded.

Taxon	Development stage	Response to increased temperature	References
<i>Crassostrea gigas</i>	2 day old larvae	Temperature has a strong effect on survival of early stages (larvae to juvenile) but adults were not affected. Growth increased as temperature increased; mortality higher at lower temperatures.	Rico-Villa <i>et al.</i> , 2009; Mizuta <i>et al.</i> , 2012.
<i>Mytilus edulis</i>	Larvae, juveniles and adults	At 25°C strong reduction in shell growth. No effect of shell breaking force but an increase in mortality between 20 and 25°C. No evidence of a relationship found in adults; increased the mortality of larvae, but also increased growth.	Wanamaker <i>et al.</i> , 2007; Rayssac <i>et al.</i> , 2010; Hiebenthal <i>et al.</i> , 2012.
<i>Mytilus galloprovincialis</i>	Adults	Increased mortality above 28°C.	Anestis <i>et al.</i> , 2007.
<i>Mytilus trossulus</i>	Larvae	Increased growth and mortality.	Rayssac <i>et al.</i> , 2010.
<i>Modiolus barbatus</i>	Adults	Significantly increased mortality above 28°C.	Anestis <i>et al.</i> , 2008.

Table 1.2: Summary of the data in Appendix 2; Table A1.1, showing the responses of different bivalve taxa to increased temperature.

Taxon	Alive or Dead	Response to increased temperature	References
<i>Leptocythere psammophila</i>	Alive	Increased temperature and salinity causes shell size and calcification to increase.	Kuhl, 1980.
<i>Cyprideis australiensis</i>	Alive	Increased temperature caused increased Mg levels.	De Deckker <i>et al.</i> , 1999.
	Dead	Increased temperature and acidic waters causes Mg to leach out of the shell.	
<i>Cyprideis torosa</i>	Alive	High temperature caused increased Mg.	De Deckker <i>et al.</i> , 1999; Marco-Barba <i>et al.</i> , 2012.
<i>Poseidonamicus</i>	Alive	Increased calcification in cooler temperatures.	Hunt & Roy, 2006.
<i>Cypria</i>	Alive	Increased calcification and moulting in warmer temperatures but shortens their life span.	Decrouy <i>et al.</i> , 2011.

Table 1.3: Summary of published data showing the responses of different ostracod taxa to increased temperature.

The taxa for which we have data each have a range of preferred water temperatures for optimal growth and survival, and this range can vary with development stage (De Deckker *et al.*, 1999; Mizuta *et al.*, 2012; Hiebenthal *et al.*, 2012). There have been a lot of laboratory studies using extant bivalve species which have produced a large quantity of information on how bivalves respond to warming oceanic temperatures (Table 1.2) however very little is known about how extant ostracods respond and this requires further study (Table 1.3).

1.5 Aim and objectives

The overall aim of this project is to investigate the fossil record across the Tr-J boundary high-CO₂ interval using $p\text{CO}_2$, $\delta^{13}\text{C}$ and palaeotemperature data to examine the hypothesis that morphological change in some marine species could be linked to ocean acidification and warming events. Results from experiments on extant taxa will assist in the interpretation of the results based on the fossil record and, potentially, identify some of the mechanisms that might be involved.

Objectives:

- To collect morphological data to investigate the size changes of two species of bivalve and one species of ostracod from strata spanning the Tr-J boundary interval in southwest England.
- To use trace element geochemistry of fossil specimens collected in the field to examine any mineralogical changes that could be attributed to changing temperature and/or $p\text{CO}_2$ levels.

- To construct a high resolution palaeotemperature curve using data collected from the fossil species and bulk rock samples combined with previously published data (Pálffy *et al.*, 2007; Korte *et al.*, 2009).
- The palaeotemperature data will be plotted along with previously published $p\text{CO}_2$ curves (e.g., McElwain *et al.*, 1999; Schaller *et al.*, 2011) to determine any relationships between changes in fossil morphology and changing temperature or $p\text{CO}_2$ levels.
- To compile the results from modern high CO_2 and high temperature laboratory experiments using relevant bivalve taxa to assist in interpreting the morphological variations identified in the bivalve fossil record.
- The effect of CO_2 enrichment and warming on aspects of growth and mineralogy will be investigated for three extant ostracod species, in order to help interpret changes in fossil ostracod morphology and mineralogy identified in the fossil record.

Chapter 2 – Geological Setting

2.1 Introduction

Tr-J boundary sections can be found in many parts of the world and have been intensively studied in North and South America, Europe (Northern and Southern Calcareous Alps) and especially in South west England. They cover a wide range of marine environments and an extensive amount of literature is available on the majority of these locations. An important element in selecting the study sites for this investigation was the presence and well-documented distribution of the same fossil taxa within large, complete sections across a range of different environments. The locations also needed to allow correlation with $p\text{CO}_2$ curves from various locations (McElwain *et al.*, 1999; Schaller *et al.*, 2011; Steinthorsdottir *et al.*, 2011).

The southwest England locations fulfil these criteria (Lyme Regis and St Audrie's Bay), because they show correlative stratigraphy and palaeontology, yet slightly different depositional environments (e.g., Lang, 1924; Hesselbo *et al.*, 2004; Warrington *et al.*, 2008). Both locations also display an extensive chronological range (Rhaetian to the end of the Hettangian, including the Tr-J boundary) with large, well exposed bedding planes containing a wide variety and abundance of fossils, which can be used to investigate any effects on marine organisms to global acidification and temperature variations (e.g., Lang, 1924; Warrington *et al.*, 2008). Furthermore, the St Audrie's Bay stratigraphy has already been correlated to the Greenland $p\text{CO}_2$ curves in several different studies (e.g., Whiteside *et al.*, 2010;

Bartolini *et al.*, 2012; Mander *et al.*, 2013), making it easier to correlate the rest of the $p\text{CO}_2$ data to these locations than to other Tr-J sections.

2.1.2 Aims and objectives

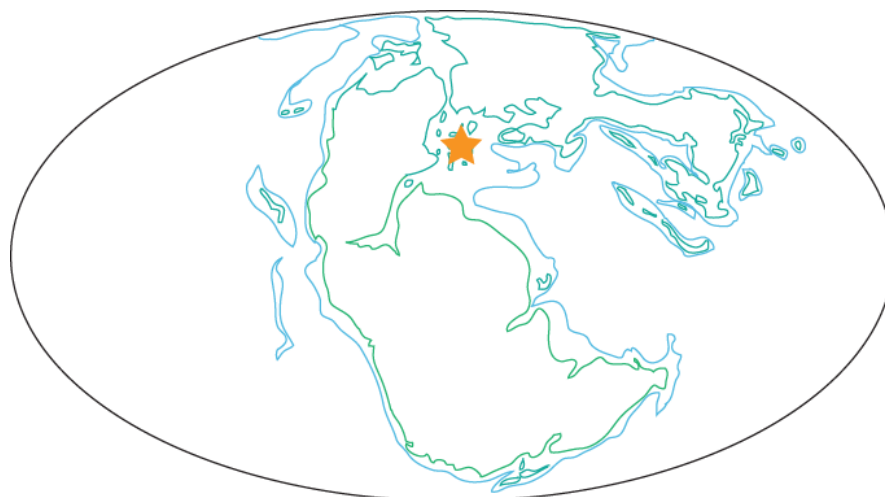
The aim of this chapter is to present an introduction to the two selected field locations. This has been constructed using published information and newly-collected field data. There is also information on how the logs from this study have been compared to published data, including the $p\text{CO}_2$ curves.

This will be achieved by:

- Presenting the locations and where they occur within the wider Early Jurassic period and reviewing the various lithology and depositional settings found in these locations.
- Investigating how the carbon and oxygen isotope results from both locations and the different magnetostratigraphy zones from St Audrie's bay correlate to the logs from this study, in addition to how the magnetostratigraphy zones correlate to those from the Newark Basin.
- Investigating how the St Audrie's Bay log can be correlated with several other key locations using the two global $\delta^{13}\text{C}_{\text{org}}$ negative excursions and how it can be correlated to the $p\text{CO}_2$ curves from various locations.

2.2 Field locations

Two different sections have been studied from southwest England: Lyme Regis (Pinhay Bay N 50°42'44.6 W 002°58'02.6 to Lyme Regis N 50°43'04.8 W 002° 56'55.2) and St Audrie's Bay (N49°46'48.01" W007°33'15.71" to Watchet N49°47'01.32" W007°33'17.29") (Figures 2.1-2.2) with the rocks at both these locations relating to the same stratigraphy (Figure 2.3). The successions at Lyme Regis and St Audrie's Bay were situated on the northwest margin of the Tethys Ocean and deposited in half-graben basins trending east-west during the Late Triassic and Early Jurassic (Hesselbo *et al.*, 2004). Both sections are bounded to the north with Palaeozoic basement rocks and by the London-Brabant landmass to the southeast. During the early Rhaetian conditions changed from lacustrine and evaporitic to mostly marine conditions (e.g., Hesselbo *et al.*, 2004; Mander *et al.*, 2008). Marine conditions then continued through to the Early Jurassic so ammonites have been used to divide the Hettangian stratigraphy into zones and subzones.



Early Jurassic $\sim 201.3 \pm 0.2\text{Ma}$

★ Southwest England

Figure 2.1: Location of southwest England during the Early Jurassic. Green lines represent landmass and blue lines represent the shelf (modified from Blakey, 2010).

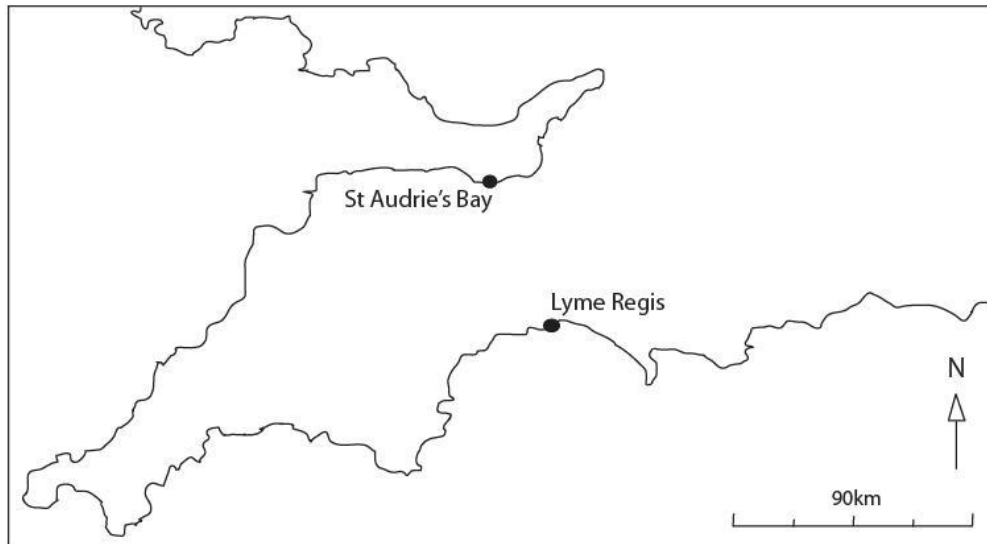


Figure 2.2: Location of Lyme Regis (Pinhay Bay N 50°42'44.6 W 002°58'02.6 to Lyme Regis N 50°43'04.8 W 002° 56'55.2) and St Audrie's Bay (N49°46'48.01" W007°33'15.71" to Watchet N49°47'01.32" W007°33'17.29") in southwest England.

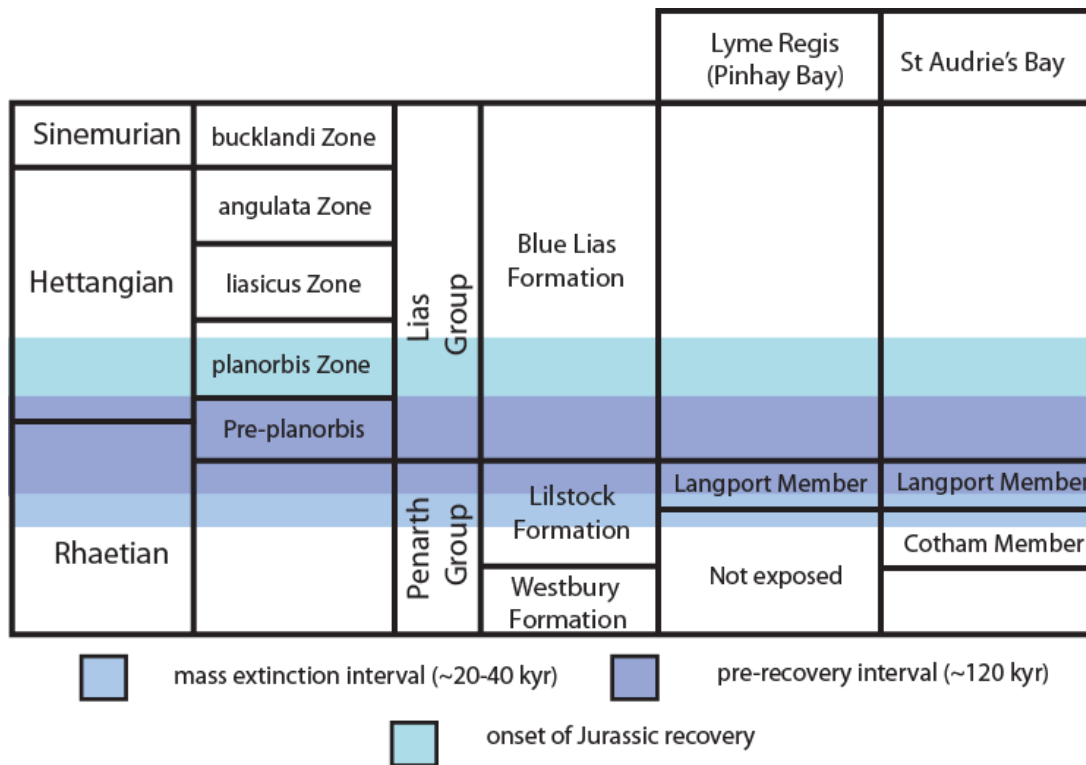


Figure 2.3: An overview of the stratigraphy of southwest England (modified from Barras and Twitchett, (2007). First and last occurrence data of the different species from Mander *et al.* (2008) and Ruhl *et al.* (2010) indicate the position of the mass extinction interval, pre-recovery interval and the onset of Jurassic recovery within the stratigraphy.

2.3 Location lithology

The lithological succession from which the morphometric data have been collected is important because the changes in the environment (e.g., sea level change, facies, etc) that are recorded through the variations in lithology could also cause morphological changes to different species through time (Patzkowsky and Holland, 2012). Fossil distributions and changes in abundance can also be affected by this variability in the stratigraphic record (Patzkowsky and Holland, 2012). Other factors (e.g., $\delta^{13}\text{C}$, $\delta^{18}\text{O}$ (temperature) and $p\text{CO}_2$) that may have caused morphological changes will also be discussed. This is because the main aim of this study is to use the $p\text{CO}_2$, $\delta^{13}\text{C}$ and palaeotemperature data to examine the hypothesis that morphological change in some marine species could be linked to ocean acidification and warming events.

2.3.2 Lyme Regis (including Pinhay Bay)

The succession at Lyme Regis (Figure 2.3), which sits in the Lyme Regis Syncline, is affected by a gentle south-easterly regional dip. This results in the beds descending to beach level along the foreshore (Lang, 1924; Hallam, 1960; Wignall, 2001). The investigated succession extends from Pinhay Bay (base of the section N $50^{\circ}42'44.6$ W $002^{\circ}58'02.6$) through to Lyme Regis in both the cliffs and across the foreshore (top of investigated section, N $50^{\circ}43'04.8$ W $002^{\circ}56'55.2$). The Lillstock Formation (formerly known as the White Lias) is exposed in the cliffs at the western end of Pinhay Bay through to the eastern end of the bay, where the boundary between the Lillstock Formation and the Blue Lias Formation dips below beach level (Figure 2.4).

The Blue Lias Formation extends from the eastern edge of Pinhay Bay at beach level through to the West Cliff, and is present in the cliffs throughout the entire area. The Late Triassic extinction level (within the Cotham Member) is not exposed between Pinhay Bay and Lyme Regis (Figure 2.5). Many of the early geologists studied this area, with the most comprehensive investigation being completed by Lang (1924). His bed numbers and names are still in use today and have been correlated with the log and bed notation that have been produced for this study. A log of the complete succession was produced over two field seasons (each comprising of 3 weeks) in 2010 and 2011 (Figure 2.5). The bed thickness data (to the nearest mm) were then digitalised using Adobe Illustrator to produce a graphic log at a scale of 1:10. Shell size data were collected in the field for *L. hisingeri* and *P. gigantea* from the limestone beds (micrite mudstones to wackestones) throughout this section. Shell size and shell thickness data were collected for *O. aspinata* from the marl and shale beds throughout this section after samples were processed in the laboratory.

The Lilstock Formation

The Lilstock Formation is Late Triassic (Rhaetian) in age (Lord and Davis, 2010), consisting of micritic mudstones and limestones with a set of complex sedimentary features including matrix supported conglomerates, channels with slumps and de-watering structures and, in the limestone beds, well-developed slumping separated by porcellanous hardgrounds (Figure 2.5) (Swift, 1999; Wignall, 2001; Gallois, 2007).

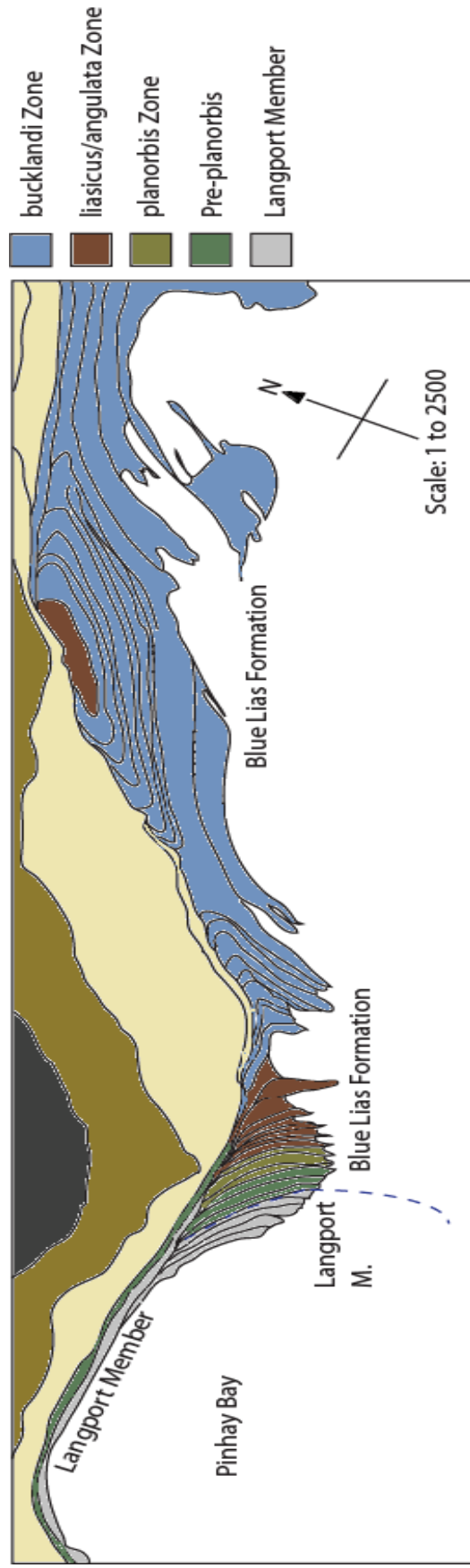


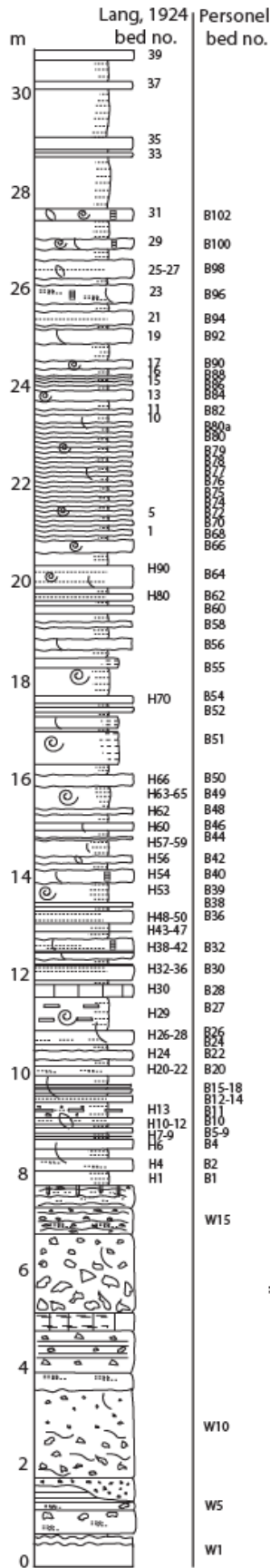
Figure 2.4: Map of the coastal section from Pinhay bay (N 50°42'44.6-W 002°58'02.6) to Lyme Regis (N 50°43'04.8-W 002° 56'55.2) identifying the positions of the various Members and Formations along the section (Google Earth, 2013).

Hardgrounds are defined as a lithified seafloor which consists of 'surfaces of syn-sedimentary cemented carbonate layers that were exposed on the seafloor' (Wilson and Palmer, 1992). Fossils are found in several horizons, mainly in winnowed concentrations in the parallel bedded remobilised and laminated limestones (Gallois, 2007). The uppermost Lillstock Formation consists of wavy-laminated limestones with intervening layers of marl and, at the top of the bed within an intra-formational conglomerate, *Diplocraterion* burrows are present. This is locally known as the Sun Bed (Lang, 1924), and forms the boundary between the Lillstock Formation (Langport Member) and the Blue Lias Formation.

The Blue Lias Formation

The Blue Lias Formation is earliest Jurassic (201.3–199.3; Hettangian to Sinemurian) in age (Figure 2.5-2.6) (Lang, 1924). Observations during this study, and from previous studies, are discussed below. The observations indicated cyclic packages consisting of limestone alternating with marl and shale beds (Figures 2.5-2.6) (e.g., Lang, 1924; Weedon, 1985; Hart, 1987; Wignall and Bond, 2008; Ruhl *et al.*, 2010). As the environment becomes more open marine through the Blue Lias succession the cyclic spacing extends probably due to increased sediment production (Hart, 1987). Paul *et al.* (2008) identified that the cyclic packages are not always symmetrical and contain a combination of diagenetic and primary features (Weedon, 1985; Hart, 1987). In general, the cyclic packages grade from laminated black shale into dark grey and pale grey marls and then into the micritic limestones.

Rhaetian		Hettangian		Sinemurian		Age
Lilstock Formation		Blue Lias Formation		bucklandi Zone		Formation
Pre-planorbis		liasicus Zone		angulata Zone		Zone
P.s. planorbis		Alsaites laqueus		Schlotheimia		Subzone
johnstoni		W. portocki		Coroniceras rotiforme		



- Echinoderms
- Brachiopods
- Ammonites
- Bivalves
- Burrows
- Wavey Laminations
- Large sized clasts
- Slumping features
- Small angular clasts
- Nodular Limestone
- Irregular top/
bottom of bed
- Limestones
- Marl/Shale



Figure 2.6: Blue Lias Formation between Pinhay Bay and Lyme Regis.

The limestone beds are diagenetically cemented and often laterally continuous. In a few places, the limestones form persistent nodule horizons that have either undulating or sharp boundaries with the marl and shale beds (Figure 2.5-2.6) (Lang, 1924; Moghadam and Paul, 2000; Paul *et al.*, 2008; Wignall and Bond 2008; Ruhl *et al.*, 2010). The laminated black shales show the most diagenetic alteration indicated by modified stable isotope values and thin pyrite rich deposits. The limestones are typically impure micrite mudstones to wackestones that are dark bluish to medium grey, with a fine-grained clay grade consistency made up of compact and hard nodular, laminated and planar bedded facies which are very fossiliferous (Figure 2.6). The proportion of siliciclastic clay and micrite minerals varies between the limestone beds. Fossil specimens include abundant *Liostrea*, *Plagiostoma*, *Gryphaea*, brachiopods, crinoids and ammonites which can be found,

¹Figure 2.5: A stratigraphical log of the Lyme Regis section with bed numbers produced during the field work completed during this study. Stratigraphy from Lang, (1924); Hart (1982) and Barras & Twitchett, (2007). *Waehneroceras portlocki* subzone = *W. portlocki* subzone, *Schlotheimia complanta/extranodosa* subzone = *Schlotheimia* and *Metophioceras conybeari* subzone = *Metophioceras* subzone. Dotted line represents position of new Tr-J boundary (Von Hillebrandt *et al.*, 2007).

densely packed, in some beds (Ager and Smith, 1973; Paul *et al.*, 2008; Page, 2010). The organic-rich shale, pale grey marls and dark grey marl beds range in thickness (from centimetres to metres; Figure 2.6). Weedon (1986) and Gallois and Paul (2009) determined that these thinly laminated beds consist of a mixture of clay minerals and marine organic matter (e.g., dinoflagellate cysts) with a limited, well preserved, calcareous fauna. The organic rich dark shales lack significant fossiliferous content and, combined with an increased pyrite content and, well developed very fine laminations indicates anoxic sea-floor conditions (Lang, 1924; Wignall and Bond 2008; Ruhl *et al.*, 2010). Those dark bituminous shales which probably indicate local, short-lived, anoxic conditions within the surface sediments explains the lack of ostracod morphological data from this section.

2.3.3 Lyme Regis depositional settings

The facies represented by the Lillstock Formation are indicative of a shallow, warm, lagoonal marine environment with varying salinity (Wignall, 2001; Hesselbo *et al.*, 2004). It has been suggested that the slump horizons and evidence of soft-sediment deformation may be due to earthquake activity (Gallois, 2007). The Blue Lias Formation, on the other hand, was deposited in a shallow, marine offshore environment (Hallam, 1995; Hallam, 1997; Wignall, 2001; Barras and Twitchett, 2007). The faunal assemblages of the Blue Lias Formation are indicative of a marine setting, even at the base of the succession where no ammonites are recorded. The data from this study and other previous studies indicate the variable water depths recorded in the

Rhaetian to Hettangian range up to a few tens of metres (Hallam, 1997; Hesselbo *et al.*, 2004; Wignall and Bond, 2008).

2.3.4 St Audrie's Bay

The section at St Audrie's Bay extends from St Audrie's Bay (N49°46'48.01" W007°33'15.71") (Figure 2.7) around the coast to Watchet (N49°47'01.32" W007°33'17.29"). The strata dip gently from the top of the south facing cliffs down on to the foreshore on the west side of St Audrie's Bay and have been locally faulted (Warrington *et al.*, 1994; Simms, 2004). This location exposes the Penarth Group (Rhaetian), which includes the Westbury Formation and the Lilstock Formation (Cotham and Langport Members). The overlying Blue Lias Formation includes the Pre-planorbis Beds, planorbis Zone, liasicus Zone and angulata Zone (Warrington *et al.*, 1994; Hounslow *et al.*, 2004). These zones have been sub-divided using ammonite assemblages (Figure 2.3, Warrington *et al.*, 1994; Page and Bloos, 1995). A log of the succession was produced over two field seasons in 2010 and 2011 (Figure 2.9). The bed thickness data (to the nearest mm) were then digitalised using Adobe Illustrator to produce a log at a scale of 1:10. Shell size data were collected in the field for *L. hisingeri* from the limestone beds (micrite mudstones to wackestones) throughout this section. Shell size and shell thickness data were collected for *O. aspinata* from the marl and shale beds throughout this section after samples were processed in the laboratory. *Plagiostoma gigantea* was not measured because this species was not abundant enough in this succession.

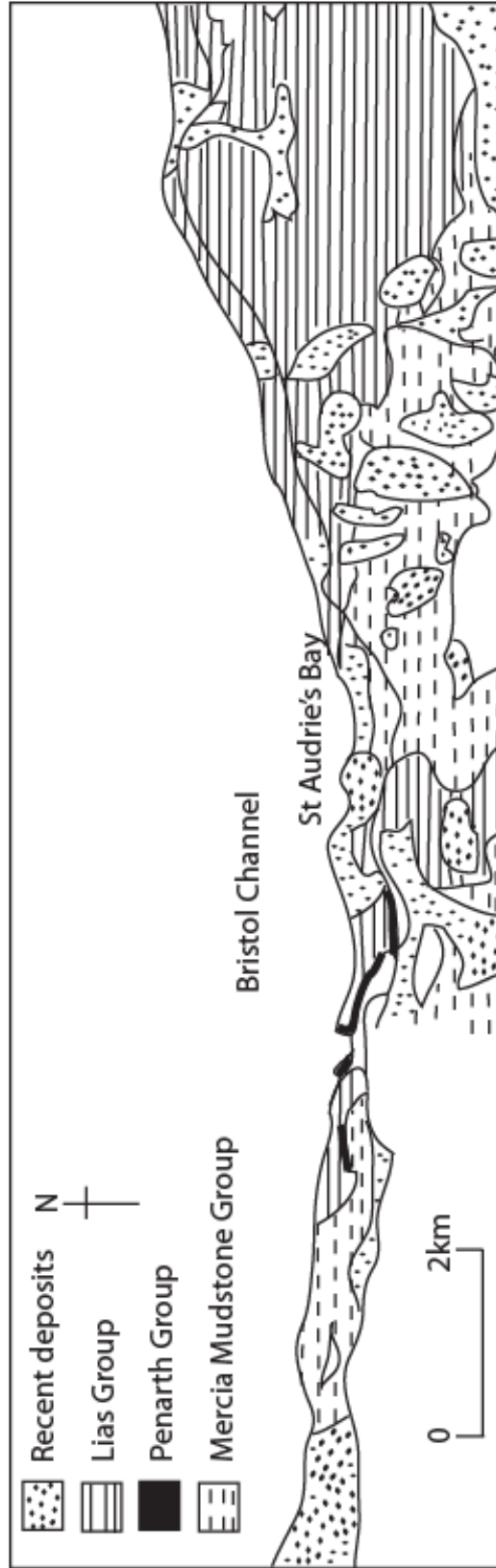


Figure 2.7: Geological map of the West Somerset coast, showing the outcrops of the Penarth Group and Lias Group on the North Somerset coast in the vicinity of St Audrie's Bay (N49°46'48.01" W007°33'15.71") (Warrington *et al.*, 2008).

The Penarth Group

The Penarth Group is a relatively new name, first introduced by the Triassic Working Group (Warrington et al., 1980; Gallois, 2009). It describes a succession situated between the terrestrial Mercia Mudstone Group and the base of the fully marine Blue Lias Formation. The succession consists of brackish to fully marine, sedimentary, argillaceous, calcareous and locally arenaceous formations (Warrington et al., 1980; Gallois, 2009). It encompasses the Westbury Formation and the Lilstock Formation (Cotham Member and Langport Member). Observations from this study and published studies are discussed below.

The Westbury Formation is predominantly formed of dark grey, calcareous, siliciclastic-rich mudstones, some interbedded limestones (bioclastic packstones and wackestones) and intraformational conglomerates (Figure 2.8-2.9) (Warrington *et al.*, 1986, 2008; Hounslow *et al.*, 2004; Mander and Twitchett, 2008). Shell beds are also common and predominantly contain bivalves (e.g., *Liostrea*, *Rhaetavicula contorta*, *Lyriomyophoria postera*) as well as vertebrate debris (e.g., fish teeth and larger marine reptiles; Hesselbo *et al.*, 2004). The boundary between the Westbury Formation and the Cotham Member is gradational, with the dark mudstones grading upwards into pale, grey-green, calcareous mudstones, thinly laminated siltstones and limestones in the lower part of the member. The lowest bed in the Cotham Member has evidence of soft sediment folding and deformed strata (SAB 2), thought to be caused by seismic shaking of unconsolidated sediments (Hesselbo *et al.*, 2004; Wignall and Bond, 2008). Other beds contain wave ripple laminations and there is limited or no fossil content (Hesselbo *et al.*,

2004; Mander and Twitchett, 2008; Wignall and Bond, 2008). Mud cracks separate the lower part of the Cotham Member from the upper part of the Cotham Member (SAB2-3) and are thought to have formed during a temporary emergence (Figure 2.8-2.9) (Warrington *et al.*, 1986; Hounslow *et al.*, 2004; Warrington *et al.*, 2008; Wignall and Bond, 2008). The upper Cotham Member consists of shales which are greenish grey in colour and thin, interbedded, mudstones and limestones. The upper part of the Cotham Member contains a limited fauna of bivalves (e.g., *Liostrea hisingeri*, *Plagiostoma* spp., *Myoconcha psilonoti*; Warrington *et al.*, 1994).

The base of the Langport Member forms a sharp contact with the underlying Cotham Member. It is predominantly composed of pale grey limestones (nodular and lenticular) and blue-grey mudstones (laminated and micritic) with some shale and dark grey mudstone (Figure 2.9) (Warrington *et al.*, 1986, 1994; Wignall and Bond, 2008). The uppermost three limestone beds are weathered a cream colour. Fossils can be found within this member, including abundant bivalves (e.g., *Liostrea*, *Plagiostoma* spp., *Myoconcha psilonoti*) in addition to echinoderms (e.g., diademopsid spines; Warrington *et al.*, 1994; Hesselbo *et al.*, 2004; Hounslow *et al.*, 2004; Warrington *et al.*, 2008). Hesselbo *et al.* (2004) have presented high resolution total organic carbon (% TOC) data from the Tr-J boundary interval. They identified very low TOC values through the Westbury Formation (approximately 0-2% TOC) except for one 'spike' of approximately 8% TOC in a medium grey mudstone within the middle of the formation. TOC values then remained low all the way through the rest of the Westbury Formation and were even lower (approximately 0% TOC) throughout the Lilstock Formation (Hesselbo *et al.*,

2004). Hesselbo *et al.* (2004) also recorded the percentage of carbonate carbon (% CARB) through the Tr-J boundary interval which showed that the majority of the Westbury Formation had very low percentages of CARB (0-10% CARB) except for six 'spikes' within the limestone beds where the % CARB peaked between 40-90% CARB. Throughout the Lilstock Formation the % CARB fluctuates from bed to bed and ranges from approximately 30-90% (Hesselbo *et al.*, 2004).

The Blue Lias Formation

At St Audrie's Bay the rock succession encompassing the Blue Lias Formation was first fully described by Palmer (1972) and then Whittaker and Green (1983), and consists of thick organic rich shale beds, blocky, fissile, pale grey marls, inter-bedded with laterally continuous dark bluish to medium grey limestone beds that form nodules and concretionary horizons (Figures 2.8, 2.9) (Simms, 2004; Warrington *et al.*, 2008; Mander and Twitchett, 2008; Wignall and Bond, 2008). The micritic limestones are compact, hard and carbonate rich with a range of fauna. The limestone concretions range from impure mudstones to wackestones. They contain a variety of marine fossils that are better preserved and less fragmented than those in the shale beds (Warrington *et al.*, 1994). Many of the fossils in the shale beds are significantly fragmented, which is due to compaction and hardening of the sediment after deposition. Ammonites can be found throughout the shale beds above the Pre-planorbis Beds (Figure 2.9) (Warrington *et al.*, 1994; Page, 2001; Hounslow *et al.*, 2004; Page, 2004; Hesselbo *et al.*, 2004; Simms, 2004; Ruhl *et al.*, 2010). The organic rich shale beds which are

suggestive of short-lived anoxic conditions would explain many of those beds with no recorded ostracod assemblages.



Figure 2.8: The Lilstock Formation and Blue Lias Formation at St Audrie's Bay

The % TOC record (Hesselbo *et al.*, 2004) through the Pre-planorbis Zone and *Psiloceras planorbis* Zone increases and decreases from bed-to-bed. Values range from 0-11 % TOC, with one large 'spike' of approximately 12% TOC in one bed consisting of dark grey laminated shale at the base of the *P. planorbis* Subzone. The percentage of CARB through the rest of the section (Pre-planorbis Zone and *Psiloceras planorbis* Zone) fluctuates from bed-to-bed and ranges from approximately 20–90% (Hesselbo *et al.*, 2004). Ruhl *et al.* (2010) suggested that the beds in this section form sedimentary rhythms or cycles, not dissimilar to those seen at Lyme Regis, and range up to several metres in thickness through the section. Where the sedimentary rhythms have not formed it is because parts of the cycle are missing (Ruhl *et al.*, 2010). The cause of the sedimentary rhythms or cycles is thought to be due to orbital climate forcing represented by 20kyr precession cycles or

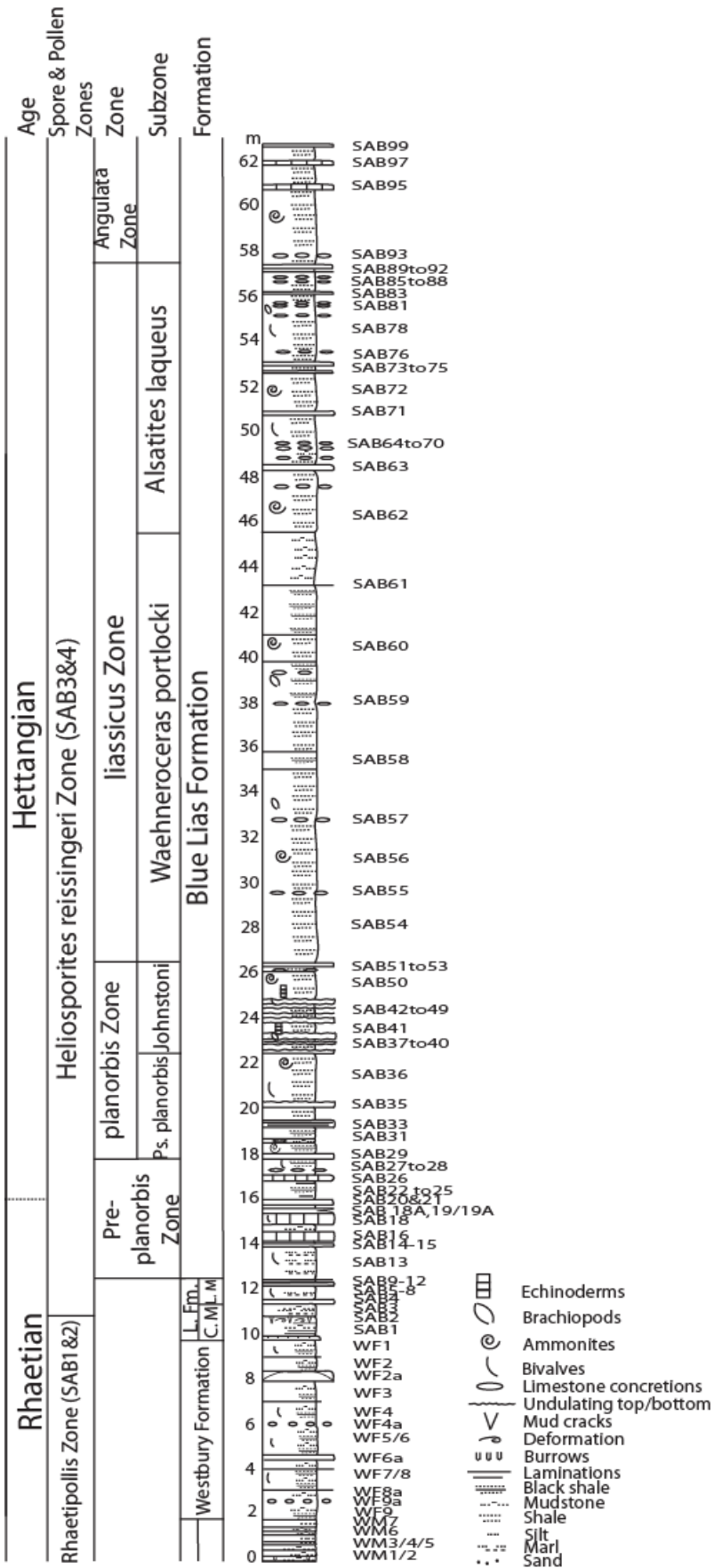
climate cycles (Weedon, 1985, 1986; Hart, 1987; Weedon *et al.*, 1999; Ruhl *et al.*, 2010).

2.3.5 St Audrie's Bay depositional setting

Deposition of the Westbury Formation occurred in a marine environment and the limestones may represent a shallower marine environment compared to the shale/marl deposits (Warrington *et al.*, 2008). The main shale/marl deposits were possibly deposited in deeper water, below wave base, with fluctuations in relative sea level or energy indicated by grain size changes (fining upwards and coarsening upwards) (Hesselbo *et al.*, 2004; Bonis *et al.*, 2010b). The lower part of the Cotham Member shows a shallowing upwards sequence from shallow water to peritidal settings, causing the sediment to dry out and produce desiccation cracks (Hesselbo *et al.*, 2004; Wignall and Bond, 2008; Bonis *et al.*, 2010b; Ruhl *et al.*, 2010). Several published studies have indicated that the soft sediment deformation found in the Cotham Member (SAB 2) and the cracks penetrating it may also reflect temporary emergence during an extra-terrestrial impact causing massive regional sediment deformation (Mayall, 1983; Simms, 2003, 2007; Warrington *et al.*, 2008). The upper part of the member is indicative of a shallow coastal environment indicated by the preserved wave ripples (Hesselbo *et al.*, 2004; Mander *et al.*, 2008; Bonis *et al.*, 2010b; Clémence *et al.*, 2010). A variety of wavelengths and amplitudes were identified within the sedimentary structures. Conditions then changed back to fully marine as sea levels rose (Hesselbo *et al.*, 2004; Mander *et al.*, 2008; Bonis *et al.*, 2010b; Clémence *et al.*, 2010).

The facies represented by the Langport Member has been interpreted in a variety of ways in a number of recent publications (e.g., Hesselbo *et al.*, 2004; Bonis *et al.*, 2010b; Clémence *et al.*, 2010). These interpretations include deposition in a shallow water, saline lagoonal environment (Gallois, 2007; Warrington *et al.*, 2008; Ruhl *et al.*, 2010), a shallow water, quiet seaway (Wignall, 2001), a record of sea level rise on a carbonate ramp (Hesselbo *et al.*, 2004; Ruhl *et al.*, 2010), or relative sea level fall and sea floor erosion causing emergence at the top of the member (Wignall and Bond, 2008). The sedimentological and fossil data identified indicate that the most likely environmental interpretation at this location is sea level rising on a carbonate ramp.

Generally, throughout the Blue Lias Formation the limestone beds and their benthic fauna reflect well-oxygenated marine seafloor conditions, whereas the shale beds and organic rich facies reflect dysaerobic-to-anoxic marine seafloor conditions (Hesselbo *et al.*, 2004; Mander and Twitchett, 2008; Warrington *et al.*, 2008; Ruhl *et al.*, 2010). Overall the section shows significant changes in sea level. The deposits in the Westbury Formation indicate sea level rise leading to a sea level fall within the lower Cotham Member (Hesselbo *et al.*, 2004). The deposits in the upper Cotham Member through to the Pre-planorbis Zone indicate a record of sustained sea level rise (Hesselbo *et al.*, 2004).



Using organic rich facies to identify dysaerobic-to-anoxic marine seafloor conditions is reasonable (Rhoads and Morse, 1971; Wignall, 1994; Hart & Fitzpatrick, 1995). Oxygenated conditions aid the breakdown of organic material which is not, therefore, preserved (Rhoads and Morse, 1971; Wignall, 1994; Hart & Fitzpatrick, 1995; Hesselbo *et al.*, 2004). Low oxygen conditions lead to the formation of pyrite framboids and restrict the action of organisms that would normally consume organic materials, allowing this organic matter to be preserved (Rhoads and Morse, 1971; Wignall, 1994; Hart & Fitzpatrick, 1995; Hesselbo *et al.*, 2004).

2.4 Carbon and oxygen isotope data from the studied sites in southwest England

The published $\delta^{18}\text{O}$ and $\delta^{13}\text{C}$ data from St Audrie's Bay and Lyme Regis described above were compiled and plotted against the logs produced during this study (vertical error less than 30cm) (Figure 2.10a,b). The exact location of each sample was determined from the published supplementary data (sample height and isotope value) by matching the bed height from their logs along with the corresponding isotope value to the equivalent bed in the logs from this study (vertical error less than 30cm) (Hesselbo *et al.*, 2002, 2004; van de Schootbrugge *et al.*, 2007; Korte *et al.*, 2009). This previously published oyster data set was then integrated with new data from *L. hisingeri*, *P. gigantea* and *O. aspinata* collected during this study and the methods and

²Figure 2.9: A stratigraphical log of the St Audrie's Bay section produced during this study with bed numbers. Stratigraphy is from Mander *et al.* (2008); Hesselbo *et al.* (2004); Barras & Twitchett, (2007) and Palmer, *pers com.* (2010). (L. Fm. = Lillstock Formation; C. M. = Cotham Member and L. M. = Langport Member). (SAB1&2) and (SAB3&4) is the sporomorph zonation scheme by Bonis *et al.* (2010b) and used by Mander *et al.*, (2013).

results can be found in Chapter 6 where they will be discussed in relationship to the geometric size data.

Korte *et al.* (2009) and van de Schootbrugge *et al.* (2007) used fossil oysters collected from Lavernock Point, Watchet and St Audrie's Bay as well as Korte *et al.* (2009) using whole rock carbonate samples from Lyme Regis, to investigate changes in $\delta^{18}\text{O}$ and $\delta^{13}\text{C}$. Korte *et al.*, (2009) and van de Schootbrugge *et al.*, (2007) both found that the $\delta^{13}\text{C}$ data from the oysters shows a positive excursion in the lower Langport Member through to the lower Blue Lias Formation. The main negative excursion occurred during the upper Pre-planorbis Beds with a decrease up to 2.2‰ (Figure 2.10a) (van de Schootbrugge *et al.*, 2007). The values then stay relatively low with only minor variations through to the planorbis Zone and the Portlocki Subzone (van de Schootbrugge *et al.*, 2007; Korte *et al.*, 2009). The $\delta^{13}\text{C}$ data from the Lyme Regis whole rock carbonate samples indicate similar trends to those found from the oysters but values were more depleted in $\delta^{13}\text{C}$ by around 2 ‰ (Korte *et al.*, 2009). Seawater $\delta^{13}\text{C}$ is thought to record changes in the re-oxidation and burial of ^{12}C -enriched organic matter within the ocean-atmosphere system. This is related to several factors including, nutrient supply, primary productivity, sea level changes, sedimentation rate, atmospheric CO_2 levels and biological isotope fractionation (e.g., Jenkyns, 1996; Hayes *et al.*, 1999; Kump and Arthur, 1999). It is also thought to be affected by the introduction of volcanic CO_2 into the ocean/atmosphere system, methane release, thermal metamorphism and/or the overturning of ^{12}C -enriched oceanic bottom waters (Knoll *et al.*, 1996; Jenkyns, 1996; Hesselbo *et al.*, 2000; McElwain *et al.*, 2005). Changes in any one or a

combination of those factors discussed above could cause shell size changes to various shelly marine species (e.g., bivalves, ostracods, gastropods, etc.). Therefore, the *L. hisingeri*, *P. gigantea* and *O. aspinata* shell size and thickness data will be compared with the $\delta^{13}\text{C}$ data.

Oysters from St Audrie's Bay were also analysed for $\delta^{18}\text{O}$ and recorded a positive trend (-0.5 to 1.5 ‰) from the lower to the upper Langport Member, where the initial negative excursion of 2.5 ‰ is found (van de Schootbrugge *et al.*, 2007; Korte *et al.*, 2009). This negative decrease is found at almost the same stratigraphic position as the main excursion in $\delta^{13}\text{C}$ values (van de Schootbrugge *et al.*, 2007). Korte *et al.* (2009) inferred that the $\delta^{18}\text{O}$ oyster values indicated bottom water temperatures range from 7°C to 14°C through the upper Langport Member and range from 12°C to 22°C from the planorbis Zone through to the Portlocki Subzone indicating a possible temperature increase in seafloor bottom waters through these sections of +8°C (van de Schootbrugge *et al.*, 2007; Korte *et al.*, 2009). At Lyme Regis, $\delta^{18}\text{O}$ for whole rock carbonate samples showed no overall trends but displayed several excursions between negative results (-4.5 ‰) and slightly less negative results (-1.5 - 2 ‰) indicating the bulk rock samples at Lyme Regis are showing less variation in the temperature of seafloor bottom waters than at St Audrie's Bay (Figure 2.10b) (Korte *et al.*, 2009).

Hesselbo *et al.* (2002) and Ruhl *et al.* (2010) produced a carbon bulk organic isotope record which indicates several excursions throughout this succession. The $\delta^{13}\text{C}$ fluctuations are coeval and the peaks and troughs can be used for trans-continental stratigraphic correlation of various stage boundaries which is why the $\delta^{13}\text{C}_{\text{org}}$ data sets of Hesselbo *et al.* (2002) and Ruhl *et al.* (2010)

are included in Figure 2.10a. The excursions identified are the initial negative excursion within the Cotham Member (~-4 ‰) and the main negative excursion in the lower Blue Lias Formation which persists throughout the *Ps. planorbis* subzone (Ruhl *et al.*, 2010). These excursions have been identified in other carbon bulk organic isotope records from other Tr-J locations specifically the GSSP and the initial negative excursion is now used as the marker for the position of the mass extinction event and the main negative excursion is used as one of several markers for the Tr-J boundary (Figure 2.11) (Pálffy *et al.*, 2001; Ward *et al.*, 2001; Hesselbo *et al.*, 2002; Guex *et al.*, 2004; Ruhl *et al.*, 2010; Črne *et al.*, 2011; Ruhl and Kurschner, 2011; Bartolini *et al.*, 2012).

Ruhl *et al.* (2010) extended the $\delta^{13}\text{C}_{\text{org}}$ curve through the rest of the Hettangian and found a continuation of the main negative excursion implying that either CAMP lasted longer than originally thought or the $\delta^{13}\text{C}_{\text{org}}$ curve is only partly related to volcanic emissions and global biogeochemical cycles may not have fully recovered (Figure 2.10a) (Ruhl *et al.*, 2010). $\delta^{13}\text{C}_{\text{org}}$ data from Kennecott Point (Queen Charlotte Islands, Canada) and Val Adrara (Italy) show a late Hettangian positive excursion which is not recorded at St Audrie's Bay which is caused by local ecological conditions and distinct changes in facies (respectively) (Ruhl *et al.*, 2010). These isotope excursions have been linked with an input of isotopically light carbon from outgassing during the initial major basaltic eruptions during the CAMP event (Hesselbo *et al.*, 2002; Ruhl and Kurschner, 2011; Bartolini *et al.*, 2012).

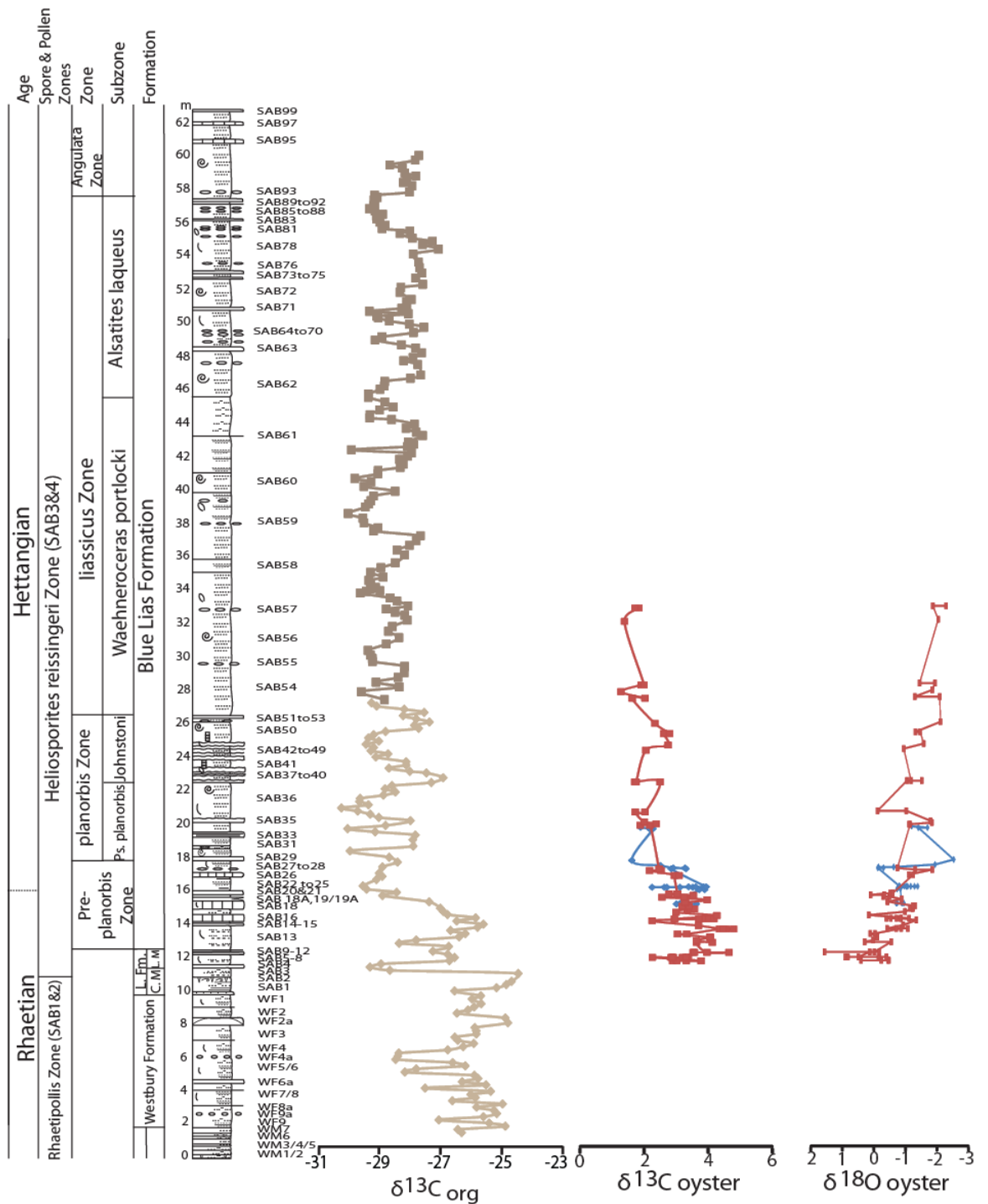


Figure 2.10a: Published $\delta^{18}O$ values and the $\delta^{13}C$ values from St Audrie's Bay. Data from Korte *et al.* (2009) ($\delta^{18}O$ and $\delta^{13}C$ oyster from St Audrie's Bay (red squares) Appendix 3: Table A3.2), Hesselbo *et al.* (2002) ($\delta^{13}C_{org}$ bulk rock from St Audrie's Bay (light brown squares)) Ruhl *et al.* (2010) ($\delta^{13}C_{org}$ bulk rock from St Audrie's Bay (dark brown squares)) (Appendix 3: Table A3.4) and van de Schootbrugge *et al.* (2007) ($\delta^{18}O$ and $\delta^{13}C$ oyster from St Audrie's Bay (blue diamonds) Appendix 3: Table A3.3). The $\delta^{13}C_{org}$ bulk rock, $\delta^{18}O$ and $\delta^{13}C$ oyster values have been correlated to the St Audrie's Bay log and bed numbers produced in this study.

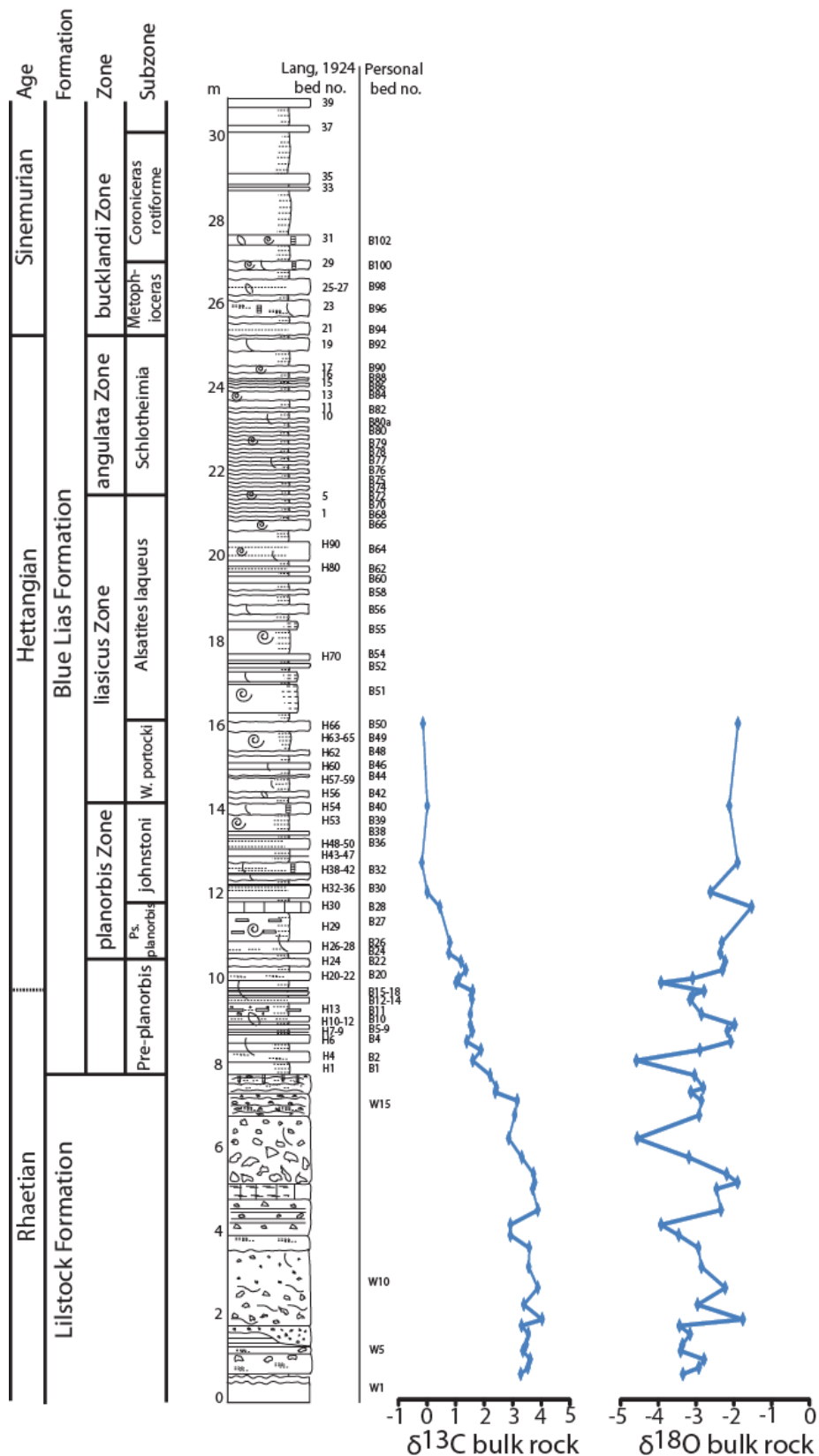


Figure 2.10b: $\delta^{18}\text{O}$ values and the $\delta^{13}\text{C}$ values from Lyme Regis. The data included in this diagram is from Korte *et al.* (2009) ($\delta^{18}\text{O}$ and $\delta^{13}\text{C}$ bulk rock from Lyme Regis (Blue lines)) (Appendix 3: Table A3.1).

2.5 Correlation of the Tr-J GSSP section to the sections studied here and other key sites including the Newark Basin and East Greenland locations.

The Kuhjoch section in Austria has been designated the Tr-J boundary Global Stratotype Section and Point (First occurrence (FO) of *Psiloceras* sp. cf. *P. spelae*; GSSP) with the Nevada section as the Auxiliary Stratotype Section and Point (ASSP) (Von Hillebrandt *et al.*, 2007, 2013). The Kuhjoch section records a well oxygenated and open marine environment with a high rate of sedimentation, well separated successive events and no syn-sedimentary disturbances to disrupt the original sequence (Von Hillebrandt *et al.*, 2007). First occurrence data of different ammonites has been used to divide the stratigraphy with the FO of *Psiloceras* sp. cf. *P. spelae* Guex at Kuhjoch designated the definition for the Tr-J boundary (Table 2.1) (Von Hillebrandt *et al.*, 2007, 2013).

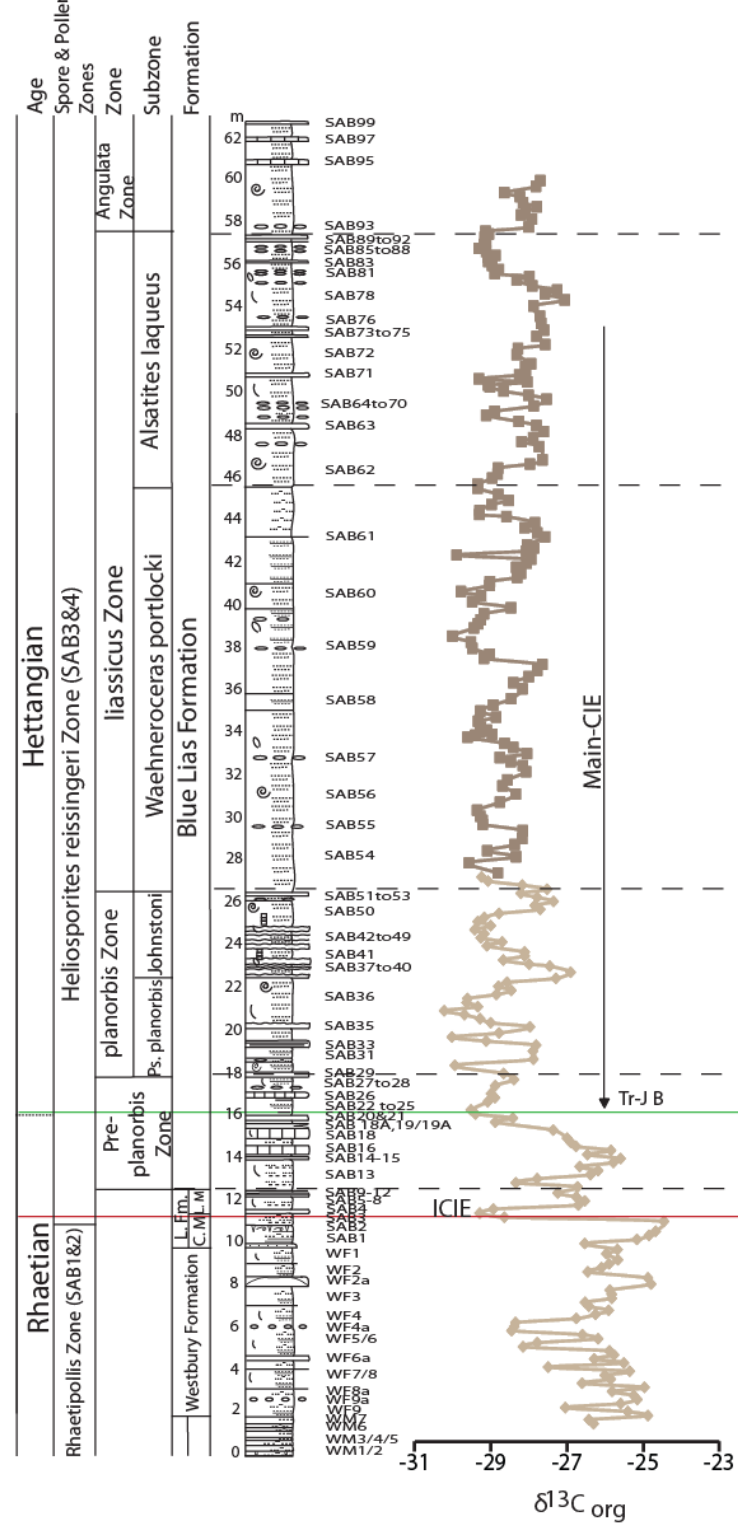
Psiloceras sp. cf. *P. spelae* Guex has been determined as the boundary marker for the base of the Jurassic because it has a short vertical range, a global distribution and is recorded in several other sections (Simms and Jeram, 2007; Von Hillebrandt *et al.*, 2007, 2013). Unfortunately, this ammonite species is not recorded in southwest England, possibly due to a reduced water depth compared to other locations, lack of oceanic connection, geographical dispersion or faunal provincialism (Clémence *et al.*, 2010). Other species of *Psiloceras* that have been found in southwest England are not recorded in the Northern Calcareous Alps (Bloos and Page, 2000; Page, 2005; Von Hillebrandt *et al.*, 2007; Korte *et al.*, 2009) (Table 2.1). McRoberts *et al.*, (2007) found that the basal Jurassic ammonite *Psiloceras* sp. cf. *P. spelae* fauna occurs at the same point as the main negative excursion (found

between two positive excursions) in both the Austria and Nevada localities and correlates with the GSSP and ASSP localities respectively (Clémence *et al.*, 2010). The first occurrence of *Cerebropollenites thiergartii* at the GSSP also has biostratigraphical value; firstly with the lowest occurrence occurring at the FO of *Psiloceras* sp. cf. *P. spelae*, secondly by being found in marine and terrestrial environments and thirdly the first occurrence correlating with the main negative excursion (Von Hillebrandt *et al.*, 2007; Bonis *et al.*, 2009; Mander *et al.*, 2013).

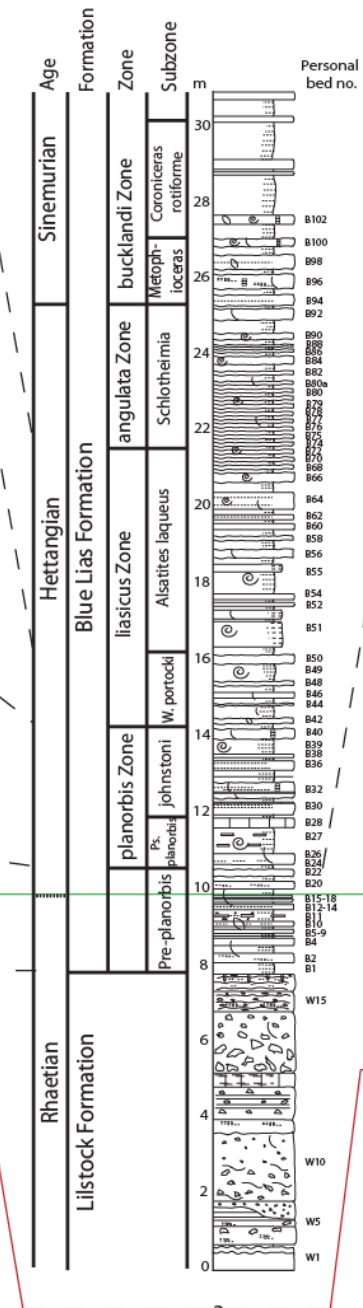
	Zones	Northern Calcareous Alps	NW Europe (UK)	North America	South America
Lower Hettangian	Planorbis	<i>Psiloceras naumanni</i>	<i>Caloceras johnstoni</i>	<i>Caloceras crassicostatum</i>	<i>Psiloceras cf. calliphylloides</i>
		<i>Psiloceras costosum</i> & <i>Psiloceras calliphylum</i>	<i>Psiloceras plicatulum</i> , <i>Psiloceras psilonotum</i> & <i>Psiloceras planorbis</i>	<i>Psiloceras polymorphum</i>	<i>Psiloceras rectocostatum</i>
					<i>Psiloceras primocostatum</i>
	Tilmani	<i>Neophyllites</i>	<i>Neophyllites</i> & <i>Psiloceras erugatum</i>	<i>Psiloceras pacificum</i>	<i>Psiloceras planocostatum</i>
		<i>Psiloceras cf. pacificum</i>	?		<i>Psiloceras tilmani</i>
		<i>Psiloceras ex gr. P. tilmani</i>		<i>Psiloceras marcouxii</i> & <i>Odoghertyceras</i>	<i>Psiloceras cf. tilmani</i> & <i>Odoghertyceras</i>
		<i>Psiloceras</i> sp. cf. <i>P. spelae</i>		<i>Psiloceras</i> sp. cf. <i>P. spelae</i>	<i>Psiloceras</i> sp. cf. <i>P. spelae</i>
Rhaetian	Marshi	<i>Choristoceras</i>		<i>Choristoceras crickmayi</i>	<i>Ch. marshi</i> & <i>Ch. crickmayi</i>

Table 2.1: Proposed correlation of ammonite zones for the Early Hettangian (modified from Von Hillebrandt *et al.*, 2007, 2013).

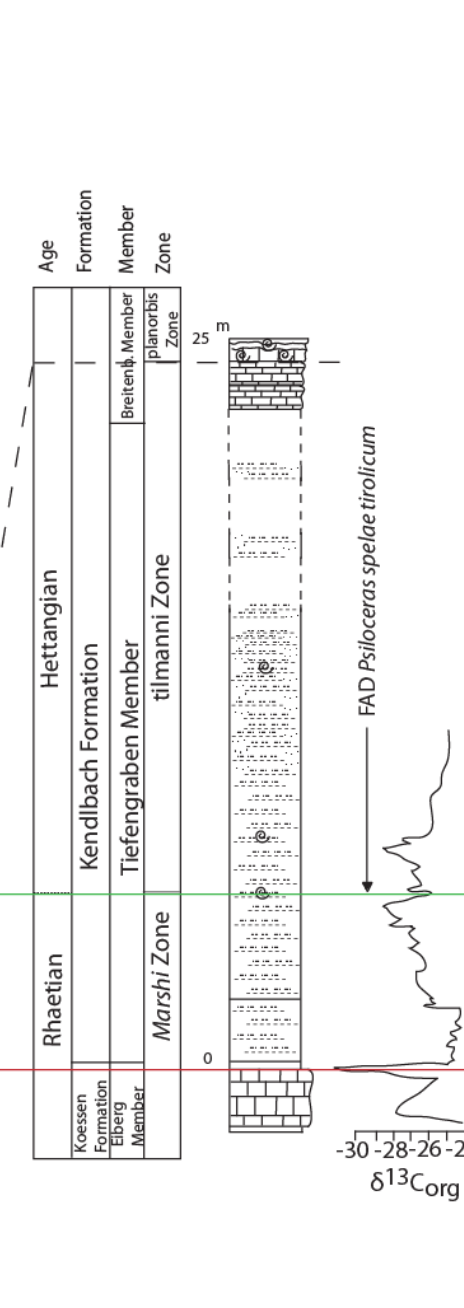
St Audrie's Bay



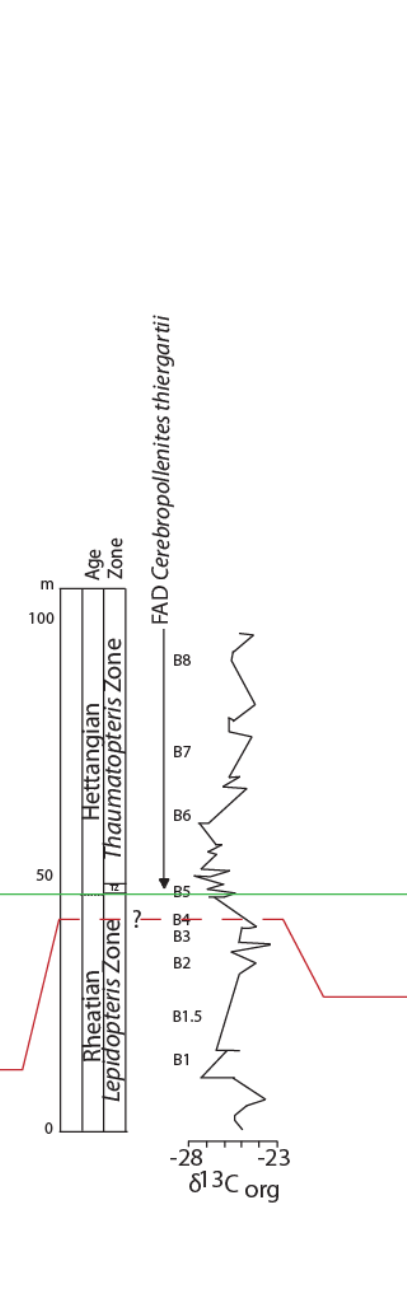
Lyme Regis



Kuhjoch Austria (GSSP)



Astartekloft East Greenland



Newark Basin

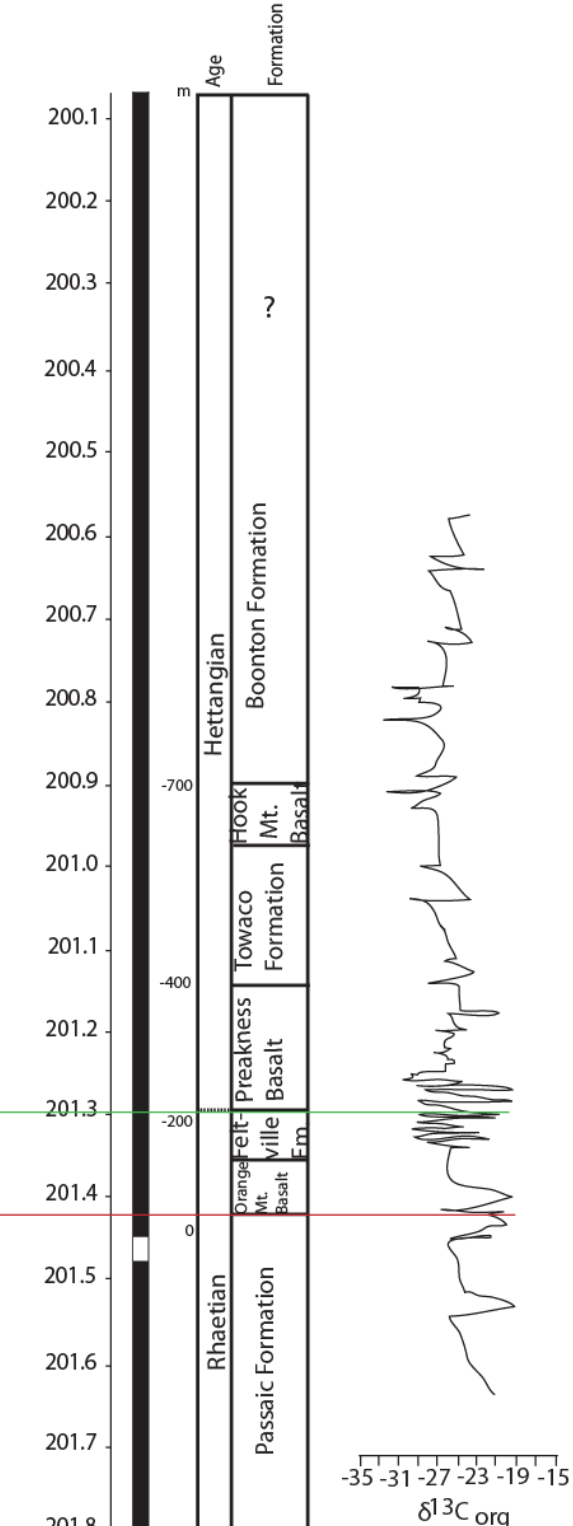


Figure 2.11: Correlation of the Tr-J southwest England sites using the main negative carbon isotope excursion (Main-CIE) found in the organic carbon isotope curves from St Audrie's Bay (Hesselbo *et al.*, 2002; Ruhl *et al.*, 2010), Kuhjoch (GSSP) (Ruhl *et al.*, 2009), Astartekløft (East Greenland) (Hesselbo *et al.*, 2002) and Newark basin (Whiteside *et al.*, 2010) which correlates with the first occurrence of *Psiloceras* cf. *spelae* Guex and *Cerebropollenites thiergartii*. The Tr-J mass extinction event is highlighted in red, green line indicates the Tr-J boundary and grey dashed lines indicate a correlation between the different stratigraphical zones.

These can be used as an alternative means of correlating the FO of *Psiloceras* sp. cf. *P. spelae* to other marine or terrestrial Tr-J sections to determine the boundary (e.g., ASSP, Newark Basin, southwest England and Astartekloft) (Figure 2.11) (Hesselbo *et al.*, 2002; Whiteside *et al.*, 2007; Pálfy *et al.*, 2007; Korte *et al.*, 2009; Bonis *et al.*, 2010b; Deenen *et al.*, 2010; Ruhl *et al.*, 2010; Črne *et al.*, 2011).

2.6 Magnetostratigraphy at St Audrie's Bay and correlation to the Newark Basin

Hounslow *et al.* (2004) determined the magnetostratigraphy for the St Audrie's Bay succession. The Penarth Group encompasses four reversed magnetozones which are also recorded in stratigraphically equivalent sections in South Wales (Hounslow *et al.*, 2004), western Germany and north eastern France (Edel and Düringer, 1997). Several studies have correlated the magnetozones from St Audrie's Bay with those of the Newark Supergroup (Figure 2.12) (Kent *et al.*, 1995; Hounslow *et al.*, 2004; Gallet *et al.*, 2007; Deenen *et al.*, 2010; International Commission on Stratigraphy, 2013). The correlation of Hounslow *et al.* (2004) magnetozones to the log from this study was accomplished by determining the exact location of each change in polarity on Hounslow *et al.* (2004) logs and matching that location to the equivalent location on the log from this study. The following discussion shows how the Newark Basin magnetozones were correlated to the St Audrie's Bay magnetozones.

Newark/
Hartford basin St Audrie's Bay

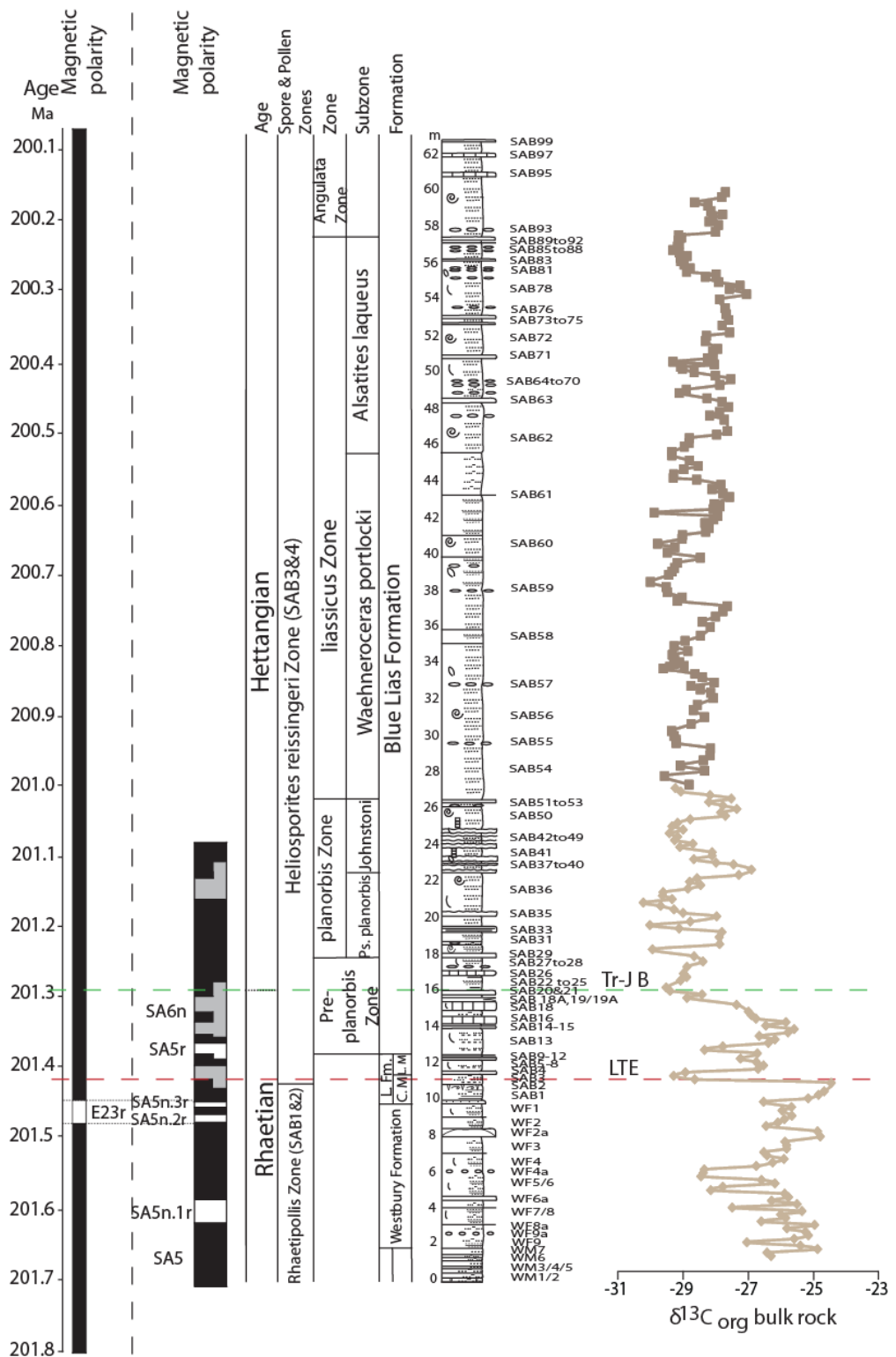


Figure 2.12: Magnetostratigraphy and the $\delta^{13}\text{C}_{\text{org}}$ curve from St Audrie's Bay correlated with the latest time calibration for the Newark Basin sequence (International Commission on stratigraphy, 2013; modified from Whiteside *et al.*, 2010; Gallet *et al.*, 2007; Hounslow *et al.*, 2004). Abbreviations include: Late Triassic extinction event (LTE) and Tr-J boundary (Tr-J B).

Using the negative shift in $\delta^{13}\text{C}_{\text{org}}$ from the continental record at Newark Basin and the corresponding initial negative carbon isotope excursion from St Audrie's Bay, the two short reversed polarity intervals (SA5n.2r & SA5n.3r) through the upper Westbury Formation to the lower Cotham Member have been correlated to the Newark Basin E23r interval (Figure 2.12) (Gallet *et al.*, 2007; Deenen *et al.*, 2010; Whiteside *et al.*, 2010). The reversed magnetic interval E23r, from the Newark Basin is made up of two very short reversed intervals separated by a short transitional-normal polarity interval but on the log is shown as one large reversed interval to match with the other publications showing this magnetostratigraphy (Kent and Olsen, 1999). This correlation has been strengthened using existing palynological records from both locations, including the upward increase in spores (Fowell *et al.*, 1994), the first and last occurrences of specific miospore taxa (e.g., *Tsugaepollenites? Pseudomassulae* and *Porcellispora longdonensis*; Hounslow *et al.*, 2004), and a monotonous *Classopollis* assemblage (Deenen *et al.*, 2010).

The majority of the polarity changes found above this point at St Audrie's Bay are interpreted as uncertain polarity changes except for the reversed polarity SA5r magnetozone (Figure 2.12) (Hounslow *et al.*, 2004). The uncertain polarity changes are inferred to represent normal polarity intervals, which correlates with the Newark Basin record (Figure 2.12) (Whiteside *et al.*, 2007, 2010). The magnetostratigraphic record at St Audrie's Bay is incomplete above the *Ps. planorbis* subzone, and correlations with the Newark Basin require the use of other data like cyclostratigraphy and $\delta^{13}\text{C}_{\text{org}}$ (Whiteside *et al.*, 2010).

2.7 $p\text{CO}_2$ correlations

To correlate the published $p\text{CO}_2$ data to the St Audrie's Bay log several methods were used. Whiteside *et al.* (2007, 2010) used the Newark Basin magnetic polarity, $\delta^{13}\text{C}$ data and plant extinction records to correlate the Greenland $p\text{CO}_2$ data with Hesselbo *et al.*'s (2002) log of St Audrie's Bay. The initial negative excursion in the $\delta^{13}\text{C}_{\text{org}}$ record and the onset of the extinction event is found above polarity zone E23r and below the oldest known CAMP basalts at the Newark Basin, whereas the main excursion occurs during the CAMP emplacement (Cohen and Coe, 2002; Whiteside *et al.*, 2007, 2010). Major negative $\delta^{13}\text{C}_{\text{org}}$ excursions in marine (Hesselbo *et al.*, 2002; Ruhl *et al.*, 2010) and terrestrial sections (McElwain *et al.*, 1999), along with the F.O of *C.thiergartii* provide a means of correlating the first increased atmospheric $p\text{CO}_2$ level and the CAMP emplacement with various sections including Astartekloft, Larne, St Audrie's Bay and the GSSP (Whiteside *et al.*, 2007, 2010; Belcher *et al.*, 2010; Steinhorsdottir *et al.*, 2011; Mander *et al.*, 2013).

The atmospheric $p\text{CO}_2$ data from Greenland (described in Chapter 1) have been correlated to the Newark Basin and thus to St Audrie's Bay using the F.O of *C.thiergartii* and the Greenland ^{13}C - depleted interval found within the $\delta^{13}\text{C}_{\text{wood}}$ data which is thought to correspond to a similar ^{13}C -depleted interval in the $\delta^{13}\text{C}_{\text{wood}}$ data from the Newark Basin (McElwain *et al.*, 2009; Belcher *et al.*, 2010; Whiteside *et al.*, 2010; Mander *et al.*, 2013). The elevated CO_2 values produced from the Greenland stomatal data correlate almost exactly to the whole CAMP episode. Bartolini *et al.* (2012) believed that the first

Greenland sample showing an increase in $p\text{CO}_2$ levels found by McElwain *et al.* (2007) corresponds to a point in the main excursion found in the planorbis Zone (log height: 20m; Bed34) which is similar to the positioning suggested by Whiteside *et al.* (2010).

Schaller *et al.* (2011) used the Newark Basin magnetic polarity data from Kent and Clemmensen (1996) and Whiteside *et al.* (2010) to correlate the McElwain *et al.* (1999) Greenland and Sweden $p\text{CO}_2$ data with the Newark Basin palaeosol $p\text{CO}_2$ data. This correlation by Schaller *et al.* (2011) enables a correlation of their $p\text{CO}_2$ data with St Audrie's Bay using the magnetic polarity record. Subsequent comparison of magnetic polarity ages with the most recent ages from the International Commission on Stratigraphy (2013) showed that they were identical.

Mander *et al.* (2013) produced a correlation between the Greenland plant beds and sporomorph assemblage zones from Astartekløft and the section at St Audrie's Bay. At Astartekløft, plant beds 1-4 represent the *Rhaetipollis-Limbosporites* Zone (Lund, 1977) which correlates with the St Audrie's Bay *Rhaetipollis* Zone (Orbell, 1973) (Beds WM1-SAB3 (from this study), and the succession up to and including the lower Cotham member) (Mander *et al.*, 2013). None of these sporomorph assemblages can be confidently correlated to those of the St Audrie's Bay succession, however, and so plant beds 1 to 4 lie within Orbell's (1973) *Rhaetipollis* Zone or Bonis' (2010) SAB1 and SAB2 zones but their exact positions cannot be determined (Figure 2.13) (Mander *et al.*, 2013; Mander, pers com., 2013). The initial carbon isotope excursion found at St Audrie's Bay is not recorded at Astartekløft but is

thought to be possibly located between plant beds 4 and 5 in a condensed interval (Mander *et al.*, 2013, fig. 5).

Plant bed 5 records the first elevated $p\text{CO}_2$ level found by McElwain *et al.* (2007). This bed also records the F.O of *C.thiergartii*, and therefore correlates with the onset of the main negative excursion at St Audrie’s Bay in the upper Pre-planorbis Beds (in this study: log height 16.2m; Bed 22) (Steinthorsdottir *et al.*, 2011; Mander *et al.*, 2013; Jaraula *et al.*, 2013). This indicates that bed 5 correlates to the lower part of Bonis *et al.* (2010) SAB3-4 Zone or within the lower part of Orbell’s, (1973) *Heliosporites* Zone (Figures 2.11-2.13).

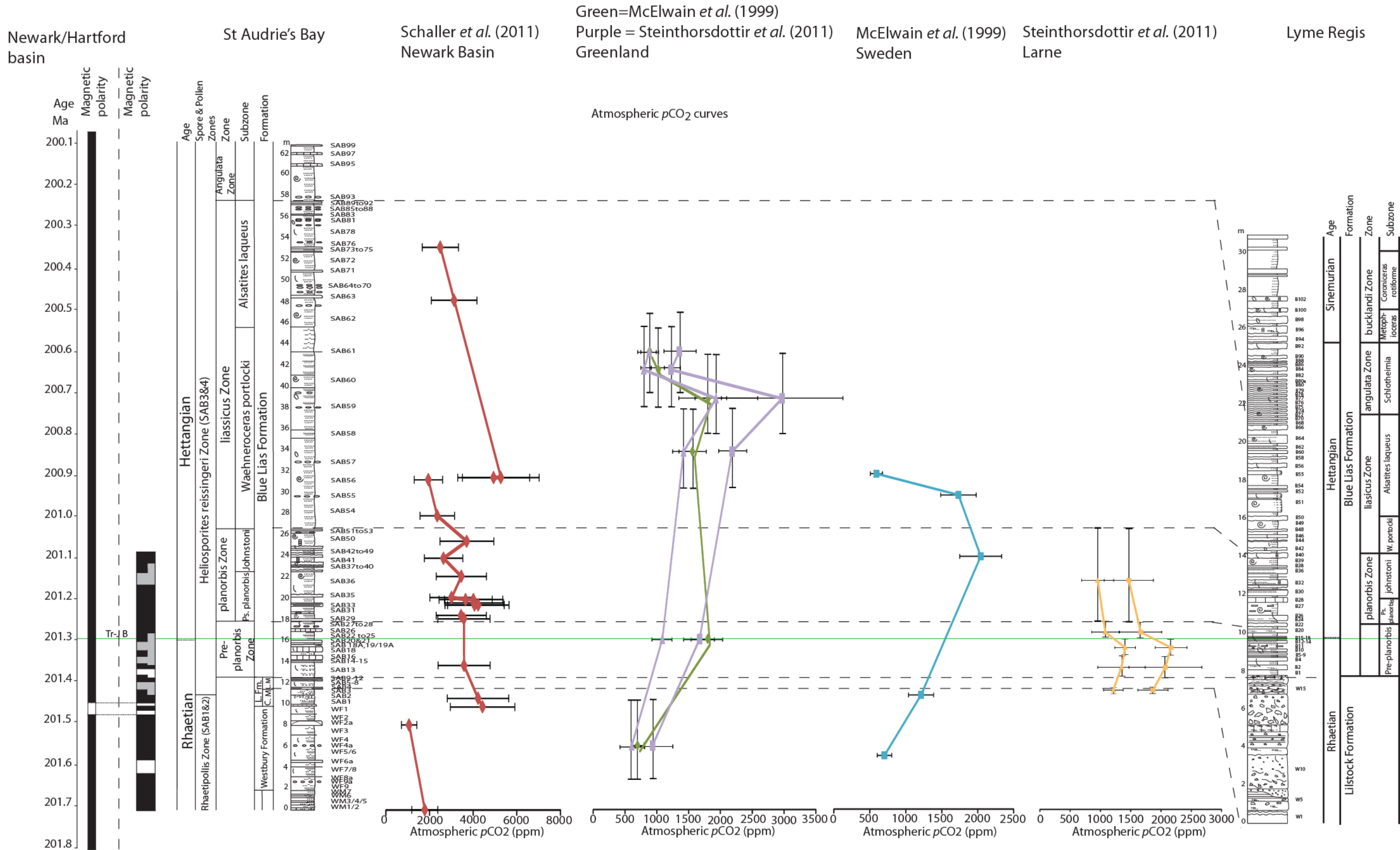
Chronostratigraphy	Astartekløft Plant Bed Schematics (McElwain <i>et al.</i> , 2007)	Astartekløft Sporomorph Zonation (Mander <i>et al.</i> , 2013)	Previous Zonation Schemes Based on Sporomorphs	
			Orbell (1973)	Bonis (2010)
Jurassic (Hettangian)	8	?	<i>Heliosporites</i> Zone	SAB4 (upper)
	7			
	6			
latest Late Rhaetian	5 F.O. <i>C. thiergartii</i>	A3		SAB4 (lower)
Triassic (Mid to Late Rhaetian)	4	A2	<i>Rhaetipollis</i> Zone	SAB3
	3			SAB3
	2	SAB2		
	1.5	SAB2		
	1	SAB1		
	1	SAB1		

Figure 2.13: Schematic correlation of the Astartekløft plant beds (from McElwain *et al.*, 2007), the Astartekløft sporomorph zonation (from Mander *et al.*, 2013), and the St Audrie’s Bay sporomorph biozonations and the F.O of *C. thiergartii* (modified from Mander *et al.*, 2013; Figure 3, p41, including the addition of the F.O of *C. thiergartii* and removal of certain columns).

Plant beds 6 to 8 cannot be confidently correlated to the St Audrie's Bay succession but they probably lie somewhere within Bonis' (2010) upper SAB4 Zone and the upper part of Orbell's (1973) *Heliosporites* Zone (Figure 2.13). Mander *et al.* (2013) results are therefore incompatible to previous studies that correlate the initial carbon isotope excursion with plant bed 1 (e.g., Bartolini *et al.*, 2012) or plant bed 3 (e.g., Whiteside *et al.*, 2010). In further communications with Dr Luke Mander (pers coms., 2013) he advised that the correlation by Schaller *et al.* (2011) should be used to produce a tighter vertical position for the rest of the McElwain *et al.* (1999) $p\text{CO}_2$ data.

Having examined previous correlations of $p\text{CO}_2$ data from different locations to St Audrie's Bay in detail, a combination of Schaller *et al.* (2011) correlation of $p\text{CO}_2$ data (from Newark Basin, Greenland and Sweden) using the Newark Basin magnetostratigraphy, Mander *et al.* (2013) palynology data for Greenland (position of F.O of *C.thiergartii*) and the negative $\delta^{13}\text{C}_{\text{org}}$ excursions seen across all of the locations (Newark Basin, Greenland, Sweden, St Audrie's Bay and Larne) will be used to position the $p\text{CO}_2$ data to the highest possible precision (e.g., nearest centimetre or metre) within the stratigraphy documented in the St Audrie's Bay logs from this investigation (Appendix 3; Table A3.5 to A3.7)³.

³Figure 2.14: The $p\text{CO}_2$ curve from Greenland, Sweden, Larne and the Newark Basin correlated with the St Audrie's Bay and Lyme Regis log from this study. The correlation was produced as previously discussed using Schaller *et al.*, (2011) correlation of all the $p\text{CO}_2$ curves with the dated magnetostratigraphy from St Audrie's Bay and Mander *et al.* (2013) palynology data. Square symbol = $p\text{CO}_2$ ppm carboniferous standard and triangle symbol = $p\text{CO}_2$ ppm modern standard for Greenland and Larne data from Steinhorsdottir *et al.* (2011).



Mander *et al.*'s (2013) correlation between Astartekølfth and St Audrie's Bay using Greenland plant bed 5, the F.O of *C.thiergartii* and the main negative excursion (Figure 2.13), allows error bars to be placed around the position of the other Greenland pCO_2 data points but not any of the other sections (Figure 2.14). Lyme Regis is correlated to St Audrie's Bay and the pCO_2 data through the same zone and subzone boundaries as well as the position of the Tr-J boundary (Appendix 3: Table A3.8 to A3.10). This method gives the best possible correlation to St Audrie's Bay and Lyme Regis logs given the limited data available at the time to do these correlations. Further improvement of this correlation method can only occur when new magnetostratigraphy, palynology and $\delta^{13}C_{org}$ data becomes available.

2.8 Further work

In the next two chapters the morphometric and geochemical data derived from three different species (*L. hisingeri*, *P. gigantea* and *O. aspinata*) is reported. This data comes from an interval that post-dates the Tr-J extinction event and extends through a period of biological recovery and continued environmental perturbation. The morphometric data from the assemblages are, therefore, from the interval that recorded the projected pCO_2 maximum and the high temperature that are recorded in the post extinction period. The faunal response during the recovery phase is, potentially, correlated with the changes in global pCO_2 and temperature.

Chapter 3 – Fossil Morphometric Studies

3.1 Introduction

Previous fossil investigations and studies on extant communities have often shown that reduced shell size and thickness are a common consequence of exposure to high CO₂ and high temperature environments. This research has sought to document size variation in a number of fossils from the post-extinction strata at both Lyme Regis and St Audrie's Bay (e.g., Wright *et al.*, 2003; Hautmann *et al.*, 2004, 2008; Pálffy., 2005; Kiessling *et al.*, 2007; Mander *et al.*, 2008; Martindale *et al.*, 2012; Greene *et al.*, 2012). There are relatively few published studies of size variations across the late Triassic extinction event and into the Hettangian, in significant enough detail, that could be used to compare with the pCO₂ and temperature curves from this interval (Mander *et al.*, 2008; Opazo, 2012).

3.1.2 Aim

The aim of this chapter is to report variations in the shell size of *Liostrea hisingeri*, *Plagiostoma gigantea* and *Ogmoconchella aspinata* through the late Triassic and into the Hettangian from the successions at Lyme Regis and St Audrie's Bay discussed in Chapter 2 (also see Section. 3.2 below).

These procedures were as follows:

- Morphometric measurements from *L. hisingeri*, *P. gigantea* (geometric shell size) and *O. aspinata* (geometric shell size and thickness) at both localities were analysed to determine any stratigraphic variation and size trends through the sections.

- Relationships were determined between these morphometric variations and the different species, across both locations.

3.2 Choice of fossil species

Previously published work on both locations (e.g., Lang, 1924; Hallam, 1989; Mander *et al.*, 2008; Lord and Davis, 2010) and preliminary field work at the start of this study were used to determine the most suitable species for study. The bivalves *L. hisingeri* and *P. gigantea* and ostracod *O. aspinata* were chosen as model organisms out of the various *Liostrea*, *Plagiostoma* and *Ogmoconchella* species available for this study as they are found in many of the beds at both St Audrie's Bay and Lyme Regis, but differ in their ecologies (epifaunal suspension feeders and opportunistic benthic species in shallow marine shelf environments). The fossil bivalve species were also chosen because a considerable amount of previous research has been conducted on roughly comparable modern species under variable pH and temperature conditions (e.g., Bamber, 1990; Green *et al.*, 2004; Kurihara *et al.*, 2007; Gazeau *et al.*, 2007; Talmage and Gobler, 2009; Ries *et al.*, 2009). Fossil ostracods were chosen because very little is known of the effects of different environmental factors including seawater pH on the biology of this group (Marco-Barba *et al.*, 2012; Hunt and Roy, 2006; De Deckker *et al.*, 1999; Bullen and Sibley, 1984).

3.3 Studied Taxa

The bivalve species *L. hisingeri* and *P. gigantea* were identified from other species in the same genera using the available literature (e.g., Lord and Davis, 2010). The ostracod species *O. aspinata* was identified from other

related taxa using the appropriate literature (e.g., Boomer and Ainsworth, 2009).

Ogmoconchella aspinata (Drexler, 1958)

Ogmoconchella aspinata is a species of ostracod that is thickly calcified, with an unornamented, smooth, ovate to sub-triangular, inflated bivalved carapace of low magnesium calcite. The left valve is slightly larger and somewhat overlaps (along the dorsal margin) the right valve which contains the antero-marginal lip (Figure 3.1a; Drexler, 1958; Lord, 1971; Hart and Hylton, 1999; Boomer and Ainsworth, 2009; Lord and Davis, 2010). They grew by moulting and produced up to eight instars between egg and adult (Athersuch *et al.*, 1989). Certain ostracod species show some sexual dimorphism but *Ogmoconchella* has unclear sexual dimorphism and so is very difficult to separate into male and female (Lord, 1971). It was an opportunistic benthic marine species living in shallow, well oxygenated marine shelf environments but tolerated a wide range of environments and salinities (Boomer and Ainsworth, 2009; Lord and Davis, 2010). It ranges from the Late Triassic through to the Early Sinemurian (Hart and Hylton, 1999; Boomer and Ainsworth, 2009; Lord and Davis, 2010). *O. aspinata* is placed within the Family Healdiidae, Superfamily Healdioidea, Suborder Metacopina, Order Podocopida, Suborder Podocopa, Class Ostracoda, Subphylum Crustacea and Phylum Arthropoda (Lord, 1971; Palaeobiology Database, accessed June, 2013).

Plagiostoma gigantea (Sowerby, 1814)

The shell of *Plagiostoma gigantea* is composed of aragonite and low magnesium calcite. It is larger in size (average valve length; 50mm) compared to others in this family, with a smooth, ovate, inflated shape and occasionally has faint radial ridges (Figure 3.1b; Sowerby, 1814; Yin and McRoberts, 2006; Lord and Davis, 2010). *P. gigantea* was an epifaunal suspension feeder, living on the substrate or hardground surfaces, with facultative or attached motility. The species is found in marine, offshore ramp/shelf, shallow/open shallow subtidal and reef environments. It ranges from the base of the Rhaetian (Upper Triassic) to the Early Tithonian (Upper Jurassic) (Palaeobiology Database, accessed June, 2013). *P. gigantea* belongs to the Genus *Plagiostoma*, Family Limidae, Superfamily Limoidea, Suborder Anomiidina, Order Pectinida, Superorder Ostreiformii, Infraclass Pteriomorpha, Subclass Autobranchia, Class Bivalvia and Phylum Mollusca (Palaeobiology Database, accessed June, 2013).

Liostrea hisingeri (Douvillé, 1904)

The shells of *Liostrea hisingeri* are elongate in shape, with a subovate outline. The shell is formed of low magnesium calcite (Figure 3.1c; Douvillé, 1904; Lord and Davis, 2010; Palaeobiology Database, accessed June, 2013). *L. hisingeri* was an epifaunal suspension feeder, cemented to the substrate or hardground as well as free living in marine and brackish environments (Palaeobiology Database, accessed June, 2013). The taxon ranges from the base of the Ladinian (Triassic) to the top of the Bartonian (Eocene; Palaeobiology Database, accessed June, 2013). *L. hisingeri* is classified in

the Genus *Liostrea*, Subfamily Gryphaeinae, Family Gryphaeidae, Superfamily Ostreoidea, Suborder Ostreidina, Order Ostreida, Superorder Ostreiformii, Infraclass Pteriomorphia, Subclass Autobranchia, Class Bivalvia and Phylum Mollusca (Palaeobiology Database, accessed June, 2013).

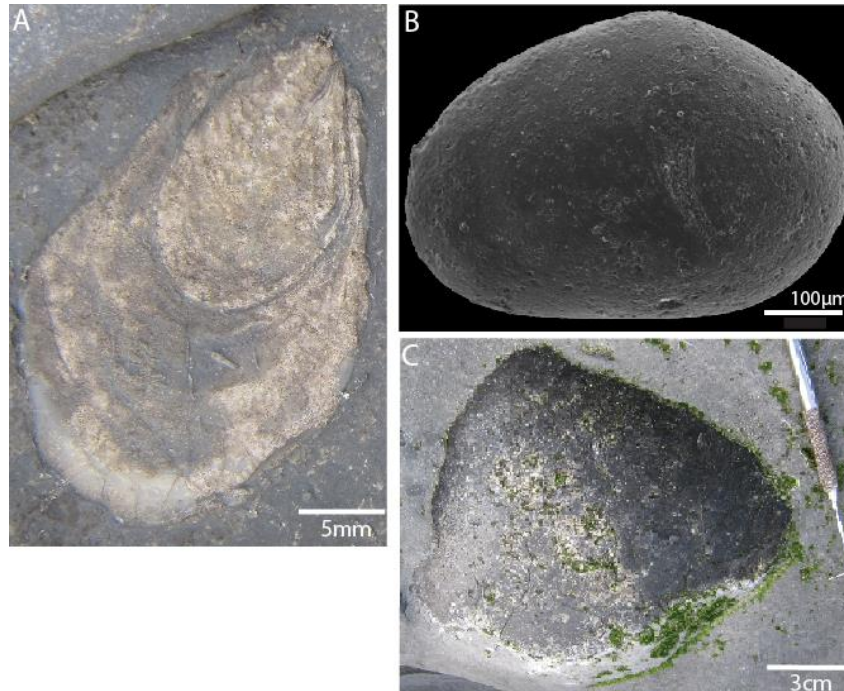


Figure 3.1: Images of the studied species (A) *L. hisingeri*, (B) *O. aspinata*, (C) *P. gigantea* (note variations in scale).

3.4 Materials and methods

3.4.2 Digestion and picking of marl samples for ostracods

At each location, 500g bulk rock samples were collected from 40 beds (for logs and sample numbers see Chapter 2.3). 250g of each sample was disaggregated to obtain ostracods and other microfossils using the white spirit technique while the remaining 250g sample was kept as a type sample (Armstrong and Brasier, 2005). The marl samples were put into clean bowls (15cm in diameter) and left in an oven at $< 40^{\circ}\text{C}$ overnight to desiccate.

Petroleum spirit (30% aliphatic hydrocarbons and 15% - 30% aromatic hydrocarbons) was then added to each bowl, which was covered with clingfilm™. After a maximum of 5 hours the white spirit was filtered (using grade 17, 270mm dial sized filter paper) to collect any loose sediment, and the white spirit re-used on the next sample. The sample was then soaked overnight in deionised water before being washed through a 63µm sieve, then filtered to remove the remaining water (using grade 17, 270mm dial sized filter paper), before being dried in an oven at 40°C for 8 hours. This process was repeated until the sample was fully disaggregated and all the clay and sediment had been removed. To confirm the sample was fully disaggregated it was checked under low power magnification (Nikon, Surry, UK) to make sure all the sediment and clay minerals had been removed and the fossils were clean.

Each disaggregated marl sample was dry sieved into >280µm, 279-180µm and 179-63 µm fractions so the maximum possible range of carapace size could be sampled and measured. To determine how many ostracods should be picked from each sample, a pilot study was performed on 350 individuals from one sample. These were picked as equally as possible from all three size fractions. The lengths and widths of the shells were measured, and the geometric mean sizes were calculated. It was established that after measuring 50 individuals from each size fraction there was no significant difference in size. Thus, a minimum of 50 individuals were picked from each of the three size fractions, giving a minimum of 150 individuals from the sample as a whole (unless the size fraction or sample was completely depleted before the minimum number was reached). The numbers were not

maximum numbers because each tray of sample had to be completely picked to avoid any form of bias before the number of ostracods could be counted leading to some samples with significantly higher number of individuals than the minimum needed. Further sample was not disaggregated when the minimum number was not reached because the total sample weight needed to be kept constant across all the samples and even if more of the sample was picked it would not guarantee the minimum ostracod number being reached in some cases.

3.4.3 Bivalve morphometrics

The length (defined as the distance from umbo to commissure tip, in a straight line) and width (defined as the maximum shell span at a right angle to the length) of individual species of *L. hisingeri* and *P. gigantea*, were measured to the nearest millimetre using digital callipers on each of the exposed beds (Figure 3.2A-B). Incomplete specimens were measured if a reasonable estimate (e.g., where the shell margin continuity can be traced, Figure 3.2D) could be made of either the length or width. Shell thickness could not be measured accurately in the field, due to weathering of the majority of the shells, so was not recorded. A pilot study measured ten individuals 10 times to estimate the errors associated with measuring specimens in the field. The errors were +/- 0.03mm for Lyme Regis and +/- 0.05mm for St Audrie's Bay for both bivalve species so all measurements will be documented to one decimal place.

The preservation of each individual (Table 3.1 & Figure 3.3) and the exact stratigraphic height it was collected from were recorded. Preservation states

were not mutually exclusive and so some specimens were allocated more than one code within the data tables (Table 3.1). The preservation states were based on descriptions of each individual specimen when in the field. Individuals where only a length or a width measurement could be made were excluded from the subsequent analysis. The preservation codes are included in Appendix 4; data tables A4.1, A4.2 and A4.22 and used in presenting the geometric shell size data for the different species at both locations.

Preservation description	Preservation code
Shell perfect	SP
Damage due to weathering	DDW
Margin damaged in places (from weathering)	MDP
Shell cracked from compression	SCC
Parts of shell obscured by sediment	PSOS
Mould of shell (occasionally with some partial shell still visible)	MS

Table 3.1: The type of preservation recorded and the coding used. For images representing the different types of preservation, see Figure 3.3.

3.4.4 Ostracod morphometrics

Each individual specimen from each size fraction was measured for length (defined as the distance from the ventral edge to dorsal hinge, in a straight line) and width (defined as the maximum shell span at a right angle to the length) using the Nikon Eclipse LV100POL microscope at 10x magnification, with Nikon Digital sight DS-U2 camera (Nikon; Surry, UK) and the NIS-elements Basic Research software and measuring tool (Nikon; Surry, UK)

(Figure 3.2C). The preservation (e.g., shell perfect: SP; shell broken: SB) and whether it was a left (LV) or right (RV) valve were also determined for every specimen. When the length and width measurements were used to produce a geometric size those individuals with only a length or width measurement were excluded.

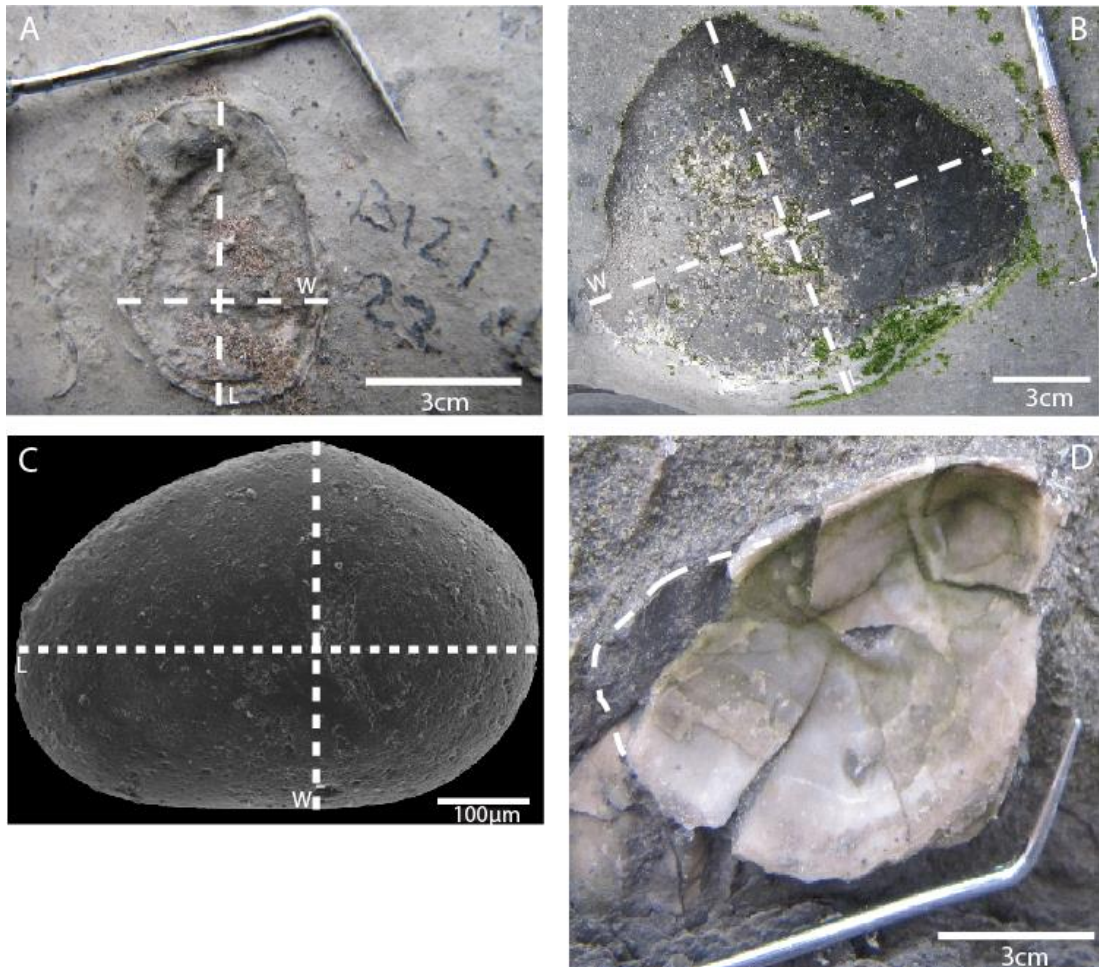


Figure 3.2: Position of length and width measurements for: (A) *L. hisingeri*, (B) *P. gigantea*, (C) *O. aspinata* (left valve) and (D) shows an example of measurements of an incomplete specimen (where the shell margin continuity can be traced).



Figure 3.3: Representative bivalve specimens showing the different types of preservation found (see Table 1 for preservation codes). A-D represent *L. hisingeri*, E represents *P. gigantea*. (A) SP = perfect preservation; (B) DDW = damage due to weathering; (C) MDP = margin damaged in places and SCC = shell cracked from compression, (D) PSOS = sediment cover round the margin; and (E) MS = an internal mould (here with some shell still intact).

The preservation codes are included in Appendix 4; data tables A4.3A-E, A4.4A-C, 23A-C and 24A-B and used when presenting the data in various graphs. An attempt was also made to identify male and female species in each of the samples from personal communications with Dr Ian Boomer, (2012), but it is very difficult to do this accurately as, to date, no one has specifically identified males or females of this species in the published literature. There was no statistically significant difference in size between those individuals thought to be male or female in the different samples, or between the left or right valve and so the data were pooled.

Ostracod carapace thickness could be accurately measured because excess sediment had been removed and specimens were undamaged after disaggregation. Double sided adhesive tape (Wilkinson, Double sided tape 50mm x 5m) was attached to a plastic rectangle with a straight line drawn down the middle (Figure 3.4). Ostracods were aligned with the black line running through the maximum length of the shell and the inner shell edge touching the tape to keep the position and orientation constant. A plastic ring was placed around the ostracods. Resin (a 4:1 mix of Araldite Resin and Hardener, measured out separately then thoroughly mixed; Opti-tec opt5001-500g, Oxfordshire, UK) was poured into the ring, over the ostracods and left to set at room temperature. Once set, the block was removed from its mould and the excess resin on the left side of the block was cut away leaving 0.5mm of resin next to the line of ostracods.

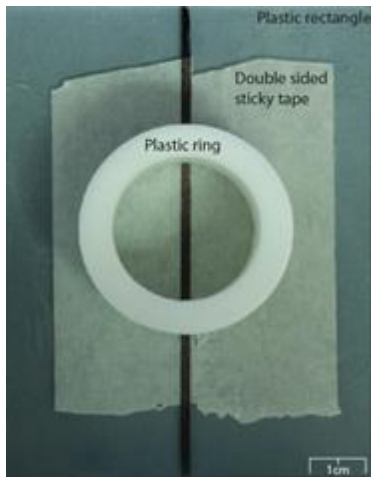


Figure 3.4: Example of the mould used to produce the resin blocks containing the fossil ostracods.

A diamond-plated Lap Master (Lap Master, Devon, UK) ground down the resin block to the anterior edge of the ostracods. Each block was finished by hand using a grinding plate and a slurry of 600 carborundum grit, to provide greater control over the delicate part of the grinding process. Each block was then polished using a polishing plate and a paste of 0.3 micron aluminium oxide (aloxite) polishing abrasive to make the ostracods visible for measuring. Each ostracod was measured in four places: at the ventral edge, the dorsal hinge and 25% and 75% away from the ventral edge along the shell length (Figure 3.5). From these four measurements an average thickness was calculated. During this process there were occasions when individuals set within the mould were unable to be measured as they were unintentionally destroyed during the grinding process so several samples have fewer than the optimum number of individuals required.

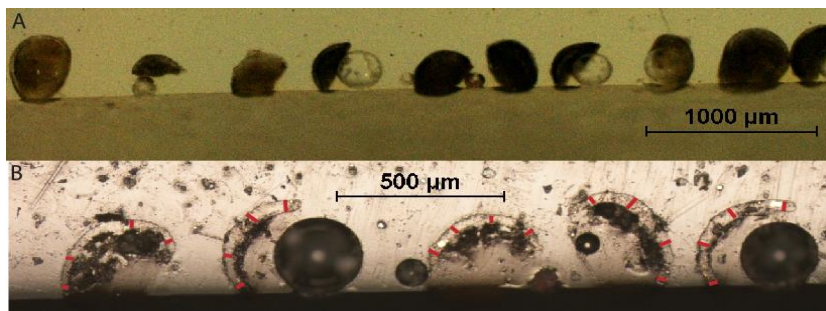


Figure 3.5: (A) Examples of several *O. aspinata* cut from the ventral edge to the dorsal hinge from sample SAB60 and (B) the red lines representing each measurement which will then give an average shell thickness.

A pilot test was undertaken using thirty random individuals (from the > 280µm size fraction) to determine how many specimens needed to be

measured. Analyse using the Kruskal-Wallis test showed that after twenty five specimens were measured there was no longer a significant difference in thickness found between the individuals. In order that the thickness measurements were not biased by only using one size fraction, but had measurements from each size fraction, twenty five individuals were taken proportionally across the three size fractions. This was calculated by dividing the total number of specimens from each size fraction by the total number of specimens in the whole sample and then multiplying by twenty five (results were round up to the nearest integer).

3.4.5 Data analysis and presentation

The length and width measurements were used to calculate a geometric mean size of each specimen ($\sqrt{\text{shell length} \times \text{shell width}}$; Jablonski, 1996) and then the mean, minimum and maximum geometric size for each sample or bed was calculated. The range of geometric shell sizes and shell thicknesses measured for each sample or each bed was also calculated. Each of the data sets (i.e. the geometric sizes for each species and ostracod shell thickness at both locations) were analysed at bed by bed scale as well as at zone and subzone scale. PAST (PALaeontological STATistical program; Hammer *et al.*, 2001) and SPSS (The Statistical Package for the Social Sciences, IBM corporation, New York, USA) were used to carry out the statistical analyses discussed below.

The statistical analyses have been completed using the geometric size data. Data from each species was tested for normal distribution (p-value: < 0.05). As the majority of these data from each sample or bed were not normally

distributed then the non-parametric Kruskal-Wallis and Mann-Whitney pairwise comparison tests were used. The Kruskal-Wallis test were used to determine whether there were any significant differences between the size variations observed throughout the section, zone or subzone, or were they just variations (outliers) around the common mean value. The Mann-Whitney pairwise comparison tests were used to determine which size variations observed in the beds and throughout the zones or subzones were significantly different to each other. General linear models were used to determine if either location or specific stratigraphical zone was important in the variation of geometric sizes found on each bed. Linear regression models were used to identify any relationships (for either location) between geometric shell size or mean shell thickness when the data was analysed at a bed by bed scale throughout the entire section as well as within each zone and with the relevant data compiled into zones and subzones. The 95th minimum, maximum and range percentile for geometric size from each bed or sample was used in the linear regression models to compensate for the variation in the number of individuals measured.

3.5 Results

The *L. hisingeri*, *P. gigantea* and *O. aspinata* geometric shell size and *O. aspinata* shell thickness results from each bed, at both locations are documented in Tables 3.2–3.5 to highlight the variation in results and numbers of individuals measured in each bed or sample.

<i>L. hisingeri</i> geometric shell size for Lyme Regis						<i>L. hisingeri</i> geometric shell size for St Audrie's Bay					
	N	Min	Max	Mean	Range		N	Min	Max	Mean	Range
LRB1	5	8.4	12.1	10.7	3.7	SAB12	40	9.3	25.7	16.4	16.5
LRB2	15	13.2	24.9	19.6	11.7	SAB16	7	10.2	17.5	14.8	7.3
LRB4	27	8.7	30.7	18.4	22.0	SAB18	12	10.5	26.1	20.1	15.6
LRB5	1	20.7	20.7	20.7		SAB18A	13	14.2	30.5	23.0	16.3
LRB6	20	13.7	31.6	20.8	17.9	SAB19A	2	22.8	27.6	25.2	4.8
LRB8	8	11.2	30.8	20.0	19.7	SAB19	46	12.4	31.3	21.6	18.8
LRB10	23	12.8	28.6	21.8	15.8	SAB20	42	11.8	34.7	24.8	22.8
LRB11	2	21.9	29.9	25.9	8.0	SAB21	7	17.5	29.9	23.4	12.4
LRB14	4	19.7	29.4	23.0	9.6	SAB22	2	18.0	26.0	22.0	8.0
LRB15	2	26.9	27.1	27.0	0.2	SAB23	6	11.9	28.5	17.9	16.6
LRB16	3	11.9	32.0	21.4	20.2	SAB24	39	13.5	44.1	26.1	30.6
LRB17	1	19.7	19.7	19.7		SAB25	8	23.6	37.8	31.1	14.2
LRB18	1	22.1	22.1	22.1		SAB26	23	13.6	39.7	23.8	26.1
LRB20	17	15.1	44.8	26.3	29.7	SAB29	3	25.7	37.7	33.0	12.1
LRB22	3	16.9	23.9	20.3	7.0	SAB35	21	10.5	28.8	17.7	18.3
LRB26	42	9.5	48.4	19.6	38.9	SAB36	2	24.2	29.4	26.8	5.2
LRB30	25	14.1	37.4	22.0	23.3	SAB41	10	13.8	26.2	18.7	12.4
LRB34	3	12.5	33.5	24.5	21.0	SAB43	3	17.0	22.0	19.0	5.0
LRB36	38	11.9	35.2	19.7	23.2	SAB63	2	9.3	18.8	14.1	9.5
LRB40	15	14.4	27.7	19.6	13.3	SAB71	1	26.8	26.8	26.8	
LRB42	15	12.7	34.7	21.2	22.0						
LRB44	2	20.1	25.5	22.8	5.4						
LRB46	33	11.2	33.0	18.7	21.8						
LRB48	9	11.4	35.1	22.2	23.7						
LRB50	20	5.9	30.3	15.7	24.4						
LRB52	46	4.4	40.6	20.0	36.1						
LRB54	34	10.7	44.4	24.0	33.7						
LRB56	43	12.7	35.4	23.0	22.7						
LRB60	17	13.8	33.0	22.0	19.2						
LRB62	4	20.4	32.4	28.4	12.1						
LRB72	1	34.4	34.4	34.4							
LRB84	4	18.3	33.3	27.0	15.0						
LRB86	4	16.8	26.2	22.4	9.4						
LRB88	7	20.8	35.0	27.0	14.2						
LRB92	1	19.0	19.0	19.0							
LRB102	23	13.3	27.7	23.9	14.4						
LRB103	1	19.4	19.4	19.4							

Table 3.2: Summary of morphometric data from Lyme Regis and St Audrie's Bay for *L. hisingeri*. Lines represent the beds separated into subzones.

<i>P. gigantea</i> geometric shell size for Lyme Regis					
	N	Min	Max	Mean	Range
LRB4	1	33.9	33.9	33.9	
LRB14	1	48.4	48.4	48.4	
LRB22	1	38.6	38.6	38.6	
LRB24	2	45.0	73.5	59.3	28.6
LRB26	2	29.6	37.9	33.8	8.3
LRB30	28	20.7	54.6	35.2	33.9
LRB32	1	53.8	53.8	53.8	
LRB34	1	57.7	57.7	57.7	
LRB36	15	14.7	39.5	25.0	24.8
LRB40	10	29.3	54.7	44.2	25.4
LRB44	1	47.8	47.8	47.8	
LRB46	8	28.5	77.7	50.1	49.2
LRB48	47	6.8	80.4	42.5	73.5
LRB50	19	23.8	74.4	48.7	50.7
LRB52	34	14.2	66.0	44.7	51.8
LRB54	19	24.6	89.7	66.9	65.1
LRB56	2	79.8	94.3	87.0	14.5
LRB60	1	57.1	57.1	57.1	
LRB72	4	76.4	114.5	93.4	38.1
LRB76	1	106.2	106.2	106.2	
LRB84	2	71.9	138.6	105.2	66.7
LRB86	1	83.8	83.8	83.8	
LRB88	10	50.4	163.5	122.5	113.2
LRB90	2	62.8	149.3	106.0	86.5
LRB94	5	51.4	160.2	108.8	108.7
LRB96	1	129.7	129.7	129.7	

Table 3.3: Summary of morphometric data from Lyme Regis and St Audrie's Bay for *P. gigantea*. Lines represent the beds separated into subzones.

<i>O. aspinata</i> geometric shell size for Lyme Regis						<i>O. aspinata</i> geometric shell size for St Audrie's Bay					
	N	Min	Max	Mean	Range		N	Min	Max	Mean	Range
LRB7	2	372.9	394.7	383.8	21.8	SAB8	69	235.4	491.9	401.7	256.5
LRB15	5	310.8	455.0	372.6	144.2	SAB11	121	305.8	500.2	431.4	194.4
LRB17	15	240.0	473.6	393.6	233.6	SAB17	4	349.8	465.0	412.9	115.1
LRB21	58	282.7	481.7	386.1	199.0	SAB26A	35	209.4	467.3	367.3	257.8
LRB23	53	234.6	500.4	384.2	265.8	SAB28	4	143.4	297.8	220.0	154.4
LRB25	91	253.2	449.9	355.5	196.7	SAB30	214	204.4	490.1	382.5	285.7
LRB27	31	283.8	476.2	383.5	192.4	SAB30A	166	210.8	473.8	357.2	262.9
LRB33	108	222.8	479.2	397.7	256.3	SAB34	54	221.2	454.4	359.2	233.2
LRB37	153	160.7	523.7	369.0	363.1	SAB40	203	249.2	506.6	390.3	257.4
LRB39	177	213.8	485.7	391.4	271.8	SAB42	198	199.0	502.5	391.6	303.5
LRB47	206	194.4	483.0	390.3	288.6	SAB44	4	326.4	477.8	398.5	151.4
LRB49	191	171.5	530.2	390.1	358.7	SAB52	212	167.4	513.3	382.4	346.0
LRB51	177	209.0	555.0	396.7	345.9	SAB60	58	233.0	484.0	361.8	251.0
LRB53	293	200.9	522.2	402.9	321.3	SAB62	253	182.2	532.2	398.9	350.0
LRB55	124	183.2	483.9	402.2	300.7	SAB64	139	158.0	497.5	395.3	339.5
LRB59	59	207.2	478.6	379.1	271.4	SAB66	211	175.0	535.8	366.0	360.9
LRB61	137	142.7	492.7	404.0	349.9	SAB68	196	205.4	523.2	383.0	317.8
LRB63	83	254.1	511.9	433.0	257.8	SAB70V.B	231	197.0	473.3	373.6	276.3
LRB67	79	290.8	584.1	422.5	293.3	SAB70V.T	205	239.3	499.6	380.8	260.3
LRB69	133	193.8	559.9	432.6	366.1	SAB74	192	208.2	528.7	416.4	320.5
LRB73	274	187.6	565.8	383.7	378.2	SAB76	217	175.7	519.2	413.9	343.5
LRB74A	108	214.0	597.1	396.1	383.1	SAB80	52	235.3	530.5	417.7	295.2
LRB75A	112	204.9	597.5	381.4	392.6	SAB82	224	189.5	528.0	395.2	338.5
LRB76A	153	235.4	548.6	394.9	313.2	SAB84	206	187.7	501.2	398.8	313.5
LRB77A	108	185.9	577.7	391.6	391.8	SAB86	180	175.0	555.7	375.3	380.8
LRB89	127	204.1	548.3	413.6	344.2	SAB88	99	255.1	504.6	384.2	249.5
LRB93	133	156.5	638.6	431.8	482.1	SAB90	290	179.9	556.0	389.0	376.1
LRB95	144	172.0	560.8	322.6	388.8	SAB94	321	182.3	616.2	365.2	433.9
LRB97	63	205.2	561.7	347.8	356.5	SAB96	26	272.0	507.6	395.8	235.6
LRB99	102	175.7	555.0	342.1	379.3	SAB98	16	269.7	419.4	318.0	149.7

Table 3.4: Summary of morphometric data from Lyme Regis and St Audrie's Bay for *O. aspinata*. Lines represent the beds separated into subzones.

<i>O. aspinata</i> shell thickness for Lyme Regis						<i>O. aspinata</i> shell thickness for St Audrie's Bay					
	N	Min	Max	Mean	Range		N	Min	Max	Mean	Range
LRB3	1	40.8	40.8	40.8		SAB8	24	12.6	50.1	24.3	37.5
LRB7	3	20.8	41.9	29.5	21.1	SAB11	22	12.7	43.5	33.4	30.8
LRB15	4	25.6	55.0	36.9	29.3	SAB17	3	25.0	44.1	31.7	19.0
LRB17	17	11.0	66.2	30.6	55.3	SAB26A	22	18.1	49.9	30.9	31.8
LRB21	22	16.2	48.8	31.7	32.6	SAB28	2	21.2	27.0	24.1	5.7
LRB23	19	15.7	53.2	35.4	37.4	SAB30A	21	11.3	47.8	22.1	36.6
LRB25	25	15.8	50.2	30.6	34.5	SAB34	20	9.8	29.4	19.3	19.6
LRB27	23	13.0	41.6	27.5	28.6	SAB40	23	14.3	50.3	32.2	36.0
LRB33	22	18.5	44.3	31.7	25.8	SAB42	23	14.2	44.2	28.1	29.9
LRB37	24	11.7	46.6	21.6	35.0	SAB44	3	30.9	45.8	36.1	14.9
LRB39	19	17.7	42.2	30.0	24.5	SAB52	25	8.3	31.0	19.5	22.7
LRB47	18	14.2	47.1	29.2	32.8	SAB60	22	10.4	38.6	24.2	28.1
LRB49	25	11.8	56.3	30.9	44.5	SAB62	22	13.0	36.8	22.0	23.9
LRB49A	20	14.7	61.2	33.2	46.5	SAB64	21	9.8	40.9	21.3	31.1
LRB51	25	10.3	44.1	25.1	33.8	SAB66	24	11.5	41.9	25.7	30.4
LRB51A	22	17.7	43.4	30.3	25.8	SAB68	24	10.7	57.0	27.0	46.3
LRB53	19	13.9	60.0	34.1	46.1	SAB70V.B	23	13.0	40.1	26.1	27.1
LRB55	24	11.9	43.5	27.6	31.6	SAB70V.T	24	12.2	43.9	27.6	31.7
LRB59	22	6.2	57.6	30.7	51.5	SAB74	24	15.9	50.1	31.0	34.2
LRB61	19	10.9	57.9	32.7	47.0	SAB76	25	13.3	57.4	26.8	44.1
LRB63	22	13.8	51.9	35.4	38.2	SAB80	25	19.1	46.3	30.3	27.2
LRB67	17	18.6	52.2	33.8	33.7	SAB82	25	10.7	46.3	29.5	35.6
LRB69	23	17.7	58.7	33.9	41.0	SAB84	23	13.8	51.0	33.6	37.3
LRB73	20	11.2	42.2	24.8	31.0	SAB86	23	15.7	59.5	32.5	43.8
LRB74A	23	13.4	52.8	27.3	39.4	SAB88	23	14.5	46.1	31.9	31.6
LRB75A	22	13.7	44.1	29.7	30.4	SAB90	23	14.9	50.9	27.7	36.1
LRB76A	14	14.5	48.1	28.8	33.6	SAB94	22	13.0	48.7	29.7	35.7
LRB77A	25	10.3	39.8	23.0	29.5	SAB96	23	11.7	43.4	26.8	31.7
LRB89	24	19.0	51.3	31.2	32.3	SAB98	24	11.8	36.6	21.1	24.8
LRB93	21	13.5	53.4	29.1	39.9						
LRB95	21	8.7	52.5	22.7	43.8						
LRB97	25	10.3	43.0	24.3	32.7						
LRB99	22	11.0	47.8	24.1	36.8						

Table 3.5: Summary of shell thickness data from Lyme Regis and St Audrie's Bay for *O. aspinata*. Lines represent the beds separated into subzones.

3.5.2 Relationships between the number of individuals measured and the minimum, maximum, mean and range of geometric sizes on each bed.

For each species there were a minimum number of individuals measured (bivalves: 20 and ostracods: 150) from each bed or sample. Some beds or samples did not yield enough individuals to meet the minimum desired threshold so in these cases as many as possible were measured. Since there is a wide variation in the number of individuals measured from each bed or sample, the minimum, maximum, mean and range of the geometric sizes of *L. hisingeri*, *P. gigantea* and *O. aspinata* may be influenced by the

number of individuals measured (Tables 3.2-3.5). The more individuals measured, the more likely outliers (extreme minimum or maximum sizes) will occur which will expand the range of geometric sizes (Tables 3.2-3.5). Regression analysis was performed to determine whether there were any significant relationships. Except those detailed in Table 3.6 and illustrated in Figure 3.6-3.9 there were no significant relationships identified.

Species	Location	Relationship	N	P	Figure
<i>P. gigantea</i>	Lyme Regis	Significant negative relationship between the minimum geometric size and number of individuals measured	26	<0.01	3.6 A
<i>P. gigantea</i>	Lyme Regis	Significant positive relationship between the range of geometric size and number of individuals measured	26	<0.05	3.6 B
<i>L. hisingeri</i> and <i>O. aspinata</i>	Lyme Regis/ St Audrie's Bay	Significant negative relationship between the minimum geometric size and number of individuals measured	37/ 20 30	<0.01/ 0.02.	3.7 A/D 3.8 A/D
<i>L. hisingeri</i> and <i>O. aspinata</i>	Lyme Regis/ St Audrie's Bay	Significant positive relationship between the range of geometric size and number of individuals measured	37/ 20 30	<0.01 <0.01	3.7 C/E 3.8 B/C
<i>L. hisingeri</i>	Lyme Regis	Significant positive relationship between the maximum geometric size and number of individuals measured.	37	<0.01	3.7 B
<i>O. aspinata</i>	St Audrie's Bay	Significant positive relationship between the maximum geometric size and number of individuals measured.	30	<0.01	3.8 E
<i>O. aspinata</i>	Lyme Regis/ St Audrie's Bay	Significant negative relationship between the minimum shell thickness and number of individuals measured	33/ 29	<0.01	3.9 A/D
<i>O. aspinata</i>	St Audrie's Bay	Significant positive relationship between the range of shell thickness and number of individuals measured	29	<0.01	3.9 C
<i>O. aspinata</i>	Lyme Regis	Significant negative relationship between the mean shell thickness and number of individuals measured	33	<0.01	3.9 B

Table 3.6: Summary of significant differences found between the numbers of individuals measured and the minimum, maximum mean and range of geometric sizes measured from each sample or bed.

Those regression models showing no significant relationships can be found in Appendix 4: Section A4.1.1, Tables A4.5-A4.8, Figure A4.1-A4.10 and Section 4.2.1, Tables A4.25-A4.27, Figure A4.13-A4.21. These results will identify where caution needs to be taken when identifying changes geometric size trends through the two sections. The geometric sizes from each bed were also grouped into zones and locations then the minimum, maximum, mean and the range of geometric sizes for each of these groupings was correlated against the total number of individuals measured throughout that zone or location (results in Appendix 4; Section A4.1.1 and Section A4.2.1).

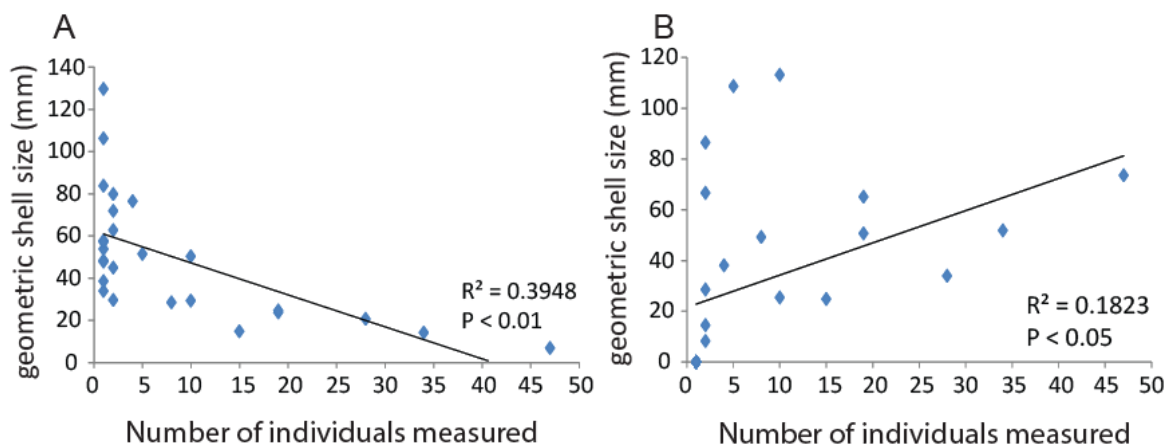


Figure 3.6: Linear regression models with trend lines showing Lyme Regis *P. gigantea* (A) minimum and (B) range of geometric sizes on each bed against the corresponding number of individuals measured in each bed (Appendix 4; Table A4.6 for statistical analysis results).

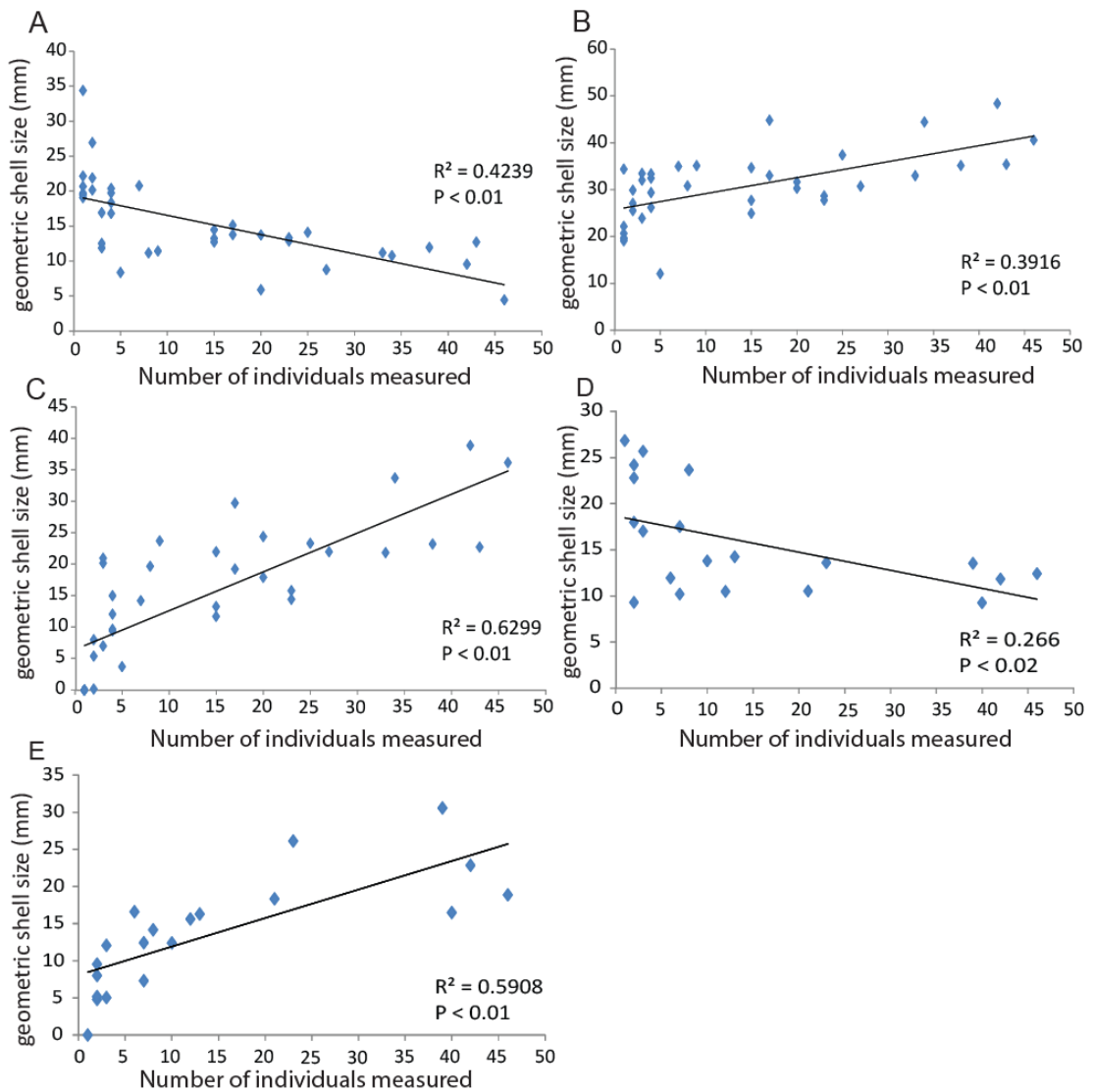


Figure 3.7: Linear regression models with trend lines showing *L. hisingeri* relationships between (A,D) minimum geometric shell size, (B) maximum geometric shell size, (C,E) range of geometric shell size and the number of individuals measured in each bed, (A-C) Lyme Regis (D-E) St Audrie's Bay (Appendix 4; Table A4.5 and A4.25 for statistical analysis results).

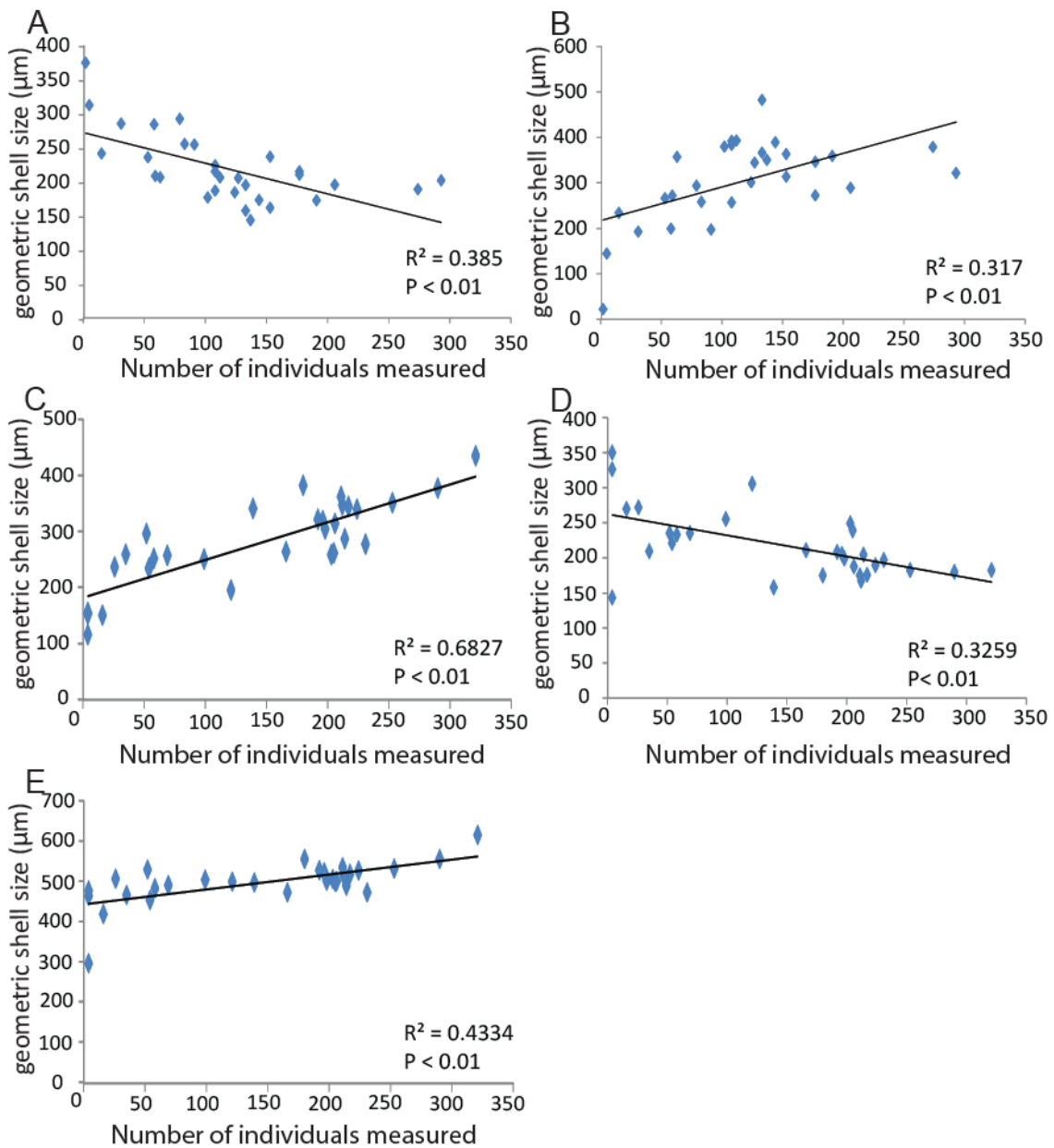


Figure 3.8: Linear regression models with trend lines showing *O. aspinata* relationships between geometric shell size and the number of individuals measured bed by bed, (A-B) Lyme Regis (C-E) St Audrie's Bay, (A/D) minimum geometric shell size, (B/C) range of geometric shell size, (E) maximum geometric shell size (Appendix 4; Table A4.7 and A4.26 for statistical analysis results).

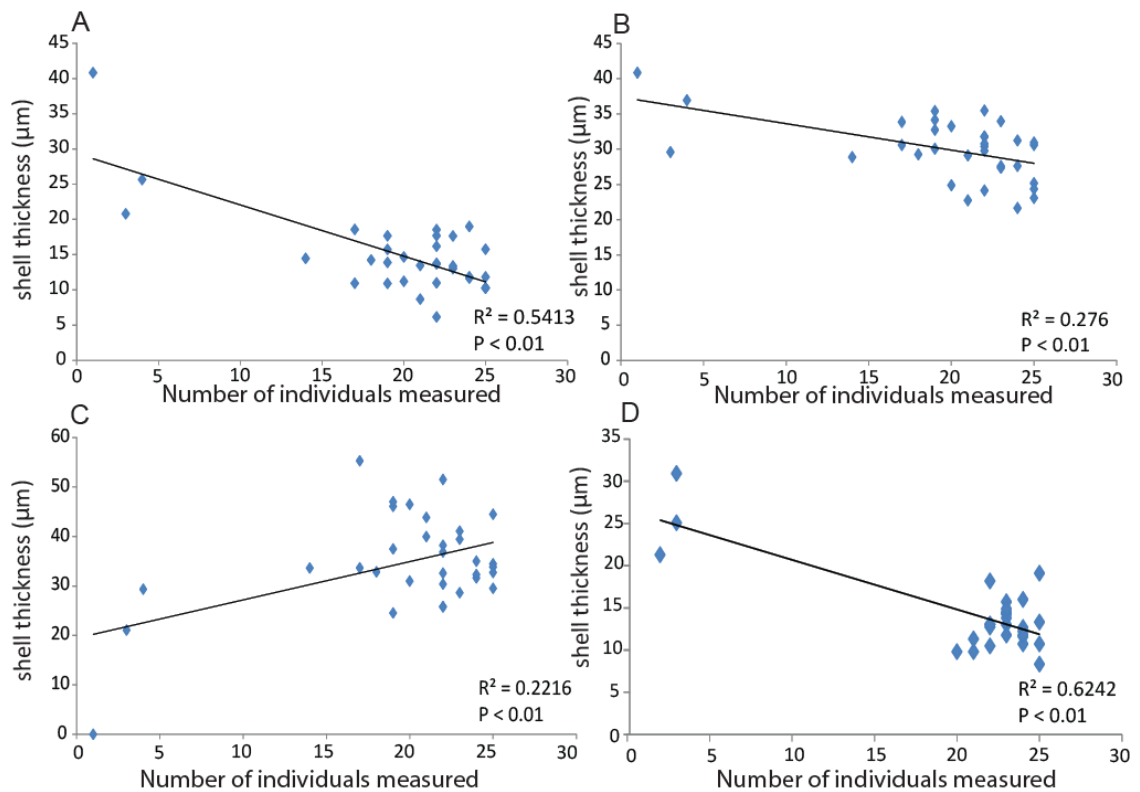


Figure 3.9: Linear regression models with trend lines showing *O. aspinata* relationships between (A/D) minimum shell thickness, (B) range of shell thicknesses, (C) mean shell thickness and the number of individuals measured bed by bed, (A-B) Lyme Regis (C-D) St Audrie's Bay (Appendix 4; Table A4.8 and A4.27 for statistical analysis results).

It is clear from this data that the minimum, maximum and range of geometric sizes measured are significantly affected by the number of individuals measured in most cases but the mean geometric size for each bed or sample is not as affected by how many individuals are measured. This is important because the mean, minimum and maximum size trends as well as the range of geometric sizes measured for *O. aspinata*, *L. hisingeri* and *P. gigantea* could be biased by the number of individuals measured which could affect any analysis trying to determine if these trends are significant. From the spread of data both the minimum and maximum numbers measured are identifying extreme outliers, with larger sizes found at both extremes for each species. The range of geometric size from each bed or sample for *L.*

hisingeri and *O. aspinata* clearly increases when more individuals are measured. This is the opposite for *P. gigantea* which found a wide range of sizes when fewer individuals were measured. For the minimum, maximum and range of geometric sizes measured this signifies that some of the data sets from various beds or samples will need to be removed from any analysis were a bed by bed approach is taken using the measurements as well as using the 95th percentile for these measurements to avoid any effect from extreme outliers (Table 3.7). The same applies to the *O. aspinata* shell thickness results but in this case for Lyme Regis only it includes the mean value (Table 3.7). It is important that the mean geometric size for each species shows no relationship to the number of individuals measured because that indicates that even those beds with very few individuals measured are still showing a common mean size to those beds with more individuals measured. For the mean geometric size this signifies that none of these data sets need to be omitted from later analysis because variations in the number of individuals measured have not caused any affected.

	Minimum and maximum number of individuals that need to be measured			
	Lyme Regis		St Audrie's Bay	
	Geometric shell size			
Species	Minimum	Maximum	Minimum	Maximum
<i>Liostrea</i>	5	17	3	N/A
<i>Plagiostoma</i>	15	2	N/A	N/A
<i>Ogmoconchella</i>	58	N/A	121	<139 / >290
	Shell thickness			
	Minimum	Mean	Minimum	
<i>Ogmoconchella</i>	14	14	20	N/A

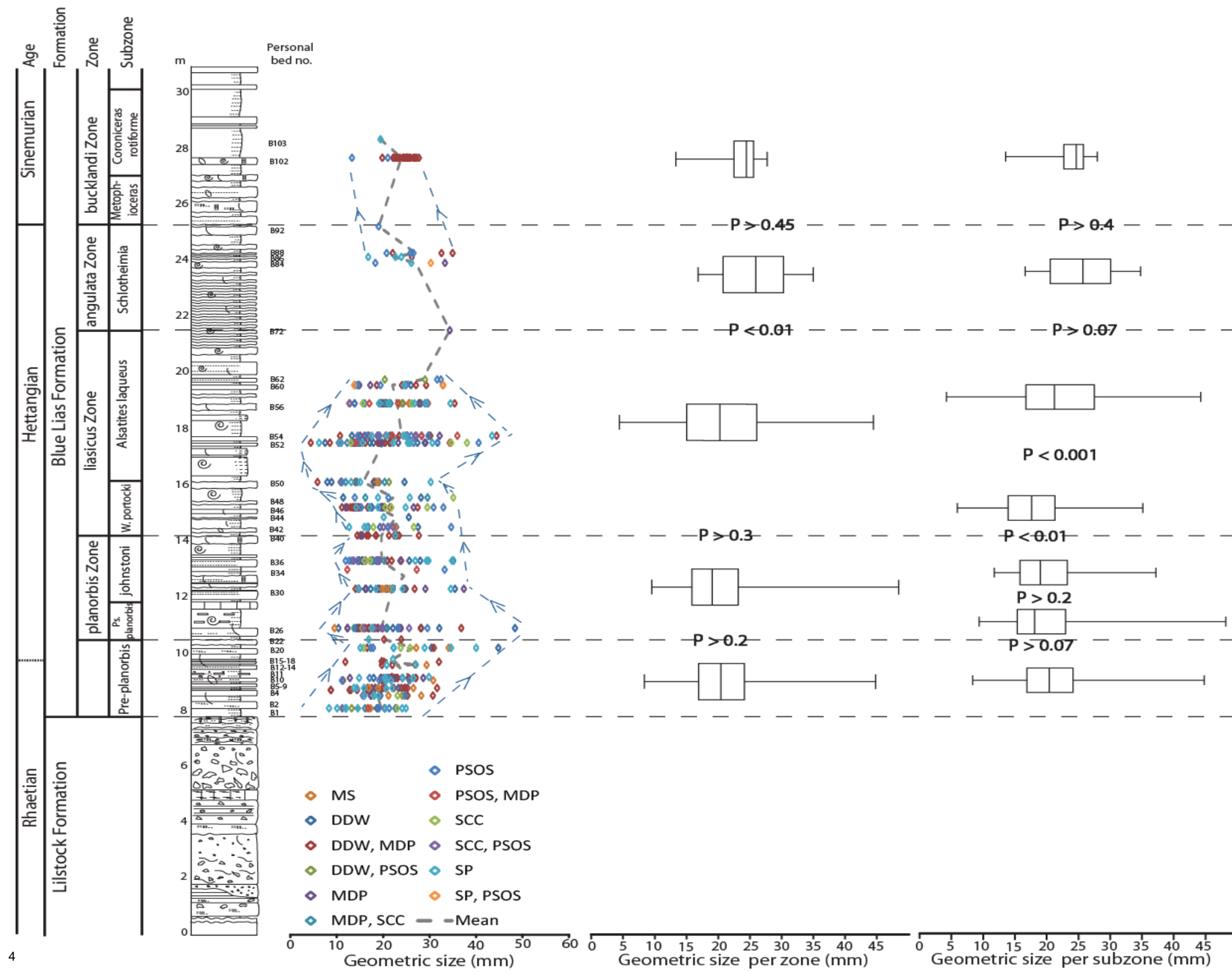
Table 3.7: Minimum number of individuals needed from each bed or sample to have no significant relationship to minimum, maximum and range of geometric sizes measured.

3.5.3 The size variations of *L. hisingeri*, *P. gigantea* and *O. aspinata* through the Lyme Regis and St Audrie's Bay sections

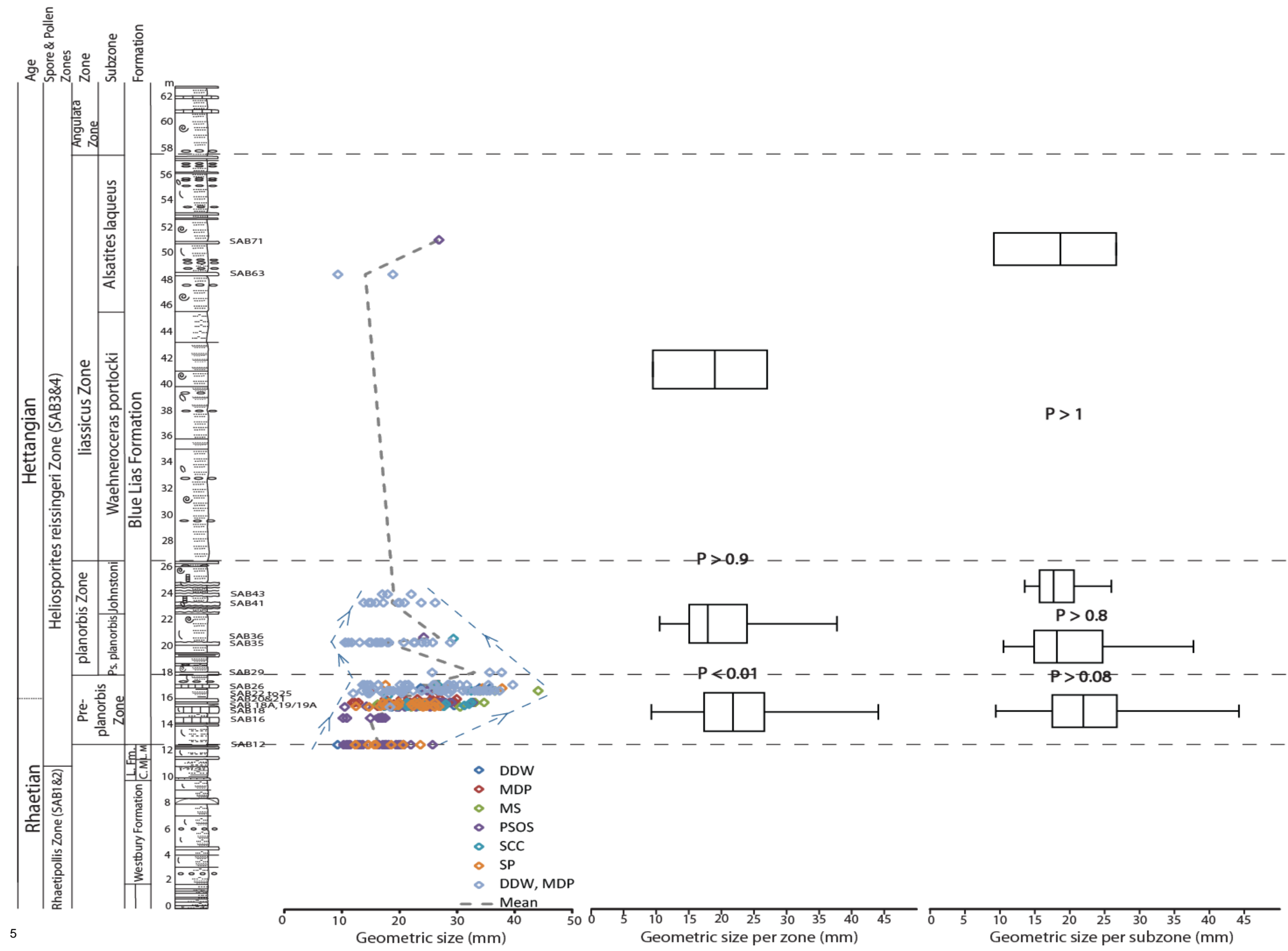
All of the geometric size and shell thickness data from both locations were used to produce box plots showing the range of geometric size and shell thickness data in each zone or subzone used in the statistical analysis (Tables 3.2-3.5 and Appendix 4: A4.1-A4.4 and A4.22-A4.24). There are several gaps in data collection as well as beds with low numbers of individuals throughout both sections which is due to some of the beds containing limited or no available specimens to measure. Except for the results and analysis detailed below in Sections 3.5.3–3.5.5 no significant difference was found between the geometric shell size or shell thickness measured from each bed through the section, from each bed within every zone as well as when comparing the geometric size and shell thickness data between zones and subzones and the various increasing and decreasing geometric shell size trends within the other zones.

3.5.4 *L. hisingeri*

The minimum, maximum and mean sizes vary throughout both sections. It is necessary to identify if these variations show an overall significant difference or were just disparities around a common mean (Figure 3.10-3.11). There was an overall significant difference in geometric shell size between the different beds from both Lyme Regis ($P < 0.001$) and St Audrie's Bay ($P < 0.001$). This was determined through the Kruskal-Wallis test and indicated that the observed trends were not representative of random outliers resulting from the sampling method.



⁴Figure 3.10: The geometric shell sizes of *L. hisingeri* measured on each bed at Lyme Regis and collated into zones and subzones (Data in Appendix 4: Table A4.1). Blue arrows placed by eye to highlight the increasing and decreasing size trends between the various beds. See Table 3.1 for preservation descriptions relating to the codes in the key above. P values represent any statistical difference between the compiled data from one zone or subzone and the following zone or subzone.



⁵Figure 3.11: The geometric shell sizes of *L. hisingeri* measured on each bed at St Audrie's Bay and collated into zones and subzones (Data in Appendix 4: Table A4.22). Blue arrows placed by eye to highlight the increasing and decreasing size trends between the various beds. See Table 3.1 for preservation descriptions relating to the codes in the key above. P values represent any statistical difference between the compiled data from one zone or subzone and the following zone or subzone.

There was an overall significant difference between the geometric sizes at the zone and subzone level at Lyme Regis ($P < 0.001$) but only zone level at St Audrie's Bay ($P < 0.05$) (Figure 3.10-3.11, Appendix 4: Table A4.10-A4.11 and A4.29-A4.30). All the individual zones at Lyme Regis show significantly ($P < 0.05$) larger geometric shell sizes to the *angulata* Zone and *bucklandi* Zone only (Figure 3.10). However, some caution needs to be taken with this result as the number of individuals measured in each zone does show a significant relationship ($P < 0.05$) to the minimum and range of geometric sizes but not to the mean or maximum geometric shell size (Appendix 4: Figure A4.5). The individual subzones at Lyme Regis show that the geometric shell sizes within the Pre-planorbis Beds, *Ps. planorbis*, *johnstoni* and *W. portlocki* subzones are both significantly bigger and smaller ($P < 0.05$) than the geometric shell sizes within the *W. portlocki*, *Alsatites laqueus*, *Schlotheimia* and *Coroniceras rotiforme* subzones (Figure 3.10). The geometric shell sizes measured within the individual zones and subzones at St Audrie's Bay were not affected by any variation in the number of individuals measured and show that the sizes within the Pre-planorbis Beds are significantly larger than those in the *planorbis* Zone and the *johnstoni* subzone ($P < 0.05$). This indicates that the decrease in size observed after the Pre-planorbis Beds is significant (Figure 3.11, Appendix 4: Table A4.29-A4.30).

To know if the increasing and decreasing trends in geometric size from both locations are significant, the geometric sizes from each bed (within each zone) were compared against each other (Figure 3.10-3.11, Appendix 4, Table A4.9A-E and A4.28A-C). The geometric sizes from one bed were

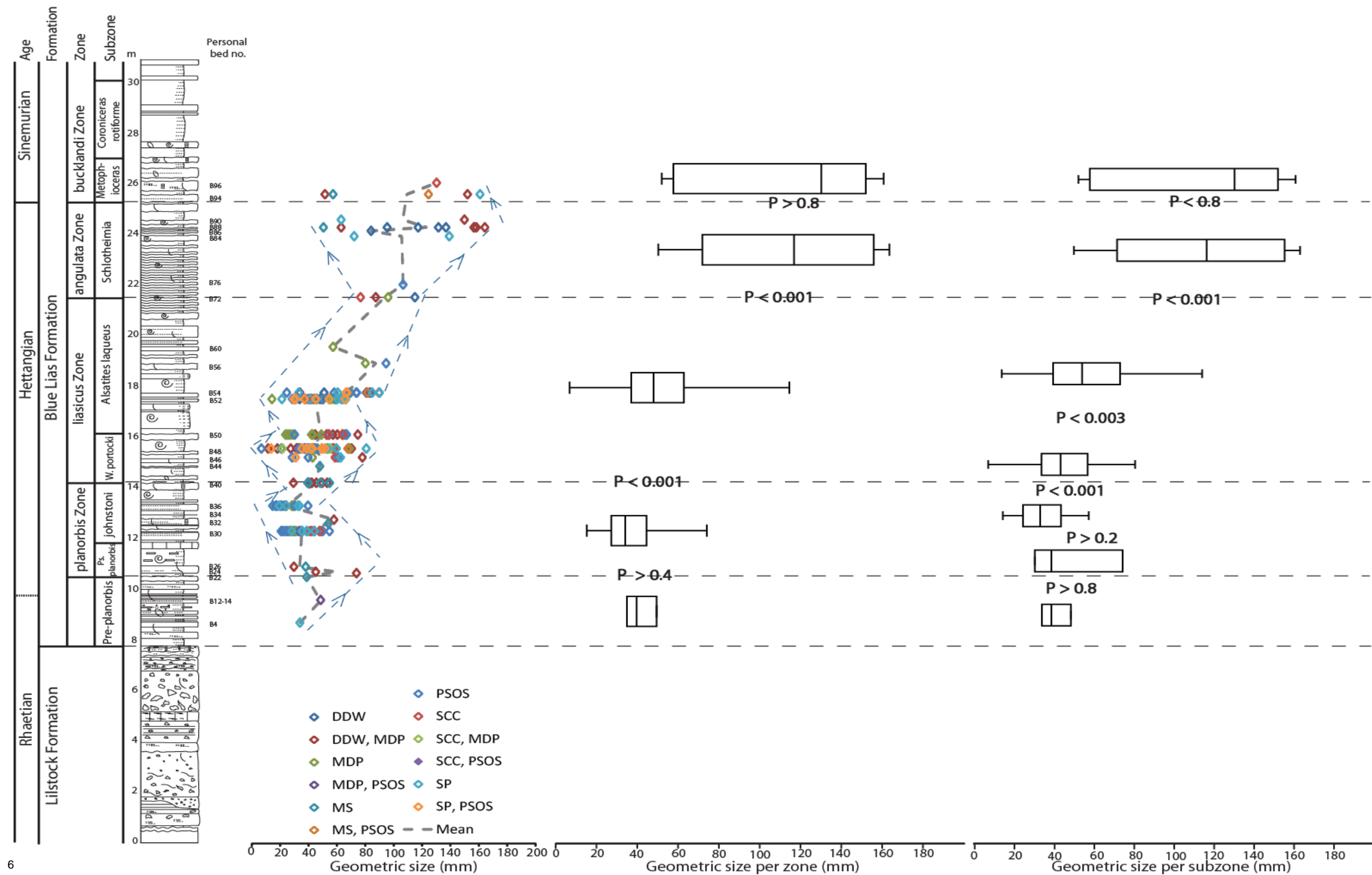
compared to the geometric sizes from the bed stratigraphically next to it (e.g., bed SAB20–SAB21/LRBL10–LRBL11). In many of these cases, but not all, any change in size seen visually between adjacent beds in the graph is actually shown to be not significant (Appendix 4, Table A4.9A-E and A4.28A-C). The observed change in size is most likely to be caused by outliers in the data set rather than a real change in size. The increasing geometric size trend in the Pre-planorbis Beds between bed 2 and bed 22 at Lyme Regis and between bed 12 and bed 26 at St Audrie's Bay was significant ($P < 0.001$) and was not due to the variation in the number of individuals measured. Many of the other beds within the Pre-planorbis Beds at both locations also show a significant difference to each other (Appendix 4, Table A4.9A and A4.28A). Through the St Audrie's Bay planorbis Zone the observed decreasing geometric shell size trend through the beds is not significant. The geometric shell sizes from various beds within the Lyme Regis liasicus Zone show a significant difference to each other ($P < 0.01$). Both increasing and decreasing trends were observed through this zone and while some were significant (e.g, between bed 52 and bed 56 ($P < 0.05$); bed 50 and bed 54 ($P < 0.001$)) others were insignificant (e.g, between bed 54 and bed 56; Appendix 4, Table A4.9C).

3.5.5 *P. gigantea*

St Audrie's Bay has no data analysis for *P. gigantea* due to low numbers of specimens being present and as such was not present in enough quantity to give an accurate representation of size through the section. The minimum, maximum and mean sizes vary throughout Lyme Regis (Figure 3.12). There

was an overall significant difference in geometric shell size between the different beds from Lyme Regis ($P < 0.001$). This was determined through the Kruskal-Wallis test and indicated that the observed trends were not just random outliers resulting from the sampling method. There was an overall significant difference between the geometric sizes at the zone and subzone level ($P < 0.001$) showing the increasing trends in geometric size are significant (Figure 3.12; Appendix 4: Table A4.13-A4.14). The majority of the different zones are significantly different to the other zones and was not due to the variation in the number of individuals measured. The planorbis Zone was significantly smaller than the liasicus Zone ($P < 0.001$) and the zones above, while the liasicus Zone is significantly smaller than the angulata Zone ($P < 0.001$) and the zones above (Figure 3.12, Appendix 4: Table A4.13).

To see if the increasing and decreasing trends in geometric size are significant, the geometric sizes from each bed (within each zone) were compared against each other (Figure 3.12, Appendix 4, Table A4.12A-D). The geometric sizes from one bed were compared to the geometric sizes from the bed stratigraphically next to it (e.g., bed LRBL30–LRBL32/LRBL50–LRBL52). In all but two of these cases (LRBL36–LRBL40/LRBL52–LRBL54), any change in size seen visually between beds next to each other in the graph is actually shown to be not significant (Appendix 4, Table A4.12A-D). The observed change in size is most likely to be caused by outliers in the data set rather than a real change in size.



⁶Figure 3.12: The geometric shell sizes of *P. gigantea* measured on each bed at Lyme Regis and collated into zones and subzones (Data in Appendix 4: Table A4.2). Blue arrows placed by eye to highlight the increasing and decreasing size trends between the various beds. See Table 3.1 for preservation descriptions relating to the codes in the key above. P values represent any statistical difference between the compiled data from one zone or subzone and the following zone or subzone.

In the planorbis Zone the decreasing geometric shell size trend between bed 30 and bed 36 ($P < 0.001$) and the increasing geometric shell size trend between bed 36 and bed 40 ($P < 0.005$) was significant and not due to the variation in the number of individuals measured (Appendix 4, Table A4.12A). The geometric shell sizes from various beds within the liasicus Zone show a significant difference to each other ($P < 0.01$). Both increasing and decreasing trends were observed through this zone and while some were significant (e.g, between bed 50 and bed 54; $P < 0.002$) others were insignificant (e.g, between bed 48 and bed 52) (Appendix 4, Table A4.12B). Upwards through the section (bed 30 through to bed 88) the geometric shell size shows an overall significant ($P < 0.001$) increase in its maximum shell size (Figure 3.12). The first (beds 4-26) and top (beds 90-96) most beds contain very few individuals and were removed from this analysis because the number of individuals measured would affect the results.

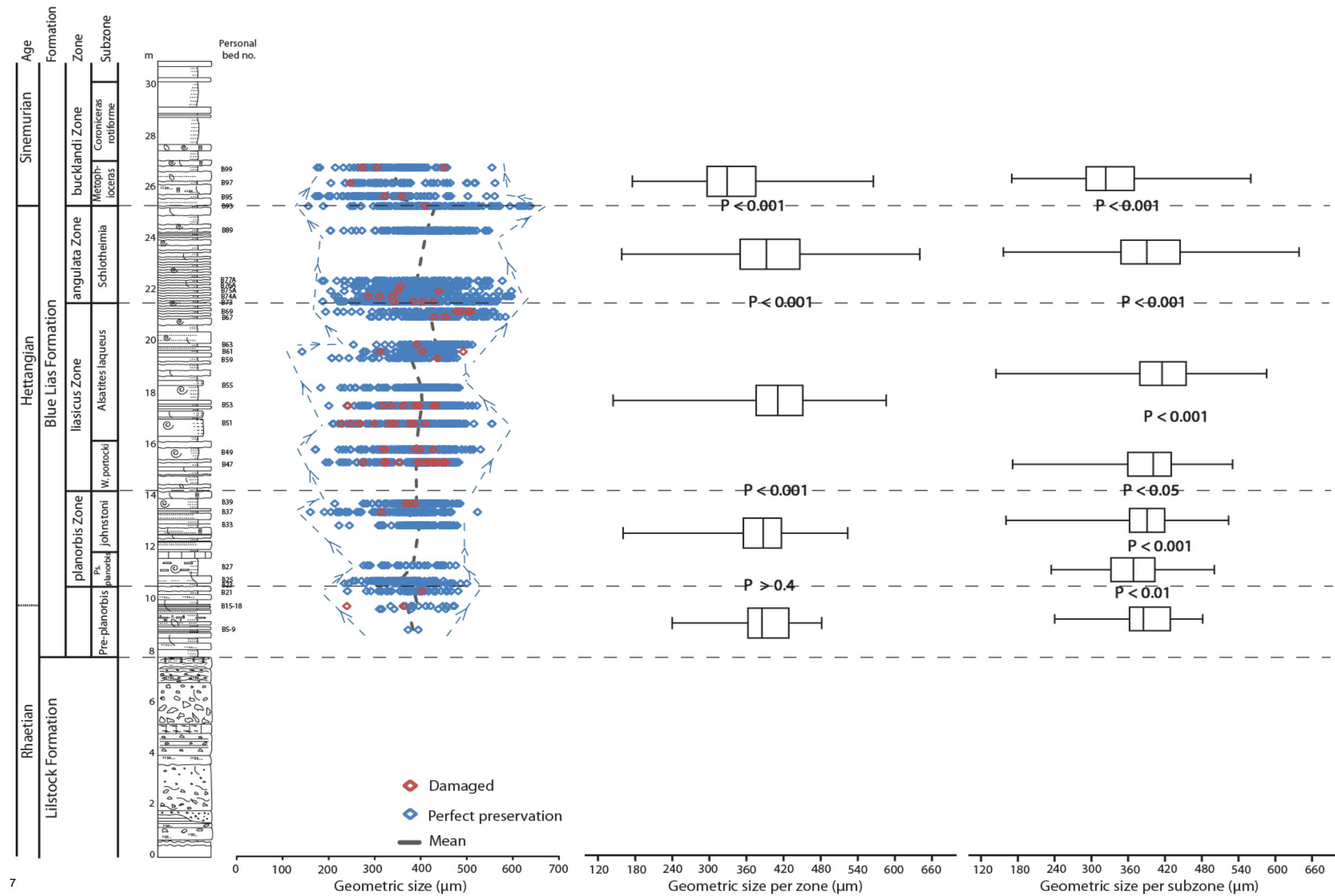
3.5.6 *O. aspinata*

The minimum, maximum and mean sizes vary throughout both sections (Figure 3.13-3.14). There was an overall significant difference in geometric shell size between the different beds from Lyme Regis and St Audrie's Bay ($P < 0.001$) which indicated that the observed trends were not just random outliers resulting from the sampling method. There was an overall significant difference between the geometric sizes at the zone and subzone level at Lyme Regis ($P < 0.001$) and at St Audrie's Bay ($P < 0.001$) (Figure 3.13-3.14, Appendix 4: Table A4.16-A4.17, A4.32-A4.33). The majority of the different zones and subzones at both locations have significantly different geometric

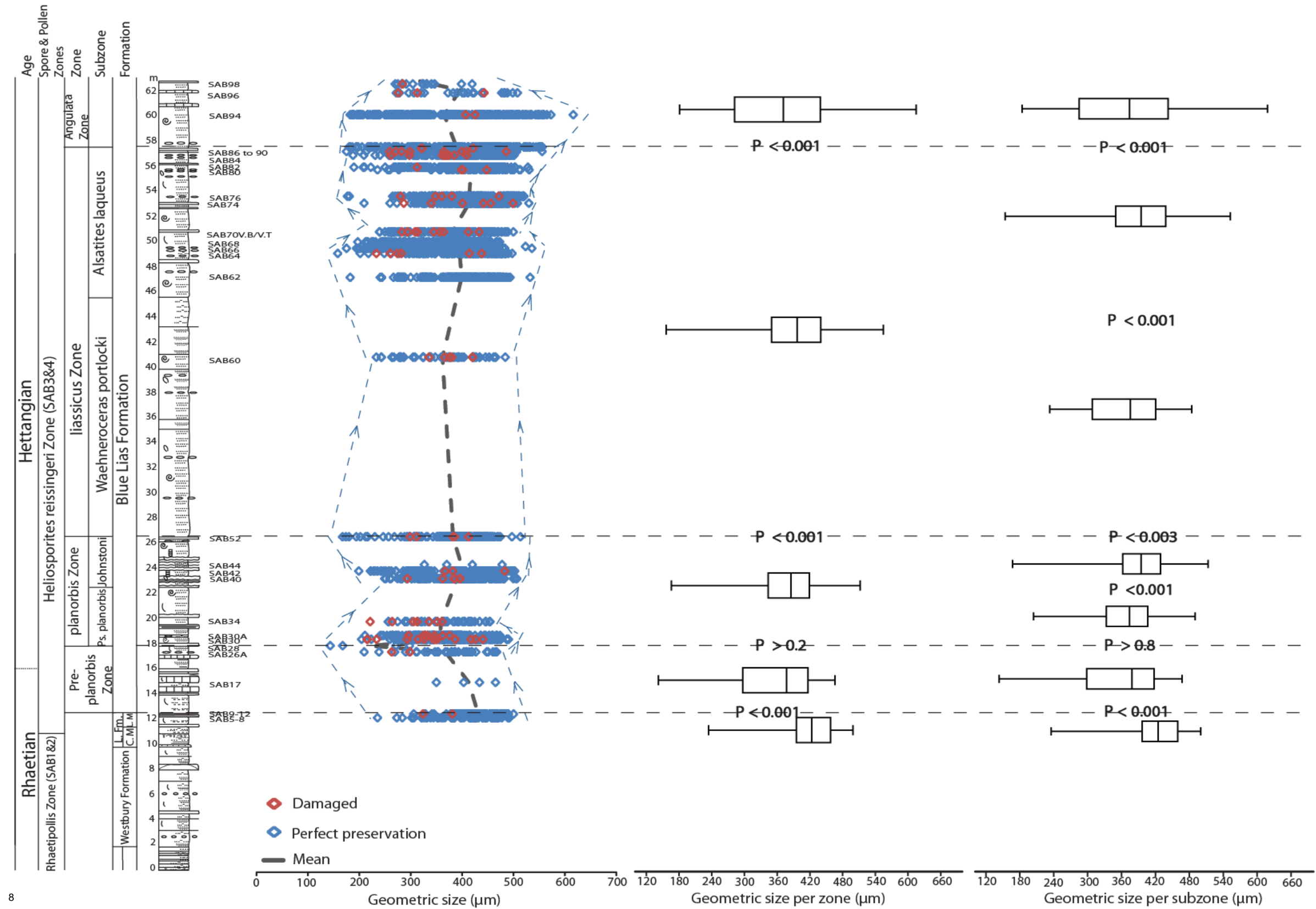
shell sizes to the other zones and was not due to the variation in the number of individuals measured (Figure 3.13-3.14, Appendix 4: Table A4.16-A4.17, A4.32-A4.33, Figure A4.7 and A4.17).

The detailed bed by bed geometric shell size variations could be an indication that certain sampled beds were missing the smallest or largest carapaces when compared to the next sampled bed (e.g., Lyme Regis; beds 89, 93 and 95, St Audrie's Bay; beds 88 and 90; Figure 3.13-3.14, 3.15A-B). The Lyme Regis bed 93 shows a higher abundance of significantly larger sizes and is missing the smaller sizes seen in bed 95 (Figure 15A). The St Audrie's Bay bed 90 shows a higher abundance of significantly smaller and larger sizes than bed 88 (Figure 15B).

To know if the increasing and decreasing trends in geometric size are significant from both localities the geometric sizes from each bed (within each zone) were compared against each other (Figure 3.13-3.14, Appendix 4, Table A4.15A-E, A4.31A-E). The geometric sizes from one bed were compared to the geometric sizes from the adjacent bed stratigraphically next to it (e.g., bed SAB74–SAB76/LRBL15–LRBL17). In a proportion of these cases, but in no way all, any change in size seen visually between beds next to each other in the graph is actually shown to be not significant (Appendix 4, Table A4.15A-E, A4.31A-E). The observed change in size is most likely to be caused by outliers in the data set rather than a real change in size. However, the data from many of the beds in the liasicus Zone specifically show the stratigraphic bed-to-bed changes in geometric size are significant (Appendix 4, Table A4.15D, A4.31D).



⁷Figure 3.13: The geometric shell sizes of *Ogmococonchella aspinata* measured on each bed at Lyme Regis and collated into zones and subzones (Data in Appendix 4: Table A4.3A-E). Blue arrows placed by eye to highlight the increasing and decreasing size trends between the various beds. P values represent any statistical difference between the compiled data from one zone or subzone and the following zone or subzone.



⁸ Figure 3.14: The geometric shell sizes of *Ogmococonchella aspinata* measured on each bed at St Audrie's Bay and collated into zones and subzones (Data in Appendix 4: Table A4.23A-C). Blue arrows placed by eye to highlight the increasing and decreasing size trends between the various beds. P values represent any statistical difference between the compiled data from one zone or subzone and the following zone or subzone.

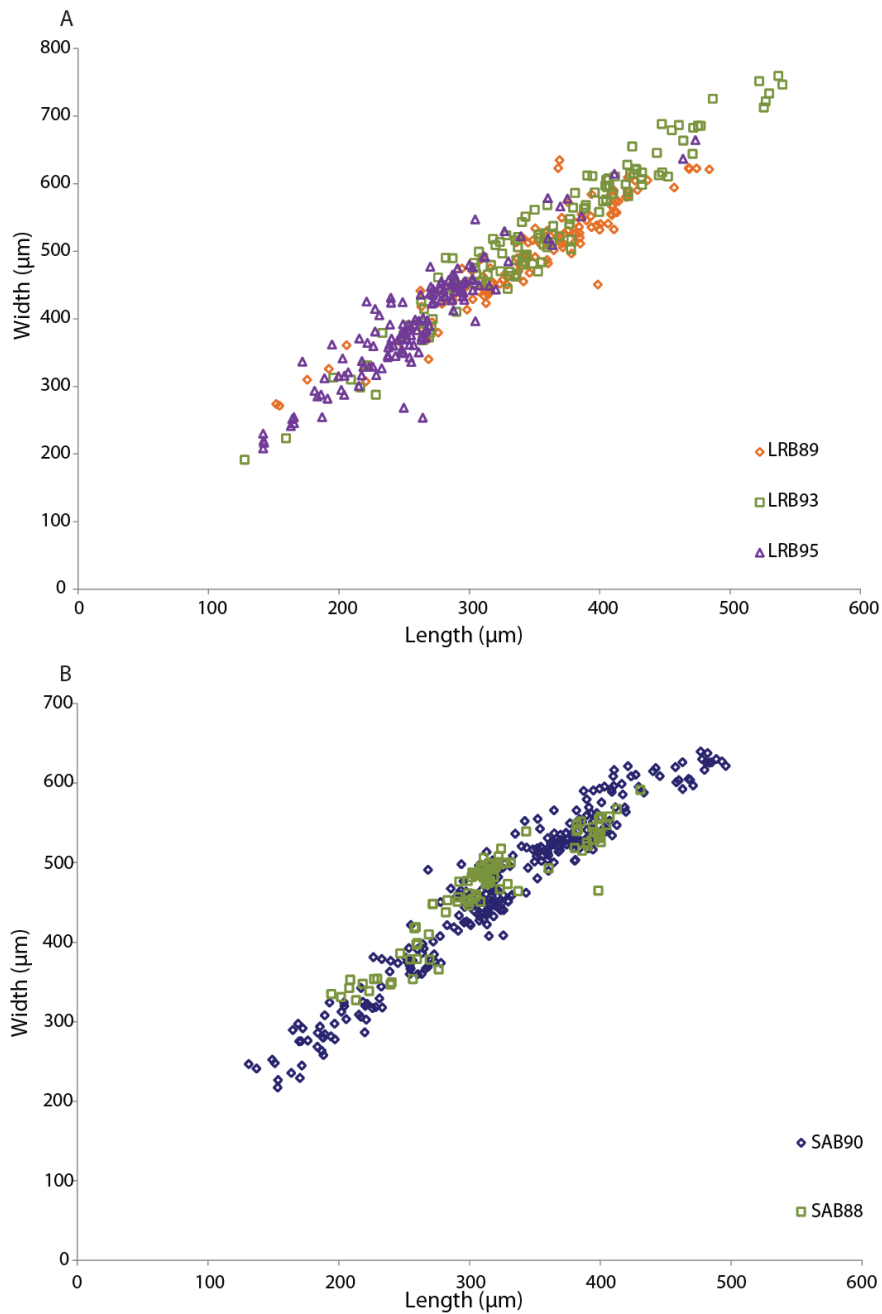


Figure 3.15: Relationships between *O. aspinata* length against width from (A) Lyme Regis, (B) St Audrie's Bay showing variations in the range of carapace sizes found and measured in each bed. These beds were chosen because they show a significantly different range of sizes to the following sampled bed above it.

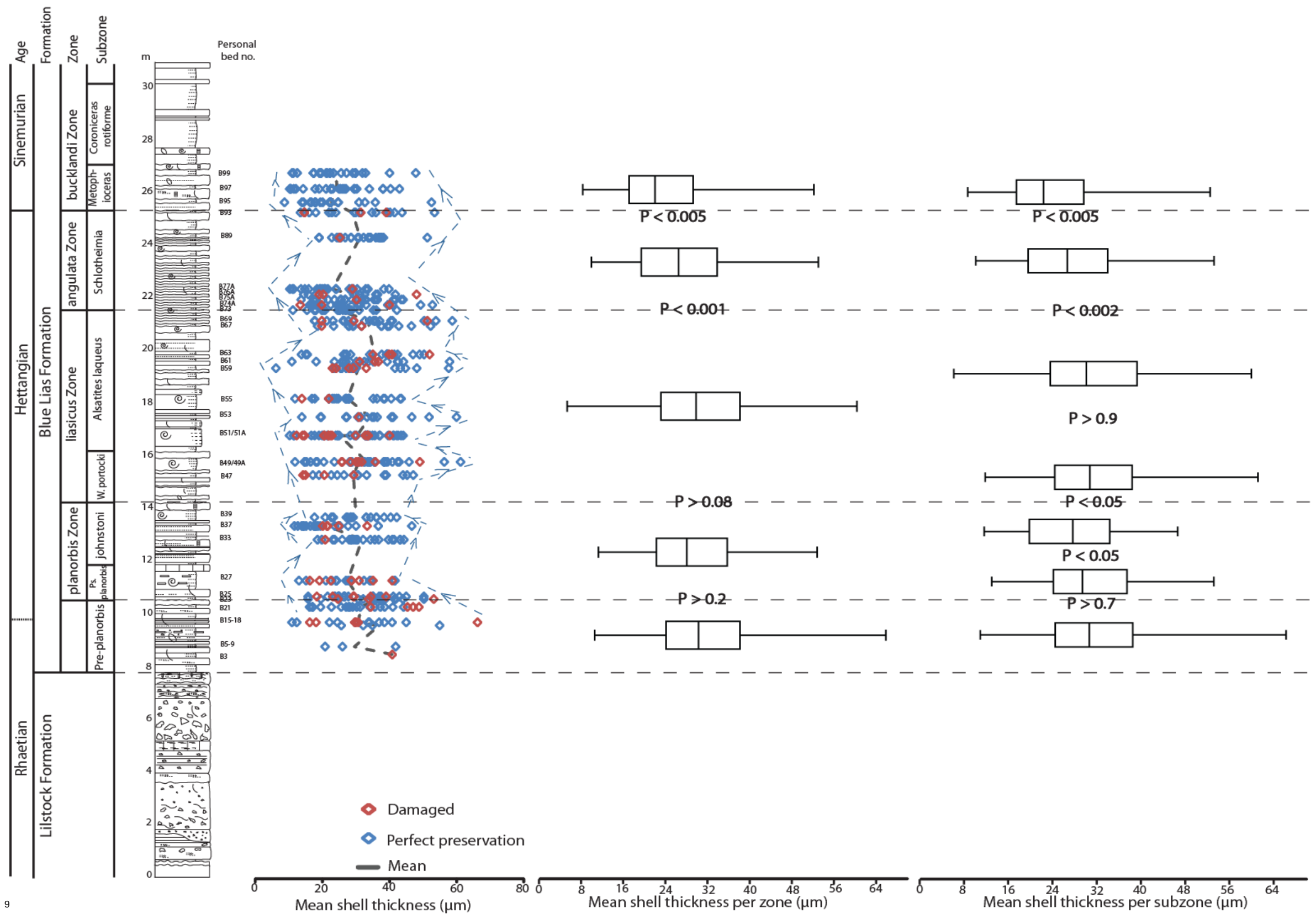
The Lilstock Formation and Pre-planorbis Beds in St Audrie's Bay both show an overall significant difference between the beds geometric shell sizes ($P < 0.001$), as well as a significant increasing geometric shell size trend between bed 8 and bed 11 ($P < 0.001$; Appendix 4, Table A4.31A) and a significant

decreasing geometric shell size trend between bed 17 and bed 28 ($P < 0.05$; Appendix 4, Table A4.31B).

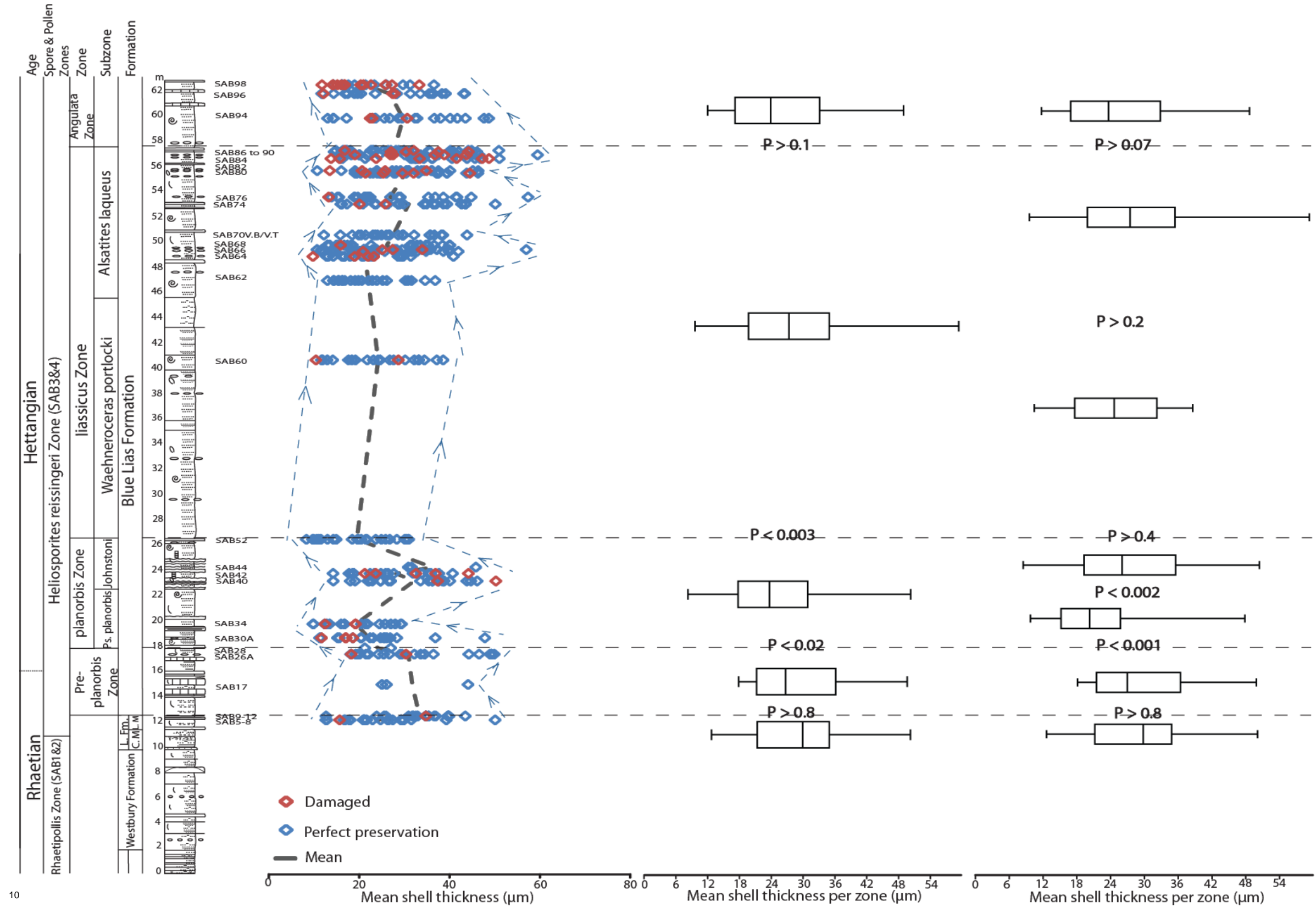
The planorbis Zone in Lyme Regis and St Audrie's Bay show an overall significant difference ($P < 0.001$) in geometric shell size from each bed. The increasing trend between beds 37-39 at Lyme Regis is significant ($P < 0.01$) but the decreasing trend between beds 27-37 is not significant. Whereas both increasing (beds 30-40) and decreasing (beds 40-52) trends at St Audrie's Bay are not significant. The significant trends are not shown to be affected by the variation in the number of individuals measured. The liasicus Zone in Lyme Regis and St Audrie's Bay show an overall significant difference ($P < 0.001$) in geometric shell size from each bed. The increasing trend (beds 47-51) and decreasing trend (beds 51-55) at Lyme Regis are not significant but the increasing trend between beds 59-67 is significant ($P < 0.001$). Whereas the increasing (beds 60-62, 70-76, 80-90) trends at St Audrie's Bay are significant ($P < 0.05$; Appendix 4, Table A4.15A-E, A4.31A-E). The angulata Zone in Lyme Regis and St Audrie's Bay show an overall significant difference ($P < 0.001$ and $P < 0.05$ respectively) in geometric shell size from each bed. The increasing trend between beds 89-93 at Lyme Regis is not significant but the decreasing trend between beds 73-89 is significant ($P < 0.02$). Whereas the decreasing trend between beds 94-98 at St Audrie's Bay is not significant but the decreasing trend between beds 96-98 is significant ($P < 0.005$; Appendix 4, Table A4.15A-E, A4.31A-E). The bucklandi Zone in Lyme Regis shows an overall significant difference ($P < 0.05$) in geometric shell size from each bed. The decreasing trend between

beds 95-99 at Lyme Regis is significant ($P < 0.01$; Appendix 4, Table A4.15A-E).

The minimum, maximum and mean shell thicknesses vary throughout both sections (Figure 3.16-3.17). There was an overall significant difference in shell thickness between the different beds from Lyme Regis and St Audrie's Bay ($P < 0.001$) which indicated that the observed trends were not just random outliers resulting from the sampling method. There was an overall significant difference between the geometric sizes at the zone and subzone level at Lyme Regis ($P < 0.001$) and at St Audrie's Bay ($P < 0.01$) (Figure 3.16-3.17). The various zones from Lyme Regis show a significant difference only to both the *angulata* Zone and the *bucklandi* Zone ($P < 0.05$; Figure 3.16, Appendix 4: Table A4.19). The various zones from St Audrie's Bay show a significant difference to the *planorbis* Zone ($P < 0.05$) and the *planorbis* Zone shows a significant difference ($P < 0.005$) to the *liasicus* zone (Figure 3.16-3.17, Appendix 4: Table A4.35). The *Ps. planorbis*, *johnstoni*, *Alsatites laqueus* and *Schlotheimia* subzones from Lyme Regis show a significant difference ($P < 0.05$) to the subzones stratigraphically above them indicating the increasing and decreasing trends between these zones are significant (Figure 3.16, Appendix 4: Table A4.20). The various subzones from St Audrie's Bay show a significant difference to the *Ps. planorbis* subzone ($P < 0.005$) and the *Ps. planorbis* subzone shows a significant difference ($P < 0.002$) to the *johnstoni* subzone (Figure 3.17, Appendix 4: Table A4.36). These significant variations were found to not be effected by the number of individuals measured (Appendix 4: Figures A4.10 and A4.20).



⁹Figure 3.16: The mean shell thickness of *Ogmococonchella aspinata* measured on each bed at Lyme Regis and collated into zones and subzones (Data in Appendix 4: Table A4.4A-C). Blue arrows placed by eye to highlight the increasing and decreasing size trends between the various beds. P values represent any statistical difference between the compiled data from one zone or subzone and the following zone or subzone.



¹⁰Figure 3.17: The mean shell thickness of *Ogmococonchella aspinata* measured on each bed at St Audrie's Bay and collated into zones and subzones (Data in Appendix 4: Table A4.24A-B). Blue arrows placed by eye to highlight the increasing and decreasing size trends between the various beds. P values represent any statistical difference between the compiled data from one zone or subzone and the following zone or subzone.

To know if the increasing and decreasing trends in shell thickness are significant from both localities the shell thickness from each bed (within each zone) were compared against each other (Figures 3.16-3.17, Appendix 4, Tables A4.18A-E and A4.34A-E). The shell thicknesses from one bed were compared to the shell thicknesses from the bed stratigraphically next to it (e.g., bed SAB80–SAB82/LRBL75A–LRBL76A). In most of these cases, but not all, any change in thickness seen visually between beds next to each other in the graph is actually shown to be not significant (Appendix 4, Tables A4.18A-E and A4.34A-E). The observed change in thickness is most likely to be caused by outliers or by variations in the number of individuals measured than a real change in thickness. The Lyme Regis and St Audrie's Bay planorbis Zone show an overall significant difference between the beds shell thickness ($P < 0.001$). However, the increasing and decreasing shell thickness trends throughout the Lyme Regis planorbis Zone (beds 23-27 and 27-37) and the decreasing shell thickness trend (bed 30-34) at St Audrie's Bay are not significant, whereas the increasing (bed 34-40) and decreasing (bed 40-52) shell thickness trends in St Audrie's Bay planorbis Zone are significant ($P < 0.001$) (Appendix 4, Tables A4.18B and A4.34C). These significant variations were found to not be effected by the number of individuals measured (Appendix 4, Table A4.21A-B).

The liasicus Zone at St Audrie's Bay shows an overall significant difference between the beds shell thicknesses ($P < 0.001$). From the observed increasing and decreasing trends through this zone at St Audrie's Bay only the decreasing trend between beds 76-84 is significant ($P < 0.05$; Appendix 4, Table A4.34D). From the observed increasing and decreasing trends through

this zone at Lyme Regis only the decreasing trends between beds 49A-51 and 53-55 and the increasing trend between beds 51-53 are significant ($P < 0.05$). The angulata Zone at Lyme Regis and St Audrie's Bay show an overall significant difference between the beds shell thickness ($P < 0.05$). However, the increasing and decreasing shell thickness trends throughout the angulata Zone at Lyme Regis (beds 73-77A and 77A-93) are not significant, whereas the increasing trend (bed 77A-89; $P < 0.01$) at Lyme Regis and the decreasing trend (bed 94-98; $P < 0.002$) at St Audrie's Bay are significant (Appendix 4, Table A4.34E).

3.6 What do the *L. hisingeri*, *P. gigantea* and *O. aspinata* size changes identified at both locations indicate?

At both locations *L. hisingeri* geometric shell size did significantly increase through the Pre-planorbis Beds but decreased through the planorbis Zone (Figures 3.10-3.11). *P. gigantea* geometric shell size significantly increased through time at Lyme Regis (Figure 3.12). There is a clear decreasing size trend through the planorbis Zone until the liasicus Zone which shows the main commencement of increasing size which continues until the upper angulata Zone where size reduced, although this reduction could be due to the limited number of individuals available to be measured (Figure 3.12). The increased *L. hisingeri* size through the Pre-planorbis Beds and the subsequent return to previously recorded smaller sizes and *P. gigantea*'s initial decrease during the planorbis Zone before increasing in size from the liasicus Zone onwards has also been seen in other studies at various locations (Hallam, 2002; Hautmann, 2004; Mander *et al.*, 2008; Opazo, 2012).

Mander *et al.* (2008) indicated this increase in size was a short-term peak within an overarching period where bivalve size was influenced by the Lilliput effect. However, Mander *et al.* (2008) study grouped all the different bivalve species together unlike this study and it is thought their short-term peak was due to the abundance of *Liostrrea* through those few specific beds at St Audrie's Bay. The Lilliput effect describes dwarfed or stunted taxa from the aftermath of an extinction event (Urbanek, 1993) and for the *L. hisingeri* species the majority of the size data from this study does show reduced sizes except for the main significant size increase through the Pre-planorbis Beds. The *P. gigantea* size data also shows reduced sizes after the extinction event however the overall size is slowly increasing back to the larger sizes as you move up the section which is different to the *L. hisingeri* species. However, *O. aspinata* showed various significant changes throughout both sections and variations include both increasing and decreasing geometric size trends which alternate up the section while shell thickness was maintained through the section with only a few variations (Figures 3.13-3.14, 3.16-3.17). These constant variations do not indicate the Lilliput effect as there is limited reduced size or stunting of individuals, which is not persistent and where reduced size or stunting is identified it is between periods of size increasing. However, other fossils including many soft-bodied species from the Tr-J interval have also shown reduced size which only recovered to larger sizes after the beginning of the angulata Zone much like the *L. hisingeri* species in this study (Barras and Twitchett, 2007).

The variations in the geometric shell size of *L. hisingeri* and *P. gigantea* and the carapace size and thickness of *O. aspinata* observed between adjacent

beds could be caused by a variety of factors that changed the environmental conditions from optimal to less than optimal. These factors include changes in sea level, seawater aragonite and calcite undersaturation, anoxia, salinity, reduced food supply, seawater pH and seawater temperature (Hallam, 1997, 2002; Hallam and Wignall, 1999; McElwain *et al.*, 1999; Radley, 2002; Hautmann, 2004; Berge *et al.*, 2006; van de Schootbrugge *et al.*, 2007; Mander *et al.*, 2008). Changes in seawater pH and seawater temperature caused by increased $p\text{CO}_2$ from the CAMP eruptions are reportedly global signatures (e.g., McElwain *et al.*, 1999; van de Schootbrugge *et al.*, 2007; Schaller *et al.*, 2011). It is these two “global signals” (changes in $p\text{CO}_2$ caused by the CAMP eruptions and palaeotemperature), that this study is attempting to identify over any changes caused by other, localised, environmental factors. This will be discussed in Chapter 4 by the identification of any significant relationships between the changes in $p\text{CO}_2$ or palaeotemperature and the shell/carapace size or thickness of *L. hisingeri*, *P. gigantea* and *O. aspinata* studied at these locations. However, it is worth mentioning some of these other local environmental factors.

Patzkowsky and Holland (2012) discussed how shell size or thickness could be affected by changes in facies between adjacent beds. The shell or carapace size and thickness of *L. hisingeri*, *P. gigantea* and *O. aspinata* species from this study also appear to fluctuate between various adjacent beds although, in most cases, these fluctuations are not significant (Figures 3.10-3.14, 3.16-3.17). Only some of the overall size trends within a zone or subzone identified in Figures 3.10-3.14, 3.16-3.17 are significant (e.g., for *L. hisingeri*: Pre-planorbis Beds between bed 2 and bed 22 at Lyme Regis and

between bed 12 and bed 26 at St Audrie's Bay ($P < .001$); Section 3.5.3 onwards gives further detail). This is not unexpected for *L. hisingeri* and *P. gigantea* as these species are known to be fairly tolerant of short term environmental change and conditions could not have passed the point of 'no return' because the species are still present. However, the changes in *O. aspinata* carapace size identified between adjacent beds show a mixture of significant and non-significant changes. This could indicate that changes in facies between adjacent beds are affecting carapace size. There are several issues with this interpretation: (1) ostracods are easily transported in the sediment and swept up by sediment eating organisms (Athersuch *et al.*, 1989); (2) ostracod abundance is also subject to seasonal variations (Athersuch *et al.*, 1989); and (3) each rock sample that ostracods were collected from probably covers < 1000 years and therefore, < 1000 life cycles. This means that the scatter of size or thickness measurements within each sample is a reflection of population changes and so any changes between adjacent beds is more likely to be just long term variability. There was also a poor recovery of the smallest *O. aspinata* instars across several beds during the disaggregation process. This could be due to adverse environmental conditions either before or after moulting or breakage during processing. It is difficult to determine at this time if the maximum or minimum shell or carapace sizes and thicknesses recorded throughout the section relate only to a specific facies. This is a result of only being able to process samples collected from the marls and shales for *O. aspinata* as the limestone samples proved impossible to disaggregate in order to extract the ostracod specimens. The reverse was an issue for *L. hisingeri* and *P. gigantea* specimens as size

data was only able to be collected from intact specimens found within the limestone samples, as those found within the marls or shales were highly fragmented and impossible to be measured.

Hesselbo *et al.* (2004) collected high resolution geochemical samples to investigate changes in the carbonate (% CARB) and total organic carbon levels (% TOC) within the St Audrie's Bay Tr–J boundary section. The % CARB measured fluctuates significantly, especially from the Cotham Member upwards, possibly as a response to primary and secondary diagenesis (Hesselbo *et al.*, 2004). Studies have shown that high levels of carbonate in sea water are needed in order for shelly organisms to continue growing, whereas low levels would indicate a biocalcification crisis and an inability to calcify, which could explain those few changes in size between adjacent beds that were significant (e.g., Hautmann, 2004; Galli *et al.*, 2005, 2007; Hautmann *et al.*, 2008; Mander *et al.*, 2008; McRoberts *et al.*, 2012).

The % TOC record from St Audrie's Bay is consistently very low (0-2%) until the Pre-planorbis Beds and onwards, where % TOC fluctuates significantly (0-12%). This is most probably due to the cyclical sedimentation (Weedon, 1985; Hart, 1987; Hesselbo *et al.*, 2004). Low % TOC (e.g., 0.2-0.4%) indicates poor organic matter preservation from biological reworking caused by animal scavengers, bioturbation by benthic fauna and aerobic bacterial degradation and, therefore, suggests oxic conditions (e.g., Demaison and Moore, 1980; Williams *et al.*, 2001; Hesselbo *et al.*, 2004; Allen and Allen, 2005). Alternatively, high % TOC (e.g., 1-25%) indicates better organic matter preservation due to slowed or little biological reworking caused by dysoxic or anoxic conditions (e.g., Demaison and Moore, 1980; Williams *et*

al., 2001; Hesselbo *et al.*, 2004; Allen and Allen, 2005). Short periods of anoxic or dysoxic conditions (e.g., oxygen levels as low as 0.3ml^{-1}) can cause reduced body size in deposit feeding organisms as a survival mechanism and it has been suggested that the recorded reduction in shell sizes during this event were a response to a slow return to normal seawater oxygen levels (Hallam, 1975; Wignall, 2001; Allen and Allen, 2005; Barras and Twitchett, 2007; Mander *et al.*, 2008). However, persistent, long term anoxia would eventually cause death and would explain the *O. aspinata* barren dark grey to black shale and bituminous clay beds at Lyme Regis and St Audrie's Bay (Rhoads and Morse, 1971; Moghadam and Paul, 2000; Wignall, 2001; Martin, 2004; Twitchett *et al.*, 2004; Allen and Allen, 2005; Mander *et al.*, 2008). Anoxic to dysoxic facies in the basal planorbis Zone at St Audrie's Bay may also explain the significant reduction in *L. hisingeri* shell size between the Pre-planorbis Beds and the planorbis Zone ($P < 0.01$).

There are several limitations present when attempting to accurately compare the published high resolution % CARB and % TOC datasets to the size and thickness data from this study. Firstly, both % CARB and % TOC were sampled multiple times throughout each bed and within some beds the results fluctuate significantly. Therefore, it is unknown exactly which of the % CARB and % TOC data points (within each bed) relates exactly to where the size measurements were taken from. This margin of error would significantly affect any results subsequently obtained through statistical analysis. Secondly, % TOC appears to be at its highest in the marls and shales where there are no bivalve data but there are ostracod data (except in the dark grey to black shale and bituminous clay beds) and is at its lowest in the

limestones where there are bivalve data but there are no ostracod data. Thirdly, at Lyme Regis there is no known % CARB and % TOC datasets, which makes it very difficult to test for a relationship between % CARB or % TOC and size or thickness data. To investigate this issue in the future, the rock samples used in this study from both Lyme Regis and St Audrie's Bay should be tested for % CARB and % TOC. This will enable the shell or carapace size and thickness data to be statistically tested against the % CARB and % TOC record.

A collapse in primary productivity, and thus a reduced food supply, has also been linked to causing a reduction in shell size and thickness (Twitchett, 2001; Hesselbo *et al.*, 2004; Aberhan *et al.*, 2007). However, the only possible evidence for such a primary productivity collapse is the negative carbon isotope excursion recorded in the Lillstock Formation, from which limited or no size or thickness data were recorded as part of this study due to the scarcity of relevant specimens (Hesselbo *et al.*, 2004; Aberhan *et al.*, 2007; Mander *et al.*, 2008). Therefore, it will be difficult to determine any relationships between the changes in shell size and thickness and variations in primary productivity at these locations.

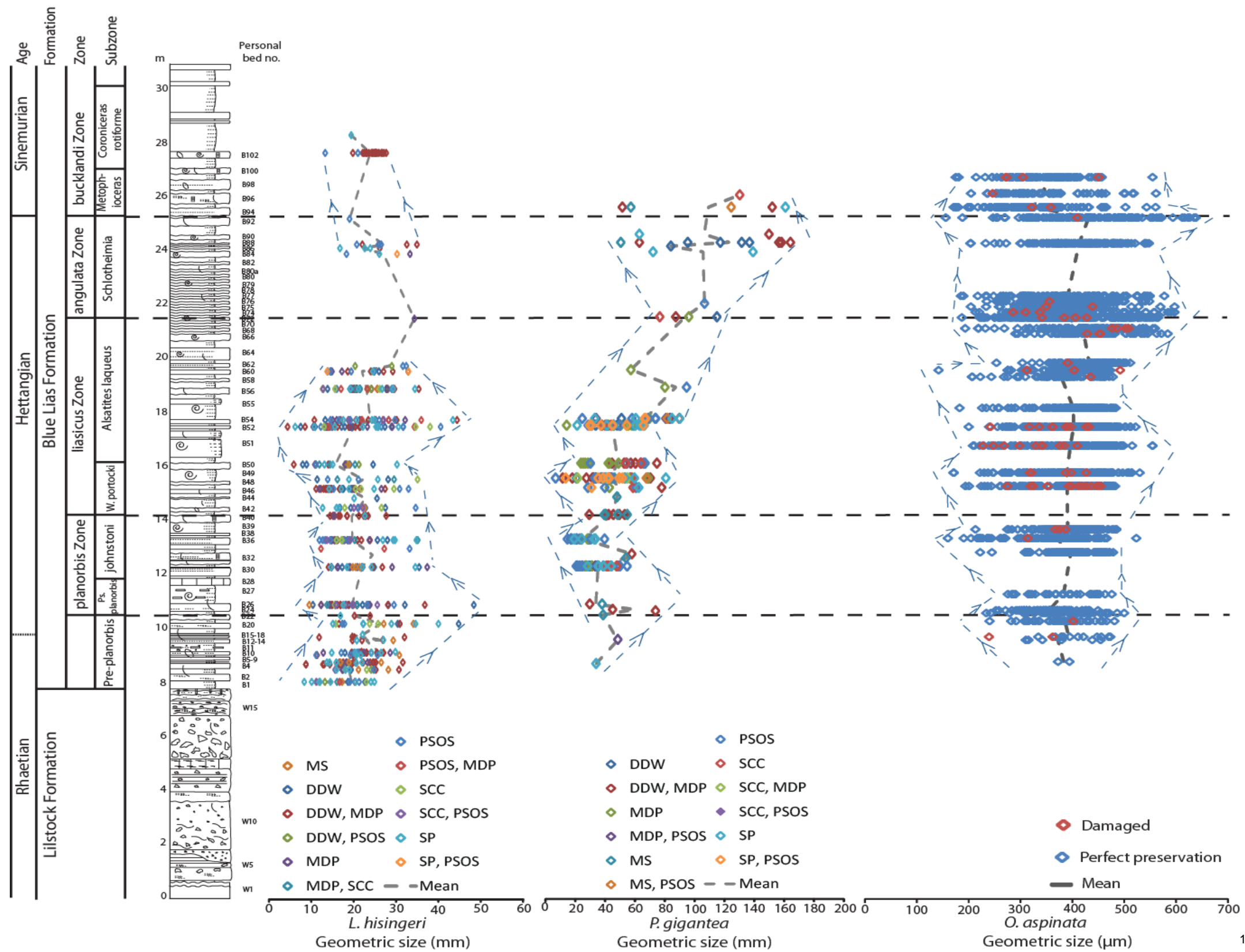
A further environmental factor which could affect size is sea level change. Bloos (1990) and Hallam (1997) interpreted sea level change from the rock record at St Audrie's Bay. Anoxic to dysoxic facies in the basal planorbis Zone indicate that sea level rise was fairly rapid (to an approximate maximum depth of 30m and well below the storm wave base), after which there was little change until the Sinemurian (Bloos, 1990; Hallam, 1997; Moghadam and Paul, 2000; Martin, 2004; Paul *et al.*, 2008; Hesselbo *et al.*,

2004). However, because all the species studied showed increasing size trends through the Pre-planorbis beds until the Planorbis Zone, these species did not seem to be adversely affected by rapid sea level rise, probably because they are tolerant to short term environmental change caused by rapid sea level rise.

Without further research in the future to identify more evidence relating to these localised environmental changes (e.g., sea level, seawater aragonite and calcite undersaturation, anoxia, salinity and reduced food supply), it is difficult to currently be able to statistically compare shell or carapace size and thickness data generated from this study with the aforementioned environmental factors in order to determine if a definitive relationship can be identified.

3.7 Identification of any significant relationships between the variations in geometric shell size or shell thickness and the different species at each location

The geometric shell size of the three species were analysed against each other to identify any relationships between the variations in size and the various life modes (Figures 3.18 and 3.19). The geometric minimum, maximum and mean shell size trends of *L. hisingeri*, *P. gigantea* and *O. aspinata* at Lyme Regis (Figure 3.18), and of *L. hisingeri* and *O. aspinata* at St Audrie's Bay record some similarities and some differences (Figure 3.19). At Lyme Regis, *L. hisingeri*, *P. gigantea* and *O. aspinata* all record a trend of increasing geometric size through the Pre-planorbis Beds. However, they all record a trend of decreasing geometric size through the planorbis Zone (Figure 3.18).



¹¹Figure 3.18: The geometric shell sizes of *L. hisingeri*, *P. gigantea* and *Ogmoconchella aspinata* measured on each bed to highlight any corresponding increasing or decreasing size trends between the three species. See Table 3.1 for preservation descriptions relating to the codes in the key above. Blue arrows placed by eye to highlight the increasing and decreasing size trends between the various beds.

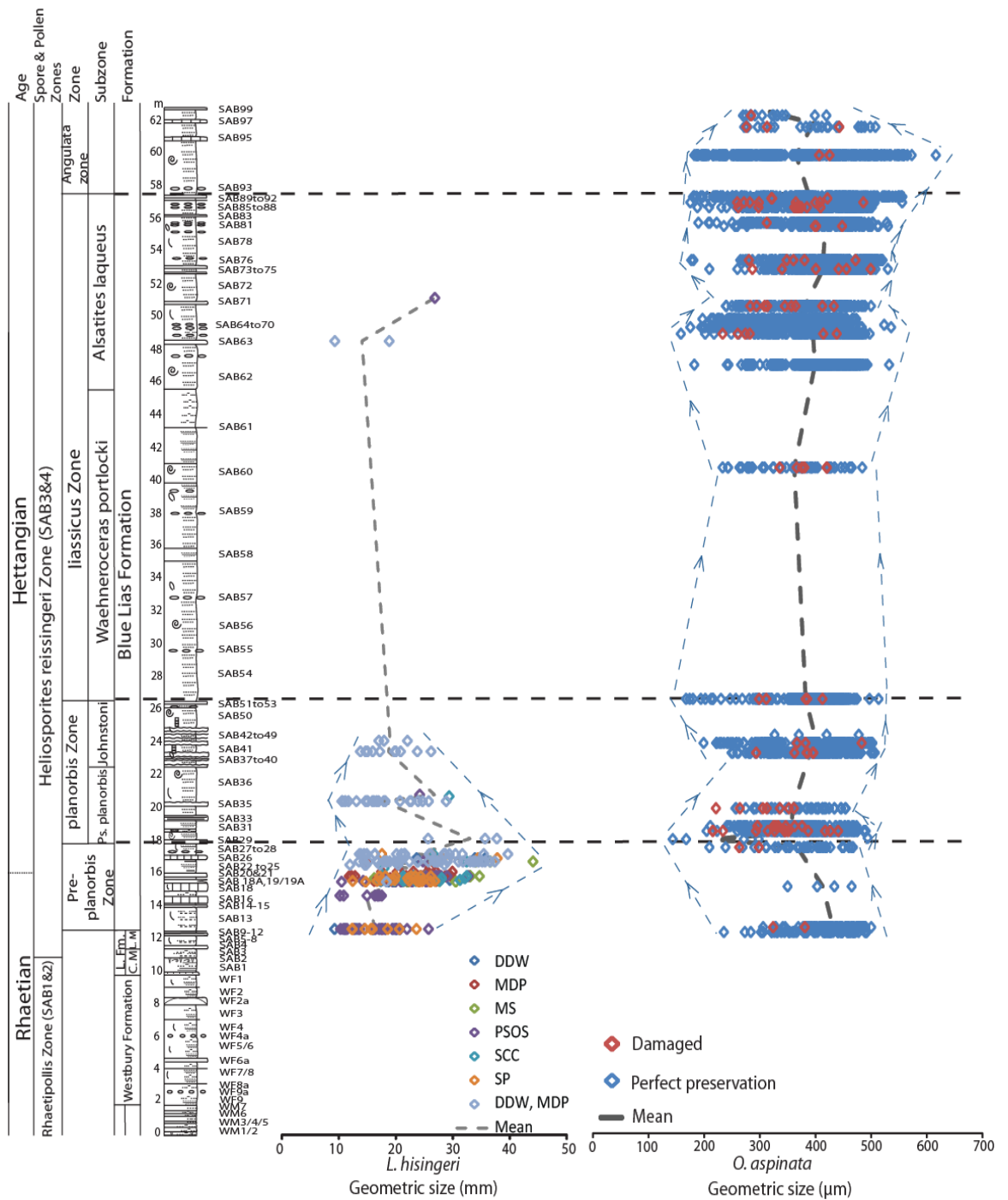


Figure 3.19: The geometric shell sizes of *L. hisingeri* and *O. aspinata* measured on each bed to highlight any corresponding increasing or decreasing size trends between the three species. See Table 3.1 for preservation descriptions relating to the codes in the key above. Blue arrows placed by eye to highlight the increasing and decreasing size trends between the various beds.

At St Audrie's Bay however, *L. hisingeri* increases in size through the Pre-planorbis Beds, whereas *O. aspinata* decreases in geometric size (Figure

3.19). Through the planorbis Zone at St Audrie's Bay *L. hisingeri* decreases in size whereas *O. aspinata* shows a decrease in size between beds 30-34 but an increase in size through beds 34-42 (Figure 3.18). Through the Lyme Regis W. portlocki subzone of the liasicus Zone, *L. hisingeri*, *P. gigantea* and *O. aspinata* all decrease in minimum geometric shell size, however both *P. gigantea* and *O. aspinata* increase in mean and maximum geometric shell size, while *L. hisingeri* records a decrease in mean and maximum geometric shell size (Figure 3.18). Through the Lyme Regis lower Alsatites laqueus subzone of the liasicus Zone, *P. gigantea* and *L. hisingeri* increase in geometric size whereas *O. aspinata* decrease in geometric size (Figure 3.18). Through the Lyme Regis upper Alsatites laqueus subzone of the liasicus Zone, *P. gigantea* and *O. aspinata* increase in geometric size whereas *L. hisingeri* decrease in geometric size (Figure 3.18). Through the Lyme Regis upper angulata Zone, *L. hisingeri* and *O. aspinata* geometric shell sizes remains moderately constant while *P. gigantean* increases (Figure 3.18). Through the Lyme Regis upper angulata Zone onwards all three species decrease in geometric shell size (Figure 3.18). Due to the lack of *L. hisingeri* data points in the St Audrie's Bay Liassic zone and onwards there are no comparisons with the *O. aspinata* data from the Liassic zone onwards.

At Lyme Regis, there is a significant positive relationship ($P < 0.05$) between the mean size of *P. gigantea* and *L. hisingeri* at the sub-zonal scale (Figure 3.20A). However, caution should be taken with this result because without the isolated large data point there is no significant relationship (Figure 3.20A). There is also a significant positive relationship ($P < 0.01$) between the 95th percentile ranges of geometric shell sizes of *O. aspinata* and *P. gigantea* at

the subzonal scale (Figure 3.20B) (Appendix 4: Table A4.21, Figure A4.12). At St Audrie's Bay there was a significant negative relationship ($P < 0.02$) between the geometric mean sizes of *O. aspinata* and *L. hisingeri* at the subzonal scale (Figure 3.21) (Appendix 4: Table A4.37, Figure A4.22).

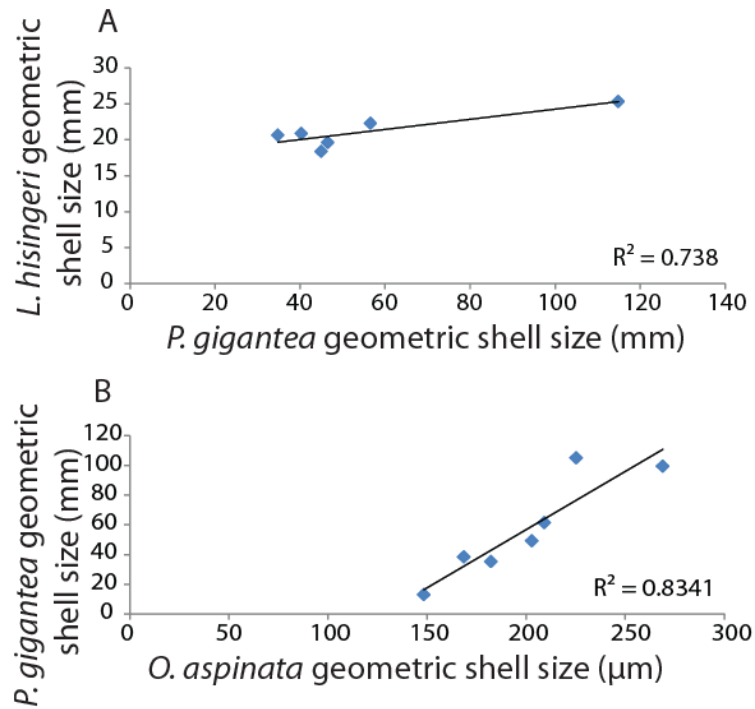


Figure 3.20: Linear regression model and trend line showing a significant relationships between Lyme Regis geometric shell size data at subzonal scale (A) mean geometric shell size from *P. gigantea* and *L. hisingeri* ($P < 0.05$), (B) 95th percentile range of geometric shell sizes from *O. aspinata* and *P. gigantea* ($P < 0.01$) (Appendix 4: Table A4.21, Figure A4.12).

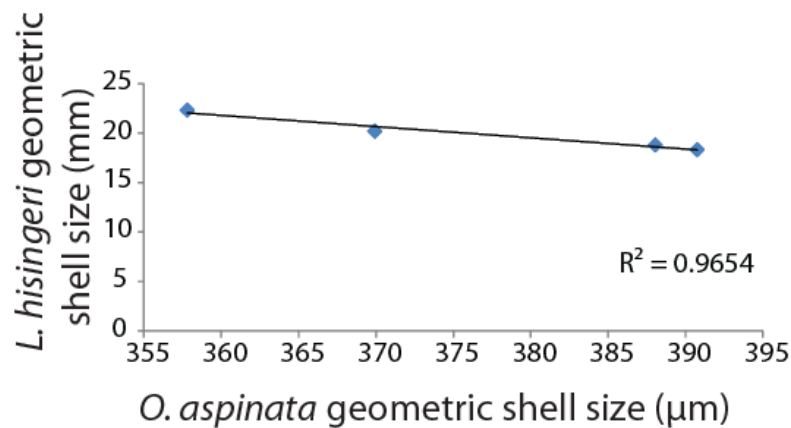


Figure 3.21: Linear regression model and trend line showing a significant relationship between St Audrie's Bay *L. hisingeri* and *O. aspinata* mean geometric shell size ($P < 0.02$) at subzonal scale (Appendix 4: Table A4.37, Figure A4.22).

These results indicate that visually many of these increasing or decreasing size trends during the Tr-J interval correlate between species. *L. hisingeri* has a positive shell size relationship to *P. gigantea* in Lyme Regis but a negative relationship to *O. aspinata* in St Audrie's Bay and *P. gigantea* has a positive relationship to *O. aspinata* at Lyme Regis. Previous studies for the Tr-J boundary have also found relationships between the extinction rates of certain species and their different life modes (Kiessling *et al.*, 2007; Greene *et al.*, 2012). It is possible that variations in environment and life mode of the different species are one reason why only a few relationships were identified. It could also be that each of the species studied reacts very differently to the same environmental changes (e.g., changes in water depth, pH, temperature or salinity). This has been noted in modern experiments specifically those studying the effects of increased temperature and high CO₂ using a variety of different species (Fabry *et al.*, 2008; Doney *et al.*, 2009; Hendriks *et al.*, 2010; Greene *et al.*, 2012 and references therein). It is thought to be due to how much physiological control a species has over their metabolic changes (Carter *et al.*, 1998; Cusack *et al.*, 2008; Findlay *et al.*, 2009, 2011).

3.8 Identification of any significant relationships between the geometric shell size or shell thickness of the same species from both Lyme Regis and St Audrie's Bay.

The identification of any significant relationships will help indicate how a change of location does or does not contribute to the variations in size found between the same species in this study.

3.8.2 *L. hisingeri*

L. hisingeri records similar variations in geometric shell size at both locations with an increasing trend through the Pre-planorbis Beds and decreasing geometric size trend through the planorbis Zone (Figure 3.22). There is no significant difference in the geometric shell size of *L. hisingeri* between the two locations even though the minimum and maximum at St Audrie's Bay are smaller than at Lyme Regis (Appendix 4: Figure A4.22). Neither the location or the stratigraphic zone they were collected from caused the overall geometric shell size of *L. hisingeri* to be smaller at St Audrie's Bay than at Lyme Regis (Appendix 4: Table A4.50). However, at the subzonal scale, the 95th percentile maximum geometric shell sizes of *L. hisingeri* from both locations show a significant negative relationship ($P < 0.05$; Figure 3.23; Appendix 4, Figure A4.27, Table A4.53). At St Audrie's Bay *L. hisingeri* records significantly larger geometric shell sizes in the Pre-planorbis Beds ($P < 0.05$) than at Lyme Regis (Figure 3.24). The other zones showed no significant difference between locations (Appendix 4: Tables A4.41-A4.43, Figures A4.22-A4.23). The negative relationship between the 95th percentile maximum geometric size for each subzone and the significantly smaller sizes in some of the St Audrie's Bay zones could be due to several reasons.

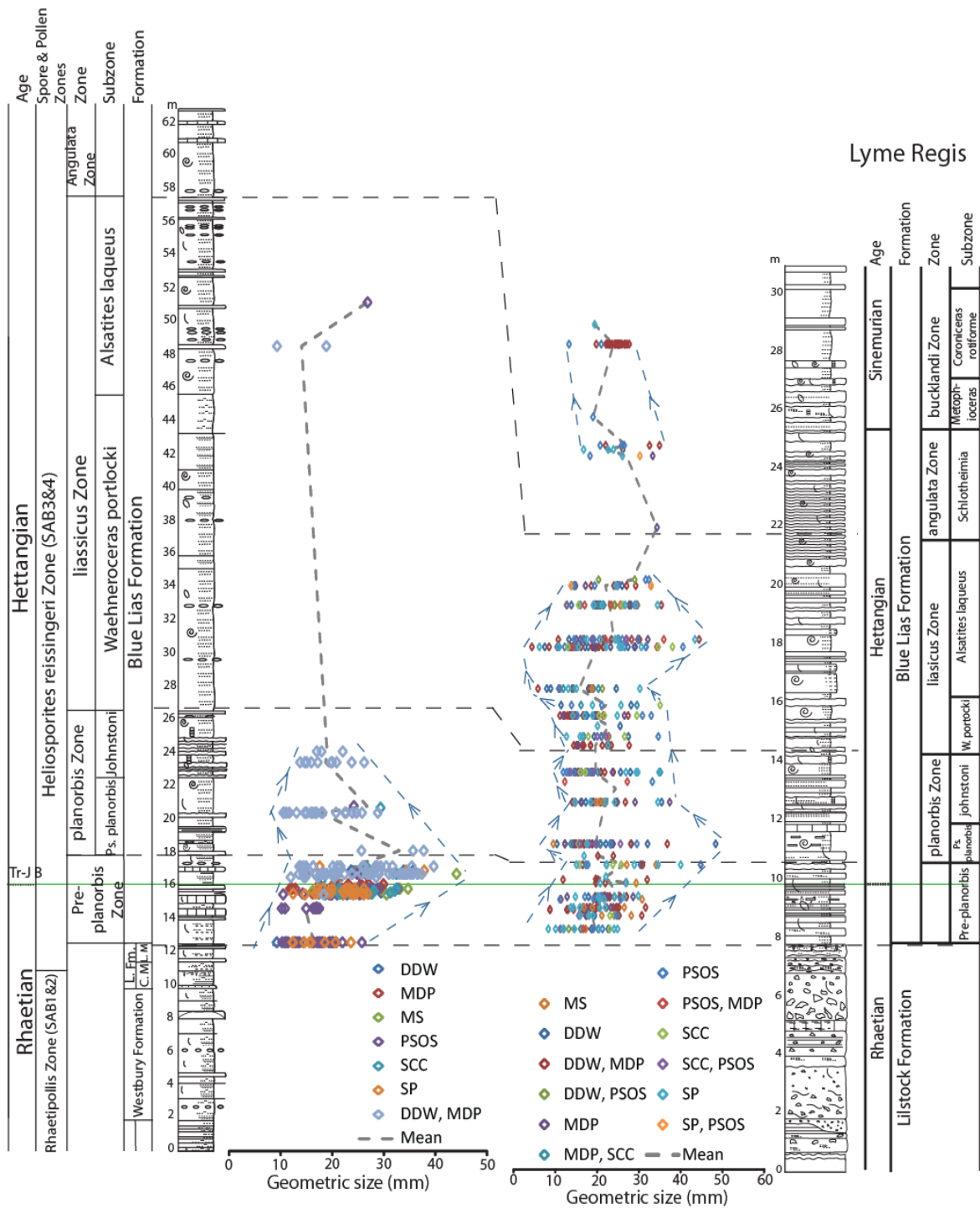


Figure 3.22: The geometric shell size data of *L. hisingeri* measured on each bed at Lyme Regis and St Audrie's Bay to determine any corresponding increasing or decreasing size trends. See Table 3.1 for preservation descriptions relating to the codes in the key above. Blue arrows placed by eye to highlight the increasing and decreasing size trends between the various beds.

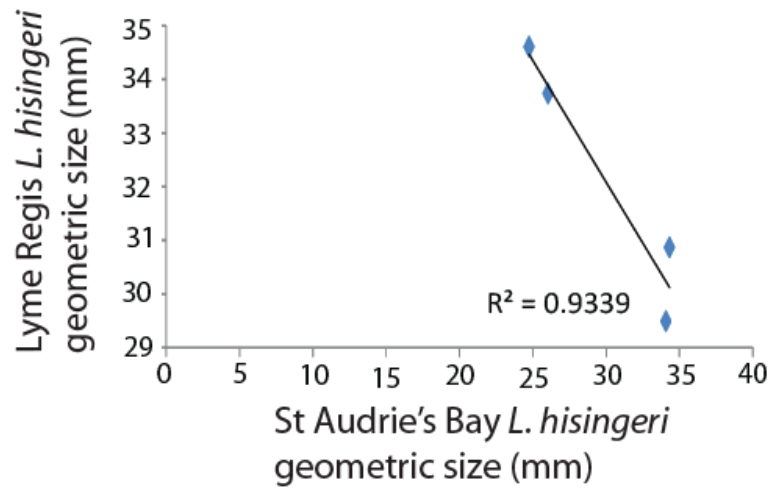


Figure 3.23: Linear regression model and trend time showing a significant relationship ($P < 0.05$) between the *L. hisingeri* 95th percentile maximum geometric size for each subzone from Lyme Regis and St Audrie's Bay.

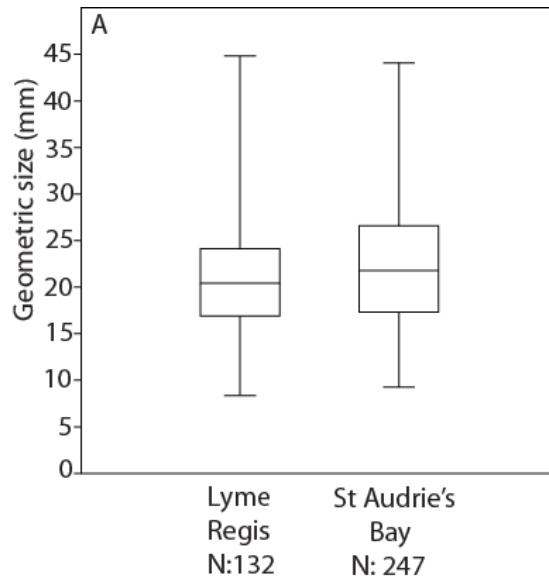


Figure 3.24: Comparison of the geometric mean shell size of *L. hisingeri* from Lyme Regis and St Audrie's Bay. (A) Pre-planorbis Beds ($P < 0.05$).

These include the possibility that the environment at St Audrie's Bay is more restricted due to either, less conducive water depths, longer periods of anoxia, adverse higher temperatures or more acidic conditions and therefore not as conducive to these species producing the larger sized shells seen at Lyme Regis (Hallam, 1995, 1997; Hesselbo *et al.*, 2004; Barras and

Twitchett, 2007; Gallois, 2007; Warrington *et al.*, 2008; Wignall and Bond, 2008; Mander *et al.*, 2008; Ruhl *et al.*, 2010).

3.8.3 *O. aspinata*

O. aspinata records some similar but also some very different variations in geometric shell size at both locations. There is opposing trends through the Pre-planorbis Beds but the same increasing trend through the planorbis Zone. The trends are opposing through most of the liasicus Zone except in the Alsatites laqueus subzone and there is a decreasing trend through the angulata Zone (Figure 3.25). There is no significant difference in the geometric shell size of *O. aspinata* between the two locations (Appendix 4: Figure A4.24, Table A4.44). Both the location and the stratigraphic zone they were collected from caused significantly smaller *O. aspinata* geometric shell sizes ($P < 0.001$) at St Audrie's Bay than at Lyme Regis (Appendix 4: Table A4.51). At the subzonal scale, the 95th percentile maximum geometric shell sizes of *O. aspinata* from both locations show a significant positive relationship ($P < 0.01$; Figure 3.26; Appendix 4, Figure A4.28, Table A4.53). The Pre-planorbis Beds and planorbis Zone show no significant difference in *O. aspinata* geometric shell size between both locations whereas the liasicus Zone and angulata Zone showed significantly smaller *O. aspinata* geometric shell sizes ($P < 0.001$) at St Audrie's Bay than at Lyme Regis (Figure 3.27; Appendix 4: Tables A4.39 and A4.45-A4.46, Figure A4.25).

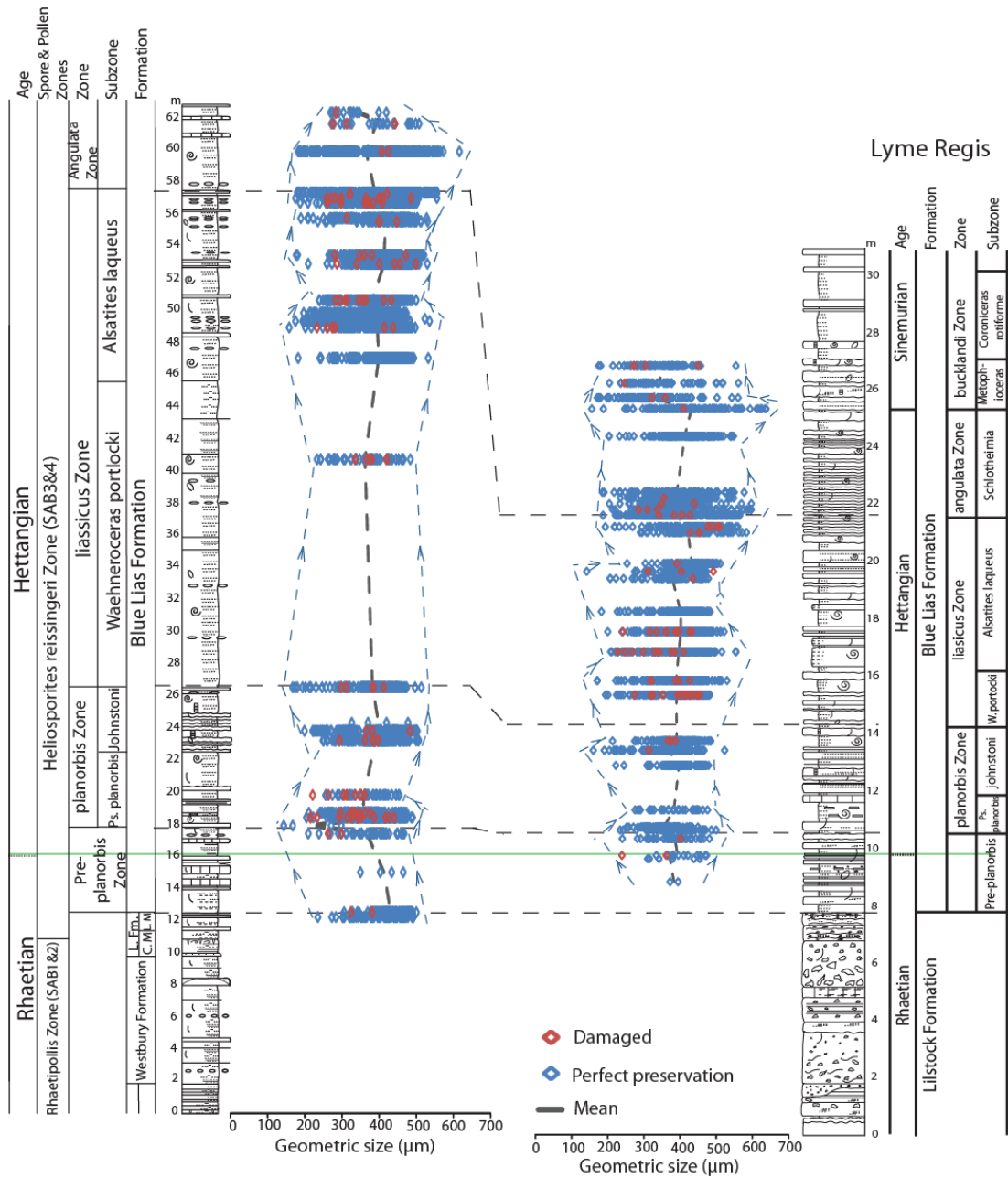


Figure 3.25: The geometric shell size data of *O. aspinata* measured on each bed at Lyme Regis and St Audrie's Bay to determine any corresponding increasing or decreasing size trends. Blue arrows placed by eye to highlight the increasing and decreasing size trends between the various beds.

O. aspinata records some similar but also some very different variations in shell thickness at both locations. There is opposing shell thickness trends through the Pre-planorbis Beds but matching increasing and decreasing shell size trends through the planorbis Zone, Liassic Zone and angulata Zone (Figure 3.28). Between the two locations there is significantly thinner *O. aspinata* shells at St Audrie's Bay ($P < 0.001$) than at Lyme Regis (Figure 3.29; Appendix 4: Table A4.47). Both the location and the stratigraphic zone the *O. aspinata* were collected from caused significantly thinner shells at St Audrie's Bay than at Lyme Regis (Appendix 4: Table A4.52). At the subzonal scale, neither the 95th percentile minimum, maximum, mean or range of *O. aspinata* shell thicknesses from both locations showed any significant relationships (Appendix 4: Tables A4.40 and A4.53, Figure A4.29). The Pre-planorbis Beds and angulata Zones show no significant difference in *O. aspinata* shell thickness at St Audrie's Bay than at Lyme Regis. However the planorbis Zone and liassic Zone showed significantly thinner shells ($P < 0.001$) at St Audrie's Bay than at Lyme Regis (Figure 3.30; Appendix 4: Tables A4.48-A4.49, Figure A4.26).

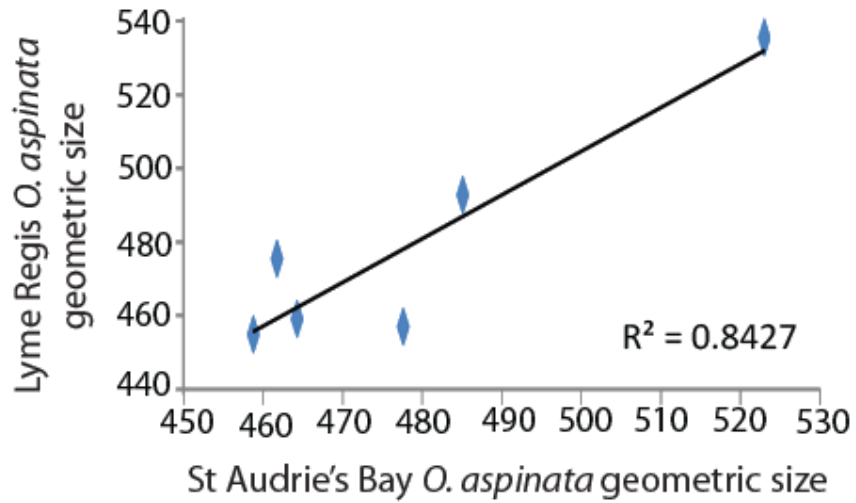


Figure 3.26: Linear regression model and trend time showing a significant relationship ($P < 0.01$) between the *O. aspinata* 95th percentile maximum geometric size for each subzone from Lyme Regis and St Audrie's Bay.

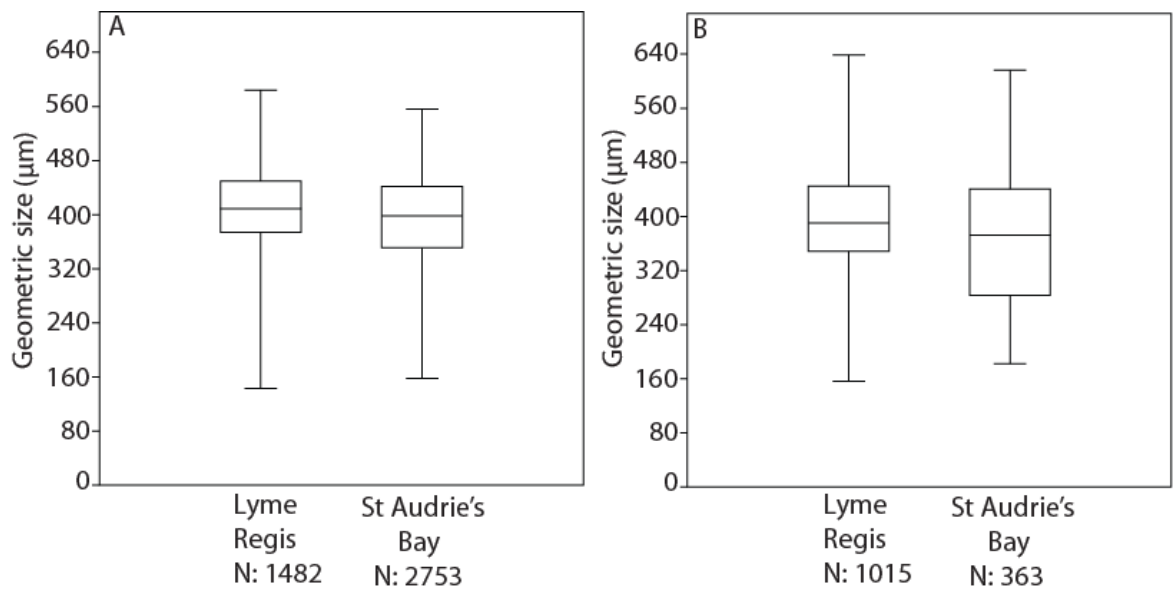


Figure 3.27: Comparison of the geometric shell size of *O. aspinata* in Lyme Regis and St Audrie's Bay (A) liasicus Zone ($P < 0.001$), (B) angulata Zone ($P < 0.001$).

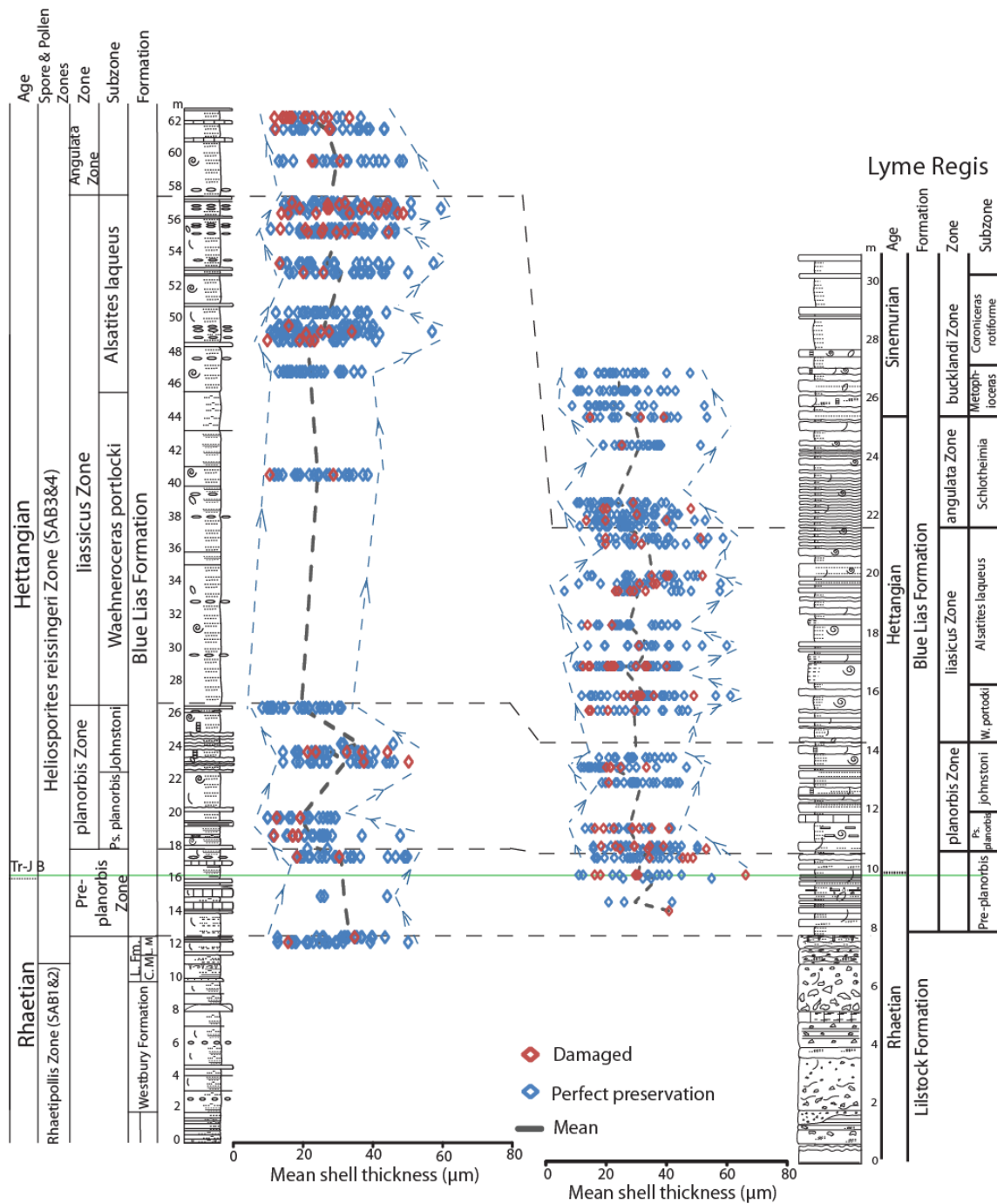


Figure 3.28: The shell thickness data of *O. aspinata* measured on each bed at Lyme Regis and St Audrie's Bay to determine any corresponding increasing or decreasing size trends. Blue arrows placed by eye to highlight the increasing and decreasing size trends between the various beds.

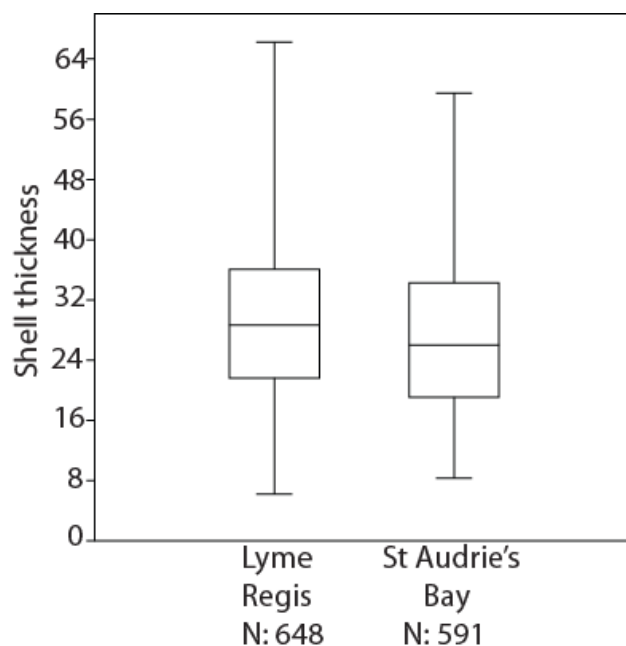


Figure 3.29: Shell thickness of *O. aspinata* at Lyme Regis and St Audrie's Bay ($P < 0.001$).

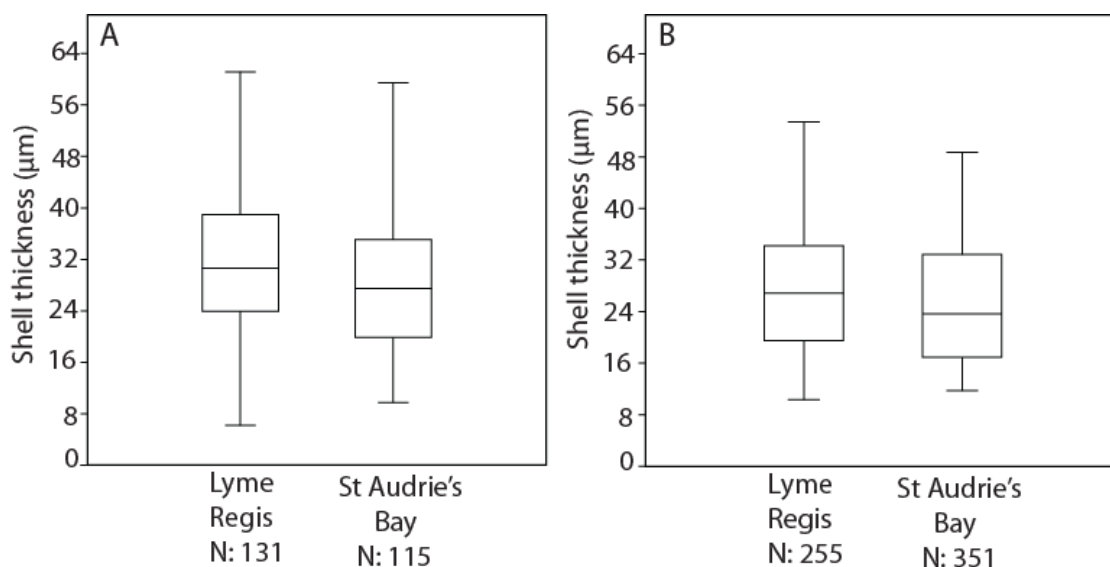


Figure 3.30: Comparison of the shell thickness of *O. aspinata* in Lyme Regis and St Audrie's Bay (A) planorbis Zone ($P < 0.001$), (B) liasicus Zone ($P < 0.001$).

The significant positive relationship between the 95th percentile maximum geometric sizes for each subzone indicates that the overriding control over the environment at both locations is similar enough that the maximum size can increase at both locations at the same time. However, the significantly

smaller sizes and thinner shells identified in certain zones at St Audrie's Bay indicates that the environment at St Audrie's Bay could be limiting or restricting the maximum *O. aspinata* sizes unlike the *O. aspinata* maximum sizes measured at Lyme Regis. However, the fact that a relationship was found between shell size and these two locations indicates that even if the St Audrie's Bay environment is restricted in some way for this species the effect is not significant enough to show no relationship when compared to Lyme Regis. Whereas for shell thickness no relationships were found either positive or negative between Lyme Regis and St Audrie's Bay which could be due to environmental restrictions at St Audrie's Bay which caused the shells to be thinner. Factors that could be limiting the maximum *O. aspinata* sizes at St Audrie's Bay include less conducive water depths, longer periods of anoxia, and changes in water temperature or more acidic seawater (Hallam, 1995, 1997; Hesselbo *et al.*, 2004; Barras and Twitchett, 2007; Gallois, 2007; Warrington *et al.*, 2008; Wignall and Bond, 2008; Mander *et al.*, 2008; Ruhl *et al.*, 2010).

The relationships or lack of relationships between the two locations for *L. hisingeri* and *O. aspinata* shell size, *O. aspinata* shell thickness and the smaller sizes and thicknesses found at St Audrie's Bay could also be attributed to global changes in marine environments due to increased atmospheric CO₂ induced through CAMP volcanism (e.g., McElwain *et al.*, 1999; Hautmann, 2004; Schaller *et al.*, 2011; Steinhorsdottir *et al.*, 2011; Greene *et al.*, 2012) emplacement rather than localised changes. CAMP is thought to have caused variations in the pH level to more acidic conditions, variations in seawater temperature or a combination of both (Hautmann,

2004; van de Schootbrugge *et al.*, 2007; Clémence *et al.*, 2010; Kiessling and Simpson, 2011). Various experimental studies using modern species have indicated variable results including decreasing and increasing shell size and thickness as well as no change in shell size and thickness when living in acidic and high temperatures conditions (e.g., Gazeau *et al.*, 2007; Wanamaker *et al.*, 2007; Kurihara *et al.*, 2008; Talmage and Gobler, 2009; Findlay *et al.*, 2009, 2011).

3.9 Summary

- All the species measured from both locations indicated significant increasing and decreasing size and thickness trends through the zones and subzones within the late Rhaetian and Hettangian. It is important to note, however, that some of the changes in size that have been identified between consecutive beds were not found to be significant, and may only be due to outliers, or variations, in the number of individuals available to be measured.
- These variations in shell size and thickness may or may not be caused by adverse changes in the environment. Several of the size trends correlate between the different species at each zone but there are a few zones where they do not. To determine the cause of these changes further research is required and this will be completed in the following Chapters 4–6. The subtle variations in shell or carapace size and/or thickness observed in a bed-by-bed context could indicate that localised lithological variations are having an effect. However, in most cases these bed-by-bed changes were not found to be significant.

Future research would be required in order to investigate these localised effects further, but that research was not included in the aim and objectives of this study. This investigation concentrated on the effects of $p\text{CO}_2$ and/or temperature on shell size and thickness.

- The maximum geometric size for *L. hisingeri* and *O. aspinata* is significantly smaller at St Audrie's Bay than at Lyme Regis and *O. aspinata* is also thinner at St Audrie's Bay than at Lyme Regis. This highlights the possibility that an environmental factor was affecting the environment significantly more at St Audrie's Bay than at Lyme Regis, reducing the ability for the largest possible shell sizes to form.

3.9.2 Further work

To understand if the changes in size and thickness could be related to the variations in $p\text{CO}_2$ and temperature the Tr-J $p\text{CO}_2$ and temperature records will be analysed in Chapter 4 alongside the size and thickness data from these three species in order to identify any relationships. Those relationships identified in Chapter 4 will be compared in Chapter 6 to the results from various modern species experiment (both those results previously published and those results from the ostracod experimental study conducted and discussed in Chapter 5) in order to help interpret what these relationships may mean and if the results indicate ocean acidification or high water temperature could of occurred during the Tr-J interval at these locations and caused the species changes identified.

Chapter 4 - Palaeoenvironmental effects on shell size and thickness of bivalves and ostracods across the Triassic-Jurassic boundary interval.

4.1 Introduction

Previous studies (e.g., Hallam, 2002; Hautmann, 2004; Kiessling *et al.*, 2007; Mander *et al.*, 2008; Hautmann *et al.*, 2008; Kiessling and Simpson, 2011) have investigated the response of benthic invertebrates to changes of $p\text{CO}_2$ and palaeotemperature during the Late Triassic and earliest Jurassic. As discussed in detail in Chapter 1 (Section 1.2.2) Hautmann (2004) found that extinction rates were exceptionally high in aragonite and high magnesium calcite organisms while organisms with shells containing a greater concentration of calcite survived better through the Tr-J extinction event (Kiessling *et al.*, 2007). It was also found that some bivalve species (e.g., *Gervillea inflata*, *Conchodon* and *Megalodon*) generally reduced their overall shell size and thickness during the Tr-J extinction event and into the Hettangian (Hallam, 2002; Hautmann, 2004). Mander *et al.* (2008) reported that bivalve shell thickness remained fairly constant through the Tr-J boundary interval but that shell size remained suppressed, except for a brief increase attributed to an influx of *Liostrea*.

4.2 Aim and objectives

In this chapter, the morphological (shell size and shell thickness) and biomineralogical (Ca and Mg) changes through the Tr-J boundary interval (see Chapter 3) are tested together with the $p\text{CO}_2$, $\delta^{13}\text{C}$ and palaeotemperature changes (derived both empirically and from the literature) from the same interval to identify any significant relationships. This will highlight any relationships between the identified morphological changes for the studied species and the latest Triassic to earliest Jurassic boundary interval high $p\text{CO}_2$ and warming event.

The objectives were established as follows:

- Palaeotemperature curves for St Audrie's Bay and Lyme Regis were derived from bivalves and ostracod stable isotope data;
- Relationships between published Tr-J boundary $p\text{CO}_2$ data and palaeotemperature data (combined from this study and previously published work) were investigated; and
- Relationships between aspects of shell morphology (size and thickness) and environmental variables ($p\text{CO}_2$ / palaeotemperature) through the Latest Triassic and Earliest Jurassic event were explored.

4.3 Materials and methods

4.3.2 Sampling material for geochemical analysis

Bivalve and ostracod fossils, as well as bulk rock samples, from St Audrie's Bay and Lyme Regis (collected as described in Sections 2.3 and 3.4.1) were subjected to geochemical analysis. Table 4.1 displays the number of

samples of each relevant species, plus bulk rock samples, collected from throughout the succession presented at Lyme Regis and St. Audrie's Bay. Geochemical samples were collected from as many beds as possible using individual shell specimens, regardless of if the specimen had been measured for shell size. These shell samples were collected from a part of the section not previously investigated in an attempt to extend the published bivalve data presented by van de Schootbrugge *et al.* (2007) and Korte *et al.* (2009). By extending the existing stable isotope data sets it also allows more of the morphological data to be correlated to temperature and $\delta^{13}\text{C}$ data. Therefore, the data from this present study were collected using the same methods as van de Schootbrugge *et al.* (2007) and Korte *et al.* (2009).

Prior to geochemical analysis, shell samples were visually inspected under low power magnification (x10 Kyowa optical microscope; Tokyo, Japan) to determine the state of preservation of each sample. Following this visual examination and using the methods of van de Schootbrugge *et al.* (2007) and Korte *et al.* (2009), the areas of each bivalve shell deemed most susceptible to diagenetic alteration were removed by scraping layers away until only smooth foliated shell layers remained. These smooth, foliated layers were targeted because they are indicative of the best shell preservation determined by van de Schootbrugge *et al.* (2007) and Korte *et al.* (2009) during their investigations. Powdered carbonate samples (mass = 200-300 μg) were then collected from each shell by flaking or drilling those best preserved areas (van de Schootbrugge *et al.*, 2007; Korte *et al.*, 2009) and then prepared for geochemical analysis.

In contrast, the most suitably preserved ostracod specimens were identified visually under low power magnification (x10) from those individuals measured for morphometric data. Those specimens with the best preservation were then identified and cleaned of as much of the remaining adherent sediment as possible. Cleaning of the specimens was accomplished by immersion in an ultrasonic bath to loosen and remove the majority of adhered sediment. Once extracted from the bath, manual removal of as much remaining sediment as possible was completed using a dental pick under low power magnification.

Unlike the bivalve analysis, the whole ostracod shell was used as the individual specimens were too small to attempt to flake or drill and the overall individual shell weight was so low. The only technique that would provide a precise sample would be laser ablation where a pit or hole of a known size can be sampled but this technique was not available. Ostracods used for geochemical analysis were only collected from samples containing >50 individuals because 10-20 individuals from each sample were required. It was necessary to use 10-20 individuals because the individual weight of each ostracod was lower than the minimum sample weight required for this test. The final stage was to sub-sample material from each of the remaining bulk rock samples that were not disaggregated in order to compare the bulk rock isotope data to the bivalve and ostracod isotope data. This bulk rock analysis was used to assist in determining if diagenetic alteration had taken place in the fossil samples. A minimum mass of 1mg was collected from a clean surface on each of the bulk rock samples and then ground down to a fine powder for geochemical analysis.

Location	No. of samples for <i>O. aspinata</i>	No. of samples for <i>L. hisingeri</i>	No. of samples for <i>P. gigantea</i>	No. of samples for bulk rock
St Audrie's Bay	21	12	15	59
Lyme Regis	24	15	15	44

Table 4.1: Number of samples collected throughout the succession at each of the field locations for *O. aspinata*, *L. hisingeri*, *P. gigantea* and bulk rock.

4.3.3 Stable isotope and trace element analyses

Stable isotopes were determined using an Optima Isotope Ratio mass spectrometer (GV Instruments) with a multiprep Gilson Multiflow carbonate auto-sampler (at Plymouth University). Carbonate powders were placed in sealed sample vials and reacted with 100% phosphoric acid at 90°C for a minimum of one hour. The evolved CO₂ was then sampled using a Gilson Multiflow carbonate auto-sampler, passed through a Thermal Conductivity Detector and analysed by the Isotope Ratio Mass Spectrometer. Samples with values below 2.0nA were omitted and, where possible, re-run. Those that were below 2.0nA and could not be re-run were removed from the final data set. The values obtained were calibrated against the Vienna Pee Dee Belemnite (VPDB) international standard NBS-19. For every 15 samples analysed, one standard was also run. The analysed standard values were then compared to the published values for NBS-19 (published values: NBS-19 = $\delta^{13}\text{C} + 1.95\text{‰}$ and $\delta^{18}\text{O} - 2.2\text{‰}$). Differences were used to correct the values of the unknown samples for any daily offset (Appendix 5: Tables A5.1-A5.2). Reproducibility for both $\delta^{13}\text{C}$ and $\delta^{18}\text{O}$ was better than 0.1‰, based upon multiple sample analysis.

4.3.4 Trace element geochemistry

For trace elemental analysis (Ca, Mg, Fe and Mn), each bivalve, ostracod and bulk rock sample was homogenised and the mass of each (mass =

0.20–1.50 mg) recorded before being dissolved in 1 mL of 4% nitric acid + 9 mL of distilled water. The prepared samples were then analysed using a Varian 752-ES ICP Optical Emission Spectrometer (ICP-OES). Prior to running the samples, the ICP-OES was calibrated using four appropriate standards of the different elements analysed, at four different concentrations (Table 4.2). The same standards were re-run between samples (one standard after every ten samples; Appendix 5: Tables A5.3-A5.4) to ensure that the ICP-OES remained within calibration throughout the testing period. Based upon the analyses of duplicate samples, reproducibility was better than 4% of the measured concentration of each element.

Standard 1	0.05ml of both the 100mg/l Strontium (Sr) solution and the multi-element mixture was diluted to 50ml (0.05/50 X 100mg/l = 0.1mg/l).
Standard 2	0.25ml of both the 100mg/l Sr and multi-element mixture diluted to 50ml. (0.25/50 x100mg/l = 0.5mg/l).
Standard 3	1ml of both the 100mg/l Sr and the multi-element mixture diluted to 50ml. (1/50 x100mg/l = 2mg/l).
Standard 4	2ml of both the 100mg/l Sr and the multi-element mixture diluted to 50ml. (2/50 x 100mg/l = 4mg/l).

Table 4.2: Details of the calibration standards used in the ICP-OES.

4.3.5 Palaeotemperature estimates

$\delta^{18}\text{O}$ values in biogenic calcite may reflect the localised palaeotemperature and salinity signal for the Late Triassic and Early Jurassic (e.g., Klein *et al.*, 1996; McRoberts *et al.*, 1997; van de Schootbrugge *et al.*, 2007; Korte *et al.*, 2009). The oxygen isotope values of calcareous marine organisms are considered a proxy for seawater palaeotemperature as the calcite is believed to have been precipitated in equilibrium with the oxygen isotope values of the ambient sea water (e.g., Klein *et al.*, 1996; Korte *et al.*, 2005; van de Schootbrugge *et al.*, 2007; Gómez *et al.*, 2009; Korte *et al.*, 2009; Price, 2010). However, $\delta^{18}\text{O}$ values from bulk rock samples are no longer thought

to provide a reliable estimate of palaeotemperature due to the possibility of significant diagenetic alteration (e.g., van de Schootbrugge *et al.*, 2007). In order to compare the stable isotope results established in this study with the stable isotope data presented by Korte *et al.* (2009), the same palaeotemperature equation refined by Anderson and Arthur (1983) was used and is shown below : -

$$T(^{\circ}\text{C}) = 16.0 - 4.14 (\delta_c - \delta_w) + 0.13 (\delta_c - \delta_w)^2$$

However, some assumptions are made with regard to a number of parameters required to be inputted into the equation and these assumptions have to be the same as those used by Korte *et al.* (2009). These assumptions are where δ_c is taken to be the oxygen isotope composition of calcite determined from primary geochemical analysis of collected samples (in the case of this study, calcite values of the bivalve and ostracod specimens) and δ_w is taken to be the oxygen isotope composition of the water, assuming $\delta^{18}\text{O}_w = -1.2\text{‰}$ (Zachos *et al.*, 2001). The $\delta^{18}\text{O}_w$ value used is -1.2‰ because the seawater pH conditions for the Tr-J boundary interval are assumed to be similar to present-day values and this is the value used by other authors (e.g., van de Schootbrugge *et al.*, 2007; Korte *et al.*, 2009). Finally, in order to check this palaeotemperature equation is correct and will produce the same palaeotemperature results identified by Korte *et al.* (2009), the raw data from their published study were inputted into this equation. The results produced were the same palaeotemperature results identified by Korte *et al.* (2009) which confirms the equation works and can be used for the data in this study.

It has been suggested that palaeotemperature change is not the only source of $\delta^{18}\text{O}$ variations, with freshwater runoff and subsequent localized changes in salinity decreasing the local seawater $\delta^{18}\text{O}$ value (e.g., Railsback *et al.*, 1989; Korte *et al.*, 2009 and references therein). The incorporation of Mg into biogenic calcite is also known to be temperature dependent, with a known exponential increase of 1°C per 10% increase in Mg/Ca, a feature identified in many calcareous marine organisms (Rosenthal *et al.*, 1997; Lea *et al.*, 1999; Lear *et al.*, 2002). The data presented by Korte *et al.* (2009) obtained from the analysis of bivalves collected from St. Audrie's Bay displayed $\delta^{18}\text{O}$ values which could be correlated with pre-existing ammonite locations from the same locality. As the appearance of ammonite specimens appear towards the top of the upward $\delta^{18}\text{O}$ trend, Korte *et al.* (2009) have inferred that the lighter $\delta^{18}\text{O}$ values are due to changes in temperature rather than salinity. If the $\delta^{18}\text{O}$ values were a result of changes in salinity, then the appearance of ammonite specimens at this point would not be expected.

4.3.6 Data analysis and presentation

Morphological data (minimum, maximum, mean and overall range of geometric size or shell thickness for the 95th percentile of the sampled specimens), Ca and Mg values from species from Lyme Regis and St. Audrie's Bay were inputted into linear regression models to identify any relationships with the $p\text{CO}_2$, $\delta^{13}\text{C}$ or palaeotemperature curves. Ca and Mg values were compared separately to the $p\text{CO}_2$, $\delta^{13}\text{C}$ or palaeotemperature curves so that the data were comparable to the experimental studies on extant species presented in Chapter 5. Linear regression models were also

used to detect any relationships between each $p\text{CO}_2$ data set and each palaeotemperature data set.

A best fit relationship was achieved by matching existing $p\text{CO}_2$, $\delta^{13}\text{C}$ and palaeotemperature data extracted from a number of published data sets with the morphological species data collected from the bed stratigraphically closest to each of the $p\text{CO}_2$, $\delta^{13}\text{C}$ and palaeotemperature data points. In this study, the morphological results are correlated to $p\text{CO}_2$ data gathered from several different locations, including Greenland. However, the results from Greenland are from 2 separate studies (see Chapter 1, Section 1.2 and Chapter 2, Section 2.7), from herein denoted as “Greenland”, referring to work completed by McElwain *et al.* (1999) and “Astartekløft”, referring to the study completed by Steinhorsdottir *et al.* (2011). The $p\text{CO}_2$ data from each of the Greenland studies come from the same section and the same beds however the $p\text{CO}_2$ values from the same bed are significantly different between the different studies. The first of the two $p\text{CO}_2$ data sets from Astartekløft was produced using a modern standard ($[\text{CO}_2]_{\text{palaeo}} = \text{SI}_{\text{NLE}}/\text{SI}_{\text{FOSSIL}} \times [\text{CO}_2]_{\text{present}}$) to calibrate palaeo- $[\text{CO}_2]$ and produce GEOCARB values relating to the Neogene and modern plants (Steinhorsdottir *et al.*, 2011). The second $p\text{CO}_2$ data set was produced using a Carboniferous standard ($[\text{CO}_2]_{\text{palaeo}} = \text{SI}_{\text{NLE}}/\text{SI}_{\text{FOSSIL}} \times 600$) to calibrate palaeo- $[\text{CO}_2]$ and produce GEOCARB values relating to the Paleozoic and Mesozoic (Steinhorsdottir *et al.*, 2011). The two palaeo- $[\text{CO}_2]$ data sets have been presented separately by Steinhorsdottir *et al.* (2011) and will, therefore, be treated as separate data sets in this study. Due to the variability between the data sets from each study it was thought to be inappropriate to take an

average value for each bed because this may skew the results. Therefore, for this study each of the published data sets from Greenland were separately correlated with the morphological data rather than grouped together.

It is also important to note that different sampling methods were used to produce the $p\text{CO}_2$ data sets: (1) palaeosol samples in the Newark basin study; and (2) Ginkgo leaves in the Sweden, Greenland, Astartekløft and Larne studies. Variations in the $p\text{CO}_2$ values between the data sets may be due to differing analytical methods, as palaeosols are known to produce higher $p\text{CO}_2$ values than Ginkgo leaves (Steinthorsdottir *et al.*, 2011; Schaller *et al.*, 2011). The morphological results are also compared to $\delta^{13}\text{C}$ and palaeotemperature data gathered from several different published studies, using slightly different methods and different species to provide a range of data from the same location, in addition to data from this study. The $\delta^{13}\text{C}$ and palaeotemperature data varied significantly between the species studied; therefore the available information has not been combined into one data set for the comparison study. Consequently, because the data were collected from various species using marginally different methods (e.g., differences in sample collection method, differences in the instruments used, difference in species sampled etc.), this required the data from each of the published studies, along with the data from this study, to be separately correlated to the morphological data, rather than grouped together.

To determine where the previously published $p\text{CO}_2$, $\delta^{13}\text{C}$ and palaeotemperature data points are within the succession from this study, these data have been correlated with the observed stratigraphy using the

methods presented in Chapter 2, Sections 2.4 and 2.7. It should be noted however, that some of the correlated $p\text{CO}_2$ curves display vertical error bars. These error bars are present on several data sets obtained through studies from terrestrial successions. This is because there is a lack of stratigraphical precision available (e.g., comparable palynology, biostratigraphy etc.) to place accurately the terrestrial $p\text{CO}_2$ data points within the Lyme Regis and St Audrie's Bay marine successions. To use those $p\text{CO}_2$ data points, the middle distance between the minimum and maximum error was calculated and correlated with the closest bed containing morphological data as some of the $p\text{CO}_2$ data points do not have species data at the same horizon. To correlate these $p\text{CO}_2$, $\delta^{13}\text{C}$ and palaeotemperature data points with the morphological data, the first closest possible bed containing species data within a maximum radius of 2 metres was used. This distance was chosen as any fossil morphological data associated with beds beyond 2 metres were deemed too far away to be relevant to the corresponding $p\text{CO}_2$, $\delta^{13}\text{C}$ and palaeotemperature point.

The individual geometric shell size and shell thickness data from each bed were not screened using the preservation codes (discussed in Chapter 3) to remove the morphological data from the worst preserved specimens before being inputted into the linear regression models. This is for several reasons including: (1) by using the geometric shell size of each individual, the worst preserved individuals with only one size measurement (either length or width) were automatically excluded; (2) the data from each bed were compiled into the mean and 95th percentile minimum, maximum and range of geometric shell size and thickness, limiting the effect of the less reliable results; and (3)

some beds contained very few individuals, therefore all of the collected individuals were required to generate a significantly large enough data set.

Data sets are considered testable if they contain 3 or more data points. Data sets with less than 3 data points are presented on the graphs but not tested for significance. Significant correlations are illustrated on the linear regression models with the use of the data trend line (line colour corresponds to the colour of the relevant data points) and both the relevant R^2 and P value. If no correlation was found no trend line was fitted and the R^2 value was presented adjacent to the graph. However, the data were still included on the appropriate graph as it is important to document that it was tested, and what the corresponding R^2 value displayed. If in one graph there are data sets depicted showing significant correlations as well as data sets showing no correlation, then those graphs are depicted in Section 4.6- 4.8 with none of the non-significant data removed. However, where a whole graph shows no correlations in any of the plotted data sets, those graphs are presented in Appendix 5: Sections A5.4.1 and A5.5.1.

4.3.7 Diagenetic versus the primary signal

It is essential to know if any of the fossil material was diagenetically altered before using it to investigate changes in palaeotemperature (Korte *et al.*, 2005; van de Schootbrugge *et al.*, 2007; Korte *et al.*, 2009; Kearsley *et al.*, 2009). Measurements of Fe and Mn from the bivalve and ostracod samples were used to detect any diagenetic signal within the samples from this study. Several published studies have previously established thresholds for Fe and Mn from bivalves (Fe > 280 ppm and Mn > 110 ppm) which are used as cut

off limits, and bivalve samples with ppm values over this should be excluded from further study (e.g., Brand and Veizer, 1980; van de Schootbrugge *et al.*, 2007; Korte *et al.*, 2009). Other thresholds have been identified (e.g., Fe > 100 / 150 / 200 / 250 ppm and Mn > 100ppm) and used in various other studies (Morrison and Brand, 1986; Brand 1989; Price and Gröcke 2002; Gröcke *et al.*, 2003; Brand *et al.*, 2003; Popp *et al.*, 1986; Korte *et al.*, 2005; Nunn and Price, 2010; Price, 2010). However, some of these studies used different marine organisms (including brachiopods and belemnites) from different time scales, which could explain the variation in the thresholds used (Morrison and Brand, 1986; Brand 1989; Price and Gröcke 2002; Gröcke *et al.*, 2003; Brand *et al.*, 2003; Popp *et al.*, 1986; Korte *et al.*, 2005; Nunn and Price, 2010; Price, 2010).

The thresholds (Fe > 280 ppm and Mn > 110 ppm) used by van de Schootbrugge *et al.* (2007) were also used in this study in order to allow comparability with their data. The trace element data (Fe and Mn) from both locations studied show the measured Fe and Mn concentrations fall largely within established thresholds for pristine biogenic calcite and are not indicative of significant diagenesis in the majority of samples (Figure 4.1; Wierzbowski, 2004; Price and Page, 2008). However, several samples exhibit elevated Fe or Mn concentrations beyond the acceptable thresholds (Fe > 280 ppm and Mn > 110 ppm) and these were excluded from further analysis. The $\delta^{18}\text{O}$ values and $\delta^{13}\text{C}$ values from *O. aspinata*, *P. gigantea*, *L. hisingeri* and bulk rock collected from both Lyme Regis and St Audrie's Bay were cross-plotted to identify any significant outliers which could determine diagenetic alteration.

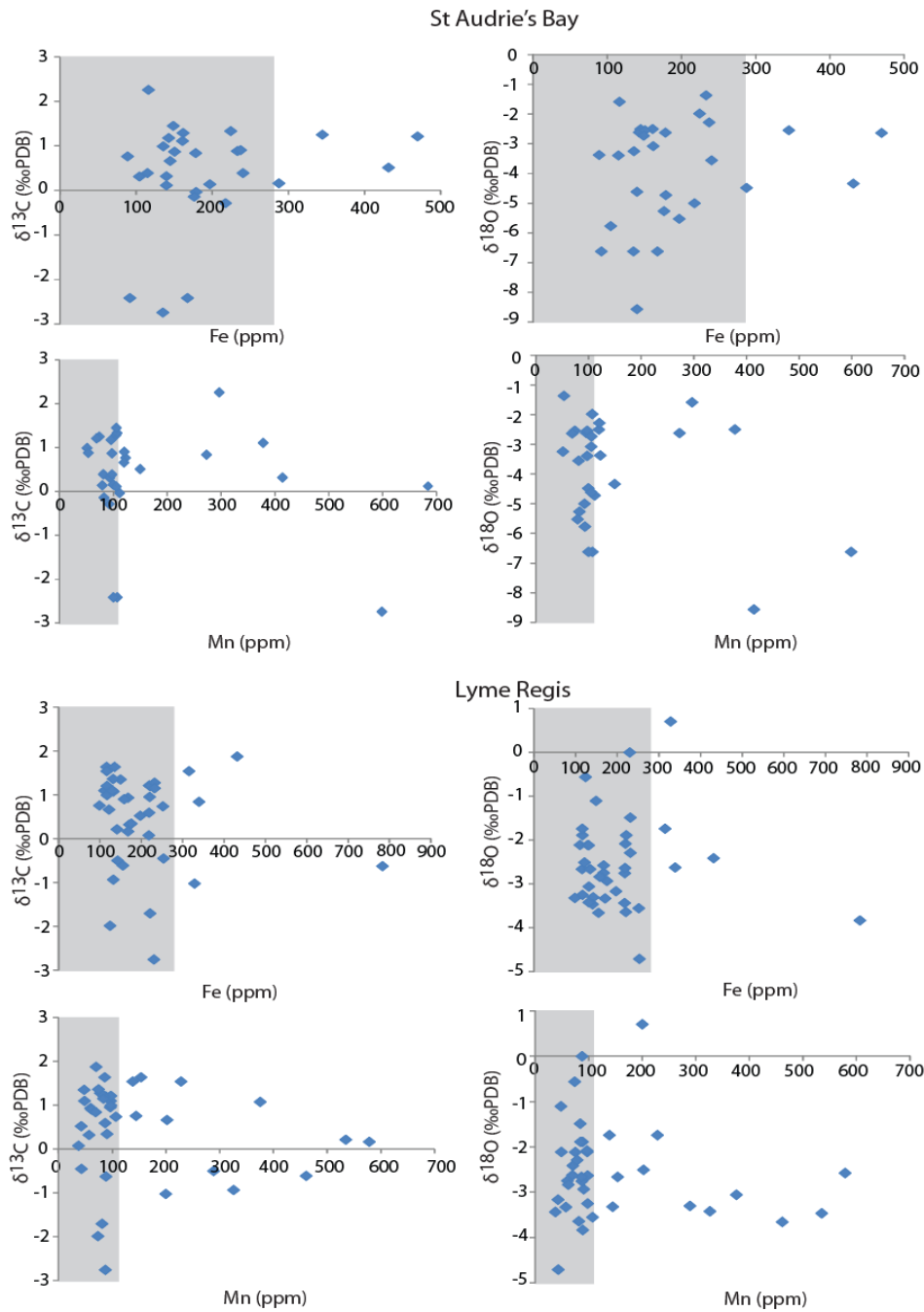


Figure 4.1: Cross plots between $\delta^{13}\text{C}$ or $\delta^{18}\text{O}$ and Mn (ppm) or Fe (ppm) for all of the samples collected from St Audrie's Bay and Lyme Regis. Each point represents an individual sample and the grey squares indicate the samples that are within the Mn and Fe thresholds used in the van de Schootbrugge *et al.* (2007) oyster study (Mn: < 110ppm; Fe: < 280ppm).

There is an acceptable threshold for oxygen and carbon isotope values which is recognised as -2.8‰ and values above this are recognised as

outliers (e.g., Morettini *et al.*, 2002; Nunn and Price, 2010). Values above this should be excluded as the data has been affected by late burial diagenetic overprinting (e.g., Morettini *et al.*, 2002; Nunn and Price, 2010). The cross-plots show a main cluster and also a number of significant outliers (Figure 4.2A–B). Samples with Fe and Mn values in excess of the accepted threshold values (Fe > 280 ppm and Mn > 110 ppm) also show $\delta^{18}\text{O}$ and $\delta^{13}\text{C}$ values beyond the accepted threshold (-2.8‰). This supports the conclusion that those samples must be recording diagenetic alteration, and should probably be discounted. When the $\delta^{18}\text{O}$ and $\delta^{13}\text{C}$ results from this investigation were plotted against the published $\delta^{18}\text{O}$ and $\delta^{13}\text{C}$ results from Lyme Regis and St Audrie's Bay (Figure 4.2C, van de Schootbrugge *et al.*, 2007 and Korte *et al.*, 2009), the majority of the values produced in this investigation show lower $\delta^{18}\text{O}$ and $\delta^{13}\text{C}$ values (Figure 4.2CD).

Several of the data sets from both locations, specifically the ostracod data sets, also show positive relationships between the $\delta^{18}\text{O}$ and $\delta^{13}\text{C}$ values. Positive relationships between the $\delta^{18}\text{O}$ and $\delta^{13}\text{C}$ in any of the data sets could indicate a level of diagenetic alteration (Malchus and Steuber, 2002). For the ostracod samples ($P < 0.02 / 0.01$), this could be due to difficulties in completely removing all of the sediment adhered to the shells coupled with the need to use the entire shell for analysis. This indicates the possibility that the primary geochemical signature identified in this investigation may not be as accurate as the previously published data and the best preserved samples used for this study may not be as well preserved as hoped. However, it should be taken into account that many of the results from this study do not stratigraphically overlap those previously published results (van

de Schootbrugge *et al.*, 2007 and Korte *et al.*, 2009). Therefore, the $\delta^{18}\text{O}$ and $\delta^{13}\text{C}$ values from further up the section may not be expected to match with those published results from lower in the section.

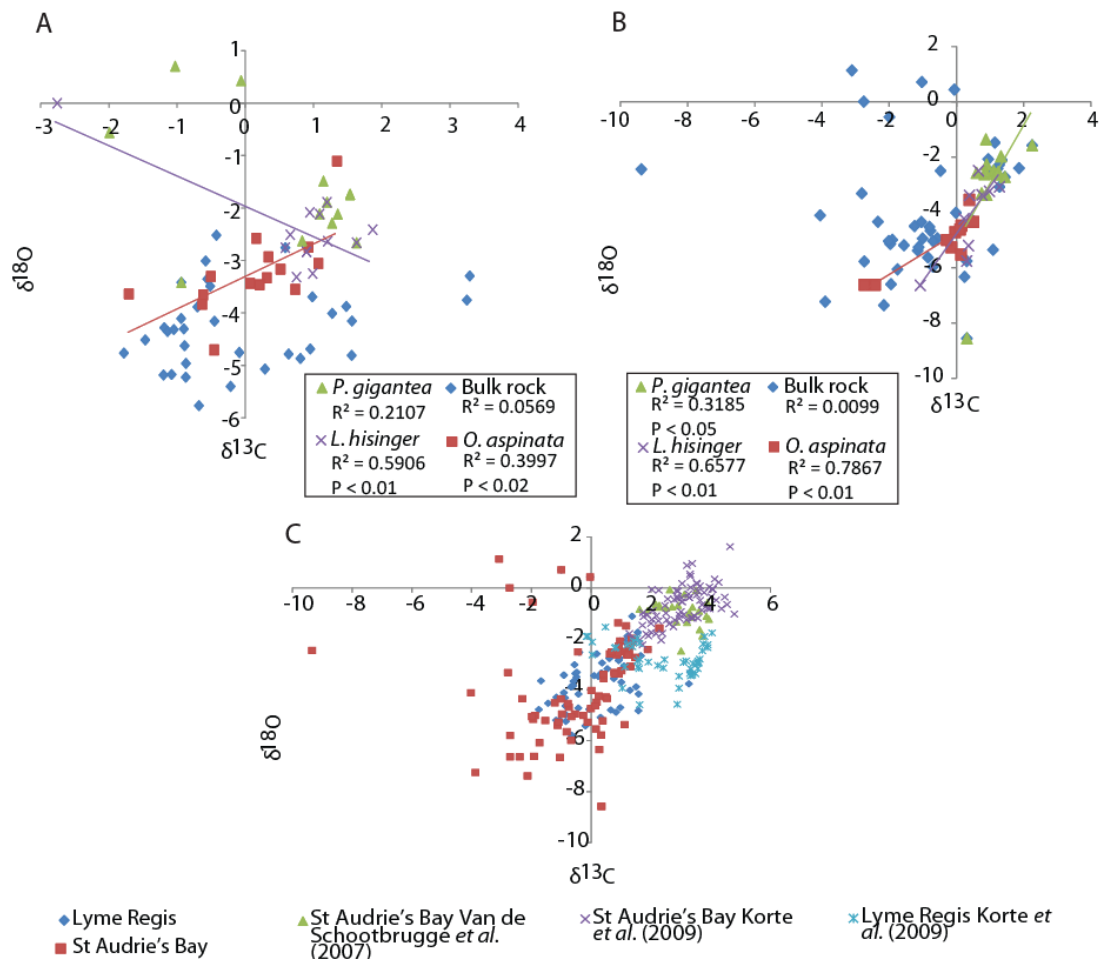


Figure 4.2: Cross plots between $\delta^{18}\text{O}$ and $\delta^{13}\text{C}_{\text{carb}}$ bulk rock and fossil samples from; (A) Lyme Regis; (B) St Audrie's Bay. Cross plots between $\delta^{18}\text{O}$ and $\delta^{13}\text{C}_{\text{carb}}$ from; (C) combined Lyme Regis and St Audrie's Bay data from this study; (D) the data from this study and the previously published southwest England data combined.

The $\delta^{18}\text{O}$ signal from calcitic shells is thought to indicate ambient palaeotemperatures, although it could also indicate variations in salinity (Korte *et al.*, 2009; Nunn and Price, 2010). Mg/Ca concentrations from calcitic shells on the other hand are also known to change with temperature but are unaffected by salinity, so could be used as a further

palaeotemperature proxy (Lear *et al.*, 2002; Nunn and Price, 2010). Several modern studies using extant species have indicated that although Mg/Ca ratios are not affected by salinity, they are affected by metabolic processes, thereby making them unreliable palaeotemperature proxies (van der Putten *et al.*, 2000; Freitas *et al.*, 2006; Korte *et al.*, 2009). Therefore, relationships between the Mg/Ca concentrations and $\delta^{18}\text{O}$ signal can indicate the temperature dependence of Mg/Ca in the calcitic shells.

Cross-plots of the Mg/Ca concentrations and $\delta^{18}\text{O}$ data from this study (all three species at both locations) show no significant relationships (Appendix 5: Figure A5.1a). This indicates several possibilities including: (1) Mg/Ca ratios are controlled by other factors not including temperature; (2) the $\delta^{18}\text{O}$ data is compromised by salinity while Mg/Ca is showing changes in temperature; and (3) both Mg/Ca and the $\delta^{18}\text{O}$ data are not showing changes in temperature (van der Putten *et al.*, 2000; Freitas *et al.*, 2006; van de Schootbrugge *et al.*, 2007; Korte *et al.*, 2009). The absence of any relationship between the bivalve Mg/Ca ratios and $\delta^{18}\text{O}$ values from both locations agrees with the data of Korte *et al.* (2009) but not that of van de Schootbrugge *et al.* (2007). However, the lack of any relationship could be due to variations in the size of the different data sets. Due to the removal of all the samples thought to be affected by diagenetic alteration this has meant that some of the sections have gaps in mineralogy and stable isotope data for certain species.

The isotope data from all the different data sets (i.e., *O. aspinata*, *P. gigantea*, *L. hisingeri*, Korte *et al.*, 2009 and van de Schootbrugge *et al.*, 2007), as well as between both locations, show some significantly different results. There

are a variety of reasons why this could be the case and this will be discussed below.

Firstly, the preservation of the samples from each data set might not be as good as initially thought and that this could be causing some of the higher palaeotemperature results. The studies by Korte *et al.* (2009) and van de Schootbrugge *et al.* (2007) indicate, in detail, how they selected the samples and removed any affected by poor preservation or apparent diagenetic alteration. There is a high level of confidence that their samples are well preserved because they give comparable results. The *O. aspinata*, *P. gigantea* and *L. hisingeri* samples were screened for poor preservation following the methods used by Korte *et al.* (2009) and van de Schootbrugge *et al.* (2007), but they do show higher palaeotemperature results. It is possible that, even after the removal of poorly preserved samples, the quality of preservation is not as good at the top of the section than at the bottom, within the Tr-J boundary interval. The *O. aspinata* samples show higher palaeotemperatures than the other species sampled which could be due to combining a number of individuals together for each sample. This may conceal the poor preservation of one, or more, of the individuals used. It could also indicate that the removal of sediment from the ostracod valves was not as successful as previously thought. This was a concern when the decision was made to use *O. aspinata* to generate an isotope record but every precaution was taken in the preparation of the material.

Secondly, the higher palaeotemperatures recorded by the *O. aspinata*, *P. gigantea* and *L. hisingeri* samples could be an accurate reflection of prevailing conditions near the top of the studied section at St Audrie's Bay,

and through out the Lyme Regis section, as there are no published records to use as a comparison. This is unlike the situation across the Tr-J boundary interval at St Audrie's Bay for which there are comparable data. Thirdly, Spero *et al.* (1998) identified from laboratory experiments that any selective dissolution of shells could affect the $\delta^{18}\text{O}$ values and produce a more positive value. This could explain some of the identified species specific differences in palaeotemperatures if the species are being affected by shell dissolution (Hautmann, 2004; Hautmann *et al.*, 2008). Fourthly, species migration during shell calcification is believed to complicate the temperature: $\delta^{18}\text{O}$ relationship. This is because the relationship requires an assumption that the shell was calcified in the same environment (Hemleben and Bijma, 1994; Spero *et al.*, 1998). However, the results from those studies were obtained using photosynthesising symbionts in plankton, whereas the results from this study were obtained using epifaunal or shallow infaunal species, which will more closely reflect the environment.

4.4 Relationships between the palaeotemperature curves and the atmospheric $p\text{CO}_2$ curves.

Many studies have suggested that atmospheric CO_2 is linked to changes in temperature and that high atmospheric $p\text{CO}_2$ would increase temperatures, as well as resulting in a degree of ocean acidification (e.g., Kump, 2000; Berner and Kothavala, 2001; Breecker *et al.*, 2010; Price *et al.*, 2013). However, the results of several studies are not consistent with this theory, suggesting temperature is independent of CO_2 variations and that instead galactic cosmic ray fluxes were the main drivers of climate change (e.g., Veizer *et al.*, 2000; Shaviv and Veizer, 2003; Royer *et al.*, 2004; Fletcher *et*

al., 2008). Elevated temperature and CO₂ could be just as detrimental to marine life singly as in combination (McElwain *et al.*, 1999; Houghton *et al.*, 2001; Palfy *et al.*, 2007; Korte *et al.*, 2009; Steinthordottir *et al.*, 2011). Fossil data (from this study and previously published) collected from both Lyme Regis and St Audrie's Bay show the palaeotemperature trend steadily increasing through the high $p\text{CO}_2$ interval and beyond, increasing even when $p\text{CO}_2$ levels decrease (Figures 4.4, 4.5). Using palaeotemperature data collected in this study and data extracted from published literature, each of the $p\text{CO}_2$ data sets were compared with the palaeotemperature data using linear regression models. However, this comparison showed no discernible relationships between the published atmospheric $p\text{CO}_2$ and the palaeotemperatures recorded in this study, or those previously published, through the Tr-J boundary interval (Appendix 5: Tables A5.5-A5.10, Figures A5.1-A5.3).

Since none of the different high palaeotemperature data sets show any relationships with the high $p\text{CO}_2$ data, it could be suggested that the $\delta^{18}\text{O}$ record used to produce the palaeotemperature curve is not recording changes in temperature alone, but also changes in salinity or variations in other environmental factors (van de Schootbrugge *et al.*, 2007; Korte *et al.*, 2009; Nunn and Price, 2010). The absence of any relationship between high palaeotemperature and high $p\text{CO}_2$ could also be due, in at least some cases, to the low numbers of correlatable data points available which, when using previously published data, was uncontrollable (Figures 4.3, 4.4; Appendix 5: Tables A5.5-A5.10, Figures A5.1-A5.3). It is also possible that for either one or a combination of the methods used, the correlations between high

palaeotemperature and high $p\text{CO}_2$ are incorrect or the basic assumptions are incorrect. However, errors caused by the basic assumptions being incorrect are unlikely. Errors from the correlation of published data to the logs generated in this study are possible due to the lack of precise biostratigraphical information and adequate tie-points. Until significant improvements are made to definitively position the pre-existing terrestrial data points within the marine successions examined in this study, a degree of variance between data points is unavoidable. Even though no relationships were detected between these two factors, independently one or both of these factors could still cause a significant detrimental impact on the shells of *L. hisingeri*, *P. gigantea* and *O. aspinata* through the Tr-J boundary interval.

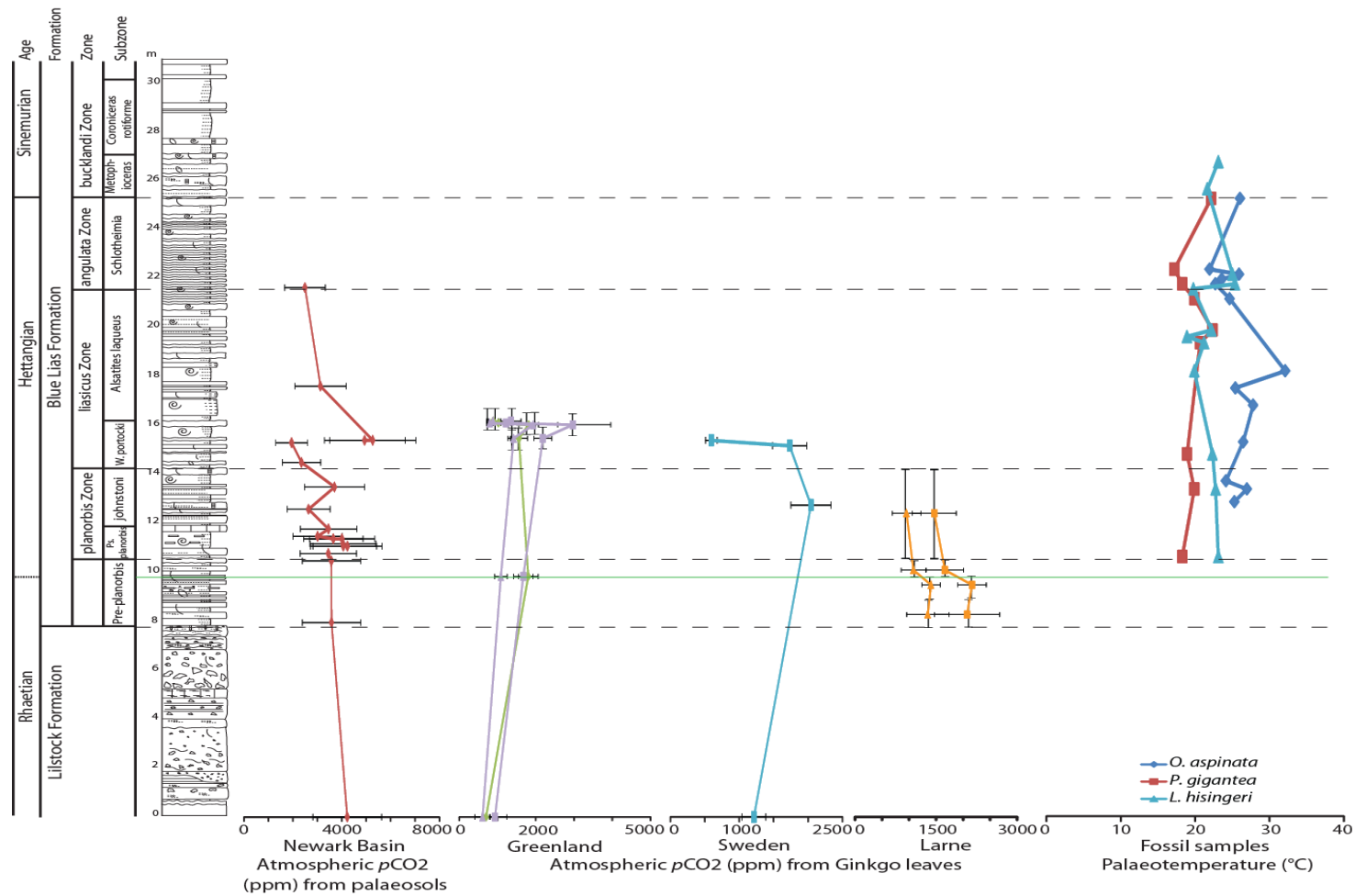


Figure 4.3: Atmospheric $p\text{CO}_2$ curves from the Newark Basin (palaeosol data), Greenland, Sweden and Larne (Ginkgo leaves data) correlated to the Lyme Regis fossil palaeotemperature curves (McElwain *et al.*, 1999; Korte *et al.*, 2009; Schaller *et al.*, 2011; Steinthorsdottir *et al.*, 2011). Green line: Tr-J boundary.

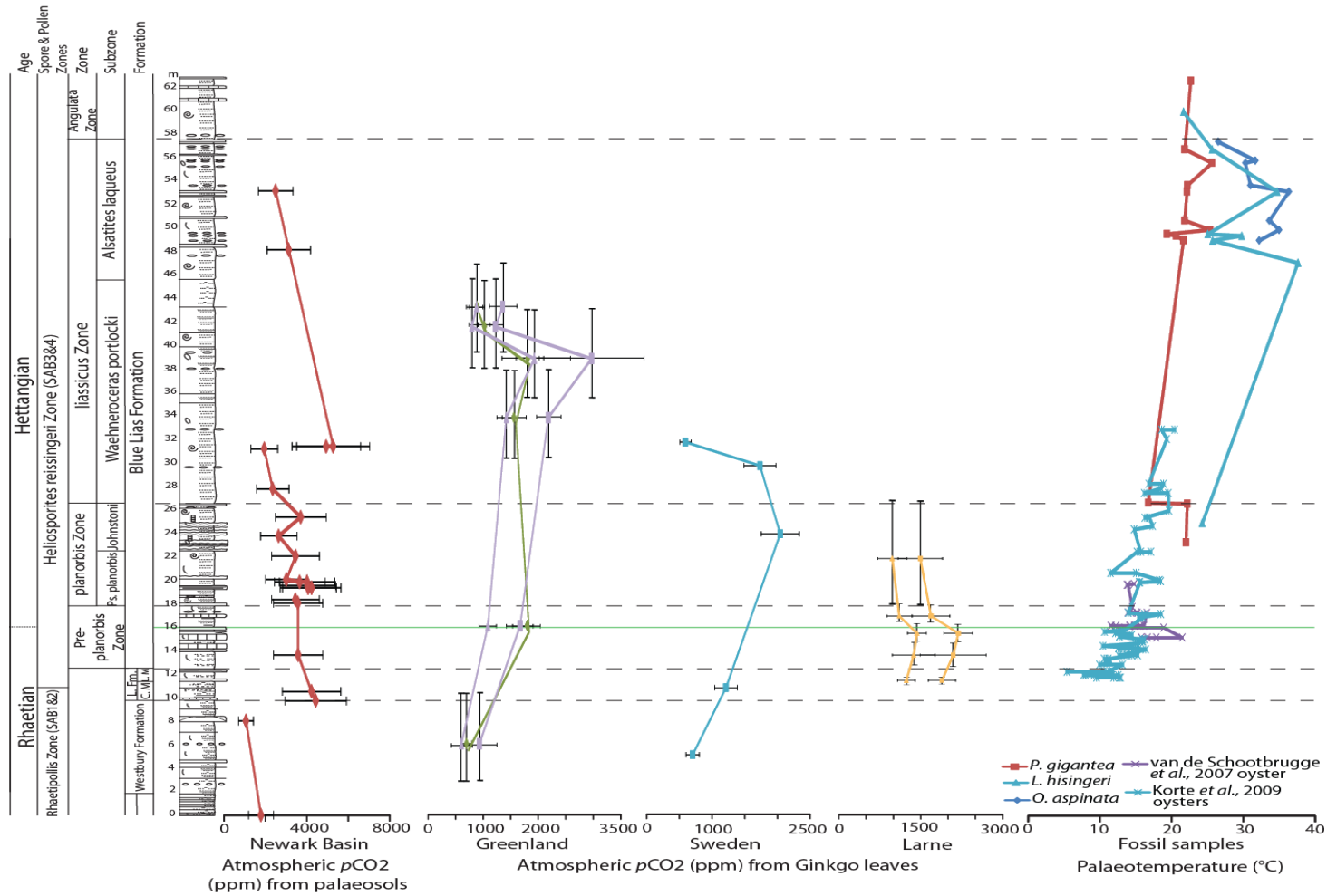


Figure 4.4: Atmospheric pCO₂ curves from the Newark Basin (palaeosol data), Greenland, Sweden and Larne (Ginkgo leaves data) correlated to the St Audrie's Bay fossil palaeotemperature curves (McElwain *et al.*, 1999; van de Schootbrugge *et al.*, 2007; Korte *et al.*, 2009; Schaller *et al.*, 2011; Steinhorsdottir *et al.*, 2011). Green line: Tr-J boundary; Lilstock Formation (L. Fm); Cotham Member (C.M); Langport Member (L.M).

4.5 Relationships between the $p\text{CO}_2$ data and the morphometric data.

All of the possible correlations between shell size or thickness of the three species from either location and the various $p\text{CO}_2$ studies were tested using linear regression models. There are 3 linear regression models for each $p\text{CO}_2$ data set displaying the minimum, maximum and mean $p\text{CO}_2$ values. Therefore, each linear regression model displays the relationship between either the minimum, maximum or mean $p\text{CO}_2$ data from one of the $p\text{CO}_2$ studies against the minimum, maximum, mean or range of shell size data. Where all of the data sets displayed on a whole graph showed no significant correlations, those graphs are presented in Appendix 5; Tables A5.11-A5.44 and Figures A5.4-A5.15. The morphometric data from this study was correlated separately to the minimum, maximum and mean $p\text{CO}_2$ data. They were investigated because it was possible that the morphometric data may only show a relationship to an extreme $p\text{CO}_2$ value (e.g., minimum or maximum) rather than the mean due to each species' differing ability to cope during adverse conditions.

4.5.2 *L. hisingeri*

Other than those relationships presented in Table 4.3 (Figures 4.5–4.6) there were no significant relationships detected between the shell size, Ca or Mg of *L. hisingeri* (from separate beds at either location) and the minimum, maximum or mean $p\text{CO}_2$ levels. The absence of any relationships between the St Audrie's Bay *L. hisingeri* geometric shell size and the various $p\text{CO}_2$ curves could be due to the limited number of $p\text{CO}_2$ data points from the section in Greenland, Sweden and Larné.

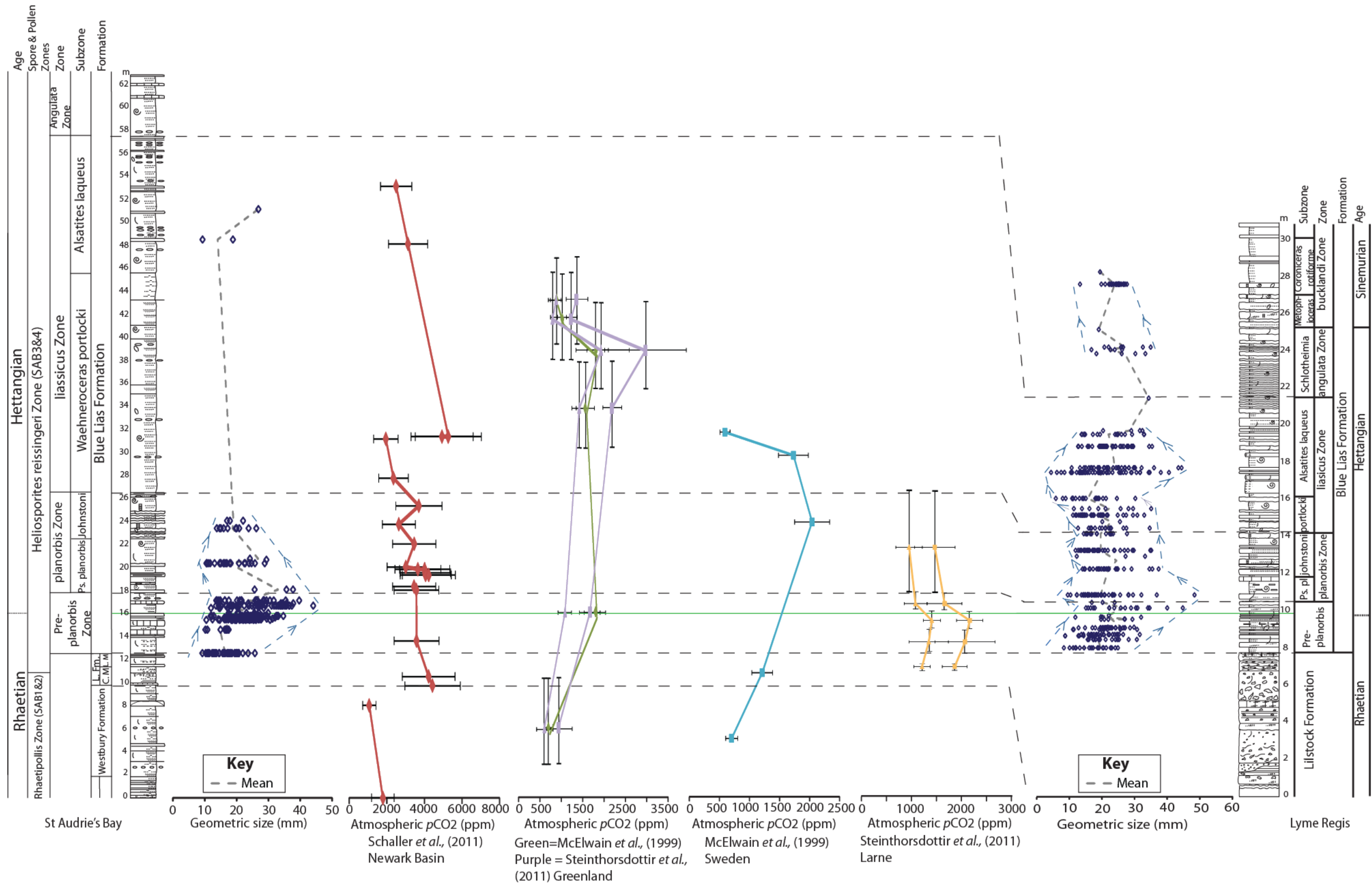


Figure 4.5: Atmospheric $p\text{CO}_2$ data from the Newark Basin (palaeosol samples), Greenland, Sweden and Larne (Ginkgo leaf samples) correlated to *L. hisingeri* geometric shell size from St Audrie's Bay and Lyme Regis (McElwain *et al.*, 1999; Schaller *et al.*, 2011; Steinthorsdottir *et al.*, 2011). The green line highlights the position of the Tr-J boundary; Ps. planorbis subzone (Ps. pl); W. portlocki (portlocki); Lilstock Formation (L. Fm); Cotham Member (C.M); Langport Member (L.M). Ca and Mg values (mg/L) were correlated to the atmospheric $p\text{CO}_2$ curves but as they showed no relationships to each other they are not visually documented on this diagram.

Species	Location	Relationships between shell geometry and $p\text{CO}_2$	No.	P	Figure
<i>L. hisingeri</i>	Lyme Regis	Positive trend between mean shell geometry and max. $p\text{CO}_2$ (Sweden data).	4	< 0.05	4.6D
<i>L. hisingeri</i>	Lyme Regis	Positive trend between mean geometric shell size and min. $p\text{CO}_2$ (Sweden data).	4	< 0.05	4.6A
<i>L. hisingeri</i>	Lyme Regis	Positive trend between mean geometric shell geometry and mean $p\text{CO}_2$ (Sweden data).	4	< 0.05	4.6C
<i>L. hisingeri</i>	Lyme Regis	Positive trend between 95 th percentile range of geometric shell geometry and max. $p\text{CO}_2$ (Astartekløft data: Carboniferous standard).	3	< 0.05	4.6B
<i>L. hisingeri</i>	Lyme Regis	Positive trend between 95 th percentile range of geometric shell geometry and max. $p\text{CO}_2$ (Astartekløft data: modern standard).	3	< 0.05	4.6E

Table 4.3: Significant relationships detected between the geometric size of *L. hisingeri* and minimum, maximum or mean $p\text{CO}_2$ levels (Figure 4.5-4.6). $p\text{CO}_2$ data from the Sweden and Astartekløft studies were conducted using Ginkgo leaves.

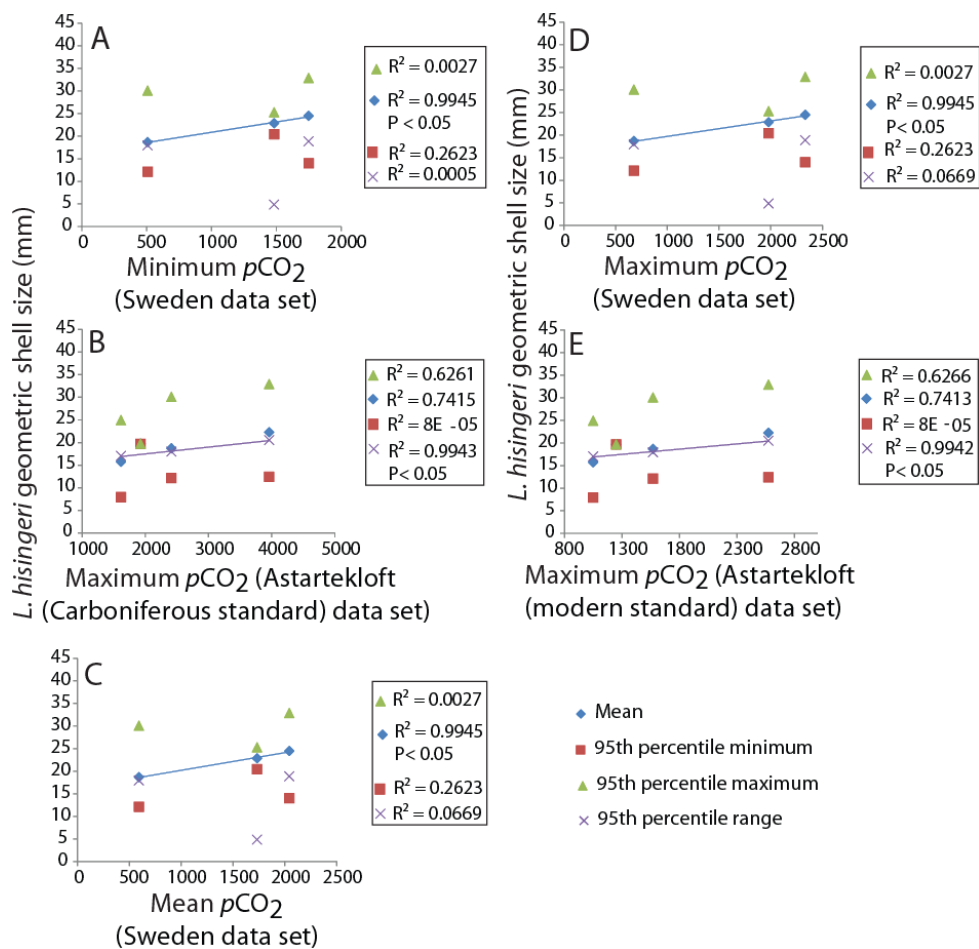


Figure 4.6: Linear regression models with positive trend lines showing one significant relationship between the geometric size of *L. hisingeri* at Lyme Regis (A-E) and the minimum, maximum or mean $p\text{CO}_2$ levels on each graph (Table 4.3). Trend lines are only included on data sets where a significant relationship was identified, however those data sets with no significant relationship were still included on the graph.

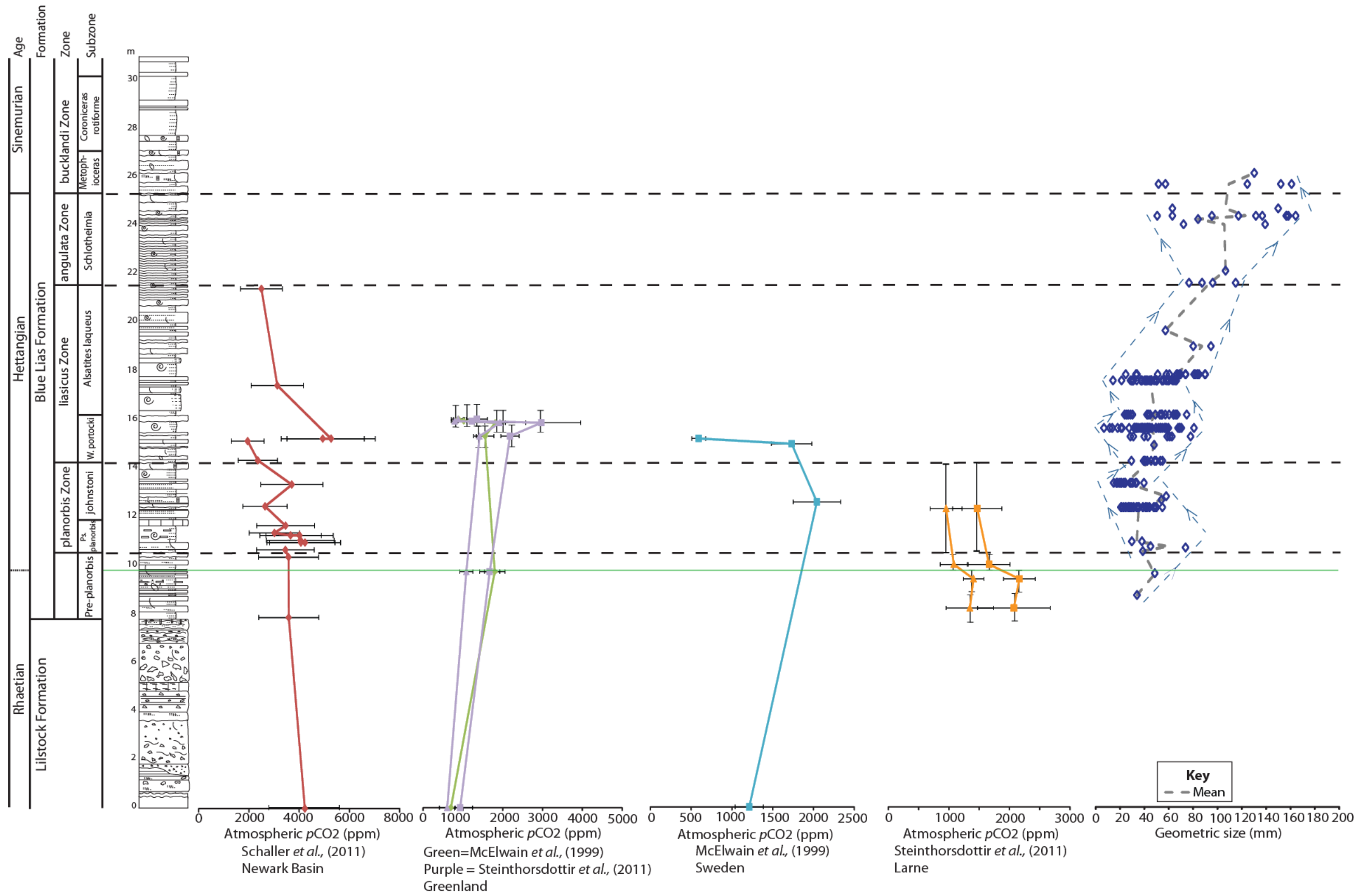


Figure 4.7: Atmospheric $p\text{CO}_2$ data from the Newark Basin (palaeosol samples), Greenland, Sweden and Larne (Ginkgo leaf samples) correlated to the *P. gigantea* geometric shell size from Lyme Regis (McElwain *et al.*, 1999; Schaller *et al.*, 2011; Steinthorsdottir *et al.*, 2011). Ca and Mg values (mg/L) were correlated to the atmospheric $p\text{CO}_2$ curves but as they showed no relationships to each other they are not visually documented on this diagram.

4.5.3 *P. gigantea*

Other than those relationships presented in Tables 4.4 (Figures 4.7–4.8) there were no relationships detected between the shell size, Ca or Mg of *P. gigantea* (from separate beds at either location) and the minimum, maximum or mean $p\text{CO}_2$ levels.

Species	Location	Relationships between shell geometry and $p\text{CO}_2$	No.	P	Figure
<i>P. gigantea</i>	Lyme Regis	Positive trend between 95 th percentile min. shell geometry and max. $p\text{CO}_2$ (Sweden data).	3	< 0.05	4.8C
<i>P. gigantea</i>	Lyme Regis	Positive trend between 95 th percentile min. shell geometry and min. $p\text{CO}_2$ (Sweden data).	3	< 0.05	4.8A
<i>P. gigantea</i>	Lyme Regis	Positive trend between 95 th percentile min. shell geometry and mean $p\text{CO}_2$ (Sweden data).	3	< 0.05	4.8B

Table 4.4: Significant relationships detected between the geometric size of *P. gigantea* and the minimum, maximum or mean $p\text{CO}_2$ levels (Figures 4.7-4.8). $p\text{CO}_2$ data from the Sweden study was conducted using Ginkgo leaves.

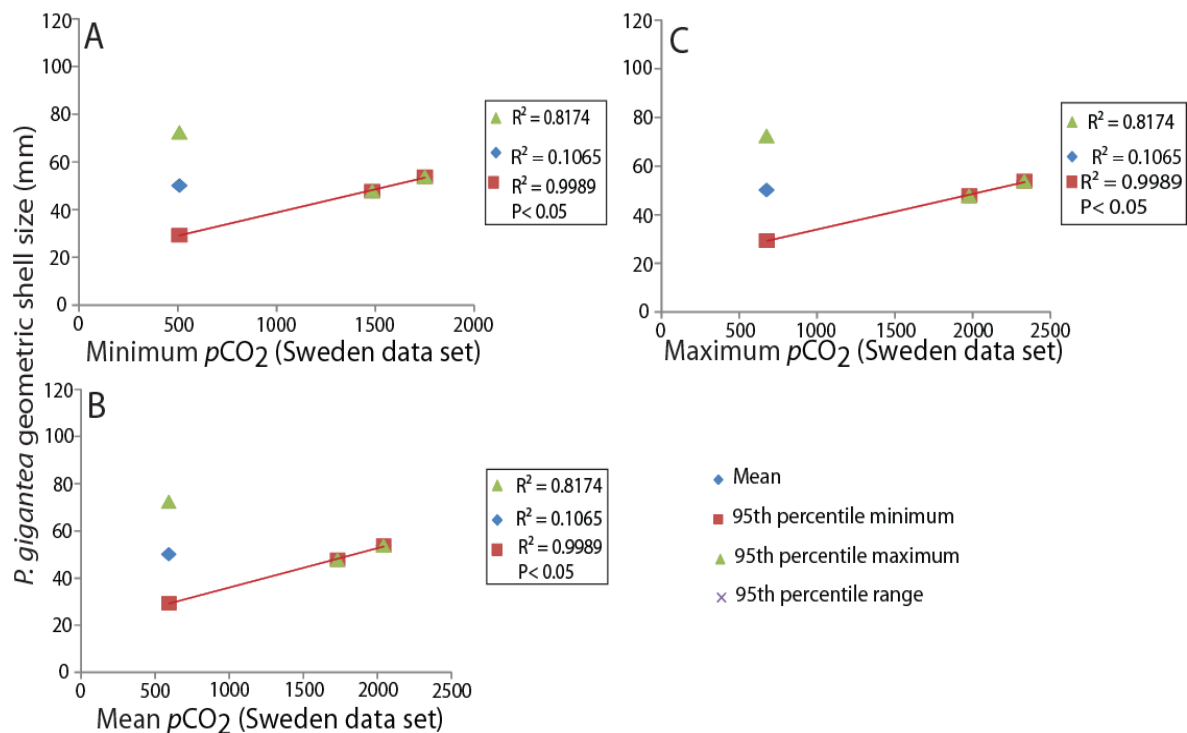


Figure 4.8: Linear regression models with positive trend lines showing one significant relationship between the geometric size of *P. gigantea* at Lyme Regis (A-C) and the minimum, maximum or mean $p\text{CO}_2$ levels on each graph (Table 4.4). Trend lines are only included on data sets where a significant relationship was identified, however those data sets with no significant relationship were still included on the graph.

4.5.4 *O. aspinata*

Other than those relationships presented in Tables 4.5A-B (Figures 4.9–4.11) there were no relationships detected between the shell size, shell thickness, Ca or Mg of *O. aspinata* (from separate beds at either location) and the minimum, maximum or mean $p\text{CO}_2$ levels.

Species	Location	Relationships between shell geometry and $p\text{CO}_2$	No.	P	Figure
<i>O. aspinata</i>	Lyme Regis	Negative trend between mean shell geometry and min. $p\text{CO}_2$ (Astartekløft data: Carboniferous standard).	4	< 0.01	4.10E
<i>O. aspinata</i>	Lyme Regis	Negative trend between mean shell geometry and min. $p\text{CO}_2$ (Astartekløft data: modern standard).	4	< 0.01	4.10F
<i>O. aspinata</i>	Lyme Regis	Negative trend between mean shell geometry and min. $p\text{CO}_2$ (Larne data: Carboniferous standard).	4	< 0.02	4.10C
<i>O. aspinata</i>	Lyme Regis	Negative trend between mean shell geometry and min. $p\text{CO}_2$ (Larne data: modern standard).	4	< 0.02	4.10D
<i>O. aspinata</i>	St Audrie's Bay	Positive trending 95 th percentile min. shell geometry and max. $p\text{CO}_2$ (Larne data: Carboniferous standard).	5	< 0.05	4.10A
<i>O. aspinata</i>	St Audrie's Bay	Positive trend between 95 th percentile min. shell geometry and max. $p\text{CO}_2$ (Larne data: modern standard).	5	< 0.05	4.10B

Table 4.5a: Significant relationships detected between the geometric size of *O. aspinata* at both locations and the minimum, maximum or mean $p\text{CO}_2$ levels (Figures 4.9–4.11). $p\text{CO}_2$ data from the Astartekløft and Larne studies were conducted using Ginkgo leaves.

Species	Location	Relationships between shell thickness and $p\text{CO}_2$	No.	P	Figure
<i>O. aspinata</i>	Lyme Regis	Positive trend between mean shell thickness and max. $p\text{CO}_2$ (Larne data: Carboniferous standard).	4	< 0.02	4.11G
<i>O. aspinata</i>	Lyme Regis	Positive trend between mean shell thickness and max. $p\text{CO}_2$ (Larne data: modern standard).	4	< 0.02	4.11H
<i>O. aspinata</i>	Lyme Regis	Positive trend between 95 th percentile max. shell thickness and mean $p\text{CO}_2$ (Greenland data).	6	< 0.05	4.11I
<i>O. aspinata</i>	Lyme Regis	Positive trend between 95 th percentile max. shell thickness and max. $p\text{CO}_2$ (Greenland data).	6	< 0.05	4.11F
<i>O. aspinata</i>	Lyme Regis	Positive trend between 95 th percentile max. shell thickness and min. $p\text{CO}_2$ (Greenland data).	6	< 0.05	4.11C
<i>O. aspinata</i>	St Audrie's Bay	Negative trend between 95 th percentile range of shell thickness and mean $p\text{CO}_2$ (Larne data: Carboniferous standard).	5	< 0.05	4.11D
<i>O. aspinata</i>	St Audrie's Bay	Negative trend between 95 th percentile range of shell thickness and mean $p\text{CO}_2$ (Larne data: modern standard).	5	< 0.05	4.11E
<i>O. aspinata</i>	St Audrie's Bay	Negative trend between 95 th percentile range of shell thickness and max. $p\text{CO}_2$ (Larne data: Carboniferous standard).	5	< 0.05	4.11A
<i>O. aspinata</i>	St Audrie's Bay	Negative trend between 95 th percentile range of shell thickness and maximum $p\text{CO}_2$ (Larne data: modern standard).	5	< 0.05	4.11B

Table 4.5b: Significant relationships detected between the shell thickness of *O. aspinata* at both locations and the minimum, maximum or mean $p\text{CO}_2$ levels (Figures 4.9–4.11). $p\text{CO}_2$ data from the Larne and Greenland studies were conducted using Ginkgo leaves.

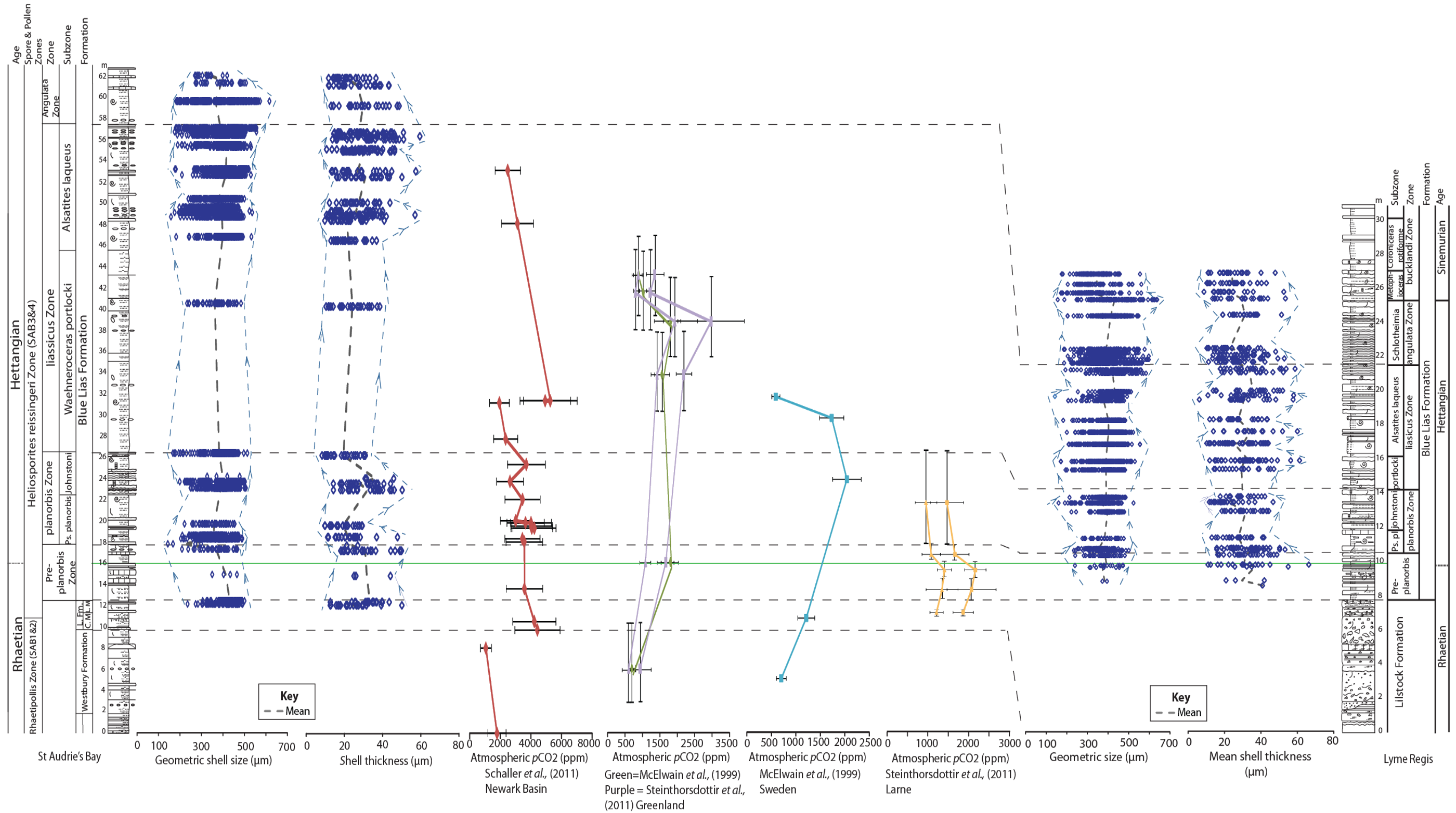


Figure 4.9: Atmospheric $p\text{CO}_2$ data from the Newark Basin (palaeosol samples), Greenland, Sweden and Larne (Ginkgo leaf samples) correlated to the *O. aspinata* geometric shell size from St Audrie's Bay and Lyme Regis (McElwain *et al.*, 1999; Schaller *et al.*, 2011; Steinhorsdottir *et al.*, 2011). The green line highlights the Tr-J boundary; Ps. planorbis subzone (Ps. pl); W. portlocki (portlocki); Lilstock Formation (L. Fm); Cotham Member (C.M); Langport Member (L.M). Ca and Mg values (mg/L) were correlated to the atmospheric $p\text{CO}_2$ curves but as they showed no relationships to each other they are not visually documented on this diagram.

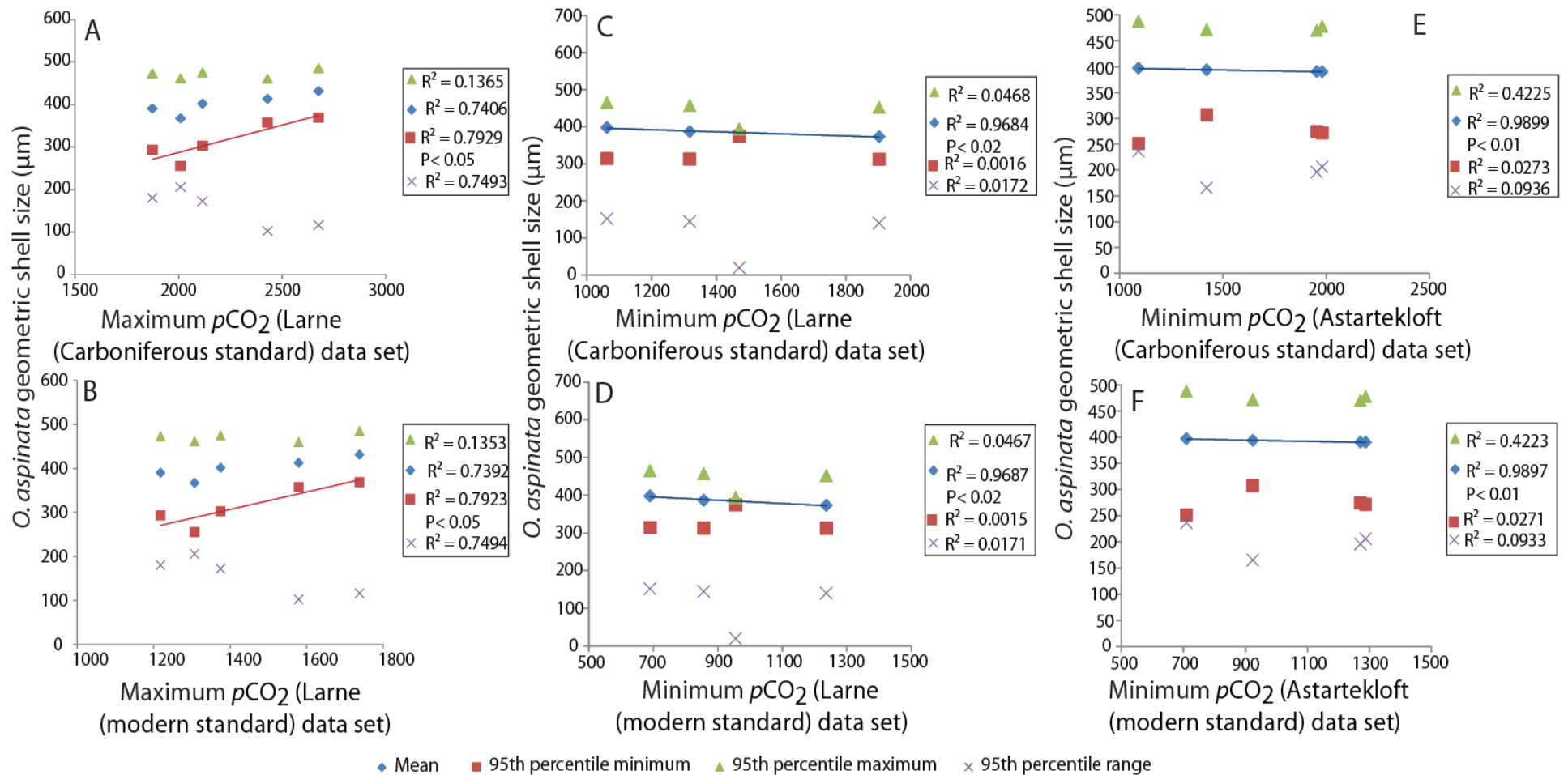


Figure 4.10: Linear regression models with positive and negative trend lines showing one significant relationship between the geometric size of *O. aspinata* from Lyme Regis (C, D, E, F) and St Audrie's Bay (A, B) and the minimum, maximum or mean pCO₂ levels on each graph (Table 4.5A). Trend lines are only included on data sets where a significant relationship was identified, however those data sets with no significant relationship were still included on the graph.

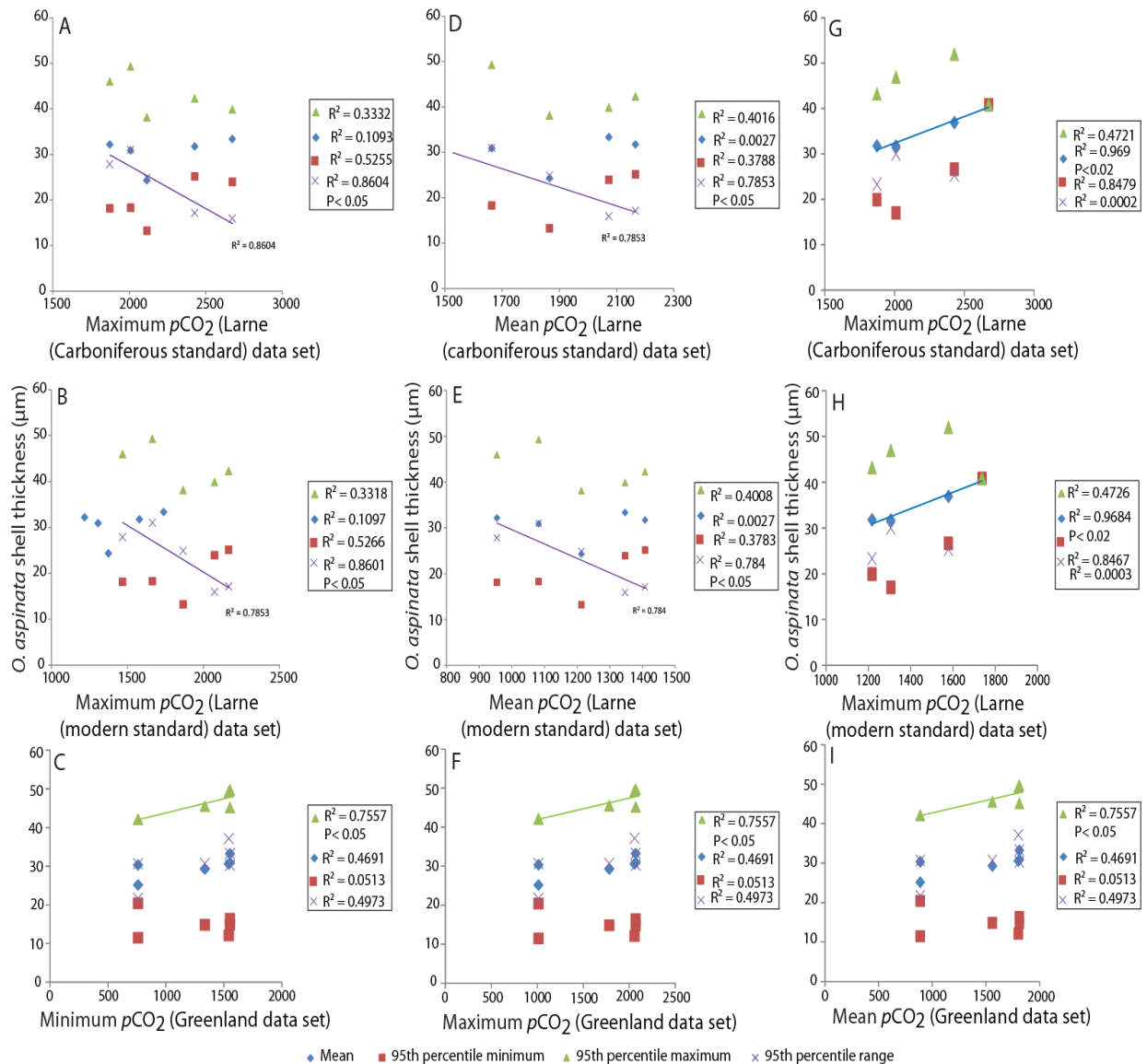


Figure 4.11: Linear regression models with positive and negative trend lines showing one significant relationship between the shell thickness of *O. aspinata* from Lyme Regis (C, F, G, H, I) and St Audrie's Bay (A, B, D, E) and the minimum, maximum or mean $p\text{CO}_2$ levels on each graph (Table 4.5B). Trend lines are only included on data sets where a significant relationship was identified, however those data sets with no significant relationship were still included on the graph.

4.5.5 Implications of relationships identified between $p\text{CO}_2$ and morphometric data.

Select geometric shell size and shell thickness data from the three species show significant relationships to the $p\text{CO}_2$ data produced from studies using Ginkgo leaves. However, no significant relationships were identified to the

$p\text{CO}_2$ data produced using palaeosols from the Newark Basin. Those relationships identified are using a very small number of data points (< 5). It was thought that the limited number of data points (< 5) in the Greenland, Sweden, Larne and Astartekløft $p\text{CO}_2$ curves may prevent the detection of any relationships between $p\text{CO}_2$ and geometric size, while the larger $p\text{CO}_2$ data set from the Newark Basin could show a more robust statistical relationship. However, the opposite was identified, possibly due to one or all of the following: (1) the significantly higher $p\text{CO}_2$ values measured in the palaeosols from the Newark Basin than those observed from ginkgoalean leaves collected from the other locations; (2) the variability in the number of correlatable data points between the different $p\text{CO}_2$ studies; (3) the possibility that the Newark Basin correlation to the logs from this study is inaccurate, however, the correlation is limited by the available data and thus is the best correlation possible until further studies can improve it; and (4) that many of the $p\text{CO}_2$ data points from the Newark Basin show similar values through parts of the section unlike the other locations which show less detail but the overall trend.

Hautmann (2004) indicated that Triassic–Jurassic seawater calcium carbonate undersaturation was due to high atmospheric CO_2 decreasing the seawater pH. This caused a reduction in bivalve shell size and thickness because of the raised energy expenditure for the biomineralisation of the shells (Hautmann, 2004). However, the bivalve results from both locations in this investigation show size increased with increasing atmospheric CO_2 (Figures 4.5–4.8, Tables 4.3–4.4). In this study, only the *O. aspinata* mean geometric shell size data from Lyme Regis corresponds with Hautmann's

(2004) hypothesis as it records a negative relationship to the minimum estimates of $p\text{CO}_2$ values at Larne and Astartekløft (Figures 4.9–4.10, Table 4.4.5A). Since the original suggestion of Hautmann (2004), further studies have also indicated a possible short-lived ocean acidification event in the Tr-J boundary interval. These investigations have found that a variety of different taxa (e.g., foraminifera, corals, sponges and calcareous nanoplankton) all display a decline in carbonate weight and shell condition, increased shell dissolution (specifically in species composed mainly of aragonite) and declining carbonate production in this interval (van de Schootbrugge *et al.*, 2007; Hautmann *et al.*, 2008; Veron, 2008; Bernasconi *et al.*, 2009; Clémence *et al.*, 2010; Kiessling and Simpson, 2011; Črne *et al.*, 2011; Greene *et al.*, 2012). However, Clémence and Hart (2013) did record a large number of aragonitic taxa throughout the Tr-J boundary interval in South-west England.

Aragonite and high-Mg calcite skeletons are known to be more soluble during periods of ocean acidification (Tucker and Wright, 1990). These differing rates of solubility led Hautmann *et al.* (2008) to speculate that increased atmospheric CO_2 during the Late Triassic caused decreased seawater pH, which specifically affected the aragonitic and high-Mg calcite skeletons of various species while alive. Decreasing seawater pH is known to reduce shell calcification in living individuals and cause shell dissolution, thinning and overall poor shell condition in both living and dead individuals (Hautmann *et al.*, 2008). However, in this present study there was no shell dissolution or poor shell condition due to ocean acidification (Chapter 3). Neither were there any relationships between the Ca or Mg content of the

shells and any of the $p\text{CO}_2$ curves for any of the species (Appendix 5: Tables A5.23 – A5.36; Figures A5.4 – A5.5, A5.8, A5.1 – A5.11).

Any poor shell condition found was identified mostly in the two bivalve species and was attributed to modern day weathering of the shells once exposed on the coast, rather than past ocean acidification. This lack of shell dissolution could be for several reasons including; (1) the site of calcification in these species occurs in areas not directly exposed to seawater: bivalves can control shell mineralization through their internal fluids which have a different chemistry to the surrounding seawater and could well be less acidic; and (2) the seawater pH did not decline to detrimental levels (e.g., Carter *et al.*, 1998; Pörtner, 2008; Greene *et al.*, 2012). The absence of poor shell preservation could also be due to these species being able to protect their shell against dissolution but at a metabolic cost: e.g., stunted size (see Findlay *et al.*, 2009). Much of the preservation data from this investigation (both bivalve and ostracod relationships) however, showed limited discernible shell damage from ocean acidification corresponding with a change in size. Kiessling *et al.* (2007) also found no evidence of extinction selectivity in skeletal mineralogy to support a biocalcification crisis in a number of Tr-J boundary interval benthic marine taxa.

Trends in bivalve shell thickness recorded by Mander *et al.* (2008) presented no significant shell thinning but instead shell thickening and therefore do not support Hautmann's (2004) hypothesis of a biocalcification crisis. The mean and 95th percentile maximum *O. aspinata* shell thickness for Lyme Regis show positive relationships to the Larne and Greenland $p\text{CO}_2$ curves, supporting Mander *et al.*'s (2008) results and contradicting Hautmann's

(2004) hypothesis. Increased shell thickness recorded times of high $p\text{CO}_2$ conditions could possibly be a survival adaptation during a high $p\text{CO}_2$ interval, even though it would require a large amount of energy which could come at a metabolic cost to other functions (Wood *et al.*, 2008; Findlay *et al.*, 2009, 2011). The *O. aspinata* data from St Audrie's Bay show reduced valve thickness during the high $p\text{CO}_2$ interval, which is based on data from the Larne succession. This tends to support the hypothesis of a biocalcification crisis.

It is possible that the lack of support for Hautmann's (2004) biocalcification hypothesis may indicate that the effects of ocean acidification are extremely species specific, as is found in modern experiments (Fabry *et al.*, 2008; Kurihara *et al.*, 2008; Doney *et al.*, 2009; Kroeker *et al.*, 2010; Hendriks *et al.*, 2010; Andersson *et al.*, 2011; Greene *et al.*, 2012) and the species investigated in the present study reacted differently to those studied by Hautmann (2004). Equally it could be that ocean acidification was less significant in southwest England than other marine locations due to other environmental factors having a more substantial effect on the species studied. This could also explain why Mander *et al.* (2008) also found no biocalcification crisis due to grouping together all of the bivalve species identified at St Audrie's Bay. The concept of significant variations in the physiological responses between different marine species to ocean acidification has been identified in many laboratory ocean acidification experiments, indicating that one hypothesis such as that of Hautmann (2004) may not be valid for all calcareous marine organisms and that it is better to

study at species level rather than group several species together (e.g., Fabry *et al.*, 2008; Kurihara *et al.*, 2008; Greene *et al.*, 2012).

4.6 Relationships between $\delta^{13}\text{C}$ and morphometric data from each species.

All of the possible correlations between shell size or thickness of the three species from either location and the various $\delta^{13}\text{C}$ studies were illustrated on linear regression models and tested for significance. Where all of the data sets displayed on a whole graph showed no significant correlations, those graphs are presented in Appendix 5: Tables A5.45–A5.60, Figure A5.16–A5.27.

4.6.2 *L. hisingeri*

No significant relationships were detected between shell size, shell thickness, Ca or Mg (at either location) and $\delta^{13}\text{C}$ for *L. hisingeri* (Figures 4.12–4.13).

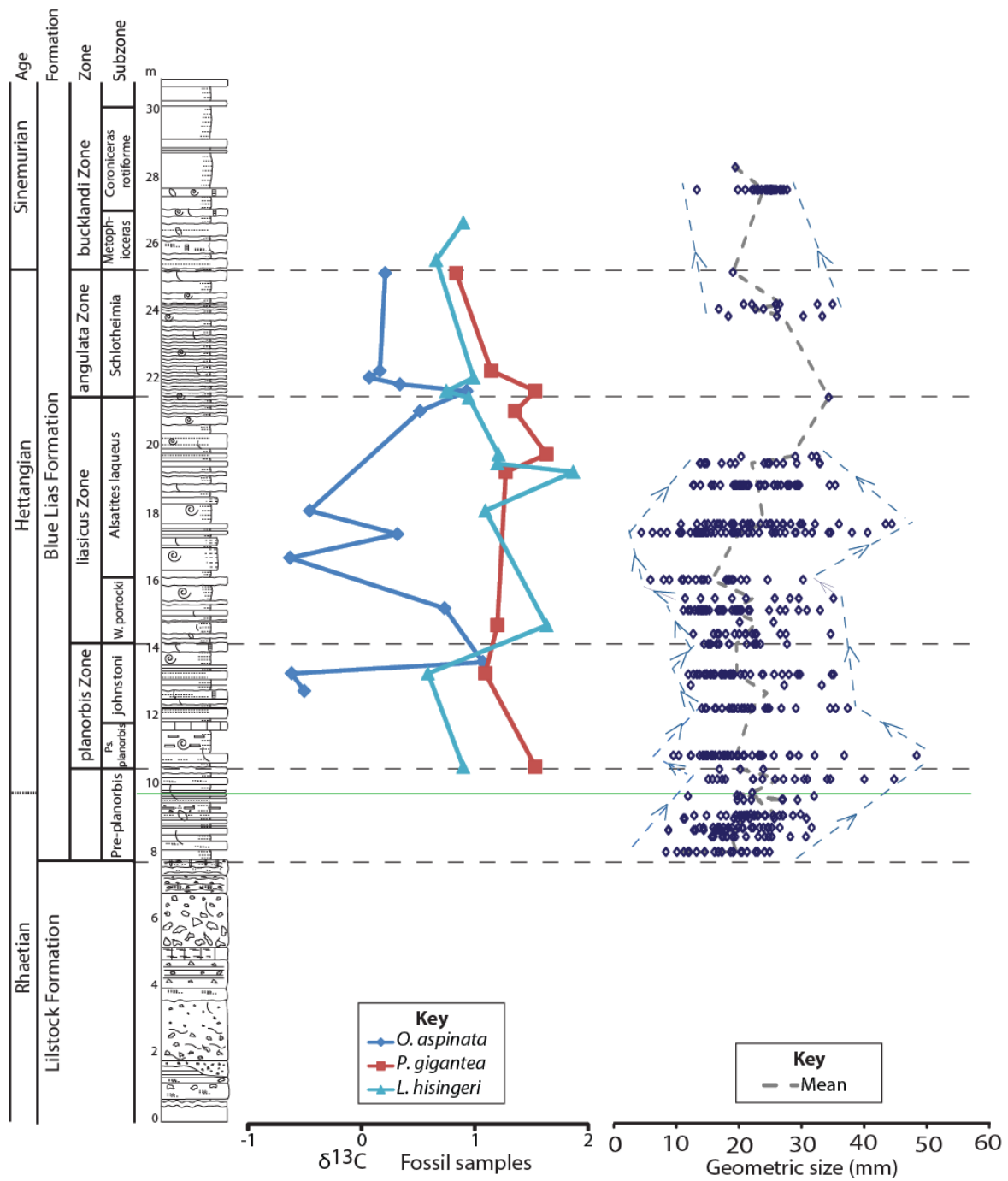


Figure 4.12: $\delta^{13}\text{C}$ curve from fossil samples (from this study) correlated to the Lyme Regis stratigraphy and *L. hisingeri* geometric shell size. The green line highlights the Tr-J boundary interval; Ps. planorbis subzone (Ps. pl); W. portlocki (portlocki). Ca and Mg values (mg/L) were correlated $\delta^{13}\text{C}$ to the curves but as they showed no relationships to each other they are not visually documented on this diagram.

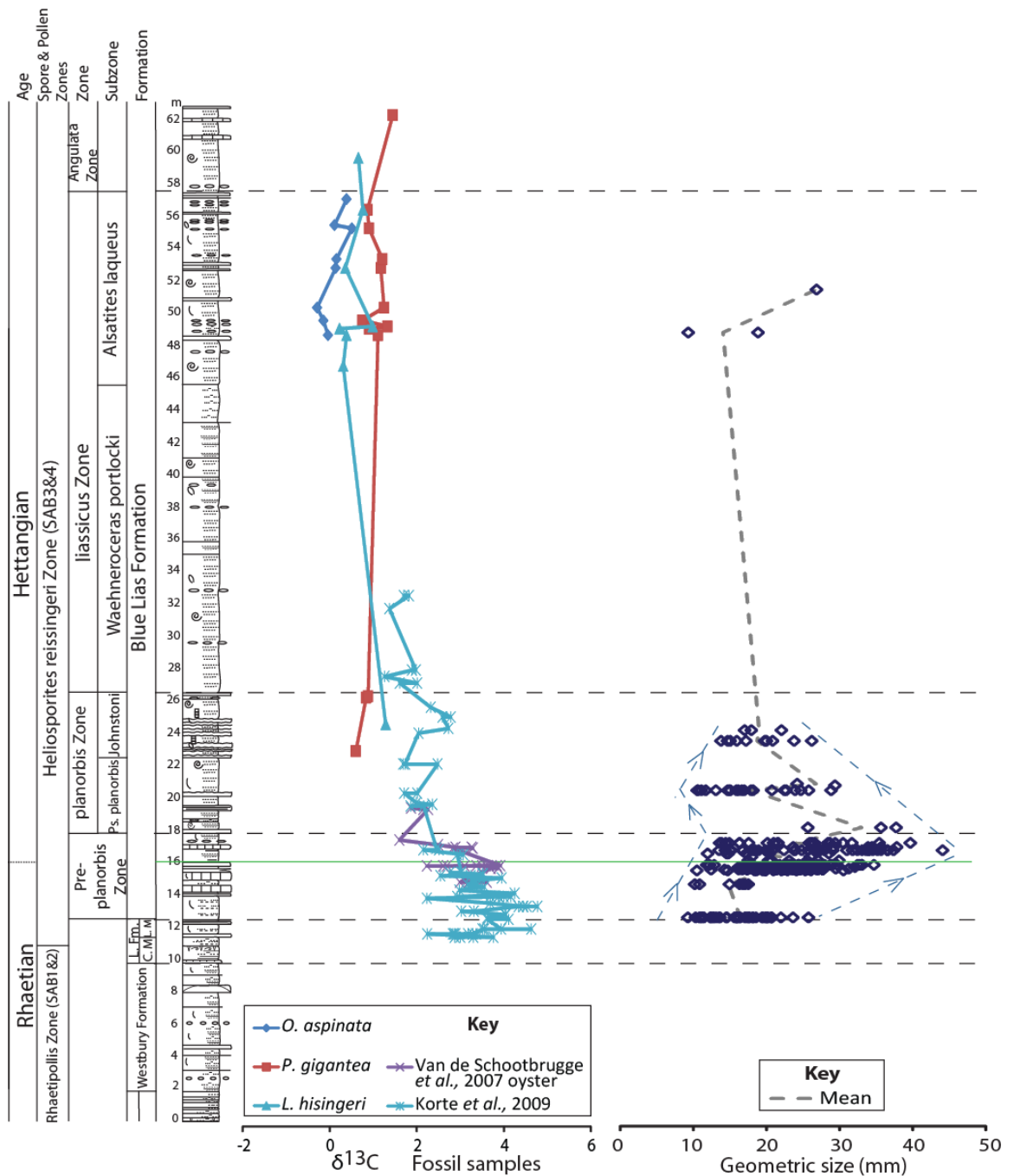


Figure 4.13: $\delta^{13}C$ curve from fossil samples (van de Schootbrugge *et al.*, 2007; Korte *et al.*, 2009 and this study) correlated to the St Audrie's Bay stratigraphy and *L. hisingeri* geometric shell size. The green line highlights the Tr-J boundary interval; Llistock Formation (L. Fm); Cotham Member (C.M); Langport Member (L.M). Ca and Mg (mg/L) values were correlated to the $\delta^{13}C$ curves but as they showed no relationships to each other they are not visually documented on this diagram.

4.6.3 *P. gigantea*

No relationships detected between shell size, shell thickness, Ca or Mg (at either location) and $\delta^{13}C$ for *P. gigantea* (Figure 4.14).

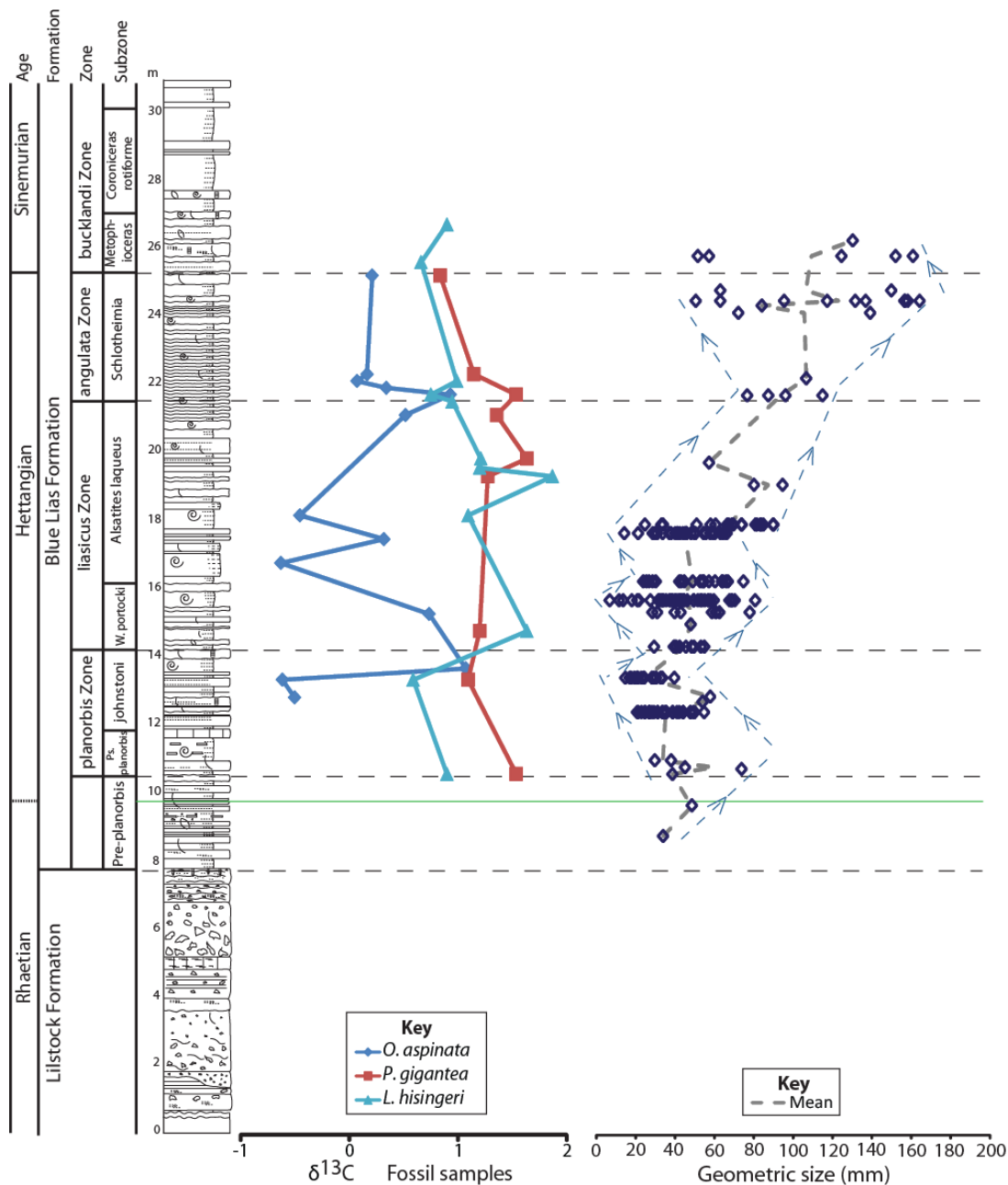


Figure 4.14: $\delta^{13}\text{C}$ curve from fossil samples (from this study) correlated to the Lyme Regis stratigraphy and *P. gigantea* geometric shell size. The green line highlights the Tr-J boundary interval; Ps. planorbis subzone (Ps. pl); W. portlocki (portlocki). Ca and Mg (mg/L) values were correlated to the $\delta^{13}\text{C}$ curves but as they showed no relationships to each other they are not visually documented on this diagram.

4.6.4 *O. aspinata*

Other than those relationships presented in Tables 4.6A–4.6C (Figures 4.15–4.20), there were no significant relationships detected between shell size, shell thickness, Ca or Mg (at either location) and $\delta^{13}\text{C}$ for *O. aspinata*.

Species	Location	Relationships between shell geometry and $\delta^{13}\text{C}$ levels	N	P	Figure
<i>O. aspinata</i>	Lyme Regis	Positive trend between 95 th percentile minimum geometric shell size and $\delta^{13}\text{C}$ levels (<i>P. gigantea</i> data set).	9	< 0.05	4.15
<i>O. aspinata</i>	St Audrie's Bay	Positive trend between 95 th percentile maximum geometric shell size and $\delta^{13}\text{C}$ levels (<i>O. aspinata</i> data set).	8	< 0.01	4.18
<i>O. aspinata</i>	St Audrie's Bay	Positive trend between Mean geometric shell size and $\delta^{13}\text{C}$ levels (Korte <i>et al.</i> (2009) data set).	8	< 0.05	4.18
<i>O. aspinata</i>	St Audrie's Bay	Positive trend between 95 th percentile minimum geometric shell size and $\delta^{13}\text{C}$ levels (van de Schootbrugge <i>et al.</i> (2007) data set).	5	< 0.05	4.18

Table 4.6a: Significant relationships detected between the geometric size of *O. aspinata* and the $\delta^{13}\text{C}$ levels (Figure 4.15–4.18).

Species	Location	Relationships between shell thickness and $\delta^{13}\text{C}$ levels	N	P	Figure
<i>O. aspinata</i>	Lyme Regis	Positive trend between 95 th percentile minimum shell thickness and $\delta^{13}\text{C}$ levels (<i>L. hisingeri</i> data set).	12	< 0.05	4.19

Table 4.6b: Significant relationships detected between the shell thickness of *O. aspinata* and the $\delta^{13}\text{C}$ levels (Figure 4.16–4.17, 4.19).

Species	Location	Relationships between shell mineralogy and $\delta^{13}\text{C}$ levels	N	P	Figure
<i>O. aspinata</i>	Lyme Regis	Negative trend between Ca levels and $\delta^{13}\text{C}$ levels (<i>P. gigantea</i> data set).	11	< 0.05	4.20
<i>O. aspinata</i>	Lyme Regis	Negative trend between Mg levels and $\delta^{13}\text{C}$ levels (<i>P. gigantea</i> data set).	11	< 0.02	4.20

Table 4.6c: Significant relationships detected between the shell mineralogy of *O. aspinata* and the $\delta^{13}\text{C}$ levels (Figure 4.15–4.16, 4.20).

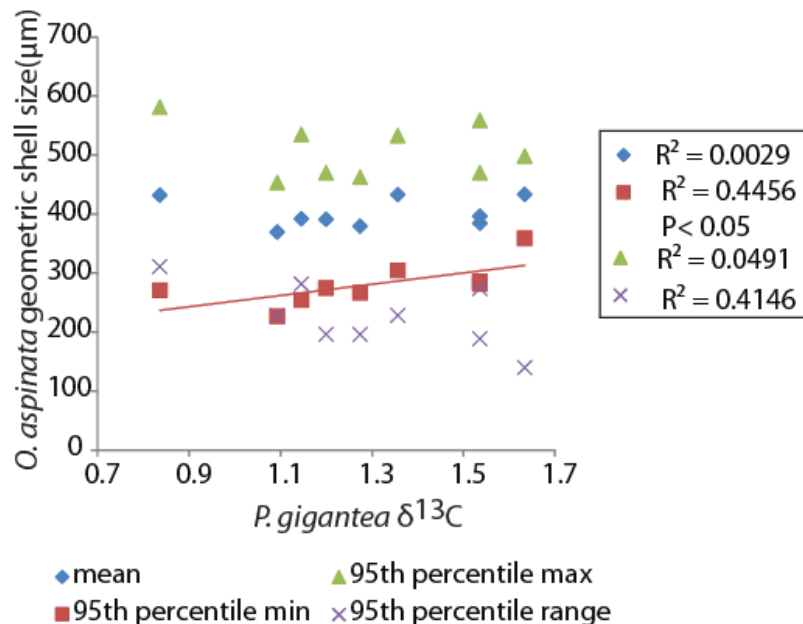


Figure 4.15: Linear regression models with positive trend lines showing one significant relationship between the geometric size of *O. aspinata* from Lyme Regis and the $\delta^{13}\text{C}$. Trend lines are only included on data sets where a significant relationship was identified, however those data sets with no significant relationship were still included on the graph.

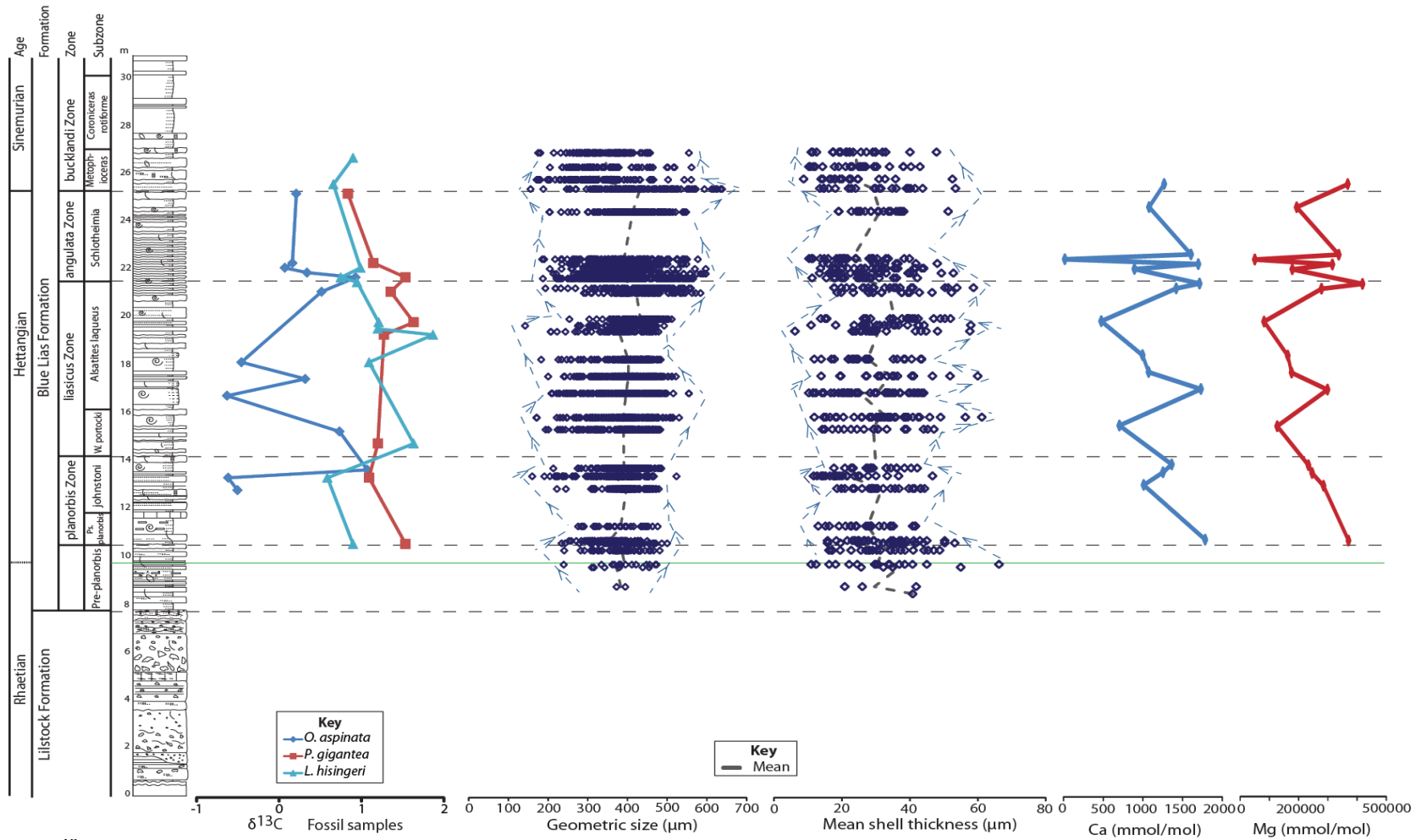


Figure 4.16: $\delta^{13}\text{C}$ curve from fossil samples (from this study) correlated to the Lyme Regis stratigraphy and *O. aspinata* geometric shell size, Ca and Mg levels (mg/L). The green line highlights the Tr-J boundary interval; Ps. planorbis subzone (Ps. pl); W. portlocki (portlocki).

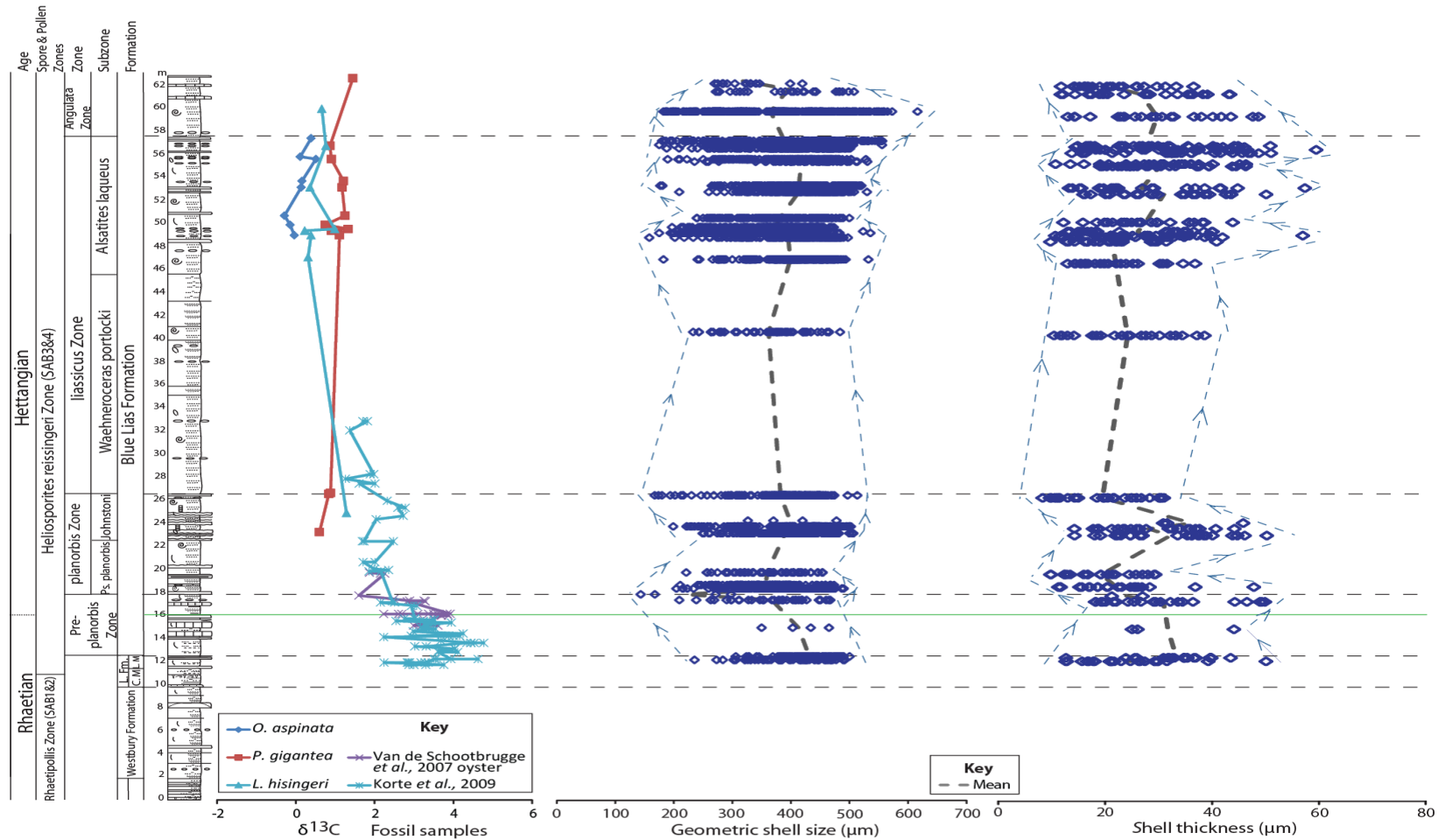


Figure 4.17: $\delta^{13}C$ curve from fossil and bulk rock samples (van de Schootbrugge *et al.*, 2007; Korte *et al.*, 2009 and this study) correlated to the St Audrie's Bay stratigraphy and *O. aspinata* geometric shell size. The green line highlights the Tr-J boundary interval; Lilstock Formation (L. Fm); Cotham Member (C.M); Langport Member (L.M). Ca and Mg values (mg/L) were correlated to the $\delta^{13}C$ curves but as they showed no relationships to each other they are not visually documented on this diagram.

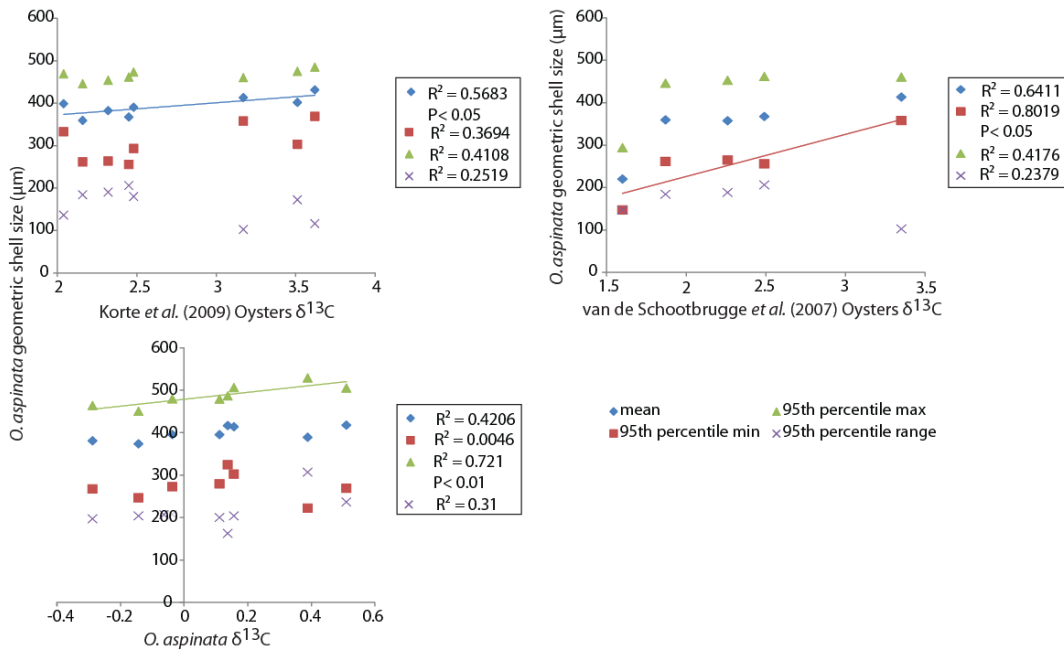


Figure 4.18: Linear regression models with positive trend lines showing one significant relationship between the geometric size of *O. aspinata* from St Audrie's Bay and the $\delta^{13}\text{C}$ on each graph. Trend lines are only included on data sets where a significant relationship was identified, however those data sets with no significant relationship were still included on the graph.

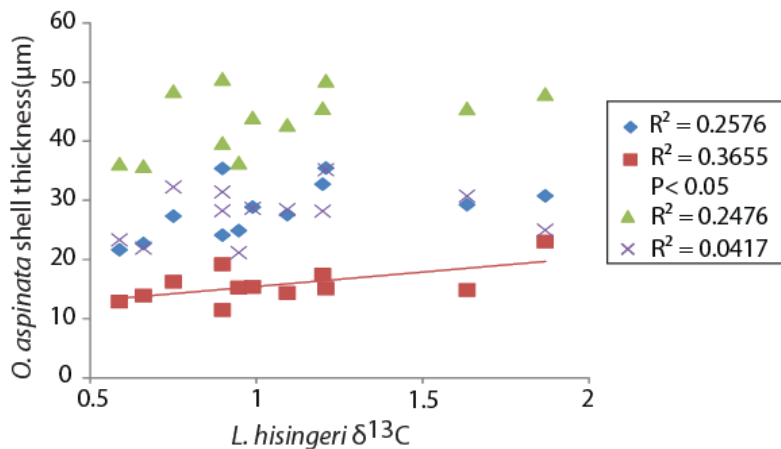


Figure 4.19: Linear regression models with positive trend lines showing one significant relationship between the shell thickness of *O. aspinata* from Lyme Regis and the $\delta^{13}\text{C}$. Trend lines are only included on data sets where a significant relationship was identified, however those data sets with no significant relationship were still included on the graph.

The changes recorded in Ca and Mg content of the *O. aspinata* valves at Lyme Regis appears to closely imitate each other (Figure 4.16). The data are not, therefore, showing the expected preferential leaching of either Ca or Mg reported by others (Hautmann, 2004; Gazeau et al., 2007; Hautmann et al., 2008). Findlay et al. (2009), however, found no significant changes in either

Mg or Ca. It is possible that another factor is causing the changes in Ca and Mg. This could be changes in the saturation state, changes in sedimentation influx or, perhaps, taphonomic changes in shell composition after the ostracod died.

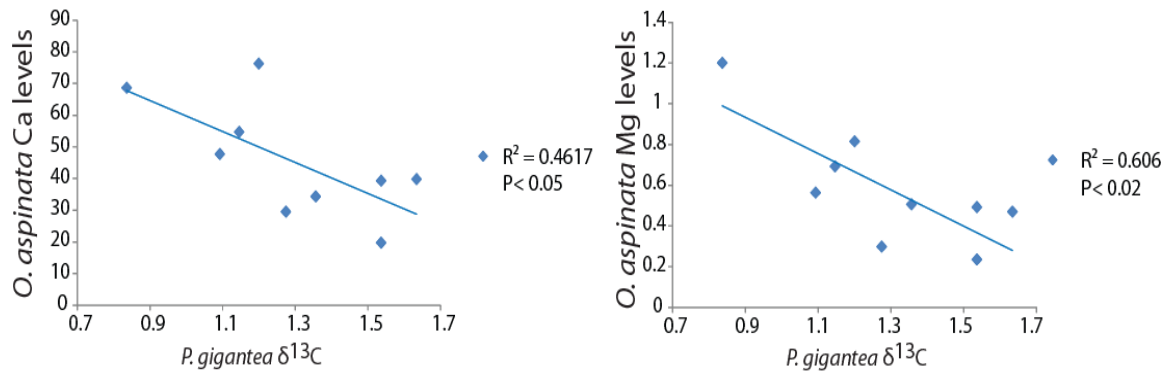


Figure 4.20: Linear regression models with negative trend lines showing one significant relationship between both the Ca and Mg levels (mg/L) of *O. aspinata* from Lyme Regis and the $\delta^{13}\text{C}$ on each graph. Trend lines are only included on data sets where a significant relationship was identified, however those data sets with no significant relationship were still included on the graph.

4.6.5 Implications of relationships identified between $\delta^{13}\text{C}$ and morphometric data.

$\delta^{13}\text{C}$ values from fossil samples are generally controlled by changes in primary productivity, atmospheric CO_2 , methane release from gas hydrates, sea level changes, plant-based carbon release and the burial and re-oxidation of ^{12}C -enriched organic matter (Knoll *et al.*, 1996; Kump and Arthur, 1999; Hesselbo *et al.*, 2000, 2002; Korte *et al.*, 2005, 2009; Hansen, 2006; van de Schootbrugge *et al.*, 2008). These controls on $\delta^{13}\text{C}$ values could help explain the positive and negative relationships found between shell size or thickness and $\delta^{13}\text{C}$ values from this study. This is because changes in primary productivity, sea level and increased $p\text{CO}_2$ causing ocean acidification could affect a species' ability to increase in size or maintain shell thickness (e.g., Hesselbo *et al.*, 2000, 2002; van de Schootbrugge *et al.*,

2008; McRoberts *et al.*, 2012). No previously published studies were identified for the Triassic-Jurassic boundary interval that have looked specifically at relationships between the shell size and/or thickness of the studied species and $\delta^{13}\text{C}$ values in the way this study has.

Several of the *O. aspinata* shell size and shell thickness data sets from Lyme Regis and St Audrie's Bay show positive relationships with a variety of the different $\delta^{13}\text{C}$ data sets (Figures 4.15, 4.18–4.19). This could be highlighting an increase in size due to increased primary productivity during a period of increased $p\text{CO}_2$ and/or an increased rate of carbon burial causing increased carbonate in the system, of which a proportion could be diagenetic carbonate (Korte *et al.*, 2005). This could mean that any change in the size of *O. aspinata* at both these locations is connected to the ocean's primary productivity levels and/or the rate of carbon burial which controls the level of carbonate in the ocean. Both *L. hisingeri* and *P. gigantea* shell size showed no significant relationships to the various $\delta^{13}\text{C}$ data sets which could be for a number of reasons including: (1) any changes in shell size for these species are not affected by the recorded changes in primary productivity and/or the rate of carbon burial; (2) the changes in primary productivity were not significant enough to effect the shell size of these species; and (3) another environmental factor (e.g., ocean acidification or palaeotemperature) is more influential on shell size for these species than changes in primary productivity.

4.7 Relationships between the palaeotemperature data and the morphometric data from each species.

All of the possible correlations between shell size or thickness of the three species from either location and the various palaeotemperature studies were illustrated on linear regression models and tested for significance. Where a whole graph detected no significant correlations in any of the plotted data sets, those graphs are presented in Appendix 5: Tables A5.45–A5.60, Figures A5.16–A5.27.

4.7.2 *L. hisingeri*

No significant relationships were detected between shell size, shell thickness, Ca or Mg (at either location) and palaeotemperature for *L. hisingeri* (Figures 4.21–4.22).

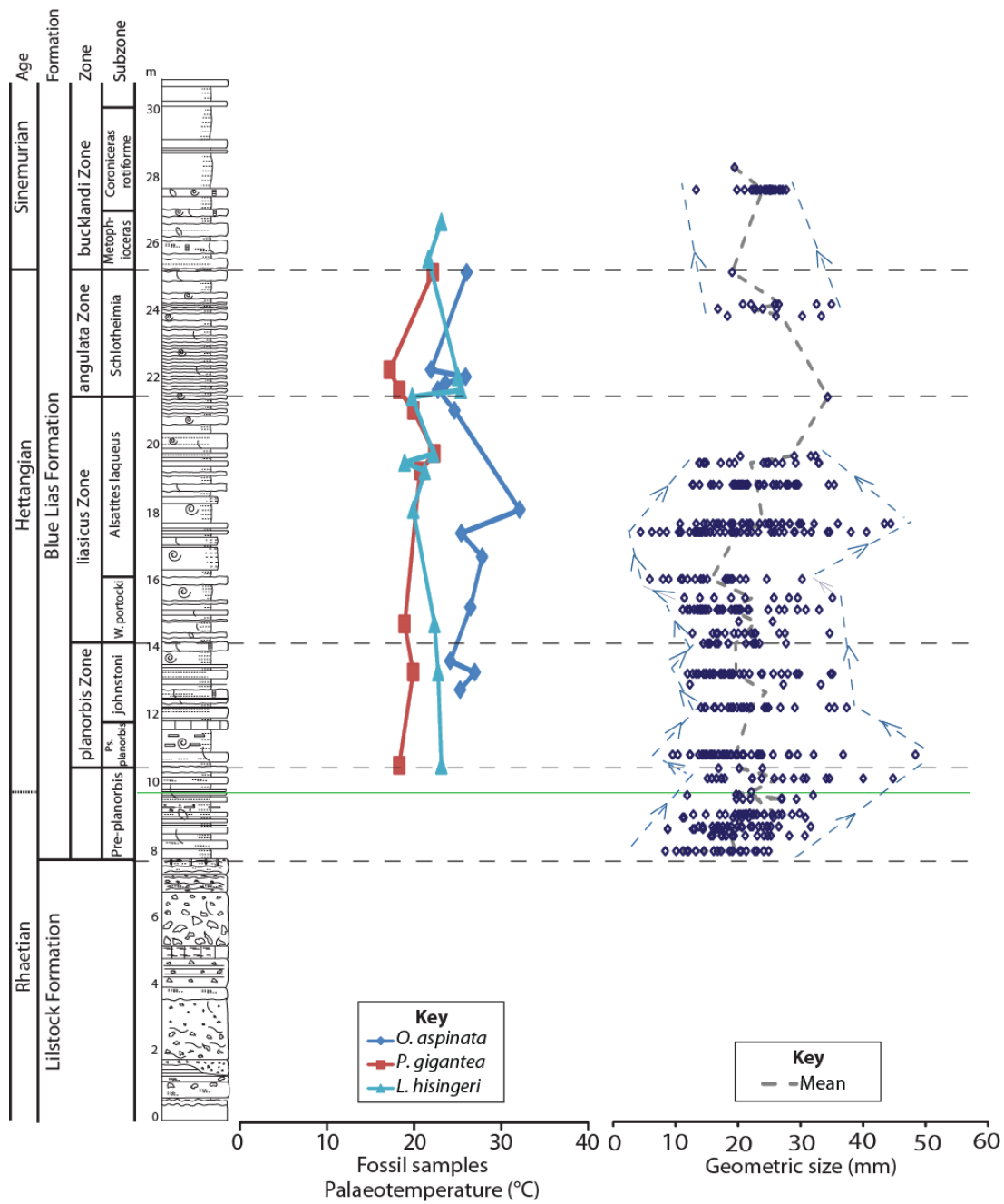


Figure 4.21: Palaeotemperature curve from fossil samples (data collected in this study) correlated to the Lyme Regis stratigraphy and *L. hisingeri* geometric shell size. The green line highlights the Tr-J boundary interval; Ps. planorbis subzone (Ps. pl); W. portlocki (portlocki). Ca and Mg values (mg/L) were correlated to the palaeotemperature curves but as they showed no relationships to each other they are not visually documented on this diagram.

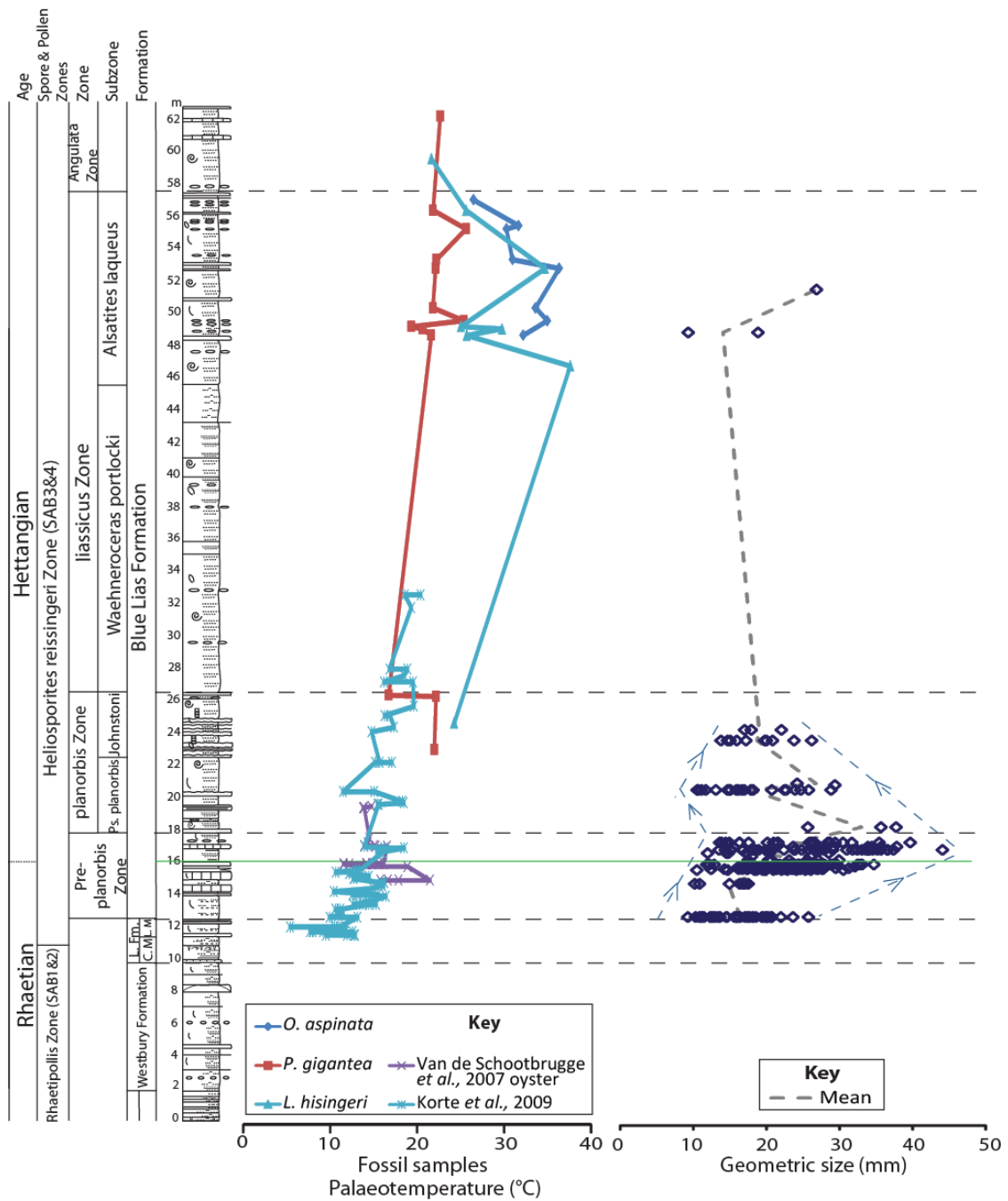


Figure 4.22: Palaeotemperature curve from fossil samples (data from van de Schootbrugge *et al.*, 2007; Korte *et al.*, 2009 and collected in this study) correlated to the St Audrie's Bay stratigraphy and *L. hisingeri* geometric shell size. The green line highlights the Tr-J boundary interval; Lilstock Formation (L. Fm); Cotham Member (C.M); Langport Member (L.M). Ca and Mg values (mg/L) were correlated to the palaeotemperature curves but as they showed no relationships to each other they are not visually documented on this diagram.

4.7.3 *P. gigantea*

Other than those relationships presented in Tables 4.7 (Figures 4.23–4.24) there were no relationships detected between shell size, shell thickness, Ca or Mg (at either location) and palaeotemperature for *P. gigantea*.

Species	Location	Relationships between shell geometry and palaeotemperature	N	P	Figure
<i>P. gigantea</i>	Lyme Regis	Positive trend between 95 th percentile range of geometric shell size and palaeotemperatures (<i>P. gigantea</i> data set).	3	< 0.05	4.23

Table 4.7: Significant relationships detected between the geometric size of *P. gigantea* and the palaeotemperature data (Figures 4.23–4.24). The low number of data points used in these correlations was because several of the relevant beds only have one shell size measurement. This meant that the range of geometric shell sizes for that bed could not be determined and therefore could not be used in these correlations.

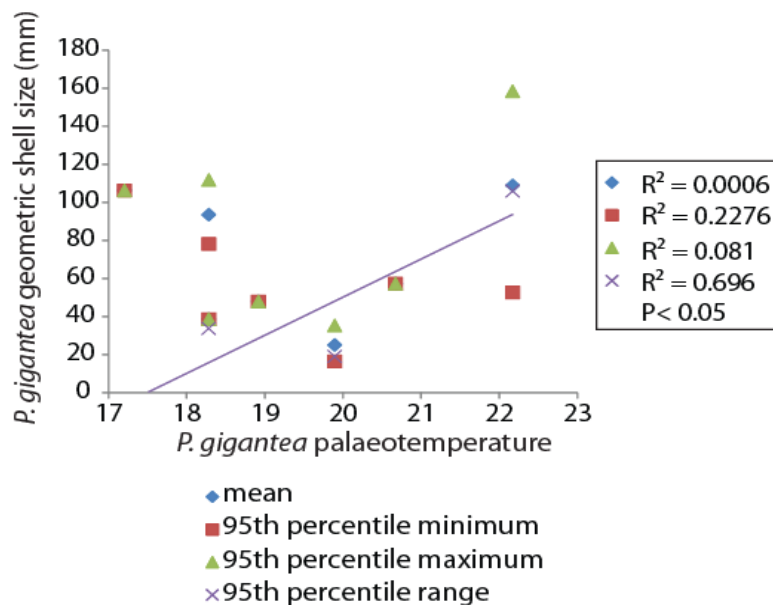


Figure 4.23: Linear regression models with positive trend lines showing one significant relationship between the geometric size of *P. gigantea* from Lyme Regis and the palaeotemperature data. Trend lines are only included on data sets where a significant relationship was identified, however those data sets with no significant relationship were still included on the graph.

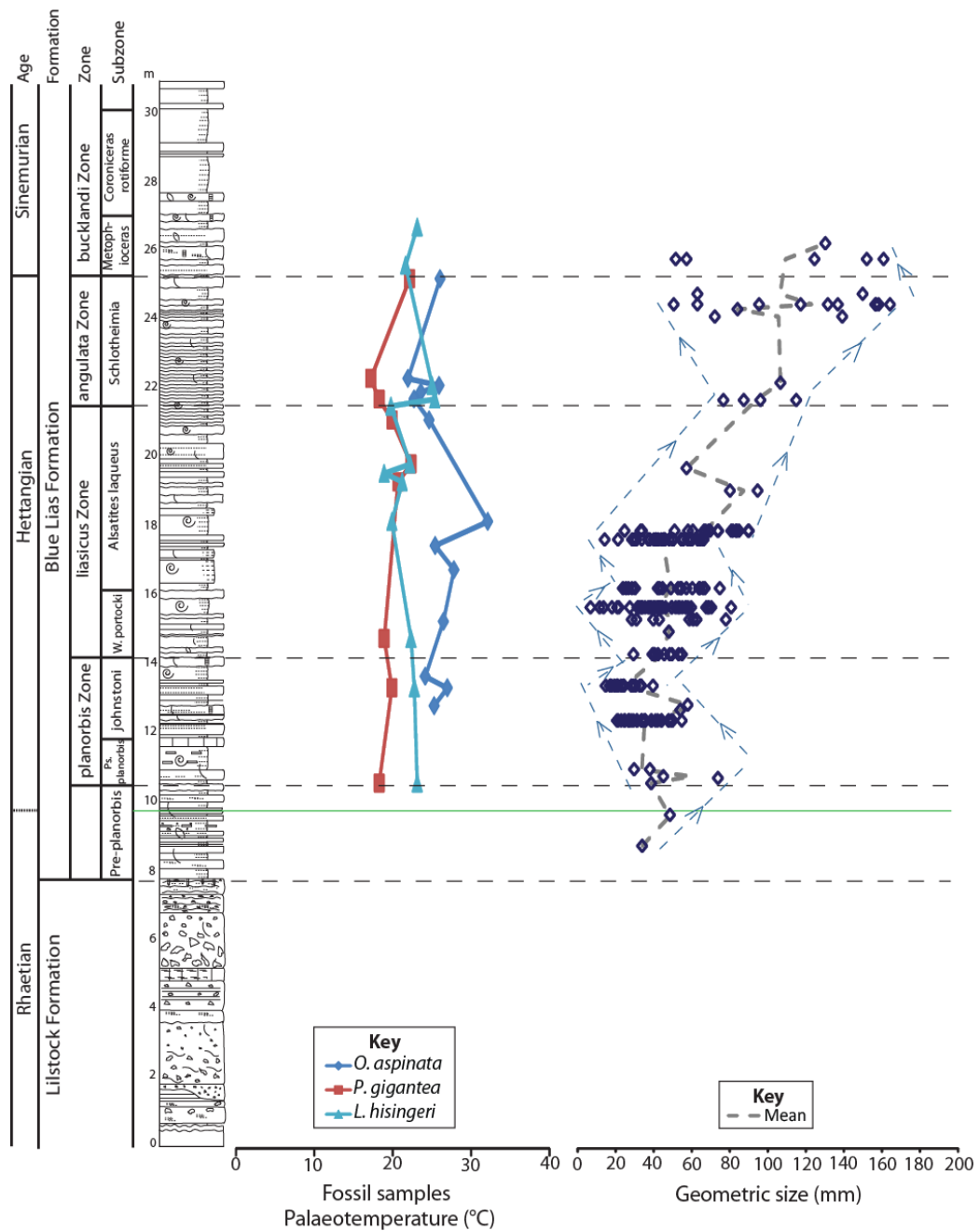


Figure 4.24: Palaeotemperature curve from fossil samples (data collected in this study) correlated to the Lyme Regis stratigraphy and *P. gigantea* geometric shell size. The green line highlights the Tr-J boundary interval; Ps. planorbis subzone (Ps. pl); W. portlocki (portlocki). Ca and Mg values (mg/L) were correlated to the palaeotemperature curves but as they showed no relationships to each other they are not visually documented on this diagram.

4.7.4 *O. aspinata*

Other than those relationships presented in Tables 4.8 (Figures 4.25–4.27) there were no relationships detected between shell size, shell thickness, Ca or Mg (at either location) and palaeotemperature for *O. aspinata*.

Species	Location	Relationships between shell geometry and palaeotemperature	N	P	Figure
<i>O. aspinata</i>	St Audrie's Bay	Negative trend between 95 th percentile maximum geometric shell size and palaeotemperature (<i>O. aspinata</i> data set).	8	< 0.02	4.27
<i>O. aspinata</i>	St Audrie's Bay	Negative trend between 95 th percentile range of geometric shell size and palaeotemperature levels (<i>O. aspinata</i> data set).	8	< 0.01	4.27

Table 4.8: Significant relationships detected between the geometric size of *O. aspinata* and the palaeotemperature (Figure 4.25–4.27).

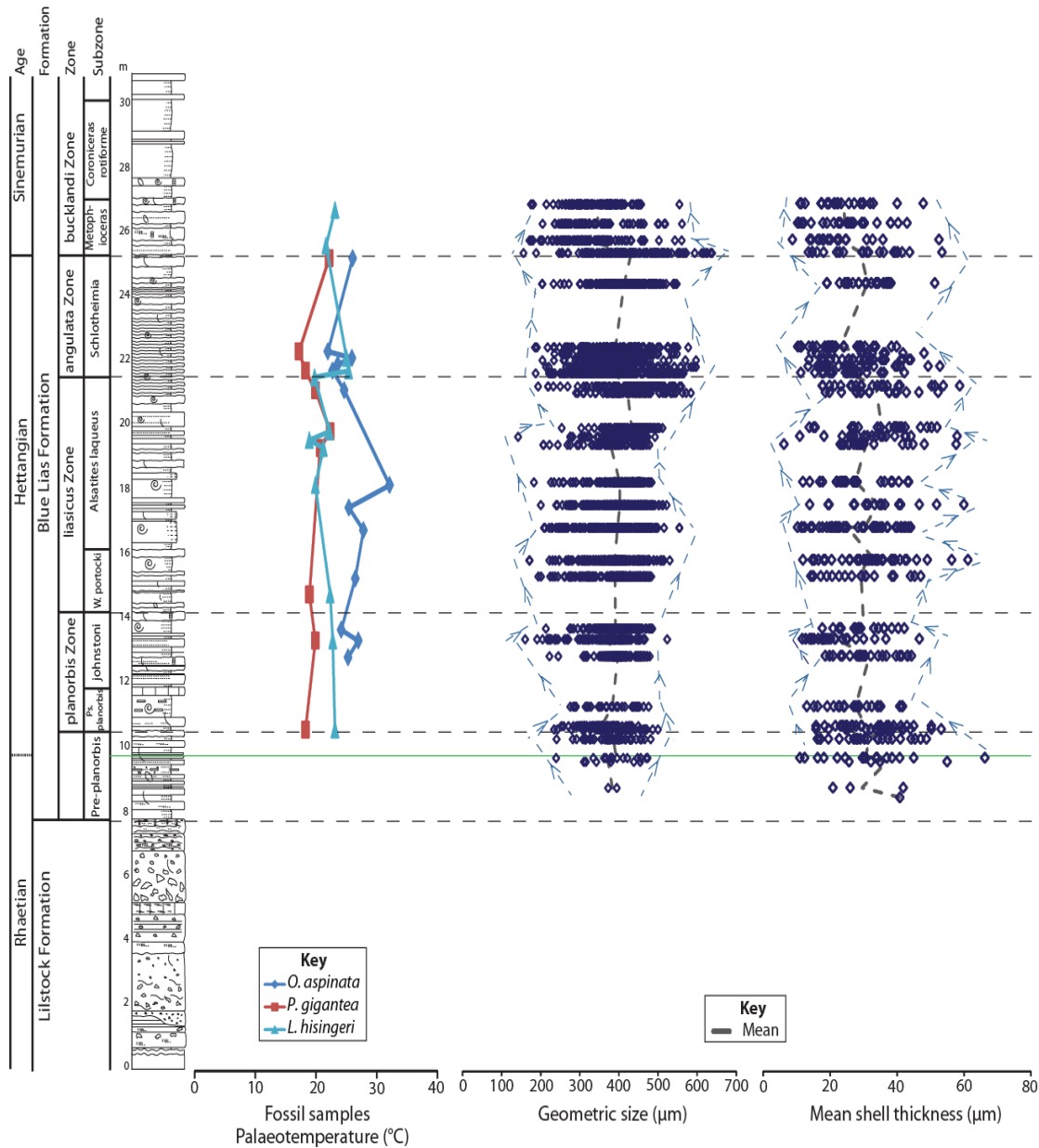


Figure 4.25: Palaeotemperature curve from fossil samples (data collected in this study) correlated to the Lyme Regis stratigraphy and *O. aspinata* geometric shell size. The green line highlights the Tr-J boundary interval; Ps. planorbis subzone (Ps. pl); W. portlocki (portlocki). Ca and Mg values were correlated to the palaeotemperature curves but as they showed no relationships to each other they are not visually documented on this diagram.

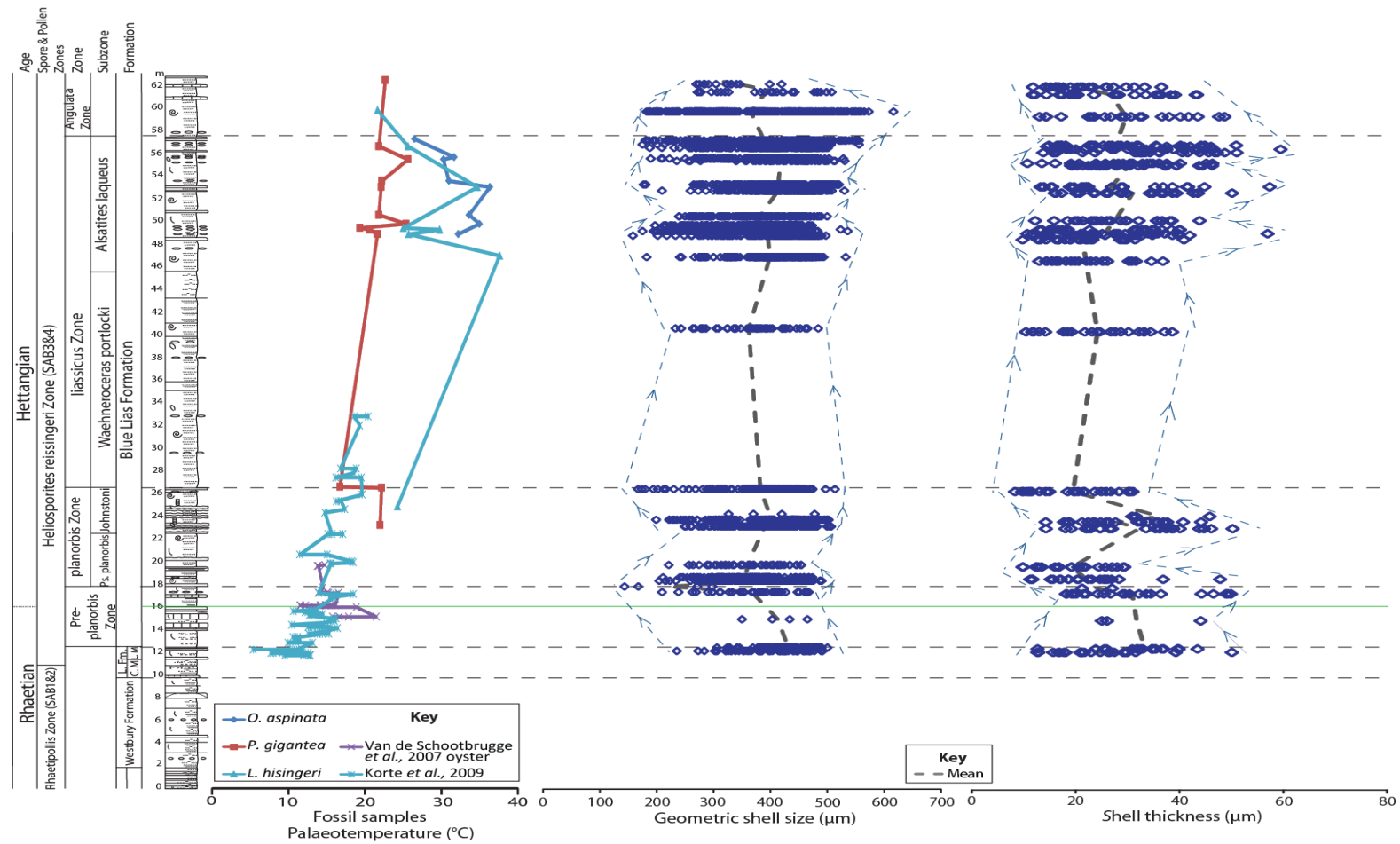


Figure 4.26: Palaeotemperature curve from fossil and bulk rock samples (data from van de Schootbrugge *et al.*, 2007; Korte *et al.*, 2009 and collected in this study) correlated to the St Audrie's Bay stratigraphy and *O. aspinata* geometric shell size. The green line highlights the Tr-J boundary interval; Lilstock Formation (L. Fm); Cotham Member (C.M); Langport Member (L.M). Ca and Mg values (mg/L) were correlated to the palaeotemperature curves but as they showed no relationships to each other they are not visually documented on this diagram.

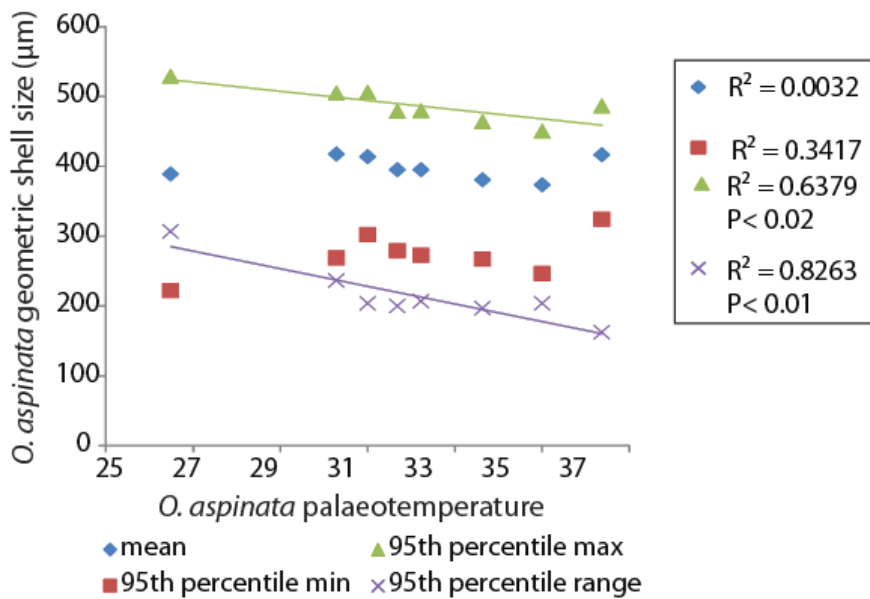


Figure 4.27: Linear regression models with negative trend lines showing two significant relationships between the geometric size of *O. aspinata* from St Audrie's Bay (A-G) and palaeotemperature. Trend lines are only included on data sets where a significant relationship was identified, however those data sets with no significant relationship were still included on the graph.

4.7.5 Implications of relationships identified between palaeotemperature and morphometric data.

$\delta^{18}\text{O}$ from fossil samples reflect changes in the seawater oxygen isotope value, which is affected by changes in palaeotemperature or changes in salinity (e.g., Palfy *et al.*, 2007; van de Schootbrugge *et al.*, 2007, 2008; Korte *et al.*, 2009). Jurassic oysters are known to be intolerant of hypersaline conditions and, along with other evidence discussed in Section 4.3.4, indicate that these locations were normal marine habitats not affected by variations in salinity (Swift and Martill, 1999; Korte *et al.*, 2009) and consequently, the $\delta^{18}\text{O}$ values should be recording only changes in temperature (Korte *et al.*, 2009). Changes in temperature could help explain the positive and negative relationships found between shell size or thickness and the $\delta^{18}\text{O}$ values from this study. This is because changes in temperature are known to affect various species' ability to increase in size or maintain

shell thickness. This has been studied in many modern experiments using extant species in experimental conditions (e.g., Hoegh-Guldberg *et al.*, 2007; Pörtner, 2008; Rayssac *et al.*, 2010). However, no previously published studies were found for the Tr-J boundary interval that have specifically investigated relationships between these species' shell size or shell thickness and $\delta^{18}\text{O}$ or palaeotemperature values as done here. The $\delta^{18}\text{O}$ values for each data set have been used in the palaeotemperature equation (discussed in Section 4.3.4) to produce the palaeotemperature data used in this study to explore any relationships between *L. hisingeri*, *P. gigantea* and *O. aspinata* shell size or thickness and palaeotemperature. *L. hisingeri* shell size and *O. aspinata* shell thickness displayed no significant relationships to the various temperature data sets, which could be for a number of reasons including: (1) any changes in shell size for these species are not affected by the recorded changes in palaeotemperature; (2) the changes in palaeotemperature were not significant enough to effect the shell size of these species; (3) the $\delta^{18}\text{O}$ values from the various data sets are not accurately representing the palaeotemperature from the Tr–J boundary interval; and (4) another environmental factor (e.g., ocean acidification or primary productivity) is more influential on shell size for these species than changes in palaeotemperature.

Increased palaeotemperature is known to result in shell damage and reduced calcification in addition to increased shell size or thickness in some modern species (each reaction is species specific; Hoegh-Guldberg *et al.*, 2007; Kiessling and Aberhan, 2007; Pörtner, 2008; Rayssac *et al.*, 2010; Kiessling and Simpson, 2011). If increased palaeotemperature does cause

increased shell size, this could go some way to explaining the positive relationships found between palaeotemperature and *P. gigantea* shell size. However, *O. aspinata* shell size exhibits a negative relationship to palaeotemperature, indicating lower palaeotemperatures are preferred for *O. aspinata* shell size to increase, with higher palaeotemperatures stunting shell size. This could possibly be because higher palaeotemperatures reduce the ability for *O. aspinata* to produce new instars due a reduced ability to calcify. The *O. aspinata* relationship results do not correspond to the modern studies, indicating that higher temperatures result in increased shell size through decreasing the time taken between the formation of each new instar. However, this metabolic adjustment resulted in a reduced life span in the ostracods (Decrouy *et al.*, 2011).

4.8 How do these Tr-J boundary interval results correlate with other perceived palaeo-ocean acidification or palaeotemperature events?

Ocean acidification is thought to have caused several other extinction events (e.g., the Permian–Triassic (P-T) and the Palaeocene–Eocene Thermal Maximum (PETM)) of variable severity and the results from those extinction events have been compared to the results from the end-Triassic extinction event (Hönisch *et al.*, 2012). A range of marine taxa from the P–T interval showed that their mean and maximum body sizes were significantly reduced during the biotic crisis before, in some cases, slowly returning to larger sizes (an example of the Lilliput effect, e.g., Schubert and Bottjer, 1995; Fraiser *et al.*, 2005; Payne, 2005; Peng *et al.*, 2007; Posenato, 2009; Metcalfe *et al.*, 2011; Song *et al.*, 2011). Several other studies of the P-T and PETM also show unbuffered and acid-sensitive extinction selectivity, specifically in reef

environments (benthic foraminifera, corals, molluscs; Bralower, 2002; Knoll *et al.*, 2007; Pelejero *et al.*, 2010; Clapham and Payne, 2011; Kiessling and Simpson, 2011). All of these results have been linked to various extreme environmental stresses and interpreted as possible evidence of ocean acidification resulting from increased $p\text{CO}_2$ (e.g., Wignall and Twitchett, 1996; Bralower, 2002; Zachos *et al.*, 2005; Knoll *et al.*, 2007; Pelejero *et al.*, 2010; Gibbs *et al.*, 2010; Clapham and Payne, 2011; Kiessling and Simpson, 2011; Metcalfe *et al.*, 2011; Retallack *et al.*, 2011; Song *et al.*, 2011). They correspond with certain studies from the Tr-J boundary interval which have also identified these factors (Hautmann, 2004; Hautmann *et al.*, 2008), but the species from this study display increasing shell size during increasing $p\text{CO}_2$ and no shell damage due to ocean acidification.

Rapid temperature increases are thought to have been associated with several other marine extinction events (e.g., the Early Toarcian and the Latest Maastrichtian) of variable severity (Abramovich and Keller, 2003; Gómez and Arias 2010), both of which have been compared to the events in the latest Triassic. The Early Toarcian is known as a period of rapidly increasing temperature where up to 85% of ostracod species progressively disappeared through a 300kyr period and modern studies have shown that increased temperature causes increases in size by decreasing the time taken between the formation of new instars, consequently reducing the life span of the ostracods (Gómez and Arias 2010; Decrouy *et al.*, 2011). Although the data collected during this study do not investigate the extinction rate of different species, *P. gigantea* geometric shell size demonstrates a positive relationship to increasing palaeotemperature. This correlates with

the increase in size observed in ostracod species during the Early Toarcian event and could lead to a similar increase in mortality. However, *O. aspinata* from St Audrie's Bay exhibited a negative relationship between maximum size and palaeotemperature, which does not correspond with the ostracod results from the Early Toarcian event. This could be due to another environmental factor influencing shell size, such as ocean acidification. Results from the Latest Maastrichtian warming event display recorded species dwarfing during periods of high palaeotemperatures (Abramovich and Keller, 2003), correlating with the *O. aspinata* results presented in this study. However, it should be noted that the study was investigating planktonic foraminifera which are a very different organism (Abramovich and Keller, 2003).

4.9 Summary

- Bivalves at both locations increased in size during a period of increasing atmospheric CO₂. However, the *O. aspinata* results show increasing size at St Audrie's Bay and decreasing sizes at Lyme Regis during increasing atmospheric CO₂.
- Bivalve size and *O. aspinata* shell thickness increased during periods of increasing pCO₂, which contradicts Hautmann's (2004) biocalcification hypothesis.
- *O. aspinata* shell size decreased in Lyme Regis, during periods of increasing pCO₂ which corresponds with Hautmann's (2004) biocalcification hypothesis.

- The variations in morphological effects to high $p\text{CO}_2$ between species could be because: (1) the response to ocean acidification is species specific as demonstrated in many modern studies; and (2) increasing shell thickness could be a possible survival adaptation during high $p\text{CO}_2$.
- As palaeotemperatures increased, *P. gigantea* shell size increased while *O. aspinata* valve size decreased. These responses confirm the findings of previous fossil and extant studies which showed that increased temperatures can cause both positive and negative species-specific effects.
- Much of the morphometric data do not show any significant relationship to either $p\text{CO}_2$ or temperature and this could mean that other environmental factors are causing the recorded changes in size and thickness. Other environmental factors that are known to generate a biological response include salinity, lithological variations and changes in sedimentation rate and sea level changes. These factors must be investigated in the future in order to determine their contribution to the changes seen in this study.

4.9.2 Further work

To interpret further the fossil shell size and shell thickness relationships to $p\text{CO}_2$ and high palaeotemperature for these species, it is necessary to relate them to the responses found during modern acidification and high temperature laboratory experiments (e.g., Greene *et al.*, 2012). There are numerous laboratory experiments using extant bivalves which can be

compared with the fossil bivalve data from this study (e.g., Green *et al.*, 2004; Gazeau *et al.*, 2007; Kurihara *et al.*, 2007; Ries *et al.*, 2009; Talmage and Gobler, 2009; Rico-Villa *et al.*, 2009; Mizuta *et al.*, 2012; Hiebenthal *et al.*, 2012). However, very few experiments have been completed using modern ostracods (e.g., Köhl., 1980; De Deckker *et al.*, 1999; Hunt and Roy., 2006; Decrouy *et al.*, 2011; Marco-Barba *et al.*, 2012) so in the following chapter (Chapter 5) we will attempt to fill this gap by studying the biological responses of three modern ostracods to high CO₂ and high temperature conditions.

Chapter 5 – Effects of elevated $p\text{CO}_2$ and temperature on three extant ostracod species.

5.1 Introduction

In Chapter 4 the variations and trends in shell size and thickness of the three calcareous marine fossils (*L. hisingeri*, *P. gigantea* and *O. aspinata*) were investigated to identify if they were responding to changes in atmospheric $p\text{CO}_2$ or palaeotemperature during the Tr-J boundary interval. There were significant relationships between the geometric shell size and shell thickness of the three different species and the different $p\text{CO}_2$ data sets as well as some of the palaeotemperature, and $\delta^{13}\text{C}$ results. To determine if these relationships between shell morphology and high $p\text{CO}_2$ or elevated palaeotemperature in the fossil record can be related to the modern day oceans, it is necessary to investigate the effect of both of these abiotic factors in relevant experimental studies using modern species.

A considerable amount of research has already been carried out investigating the effects of elevated atmospheric CO_2 on aspects of modern bivalve biology but not on modern ostracod biology. The studies of bivalves showed that, not without exceptions (Findlay *et al.*, 2011), there was reduced carapace growth, increased carapace dissolution and increased mortality upon exposure to high CO_2 or high temperature singly, or in combination (see Chapter 1 and Appendices 1–2 for a more detailed summary of what has been found; e.g., Gazeau *et al.*, 2007; Kurihara *et al.*, 2007; Talmage and Gobler, 2009; Findlay *et al.*, 2011; Hiebenthal *et al.*, 2012). In comparison with the bivalves few studies have investigated the effects of

temperature and CO₂ (singly or in combination) on either fossil or extant ostracod biology and of those, most have studied temperature (Kühl, 1980; Bullen and Sibley, 1984; De Deckker *et al.*, 1999; Gómez and Arias 2010; Marco-Barba *et al.*, 2012).

Fossil studies show that a significant increase in temperature during the earliest Toarcian coincided with increased mortality while variations in the palaeoceanographic conditions during the middle Late Triassic are important in preservation, i.e. increased Mg levels lead to dolomite formation, whereas high temperatures with acidic waters cause Mg to significantly leach out of the carapaces of *Cyprideis australiensis* (De Deckker *et al.*, 1999; Gómez and Arias, 2010; Iannace *et al.*, 2011). CO₂ and temperature related changes in the mineralogy of the carapace of live organisms is very different the carapaces of dead organisms (Findlay *et al.*, 2009, 2011). Dead ostracods (*Cyprideis australiensis* and equivalent fossil species) deposited in high temperatures combined with high CO₂ showed significant leaching of Mg from the carapace whereas high water temperatures with higher Mg/Ca ratios (> 20 Mg/Ca ratios) increase the Mg in the carapaces of living *Cyprideis torosa* (Bullen and Sibley, 1984; De Deckker *et al.*, 1999; Marco-Barba *et al.*, 2012).

Studies using carapaces have found that, for a significant increase in Mg to occur, the living species *Cyprideis australiensis* required a 1°C increase in temperature (De Deckker *et al.*, 1999; Marco-Barba *et al.*, 2012). Dead foraminifera however, needed < 24 hrs at 250°C to cause a significant increase in Mg (Bullen and Sibley, 1984). However, Ca levels in live individuals from several species (e.g., *Littorina littorea*, *Carcinus maenas*,

Amphiura filiformis, *Mytilus edulis*, *Semibalanus balanoides*) stay constant or, in a few cases, increase due to elevated CO₂ (Bibby *et al.*, 2007; Wood *et al.*, 2008; Findlay *et al.*, 2009, 2011). Analyses of the carapaces of dead individuals indicate that Ca levels decrease over a period of 7 days (Findlay *et al.*, 2009, 2011). Increasing temperature irrespective of salinity resulted in increased calcification, increased carapace size and greater mortality for several (but not all) ostracod species (Kühl 1980; Frenzel and Boomer, 2005; Hunt and Roy, 2006; Decrouy *et al.*, 2011).

Consequently, there is a clear need to investigate how modern day ostracods might respond to both future ocean acidification and elevated water temperature (IPCC 2007). In one hundred years' time the ocean water temperature is expected to have increased on average by 4°C from 15°C to 19°C, while estimated elevated CO₂ values will range from 900 – 1200 ppm and are expected to produce an average seawater pH of 7.7 at 15°C and pH of 7.8 at 19°C (Riebesell *et al.*, 2010; Houghton *et al.*, 2001). Ostracods are a key organism in both marine and freshwater ecosystems, acting as important detritivores and as a food source for other organisms (Reyment, 1966; Kornicker and Sohn, 1971; Neale, 1983; Leonard, 1983; Athersuch *et al.*, 1989)

5.2 Aim and objectives

The aim of this chapter is to investigate the effects of elevated CO₂ and temperature on the growth, carapace thickness, mineralogy (Mg and Ca levels) and carapace preservation of modern ostracods. These results will

then be used in Chapter 6 to interpret the fossil ostracod results from the suspected ocean acidification interval presented in Chapter 4.

This was carried out as follows:

- Three ostracod species were kept at two nominal temperatures (average: $T = 15$ or 19°C and two nominal pH values (average pH = 8.0 (controls) or 7.7 (acidified) for either 21 or 95 days.
- After either 21 or 95 days ostracods (live and dead) were removed and their carapace dimensions (length and width) and carapace thickness measured. Each individual also had their carapace preservation recorded and the percentage of Mg and Ca in the carapace measured.
- Data for each of these parameters were collected from individuals sampled from the field and before they were introduced into any experiment so that the data from the experiments can be compared to these results to determine how much morphological change has occurred since starting the experiment.

5.3 Choice of experimental species

Preliminary experiments found that fully marine ostracods were very sensitive to environmental perturbation and did not do well in laboratory culture. It was important to use more lab-tolerant species, preferably from habitats close to the laboratory (i.e., could be returned to the laboratory within an hour of capture). Unfortunately none of the species readily

available in the Plymouth area are closely related to any of the fossil genera from the Tr-J (see Chapter 3). Consequently, three ostracod species belonging to the genus *Leptocythere* (described below), were collected from a coastal/estuarine environment (the Plym Estuary) because they were; (a) relatively laboratory-hardy, (b) relatively easy to collect in large numbers, and (c) were located in habitats that are in close proximity to the laboratory.

5.3.2 *Leptocythere* sp.

The identification of this species was difficult so advice was sought from Professor David Horne (Queen Mary College, University of London). He was unsure about the identification but was positive that it was a species of *Leptocythere*. He tentatively suggested that it could possibly be *Leptocythere castanea* but many of the identifying features for this unidentified species do not fit with the description of *L. castanea* (Athersuch *et al.*, 1989). The features that separate this species from *L. castanea* include; the pores and fossae which seem larger and differently spaced, the posterior margin seems slightly more compressed and the dorsal and ventral margin seems straighter, less curved or sloping. There are two possibilities: (1) it could be *L. castanea* but there is a greater degree of previously un-recognised phenotypic plasticity, or, (2) it could be an undescribed species of *Leptocythere*. Consequently this species will be referred to as *Leptocythere* sp. For a full description of this species refer to field collected section (Section 5.5.2) and Figure. 5.1.

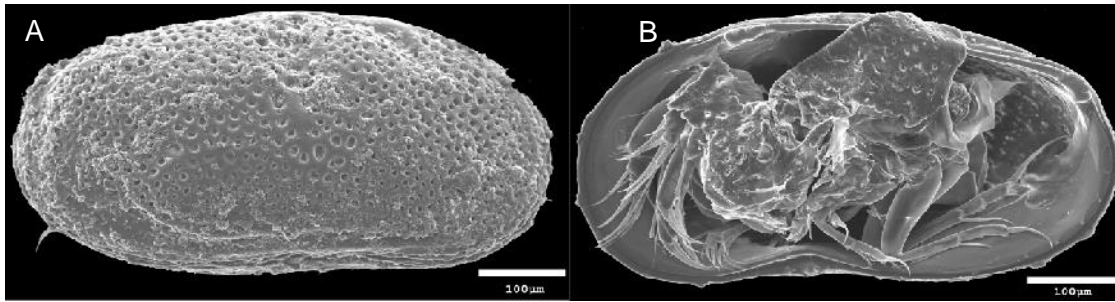


Figure 5.1: *Leptocythere* sp. (A) Right valve external view, (B) Right valve, internal view showing arrangement of the appendages which is required for identification purposes (Scale is 100μm).

5.3.3 *Leptocythere castanea* (Sars, 1866)

Leptocythere castanea has a large thin shelled and finely pitted carapace (approx. length: 400 – 500 μm). The width of the carapace is relatively high in proportion to length, with a distinct post-ocular and dorsomedian sulci but weak posteroventral alar protuberances (Figure 5.2; Oertli, 1985; Athersuch *et al.*, 1989). The colour of the carapace is buff, dark brown or white in live individuals and the ventral margin is almost straight anteriorly but strongly convex posteriorly (Oertli, 1985; Athersuch *et al.*, 1989).

Distribution: It is found exclusively in brackish water, estuarine and salt marsh environments, usually associated with mud and algae. It is common in northwest European estuaries (Athersuch *et al.*, 1989). The individuals pictured here were collected from the Plym Estuary (England).

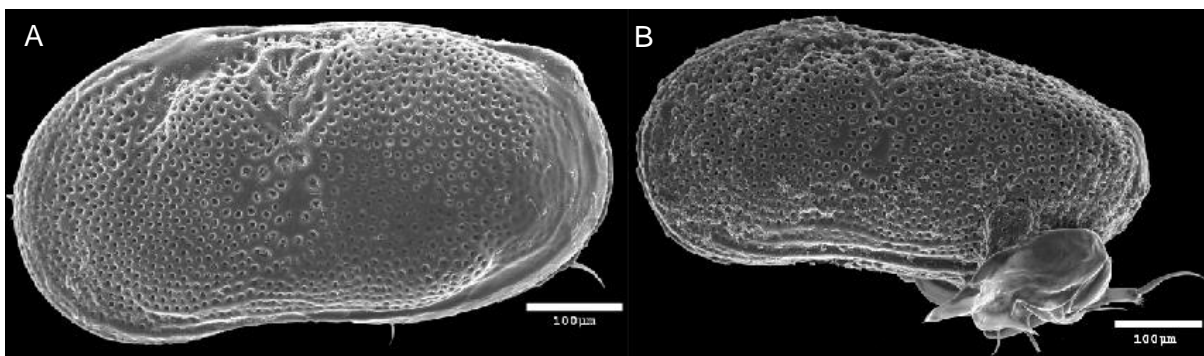


Figure 5.2: *Leptocythere castanea*. (A) Left valve, external view, (B) Left valve, external view showing appendages protruding which aid identification (Scale is 100μm).

5.3.4 *Leptocythere lacertosa* (Hirschmann, 1912)

Diagnosis: *Leptocythere lacertosa* has a small (approx. Geometric carapace size: 150 – 250 μm) robust carapace with smooth reticulate or pitted ornament in female individuals while only finely pitted in male individuals (Oertli, 1985; Athersuch *et al.*, 1989). The dorsal view of the posterior margin is somewhat truncated. The colour of the carapace is a buff to dark brown. The post-ocular and dorsomedian sulci and the posteroventral alar protuberances are either weak or completely absent and the ventral margin is concave with straight sections (Figure 5.3; Oertli, 1985; Athersuch *et al.*, 1989).

Distribution: *Leptocythere lacertosa* is tolerant of a wide range of salinities and is normally, though not exclusively, found in estuarine conditions in mud or fine sand. It is common in northwest European estuaries (Athersuch *et al.*, 1989). The individuals were collected from the Plym Estuary (England).

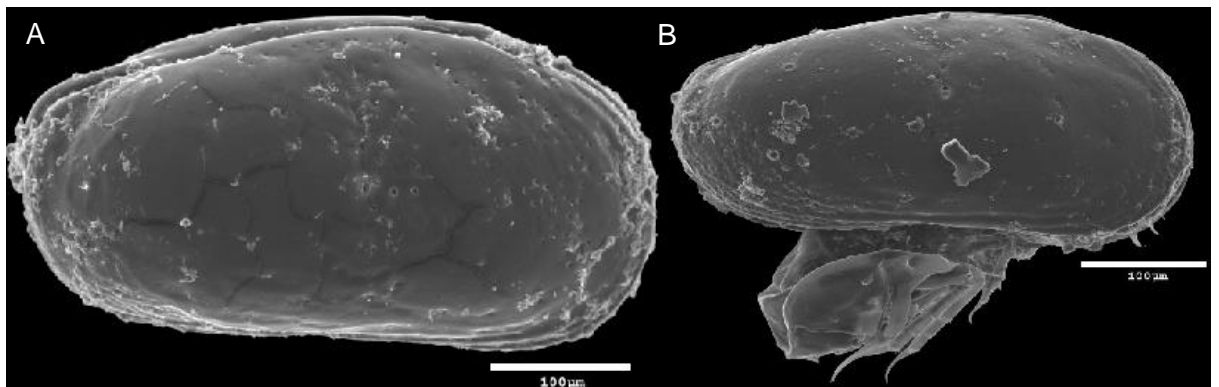


Figure 5.3: *Leptocythere lacertosa*. (A) Right valve, external view, (B) Right valve, external view showing appendages which aid identification (Scale is 100 μm).

5.4 Materials and methods

5.4.2 Animal material

Sediment samples were collected in February (2012) at around 3pm, using a hand-held trowel from the surface (upper 2 cm) of the mid-shore mudflats, of the Plym Estuary, Devon, UK (Lat. 50.371911° Long. -4.104514°) during a low tide . Also collected was some of the surrounding standing water (S = 32.8 ‰ measured using a refractometer (D-D H2Ocean Salinity; Essex, UK)). Mud and water samples were transported to the laboratory at Plymouth University in plastic tubs (vol. = 900 ml) with sealed lids within one hour of collection. Upon arrival, sediment samples were placed in a controlled temperature environment (T = 10°C) and each tub half-filled with mud, overlain with sea water, was supplied with an aeration stone.

To remove individual ostracods sub-samples of sediment (approx. vol. = 0.5 ml) were removed from the plastic tubs using a pipette and transferred to a shallow glass dish (diam. = 8 cm, depth = 1.5 cm) half-filled with sea water (S = 34 ‰). Individual ostracods were located and removed manually from sediment samples under low power magnification (x 10 – x 40) using a glass pipette. They were then removed to glass vials (vol. = 28 ml, 50 individuals per vial) where they were kept in continuously (but gently) aerated sea water (S = 34 ‰) in a controlled temperature environment (T = 10°C). After sorting, species were identified using the key of Athersuch *et al.* (1989), and individuals redistributed, according to species, into a second set of glass vials (vol. = 28 ml, S = 34 ‰). Species identification was subsequently confirmed by Professor David Horne (Queen Mary, University of London).

Those individuals from each species that were discovered to be dead upon identification were not put in the treatments, but instead were measured for carapace size and thickness to provide an indication of pre-treatment size.

The water temperature within the glass vials that the ostracods were living in was gradually increased from 10 to 15°C (to avoid temperature shock-related mortality) by transferring the glass vials from the 10°C to the 15°C temperature controlled room and keeping them there for 28 days. The individuals were introduced into the cages and the experimental apparatus, described below.

5.4.3 Experimental cages

Individuals of three ostracod species, *Leptocythere* sp., *L. castanea*, and *L. lacertosa* (Figures 5.1, 5.2, 5.3) were removed from the glass vials and placed into specially-constructed cages using a pipette, (N = 6, 1–2 individuals per species but preferably two where possible) for introduction into the experimental mesocosm described below. Each cage was constructed from green plastic tubing (length = 25 mm, diam. = 20 mm, see Figure 5.4). Mesh (total area = 3 cm² mesh size = 54 µm) was secured over each end of the tube using two plastic rings (width = 5 mm, diam. = 15 mm). The mesh prevented the ostracods escaping from the tube. The plastic rings were easy to remove and replace allowing ready access to the cage, for the introduction and removal of food every 14 days.

The extent to which the water flow was impeded by the mesh around each end of the cage was tested as follows; 0.5 ml of sediment was pipetted into a cage with 3 drops of blue food dye (Supercooks; Leeds, England). This was

left in an aquaria (length = 14 cm, width = 20 cm, height = 14 cm; the same as those used in the experimental mesocosm during the final experiment) filled with the same natural untreated sea water from Plymouth Sound that was used in the experimental mesocosm. An aeration stone was introduced to gently aerate and cause the water in the tank to flow through the mesh placed around each end of the cages. This was left running overnight to determine if the mesh impeded the flow of water through the cage. Water flow through the cage was deemed acceptable because the water in the aquaria had turned the same blue colour as the dye placed inside the cage, indicating that the water was able to flow through the mesh unimpeded. A further test using live ostracods and detritus was applied to the cages to check that the flow indicated in the first flow test was sufficient for the ostracods to survive. Six ostracods and 0.5ml of detritus were introduced into the same cage (used for the first water flow test) and placed in the experimental mesocosm for one week. After one week the cage was removed from the experimental mesocosm, the ostracods were removed from the cage and checked to confirm they were still live. The ostracods were found alive which indicated that the cage and mesh was suitable for the experiment and would not be responsible for mortality related to lack of oxygen.

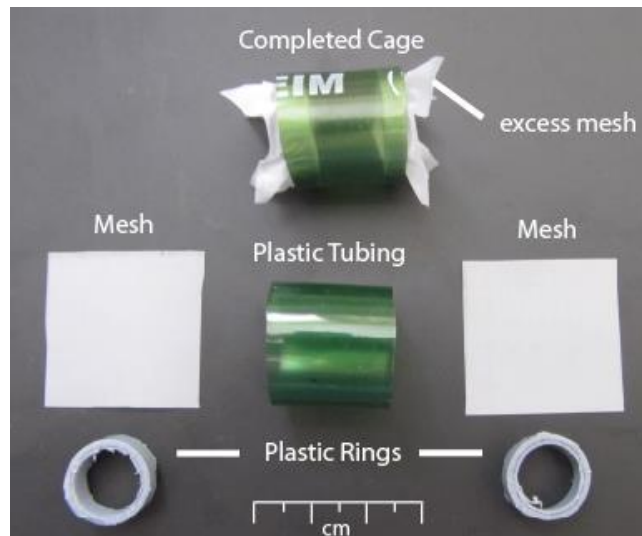


Figure 5.4: Components used to construct the cages and a constructed cage.

5.4.4 Experimental mesocosm set-up

One hundred and eighty cages were equally distributed between twelve experimental aquaria which were then placed (length = 14 cm, width = 20 cm, height = 14 cm) into the four shallow plastic trays within the CO₂ and Temperature Equilibration System pictured in Figure 5.5. Natural un-treated sea water drawn from Plymouth Sound was transported by commercial tanker to Plymouth University and held in tanks before being transferred into the plastic trays and sump through a hose. The sea water (S = 34 ‰) was pumped from the sump through a chiller (B in Figure 5.5; ± 1°C; BOYU, L series water chiller; Raoping Guangdong China) into four shallow plastic trays (A in Figure 5.5, length = 180 cm, width = 75 cm, height = 12 cm). These housed either four or two experimental aquaria (C in Figure 5.5 length = 14 cm, width = 20 cm, height = 14 cm) and acted as a water bath to maintain the aquaria water at an almost constant temperature (approx. plus or minus 0.5°C for both temperatures). There was a header tank (made of high density polyethelene (HDPE), dimensions: length = 52 cm, width = 42 cm, depth = 43 cm) for each experimental treatment and a separate loop of

water run from the first two trays (15°C and 19°C) up to the header tank supply lines (D in Figure 5.5) which feed into the header tanks. The header tanks feed water into the supply lines suspended above the trays (E in Figure 5.5) and the supply lines feed through saddle valves into nitrile tubing (F in Figure 4.5) and then into the aquaria. The water flow through the nitrile tubing was maintained at 80 ml.min⁻¹ by timing how long (timed using a digital stop watch - Traceable: Texas, USA) it took to collect a known amount of water (using a measuring cylinder) through each tube, every two days. If the flow rate needed to be adjusted the saddle valve in the supply line was used to increase or decrease the flow accordingly and then the flow rate was timed again to confirm the correct flow rate had been achieved.

Upon entering the aquaria (C in Figure 5.5), the water flows out through overflow vents in the lid and into the tray before overflowing the tray (G in Figure 5.5) and returning to the sump. The water temperature in the trays and header tanks was controlled using a number of heating units (Eheim: aquarium glass stick heaters; Deizisau, Germany). Two heaters were set up in each of the two 19°C trays and header tanks to maintain the water temperature at a constant 19°C. As the room temperature fluctuates it can cause the water temperature to fluctuate away from the desired temperatures, so chillers (BOYU: L series water chiller; Raoping Guangdong China) were used to maintain the temperature of the water being pumped into the trays and header tanks of each system to within 1°C of the desired temperature. Temperature was measured daily in each aquaria using a digital thermometer (Traceable, precision of two decimal places; Texas, USA).

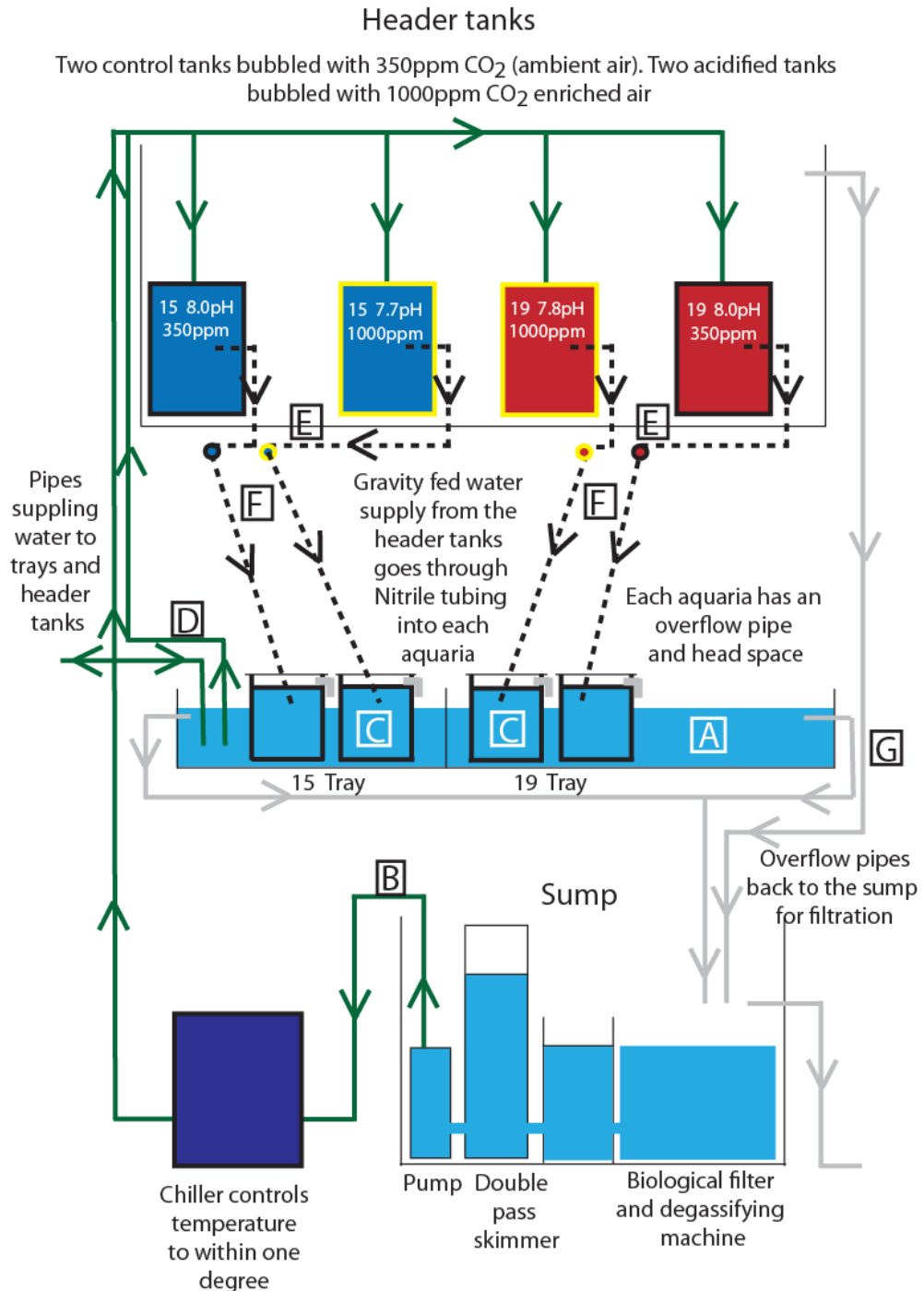


Figure 5.5: Schematic of CO₂ & Temperature Equilibration System. Letters A-F highlight parts of the diagram in the main text; green lines and arrows indicate the pipes supplying the trays and header tanks and the direction of water flow; grey coloured lines and arrows indicate the overflow pipes and the direction of water flow; dashed lines with arrows represent the supply lines and nitrile tubing that go from the header tanks to the aquaria's along with the direction of water flow. Header tanks (coloured rectangles) and saddle valve (coloured circles) colours represent the different treatments: blue = 15°C, red = 19°C, blue or red with black outline = 8.0 pH/350 ppm and blue or red with yellow outline = 7.7-7.8 pH/1000 ppm. Light blue colour in trays and sump indicates containers the water flows into. Dark blue square next to the sump designates the chiller the water flows through.

To produce a standard CO₂ concentration, the sea water in the header tanks was equilibrated with untreated air (350 ppm CO₂). To increase the pCO₂ (ppm) concentration in the sea water, air was mixed with CO₂ from a cylinder to produce CO₂ enriched air. A CO₂ cylinder was attached to a gas regulator (10 Bar, BOC 8500; UK) and the gas was bubbled into a Buchnar flask (2000 ml) and mixed with untreated air which produced the CO₂ enriched air. The regulator was then manually adjusted accordingly to maintain the accepted ppm range explained above. The CO₂ enriched air was then measured using a CO₂ gas analyser (Licor, LI-820; Nebraska, USA. range of 0 - 20,000ppm CO₂ and precision: RMS Noise at 370ppm with 1 second signal filtering: <1ppm; accuracy: <3% of reading). The header tanks were aerated with enriched air or normal air at a rate of 1400 L/per min which is split equally between untreated air and enriched air and was then bubbled into all eight header tanks using a 12 inch air stone (Algarde aquatic products, Nottingham, UK).

5.4.5 Measurement of pH, salinity, oxygen and total alkalinity

The pH of water in all of the experimental aquaria containing the cages was measured five days out of every seven using a pH combination electrode and meter, and water in the header tanks were measured once a week (Seven Easy Mettler Toledo pH meter with auto temperature compensation, Ohio, USA; precision: two decimal places, accuracy: pH = ± 0.01, mV = ± 1 and T = ± 0.5°C). The pH meter was calibrated using three standard buffers (Mettler-Toledo pH buffer, Ohio, USA; at 25°C = pH 4.01, pH 7 and pH 9.21). A temperature probe coupled to the pH meter automatically corrected the pH measurement for temperature differences. The salinity and oxygen of the

seawater in each of the experimental aquaria were measured at the same time as the pH using a refractometer (D-D H₂Ocean Salinity; Essex, UK) and O₂ meter (HACH LDO HQ10; Dusseldorf, Germany) respectively.

Seawater samples for measurement of total alkalinity (TA) were taken once every seven days from every experimental aquaria containing ostracod cages and once every two to three weeks from every header tank and both sumps. Borosilicate bottles (125ml) were filled with sea water from each experimental aquaria tank, the header tanks and both sumps. Mercuric chloride (30 µl, 0.02 % of sample volume from a saturated solution) was added to each borosilicate bottle to poison every sample. The bottle was shaken well to completely mix the mercuric chloride and sea water and then placed in a Fisher Scientific water bath (Loughborough, UK) to bring the sample water up to 25°C in order to measure accurately the TA of every sample. Every 0.25 ml sample was measured once for TA using an automatic titrator (equipment for the titration system: APOLLO SciTech: Seawater gran titration Alkalinity titrator and computer program (Georgia, USA) with a Thermo scientific calibration meter attached (Massachusetts, USA)). Any samples recording an unusual result were re-run a second time to confirm the result (Appendix 6, Table A6.1).

5.4.6 Experimental protocol

One hundred and eighty cages, each containing between 1–2 individuals of each ostracod species, were placed equally between all the treatments. The number of individuals found for each species was different, so 138 of the cages contained individuals of all three species, 17 contained individuals of

two species (*L. castanea*, *L. lacertosa*) and 25 contained individuals of one species (*L. castanea*) which were then equally distributed between all the treatments.

When the cages were moved from the 15°C temperature controlled room and placed in both initial temperatures (15°C and 18°C) in the experimental mesocosm, the cages were maintained in non-acidified sea water. All of the cages were kept in non-acidified sea water for five days to allow the ostracods to settle and acclimatise, particularly to the higher temperature. After 5 days, the CO₂ was turned on in the header tanks for the relevant half of all the experimental aquaria (across both temperatures). After a further two week period to allow those ostracods to settle into the acidified sea water, the temperature in the warm tanks was increased from 18°C to the required 19°C. From this point on the temperatures and pH levels were kept constant for the entire duration of both the 21 day and the 95 day experiment.

Every 14 days one of the plastic rings was carefully removed from the tube and the surrounding mesh pushed aside to allow the introduction of approx. 0.5 ml of food into each cage, using a pipette to transfer the specially prepared food from its holding container. The food used was a mixture of detritus and natural seawater from the remaining sediment. The sediment was searched through in detail using a microscope to remove all visible living organisms (e.g., worms, gastropods, arthropods).

After 21 days, fifteen cages were removed from each treatment and after 95 days the remaining thirty cages were removed from each treatment. When the cages were removed from the treatment, the plastic ring and mesh was

removed from each cage and the content emptied into a plastic tub specific to each treatment (diameter = 18 cm, depth = 6 cm) containing 2 cm depth of natural sea water. Each tube and the mesh from both ends was flushed out with further sea water into the plastic tub to ensure that no ostracods or any food was left attached to the cage. Using a pipette, 2 ml of the content from the cages from one treatment was removed from the plastic tub and placed in a glass Petri dish (diameter = 8 cm, depth = 1.5 cm) half filled with sea water and examined under low power magnification to locate all of the ostracods. When an ostracod was located it was identified as either dead or alive and then removed using a pipette with as little of the detritus as possible to a glass vial labelled as either 'dead' or 'alive' and the relevant treatment. This was repeated until all of the sediment from the plastic tub had been transferred to the glass Petri dish, searched through and the ostracods removed. This process was repeated for every cage from each of the treatments until all of the sediment and sea water had been thoroughly inspected and all of the ostracods removed and placed in the relevant vials.

All of the vials (containing both live and dead individuals) were then filled with deionised water and left for 24 hours before the deionised water was removed and replaced with fresh deionised water. This cleaned the ostracods in the vial of anything that may have affected the mineralogy of the carapace as well as fully removing any sea water in the vial. The ostracods were left in the vials for a further 2 days allowing those ostracods that were alive on removal from the system to die. The content of each vial that was labelled 'dead' on retrieval was then placed into a relevantly labelled glass Petri dish and examined again under low power magnification to locate and

identify each of the ostracods. As each ostracod was identified it was moved, using a paintbrush, to the relevant specimen side (labelled: found dead on retrieval) and placed in an individual specimen square ready to be measured.

The glass vials labelled 'live' on retrieval were treated in the same way but, during this process, the ostracods were checked to ensure that they were finally dead before being placed on the relevant specimen slides (labelled: found live on retrieval). From this it was clear that not all of the ostracods placed in the system had been retrieved and there could be several reasons for this. It is possible that, when some of the individuals died, their carapaces broke up due to dissolution destroying the carapaces structural integrity as well as the logistical difficulties that came with recovering every individual from all of the cages. The main logistical difficulty is that the specimens are very small and the surrounding sediment can hide individual specimens whether they are alive or dead. This meant that for some treatments and species, significantly fewer specimens were retrieved at the end of the experiment even though extremely thorough inspections of the sediment were undertaken.

5.4.7 Ostracod morphometrics

Each individual was placed on a specimen slide and both valves measured under low power magnification (10x (Nikon Eclipse LV100POL microscope, Nikon Digital sight DS-U2 camera; Surrey, UK)). The maximum width (defined as ventral edge to dorsal hinge in a straight line) and maximum length (defined as the carapace span at a right angle to the width line) of both carapaces was determined (error margin: 2 μ m) using the NIS-elements

Basic Research microscope software (Nikon; Surrey, UK) that incorporates a measuring tool (Figure 5.6).

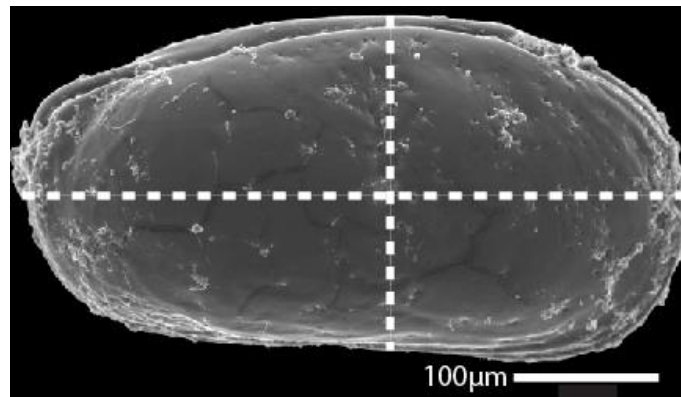
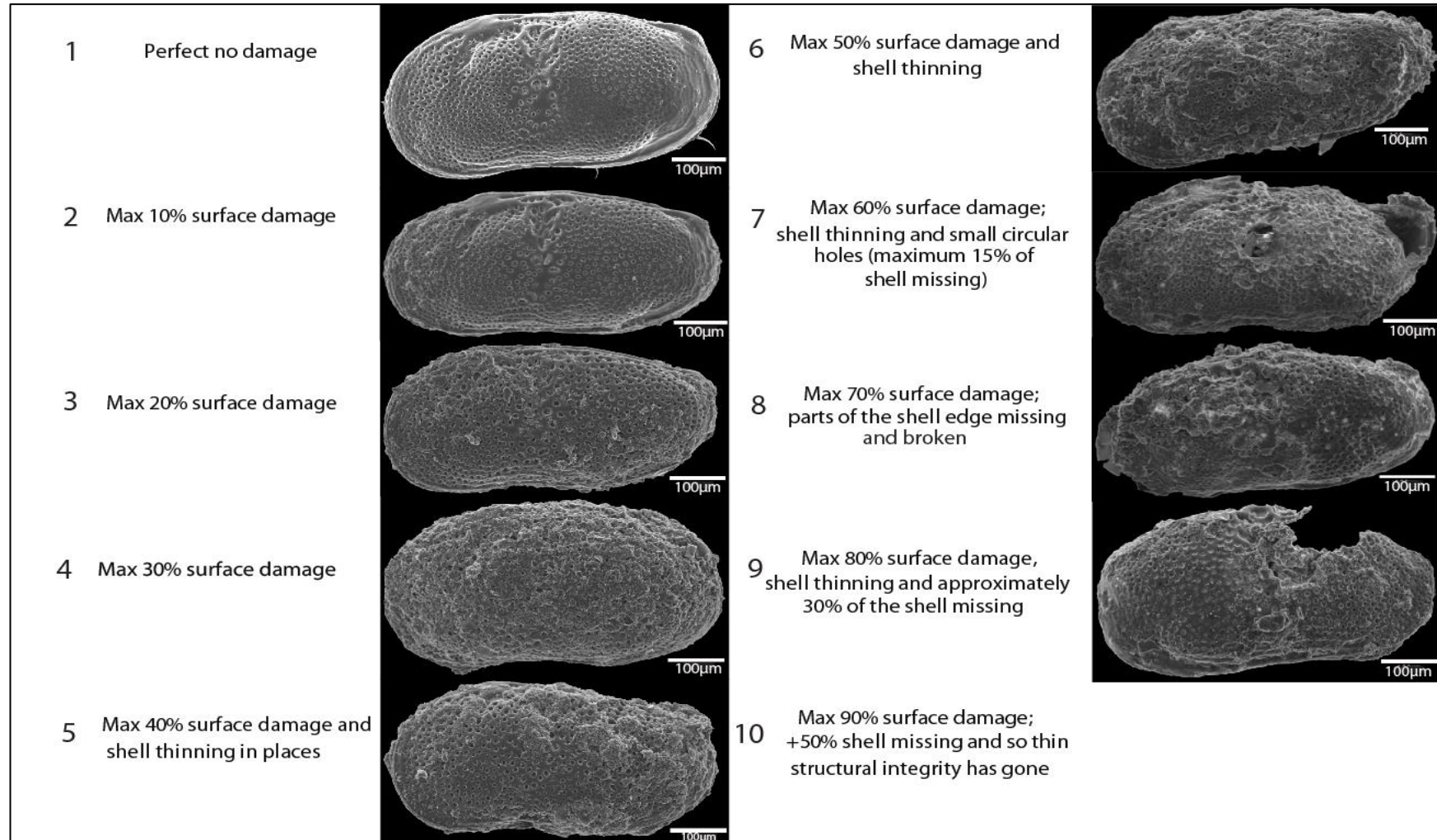


Figure 5.6: SEM image of the recorded measurements for carapace width (vertical line) and length (horizontal line) measurements were taken from (*L. lacertosa*; right valve, external view).

To determine accurately the different degrees of carapace preservation/damage of each specimen, a preservation scale (detailed below) was produced to rank the preservation (Figure 5.7). This scale was produced from a combination of observing the specimens collected from the different treatments and determining the level of change in the preservation between specimens (e.g., increments in preservation of every: maximum 5 % or 10 % or 15 % or 20 % damage etc.) as well as incorporating relevant schemes from published preservation scales. These scales could not be used in their entirety because they were not based on using ostracods but on completely different organisms (e.g., foraminifera, pteropods, bivalves). From this an incremental scale of preservation (1–10 %, 11–20 %, 21–30 % onwards) was produced as this illustrates the maximum variations in preservation seen. The scale consisted of limited 1–10 % surface damage (rank 2) all the way through to 90 % surface damage with +50 % of the carapace missing (rank 10; Figure 5.7).



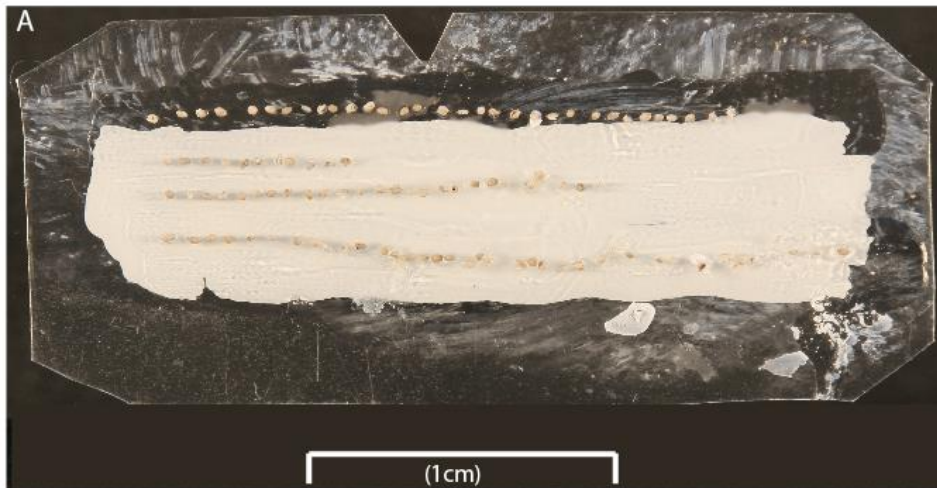
¹²Figure 5.7: The ostracod preservation scale. Note: ten has no image as the individual specimens ranked at scale ten were too delicate (as they had lost all structural integrity) to be moved onto a stub for SEM imaging and would not light photograph well enough.

Each ostracod was assessed visually under low power magnification to determine the carapace preservation rank using the scale produced in this study (Figure 5.7). After all the individuals had been measured and their level of preservation determined, one of each species was kept as an example individual and the remaining ostracods were then placed in resin blocks for sectioning to determine the carapace thickness and carapace mineralogy as described below.

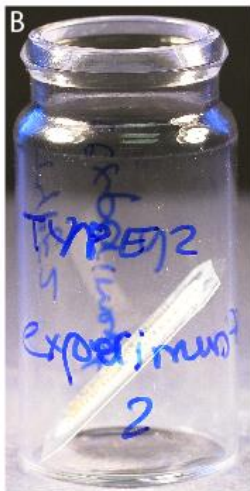
5.4.8 Preparation of resin blocks for carapace thickness measurements

To produce the resin blocks containing the ostracod carapaces several steps were taken. Stage 1: cyanoacrylate adhesive (Loctite; Hatfield, UK) was applied to a 2.6 cm X 1.5 cm piece of thin, clear plastic and the ostracods fixed to it in lines on their anterior edge. This meant that for each experiment all the individuals for one species fitted on to the same piece of plastic, with each line of individuals representing a different treatment and whether the individual had been found alive or dead (Figure 5.8A). This was repeated for each species and both experiments so for each species there was two clear pieces of plastic one for each experiment. Stage 2, Part 1: each piece of plastic with ostracods attached was then put in a glass vial (vol. = 20 ml) with 2% glutaraldehyde fixative and then topped up with deionised water and left for 1.5 hrs (Figure 5.8B). After 1.5 hrs the fixative was washed off each piece of plastic with ostracods attached using deionised water and then the plastic with ostracods attached was placed in 30 % ethanol for 15 min. Every 15 min the percentage of ethanol was increased in steps through 50, 70, 90 and 100 % to dehydrate the ostracods.

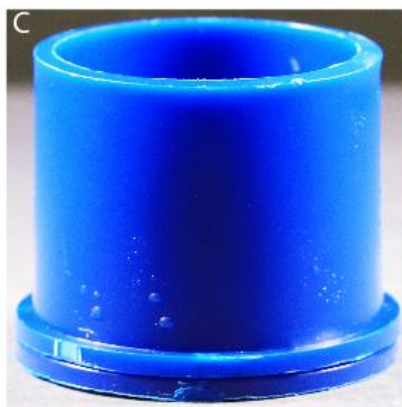
Ostracod carapaces attached to plastic slip



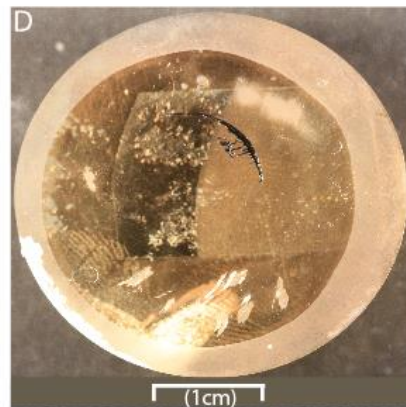
Glass vial containing the plastic slip



Resin mould



Polished resin block



SEM image of resin block with thickness measurement locations on each ostracod

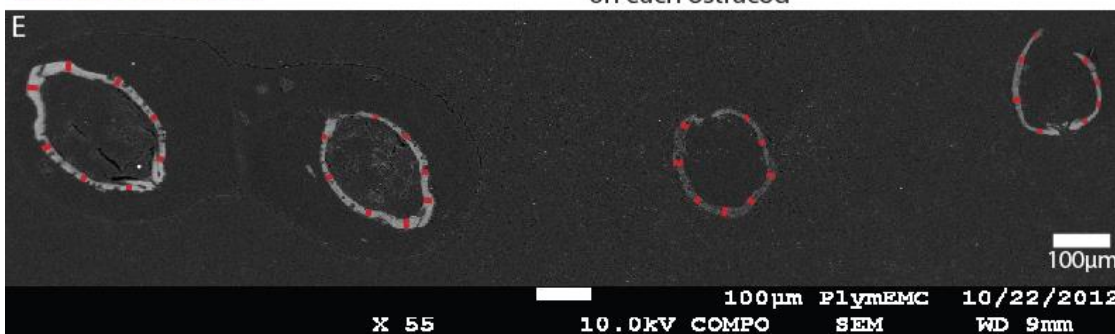


Figure 5.8: Photographs and titles illustrating how ostracod carapaces were encased in a resin block; (A) Stage 1, (B) Stage 2, (C) Stage 3, (D) Stage 4 and (E) Stage 5.

Stage 2, Part 2: each piece of plastic with ostracods attached was then immersed overnight in a 30 % resin (Agar scientific; Agar low viscosity resin; Essex, UK), 70 % ethanol mix to commence the infiltration process. After 24 hrs the mixture was changed to 50 % resin 50 % ethanol then, after a further

24 hrs to 70 % resin 30 % ethanol and after a final 24 hrs to 100 % resin. Stage 3: moulds were given relevant labels according to which species and which experiment the mould would contain and fresh 100 % resin was poured inside (diam. = 33 mm; height = 40 mm). Each piece of plastic with ostracods attached was placed into the correspondingly labelled mould with the posterior edge of the ostracods touching the base of the mould and left to set at $T = 45^{\circ}\text{C}$ for 24 hrs (Figure 5.8C).

Stage 4: once the resin block was set and removed from its mould, it was ground down until the ostracod carapaces were sectioned through to the carapace in a straight line. To grind and polish the resin blocks, 800 grit paper was fixed to a Buehler Beta grinder/polisher (Illinois, USA) and the blocks ground down until the individuals were around three quarters of their original length. Finer grinding was completed using 1200 grit paper until the ostracods were nearly half of their original length. Finally, each resin block had to be polished down to a condition suitable for imaging in the Scanning Electron microscope (SEM) using firstly a woven nylon cloth with $6\mu\text{m}$ DP spray and then a short pile (man-made) cloth with $1\mu\text{m}$ DP spray. Each resin block was carbon coated using an Emitech K450X rotary carbon coater (Quorum Technologies Ltd, West Sussex, UK) to prepare the surface of each resin block (containing the ostracod individuals from each treatment) for the SEM (JEOL JSM-7001F Field Emission Scanning Electron microscope; Tokyo, Japan).

Stage 5: carapace thickness was measured from the inner edge of the carapace to the outer edge of the carapace at four equally spaced intervals along the carapace length using images generated by an SEM and the SEM

measuring tool (JEOL JSM-7001F Field Emission Scanning Electron microscope; Tokyo, Japan) (Figure 5.8E). A carapace thickness measurement was taken at the extreme dorsal and ventral edges and then at points 25% and 75% away from the extreme dorsal edge. These values were then used to calculate an average carapace thickness for each carapace.

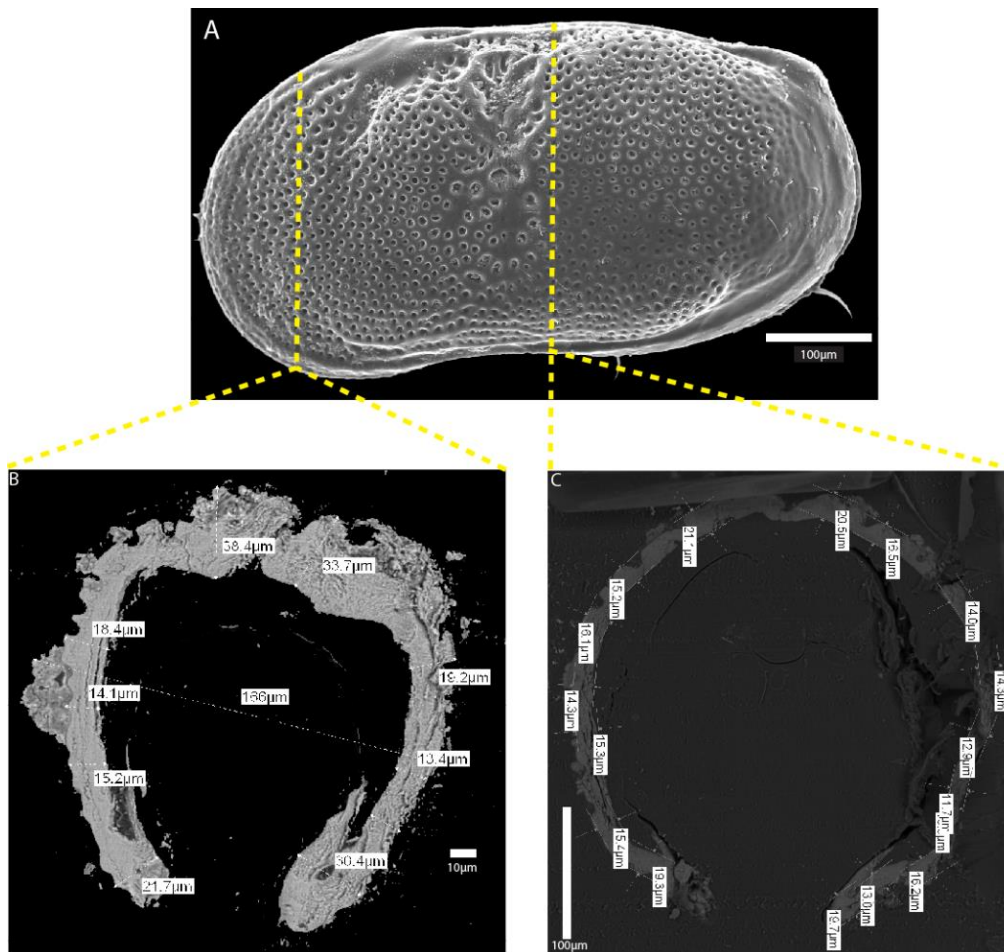


Figure 5.9: Two different sections through one ostracod valve (A) the ostracod carapace before cutting (yellow dashed lines show the position of the corresponding images below which are sections through the carapace), (B) image of ostracod carapace cut through posterior edge, (C) image of the ostracod carapace through the middle.

A pilot study was undertaken to determine the correct portion of the carapace to measure for carapace thickness (Figure 5.9A). Four individuals that had not gone into the treatments were used to determine how much of the ostracod carapace needed to be ground away to get an accurate thickness

measurement (Figure 5.9A). In the first trial the block was only ground down so the posterior edge of the carapace was removed and then measured for carapace thickness as previously explained (Figure 5.9B). In the second trial, the same block was then ground down again to the middle of the specimens and again measured as previously explained (Figure 5.9C). From this experiment it was decided that the blocks had to be ground down to the middle of the specimens as it gave a much clearer image and a more accurate measurement than at the posterior edge.

5.4.9 Carapace mineralogy

The Magnesium (Mg) and Calcium (Ca) content of the carapace were determined using, a Varian 752-ES ICP Optical Emission Spectrometer (ICPOES, Agilent Technologies; Santa Clara, USA). First a pilot study was undertaken to determine the amount of material required to allow the ICPOES to produce realistic results as one ostracod would not be enough. Five and ten individuals of each species from the field collected specimens were picked out of the sediment and tested as well as an example of the sediment from which they were collected. The mass of each of the combined ostracod samples was recorded in milligrams after which 1 ml of HCl (10 %) was added and left for 2 hrs to dissolve the samples. This was then diluted with deionised water to 10 ml, mixed well and tested (in duplicate) along with four reference standards constructed using a multi-element solution and a strontium carbonate solution. The strontium solution was prepared by diluting 0.5 ml of 10,000 mg.l⁻¹ SrCO₃ to 50 ml with HNO₃ (2 %). The table below shows how the four different standards were prepared (Table 5.1).

Standards	Preparation methods
Standard 1	0.05 ml of both the 100 mg/l Sr solution and the multi-element standard was diluted to 50ml ($0.05/50 \times 100 \text{ mg/l} = 0.1 \text{ mg/l}$).
Standard 2	0.25 ml of both the 100 mg/l Sr and multi-element mixture diluted to 50 ml. ($0.25/50 \times 100 \text{ mg/l} = 0.5 \text{ mg/l}$).
Standard 3	1 ml of both the 100 mg/l Sr and the multi-element mixture diluted to 50 ml. ($1/50 \times 100 \text{ mg/l} = 2 \text{ mg/l}$).
Standard 4	2 ml of both the 100 mg/l Sr and the multi-element mixture diluted to 50 ml. ($2/50 \times 100 \text{ mg/l} = 4 \text{ mg/l}$).

Table 5.1: Preparation of calibration standards for trace element geochemistry.

Results are expressed as mg kg^{-1} . It was estimated from this that only five individuals per treatment would be needed to acquire the relevant concentrations for the machine (Appendix 6, Table A6.2). It was realised that not enough individuals were present to complete both elemental and carapace thickness analysis for each treatment due to the destructive nature of the ICPOES analysis (Agilent Technologies; Santa Clara, USA). For this reason a different method was attempted to determine the mineralogical composition of the carapaces (described below).

One specimen of each species from the field collected samples and one specimen from every treatment and treatment sub-group (live and dead) was placed on a stub for the SEM. Each stub was carbon coated using an Emitech K450X rotary carbon coater (Quorum Technologies Ltd, West Sussex, UK) to prepare the surface for the SEM. Each specimen was then photographed and the carapace surface analysed for elemental analysis using the Oxford instruments AZtec X-ray micro analysis (High Wickham, UK) which is attached to the JEOL JSM-7001F Field Emission Scanning Electron Microscope (Tokyo, Japan). To complete this, ten different points on the cleanest area (determined visually) of the carapace surface were analysed to produce a mean result for each element. The problem with this method is that once the individuals are attached to the stub, and carbon coated, their

carapace thickness could not be measured. This was a problem because it was important in this investigation to have elemental analysis, carapace size and carapace thickness measurements all from the same specimen. Consequently it was decided that when measuring for carapace thickness, elemental analysis would be conducted through the carapace's thickness rather than on the carapace's surface which solved the issue of having small numbers of individuals. Elemental analysis was conducted where carapace thickness measurements were taken with a minimum of ten points analysed through the thickness of the carapace.

5.4.10 Data manipulation

PAST (PAlaeontological STatistical program; Hammer *et al.*, 2001) and SPSS (The Statistical Package for the Social Sciences, IBM corporation, New York, USA) were used to carry out the statistical analysis on the data sets. To determine if the results for geometric carapace size, carapace thickness, percentage of Mg and Ca in the carapace and preservation (see Appendix 6: Tables A6.3A-E, A6.10A-E and A6.18A-E for raw species data) show any statistically significant difference between the four treatments, the length of treatment or live or dead, the Kruskal-Wallis and the Mann-Whitney pairwise comparison test was used. To investigate any significant relationships between the different measurements, linear regression models were used to compare all the different measurements (except preservation) against each other. Preservation had to be analysed differently using Spearman's rank because the preservation is a ranked number unlike the rest of the data sets which are measurements. General linear models were

used to investigate which was the principal controlling factor on the geometric carapace size, carapace thickness, average Mg, average Ca and carapace preservation results (e.g., a specific treatment, length of treatment or if they were collected live or dead) (Appendix 6: Figures A6.1–A6.5, A6.12–A6.16 and A6.22–A6.26 A–B analysed data for all three species).

5.5 Results

5.5.2 Field collected individuals

These data are for individuals collected from the field but not placed in the experimental mesocosm.

5.5.3 *Leptocythere* sp.

From the 40 field collected individuals of *Leptocythere* sp. there was a geometric carapace size range of 401.55–473.08 μm , a mean carapace thickness range of 9.44–15.18 μm from the 30 measured, average Mg values ranging from 0.58–1.09 % and average Ca values ranging from 46.32–69.22 %. Images of perfect preservation can be seen in (Figure 5.10A).

5.5.4 *L. castanea*

From the 45 field collected individuals of *L. castanea* there was a geometric carapace size range of 411.37–486.62 μm , a mean carapace thickness range of 8.96–17.43 μm from the 31 individuals measured, average Mg values ranging from 0.43–1.33 % and average Ca values ranging between 47.6–77.95 %. Images of perfect preservation can be seen in (Figure 5.10B).

5.5.5 *L. lacertosa*

From the 14 field collected individuals of *L. lacertosa* there was a geometric carapace size range between 189.15–275.48 μm , a mean carapace thickness range between 7.09–11.25 μm from the 6 measured, average Mg values range between 0.43–0.68 % and average Ca values range from 56.84–75.11 %. Images of perfect preservation can be seen in (Figure 5.10C).

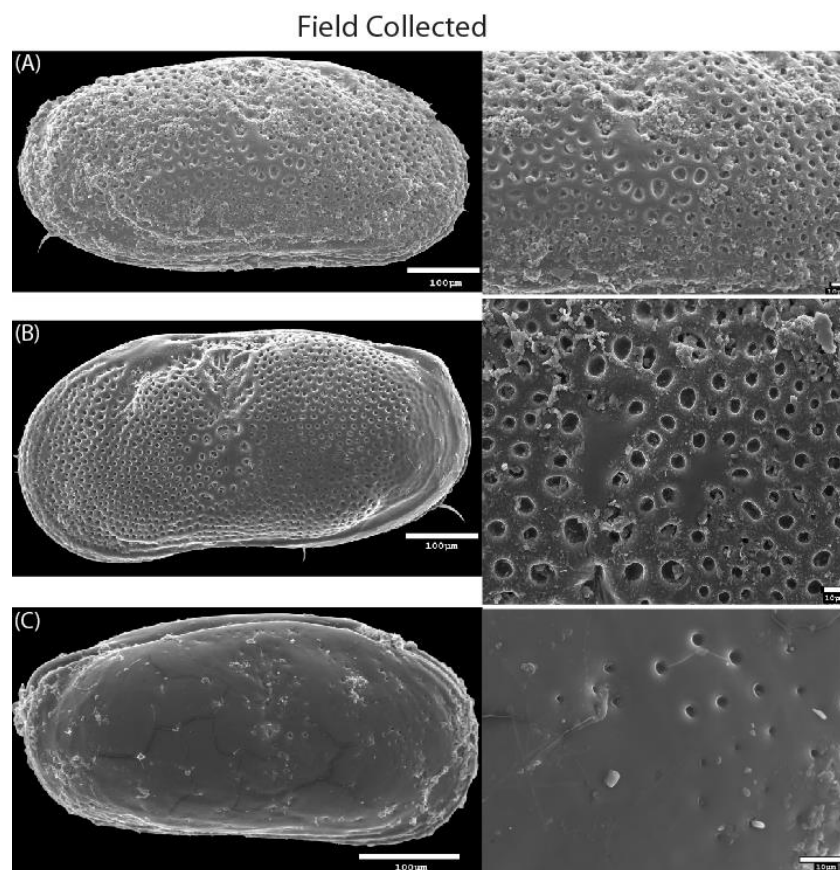


Figure 5.10: Carapace preservation of the different field collected species (A) *Leptocythere* sp., (B) *L. castanea*, (C) *L. lacertosa* (Scale: 100 μm for carapace image, 10 μm for surface detail).

5.6 Effects of elevated CO_2 and temperature on survival.

Survival was comparatively low for all three species in each treatment (including controls) after 21 days. No individuals survived 95 days in any

treatment even though their life cycle is reported to be significantly longer than this (Figure 5.11). *L. lacertosa* survived best in culture. There was little effect of temperature on survival of *Leptocythere* sp. but no individuals survived 21 days under high CO₂ conditions. In the case of *L. lacertosa* and *L. castanea* there was a reduction in survival only in the high temperature control, with survival in the high temperature and CO₂ condition being similar to survival at the lower temperature, irrespective of whether the water was acidified or not.

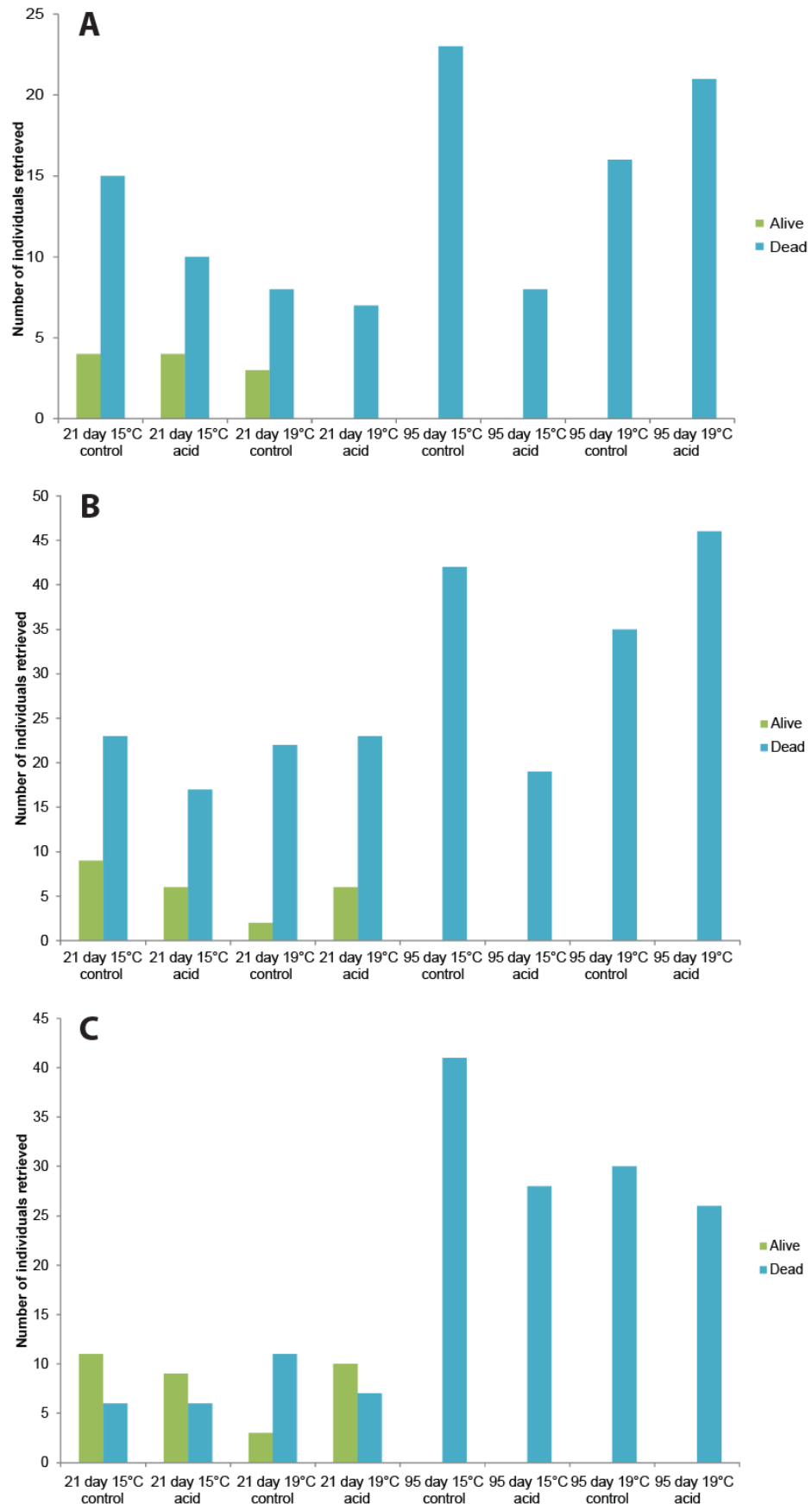


Figure 5.11: Survival of (A) *Leptocythere* sp., (B) *L. castanea*, (C) *L. lacertosa* in the treatments upon retrieval from the system after either 21 day or 95 days.

5.6.2 Effect of elevated CO₂ and temperature on ostracod morphometrics for living individuals.

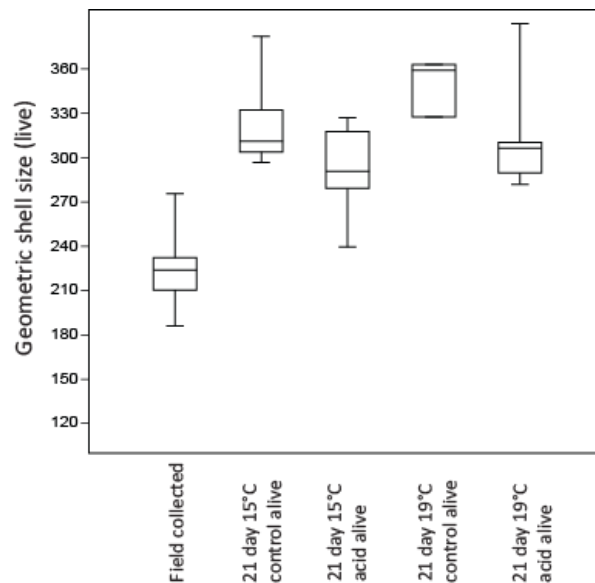


Figure 5.12: *L. lacertosa*: The box and whisker plot displays the geometric carapace size data (µm) showing the minimum, maximum, median and first and third quartile of the data from each treatment.

There was a significant difference in geometric carapace size (including field collected data) for *L. lacertosa* ($P < 0.001$) due to high CO₂ but not temperature (Figure 5.12). Ostracods grew whilst in the mesocosm and that growth was compromised by high CO₂. However, there was no further significant difference found for ostracod morphometrics between treatments and for other species. Neither of the other two species grew in the mesocosm. These data are presented in Table 5.2 with the full results of the statistical tests presented in Appendix 6: Figures A6.6–A6.7, A6.16–A6.17, A6.27 and Tables A6.19, A6.40–A6.41.

5.6.3 Effect of elevated CO₂ and temperature on live ostracod mineralogy.

There was a significant difference in Mg for *L. lacertosa* ($P < 0.005$; Figure 5.13; including field collected data) as a result of high CO₂ and high

temperature conditions. Except for those detailed below, there was no significant difference found for ostracod mineralogy between treatments and these data are recorded in Table 5.3 with the full results of the statistical tests presented in Appendix 6: Figures A6.8–A6.9, 1 A6.8–A6.19, A6.29 and Table A6.20.

<i>Leptocythere</i> sp. Live geometric carapace size (µm)								
	N	Min	Max	Mean	Stand. dev.	Median	25 percentile	75 percentile
field collected	40	401.55	473.08	433.21	18.29	429.03	418.99	446.82
21 day 15°C control live	4	379.07	466.15	432.17	37.70	441.72	392.90	461.88
21 day 15°C acid live	4	417.25	451.86	437.30	14.60	440.04	422.37	449.49
21 day 19°C control live	3	423.88	440.84	430.78	8.91	427.61	423.88	440.84
<i>Leptocythere</i> sp. Live carapace thickness (µm)								
field collected	30	9.44	15.18	12.57	1.43	12.68	11.65	13.54
21 day 15°C control live	2	8.66	9.89	9.28	0.87	9.28	6.5	7.42
21 day 15°C acid live	2	11.63	14	12.82	1.68	12.82	8.72	10.5
<i>L. castanea</i> Live geometric carapace size (µm)								
field collected	45	411.37	486.62	440.37	15.51	439.98	431.15	450.14
21 day 15°C control live	9	380.64	451.75	428.35	22.60	432.66	415.61	448.69
21 day 15°C acid live	6	383.47	456.31	428.87	30.4	442.94	394.38	451.23
21 day 19°C control live	2	393.66	421.21	407.44	19.48	407.44	295.23	425.65
21 day 19°C acid live	6	427.54	448.11	438.76	7.53	439.29	431.97	445.69
<i>L. castanea</i> Live carapace thickness (µm)								
field collected	31	8.96	17.43	11.79	1.94	11.88	10.04	12.68
21 day 15°C control live	7	6.39	11.8	9.39	2.23	9.33	6.74	11.57
21 day 15°C acid live	4	5.54	13.85	8.33	3.87	6.97	5.59	12.44
21 day 19°C acid live	4	6.96	13.45	10.62	2.79	11.04	7.76	13.07
<i>L. lacertosa</i> Live carapace thickness (µm)								
field collected	6	7.09	11.25	9.43	1.41	9.77	8.29	10.33
21 day 15°C control live	9	6.50	10.85	8.15	1.42	8.01	6.90	9.18
21 day 15°C acid live	7	5.66	12.16	9.01	2.15	9.65	6.91	10.02
21 day 19°C control live	3	327.42	362.94	349.80	19.48	359.05	327.42	362.94
21 day 19°C acid live	8	5.50	13.35	8.71	2.62	8.45	6.14	10.37

Table 5.2: The ostracod morphometrics data for the three species where no statistically significant differences were found between treatments.

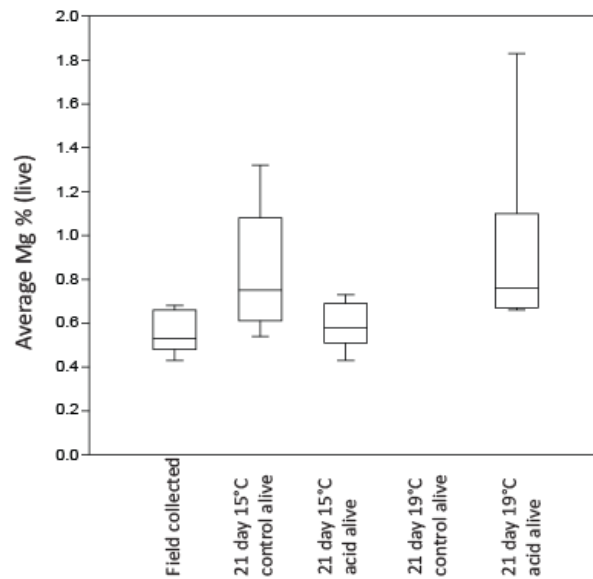


Figure 5.13: *L. lacertosa*: The box and whisker plot displays the live average Mg data (%) showing the minimum, maximum, median and first and third quartile of the data in each treatment. There were insufficient data to plot the 21 day, 19°C control live results.

<i>Leptocythere</i> sp. Live average Mg (%)								
	N	Min	Max	Mean	Stand. dev.	Median	25 percentile	75 percentile
Field collected	31	0.58	1.09	0.83	0.13	0.82	0.73	0.94
21 day 15°C control live	2	0.83	0.87	0.85	0.03	0.85	0.62	0.65
<i>Leptocythere</i> sp. Live average Ca (%)								
Field collected	31	46.32	69.22	54.13	6.80	51.82	48.16	57.65
21 day 15°C control live	2	56.32	68.95	62.64	8.93	62.64	42.24	51.71
21 day 15°C acid live	2	48.83	50.99	49.91	1.53	49.91	36.62	38.24
<i>L. castanea</i> Live average Mg (%)								
Field collected	30	0.43	1.33	0.81	0.19	0.78	0.71	0.96
21 day 15°C control live	7	0.60	1.46	0.97	0.37	0.76	0.66	1.41
21 day 15°C acid live	4	0.69	1.95	1.08	0.58	0.85	0.72	1.68
21 day 19°C acid live	4	0.82	0.96	0.88	0.06	0.87	0.83	0.94
<i>L. castanea</i> Live average Ca (%)								
Field collected	31	47.60	77.95	57.13	7.28	55.32	50.94	62.37
21 day 15°C control live	7	49.66	67.71	58.98	6.35	58.19	52.71	63.84
21 day 15°C acid live	4	51.48	61.26	55.95	4.08	55.53	52.28	60.04
21 day 19°C acid live	4	43.88	61.22	54.78	7.61	57.02	46.83	60.50
<i>L. lacertosa</i> Live average Ca (%)								
Field collected	6	56.84	75.11	66.59	6.63	68.75	59.74	70.84
21 day 15°C control live	9	51.65	70.05	57.93	7.07	54.94	51.88	64.77
21 day 15°C acid live	7	48.08	80.22	66.14	13.22	68.91	48.59	79.26
21 day 19°C acid live	9	50.78	70.56	59.41	6.75	57.96	54.03	65.07

Table 5.3: The ostracod mineralogy data for the three species where no statistically significant differences were found between treatments.

5.6.4 Effect of elevated CO₂ and temperature on carapace condition of live ostracods.

Presented in Figures 5.14–5.19 are the effects of 21 days exposure to high CO₂ and temperature conditions on carapace condition for all three species. There was a significant difference in carapace condition of both *Leptocythere* sp. ($P < 0.001$) and *L. castanea* ($P < 0.001$; including field collected data) as a result of high CO₂ and temperature conditions. Carapace surface quality was poorer in high CO₂ conditions and this was even more marked at the higher temperature. There was a significant difference in carapace condition for *L. lacertosa* ($P < 0.001$) (including field collected data) as a result of either high CO₂ or temperature conditions combined.

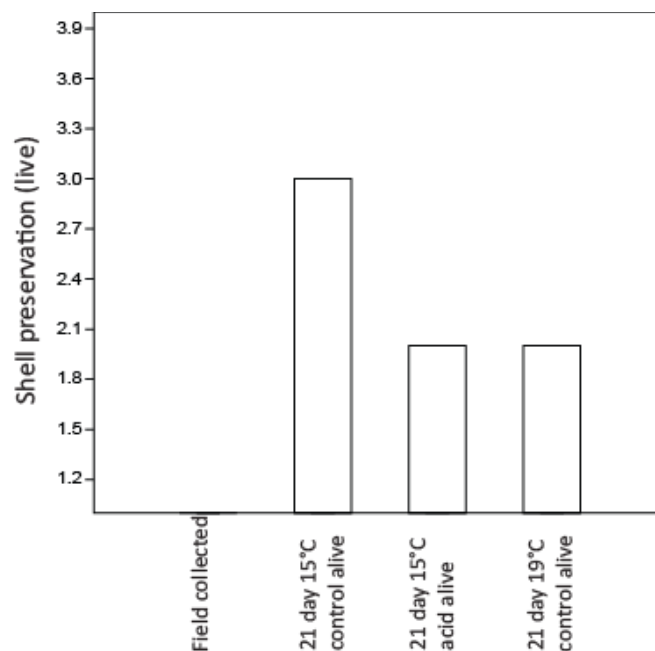


Figure 5.14: *Leptocythere* sp.: The box and whisker plot displays the live carapace condition data showing the minimum, maximum, median and first and third quartile of the data from each treatment set. Full results of the statistical tests are presented in Appendix 6; Table A6.4.

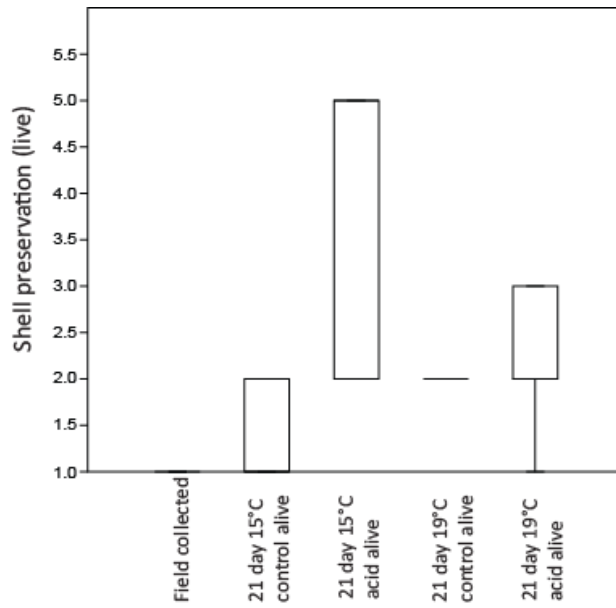


Figure 5.15: *L. castanea*: The box and whisker plot displays the live carapace preservation data showing the minimum, maximum, median and first and third quartile of the data from each treatment. The 19°C control alive box and whisker is only a line due to lack of a wide spread of preservation data from that treatment. Full results of the statistical tests are presented in Appendix 6; Table A6.11.

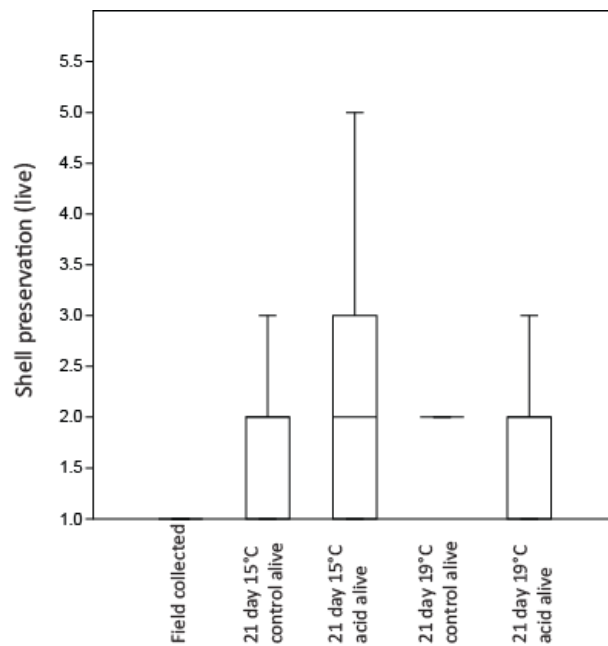


Figure 5.16: *L. lacertosa*: The box and whisker plot displays the live carapace preservation data showing the minimum, maximum, median and first and third quartile of the data from each treatment. The 19°C control alive box and whisker is only a line due to lack of a wide spread of preservation data from that treatment. Full results of the statistical tests are presented in Appendix 6; Table A6.21.

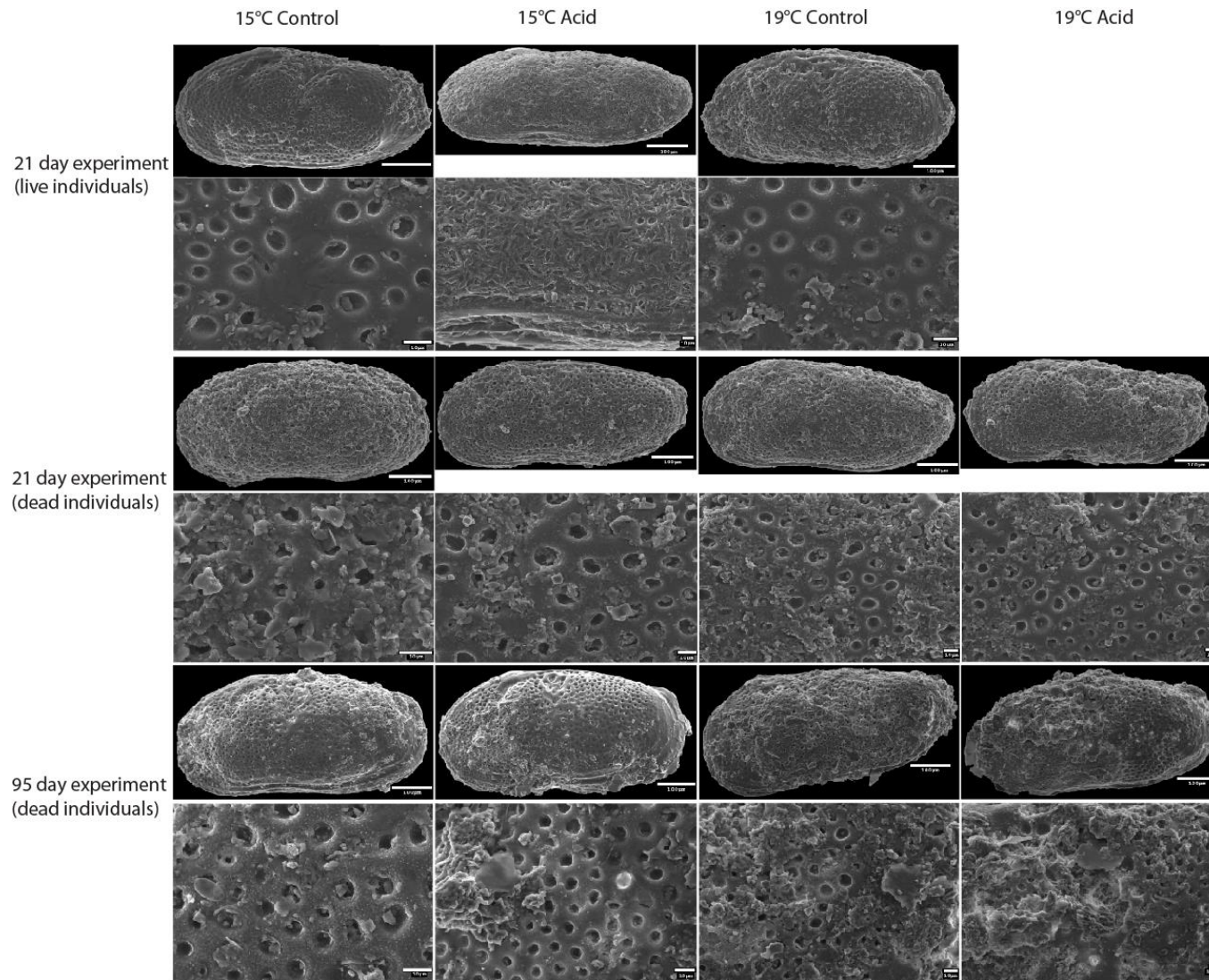


Figure 5.17: Images of *Leptocythere* sp. showing examples of the preservation found when individuals both live and dead were collected from the experiments at 21 days and then 95 days. Scale bars for full image of ostracods are 100 μ m and detailed shell surface images are 10 μ m.

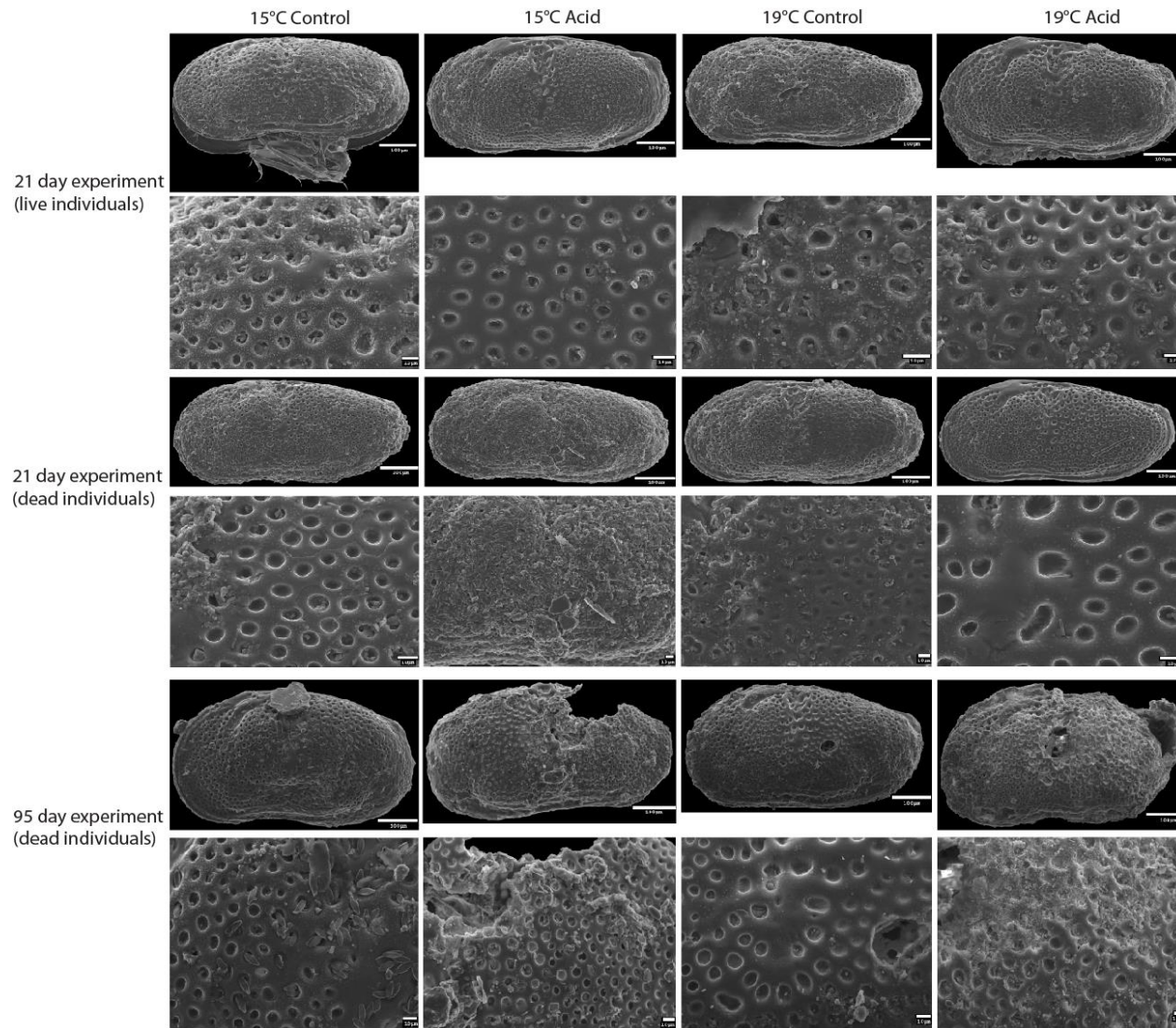


Figure 5.18: Images of *L. castanea* showing examples of the preservation found when individuals both live and dead were collected from the experiments at 21 days and then 95 days. Scale bars for full image of ostracods are 100 μ m and detailed shell surface images are 10 μ m.

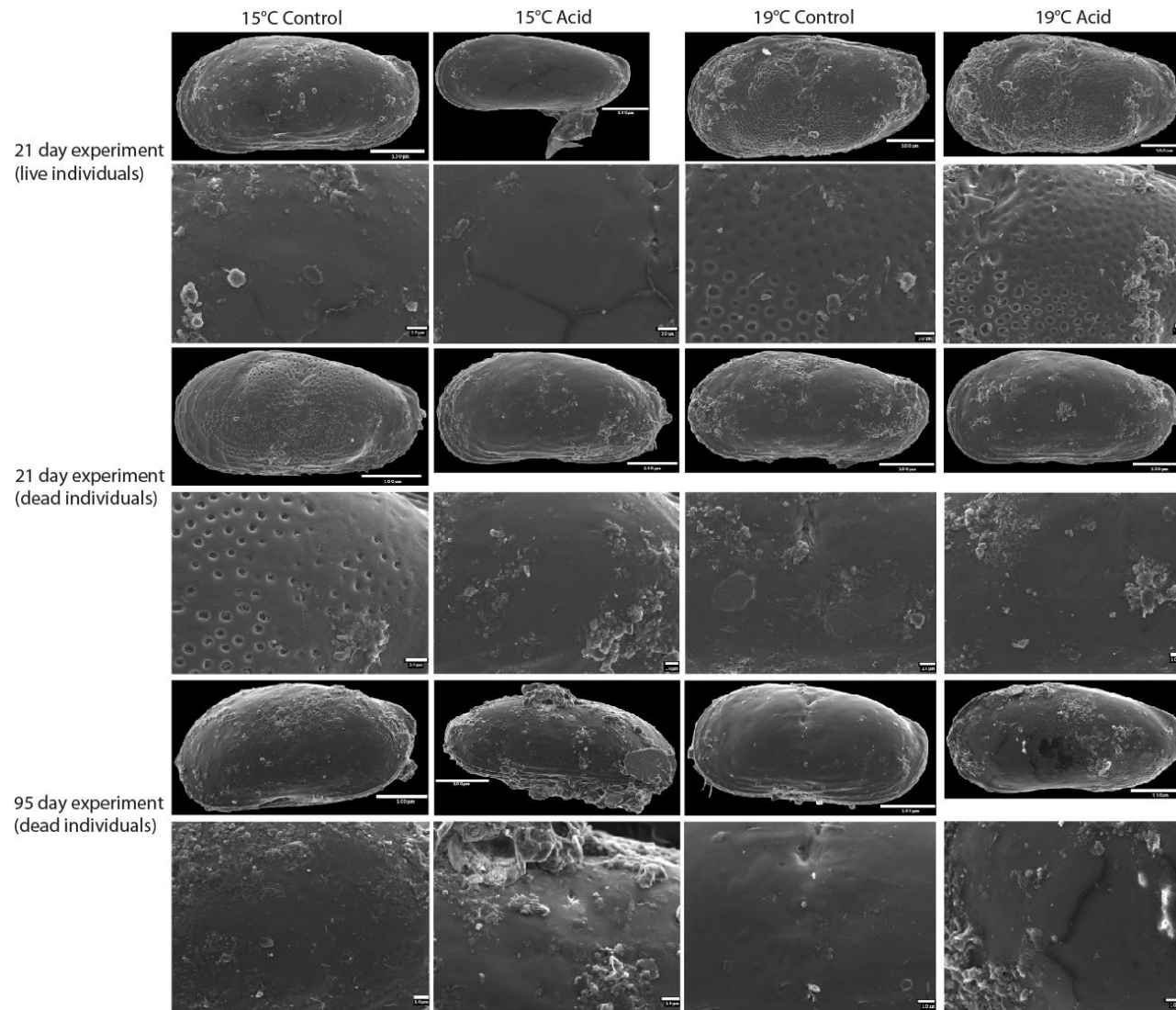


Figure 5.19: Images of *L. lacertosa* showing examples of the preservation found when individuals both live and dead were collected from the experiments at 21 days and then 95 days. Scale bars for full image of ostracods are 100 μ m and detailed shell surface images are 10 μ m.

5.7 Effect of exposure to elevated CO₂ and temperature conditions on the carapaces of dead individuals over 21 days and 95 days?

All data presented in this section are from the carapaces of dead individuals and so preservation has been analysed before carapace size as it is the most likely component to be altered post-harvest. Except for those detailed below there was no significant difference found for ostracod preservation, morphometrics and mineralogy between treatments and these data are recorded in Table 5.4 with the full results of the statistical tests presented in Appendix 6; Tables A6.5–A6.8, A6.12–A6.16, A6.22–A6.25 and Figure A6.28.

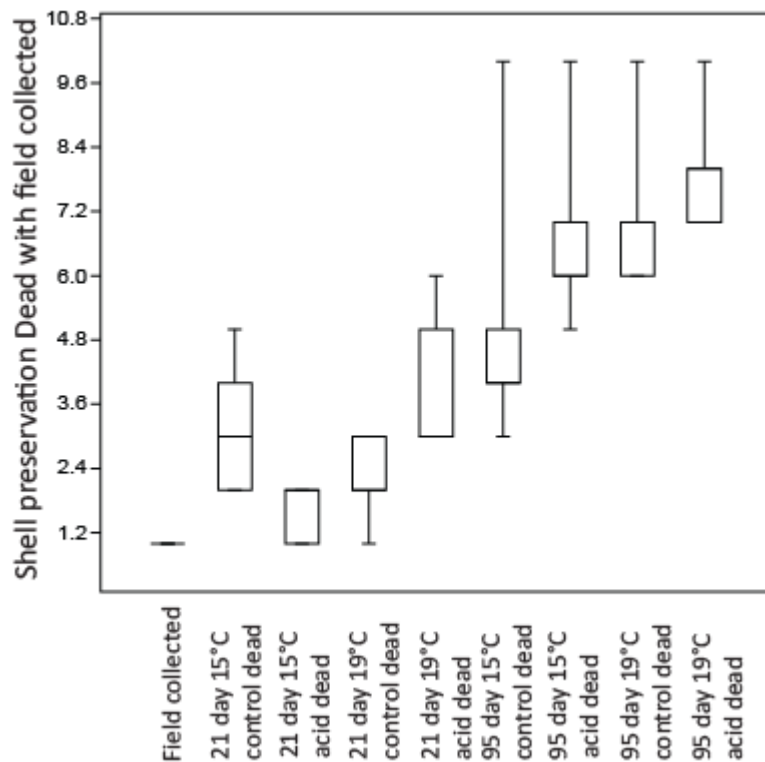


Figure 5.20: *Leptocythere* sp.: The box and whisker plot displays the dead carapace preservation data showing the minimum, maximum, median and first and third quartile of the data from each treatment set. The field collected box and whisker is only a line due to lack of a wide spread of preservation data from that treatment.

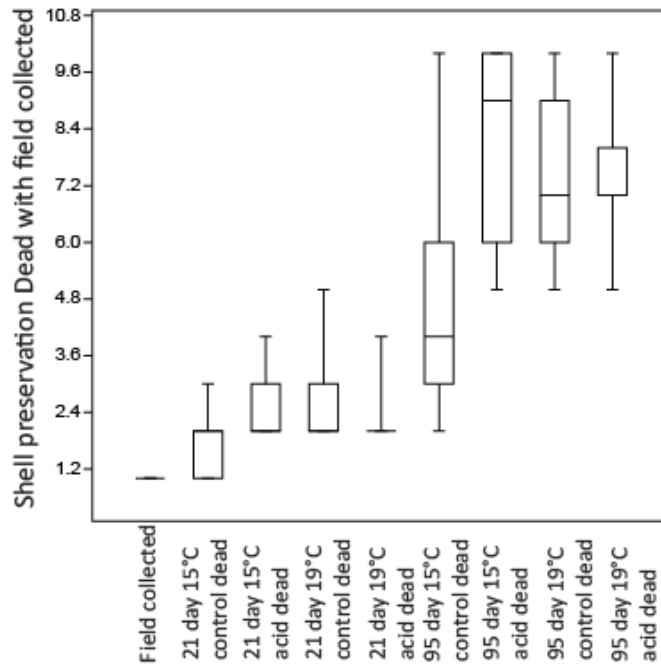


Figure 5.21: *L. castanea*: The box and whisker plot displays the dead carapace preservation data showing the minimum, maximum, median and first and third quartile of the data from each treatment. The field collected box and whisker is only a line due to lack of a wide spread of preservation data from that treatment.

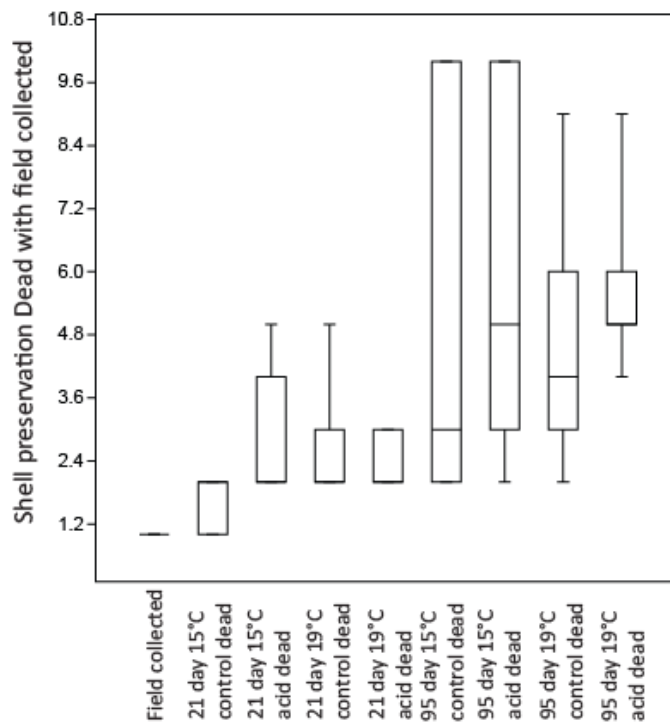


Figure 5.22: *L. lacertosa*: The box and whisker plot displays the dead carapace preservation data showing the minimum, maximum, median and first and third quartile of the data from each treatment. The field collected box and whisker is only a line due to lack of a wide spread of preservation data from that treatment.

Preservation: The carapace preservation of *Leptocythere* sp., *L. castanea* and *L. lacertosa* throughout the different treatments was significantly affected by how long they were kept in the experimental conditions ($P < 0.001$ in each case). Carapace preservation deteriorated after 21 days exposure to high temperature for *L. lacertosa* ($P < 0.02$), *Leptocythere* sp. ($P < 0.05$) and *L. castanea* ($P < 0.02$) and was reduced further by exposure to high CO₂ conditions ($P < 0.001$ in each case; Figures 5.20–5.22 for all three species after 21 days). There was a significant decrease in carapace preservation after 95 days for *Leptocythere* sp. and *L. castanea* due to higher temperatures and high CO₂ conditions ($P < 0.001$ and $P < 0.05$ respectively and $P < 0.001$ for both species). However for *L. lacertosa* only high CO₂ conditions resulted in a significant deterioration after 95 days ($P < 0.014$; Figures 5.20–5.22 for all three species after 95 days).

Carapace preservation had significantly deteriorated (in each treatment and depending on treatment duration) when compared with the field collected individuals as a result of high CO₂ conditions, temperature and treatment length ($P < 0.001$ for all three species). Preservation of the carapaces of dead individuals had significantly deteriorated (in each treatment and both treatment lengths) when compared with carapace preservation in live individuals as a result of high CO₂ conditions, temperature and treatment length ($P < 0.001$ for all three species).

Geometric carapace size: The geometric carapace size of dead *Leptocythere* sp. ($P < 0.01$), *L. castanea* ($P < 0.05$) and *L. lacertosa* ($P < 0.002$) (within all the treatments) was significantly reduced the longer the carapaces had been in the experimental conditions. There was a significant difference in

geometric size for *L. castanea* which was attributable to high CO₂ conditions after 21 days ($P < 0.02$) and after 95 days ($P < 0.003$) as well as temperature after 95 days ($P < 0.01$; Figure 5.24). Geometric carapace size (in each treatment and both treatment lengths) was significantly reduced compared against the field collected individuals ($P < 0.05$, $P < 0.001$ and $P < 0.001$ respectively; Figures 5.23–5.25) as a result of high CO₂ conditions, temperature and treatment length.

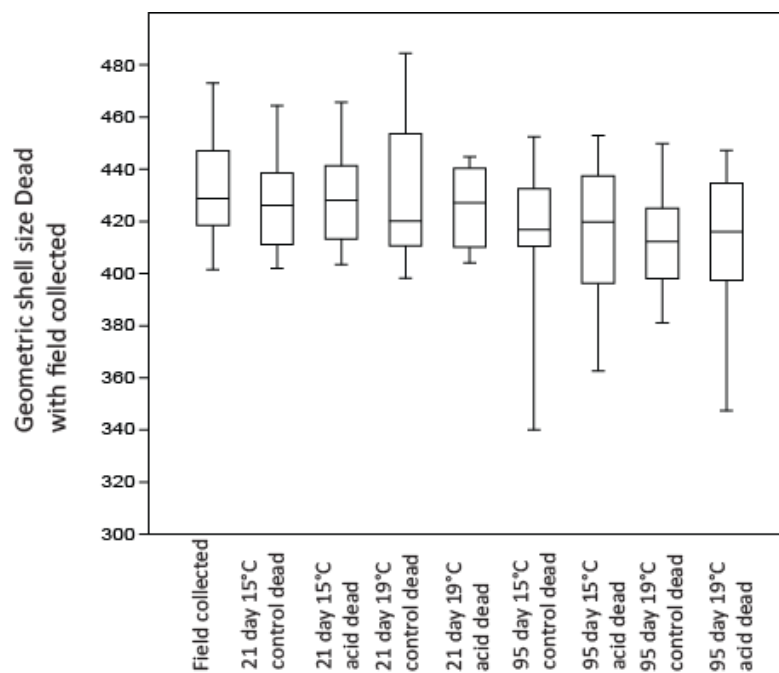


Figure 5.23: *Leptocythere* sp.: The box and whisker plot illustrates the dead geometric carapace size data (μm) showing the minimum, maximum, median and first and third quartile of the data from each treatment.

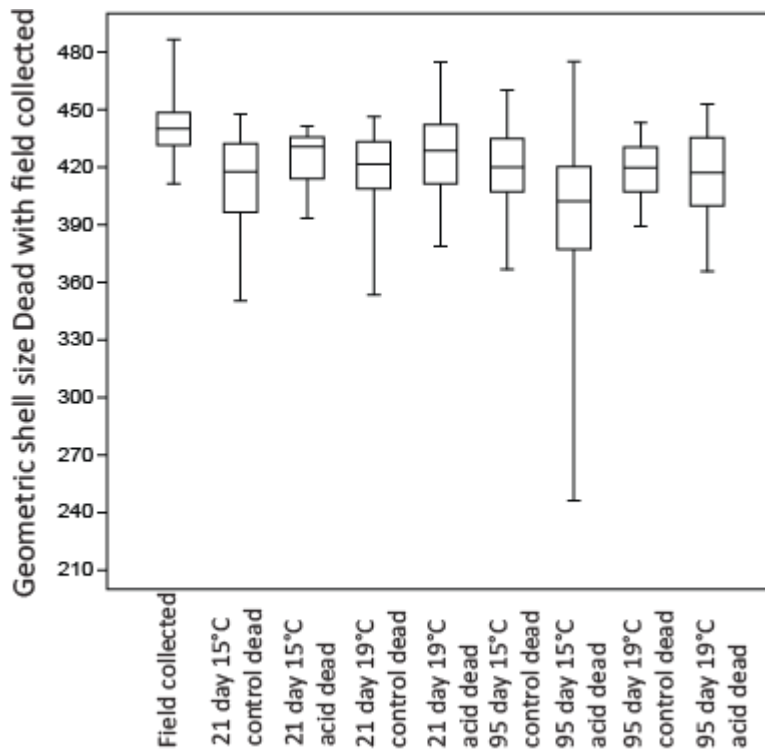


Figure 5.24: *L. castanea*: The box and whisker plot illustrates the dead geometric carapace size data (μm) showing the minimum, maximum, median and first and third quartile of the data from each treatment.

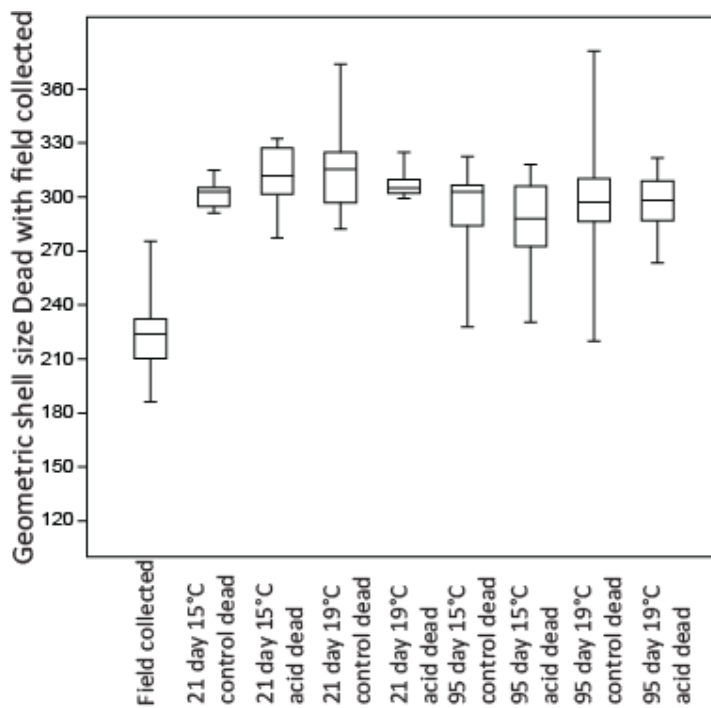


Figure 5.25: *L. lacertosa*: The box and whisker plot illustrates the dead geometric carapace size data (μm) showing the minimum, maximum, median and first and third quartile of the data from each treatment.

The geometric size of the carapace of the dead individuals (in each treatment and both treatment lengths) was significantly less than that of live individuals ($P < 0.05$ in each case; Figures 5.23–5.25). For *L. castanea* geometric carapace size decreased further for dead individuals in the high CO₂ conditions ($P < 0.001$) whereas *L. lacertosa* was affected across all of the treatments ($P < 0.002$ in each case). *Leptocythere* sp. shows a significant effect between dead and live individuals but the results do not indicate which factor is causing this significant effect.

<i>Leptocythere</i> sp. Dead carapace thickness (µm)								
	N	Min	Max	Mean	Stand. dev.	Median	25 percentile	75 percentile
21 day_15°C control dead	13	7.38	14.20	12.01	2.59	13.53	9.52	13.94
21 day 15°C acid dead	8	9.46	14.60	11.97	1.88	11.37	10.64	14.12
21 day 19°C control dead	6	12.13	14.20	13.07	0.73	13.12	12.37	13.60
21 day 19°C acid dead	5	8.87	15.00	12.20	2.35	12.50	9.99	14.27
95 day 15°C control dead	18	8.06	16.15	12.74	2.33	13.64	11.35	14.10
95 day 15°C acid dead	5	8.89	12.30	10.67	1.51	10.48	9.24	12.20
95 day 19°C control dead	11	9.28	13.45	11.60	1.10	11.72	10.88	12.48
95 day 19°C acid dead	15	8.07	15.45	11.30	1.95	11.13	10.22	12.70
<i>L. lacertosa</i> Dead carapace thickness (µm)								
21 day 15°C control dead	4	8.32	11.68	10.07	1.39	10.13	8.70	11.37
21 day 15°C acid dead	3	9.49	10.55	9.89	0.58	9.63	9.49	10.55
21 day 19°C control dead	8	6.78	11.54	8.86	1.99	8.57	6.91	10.88
21 day 19°C acid dead	5	8.01	10.88	9.75	1.10	10.05	8.74	10.61
95 day 15°C control dead	26	6.54	11.65	9.20	1.54	9.18	7.85	10.37
95 day 15°C acid dead	16	4.07	12.03	8.29	2.61	9.00	5.48	10.50
95 day 19°C control dead	25	5.45	12.20	8.36	1.90	8.06	6.65	9.71
95 day 19°C acid dead	23	4.93	11.70	8.98	1.88	8.82	7.70	10.51

Table 5.4: The ostracod carapace thickness data for the three species where no statistically significant differences were found between treatments.

Carapace thickness: After 21 days there was a significant difference in carapace thickness in *L. castanea* as a result of both high CO₂ conditions ($P < 0.005$) and temperature ($P < 0.02$; Figure 5.26). Treatment length and CO₂

combined produced significantly thinner carapaces for *L. castanea* ($P < 0.005$). Carapace thickness was also significantly thinner (in each treatment and both treatment lengths) than the field collected individuals ($P < 0.005$) (Figure 5.26). Carapace thickness from live and dead individuals (in each treatment and both treatment lengths) show a significant thinning as a result of high CO_2 conditions when combined with both the live and dead data ($P < 0.005$).

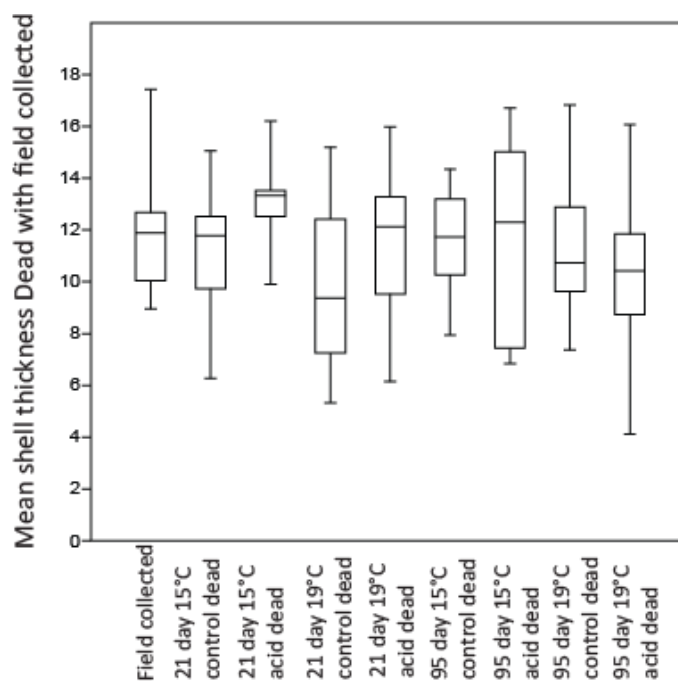


Figure 5.26: *L. castanea*: The box and whisker plot illustrates the dead mean carapace thickness data (μm) showing the minimum, maximum, median and first and third quartile of the data from each treatment set.

Mg: When combined, the treatment length, temperature and high CO_2 conditions had a significant effect on the average Mg levels for *Leptocythere* sp. ($P < 0.001$), *L. castanea* ($P < 0.001$) and *L. lacertosa* ($P < 0.001$) because all increased with exposure time. Average Mg values for *L. castanea* and *L. lacertosa* significantly changed as a result of 21 days exposure to elevated high CO_2 conditions and temperature with average Mg

increasing in acidified, high temperature conditions (21 days = $P < 0.02$ and $P < 0.05$ respectively; Figures 5.27–5.29). Average Mg values for *Leptocythere* sp., *L. castanea* and *L. lacertosa* were all significantly greater as a result of 95 days exposure to high CO₂ conditions and temperature ($P < 0.001$ for all three species, in each case; Figures 5.27–5.29). Increasing treatment lengths combined with acidified higher temperatures caused the average Mg to significantly increase in comparison to the levels in the field collected individuals ($P < 0.001$ for all three species; Figures 5.27–5.29). The overall significant difference in average Mg levels found between live and dead individuals combined (across each treatment and both treatment lengths; $P < 0.001$ for all three species) is due to treatment length combined with high CO₂, high temperature waters.

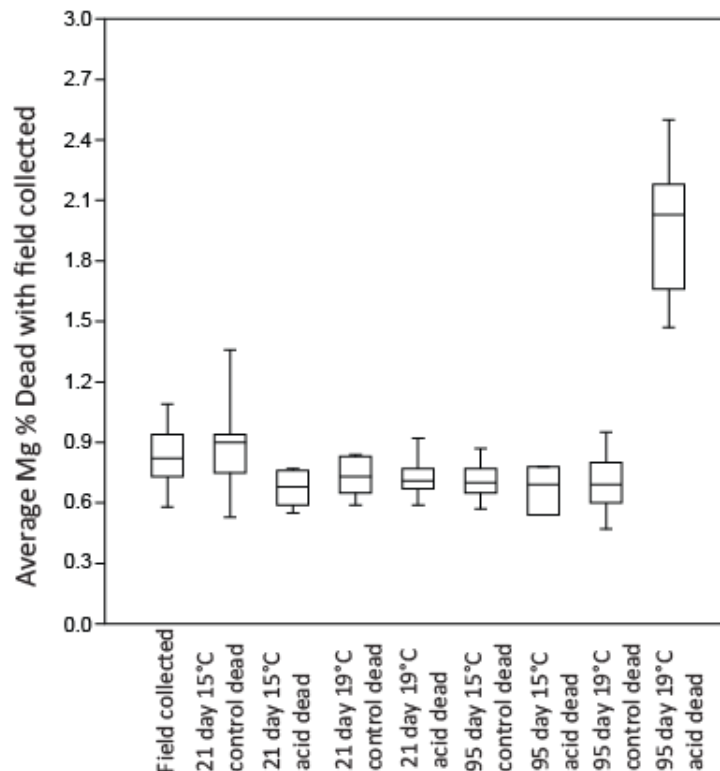


Figure 5.27: *Leptocythere* sp.: The box and whisker plot illustrates the dead average Mg data (%) showing the minimum, maximum, median and first and third quartile of the data from each treatment.

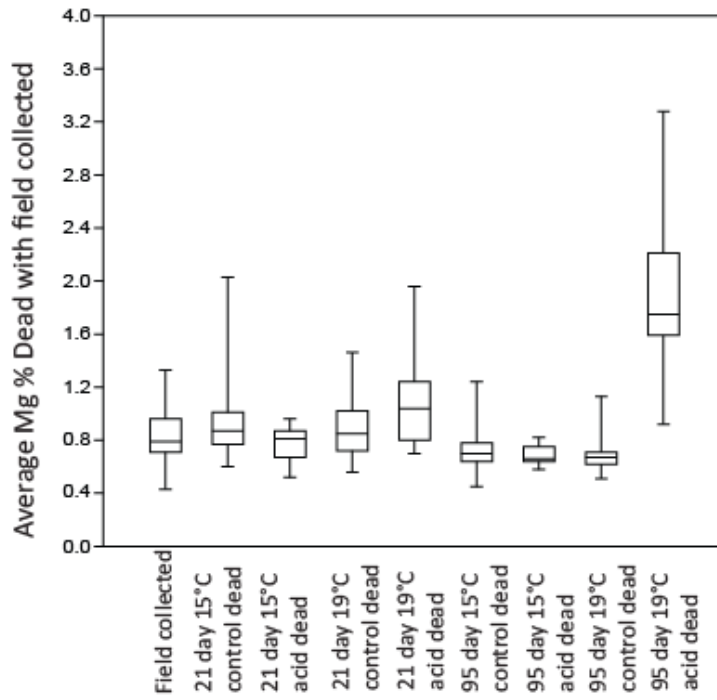


Figure 5.28: *L. castanea*: The box and whisker plot illustrates the dead average Mg data (%) showing the minimum, maximum, median and first and third quartile of the data from each treatment.

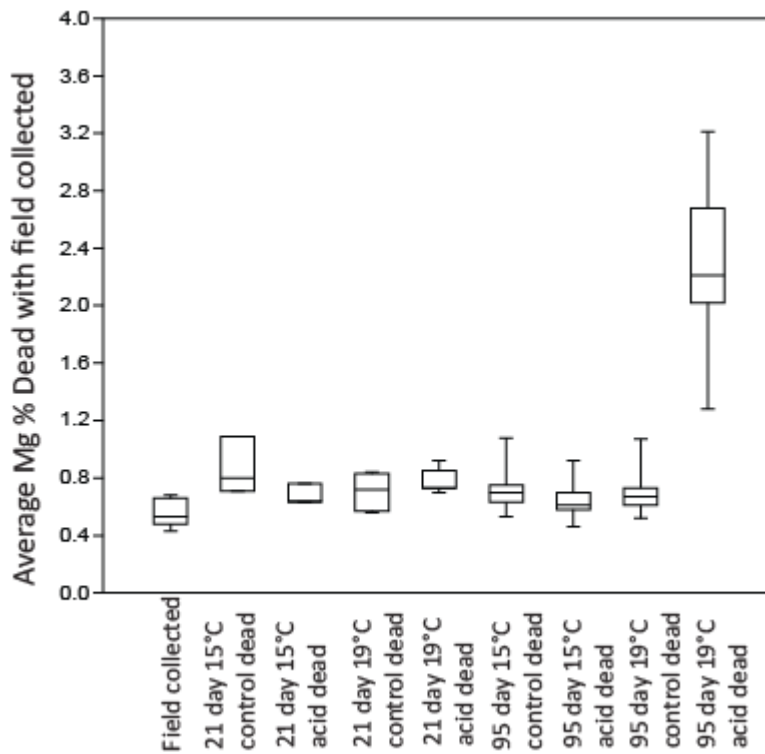


Figure 5.29: *L. lacertosa*: The box and whisker plot illustrates the dead average Mg data (%) showing the minimum, maximum, median and first and third quartile of the data from each treatment.

Ca: Average Ca in *L. lacertosa* had decreased significantly after 21 days in elevated CO₂ (P < 0.01). Decreasing Ca levels were also caused by a combination of high CO₂ conditions and the survival results as well as a combination of high CO₂ conditions temperature (P < 0.002). Longer exposure to experimental treatments resulted in a significant decrease in average Ca levels across all the different treatments for *Leptocythere* sp. (P < 0.01 in each case) with increased temperature after 95 days specifically showing a significant decrease (P < 0.05; Figure 5.30).

Average Ca (across each treatment and both treatment lengths) decreased significantly when compared against the field collected individuals for *Leptocythere* sp., *L. castanea* and *L. lacertosa* (P < 0.05, P < 0.005 and P < 0.001 respectively; Figures 5.31–5.33) likely as a combination of high CO₂ conditions, temperature and treatment length. Average Ca (across each treatment and both treatment lengths) of the carapaces of dead individuals was significantly lower compared with those of live individuals (P < 0.05, P < 0.001 and P < 0.001 respectively; Figures 5.30–5.32). For *L. castanea* an increase in temperature resulted in a significant decrease in Ca. However it was elevated CO₂ which resulted in a significant decrease in Ca in *L. lacertosa*.

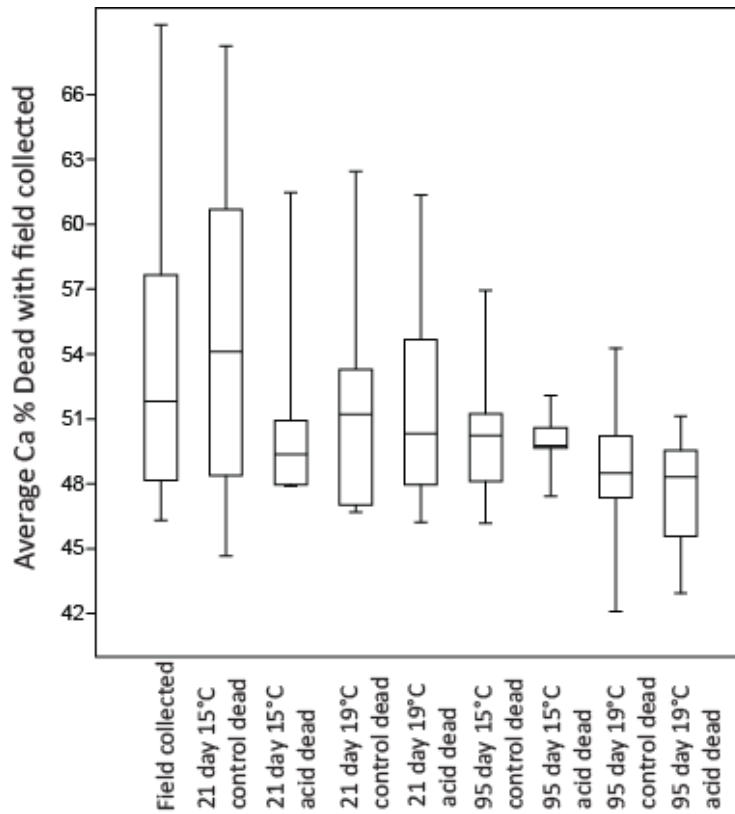


Figure 5.30: *Leptocythere* sp.: The box and whisker plot illustrates the dead average Ca data (%) showing the minimum, maximum, median and first and third quartile of the data from each treatment.

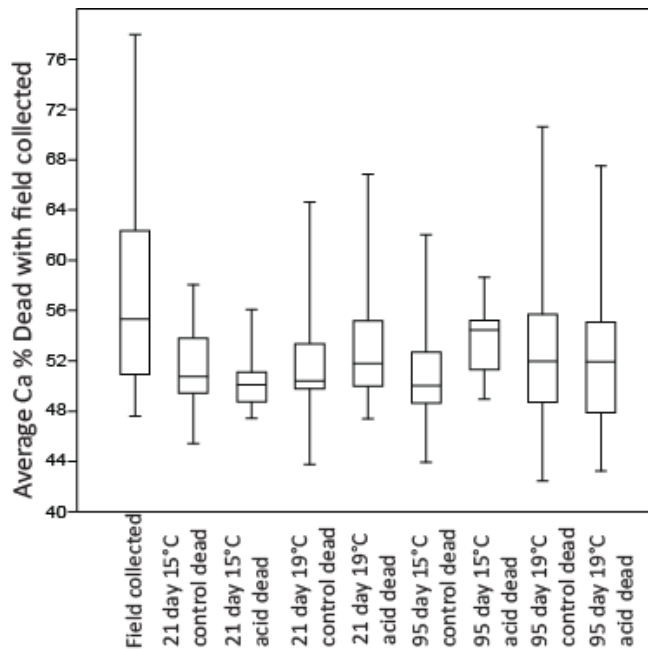


Figure 5.31: *L. castanea*: The box and whisker plot illustrates the dead average Ca data (%) showing the minimum, maximum, median and first and third quartile of the data from each treatment.

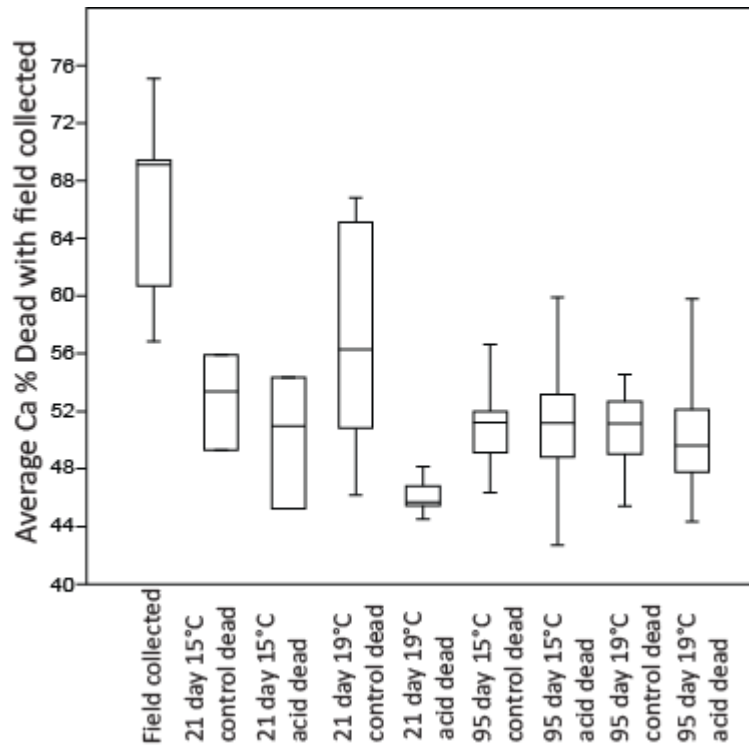


Figure 5.32: *L. lacertosa*: The box and whisker plot illustrates the dead average Ca data (%) showing the minimum, maximum, median and first and third quartile of the data from each treatment.

5.8 Significant relationships between the variations in geometric carapace size, thickness, average Ca, and Mg and preservation for each species.

All of the results for these statistical analyses are in Appendix 6; Tables A6.9, A6.17 and A6.26. There were no significant relationships detected between any two of geometric carapace size, carapace thickness, average Mg and Ca and carapace preservation for live, dead and all the data for each species except for those presented below in Table 5.5. Where there was no significant relationship detected the data are presented in Appendix 6; Figures A6.10–A6.11, A6.20–A6.21 and A6.30–A6.31.

Species	Relationship	N	P	Figure
<i>Leptocythere</i> sp., <i>L. lacertosa</i>	negative relationship between preservation state and dead geometric carapace size	99, 144	P< 0.02/ 0.001	5.33B, 5.34E
	negative relationship between preservation state and all the geometric carapace size data	150, 191	P< 0.001	5.33A 5.34F
<i>L. castanea</i>	negative relationship between preservation state and all the geometric carapace size	261	P< 0.001	5.35D
<i>L. lacertosa</i>	negative relationship between preservation state and the live carapace thickness	47	P< 0.008	5.34H
<i>Leptocythere</i> sp., <i>L. castanea</i> , <i>L. lacertosa</i>	negative relationship between preservation state and dead carapace thickness	81, 207, 110	P< 0.05	5.33 F, 5.35B, 5.34I
<i>Leptocythere</i> sp., <i>L. lacertosa</i>	negative relationship between preservation state and all the carapace thicknesses	116, 141	P< 0.05	5.33E, 5.34G,
<i>Leptocythere</i> sp., <i>L. lacertosa</i>	negative relationship between preservation state and dead average Ca	85, 121	P< 0.005, P< 0.05	5.33 D 5.34D
	negative relationship between preservation state and all of the average Ca	119, 152	P< 0.001	5.33C 5.34C
<i>L. castanea</i> , <i>Leptocythere lacertos</i>	positive relationship between preservation state and all the average Mg	205, 133	P< 0.02	5.35C, 5.34A
<i>Leptocythere</i> sp., <i>L. lacertosa</i>	positive relationship between preservation state and the dead average Mg	78 103	P< 0.001 and P< 0.05	5.33G, 5.34B
<i>L. castanea</i>	positive relationship between geometric carapace size and all the data combined for the mean carapace thickness data	191	P< 0.05	5.37A, B
	positive relationship between geometric carapace size and the live mean carapace thickness data	47	P< 0.01	
<i>Leptocythere</i> sp., <i>L. lacertosa</i>	positive relationship between geometric carapace size data and the mean carapace thickness data for the dead individuals	78, 103	P< 0.05, P< 0.05	5.36A, 5.38B
<i>Leptocythere</i> sp.	positive relationship between mean carapace thickness data and the dead data for average Ca	80	P< 0.02	5.36B
<i>L. lacertosa</i>	positive relationship between mean carapace thickness data and the dead data for average Ca	110	P< 0.01	5.38A
<i>L. castanea</i>	negative relationship between geometric carapace size data and the live data for the average Mg	46	P< 0.01	5.37C
<i>Leptocythere</i> sp.	positive relationship between geometric carapace size data and the dead individuals for the average Mg	77	P< 0.01	5.36C
<i>L. castanea</i>	negative relationship between mean carapace thickness data and the live data for average Mg	46	P< 0.01	5.37E
<i>L. castanea</i>	negative relationship between mean carapace thickness data and the dead data for average Mg	144	P< 0.01	5.36F
<i>Leptocythere</i> sp., <i>L. castanea</i>	negative relationship between mean carapace thickness data and all of the data combined for average Mg	107 190	P< 0.05, P< 0.01	5.37E, D

Table 5.5: significant relationships between any two of geometric carapace size, carapace thickness, average Mg and Ca and carapace preservation for live, dead and all the data for each species.

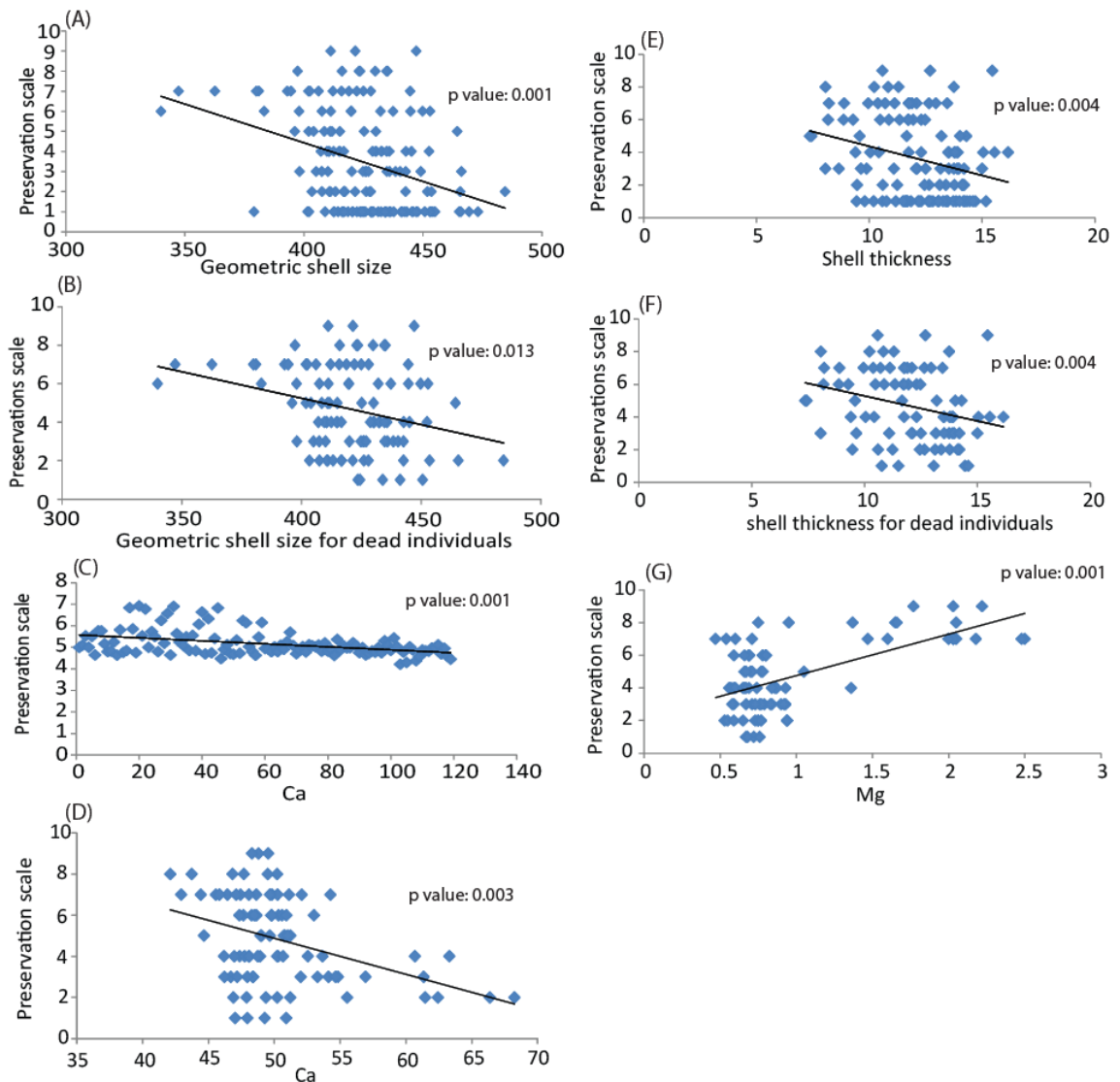
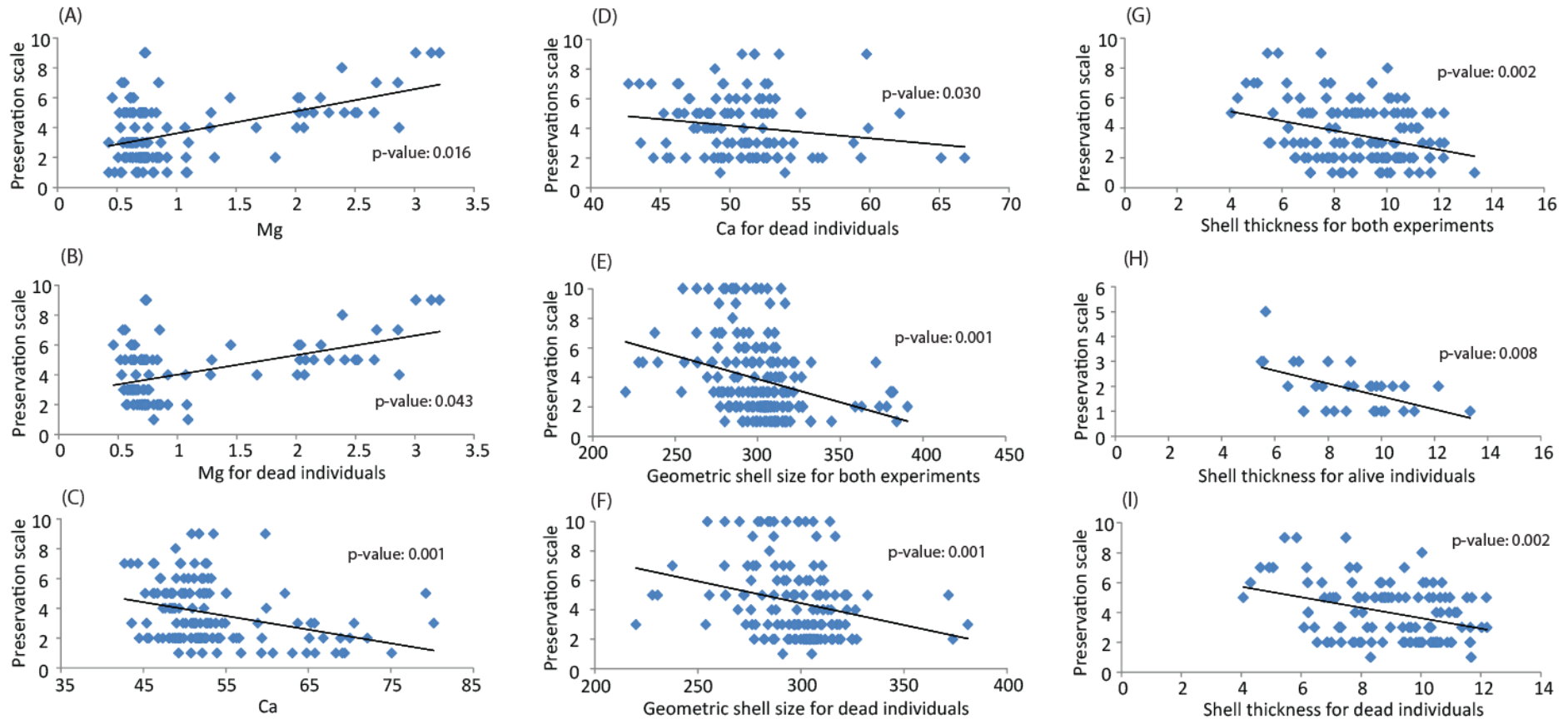


Figure 5.33: *Leptocythere* sp.: Linear regression models and Spearman's rank results (p-values) from comparing all the different data sets ((A) Geometric shell size for both experiments; (B) dead individuals, (E) Mean shell thickness for both experiments; (F) for dead individuals, (G) Average Mg % for dead individuals, and (C) Ca % for both experiments; (D) for dead individuals) against the relevant preservation rank to determine if there are any relationships or trends between the different data sets and preservation. Trend lines on the linear regression models indicate that the data show a significant relationship.



¹³Figure 5.34: *L. lacertosa*: Linear regression models and Spearman's rank results (p-values) from comparing all the different data sets ((E) Geometric shell size for both experiments; (F) for dead individuals, (G) Mean shell thickness for both experiments; (H) for alive individuals; (I) for dead individuals (A) Average Mg % for both experiments; (B) for dead individuals, and (C) Ca % for both experiments; (D) for dead individuals) against the relevant preservation rank to determine if there are any relationships or trends between the different data sets and preservation. Trend lines on the linear regression models indicate that the data show a significant relationship.

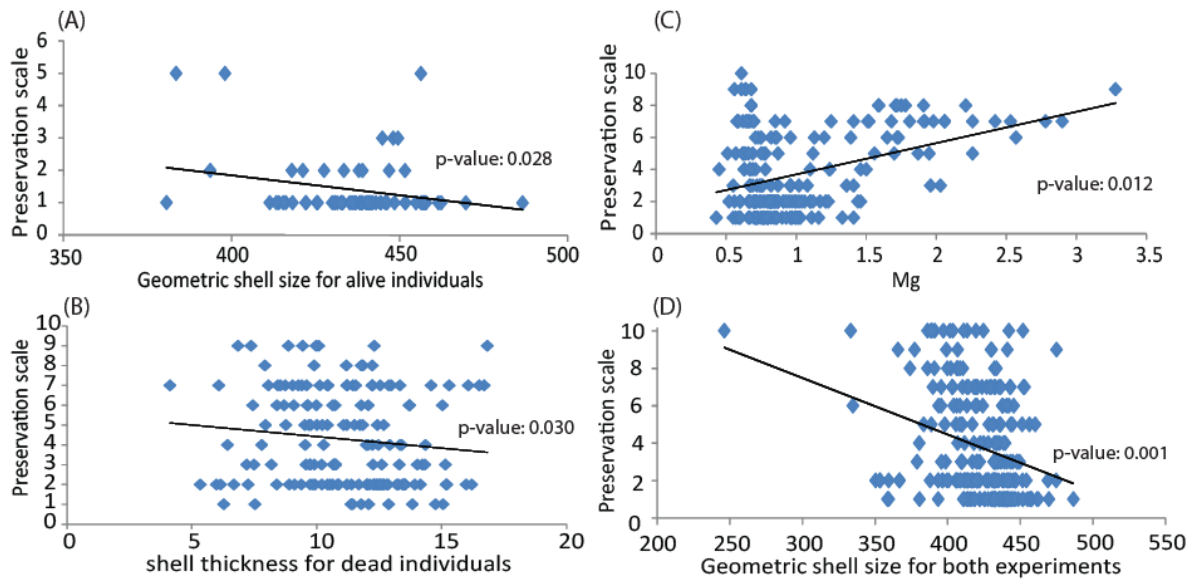


Figure 5.35: *L. castanea*: Linear regression models and Spearmans rank results (p-values) from comparing all the different data sets ((A) Geometric carapace size for alive individuals; (D) for both experiments, (B) Mean carapace thickness for dead individuals, (C) Average Mg for both experiments) against the relevant preservation rank to determine if there are any relationships or trends between the different data sets and preservation. Trend lines on the linear regression models indicate that the data show a significant relationship.

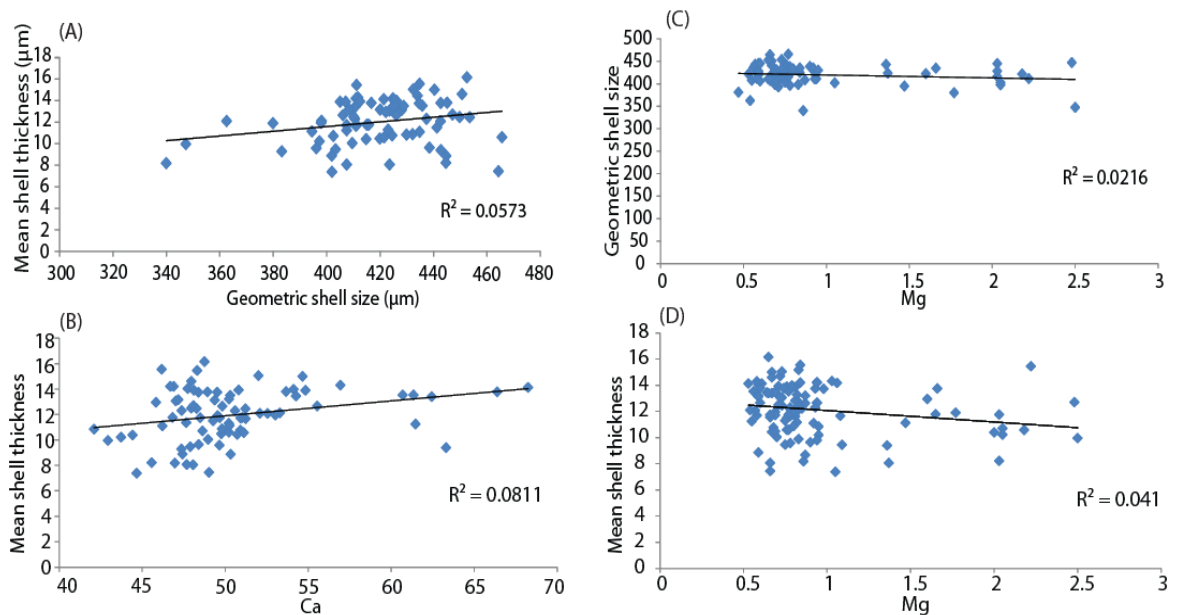


Figure 5.36: *Leptocythere* sp.: Linear regression models comparing all the data against each other to determine if there are any relationships or trends between the different data sets (Geometric shell size, Mean shell thickness, Average Mg and Ca %) (A, B, C) dead individuals, (D) both experiments. Trend lines on the linear regression models indicate that the data show a significant relationship.

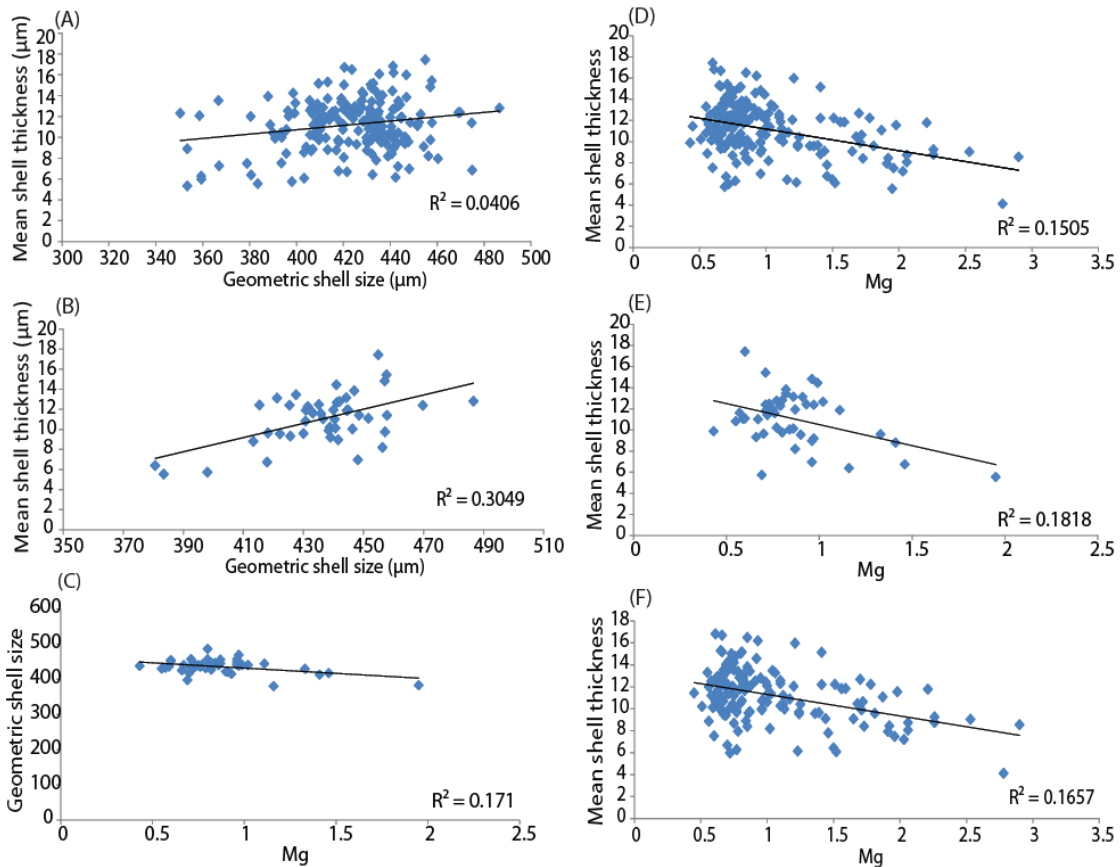


Figure 5.37: *L. castanea*: Linear regression models comparing all the data against each other to determine if there are any relationships or trends between the different data sets (Geometric shell size, Mean shell thickness, Average Mg and Ca %) (F) dead individuals, (B, E, C) alive individuals, (A, D) both experiments. Trend lines on the linear regression models indicate that the data show a significant relationship.

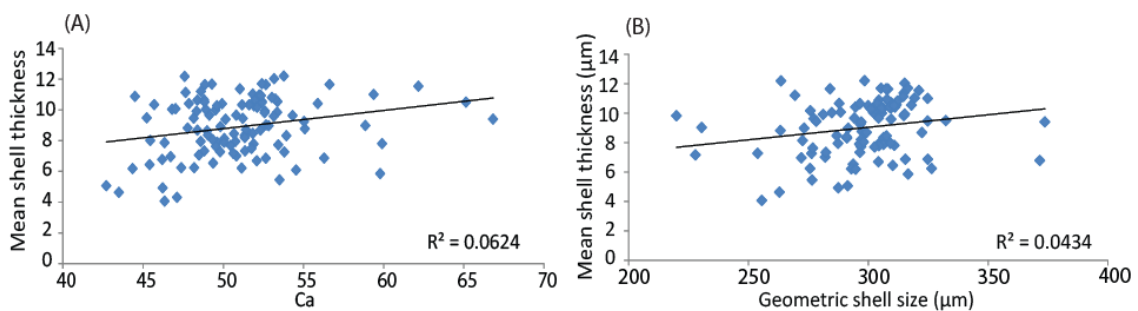


Figure 5.38: *L. lacertosa*: Linear regression models comparing all the data against each other to determine if there are any relationships or trends between the different data sets (Geometric shell size, Mean shell thickness, Average Ca %) (A, B) dead individuals. Trend lines on the linear regression models indicate that the data show a significant relationship.

5.9 Discussion

5.9.2 Survival

The survival of *Leptocythere* sp., *L. castanea* and *L. lacertosa* was generally poor in culture, with a small number of individuals surviving after 21 days, even in control conditions and no individuals that survived to 95 days. It is concluded that although these species were the hardiest available they are not amenable to medium term culture. However, there were differences between the species as well as treatment length; *L. lacertosa* showed the highest survival numbers in each of the experimental treatments after 21 days while *Leptocythere* sp. has the lowest survival numbers. Between the various treatments the high temperature treatments show the lowest survival for *L. castanea* and *L. lacertosa* whereas for *Leptocythere* sp. it was both acidic and high temperature treatments with the lowest survival. After 95 days the individuals from all three species had died.

There are few studies with which to compare these survival data, although De Deckker *et al.* (1999) found that *Cyprideis australiensis* died within 33 days of introduction into a mesocosm. Although they were not fed and were not living in high CO₂ or high temperature conditions many of the ostracods moulted during captivity. The ostracods used in this investigation showed poor survival rates, even though their food was present in excess. This rules out starvation as a reason for mortality (De Deckker *et al.*, 1999).

Other crustaceans and calcifying reefal organisms show significant variation in survival rates under similar conditions (e.g., barnacles, 69–97% - survival depended on the treatment; corals, >95% - no differences between

treatments; echinoids, >95% - any mortality due to lower pH combined with treatment length. These data are based on the research undertaken by Shirayama and Thornton (2005), Findlay *et al.* (2008), Jokie *et al.* (2008) and Wood *et al.* (2008). In general, the survival rates are better than those recorded for *Leptocythere* sp., *L. castanea* and *L. lacertosa* in this investigation. However, several experimental studies of bivalves and crustaceans (barnacles, copepods, krill) indicated larval to juvenile stages were severely affected by increased temperature and CO₂ while the adults were less affected by increased temperature than CO₂ (Anestis *et al.*, 2007, 2008; Findlay *et al.*, 2008; Rayssac *et al.*, 2010; Mizuta *et al.*, 2012; Hiebenthal *et al.*, 2012). Several echinoids, deep sea urchins, krill and *Conchoecia* sp. also identified increased mortality after a prolonged period of exposure to low pH/high CO₂ (e.g., several months for echinoids, up to 144 hrs for *Conchoecia* sp.; Yamada and Ikeda, 1999; Barry *et al.*, 2002; Shirayama and Thornton, 2005).

There are a number of potential reasons for the poor survival of the ostracod species in this study; Firstly, while abundant food appeared to be available, and that food was similar to the material available in situ, it is still possible that feeding behaviour itself was disrupted by being brought into the laboratory and so the ostracods were not able to access it in the quantities required. Few studies have been completed on how feeding behaviour could be disrupted while ostracods live in laboratory conditions. Within these few studies, Roca and Danielopol (1991) found that laboratory conditions did disrupt the feeding of *Cypridopsis vidua* causing high mortality (half of the specimens were dead after 3 days). However, Vannier *et al.* (1998) found

that the feeding of *Vargula hilgendorfi* was not disrupted and they were attracted to a wide range of natural food sources including vegetation and scavenging on dead animals. They are also able to ingest large quantities of food at one time and survive several weeks of starvation (Vannier *et al.*, 1998). What has not been determined from these studies is whether increased CO₂ or increased temperature is affecting the ostracods ability to find food, to feed and take up the relevant nutrients. A few studies have been completed investigating this but not with any ostracod species. The two species used indicated that feeding was impaired (*Strongylocentrotus droebachiensis*) or there was an energetic trade off (*Amphiura filiformis*) associated with living in a high CO₂ environment (Dupont and Thorndyke, 2008; Wood *et al.*, 2008).

Secondly; *L. lacertosa*, *Leptocythere* sp. and *L. castanea* are brackish-water species found in estuarine-intertidal environments and tolerant of variable salinities (Athersuch *et al.*, 1989). Consequently they are adapted to living through periods of exposure in the mud flats, regular temperature variations as they are mostly eurythermic (Frenzel and Boomer, 2005) and tidal effects (all of which were not part the experimental mesocosm). This could indicate that they reacted adversely to relocation to a more constant environment even though they are known to survive outside of their normal habitat for days or weeks at a time (Theisen, 1966; Kornicker and Sohn, 1971; Athersuch *et al.*, 1989; Frenzel and Boomer, 2005; Pörtner and Farrell, 2008; Findlay *et al.*, 2011).

Thirdly; other shelled organisms have shown that the larger shelled individuals are better able to cope with the adverse conditions but the results

from this study show that if ostracod carapace size was a factor in survival then the smallest species (*L. lacertosa*) appears to be best able to cope rather than the larger species (*Leptocythere* sp., *L. castanea*) (Mizuta *et al.*, 2012; Hiebenthal *et al.*, 2012; Rayssac *et al.*, 2010; Fabry *et al.*, 2008; Findlay *et al.*, 2008; Anestis *et al.*, 2008, 2007).

5.9.3 Carapace condition in live individuals

Carapace condition for *L. lacertosa*, *Leptocythere* sp. and *L. castanea* for all the different treatments was significantly worse than observed for field collected specimens, with *L. castanea* showing the poorest conditions during exposure to elevated CO₂. This corresponds well with the fact that survival in culture was so poor even in the controls. *L. lacertosa* shows the best condition across all the treatments. Passlow (1997) discovered that some deep sea ostracod species protect their carapaces by accumulating fine-grained carbonate phytoplankton detritus on their outer surfaces during high CO₂ conditions. SEM images from this study also showed a layer of easily removable detritus covering the carapace of *L. lacertosa*. It is not clear if *L. lacertosa* purposely cover their carapaces in a fine grained detritus for protection or if it is merely a result of burrowing through the sediment. The type of detritus covering the carapaces is a mixture of clay minerals, diatoms, phytoplankton and organic material (e.g., decomposed algae) and since it is easily removable with no clear form of attachment presumably it is unlikely to provide a significant amount of prolonged protection from ocean acidification.

The ostracod carapace consists of two dorsally articulated valves composed of a calcium carbonate layer called the procuticle which is bound internally

and externally with chitinous layers (80–90% calcium carbonate / 2–15% chitin and proteins) (Rosenfeld, 1982; Keyser, 1982; Bennett *et al.*, 2011; Decrouy *et al.*, 2011). The calcite layers contain the pores and sensory bristles which protrude through the chitinous layer and the epicuticle outer layer (Keyser, 1982; Bennett *et al.*, 2011; Decrouy *et al.*, 2011). When no calcification occurs the surrounding chitinous layers give the appearance of a lack of sieve pores (Keyser, 1982; Bennett *et al.*, 2011; Decrouy *et al.*, 2011). There are a wide variety of pores (e.g., normal, simple, sieve and exocrine pores) that can be found flush, raised or recessed on the valve surface (Athersuch *et al.*, 1989). The mineralogy of the new carapace is normally secreted by the epidermis from the surrounding water within a few hours of the original moulting and it stores information on the surrounding water temperatures and chemistry (Rosenfeld, 1982; Frenzel and Boomer, 2005; Decrouy *et al.*, 2011; Marco-Barba *et al.*, 2012). A layer of granules consisting of calcite and apatitic calcium orthophosphate are found along the internal side and thought to be used in the construction of new carapaces (Rosenfeld, 1982; Decrouy *et al.*, 2011). The preservation of ostracod carapaces in the fossil record is thought to be connected to the chitinous layer enveloping the calcitic layers (Rosenfeld, 1982) indicating that the *L. lacertosa* carapaces might comprise of a thicker chitinous layer causing improved preservation than *Leptocythere* sp. and *L. castanea*. From these studies variations in the thickness of the chitinous layer between the different species is more likely to improve the carapaces preservation than a purposeful accumulation of detritus with this composition.

Elevated CO₂ has similarly been found to have a detrimental impact on the shell condition of a range of living shelly marine organisms. Various bivalve species (e.g., *Mercenaria mercenaria*, *Ostrea edulis*, *Crassostrea gigas*) have been reported as showing that increased CO₂ environments have caused increased shell dissolution randomly across the shell surface while alive. This was identified from reduced carapace weight, reduced mineralogy, flaky appearance of the carapaces as well as pitting and significantly more fragile carapace edges, all of which leads to higher mortality rates (Bamber, 1990; Green *et al.*, 2004; Hiebenthal *et al.*, 2012). The pteropod species *Limacina helicina antarctica* and *Clio pyramidata* showed significant shell damage (type 1; aragonite crystals missing, porosity increased, type 2; dissolution through to the prismatic layer, type 3; gaps within prismatic layer causing significant carapace frailness) during high CO₂ events (1200 ppm over 14 days), while the foraminifera *Orbulina universa* and *Globigerinoides sacculifer* showed decreasing test mass due to increased dissolution during high pCO₂ (740 ppm) conditions (Spero *et al.*, 1997; Bijma *et al.*, 1999, 2002; Feely *et al.*, 2004; Orr *et al.*, 2005; Fabry *et al.*, 2008; Guinotte and Fabry, 2008; Bednaršek *et al.*, 2012).

Ries *et al.* (2009) also observed net shell dissolution after 60 days in their highest pCO₂ treatment (2856 ±54 ppm) across a wide range of species (hard and soft clams, conchs, pencil urchins, periwinkles and whelks) but was unable to determine how these changes would impact survival. The skeleton building of many coral species including *Oculina patagonica* and *Madracis pharencis* are known to be significantly susceptible to damage and complete dissolution due to high pCO₂ (Fine and Tchernov, 2007; Guinotte

and Fabry, 2008). This is not thought to affect mortality as the polyps have been found to survive without skeletons until the environment is such that skeletal building can occur rather than try to maintain their skeleton during adverse conditions (Fine and Tchernov, 2007; Guinotte and Fabry, 2008). The detrimental impact of high $p\text{CO}_2$ on the shell condition of the various species discussed above and the results found in this study are very similar but the relationship between treatment length, level of $p\text{CO}_2$ in the water and decreasing carapace condition is species specific even within the same class or genus.

5.9.4 Variations in the carapace size of live individuals

From the three species studied, only *L. lacertosa* showed any significant increase in carapace size after 21 days in the mesocosm with the most significant increase occurring in the non-acidified conditions at both temperatures. This indicates that *L. lacertosa* is a quite hardy species compared with *Leptocythere* sp. and *L. castanea* where no significant growth was detected.

There appears to be no published research on the effect of increased CO_2 on variations in ostracod carapace size. However, a few publications have been found that reported on the impact of changing temperatures on variation in ostracod carapace size (e.g., Kühl, 1980; Frenzel and Boomer, 2005; Hunt and Roy, 2006; Decrouy *et al.*, 2011). From those studies that have investigated the effect of temperature variations on carapace size using several different ostracod species, the generally observed trend comprised of a positive relationship between carapace size and temperature (Kuhl, 1980;

Frenzel and Boomer, 2005; Decrouy *et al.*, 2011). Specifically the body size of ostracod genera *Poseidonamicus* and species *Cypria ophthalmica* forma *lacustris* was found to react completely differently to each other to changes in temperature (Hunt and Roy, 2006; Decrouy *et al.*, 2011). *Cypria ophthalmica* forma *lacustris* showed a positive relationship between increasing temperature and carapace size but this lead to a reduced life span, whereas *Poseidonamicus* showed larger carapace sizes during colder water temperatures in deeper water depths (Hunt and Roy, 2006; Decrouy *et al.*, 2011). K hl (1980) determined that a simultaneous increase in localised temperature and salinity resulted in increased size and calcification of *Leptocythere psammophila* carapaces. These studies do not correlate with the growth results for *L. lacertosa* from this investigation because neither water temperature showed a significant species specific response and salinity was kept constant. This could indicate that *L. lacertosa* growth is temperature insensitive. This would, perhaps, be expected as *L. lacertosa* lives in coastal/estuarine environments and has evolved to cope with highly variable environmental conditions.

Various other calcifying marine organisms have been studied to determine any changes in body size while living in high CO₂ or high temperature conditions and have shown both increasing as well as decreasing body size as a response to the adverse conditions (e.g., Gazeau *et al.*, 2007; Talmage and Gobler, 2009; Findlay *et al.*, 2009, 2011; Hiebenthal *et al.*, 2012). Several studies using bivalves (e.g., *Mytilus galloprovincialis*, *Mytilus edulis*, *Mytilus trossulus*, *Crassostrea gigas*, *Clinocardium nuttallii*) have shown growth continued during high CO₂, high temperature events and in some

cases show a positive size relationship to increased temperature but often at a slower rate (Michaelidis *et al.*, 2005; Fabry *et al.*, 2008; Rico-Villa *et al.*, 2009; Rayssac *et al.*, 2010). Some species of crustaceans (e.g., *Acartia tsuensis*, *Calanus finmarchicus*, *Amphibalanus Amphitrite*, & *Gammarus locusta*) show no specific relationship to either high CO₂ or temperature (Mayor *et al.*, 2007; Kurihara and Ishimatsu, 2007; Hauton *et al.*, 2009; McDonald *et al.*, 2009; Whiteley, 2011). Since other marine organisms have shown an ability to increase size in high CO₂ and high temperature conditions even if it is at a slower rate this correlates well with the *L. lacertosa* results which also show size increasing although it is unknown in this study if the rate of increase has varied from the norm. The results from *L. lacertosa* though do not correlate with many high CO₂ or temperature studies which highlight reduced carapace size and rate of growth for bivalves (e.g., *Haliotis laevis*, *Mytilus galloprovincialis*, *Mytilus edulis*, *Argopecten irradians*, *Ostrea edulis*, *Crassostrea virginica*) and decreased growth rate due to decreasing moulting frequency and increased intermoult periods several crustaceans (e.g., *Palaemon pacificus*, *Penaeus occidentalis* & *Penaeus monodon*) (Wickins, 1984; Bamber, 1990; Harris *et al.*, 1999; Kurihara *et al.*, 2008; Talmage and Gobler, 2009; Whiteley, 2011; Hiebenthal *et al.*, 2012).

The absence of growth across all the treatments for *Leptocythere* sp. and *L. castanea* could be the result of the energy being diverted to counteract increased dissolution rates rather than impaired calcification which has also been identified in other shelled organisms (Findlay *et al.*, 2009, 2011). This corresponds well with the fact that carapace condition was also poor across

all the different treatments for both these species. Frenzel and Boomer (2005) showed that ostracods living in salinity values beyond their optimum stopped growing (in the majority of cases), however the salinity was kept constant in this study so should not be contributing to the reduced carapace size seen in the Frenzel and Boomer, (2005) study. Also *Leptocythere* sp. and *L. castanea* came from estuarine environments where the salinity of the water could vary over time due to changes in the amount of fresh water coming from upstream. However the results from their study do suggest that the lack of growth for *Leptocythere* sp. and *L. castanea* could be caused by other environmental factors being far from optimum within the mesocosm causing these species to live at their tolerance limit. *Penaeus occidentalis* and *Penaeus monodon*'s decreasing moulting frequency though increased intermoult periods during long periods of high CO₂ was identified by Wickins (1984). This survival mechanism in less than optimal conditions could be common for any species that grows through moulting. However, the published literature is unclear as to whether all other crustaceans are capable of changing their inter-moult periods as reported for *Penaeus occidentalis* and *Penaeus monodon*. If other species do adjust their intermoult periods while living in less than optimum conditions, this could explain the lack of growth but continued survival found throughout all the treatments for *Leptocythere* sp. and *L. castanea* in this study.

The results from this investigation do not confirm the results from the few other published studies that have used a variety of ostracod species. Some of the results, however, do correspond with those using a variety of other marine organisms (Kühl, 1980; Frenzel and Boomer, 2005; Hunt and Roy,

2006; Decrouy *et al.*, 2011). *Leptocythere* sp. and *L. castanea* could possibly be living at their tolerance limit in all the treatments because they have not grown and could have adjusted the length of their intermoult period to reduce energy expenditure in order to survive. *L. lacertosa* could be temperature insensitive because they grew equally between both temperatures. It is important to note that this experiment did not persist through several life cycles, due mainly to the poor survival of the ostracod species in the treatment system and the limited time available for the study. Thus, carapace size could only increase while the specimens were alive and shell diminution, due to elevated CO₂ and/or temperature change, would be difficult to observe. This makes the interpretation of the morphometric results extremely difficult.

5.9.5 Variations in the carapace thickness of live individuals

There were no significant changes in carapace thickness for each species after 21 days in the various treatments. Additionally there were no significant changes observed in carapace thickness between the different treatments for each species, even when a species carapace size and condition was compromised. There was also no difference between the carapace thicknesses of the different species regardless of if the carapace size increased (*L. lacertosa*) or not (*Leptocythere* sp. and *L. castanea*).

The lack of significant carapace thickness changes found in any of the treatments and specifically the high CO₂ treatments seems contradictory to what has been found for other shelled organisms (e.g., bivalves, corals, planktonic foraminifera) where there are high levels of shell dissolution

causing reduced shell thickness combined with reduced shell size during high CO₂ periods (e.g., Bamber, 1990; Spero *et al.*, 1997; Bijma *et al.*, 1999, 2002; Hallam, 2002; Green *et al.*, 2004; Hautmann, 2004; Fine and Tchernov, 2007; Gazeau *et al.*, 2007; Talmage and Gobler, 2009; Greene *et al.*, 2012). High CO₂ has also been found to not only cause carapace thinning but disrupt the ability of intertidal gastropods to increase carapace thickness which is important because they produce thicker carapaces when in the presence of predators as a form of protection (Bibby *et al.*, 2007). Several studies have also found a reduction in carapace thickness is often linked with reduced or altered carapace mineralogy (e.g., Bamber, 1990; Green *et al.*, 2004; Hautmann, 2004; Gazeau *et al.*, 2007; Talmage and Gobler, 2009). However, this study shows no significant changes in carapace thickness and so the reported changes in Mg or Ca must not be related to carapace thickness. Several species, including *Littorina littorea*, have shown that shell thickness can be maintained and even increase while living in high CO₂ conditions (McDonald *et al.*, 2009; Maier *et al.*, 2009; Findlay *et al.*, 2011). This is because calcification continues which reduces the effect of shell dissolution (McDonald *et al.*, 2009; Maier *et al.*, 2009; Findlay *et al.*, 2011). This agrees with the results from this study which showed that there were no significant variations in carapace thickness between the different treatments, regardless of any changes in carapace condition or carapace size.

5.9.6 Variations in the carapace mineralogy of live individuals

L. lacertosa showed the only significant increase in Mg levels. This was observed in the 15°C control and 19°C acid treatments when compared to

the initial levels measured in the field collected individuals. Additionally the 19°C acidic treatment and 15°C control treatment shows significantly higher levels of Mg in the carapace than the other treatments with the high temperature treatment showing the highest Mg levels out of all of the various treatments and this shows no relationship to increased size. However, there were no significant changes in Mg levels observed in *Leptocythere* sp. and *L. castanea* after completion of the various treatments when compared to the initial levels measured in the field collected individuals. Additionally there were no changes observed in Mg levels between the different treatments for *Leptocythere* sp. and *L. castanea*, even though their carapace size and condition was compromised. There were no significant changes in Ca levels observed after completion of the various treatments when compared to the initial levels measured in the field collected individuals of each species. Additionally there were no changes observed in Ca levels between the different treatments for each species, even when a species carapace size and condition was compromised. There was also no difference between the Ca levels of *L. lacertosa* which increased its carapace size and had the best carapace condition and the other species (*Leptocythere* sp. and *L. castanea*) which did not increase their carapace size and had worse carapace condition. Several other ostracod studies have investigated the uptake of Mg including De Deckker *et al.* (1999) which have shown that the uptake of Mg varies according to environmental conditions. *Cyprideis australiensis* and other brackish water ostracods showed Mg increased after temperature increased. However, this temperature dependency can be masked or changed by small changes in the waters Mg/Ca ratio or salinity (Chivas *et al.*, 1983; Reyment,

1966; De Deckker *et al.*, 1999; Janz and Vennemann, 2005; Decrouy *et al.*, 2011; Marco-Barba *et al.*, 2012). De Deckker *et al.* (1999) also indicated that these ostracods must be able to calcify out of thermodynamic equilibrium because they cannot change their mineralogy to high Mg/Ca ratios.

The relationship between increased temperature and increased Mg found in previous studies partially explains the results from this study because increased Mg is found in one of the high temperature treatments. However, these other studies do not explain why the increase in Mg is found in only one of the three species (*L. lacertosa*) and only in the high temperature, high CO₂ treatment instead of both high temperature treatments. The possibility that changes in the Mg/Ca ratios or salinity could be masking an increase in Mg (e.g., De Deckker *et al.*, 1999; Janz and Vennemann, 2005) in the non-acidic high temperature treatment is unlikely as the ratio; salinity and type of seawater were kept constant across all of the treatments. This indicates that variations in seawater pH could well be another important factor in Mg uptake when combined with high temperature.

The maintenance or increase in Ca and Mg levels found within the carapaces of these ostracod species agrees with other published studies (e.g., Bibby *et al.*, 2007; Wood *et al.*, 2008; McDonald *et al.*, 2009; Arnold *et al.*, 2009; Findlay *et al.*, 2009, 2011) derived from a variety of other marine organisms (e.g., lobsters, limpets, barnacles, mussels and brittle stars) that have been used to investigate changes in mineralogy during high CO₂ events. The results of these investigations showed constant or increasing levels of calcium in the shells or carapaces of living lobsters, limpets, barnacles, mussels and brittle stars during high CO₂ events, even when the

water has lower calcite and aragonite saturation states (Bibby *et al.*, 2007; Wood *et al.*, 2008; McDonald *et al.*, 2009; Arnold *et al.*, 2009; Findlay *et al.*, 2009, 2011). It is believed that these species were able to produce extra CaCO_3 to replace what was lost through dissolution to keep the levels in the carapace constant (Lewis and Cerrato, 1997; Pörtner, 2008; Findlay *et al.*, 2009, 2011). This indicates many species are able to exert a form of biological control over dissolution even if the energy used is detrimental to the organism in other ways (Lewis and Cerrato, 1997; Pörtner, 2008). This could explain how *L. lacertosa*, *Leptocythere* sp. and *L. castanea* were able to maintain or increase the Ca and Mg levels in their carapaces. It could also possibly suggest another reason why *Leptocythere* sp. and *L. castanea* did not grow in culture because the energy normally used for growth was instead used to maintain the Ca and Mg levels in the carapace while living at their tolerance limits.

5.9.7 Carapace preservation when dead

This study shows that the carapaces of dead ostracods react differently to those of live animals when exposed to elevated CO_2 and/or elevated temperatures. After death, both the high temperature and high CO_2 conditions caused carapace preservation to deteriorate even more significantly. Ca levels within the carapace significantly reduced and, between 21 and 95 days, carapace size decreased. However, after 95 days, Mg levels in the carapace increased due to a combination of high CO_2 and high temperature conditions. The level of carapace size reduction after death (between 21 and 95 days) varied among the different species with *L.*

lacertosa showing the least change in carapace size. The cause of the reduction in Ca levels also varied between species with high CO₂ across both temperatures for *L. lacertosa* and both high temperature treatments for *Leptocythere* sp. causing a reduction in Ca within the carapaces. Significant reductions in carapace thickness were limited to *L. castanea* individuals that had undergone the high temperature treatments for 95 days.

Previous studies have also shown that the shells of various other organisms (including limpets, mussels and brittle stars) react adversely in high CO₂ and high temperature conditions once the organism has died (Bibby *et al.*, 2007; Wood *et al.*, 2008; McDonald *et al.*, 2009; Findlay *et al.*, 2009, 2011). All of these studies have shown that the principal adverse reaction after death is increased dissolution leading to poor shell preservation, a reduced shell size, thickness and leaching of certain minerals (Bibby *et al.*, 2007; Wood *et al.*, 2008; McDonald *et al.*, 2009; Findlay *et al.*, 2009, 2011). These findings correspond with many of the results from this study indicating that carapaces of various dead organisms living in different environments react in the same way to high CO₂ and high temperature conditions.

However, the carapace thickness of *L. lacertosa* and *Leptocythere* sp. does not display the anticipated significant thinning after death, although the geometric carapace size has reduced and preservation has deteriorated. This lack of carapace thinning does not correspond with published experimental studies (e.g., Bibby *et al.*, 2007) using dead organisms (e.g., *Littorina littorea*) or with the *L. castanea* carapace thickness results from this study which records the expected carapace thinning. It is unclear why the carapace thickness of these two species shows no significant thinning while

recording other detrimental changes to their carapaces and while *L. castanea* shows both thinning and reduced preservation quality. One possible reason for a lack of significant thinning is the way their carapace is constructed and its composition (as previously explained; Rosenfeld, 1982). However, if this was the case there would be improved carapace preservation quality and a stable carapace size, both of which have not been identified.

The increase in Mg found in the carapaces of *L. lacertosa*, *Leptocythere* sp. and *L. castanea* that were deposited in the high CO₂, high temperature treatment also contradicts previous studies which indicate Mg leaching from the carapaces. De Deckker *et al.* (1999) investigated the dissolution of dead ostracod valves (recent species and fossil species; *Cyprideis*) and identified that high CO₂ causes significant leaching of Mg from the valve. This suggests that something else, possibly the higher temperature conditions, is counteracting the leaching effect of high CO₂. This has resulted in increased Mg levels forming as a part of the carapace preservation process. This agrees with Bullen and Sibley's (1984) study which indicated that short periods of time (<24hrs) at very high temperatures (250°C) converts low/high-Mg calcite within the tests of dead foraminifera to well-ordered dolomite. Although the Bullen and Sibley (1984) study uses significantly higher temperatures than this study, it is possible that if the experiment had been completed using lower temperatures (19–20°C) in acidic conditions the same results would have been produced but after a much longer time period (e.g., 95 days) so long as the carapaces did not dissolve in the acidic conditions first. It is also possible that this increase in Mg levels is the first

indication of valve preservation commencing and could fit into one of the 6 diagenetic stages identified by Bennett *et al.* (2011) in fossil ostracods from the Carboniferous. The stages range from neomorphic calcite replacing the original calcite in early shallow burial, ferroan dolomite forming with the original calcium carbonate replaced with magnesium carbonate to sphalerite and barite forming during much later burial and hydrothermal alteration in Mg bearing waters and higher temperatures (Al-Aasm *et al.*, 2000; Gregg *et al.*, 2001; Machel and Lonnee, 2002; Al-Aasm, 2003; Flèugel and Munnecke 2010; Bennett *et al.*, 2011; Iannace *et al.*, 2011).

The Mg/Ca ratios from the *L. lacertosa*, *Leptocythere* sp. and *L. castanea* carapaces that showed significant changes in their mineralogy indicate that the percentage of Mg in the carapace has not increased substantially enough to produce high Mg/Ca ratios or indicate dolomite formation. This could mean that if this level of increased Mg is a preservation signal it would only be indicating the commencement of preservation rather than any significant changes like dolomite formation. It also suggests that the 19°C temperature is not high enough to form dolomite in the carapaces over 95 days but these results show it is enough to start increasing Mg levels when combined with high CO₂ (Bullen and Sibley, 1984; Gregg *et al.*, 2001).

5.9.8 Summary

- A difference was identified between how the carapaces of dead ostracods and live ostracods react to periods of high CO₂ and high temperatures.

- Survival was poor after 21 days and, after 95 days, all of the individuals had died. After 21 days the three species were probably living in a far from optimum environment, especially *Leptocythere* sp. and *L. castanea*.
- After 21 days the live *L. lacertosa* individuals continued to grow and they appear to be temperature insensitive. However, *Leptocythere* sp. and *L. castanea* showed no growth, indicating they were either living at their tolerance limit or using that energy to counteract increased shell dissolution.
- Dead individuals after 95 days preservation, shell size and Ca levels had all drastically deteriorated across high temperature and high CO₂ conditions. However, Mg levels increased in the high CO₂, high temperature treatment, which is the opposite of other high CO₂ studies that showed leaching and indicates that high temperatures could be counteracting the known leaching effect of high CO₂.

5.9.9 Further work

These alive and dead results can also be used to help interpret the results from the fossil record specifically the ostracod results discussed in Chapter 4. If the same trends are found in the fossil record as have been found here this will help interpret whether other past extinction events could be due to ocean acidification and or high water temperatures. The following chapter (Chapter 6) will bring together the work discussed in Chapters 3–5 to attempt to determine whether the Tr-J extinction event was affected in any way by ocean acidification or high water temperatures.

Chapter 6 – Discussion

6.1 Introduction

Several authors have suggested ocean acidification may have occurred across the Tr-J boundary interval as a result of the CAMP eruptive phase causing a massive release of CO₂ into the atmosphere (Hautmann, 2004; van de Schootbrugge *et al.*, 2007; Hautmann *et al.*, 2008; Kiessling and Simpson, 2011; Greene *et al.*, 2012). Evidence presented for the ocean acidification hypothesis includes global scarcity of carbonate, selective organism extinction and the state of shelly marine organisms (shell size, shell thickness, preservation; Hautmann, 2004; Hautmann *et al.*, 2008). The results from this investigation (detailed below) attempt to identify further evidence of ocean acidification and/or high palaeotemperature from specific marine species throughout the Tr-J boundary interval.

This research has determined that *L. hisingeri* and *P. gigantea* shell size in the Lyme Regis area increased as $p\text{CO}_2$ increased, while only *P. gigantea* shell size increased as palaeotemperature increased (Chapters 3–4, Figure 6.1). However, *O. aspinata* specimens, collected from St Audrie's Bay, displayed increased shell size as $p\text{CO}_2$ increased but decreased shell size as palaeotemperature increased (Chapters 3–4, Figure 6.1). *O. aspinata* shell thickness decreased as $p\text{CO}_2$ increased, but showed no discernable relationships to changes in palaeotemperature (Chapters 3–4, Figure 6.1). Conversely, specimens of *O. aspinata* collected from Lyme Regis showed a decrease in shell size but increased shell thickness as $p\text{CO}_2$ increased but

neither shell size or thickness showed any discernable relationships to changes in palaeotemperature (Chapters 3–4, Figure 6.1). The preservation of all three species was not found to show any effects from acidification, with Ca and Mg within the shells presenting no discernable relationship to either $p\text{CO}_2$ or palaeotemperature (Chapters 3–4, Figure 6.1). In order to interpret these fossil results correctly, it is important to use evidence from species in modern high CO_2 and high temperature experiments (Chapters 5–6) or evidence from naturally occurring acidification areas.

Laboratory experiments (previously published by other authors and Chapter 5) have identified a complex range of morphological impacts caused by ocean acidification and high temperatures, which include changes in size, survival rates and biomineralization (e.g., Fabry *et al.*, 2008; Hendriks *et al.*, 2010; Findlay *et al.*, 2011; Greene *et al.*, 2012 as well as references given in Table 6.1). Specifically, Chapter 5 showed reduced survival and shell condition in the species *Leptocythere* sp. and *L. castanea*, while the overall size, thickness and Ca and Mg percentages present within the shells did not significantly change. Conversely, *L. lacertosa* displayed increased survival rates, higher percentages of shell Mg and increased size while displaying no significant changes in shell thickness. It should be noted, however, that the overall condition of the shells deteriorated over the course of the experiment. A comparison of these fossil results and the modern species results is made over the subsequent two sections. This will identify any evidence of ocean acidification and/or high palaeotemperature in specific marine species throughout this Tr-J boundary interval.

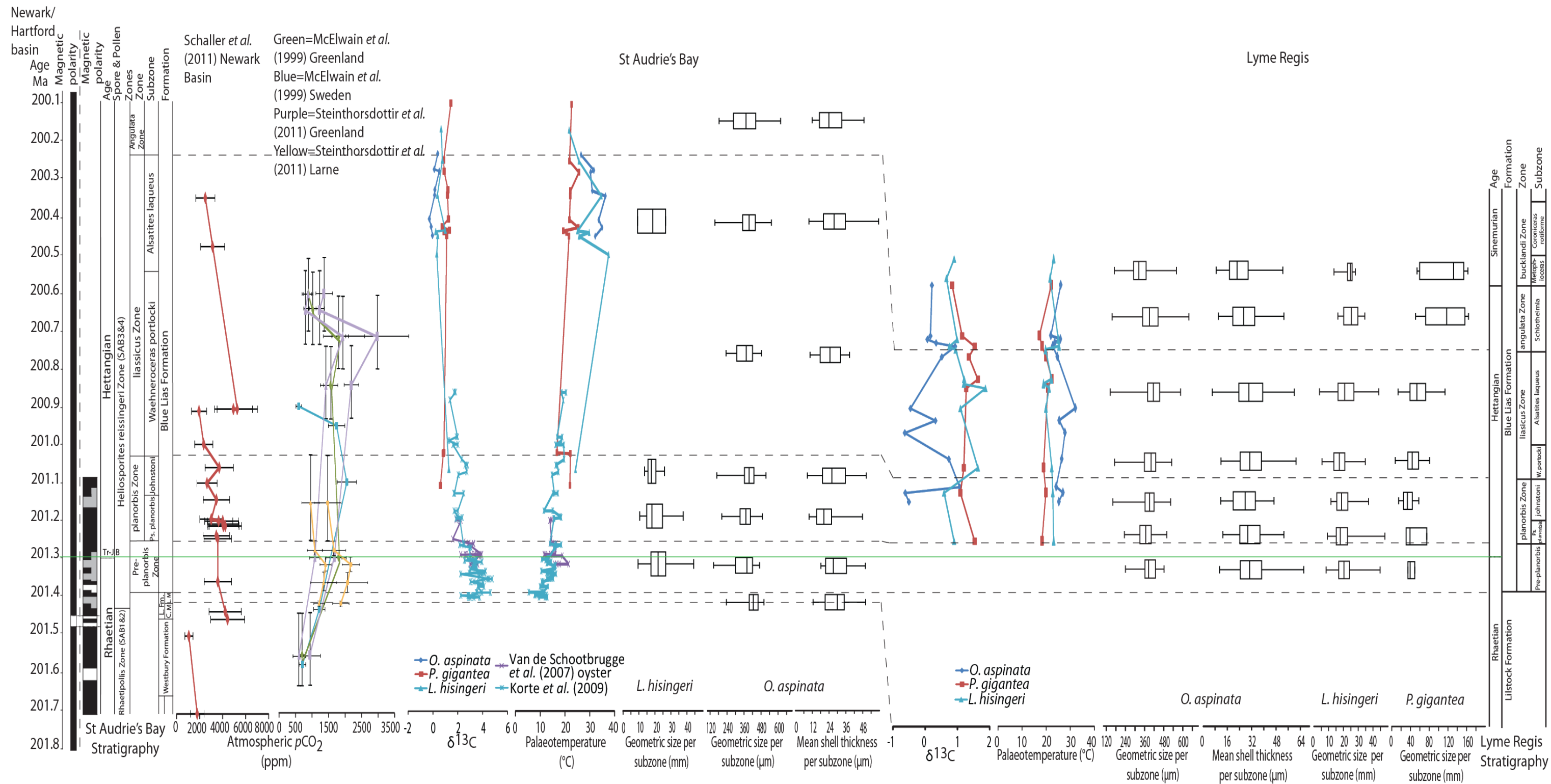


Figure 6.1: Summary diagram showing the key changes during the Tr-J boundary interval at St Audrie's Bay and Lyme Regis. The key changes documented includes the pCO_2 data from Greenland (McElwain *et al.*, 1999; Steinthorsdottir *et al.*, 2011), Sweden (McElwain *et al.*, 1999), Larne (Steinthorsdottir *et al.*, 2011) and the Newark Basin (Schaller *et al.*, 2011), $\delta^{13}C$ and palaeotemperature data (previously published and from this study) from St Audrie's Bay (van de Schootbrugge *et al.*, 2007; Korte *et al.*, 2009) and Lyme Regis and the morphological results from *O. aspinata* (geometric size and thickness), *L. hisingeri* (geometric size) and *P. gigantea* (geometric size) plotted against time (Ma), stratigraphic zones and subzones

6.2 Aims and objectives

The results from Chapters 3–5 will be utilised to determine if ocean acidification and/or high palaeotemperature occurred during the Tr-J boundary greenhouse interval.

This was done as follows:

- Comparison of all of the results (shell size, thickness, survival, calcification, shell dissolution, $p\text{CO}_2$ and palaeotemperature) presented in Chapter 4 (and summarised in Section 6.1, Figure 6.1) with those presented from modern high CO_2 and high temperature experiments using living marine and estuarine organisms (both pre-published data and those documented in Chapter 5).
- Comparison of all of the results (shell size, thickness, calcification, shell dissolution, $p\text{CO}_2$ and palaeotemperature) presented in Chapter 4 (and summarised in Section 6.1, Figure 6.1) with the results from dead modern marine and estuarine species (e.g., *Mytilus edulis*, *Littorina littorea* and *L. castanea* among others) deposited in high CO_2 and high temperature laboratory experiments (both pre-published data and those documented in Chapter 5).








































6.3 Comparison of fossil relationships (Chapter 4) with the results from laboratory experiments using living organisms.

Table 6.1 summarises the key results (e.g., changes in marine organisms survival, calcification, shell dissolution, shell size and shell thickness) from both the various modern high CO_2 and high temperature experiments using

living specimens (published and those reported in Chapter 5), and the fossil relationships identified and discussed in Chapter 4 (Figure 6.1). Various Tr-J boundary interval studies that investigated potential evidence for, and against, a biocalcification crisis showed that species vary in their responses (e.g., Hautmann, 2004; van de Schootbrugge *et al.*, 2007; Hautmann *et al.*, 2008; Mander *et al.*, 2008). This supports the results of the laboratory experiments undertaken in this research and those previously published, which found that the effects of ocean acidification on shelly organisms are very species specific (e.g., Lucas *et al.*, 2007; van de Schootbrugge *et al.*, 2007; Mander *et al.*, 2008; Črne *et al.*, 2011, plus all references in Table 6.1).

The comparison of the fossil data with the results from the laboratory experiments indicates that ocean acidification could have been affecting marine species during the Tr-J boundary interval. Evidence for this comes from: (1) laboratory studies identifying that size can increase during lowered pH conditions (e.g., *L. lacertosa* and *Mytilus galloprovincialis*), which supports the results from this research (shell size continued to increase through a high $p\text{CO}_2$ period) (Table 6.1; Pörtner, 2008; Findlay *et al.*, 2009, 2011); and (2) the Findlay *et al.* (2011) study showing increased shell thickness during lower pH conditions, which supports the relationship identified between increasing *O. aspinata* shell thickness from Lyme Regis and increasing $p\text{CO}_2$ values (Table 6.1).

Published modern experiments							Fossil relationships to $p\text{CO}_2$ or temperature from the Tr-J boundary interval			
Taxa	Survival	Calcification	Shell dissolution	Size	Shell thickness	References	Shell Size	Shell thickness	Ca & Mg	Shell dissolution
<i>Mercenaria mercenaria</i>	↓		↑			Green <i>et al.</i> , 2004; Talmage & Gobler, 2009.				
<i>Crassostrea gigas</i>	↓ ↑	↓	↑	↓ ↑		Bamber, 1990; Gazeau <i>et al.</i> , 2007; Rico-Villa <i>et al.</i> , 2009; Mizuta <i>et al.</i> , 2012.				
<i>Crassostrea virginica</i>		↓		↓		Kurihara <i>et al.</i> , 2007; Ries <i>et al.</i> , 2009; Talmage & Gobler, 2009.	↑ ↔		↔ ↔	↔ ↔
<i>Ostrea edulis</i>	↕		↑	↓		Bamber, 1990.	↑ ↑		↔ ↔	↔ ↔
<i>Mytilus edulis</i>	↓ ↓	↓	↑	↓ ↓		Bamber, 1990; Berge <i>et al.</i> , 2006; Gazeau <i>et al.</i> , 2007; Wanamaker <i>et al.</i> , 2007; Beesley <i>et al.</i> , 2008; Bibby <i>et al.</i> , 2008; Findlay <i>et al.</i> , 2009; Ries <i>et al.</i> , 2009; Rayssac <i>et al.</i> , 2010; Findlay <i>et al.</i> , 2011; Hiebenthal <i>et al.</i> , 2012.	↕ ↓	↕ ↔	↔ ↔	↔ ↔
<i>Mytilus galloprovincialis</i>	↓			↑		Michaelidis <i>et al.</i> , 2005; Anestis <i>et al.</i> , 2007; Kurihara <i>et al.</i> , 2008; Range <i>et al.</i> , 2012.				
<i>Mytilus trossulus</i>	↓			↑		Rayssac <i>et al.</i> , 2010.				

Published modern experiments							Fossil relationships to $p\text{CO}_2$ or temperature from the Tr-J boundary interval			
Taxa	Survival	Calcification	Shell dissolution	Size	Shell thickness	References	Shell Size	Shell thickness	Ca & Mg	Shell dissolution
<i>Modiolus barbatus</i>						Anestis <i>et al.</i> , 2008.				
Gastropods						Doney <i>et al.</i> , 2009; Kroeker <i>et al.</i> , 2010; Andersson <i>et al.</i> , 2011.				
Corals						Fine & Tchernov, 2007; Guinotte & Fabry, 2008; Doney <i>et al.</i> , 2009; Kroeker <i>et al.</i> , 2010; Hendriks <i>et al.</i> , 2010; Andersson <i>et al.</i> , 2011.				
Foraminifera						Doney <i>et al.</i> , 2009; Andersson <i>et al.</i> , 2011.	 		 	 
Echinoderms						Doney <i>et al.</i> , 2009; Kroeker <i>et al.</i> , 2010; Andersson <i>et al.</i> , 2011.	 		 	 
Crustaceans						Kroeker <i>et al.</i> , 2010; Andersson <i>et al.</i> , 2011.	 	 	 	 
<i>Limacina helicina antarctica</i>						Bednaršek <i>et al.</i> , 2012.				
<i>Clio pyramidata</i>						Bednaršek <i>et al.</i> , 2012.				
<i>Orbulina universa</i>						Spero <i>et al.</i> , 1997; Bijma <i>et al.</i> , 1999, 2002.				
<i>Globigerinoides sacculifer</i>						Bijma <i>et al.</i> , 1999, 2002.				

Published modern experiments							Fossil relationships to $p\text{CO}_2$ or temperature from the Tr-J boundary interval			
Taxa	Survival	Calcification	Shell dissolution	Size	Shell thickness	References	Shell Size	Shell thickness	Ca & Mg	Shell dissolution
<i>Leptocythere psammophila</i>		↑		↑		Kühl, 1980.				
<i>Cyprideis australiensis</i>		Mg ↑				Chivas <i>et al.</i> , 1983; Reyment, 1996; De Deckker <i>et al.</i> , 1999; Janz & Vennemann, 2005.	↑ ↔		↔ ↔	↔ ↔
<i>Cyprideis-torosa</i>		Mg ↑				De Deckker <i>et al.</i> , 1999; Marco-Barba <i>et al.</i> , 2012.	↑ ↑		↔ ↔	↔ ↔
<i>Poseidonamicus</i>		↓				Hunt & Roy, 2006.	↕ ↓	↕ ↔	↔ ↔	↔ ↔
<i>Cypria</i>	↓	↑		↑		Decrouy <i>et al.</i> , 2011.				
Ostracod modern experiment results identified in Chapter 5										
<i>Leptocythere</i> sp.	↓ ↓ ↓	↔ ↔	↑ ↑ ↑	↔ ↔	↔ ↔	Reported in Chapter 5	↑ ↔		↔ ↔	↔ ↔
<i>L. castanea</i>	↓ ↓ ↓	↔ ↔	↑ ↑ ↑	↔ ↔	↔ ↔		↑ ↑		↔ ↔	↔ ↔
<i>L. lacertosa</i>	↑ ↑ ↑	Mg ↑ ↑ ↑	↑ ↑ ↑	↑ ↑ ↑	↔ ↔		↕ ↓	↕ ↔	↔ ↔	↔ ↔

Table 6.1: Living marine organism responses to modern $p\text{CO}_2$ and temperature experiments (previously published and from Chapter 5) and the morphological results discussed in Chapter 4 from the Tr-J boundary interval. Arrows pointing downwards represent a decrease, arrows pointing upwards represent an increase and horizontal arrows represent no result and/or no change. Blue edged arrows represent increased $p\text{CO}_2$, red edged arrows represent increased temperature, dark blue and dark red mix represent $p\text{CO}_2$ and temperature combined, arrows infilled with orange represent *L. hisingeri*, arrows infilled with purple represent *P. gigantea*, arrows infilled with green represent *O. aspinata*.

If the studied species from the Tr-J boundary interval are not displaying the predicted reactions (discussed in published studies referenced in Table 6.1; e.g., Bamber, 1990; Berge *et al.*, 2006; Wanamaker *et al.*, 2007; Beesley *et al.*, 2008; Findlay *et al.*, 2009; Ries *et al.*, 2009; Findlay *et al.*, 2011) to increased $p\text{CO}_2$ and ocean acidification, then this suggests that another environmental factor (e.g., temperature) is more significant for these species. The comparisons of the fossil data with those results from laboratory experiments suggest that high palaeotemperatures were affecting the size of *P. gigantea* and *O. aspinata* during the Tr-J boundary interval. Palaeotemperature appears to be reversing the predicted negative effect from ocean acidification and causing *P. gigantea* size to increase irrespective of the pH conditions. Conversely, high palaeotemperatures appear to be limiting the increase in size of *O. aspinata*. Evidence for this comes from: (1) increasing bivalve and ostracod size identified in the modern high temperature experiments (Table 6.1 and references therein) correlates with the increasing size during high palaeotemperature identified for *P. gigantea* (Table 6.1); and (2) each species have a different maximum temperature over which a negative effect occurs (e.g., Kühl., 1980; Wanamaker *et al.*, 2007; Anestis *et al.*, 2008; Rayssac *et al.*, 2010; Decrouy *et al.*, 2011; Hiebenthal *et al.*, 2012). This could explain the *O. aspinata* shell size data (i.e. the observed negative relationship to palaeotemperature) if *O. aspinata* was living for any length of time in conditions beyond their most favourable palaeotemperature (Table 6.1).

Table 6.1 also shows that many of the results from the modern laboratory experiments and Hautmann's (2004) biocalcification hypothesis for the Tr-J

boundary interval do not support the results reported in Chapter 4. There could be several reasons for this which include: (1) seawater pH was not low enough to effect shell size at either location, unlike the pH values used in the laboratory experiments; (2) any effects on shell size are very species specific, as identified from the laboratory experiments (e.g., bivalve species), so it is not surprising that the data from fossil species do not correspond with those from the extant species (Table 6.1 and references therein); (3) other environmental factors (e.g., food supply, dissolved O₂, changes in temperature, sea level variation, sedimentation rate or another change in environment) could be significantly influencing any changes in shell size; and (4) it is possible that *L. hisingeri*, *P. gigantea* and *O. aspinata* may have evolved, over time, to survive adverse conditions. This would be almost impossible to identify accurately.

One such example of results which are not supported by evidence from modern studies is changes in the Ca and Mg content of the carapaces. There was no evident changes in Ca or Mg levels and no indication of poor shell preservation in fossil ostracods due to changing $p\text{CO}_2$ (Chapter 4). This is not supported by the results from the laboratory experiments. These results exhibited decreased carapace or shell preservation quality and decreased levels of Ca and Mg within the carapaces or shells (Wood *et al.*, 2008; Ries *et al.*, 2009; Nienhuis *et al.*, 2010; Greene *et al.*, 2012). Several species used in the laboratory experiments also showed an increase in calcification, but at an apparent metabolic cost to other physiological factors (Wood *et al.*, 2008; Findlay *et al.*, 2009; Ries *et al.*, 2009; Nienhuis *et al.*, 2010; Greene *et al.*, 2012). How significant the metabolic cost for a species

will be depends considerably on whether those organisms have: (1) shells or carapaces in direct contact with seawater; (2) shells or carapaces lacking a protective organic coating as seen on some ostracod and bivalve species; and (3) how and where on the shell or carapace these various species have physiological control over biomineralization (Pörtner, 2008; Tunnicliffe *et al.*, 2009; Findlay *et al.*, 2009; Ries *et al.*, 2009; Greene *et al.*, 2012). As a result, therefore, other factors may have had a more significant effect on the shell or carapace condition of the species studied through the Tr-J boundary interval.

6.4 Comparison of fossil relationships (Chapter 4) with the results from laboratory experiments using deceased organisms.

The comparison of fossil relationships with the results from modern deceased organisms has been investigated to explain why only some of the fossil morphometric results from the Tr-J boundary interval correlate to the results from those modern experiments using living individuals. It is possible that the fossil record could be recording what happened to an organism's shell after death. This is because it is unknown how long each individual fossil ostracod was deceased prior to burial or the time between the deposition of a moulted carapace and its subsequent burial. It is also unknown if there were any chemical impacts from within the sediments and any effects can go on for a long time. It has been shown in several laboratory experiments that shells deteriorate more rapidly after death (Bamber, 1990; De Deckker *et al.*, 1999; Bibby *et al.*, 2007). Chapter 5 clearly shows that environmental conditions affected shell morphology of living ostracods in a different way from those of dead individuals.

Published modern experiments						Fossil relationships to $p\text{CO}_2$ or temperature from the Tr-J boundary interval			
Taxa	Calcification	Shell dissolution	Size	Shell thickness	References	Shell size	Shell thickness	Ca & Mg	Shell dissolution
<i>Mytilus edulis</i>	Calcium carbonate ↓				Bamber, 1990.				
<i>Littorina littorea</i>				↓	Bibby <i>et al.</i> , 2007.	↑ ↔		↔ ↔	↔ ↔
<i>Cyprideis australiensis</i>	Mg ↓ ↑				De Deckker <i>et al.</i> , 1999.	↕ ↓	↕ ↔	↔ ↔	↔ ↔
Ostracod modern experiment results identified in Chapter 5									
<i>Leptocythere</i> sp	Ca ↓ ↓ ↓ ↑ Mg ↔ ↑	↑ ↑ ↑	↓ ↓ ↓	↔ ↔	Reported in Chapter 5	↑ ↔		↔ ↔	↔ ↔
<i>L. castanea</i>	Ca ↓ ↓ ↓ ↑ Mg ↔ ↑	↑ ↑ ↑	↓ ↓ ↓	↓ ↓ ↓		↑ ↑		↔ ↔	↔ ↔
<i>L. lacertosa</i>	Ca ↓ ↓ ↓ ↑ Mg ↔ ↑	↑ ↑ ↑	↓ ↓ ↓	↔ ↔		↕ ↓	↕ ↔	↔ ↔	↔ ↔

Table 6.2: Deceased marine organism responses compared to modern $p\text{CO}_2$ and temperature experiments (previously published and from Chapter 5) and the morphological results discussed in Chapter 4 from the Tr-J boundary interval. Arrows pointing downwards represent a decrease, arrows pointing upwards represent an increase and horizontal arrows represent no result and/or no change. Blue edged arrows represent increased $p\text{CO}_2$, red edged arrows represent increased temperature, dark blue and dark red mix represent $p\text{CO}_2$ and temperature combined, arrows infilled with orange represent *L. hisingeri*, arrows infilled with purple represent *P. gigantea*, arrows infilled with green represent *O. aspinata*.

Table 6.2 summarises the key points (e.g., changes in marine organisms survival, calcification, shell dissolution, shell size and shell thickness) from both the various modern high CO₂ and high temperature experiments using deceased specimens (published and those reported in Chapter 5) and the fossil relationships identified in this research (Chapter 4, Figure 6.1). The comparisons of the fossil results with those results from the laboratory experiments using shells from deceased organisms show no correlations because only living organisms can increase their shell size and both *L. hisingeri* and *P. gigantea* show shell size increasing. However, the reduced shell size of *O. aspinata* could be indicating that the beds contained a combination of moulted carapaces from various generations that had been deposited in the sediment for some time, along with recently deceased ostracods also from various generations. Evidence for this comes from: (1) *L. hisingeri* and *P. gigantea* shell size continuing to increase during high pCO₂ and high temperature conditions; whereas modern species showed size decreasing in all conditions once deceased due to deteriorating preservation specifically around the shell edge (Table 6.2 and references therein); and (2) *O. aspinata* results from Lyme Regis showed reduced shell size during periods of high pCO₂, while at St Audrie's Bay there was reduced shell size during periods of higher palaeotemperature, which agrees with the dead ostracod results reported in Chapter 5 which show reduced shell size during high pCO₂ and high temperature conditions (Table 6.2). The results presented in Chapter 5 indicated that the longer an empty carapace is deposited in adverse conditions, the smaller it becomes, due to poor preservation of the carapace edges or shell shrinkage.

However, the rest of the fossil results in Table 6.2 are not supported by the modern experiment data. This could be because: (1) *O. aspinata* increase their overall size through moulting their carapace unlike the bivalve species, resulting in the deposition of numerous empty carapaces on the seafloor which are unprotected from any environmental effects; (2) there may be a higher proportion of moulted carapaces in a bed than shells of just deceased ostracods; and (3) how strong an effect either factor has and how quickly their shells deteriorate varies greatly between species.

6.5 Summary

Overall the data shows evidence that both high $p\text{CO}_2$ and high palaeotemperature may be contributing to the morphological changes recorded (Table 6.1). This makes it very difficult to separate out which factor ($p\text{CO}_2$ or temperature) is the primary cause of the changes in shell size or thickness observed throughout the Tr-J boundary interval. It is also possible that one of the factors is so important to a species' ability to increase shell size, that it is cancelling out or exacerbating the negative or positive effect of the other factor. For instance, Kiessling and Simpson (2011) indicated that a combination of ocean acidification and high temperature would significantly affect many species.

The fossil shell size evidence indicates that ocean acidification and high temperatures could be significant during the Tr-J boundary interval, but it is not definitive enough to demonstrate acidification in the rock record without an appropriate trigger mechanism (Greene *et al.*, 2012). The CAMP eruptive phase that occurred during the Tr-J boundary interval is thought to have

produced the quantity of atmospheric CO₂ required to cause ocean acidification and undersaturation, leading to increased dissolution and increased extinction of acid sensitive species, accompanied by increased oceanic palaeotemperatures (e.g., McElwain *et al.*, 1999; Hautmann, 2004; Schaller *et al.*, 2011; Steinhorsdottir *et al.*, 2011; Greene *et al.*, 2012). Evidence from other, more modern events, have identified that volcanism can cause localised ocean acidification along with the extinction of specific marine taxa which are then, subsequently, preserved in the ocean sediments (Wall-Palmer *et al.*, 2011; Greene *et al.*, 2012).

Chapter 7 - Conclusions

The aim of this project was to determine if morphological changes in several marine species from the Tr-J boundary interval could be linked to ocean acidification and warming events, with results from experiments on extant taxa assisting in the interpretation of the fossil record. In order to investigate this aim the geometric shell size of three species (*L. hisingeri*, *P. gigantea* and *O. aspinata*) collected from various beds through the Tr-J boundary interval from the successions exposed at St Audrie's Bay and Lyme Regis (Chapter 3) was measured. These data were correlated to $p\text{CO}_2$ and palaeotemperature data to identify any relationships between the changes in $p\text{CO}_2$ or temperature and the geometric shell size of the studied species (Chapter 4). The potential relationships were then compared with the results from a series of laboratory experiments (both published and those reported in Chapter 5). The key findings from this investigation are detailed below:

- The laboratory experiments on ostracods identified a difference between how the carapaces of dead ostracods and those still living react to periods of high CO_2 conditions and high temperatures. Survival rates were poor after 21 days, and after 95 days all of the individuals had died. Only *L. lacertosa* continued to grow after 21 days and growth was temperature insensitive. The three species were probably living in a far from optimum environment after 21 days, especially *Leptocythere* sp. and *L. castanea*.
- Once dead, preservation quality, shell size and Ca levels all deteriorated drastically in the high temperature and high CO_2

conditions (especially after 95 days). However, Mg levels increased in the high CO₂, high temperature treatment, indicating that higher temperatures could be counteracting the known leaching effect of high CO₂ conditions.

- When the data from fossil and modern results are combined, there is evidence that a period of ocean acidification could have occurred within the Tr-J boundary interval and caused the variations in size seen in *L. hisingeri*, *P. gigantea* and *O. aspinata* (Chapter 4, 6).

Evidence for this conclusion comes from:

(1) positive relationships identified between both *L. hisingeri* and *P. gigantea* shell size and pCO₂ from Lyme Regis (Chapter 4); and (2) positive and negative relationships between *O. aspinata* shell size or shell thickness and pCO₂ from St Audrie's Bay and Lyme Regis (Chapter 4). These results correspond to data collected from high CO₂ experiments (Chapters 5, 6) which identified that size can still increase during periods of ocean acidification.

- The evidence does not, however, indicate that ocean acidification was the primary cause of the changes observed in the marine realm through the Tr-J boundary interval as high palaeotemperatures were also having an effect on the species studied (Chapters 4, 6). Evidence for this comes from:

(1) positive relationship identified between *P. gigantea* geometric shell size and palaeotemperature from Lyme Regis (Chapter 4); and (2) the negative relationship identified between the geometric shell size of *O. aspinata* and palaeotemperatures from St Audrie's Bay (Chapter 4).

The results from this study correspond to data derived from high temperature experiments (Chapters 5, 6) which identified that shell size can be affected both positively and negatively by high palaeotemperatures.

- There is clear evidence for both ocean acidification and high palaeotemperatures affecting species' shell size and thickness, although it is unclear which is having the most significant effect on the environment. Further work will be required in order to determine which of these factors is the most important and to determine if any other environmental factors (e.g., changes in sea level, sedimentation rates, oxygen concentrations, food supply etc) are also having a significant effect on the shell size and thickness of the recorded species.
- It is also important to realise that the $p\text{CO}_2$ data, especially the data from ginkgoalean leaves, have a very low sampling resolution and that this is having a significant effect on the results. This low sampling resolution also makes it difficult to compare the $p\text{CO}_2$ data to the fossil morphometric data. Until higher resolution sampling of ginkgoalean leaves is conducted this issue remains unresolved.

Proposed further work:

- (1) Further research is required at other Tr-J boundary interval sections to determine if the same relationships are found. In some cases the same, or comparable, species may be present, which would allow direct comparison. A more dispersed data set could then identify clear evidence for, or against, whether ocean acidification and high

palaeotemperatures were affecting species globally, regionally or locally during the Tr-J boundary interval.

- (2) It would be useful to compare the fossil morphometric data to any other plausible changes in environment (e.g., changes in sea level, sedimentation rate, oxygen concentrations, food supply etc). Results from such an analysis may explain the few significant bed-by-bed changes in size recorded, especially where no relationship was found to changes in $p\text{CO}_2$ and temperature. This was not investigated in this study because the main aim of the work was to test the ocean acidification hypothesis.
- (3) Additionally, there is a need for more stomatal and palaeosol (pedogenic carbonate) data in order to elaborate on and improve the resolution of the already published datasets, as well as the need for more acidification evidence collected from a greater range of localities and palaeo water depths to further try and understand and expand upon the results presented in this study.

Appendix 1 – Summary of previously published modern high CO₂ experiments using bivalves (relates to Chapter 1)

Table A1.1: modern experiments using bivalves and increased CO₂ (Presented in Section 1.4).

Taxon	Mineralogy and development stage	Experiment type	Response to changes in pCO ₂	References	What was measured and other notes
<i>Mercenaria mercenaria</i>	Larval stage	Four 1 litre beakers containing filtered seawater had CO ₂ gas mixtures continuously pumped into them at 3 different levels (high, moderate and ambient). 100 larvae were placed in each bucket and twice weekly the condition and development stage was determined visually. When 50% had metamorphosed 15 were selected to be measured.	Larvae survivorship significantly decreased with increased CO ₂ when compared with larvae survivorship living in ambient CO ₂ levels. It was also found to cause delays in metamorphosis.	Talmage & Gobler, 2009	
	Juvenile specimens (0.2mm, 0.3mm, 1mm & 2mm)	Populations were introduced into sediments under saturated and saturated with aragonite. Sediment was collected from an intertidal mud flat along the coast. A linear regression analysis is used to examine mortality over time. Differences in mortality between treatments were analysed using covariance (ANCOVA).	Shell dissolution may lead to increased mortality for just set juveniles and very small individuals. In under saturated treatments significant mortality in every size class was found. Different rates of mortality were found for different size populations	Green <i>et al.</i> , 2004	Measured the impact of the saturation state and dissolution on their survivorship.

Taxon	Mineralogy and development stage	Experiment type	Response to changes in $p\text{CO}_2$	References	What was measured and other notes
<i>Crassostrea gigas</i>	Adults and juveniles specimens. Mainly calcite shells	Specimens were collected and placed in two aquarium tanks $p\text{CO}_2$ levels were set at desired levels by moderating CO_2 -free air bubbling in to the tanks. Incubations lasted for 2hrs 2 or 3 times a day. Net calcification rates were estimated using the alkalinity anomaly technique.	Calcification rates decline linearly with increased $p\text{CO}_2$ 10% by the end of the century. It was found to dissolve at $p\text{CO}_2$ values exceeding threshold values of ~1800 ppmv but at a slower rate than <i>Mytilus edulis</i> .	Gazeau <i>et al.</i> , 2007	740ppmv, IPCC IS92a scenario, net calcification was measured.
	Young hatchery reared stock ~1cm in size.	Maintained in a 2-1 aquaria seawater between pH 5.4-8.2 for 60 days. Survival registered as those showing movement within 24hrs of return to normal water. Shell weights were determined as dry weights. Shell size measured as area of the shell. Growth was determined by the presence or absence of the shell edge having finger like extentions.	Significant mortalities found at pH ≤ 6 . Mortality of large specimens increases with exposure time, increased specimen size. Growth rate and thus shell size was reduced, tissue weight loss & shell dissolution also found at pH ≤ 7 .	Bamber, 1990	
<i>Crassostrea virginica</i>	Low magnesium calcite	Species were reared for 60 days in isothermal experimental seawaters equilibrated with average modern $p\text{CO}_2$ values which were then changed up to 10 times pre industrial levels. The net rate of calcification was measured from changes in the buoyant weight and confirmed with dry weight.	Net calcification was found to decrease as $p\text{CO}_2$ levels increased.	Ries <i>et al.</i> , 2009	The net rate of calcification (total calcification minus total dissolution).

Taxon	Mineralogy and development stage	Experiment type	Response to changes in $p\text{CO}_2$	References	What was measured and other notes
	Larval stage	Four 1 litre beakers containing filtered seawater had CO_2 gas mixtures continuously pumped into them at 3 different levels (high, moderate and ambient). 100 larvae were placed in each bucket and twice weekly the condition and development stage was determined visually. When 50% had metamorphosed 15 were selected to be measured.	The metamorphosis rate of the larvae was significantly delayed by high CO_2 levels. After 2 weeks a third of those in current CO_2 levels had metamorphosed unlike the 6% in high CO_2 levels. They were also significantly smaller than those grown at ambient CO_2 levels. But there was less of a difference in survivorship at the different CO_2 levels.	Talmage & Gobler, 2009	
	Larval stage	Developing embryos were placed in vials and fixed with 10% neutralized formalin seawater at 2, 3, 8, 24 & 48 hrs. A morphological criterion is used to differentiate normal and abnormal larvae. Normal was measured for shell length and height and at 24-48 hrs were analysed for the degree of shell mineralisation.	Increased $p\text{CO}_2$ to pH 7.4 was found to severely impact the early development (embryogenesis stage) of the oyster as it is more sensitive to environmental disturbances than adults. Shell mineralisation and growth was severely inhibited compared to the control group.	Kurihara <i>et al.</i> , 2007	Larvae were categorized into fully, partially and none mineralized.
<i>Ostrea edulis</i>	Three different ages used (newly settled spat small ~1cm across, larger 4cm across)	Maintained in 2-1 aquaria in seawater between pH 5.4-8.2 for 60 days. Survival registered as those showing movement within 24hrs of return to normal water. Shell weights were determined as dry weights. Shell size measured as length using vernier callipers. Growth was measured from	Significant mortalities found at pH \leq 6.9 but survival improves with size. Mortality of large specimens increases with exposure time & increasing temperature. Growth rate and thus shell size was reduced, tissue weight loss & shell dissolution also found at pH \leq 7.	Bamber, 1990	

Taxon	Mineralogy and development stage	Experiment type	Response to changes in $p\text{CO}_2$	References	What was measured and other notes
		the width of new shell after the pallial line as a proportion of remaining shell length.			
<i>Mytilus edulis</i>	Young specimens	A 2-factorial fully crossed 3 month experiment with both temperature (7.5, 10, 16, 20 and 25°C) and 3 $p\text{CO}_2$ levels (391 μatm , 869 μatm and 1,358 μatm). Bivalves were cultured and fed five days a week and lived in a flow-through system. Shell height was measured with callipers (dorso ventral axis)	At 25°C and 1,358 μatm $p\text{CO}_2$ level all shell growth was hindered, different $p\text{CO}_2$ levels had no effect on the shells breaking force. Growth had a negative correlation with CaCO_3 saturation and carbonate ion concentration. There was a negative correlation between shell growth and Lipofuscin accumulation but it positively correlated with mortality. Mortality is negatively correlated with shell growth, no correlation with shell breaking force and positively correlated with Lipofuscin accumulation.	Hiebenthal <i>et al.</i> , (2012)	Seawater $p\text{CO}_2$ and temperature on shell growth, shell stability, condition and cellular stress
	Alive and dead individuals	Specimens were placed in acidified water at pH levels 8.0, 7.8, 7.6 and 6.8 for 60 days. CO_2 was bubbled into header tanks which went to the experimental containers. Calcium carbonate composition estimated by analysing the calcium ion concentrations as a proxy for any changes in calcification or dissolution	As pH decreased calcium carbonate does not differ significantly compared to controls despite lower calcite and aragonite saturation states in live individuals (levels were maintained), at the cost of reduced health. Isolated shells decreased compared to controls at 1.5% day^{-1}	Findlay <i>et al.</i> , 2011	calcium carbonate composition of alive and dead specimens

Taxon	Mineralogy and development stage	Experiment type	Response to changes in $p\text{CO}_2$	References	What was measured and other notes
		Specimens were placed in acidified water using a pH adjustment for 40 days. Calcium concentrations were measured by dissolving the shells in 10% nitric acid then drying and weighing. Using an atomic absorption spectrophotometer the total calcium concentration is measured.	No significant changes in the calcium concentrations found in live specimens compared to the controls even with lower saturation states.	Findlay <i>et al.</i> , 2009	Measured calcium (Ca^{2+}) concentration in the calcified structures or shell morphological parameters as a proxy.
	Low magnesium calcite and aragonite	Species were reared for 60 days in isothermal experimental seawaters equilibrated with average modern $p\text{CO}_2$ values which were then changed up to 10 times pre industrial levels. The net rate of calcification was measured from changes in the buoyant weight and confirmed with dry weight.	No significant trend was found in response to elevated $p\text{CO}_2$ levels.	Ries <i>et al.</i> , 2009	The net rate of calcification (total calcification minus total dissolution).
	Adult specimens	Specimens were placed in tanks with flowing seawater to which additional CO_2 was added. Mussel health was analysed using NRR assay for lysosomal membrane stability and histopathological analysis of reproduction, digestion and respiratory tissues.	No impact on tissue structures was found, but reduced health measured from NRR assay was found thought to be due to elevated calcium ion levels in the haemolymph which is generated from the shell dissolution. Over long periods there's an energetic cost which causes reduced shell growth so long term changes are more significant to survival.	Beesley <i>et al.</i> , 2008	The health was monitored over a 60 day period.

Taxon	Mineralogy and development stage	Experiment type	Response to changes in $p\text{CO}_2$	References	What was measured and other notes
	Specimens between 40-50mm in shell length were used.	Placed in acidified water using CO_2 for 32 days to measure the effects of medium term hypercapnia. pH 7.7, 7.5, 6.7	Levels of phagocytosis increased significantly suggesting an immune response. This response was suppressed when they were exposed to acidified seawater. No other effects on the other immune-surveillance parameters measured.	Bibby <i>et al.</i> , 2008	How hypercapnia affects the immune response. immune-surveillance parameters measured were superoxide anion production, total and differential cell counts.
	Juvenile and adult specimens. 83% aragonitic shell.	Specimens were collected and placed in two aquarium tanks $p\text{CO}_2$ levels were set by moderating CO_2 -free air bubbling in to the tanks. Incubations lasted for 2 hrs 2 or 3 times a day. Net calcification rates were estimated using the alkalinity anomaly technique.	Calcification rates decline linearly with increased $p\text{CO}_2$ 25% by the end of the century. It was found to dissolve at $p\text{CO}_2$ values exceeding threshold values of ~1800 ppmv.	Gazeau <i>et al.</i> , 2007	740ppmv, IPCC IS92a scenario, net calcification was measured. The duration of the experiment did not allow for any potential adaptation.
	Specimens ranged in size from 8.5-25mm.	Specimens placed in aquarias filled with seawater that had increased levels of CO_2 introduced to give 5 different levels of pH between 6.7-8.1. Shell length was measured at the start and end of the 44 day period. Two size groups for each pH treatment 11mm mean for the small group 21mm mean for large group.	The growth was much larger in smaller specimens than large. Relative growth as a function of pH was similar in the two size groups differences may be random variations between samples. Reduction of pH affected growth negatively especially at lowest values. Virtually no growth at pH 6.7 was found. Effects set in between pH 7.4-7.1. pH 7.4-7.6 no significant difference in growth from pH 8.1 found.	Berge <i>et al.</i> , 2006	Measured shell growth in increased CO_2 seawater.

Taxon	Mineralogy and development stage	Experiment type	Response to changes in $p\text{CO}_2$	References	What was measured and other notes
	Collected from an estuary and segregated into large ~5cm and small up to 2.5cm.	Maintained in seawater between pH 5.4-8.2 for 60 days. Survival registered as those showing movement within 24 hrs of return to normal water. Shell weights were determined as dry weights. Shell size measured as length using vernier callipers.	Significant mortalities found at pH ≤ 6.6 . Mortality of large specimen's increases with exposure time is significantly higher at temperatures of 14°C than 9.2°C. Growth rate and thus shell size was reduced, tissue weight loss & shell dissolution also found at pH ≤ 7 .	Bamber, 1990	
<i>Mytilus galloprovincialis</i>	Juvenile 6 months old	Bivalve hatchery used filled with seawater pumped from the Ria Formosa lagoon. Reduced pH levels of 0.3 and 0.6 pH units were used as well as one control level stocked with 200 individuals in a flow through system. Length width height and live weight were measured at the start and 4 other occasions	Increased growth rates in the 0.6 pH treatment towards the end of the experiment. After 84 days no significant differences in pH levels were found for increments of size or weight. Shell weight decreased with pH levels but only for the inorganic component this increased with the individual's size.	Range <i>et al.</i> , 2012	Coastal lagoon environment
	Embryos were used.	Incubation occurred for 144 hrs in both high CO ₂ seawater (2000 ppm, pH 7.4) and control levels. Ordinary light, polarised light and scanning electron	Development at trochophore stage was delayed as shell formed. Veliger larvae in high CO ₂ showed morphological anomalies including	Kurihara <i>et al.</i> , 2008	Effects of CO ₂ rich seawater on early development. Compared embryogenesis, larval

Taxon	Mineralogy and development stage	Experiment type	Response to changes in $p\text{CO}_2$	References	What was measured and other notes
		microscopy were used to examine the embryos.	malformation of the shells & convex hinge. Height and length were smaller respectively compared to the control.		growth & morphology.
	Juvenile and adult specimens	An equal amount of specimens were placed into two tanks one as a control and one under hypercapnia conditions. The pH was set at 7.3 and mussel growth was measured regularly as well as total body weight	Shell growth increased progressively but at a slower rate in a hypercapnic environment compared to the control environment. The relationship between the length and weight show an exponential regular growth rate in both tanks and was not statistically different which suggests reduced shell growth is linked to decreasing soft body growth under hypercapnia.	Michaelidis <i>et al.</i> , 2005	Shell length, width and height were measured. Shell length was used for size frequency histograms
<i>Argopecten irradians</i>	Larval stage	Four 1 litre beakers containing filtered seawater had CO_2 gas mixtures continuously pumped into them at 3 different levels (high, moderate and ambient). 100 larvae were placed in each bucket and twice weekly the condition and development stage was determined visually. When 50% had metamorphosed 15 were selected to be measured.	The specimens were found to be very sensitive to high CO_2 levels very few survived to metamorphosis were as 52% survived in ambient CO_2 levels. Development rates were also found to be decreased. Size was also severely reduced to half the size of those in ambient levels.	Talmage & Gobler, 2009	

Appendix 2 – Summary of previously published modern temperature experiments using bivalves (relates to Chapter 1)

Table A2.1: modern experiments using bivalves and increased temperature (Presented in Section 1.4.1).

Taxon	Mineralogy and development stage	Experiment type	Response to changes in $p\text{CO}_2$	Authors References	What was measured and other notes
<i>Crassostrea gigas</i>		Commercial farming techniques, classified into four classes according to shell length (seed, juvenile, adult and marketable) daily sea surface temperatures were determined within the farming area at 50cm depth.	Temperature has a strong effect on survival of early stages. Mean temperature showed a negative relation to crop survival in seed to juvenile stage (temperature 20.0 to 21.3°C) and possibly at juvenile to adult stage (temperature 19.6 and 20.9°C). adult to marketable was not affected	Mizuta <i>et al.</i> , 2012	temperature
	2 day old Larvae	Placed in an Ifremer experimental hatchery at 19°C for 6 weeks for conditioning. A flow through culture system was used for experiments in conical tanks with each tank surveyed 6-7 times per day. Reared at 5 different temperatures (17°C, 22°C, 25°C, 27°C, and 32°C).	Mortality was 10% greater within 22-32°C temperature range and 20% greater at 17°C. Larval growth was expressed during the exotrophic period in which a linear relationship with temperature was found. Larval growth increased as temperature increased. Metamorphosis follows the same trend as growth.	Rico-Villa <i>et al.</i> , 2009	Shell length, growth rate, mortality and metamorphosis were measured against increasing temperature.
<i>Mytilus edulis</i>	Young specimens	A 2-factorial fully crossed 3 month experiment with both temperature (7.5, 10, 16, 20 and 25°C) and 3 $p\text{CO}_2$ levels	Strong reduction in shell growth at 25°C compared to lower temperatures. Temperature had	Hiebenthal <i>et al.</i> , (2012)	Seawater $p\text{CO}_2$ and temperature on shell growth, shell stability,

Taxon	Mineralogy and development stage	Experiment type	Response to changes in $p\text{CO}_2$	Authors References	What was measured and other notes
		(391 μatm , 869 μatm and 1,358 μatm). Bivalves were cultured and fed five days a week and lived in a flow-through system. Shell height was measured with callipers (dorso ventral axis)	no effect on the shells breaking force. Mortality drastically increased between 20 and 25°C		condition and cellular stress
	Larvae	One experiment they were reared in jars and placed in water baths kept at a constant temperatures of 10°C, 17°C, 24°C till the dissoconch stage. Growth and survival was measured every 5 days by collected sub samples. For the second experiment the larvae from the first experiment were placed in 6 new aquaria maintained at the same temperatures to allow settlement and metamorphosis. Growth and survival were measured the same as before.	Survived significantly better at 24°C than the survival rate at 10°C. 17°C was the optimum survival temperature with 74% compared to <46% at the other temperatures. After 200 days till the end it grew in similar patterns regardless of different temperatures. Growth was found to be positively correlated with temperature (3 μm at 10°C, 5 μm at 17°C and 7 μm at 24°C). Temperature was found to affect larval stage mortality more significantly than specimens at a post larval stage.	Rayssac <i>et al.</i> , 2010	The effect of temperature on growth and survival.
	1,000 adult and juvenile sized specimens.	Recirculating water bath system was used to achieve four temperature settings (4°C, 8°C, 12°C and 15°C). 3 large containers pumped seawater to water baths at specific temperatures. 30 juveniles were placed in each tank and cultured for 5 months. 6 adults were placed in separate tanks for 6	From bulk growth measurements it was found there was no significant evidence of a relationship between temperature and shell length or growth. Growth rates were dissimilar between adults and juveniles with juveniles growing faster than	Wanamaker <i>et al.</i> , 2007	Growth rates and shell length compared to increasing temperatures.

Taxon	Mineralogy and development stage	Experiment type	Response to changes in $p\text{CO}_2$	Authors References	What was measured and other notes
		months. Water was changed weekly. Specimens were treated with a biomarker before it started to determine future shell growth and the original shell length was measured and then measured monthly with digital callipers.	adults.		
<i>Mytilus galloprovincialis</i>	Adult specimens	Kept in aquariums under normal condition 2 weeks prior to experiment. Placed in 6 aquaria at temperatures warming slowly up to 18°C, 20°C, 24°C, 26°C, 28°C, and 30°C. Mortality was checked every day for 30 days. Mussels that when stimulated didn't close were considered dead.	Very few die below 26°C. 5% within 5 days and 20% after 30 days started to die at 26°C. Mortality increased significantly at acclimation to 28°C, 20% by day 5, 30% after 30 days. 80% dies after 15 days at 30°C.	Anestis <i>et al.</i> , 2007	Mortality responses to long term acclimation at increased ambient temperature
<i>Mytilus trossulus</i>	Larvae	One experiment they were reared in jars and placed in water baths kept at a constant temperatures of 10°C, 17°C, 24°C till the dissoconch stage. Growth and survival was measured every 5 days by collecting sub samples. For the second experiment the larvae from the first experiment were placed in 6 new aquaria maintained at the same temperatures to allow settlement and metamorphosis. Growth and survival were measured the same as before.	Highest survival was at both 10°C and 17°C with lowest at 24°C which was 19%. After 200 days till the end it grew in similar patterns regardless of different temperatures. Growth was found to be positively correlated with temperature (3µm at 10°C, 5µm at 17°C and 7µm at 24°C). Temperature was found to affect larval stage mortality more significantly than specimens at a post larval stage.	Rayssac <i>et al.</i> , 2010	The effect of temperature on growth and survival.

Taxon	Mineralogy and development stage	Experiment type	Response to changes in $p\text{CO}_2$	Authors References	What was measured and other notes
<i>Modiolus barbatus</i>	Adult specimens (55-60mm)	Held in aquariums for 2 weeks in normal conditions before experiments. Placed in 6 aquaria brought to 18°C, 20°C, 24°C, 26°C, 28°C, 30°C in temperature slowly. Mortality checked every day for 30 days.	No mortality up to 24°C. 3% dies at 26°C. Significant mortality increased at 28°C and 30°C with 10% to 20% mortality after 30 days.	Anestis <i>et al.</i> , 2008	Mortality responses to long term acclimation at increased ambient temperature
<i>Clinocardium nuttallii</i>	Larvae	Placed in rearing containers that were then placed in the holding tanks that were used to regulate temperature. Temperatures used in the tanks were 5.9, 10.2, 14.2, 18.2, 21.9 & 26.3°C. Larval rearing was terminated at the pediveliger stage so survival rates at temperatures could be compared at the same development stage and time. Seawater changes every other day and 4 subsamples taken to determine shell length and survival rate.	Larval growth increased with increasing temperature and growth was found to be reliant on the temperature it was reared in. The time it took to reach pediveliger stage was shorter at higher temperatures than lower temperatures. Survival to settlement stage was unaffected by temperature except at the highest temperature where larvae failed to survive after day 6. Optimum temperature for growth was 21.9°C but the survival rate was significantly lower.	Liu <i>et al.</i> , 2010	Temperature against growth and survival of larvae

Appendix 3 – Previously published data correlated to Lyme Regis and St Audrie’s Bay (relates to Chapter 2)

A3.1: Previously published isotope data from Lyme Regis and St Audrie’s Bay

Table A3.1: Korte *et al.* (2009) bulk rock from Lyme Regis with the corresponding bed heights from the logs produced from this study.

Korte <i>et al.</i> (2009) bulk rock from Lyme Regis			
$\delta^{13}\text{C}$	Bed height for this study’s logs	$\delta^{18}\text{O}$	Bed height for this study’s logs
3.28	0.6	-3.35	0.6
3.53	0.75	-2.93	0.75
3.61	0.95	-2.79	0.95
3.36	1.15	-3.41	1.15
3.47	1.3	-3.36	1.3
3.55	1.55	-3.16	1.55
3.31	1.75	-3.44	1.75
4.03	1.9	-1.76	1.9
3.39	2.25	-2.96	2.25
3.88	2.65	-2.23	2.65
3.56	3.15	-2.86	3.15
3.58	3.6	-2.94	3.6
2.92	3.9	-3.46	3.9
2.92	4.15	-3.93	4.15
3.88	4.5	-2.34	4.5
3.7	5	-2.46	5
3.77	5.15	-1.9	5.15
3.73	5.35	-2.19	5.35
3.32	5.75	-3.19	5.75
2.86	6.2	-4.56	6.2
3.07	6.75	-2.92	6.75
3.16	7.1	-2.86	7.1
2.39	7.3	-3.14	7.3
2.43	7.4	-2.81	7.4
2.21	7.7	-3.04	7.7
1.6	8.05	-4.58	8.05
1.89	8.3	-2.9	8.3
1.39	8.5	-2.08	8.5
1.59	8.75	-2.17	8.75
1.52	8.9	-1.98	8.9
1.52	9.15	-2.86	9.15
1.58	9.5	-3.16	9.5
1.55	9.6	-3.09	9.6
1.6	9.7	-2.79	9.7
1.02	9.9	-3.93	9.9
1.11	10	-3.09	10
1.36	10.2	-2.3	10.2
1.19	10.4	-2.23	10.4
0.77	10.6	-2.36	10.6
0.8	10.85	-2.32	10.85
0.45	11.7	-1.53	11.7
0.01	12.05	-2.62	12.05
-0.18	12.75	-1.9	12.75

0.01	14.1	-2.12	14.1
-0.14	16.05	-1.89	16.05

Table A3.2: Korte *et al.* (2009) oysters from St Audrie's Bay with the corresponding bed heights from the logs produced from this study.

Korte <i>et al.</i> (2009) oysters from St Audrie's Bay			
$\delta^{13}\text{C}$	Bed height for this study's logs	$\delta^{18}\text{O}$	Bed height for this study's logs
2.87	11.7	-0.42	11.7
3.3	11.7	0.46	11.7
3	11.7	-0.39	11.7
3.76	11.7	-0.18	11.7
2.24	11.9	-0.09	11.9
2.89	11.9	-0.12	11.9
3.18	11.9	0.88	11.9
2.83	11.9	-0.1	11.9
2.86	11.9	-0.34	11.9
3.36	11.9	0.96	11.9
3.29	11.9	0.55	11.9
3.51	12.2	0.19	12.2
3.55	12.2	-0.12	12.2
4.63	12.2	1.62	12.2
3.94	12.2	0.04	12.2
3.62	12.8	-0.49	12.8
4.11	12.8	0.35	12.8
3.62	12.9	0.08	12.9
4.04	13.1	-0.05	13.1
4.04	13.1	-0.05	13.1
4.04	13.1	-0.05	13.1
4.04	13.1	-0.05	13.1
3.02	13.3	0.17	13.3
3.31	13.3	0.02	13.3
4.34	13.6	-0.81	13.6
4.53	13.6	-0.65	13.6
4.77	13.6	-1.02	13.6
4.45	13.6	-0.36	13.6
3.68	13.8	-0.87	13.8
2.23	14.1	-1.29	14.1
3.88	14.2	-0.8	14.2
3.88	14.2	-0.8	14.2
3.69	14.2	-0.66	14.2
4	14.2	-0.34	14.2
4.16	14.2	-0.48	14.2
2.93	14.2	-1.06	14.2
4.25	14.4	0.22	14.4
2.98	14.6	-0.93	14.6
3.33	14.8	-1.17	14.8
3.33	14.8	-1.17	14.8
3.43	14.8	-1.09	14.8
3.55	14.8	-1.18	14.8
3.17	14.95	-1.25	14.95
3.38	14.95	-1.18	14.95
3.26	15.2	-0.38	15.2
3.26	15.2	-0.38	15.2
3.95	15.35	-0.82	15.35
2.54	15.5	-0.43	15.5
3.24	15.5	-0.24	15.5

Korte <i>et al.</i> (2009) oysters from St Audrie's Bay			
$\delta^{13}\text{C}$	Bed height for this study's logs	$\delta^{18}\text{O}$	Bed height for this study's logs
3.51	15.6	-0.27	15.6
3.52	15.6	0.16	15.6
2.76	15.7	-0.46	15.7
3.02	15.7	-0.54	15.7
3.02	15.7	-0.54	15.7
2.93	16.8	-1.19	16.8
3.07	16.8	-1.05	16.8
2.15	17.1	-1.79	17.1
2.51	17.1	-1.25	17.1
2.45	17.2	-0.69	17.2
2.16	19.8	-1.09	19.8
1.86	19.8	-1.06	19.8
2.36	19.9	-1.78	19.9
1.99	20	-1.74	20
1.71	20.6	-0.97	20.6
2.01	20.6	-0.06	20.6
2.48	22.4	-0.99	22.4
1.69	22.4	-1.46	22.4
1.73	22.4	-1.12	22.4
2.04	24.3	-0.89	24.3
2.73	24.6	-1.52	24.6
2.59	25.3	-1.41	25.3
2.78	25.3	-1.26	25.3
2.32	25.9	-2.05	25.9
1.61	27.4	-2.03	27.4
2.01	27.4	-1.24	27.4
1.26	27.8	-1.79	27.8
1.89	28.2	-1.88	28.2
1.98	28.2	-1.39	28.2
1.37	32	-1.98	32
1.82	32.8	-1.81	32.8
1.7	32.8	-2.23	32.8

Table A3.3: van de Schootbrugge *et al.* (2007) oysters from St Audrie's Bay with the corresponding bed heights from the logs produced from this study.

van de Schootbrugge <i>et al.</i> (2007) oyster from St Audrie's Bay			
$\delta^{13}\text{C}$	Bed height for this study's logs	$\delta^{18}\text{O}$	Bed height for this study's logs
3.35	15.1	-1.14	15.1
3.61	15.1	-1.64	15.1
3.19	15.1	-1.35	15.1
2.99	15.1	-2.47	15.1
3.7	15.95	-1.88	15.95
3.87	15.95	-0.57	15.95
3.5	16.1	-0.09	16.1
3.1	16.1	-0.25	16.1
2.61	16.1	-0.07	16.1
2.23	16.1	-0.75	16.1
2.69	16.1	-0.74	16.1
3.37	16.12	-0.75	16.12
3.59	16.12	-0.91	16.12
3.84	16.12	-1.11	16.12
3.92	16.12	-1.23	16.12
2.83	17.2	-1.33	17.2
3.29	17.2	-1.01	17.2

van de Schootbrugge <i>et al.</i> (2007) oyster from St Audrie's Bay			
$\delta^{13}\text{C}$	Bed height for this study's logs	$\delta^{18}\text{O}$	Bed height for this study's logs
3.26	17.25	-0.97	17.25
2.89	17.25	-0.68	17.25
2.49	17.4	-0.78	17.4
1.6	17.7	-0.83	17.7
2.26	19.6	-0.68	19.6
2.15	19.6	-0.65	19.6
1.87	19.68	-0.89	19.68

Table A3.4: Hesselbo *et al.* (2002) and Ruhl *et al.* (2010) $\delta^{13}\text{Corg}$ bulk rock from St Audrie's Bay with the corresponding bed heights from the logs produced from this study.

Hesselbo <i>et al.</i> (2002) from St Audrie's Bay		Ruhl <i>et al.</i> (2010) from St Audrie's Bay	
$\delta^{13}\text{Corg}$ bulk rock	Bed height for this study's logs	$\delta^{13}\text{Corg}$ bulk rock	Bed height for this study's logs
-29.25	27.9	-27.707	62.3
-29.08	27.7	-27.824	62
-28.18	27.5	-28.655	61.7
-27.53	27.3	-28.245	61.5
-28.22	27.1	-28.159	61.2
-27.79	26.9	-27.797	61
-27.36	26.7	-28.094	60.8
-27.85	26.5	-28.21	60.6
-27.71	26.3	-27.925	60.4
-28.79	26.1	-28.012	60
-29.18	25.9	-29.148	59.8
-29.35	25.7	-29.061	59.66
-29.01	25.5	-29.167	59.5
-29.43	25.3	-29.131	59.3
-29.18	25.1	-29.178	59.15
-29.27	24.9	-29.323	58.95
-28.71	24.7	-29.132	58.8
-29.11	24.5	-28.888	58.6
-28.12	24.2	-29.092	58.5
-28.12	24	-29.078	58.3
-28.68	23.8	-28.973	58.1
-28	23.6	-28.796	57.9
-27.46	23.5	-28.902	57.7
-26.91	23.2	-27.997	57.55
-27.3	22.9	-28.327	57.4
-28.58	22.7	-27.919	57.1
-28.81	22.5	-27.261	56.9
-28.47	22.3	-27.588	56.7
-28.86	22.1	-27.064	56.4
-29.62	21.9	-27.889	56.1
-29.64	21.7	-27.718	55.6
-29.35	21.5	-27.684	55.25
-30.23	21.3	-27.608	54.9
-29.7	21.1	-27.807	54.6
-29.29	20.9	-27.577	54.2
-29.01	20.7	-28.294	54
-27.98	20.5	-28.324	53.7
-28.79	20.2	-27.951	53.25
-30.03	20	-28.103	53.1
-29.13	19.8	-28.092	52.9
-27.82	19.6	-28.26	52.7

Hesselbo <i>et al.</i> (2002) from St Audrie's Bay		Ruhl <i>et al.</i> (2010) from St Audrie's Bay	
$\delta^{13}\text{C}$org bulk rock	Bed height for this study's logs	$\delta^{13}\text{C}$org bulk rock	Bed height for this study's logs
-27.9	19.3	-29.321	52.5
-27.89	18.9	-28.051	52.35
-29.95	18.6	-29.082	52.2
-28.67	18.2	-29.03	52.1
-28.4	17.9	-28.668	51.9
-28.89	17.6	-28.016	51.7
-29	17.2	-27.541	51.5
-28.9	17	-27.88	51.17
-29.09	16.8	-28.908	50.9
-29.53	16.4	-29.132	50.7
-29.41	16.2	-28.273	50.4
-28.43	16	-27.81	50.2
-28.89	15.8	-27.614	49.9
-27.37	15.4	-27.893	49.6
-27	15	-28.199	49.4
-26.91	14.8	-27.743	49.16
-26.77	14.6	-27.649	48.5
-25.85	14.4	-27.978	48.3
-26.47	14.2	-28.815	48.1
-25.6	14	-28.827	47.8
-25.79	13.8	-28.971	47.6
-26.67	13.6	-29.354	47.3
-26.19	13.4	-29.356	47.1
-26.39	13.2	-28.813	46.8
-27.79	13	-28.54	46.5
-28.35	12.8	-28.991	46.3
-26.73	12.6	-29.3	46
-27.25	12.3	-29.308	45.8
-26.76	12.1	-28.595	45.7
-26.54	11.9	-27.845	45.4
-26.71	11.7	-28.124	45.15
-28.94	11.5	-27.788	44.9
-29.3	11.3	-27.583	44.7
-28.65	11.1	-28.052	44.3
-24.46	10.9	-27.873	44.15
-24.68	10.4	-28.076	44
-24.85	10.2	-29.9	43.8
-25.17	10	-27.947	43.6
-26.54	9.8	-28.068	43.4
-25.68	9.5	-28.339	43.2
-25.97	9.3	-28.214	42.9
-25.67	9	-28.314	42.7
-25.9	8.8	-29.029	42.5
-26.1	8.6	-29.039	42.3
-26.46	8.4	-29.793	42
-24.88	8.1	-29.26	41.8
-24.8	7.8	-29.499	41.5
-25.88	7.5	-28.478	41.2
-25.83	7.3	-29.187	40.9
-25.83	7.1	-29.269	40.6
-26.53	6.9	-29.345	40.4
-26.43	6.7	-29.453	40.2
-25.91	6.5	-30.011	39.8
-26.26	6.3	-29.529	39.5

Hesselbo <i>et al.</i> (2002) from St Audrie's Bay		Ruhl <i>et al.</i> (2010) from St Audrie's Bay	
$\delta^{13}\text{Corg}$ bulk rock	Bed height for this study's logs	$\delta^{13}\text{Corg}$ bulk rock	Bed height for this study's logs
-26.76	6.1	-29.492	39.2
-28.36	5.9	-29.041	38.9
-28.39	5.7	-29.188	38.7
-28.46	5.5	-27.653	38.4
-26.6	5.3	-27.79	38.1
-26.19	5.1	-28.011	37.8
-27.79	4.9	-28.415	37.5
-28.16	4.7	-28.173	37.2
-25.89	4.5	-28.472	36.7
-25.77	4.3	-28.944	36.4
-26.29	4.1	-29.282	36.1
-25.51	3.9	-28.865	35.8
-27.5	3.7	-29.339	35.6
-25.36	3.5	-29.267	35.3
-26.01	3.3	-29.115	35.15
-25.86	3.1	-29.287	35.05
-26.61	2.9	-28.973	34.95
-24.97	2.7	-29.418	34.9
-25.82	2.5	-29.618	34.8
-25.25	2.3	-28.642	34.5
-25.16	2.1	-28.419	34.3
-25.6	1.9	-28.058	34
-27.05	1.7	-28.772	33.8
-25.41	1.5	-28.482	33.6
-24.88	1.3	-28.163	33.4
-26.43	1.1	-28.082	33.1
-26.31	0.9	-28.57	32.7
		-28.697237	32.4
		-28.356163	32
		-28.76684	31.6
		-29.366781	31.2
		-29.281804	30.9
		-29.224134	30.7
		-29.220234	30.5
		-28.170162	30.2
		-28.181282	29.8
		-28.384294	29.5
		-29.101462	29.2
		-28.345099	28.9
		-29.579451	28.6
		-28.823661	28.1

A3.2: Previously published $p\text{CO}_2$ data correlated to Lyme Regis and St Audrie's Bay

Table A3.5: McElwain *et al.* (1999) $p\text{CO}_2$ levels for the Greenland and Sweden sections and corresponding bed heights from the St Audrie's Bay logs.

McElwain <i>et al.</i> (1999)			
Greenland bed height	Error value	$p\text{CO}_2$ ppm	St Audrie's Bay Bed height
69	99.75	698.25	6
50	257.25	1800.75	16
32	222.75	1559.25	33.6
25	258.75	1811.25	38.6
22.5	146.25	1023.75	41.3
20	126.75	887.25	43
Sweden bed height			
6	100.5	703.5	5
8	173.25	1212.75	10.7
12	291.75	2042.25	23.8
14	247.5	1732.5	29.6
15	84.75	593.25	31.6

Table A3.6: Schaller *et al.* (2011) $p\text{CO}_2$ levels for the Newark Basin and corresponding bed heights from the St Audrie's Bay logs.

Schaller <i>et al.</i> (2011) for the Newark Basin				
Sample number	$p\text{CO}_2$ S(z) = 3000 (\pm 1000ppm)	S(z) "+/-" 1000 ppm	St Audrie's Bay bed height	"Absolute" Time (Myr)
NBPT3-250	2496	831.9168	53	200.3626
NBC134-192	3131	1043.562	48	200.4778
NBPT9-453	5273	1757.491	31.3	200.9062
NBC104-123	4941	1650.835	31.3	200.9062
Hook Mountain Basalt				
NTPT12-239	1949	649.6017	31.1	200.9143
NTC129-223	2356	785.2548	27.7	201.0247
NTC128-221	3708	1235.876	25.3	201.0743
NTC101-128	2642	880.5786	23.7	201.1184
NTC127-192	3460	1153.218	22	201.163
NTPT16-266	3014	1004.566	20	201.1999
NTC125-110	3657	1218.878	19.8	201.2116
NTC100-195	4015	1338.2	19.8	201.2116
NTPT16-340	4050	1349.865	19.5	201.2157
NTC124-73	4070	1356.531	19.3	201.2263
NTC125-170	4234	1411.192	19.3	201.2263
Preakness Basalt				
NFPTI3-156	3453	1150.885	18.3	201.2566
NFDH9-105	3577	1192.214	18	201.2775
NFC93-134	3584	1194.547	13.6	201.3878
NFPT26-169	4228	1409.192	10.5	201.4538
NFPT26-245	4434	1477.852	9.7	201.4895
Orange Mountain Basalt				
NPEX	1065	355	8	201.5091
NPMART-1342	1787	596	0	201.7261

Table A3.7: Steinhorsdottir *et al.* (2011) $p\text{CO}_2$ levels for Larne in Northern Ireland and corresponding bed heights from the St Audrie's Bay logs.

Steinhorsdottir <i>et al.</i> (2011)						
Astartekloft Greenland bed number	Error value	$p\text{CO}_2$ ppm carboniferous standard	St Audrie's Bay Bed height	Error value	$p\text{CO}_2$ ppm modern standard	St Audrie's Bay Bed height
Bed 8	262	1354	43	170	880	43
Bed 7	131	1223	41.3	85	795	41.3
Bed 6	989	2971	38.6	643	1931	38.6
Bed 5	229	2184	33.6	149	1420	33.6
Bed 4	251	1673	16	163	1087	16
Bed 3	307	932	6	200	606	6
Larne Northern Ireland bed numbers						
A10	406	1468	22	264	954	22
G5	346	1664	17	225	1082	17
G3	263	2166	15.5	171	1408	15.5
WL5	602	2073	13.6	391	1347	13.6
WL2	250	1866	11.4	162	1213	11.4

Table A3.8: McElwain *et al.* (1999) $p\text{CO}_2$ levels for the Greenland and Sweden sections and corresponding bed heights from the Lyme Regis logs.

McElwain <i>et al.</i> (1999)			
Greenland bed height	Error value	$p\text{CO}_2$ ppm	Lyme Regis Bed height
69	99.75	698.25	0
50	257.25	1800.75	9.72
32	222.75	1559.25	15.3
25	258.75	1811.25	15.85
22.5	146.25	1023.75	15.92
20	126.75	887.25	16
Sweden bed height			
8	173.25	1212.75	0
12	291.75	2042.25	12.6
14	247.5	1732.5	15
15	84.75	593.25	15.22

Table A3.9: Schaller *et al.* (2011) $p\text{CO}_2$ levels for the Newark Basin and corresponding bed heights from the Lyme Regis logs.

Schaller <i>et al.</i> (2011) for the Newark Basin				
Sample number	$p\text{CO}_2$ S(z) = 3000 (\pm 1000ppm)	S(z)" +/-" 1000 ppm	Lyme Regis bed height	"Absolute" Time (Myr)
NBPT3-250	2496	831.9168	21.5	200.3626
NBC134-192	3131	1043.5623	17.5	200.4778
NBPT9-453	5273	1757.4909	15.3	200.9062
NBC104-123	4941	1650.8349	15.3	200.9062
Hook Mountain Basalt				
NTP12-239	1949	649.6017	15.2	200.9143
NTC129-223	2356	785.2548	14.4	201.0247
NTC128-221	3708	1235.8764	13.4	201.0743
NTC101-128	2642	880.5786	12.5	201.1184
NTC127-192	3460	1153.218	11.7	201.163
NTP16-266	3014	1004.5662	11.4	201.1999
NTC125-110	3657	1218.8781	11.3	201.2116
NTC100-195	4015	1338.1995	11.3	201.2116
NTP16-340	4050	1349.865	11.1	201.2157
NTC124-73	4070	1356.531	11	201.2263
NTC125-170	4234	1411.1922	11	201.2263
Preakness Basalt				
NFPT13-156	3453	1150.8849	10.7	201.2566
NFDH9-105	3577	1192.2141	10.4	201.2775
NFC93-134	3584	1194.5472	7.9	201.3878
NFPT26-169	4228	1409.1924	0	201.4538

Table A3.10: Steinthorsdottir *et al.* (2011) $p\text{CO}_2$ levels for Larne in Northern Ireland and corresponding bed heights from the Lyme Regis logs.

Steinthorsdottir <i>et al.</i> (2011)						
Astartekloft Greenland bed number	Error value	$p\text{CO}_2$ ppm carbonifero us standard	Lyme Regis Bed height	Error value	$p\text{CO}_2$ ppm modern standard	Lyme Regis Bed height
Bed 8	262	1354	16	170	880	16
Bed 7	131	1223	15.92	85	795	15.92
Bed 6	989	2971	15.85	643	1931	15.85
Bed 5	229	2184	15.3	149	1420	15.3
Bed 4	251	1673	9.72	163	1087	9.72
Bed 3	307	932	0	200	606	0
Larne Northern Ireland bed numbers						
A10	406	1468	12.3	264	954	12.3
G5	346	1664	10	225	1082	10
G3	263	2166	9.4	171	1408	9.4
WL5	602	2073	8.2	391	1347	8.2

Appendix 4 – Raw fossil data collected from both locations and the corresponding analysis of the results (relates to Chapter 3)

A4.1: Lyme Regis raw fossil data

Table A4.1: *L. hisingeri* geometric shell size data from every individual per bed in Lyme Regis with the corresponding stratigraphic zones, subzones and bed height. (Presented in Section 3.5.3) (Measured in mm)

<i>L. hisingeri</i>					
Zone	Subzone	Bed N.	Bed height	Geometric shell size	Shell preservation
Pre-planorbis		LRB 1	8.05	11.2	SP
			8.05	12.1	SP
			8.05	10.1	SP
			8.05	8.4	SP
			8.05	11.9	SP
		LRB 2	8.50	17.3	PSOS
			8.50	19.1	PSOS
			8.50	21.3	SP
			8.50	20.5	SCC
			8.50	16.7	SCC
			8.50	23.0	MS
			8.50	16.1	MDP
			8.50	13.2	SP
			8.50	24.9	SP
			8.50	14.6	DDW, MDP
			8.50	22.7	MDP
			8.50	20.3	DDW
			8.50	21.4	DDW
			8.50	18.7	SP
			8.50	24.1	SP
		LRB 4	8.70	18.1	SP
			8.70	18.0	SCC
			8.70	23.1	SCC, PSOS
			8.70	15.6	SCC, PSOS
			8.70	17.3	MDP
			8.70	28.2	MS
			8.70	19.4	DDW
			8.70	30.7	DDW, MDP
			8.70	17.5	MDP, SCC
			8.70	19.0	SP
			8.70	16.0	SP
			8.70	24.8	PSOS
			8.70	21.2	MS
			8.70	25.3	DDW, PSOS
			8.70	24.1	DDW, PSOS
			8.70	17.9	MDP
			8.70	18.0	DDW, PSOS
			8.70	16.1	DDW, MDP
			8.70	16.5	DDW, MDP
			8.70	8.7	DDW, MDP
			8.70	16.4	DDW, MDP
			8.70	12.8	DDW, MDP
			8.70	13.0	DDW, MDP
		8.70	14.4	DDW, MDP	
		8.70	16.9	DDW, MDP	
		8.70	19.5	DDW, MDP	
		8.70	8.7	DDW, MDP	
		LRB 5	8.75	20.7	SP
		LRB 6	8.77	22.0	SP
			8.77	25.2	DDW, MDP

<i>L. hisingeri</i>					
Zone	Subzone	Bed N.	Bed height	Geometric shell size	Shell preservation
			8.77	20.5	DDW, MDP
			8.77	17.6	DDW, MDP
			8.77	18.3	DDW, MDP
			8.77	31.6	DDW, MDP
			8.77	13.7	SP
			8.77	23.9	DDW, MDP
			8.77	22.3	DDW, MDP
			8.77	26.5	MS, DDW, MDP
			8.77	15.9	SP
			8.77	16.9	MS
			8.77	24.6	DDW, MDP
			8.77	23.3	MDP
			8.77	16.6	MDP
			8.77	18.3	MDP
			8.77	14.3	SP
			8.77	18.9	OMI, CSM
			8.77	24.7	DDW, MDP
			8.77	19.9	DDW, MDP
			9.04	21.7	SP
			9.04	20.6	SP
			9.04	19.2	PSOS
			9.04	11.2	PSOS
			9.04	25.6	PSOS
			9.04	19.8	DDW, MDP
			9.04	30.8	MS
			9.04	11.4	DDW, MDP
			9.13	20.8	PSOS
			9.13	20.1	PSOS
			9.13	21.1	PSOS
			9.13	26.5	SP
			9.13	24.2	SP
			9.13	28.6	MDP
			9.13	22.4	MDP
			9.13	12.8	MDP
			9.13	24.1	MDP
			9.13	19.5	DDW
			9.13	18.0	DDW
			9.13	17.1	PSOS
			9.13	27.1	DDW, MDP
			9.13	23.0	DDW, MDP
			9.13	19.6	DDW, MDP
			9.13	14.8	SP
			9.13	27.0	DDW, MDP
			9.13	22.5	DDW, MDP
			9.13	20.4	SP
			9.13	23.1	DDW, MDP
			9.13	25.5	DDW, MDP
			9.13	21.4	DDW, MDP
			9.13	21.3	DDW, MDP
			9.16	21.9	SP
			9.16	29.9	DDW, MDP
			9.59	19.7	DDW, MDP
			9.59	29.4	MS
			9.59	20.8	SP
			9.59	22.0	DDW, MDP
			9.60	27.1	SP
			9.60	26.9	DDW, MDP
			9.70	32.0	DDW, MDP
			9.70	20.2	DDW, MDP
			9.70	11.9	DDW, MDP
			9.72	19.7	DDW, MDP
			9.80	22.1	SP
			10.20	30.4	DDW
			10.20	22.2	SP
			10.20	28.9	SP
			10.20	23.8	SCC
			10.20	34.6	SP
			10.20	34.1	SCC, MS

<i>L. hisingeri</i>							
Zone	Subzone	Bed N.	Bed height	Geometric shell size	Shell preservation		
			10.20	25.8	SCC		
			10.20	27.1	SCC, MS		
			10.20	17.8	PSOS		
			10.20	31.0	DDW, MDP		
			10.20	44.8	DDW		
			10.20	16.6	DDW, MDP		
			10.20	15.1	SP		
			10.20	15.8	SCC		
			10.20	17.3	PSOS		
			10.20	40.0	SP		
		10.20	22.3	SP			
		10.50	16.9	SP			
				LRB 22	10.50	23.9	DDW, MDP
10.50	20.2				DDW, MDP		
planorbis Zone	Ps. planorbis subzone			LRB 26	10.90	23.2	PSOS
					10.90	23.1	PSOS
					10.90	29.6	PSOS
					10.90	19.7	PSOS
					10.90	15.7	DDW, MDP
					10.90	36.8	DDW, MDP
					10.90	16.9	DDW, MDP
					10.90	12.3	DDW, MDP
					10.90	14.5	DDW
					10.90	10.2	DDW
					10.90	48.4	DDW
		10.90	18.3		DDW		
		10.90	10.4		DDW		
		10.90	18.9		DDW		
		10.90	28.2		DDW		
		10.90	23.5		DDW		
		10.90	20.9		SCC, MDP		
		10.90	13.7		SCC, MDP		
		10.90	15.5		SCC		
		10.90	17.7		SCC		
		10.90	18.1		SCC, PSOS		
		10.90	9.5		MS		
		10.90	12.3		MDP		
		10.90	15.8		SCC, PSOS		
		10.90	20.9		MDP		
		10.90	23.9		MDP		
		10.90	20.7		MDP		
		10.90	14.2		MDP		
		10.90	17.5		SP		
		10.90	25.6		SCC, PSOS		
		10.90	19.8		SCC, PSOS		
		10.90	16.9		DDW, MDP		
		10.90	18.8		DDW, MDP		
10.90	15.0	DDW, MDP					
10.90	28.1	DDW, MDP					
10.90	16.9	DDW, MDP					
10.90	14.8	DDW, MDP					
10.90	23.2	DDW, MDP					
10.90	16.2	DDW, MDP					
10.90	19.9	DDW, MDP					
10.90	22.1	DDW					
10.90	15.7	DDW					
	C. johnstoni subzone	LRB 30	12.30	14.8	DDW		
			12.30	17.3	DDW		
			12.30	16.4	DDW		
			12.30	22.1	DDW		
			12.30	20.9	DDW		
			12.30	14.7	DDW		
			12.30	18.9	DDW		
			12.30	29.1	MDP		
			12.30	19.2	MDP		
			12.30	37.4	MDP		
12.30	16.2	MDP					
12.30	18.4	SP					

<i>L. hisingeri</i>					
Zone	Subzone	Bed N.	Bed height	Geometric shell size	Shell preservation
			12.30	34.6	SP
			12.30	22.0	DDW, MDP
			12.30	26.8	DDW, MDP
			12.30	24.6	DDW, MDP
			12.30	14.7	SP
			12.30	14.1	DDW, MDP
			12.30	21.4	MS
			12.30	20.5	MS
			12.30	19.8	MS
			12.30	22.1	SP
			12.30	24.2	SP
			12.30	24.9	DDW
			12.30	35.5	DDW
		LRB 34	12.75	33.5	PSOS, MDP
			12.75	27.5	PSOS, MDP
			12.75	12.5	PSOS, MDP
			13.30	19.2	PSOS, SCC
			13.30	13.7	PSOS, SCC
			13.30	16.0	PSOS
			13.30	17.7	PSOS
			13.30	15.5	DDW, MDP
			13.30	14.5	PSOS
			13.30	21.8	DDW, MDP
			13.30	11.9	PSOS
			13.30	13.3	PSOS
			13.30	15.5	MDP
			13.30	18.5	MDP
			13.30	23.7	MDP
			13.30	35.2	SCC, MDP
			13.30	20.3	SCC, MDP
			13.30	17.9	DDW, MDP
			13.30	17.4	DDW, MDP
			13.30	20.9	DDW, MDP
			13.30	14.5	DDW, MDP
			13.30	15.5	DDW, MDP
			13.30	16.2	DDW, MDP
			13.30	19.0	DDW, MDP
			13.30	17.2	SCC
			13.30	17.2	SCC
			13.30	12.7	PSOS
			13.30	18.7	PSOS
			13.30	19.2	MDP
			13.30	16.0	SCC
			13.30	14.8	MDP
			13.30	18.7	MDP
			13.30	25.6	DDW
			13.30	20.9	DDW, MDP
			13.30	23.9	DDW, MDP
			13.30	28.0	DDW
			13.30	29.8	SP
			13.30	26.9	SP
			13.30	34.8	SP
			13.30	29.4	SP
			13.30	14.9	DDW
			14.20	15.4	MDP
			14.20	21.3	DDW, MDP
			14.20	15.5	DDW, MDP
			14.20	18.4	DDW, MDP
			14.20	15.1	DDW, MDP
			14.20	16.5	DDW, MDP
			14.20	23.4	DDW, MDP
			14.20	27.7	DDW, MDP
			14.20	18.5	DDW, MDP
			14.20	22.9	DDW, MDP
			14.20	22.7	SP
			14.20	22.8	DDW, MDP
			14.20	16.8	DDW, MDP
			14.20	14.4	DDW, MDP
		LRB 40			

<i>L. hisingeri</i>							
Zone	Subzone	Bed N.	Bed height	Geometric shell size	Shell preservation		
		LRB 42	14.20	22.4	DDW, MDP		
			14.50	26.6	SCC		
			14.50	17.9	SCC		
			14.50	20.1	SCC, PSOS		
			14.50	22.2	SCC, PSOS		
			14.50	22.8	DDW		
			14.50	27.5	DDW		
			14.50	16.8	DDW		
			14.50	19.3	DDW		
			14.50	16.6	SP		
			14.50	16.0	SP		
			14.50	12.7	SP		
			14.50	21.1	PSOS		
			14.50	34.7	PSOS		
		14.50	22.6	MS			
		14.50	21.0	MDP			
		liasicus Zone	W. portlocki subzone	LRB 44	14.85	20.1	SP
					14.85	25.5	DDW
				LRB 46	15.20	21.5	DDW, MDP
					15.20	13.9	DDW, MDP
					15.20	13.6	DDW, MDP
					15.20	11.2	DDW, MDP
					15.20	12.3	DDW, MDP
					15.20	14.0	DDW, MDP
					15.20	14.4	DDW, MDP
					15.20	12.9	DDW, MDP
					15.20	13.4	DDW, MDP
					15.20	14.8	DDW
15.20	19.7				DDW		
15.20	19.4				DDW		
15.20	18.9				SP		
15.20	17.1				SP		
15.20	14.2				SP		
15.20	27.4				DDW, MDP		
15.20	16.7				DDW, MDP		
15.20	20.3				DDW, MDP		
15.20	16.7				DDW		
15.20	17.6				DDW		
15.20	17.5				DDW		
15.20	24.8				SP		
15.20	20.5				SCC		
15.20	15.3				PSOS		
15.20	30.9				PSOS		
15.20	33.0				PSOS		
15.20	21.8				SCC		
15.20	29.5				SCC		
15.20	19.8				MDP		
15.20	11.9				MDP		
15.20	26.6			MDP			
15.20	14.7			DDW, MDP			
15.20	20.1			DDW			
LRB 48	15.55			25.7	SP		
	15.55			28.2	DDW		
	15.55			11.4	DDW		
	15.55			21.1	PSOS		
	15.55			13.9	PSOS		
	15.55			29.6	MDP, SCC		
	15.55			16.2	MDP, SCC		
	15.55			35.1	SCC		
LRB 50	15.55			18.9	SP		
	16.10			5.9	DDW, MDP		
	16.10			18.3	DDW, MDP		
	16.10			11.1	PSOS		
	16.10			10.9	MDP		
	16.10	13.1	SP				
	16.10	14.4	MDP, SCC				
16.10	11.9	MDP, SCC					
16.10	20.3	MDP, SCC					

<i>L. hisingeri</i>					
Zone	Subzone	Bed N.	Bed height	Geometric shell size	Shell preservation
			16.10	18.9	MS
			16.10	18.0	MDP
			16.10	19.1	DDW
			16.10	24.6	DDW
			16.10	8.0	DDW
			16.10	15.1	SP
			16.10	8.9	DDW
			16.10	21.3	DDW, PSOS
			16.10	18.5	DDW, PSOS
			16.10	11.1	DDW, PSOS
			16.10	30.3	SP
			16.10	14.0	DDW, MDP
			17.50	21.4	DDW, MDP
			17.50	13.6	DDW, MDP
			17.50	12.3	PSOS
			17.50	29.1	MDP
			17.50	13.3	PSOS
			17.50	21.5	DDW, MDP
			17.50	13.8	DDW, MDP
			17.50	17.2	DDW
			17.50	17.9	DDW
			17.50	7.5	DDW
			17.50	25.9	SP
			17.50	19.3	MDP
			17.50	14.8	PSOS
			17.50	29.0	DDW
			17.50	27.4	DDW
			17.50	25.3	SP
			17.50	10.7	SP
			17.50	6.2	SP
			17.50	23.2	MDP
			17.50	13.2	DDW
			17.50	19.2	DDW, MDP
			17.50	14.1	PSOS, MDP
			17.50	20.4	DDW, MDP
			17.50	15.6	SP
			17.50	18.9	DDW, MDP
			17.50	10.5	MDP
			17.50	19.0	DDW
			17.50	21.6	DDW
			17.50	19.8	DDW
			17.50	10.9	DDW
			17.50	4.4	DDW, MDP
			17.50	8.5	DDW, MDP
			17.50	16.2	DDW, MDP
			17.50	15.0	DDW, MDP
			17.50	14.3	DDW, MDP
			17.50	13.0	SCC
			17.50	31.7	PSOS
			17.50	25.8	PSOS
			17.50	34.4	PSOS, MDP
			17.50	40.6	PSOS
			17.50	30.6	SP
			17.50	34.7	SCC
			17.50	38.1	SCC
			17.50	22.2	SP
			17.50	31.7	PSOS
			17.50	26.6	PSOS
			17.75	14.5	PSOS
			17.75	26.0	PSOS
			17.75	21.4	DDW
			17.75	13.3	DDW
			17.75	27.1	SCC, PSOS
			17.75	16.9	DDW, MDP
			17.75	44.4	DDW, MDP
			17.75	17.6	SP
			17.75	21.9	DDW, MDP
			17.75	23.5	DDW, MDP

<i>L. hisingeri</i>					
Zone	Subzone	Bed N.	Bed height	Geometric shell size	Shell preservation
			17.75	18.8	SCC, PSOS
			17.75	10.7	DDW, MDP
			17.75	19.3	PSOS
			17.75	20.6	DDW, MDP
			17.75	24.9	SP
			17.75	43.5	SP
			17.75	27.0	DDW, MDP
			17.75	16.6	MDP
			17.75	20.8	PSOS
			17.75	25.0	SP
			17.75	29.8	DDW, MDP
			17.75	30.2	DDW, MDP
			17.75	24.9	DDW, MDP
			17.75	25.2	DDW, MDP
			17.75	28.3	MDP
			17.75	36.0	PSOS, MDP
			17.75	22.0	PSOS, MDP
			17.75	24.4	PSOS, MDP
			17.75	16.0	SP
			17.75	15.1	MDP
			17.75	32.2	MDP
			17.75	19.0	MDP
			17.75	28.3	DDW
			17.75	29.8	DDW
			18.90	19.4	PSOS, DDW
			18.90	12.7	PSOS, DDW
			18.90	23.5	PSOS, DDW
			18.90	25.6	DDW, MDP
			18.90	19.7	DDW, MDP
			18.90	24.1	PSOS, DDW
			18.90	29.3	PSOS
			18.90	29.0	PSOS
			18.90	19.1	PSOS
			18.90	19.3	SP
			18.90	25.6	MS
			18.90	20.5	MDP, SCC
			18.90	21.6	MDP, SCC
			18.90	19.5	MDP
			18.90	26.7	SP
			18.90	20.7	DDW, MDP
			18.90	27.9	DDW, MDP
			18.90	28.2	PSOS, DDW
			18.90	35.4	DDW, MDP
			18.90	19.5	DDW, MDP
			18.90	29.7	DDW, MDP
		LRB 56	18.90	24.2	DDW, MDP
			18.90	21.4	DDW, MDP
			18.90	26.2	SCC
			18.90	15.6	SCC
			18.90	12.8	SCC, PSOS
			18.90	29.4	SCC, PSOS
			18.90	29.4	MS
			18.90	17.0	MDP, PSOS
			18.90	23.2	MDP, PSOS
			18.90	28.0	MDP
			18.90	29.3	SP
			18.90	34.5	SP
			18.90	21.2	SP
			18.90	20.7	DDW, MDP
			18.90	20.2	DDW, MDP
			18.90	16.0	PSOS
			18.90	20.2	DDW
			18.90	27.7	DDW
			18.90	13.9	DDW
			18.90	20.8	DDW
			18.90	20.0	DDW
			18.90	21.5	MDP
		LRB 60	19.55	17.2	MDP

<i>L. hisingeri</i>						
Zone	Subzone	Bed N.	Bed height	Geometric shell size	Shell preservation	
			19.55	14.9	MDP	
			19.55	13.9	PSOS	
			19.55	24.9	PSOS	
			19.55	24.6	SP, PSOS	
			19.55	13.8	SP, PSOS	
			19.55	24.1	DDW, MDP	
			19.55	29.3	DDW, MDP	
			19.55	27.1	DDW, MDP	
			19.55	33.0	SP, PSOS	
			19.55	26.0	DDW	
			19.55	32.9	DDW, MDP	
			19.55	18.6	DDW, MDP	
			19.55	14.6	DDW	
			19.55	24.9	DDW	
			19.55	19.4	PSOS	
		19.55	14.5	PSOS		
		LRB 62	19.75	32.4	PSOS	
			19.75	31.6	PSOS	
			19.75	20.4	DDW, PSOS	
			19.75	29.0	DDW, PSOS	
LRB 72	21.50	34.4	MDP			
angulata Zone	Schlotheimia angulata subzone	LRB 84	23.90	33.3	MDP	
			23.90	30.3	SP, PSOS	
			23.90	26.1	SP	
			23.90	18.3	PSOS	
		LRB 86	24.11	22.6	SP	
			24.11	26.2	DDW, MDP	
			24.11	23.9	SP	
		LRB 88	24.11	16.8	SP	
			24.25	22.1	DDW, MDP	
			24.25	26.0	MDP	
			24.25	32.6	DDW, MDP	
			24.25	35.0	DDW, MDP	
			24.25	26.5	PSOS	
		LRB 92	24.25	25.9	PSOS	
			24.25	20.8	PSOS	
25.20	19.0		PSOS			
bucklandi Zone	Coroniceras rotiforme subzone		LRB 102	27.64	26.0	DDW, MDP
				27.64	25.6	DDW, MDP
		27.64		23.1	DDW, MDP	
		27.64		22.9	DDW, MDP	
		27.64		22.5	DDW, MDP	
		27.64		25.2	DDW, MDP	
		27.64		27.7	DDW, MDP	
		27.64		21.0	PSOS	
		27.64		13.3	PSOS	
		27.64		24.2	DDW, MDP	
		27.64		25.2	DDW, MDP	
		27.64		25.0	DDW, MDP	
		27.64		27.2	DDW, MDP	
		27.64		22.2	DDW, MDP	
		27.64		24.6	DDW, MDP	
		27.64		19.8	DDW, MDP	
		27.64		26.6	DDW, MDP	
		27.64		26.8	DDW, MDP	
		27.64	24.4	DDW, MDP		
		27.64	23.6	DDW, MDP		
27.64	25.2	DDW, MDP				
27.64	23.0	DDW, MDP				
27.64	25.0	DDW, MDP				
LRB 103	28.30	19.4	SP			

Table A4.2: *P. gigantea* geometric shell size data from every individual per bed in Lyme Regis with the corresponding stratigraphic zones, subzones and bed height. (Presented in Section 3.5.4) (Measured in mm)

<i>P. gigantea</i>						
Zone	Subzone	Bed N.	Bed height	Geometric shell size	Shell preservation	
Pre-planorbis		LRB 4	8.70	33.9	SP	
		LRB 14	9.56	48.4	MDP, PSOS	
		LRB 22	10.50	38.6	MS	
planorbis Zone	Ps. planorbis subzone	LRB 24	10.70	45.0	DDW, MDP	
			10.70	73.5	DDW, MDP	
		LRB 26	10.90	37.9	MS	
			10.90	29.6	DDW, MDP	
		C. johnstoni subzone	LRB 30	12.30	24.8	PSOS
				12.30	49.8	PSOS
	12.30			34.7	PSOS	
	12.30			38.6	SP	
	12.30			42.0	SCC	
	12.30			33.5	MDP, SCC	
	12.30			47.5	MDP	
	12.30			33.5	MDP	
	12.30			26.7	DDW, MDP	
	12.30			40.8	SCC	
	12.30			23.0	PSOS	
	12.30			29.3	DDW	
	12.30			31.0	DDW	
	12.30			21.4	DDW	
	12.30			31.2	MDP	
	12.30			26.8	MDP	
	12.30			28.2	SP	
	12.30			44.0	SP	
	12.30			54.6	PSOS	
	12.30			47.8	SCC	
	12.30			49.1	PSOS	
	12.30			43.9	MDP, PSOS	
	12.30			24.6	MDP, PSOS	
	12.30			35.4	DDW, MDP	
	12.30			20.7	PSOS	
	12.30			27.1	DDW, MDP	
	12.30			38.8	SP	
	12.30			35.5	SP	
	LRB 32			12.60	53.8	MS
	LRB 34			12.75	57.7	DDW, MDP
	LRB 36			13.30	32.6	SP
				13.30	17.7	PSOS
				13.30	30.3	PSOS
				13.30	24.3	SP
		13.30	17.0	DDW		
		13.30	14.7	PSOS		
		13.30	20.6	PSOS		
		13.30	24.1	SCC		
		13.30	28.2	MDP		
		13.30	39.5	PSOS		
		13.30	29.1	DDW		
		13.30	22.8	MS		
		13.30	19.4	SP		
		13.30	21.1	PSOS		
	LRB 40	14.20	33.5	SP		
		14.20	40.5	DDW, MDP		
14.20		40.0	MS			
14.20		39.3	MS			
14.20		42.2	DDW, MDP			
14.20		52.9	DDW, MDP			
14.20		49.4	DDW, MDP			
14.20		48.2	MS			
14.20	54.7	MS				
14.20	45.4	DDW, MDP				
14.20	29.3	DDW, MDP				
liasicus Zone	W. portlocki	LRB 44	14.85	47.8	MS	

<i>P. gigantea</i>					
Zone	Subzone	Bed N.	Bed height	Geometric shell size	Shell preservation
	subzone	LRB 46	15.20	62.3	SP
			15.20	30.8	SP, PSOS
			15.20	28.5	PSOS
			15.20	60.5	PSOS
			15.20	39.7	PSOS
			15.20	42.7	MDP
			15.20	58.6	SCC
		LRB 48	15.20	77.7	DDW, MDP
			15.55	70.1	DDW, MDP
			15.55	46.0	MS
			15.55	67.4	MS, MDP
			15.55	80.4	SP
			15.55	33.1	PSOS
			15.55	37.6	PSOS
			15.55	53.4	MDP
			15.55	56.7	MDP
			15.55	20.7	MS
			15.55	38.3	DDW
			15.55	44.3	DDW
			15.55	37.0	PSOS
			15.55	52.7	SP
			15.55	13.7	SP, PSOS
			15.55	11.6	DDW, MDP
			15.55	32.1	DDW, MDP
			15.55	27.4	DDW, MDP
			15.55	42.4	DDW, MDP
			15.55	31.4	DDW, MDP
			15.55	41.6	SP, PSOS
			15.55	49.2	SP, PSOS
			15.55	42.6	SP, PSOS
			15.55	35.3	SP, PSOS
			15.55	51.4	SP, PSOS
			15.55	49.4	SP, PSOS
			15.55	6.8	PSOS
			15.55	40.5	SP
			15.55	44.3	PSOS
			15.55	37.1	SCC, PSOS
			15.55	38.4	SCC, PSOS
			15.55	57.8	SCC
			15.55	54.8	SCC, MDP
			15.55	21.6	SCC, MDP
		15.55	43.4	DDW, MDP	
		15.55	18.0	DDW, MDP	
		15.55	56.6	DDW, MDP	
		15.55	39.8	PSOS	
		15.55	34.0	PSOS	
		15.55	33.6	MS	
		15.55	59.5	SP	
		15.55	38.5	SP, PSOS	
		15.55	68.4	MDP	
		15.55	43.1	SCC, PSOS	
15.55	31.9	DDW			
15.55	42.6	DDW			
15.55	68.7	MDP			
15.55	53.3	SCC, PSOS			
LRB 50	16.10	65.6	PSOS		
	16.10	30.2	PSOS		
	16.10	54.4	PSOS		
	16.10	66.6	PSOS		
	16.10	23.8	MDP		
	16.10	42.9	MDP		
	16.10	42.0	MDP		
	16.10	25.4	MDP		
	16.10	26.7	MDP		
	16.10	28.5	MDP		
16.10	48.9	MDP			
16.10	60.1	DDW, MDP			
16.10	63.7	DDW, MDP			

<i>P. gigantea</i>					
Zone	Subzone	Bed N.	Bed height	Geometric shell size	Shell preservation
			16.10	57.0	DDW, MDP
			16.10	74.4	DDW, MDP
			16.10	44.5	DDW, MDP
			16.10	52.6	DDW, MDP
			16.10	53.8	SCC
			16.10	64.0	SCC
			17.50	37.4	SCC
			17.50	30.8	PSOS
			17.50	49.8	PSOS
			17.50	28.6	PSOS
			17.50	41.4	PSOS
			17.50	54.4	SP, PSOS
			17.50	44.9	SP, PSOS
			17.50	30.6	SP, PSOS
			17.50	29.6	SP, PSOS
			17.50	29.9	SP, PSOS
			17.50	48.0	DDW
			17.50	49.7	DDW
			17.50	33.6	DDW
			17.50	55.5	MDP
			17.50	14.2	MDP
			17.50	50.2	MDP
			17.50	45.6	SP
			17.50	40.9	SP
			17.50	66.0	SP
			17.50	60.0	SP
			17.50	43.8	SCC
			17.50	59.1	MS
			17.50	45.4	SP
			17.50	21.3	SP
			17.50	62.9	SP
			17.50	65.5	SP, PSOS
			17.50	37.1	SP, PSOS
			17.50	40.0	SCC
			17.50	54.5	MDP
			17.50	42.3	MDP
			17.50	64.1	SP
			17.50	37.9	MDP
			17.50	57.7	MDP
			17.50	45.7	MDP, PSOS
			17.75	33.8	MDP, PSOS
			17.75	50.8	DDW
			17.75	68.6	PSOS
			17.75	24.6	PSOS
			17.75	89.3	SCC
			17.75	33.0	SP
			17.75	73.7	PSOS
			17.75	80.5	MDP, PSOS
			17.75	83.4	MDP, PSOS
			17.75	82.9	MDP, PSOS
			17.75	73.4	PSOS
			17.75	69.4	MDP
			17.75	89.7	SP
			17.75	81.3	MS, PSOS
			17.75	60.4	SP
			17.75	84.6	SP
			17.75	66.2	SP, PSOS
			17.75	67.0	SP, PSOS
			17.75	57.9	PSOS
			18.90	94.3	PSOS
			18.90	79.8	MDP
			19.55	57.1	MDP
			21.50	76.4	SCC
			21.50	95.7	MDP
			21.50	87.1	DDW, MDP
			21.50	114.5	DDW
angulata Zone	Schlotheimia angulata subzone	LRB 76	22.00	106.2	PSOS
		LRB 84	23.90	71.9	SP

<i>P. gigantea</i>					
Zone	Subzone	Bed N.	Bed height	Geometric shell size	Shell preservation
			23.90	138.6	SP
		LRB 86	24.11	83.8	DDW
		LRB 88	24.25	62.8	DDW, MDP
			24.25	157.6	DDW, MDP
			24.25	163.5	DDW, MDP
			24.25	131.0	DDW
			24.25	155.9	DDW, MDP
			24.25	136.2	DDW
			24.25	95.0	DDW
			24.25	116.8	DDW
			24.25	156.1	DDW
			24.25	50.4	MS
		LRB 90	24.55	149.3	DDW, MDP
			24.55	62.8	SP
		bucklandi Zone	Metophioceras conybeari subzone	LRB 94	25.55
25.55	51.4				DDW, MDP
25.55	151.4				DDW, PSOS
25.55	124.1				OMI, CSM
25.55	160.2				SP
LRB 96	26.00			129.7	SCC

Table A4.3 A-E: *O. aspinata* geometric shell size data from every individual per bed in Lyme Regis with the corresponding stratigraphic zones, subzones and bed height. (Presented in Section 3.5.5) (Measured in μm)

(A)						<i>O. aspinata</i>					
Zone	Subzone	Bed N.	Bed height	Geometric shell size	Shell preservation	Zone	Subzone	Bed N.	Bed height	Geometric shell size	Shell preservation
Pre-planorbis		B7	8.8	394.7	LV, SP	planorbis Zone	johnstoni subzone	B33	12.85	276.3	LV, SP
			8.8	372.9	RV, SP				12.85	400.5	RV, SP
		B15	9.6	438.8	LV, SP				12.85	396.0	RV, SP
			9.6	455.0	RV, SP				12.85	390.1	RV, SP
			9.6	342.7	RV, SP				12.85	407.4	RV, SP
			9.6	315.8	LV, SP				12.85	377.3	LV, SP
			9.6	310.8	LV, SP				12.85	445.4	LV, SP
			9.6	310.8	LV, SP				12.85	455.4	LV, SP
		B17	9.72	379.6	LV, SP				12.85	472.6	RV, SP
			9.72	447.9	LV, SP				12.85	472.6	RV, SP
			9.72	421.9	LV, SP				12.85	407.5	LV, SP
			9.72	470.6	LV, SP				12.85	389.0	LV, SP
			9.72	473.6	LV, SP				12.85	396.9	RV, SP
			9.72	456.1	LV, SP				12.85	373.4	LV, SP
			9.72	380.1	RV, SP				12.85	355.7	RV, SP
			9.72	334.9	LV, SP				12.85	313.6	RV, SP
			9.72	395.5	RV, SP				12.85	308.9	RV, SP
			9.72	367.7	LV, SP				12.85	359.9	RV, SP
			9.72	379.1	RV, SP				12.85	420.6	RV, SP
			9.72	362.3	SB				12.85	370.5	RV, SP
			9.72	383.6	RV, SP				12.85	364.7	LV, SP
			9.72	240.0	SB				12.85	315.4	RV, SP
		B21	9.72	411.3	RV, SP				12.85	403.1	LV, SP
			10.3	400.2	LV, SP				12.85	313.5	RV, SP
			10.3	371.4	RV, SP				12.85	354.6	RV, SP
			10.3	408.6	LV, SP				12.85	318.1	LV, SP
			10.3	397.3	RV, SP				12.85	375.6	LV, SP
			10.3	456.5	LV, SP				12.85	383.8	LV, SP
			10.3	466.4	LV, SP				12.85	383.0	LV, SP
			10.3	481.7	RV, SP				12.85	349.9	LV, SP
			10.3	430.5	LV, SP				12.85	222.8	RV, SP
			10.3	392.3	RV, SP				12.85	245.5	RV, SP
			10.3	455.1	LV, SP				12.85	402.5	LV, SP
			10.3	458.6	LV, SP				12.85	425.3	LV, SP
			10.3	428.5	RV, SP				12.85	411.4	LV, SP
			10.3	429.0	LV, SP				12.85	365.7	RV, SP

(A)						<i>O. aspinata</i>					
Zone	Subzone	Bed N.	Bed height	Geometric shell size	Shell preservation	Zone	Subzone	Bed N.	Bed height	Geometric shell size	Shell preservation
			10.3	403.4	RV, SP				12.85	455.9	RV, SP
			10.3	374.1	RV, SP				12.85	386.0	RV, SP
			10.3	444.5	LV, SP				12.85	369.4	RV, SP
			10.3	428.5	LV, SP				12.85	390.6	LV, SP
			10.3	431.4	RV, SP				12.85	443.6	LV, SP
			10.3	417.8	RV, SP				12.85	445.3	LV, SP
			10.3	433.8	RV, SP				12.85	460.0	RV, SP
			10.3	416.3	RV, SP				12.85	450.4	RV, SP
			10.3	431.2	RV, SP				12.85	378.4	LV, SP
			10.3	398.2	RV, SP				12.85	404.6	RV, SP
			10.3	401.6	RV, SP				12.85	413.0	LV, SP
			10.3	417.4	LV, SP				12.85	464.6	RV, SP
			10.3	431.8	RV, SP				12.85	404.4	LV, SP
			10.3	378.7	LV, SP				12.85	455.8	RV, SP
			10.3	385.6	RV, SP				12.85	472.0	RV, SP
			10.3	376.4	RV, SP				12.85	393.4	RV, SP
			10.3	376.1	RV, SP				12.85	449.6	LV, SP
			10.3	364.2	RV, SP				12.85	453.3	LV, SP
			10.3	371.7	LV, SP				12.85	471.8	LV, SP
			10.3	370.3	RV, SP				12.85	403.4	LV, SP
			10.3	369.9	RV, SP				12.85	387.1	RV, SP
			10.3	399.2	RV, SP				12.85	420.5	LV, SP
			10.3	379.1	RV, SP				12.85	409.2	RV, SP
			10.3	313.5	RV, SP				12.85	461.4	RV, SP
			10.3	327.4	RV, SP				12.85	391.9	LV, SP
			10.3	308.3	LV, SP				12.85	380.8	RV, SP
			10.3	393.9	LV, SP				12.85	392.9	RV, SP
			10.3	370.5	RV, SP				12.85	396.3	LV, SP
			10.3	365.4	RV, SP				12.85	397.9	RV, SP
			10.3	315.7	RV, SP				12.85	405.9	LV, SP
			10.3	335.4	LV, SP				12.85	392.6	RV, SP
			10.3	373.8	LV, SP				12.85	388.4	LV, SP
			10.3	402.0	RV, SP				12.85	479.2	RV, SP
			10.3	328.9	RV, SP				12.85	415.3	LV, SP
			10.3	388.5	RV, SP				12.85	399.8	RV, SP
			10.3	354.8	RV, SP				12.85	419.1	RV, SP
			10.3	325.1	RV, SP				12.85	395.0	RV, SP
			10.3	357.0	RV, SP				12.85	430.1	LV, SP
			10.3	384.8	RV, SP				12.85	448.7	RV, SP

(A)						<i>O. aspinata</i>					
Zone	Subzone	Bed N.	Bed height	Geometric shell size	Shell preservation	Zone	Subzone	Bed N.	Bed height	Geometric shell size	Shell preservation
			10.6	393.3	RV, SP				13.37	413.4	LV, SP
			10.6	360.7	RV, SP				13.37	387.0	LV, SP
			10.6	365.0	RV, SP				13.37	523.7	LV, SP
			10.6	369.2	LV, SP				13.37	452.1	LV, SP
			10.6	327.5	RV, SP				13.37	378.8	LV, SP
			10.6	373.7	RV, SP				13.37	323.5	RV, SP
			10.6	345.8	LV, SP				13.37	347.9	LV, SP
			10.6	308.6	RV, SP				13.37	346.7	RV, SP
			10.6	327.0	RV, SP				13.37	383.5	LV, SP
			10.6	353.8	RV, SP				13.37	374.9	RV, SP
			10.6	369.0	RV, SP				13.37	322.4	RV, SP
			10.6	306.7	LV, SP				13.37	454.2	RV, SP
			10.6	358.2	RV, SP				13.37	334.0	RV, SP
			10.6	312.2	RV, SP				13.37	295.6	RV, SP
			10.6	373.4	RV, SP				13.37	384.4	LV, SP
			10.6	349.2	RV, SP				13.37	390.4	LV, SP
			10.6	243.3	RV, SP				13.37	271.3	LV, SP
			10.6	357.8	RV, SP				13.37	263.0	RV, SP
			10.6	356.5	RV, SP				13.37	347.7	LV, SP
			10.6	234.6	RV, SP				13.37	399.8	RV, SP
			10.7	279.6	RV, SP				13.37	324.3	RV, SP
			10.7	384.5	RV, SP				13.37	390.0	LV, SP
			10.7	425.7	RV, SP				13.37	333.0	LV, SP
			10.7	395.4	RV, SP				13.37	301.7	LV, SP
			10.7	386.2	RV, SP				13.37	351.8	LV, SP
			10.7	302.4	LV, SP				13.37	307.9	RV, SP
			10.7	387.9	RV, SP				13.37	404.0	LV, SP
			10.7	383.6	LV, SP				13.37	309.2	LV, SP
			10.7	393.9	LV, SP				13.37	373.5	RV, SP
			10.7	376.5	LV, SP				13.37	359.5	RV, SP
			10.7	375.1	LV, SP				13.37	402.3	LV, SP
			10.7	291.6	LV, SP				13.37	222.7	RV, SP
			10.7	355.2	LV, SP				13.37	355.0	LV, SP
			10.7	311.9	LV, SP				13.37	319.6	RV, SP
			10.7	344.3	LV, SP				13.37	361.3	RV, SP
			10.7	345.1	RV, SP				13.37	350.7	RV, SP
			10.7	347.9	LV, SP				13.37	364.3	RV, SP
			10.7	449.9	LV, SP				13.37	412.9	RV, SP
			10.7	340.2	RV, SP				13.37	324.2	LV, SP

(A)						<i>O. aspinata</i>					
Zone	Subzone	Bed N.	Bed height	Geometric shell size	Shell preservation	Zone	Subzone	Bed N.	Bed height	Geometric shell size	Shell preservation
			10.7	283.8	LV, SP				13.37	369.9	SB
			10.7	307.4	LV, SP				13.37	417.3	LV, SP
			10.7	306.8	LV, SP				13.37	372.2	RV, SP
			10.7	253.2	LV, SP				13.37	353.8	RV, SP
			10.7	408.6	LV, SP				13.37	379.1	LV, SP
			10.7	398.3	LV, SP				13.37	342.2	LV, SP
			10.7	426.8	RV, SP				13.37	449.0	LV, SP
			10.7	398.6	RV, SP				13.37	309.2	RV, SP
			10.7	418.5	LV, SP				13.37	466.6	RV, SP
			10.7	365.9	RV, SP				13.37	390.5	LV, SP
			10.7	425.3	RV, SP				13.37	365.2	RV, SP
			10.7	317.4	LV, SP				13.37	390.3	LV, SP
			10.7	371.2	LV, SP				13.37	410.0	LV, SP
			10.7	419.4	LV, SP				13.37	318.5	LV, SP
			10.7	434.0	LV, SP				13.37	378.5	RV, SP
			10.7	396.1	LV, SP				13.37	377.0	RV, SP
			10.7	387.1	RV, SP				13.37	382.3	RV, SP
			10.7	398.8	LV, SP				13.37	268.8	RV, SP
			10.7	391.3	RV, SP				13.37	358.8	LV, SP
			10.7	390.2	LV, SP				13.37	374.7	RV, SP
			10.7	371.6	RV, SP				13.37	369.4	RV, SP
			10.7	385.1	RV, SP				13.37	322.4	LV, SP
			10.7	370.1	LV, SP				13.37	354.0	LV, SP
			10.7	379.6	RV, SP				13.37	377.6	RV, SP
			10.7	359.1	RV, SP				13.37	300.3	RV, SP
			10.7	364.8	LV, SP				13.37	350.7	LV, SP
			10.7	428.3	RV, SP				13.37	340.3	LV, SP
			10.7	351.1	RV, SP				13.37	363.7	LV, SP
			10.7	431.9	RV, SP				13.37	314.0	RV, SP
			10.7	393.6	LV, SP				13.37	329.9	RV, SP
			10.7	432.7	RV, SP				13.37	313.8	RV, SP
			10.7	385.6	RV, SP				13.37	240.1	RV, SP
			10.7	338.7	LV, SP				13.37	268.4	LV, SP
			10.7	370.9	LV, SP				13.37	369.1	RV, SP
			10.7	348.0	RV, SP				13.37	219.0	RV, SP
			10.7	382.4	LV, SP				13.37	236.3	RV, SP
			10.7	351.5	RV, SP				13.37	222.1	RV, SP
			10.7	334.2	RV, SP				13.37	205.3	RV, SP
			10.7	326.4	RV, SP				13.37	224.2	RV, SP

(A)						<i>O. aspinata</i>					
Zone	Subzone	Bed N.	Bed height	Geometric shell size	Shell preservation	Zone	Subzone	Bed N.	Bed height	Geometric shell size	Shell preservation
			10.7	334.7	RV, SP				13.37	160.7	RV, SP
			10.7	355.9	LV, SP				13.37	244.8	RV, SP
			10.7	349.9	LV, SP				13.37	217.1	RV, SP
			10.7	317.3	RV, SP				13.37	399.7	LV, SP
			10.7	339.1	LV, SP				13.37	239.9	RV, SP
			10.7	345.2	RV, SP				13.37	191.3	RV, SP
			10.7	331.9	RV, SP				13.37	236.6	LV, SP
			10.7	331.9	RV, SP				13.37	227.6	RV, SP
			10.7	357.3	LV, SP				13.37	384.1	RV, SP
			10.7	303.7	RV, SP				13.37	409.6	RV, SP
			10.7	344.3	LV, SP				13.37	407.4	LV, SP
			10.7	345.0	LV, SP				13.37	443.3	RV, SP
			10.7	312.5	RV, SP				13.37	444.0	LV, SP
			10.7	294.5	RV, SP				13.37	386.5	RV, SP
			10.7	308.0	RV, SP				13.37	407.2	RV, SP
			10.7	326.8	LV, SP				13.37	402.4	RV, SP
			10.7	307.1	RV, SP				13.37	421.8	RV, SP
			10.7	311.9	RV, SP				13.37	387.0	RV, SP
			10.7	297.7	LV, SP				13.37	450.2	LV, SP
			10.7	271.6	RV, SP				13.37	398.0	RV, SP
			10.7	357.2	LV, SP				13.37	455.2	RV, SP
			10.7	258.9	LV, SP				13.37	465.2	LV, SP
			10.7	358.9	LV, SP				13.37	392.5	RV, SP
			10.7	299.4	RV, SP				13.37	411.1	RV, SP
			10.7	312.3	LV, SP				13.37	361.5	RV, SP
			10.7	363.4	RV, SP				13.37	376.5	RV, SP
			10.7	355.3	LV, SP				13.37	378.0	LV, SP
			10.7	354.9	LV, SP				13.37	374.4	RV, SP
			10.7	302.5	RV, SP				13.37	425.4	RV, SP
			10.7	359.0	RV, SP				13.37	400.5	RV, SP
			10.7	318.6	RV, SP				13.37	426.8	LV, SP
			10.7	355.8	RV, SP				13.37	368.3	RV, SP
			10.7	384.8	LV, SP				13.37	420.3	RV, SP
			11.3	317.1	LV, SP				13.37	400.8	LV, SP
			11.3	350.8	RV, SP				13.37	355.7	LV, SP
		B27	11.3	394.1	LV, SP				13.37	421.6	LV, SP
			11.3	287.4	LV, SP				13.37	419.5	RV, SP
			11.3	397.5	LV, SP				13.37	314.5	RV, SP
			11.3	446.7	LV, SP				13.37	386.3	LV, SP

(A)						<i>O. aspinata</i>					
Zone	Subzone	Bed N.	Bed height	Geometric shell size	Shell preservation	Zone	Subzone	Bed N.	Bed height	Geometric shell size	Shell preservation
			11.3	348.3	LV, SP				13.37	452.0	RV, SP
			11.3	434.1	RV, SP				13.37	390.4	LV, SP
			11.3	408.5	LV, SP				13.37	454.2	RV, SP
			11.3	415.9	LV, SP				13.37	432.2	LV, SP
			11.3	369.2	LV, SP				13.37	388.6	LV, SP
			11.3	463.5	LV, SP				13.37	448.7	RV, SP
			11.3	384.2	LV, SP				13.37	415.4	RV, SP
			11.3	283.8	RV, SP				13.37	447.6	RV, SP
			11.3	290.9	LV, SP				13.37	408.7	LV, SP
			11.3	448.8	LV, SP				13.37	379.2	LV, SP
			11.3	448.0	LV, SP				13.37	393.0	RV, SP
			11.3	437.9	LV, SP				13.37	389.4	RV, SP
			11.3	476.2	LV, SP				13.37	403.1	RV, SP
			11.3	452.6	RV, SP				13.37	424.1	RV, SP
			11.3	397.7	LV, SP				13.37	385.8	LV, SP
			11.3	368.4	LV, SP				13.37	406.8	LV, SP
			11.3	442.5	LV, SP				13.37	432.5	RV, SP
			11.3	435.4	RV, SP				13.37	429.6	LV, SP
			11.3	380.7	RV, SP				13.37	401.6	LV, SP
			11.3	367.3	RV, SP				13.37	409.3	RV, SP
			11.3	322.4	RV, SP				13.37	447.2	LV, SP
			11.3	356.1	LV, SP				13.37	429.5	RV, SP
			11.3	318.3	RV, SP				13.37	396.2	RV, SP
			11.3	328.8	LV, SP				13.37	390.5	RV, SP
			11.3	315.3	LV, SP				13.37	452.6	LV, SP
									13.37	414.2	RV, SP
									13.37	405.9	RV, SP
									13.37	414.4	LV, SP
									13.37	462.4	LV, SP
									13.37	372.8	RV, SP
									13.37	261.5	RV, SP

(B)																	
<i>O. aspinata</i>																	
Zone	Subzone	Bed N.	Bed H.	Geometric shell size	Shell pres.	Zone	Subzone	Bed N.	Bed H.	Geometric shell size	Shell pres.	Zone	Subzone	Bed N.	Bed H.	Geometric shell size	Shell pres.
planorbis Zone	C. johnstoni subzone	B39	13.7	399.7	LV, SP	liasicus Zone	W. portlocki subzone	B47	15.3	468.0	LV, SP	liasicus Zone	W. portlocki subzone	B49	15.8	431.1	LV, SP
			13.7	459.5	LV, SP				15.3	383.9	RV, SP				15.8	461.2	RV, SP
			13.7	449.8	LV, SP				15.3	410.7	RV, SP				15.8	476.2	RV, SP

(B)						<i>O. aspinata</i>											
Zone	Subzone	Bed N.	Bed H.	Geometric shell size	Shell pres.	Zone	Subzone	Bed N.	Bed H.	Geometric shell size	Shell pres.	Zone	Subzone	Bed N.	Bed H.	Geometric shell size	Shell pres.
			13.7	437.9	RV, SP				15.3	434.3	LV, SP				15.8	391.7	RV, SP
			13.7	401.6	LV, SP				15.3	444.8	LV, SP				15.8	448.4	LV, SP
			13.7	480.1	LV, SP				15.3	478.8	LV, SP				15.8	433.7	RV, SP
			13.7	433.8	LV, SP				15.3	478.1	LV, SP				15.8	452.1	RV, SP
			13.7	437.3	RV, SP				15.3	397.3	LV, SP				15.8	413.7	LV, SP
			13.7	443.4	RV, SP				15.3	428.1	RV, SP				15.8	451.7	LV, SP
			13.7	421.5	RV, SP				15.3	398.3	LV, SP				15.8	477.3	RV, SP
			13.7	428.6	LV, SP				15.3	446.6	RV, SP				15.8	364.4	RV, SP
			13.7	451.3	RV, SP				15.3	392.8	LV, SP				15.8	389.4	RV, SP
			13.7	470.4	RV, SP				15.3	415.3	LV, SP				15.8	298.6	RV, SP
			13.7	435.8	SB				15.3	479.6	SB				15.8	379.5	RV, SP
			13.7	390.6	RV, SP				15.3	393.6	RV, SP				15.8	337.2	RV, SP
			13.7	382.4	LV, SP				15.3	448.7	RV, SP				15.8	427.1	LV, SP
			13.7	407.9	LV, SP				15.3	411.1	SB				15.8	365.4	RV, SP
			13.7	391.4	LV, SP				15.3	463.9	LV, SP				15.8	417.7	RV, SP
			13.7	437.1	LV, SP				15.3	387.6	SB				15.8	370.3	RV, SP
			13.7	423.4	RV, SP				15.3	455.0	RV, SP				15.8	328.5	RV, SP
			13.7	394.6	LV, SP				15.3	412.7	LV, SP				15.8	397.6	LV, SP
			13.7	417.7	LV, SP				15.3	399.9	LV, SP				15.8	319.3	RV, SP
			13.7	436.4	LV, SP				15.3	455.1	LV, SP				15.8	364.4	RV, SP
			13.7	394.9	RV, SP				15.3	423.2	RV, SP				15.8	395.5	RV, SP
			13.7	453.2	RV, SP				15.3	462.6	LV, SP				15.8	348.6	LV, SP
			13.7	395.0	LV, SP				15.3	483.0	RV, SP				15.8	408.4	LV, SP
			13.7	352.9	LV, SP				15.3	412.9	RV, SP				15.8	383.6	RV, SP
			13.7	376.2	RV, SP				15.3	473.0	RV, SP				15.8	326.8	RV, SP
			13.7	370.0	RV, SP				15.3	402.9	LV, SP				15.8	373.2	RV, SB
			13.7	345.7	RV, SP				15.3	455.8	LV, SP				15.8	385.3	LV, SP
			13.7	311.3	LV, SP				15.3	465.7	RV, SP				15.8	365.9	RV, SP
			13.7	323.7	LV, SP				15.3	426.3	LV, SP				15.8	395.7	RV, SP
			13.7	284.2	RV, SP				15.3	469.6	LV, SP				15.8	463.7	RV, SP
			13.7	385.6	RV, SP				15.3	426.6	RV, SP				15.8	412.5	RV, SP
			13.7	373.8	RV, SP				15.3	411.7	RV, SP				15.8	374.2	RV, SP
			13.7	410.2	LV, SP				15.3	431.0	RV, SP				15.8	309.5	RV, SP
			13.7	380.4	RV, SP				15.3	416.1	LV, SP				15.8	306.0	LV, SP
			13.7	294.9	LV, SP				15.3	440.3	SB				15.8	360.3	LV, SP
			13.7	350.4	RV, SP				15.3	447.5	RV, SP				15.8	400.1	RV, SP
			13.7	362.5	RV, SP				15.3	439.8	SB				15.8	307.2	RV, SP
			13.7	400.8	LV, SP				15.3	475.2	LV, SP				15.8	404.8	RV, SP
			13.7	386.0	LV, SP				15.3	428.5	RV, SP				15.8	407.4	RV, SP

(B)						<i>O. aspinata</i>											
Zone	Subzone	Bed N.	Bed H.	Geometric shell size	Shell pres.	Zone	Subzone	Bed N.	Bed H.	Geometric shell size	Shell pres.	Zone	Subzone	Bed N.	Bed H.	Geometric shell size	Shell pres.
			13.7	428.0	LV, SP				15.3	471.2	LV, SP				15.8	398.3	LV, SP
			13.7	363.0	RV, SP				15.3	412.3	LV, SP				15.8	319.7	RV, SP
			13.7	404.5	LV, SP				15.3	382.2	RV, SP				15.8	406.9	LV, SP
			13.7	368.4	LV, SP				15.3	387.1	SB				15.8	394.8	LV, SP
			13.7	326.3	LV, SP				15.3	385.7	RV, SP				15.8	335.8	RV, SP
			13.7	213.8	LV, SP				15.3	411.4	LV, SP				15.8	397.8	RV, SP
			13.7	368.5	RV, SP				15.3	469.9	RV, SP				15.8	372.5	RV, SP
			13.7	389.1	LV, SP				15.3	404.5	SB				15.8	366.3	LV, SP
			13.7	370.2	LV, SP				15.3	443.2	LV, SP				15.8	410.4	LV, SP
			13.7	360.0	RV, SP				15.3	404.7	LV, SP				15.8	386.0	RV, SP
			13.7	358.6	LV, SP				15.3	422.6	LV, SP				15.8	278.0	RV, SP
			13.7	406.2	RV, SP				15.3	379.5	LV, SP				15.8	393.4	RV, SP
			13.7	401.8	LV, SP				15.3	393.4	LV, SP				15.8	312.8	RV, SP
			13.7	362.4	LV, SP				15.3	396.8	RV, SP				15.8	399.2	LV, SP
			13.7	390.4	LV, SP				15.3	409.8	LV, SP				15.8	335.7	RV, SP
			13.7	395.2	RV, SP				15.3	427.7	RV, SP				15.8	381.4	LV, SP
			13.7	369.8	LV, SP				15.3	448.0	LV, SP				15.8	342.4	RV, SP
			13.7	364.3	LV, SP				15.3	316.6	RV, SP				15.8	409.4	LV, SP
			13.7	357.7	LV, SP				15.3	321.6	RV.2				15.8	401.1	RV, SP
			13.7	350.5	RV, SP				15.3	448.7	RV, SP				15.8	357.0	RV, SP
			13.7	391.4	LV, SP				15.3	385.0	LV, SP				15.8	376.1	RV, SP
			13.7	411.3	RV, SP				15.3	375.7	RV, SP				15.8	305.1	RV, SP
			13.7	360.6	RV, SP				15.3	405.9	LV, SP				15.8	313.0	LV, SP
			13.7	386.4	RV, SP				15.3	318.3	RV, SP				15.8	408.9	LV, SP
			13.7	320.9	LV, SP				15.3	324.0	SB				15.8	271.7	RV, SP
			13.7	342.4	RV, SP				15.3	382.9	LV, SP				15.8	295.3	RV, SP
			13.7	374.0	RV, SP				15.3	412.4	RV, SP				15.8	417.9	RV, SP
			13.7	373.3	LV, SP				15.3	321.2	RV, SP				15.8	269.8	RV, SP
			13.7	339.4	RV, SP				15.3	299.0	LV, SP				15.8	265.3	RV, SP
			13.7	387.2	LV, SP				15.3	369.5	RV, SP				15.8	271.6	RV, SP
			13.7	386.0	LV, SP				15.3	412.0	LV, SP				15.8	222.5	RV, SP
			13.7	375.1	RV, SP				15.3	337.1	LV, SP				15.8	230.6	RV, SP
			13.7	360.3	LV, SP				15.3	385.9	LV, SP				15.8	237.9	RV, SP
			13.7	373.2	LV, SP				15.3	314.9	LV, SP				15.8	247.0	LV, SP
			13.7	277.6	LV, SP				15.3	415.3	LV, SP				15.8	474.5	SB
			13.7	361.0	RV, SP				15.3	406.7	LV, SP				15.8	248.4	RV, SP
			13.7	356.8	RV, SP				15.3	275.1	LV, SP				15.8	272.7	RV, SP
			13.7	308.1	RV, SP				15.3	370.9	RV, SP				15.8	172.0	RV, SP
			13.7	368.5	LV, SP				15.3	333.8	LV, SP				15.8	171.5	LV, SP

(B)						<i>O. aspinata</i>											
Zone	Subzone	Bed N.	Bed H.	Geometric shell size	Shell pres.	Zone	Subzone	Bed N.	Bed H.	Geometric shell size	Shell pres.	Zone	Subzone	Bed N.	Bed H.	Geometric shell size	Shell pres.
			13.7	383.6	RV, SP				15.3	412.8	LV, SP				15.8	394.3	RV, SP
			13.7	388.5	RV, SP				15.3	333.9	LV, SP				15.8	408.2	RV, SP
			13.7	381.1	LV, SP				15.3	405.2	LV, SP				15.8	363.9	RV, SP
			13.7	328.2	RV, SP				15.3	341.6	LV, SP				15.8	438.1	LV, SP
			13.7	275.2	RV, SP				15.3	331.0	LV, SP				15.8	404.3	RV, SP
			13.7	356.5	LV, SP				15.3	393.7	LV, SP				15.8	399.2	RV, SP
			13.7	367.8	LV, SP				15.3	379.2	RV, SP				15.8	448.7	RV, SP
			13.7	362.8	LV, SP				15.3	409.9	LV, SP				15.8	462.8	SB
			13.7	335.6	LV, SP				15.3	340.6	SB				15.8	413.9	LV, SP
			13.7	404.4	RV, SP				15.3	304.7	RV, SP				15.8	440.3	RV, SP
			13.7	357.0	RV, SP				15.3	327.6	LV, SP				15.8	439.0	RV, SP
			13.7	389.0	RV, SP				15.3	287.4	LV, SP				15.8	397.8	RV, SP
			13.7	366.4	LV, SP				15.3	310.3	RV, SP				15.8	454.8	RV, SP
			13.7	374.9	LV, SP				15.3	368.4	LV, SP				15.8	406.1	RV, SP
			13.7	359.2	LV, SP				15.3	337.5	LV, SP				15.8	342.8	RV, SP
			13.7	367.2	RV, SP				15.3	449.3	RV, SP				15.8	407.0	RV, SP
			13.7	370.0	LV, SP				15.3	324.7	LV, SP				15.8	353.7	RV, SP
			13.7	323.9	SB				15.3	321.2	RV, SP				15.8	359.4	RV, SP
			13.7	378.4	LV, SP				15.3	287.5	LV, SP				15.8	470.5	RV, SP
			13.7	398.0	RV, SP				15.3	413.4	LV, SP				15.8	443.3	RV, SP
			13.7	372.1	LV, SP				15.3	320.2	RV, SP				15.8	401.9	RV, SP
			13.7	438.1	RV, SP				15.3	403.0	LV, SP				15.8	462.2	RV, SP
			13.7	309.5	RV, SP				15.3	406.0	RV, SP				15.8	459.0	RV, SP
			13.7	406.6	LV, SP				15.3	418.7	RV, SP				15.8	333.4	LV, SP
			13.7	348.6	LV, SP				15.3	403.0	LV, SP				15.8	464.2	RV, SP
			13.7	372.4	LV, SP				15.3	356.8	LV, SP				15.8	410.2	RV, SP
			13.7	346.6	LV, SP				15.3	377.9	LV, SP				15.8	425.9	LV, SP
			13.7	356.6	LV, SP				15.3	326.7	RV, SP				15.8	449.9	RV, SP
			13.7	307.4	LV, SP				15.3	396.0	RV, SP				15.8	389.3	LV, SP
			13.7	443.5	LV, SP				15.3	392.1	LV, SP				15.8	391.2	RV, SP
			13.7	378.3	RV, SP				15.3	324.0	RV, SP				15.8	341.2	RV, SP
			13.7	364.3	RV, SP				15.3	410.1	LV, SP				15.8	420.3	RV, SP
			13.7	393.7	LV, SP				15.3	301.0	LV, SP				15.8	428.1	RV, SP
			13.7	431.5	RV, SP				15.3	379.6	LV, SP				15.8	451.3	RV, SP
			13.7	433.6	RV, SP				15.3	381.6	RV, SP				15.8	376.9	LV, SP
			13.7	428.4	LV, SP				15.3	279.3	LV, SP				15.8	282.0	RV, SP
			13.7	424.3	LV, SP				15.3	290.3	LV, SP				15.8	448.7	RV, SP
			13.7	422.1	LV, SP				15.3	393.8	LV, SP				15.8	402.3	RV, SP
			13.7	390.5	RV, SP				15.3	462.2	LV, SP				15.8	437.0	RV, SP

(B)						<i>O. aspinata</i>											
Zone	Subzone	Bed N.	Bed H.	Geometric shell size	Shell pres.	Zone	Subzone	Bed N.	Bed H.	Geometric shell size	Shell pres.	Zone	Subzone	Bed N.	Bed H.	Geometric shell size	Shell pres.
			13.7	416.6	RV, SP				15.3	377.8	LV, SP				15.8	421.9	RV, SP
			13.7	434.7	RV, SP				15.3	398.4	LV, SP				15.8	514.4	RV, SP
			13.7	427.6	RV, SP				15.3	400.9	LV, SP				15.8	377.9	RV, SP
			13.7	386.0	RV, SP				15.3	382.5	LV, SP				15.8	468.1	RV, SP
			13.7	325.8	RV, SP				15.3	328.1	RV, SP				15.8	363.9	LV, SP
			13.7	379.6	RV, SP				15.3	374.7	LV, SP				15.8	374.4	RV, SP
			13.7	379.0	RV, SP				15.3	380.4	LV, SP				15.8	412.0	LV, SP
			13.7	438.6	RV, SP				15.3	382.6	RV, SP				15.8	362.5	RV, SP
			13.7	383.7	LV, SP				15.3	333.4	RV, SP				15.8	506.1	RV, SP
			13.7	416.4	RV, SP				15.3	380.6	RV, SP				15.8	378.4	RV, SP
			13.7	394.3	RV, SP				15.3	320.2	RV, SP				15.8	379.6	RV, SP
			13.7	468.1	RV, SP				15.3	409.9	RV, SP				15.8	461.5	LV, SP
			13.7	403.0	RV, SP				15.3	319.1	LV, SP				15.8	384.9	RV, SP
			13.7	402.0	RV, SP				15.3	304.3	RV, SP				15.8	395.4	RV, SP
			13.7	399.1	RV, SP				15.3	372.3	LV, SP				15.8	396.1	RV, SP
			13.7	442.0	RV, SP				15.3	260.4	RV, SP				15.8	401.2	RV, SP
			13.7	393.3	RV, SP				15.3	194.4	RV, SP				15.8	402.5	RV, SP
			13.7	477.3	LV, SP				15.3	397.1	RV, SP				15.8	393.3	RV, SP
			13.7	416.4	RV, SP				15.3	201.3	LV, SP				15.8	325.3	LV, SP
			13.7	435.4	RV, SP				15.3	281.4	RV, SP				15.8	399.0	RV, SP
			13.7	407.9	RV, SP				15.3	224.8	RV, SP				15.8	321.6	RV, SP
			13.7	443.3	RV, SP				15.3	276.8	LV, SP				15.8	312.4	LV, SP
			13.7	427.2	LV, SP				15.3	244.4	SB				15.8	296.2	LV, SP
			13.7	411.4	RV, SP				15.3	272.5	LV, SP				15.8	400.3	LV, SP
			13.7	418.1	LV, SP				15.3	272.2	LV, SP				15.8	314.4	RV, SP
			13.7	424.2	LV, SP				15.3	430.2	RV, SP				15.8	354.5	LV, SP
			13.7	428.5	RV, SP				15.3	298.9	RV, SP				15.8	298.8	LV, SP
			13.7	484.3	LV, SP				15.3	262.6	RV, SP				15.8	456.4	LV, SP
			13.7	419.9	RV, SP				15.3	237.1	LV, SP				15.8	452.3	LV, SP
			13.7	402.2	RV, SP				15.3	277.6	SB				15.8	439.0	RV, SP
			13.7	395.4	RV, SP				15.3	231.0	LV, SP				15.8	445.5	LV, SP
			13.7	384.4	LV, SP				15.3	273.7	LV, SP				15.8	396.5	LV, SP
			13.7	401.8	RV, SP				15.3	308.0	RV, SP				15.8	385.8	RV, SP
			13.7	390.3	RV, SP				15.3	437.2	RV, SP				15.8	421.6	RV, SP
			13.7	443.3	RV, SP				15.3	417.6	LV, SP				15.8	429.5	LV, SP
			13.7	440.6	RV, SP				15.3	395.9	LV, SP				15.8	489.7	LV, SP
			13.7	408.3	RV, SP				15.3	427.2	RV, SP				15.8	497.4	RV, SP
			13.7	446.6	RV, SP				15.3	417.3	RV, SP				15.8	405.9	RV, SP
			13.7	485.7	RV, SP				15.3	457.3	SB				15.8	414.2	RV, SP

(B)						<i>O. aspinata</i>											
Zone	Subzone	Bed N.	Bed H.	Geometric shell size	Shell pres.	Zone	Subzone	Bed N.	Bed H.	Geometric shell size	Shell pres.	Zone	Subzone	Bed N.	Bed H.	Geometric shell size	Shell pres.
			13.7	448.8	RV, SP				15.3	429.3	RV, SP				15.8	415.1	LV, SP
			13.7	459.2	RV, SP				15.3	467.7	LV, SP				15.8	380.7	LV, SP
			13.7	436.2	SB				15.3	429.3	RV, SP				15.8	389.8	LV, SP
			13.7	372.9	RV, SP				15.3	402.3	RV, SP				15.8	478.7	LV, SP
			13.7	394.4	RV, SP				15.3	408.8	LV, SP				15.8	477.5	RV, SP
			13.7	414.9	RV, SP				15.3	436.7	RV, SP				15.8	464.7	LV, SP
			13.7	440.8	RV, SP				15.3	394.0	SB				15.8	455.6	LV, SP
			13.7	371.3	RV, SP				15.3	352.2	RV, SP				15.8	449.7	RV, SP
			13.7	419.5	RV, SP				15.3	475.7	RV, SP				15.8	476.6	LV, SP
			13.7	422.7	RV, SP				15.3	412.6	RV, SP				15.8	515.1	LV, SP
			13.7	449.1	LV, SP				15.3	453.4	RV, SP				15.8	437.7	RV, SP
			13.7	456.0	RV, SP				15.3	464.2	RV, SP				15.8	530.2	RV, SP
			13.7	352.3	RV, SP				15.3	419.3	SB				15.8	452.5	SB
			13.7	354.7	RV, SP				15.3	450.5	RV, SP				15.8	387.9	LV, SP
			13.7	400.2	RV, SP				15.3	389.6	RV, SP				15.8	352.9	LV, SP
			13.7	389.8	RV, SP				15.3	378.9	RV, SP				15.8	508.8	SB
			13.7	393.2	RV, SP				15.3	428.6	LV, SP				15.8	318.6	LV, SP
			13.7	404.8	RV, SP				15.3	427.3	RV, SP				15.8	347.8	LV, SP
									15.3	465.7	RV, SP				15.8	415.9	LV, SP
									15.3	479.9	LV, SP				15.8	392.9	LV, SP
									15.3	452.4	RV, SP				15.8	420.7	RV, SP
									15.3	462.0	RV, SP				15.8	475.6	RV, SP
									15.3	456.4	RV, SP				15.8	347.6	LV, SP
									15.3	417.0	RV, SP				15.8	407.1	RV, SP
									15.3	463.3	LV, SP				15.8	396.0	LV, SP
									15.3	417.8	RV, SP				15.8	397.2	LV, SP
									15.3	401.3	RV, SP				15.8	405.8	RV, SP
									15.3	401.7	LV, SP				15.8	403.4	LV, SP
									15.3	432.2	SB				15.8	488.6	RV, SP
									15.3	410.2	LV, SP				15.8	412.7	LV, SP
									15.3	474.3	RV, SP				15.8	473.7	RV, SP
									15.3	404.7	RV, SP				15.8	354.6	LV, SP
									15.3	454.4	LV, SP						
									15.3	446.0	LV, SP						
									15.3	398.2	RV, SP						
									15.3	461.8	RV, SP						
									15.3	411.7	LV, SP						
									15.3	410.0	RV, SP						
									15.3	417.3	LV, SP						

(B)						<i>O. aspinata</i>											
Zone	Subzone	Bed N.	Bed H.	Geometric shell size	Shell pres.	Zone	Subzone	Bed N.	Bed H.	Geometric shell size	Shell pres.	Zone	Subzone	Bed N.	Bed H.	Geometric shell size	Shell pres.
									15.3	401.0	LV, SP						
									15.3	426.6	RV, SP						
									15.3	395.1	RV, SP						
									15.3	407.4	LV, SP						
									15.3	454.2	RV, SP						
									15.3	409.1	RV, SP						
									15.3	389.0	RV, SP						
									15.3	438.4	RV, SP						

(C)						<i>O. aspinata</i>					
Zone	Subzone	Bed N.	Bed height	Geometric shell size	Shell preservation	Zone	Subzone	Bed N.	Bed height	Geometric shell size	Shell preservation
liasicus Zone	Alsatites laqueus subzone	B51	16.8	509.6	LV, SP	liasicus Zone	Alsatites laqueus subzone	B53	17.5	393.8	LV, SP
			16.8	486.5	RV, SP				17.5	320.5	RV, SP
			16.8	420.7	LV, SP				17.5	455.0	LV, SP
			16.8	401.6	LV, SP				17.5	283.7	LV, SP
			16.8	432.5	LV, SP				17.5	317.7	RV, SP
			16.8	555.0	LV, SP				17.5	371.4	RV, SP
			16.8	445.1	LV, SP				17.5	414.4	LV, SP
			16.8	430.9	RV, SP				17.5	320.7	RV, SP
			16.8	411.5	RV, SP				17.5	393.2	LV, SP
			16.8	415.2	RV, SP				17.5	363.7	LV, SP
			16.8	387.0	RV, SP				17.5	397.2	LV, SP
			16.8	343.8	RV, SP				17.5	465.3	LV, SP
			16.8	383.1	LV, SP				17.5	330.5	LV, SP
			16.8	336.5	LV, SP				17.5	352.0	LV, SP
			16.8	313.7	LV, SP				17.5	376.0	RV, SP
			16.8	400.4	RV, SP				17.5	399.6	RV, SP
			16.8	367.5	LV, SP				17.5	362.5	LV, SP
			16.8	332.0	RV, SP				17.5	413.9	RV, SP
			16.8	375.9	LV, SP				17.5	367.5	LV, SP
			16.8	338.9	LV, SP				17.5	391.8	LV, SP
			16.8	397.4	LV, SP				17.5	379.5	LV, SP
			16.8	424.6	RV, SP				17.5	382.0	LV, SP
			16.8	389.3	LV, SP				17.5	370.1	RV, SP
			16.8	402.4	RV, SP				17.5	388.5	LV, SP
			16.8	351.3	LV, SP				17.5	459.6	LV, SP
			16.8	307.8	LV, SP				17.5	438.4	LV, SP

(C)			<i>O. aspinata</i>								
Zone	Subzone	Bed N.	Bed height	Geometric shell size	Shell preservation	Zone	Subzone	Bed N.	Bed height	Geometric shell size	Shell preservation
			16.8	281.2	LV, SP				17.5	289.2	RV, SP
			16.8	385.0	RV, SP				17.5	376.6	RV, SP
			16.8	300.3	RV, SP				17.5	320.1	LV, SP
			16.8	347.6	RV, SP				17.5	400.7	LV, SP
			16.8	398.5	RV, SP				17.5	391.3	RV, SP
			16.8	298.4	RV, SP				17.5	394.9	LV, SP
			16.8	376.5	RV, SP				17.5	389.0	LV, SP
			16.8	401.0	RV, SP				17.5	361.1	LV, SP
			16.8	376.3	RV, SP				17.5	317.2	RV, SP
			16.8	330.3	LV, SP				17.5	427.3	LV, SP
			16.8	337.8	RV, SP				17.5	335.8	RV, SP
			16.8	394.3	RV, SP				17.5	385.6	LV, SP
			16.8	408.0	RV, SP				17.5	326.7	RV, SP
			16.8	472.1	LV, SP				17.5	368.9	RV, SP
			16.8	362.3	RV, SP				17.5	469.5	RV, SP
			16.8	371.8	RV, SP				17.5	362.2	RV, SP
			16.8	374.0	LV, SP				17.5	370.7	RV, SP
			16.8	332.6	LV, SP				17.5	338.8	RV, SP
			16.8	351.8	LV, SP				17.5	392.3	RV, SP
			16.8	383.5	LV, SP				17.5	397.2	LV, SP
			16.8	372.2	RV, SP				17.5	356.5	RV, SP
			16.8	360.7	RV, SP				17.5	350.0	RV, SP
			16.8	411.5	LV, SP				17.5	363.4	LV, SP
			16.8	369.3	RV, SP				17.5	317.6	LV, SP
			16.8	338.6	LV, SP				17.5	414.3	RV, SP
			16.8	330.5	LV, SP				17.5	401.2	RV, SP
			16.8	264.4	LV, SP				17.5	386.6	LV, SP
			16.8	313.4	LV, SP				17.5	363.0	RV, SP
			16.8	388.9	LV, SP				17.5	400.7	RV, SP
			16.8	468.6	LV, SP				17.5	368.3	RV, SP
			16.8	359.4	LV, SP				17.5	451.0	RV, SP
			16.8	341.0	LV, SP				17.5	305.1	RV, SP
			16.8	392.9	LV, SP				17.5	342.3	SB
			16.8	256.9	RV, SP				17.5	377.2	RV, SP
			16.8	416.5	RV, SP				17.5	402.0	RV, SP
			16.8	283.6	RV, SP				17.5	319.9	RV, SP
			16.8	291.0	LV, SP				17.5	335.8	LV, SP
			16.8	209.0	LV, SP				17.5	331.3	RV, SP
			16.8	288.7	LV, SP				17.5	411.0	RV, SP

(C)			<i>O. aspinata</i>								
Zone	Subzone	Bed N.	Bed height	Geometric shell size	Shell preservation	Zone	Subzone	Bed N.	Bed height	Geometric shell size	Shell preservation
			16.8	261.2	RV, SP				17.5	330.1	RV, SP
			16.8	251.9	RV, SP				17.5	458.2	LV, SP
			16.8	269.7	RV, SP				17.5	322.4	RV, SP
			16.8	483.8	RV, SP				17.5	403.5	RV, SP
			16.8	227.8	LV, SP				17.5	308.4	RV, SP
			16.8	247.5	LV, SP				17.5	323.2	LV, SP
			16.8	244.3	LV, SP				17.5	372.9	RV, SP
			16.8	239.3	LV, SP				17.5	365.2	RV, SP
			16.8	248.1	LV, SP				17.5	391.9	RV, SP
			16.8	211.6	LV, SP				17.5	380.9	SB
			16.8	495.7	RV, SP				17.5	455.3	RV, SP
			16.8	441.9	RV, SP				17.5	369.1	RV, SP
			16.8	448.9	LV, SP				17.5	323.8	RV, SP
			16.8	430.4	RV, SP				17.5	335.5	RV, SP
			16.8	479.5	LV, SP				17.5	315.3	LV, SP
			16.8	415.5	LV, SP				17.5	394.4	LV, SP
			16.8	354.0	RV, SP				17.5	308.4	RV, SP
			16.8	438.5	RV, SP				17.5	389.6	RV, SP
			16.8	425.2	RV, SP				17.5	386.7	RV, SP
			16.8	396.1	RV, SP				17.5	424.2	RV, SP
			16.8	460.1	SB				17.5	346.8	RV, SP
			16.8	412.7	SB				17.5	398.8	RV, SP
			16.8	425.8	RV, SP				17.5	401.7	RV, SP
			16.8	423.4	LV, SP				17.5	397.6	RV, SP
			16.8	339.5	RV, SP				17.5	380.1	SB
			16.8	404.4	RV, SP				17.5	399.3	RV, SP
			16.8	387.7	RV, SP				17.5	390.3	SB
			16.8	462.1	LV, SP				17.5	382.3	SB
			16.8	473.2	RV, SP				17.5	415.6	LV, SP
			16.8	406.0	RV, SP				17.5	323.3	RV, SP
			16.8	302.6	RV, SP				17.5	374.7	RV, SP
			16.8	450.4	RV, SP				17.5	313.0	RV, SP
			16.8	482.9	LV, SP				17.5	381.7	RV, SP
			16.8	470.6	RV, SP				17.5	309.5	LV, SP
			16.8	323.0	RV, SP				17.5	380.2	LV, SP
			16.8	443.6	RV, SP				17.5	392.7	RV, SP
			16.8	418.2	RV, SP				17.5	454.8	SB
			16.8	430.7	RV, SP				17.5	308.7	LV, SP
			16.8	257.7	RV, SP				17.5	432.4	LV, SP

(C)			<i>O. aspinata</i>								
Zone	Subzone	Bed N.	Bed height	Geometric shell size	Shell preservation	Zone	Subzone	Bed N.	Bed height	Geometric shell size	Shell preservation
			16.8	230.1	LV, SP				17.5	278.3	RV, SP
			16.8	470.8	SB				17.5	280.8	RV, SP
			16.8	221.9	RV, SP				17.5	273.1	RV, SP
			16.8	485.5	LV, SP				17.5	449.3	RV, SP
			16.8	457.2	SB				17.5	266.1	RV, SP
			16.8	439.1	RV, SP				17.5	256.2	RV, SP
			16.8	496.2	RV, SP				17.5	240.2	RV, SP
			16.8	443.3	SB				17.5	361.5	RV, SP
			16.8	472.3	LV, SP				17.5	242.6	RV, SP
			16.8	477.8	RV, SP				17.5	200.9	RV, SP
			16.8	426.6	RV, SP				17.5	279.3	RV, SP
			16.8	388.0	RV, SP				17.5	271.8	LV, SP
			16.8	464.6	RV, SP				17.5	274.8	LV, SP
			16.8	396.9	RV, SP				17.5	462.1	RV, SP
			16.8	427.2	RV, SP				17.5	428.3	RV, SP
			16.8	419.7	RV, SP				17.5	440.7	LV, SP
			16.8	481.9	RV, SP				17.5	388.5	LV, SP
			16.8	492.2	RV, SP				17.5	415.4	RV, SP
			16.8	438.2	RV, SP				17.5	423.9	RV, SP
			16.8	480.4	RV, SP				17.5	432.4	RV, SP
			16.8	422.9	RV, SP				17.5	484.1	LV, SP
			16.8	421.2	LV, SP				17.5	421.5	RV, SP
			16.8	380.0	SB				17.5	488.8	RV, SP
			16.8	409.8	LV, SP				17.5	435.2	RV, SP
			16.8	483.1	RV, SP				17.5	413.2	RV, SP
			16.8	409.4	RV, SP				17.5	455.3	RV, SP
			16.8	472.5	RV, SP				17.5	389.5	RV, SP
			16.8	460.6	SB				17.5	511.8	RV, SP
			16.8	447.2	RV, SP				17.5	473.2	RV, SP
			16.8	484.2	LV, SP				17.5	392.7	RV, SP
			16.8	439.8	LV, SP				17.5	485.8	RV, SP
			16.8	409.3	LV, SP				17.5	450.5	RV, SP
			16.8	475.0	LV, SP				17.5	469.0	RV, SP
			16.8	467.4	RV, SP				17.5	463.9	RV, SP
			16.8	462.5	LV, SP				17.5	472.1	RV, SP
			16.8	328.2	LV, SP				17.5	406.1	RV, SP
			16.8	327.7	RV, SP				17.5	455.3	RV, SP
			16.8	373.4	SB				17.5	410.0	RV, SP
			16.8	322.9	RV, SP				17.5	469.2	RV, SP

(C)						<i>O. aspinata</i>					
Zone	Subzone	Bed N.	Bed height	Geometric shell size	Shell preservation	Zone	Subzone	Bed N.	Bed height	Geometric shell size	Shell preservation
			16.8	341.9	LV, SP				17.5	347.6	RV, SP
			16.8	343.0	LV, SP				17.5	446.9	LV, SP
			16.8	384.3	SB				17.5	442.6	RV, SP
			16.8	386.5	RV, SP				17.5	414.2	RV, SP
			16.8	301.9	LV, SP				17.5	402.7	RV, SP
			16.8	466.5	LV, SP				17.5	501.8	RV, SP
			16.8	554.8	LV, SP				17.5	403.7	RV, SP
			16.8	477.2	LV, SP				17.5	385.3	RV, SP
			16.8	468.1	LV, SP				17.5	439.8	RV, SP
			16.8	441.1	LV, SP				17.5	456.3	SB
			16.8	478.5	LV, SP				17.5	471.5	LV, SP
			16.8	451.8	RV, SP				17.5	454.1	RV, SP
			16.8	426.3	LV, SP				17.5	405.0	RV, SP
			16.8	482.3	LV, SP				17.5	454.5	RV, SP
			16.8	415.3	LV, SP				17.5	404.9	RV, SP
			16.8	463.9	RV, SP				17.5	449.5	LV, SP
			16.8	420.6	LV, SP				17.5	407.8	SB
			16.8	499.3	LV, SP				17.5	451.0	SB
			16.8	484.6	RV, SP				17.5	402.8	RV, SP
			16.8	428.5	LV, SP				17.5	409.4	RV, SP
			16.8	422.2	SB				17.5	399.9	RV, SP
			16.8	409.8	LV, SP				17.5	422.7	RV, SP
			16.8	415.0	LV, SP				17.5	423.7	RV, SP
			16.8	467.3	LV, SP				17.5	418.0	RV, SP
			16.8	445.4	LV, SP				18.2	396.5	LV, SP
			16.8	483.4	LV, SP				18.2	392.9	RV, SP
			16.8	452.3	LV, SP				18.2	441.3	LV, SP
			16.8	423.8	LV, SP				18.2	477.4	LV, SP
			16.8	515.8	LV, SP				18.2	475.4	LV, SP
			16.8	360.1	LV, SP				18.2	436.0	RV, SP
			16.8	455.6	LV, SP				18.2	415.1	RV, SP
			16.8	397.0	SB				18.2	449.9	LV, SP
			16.8	268.6	LV, SP				18.2	414.8	LV, SP
			16.8	494.1	LV, SP				18.2	438.7	RV, SP
			17.5	418.9	LV, SP				18.2	323.2	LV, SP
		B53	17.5	472.5	LV, SP				18.2	367.3	LV, SP
			17.5	466.8	RV, SP				18.2	377.0	LV, SP
			17.5	405.8	LV, SP				18.2	387.3	LV, SP
			17.5	522.2	RV, SP				18.2	394.1	RV, SP

(C)		<i>O. aspinata</i>									
Zone	Subzone	Bed N.	Bed height	Geometric shell size	Shell preservation	Zone	Subzone	Bed N.	Bed height	Geometric shell size	Shell preservation
			17.5	426.5	RV, SP				18.2	450.5	RV, SP
			17.5	413.9	RV, SP				18.2	349.8	RV, SP
			17.5	429.8	LV, SP				18.2	391.7	RV, SP
			17.5	417.5	LV, SP				18.2	368.2	LV, SP
			17.5	473.9	LV, SP				18.2	372.7	RV, SP
			17.5	492.3	LV, SP				18.2	362.6	LV, SP
			17.5	422.8	LV, SP				18.2	401.6	LV, SP
			17.5	410.2	RV, SP				18.2	310.3	RV, SP
			17.5	428.7	LV, SP				18.2	308.2	LV, SP
			17.5	453.4	LV, SP				18.2	364.0	LV, SP
			17.5	419.0	LV, SP				18.2	406.5	RV, SP
			17.5	412.4	RV, SP				18.2	364.2	RV, SP
			17.5	410.4	LV, SP				18.2	388.0	LV, SP
			17.5	458.8	RV, SP				18.2	387.0	LV, SP
			17.5	421.0	LV, SP				18.2	344.3	RV, SP
			17.5	476.9	RV, SP				18.2	435.2	RV, SP
			17.5	487.1	LV, SP				18.2	352.6	RV, SP
			17.5	393.5	LV, SP				18.2	379.8	RV, SP
			17.5	482.0	LV, SP				18.2	356.4	LV, SP
			17.5	440.6	LV, SP				18.2	327.6	LV, SP
			17.5	469.6	LV, SP				18.2	317.4	RV, SP
			17.5	446.8	LV, SP				18.2	456.8	LV, SP
			17.5	457.1	LV, SP				18.2	289.9	LV, SP
			17.5	426.7	RV, SP				18.2	282.8	LV, SP
			17.5	449.1	RV, SP				18.2	308.0	LV, SP
			17.5	424.8	RV, SP				18.2	276.5	RV, SP
			17.5	403.5	LV, SP				18.2	257.3	RV, SP
			17.5	463.5	LV, SP				18.2	226.7	RV, SP
			17.5	424.2	RV, SP				18.2	450.6	RV, SP
			17.5	449.2	RV, SP				18.2	234.6	RV, SP
			17.5	410.4	LV, SP				18.2	247.4	LV, SP
			17.5	448.7	SB				18.2	259.5	LV, SP
			17.5	384.6	RV, SP				18.2	183.2	LV, SP
			17.5	435.5	RV, SP				18.2	290.9	LV, SP
			17.5	403.1	RV, SP				18.2	385.7	LV, SP
			17.5	441.9	LV, SP				18.2	389.4	RV, SP
			17.5	462.6	RV, SP				18.2	408.4	LV, SP
			17.5	408.8	LV, SP				18.2	377.4	LV, SP
			17.5	481.2	LV, SP				18.2	419.0	RV, SP

(C)				<i>O. aspinata</i>							
Zone	Subzone	Bed N.	Bed height	Geometric shell size	Shell preservation	Zone	Subzone	Bed N.	Bed height	Geometric shell size	Shell preservation
			17.5	423.8	RV, SP				18.2	433.8	LV, SP
			17.5	413.9	LV, SP				18.2	421.7	RV, SP
			17.5	512.8	SB				18.2	464.5	RV, SP
			17.5	441.3	LV, SP				18.2	451.6	LV, SP
			17.5	473.0	LV, SP				18.2	446.8	LV, SP
			17.5	460.4	LV, SP				18.2	458.3	RV, SP
			17.5	422.2	RV, SP				18.2	457.0	LV, SP
			17.5	486.2	LV, SP				18.2	437.0	LV, SP
			17.5	413.5	LV, SP				18.2	402.0	RV, SP
			17.5	421.1	LV, SP				18.2	431.2	LV, SP
			17.5	418.9	LV, SP				18.2	435.0	RV, SP
			17.5	416.1	RV, SP				18.2	408.3	LV, SP
			17.5	454.8	LV, SP				18.2	450.6	RV, SP
			17.5	434.5	RV, SP				18.2	446.1	RV, SP
			17.5	469.4	LV, SP				18.2	398.7	LV, SP
			17.5	455.0	RV, SP				18.2	459.8	RV, SP
			17.5	410.2	LV, SP				18.2	460.5	LV, SP
			17.5	470.1	RV, SP				18.2	407.7	RV, SP
			17.5	465.0	LV, SP				18.2	455.2	LV, SP
			17.5	439.3	RV, SP				18.2	444.1	RV, SP
			17.5	413.5	LV, SP				18.2	452.7	LV, SP
			17.5	434.8	RV, SP				18.2	483.9	LV, SP
			17.5	393.6	LV, SP				18.2	451.4	LV, SP
			17.5	425.2	LV, SP				18.2	447.8	LV, SP
			17.5	470.1	LV, SP				18.2	426.1	RV, SP
			17.5	433.8	LV, SP				18.2	427.9	RV, SP
			17.5	461.5	LV, SP				18.2	417.8	LV, SP
			17.5	445.4	LV, SP				18.2	443.9	RV, SP
			17.5	467.8	LV, SP				18.2	383.6	LV, SP
			17.5	462.7	RV, SP				18.2	452.5	LV, SP
			17.5	481.9	RV, SP				18.2	434.4	RV, SP
			17.5	422.8	RV, SP				18.2	453.3	LV, SP
			17.5	460.6	LV, SP				18.2	454.2	LV, SP
			17.5	484.5	RV, SP				18.2	448.9	RV, SP
			17.5	391.6	RV, SP				18.2	436.9	RV, SP
			17.5	426.7	RV, SP				18.2	398.0	RV, SP
			17.5	468.9	RV, SP				18.2	443.9	LV, SP
			17.5	428.9	RV, SP				18.2	461.6	LV, SP
			17.5	460.5	RV, SP				18.2	390.4	LV, SP

(C)		<i>O. aspinata</i>									
Zone	Subzone	Bed N.	Bed height	Geometric shell size	Shell preservation	Zone	Subzone	Bed N.	Bed height	Geometric shell size	Shell preservation
			17.5	441.7	LV, SP				18.2	433.0	LV, SP
			17.5	448.5	RV, SP				18.2	473.3	LV, SP
			17.5	482.2	LV, SP				18.2	409.7	RV, SP
			17.5	411.8	LV, SP				18.2	452.9	RV, SP
			17.5	393.6	RV, SP				18.2	438.0	RV, SP
			17.5	467.2	RV, SP				18.2	419.7	RV, SP
			17.5	400.5	LV, SP				18.2	454.4	RV, SP
			17.5	503.4	LV, SP				18.2	406.7	RV, SP
			17.5	393.3	LV, SP				18.2	452.8	RV, SP
			17.5	405.6	LV, SP				18.2	401.2	RV, SP
			17.5	473.4	LV, SP				18.2	432.5	RV, SP
			17.5	462.0	LV, SP				18.2	448.9	RV, SP
			17.5	398.1	LV, SP				18.2	397.2	RV, SP
			17.5	423.7	LV, SP				18.2	413.5	RV, SP
			17.5	440.6	LV, SP				18.2	409.5	RV, SP
			17.5	369.8	LV, SP				18.2	406.0	RV, SP
			17.5	392.0	LV, SP				18.2	436.6	RV, SP
			17.5	390.5	LV, SP				18.2	419.8	RV, SP
			17.5	384.1	RV, SP				18.2	387.3	RV, SP
			17.5	372.6	LV, SP				18.2	399.7	RV, SP
			17.5	377.3	RV, SP				18.2	368.8	LV, SP
			17.5	394.0	RV, SP				18.2	415.4	RV, SP
			17.5	401.1	RV, SP				18.2	390.4	RV, SP
			17.5	376.0	RV, SP				18.2	480.1	RV, SP
			17.5	379.5	LV, SP				18.2	392.2	LV, SP
			17.5	347.5	RV, SP				18.2	424.6	RV, SP
			17.5	390.7	RV, SP				18.2	467.6	LV, SP
			17.5	397.8	LV, SP				18.2	397.0	RV, SP
			17.5	327.9	LV, SP				18.2	449.4	RV, SP
			17.5	336.0	LV, SP				18.2	423.4	RV, SP
			17.5	457.5	RV, SP				18.2	417.1	LV, SP
			17.5	335.2	RV, SP						
			17.5	384.7	LV, SP						
			17.5	377.6	LV, SP						
			17.5	378.1	LV, SP						
			17.5	417.1	RV, SP						
			17.5	314.1	LV, SP						
			17.5	319.9	RV, SP						
			17.5	411.9	RV, SP						

(C)						<i>O. aspinata</i>					
Zone	Subzone	Bed N.	Bed height	Geometric shell size	Shell preservation	Zone	Subzone	Bed N.	Bed height	Geometric shell size	Shell preservation
			17.5	401.6	RV, SP						
			17.5	365.9	RV, SP						
			17.5	336.5	RV, SP						
			17.5	377.9	RV, SP						

(D)																	
						<i>O. aspinata</i>											
Zone	Subzone	Bed N.	Bed H.	Geometric shell size	Shell pres.	Zone	Subzone	Bed N.	Bed H.	Geometric shell size	Shell pres.	Zone	Subzone	Bed N.	Bed H.	Geometric shell size	Shell pres.
liasicus Zone	Alsatites laqueus subzone	B59	19.35	427.7	LV, SP	angulata Zone	Schlothe- imia angulata subzone	B73	21.55	404.5	LV, SP	angulata Zone	Schlothe- -imia angulata subzone	B76 A	22.15	350.0	RV, SP
			19.35	460.5	LV, SP				21.55	386.3	LV, SP				22.15	477.5	RV, SP
			19.35	478.6	LV, SP				21.55	429.7	RV, SP				22.15	429.1	RV, SP
			19.35	369.3	SB				21.55	428.3	SB				22.15	447.3	LV, SP
			19.35	435.3	LV, SP				21.55	424.7	LV, SP				22.15	458.6	RV, SP
			19.35	457.4	RV, SP				21.55	422.0	RV, SP				22.15	415.9	RV, SP
			19.35	404.0	LV, SP				21.55	515.9	RV, SP				22.15	428.3	RV, SP
			19.35	452.8	LV, SP				21.55	520.3	RV, SP				22.15	548.6	RV, SP
			19.35	471.5	LV, SP				21.55	561.4	LV, SP				22.15	437.5	RV, SP
			19.35	448.0	LV, SP				21.55	380.3	LV, SP				22.15	541.2	LV, SP
			19.35	421.2	RV, SP				21.55	498.5	RV, SP				22.15	462.1	RV, SP
			19.35	409.2	LV, SP				21.55	441.8	RV, SP				22.15	454.6	LV, SP
			19.35	375.6	RV, SP				21.55	351.9	SB				22.15	473.1	RV, SP
			19.35	417.1	LV, SP				21.55	400.8	LV, SP				22.15	358.0	LV, SP
			19.35	464.0	LV, SP				21.55	256.7	RV, SP				22.15	421.0	LV, SP
			19.35	442.0	LV, SP				21.55	527.1	RV, SP				22.15	372.9	LV, SP
			19.35	436.7	LV, SP				21.55	459.2	RV, SP				22.15	387.0	RV, SP
			19.35	439.2	LV, SP				21.55	565.8	LV, SP				22.15	443.2	LV, SP
			19.35	416.1	LV, SP				21.55	527.1	LV, SP				22.15	400.3	LV, SP
			19.35	435.8	LV, SP				21.55	460.2	RV, SP				22.15	379.7	RV, SP
			19.35	461.9	RV, SP				21.55	456.1	RV, SP				22.15	353.0	RV, SP
			19.35	390.2	RV, SP				21.55	431.7	RV, SP				22.15	434.4	RV, SP
			19.35	381.8	LV, SP				21.55	476.2	RV, SP				22.15	333.9	RV, SP
			19.35	455.2	RV, SP				21.55	387.8	RV, SP				22.15	347.3	LV, SP
			19.35	403.2	RV, SP				21.55	433.2	LV, SP				22.15	454.6	RV, SP
			19.35	391.1	RV, SP				21.55	440.4	RV, SP				22.15	436.9	LV, SP
			19.35	389.5	RV, SP				21.55	406.0	LV, SP				22.15	451.3	RV, SP
			19.35	383.1	RV, SP				21.55	549.9	RV, SP				22.15	455.8	RV, SP
19.35	355.0	RV, SP	21.55	532.4	LV, SP	22.15	375.3	LV, SP									
19.35	351.0	RV, SP	21.55	361.3	LV, SP	22.15	387.2	LV, SP									
19.35	268.9	RV, SP	21.55	388.2	RV, SP	22.15	378.0	LV, SP									

(D)						<i>O. aspinata</i>											
Zone	Subzone	Bed N.	Bed H.	Geometric shell size	Shell pres.	Zone	Subzone	Bed N.	Bed H.	Geometric shell size	Shell pres.	Zone	Subzone	Bed N.	Bed H.	Geometric shell size	Shell pres.
			19.35	366.2	RV, SP				21.55	377.8	RV, SP				22.15	385.3	LV, SP
			19.35	389.3	RV, SP				21.55	433.3	RV, SP				22.15	398.2	RV, SP
			19.35	309.7	RV, SP				21.55	546.2	RV, SP				22.15	417.7	LV, SP
			19.35	400.1	LV, SP				21.55	478.0	RV, SP				22.15	376.8	RV, SP
			19.35	347.7	LV, SP				21.55	503.6	RV, SP				22.15	362.6	LV, SP
			19.35	294.9	LV, SP				21.55	403.7	RV, SP				22.15	363.7	RV, SP
			19.35	276.1	RV, SP				21.55	382.6	RV, SP				22.15	320.2	LV, SP
			19.35	366.1	RV, SP				21.55	538.0	RV, SP				22.15	305.7	LV, SP
			19.35	341.0	RV, SP				21.55	413.2	RV, SP				22.15	344.3	LV, SP
			19.35	388.7	RV, SP				21.55	474.0	RV, SP				22.15	324.7	RV, SP
			19.35	369.8	LV, SP				21.55	481.8	LV, SP				22.15	384.6	LV, SP
			19.35	330.4	RV, SP				21.55	511.1	RV, SP				22.15	429.1	LV, SP
			19.35	366.9	LV, SP				21.55	505.6	RV, SP				22.15	350.7	LV, SP
			19.35	351.2	RV, SP				21.55	414.8	LV, SP				22.15	344.0	LV, SP
			19.35	366.1	RV, SP				21.55	384.8	LV, SP				22.15	312.3	RV, SP
			19.35	334.0	RV, SP				21.55	403.6	RV, SP				22.15	318.9	RV, SP
			19.35	298.1	LV, SP				21.55	392.2	RV, SP				22.15	281.3	LV, SP
			19.35	365.0	RV, SP				21.55	380.5	LV, SP				22.15	319.8	RV, SP
			19.35	351.9	LV, SP				21.55	260.9	RV, SP				22.15	386.7	LV, SP
			19.35	396.9	RV, SP				21.55	391.6	RV, SP				22.15	363.3	LV, SP
			19.35	394.7	RV, SP				21.55	399.3	LV, SP				22.15	335.4	LV, SP
			19.35	344.9	RV, SP				21.55	333.8	LV, SP				22.15	391.3	RV, SP
			19.35	293.6	RV, SP				21.55	319.6	RV, SP				22.15	342.4	RV, SP
			19.35	380.2	RV, SP				21.55	368.3	LV, SP				22.15	351.8	RV, SP
			19.35	374.2	RV, SP				21.55	292.6	RV, SP				22.15	388.2	LV, SP
			19.35	244.2	RV, SP				21.55	317.6	LV, SP				22.15	353.6	RV, SP
			19.35	223.0	RV, SP				21.55	375.2	RV, SP				22.15	343.1	LV, SP
			19.35	207.2	RV, SP				21.55	384.6	RV, SP				22.15	375.1	LV, SP
			19.6	207.7	LV, SP				21.55	406.0	LV, SP				22.15	256.0	LV, SP
			19.6	473.6	RV, SP				21.55	349.7	LV, SP				22.15	327.4	LV, SP
			19.6	420.6	LV, SP				21.55	344.9	LV, SP				22.15	330.0	LV, SP
			19.6	463.8	LV, SP				21.55	270.4	RV, SP				22.15	300.7	LV, SP
			19.6	454.0	LV, SP				21.55	373.6	RV, SP				22.15	372.0	RV, SP
		B61	19.6	430.6	LV, SP				21.55	324.2	RV, SP				22.15	377.1	LV, SP
			19.6	399.3	LV, SP				21.55	379.4	RV, SP				22.15	343.0	RV, SP
			19.6	444.4	LV, SP				21.55	348.2	LV, SP				22.15	361.7	LV, SP
			19.6	363.4	LV, SP				21.55	354.6	RV, SP				22.15	392.9	RV, SP
			19.6	403.4	LV, SP				21.55	488.0	LV, SP				22.15	363.5	RV, SP
			19.6	452.5	LV, SP				21.55	316.2	RV, SP				22.15	340.0	LV, SP

(D)						<i>O. aspinata</i>											
Zone	Subzone	Bed N.	Bed H.	Geometric shell size	Shell pres.	Zone	Subzone	Bed N.	Bed H.	Geometric shell size	Shell pres.	Zone	Subzone	Bed N.	Bed H.	Geometric shell size	Shell pres.
			19.6	464.5	RV, SP				21.55	314.5	RV, SP				22.15	333.2	RV, SP
			19.6	417.5	LV, SP				21.55	383.6	LV, SP				22.15	343.4	LV, SP
			19.6	420.0	RV, SP				21.55	341.9	RV, SP				22.15	317.1	LV, SP
			19.6	381.2	RV, SP				21.55	336.4	RV, SP				22.15	363.7	LV, SP
			19.6	402.7	RV, SP				21.55	320.1	RV, SP				22.15	420.0	LV, SP
			19.6	430.8	RV, SP				21.55	340.0	LV, SP				22.15	266.8	LV, SP
			19.6	437.1	RV, SP				21.55	300.6	RV, SP				22.15	349.1	RV, SP
			19.6	450.0	RV, SP				21.55	527.7	LV, SP				22.15	356.4	LV, SP
			19.6	405.9	LV, SP				21.55	329.3	RV, SP				22.15	309.5	LV, SP
			19.6	456.7	LV, SP				21.55	351.6	RV, SP				22.15	264.7	LV, SP
			19.6	458.4	LV, SP				21.55	372.6	RV, SP				22.15	259.2	LV, SP
			19.6	404.1	LV, SP				21.55	299.8	RV, SP				22.15	254.4	LV, SP
			19.6	426.5	LV, SP				21.55	346.4	LV, SP				22.15	303.0	LV, SP
			19.6	447.1	LV, SP				21.55	330.9	RV, SP				22.15	272.4	LV, SP
			19.6	452.5	LV, SP				21.55	335.7	RV, SP				22.15	235.4	LV, SP
			19.6	457.2	LV, SP				21.55	276.2	LV, SP				22.15	371.5	LV, SP
			19.6	454.5	LV, SP				21.55	564.5	RV, SP				22.15	444.4	LV, SP
			19.6	377.3	LV, SP				21.55	323.4	RV, SP				22.15	429.3	RV, SP
			19.6	436.8	RV, SP				21.55	348.6	RV, SP				22.15	377.3	RV, SP
			19.6	454.1	LV, SP				21.55	404.4	RV, SP				22.15	392.8	LV, SP
			19.6	393.7	LV, SP				21.55	365.0	RV, SP				22.15	404.1	LV, SP
			19.6	386.4	LV, SP				21.55	305.6	RV, SP				22.15	383.2	RV, SP
			19.6	404.3	SB				21.55	371.0	LV, SP				22.15	393.0	LV, SP
			19.6	325.9	LV, SP				21.55	396.0	RV, SP				22.15	402.0	LV, SP
			19.6	379.1	LV, SP				21.55	331.1	LV, SP				22.15	409.2	LV, SP
			19.6	365.4	RV, SP				21.55	312.4	RV, SP				22.15	439.5	RV, SP
			19.6	357.9	RV, SP				21.55	405.7	RV, SP				22.15	426.5	LV, SP
			19.6	370.0	RV, SP				21.55	347.8	LV, SP				22.15	374.1	RV, SP
			19.6	310.4	LV, SP				21.55	341.9	RV, SP				22.15	399.3	LV, SP
			19.6	276.5	LV, SP				21.55	338.2	RV, SP				22.15	440.7	LV, SP
			19.6	344.3	LV, SP				21.55	281.0	LV, SP				22.15	434.0	LV, SP
			19.6	462.0	LV, SP				21.55	349.9	RV, SP				22.15	415.2	RV, SP
			19.6	359.9	RV, SP				21.55	339.4	RV, SP				22.15	462.0	LV, SP
			19.6	403.4	RV, SP				21.55	335.4	RV, SP				22.15	393.0	LV, SP
			19.6	348.2	LV, SP				21.55	372.3	RV, SP				22.15	430.9	LV, SP
			19.6	368.8	LV, SP				21.55	420.7	LV, SP				22.15	395.8	RV, SP
			19.6	373.8	LV, SP				21.55	372.8	RV, SP				22.15	464.0	RV, SP
			19.6	320.8	RV, SP				21.55	348.2	RV, SP				22.15	441.4	RV, SP
			19.6	409.1	LV, SP				21.55	345.9	RV, SP				22.15	409.1	RV, SP

(D)						<i>O. aspinata</i>											
Zone	Subzone	Bed N.	Bed H.	Geometric shell size	Shell pres.	Zone	Subzone	Bed N.	Bed H.	Geometric shell size	Shell pres.	Zone	Subzone	Bed N.	Bed H.	Geometric shell size	Shell pres.
			19.6	368.3	SB				21.55	298.3	RV, SP				22.15	415.3	LV, SP
			19.6	276.2	RV, SP				21.55	304.8	RV, SP				22.15	535.9	RV, SP
			19.6	367.7	RV, SP				21.55	352.6	LV, SP				22.15	358.8	LV, SP
			19.6	382.8	LV, SP				21.55	363.6	RV, SP				22.15	497.2	RV, SP
			19.6	360.4	RV, SP				21.55	279.8	RV, SP				22.15	484.1	RV, SP
			19.6	448.0	RV, SP				21.55	502.9	RV, SP				22.15	413.8	LV, SP
			19.6	378.6	RV, SP				21.55	340.8	LV, SP				22.15	400.1	LV, SP
			19.6	303.0	LV, SP				21.55	315.9	RV, SP				22.15	390.0	LV, SP
			19.6	312.6	RV, SP				21.55	372.9	RV, SP				22.15	377.5	LV, SP
			19.6	304.5	LV, SP				21.55	325.1	RV, SP				22.15	442.9	LV, SP
			19.6	314.4	LV, SP				21.55	382.0	RV, SP				22.15	435.8	RV, SP
			19.6	360.6	RV, SP				21.55	345.9	SB				22.15	455.3	RV, SP
			19.6	363.8	LV, SP				21.55	514.1	RV, SP				22.15	398.5	LV, SP
			19.6	387.7	LV, SP				21.55	308.2	LV, SP				22.15	403.8	RV, SP
			19.6	275.8	LV, SP				21.55	379.1	RV, SP				22.15	404.4	RV, SP
			19.6	282.4	RV, SP				21.55	308.6	LV, SP				22.15	480.8	RV, SP
			19.6	142.7	RV, SP				21.55	363.7	RV, SP				22.15	387.9	LV, SP
			19.6	404.9	RV, SP				21.55	398.1	RV, SP				22.15	367.9	LV, SP
			19.6	409.2	RV, SP				21.55	302.9	LV, SP				22.15	458.7	RV, SP
			19.6	393.3	LV, SP				21.55	391.5	LV, SP				22.15	463.3	RV, SP
			19.6	399.0	LV, SP				21.55	380.2	RV, SP				22.15	435.5	LV, SP
			19.6	382.8	RV, SP				21.55	358.7	LV, SP				22.15	476.4	LV, SP
			19.6	450.9	LV, SP				21.55	482.7	LV, SP				22.15	433.9	LV, SP
			19.6	459.0	RV, SP				21.55	377.1	RV, SP				22.15	399.9	RV, SP
			19.6	447.0	LV, SP				21.55	314.4	RV, SP				22.15	378.7	LV, SP
			19.6	461.4	RV, SP				21.55	260.8	RV, SP				22.15	385.5	RV, SP
			19.6	442.0	RV, SP				21.55	325.6	RV, SP				22.15	397.0	RV, SP
			19.6	386.7	RV, SP				21.55	340.0	RV, SP				22.15	426.4	RV, SP
			19.6	447.8	LV, SP				21.55	369.5	RV, SP				22.15	393.8	RV, SP
			19.6	452.8	RV, SP				21.55	328.3	LV, SP				22.15	427.1	RV, SP
			19.6	440.5	RV, SP				21.55	343.0	LV, SP				22.15	360.5	LV, SP
			19.6	469.8	RV, SP				21.55	322.9	RV, SP				22.15	489.0	LV, SP
			19.6	389.0	LV, SP				21.55	351.5	LV, SP				22.15	489.8	RV, SP
			19.6	468.8	LV, SP				21.55	488.6	LV, SP				22.15	501.4	RV, SP
			19.6	449.4	RV, SP				21.55	301.6	RV, SP				22.15	438.3	RV, SP
			19.6	452.1	LV, SP				21.55	339.6	RV, SP				22.15	397.7	RV, SP
			19.6	492.7	LV, SP				21.55	329.7	RV, SP				22.15	387.0	SB
			19.6	396.6	LV, SP				21.55	347.3	RV, SP				22.15	436.3	RV, SP
			19.6	391.4	LV, SP				21.55	358.1	RV, SP				22.15	435.0	RV, SP

(D)						<i>O. aspinata</i>											
Zone	Subzone	Bed N.	Bed H.	Geometric shell size	Shell pres.	Zone	Subzone	Bed N.	Bed H.	Geometric shell size	Shell pres.	Zone	Subzone	Bed N.	Bed H.	Geometric shell size	Shell pres.
			19.6	406.3	LV, SP				21.55	328.2	RV, SP				22.15	475.5	RV, SP
			19.6	401.7	RV, SP				21.55	303.5	RV, SP				22.15	428.1	LV, SP
			19.6	410.9	LV, SP				21.55	446.7	LV, SP				22.15	479.6	LV, SP
			19.6	400.7	LV, SP				21.55	387.9	RV, SP				22.15	499.1	LV, SP
			19.6	384.7	LV, SP				21.55	291.2	LV, SP				22.15	466.9	RV, SP
			19.6	421.6	LV, SP				21.55	336.4	RV, SP				22.35	370.0	RV, SP
			19.6	451.7	LV, SP				21.55	363.1	RV, SP				22.35	370.5	RV, SP
			19.6	397.2	RV, SP				21.55	355.5	RV, SP				22.35	405.1	RV, SP
			19.6	392.7	LV, SP				21.55	364.2	RV, SP				22.35	523.9	RV, SP
			19.6	455.2	RV, SP				21.55	346.1	LV, SP				22.35	439.7	LV, SP
			19.6	471.7	LV, SP				21.55	301.6	RV, SP				22.35	461.5	LV, SP
			19.6	433.8	LV, SP				21.55	554.5	RV, SP				22.35	526.4	RV, SP
			19.6	380.5	RV, SP				21.55	343.2	RV, SP				22.35	542.7	LV, SP
			19.6	471.4	LV, SP				21.55	331.3	RV, SP				22.35	411.9	RV, SP
			19.6	403.9	LV, SP				21.55	302.9	RV, SP				22.35	443.6	LV, SP
			19.6	394.1	LV, SP				21.55	354.3	LV, SP				22.35	335.1	LV, SP
			19.6	443.3	RV, SP				21.55	319.6	RV, SP				22.35	218.2	LV, SP
			19.6	396.0	LV, SP				21.55	295.2	LV, SP				22.35	326.2	LV, SP
			19.6	408.6	RV, SP				21.55	327.1	LV, SP				22.35	364.0	LV, SP
			19.6	383.5	LV, SP				21.55	360.7	SB				22.35	367.2	LV, SP
			19.6	460.6	RV, SP				21.55	382.0	LV, SP				22.35	283.0	LV, SP
			19.6	366.9	RV, SP				21.55	282.8	RV, SP				22.35	345.0	LV, SP
			19.6	460.6	RV, SP				21.55	304.6	RV, SP				22.35	316.3	LV, SP
			19.6	395.9	RV, SP				21.55	321.3	LV, SP				22.35	461.9	LV, SP
			19.6	406.9	RV, SP				21.55	367.5	RV, SP				22.35	300.3	RV, SP
			19.6	381.8	LV, SP				21.55	385.5	RV, SP				22.35	314.1	LV, SP
			19.6	466.8	LV, SP				21.55	364.8	RV, SP				22.35	309.7	LV, SP
			19.6	453.9	RV, SP				21.55	408.3	LV, SP				22.35	389.2	RV, SP
			19.6	398.3	RV, SP				21.55	392.8	RV, SP				22.35	315.5	RV, SP
			19.6	416.0	RV, SP				21.55	329.9	RV, SP				22.35	386.1	LV, SP
			19.6	398.2	RV, SP				21.55	377.4	RV, SP				22.35	351.2	LV, SP
			19.6	467.6	RV, SP				21.55	339.8	LV, SP				22.35	372.0	LV, SP
			19.6	433.3	RV, SP				21.55	357.2	RV, SP				22.35	304.9	LV, SP
			19.6	410.9	RV, SP				21.55	328.4	LV, SP				22.35	546.1	LV, SP
			19.6	444.2	RV, SP				21.55	360.0	RV, SP				22.35	368.9	LV, SP
			19.6	400.1	RV, SP				21.55	330.3	LV, SP				22.35	352.3	LV, SP
			19.6	371.3	RV, SP				21.55	362.4	RV, SP				22.35	190.5	LV, SP
			19.6	411.2	RV, SP				21.55	287.1	LV, SP				22.35	272.9	RV, SP
			19.6	454.1	RV, SP				21.55	357.9	LV, SP				22.35	386.6	RV, SP

B77
A

(D)						<i>O. aspinata</i>											
Zone	Subzone	Bed N.	Bed H.	Geometric shell size	Shell pres.	Zone	Subzone	Bed N.	Bed H.	Geometric shell size	Shell pres.	Zone	Subzone	Bed N.	Bed H.	Geometric shell size	Shell pres.
			19.6	411.8	RV, SP				21.55	424.8	RV, SP				22.35	266.9	RV, SP
			19.6	375.8	SB				21.55	340.5	LV, SP				22.35	267.5	LV, SP
			19.6	450.9	RV, SP				21.55	352.1	RV, SP				22.35	334.1	RV, SP
			19.6	388.6	RV, SP				21.55	283.3	RV, SP				22.35	449.4	LV, SP
			19.6	456.6	RV, SP				21.55	381.3	RV, SP				22.35	262.2	LV, SP
			19.6	433.5	LV, SP				21.55	354.1	RV, SP				22.35	235.8	RV, SP
			19.6	441.8	RV, SP				21.55	259.7	RV, SP				22.35	248.7	LV, SP
			19.6	457.2	RV, SP				21.55	354.2	LV, SP				22.35	232.9	LV, SP
			19.6	392.8	RV, SP				21.55	323.2	RV, SP				22.35	185.9	LV, SP
			19.87	457.4	LV, SP				21.55	349.5	LV, SP				22.35	440.2	LV, SP
			19.87	442.5	RV, SP				21.55	260.6	LV, SP				22.35	432.1	LV, SP
			19.87	450.1	LV, SP				21.55	305.2	RV, SP				22.35	439.8	RV, SP
			19.87	476.7	LV, SP				21.55	355.7	RV, SP				22.35	451.2	RV, SP
			19.87	459.1	LV, SP				21.55	259.1	RV, SP				22.35	525.1	LV, SP
			19.87	464.1	RV, SP				21.55	230.6	RV, SP				22.35	498.8	LV, SP
			19.87	406.5	RV, SP				21.55	263.5	RV, SP				22.35	426.4	RV, SP
			19.87	448.4	LV, SP				21.55	266.2	RV, SP				22.35	451.5	RV, SP
			19.87	501.5	RV, SP				21.55	250.4	RV, SP				22.35	432.2	RV, SP
			19.87	481.0	RV, SP				21.55	228.7	RV, SP				22.35	440.5	LV, SP
			19.87	438.2	RV, SP				21.55	421.5	RV, SP				22.35	550.1	LV, SP
			19.87	375.1	RV, SP				21.55	250.4	RV, SP				22.35	538.8	RV, SP
			19.87	388.5	RV, SP				21.55	231.4	LV, SP				22.35	304.1	LV, SP
			19.87	363.3	RV, SP				21.55	225.5	RV, SP				22.35	476.6	LV, SP
		B63	19.87	392.4	LV, SP				21.55	224.3	RV, SP				22.35	424.3	RV, SP
			19.87	366.3	LV, SP				21.55	236.4	LV, SP				22.35	450.5	LV, SP
			19.87	462.2	RV, SP				21.55	300.4	RV, SP				22.35	479.9	LV, SP
			19.87	373.5	RV, SP				21.55	230.8	RV, SP				22.35	503.0	LV, SP
			19.87	377.7	RV, SP				21.55	187.6	RV, SP				22.35	443.8	RV, SP
			19.87	322.6	RV, SP				21.55	250.4	LV, SP				22.35	434.5	LV, SP
			19.87	416.2	RV, SP				21.55	409.3	RV, SP				22.35	392.2	RV, SP
			19.87	443.2	LV, SP				21.55	221.7	RV, SP				22.35	402.5	LV, SP
			19.87	458.1	RV, SP				21.55	405.7	RV, SP				22.35	369.8	RV, SP
			19.87	482.9	LV, SP				21.55	402.7	RV, SP				22.35	452.3	RV, SP
			19.87	498.9	LV, SP				21.55	399.4	LV, SP				22.35	577.7	RV, SP
			19.87	415.0	LV, SP				21.55	375.2	LV, SP				22.35	410.3	RV, SP
			19.87	442.5	RV, SP				21.55	398.9	LV, SP				22.35	450.4	RV, SP
			19.87	455.1	RV, SP				21.55	496.6	RV, SP				22.35	377.2	RV, SP
			19.87	460.7	LV, SP				21.55	550.7	RV, SP				22.35	505.6	LV, SP
			19.87	394.7	RV, SP				21.55	500.7	LV, SP				22.35	441.5	LV, SP

(D)						<i>O. aspinata</i>												
Zone	Subzone	Bed N.	Bed H.	Geometric shell size	Shell pres.	Zone	Subzone	Bed N.	Bed H.	Geometric shell size	Shell pres.	Zone	Subzone	Bed N.	Bed H.	Geometric shell size	Shell pres.	
			19.87	488.0	RV, SP				21.55	444.6	RV, SP					22.35	429.5	LV, SP
			19.87	431.7	LV, SP				21.55	417.0	RV, SP					22.35	464.4	LV, SP
			19.87	415.3	LV, SP				21.55	392.6	RV, SP					22.35	485.9	RV, SP
			19.87	400.2	LV, SP				21.55	482.2	RV, SP					22.35	395.6	RV, SP
			19.87	511.9	LV, SP				21.55	399.2	RV, SP					22.35	415.1	LV, SP
			19.87	402.7	LV, SP				21.55	427.3	LV, SP					22.35	477.4	RV, SP
			19.87	423.3	RV, SP				21.55	462.5	LV, SP					22.35	389.4	RV, SP
			19.87	503.9	RV, SP				21.55	386.0	RV, SP					22.35	412.6	RV, SP
			19.87	421.1	RV, SP				21.55	482.8	LV, SP					22.35	479.4	LV, SP
			19.87	449.8	LV, SP				21.55	392.1	RV, SP					22.35	451.1	RV, SP
			19.87	464.9	RV, SP				21.55	541.3	LV, SP					22.35	459.4	LV, SP
			19.87	460.6	RV, SP				21.55	541.7	LV, SP					22.35	448.4	RV, SP
			19.87	488.6	LV, SP				21.55	386.2	RV, SP					22.35	539.4	RV, SP
			19.87	452.1	RV, SP				21.55	531.3	RV, SP					22.35	526.6	LV, SP
			19.87	481.4	RV, SP				21.55	512.2	LV, SP					22.35	382.2	RV, SP
			19.87	447.9	LV, SP				21.55	477.9	LV, SP					22.35	369.0	RV, SP
			19.87	433.0	LV, SP				21.55	496.7	RV, SP					22.35	360.4	RV, SP
			19.87	436.0	RV, SP				21.55	402.2	RV, SP					22.35	360.6	LV, SP
			19.87	413.4	RV, SP				21.55	399.9	RV, SP					22.35	307.9	LV, SP
			19.87	377.9	LV, SP				21.55	402.9	RV, SP					22.35	380.6	LV, SP
			19.87	423.0	LV, SP				21.55	509.6	RV, SP					22.35	279.1	LV, SP
			19.87	488.5	RV, SP				21.55	556.5	RV, SP					22.35	352.1	RV, SP
			19.87	442.9	LV, SP				21.55	478.3	LV, SP					22.35	354.0	LV, SP
			19.87	432.1	LV, SP				21.55	427.9	RV, SP					22.35	308.2	RV, SP
			19.87	498.2	RV, SP				21.55	526.7	RV, SP					22.35	320.6	LV, SP
			19.87	470.5	RV, SP				21.55	410.0	RV, SP					22.35	311.4	LV, SP
			19.87	460.5	SB				21.55	419.2	LV, SP					22.35	385.6	LV, SP
			19.87	461.0	RV, SP				21.55	436.8	RV, SP					22.35	318.8	RV, SP
			19.87	474.3	RV, SP				21.55	511.8	LV, SP					22.35	383.4	LV, SP
			19.87	443.6	RV, SP				21.55	430.5	LV, SP					22.35	362.6	LV, SP
			19.87	479.1	LV, SP				21.55	544.6	LV, SP					22.35	369.0	LV, SP
			19.87	452.6	LV, SP				21.55	457.2	RV, SP					22.35	342.9	RV, SP
			19.87	472.6	LV, SP				21.55	393.0	RV, SP					22.35	383.0	RV, SP
			19.87	447.6	RV, SP				21.55	526.8	RV, SP					22.35	304.5	LV, SP
			19.87	396.5	RV, SP				21.55	441.5	RV, SP					22.35	307.9	RV, SP
			19.87	391.7	LV, SP				21.55	490.3	RV, SP					24.3	323.1	RV, SP
			19.87	436.2	RV, SP				21.55	396.0	RV, SP					24.3	479.3	RV, SP
			19.87	477.0	LV, SP				21.55	500.5	RV, SP					24.3	461.1	LV, SP
			19.87	469.6	RV, SP				21.55	404.7	RV, SP					24.3	443.8	LV, SP

(D)						<i>O. aspinata</i>											
Zone	Subzone	Bed N.	Bed H.	Geometric shell size	Shell pres.	Zone	Subzone	Bed N.	Bed H.	Geometric shell size	Shell pres.	Zone	Subzone	Bed N.	Bed H.	Geometric shell size	Shell pres.
			19.87	493.2	RV, SP				21.55	494.3	RV, SP				24.3	385.0	LV, SP
			19.87	491.1	RV, SP				21.55	518.2	RV, SP				24.3	438.8	RV, SP
			19.87	466.1	RV, SP				21.55	513.1	RV, SP				24.3	416.8	LV, SP
			19.87	367.7	RV, SP				21.55	493.8	LV, SP				24.3	494.1	RV, SP
			19.87	409.3	RV, SP				21.55	482.6	RV, SP				24.3	382.3	RV, SP
			19.87	304.3	RV, SP				21.55	435.5	LV, SP				24.3	438.4	LV, SP
			19.87	354.8	RV, SP				21.55	387.4	LV, SP				24.3	508.0	LV, SP
			19.87	254.1	LV, SP				21.55	435.4	LV, SP				24.3	486.8	RV, SP
			19.87	401.0	LV, SP				21.55	377.8	RV, SP				24.3	431.4	LV, SP
			19.87	392.2	RV, SP				21.75	437.8	LV, SP				24.3	461.1	RV, SP
			19.87	380.1	RV, SP				21.75	517.1	LV, SP				24.3	379.1	LV, SP
			19.87	395.0	RV, SP				21.75	471.2	LV, SP				24.3	497.6	RV, SP
			19.87	436.6	RV, SP				21.75	498.0	RV, SP				24.3	484.1	LV, SP
			19.87	357.8	LV, SP				21.75	558.9	LV, SP				24.3	451.4	LV, SP
			20.95	337.5	LV, SP				21.75	421.5	LV, SP				24.3	386.0	LV, SP
			20.95	438.3	LV, SP				21.75	415.6	RV, SP				24.3	433.4	RV, SP
			20.95	461.5	RV, SP				21.75	557.5	RV, SP				24.3	478.9	RV, SP
			20.95	444.8	RV, 3				21.75	502.8	LV, SP				24.3	548.3	RV, SP
			20.95	429.0	RV, SP				21.75	360.7	LV, SP				24.3	344.6	RV, SP
			20.95	397.4	LV, SP				21.75	339.2	RV, SP				24.3	327.4	RV, SP
			20.95	503.1	RV, SP				21.75	298.2	RV, SP				24.3	351.2	LV, SP
			20.95	545.8	RV, SP				21.75	381.7	RV, SP				24.3	355.8	LV, SP
			20.95	405.3	LV, SP				21.75	265.4	LV, SP				24.3	340.6	LV, SP
			20.95	359.2	LV, SP				21.75	306.3	RV, SP				24.3	272.6	RV, SP
			20.95	311.0	RV, SP			B74	21.75	381.5	RV, SP				24.3	351.8	LV, SP
			20.95	368.5	RV, SP			A	21.75	369.7	RV, SP				24.3	442.3	RV, SP
		B67	20.95	327.7	RV, SP				21.75	272.8	LV, SP				24.3	314.5	RV, SP
			20.95	387.3	RV, SP				21.75	430.4	LV, SP				24.3	318.2	RV, SP
			20.95	388.5	LV, SP				21.75	363.6	RV, SP				24.3	302.4	RV, SP
			20.95	295.5	LV, SP				21.75	310.9	RV, SP				24.3	260.5	RV, SP
			20.95	419.4	RV, SP				21.75	336.1	RV, SP				24.3	374.3	RV, SP
			20.95	340.3	RV, SP				21.75	371.0	RV, SP				24.3	446.3	LV, SP
			20.95	480.0	LV, SP				21.75	303.0	RV, SP				24.3	448.3	RV, SP
			20.95	468.9	RV, SP				21.75	392.3	RV, SP				24.3	372.5	RV, SP
			20.95	533.5	RV, SP				21.75	394.4	RV, SP				24.3	323.8	RV, SP
			20.95	426.2	LV, SP				21.75	346.2	LV, SP				24.3	362.3	RV, SP
			20.95	402.9	RV, SP				21.75	341.9	RV, SP				24.3	331.6	LV, SP
			20.95	290.8	LV, SP				21.75	305.9	RV, SP				24.3	300.5	RV, SP
			20.95	481.8	LV, SP				21.75	352.5	LV, SP				24.3	250.4	LV, SP

(D)																	
<i>O. aspinata</i>																	
Zone	Subzone	Bed N.	Bed H.	Geometric shell size	Shell pres.	Zone	Subzone	Bed N.	Bed H.	Geometric shell size	Shell pres.	Zone	Subzone	Bed N.	Bed H.	Geometric shell size	Shell pres.
			20.95	445.6	LV, SP				21.75	377.4	RV, SP				24.3	233.4	LV, SP
			20.95	533.2	LV, SP				21.75	341.3	LV, SP				24.3	204.1	RV, SP
			20.95	512.6	SB				21.75	350.9	LV, SP				24.3	521.2	LV, SP
			20.95	466.3	SB				21.75	471.3	LV, SP				24.3	204.7	LV, SP
			20.95	403.2	LV, SP				21.75	392.0	LV, SP				24.3	433.5	RV, SP
			20.95	411.0	RV, SP				21.75	349.2	LV, SP				24.3	394.1	LV, SP
			20.95	504.2	RV, SP				21.75	386.9	RV, SP				24.3	494.8	RV, SP
			20.95	388.4	RV, SP				21.75	376.9	RV, SP				24.3	465.7	RV, SP
			20.95	385.6	LV, SP				21.75	278.9	RV, SP				24.3	431.8	RV, SP
			20.95	539.4	RV, SP				21.75	214.0	RV, SP				24.3	373.3	RV, SP
			20.95	475.9	LV, SP				21.75	221.1	RV, SP				24.3	482.6	LV, SP
			20.95	470.0	RV, SP				21.75	383.0	LV, SP				24.3	467.7	LV, SP
			20.95	452.7	LV,, SB				21.75	392.0	LV, SP				24.3	355.5	LV, SP
			20.95	454.5	RV, SP				21.75	575.7	LV, SP				24.3	394.3	LV, SP
			20.95	517.9	LV, SP				21.75	391.8	LV, SP				24.3	405.9	RV, SP
			20.95	404.6	RV, SP				21.75	430.7	LV, SP				24.3	446.9	RV, SP
			20.95	398.2	RV, SP				21.75	420.2	LV, SP				24.3	406.1	RV, SP
			20.95	521.6	LV, SP				21.75	468.1	RV, SP				24.3	343.3	LV, SP
			20.95	395.8	RV, SP				21.75	465.6	RV, SP				24.3	365.4	LV, SP
			20.95	424.6	RV, SP				21.75	487.8	RV, SP				24.3	373.7	RV, SP
			20.95	572.1	RV, SP				21.75	366.6	RV, SP				24.3	411.9	RV, SP
			20.95	450.9	LV, SP				21.75	501.2	RV, SP				24.3	363.8	LV, SP
			20.95	435.2	LV, SP				21.75	471.8	LV, SP				24.3	468.8	RV, SP
			20.95	403.3	RV, SP				21.75	519.9	SB				24.3	476.2	RV, SP
			20.95	563.0	LV, SP				21.75	438.3	LV, SP				24.3	462.8	RV, SP
			20.95	456.8	RV, SP				21.75	597.1	LV, SP				24.3	367.6	LV, SP
			20.95	475.7	RV, SP				21.75	407.3	LV, SP				24.3	450.1	LV, SP
			20.95	422.0	RV, SP				21.75	402.5	RV, SP				24.3	378.3	RV, SP
			20.95	464.5	RV, SP				21.75	590.4	RV, SP				24.3	350.5	RV, SP
			20.95	442.0	LV, SP				21.75	436.2	LV, SP				24.3	371.7	RV, SP
			20.95	584.1	RV, SP				21.75	393.2	RV, SP				24.3	459.2	LV, SP
			20.95	422.7	RV, SP				21.75	438.5	LV, SP				24.3	540.3	LV, SP
			20.95	381.5	LV, SP				21.75	501.4	LV, SP				24.3	429.0	RV, SP
			20.95	360.1	RV, SP				21.75	450.9	RV, SP				24.3	454.8	LV, SP
			20.95	372.6	RV, SP				21.75	542.3	RV, SP				24.3	388.2	RV, SP
			20.95	395.8	LV, SP				21.75	450.9	RV, SP				24.3	420.9	RV, SP
			20.95	398.8	RV, SP				21.75	446.8	RV, SP				24.3	423.8	LV, SP
			20.95	387.5	RV, SP				21.75	597.0	SB				24.3	435.6	RV, SP
			20.95	380.9	RV, SP				21.75	361.2	LV, SP				24.3	479.6	RV, SP

(D)						<i>O. aspinata</i>											
Zone	Subzone	Bed N.	Bed H.	Geometric shell size	Shell pres.	Zone	Subzone	Bed N.	Bed H.	Geometric shell size	Shell pres.	Zone	Subzone	Bed N.	Bed H.	Geometric shell size	Shell pres.
			20.95	308.1	RV, SP				21.75	395.5	LV, SP				24.3	492.3	RV, SP
			20.95	385.9	RV, SP				21.75	480.5	RV, SP				24.3	462.8	RV, SP
			20.95	403.5	LV, SP				21.75	523.1	SB				24.3	426.2	LV, SP
			20.95	386.4	LV, SP				21.75	466.7	RV, SP				24.3	476.1	RV, SP
			20.95	393.6	LV, SP				21.75	423.1	LV, SP				24.3	389.8	RV, SP
			20.95	340.6	LV, SP				21.75	429.3	RV, SP				24.3	479.7	LV, SP
			20.95	340.9	LV, SP				21.75	541.7	LV, SP				24.3	436.7	RV, SP
			20.95	368.6	LV, SP				21.75	414.3	RV, SP				24.3	463.7	RV, SP
			20.95	402.1	RV, SP				21.75	425.4	LV, SP				24.3	410.9	RV, SP
			20.95	399.8	RV, SP				21.75	584.7	RV, SP				24.3	387.5	RV, SP
			20.95	371.6	RV, SP				21.75	356.5	LV, SP				24.3	465.2	RV, SP
			20.95	398.0	LV, SP				21.75	328.4	RV, SP				24.3	372.0	RV, SP
			20.95	400.9	RV, SP				21.75	305.5	RV, SP				24.3	367.9	LV, SP
			20.95	374.5	RV, SP				21.75	307.6	LV, SP				24.3	427.8	LV, SP
			20.95	383.6	LV, SP				21.75	338.0	RV, SP				24.3	415.2	LV, SP
			21.15	385.1	RV, SP				21.75	331.0	RV, SP				24.3	425.3	RV, SP
			21.15	444.3	RV, SP				21.75	340.5	RV, SP				24.3	453.9	LV, SP
			21.15	449.1	RV, SP				21.75	391.9	LV, SP				24.3	491.0	RV, SP
			21.15	414.7	LV, SP				21.75	353.9	LV, SP				24.3	436.3	RV, SP
			21.15	489.7	SB				21.75	297.0	RV, SP				24.3	415.0	LV, SP
			21.15	477.3	SB				21.75	396.7	RV, SP				24.3	506.8	RV, SP
			21.15	509.1	LV, SP				21.75	292.8	RV, SP				24.3	503.2	RV, SP
			21.15	459.5	LV, SP				21.75	300.4	RV, SP				24.3	493.6	RV, SP
			21.15	420.5	LV, SP				21.75	337.9	RV, SP				24.3	514.0	RV, SP
			21.15	399.7	LV, SP				21.75	299.2	RV, SP				24.3	424.1	RV, SP
			21.15	444.0	RV, SP				21.75	371.6	RV, SP				24.3	436.4	RV, SP
		B69	21.15	466.9	LV, SP				21.75	317.7	RV, SP				24.3	403.1	RV, SP
			21.15	508.1	LV, SP				21.75	284.5	LV, SP				24.3	420.7	RV, SP
			21.15	425.4	RV, SP				21.75	310.4	LV, SP				24.3	402.6	RV, SP
			21.15	535.9	RV, SP				21.75	387.0	RV, SP				24.3	429.1	LV, SP
			21.15	475.1	LV, SP				21.75	377.4	RV, SP				24.3	487.7	RV, SP
			21.15	421.3	RV, SP				21.75	381.4	RV, SP				24.3	447.5	RV, SP
			21.15	455.2	RV, SP				21.75	286.0	RV, SP				24.3	360.4	LV, SP
			21.15	482.4	SB				21.75	333.1	LV, SP				24.3	432.5	LV, SP
			21.15	542.8	RV, SP				21.75	343.1	LV, SP				24.3	379.9	LV, SP
			21.15	424.0	LV, SP				21.75	372.1	RV, SP				24.3	370.2	RV, SP
			21.15	386.6	RV, SP				21.75	297.1	LV, SP				24.3	543.4	RV, SP
			21.15	541.7	RV, SP				21.75	411.1	LV, SP				24.3	418.7	RV, SP
			21.15	516.4	LV, SP				21.75	357.0	LV, SP				24.3	442.9	RV, SP

(D)																	
<i>O. aspinata</i>																	
Zone	Subzone	Bed N.	Bed H.	Geometric shell size	Shell pres.	Zone	Subzone	Bed N.	Bed H.	Geometric shell size	Shell pres.	Zone	Subzone	Bed N.	Bed H.	Geometric shell size	Shell pres.
			21.15	414.8	RV, SP				21.95	354.0	LV, SP				24.3	374.1	RV, SP
			21.15	425.6	RV, SP				21.95	459.2	RV, SP				24.3	377.2	LV, SP
			21.15	417.8	LV, SP				21.95	375.0	LV, SP				24.3	398.7	RV, SP
			21.15	429.9	RV, SP				21.95	473.2	LV, SP				24.3	398.5	LV, SP
			21.15	460.9	RV, SP				21.95	425.5	RV, SP				24.3	539.7	LV, SP
			21.15	448.7	LV, SP				21.95	406.6	LV, SP				24.3	390.5	RV, SP
			21.15	507.5	LV, SP				21.95	433.8	RV, SP				25.25	481.4	RV, SP
			21.15	366.8	RV, SP				21.95	528.0	LV, SP				25.25	442.5	RV, SP
			21.15	348.7	SB				21.95	479.8	LV, SP				25.25	395.7	LV, SP
			21.15	346.1	RV, SP				21.95	384.9	RV, SP				25.25	434.0	LV, SP
			21.15	420.4	LV, SP				21.95	460.3	LV, SP				25.25	393.9	LV, SP
			21.15	316.8	RV, SP				21.95	371.6	LV, SP				25.25	394.3	RV, SP
			21.15	319.1	RV, SP				21.95	322.0	RV, SP				25.25	472.2	RV, SP
			21.15	343.4	LV, SP				21.95	377.7	LV, SP				25.25	390.3	RV, SP
			21.15	529.9	RV, SP				21.95	386.3	LV, SP				25.25	406.1	RV, SP
			21.15	250.5	RV, SP				21.95	376.4	LV, SP				25.25	432.3	RV, SP
			21.15	374.5	LV, SP				21.95	297.8	LV, SP				25.25	439.0	RV, SP
			21.15	356.6	LV, SP				21.95	377.4	RV, SP				25.25	556.0	RV, SP
			21.15	331.6	LV, SP				21.95	370.6	LV, SP				25.25	489.0	RV, SP
			21.15	350.2	LV, SP			B75	21.95	350.0	RV, SP				25.25	570.9	RV, SP
			21.15	363.1	LV, SP			A	21.95	291.5	RV, SP				25.25	489.9	RV, SP
			21.15	375.4	RV, SP				21.95	374.7	LV, SP				25.25	483.2	RV, SP
			21.15	428.5	LV, SP				21.95	350.4	LV, SP				25.25	483.2	RV, SP
			21.15	295.0	LV, SP				21.95	304.6	LV, SP				25.25	535.2	LV, SP
			21.15	340.1	RV, SP				21.95	321.9	RV, SP				25.25	368.2	RV, SP
			21.15	394.0	LV, SP				21.95	372.8	LV, SP				25.25	361.4	LV, SP
			21.15	362.4	LV, SP				21.95	289.5	RV, SP				25.25	527.6	RV, SP
			21.15	310.4	RV, SP				21.95	372.8	RV, SP				25.25	375.0	RV, SP
			21.15	391.9	RV, SP				21.95	351.4	RV, SP				25.25	297.5	LV, SP
			21.15	490.4	RV, SP				21.95	339.0	RV, SP				25.25	350.4	LV, SP
			21.15	413.5	RV, SP				21.95	376.5	RV, SP				25.25	391.7	RV, SP
			21.15	346.9	LV, SP				21.95	452.3	LV, SP				25.25	318.1	RV, SP
			21.15	269.4	LV, SP				21.95	369.2	RV, SP				25.25	472.7	RV, SP
			21.15	219.3	LV, SP				21.95	371.9	LV, SP				25.25	371.8	LV, SP
			21.15	219.4	LV, SP				21.95	358.1	LV, SP				25.25	380.5	RV, SP
			21.15	193.8	RV, SP				21.95	365.8	RV, SP				25.25	322.8	RV, SP
			21.15	232.8	RV, SP				21.95	320.9	RV, SP				25.25	390.5	RV, SP
			21.15	447.0	RV, SP				21.95	402.4	RV, SP				25.25	358.4	LV, SP
			21.15	480.6	LV, SP				21.95	357.4	LV, SP				25.25	256.3	RV, SP
															25.25	320.1	LV, SP

(D)						<i>O. aspinata</i>											
Zone	Subzone	Bed N.	Bed H.	Geometric shell size	Shell pres.	Zone	Subzone	Bed N.	Bed H.	Geometric shell size	Shell pres.	Zone	Subzone	Bed N.	Bed H.	Geometric shell size	Shell pres.
			21.15	491.5	LV, SP				21.95	362.6	RV, SP				25.25	406.3	RV, SP
			21.15	414.7	RV, SP				21.95	234.3	SB				25.25	335.2	LV, SP
			21.15	502.8	LV, SP				21.95	261.6	LV, SP				25.25	329.6	LV, SP
			21.15	393.0	LV, SP				21.95	204.9	RV, SP				25.25	382.6	LV, SP
			21.15	392.2	LV, SP				21.95	301.3	LV, SP				25.25	382.9	LV, SP
			21.15	477.9	LV, SP				21.95	259.2	LV, SP				25.25	370.9	RV, SP
			21.15	467.7	LV, SP				21.95	404.1	LV, SP				25.25	324.6	LV, SP
			21.15	484.1	RV, SP				21.95	444.1	LV, SP				25.25	345.0	LV, SP
			21.15	459.1	RV, SP				21.95	374.3	RV, SP				25.25	331.6	RV, SP
			21.15	427.5	RV, SP				21.95	432.9	RV, SP				25.25	311.9	RV, SP
			21.15	537.1	LV, SP				21.95	514.4	LV, SP				25.25	356.9	RV, SP
			21.15	443.7	LV, SP				21.95	421.7	LV, SP				25.25	482.1	RV, SP
			21.15	468.3	RV, SP				21.95	409.9	LV, SP				25.25	314.6	SB
			21.15	413.6	LV, SP				21.95	437.2	LV, SP				25.25	344.1	RV, SP
			21.15	386.8	RV, SP				21.95	449.5	RV, SP				25.25	362.5	RV, SP
			21.15	377.8	LV, SP				21.95	429.5	LV, SP				25.25	375.7	RV, SP
			21.15	486.6	RV, SP				21.95	389.8	RV, SP				25.25	319.0	RV, SP
			21.15	426.3	LV, SP				21.95	411.7	LV, SP				25.25	306.2	RV, SP
			21.15	363.0	RV, SP				21.95	450.8	RV, SP				25.25	316.6	RV, SP
			21.15	389.4	RV, SP				21.95	414.6	LV, SP				25.25	156.5	LV, SP
			21.15	458.7	LV, SP				21.95	406.3	LV, SP				25.25	247.6	RV, SP
			21.15	495.4	LV, SP				21.95	391.1	RV, SP				25.25	442.4	LV, SP
			21.15	500.0	RV, SP				21.95	570.1	LV, SP				25.25	254.1	RV, SP
			21.15	495.6	LV, SP				21.95	399.2	RV, SP				25.25	254.8	RV, SP
			21.15	464.7	RV, SP				21.95	452.8	RV, SP				25.25	269.7	LV, SP
			21.15	516.5	RV, SP				21.95	381.3	RV, SP				25.25	188.7	LV, SP
			21.15	428.2	LV, SP				21.95	444.0	RV, SP				25.25	391.7	RV, SP
			21.15	460.5	RV, SP				21.95	442.9	RV, SP				25.25	416.0	LV, SP
			21.15	420.9	LV, SP				21.95	374.9	RV, SP				25.25	402.0	RV, SP
			21.15	418.4	RV, SP				21.95	358.6	SB				25.25	572.1	LV, SP
			21.15	474.2	LV, SP				21.95	376.7	LV, SP				25.25	435.9	LV, SP
			21.15	443.8	LV, SP				21.95	439.1	RV, SP				25.25	555.0	RV, SP
			21.15	515.3	RV, SP				21.95	597.5	LV, SP				25.25	516.4	RV, SP
			21.15	459.7	LV, SP				21.95	439.1	LV, SP				25.25	413.0	LV, SP
			21.15	496.2	RV, SP				21.95	379.8	LV, SP				25.25	612.3	LV, SP
			21.15	494.6	RV, SP				21.95	416.1	RV, SP				25.25	480.5	RV, SP
			21.15	422.7	RV, SP				21.95	417.1	RV, SP				25.25	550.9	LV, SP
			21.15	432.0	RV, SP				21.95	454.0	LV, SP				25.25	515.8	LV, SP
			21.15	392.6	RV, SP				21.95	350.3	RV, SP				25.25	452.2	LV, SP

(D)						<i>O. aspinata</i>											
Zone	Subzone	Bed N.	Bed H.	Geometric shell size	Shell pres.	Zone	Subzone	Bed N.	Bed H.	Geometric shell size	Shell pres.	Zone	Subzone	Bed N.	Bed H.	Geometric shell size	Shell pres.
			21.15	514.4	LV, SP				21.95	399.5	RV, SP				25.25	412.7	LV, SP
			21.15	473.9	RV, SP				21.95	357.0	LV, SP				25.25	375.6	RV, SP
			21.15	448.6	LV, SP				21.95	406.8	RV, SP				25.25	407.7	RV, SP
			21.15	474.1	RV, SP				21.95	392.1	RV, SP				25.25	491.3	RV, SP
			21.15	413.9	RV, SP				21.95	387.8	RV, SP				25.25	436.6	LV, SP
			21.15	444.3	RV, SP				21.95	411.7	RV, SP				25.25	555.0	RV, SP
			21.15	440.6	RV, SP				21.95	402.8	LV, SP				25.25	414.7	LV, SP
			21.15	452.3	RV, SP				21.95	385.8	LV, SP				25.25	623.4	RV, SP
			21.15	444.8	LV, SP				21.95	348.8	LV, SP				25.25	497.8	RV, SP
			21.15	559.9	RV, SP				21.95	357.2	RV, SP				25.25	512.1	RV, SP
			21.15	484.9	LV, SP				21.95	259.7	LV, SP				25.25	429.9	RV, SP
			21.15	476.5	RV, SP				21.95	372.5	LV, SP				25.25	404.8	RV, SP
			21.15	555.4	RV, SP				21.95	379.6	RV, SP				25.25	382.6	RV, SP
			21.15	424.2	RV, SP				21.95	346.4	RV, SP				25.25	493.0	RV, SP
			21.15	438.4	RV, SP				21.95	382.1	LV, SP				25.25	414.8	RV, SP
			21.15	491.5	RV, SP				21.95	355.9	RV, SP				25.25	562.5	RV, SP
			21.15	436.6	RV, SP				21.95	355.7	LV, SP				25.25	525.6	RV, SP
			21.15	492.8	LV, SP				21.95	322.5	LV, SP				25.25	409.9	LV, SP
			21.15	490.3	RV, SP				21.95	347.0	RV, SP				25.25	467.3	LV, SP
			21.15	489.4	RV, SP				21.95	335.9	LV, SP				25.25	426.6	RV, SP
			21.15	427.9	RV, SP				21.95	379.5	LV, SP				25.25	522.3	RV, SP
			21.15	536.5	RV, SP				21.95	330.3	RV, SP				25.25	491.1	RV, SP
			21.15	457.4	RV, SP				21.95	349.6	LV, SP				25.25	434.9	RV, SP
			21.15	449.9	RV, SP				21.95	355.4	LV, SP				25.25	594.3	LV, SP
			21.15	478.8	LV, SP				21.95	390.5	RV, SP				25.25	491.0	RV, SP
			21.15	504.0	RV, SP				21.95	354.2	RV, SP				25.25	617.0	RV, SP
			21.15	486.6	RV, SP				21.95	326.7	RV, SP				25.25	514.2	RV, SP
			21.15	425.5	LV, SP				21.95	371.6	RV, SP				25.25	508.5	LV, SP
			21.15	480.9	RV, SP				21.95	374.3	LV, SP				25.25	525.6	RV, SP
			21.15	387.7	LV, SP				21.95	363.6	RV, SP				25.25	454.5	LV, SP
			21.15	447.4	LV, SP				21.95	368.1	RV, SP				25.25	429.3	RV, SP
									21.95	364.7	RV, SP				25.25	626.6	RV, SP
									21.95	290.4	RV, SP				25.25	515.5	LV, SP
									21.95	343.6	RV, SP				25.25	638.6	RV, SP
															25.25	403.7	RV, SP
															25.25	501.4	RV, SP
															25.25	635.0	RV, SP
															25.25	567.5	LV, SP
															25.25	468.4	LV, SP

(D)						<i>O. aspinata</i>												
Zone	Subzone	Bed N.	Bed H.	Geometric shell size	Shell pres.	Zone	Subzone	Bed N.	Bed H.	Geometric shell size	Shell pres.	Zone	Subzone	Bed N.	Bed H.	Geometric shell size	Shell pres.	
																25.25	510.1	LV, SP
																25.25	430.3	LV, SP
																25.25	389.7	RV, SP
																25.25	404.6	LV, SP
																25.25	488.8	LV, SP
																25.25	462.9	LV, SP
																25.25	495.3	RV, SP
																25.25	501.5	LV, SP
																25.25	409.8	RV, SP
																25.25	482.3	LV, SP
																25.25	470.3	RV, SP
																25.25	451.1	LV, SP
																25.25	377.3	RV, SP
																25.25	511.7	RV, SP
																25.25	411.5	RV, SP
																25.25	407.1	RV, SP
																25.25	495.2	RV, SP
																25.25	426.6	RV, SP
																25.25	497.3	LV, SP
																25.25	419.3	LV, SP
																25.25	443.3	LV, SP
																25.25	271.1	LV, SP

(E)											
<i>O. aspinata</i>											
Zone	Subzone	Bed N.	Bed height	Geometric shell size	Shell preservation	Zone	Subzone	Bed N.	Bed height	Geometric shell size	Shell preservation
bucklandi Zone	Metophioceras conybeari subzone	B95	25.64	457.6	LV, SP	bucklandi Zone	Metophioceras conybeari subzone	B97	26.15	499.7	RV, SP
			25.64	391.6	RV, SP				26.15	561.7	RV, SP
			25.64	371.5	LV, SP				26.15	518.9	RV, SP
			25.64	502.7	LV, SP				26.15	428.3	LV, SP
			25.64	359.0	SB				26.15	412.1	RV, SP
			25.64	461.5	RV, SP				26.15	410.6	RV, SP
			25.64	262.4	RV, SP				26.15	369.1	LV, SP
			25.64	309.8	RV, SP				26.15	377.7	LV, SP
			25.64	360.0	LV, SP				26.15	464.5	RV, SP
			25.64	291.7	LV, SP				26.15	516.5	LV, SP
			25.64	348.7	RV, SP				26.15	422.0	LV, SP
			25.64	259.1	RV, SP				26.15	502.3	LV, SP
			25.64	338.6	LV, SP				26.15	457.2	LV, SP

(E)			<i>O. aspinata</i>								
Zone	Subzone	Bed N.	Bed height	Geometric shell size	Shell preservation	Zone	Subzone	Bed N.	Bed height	Geometric shell size	Shell preservation
			25.64	294.7	LV, SP				26.15	457.1	LV, SP
			25.64	294.1	LV, SP				26.15	261.3	RV, SP
			25.64	432.4	RV, SP				26.15	450.0	RV, SP
			25.64	326.3	RV, SP				26.15	363.2	RV, SP
			25.64	317.7	LV, SP				26.15	364.1	RV, SP
			25.64	306.0	RV, SP				26.15	457.0	LV, SP
			25.64	308.9	LV, SP				26.15	378.0	RV, SP
			25.64	268.3	RV, SP				26.15	437.1	LV, SP
			25.64	356.2	RV, SP				26.15	356.2	RV, SP
			25.64	325.1	RV, SP				26.15	301.1	LV, SP
			25.64	347.9	RV, SP				26.15	372.9	RV, SP
			25.64	242.9	LV, SP				26.15	357.0	RV, SP
			25.64	543.6	RV, SP				26.15	363.9	LV, SP
			25.64	379.5	RV, SP				26.15	339.0	RV, SP
			25.64	304.9	LV, SP				26.15	236.1	RV, SP
			25.64	295.3	RV, SP				26.15	365.3	LV, SP
			25.64	295.3	RV, SP				26.15	355.5	LV, SP
			25.64	300.8	LV, SP				26.15	313.2	RV, SP
			25.64	306.8	RV, SP				26.15	309.3	LV, SP
			25.64	347.5	LV, SP				26.15	314.1	RV, SP
			25.64	315.1	LV, SP				26.15	323.0	RV, SP
			25.64	456.6	RV, SP				26.15	336.1	RV, SP
			25.64	349.3	RV, SP				26.15	298.2	LV, SP
			25.64	263.2	LV, SP				26.15	291.9	LV, SP
			25.64	259.0	LV, SP				26.15	342.8	LV, SP
			25.64	349.7	RV, SP				26.15	237.3	RV, SP
			25.64	364.0	RV, SP				26.15	271.0	RV, SP
			25.64	285.6	RV, SP				26.15	297.8	RV, SP
			25.64	295.1	RV, SP				26.15	246.7	SB
			25.64	325.7	RV, SP				26.15	305.0	LV, SP
			25.64	360.7	RV, SP				26.15	306.4	LV, SP
			25.64	269.2	LV, SP				26.15	263.3	RV, SP
			25.64	352.3	RV, SP				26.15	326.6	RV, SP
			25.64	315.7	RV, SP				26.15	339.8	RV, SP
			25.64	320.6	LV, SP				26.15	273.7	LV, SP
			25.64	293.1	RV, SP				26.15	257.2	RV, SP
			25.64	305.8	LV, SP				26.15	267.6	RV, SP
			25.64	366.0	RV, SP				26.15	278.0	LV, SP
			25.64	372.8	LV, SP				26.15	287.0	LV, SP

(E)			<i>O. aspinata</i>								
Zone	Subzone	Bed N.	Bed height	Geometric shell size	Shell preservation	Zone	Subzone	Bed N.	Bed height	Geometric shell size	Shell preservation
			25.64	351.6	LV, SP				26.15	316.0	RV, SP
			25.64	368.0	RV, SP				26.15	323.4	RV, SP
			25.64	400.1	RV, SP				26.15	307.2	RV, SP
			25.64	284.3	RV, SP				26.15	205.2	RV, SP
			25.64	265.5	RV, SP				26.15	360.1	LV, SP
			25.64	282.8	RV, SP				26.15	253.5	RV, SP
			25.64	244.0	RV, SP				26.15	264.3	RV, SP
			25.64	175.8	RV, SP				26.15	377.2	LV, SP
			25.64	176.9	LV, SP				26.15	253.0	RV, SP
			25.64	205.3	RV, SP				26.15	299.4	LV, SP
			25.64	242.3	RV, SP				26.15	313.5	RV, SP
			25.64	218.3	RV, SP				26.75	302.9	LV, SP
			25.64	254.4	LV, SP				26.75	395.3	LV, SP
			25.64	391.5	RV, SP				26.75	369.5	LV, SP
			25.64	232.2	LV, SP				26.75	408.0	RV, SP
			25.64	285.4	RV, SP				26.75	408.2	SB
			25.64	228.9	LV, SP				26.75	450.9	LV, SP
			25.64	203.4	RV, SP				26.75	555.0	LV, SP
			25.64	230.7	RV, SP				26.75	404.5	LV, SP
			25.64	240.6	RV, SP				26.75	449.1	RV, SP
			25.64	198.5	LV, SP				26.75	379.8	RV, SP
			25.64	172.0	LV, SP				26.75	383.4	LV, SP
			25.64	560.8	RV, SP				26.75	265.3	RV, SP
			25.64	201.7	SB				26.75	392.7	LV, SP
			25.64	180.8	LV, SP				26.75	352.6	RV, SP
			25.64	231.6	RV, SP			B99	26.75	214.9	LV, SP
			25.64	379.5	LV, SP				26.75	175.7	LV, SP
			25.64	416.2	RV, SP				26.75	181.3	LV, SP
			25.64	421.2	RV, SP				26.75	457.2	LV, SP
			25.64	430.4	LV, SP				26.75	383.3	RV, SP
			25.64	408.1	LV, SP				26.75	415.3	LV, SP
			25.64	465.7	LV, SP				26.75	398.3	LV, SP
			25.64	286.8	RV, SP				26.75	437.2	LV, SP
			25.64	304.9	RV, SP				26.75	403.2	RV, SP
			25.64	271.0	LV, SP				26.75	376.6	LV, SP
			25.64	344.8	RV, SP				26.75	445.0	LV, SP
			25.64	366.8	LV, SP				26.75	451.7	RV, SP
			25.64	289.8	RV, SP				26.75	455.4	LV, SP
			25.64	272.8	RV, SP				26.75	410.3	SB

(E)			<i>O. aspinata</i>								
Zone	Subzone	Bed N.	Bed height	Geometric shell size	Shell preservation	Zone	Subzone	Bed N.	Bed height	Geometric shell size	Shell preservation
			25.64	314.7	RV, SP				26.75	380.8	RV, SP
			25.64	371.8	LV, SP				26.75	409.3	LV, SP
			25.64	254.0	LV, SP				26.75	432.3	RV, SP
			25.64	312.5	RV, SP				26.75	396.7	RV, SP
			25.64	271.0	LV, SP				26.75	393.1	RV, SP
			25.64	275.9	LV, SP				26.75	388.1	RV, SP
			25.64	314.9	LV, SP				26.75	272.4	LV, SP
			25.64	376.2	RV, SP				26.75	391.0	RV, SP
			25.64	321.6	LV, SP				26.75	338.0	LV, SP
			25.64	296.9	RV, SP				26.75	318.1	LV, SP
			25.64	323.7	RV, SP				26.75	273.1	LV, SP
			25.64	313.9	RV, SP				26.75	285.4	LV, SP
			25.64	321.2	RV, SP				26.75	331.2	RV, SP
			25.64	257.8	LV, SP				26.75	278.3	RV, SP
			25.64	365.2	LV, SP				26.75	311.5	RV, SP
			25.64	307.3	LV, SP				26.75	371.2	RV, SP
			25.64	365.7	LV, SP				26.75	232.5	RV, SP
			25.64	303.1	RV, SP				26.75	280.8	RV, SP
			25.64	360.2	LV, SP				26.75	365.8	RV, SP
			25.64	344.5	LV, SP				26.75	303.5	LV, SP
			25.64	338.3	RV, SP				26.75	376.7	RV, SP
			25.64	360.0	RV, SP				26.75	371.5	LV, SP
			25.64	340.1	LV, SP				26.75	358.7	LV, SP
			25.64	376.9	RV, SP				26.75	300.5	LV, SP
			25.64	303.9	RV, SP				26.75	313.4	LV, SP
			25.64	319.0	LV, SP				26.75	331.3	RV, SP
			25.64	350.6	RV, SP				26.75	330.3	RV, SP
			25.64	311.9	LV, SP				26.75	372.6	LV, SP
			25.64	366.0	RV, SP				26.75	356.7	RV, SP
			25.64	356.0	LV, SP				26.75	263.1	LV, SP
			25.64	371.7	LV, SP				26.75	369.4	RV, SP
			25.64	361.1	LV, SP				26.75	333.0	RV, SP
			25.64	250.9	LV, SP				26.75	325.2	SB
			25.64	357.0	RV, SP				26.75	390.6	RV, SP
			25.64	354.8	RV, SP				26.75	295.5	RV, SP
			25.64	347.0	LV, SP				26.75	264.4	LV, SP
			25.64	360.2	LV, SP				26.75	322.5	RV, SP
			25.64	343.6	RV, SP				26.75	378.4	RV, SP
			25.64	295.4	LV, SP				26.75	355.4	RV, SP

(E)			<i>O. aspinata</i>								
Zone	Subzone	Bed N.	Bed height	Geometric shell size	Shell preservation	Zone	Subzone	Bed N.	Bed height	Geometric shell size	Shell preservation
			25.64	302.6	RV, SP				26.75	305.4	RV, SP
			25.64	359.8	RV, SP				26.75	272.1	RV, SP
			25.64	344.1	LV, SP				26.75	293.0	SB
			25.64	313.8	RV, SP				26.75	305.0	LV, SP
			25.64	356.0	RV, SP				26.75	391.8	LV, SP
			25.64	306.1	LV, SP				26.75	314.6	RV, SP
			25.64	357.5	RV, SP				26.75	292.3	LV, SP
			25.64	347.6	RV, SP				26.75	302.5	LV, SP
			25.64	307.7	LV, SP				26.75	255.1	RV, SP
			25.64	307.1	RV, SP				26.75	273.7	RV, SP
			25.64	298.5	LV, SP				26.75	361.3	LV, SP
			25.64	322.2	RV, SP				26.75	372.5	LV, SP
			25.64	318.9	LV, SP				26.75	285.5	RV, SP
			25.64	362.3	RV, SP				26.75	299.8	RV, SP
									26.75	352.5	RV, SP
									26.75	279.4	LV, SP
									26.75	316.4	RV, SP
									26.75	292.3	LV, SP
									26.75	246.1	RV, SP
									26.75	376.6	RV, SP
									26.75	318.8	RV, SP
									26.75	299.4	RV, SP
									26.75	379.9	RV, SP
									26.75	302.6	RV, SP
									26.75	344.7	RV, SP
									26.75	376.0	LV, SP
									26.75	297.3	RV, SP
									26.75	367.0	LV, SP
									26.75	245.6	RV, SP
									26.75	280.9	LV, SP
									26.75	317.4	RV, SP
									26.75	348.9	LV, SP
									26.75	330.3	LV, SP
									26.75	320.8	LV, SP
									26.75	295.6	LV, SP

(A)						<i>O. aspinata</i>					
Zone	Subzone	Bed N.	Bed height	Shell thickness	Shell preservation	Zone	Subzone	Bed N.	Bed height	Shell thickness	Shell preservation
planorbis Zone	Ps. planorbis subzone	B23	10.3	41.0	LV, SP				15.8	30.0	SB
			10.3	28.1	RV, SP				15.8	28.3	LV, SP
			10.3	25.6	RV, SP				15.8	32.6	RV, SP
			10.3	29.0	LV, SP				15.8	18.5	RV, SP
			10.3	19.5	RV, SP				15.8	31.7	SB
			10.3	22.7	RV, SP				15.8	15.3	RV, SP
			10.3	27.8	RV, SP				15.8	11.8	RV, SP
			10.3	16.2	RV, SP				15.8	14.7	RV, SP
			10.3	17.1	RV, SP				15.8	31.3	LV, SP
			10.3	45.4	SB				15.8	35.5	LV, SP
			10.3	34.4	SB				15.8	38.9	LV, SP
			10.3	17.0	LV, SP				15.8	38.4	RV, SP
			10.6	36.8	RV, SP				15.8	14.7	LV, SP
		10.6	33.8	SB	15.8			16.5	RV, SP		
		10.6	32.2	LV, SP	15.8			40.8	RV, SP		
		10.6	41.5	LV, SP	15.8			25.9	SB		
		10.6	41.5	RV, SP	15.8			61.2	LV, SP		
		10.6	37.8	RV, SP	15.8			20.4	LV, SP		
		10.6	35.0	LV, SP	15.8			38.3	RV, SP		
		10.6	44.0	RV, SP	15.8			18.1	LV, SP		
		10.6	30.7	LV, SP	15.8			38.5	LV, SP		
		10.6	53.2	SB	15.8			35.8	SB		
		10.6	33.8	LV, SP	15.8			28.5	LV, SP		
10.6	24.6	SB	15.8	25.7	SB						
10.6	36.3	RV, SP	15.8	42.9	LV, SP						
10.6	50.2	RV, SP	15.8	28.4	SB						
10.6	15.7	RV, SP	15.8	49.0	SB						
10.6	41.8	RV, SP	15.8	35.7	RV, SP						
10.6	19.5	RV, SP	16.8	42.6	LV, SP						
10.6	24.9	RV, SP	16.8	19.9	RV, SP						
10.6	38.7	RV, SP	16.8	34.9	LV, SP						
B25		10.7	37.5	RV, SP	16.8	16.7	LV, SP				
		10.7	50.2	RV, SP	16.8	34.1	LV, SP				
		10.7	26.6	RV, SP	16.8	44.1	RV, SP				
		10.7	24.8	RV, SP	16.8	10.3	LV, SP				
		10.7	35.1	RV, SP	16.8	39.6	RV, SP				
		10.7	44.9	LV, SP	16.8	14.5	LV, SP				
		10.7	42.9	RV, SP	16.8	30.2	LV, SP				
10.7	35.1	LV, SP	16.8	37.2	LV, SP						
					Alsatites laqueus subzone						

(A)						<i>O. aspinata</i>					
Zone	Subzone	Bed N.	Bed height	Shell thickness	Shell preservation	Zone	Subzone	Bed N.	Bed height	Shell thickness	Shell preservation
			10.7	29.5	SB				16.8	24.6	RV, SP
			10.7	34.4	SB				16.8	25.0	RV, SP
			10.7	26.7	RV, SP				16.8	35.6	RV, SP
			10.7	29.2	SB				16.8	20.5	RV, SP
			10.7	18.3	SB				16.8	14.1	SB
			10.7	24.7	LV, SP				16.8	29.9	SB
			10.7	15.8	RV, SP				16.8	11.5	RV, SP
			10.7	39.0	SB				16.8	22.4	SB
			10.7	27.8	RV, SP				16.8	14.7	SB
			10.7	36.9	LV, SP				16.8	22.8	SB
			10.7	41.1	RV, SP				16.8	12.3	SB
			10.7	23.8	RV, SP				16.8	11.5	LV, SP
			10.7	21.6	LV, SP				16.8	40.1	SB
			10.7	26.4	RV, SP				16.8	19.0	RV, SP
			10.7	23.7	RV, SP				16.8	29.5	LV, SP
			10.7	23.1	SB				16.8	17.7	LV, SP
			10.7	25.1	RV, SP				16.8	41.3	LV, SP
			11.3	24.2	LV, SP				16.8	33.1	LV, SP
			11.3	41.6	LV, SP				16.8	33.6	SB
			11.3	27.7	LV, SP				16.8	37.0	LV, SP
			11.3	28.3	LV, SP				16.8	33.4	LV, SP
			11.3	24.0	LV, SP				16.8	33.1	RV, SP
			11.3	34.1	RV, SP				16.8	33.5	SB
			11.3	22.8	LV, SP				16.8	42.2	LV, SP
			11.3	41.4	LV, SP				16.8	24.0	LV, SP
			11.3	21.0	LV, SP				16.8	20.4	SB
			11.3	40.8	SB				16.8	21.7	SB
			11.3	27.0	LV, SP				16.8	21.5	LV, SP
			11.3	30.9	SB				16.8	28.3	RV, SP
			11.3	32.4	LV, SP				16.8	43.4	LV, SP
			11.3	28.6	SB				16.8	32.8	SB
			11.3	35.1	SB				16.8	20.7	SB
			11.3	19.1	SB				16.8	41.0	LV, SP
			11.3	34.5	RV, SP				16.8	32.7	LV, SP
			11.3	24.3	RV, SP				16.8	21.8	SB
			11.3	13.0	RV, SP				16.8	24.4	LV, SP
			11.3	28.7	SB				17.5	33.3	RV, SP
			11.3	22.5	SB				17.5	31.4	LV, SP
			11.3	15.1	RV, SP				17.5	35.4	RV, SP

(A)						<i>O. aspinata</i>					
Zone	Subzone	Bed N.	Bed height	Shell thickness	Shell preservation	Zone	Subzone	Bed N.	Bed height	Shell thickness	Shell preservation
			11.3	16.3	SB				17.5	27.3	LV, SP
			12.85	20.9	SB				17.5	41.1	LV, SP
			12.85	35.6	LV, SP				17.5	30.9	SB
			12.85	41.4	LV, SP				17.5	34.8	LV, SP
			12.85	28.6	LV, SP				17.5	60.0	LV, SP
			12.85	29.3	LV, SP				17.5	19.4	LV, SP
			12.85	40.8	LV, SP				17.5	40.8	LV, SP
			12.85	39.7	RV, SP				17.5	36.4	LV, SP
			12.85	34.3	RV, SP				17.5	51.8	LV, SP
			12.85	36.8	LV, SP				17.5	27.0	LV, SP
			12.85	43.1	LV, SP				17.5	30.6	LV, SP
			12.85	32.1	LV, SP				17.5	27.2	RV, SP
			12.85	44.3	RV, SP				17.5	19.7	RV, SP
			12.85	30.0	RV, SP				17.5	13.9	LV, SP
			12.85	18.5	RV, SP				17.5	46.7	RV, SP
			12.85	43.2	RV, SP				17.5	40.5	RV, SP
			12.85	23.1	RV, SP				18.2	23.5	RV, SP
			12.85	23.7	RV, SP				18.2	17.7	RV, SP
			12.85	19.8	RV, SP				18.2	43.1	RV, SP
			12.85	30.5	RV, SP				18.2	22.0	LV, SP
			12.85	28.0	RV, SP				18.2	28.0	RV, SP
			12.85	25.9	LV, SP				18.2	40.5	LV, SP
			12.85	28.7	RV, SP				18.2	24.8	LV, SP
			13.37	23.7	RV, SP				18.2	21.9	RV, SP
			13.37	27.7	LV, SP				18.2	38.2	LV, SP
			13.37	15.1	RV, SP				18.2	35.1	LV, SP
			13.37	17.7	RV, SP				18.2	22.9	RV, SP
			13.37	13.8	LV, SP				18.2	26.8	RV, SP
			13.37	19.3	LV, SP				18.2	38.6	LV, SP
			13.37	33.3	SB				18.2	27.1	LV, SP
			13.37	18.0	LV, SP				18.2	21.9	SB
			13.37	24.8	SB				18.2	27.9	RV, SP
			13.37	18.7	LV, SP				18.2	24.2	LV, SP
			13.37	46.6	LV, SP				18.2	43.5	LV, SP
			13.37	21.4	SB				18.2	16.9	LV, SP
			13.37	21.6	SB				18.2	36.3	RV, SP
			13.37	20.1	SB				18.2	27.2	RV, SP
			13.37	30.0	RV, SP				18.2	13.9	SB
			13.37	17.5	RV, SP				18.2	11.9	RV, SP

(A)						<i>O. aspinata</i>						
Zone	Subzone	Bed N.	Bed height	Shell thickness	Shell preservation	Zone	Subzone	Bed N.	Bed height	Shell thickness	Shell preservation	
			13.37	12.7	RV, SP			B59	18.2	27.7	LV, SP	
			13.37	36.7	RV, SP				19.35	48.1	LV, SP	
			13.37	18.1	RV, SP				19.35	44.8	LV, SP	
			13.37	16.4	RV, SP				19.35	25.7	LV, SP	
			13.37	14.3	RV, SP				19.35	43.3	LV, SP	
			13.37	14.5	LV, SP				19.35	33.1	SB	
			13.37	25.2	RV, SP				19.35	28.7	LV, SP	
		B39		13.37	11.7				RV, SP	19.35	30.0	RV, SP
				13.7	36.0				RV, SP	19.35	41.6	LV, SP
				13.7	28.5				RV, SP	19.35	57.6	LV, SP
				13.7	29.2				RV, SP	19.35	29.4	RV, SP
				13.7	33.1				LV, SP	19.35	29.8	RV, SP
				13.7	33.0				RV, SP	19.35	25.8	RV, SP
				13.7	36.1				LV, SP	19.35	29.2	SB
				13.7	27.6				RV, SP	19.35	27.9	SB
				13.7	28.7				LV, SP	19.35	27.1	RV, SP
				13.7	28.4				RV, SP	19.35	6.2	RV, SP
				13.7	38.4				RV, SP	19.35	25.4	RV, SP
				13.7	40.3				LV, SP	19.35	23.0	SB
				13.7	34.4				LV, SP	19.35	23.3	RV, SP
				13.7	22.9				LV, SP	19.35	28.5	RV, SP
				13.7	42.2				LV, SP	19.35	24.1	SB
				13.7	20.9				LV, SP	19.35	23.9	RV, SP
				13.7	23.3				RV, SP			
				13.7	27.1				LV, SP			
				13.7	22.7				RV, SP			
				13.7	17.7				LV, SP			

(B)						<i>O. aspinata</i>					
Zone	Subzone	Bed N.	Bed height	Shell thickness	Shell preservation	Zone	Subzone	Bed N.	Bed height	Shell thickness	Shell preservation
liasicus Zone	Alsatites laqueus subzone	B61	19.6	44.2	LV, SP	angulata Zone	Schlotheimia angulata subzone	B73	21.55	24.6	RV, SP
			19.6	28.2	LV, SP				21.55	36.0	RV, SP
			19.6	35.7	SB				21.55	35.2	RV, SP
			19.6	57.9	LV, SP				21.55	17.6	RV, SP
			19.6	42.4	LV, SP				21.55	28.0	LV, SP
			19.6	32.5	LV, SP				21.55	25.2	RV, SP
			19.6	23.6	RV, SP				21.55	42.2	LV, SP

(B)						<i>O. aspinata</i>					
Zone	Subzone	Bed N.	Bed height	Shell thickness	Shell preservation	Zone	Subzone	Bed N.	Bed height	Shell thickness	Shell preservation
			19.6	31.1	SB				21.55	30.9	RV, SP
			19.6	27.0	LV, SP				21.55	28.6	LV, SP
			19.6	25.8	LV, SP				21.55	17.9	LV, SP
			19.6	39.3	LV, SP				21.55	20.3	LV, SP
			19.6	36.7	SB				21.55	20.8	RV, SP
			19.6	30.2	LV, SP				21.55	19.8	RV, SP
			19.6	35.2	RV, SP				21.55	15.4	RV, SP
			19.6	42.6	RV, SP				21.55	27.1	LV, SP
			19.6	10.9	LV, SP				21.55	25.0	RV, SP
			19.6	33.7	LV, SP				21.55	26.1	LV, SP
			19.6	18.1	LV, SP				21.55	26.9	RV, SP
			19.6	26.2	RV, SP				21.55	18.0	RV, SP
			19.87	39.3	RV, SP				21.55	11.2	LV, SP
			19.87	39.1	RV, SP				21.75	40.9	LV, SP
			19.87	27.2	RV, SP				21.75	40.0	SB
			19.87	26.3	RV, SP				21.75	31.4	RV, SP
			19.87	34.1	LV, SP				21.75	18.4	RV, SP
			19.87	49.0	RV, SP				21.75	25.6	RV, SP
			19.87	41.4	LV, SP				21.75	52.8	RV, SP
			19.87	50.3	LV, SP				21.75	49.3	RV, SP
			19.87	51.9	SB				21.75	28.9	LV, SP
			19.87	42.4	LV, SP				21.75	39.5	RV, SP
			19.87	39.2	RV, SP				21.75	22.5	RV, SP
			19.87	15.1	RV, SP				21.75	30.5	LV, SP
			19.87	39.7	LV, SP			B74A	21.75	19.8	SB
			19.87	47.0	RV, SP				21.75	25.0	RV, SP
			19.87	39.9	SB				21.75	17.4	RV, SP
			19.87	35.0	SB				21.75	24.3	RV, SP
			19.87	15.5	LV, SP				21.75	13.4	SB
			19.87	37.7	RV, SP				21.75	26.4	LV, SP
			19.87	40.7	SB				21.75	33.0	LV, SP
			19.87	13.8	RV, SP				21.75	16.9	LV, SP
			19.87	26.8	LV, SP				21.75	19.0	LV, SP
			19.87	28.4	RV, SP				21.75	16.1	RV, SP
			20.95	37.5	LV, SP				21.75	18.8	LV, SP
			20.95	52.2	LV, SP				21.75	18.1	RV, SP
			20.95	31.7	SB				21.95	41.2	LV, SP
			20.95	29.0	RV, SP			B75A	21.95	26.9	RV, SP
			20.95	19.8	SB				21.95	28.8	LV, SP

(B)						<i>O. aspinata</i>					
Zone	Subzone	Bed N.	Bed height	Shell thickness	Shell preservation	Zone	Subzone	Bed N.	Bed height	Shell thickness	Shell preservation
			20.95	29.3	LV, SP				21.95	44.1	RV, SP
			20.95	39.5	RV, SP				21.95	33.0	RV, SP
			20.95	42.8	RV, SP				21.95	32.7	LV, SP
			20.95	40.0	LV, SP				21.95	41.7	LV, SP
			20.95	37.7	RV, SP				21.95	18.2	LV, SP
			20.95	18.6	LV, SP				21.95	30.2	SB
			20.95	46.5	RV, SP				21.95	36.4	RV, SP
			20.95	23.4	RV, SP				21.95	35.4	LV, SP
			20.95	27.8	LV, SP				21.95	25.4	LV, SP
			20.95	31.6	RV, SP				21.95	31.8	RV, SP
			20.95	28.0	LV, SP				21.95	26.7	LV, SP
			20.95	39.4	RV, SP				21.95	25.6	LV, SP
			21.15	50.3	RV, SP				21.95	20.1	LV, SP
			21.15	35.6	RV, SP				21.95	21.7	RV, SP
			21.15	51.3	SB				21.95	23.6	LV, SP
			21.15	19.8	SB				21.95	35.9	RV, SP
			21.15	37.1	RV, SP				21.95	43.5	RV, SP
			21.15	40.9	RV, SP				21.95	17.4	RV, SP
			21.15	35.2	RV, SP				21.95	13.7	RV, SP
			21.15	53.8	LV, SP				22.15	41.8	RV, SP
			21.15	34.1	RV, SP				22.15	29.3	LV, SP
			21.15	26.1	RV, SP				22.15	35.9	RV, SP
			21.15	40.4	LV, SP				22.15	18.0	LV, SP
		B69	21.15	58.7	RV, SP				22.15	31.1	LV, SP
			21.15	36.0	RV, SP				22.15	32.6	RV, SP
			21.15	27.7	LV, SP				22.15	36.5	LV, SP
			21.15	29.1	LV, SP			B76A	22.15	48.1	SB
			21.15	21.3	RV, SP				22.15	29.9	LV, SP
			21.15	29.4	SB				22.15	19.0	SB
			21.15	32.6	RV, SP				22.15	20.2	SB
			21.15	35.7	RV, SP				22.15	15.8	RV, SP
			21.15	17.8	LV, SP				22.15	31.1	LV, SP
			21.15	26.5	RV, SP				22.15	14.5	RV, SP
			21.15	23.2	LV, SP						
			21.15	17.7	RV, SP						

(C)		<i>O. aspinata</i>									
Zone	Subzone	Bed N.	Bed height	Geometric shell size	Shell preservation	Zone	Subzone	Bed N.	Bed height	Geometric shell size	Shell preservation
angulata Zone	Schlotheimia angulata subzone	B77A	22.35	30.4	LV, SP	bucklandi Zone	Metophioceras conybeari subzone	B95	25.64	22.1	LV, SP
			22.35	39.8	LV, SP				25.64	17.8	RV, SP
			22.35	20.6	LV, SP				25.64	22.6	LV, SP
			22.35	28.7	LV, SP				25.64	52.5	LV, SP
			22.35	19.2	RV, SP				25.64	35.8	LV, SP
			22.35	29.0	SB				25.64	22.2	RV, SP
			22.35	21.6	LV, SP				25.64	32.7	LV, SP
			22.35	38.3	LV, SP				25.64	22.5	LV, SP
			22.35	33.6	RV, SP				25.64	22.4	LV, SP
			22.35	32.9	RV, SP				25.64	16.7	RV, SP
			22.35	20.9	LV, SP				25.64	18.0	RV, SP
			22.35	24.1	LV, SP				25.64	18.0	RV, SP
			22.35	28.0	LV, SP				25.64	24.8	RV, SP
			22.35	14.8	RV, SP				25.64	30.9	RV, SP
			22.35	19.5	LV, SP				25.64	19.4	RV, SP
			22.35	15.9	LV, SP				25.64	14.4	RV, SP
			22.35	13.6	LV, SP				25.64	16.4	LV, SP
			22.35	10.3	RV, SP				25.64	24.6	RV, SP
			22.35	29.2	LV, SP				25.64	20.1	LV, SP
			22.35	20.0	RV, SP				25.64	13.9	LV, SP
		22.35	18.4	LV, SP	25.64			8.7	LV, SP		
		22.35	11.1	RV, SP	26.15			10.6	RV, SP		
		22.35	11.4	RV, SP	26.15			40.3	LV, SP		
		22.35	24.0	RV, SP	26.15			26.5	RV, SP		
		22.35	20.6	RV, SP	26.15			17.8	RV, SP		
		B89	B89	24.3	30.5			RV, SP	26.15	29.4	LV, SP
				24.3	35.9			RV, SP	26.15	14.3	RV, SP
				24.3	32.3			RV, SP	26.15	26.0	LV, SP
				24.3	37.1			RV, SP	26.15	25.0	LV, SP
				24.3	25.2			SB	26.15	38.1	LV, SP
				24.3	36.7			LV, SP	26.15	38.0	LV, SP
				24.3	22.8			LV, SP	26.15	34.0	LV, SP
				24.3	38.2			LV, SP	26.15	22.5	RV, SP
				24.3	24.3			RV, SP	26.15	19.1	LV, SP
24.3	25.5			LV, SP	26.15	43.0	RV, SP				
24.3	24.9			RV, SP	26.15	25.4	LV, SP				
24.3	37.7			RV, SP	26.15	21.1	RV, SP				

(C)						<i>O. aspinata</i>					
Zone	Subzone	Bed N.	Bed height	Geometric shell size	Shell preservation	Zone	Subzone	Bed N.	Bed height	Geometric shell size	Shell preservation
			24.3	33.8	RV, SP				26.15	30.2	RV, SP
			24.3	51.3	RV, SP				26.15	27.0	LV, SP
			24.3	37.4	RV, SP				26.15	10.5	LV, SP
			24.3	28.5	RV, SP				26.15	22.6	LV, SP
			24.3	33.7	LV, SP				26.15	10.3	RV, SP
			24.3	26.8	RV, SP				26.15	29.7	RV, SP
			24.3	34.4	LV, SP				26.15	23.1	LV, SP
			24.3	19.0	RV, SP				26.15	11.5	LV, SP
			24.3	28.5	LV, SP				26.15	12.1	RV, SP
			24.3	34.2	RV, SP				26.75	19.7	LV, SP
			24.3	19.0	RV, SP				26.75	21.1	LV, SP
			24.3	30.9	RV, SP				26.75	29.8	LV, SP
			25.25	14.7	LV, SP				26.75	47.8	RV, SP
			25.25	34.8	RV, SP				26.75	31.9	LV, SP
			25.25	31.0	LV, SP				26.75	32.9	LV, SP
			25.25	31.5	SB				26.75	17.3	LV, SP
			25.25	14.6	SB				26.75	27.2	LV, SP
			25.25	41.5	RV, SP				26.75	11.0	RV, SP
			25.25	53.4	LV, SP				26.75	25.6	RV, SP
			25.25	39.5	LV, SP				26.75	40.0	LV, SP
			25.25	40.2	RV, SP				26.75	22.4	LV, SP
			25.25	43.7	RV, SP				26.75	29.1	RV, SP
			25.25	18.0	RV, SP				26.75	19.1	RV, SP
			25.25	36.0	LV, SP				26.75	29.9	RV, SP
			25.25	24.0	RV, SP				26.75	21.4	LV, SP
			25.25	22.8	RV, SP				26.75	17.4	RV, SP
			25.25	29.5	RV, SP				26.75	23.3	LV, SP
			25.25	39.0	SB				26.75	22.2	RV, SP
			25.25	21.9	RV, SP				26.75	11.4	RV, SP
			25.25	14.7	SB				26.75	17.5	RV, SP
			25.25	16.1	LV, SP				26.75	12.5	RV, SP
			25.25	13.5	RV, SP						
			25.25	29.9	RV, SP						

A4.1.2: Relationships between the fossil size recorded and the number of individuals measured at Lyme Regis.

Table A4.5: *L. hisingeri* geometric shell size results from the statistical analysis when determining any relationship between the mean, min, max and range and the number of individuals measured in Lyme Regis. (Presented in Section 3.5.1)

Correlation question	Number of individuals	R ² value
Minimum geometric <i>L. hisingeri</i> shell size against the number of individuals measured on each bed	37	0.4239
Maximum geometric <i>L. hisingeri</i> shell size against the number of individuals measured on each bed	37	0.3916
Mean geometric <i>L. hisingeri</i> shell size against the number of individuals measured on each bed	37	0.0541
Range geometric <i>L. hisingeri</i> shell size against the number of individuals measured on each bed	37	0.6299
Minimum geometric <i>L. hisingeri</i> shell size against the number of individuals measured on each bed in the Pre-planorbis Zone	15	0.371
Maximum geometric <i>L. hisingeri</i> shell size against the number of individuals measured on each bed in the Pre-planorbis Zone	15	0.2134
Mean geometric <i>L. hisingeri</i> shell size against the number of individuals measured on each bed in the Pre-planorbis Zone	15	0.0069
Range geometric <i>L. hisingeri</i> shell size against the number of individuals measured on each bed in the Pre-planorbis Zone	15	0.5028
Minimum geometric <i>L. hisingeri</i> shell size against the number of individuals measured on each bed in the Planorbis Zone	6	0.3608
Maximum geometric <i>L. hisingeri</i> shell size against the number of individuals measured on each bed in the Planorbis Zone	6	0.479
Mean geometric <i>L. hisingeri</i> shell size against the number of individuals measured on each bed in the Planorbis Zone	6	0.5159
Range geometric <i>L. hisingeri</i> shell size against the number of individuals measured on each bed in the Planorbis Zone	6	0.4781
Minimum geometric <i>L. hisingeri</i> shell size against the number of individuals measured on each bed in the liasicus Zone	10	0.4927
Maximum geometric <i>L. hisingeri</i> shell size against the number of individuals measured on each bed in the liasicus Zone	10	0.3797
Mean geometric <i>L. hisingeri</i> shell size against the number of individuals measured on each bed in the liasicus Zone	10	0.262
Range geometric <i>L. hisingeri</i> shell size against the number of individuals measured on each bed in the liasicus Zone	10	0.6644
Minimum geometric <i>L. hisingeri</i> shell size against the number of individuals measured on each bed in the angulata Zone	4	0.1801
Maximum geometric <i>L. hisingeri</i> shell size against the number of individuals measured on each bed in the angulata Zone	4	0.7926
Mean geometric <i>L. hisingeri</i> shell size against the number of individuals measured on each bed in the angulata Zone	4	0.6988
Range geometric <i>L. hisingeri</i> shell size against the number of individuals measured on each bed in the angulata Zone	4	0.7074
Minimum geometric <i>L. hisingeri</i> shell size against the number of individuals measured on each bed in the bucklandi Zone	2	1
Maximum geometric <i>L. hisingeri</i> shell size against the number of individuals measured on each bed in the bucklandi Zone	2	1
Mean geometric <i>L. hisingeri</i> shell size against the number of individuals measured on each bed in the bucklandi Zone	2	1
Range geometric <i>L. hisingeri</i> shell size against the number of individuals measured on each bed in the bucklandi Zone	2	1
Minimum geometric <i>L. hisingeri</i> shell size against the number of individuals measured in each zone	5	0.9334
Maximum geometric <i>L. hisingeri</i> shell size against the number of individuals measured in each zone	5	0.6868
Mean geometric <i>L. hisingeri</i> shell size against the number of individuals measured in each zone	5	0.7574
Range geometric <i>L. hisingeri</i> shell size against the number of individuals measured in each zone	5	0.8981

Relationships between *Liostrea* geometric shell size and the number of individuals measured on each zone

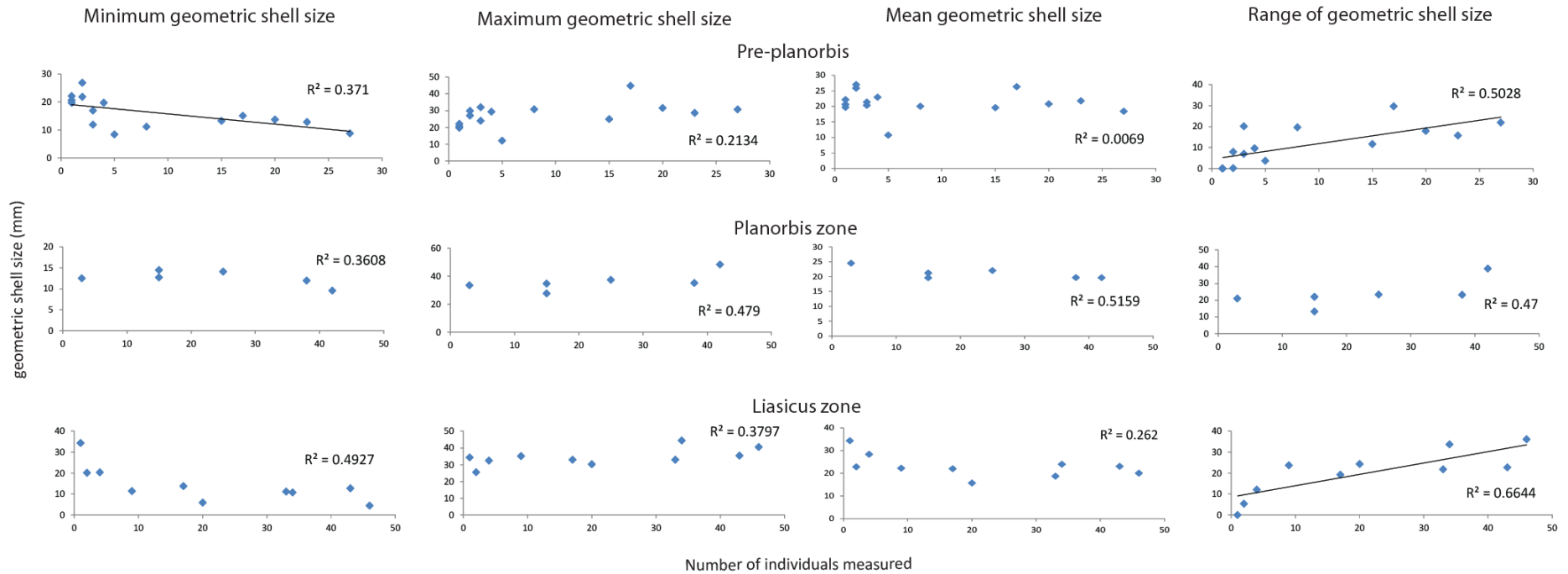


Figure A4.1A: *L. hisingeri* geometric shell size data (the mean, minimum, maximum and range of geometric shell size versus the number of individuals measured from each bed in Pre-planorbis Zone, Planorbis Zone and liasicus Zone) from Lyme Regis (Presented in Section 3.5.1).

Relationships between *Liostrea* geometric shell size and the number of individuals measured on each zone

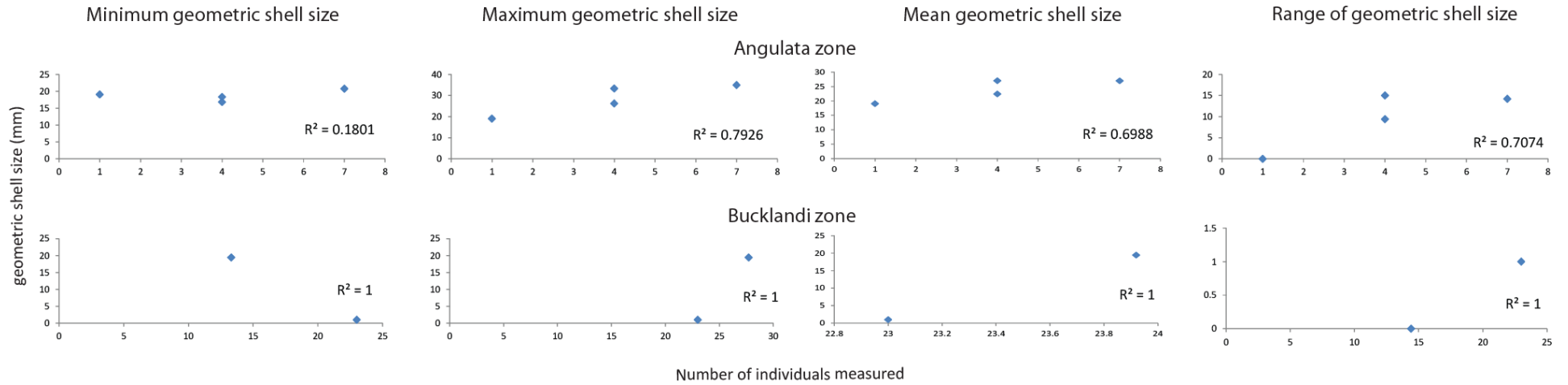


Figure A4.1B: *L. hisingeri* geometric shell size data (the mean, minimum, maximum and range of geometric shell size versus the number of individuals measured from each bed in angulata Zone and bucklandi Zone) from Lyme Regis (Presented in Section 3.5.1).

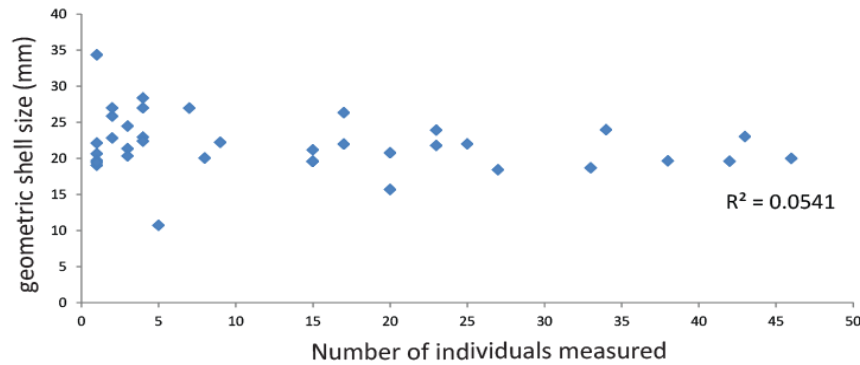


Figure A4.2: Lyme Regis, *L. hisingeri* mean geometric size on each bed versus the corresponding number of individuals measured in each bed (Presented in Section 3.5.1).

Table A4.6: *P. gigantea* geometric shell size results from the statistical analysis when determining any relationship between the mean, min, max and range and the number of individuals measured in Lyme Regis. (Presented in Section 3.5.1)

Correlation question	Number of individuals	R ² value
Minimum geometric <i>P. gigantea</i> shell size against the number of individuals measured on each bed	26	0.3948
Maximum geometric <i>P. gigantea</i> shell size against the number of individuals measured on each bed	26	0.1107
Mean geometric <i>P. gigantea</i> shell size against the number of individuals measured on each bed	26	0.0063
Range geometric <i>P. gigantea</i> shell size against the number of individuals measured on each bed	26	0.1823
Minimum geometric <i>P. gigantea</i> shell size against the number of individuals measured on each bed in the Pre-planorbis Zone	3	#N/A
Maximum geometric <i>P. gigantea</i> shell size against the number of individuals measured on each bed in the Pre-planorbis Zone	3	#N/A
Mean geometric <i>P. gigantea</i> shell size against the number of individuals measured on each bed in the Pre-planorbis Zone	3	#N/A
Range geometric <i>P. gigantea</i> shell size against the number of individuals measured on each bed in the Pre-planorbis Zone	3	#N/A
Minimum geometric <i>P. gigantea</i> shell size against the number of individuals measured on each bed in the Planorbis Zone	7	0.5667
Maximum geometric <i>P. gigantea</i> shell size against the number of individuals measured on each bed in the Planorbis Zone	7	0.0316
Mean geometric <i>P. gigantea</i> shell size against the number of individuals measured on each bed in the Planorbis Zone	7	0.3859
Range geometric <i>P. gigantea</i> shell size against the number of individuals measured on each bed in the Planorbis Zone	7	0.5304
Minimum geometric <i>P. gigantea</i> shell size against the number of individuals measured on each bed in the liasicus Zone	9	0.6743
Maximum geometric <i>P. gigantea</i> shell size against the number of individuals measured on each bed in the liasicus Zone	9	0.00003
Mean geometric <i>P. gigantea</i> shell size against the number of individuals measured on each bed in the liasicus Zone	9	0.282
Range geometric <i>P. gigantea</i> shell size against the number of individuals measured on each bed in the liasicus Zone	9	0.6386
Minimum geometric <i>P. gigantea</i> shell size against the number of individuals measured on each bed in the angulata Zone	5	0.5261
Maximum geometric <i>P. gigantea</i> shell size against the number of individuals measured on each bed in the angulata Zone	5	0.4856
Mean geometric <i>P. gigantea</i> shell size against the number of individuals measured on each bed in the angulata Zone	5	0.5652
Range geometric <i>P. gigantea</i> shell size against the number of individuals measured on each bed in the angulata Zone	5	0.5533
Minimum geometric <i>P. gigantea</i> shell size against the number of individuals measured on each bed in the bucklandi Zone	2	1
Maximum geometric <i>P. gigantea</i> shell size against the number of individuals measured on each bed in the bucklandi Zone	2	1
Mean geometric <i>P. gigantea</i> shell size against the number of individuals measured on each bed in the bucklandi Zone	2	1
Range geometric <i>P. gigantea</i> shell size against the number of individuals measured on each bed in the bucklandi Zone	2	1
Minimum geometric <i>P. gigantea</i> shell size against the number of individuals measured in each zone	5	0.7353
Maximum geometric <i>P. gigantea</i> shell size against the number of individuals measured in each zone	5	0.0079
Mean geometric <i>P. gigantea</i> shell size against the number of individuals measured in each zone	5	0.2026
Range geometric <i>P. gigantea</i> shell size against the number of individuals measured in each zone	5	0.0889

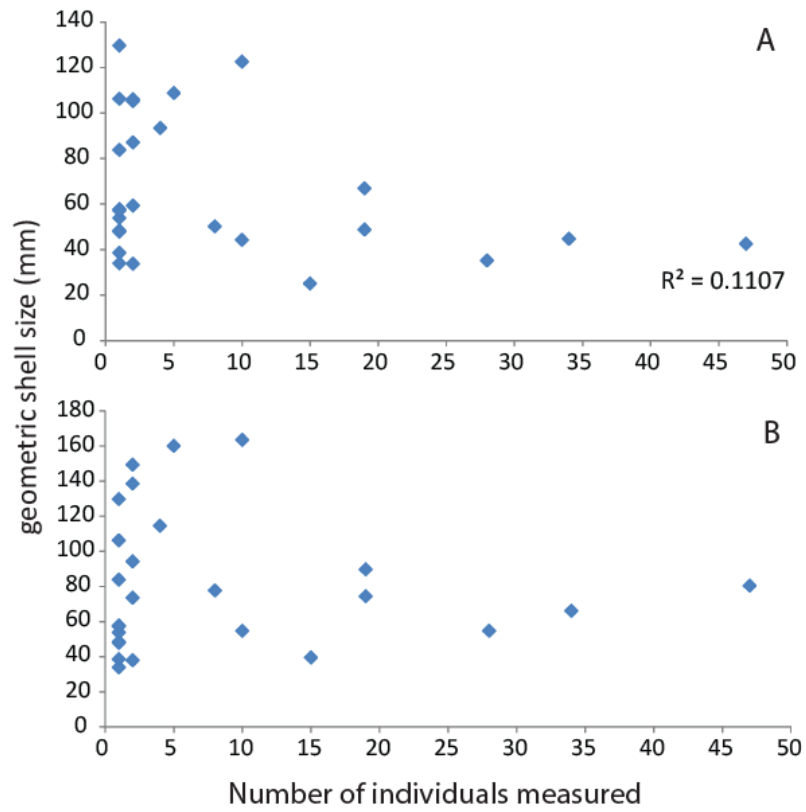


Figure A4.3: Lyme Regis *P. gigantea* (A) mean and (B) maximum geometric sizes on each bed versus the corresponding number of individuals measured in each bed (Presented in Section 3.5.1).

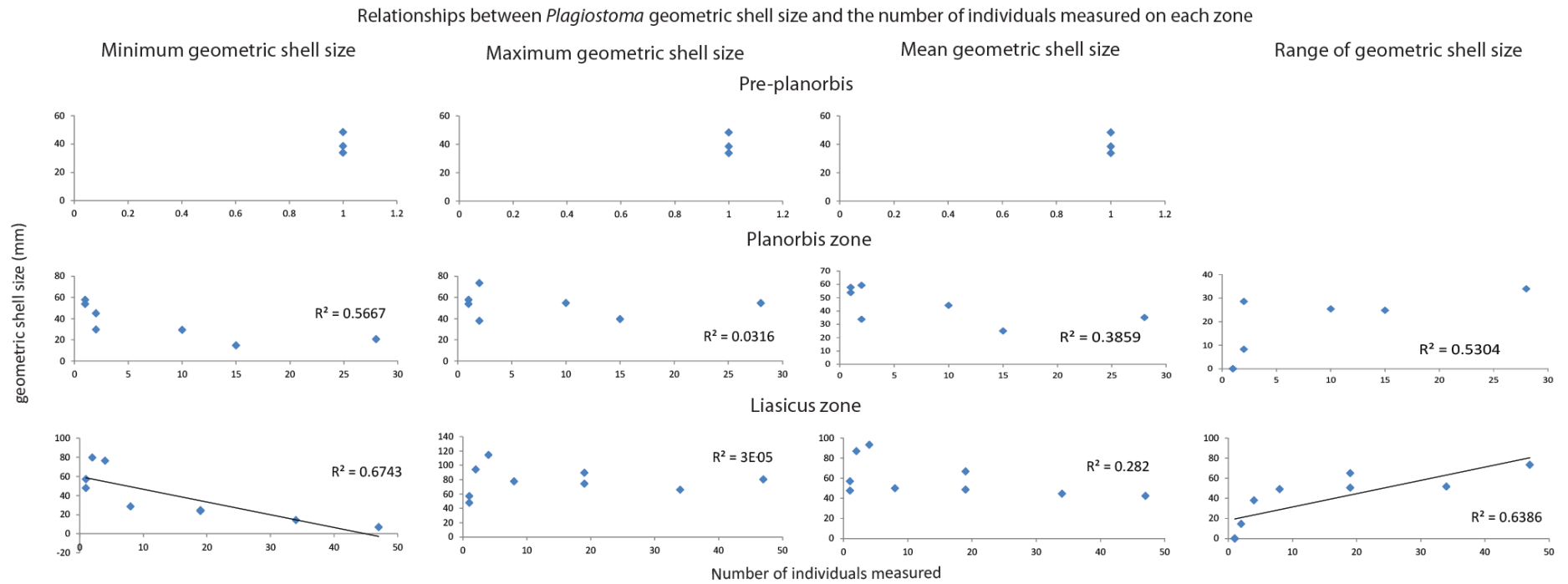


Figure A4.4A: *P. gigantea* geometric shell size data (the mean, minimum, maximum and range of geometric shell size versus the number of individuals measured from each bed in Pre-planorbis Zone, Planorbis Zone and Liasicus Zone) from Lyme Regis (Presented in Section 3.5.1).

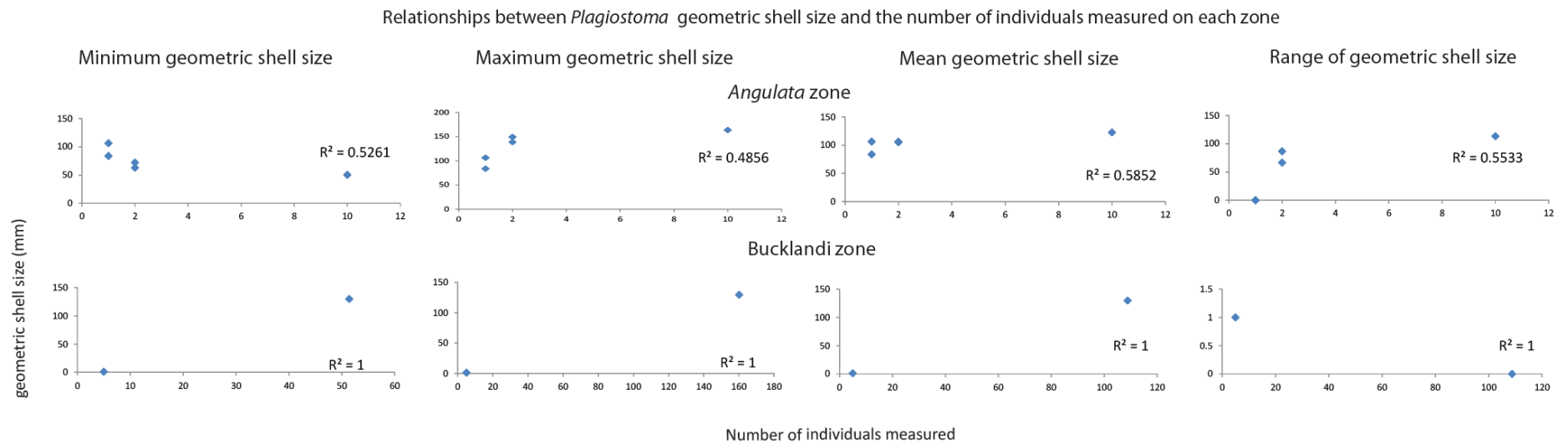


Figure A4.4B: *P. gigantea* geometric shell size data (the mean, minimum, maximum and range of geometric shell size versus the number of individuals measured from each bed in each angulata Zone and bucklandi Zone) from Lyme Regis (Presented in Section 3.5.1).

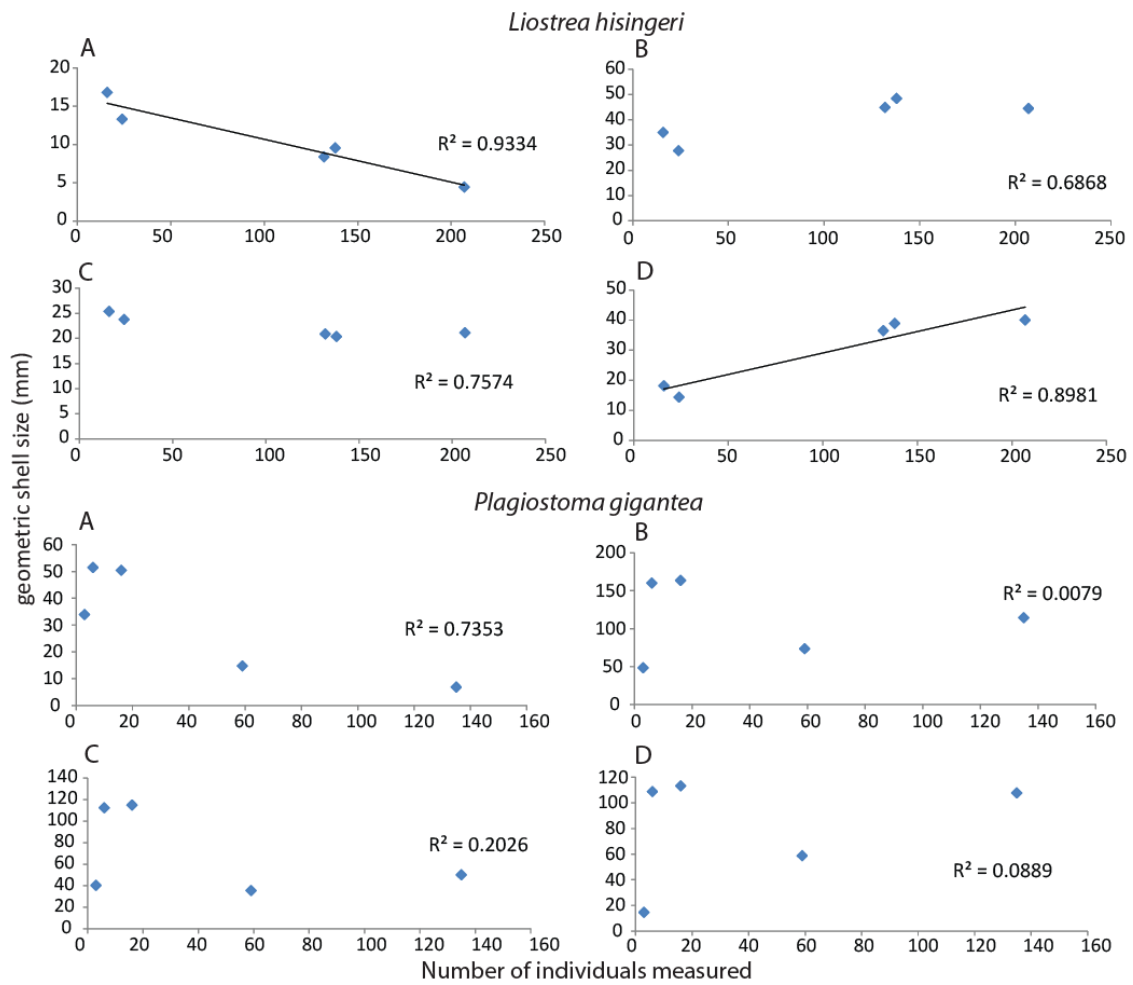


Figure A4.5: *L. hisingeri* and *P. gigantea* geometric shell size data (A) minimum, (B) maximum, (C) mean, and (D) range of geometric shell size versus the number of individuals measured in each zone from Lyme Regis (Presented in Section 3.5.1).

Table A4.7: *O. aspinata* geometric shell size results from the statistical analysis when determining any relationship between the mean, min, max and range and the number of individuals measured in Lyme Regis (Presented in Section 3.5.1).

Correlation question	Number of individuals	R ² value
Minimum geometric <i>O. aspinata</i> shell size against the number of individuals measured on each bed	30	0.385
Maximum geometric <i>O. aspinata</i> shell size against the number of individuals measured on each bed	30	0.1432
Mean geometric <i>O. aspinata</i> shell size against the number of individuals measured on each bed	30	0.0161
Range geometric <i>O. aspinata</i> shell size against the number of individuals measured on each bed	30	0.317
Minimum geometric <i>O. aspinata</i> shell size against the number of individuals measured on each bed in the Pre-planorbis Zone	4	0.1787
Maximum geometric <i>O. aspinata</i> shell size against the number of individuals measured on each bed in the Pre-planorbis Zone	4	0.4301
Mean geometric <i>O. aspinata</i> shell size against the number of individuals measured on each bed in the Pre-planorbis Zone	4	0.0935
Range geometric <i>O. aspinata</i> shell size against the number of individuals measured on each bed in the Pre-planorbis Zone	4	0.2825
Minimum geometric <i>O. aspinata</i> shell size against the number of individuals measured on each bed in the Planorbis Zone	6	0.6108
Maximum geometric <i>O. aspinata</i> shell size against the number of individuals measured on each bed in the Planorbis Zone	6	0.1035
Mean geometric <i>O. aspinata</i> shell size against the number of individuals measured on each bed in the Planorbis Zone	6	0.0025
Range geometric <i>O. aspinata</i> shell size against the number of individuals measured on each bed in the Planorbis Zone	6	0.4197
Minimum geometric <i>O. aspinata</i> shell size against the number of individuals measured on each bed in the liasicus Zone	10	0.157
Maximum geometric <i>O. aspinata</i> shell size against the number of individuals measured on each bed in the liasicus Zone	10	0.000001
Mean geometric <i>O. aspinata</i> shell size against the number of individuals measured on each bed in the liasicus Zone	10	0.0703
Range geometric <i>O. aspinata</i> shell size against the number of individuals measured on each bed in the liasicus Zone	10	0.1828
Minimum geometric <i>O. aspinata</i> shell size against the number of individuals measured on each bed in the angulata Zone	7	0.0134
Maximum geometric <i>O. aspinata</i> shell size against the number of individuals measured on each bed in the angulata Zone	7	0.0853
Mean geometric <i>O. aspinata</i> shell size against the number of individuals measured on each bed in the angulata Zone	7	0.0721
Range geometric <i>O. aspinata</i> shell size against the number of individuals measured on each bed in the angulata Zone	7	0.0155
Minimum geometric <i>O. aspinata</i> shell size against the number of individuals measured on each bed in the bucklandi Zone	3	0.0134
Maximum geometric <i>O. aspinata</i> shell size against the number of individuals measured on each bed in the bucklandi Zone	3	0.011
Mean geometric <i>O. aspinata</i> shell size against the number of individuals measured on each bed in the bucklandi Zone	3	0.921
Range geometric <i>O. aspinata</i> shell size against the number of individuals measured on each bed in the bucklandi Zone	3	0.9372
Minimum geometric <i>O. aspinata</i> shell size against the number of individuals measured in each zone	5	0.6504
Maximum geometric <i>O. aspinata</i> shell size against the number of individuals measured in each zone	5	0.5027
Mean geometric <i>O. aspinata</i> shell size against the number of individuals measured in each zone	5	0.3733
Range geometric <i>O. aspinata</i> shell size against the number of individuals measured in each zone	5	0.6335

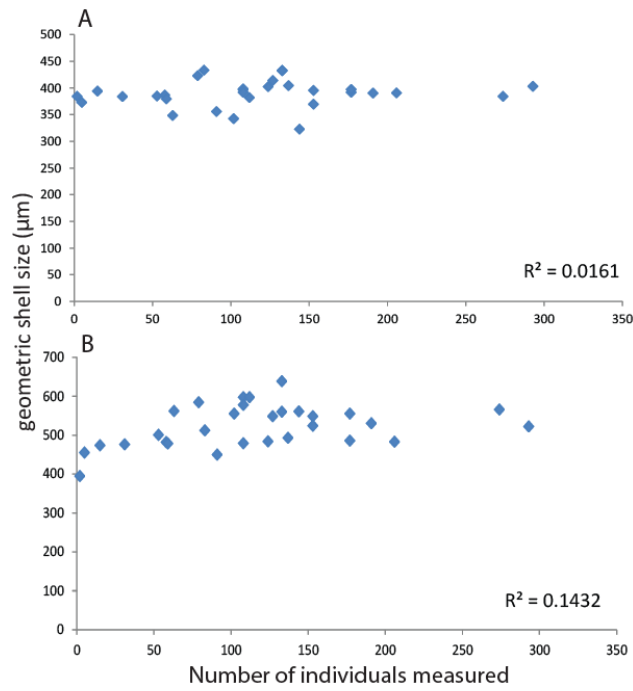


Figure A4.6: Lyme Regis, *O. aspinata* (A) mean and (B) maximum geometric sizes on each bed and the corresponding number of individuals measured in each bed (Presented in Section 3.5.1).

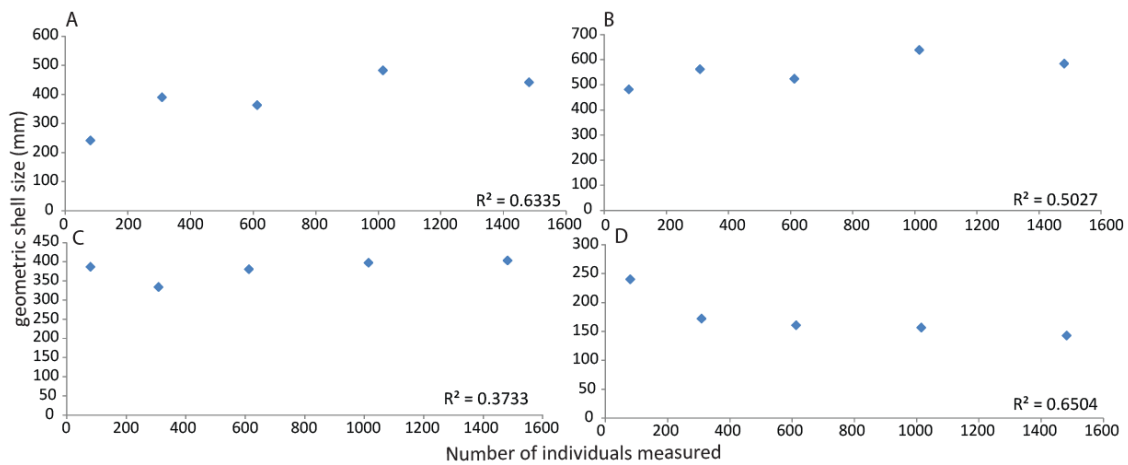
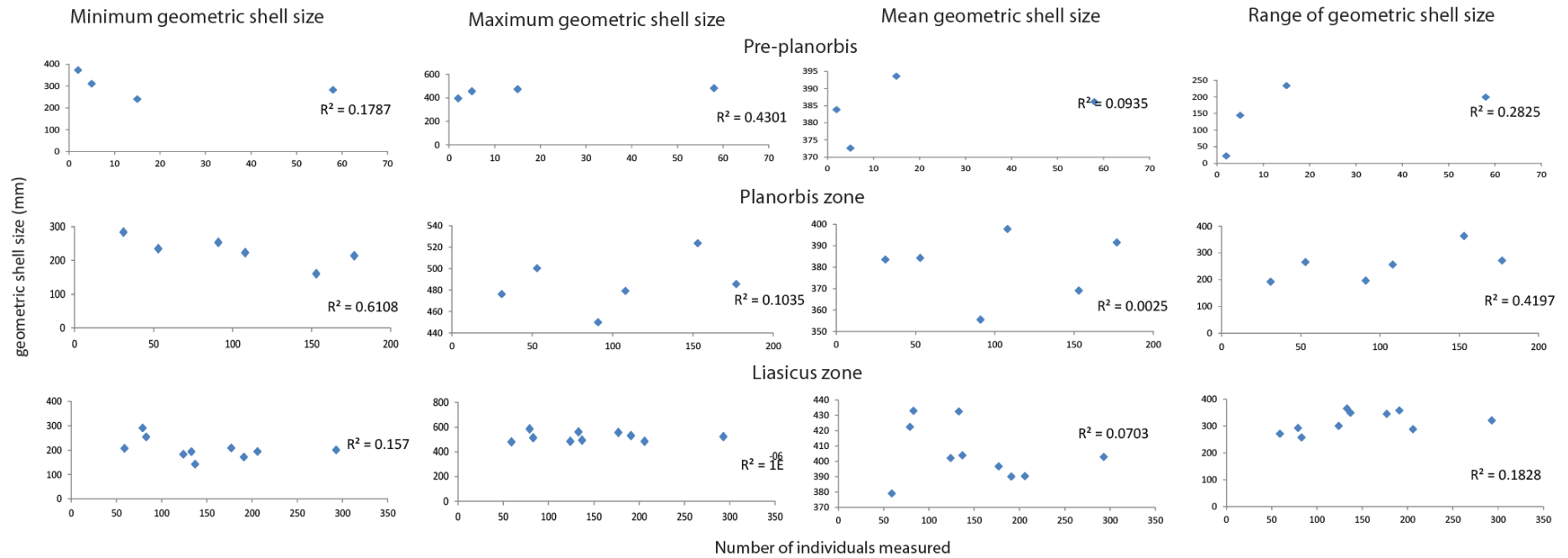


Figure A4.7: *O. aspinata* geometric shell size data (C) mean, (D) minimum, (B) maximum and (A) range of geometric shell size versus the number of individuals measured in each zone) from Lyme Regis (Presented in Section 3.5.1).

Relationships between *Ogmoconchella* geometric shell size and the number of individuals measured on each zoneFigure A4.8A: *O. aspinata* geometric shell size data (the mean, minimum, maximum and range of geometric shell size verses the number of individuals measured from each bed in each Pre-planorbis Zone, Planorbis Zone and Liasicus Zone) from Lyme Regis (Presented in Section 3.5.1).

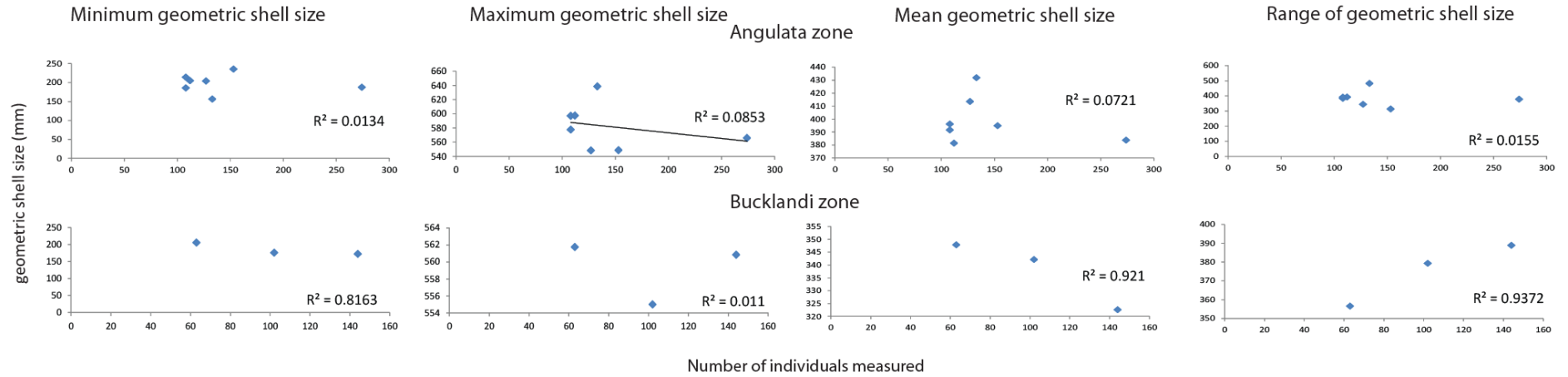
Relationships between *Ogmoconchella* geometric shell size and the number of individuals measured on each zoneFigure A4.8B: *O. aspinata* geometric shell size data (the mean, minimum, maximum and range of geometric shell size versus the number of individuals measured from each bed in each angulata Zone and bucklandi Zone) from Lyme Regis (Presented in Section 3.5.1).

Table A4.8: *O. aspinata* shell thickness results from the statistical analysis when determining any relationship between the mean, min, max and range and the number of individuals measured in Lyme Regis (Presented in Section 3.5.1).

Correlation question	Number of individuals	R ² value
Minimum <i>O. aspinata</i> shell thickness against the number of individuals measured on each bed	33	0.5413
Maximum <i>O. aspinata</i> shell thickness against the number of individuals measured on each bed	33	0.006
Mean <i>O. aspinata</i> shell thickness against the number of individuals measured on each bed	33	0.276
Range <i>O. aspinata</i> shell thickness against the number of individuals measured on each bed	33	0.2216
Minimum <i>O. aspinata</i> shell thickness against the number of individuals measured on each bed in the Pre-planorbis Zone	5	0.5755
Maximum <i>O. aspinata</i> shell thickness against the number of individuals measured on each bed in the Pre-planorbis Zone	5	0.2825
Mean <i>O. aspinata</i> shell thickness against the number of individuals measured on each bed in the Pre-planorbis Zone	5	0.3004
Range <i>O. aspinata</i> shell thickness against the number of individuals measured on each bed in the Pre-planorbis Zone	5	0.506
Minimum <i>O. aspinata</i> shell thickness against the number of individuals measured on each bed in the Planorbis Zone	6	0.2463
Maximum <i>O. aspinata</i> shell thickness against the number of individuals measured on each bed in the Planorbis Zone	6	0.00005
Mean <i>O. aspinata</i> shell thickness against the number of individuals measured on each bed in the Planorbis Zone	6	0.3327
Range <i>O. aspinata</i> shell thickness against the number of individuals measured on each bed in the Planorbis Zone	6	0.0564
Minimum <i>O. aspinata</i> shell thickness against the number of individuals measured on each bed in the liasicus Zone	12	0.1308
Maximum <i>O. aspinata</i> shell thickness against the number of individuals measured on each bed in the liasicus Zone	12	0.0773
Mean <i>O. aspinata</i> shell thickness against the number of individuals measured on each bed in the liasicus Zone	12	0.2402
Range <i>O. aspinata</i> shell thickness against the number of individuals measured on each bed in the liasicus Zone	12	0.0057
Minimum <i>O. aspinata</i> shell thickness against the number of individuals measured on each bed in the angulata Zone	7	0.0003
Maximum <i>O. aspinata</i> shell thickness against the number of individuals measured on each bed in the angulata Zone	7	0.0081
Mean <i>O. aspinata</i> shell thickness against the number of individuals measured on each bed in the angulata Zone	7	0.0373
Range <i>O. aspinata</i> shell thickness against the number of individuals measured on each bed in the angulata Zone	7	0.0106
Minimum <i>O. aspinata</i> shell thickness against the number of individuals measured on each bed in the bucklandi Zone	3	0.1892
Maximum <i>O. aspinata</i> shell thickness against the number of individuals measured on each bed in the bucklandi Zone	3	0.9279
Mean <i>O. aspinata</i> shell thickness against the number of individuals measured on each bed in the bucklandi Zone	3	0.05993
Range <i>O. aspinata</i> shell thickness against the number of individuals measured on each bed in the bucklandi Zone	3	0.8268
Minimum <i>O. aspinata</i> shell thickness against the number of individuals measured in each zone	5	0.0386
Maximum <i>O. aspinata</i> shell thickness against the number of individuals measured in each zone	5	0.0003
Mean <i>O. aspinata</i> shell thickness against the number of individuals measured in each zone	5	0.4294
Range <i>O. aspinata</i> shell thickness against the number of individuals measured in each zone	5	0.1069

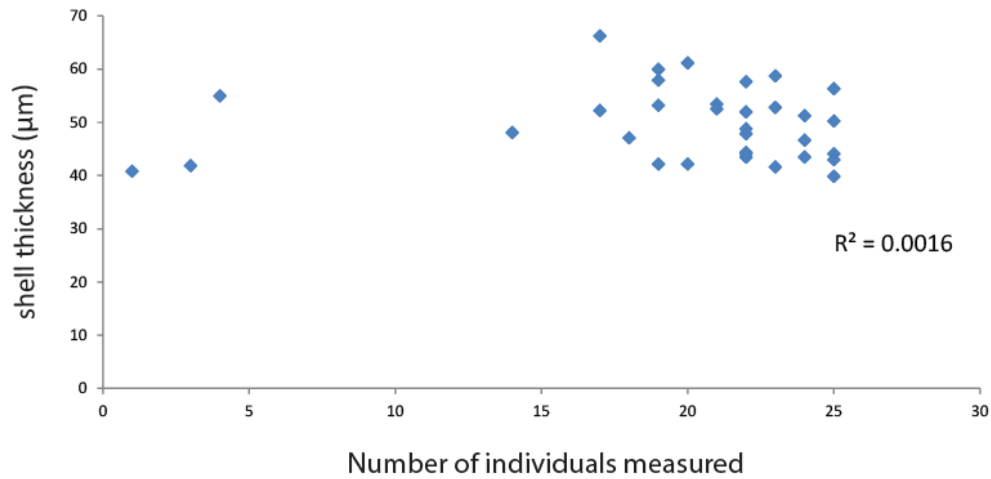


Figure A4.9: Lyme Regis, *O. aspinata* maximum shell thickness on each bed verses the corresponding number of individuals measured in each bed (Presented in Section 3.5.1).

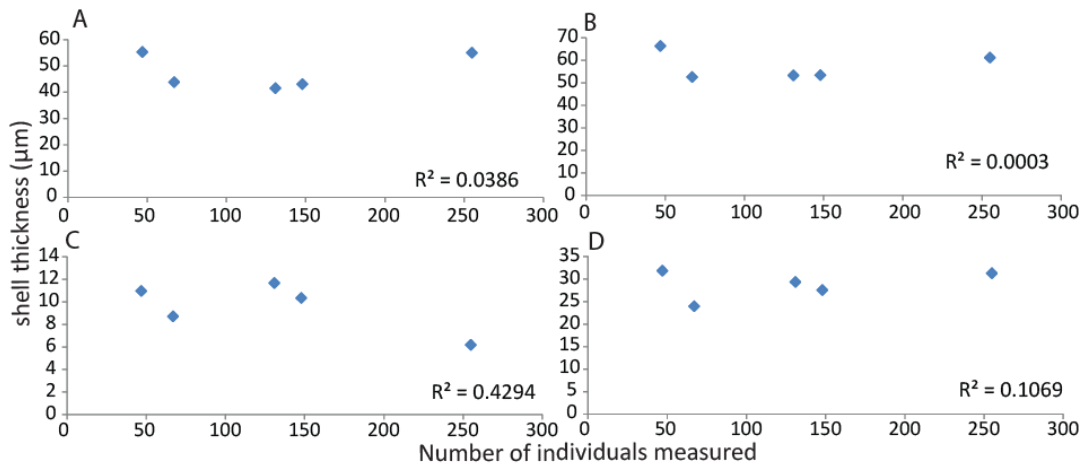


Figure A4.10: *O. aspinata* geometric shell thickness data (D) mean, (C) minimum, (B) maximum and (A) range of geometric shell size verses the number of individuals measured in each zone from Lyme Regis (Presented in Section 3.5.1).

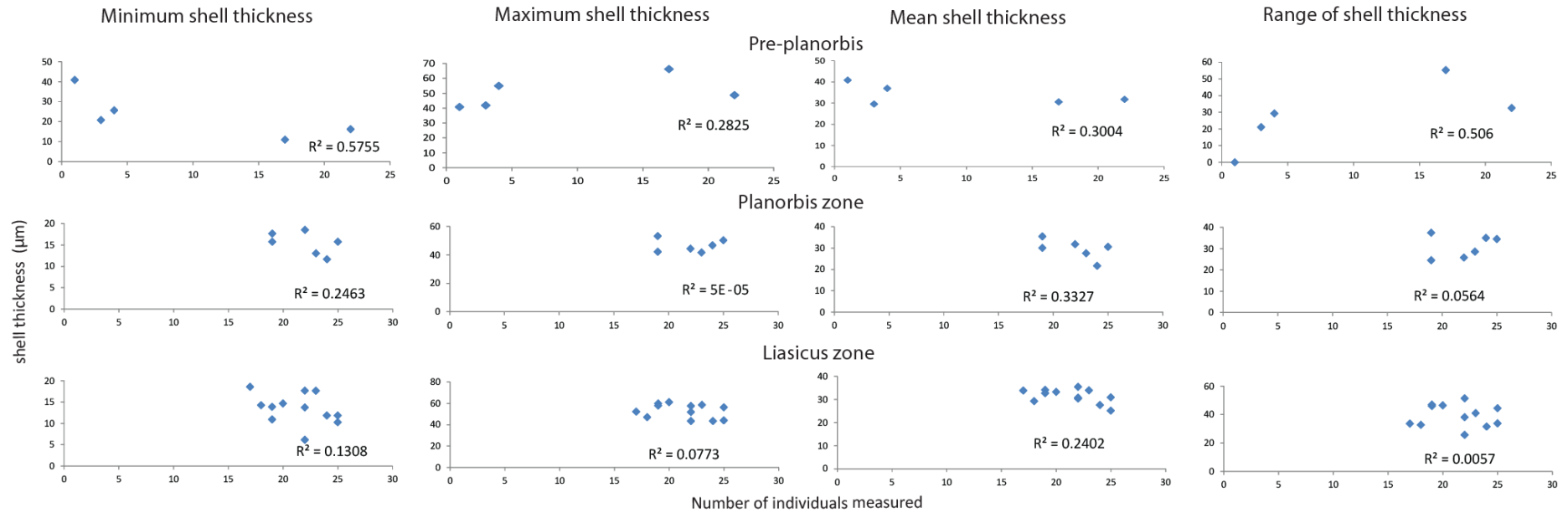
Relationships between *Ogmoconchella* shell thickness and the number of individuals measured on each zoneFigure A4.11A: *O. aspinata* shell thickness data (the mean, minimum, maximum and range of geometric shell size verses the number of individuals measured from each bed in each Pre-planorbis Zone, Planorbis Zone and liasicus Zone) from Lyme Regis (Presented in Section 3.5.1).

Table A4.9B: *L. hisingeri* statistical results from the geometric shell size from every bed within the Planorbis Zone from Lyme Regis using the Kruskal-Wallis and the Mann Whitney tests (Presented in Section 3.5.3).

Planorbis Zone					
H (chl ²)	4.978	Hc (tie corrected)	4.978	p(same)	0.4186
	LRBL BED30	LRBL BED34	LRBL BED36	LRBL BED40	LRBL BED42
LRBL BED26	0.09068	0.3999	0.8889	0.7103	0.1951
LRBL BED30		0.7103	0.09596	0.4341	0.9554
LRBL BED34			0.5315	0.4772	0.6356
LRBL BED36				0.7297	0.1762
LRBL BED40					0.5897

Table A4.9C: *L. hisingeri* statistical results from the geometric shell size from every bed within the liasicus Zone from Lyme Regis using the Kruskal-Wallis and the Mann Whitney tests (Presented in Section 3.5.3).

liasicus Zone									
H (chl ²)	33.44	Hc (tie corrected)	33.44	p(same)	0.000112				
	LRBL BED46	LRBL BED48	LRBL BED50	LRBL BED52	LRBL BED54	LRBL BED56	LRBL BED60	LRBL BED62	LRBL BED72
LRBL BED44	0.2136	0.9062	0.09772	0.519	0.9725	0.8905	0.7398	0.2472	0.5403
LRBL BED46		0.2698	0.07971	0.6368	0.00226	0.0008604	0.1057	0.01177	0.1029
LRBL BED48			0.0403	0.446	0.6014	0.7167	0.9142	0.1897	0.2963
LRBL BED50				0.05161	0.0001516	0.0000266	0.007661	0.005963	0.1167
LRBL BED52					0.03265	0.02581	0.2959	0.05573	0.1506
LRBL BED54						0.7622	0.3739	0.1469	0.1813
LRBL BED56							0.4505	0.07625	0.1346
LRBL BED60								0.117	0.1231
LRBL BED62									0.2888

Table A4.9D-E: *L. hisingeri* statistical results from the geometric shell size from every bed within the (D) angulata Zone and (E) bucklandi Zone from Lyme Regis using the Kruskal-Wallis and the Mann Whitney tests (Presented in Section 3.5.3).

(D) Angulata Zone			
H (chl ²)	3.08	Hc (tie corrected)	3.08
p(same)	0.3794		
	LRBL BED86	LRBL BED88	LRBL BED92
LRBL BED84	0.3123	0.9247	0.7237
LRBL BED86		0.2986	0.7237
LRBL BED88			0.1904

(E) bucklandi Zone	
H (chl ²)	2.301
Hc (tie corrected)	2.301
p(same)	0.1293
	LRBLBED 103
LRBL BED102	0.1486
LRBLBED 103	

Table A4.10: Kruskal-Wallis and Mann Whitney results for the compiled *L. hisingeri* geometric Zone data in Lyme Regis (Presented in Section 3.5.3).

H (chi ²)	20.1	Hc (tie corrected)	20.1	p(same)	0.0004782
	planorbis Zone	liasicus Zone	angulata Zone	bucklandi Zone	
Pre-planorbis Zone	0.1594	0.9905	0.003741	0.001283	
planorbis Zone		0.298	0.001004	0.0001278	
liasicus Zone			0.01161	0.0194	
angulata Zone				0.4477	

Table A4.11: Kruskal-Wallis and Mann Whitney results for the compiled *L. hisingeri* geometric subzone data in Lyme Regis (Presented in Section 3.5.3).

H (chi ²)	38	Hc (tie corrected)	38	p(same)	0.00000112	
	Ps. planorbis	C. johnstoni	W. portlocki	Alsatites laqueus	Schlotheimia angulata	Coroniceras rotiforme
Pre-planorbis Zone	0.07204	0.4271	0.003468	0.09518	0.003741	0.001283
Ps. planorbis		0.2335	0.371	0.01073	0.000715	0.0001948
johnstoni			0.01162	0.04944	0.002722	0.0004765
W. portlocki				0.0002096	0.0001707	0.0000508
Alsatites laqueus					0.07176	0.1836
Schlotheimia						0.4477

Table A4.12A: *P. gigantea* statistical results from the geometric shell size from every bed within the Planorbis Zone from Lyme Regis using the Kruskal-Wallis and the Mann Whitney tests (Presented in Section 3.5.4).

Planorbis Zone						
H (chi ²)	28	Hc (tie corrected)	28	p(same)	0.0000941	
	LRBL BED26	LRBL BED30	LRBL BED32	LRBL BED34	LRBL BED36	LRBL BED40
LRBL BED24	0.2453	0.06139	0.5403	0.5403	0.03065	0.3337
LRBL BED26		0.9668	0.5403	0.5403	0.1567	0.1071
LRBL BED30			0.1352	0.1066	0.0008828	0.01232
LRBL BED32				1	0.1289	0.2684
LRBL BED34					0.1289	0.1547
LRBL BED36						0.000116

Table A4.12B: *P. gigantea* statistical results from the geometric shell size from every bed within the liasicus Zone from Lyme Regis using the Kruskal-Wallis and the Mann Whitney tests (Presented in Section 3.5.4).

liasicus Zone								
H (chi^2)	36.89	Hc (tie corrected)	36.89	p(same)	0.0000121			
	LRBL BED46	LRBL BED48	LRBL BED50	LRBL BED52	LRBL BED54	LRBL BED56	LRBL BED60	LRBL BED72
LRBL BED44	0.8465	0.6134	0.8623	0.8045	0.2981	0.5403	1	0.2888
LRBL BED46		0.3103	0.8944	0.5322	0.04092	0.05019	0.8465	0.01379
LRBL BED48			0.1609	0.4878	0.0000377	0.0215	0.2481	0.001192
LRBL BED50				0.3684	0.00197	0.02666	0.6029	0.002353
LRBL BED52					0.0000548	0.02069	0.3469	0.001324
LRBL BED54						0.1683	0.3859	0.0208
LRBL BED56							0.5403	0.817
LRBL BED60								0.2888

Table A4.12C-D: *P. gigantea* statistical results from the geometric shell size from every bed within (C) angulata Zone and (D) bucklandi Zone from Lyme Regis using the Kruskal-Wallis and the Mann Whitney tests (Presented in Section 3.5.4).

(C) angulata Zone					
H (chi^2)	1.174	Hc (tie corrected)	1.174	p(same)	0.8824
	LRBL BED84	LRBL BED86	LRBL BED88	LRBL BED90	
LRBL BED76	0.5403	1	0.6353	0.5403	
LRBL BED84		0.5403	0.7473	0.6985	
LRBL BED86			0.4292	0.5403	
LRBL BED88				0.7473	

(D) bucklandi Zone	
H (chi^2)	0.08571
Hc (tie corrected)	0.08571
p(same)	0.7697
	LRBL BED96
LRBL BED94	1

Table A4.13: Kruskal-Wallis and Mann Whitney results for the compiled *P. gigantea* geometric zone data in Lyme Regis (Presented in Section 3.5.4).

H (chi^2)	68.91	Hc (tie corrected)	68.91	p(same)	3.86 x 10 ⁻¹⁴
	planorbis Zone	liasicus Zone	angulata Zone	bucklandi Zone	
Pre-planorbis Zone	0.4122	0.3577	0.008605	0.02819	
planorbis Zone		0.000000182	0.0000000221	0.0001342	
liasicus Zone			0.000000245	0.002297	
angulata Zone				0.8538	

Table A4.15D-E: *O. aspinata* statistical results from the geometric shell size from every bed within the angulata Zone and bucklandi Zone from Lyme Regis using the Kruskal-Wallis and the Mann Whitney tests (Presented in Section 3.5.5).

(D) angulata Zone						
H (chi ²)	49.81	Hc (tie corrected)	49.81	p(same)	0.0000000512	
	LRBL BED74A	LRBL BED75A	LRBL BED76A	LRBL BED77A	LRBL BED89	LRBL BED93
LRBL BED73	0.2481	0.6586	0.01878	0.2349	0.0000135	0.000000923
LRBL BED74A		0.3856	0.4684	0.9176	0.01156	0.00064
LRBL BED75A			0.0265	0.2426	0.00000905	0.00000366
LRBL BED76A				0.7423	0.005959	0.0000944
LRBL BED77A					0.0241	0.000728
LRBL BED89						0.09466

(E) bucklandi Zone		
H (chi ²)	7.326	
Hc (tie corrected)	7.326	
p(same)	0.02565	
	LRBL BED97	LRBL BED99
LRBL BED95	0.08895	0.009426
LRBL BED97		0.8261

Table A4.16: Kruskal-Wallis and Mann Whitney results for the compiled *O. aspinata* geometric zone data in Lyme Regis (Presented in Section 3.5.5).

H (chi ²)	298.9	Hc (tie corrected)	298.9	p(same)	1.90 x 10 ⁻⁶³
	planorbis Zone	liasicus Zone	angulata Zone	bucklandi Zone	
Pre-planorbis Zone	0.4796	0.001515	0.3365	2.44 x 10 ⁻¹²	
planorbis Zone		8.53 x 10 ⁻²⁰	0.000696	8.43 x 10 ⁻³⁰	
liasicus Zone			0.0000538	2.79 x 10 ⁻⁵⁷	
angulata Zone				1.61 x 10 ⁻³⁶	

Table A4.17: Kruskal-Wallis and Mann Whitney results for the compiled *O. aspinata* geometric subzone data in Lyme Regis (Presented in Section 3.5.5).

H (chi ²)	329.5	Hc (tie corrected)	329.5	p(same)	3.87 x 10 ⁻⁶⁸	
	Ps. planorbis	johnstoni	W. portlocki	Alsatites laqueus	Schlotheimia	Metophioceras
Pre-planorbis Zone	0.007865	0.8318	0.1981	0.0001486	0.3365	2.44 x 10 ⁻¹²
Ps. planorbis		0.0000149	0.00000988	7.44 x 10 ⁻¹⁸	0.00000232	0.00000000346
johnstoni			0.02835	1.51 x 10 ⁻¹⁴	0.1225	1.19 x 10 ⁻³¹
W. portlocki				0.00000195	0.9086	2.65 x 10 ⁻³⁰
Alsatites laqueus					0.00000195	4.79 x 10 ⁻⁵⁹
Schlotheimia						1.61 x 10 ⁻³⁶

Table A4.18A-B: *O. aspinata* statistical results from the shell thickness from every bed within the (A) Pre-planorbis Zone and (B) Planorbis Zone from Lyme Regis using the Kruskal-Wallis and the Mann Whitney tests (Presented in Section 3.5.5).

(A) Pre-planorbis Zone					
H (chi ²)	2.168	Hc (tie corrected)	2.168	p(same)	0.705
	LRBL BED7	LRBL BED15	LRBL BED17	LRBL BED21	
LRBL BED3	1	0.7237	0.2475	0.407	
LRBL BED7		0.5959	1	0.7067	
LRBL BED15			0.3949	0.4996	
LRBL BED17				0.5808	

(B) Planorbis Zone					
H (chi ²)	28.25	Hc (tie corrected)	28.25	p(same)	0.0000326
	LRBL BED25	LRBL BED27	LRBL BED33	LRBL BED37	LRBL BED39
LRBL BED23	0.1046	0.006852	0.1782	0.0000575	0.04712
LRBL BED25		0.2925	0.5155	0.0003306	0.9433
LRBL BED27			0.1094	0.009718	0.3002
LRBL BED33				0.0001487	0.4252
LRBL BED37					0.0008432

Table A4.18C: *O. aspinata* statistical results from the shell thickness from every bed within the liasicus Zone from Lyme Regis using the Kruskal-Wallis and the Mann Whitney tests (Presented in Section 3.5.5).

liasicus Zone											
H (chi ²)	19.42	Hc (tie corrected)	19.42	p(same)	0.05391						
	LRBL BED49	LRBL BED49A	LRBL BED51	LRBL BED51A	LRBL BED53	LRBL BED55	LRBL BED59	LRBL BED61	LRBL BED63	LRBL BED67	LRBL BED69
LRBL BED47	0.4527	0.3726	0.2049	0.615	0.1668	0.5335	0.7962	0.3234	0.07062	0.2283	0.232
LRBL BED49		0.3669	0.09519	0.8898	0.3679	0.1416	0.332	0.5858	0.07162	0.4122	0.3749
LRBL BED49A			0.02594	0.4131	0.944	0.09194	0.4276	0.8441	0.3077	0.726	0.9903
LRBL BED51				0.1122	0.02023	0.3125	0.08228	0.03927	0.003612	0.01971	0.01864
LRBL BED51A					0.3955	0.3972	0.9719	0.4102	0.06203	0.4034	0.4072
LRBL BED53						0.04899	0.1956	0.7261	0.539	0.9495	0.8795
LRBL BED55							0.1436	0.08036	0.01257	0.03103	0.08474
LRBL BED59								0.3017	0.1185	0.2882	0.3698
LRBL BED61									0.2665	0.6573	0.8995
LRBL BED63										0.5615	0.4334
LRBL BED67											0.7844

Table A4.18D-E: *O. aspinata* statistical results from the shell thickness from every bed within the (D) angulata Zone and (E) bucklandi Zone from Lyme Regis using the Kruskal-Wallis and the Mann Whitney tests (Presented in Section 3.5.5).

(D) angulata Zone						
H (chi ²)	13.26	Hc (tie corrected)	13.26	p(same)	0.03915	
	LRBL BED74A	LRBL BED75A	LRBL BED76A	LRBL BED77A	LRBL BED89	LRBL BED93
LRBL BED73	0.7608	0.06787	0.2015	0.545	0.01128	0.2791
LRBL BED74A		0.2201	0.5624	0.274	0.06259	0.707
LRBL BED75A			0.8329	0.01553	0.5601	0.7246
LRBL BED76A				0.1042	0.4226	0.9866
LRBL BED77A					0.001423	0.07056
LRBL BED89						0.5466

(E) bucklandi Zone		
H (chi ²)	0.9389	
Hc (tie corrected)	0.9389	
p(same)	0.6253	
	LRBL BED97	LRBL BED99
LRBL BED95	0.3104	0.568
LRBL BED97		0.873

Table A4.19: Kruskal-Wallis and Mann Whitney results for the compiled *O. aspinata* shell thickness zone data in Lyme Regis (Presented in Section 3.5.5).

H (chi ²)	36.67	Hc (tie corrected)	36.67	p(same)	0.00000211
	planorbis Zone	liasicus Zone	angulata Zone	bucklandi Zone	
Pre-planorbis Zone	0.1848	0.816	0.02424	0.0000918	
planorbis Zone		0.07641	0.1575	0.0000580	
liasicus Zone			0.000771	0.000000733	
angulata Zone				0.004009	

Table A4.20: Kruskal-Wallis and Mann Whitney results for the compiled *O. aspinata* shell thickness subzone data in Lyme Regis (Presented in Section 3.5.5).

H (chi ²)	40.34	Hc (tie corrected)	40.34	p(same)	0.00000391	
	Ps. planorbis	C. johnstoni	W. portlocki	Alsatites laqueus	Schlotheimia angulata	Metophioceras conybeari
Pre-planorbis Zone	0.7126	0.04501	0.8514	0.8202	0.02424	0.0000918
Ps. planorbis		0.04189	0.8815	0.8137	0.02182	0.0000974
C. johnstoni			0.0448	0.01427	0.9751	0.01272
W. portlocki				0.9961	0.0239	0.0000282
Alsatites laqueus					0.001391	0.00000193
Schlotheimia						0.004009

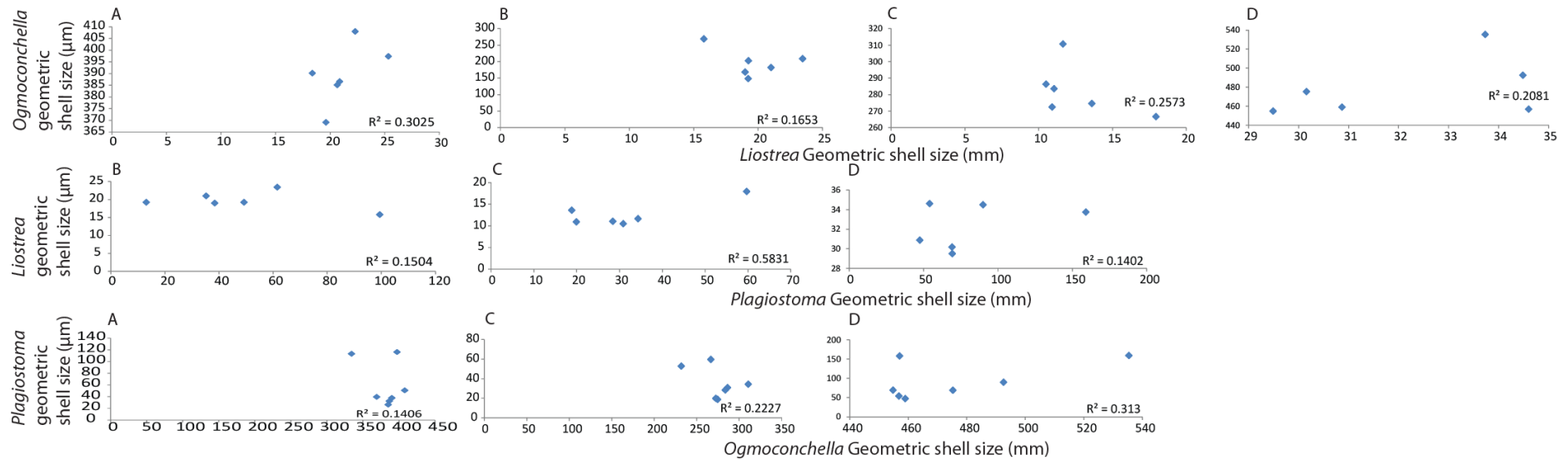


Figure A4.12: The (A) mean, (B) 95th percentile range, (C) 95th percentile minimum and (D) 95th percentile maximum *L. hisingeri*, *P. gigantea* and *O. aspinata* geometric size for each subzone, correlated against each other to determine any statistical correlation between the three species growth patterns at Lyme Regis (Presented in Section 3.7).

Table A4.21: Geometric shell size data from all three species compared against each other to determine any relationships in growth in Lyme Regis (Presented in Section 3.7).

Correlation question	Number of individuals	R ² value
mean <i>P. gigantea</i> versus mean <i>L. hisingeri</i> geometric size	6	0.738
95 th percentile range <i>P. gigantea</i> versus the 95 th percentile range <i>L. hisingeri</i> geometric size	6	0.1504
95 th percentile minimum <i>P. gigantea</i> versus the 95 th percentile minimum <i>L. hisingeri</i> geometric size	6	0.5831
95 th percentile maximum <i>P. gigantea</i> versus the 95 th percentile maximum <i>L. hisingeri</i> geometric size	6	0.1402
mean <i>O. aspinata</i> versus mean <i>P. gigantea</i> geometric size	7	0.1406
95 th percentile range <i>O. aspinata</i> versus the 95 th percentile range <i>P. gigantea</i> geometric size	7	0.8341
95 th percentile minimum <i>O. aspinata</i> versus the 95 th percentile minimum <i>P. gigantea</i> geometric size	7	0.2227
95 th percentile maximum <i>O. aspinata</i> versus the 95 th percentile maximum <i>P. gigantea</i> geometric size	7	0.313
mean <i>L. hisingeri</i> versus mean <i>O. aspinata</i> geometric size	6	0.3025
95 th percentile range <i>L. hisingeri</i> versus the 95 th percentile range <i>O. aspinata</i> geometric size	6	0.1653
95 th percentile minimum <i>L. hisingeri</i> versus the 95 th percentile minimum <i>O. aspinata</i> geometric size	6	0.2573
95 th percentile maximum <i>L. hisingeri</i> versus the 95 th percentile maximum <i>O. aspinata</i> geometric size	6	0.2081

A4.2: St Audrie's Bay raw fossil data

Table A4.22: *L. hisingeri* geometric shell size data from every individual per bed in St Audrie's Bay with the corresponding stratigraphic zones, subzones and bed height (Presented in Section 3.5.3) (measured in mm).

<i>L. hisingeri</i>						
Zone	Subzone	Bed N.	Bed height	Geometric shell size	Shell preservation	
Pre-planorbis		SAB12	12.55	18.5	SP, PSOS	
			12.55	22.0	PSOS	
			12.55	20.1	DDW	
			12.55	16.0	DDW	
			12.55	14.5	PSOS	
			12.55	11.5	OMI, ISCS	
			12.55	13.6	PSOS	
			12.55	15.9	SP	
			12.55	17.0	PSOS	
			12.55	16.3	PSOS	
			12.55	18.1	DDW	
			12.55	19.8	PSOS	
			12.55	25.7	PSOS	
			12.55	12.3	SP	
			12.55	13.5	PSOS	
			12.55	20.6	SP	
			12.55	12.4	SP	
			12.55	23.6	SP	
			12.55	15.6	SP	
			12.55	14.6	SP	
			12.55	17.6	MDP	
			12.55	20.7	DDW	
			12.55	19.4	PSOS	
			12.55	11.2	PSOS	
			12.55	10.3	PSOS	
			12.55	13.1	DDW	
			12.55	15.9	DDW	
			12.55	9.3	DDW	
			12.55	11.0	DDW	
			12.55	17.7	PSOS	
			12.55	19.5	DDW	
			12.55	20.7	PSOS	
			12.55	10.8	PSOS	
		12.55	12.8	PSOS		
		12.55	18.1	PSOS		
		12.55	12.6	PSOS		
		12.55	16.4	PSOS		
		12.55	20.1	PSOS		
		12.55	17.3	DDW		
		12.55	20.0	DDW		
		14.6	SAB16	14.6	17.5	PSOS
		14.6		14.9	PSOS	
		14.6		17.0	PSOS	
		14.6		16.3	PSOS	
		14.6		16.8	PSOS	
		14.6		10.2	PSOS	
		14.6	10.8	PSOS		
		15.45	SAB18	15.45	25.3	PSOS
		15.45		19.8	PSOS	
		15.45		18.6	DDW	
15.45	18.3	DDW, MDP				
15.45	19.9	OMI, CSM				
15.45	19.5	PSOS				
15.45	10.5	PSOS				
15.45	22.9	PSOS				
15.45	22.1	MS				
15.45	26.1	SP				
15.45	14.7	SP				
15.45	24.1	SP				
15.5	SAB18A	15.5	25.6	MDP		

<i>L. hisingeri</i>					
Zone	Subzone	Bed N.	Bed height	Geometric shell size	Shell preservation
			15.5	17.4	PSOS
			15.5	22.3	PSOS
			15.5	26.1	SP
			15.5	26.8	SP
			15.5	22.1	MDP
			15.5	21.3	SCC
			15.5	14.2	PSOS
			15.5	23.7	SP
			15.5	27.7	SCC
			15.5	20.9	OMI, ISCS
			15.5	30.5	MS
			15.5	19.7	SCC
		SAB19A	15.57	22.8	PSOS
			15.57	27.6	MDP
			15.67	26.3	DDW
			15.67	20.2	DDW
			15.67	25.0	PSOS
			15.67	31.3	SCC
			15.67	21.8	PSOS
			15.67	19.2	SP
			15.67	18.4	MDP
			15.67	17.3	SP
			15.67	21.1	DDW
			15.67	16.9	DDW
			15.67	19.4	DDW
			15.67	26.2	DDW
			15.67	18.5	DDW
			15.67	19.9	DDW
			15.67	21.2	MDP
			15.67	29.5	DDW
			15.67	17.7	DDW
			15.67	26.0	DDW
			15.67	23.5	DDW
			15.67	19.8	SP
			15.67	22.4	DDW
			15.67	19.9	PSOS
			15.67	16.3	DDW
		SAB19	15.67	18.7	MDP
			15.67	27.1	MDP
			15.67	12.4	SP
			15.67	17.3	SCC
			15.67	16.7	SP
			15.67	24.6	SP
			15.67	22.4	SP
			15.67	24.6	SP
			15.67	16.2	MDP, SCC
			15.67	21.4	MDP
			15.67	23.4	SCC
			15.67	27.6	MS
			15.67	23.2	MS
			15.67	22.1	SP
			15.67	24.0	SCC
			15.67	16.2	PSOS, MS
			15.67	21.6	SCC
			15.67	17.3	MDP, MS
			15.67	19.0	MDP
			15.67	22.7	PSOS
			15.67	26.4	PSOS
			15.67	26.0	MDP
			15.67	23.1	PSOS
		SAB20	15.8	23.2	SCP, OLMD, PCSM
			15.8	21.8	MDP
			15.8	25.3	PSOS
			15.8	25.2	PSOS, MS
			15.8	28.0	SCC, PSOS
			15.8	32.1	SCC, MDP
			15.8	28.0	SCC, MDP
			15.8	11.8	MDP, PSOS

<i>L. hisingeri</i>					
Zone	Subzone	Bed N.	Bed height	Geometric shell size	Shell preservation
			15.8	12.2	MDP
			15.8	32.4	SCC, PSOS
			15.8	21.3	SCC, PSOS
			15.8	23.1	DDW
			15.8	29.0	PSOS
			15.8	17.6	PSOS
			15.8	32.7	PSOS
			15.8	24.3	PSOS
			15.8	26.4	PSOS
			15.8	24.5	PSOS
			15.8	26.2	DDW
			15.8	27.9	PSOS
			15.8	33.0	MS
			15.8	27.0	MDP
			15.8	23.4	SP
			15.8	23.0	PSOS
			15.8	33.1	MS
			15.8	23.1	PSOS
			15.8	22.7	SP
			15.8	29.6	MDP
			15.8	17.8	MDP
			15.8	23.8	MDP
			15.8	28.7	MDP
			15.8	27.6	PSOS
			15.8	27.2	PSOS
			15.8	27.0	PSOS
			15.8	26.1	MDP
			15.8	12.8	MDP
			15.8	34.7	MS
			15.8	18.2	SP
			15.8	19.9	SP
			15.8	26.1	SP
			15.8	24.4	SP
			15.8	17.1	SP
		SAB21	16.07	17.5	MDP
			16.07	20.3	MDP
			16.07	27.1	MDP
			16.07	23.1	MDP
			16.07	20.7	MDP
			16.07	25.6	MDP
			16.07	29.9	MDP
		SAB22	16.3	26.0	MDP
			16.3	18.0	SCC
		SAB23	16.5	11.9	DDW, MDP
			16.5	17.2	DDW, MDP
			16.5	20.4	DDW, MDP
			16.5	28.5	DDW, MDP
			16.5	14.5	DDW, MDP
			16.5	14.8	DDW, MDP
		SAB24	16.7	32.4	SCC, PSOS
			16.7	36.5	DDW, MDP
			16.7	27.9	DDW, MDP
			16.7	23.8	DDW, MDP
			16.7	16.7	DDW, MDP
			16.7	37.4	DDW, MDP
			16.7	17.9	DDW, MDP
			16.7	15.2	DDW, MDP
			16.7	27.2	DDW, MDP
			16.7	23.9	DDW, MDP
			16.7	18.2	DDW, MDP
			16.7	22.4	DDW, MDP
			16.7	34.0	DDW, MDP
			16.7	14.4	DDW, MDP
			16.7	27.1	DDW, MDP
			16.7	33.6	DDW, MDP
			16.7	27.4	DDW, MDP
			16.7	20.3	DDW, MDP
			16.7	18.5	DDW, MDP

<i>L. hisingeri</i>					
Zone	Subzone	Bed N.	Bed height	Geometric shell size	Shell preservation
			16.7	16.7	DDW, MDP
			16.7	26.7	DDW, MDP
			16.7	44.1	MS
			16.7	33.1	DDW, MDP
			16.7	34.5	DDW, MDP
			16.7	25.7	DDW, MDP
			16.7	20.7	DDW, MDP
			16.7	35.2	DDW, MDP
			16.7	13.5	DDW, MDP
			16.7	18.9	DDW, MDP
			16.7	31.8	DDW, MDP
			16.7	35.7	DDW, MDP
			16.7	16.8	DDW, MDP
			16.7	19.9	DDW, MDP
			16.7	31.0	DDW, MDP
			16.7	29.0	DDW, MDP
			16.7	24.8	PSOS
			16.7	36.6	MS
			16.7	15.0	MDP
		16.7	34.0	MS	
		SAB25	16.9	26.4	MS
			16.9	29.2	DDW, MDP
			16.9	33.9	DDW
			16.9	23.6	DDW
			16.9	34.4	SP
			16.9	35.7	DWW
			16.9	37.8	SP
		SAB26	16.9	28.2	SP
			17.15	30.5	DDW, MDP
			17.15	16.3	DDW, MDP
			17.15	13.9	DDW, MDP
			17.15	14.4	DDW, MDP
			17.15	14.9	DDW, MDP
			17.15	21.0	DDW, MDP
			17.15	25.9	DDW, MDP
			17.15	39.7	DDW, MDP, PSOS
			17.15	29.4	DDW, MDP
			17.15	13.6	DDW, MDP
			17.15	21.5	DDW, MDP
			17.15	26.2	DDW, MDP
			17.15	35.4	DDW, MDP, PSOS
			17.15	26.2	SP
			17.15	17.6	SP
			17.15	31.7	DDW, MDP
17.15	28.7		DDW, MDP		
17.15	20.1		DDW, MDP		
17.15	16.3		DDW, MDP, PSOS		
17.15	28.4	DDW, MDP			
17.15	28.4	DDW, MDP			
17.15	21.6	DDW, MDP			
17.15	26.6	SCC			
planorbis Zone	Ps. planorbis subzone	SAB29	18.1	37.7	DDW, MDP
			18.1	25.7	DDW, MDP
			18.1	35.6	DDW, MDP
		SAB35	20.4	11.7	DDW, MDP
			20.4	10.6	DDW, MDP
			20.4	13.1	DDW, MDP
			20.4	28.8	DDW, MDP
			20.4	16.6	DDW, MDP
			20.4	10.5	DDW, MDP
			20.4	15.1	DDW, MDP
			20.4	22.4	DDW, MDP
			20.4	17.0	DDW, MDP
			20.4	23.9	DDW, MDP
			20.4	11.1	DDW, MDP
			20.4	25.8	DDW, MDP
			20.4	24.7	DDW, MDP
			20.4	20.7	DDW, MDP

<i>L. hisingeri</i>					
Zone	Subzone	Bed N.	Bed height	Geometric shell size	Shell preservation
			20.4	14.7	DDW, MDP
			20.4	15.9	DDW, MDP
			20.4	17.9	DDW, MDP
			20.4	14.9	DDW, MDP
			20.4	16.1	DDW, MDP
			20.4	18.1	DDW, MDP
			20.4	22.7	DDW, MDP
		SAB36	20.8	29.4	SCC
			20.8	24.2	PSOS
			23.45	14.7	DDW, MDP
	C. johnstoni subzone	SAB41	23.45	17.2	DDW, MDP
			23.45	20.0	DDW, MDP
			23.45	20.8	DDW, MDP
			23.45	23.8	DDW, MDP
			23.45	19.8	DDW, MDP
			23.45	13.8	DDW, MDP
			23.45	26.2	DDW, MDP
			23.45	15.0	DDW, MDP
		SAB43	23.45	15.9	DDW, MDP
			24.11	22.0	DDW, MDP
		SAB43	24.11	17.0	DDW, MDP
			24.11	17.9	DDW, MDP
			24.11	17.9	DDW, MDP
liasicus Zone	Alsatites laqueus subzone	SAB63	48.65	9.3	DDW, MDP
			48.65	18.8	DDW, MDP
		SAB71	51.3	26.8	PSOS

Table A4.23 A-C: *O. aspinata* geometric shell size from every individual per bed in St Audrie's Bay with the corresponding stratigraphic zones, subzones and bed height (Presented in Section 3.5.5) (measured in μm).

(A)						<i>O. aspinata</i>					
Zone	Subzone	Bed N.	Bed height	Geometric shell size	Shell preservation	Zone	Subzone	Bed N.	Bed height	Geometric shell size	Shell preservation
Lilstock Formation	Langport Member	SAB8	12.2	398.5	RV, SP	planorbis Zone	C. johnstoni subzone	SAB40	23.2	423.3	RV, SP
			12.2	416.6	RV, SP				23.2	412.9	RV, SP
			12.2	446.1	LV, SP				23.2	412.0	RV, SP
			12.2	456.8	LV, SP				23.2	481.4	LV, SP
			12.2	490.7	LV, SP				23.2	421.5	RV, SP
			12.2	462.9	LV, SP				23.2	404.5	RV, SP
			12.2	414.0	LV, SP				23.2	473.7	LV, SP
			12.2	425.9	RV, SP				23.2	401.4	LV, SP
			12.2	431.7	LV, SP				23.2	413.5	RV, SP
			12.2	491.9	RV, SP				23.2	443.7	LV, SP
			12.2	423.8	LV, SP				23.2	499.6	LV, SP
			12.2	463.5	LV, SP				23.2	431.6	LV, SP
			12.2	352.3	RV, SP				23.2	385.5	RV, SP
			12.2	403.5	LV, SP				23.2	384.2	SB
			12.2	442.3	LV, SP				23.2	408.1	RV, SP
			12.2	420.4	LV, SP				23.2	410.9	RV, SP
			12.2	471.5	LV, SP				23.2	415.2	RV, SP
			12.2	423.9	RV, SP				23.2	445.3	RV, SP
			12.2	421.2	RV, SP				23.2	442.8	RV, SP
			12.2	448.2	LV, SP				23.2	400.2	LV, SP
			12.2	477.3	LV, SP				23.2	408.1	RV, SP
			12.2	383.0	RV, SP				23.2	434.7	RV, SP
			12.2	440.0	LV, SP				23.2	410.0	LV, SP
			12.2	427.2	RV, SP				23.2	410.0	LV, SP
			12.2	459.2	LV, SP				23.2	382.8	LV, SP
			12.2	415.6	LV, SP				23.2	445.4	LV, SP
			12.2	468.5	RV, SP				23.2	456.7	LV, SP
			12.2	447.7	LV, SP				23.2	424.5	LV, SP
			12.2	425.9	RV, SP				23.2	390.0	LV, SP
			12.2	489.0	RV, SP				23.2	413.3	RV, SP
			12.2	446.1	RV, SP				23.2	412.6	RV, SP
			12.2	416.7	LV, SP				23.2	479.8	RV, SP
12.2	469.4	LV, SP	23.2	439.8	LV, SP						
12.2	399.7	LV, SP	23.2	401.9	LV, SP						
12.2	428.2	LV, SP	23.2	474.9	LV, SP						
								23.2	456.1	LV, SP	

(A)		<i>O. aspinata</i>									
Zone	Subzone	Bed N.	Bed height	Geometric shell size	Shell preservation	Zone	Subzone	Bed N.	Bed height	Geometric shell size	Shell preservation
			12.2	458.2	LV, SP				23.2	422.4	RV, SP
			12.2	440.1	RV, SP				23.2	465.1	RV, SP
			12.2	467.2	LV, SP				23.2	410.8	RV, SP
			12.2	446.4	RV, SP				23.2	432.3	RV, SP
			12.2	417.3	LV, SP				23.2	475.5	LV, SP
			12.2	467.9	LV, SP				23.2	479.9	LV, SP
			12.2	396.8	RV, SP				23.2	467.0	LV, SP
			12.2	459.9	RV, SP				23.2	425.3	RV, SP
			12.2	326.1	RV, SP				23.2	401.0	LV, SP
			12.2	381.3	LV, SP				23.2	423.9	RV, SP
			12.2	379.1	LV, SP				23.2	455.6	LV, SP
			12.2	331.6	LV, SP				23.2	366.0	RV, SP
			12.2	344.5	RV, SP				23.2	396.5	LV, SP
			12.2	302.0	LV, SP				23.2	506.6	LV, SP
			12.2	353.8	RV, SP				23.2	416.2	RV, SP
			12.2	321.6	RV, SP				23.2	418.0	RV, SP
			12.2	306.0	RV, SP				23.2	385.3	LV, SP
			12.2	362.1	RV, SP				23.2	437.4	RV, SP
			12.2	381.4	LV, SP				23.2	373.8	RV, SP
			12.2	283.7	RV, SP				23.2	404.6	RV, SP
			12.2	385.1	LV, SP				23.2	356.5	RV, SP
			12.2	381.0	RV, SP				23.2	427.5	RV, SP
			12.2	303.8	RV, SP				23.2	424.7	RV, SP
			12.2	366.2	RV, SP				23.2	405.9	LV, SP
			12.2	378.9	RV, SP				23.2	453.0	RV, SP
			12.2	384.0	RV, SP				23.2	439.1	RV, SP
			12.2	330.9	LV, SP				23.2	436.9	LV, SP
			12.2	235.4	LV, SP				23.2	454.0	LV, SP
			12.2	384.3	RV, SP				23.2	394.3	RV, SP
			12.2	320.9	LV, SP				23.2	457.5	LV, SP
			12.2	359.1	LV, SP				23.2	360.3	RV, SP
			12.2	338.5	LV, SP				23.2	454.4	RV, SP
			12.2	352.6	LV, SP				23.2	462.1	LV, SP
			12.2	272.9	LV, SP				23.2	438.4	RV, SP
			12.5	448.3	LV, SP				23.2	462.6	LV, SP
		SAB11	12.5	409.5	LV, SP				23.2	404.3	RV, SP
			12.5	424.7	RV, SP				23.2	419.5	LV, SP
			12.5	468.6	LV, SP				23.2	416.4	LV, SP
			12.5	475.6	LV, SP				23.2	400.0	LV, SP

(A)		<i>O. aspinata</i>									
Zone	Subzone	Bed N.	Bed height	Geometric shell size	Shell preservation	Zone	Subzone	Bed N.	Bed height	Geometric shell size	Shell preservation
			12.5	428.3	RV, SP				23.2	430.2	LV, SP
			12.5	398.4	RV, SP				23.2	481.3	LV, SP
			12.5	474.1	LV, SP				23.2	408.0	LV, SP
			12.5	443.8	RV, SP				23.2	406.9	LV, SP
			12.5	405.9	RV, SP				23.2	471.7	LV, SP
			12.5	478.7	LV, SP				23.2	414.0	RV, SP
			12.5	467.1	LV, SP				23.2	410.2	RV, SP
			12.5	485.7	LV, SP				23.2	417.1	LV, SP
			12.5	424.6	RV, SP				23.2	403.8	RV, SP
			12.5	425.7	RV, SP				23.2	434.5	LV, SP
			12.5	453.5	LV, SP				23.2	405.4	LV, SP
			12.5	438.4	LV, SP				23.2	361.4	LV, SP
			12.5	446.6	RV, SP				23.2	395.3	SB
			12.5	474.7	LV, SP				23.2	467.3	LV, SP
			12.5	465.4	LV, SP				23.2	430.2	RV, 1
			12.5	424.4	RV, SP				23.2	457.2	LV, SP
			12.5	468.0	RV, SP				23.2	470.9	RV, SP
			12.5	417.2	LV, SP				23.2	467.4	LV, SP
			12.5	429.0	RV, SP				23.2	416.5	LV, SP
			12.5	419.6	RV, SP				23.2	456.4	LV, SP
			12.5	439.1	RV, SP				23.2	397.3	RV, SP
			12.5	401.9	LV, SP				23.2	410.2	LV, SP
			12.5	418.0	RV, SP				23.2	403.9	LV, SP
			12.5	420.6	RV, SP				23.2	422.9	LV, SP
			12.5	478.5	LV, SP				23.2	385.4	SB
			12.5	454.4	RV, SP				23.2	419.2	RV, SP
			12.5	466.9	LV, SP				23.2	504.3	LV, SP
			12.5	423.5	LV, SP				23.2	401.9	LV, SP
			12.5	460.9	RV, SP				23.2	399.6	LV, SP
			12.5	407.0	LV, SP				23.2	416.4	RV, SP
			12.5	469.6	RV, SP				23.2	415.1	LV, SP
			12.5	476.3	LV, SP				23.2	335.2	RV, SP
			12.5	435.5	RV, SP				23.2	481.7	LV, SP
			12.5	428.0	RV, SP				23.2	324.7	LV, SP
			12.5	480.4	RV, SP				23.2	370.0	RV, SP
			12.5	444.6	RV, SP				23.2	378.4	RV, SP
			12.5	436.8	RV, SP				23.2	386.8	RV, SP
			12.5	423.4	RV, SP				23.2	368.1	RV, SP
			12.5	459.5	RV, SP				23.2	362.5	RV, SP

(A)			<i>O. aspinata</i>								
Zone	Subzone	Bed N.	Bed height	Geometric shell size	Shell preservation	Zone	Subzone	Bed N.	Bed height	Geometric shell size	Shell preservation
			12.5	446.9	RV, SP				23.2	372.5	RV, SP
			12.5	475.7	LV, SP				23.2	385.0	RV, SP
			12.5	424.2	RV, SP				23.2	331.3	LV, SP
			12.5	419.3	RV, SP				23.2	363.0	RV, SP
			12.5	417.8	RV, SP				23.2	378.8	LV, SP
			12.5	477.9	LV, SP				23.2	359.2	RV, SP
			12.5	412.8	RV, SP				23.2	377.4	RV, SP
			12.5	426.7	RV, SP				23.2	371.6	RV, SP
			12.5	473.6	LV, SP				23.2	353.1	RV, SP
			12.5	483.1	RV, SP				23.2	358.8	RV, SP
			12.5	490.0	RV, SP				23.2	369.6	RV, SP
			12.5	422.2	RV, SP				23.2	396.2	SB
			12.5	382.9	RV, SP				23.2	293.3	SB
			12.5	424.7	RV, SP				23.2	358.0	RV, SP
			12.5	477.9	LV, SP				23.2	406.5	RV, SP
			12.5	414.4	RV, SP				23.2	358.2	RV, SP
			12.5	385.1	RV, SP				23.2	378.3	RV, SP
			12.5	428.3	RV, SP				23.2	382.2	RV, SP
			12.5	388.9	LV, SP				23.2	365.3	RV, SP
			12.5	464.3	LV, SP				23.2	362.0	RV, SP
			12.5	441.8	RV, SP				23.2	317.1	RV, SP
			12.5	459.3	RV, SP				23.2	321.5	RV, SP
			12.5	446.6	LV, SP				23.2	375.4	RV, SP
			12.5	421.2	RV, SP				23.2	394.7	RV, SP
			12.5	453.3	RV, SP				23.2	345.7	RV, SP
			12.5	369.1	LV, SP				23.2	364.8	RV, SP
			12.5	430.5	LV, SP				23.2	345.6	RV, SP
			12.5	421.9	RV, SP				23.2	374.9	RV, SP
			12.5	409.4	RV, SP				23.2	402.0	RV, SP
			12.5	485.2	LV, SP				23.2	372.2	RV, SP
			12.5	398.6	RV, SP				23.2	376.7	RV, SP
			12.5	397.2	LV, SP				23.2	367.4	RV, SP
			12.5	413.7	LV, SP				23.2	318.4	LV, SP
			12.5	481.1	LV, SP				23.2	384.8	RV, SP
			12.5	456.6	LV, SP				23.2	365.7	RV, SP
			12.5	489.6	RV, SP				23.2	388.3	RV, SP
			12.5	438.1	RV, SP				23.2	376.9	RV, SP
			12.5	387.0	RV, SP				23.2	361.6	RV, SP
			12.5	484.0	LV, SP				23.2	318.0	LV, SP

(A)						<i>O. aspinata</i>					
Zone	Subzone	Bed N.	Bed height	Geometric shell size	Shell preservation	Zone	Subzone	Bed N.	Bed height	Geometric shell size	Shell preservation
			12.5	425.7	RV, SP				23.2	316.7	RV, SP
			12.5	444.6	LV, SP				23.2	395.8	RV, SP
			12.5	500.2	LV, SP				23.2	397.6	RV, SP
			12.5	455.9	RV, SP				23.2	383.7	RV, SP
			12.5	464.4	LV, SP				23.2	282.7	RV, SP
			12.5	410.2	RV, SP				23.2	368.4	RV, SP
			12.5	486.5	RV, SP				23.2	318.7	LV, SP
			12.5	415.2	RV, SP				23.2	307.5	RV, SP
			12.5	419.8	RV, SP				23.2	385.0	RV, SP
			12.5	424.7	RV, SP				23.2	327.6	LV, SP
			12.5	429.4	RV, SP				23.2	385.0	RV, SP
			12.5	416.4	RV, SP				23.2	324.0	RV, SP
			12.5	419.0	RV, SP				23.2	379.2	RV, SP
			12.5	436.8	RV, SP				23.2	301.4	LV, SP
			12.5	392.2	RV, SP				23.2	399.7	LV, SP
			12.5	433.2	LV, SP				23.2	370.8	RV, SP
			12.5	418.7	RV, SP				23.2	387.7	RV, SP
			12.5	487.6	LV, SP				23.2	395.7	RV, SP
			12.5	465.6	LV, SP				23.2	318.9	LV, SP
			12.5	477.2	LV, SP				23.2	336.9	LV, SP
			12.5	480.3	LV, SP				23.2	381.8	LV, SP
			12.5	473.8	LV, SP				23.2	302.0	RV, SP
			12.5	396.5	RV, SP				23.2	376.3	RV, SP
			12.5	382.5	RV, SP				23.2	402.8	RV, SP
			12.5	305.8	RV, SP				23.2	370.8	RV, SP
			12.5	379.7	RV, SP				23.2	389.6	LV, SP
			12.5	393.5	RV, SP				23.2	374.7	LV, SP
			12.5	392.2	RV, SP				23.2	383.4	RV, SP
			12.5	345.5	LV, SP				23.2	372.4	RV, SP
			12.5	412.7	RV, SP				23.2	351.2	RV, SP
			12.5	341.1	RV, SP				23.2	327.8	RV, SP
			12.5	328.5	RV, SP				23.2	371.8	RV, SP
			12.5	323.7	SB				23.2	362.2	SB
			12.5	380.8	SB				23.2	386.7	RV, SP
			12.5	402.0	SB				23.2	328.9	LV, SP
			12.5	327.6	RV, SP				23.2	375.9	RV, SP
			12.5	389.0	RV, SP				23.2	382.2	LV, SP
			12.5	377.3	RV, SP				23.2	315.0	RV, SP
Pre-planorbis		SAB17	15	433.8	RV, SP				23.2	315.0	RV, SP

(A)						<i>O. aspinata</i>					
Zone	Subzone	Bed N.	Bed height	Geometric shell size	Shell preservation	Zone	Subzone	Bed N.	Bed height	Geometric shell size	Shell preservation
planorbis Zone	Ps. planorbis subzone	SAB30	17.9	297.8	RV, SP				23.8	428.4	RV, SP
			17.9	167.6	LV, SP				23.8	390.9	RV, SP
			17.9	143.4	RV, SP				23.8	496.1	LV, SP
			18.4	456.5	LV, SP				23.8	392.8	RV, SP
			18.4	384.3	RV, SP				23.8	457.3	RV, SP
			18.4	415.9	LV, SP				23.8	439.5	LV, SP
			18.4	441.2	LV, SP				23.8	417.1	RV, SP
			18.4	420.4	LV, SP				23.8	502.5	LV, SP
			18.4	381.9	LV, SP				23.8	438.6	RV, SP
			18.4	444.7	LV, SP				23.8	445.8	RV, SP
			18.4	385.2	RV, SP				23.8	483.9	LV, SP
			18.4	468.9	LV, SP				23.8	399.1	RV, SP
			18.4	396.9	RV, SP				23.8	366.7	SB
			18.4	395.4	LV, SP				23.8	377.0	RV, SP
			18.4	490.1	LV, SP				23.8	420.6	RV, SP
			18.4	467.1	RV, SP				23.8	376.7	SB
			18.4	382.2	LV, SP				23.8	448.5	RV, SP
			18.4	382.0	LV, SP				23.8	417.7	LV, SP
			18.4	417.1	SB				23.8	373.7	RV, SP
			18.4	426.1	SB				23.8	294.8	RV, SP
			18.4	359.6	RV, SP				23.8	420.3	LV, SP
			18.4	466.3	LV, SP				23.8	419.4	RV, SP
			18.4	443.5	RV, SP				23.8	406.8	RV, SP
			18.4	464.3	RV, SP				23.8	375.6	RV, SP
			18.4	446.8	LV, SP				23.8	474.8	LV, SP
			18.4	366.5	RV, SP				23.8	436.8	LV, SP
			18.4	440.4	RV, SP				23.8	477.7	RV, SP
			18.4	351.5	SB				23.8	477.7	LV, SP
			18.4	443.8	LV, SP				23.8	416.5	LV, SP
			18.4	419.9	RV, SP				23.8	500.5	LV, SP
			18.4	430.2	LV, SP				23.8	453.6	LV, SP
			18.4	402.7	LV, SP				23.8	427.0	RV, SP
			18.4	470.1	LV, SP				23.8	447.8	RV, SP
			18.4	389.4	RV, SP				23.8	446.4	LV, SP
18.4	439.7	RV, SP	23.8	450.1	LV, SP						
18.4	452.4	LV, SP	23.8	441.2	RV, SP						
18.4	409.1	LV, SP	23.8	445.0	RV, SP						
18.4	386.2	LV, SP	23.8	498.1	LV, SP						
18.4	441.8	RV, SP	23.8	476.5	LV, SP						

(A)		<i>O. aspinata</i>									
Zone	Subzone	Bed N.	Bed height	Geometric shell size	Shell preservation	Zone	Subzone	Bed N.	Bed height	Geometric shell size	Shell preservation
			18.4	402.7	LV, SP				23.8	446.7	RV, SP
			18.4	417.7	RV, SP				23.8	467.4	RV, SP
			18.4	364.4	LV, SP				23.8	326.0	LV, SP
			18.4	395.1	LV, SP				23.8	399.1	RV, SP
			18.4	475.3	RV, SP				23.8	451.8	RV, SP
			18.4	390.0	RV, SP				23.8	489.7	LV, SP
			18.4	428.3	LV, SP				23.8	436.0	LV, SP
			18.4	456.5	RV, SP				23.8	494.5	RV, SP
			18.4	392.9	LV, SP				23.8	404.2	RV, SP
			18.4	413.2	LV, SP				23.8	486.0	RV, SP
			18.4	418.7	RV, SP				23.8	500.4	LV, SP
			18.4	428.9	LV, SP				23.8	422.1	LV, SP
			18.4	405.4	RV, SP				23.8	441.5	RV, SP
			18.4	364.7	RV, SP				23.8	466.4	LV, SP
			18.4	393.3	RV, SP				23.8	406.8	LV, SP
			18.4	453.6	LV, SP				23.8	467.3	RV, SP
			18.4	411.2	RV, SP				23.8	397.8	LV, SP
			18.4	387.0	RV, SP				23.8	417.1	RV, SP
			18.4	441.7	LV, SP				23.8	463.5	LV, SP
			18.4	427.5	LV, SP				23.8	398.2	LV, SP
			18.4	432.7	RV, SP				23.8	443.8	RV, SP
			18.4	464.1	LV, SP				23.8	434.6	RV, SP
			18.4	388.7	RV, SP				23.8	364.2	LV, SP
			18.4	372.6	RV, SP				23.8	477.6	RV, SP
			18.4	337.7	RV, SP				23.8	459.1	LV, SP
			18.4	356.4	LV, SP				23.8	486.5	RV, SP
			18.4	452.2	LV, SP				23.8	436.8	LV, SP
			18.4	365.2	LV, SP				23.8	429.1	RV, SP
			18.4	399.9	RV, SP				23.8	430.7	RV, SP
			18.4	432.4	LV, SP				23.8	448.2	RV, SP
			18.4	413.6	RV, SP				23.8	385.4	LV, SP
			18.4	402.2	RV, SP				23.8	401.9	LV, SP
			18.4	436.3	LV, SP				23.8	439.2	RV, SP
			18.4	436.2	LV, SP				23.8	418.9	LV, SP
			18.4	406.1	LV, SP				23.8	379.6	LV, SP
			18.4	417.6	RV, SP				23.8	479.1	LV, SP
			18.4	417.2	LV, SP				23.8	415.5	RV, SP
			18.4	389.0	RV, SP				23.8	419.6	RV, SP
			18.4	460.0	LV, SP				23.8	499.6	RV, SP

(A)		<i>O. aspinata</i>									
Zone	Subzone	Bed N.	Bed height	Geometric shell size	Shell preservation	Zone	Subzone	Bed N.	Bed height	Geometric shell size	Shell preservation
			18.4	386.6	RV, SP				23.8	406.0	LV, SP
			18.4	416.9	RV, SP				23.8	393.3	RV, SP
			18.4	420.8	RV, SP				23.8	382.0	RV, SP
			18.4	362.5	RV, SP				23.8	422.7	SB
			18.4	411.8	RV, SP				23.8	379.3	LV, SP
			18.4	412.7	RV, SP				23.8	422.7	LV, SP
			18.4	487.0	RV, SP				23.8	428.3	RV, SP
			18.4	425.3	LV, SP				23.8	452.1	RV, SP
			18.4	399.1	RV, SP				23.8	447.9	LV, SP
			18.4	415.8	RV, SP				23.8	428.7	RV, SP
			18.4	425.5	LV, SP				23.8	406.4	RV, SP
			18.4	403.6	RV, SP				23.8	461.8	RV, SP
			18.4	342.6	LV, SP				23.8	425.3	LV, SP
			18.4	395.8	RV, SP				23.8	441.4	RV, SP
			18.4	414.9	RV, SP				23.8	449.4	RV, SP
			18.4	382.9	RV, SP				23.8	493.8	RV, SP
			18.4	385.9	RV, SP				23.8	439.7	LV, SP
			18.4	413.4	RV, SP				23.8	395.4	RV, SP
			18.4	387.1	RV, SP				23.8	292.1	LV, SP
			18.4	398.7	RV, SP				23.8	315.0	LV, SP
			18.4	417.6	LV, SP				23.8	316.6	RV, SP
			18.4	428.7	LV, SP				23.8	316.2	RV, SP
			18.4	412.4	LV, SP				23.8	328.8	LV, SP
			18.4	367.0	LV, SP				23.8	324.4	RV, SP
			18.4	455.9	LV, SP				23.8	335.4	LV, SP
			18.4	401.4	RV, SP				23.8	313.2	LV, SP
			18.4	383.4	RV, SP				23.8	327.2	RV, SP
			18.4	441.7	LV, SP				23.8	370.0	LV, SP
			18.4	364.9	RV, SP				23.8	397.0	RV, SP
			18.4	441.6	RV, SP				23.8	318.7	LV, SP
			18.4	378.3	LV, SP				23.8	389.1	LV, SP
			18.4	458.5	RV, SP				23.8	387.7	RV, SP
			18.4	460.8	LV, SP				23.8	324.5	RV, SP
			18.4	471.0	LV, SP				23.8	394.8	RV, SP
			18.4	474.9	LV, SP				23.8	308.7	RV, SP
			18.4	377.3	LV, SP				23.8	290.9	LV, SP
			18.4	441.9	LV, SP				23.8	401.3	RV, SP
			18.4	395.2	RV, SP				23.8	340.2	RV, SP
			18.4	409.2	LV, SP				23.8	310.5	LV, SP

(A)		<i>O. aspinata</i>									
Zone	Subzone	Bed N.	Bed height	Geometric shell size	Shell preservation	Zone	Subzone	Bed N.	Bed height	Geometric shell size	Shell preservation
			18.4	401.8	RV, SP				23.8	310.1	LV, SP
			18.4	469.1	LV, SP				23.8	308.0	RV, SP
			18.4	428.8	LV, SP				23.8	346.1	LV, SP
			18.4	433.5	RV, SP				23.8	305.1	RV, SP
			18.4	422.2	LV, SP				23.8	367.2	LV, SP
			18.4	487.3	LV, SP				23.8	309.5	LV, SP
			18.4	473.8	LV, SP				23.8	285.3	RV, SP
			18.4	447.7	LV, SP				23.8	262.4	RV, SP
			18.4	406.3	LV, SP				23.8	391.8	RV, SP
			18.4	374.8	LV, SP				23.8	328.2	RV, SP
			18.4	328.4	RV, SP				23.8	392.6	LV, SP
			18.4	338.1	LV, SP				23.8	372.1	RV, SP
			18.4	307.0	LV, SP				23.8	329.8	RV, SP
			18.4	371.6	LV, SP				23.8	385.5	RV, SP
			18.4	332.0	LV, SP				23.8	382.9	RV, SP
			18.4	330.7	RV, SP				23.8	297.7	RV, SP
			18.4	342.9	LV, SP				23.8	333.7	RV, SP
			18.4	366.4	RV, SP				23.8	377.1	LV, SP
			18.4	388.6	RV, SP				23.8	370.4	LV, SP
			18.4	379.0	RV, SP				23.8	303.3	RV, SP
			18.4	306.9	LV, SP				23.8	325.8	LV, SP
			18.4	382.3	RV, SP				23.8	326.3	LV, SP
			18.4	345.2	LV, SP				23.8	313.7	LV, SP
			18.4	382.5	RV, SP				23.8	404.3	RV, SP
			18.4	316.9	RV, SP				23.8	327.3	RV, SP
			18.4	377.8	RV, SP				23.8	324.5	RV, SP
			18.4	293.1	SB				23.8	321.7	LV, SP
			18.4	345.6	SB				23.8	327.7	RV, SP
			18.4	395.8	RV, SP				23.8	369.6	RV, SP
			18.4	379.9	RV, SP				23.8	323.8	RV, SP
			18.4	382.6	RV, SP				23.8	369.7	RV, SP
			18.4	338.4	LV, SP				23.8	483.0	LV, SP
			18.4	349.0	LV, SP				23.8	402.4	SB
			18.4	285.8	RV, SP				23.8	397.8	RV, SP
			18.4	341.0	RV, SP				23.8	371.6	RV, SP
			18.4	363.8	RV, SP				23.8	303.6	LV, SP
			18.4	322.9	RV, SP				23.8	300.5	RV, SP
			18.4	366.4	RV, SP				23.8	373.9	RV, SP
			18.4	326.0	LV, SP				23.8	337.3	RV, SP

(A)		<i>O. aspinata</i>									
Zone	Subzone	Bed N.	Bed height	Geometric shell size	Shell preservation	Zone	Subzone	Bed N.	Bed height	Geometric shell size	Shell preservation
			18.4	370.1	RV, SP				23.8	390.1	RV, SP
			18.4	312.1	RV, SP				23.8	303.0	LV, SP
			18.4	378.7	RV, SP				23.8	257.6	LV, SP
			18.4	306.9	LV, SP				23.8	230.7	RV, SP
			18.4	345.0	SB				23.8	199.0	RV, SP
			18.4	361.9	RV, SP				23.8	251.5	RV, SP
			18.4	364.2	RV, SP				23.8	235.3	RV, SP
			18.4	344.5	RV, SP				23.8	243.1	RV, SP
			18.4	363.3	RV, SP				23.8	227.5	RV, SP
			18.4	287.0	LV, SP				23.8	257.6	RV, SP
			18.4	394.6	LV, SP				23.8	271.4	RV, SP
			18.4	380.5	RV, SP				23.8	247.6	RV, SP
			18.4	337.1	RV, SP				23.8	270.3	RV, SP
			18.4	380.8	LV, SP				23.8	222.2	RV, SP
			18.4	363.2	RV, SP				23.8	221.9	RV, SP
			18.4	344.0	LV, SP				23.8	241.2	LV, SP
			18.4	310.1	RV, SP				24.3	477.8	LV, SP
			18.4	326.4	RV, SP			SAB44	24.3	419.8	RV, SP
			18.4	378.3	RV, SP				24.3	370.1	RV, SP
			18.4	344.4	SB				24.3	326.4	LV, SP
			18.4	313.3	RV, SP				26.5	399.0	LV, SP
			18.4	365.8	RV, SP				26.5	436.4	LV, SP
			18.4	386.7	SB				26.5	387.1	LV, SP
			18.4	293.8	RV, SP				26.5	438.6	RV, SP
			18.4	259.4	RV, SP				26.5	388.8	LV, SP
			18.4	339.8	RV, SP				26.5	470.9	LV, SP
			18.4	355.7	RV, SP				26.5	430.9	LV, SP
			18.4	395.6	RV, SP				26.5	398.8	RV, SP
			18.4	329.8	RV, SP				26.5	448.4	RV, SP
			18.4	440.6	SB			SAB52	26.5	414.5	RV, SP
			18.4	354.8	RV, SP				26.5	379.6	LV, SP
			18.4	372.5	LV, SP				26.5	423.9	LV, SP
			18.4	279.8	LV, SP				26.5	375.6	RV, SP
			18.4	372.9	RV, SP				26.5	412.3	RV, SP
			18.4	327.9	RV, SP				26.5	389.7	LV, SP
			18.4	379.1	LV, SP				26.5	445.8	LV, SP
			18.4	319.0	RV, SP				26.5	403.6	LV, SP
			18.4	359.0	LV, SP				26.5	448.0	RV, SP
			18.4	391.8	LV, SP				26.5	412.4	SB

(A)		<i>O. aspinata</i>									
Zone	Subzone	Bed N.	Bed height	Geometric shell size	Shell preservation	Zone	Subzone	Bed N.	Bed height	Geometric shell size	Shell preservation
			18.7	405.3	RV, SP				26.5	395.3	LV, SP
			18.7	356.1	RV, SP				26.5	397.3	RV, SP
			18.7	397.7	LV, SP				26.5	386.4	RV, SP
			18.7	466.1	LV, SP				26.5	407.9	LV, SP
			18.7	459.0	RV, SP				26.5	407.0	LV, SP
			18.7	383.8	LV, SP				26.5	390.8	LV, SP
			18.7	399.1	RV, SP				26.5	402.1	RV, SP
			18.7	380.7	RV, SP				26.5	424.1	RV, SP
			18.7	375.9	RV, SP				26.5	391.9	RV, SP
			18.7	354.8	LV, SP				26.5	408.4	LV, SP
			18.7	452.2	LV, SP				26.5	407.9	LV, SP
			18.7	388.9	RV, SP				26.5	418.9	RV, SP
			18.7	368.0	LV, SP				26.5	404.7	RV, SP
			18.7	380.8	RV, SP				26.5	370.8	RV, SP
			18.7	379.2	RV, SP				26.5	440.6	RV, SP
			18.7	398.7	LV, SP				26.5	362.8	LV, SP
			18.7	393.4	RV, SP				26.5	389.7	LV, SP
			18.7	473.8	LV, SP				26.5	392.5	LV, SP
			18.7	399.0	LV, SP				26.5	389.7	RV, SP
			18.7	390.5	LV, SP				26.5	409.6	RV, SP
			18.7	398.3	LV, SP				26.5	359.8	LV, SP
			18.7	391.9	RV, SP				26.5	450.9	LV, SP
			18.7	401.3	RV, SP				26.5	353.2	LV, SP
			18.7	458.6	RV, SP				26.5	332.8	LV, SP
			18.7	363.9	LV, SP				26.5	395.2	LV, SP
			18.7	373.1	LV, SP				26.5	445.9	LV, SP
			18.7	459.6	RV, SP				26.5	453.5	LV, SP
			18.7	452.7	RV, SP				26.5	392.5	RV, SP
			18.7	380.4	LV, SP				26.5	374.3	LV, SP
			18.7	405.0	RV, SP				26.5	448.5	LV, SP
			18.7	380.6	LV, SP				26.5	387.0	LV, SP
			18.7	415.7	LV, SP				26.5	446.2	LV, SP
			18.7	360.1	LV, SP				26.5	417.7	LV, SP
			18.7	376.2	RV, SP				26.5	450.8	LV, SP
			18.7	415.7	RV, SP				26.5	447.3	LV, SP
			18.7	367.0	LV, SP				26.5	433.7	RV, SP
			18.7	295.6	SB				26.5	463.3	LV, SP
			18.7	362.9	LV, SP				26.5	412.2	RV, SP
			18.7	436.1	RV, SP				26.5	432.4	LV, SP

(A)		<i>O. aspinata</i>									
Zone	Subzone	Bed N.	Bed height	Geometric shell size	Shell preservation	Zone	Subzone	Bed N.	Bed height	Geometric shell size	Shell preservation
			18.7	391.4	RV, SP				26.5	389.8	LV, SP
			18.7	443.2	LV, SP				26.5	415.0	RV, SP
			18.7	355.8	RV, SP				26.5	444.1	LV, SP
			18.7	342.9	RV, SP				26.5	413.9	LV, SP
			18.7	369.0	RV, SP				26.5	395.0	LV, SP
			18.7	425.2	LV, SP				26.5	426.0	LV, SP
			18.7	395.2	LV, SP				26.5	415.6	LV, SP
			18.7	395.7	RV, SP				26.5	429.3	RV, SP
			18.7	458.2	LV, SP				26.5	425.9	LV, SP
			18.7	355.1	RV, SP				26.5	405.9	RV, SP
			18.7	393.2	LV, SP				26.5	397.4	LV, SP
			18.7	397.4	RV, SP				26.5	383.1	LV, SP
			18.7	346.4	LV, SP				26.5	375.5	LV, SP
			18.7	392.1	LV, SP				26.5	384.0	LV, SP
			18.7	408.7	RV, SP				26.5	367.7	LV, SP
			18.7	413.5	RV, SP				26.5	401.1	RV, SP
			18.7	395.1	LV, SP				26.5	386.7	RV, SP
			18.7	343.8	RV, SP				26.5	390.1	LV, SP
			18.7	299.5	RV, SP				26.5	445.5	LV, SP
			18.7	372.8	LV, SP				26.5	390.9	RV, SP
			18.7	317.7	RV, SP				26.5	448.8	LV, SP
			18.7	369.2	LV, SP				26.5	455.2	LV, SP
			18.7	312.5	RV, SP				26.5	449.4	LV, SP
			18.7	328.9	LV, SP				26.5	422.4	RV, SP
			18.7	317.0	RV, SP				26.5	403.0	RV, SP
			18.7	346.4	SB				26.5	449.1	LV, SP
			18.7	357.9	LV, SP				26.5	415.7	LV, SP
			18.7	341.2	RV, SP				26.5	406.1	RV, SP
			18.7	297.3	RV, SP				26.5	415.2	LV, SP
			18.7	338.3	RV, SP				26.5	443.8	LV, SP
			18.7	336.6	LV, SP				26.5	431.5	LV, SP
			18.7	345.0	RV, SP				26.5	390.0	LV, SP
			18.7	342.3	LV, SP				26.5	360.7	LV, SP
			18.7	327.0	RV, SP				26.5	424.1	LV, SP
			18.7	308.1	RV, SP				26.5	458.5	LV, SP
			18.7	364.7	RV, SP				26.5	389.1	RV, SP
			18.7	371.4	RV, SP				26.5	370.5	LV, SP
			18.7	340.4	LV, SP				26.5	388.5	LV, SP
			18.7	378.9	RV, SP				26.5	357.9	LV, SP

(A)						<i>O. aspinata</i>					
Zone	Subzone	Bed N.	Bed height	Geometric shell size	Shell preservation	Zone	Subzone	Bed N.	Bed height	Geometric shell size	Shell preservation
			18.7	314.0	LV, SP				26.5	388.6	LV, SP
			18.7	359.9	RV, SP				26.5	397.5	LV, SP
			18.7	334.2	LV, SP				26.5	380.0	LV, SP
			18.7	386.8	RV, SP				26.5	312.1	RV, SP
			18.7	374.2	LV, SP				26.5	256.8	LV, SP
			18.7	377.8	RV, SP				26.5	321.5	RV, SP
			18.7	327.2	LV, SP				26.5	382.6	RV, SP
			18.7	368.7	RV, SP				26.5	373.3	RV, SP
			18.7	342.5	RV, SP				26.5	375.4	RV, SP
			18.7	336.5	RV, SP				26.5	379.1	RV, SP
			18.7	308.0	RV, SP				26.5	382.2	SB
			18.7	265.9	RV, SP				26.5	308.8	RV, SP
			18.7	374.0	RV, SP				26.5	355.5	RV, SP
			18.7	306.2	RV, SP				26.5	296.8	RV, SP
			18.7	372.3	RV, SP				26.5	369.9	RV, SP
			18.7	309.1	LV, SP				26.5	307.3	LV, SP
			18.7	344.8	LV, SP				26.5	387.7	RV, SP
			18.7	328.2	RV, SB				26.5	351.1	RV, SP
			18.7	332.9	RV, SB				26.5	353.3	RV, SP
			18.7	270.7	LV, SP				26.5	385.2	RV, SP
			18.7	314.3	LV, SP				26.5	391.0	RV, SP
			18.7	367.6	RV, SP				26.5	496.9	LV, SP
			18.7	391.0	RV, SP				26.5	330.1	RV, SP
			18.7	348.8	RV, SP				26.5	305.5	LV, SP
			18.7	327.9	RV, SP				26.5	358.7	RV, SP
			18.7	260.5	LV, SP				26.5	366.9	LV, SP
			18.7	332.5	RV, SP				26.5	317.0	LV, SP
			18.7	295.2	LV, SP				26.5	307.6	RV, SP
			18.7	320.9	LV, SP				26.5	387.3	RV, SP
			18.7	387.5	RV, SP				26.5	280.6	LV, SP
			18.7	304.4	RV, SP				26.5	316.1	LV, SP
			18.7	346.0	RV, SP				26.5	378.7	RV, SP
			18.7	310.4	LV, SP				26.5	390.8	LV, SP
			18.7	376.6	RV, SP				26.5	268.1	RV, SP
			18.7	315.9	RV, SP				26.5	377.7	RV, SP
			18.7	362.3	SB				26.5	311.6	RV, SP
			18.7	324.7	SB				26.5	372.3	RV, SP
			18.7	332.3	LV, SP				26.5	287.8	RV, SP
			18.7	317.2	RV, SP				26.5	314.6	LV, SP

(A)						<i>O. aspinata</i>					
Zone	Subzone	Bed N.	Bed height	Geometric shell size	Shell preservation	Zone	Subzone	Bed N.	Bed height	Geometric shell size	Shell preservation
			18.7	364.7	LV, SP				26.5	298.7	SB
			18.7	352.9	RV, SP				26.5	293.7	LV, SP
			18.7	276.0	LV, SP				26.5	378.5	LV, SP
			18.7	290.8	RV, SP				26.5	296.8	RV, SP
			18.7	350.0	LV, SP				26.5	320.3	RV, SP
			18.7	387.9	RV, SP				26.5	362.5	RV, SP
			18.7	385.1	RV, SP				26.5	400.3	RV, SP
			18.7	314.6	LV, SP				26.5	359.0	LV, SP
			18.7	367.5	RV, SP				26.5	343.2	RV, SP
			18.7	328.2	RV, SP				26.5	311.6	SB
			18.7	342.3	RV, SP				26.5	321.2	RV, SP
			18.7	283.5	LV, SP				26.5	299.1	LV, SP
			18.7	345.1	LV, SP				26.5	422.0	LV, SP
			18.7	322.3	LV, SP				26.5	320.6	LV, SP
			18.7	305.9	RV, SP				26.5	383.7	LV, SP
			18.7	265.1	LV, SP				26.5	356.7	LV, SP
			18.7	314.4	LV, SP				26.5	356.1	LV, SP
			18.7	298.4	RV, SP				26.5	368.4	RV, SP
			18.7	311.3	RV, SP				26.5	383.7	LV, SP
			18.7	369.8	RV, SP				26.5	390.8	RV, SP
			18.7	273.3	RV, SP				26.5	381.2	RV, SP
			18.7	308.8	RV, SP				26.5	365.8	LV, SP
			18.7	210.8	RV, SP				26.5	292.2	RV, SP
			18.7	263.6	LV, SP				26.5	356.5	RV, SP
			18.7	243.5	RV, SP				26.5	389.3	RV, SP
			18.7	240.6	RV, SP				26.5	379.2	RV, SP
			18.7	271.2	RV, SP				26.5	367.7	RV, SP
			18.7	264.3	LV, SP				26.5	363.9	RV, SP
			18.7	246.7	RV, SP				26.5	193.9	LV, SP
			18.7	276.6	RV, SP				26.5	212.3	RV, SP
			18.7	253.6	RV, SP				26.5	179.8	LV, SP
			18.7	260.5	RV, SP				26.5	167.4	LV, SP
			19.8	412.2	LV, SP				26.5	214.9	LV, SP
			19.8	393.9	RV, SP				26.5	216.1	RV, SP
			19.8	453.3	LV, SP				26.5	230.1	RV, SP
		SAB34	19.8	404.1	LV, SP				26.5	173.7	RV, SP
			19.8	415.2	LV, SP				26.5	246.4	RV, SP
			19.8	424.3	RV, SP				26.5	202.0	RV, SP
			19.8	385.1	RV, SP						

(A)			<i>O. aspinata</i>								
Zone	Subzone	Bed N.	Bed height	Geometric shell size	Shell preservation	Zone	Subzone	Bed N.	Bed height	Geometric shell size	Shell preservation
			19.8	412.6	LV, SP						
			19.8	418.6	LV, SP						
			19.8	434.2	LV, SP						
			19.8	445.3	LV, SP						
			19.8	400.8	RV, SP						
			19.8	391.5	LV, SP						
			19.8	416.6	LV, SP						
			19.8	446.3	LV, SP						
			19.8	403.7	LV, SP						
			19.8	433.6	LV, SP						
			19.8	454.4	LV, SP						
			19.8	383.1	RV, SP						
			19.8	405.1	RV, SP						
			19.8	391.5	RV, SP						
			19.8	362.6	RV, SP						
			19.8	383.6	RV, SP						
			19.8	274.4	RV, SP						
			19.8	257.3	LV, SP						
			19.8	352.2	SB						
			19.8	292.8	RV, SP						
			19.8	348.6	RV, SP						
			19.8	321.7	RV, SP						
			19.8	369.2	RV, SP						
			19.8	371.4	RV, SP						
			19.8	334.0	RV, SP						
			19.8	335.5	LV, SP						
			19.8	305.3	SB						
			19.8	263.9	SB						
			19.8	347.5	RV, SP						
			19.8	320.1	LV, SP						
			19.8	289.0	LV, SP						
			19.8	288.5	RV, SP						
			19.8	336.0	SB						
			19.8	289.9	RV, SP						
			19.8	312.4	SB						
			19.8	365.6	RV, SP						
			19.8	361.2	SB						
			19.8	351.2	RV, SP						
			19.8	314.3	LV, SP						

(A)						<i>O. aspinata</i>					
Zone	Subzone	Bed N.	Bed height	Geometric shell size	Shell preservation	Zone	Subzone	Bed N.	Bed height	Geometric shell size	Shell preservation
			19.8	362.0	RV, SP						
			19.8	320.9	RV, SP						
			19.8	370.6	RV, SP						
			19.8	364.6	RV, SP						
			19.8	327.2	LV, SP						
			19.8	302.0	RV, SP						
			19.8	221.2	SB						
			19.8	256.2	LV, SP						

(B)						<i>O. aspinata</i>					
Zone	Subzone	Bed N.	Bed height	Geometric shell size	Shell preservation	Zone	Subzone	Bed N.	Bed height	Geometric shell size	Shell preservation
liasicus Zone	W. portlocki subzone	SAB60	40.7	375.9	LV, SP	liasicus Zone	Alsatites laqueus subzone	SAB70V.T	50.6	424.6	RV, SP
			40.7	394.6	LV, SP				50.6	433.7	LV, SP
			40.7	389.9	LV, SP				50.6	413.6	RV, SP
			40.7	377.9	LV, SP				50.6	373.0	LV, SP
			40.7	484.0	RV, SP				50.6	400.9	RV, SP
			40.7	366.1	SB				50.6	393.2	RV, SP
			40.7	434.0	LV, SP				50.6	391.5	RV, SP
			40.7	392.3	LV, SP				50.6	482.4	RV, SP
			40.7	359.0	LV, SP				50.6	444.2	LV, SP
			40.7	461.2	LV, SP				50.6	366.1	LV, SP
			40.7	421.1	RV, SP				50.6	454.9	LV, SP
			40.7	464.6	RV, SP				50.6	423.1	LV, SP
			40.7	434.1	LV, SP				50.6	433.4	LV, SP
			40.7	382.4	RV, SP				50.6	402.7	RV, SP
			40.7	426.3	RV, SP				50.6	460.3	LV, SP
			40.7	452.7	LV, SP				50.6	399.0	RV, SP
			40.7	423.2	RV, SP				50.6	463.7	LV, SP
			40.7	465.2	LV, SP				50.6	447.0	LV, SP
			40.7	392.6	RV, SP				50.6	394.3	LV, SP
			40.7	445.6	LV, SP				50.6	485.5	LV, SP
			40.7	421.3	RV, SP				50.6	389.5	LV, SP
			40.7	419.9	SB				50.6	378.3	LV, SP
			40.7	338.6	LV, SP				50.6	451.8	LV, SP
			40.7	428.0	LV, SP				50.6	379.3	RV, SP
40.7	385.0	RV, SP	50.6	391.7	RV, SP						

(B)						<i>O. aspinata</i>					
Zone	Subzone	Bed N.	Bed height	Geometric shell size	Shell preservation	Zone	Subzone	Bed N.	Bed height	Geometric shell size	Shell preservation
			47	443.2	LV, SP				50.6	382.8	RV, SP
			47	473.8	LV, SP				50.6	443.6	RV, SP
			47	448.3	RV, SP				50.6	387.1	RV, SP
			47	416.2	LV, SP				50.6	420.2	LV, SP
			47	398.0	RV, SP				50.6	380.4	RV, SP
			47	380.2	LV, SP				50.6	425.4	LV, SP
			47	480.6	RV, SP				50.6	410.8	RV, SP
			47	454.8	LV, SP				50.6	365.9	LV, SP
			47	389.8	LV, SP				50.6	407.8	RV, SP
			47	404.7	RV, SP				50.6	470.6	RV, SP
			47	395.9	LV, SP				50.6	422.5	RV, SP
			47	391.4	RV, SP				50.6	407.7	RV, SP
			47	443.3	RV, SP				50.6	431.3	LV, SP
			47	480.5	RV, SP				50.6	447.5	LV, SP
			47	421.5	LV, SP				50.6	435.2	LV, SP
			47	469.6	RV, SP				50.6	371.7	RV, SP
			47	461.2	LV, SP				50.6	392.0	RV, SP
			47	415.5	RV, SP				50.6	363.8	RV, SP
			47	465.3	LV, SP				50.6	386.9	LV, SP
			47	449.6	RV, SP				50.6	462.8	LV, SP
			47	389.7	LV, SP				50.6	470.0	LV, SP
			47	405.3	RV, SP				50.6	407.5	LV, SP
			47	453.9	RV, SP				50.6	383.0	LV, SP
			47	412.9	RV, SP				50.6	444.7	LV, SP
			47	472.2	LV, SP				50.6	346.0	RV, SP
			47	415.7	RV, SP				50.6	375.2	RV, SP
			47	430.8	RV, SP				50.6	438.5	LV, SP
			47	462.4	LV, SP				50.6	457.2	LV, SP
			47	417.2	RV, SP				50.6	444.1	LV, SP
			47	462.7	LV, SP				50.6	394.9	RV, SP
			47	409.9	RV, SP				50.6	293.9	LV, SP
			47	395.5	LV, SP				50.6	437.3	LV, SP
			47	409.8	RV, SP				50.6	432.8	SB
			47	430.1	LV, SP				50.6	437.2	RV, SP
			47	449.7	LV, SP				50.6	446.8	LV, SP
			47	398.9	RV, SP				50.6	394.1	RV, SP
			47	409.4	LV, SP				50.6	413.0	RV, SP
			47	439.3	LV, SP				50.6	499.6	RV, SP
			47	486.0	LV, SP				50.6	399.2	RV, SP

(B)						<i>O. aspinata</i>					
Zone	Subzone	Bed N.	Bed height	Geometric shell size	Shell preservation	Zone	Subzone	Bed N.	Bed height	Geometric shell size	Shell preservation
			47	403.8	RV, SP				50.6	434.7	RV, SP
			47	378.0	RV, SP				50.6	476.5	LV, SP
			47	452.5	LV, SP				50.6	454.7	LV, SP
			47	451.3	RV, SP				50.6	384.0	RV, SP
			47	458.6	LV, SP				50.6	436.5	LV, SP
			47	476.1	LV, SP				50.6	410.3	RV, SP
			47	467.4	RV, SP				50.6	384.1	LV, SP
			47	447.1	LV, SP				50.6	488.8	LV, SP
			47	405.0	RV, SP				50.6	477.1	LV, SP
			47	422.8	RV, SP				50.6	423.4	RV, SP
			47	403.0	LV, SP				50.6	433.4	LV, SP
			47	422.9	LV, SP				50.6	457.2	LV, SP
			47	448.0	LV, SP				50.6	392.9	RV, SP
			47	423.6	RV, SP				50.6	442.6	LV, SP
			47	409.7	RV, SP				50.6	374.0	LV, SP
			47	410.3	RV, SP				50.6	292.6	LV, SP
			47	437.9	LV, SP				50.6	347.7	RV, SP
			47	463.9	LV, SP				50.6	325.4	RV, SP
			47	455.2	LV, SP				50.6	393.5	RV, SP
			47	426.7	LV, SP				50.6	377.5	RV, SP
			47	428.9	RV, SP				50.6	356.6	SB
			47	438.6	LV, SP				50.6	296.7	LV, SP
			47	400.9	LV, SP				50.6	316.4	LV, SP
			47	443.8	LV, SP				50.6	289.1	RV, SP
			47	407.0	RV, SP				50.6	371.4	RV, SP
			47	463.4	LV, SP				50.6	343.3	RV, SP
			47	398.4	LV, SP				50.6	349.0	RV, SP
			47	426.2	LV, SP				50.6	381.3	RV, SP
			47	489.8	LV, SP				50.6	354.3	RV, SP
			47	387.2	LV, SP				50.6	292.5	RV, SP
			47	532.2	LV, SP				50.6	350.3	LV, SP
			47	416.3	RV, SP				50.6	377.9	LV, SP
			47	436.0	RV, SP				50.6	294.8	LV, SP
			47	391.4	LV, SP				50.6	412.1	SB
			47	454.8	RV, SP				50.6	311.5	LV, SP
			47	453.1	RV, SP				50.6	319.7	RV, SP
			47	370.8	LV, SP				50.6	390.8	RV, SP
			47	474.4	LV, SP				50.6	339.9	LV, SP
			47	451.3	RV, SP				50.6	313.2	SB

(B)						<i>O. aspinata</i>					
Zone	Subzone	Bed N.	Bed height	Geometric shell size	Shell preservation	Zone	Subzone	Bed N.	Bed height	Geometric shell size	Shell preservation
			47	397.8	LV, SP				50.6	373.7	RV, SP
			47	415.4	LV, SP				50.6	356.6	RV, SP
			47	377.1	LV, SP				50.6	383.7	RV, SP
			47	446.9	RV, SP				50.6	385.0	RV, SP
			47	376.2	RV, SP				50.6	279.4	RV, SP
			47	418.3	RV, SP				50.6	355.1	RV, SP
			47	471.4	RV, SP				50.6	359.8	LV, SP
			47	409.7	RV, SP				50.6	365.1	RV, SP
			47	415.3	LV, SP				50.6	360.4	LV, SP
			47	474.0	LV, SP				50.6	345.0	SB
			47	376.4	RV, SP				50.6	249.8	RV, SP
			47	426.8	RV, SP				50.6	360.7	RV, SP
			47	474.0	RV, SP				50.6	353.2	RV, SP
			47	384.9	RV, SP				50.6	352.3	LV, SP
			47	424.1	RV, SP				50.6	308.4	SB
			47	441.0	LV, SP				50.6	348.6	RV, SP
			47	428.6	RV, SP				50.6	294.1	SB
			47	484.5	LV, SP				50.6	445.6	LV, SP
			47	391.9	RV, SP				50.6	262.8	RV, SP
			47	460.5	RV, SP				50.6	261.3	RV, SP
			47	450.5	LV, SP				50.6	370.0	RV, SP
			47	422.7	RV, SP				50.6	239.5	RV, SP
			47	406.1	LV, SP				50.6	363.3	RV, SP
			47	431.2	RV, SP				50.6	265.3	RV, SP
			47	451.1	RV, SP				50.6	370.6	RV, SP
			47	399.2	LV, SP				50.6	351.0	RV, SP
			47	452.2	LV, SP				50.6	358.0	RV, SP
			47	418.4	RV, SP				50.6	370.3	RV, SP
			47	393.9	RV, SP				50.6	265.4	LV, SP
			47	462.5	LV, SP				50.6	354.6	RV, SP
			47	411.2	RV, SP				50.6	319.5	LV, SP
			47	382.6	LV, SP				50.6	373.5	RV, SP
			47	402.0	LV, SP				50.6	358.1	RV, SP
			47	426.3	RV, SP				50.6	351.5	RV, SP
			47	459.7	RV, SP				50.6	357.7	RV, SP
			47	419.3	RV, SP				50.6	325.2	LV, SP
			47	368.4	LV, SP				50.6	379.8	RV, SP
			47	480.0	LV, SP				50.6	319.0	LV, SP
			47	442.6	RV, SP				50.6	381.5	RV, SP

(B)						<i>O. aspinata</i>					
Zone	Subzone	Bed N.	Bed height	Geometric shell size	Shell preservation	Zone	Subzone	Bed N.	Bed height	Geometric shell size	Shell preservation
			47	413.0	RV, SP				50.6	314.2	RV, SP
			47	450.0	LV, SP				50.6	274.7	LV, SP
			47	461.4	LV, SP				50.6	327.9	RV, SP
			47	387.3	RV, SP				50.6	288.0	LV, SP
			47	400.1	RV, SP				50.6	378.9	RV, SP
			47	453.8	LV, SP				50.6	321.8	RV, SP
			47	462.9	LV, SP				50.6	364.0	SB
			47	459.0	LV, SP				50.6	334.5	RV, SP
			47	467.4	LV, SP				50.6	386.4	RV, SP
			47	428.0	RV, SP				50.6	277.6	RV, SP
			47	441.9	RV, SP				50.6	380.1	RV, SP
			47	390.8	LV, SP				50.6	298.9	LV, SP
			47	391.1	LV, SB				50.6	312.9	RV, SP
			47	456.0	LV, SP				50.6	317.0	RV, SP
			47	407.0	RV, SP				50.6	282.8	SB
			47	400.0	RV, SP				50.6	266.6	RV, SP
			47	410.6	LV, SP				50.6	318.4	LV, SP
			47	340.0	RV, SP				50.6	358.9	RV, SP
			47	367.4	LV, SP				50.6	268.2	RV, SP
			47	472.3	LV, SP				50.6	257.4	RV, SP
			47	400.9	RV, SP				50.6	270.2	LV, SP
			47	400.0	RV, SP				50.6	256.6	LV, SP
			47	389.3	LV, SP				50.6	239.3	RV, SP
			47	380.7	RV, SP				50.6	261.7	RV, SP
			47	419.6	LV, SP				53.05	481.9	LV, SP
			47	397.3	RV, SP				53.05	454.0	LV, SP
			47	469.7	LV, SP				53.05	373.1	LV, SP
			47	388.7	LV, SP				53.05	410.6	RV, SP
			47	423.8	RV, SP				53.05	393.4	LV, SP
			47	440.7	RV, SP				53.05	506.7	LV, SP
			47	453.4	LV, SP				53.05	472.4	LV, SP
			47	433.7	RV, SP				53.05	471.5	LV, SP
			47	374.2	LV, SP				53.05	472.6	LV, SP
			47	386.7	RV, SP				53.05	463.1	LV, SP
			47	397.7	LV, SP				53.05	476.7	LV, SP
			47	400.9	RV, SP				53.05	459.3	LV, SP
			47	403.4	LV, SP				53.05	392.1	LV, SP
			47	405.8	RV, SP				53.05	441.4	LV, SP
			47	413.8	LV, SP				53.05	413.9	RV, SP

(B)						<i>O. aspinata</i>					
Zone	Subzone	Bed N.	Bed height	Geometric shell size	Shell preservation	Zone	Subzone	Bed N.	Bed height	Geometric shell size	Shell preservation
			47	438.2	LV, SP				53.05	406.3	LV, SP
			47	434.3	RV, SP				53.05	446.9	LV, SP
			47	434.2	RV, SP				53.05	456.0	LV, SP
			47	493.4	RV, SP				53.05	389.7	LV, SP
			47	478.3	LV, SP				53.05	468.7	LV, SP
			47	388.1	LV, SP				53.05	389.7	LV, SP
			47	423.6	RV, SP				53.05	446.2	RV, SP
			47	405.9	RV, SP				53.05	426.6	LV, SP
			47	455.2	LV, SP				53.05	484.9	RV, SP
			47	468.0	LV, SP				53.05	469.6	LV, SP
			47	407.5	RV, SP				53.05	358.3	LV, SP
			47	408.9	RV, SP				53.05	473.2	LV, SP
			47	359.4	RV, SP				53.05	464.1	RV, SP
			47	438.7	RV, SP				53.05	374.3	RV, SP
			47	372.1	LV, SP				53.05	459.6	RV, SP
			47	413.0	RV, SP				53.05	415.4	LV, SP
			47	412.0	RV, SP				53.05	443.1	RV, SP
			47	438.2	RV, SP				53.05	390.0	LV, SP
			47	438.6	RV, SP				53.05	436.1	LV, SP
			47	402.5	RV, SP				53.05	410.0	RV, SP
			47	443.7	RV, SP				53.05	426.3	RV, SP
			47	380.1	LV, SP				53.05	440.6	LV, SP
			47	299.8	RV, SP				53.05	398.2	LV, SP
			47	338.9	LV, SP				53.05	449.2	LV, SP
			47	322.2	RV, SP				53.05	451.5	LV, SP
			47	388.2	RV, SP				53.05	489.7	LV, SP
			47	276.8	LV, SP				53.05	485.0	LV, SP
			47	375.1	RV, SP				53.05	474.5	LV, SP
			47	275.5	RV, SP				53.05	421.9	RV, SP
			47	274.3	RV, SP				53.05	407.0	RV, SP
			47	328.8	RV, SP				53.05	486.8	LV, SP
			47	391.7	RV, SP				53.05	404.9	LV, SP
			47	373.8	RV, SP				53.05	447.2	LV, SP
			47	364.9	LV, SP				53.05	466.0	LV, SP
			47	325.1	LV, SP				53.05	501.3	LV, SB
			47	326.2	RV, SP				53.05	401.9	RV, SP
			47	323.8	RV, SP				53.05	452.7	LV, SP
			47	386.9	RV, SP				53.05	411.4	RV, SP
			47	280.8	RV, SP				53.05	475.3	LV, SP

(B)						<i>O. aspinata</i>					
Zone	Subzone	Bed N.	Bed height	Geometric shell size	Shell preservation	Zone	Subzone	Bed N.	Bed height	Geometric shell size	Shell preservation
			47	362.6	LV, SP				53.05	416.4	RV, SP
			47	373.6	RV, SP				53.05	417.9	RV, SP
			47	331.6	RV, SP				53.05	433.3	RV, SP
			47	341.8	RV, SP				53.05	421.6	RV, SP
			47	240.9	RV, SP				53.05	475.2	LV, SP
			47	286.8	RV, SP				53.05	468.9	LV, SP
			47	332.0	LV, SP				53.05	460.4	LV, SP
			47	375.8	RV, SP				53.05	427.6	RV, SP
			47	363.3	RV, SP				53.05	471.9	RV, SP
			47	286.4	LV, SP				53.05	462.8	LV, SP
			47	330.2	RV, SP				53.05	457.6	RV, SP
			47	335.8	RV, SP				53.05	528.7	LV, SP
			47	333.1	RV, SP				53.05	475.2	LV, SP
			47	373.6	RV, SP				53.05	464.6	LV, SP
			47	277.5	RV, SP				53.05	425.2	RV, SP
			47	330.1	RV, SP				53.05	391.8	RV, SP
			47	377.8	RV, SP				53.05	490.2	LV, SP
			47	334.7	LV, SP				53.05	414.8	RV, SP
			47	381.9	RV, SP				53.05	497.9	SB
			47	282.1	RV, SP				53.05	445.6	LV, SP
			47	325.0	LV, SP				53.05	390.2	LV, SP
			47	374.1	RV, SP				53.05	471.3	LV, SP
			47	329.4	LV, SP				53.05	452.3	LV, SP
			47	322.5	LV, SP				53.05	456.9	LV, SP
			47	319.1	LV, SP				53.05	487.9	LV, SP
			47	372.5	RV, SP				53.05	440.3	RV, SB
			47	372.2	RV, SP				53.05	397.2	RV, SP
			47	374.0	LV, SP				53.05	449.5	LV, SP
			47	274.2	RV, SP				53.05	488.0	LV, SP
			47	320.2	LV, SP				53.05	460.8	LV, SP
			47	285.4	RV, SP				53.05	458.8	LV, SP
			47	328.2	LV, SP				53.05	472.8	LV, SP
			47	338.5	LV, SP				53.05	393.1	LV, SP
			47	382.0	RV, SP				53.05	430.0	LV, SP
			47	288.9	LV, SP				53.05	486.1	LV, SP
			47	330.1	RV, SP				53.05	401.7	LV, SP
			47	346.3	RV, SP				53.05	478.0	LV, SP
			47	362.6	RV, SP				53.05	471.4	LV, SP
			47	382.8	RV, SP				53.05	426.1	RV, SP

(B)						<i>O. aspinata</i>					
Zone	Subzone	Bed N.	Bed height	Geometric shell size	Shell preservation	Zone	Subzone	Bed N.	Bed height	Geometric shell size	Shell preservation
			47	277.4	RV, SP				53.05	424.6	LV, SP
			47	323.7	LV, SP				53.05	406.9	RV, SP
			47	311.6	RV, SP				53.05	459.1	LV, SP
			47	385.9	LV, SP				53.05	437.0	LV, SP
			47	337.7	LV, SP				53.05	399.3	RV, SP
			47	243.9	RV, SP				53.05	454.4	LV, SP
			47	322.4	RV, SP				53.05	430.6	LV, SP
			47	371.3	LV, SP				53.05	440.4	RV, SP
			47	280.1	RV, SP				53.05	477.7	LV, SP
			47	277.0	LV, SP				53.05	454.7	SB
			47	182.2	LV, SP				53.05	454.0	LV, SP
			47	266.4	RV, SP				53.05	465.3	LV, SP
			47	284.5	LV, SP				53.05	441.2	LV, SP
			48.9	391.4	LV, SP				53.05	456.4	LV, SP
			48.9	461.5	LV, SP				53.05	402.4	LV, SP
			48.9	453.5	LV, SP				53.05	395.5	RV, SP
			48.9	364.3	LV, SP				53.05	459.4	LV, SP
			48.9	416.3	RV, SP				53.05	464.7	LV, SP
			48.9	417.6	RV, SP				53.05	414.4	LV, SP
			48.9	348.0	RV, SP				53.05	446.1	LV, SP
			48.9	426.2	LV, SP				53.05	394.4	LV, SP
			48.9	469.4	RV, SP				53.05	480.0	RV, SP
			48.9	467.2	LV, SP				53.05	453.6	LV, SP
			48.9	421.6	RV, SP				53.05	477.1	LV, SP
			48.9	428.2	RV, SP				53.05	436.3	LV, SP
			48.9	477.9	LV, SP				53.05	374.2	RV, SP
			48.9	466.6	LV, SB				53.05	461.9	LV, SP
			48.9	297.2	RV, SP				53.05	430.5	RV, SP
			48.9	425.4	LV, SB				53.05	395.3	RV, SP
			48.9	405.6	RV, SP				53.05	425.1	LV, SP
			48.9	415.8	RV, SP				53.05	450.5	LV, SP
			48.9	441.2	RV, SP				53.05	409.9	RV, SP
			48.9	399.7	LV, SP				53.05	416.6	RV, SP
			48.9	408.3	LV, SP				53.05	464.9	LV, SP
			48.9	465.6	LV, SP				53.05	391.9	LV, SP
			48.9	370.7	RV, SP				53.05	483.7	LV, SP
			48.9	464.0	LV, SP				53.05	432.6	LV, SP
			48.9	392.6	LV, SP				53.05	465.2	LV, SP
			48.9	420.9	LV, SP				53.05	364.8	RV, SP

(B)						<i>O. aspinata</i>					
Zone	Subzone	Bed N.	Bed height	Geometric shell size	Shell preservation	Zone	Subzone	Bed N.	Bed height	Geometric shell size	Shell preservation
			48.9	431.1	LV, SP				53.05	496.6	LV, SP
			48.9	477.0	RV, SP				53.05	401.7	RV, SP
			48.9	438.4	RV, SP				53.05	427.5	RV, SP
			48.9	406.0	LV, SP				53.05	416.0	LV, SP
			48.9	400.3	RV, SP				53.05	458.4	RV, SP
			48.9	444.5	RV, SP				53.05	399.4	SB
			48.9	380.4	RV, SP				53.05	373.8	RV, SP
			48.9	453.3	RV, SP				53.05	362.4	RV, SP
			48.9	479.0	RV, SP				53.05	393.1	RV, SP
			48.9	483.5	LV, SP				53.05	376.2	RV, SP
			48.9	426.7	LV, SP				53.05	367.8	RV, SP
			48.9	423.0	LV, SP				53.05	342.6	RV, SP
			48.9	471.6	RV, SP				53.05	376.8	RV, SP
			48.9	414.6	RV, SP				53.05	378.1	RV, SP
			48.9	431.3	LV, SP				53.05	433.2	RV, SP
			48.9	475.2	LV, SP				53.05	320.7	RV, SP
			48.9	426.5	RV, SP				53.05	324.6	RV, SP
			48.9	469.6	LV, SP				53.05	405.7	RV, SP
			48.9	450.1	RV, SP				53.05	350.4	RV, SP
			48.9	370.6	RV, SP				53.05	350.8	RV, SP
			48.9	399.0	LV, SP				53.05	366.3	RV, SP
			48.9	476.1	LV, SP				53.05	377.2	RV, SP
			48.9	449.5	LV, SP				53.05	326.0	LV, SP
			48.9	380.0	RV, SP				53.05	355.7	RV, SP
			48.9	422.1	RV, SP				53.05	309.7	LV, SP
			48.9	482.2	RV, SP				53.05	399.9	RV, SP
			48.9	476.8	RV, SP				53.05	326.6	RV, SP
			48.9	399.9	RV, SP				53.05	372.7	RV, SP
			48.9	450.8	LV, SP				53.05	381.1	RV, SP
			48.9	484.2	LV, SP				53.05	379.6	RV, SP
			48.9	477.5	RV, SP				53.05	329.3	RV, SP
			48.9	460.0	LV, SP				53.05	350.8	RV, SP
			48.9	380.6	LV, SP				53.05	363.3	RV, SP
			48.9	474.5	LV, SP				53.05	356.3	LV, SP
			48.9	432.0	RV, SP				53.05	372.1	RV, SP
			48.9	422.8	LV, SP				53.05	390.2	LV, SP
			48.9	457.5	LV, SP				53.05	335.5	LV, SP
			48.9	497.5	RV, SP				53.05	365.3	RV, SP
			48.9	385.8	RV, SP				53.05	387.0	RV, SP

(B)						<i>O. aspinata</i>					
Zone	Subzone	Bed N.	Bed height	Geometric shell size	Shell preservation	Zone	Subzone	Bed N.	Bed height	Geometric shell size	Shell preservation
			48.9	429.6	LV, SP				53.05	323.4	RV, SP
			48.9	437.5	LV, SP				53.05	388.5	RV, SP
			48.9	401.7	RV, SP				53.05	396.8	RV, SP
			48.9	483.7	RV, SP				53.05	372.9	RV, SP
			48.9	465.7	LV, SP				53.05	385.4	RV, SP
			48.9	472.9	LV, SP				53.05	341.6	RV, SP
			48.9	415.1	RV, SP				53.05	298.5	RV, SP
			48.9	419.9	RV, SP				53.05	385.1	RV, SP
			48.9	407.8	RV, SP				53.05	365.2	RV, SP
			48.9	410.1	RV, SP				53.05	367.2	RV, SP
			48.9	457.1	LV, SP				53.05	305.6	RV, SP
			48.9	409.3	LV, SP				53.05	342.7	RV, SP
			48.9	438.0	SB				53.05	371.7	LV, SP
			48.9	489.9	LV, SP				53.05	372.1	LV, SP
			48.9	449.8	RV, SP				53.05	324.6	RV, SP
			48.9	429.6	LV, SP				53.05	338.6	SB
			48.9	410.9	RV, SP				53.05	314.2	RV, SP
			48.9	476.7	LV, SP				53.05	258.5	RV, SP
			48.9	485.7	LV, SP				53.05	285.4	SB
			48.9	458.8	LV, SP				53.05	208.2	LV, SP
			48.9	462.3	LV, SP				53.05	272.0	RV, SP
			48.9	391.9	RV, SP				53.6	504.6	LV, SP
			48.9	446.3	LV, SP				53.6	444.4	RV, SP
			48.9	421.6	RV, SP				53.6	473.9	RV, SP
			48.9	434.9	LV, SP				53.6	381.7	LV, SP
			48.9	413.9	RV, SB				53.6	478.9	RV, SP
			48.9	248.6	RV, SP				53.6	493.8	RV, SP
			48.9	311.4	RV, SP				53.6	393.6	RV, SP
			48.9	306.6	RV, SP				53.6	492.4	RV, SP
			48.9	324.7	LV, SP				53.6	481.5	LV, SP
			48.9	366.9	RV, SP			SAB76	53.6	399.3	LV, SP
			48.9	332.8	LV, SP				53.6	489.0	LV, SP
			48.9	360.1	RV, SP				53.6	484.7	LV, SP
			48.9	324.8	LV, SP				53.6	397.3	RV, SP
			48.9	371.7	LV, SP				53.6	398.1	LV, SP
			48.9	396.8	RV, SP				53.6	421.6	RV, SP
			48.9	373.5	RV, SP				53.6	430.5	RV, SP
			48.9	347.7	LV, SP				53.6	409.7	RV, SP
			48.9	369.3	RV, SP				53.6	500.4	LV, SP

(B)						<i>O. aspinata</i>					
Zone	Subzone	Bed N.	Bed height	Geometric shell size	Shell preservation	Zone	Subzone	Bed N.	Bed height	Geometric shell size	Shell preservation
			48.9	346.1	LV, SP				53.6	484.6	LV, SP
			48.9	384.5	RV, SP				53.6	449.3	LV, SP
			48.9	297.1	RV, SP				53.6	395.5	LV, SP
			48.9	318.4	RV, SP				53.6	489.2	LV, SP
			48.9	260.3	SB				53.6	460.2	LV, SP
			48.9	375.1	LV, SP				53.6	427.8	RV, SP
			48.9	333.4	RV, SP				53.6	442.6	RV, SP
			48.9	303.9	RV, SP				53.6	492.2	RV, SP
			48.9	290.4	RV, SP				53.6	437.2	RV, SP
			48.9	380.2	RV, SP				53.6	496.9	RV, SP
			48.9	277.5	RV, SP				53.6	437.9	LV, SP
			48.9	362.0	RV, SP				53.6	470.9	RV, SB
			48.9	370.8	RV, SP				53.6	509.6	LV, SP
			48.9	374.9	RV, SP				53.6	437.9	RV, SP
			48.9	382.8	RV, SP				53.6	432.0	RV, SP
			48.9	326.6	RV, SP				53.6	472.8	LV, SP
			48.9	317.6	LV, SP				53.6	443.0	RV, SP
			48.9	315.3	LV, SP				53.6	519.2	LV, SP
			48.9	290.1	RV, SP				53.6	495.3	LV, SP
			48.9	329.7	LV, SP				53.6	427.6	LV, SP
			48.9	273.9	SB				53.6	445.5	RV, SP
			48.9	340.7	RV, SP				53.6	506.5	LV, SP
			48.9	407.1	RV, SP				53.6	518.2	RV, SP
			48.9	323.5	RV, SP				53.6	408.4	RV, SP
			48.9	296.7	LV, SP				53.6	497.0	LV, SP
			48.9	328.5	LV, SP				53.6	393.5	LV, SP
			48.9	363.8	RV, SP				53.6	438.5	RV, SP
			48.9	282.0	SB				53.6	430.4	RV, SP
			48.9	314.9	LV, SP				53.6	440.5	RV, SP
			48.9	373.2	RV, SP				53.6	427.2	RV, SP
			48.9	158.0	RV, SP				53.6	423.3	RV, SP
			48.9	201.6	RV, SP				53.6	391.7	RV, SP
			48.9	217.7	LV, SP				53.6	435.4	RV, SP
			48.9	262.1	LV, SP				53.6	435.6	RV, SP
			48.9	233.0	SB				53.6	425.2	RV, SP
		SAB66	49.3	396.5	RV, SP				53.6	423.1	LV, SP
			49.3	391.8	RV, SP				53.6	420.3	RV, SP
			49.3	417.9	RV, SP				53.6	420.9	LV, SP
			49.3	375.4	RV, SP				53.6	486.2	RV, SP

(B)						<i>O. aspinata</i>					
Zone	Subzone	Bed N.	Bed height	Geometric shell size	Shell preservation	Zone	Subzone	Bed N.	Bed height	Geometric shell size	Shell preservation
			49.3	424.1	RV, SP				53.6	368.0	LV, SP
			49.3	419.7	LV, SP				53.6	478.3	LV, SP
			49.3	440.5	LV, SP				53.6	394.9	LV, SP
			49.3	391.5	RV, SP				53.6	502.7	LV, SP
			49.3	390.1	RV, SP				53.6	496.8	RV, SP
			49.3	425.9	RV, SP				53.6	457.8	LV, SP
			49.3	457.2	LV, SP				53.6	489.9	LV, SP
			49.3	426.1	LV, SP				53.6	422.3	LV, SP
			49.3	393.1	LV, SP				53.6	488.2	LV, SP
			49.3	448.2	LV, SP				53.6	454.0	LV, SP
			49.3	396.5	RV, SP				53.6	388.9	LV, SP
			49.3	355.7	LV, SP				53.6	428.8	RV, SP
			49.3	456.0	LV, SP				53.6	459.8	RV, SP
			49.3	439.2	LV, SP				53.6	460.3	LV, SP
			49.3	365.8	RV, SP				53.6	448.6	LV, SP
			49.3	423.2	LV, SP				53.6	431.4	RV, SP
			49.3	405.7	RV, SP				53.6	418.1	RV, SP
			49.3	434.0	LV, SP				53.6	430.1	RV, SP
			49.3	444.2	LV, SP				53.6	469.6	LV, SP
			49.3	449.2	LV, SP				53.6	494.3	LV, SP
			49.3	317.5	LV, SP				53.6	504.6	LV, SP
			49.3	448.2	LV, SP				53.6	485.9	RV, SP
			49.3	443.9	LV, SP				53.6	487.4	RV, SP
			49.3	378.7	RV, SP				53.6	508.5	LV, SP
			49.3	396.9	RV, SP				53.6	517.9	LV, SP
			49.3	374.8	RV, SP				53.6	515.3	LV, SP
			49.3	407.6	RV, SP				53.6	452.4	LV, SP
			49.3	432.0	RV, SP				53.6	488.7	LV, SP
			49.3	400.0	RV, SP				53.6	416.9	LV, SP
			49.3	445.5	LV, SP				53.6	500.4	RV, SP
			49.3	441.8	LV, SP				53.6	449.9	RV, SP
			49.3	449.0	LV, SP				53.6	493.8	LV, SP
			49.3	439.5	LV, SP				53.6	435.0	RV, SP
			49.3	407.6	RV, SP				53.6	474.9	RV, SP
			49.3	443.3	LV, SP				53.6	407.7	LV, SP
			49.3	379.1	RV, SP				53.6	405.0	LV, SP
			49.3	438.0	LV, SP				53.6	436.0	RV, SP
			49.3	458.4	LV, SP				53.6	413.3	RV, SP
			49.3	439.3	LV, SP				53.6	480.5	RV, SP

(B)						<i>O. aspinata</i>					
Zone	Subzone	Bed N.	Bed height	Geometric shell size	Shell preservation	Zone	Subzone	Bed N.	Bed height	Geometric shell size	Shell preservation
			49.3	416.3	RV, SP				53.6	441.3	RV, SP
			49.3	400.4	RV, SP				53.6	411.7	LV, SP
			49.3	399.3	LV, SP				53.6	483.6	LV, SP
			49.3	399.8	LV, SP				53.6	479.7	LV, SP
			49.3	398.1	RV, SP				53.6	480.8	RV, SP
			49.3	432.9	RV, SP				53.6	422.1	RV, SP
			49.3	395.3	LV, SP				53.6	516.1	RV, SP
			49.3	389.5	RV, SP				53.6	419.0	RV, SP
			49.3	417.7	RV, SP				53.6	506.0	LV, SP
			49.3	377.7	RV, SP				53.6	491.0	LV, SP
			49.3	431.3	LV, SP				53.6	488.7	RV, SP
			49.3	434.0	LV, SP				53.6	404.9	LV, SP
			49.3	397.2	LV, SP				53.6	485.5	RV, SP
			49.3	450.5	LV, SP				53.6	427.4	RV, SP
			49.3	399.5	RV, SP				53.6	437.6	RV, SP
			49.3	483.2	LV, SP				53.6	407.1	LV, SP
			49.3	408.5	RV, SP				53.6	430.9	RV, SP
			49.3	357.2	LV, SP				53.6	488.7	LV, SP
			49.3	393.3	RV, SP				53.6	457.3	LV, SP
			49.3	452.7	LV, SP				53.6	455.8	LV, SP
			49.3	422.2	RV, SP				53.6	368.9	RV, SP
			49.3	415.3	RV, SP				53.6	432.0	RV, SP
			49.3	416.6	LV, SP				53.6	428.4	RV, SP
			49.3	394.3	RV, SP				53.6	512.1	LV, SP
			49.3	441.8	RV, SP				53.6	509.8	LV, SP
			49.3	450.9	LV, SP				53.6	500.1	RV, SP
			49.3	388.5	RV, SP				53.6	420.5	LV, SP
			49.3	433.1	LV, SP				53.6	435.1	RV, SP
			49.3	445.0	LV, SP				53.6	498.6	LV, SP
			49.3	442.2	LV, SP				53.6	434.4	RV, SP
			49.3	446.9	LV, SP				53.6	473.5	RV, SP
			49.3	439.2	LV, SP				53.6	501.0	LV, SP
			49.3	421.7	LV, SP				53.6	376.2	RV, SP
			49.3	416.1	RV, SP				53.6	404.2	LV, SP
			49.3	411.8	RV, SP				53.6	416.4	LV, SP
			49.3	472.4	LV, SP				53.6	499.9	LV, SP
			49.3	480.0	LV, SP				53.6	427.1	LV, SP
			49.3	373.0	RV, SP				53.6	485.4	LV, SP
			49.3	424.1	LV, SP				53.6	411.6	LV, SP

(B)						<i>O. aspinata</i>					
Zone	Subzone	Bed N.	Bed height	Geometric shell size	Shell preservation	Zone	Subzone	Bed N.	Bed height	Geometric shell size	Shell preservation
			49.3	410.7	RV, SP				53.6	445.8	RV, SP
			49.3	432.0	LV, SP				53.6	435.3	RV, SP
			49.3	425.5	LV, SP				53.6	402.6	LV, SP
			49.3	416.2	RV, SP				53.6	496.4	LV, SP
			49.3	409.0	LV, SP				53.6	421.6	RV, SP
			49.3	390.5	RV, SP				53.6	508.9	RV, SP
			49.3	408.0	LV, SP				53.6	433.3	LV, SP
			49.3	432.7	LV, SP				53.6	295.6	LV, SP
			49.3	447.2	LV, SP				53.6	359.0	LV, SP
			49.3	428.3	RV, SP				53.6	336.9	RV, SP
			49.3	414.2	RV, SP				53.6	353.6	RV, SP
			49.3	429.6	RV, SP				53.6	303.3	RV, SP
			49.3	388.4	LV, SP				53.6	279.2	SB
			49.3	389.2	RV, SP				53.6	393.3	RV, SP
			49.3	369.4	RV, SP				53.6	345.4	RV, SP
			49.3	420.6	RV, SP				53.6	327.3	RV, SP
			49.3	396.1	LV, SP				53.6	349.2	RV, SP
			49.3	450.4	LV, SP				53.6	388.3	RV, SP
			49.3	437.4	LV, SP				53.6	347.0	RV, SP
			49.3	424.5	LV, SP				53.6	346.3	RV, SP
			49.3	443.0	LV, SP				53.6	343.6	LV, SP
			49.3	383.4	RV, SP				53.6	374.1	RV, SP
			49.3	402.1	RV, SP				53.6	347.2	SB
			49.3	380.8	RV, SP				53.6	387.1	RV, SP
			49.3	421.4	RV, SP				53.6	335.9	LV, SP
			49.3	370.3	LV, SP				53.6	340.0	RV, SP
			49.3	428.2	RV, SP				53.6	379.2	SB
			49.3	433.8	RV, SP				53.6	359.1	SB
			49.3	430.6	LV, SP				53.6	363.2	RV, SP
			49.3	451.5	LV, SP				53.6	377.7	RV, SP
			49.3	433.1	LV, SP				53.6	377.8	RV, SP
			49.3	357.5	LV, SP				53.6	368.5	RV, SP
			49.3	414.0	RV, SP				53.6	320.2	RV, SP
			49.3	365.8	RV, SP				53.6	319.3	RV, SP
			49.3	416.9	LV, SP				53.6	309.9	RV, SP
			49.3	535.8	RV, SP				53.6	268.2	RV, SP
			49.3	382.0	RV, SP				53.6	306.2	RV, SP
			49.3	380.7	RV, SP				53.6	383.3	RV, SP
			49.3	440.6	RV, SP				53.6	285.4	LV, SP

(B)						<i>O. aspinata</i>					
Zone	Subzone	Bed N.	Bed height	Geometric shell size	Shell preservation	Zone	Subzone	Bed N.	Bed height	Geometric shell size	Shell preservation
			49.3	286.5	RV, SP				53.6	364.1	RV, SP
			49.3	320.4	LV, SP				53.6	335.0	LV, SP
			49.3	385.7	RV, SP				53.6	394.4	RV, SP
			49.3	348.9	RV, SP				53.6	319.3	RV, SP
			49.3	312.2	RV, SP				53.6	335.5	RV, SP
			49.3	326.7	RV, SP				53.6	275.8	RV, SP
			49.3	293.8	LV, SP				53.6	378.1	RV, SP
			49.3	317.0	LV, SP				53.6	340.9	RV, SP
			49.3	317.8	LV, SP				53.6	297.9	RV, SP
			49.3	246.5	RV, SP				53.6	339.1	RV, SP
			49.3	373.4	LV, SP				53.6	395.1	RV, SP
			49.3	295.0	LV, SP				53.6	342.9	LV, SP
			49.3	292.4	RV, SP				53.6	381.1	RV, SP
			49.3	332.1	RV, SP				53.6	382.9	RV, SP
			49.3	361.8	RV, SP				53.6	340.0	LV, SP
			49.3	342.9	LV, SP				53.6	382.2	RV, SP
			49.3	303.5	LV, SP				53.6	304.6	RV, SP
			49.3	302.1	LV, SP				53.6	342.4	RV, SP
			49.3	376.5	RV, SP				53.6	346.3	RV, SP
			49.3	344.4	LV, SP				53.6	333.6	LV, SP
			49.3	305.3	RV, SP				53.6	354.4	LV, SP
			49.3	308.2	RV, SP				53.6	322.3	RV, SP
			49.3	329.3	RV, SP				53.6	340.0	LV, SP
			49.3	309.2	RV, SP				53.6	389.2	RV, SP
			49.3	289.6	RV, SP				53.6	391.2	RV, SP
			49.3	298.7	LV, SP				53.6	341.8	RV, SP
			49.3	307.0	LV, SP				53.6	366.5	RV, SP
			49.3	322.3	RV, SP				53.6	316.3	RV, SP
			49.3	334.7	RV, SP				53.6	363.4	LV, SP
			49.3	373.6	RV, SP				53.6	369.6	RV, SP
			49.3	264.5	RV, SP				53.6	371.0	LV, SP
			49.3	355.2	LV, SP				53.6	387.4	LV, SP
			49.3	325.8	RV, SP				53.6	326.5	LV, SP
			49.3	317.8	RV, SP				53.6	341.8	RV, SP
			49.3	396.9	RV, SP				53.6	345.6	RV, SP
			49.3	373.8	RV, SP				53.6	279.2	RV, SP
			49.3	292.4	RV, SP				53.6	263.7	RV, SP
			49.3	253.3	RV, SP				53.6	394.1	RV, SP
			49.3	367.1	RV, SP				53.6	326.9	LV, SP

(B)						<i>O. aspinata</i>					
Zone	Subzone	Bed N.	Bed height	Geometric shell size	Shell preservation	Zone	Subzone	Bed N.	Bed height	Geometric shell size	Shell preservation
			49.3	306.3	RV, SP				53.6	361.4	RV, SP
			49.3	369.8	RV, SP				53.6	175.7	LV, SP
			49.3	329.5	RV, SP				53.6	179.5	RV, SP
			49.3	308.2	LV, SP				53.6	272.6	RV, SP
			49.3	312.7	RV, SP				55.5	478.8	LV, SP
			49.3	326.0	RV, SP				55.5	355.9	RV, SP
			49.3	313.6	RV, SP				55.5	400.2	RV, SP
			49.3	372.2	RV, SP				55.5	462.0	RV, SP
			49.3	362.6	RV, SP				55.5	513.4	LV, SP
			49.3	369.9	RV, SP				55.5	390.6	RV, SP
			49.3	265.8	RV, SP				55.5	486.5	LV, SP
			49.3	342.2	LV, SP				55.5	423.0	RV, SP
			49.3	217.8	LV, SP				55.5	471.9	LV, SP
			49.3	377.7	LV, SP				55.5	398.7	SB
			49.3	278.3	RV, SP				55.5	449.6	LV, SP
			49.3	312.2	RV, SP				55.5	423.2	LV, SP
			49.3	303.7	RV, SP				55.5	255.5	LV, SP
			49.3	275.0	LV, SP				55.5	511.0	LV, SP
			49.3	314.1	LV, SP				55.5	423.0	RV, SP
			49.3	317.2	RV, SP				55.5	446.9	LV, SP
			49.3	316.4	RV, SP				55.5	426.8	LV, SP
			49.3	309.4	RV, SP				55.5	391.4	RV, SP
			49.3	297.9	LV, SP				55.5	438.2	LV, SP
			49.3	381.6	RV, SP				55.5	401.2	SB
			49.3	256.7	RV, SP				55.5	466.0	LV, SP
			49.3	290.0	RV, SP				55.5	500.3	LV, SP
			49.3	384.1	RV, SP				55.5	339.9	RV, SP
			49.3	245.0	RV, SP				55.5	357.8	LV, SP
			49.3	224.1	RV, SP				55.5	405.0	RV, SP
			49.3	229.5	RV, SP				55.5	444.0	RV, SP
			49.3	236.9	LV, SP				55.5	458.0	LV, SP
			49.3	276.6	RV, SP				55.5	423.3	LV, SP
			49.3	210.0	LV, SP				55.5	483.9	LV, SP
			49.3	201.1	LV, SP				55.5	447.7	SB
			49.3	252.0	LV, SP				55.5	496.5	LV, SP
			49.3	175.0	LV, SP				55.5	454.2	LV, SP
			49.3	211.9	RV, SP				55.5	530.5	LV, SP
			49.3	230.2	RV, SP				55.5	464.4	LV, SP
			49.3	194.4	RV, SP				55.5	370.3	RV, SP

(B)						<i>O. aspinata</i>					
Zone	Subzone	Bed N.	Bed height	Geometric shell size	Shell preservation	Zone	Subzone	Bed N.	Bed height	Geometric shell size	Shell preservation
			49.3	225.8	RV, SP				55.5	461.3	LV, SP
			49.3	198.3	RV, SP				55.5	415.9	RV, SP
			49.3	209.9	LV, SP				55.5	382.9	RV, SP
			49.3	215.0	RV, SP				55.5	435.8	RV, SP
			49.3	239.9	LV, SP				55.5	412.0	RV, SP
			49.3	228.8	LV, SP				55.5	447.8	RV, SP
			49.3	262.4	LV, SP				55.5	373.8	LV, SP
			49.3	260.2	RV, SP				55.5	495.1	LV, SP
			49.3	221.4	RV, SP				55.5	392.7	RV, SP
			49.3	273.5	RV, SP				55.5	399.7	RV, SP
			49.3	239.3	RV, SP				55.5	380.0	RV, SP
			49.3	276.5	LV, SP				55.5	276.7	RV, SP
			49.44	523.2	RV, SP				55.5	235.3	LV, SP
			49.44	430.1	RV, SP				55.5	259.3	LV, SP
			49.44	385.0	LV, SP				55.5	400.7	RV, SP
			49.44	408.7	RV, SP				55.5	339.6	RV, SP
			49.44	444.7	LV, SP				55.5	422.4	RV, SP
			49.44	410.9	RV, SP				55.7	458.1	LV, SP
			49.44	454.3	LV, SP				55.7	459.1	LV, SP
			49.44	452.0	RV, SP				55.7	419.4	LV, SP
			49.44	452.8	LV, SP				55.7	418.1	RV, SP
			49.44	426.8	LV, SP				55.7	410.3	LV, SP
			49.44	447.2	LV, SP				55.7	461.7	LV, SP
			49.44	441.7	RV, SP				55.7	465.0	RV, SP
			49.44	442.7	LV, SP				55.7	480.8	RV, SP
			49.44	397.1	LV, SP				55.7	378.4	RV, SP
			49.44	398.5	RV, SP				55.7	466.2	LV, SP
			49.44	431.3	LV, SP				55.7	385.2	RV, SP
			49.44	357.2	LV, SP				55.7	471.6	LV, SP
			49.44	437.6	LV, SP				55.7	467.3	RV, SP
			49.44	388.8	RV, SP				55.7	456.0	LV, SP
			49.44	367.4	LV, SP				55.7	412.3	RV, SP
			49.44	391.7	LV, SP				55.7	480.0	LV, SP
			49.44	459.3	RV, SP				55.7	394.1	LV, SP
			49.44	386.3	LV, SP				55.7	383.1	RV, SP
			49.44	433.5	LV, SP				55.7	452.3	LV, SP
			49.44	435.5	LV, SP				55.7	410.6	RV, SP
			49.44	442.9	LV, SP				55.7	456.2	RV, SP
			49.44	354.9	LV, SP				55.7	462.7	LV, SP

(B)						<i>O. aspinata</i>					
Zone	Subzone	Bed N.	Bed height	Geometric shell size	Shell preservation	Zone	Subzone	Bed N.	Bed height	Geometric shell size	Shell preservation
			49.44	388.3	LV, SP				55.7	436.4	LV, SP
			49.44	400.6	RV, SP				55.7	370.5	RV, SP
			49.44	404.5	RV, SP				55.7	399.9	RV, SP
			49.44	461.9	RV, SP				55.7	431.2	RV, SP
			49.44	436.7	LV, SP				55.7	478.9	LV, SP
			49.44	449.5	LV, SP				55.7	374.3	RV, SP
			49.44	358.8	LV, SP				55.7	459.4	LV, SP
			49.44	434.7	LV, SP				55.7	450.1	RV, SP
			49.44	397.3	RV, SP				55.7	389.6	RV, SP
			49.44	452.6	LV, SP				55.7	440.0	RV, SP
			49.44	423.6	LV, SP				55.7	383.0	LV, SP
			49.44	468.8	LV, SP				55.7	406.6	RV, SP
			49.44	445.2	LV, SP				55.7	470.6	LV, SP
			49.44	446.7	LV, SP				55.7	460.8	LV, SP
			49.44	410.3	RV, SP				55.7	487.8	RV, SP
			49.44	429.2	LV, SP				55.7	388.8	LV, SP
			49.44	444.2	LV, SP				55.7	408.6	RV, SP
			49.44	437.7	LV, SP				55.7	414.4	RV, SP
			49.44	412.1	RV, SP				55.7	414.8	RV, SP
			49.44	445.6	LV, SP				55.7	427.3	RV, SP
			49.44	436.5	RV, SP				55.7	434.8	RV, SP
			49.44	381.6	LV, SP				55.7	502.4	RV, SP
			49.44	467.6	LV, SP				55.7	427.6	RV, SP
			49.44	449.2	LV, SP				55.7	402.3	LV, SP
			49.44	398.9	RV, SP				55.7	482.0	LV, SP
			49.44	441.9	LV, SP				55.7	467.9	LV, SP
			49.44	442.1	RV, SP				55.7	462.1	RV, SP
			49.44	441.8	LV, SP				55.7	495.5	LV, SP
			49.44	449.6	RV, SP				55.7	403.8	RV, SP
			49.44	452.8	RV, SP				55.7	446.5	LV, SP
			49.44	439.8	LV, SP				55.7	475.2	RV, SP
			49.44	381.4	LV, SP				55.7	456.5	LV, SP
			49.44	455.3	LV, SP				55.7	431.8	RV, SP
			49.44	408.4	RV, SP				55.7	465.0	LV, SP
			49.44	376.5	LV, SP				55.7	402.0	LV, SP
			49.44	453.3	RV, SP				55.7	400.9	RV, SP
			49.44	386.5	RV, SP				55.7	410.7	RV, SP
			49.44	395.0	LV, SP				55.7	472.9	LV, SP
			49.44	428.1	LV, SP				55.7	482.9	LV, SP

(B)						<i>O. aspinata</i>					
Zone	Subzone	Bed N.	Bed height	Geometric shell size	Shell preservation	Zone	Subzone	Bed N.	Bed height	Geometric shell size	Shell preservation
			49.44	439.9	LV, SP				55.7	419.8	RV, SP
			49.44	427.4	LV, SP				55.7	436.9	LV, SP
			49.44	448.0	LV, SP				55.7	384.2	LV, SP
			49.44	369.6	RV, SP				55.7	434.8	RV, SP
			49.44	442.7	LV, SP				55.7	325.7	RV, SP
			49.44	399.5	RV, SP				55.7	440.3	RV, SP
			49.44	439.3	RV, SP				55.7	421.3	LV, SP
			49.44	404.7	RV, SP				55.7	416.4	RV, SP
			49.44	444.6	LV, SP				55.7	414.9	RV, SP
			49.44	446.1	LV, SP				55.7	421.7	RV, SP
			49.44	440.6	LV, SP				55.7	458.8	RV, SP
			49.44	437.6	LV, SP				55.7	425.4	RV, SP
			49.44	447.4	LV, SP				55.7	414.0	RV, SP
			49.44	428.4	RV, SP				55.7	447.3	RV, SP
			49.44	388.8	LV, SP				55.7	438.5	LV, SP
			49.44	448.7	LV, SP				55.7	459.7	RV, SP
			49.44	415.4	RV, SP				55.7	435.1	RV, SP
			49.44	384.0	LV, SP				55.7	365.9	LV, SP
			49.44	455.3	LV, SP				55.7	412.7	RV, SP
			49.44	453.5	LV, SP				55.7	424.3	RV, SP
			49.44	451.5	LV, SP				55.7	456.9	RV, SP
			49.44	457.4	LV, SP				55.7	398.8	RV, SP
			49.44	402.6	RV, SP				55.7	403.2	LV, SP
			49.44	451.3	LV, SP				55.7	429.7	RV, SP
			49.44	451.8	LV, SP				55.7	433.6	RV, SP
			49.44	456.4	LV, SP				55.7	480.8	LV, SP
			49.44	438.6	LV, SP				55.7	474.6	LV, SP
			49.44	452.1	LV, SP				55.7	396.5	LV, SP
			49.44	415.2	RV, SP				55.7	419.0	RV, SP
			49.44	439.4	LV, SP				55.7	412.6	RV, SP
			49.44	389.6	LV, SP				55.7	441.3	RV, SP
			49.44	286.4	RV, SP				55.7	468.4	LV, SP
			49.44	354.1	LV, SP				55.7	390.2	RV, SP
			49.44	306.7	RV, SP				55.7	436.6	LV, SP
			49.44	311.0	RV, SP				55.7	471.4	LV, SP
			49.44	365.4	RV, SP				55.7	482.9	LV, SP
			49.44	372.1	LV, SP				55.7	424.5	RV, SP
			49.44	302.4	RV, SP				55.7	404.1	RV, SP
			49.44	363.4	RV, SP				55.7	467.1	LV, SP

(B)						<i>O. aspinata</i>					
Zone	Subzone	Bed N.	Bed height	Geometric shell size	Shell preservation	Zone	Subzone	Bed N.	Bed height	Geometric shell size	Shell preservation
			49.44	353.8	RV, SP				55.7	468.4	LV, SP
			49.44	319.1	LV, SP				55.7	410.5	RV, SP
			49.44	383.6	LV, SP				55.7	410.2	RV, SP
			49.44	396.5	RV, SP				55.7	452.6	LV, SP
			49.44	330.1	RV, SP				55.7	416.1	RV, SP
			49.44	264.6	LV, SP				55.7	424.6	RV, SP
			49.44	308.0	RV, SP				55.7	453.7	RV, SP
			49.44	377.7	RV, SP				55.7	424.6	LV, SP
			49.44	388.1	RV, SP				55.7	528.0	RV, SP
			49.44	366.2	RV, SP				55.7	445.6	LV, SP
			49.44	281.1	RV, SP				55.7	418.5	RV, SP
			49.44	388.5	RV, SP				55.7	366.4	RV, SP
			49.44	364.0	RV, SP				55.7	406.7	LV, SP
			49.44	315.2	RV, SP				55.7	503.1	RV, SP
			49.44	336.4	RV, SP				55.7	388.4	LV, SP
			49.44	270.1	LV, SP				55.7	435.6	RV, SP
			49.44	367.3	RV, SP				55.7	476.8	LV, SP
			49.44	319.3	RV, SP				55.7	469.8	LV, SP
			49.44	329.1	RV, SP				55.7	456.3	RV, SP
			49.44	320.2	LV, SP				55.7	426.7	RV, SP
			49.44	368.2	RV, SP				55.7	407.8	LV, SP
			49.44	392.0	RV, SP				55.7	464.3	RV, SP
			49.44	317.8	LV, SP				55.7	395.7	LV, SP
			49.44	308.2	RV, SP				55.7	464.0	LV, SP
			49.44	288.0	RV, SP				55.7	440.0	LV, SP
			49.44	316.5	RV, SP				55.7	477.6	LV, SP
			49.44	384.0	RV, SP				55.7	411.9	LV, SP
			49.44	318.4	LV, SP				55.7	370.6	RV, SP
			49.44	399.7	RV, SP				55.7	455.5	LV, SP
			49.44	382.2	LV, SP				55.7	446.8	RV, SP
			49.44	390.7	RV, SP				55.7	448.6	RV, SP
			49.44	350.7	RV, SP				55.7	476.3	RV, SP
			49.44	397.8	RV, SP				55.7	397.4	RV, SP
			49.44	359.7	LV, SP				55.7	469.4	RV, SP
			49.44	326.0	LV, SP				55.7	426.1	RV, SP
			49.44	337.2	LV, SP				55.7	430.8	LV, SP
			49.44	378.1	LV, SP				55.7	477.2	LV, SP
			49.44	389.4	RV, SP				55.7	387.8	RV, SP
			49.44	374.5	RV, SP				55.7	444.0	LV, SP

(B)						<i>O. aspinata</i>					
Zone	Subzone	Bed N.	Bed height	Geometric shell size	Shell preservation	Zone	Subzone	Bed N.	Bed height	Geometric shell size	Shell preservation
			49.44	399.5	RV, SP				55.7	433.1	RV, SP
			49.44	331.6	RV, SP				55.7	418.2	RV, SP
			49.44	391.5	RV, SP				55.7	433.5	RV, SP
			49.44	279.8	RV, SP				55.7	468.4	RV, SP
			49.44	413.3	LV, SP				55.7	399.3	RV, SP
			49.44	317.5	RV, SP				55.7	362.0	LV, SP
			49.44	323.3	RV, SP				55.7	371.3	RV, SP
			49.44	291.5	RV, SP				55.7	431.7	RV, SP
			49.44	259.9	LV, SP				55.7	373.9	RV, SP
			49.44	365.1	RV, SP				55.7	301.1	RV, SP
			49.44	364.3	LV, SP				55.7	325.5	LV, SP
			49.44	296.5	RV, SP				55.7	393.5	RV, SP
			49.44	372.3	RV, SP				55.7	371.3	RV, SP
			49.44	399.4	LV, SP				55.7	357.9	RV, SP
			49.44	365.3	RV, SP				55.7	319.9	LV, SP
			49.44	360.2	LV, SP				55.7	372.8	LV, SP
			49.44	333.7	RV, SP				55.7	360.8	LV, SP
			49.44	390.3	RV, SP				55.7	331.6	RV, SP
			49.44	365.8	RV, SP				55.7	369.1	RV, SP
			49.44	368.6	LV, SP				55.7	320.4	LV, SP
			49.44	334.6	LV, SP				55.7	375.7	LV, SP
			49.44	315.3	RV, SP				55.7	327.4	RV, SP
			49.44	326.7	LV, SP				55.7	328.5	RV, SP
			49.44	381.1	RV, SP				55.7	282.4	LV, SP
			49.44	400.5	RV, SP				55.7	315.9	LV, SP
			49.44	362.2	RV, SP				55.7	293.7	RV, SP
			49.44	391.5	LV, SP				55.7	333.7	LV, SP
			49.44	302.8	RV, SP				55.7	312.4	SB
			49.44	265.2	RV, SP				55.7	345.8	RV, SP
			49.44	297.1	RV, SP				55.7	386.3	RV, SP
			49.44	396.7	LV, SP				55.7	287.1	LV, SP
			49.44	380.6	RV, SP				55.7	369.4	RV, SP
			49.44	380.5	RV, SP				55.7	327.0	RV, SP
			49.44	340.8	LV, SP				55.7	316.7	RV, SP
			49.44	266.6	RV, SP				55.7	288.6	LV, SP
			49.44	392.7	RV, SP				55.7	322.1	LV, SP
			49.44	377.2	RV, SP				55.7	298.0	LV, SP
			49.44	398.6	RV, SP				55.7	275.6	LV, SP
			49.44	231.6	RV, SP				55.7	325.9	RV, SP

(B)						<i>O. aspinata</i>					
Zone	Subzone	Bed N.	Bed height	Geometric shell size	Shell preservation	Zone	Subzone	Bed N.	Bed height	Geometric shell size	Shell preservation
			49.44	280.0	RV, SP				55.7	393.1	RV, SP
			49.44	382.4	LV, SP				55.7	362.5	RV, SP
			49.44	346.5	RV, SP				55.7	380.0	RV, SP
			49.44	382.7	LV, SP				55.7	371.1	RV, SP
			49.44	343.7	RV, SP				55.7	310.8	RV, SP
			49.44	378.5	RV, SP				55.7	317.6	LV, SP
			49.44	277.8	RV, SP				55.7	357.3	LV, SP
			49.44	312.3	LV, SP				55.7	313.1	LV, SP
			49.44	268.4	LV, SP				55.7	266.7	LV, SP
			49.44	260.1	RV, SP				55.7	250.2	RV, SP
			49.44	248.8	RV, SP				55.7	338.2	RV, SP
			49.44	230.6	RV, SP				55.7	271.4	LV, SP
			49.44	205.4	LV, SP				55.7	277.9	LV, SP
			49.8	445.2	LV, SP				55.7	360.7	LV, SP
			49.8	398.9	RV, SP				55.7	378.1	RV, SP
			49.8	401.8	RV, SP				55.7	325.1	LV, SP
			49.8	435.5	LV, SP				55.7	285.3	LV, SP
			49.8	444.8	LV, SP				55.7	302.3	LV, SP
			49.8	441.2	LV, SP				55.7	280.3	RV, SP
			49.8	383.4	RV, SP				55.7	361.1	RV, SP
			49.8	396.1	RV, SP				55.7	399.3	LV, SP
			49.8	395.6	RV, SP				55.7	376.7	RV, SP
			49.8	394.4	LV, SP				55.7	284.0	LV, SP
			49.8	409.5	RV, SP				55.7	374.0	RV, SP
			49.8	374.5	RV, SP				55.7	371.2	LV, SP
			49.8	397.9	LV, SP				55.7	268.3	LV, SP
		SAB70V.B	49.8	377.5	LV, SP				55.7	271.0	RV, SP
			49.8	424.0	LV, SP				55.7	345.9	LV, SP
			49.8	433.7	LV, SP				55.7	293.3	RV, SP
			49.8	452.4	LV, SP				55.7	324.1	LV, SP
			49.8	443.2	LV, SP				55.7	295.5	LV, SP
			49.8	389.5	LV, SP				55.7	380.1	RV, SP
			49.8	440.4	RV, SP				55.7	300.8	RV, SP
			49.8	405.9	LV, SP				55.7	338.6	LV, SP
			49.8	418.7	RV, SP				55.7	330.1	LV, SP
			49.8	353.4	LV, SP				55.7	282.5	RV, SP
			49.8	395.0	RV, SP				55.7	286.6	LV, SP
			49.8	438.0	LV, SP				55.7	357.5	LV, SP
			49.8	401.1	RV, SP				55.7	306.8	LV, SP

(B)						<i>O. aspinata</i>					
Zone	Subzone	Bed N.	Bed height	Geometric shell size	Shell preservation	Zone	Subzone	Bed N.	Bed height	Geometric shell size	Shell preservation
			49.8	413.2	RV, SP				55.7	324.8	RV, SP
			49.8	388.5	RV, SP				55.7	355.0	RV, SP
			49.8	431.4	RV, SP				55.7	189.5	RV, SP
			49.8	398.3	RV, SP				55.7	222.3	RV, SP
			49.8	408.8	RV, SP				55.7	210.3	RV, SP
			49.8	454.9	LV, SP				55.7	207.6	RV, SP
			49.8	382.5	RV, SP				55.7	278.7	RV, SP
			49.8	425.8	LV, SP				56.65	392.1	RV, SP
			49.8	393.4	RV, SP				56.65	466.8	LV, SP
			49.8	441.5	LV, SP				56.65	387.0	RV, SP
			49.8	401.8	RV, SP				56.65	413.9	RV, SP
			49.8	446.2	LV, SP				56.65	405.7	RV, SP
			49.8	398.6	RV, SP				56.65	412.8	RV, SP
			49.8	443.5	LV, SP				56.65	395.7	LV, SP
			49.8	389.3	RV, SP				56.65	458.5	LV, SP
			49.8	448.4	LV, SP				56.65	418.2	RV, SP
			49.8	445.0	LV, SP				56.65	408.4	RV, SP
			49.8	455.1	LV, SP				56.65	492.3	LV, SP
			49.8	445.1	LV, SP				56.65	426.3	RV, SP
			49.8	415.1	LV, SP				56.65	400.8	RV, SP
			49.8	402.0	RV, SP				56.65	410.8	RV, SP
			49.8	447.1	LV, SP				56.65	454.9	LV, SP
			49.8	394.8	RV, SP				56.65	404.5	RV, SP
			49.8	430.5	LV, SP				56.65	414.5	RV, SP
			49.8	456.0	LV, SP				56.65	405.7	RV, SP
			49.8	405.6	RV, SP				56.65	449.1	LV, SP
			49.8	402.1	RV, SP				56.65	407.4	RV, SP
			49.8	443.2	LV, SP				56.65	424.1	RV, SP
			49.8	466.5	LV, SP				56.65	415.2	LV, SP
			49.8	421.5	LV, SP				56.65	390.1	RV, SP
			49.8	426.6	RV, SP				56.65	465.9	LV, SP
			49.8	431.6	LV, SP				56.65	411.9	RV, SP
			49.8	405.6	RV, SP				56.65	381.7	RV, SP
			49.8	396.8	RV, SP				56.65	390.5	RV, SP
			49.8	427.8	RV, SP				56.65	462.6	LV, SP
			49.8	440.8	LV, SP				56.65	488.0	LV, SP
			49.8	430.5	LV, SP				56.65	472.6	RV, SP
			49.8	419.1	LV, SP				56.65	501.2	LV, SP
			49.8	384.6	RV, SP				56.65	454.3	LV, SP

(B)						<i>O. aspinata</i>					
Zone	Subzone	Bed N.	Bed height	Geometric shell size	Shell preservation	Zone	Subzone	Bed N.	Bed height	Geometric shell size	Shell preservation
			49.8	402.8	RV, SP				56.65	469.3	LV, SP
			49.8	419.5	RV, SP				56.65	455.0	LV, SP
			49.8	424.5	LV, SP				56.65	436.6	LV, SP
			49.8	434.3	RV, SP				56.65	385.1	RV, SP
			49.8	422.6	LV, SP				56.65	454.2	RV, SP
			49.8	449.3	LV, SP				56.65	445.6	LV, SP
			49.8	418.2	RV, SP				56.65	430.2	RV, SP
			49.8	454.4	LV, SP				56.65	467.3	LV, SP
			49.8	439.9	RV, SP				56.65	446.1	LV, SP
			49.8	397.3	LV, SP				56.65	394.6	RV, SP
			49.8	416.2	LV, SP				56.65	455.0	LV, SP
			49.8	408.6	RV, SP				56.65	425.6	RV, SP
			49.8	408.8	RV, SP				56.65	414.5	RV, SP
			49.8	383.2	RV, SP				56.65	418.5	RV, SP
			49.8	418.0	LV, SP				56.65	408.9	RV, SB
			49.8	466.3	LV, SP				56.65	418.6	RV, SP
			49.8	442.6	RV, SP				56.65	485.2	RV, SP
			49.8	408.6	RV, SP				56.65	465.8	LV, SP
			49.8	392.9	RV, SP				56.65	496.1	LV, SP
			49.8	469.3	LV, SP				56.65	397.4	LV, SP
			49.8	425.2	LV, SP				56.65	453.6	RV, SP
			49.8	418.0	LV, SP				56.65	472.3	LV, SP
			49.8	378.9	LV, SP				56.65	466.5	RV, SP
			49.8	451.2	LV, SP				56.65	443.0	LV, SP
			49.8	426.1	RV, SP				56.65	471.7	RV, SP
			49.8	404.0	RV, SP				56.65	466.8	LV, SP
			49.8	432.2	LV, SP				56.65	461.6	LV, SP
			49.8	398.6	RV, SP				56.65	427.9	RV, SP
			49.8	439.2	RV, SP				56.65	329.1	LV, SP
			49.8	432.6	LV, SP				56.65	447.0	LV, SP
			49.8	433.3	LV, SP				56.65	444.7	LV, SP
			49.8	403.9	RV, SP				56.65	465.8	LV, SP
			49.8	454.3	LV, SP				56.65	482.3	LV, SP
			49.8	428.6	LV, SP				56.65	498.8	LV, SP
			49.8	396.5	RV, SP				56.65	469.9	LV, SP
			49.8	440.0	LV, SP				56.65	400.3	LV, SP
			49.8	440.8	RV, SP				56.65	403.8	RV, SP
			49.8	421.1	RV, SP				56.65	422.1	RV, SP
			49.8	419.6	LV, SP				56.65	411.0	LV, SP

(B)						<i>O. aspinata</i>					
Zone	Subzone	Bed N.	Bed height	Geometric shell size	Shell preservation	Zone	Subzone	Bed N.	Bed height	Geometric shell size	Shell preservation
			49.8	442.5	LV, SP				56.65	421.2	RV, SP
			49.8	424.0	LV, SP				56.65	427.8	LV, SP
			49.8	439.1	LV, SP				56.65	439.1	LV, SP
			49.8	437.6	LV, SP				56.65	411.5	RV, SP
			49.8	439.3	RV, SP				56.65	472.2	RV, SP
			49.8	410.6	RV, SP				56.65	408.9	LV, SP
			49.8	441.8	LV, SP				56.65	490.8	LV, SP
			49.8	391.0	RV, SP				56.65	445.3	LV, SP
			49.8	442.0	LV, SP				56.65	408.0	RV, SP
			49.8	456.0	LV, SP				56.65	395.5	RV, SP
			49.8	413.4	RV, SP				56.65	484.4	LV, SP
			49.8	409.6	RV, SP				56.65	455.8	LV, SP
			49.8	388.6	RV, SP				56.65	481.8	LV, SP
			49.8	436.4	LV, SP				56.65	455.6	LV, SP
			49.8	353.2	RV, SP				56.65	384.4	LV, SP
			49.8	381.2	RV, SP				56.65	466.7	LV, SP
			49.8	325.4	RV, SP				56.65	465.2	LV, SP
			49.8	392.8	LV, SP				56.65	469.2	LV, SP
			49.8	305.5	RV, SP				56.65	466.2	LV, SP
			49.8	359.8	LV, SP				56.65	403.3	RV, SP
			49.8	387.3	RV, SP				56.65	411.7	RV, SP
			49.8	364.1	RV, SP				56.65	467.0	LV, SP
			49.8	302.9	RV, SP				56.65	394.9	RV, SP
			49.8	279.1	RV, SP				56.65	419.0	RV, SP
			49.8	361.6	RV, SP				56.65	415.7	RV, SP
			49.8	366.7	RV, SP				56.65	464.3	RV, SP
			49.8	350.1	RV, SP				56.65	443.4	LV, SP
			49.8	226.1	RV, SP				56.65	404.7	RV, SP
			49.8	334.0	RV, SP				56.65	398.3	RV, SP
			49.8	360.2	RV, SP				56.65	455.7	LV, SP
			49.8	345.6	RV, SP				56.65	445.6	LV, SP
			49.8	367.1	RV, SP				56.65	462.0	LV, SP
			49.8	377.2	LV, SP				56.65	412.5	RV, SP
			49.8	306.5	RV, SP				56.65	475.7	LV, SP
			49.8	369.2	RV, SP				56.65	400.4	RV, SP
			49.8	295.8	RV, SP				56.65	456.5	LV, SP
			49.8	362.2	LV, SP				56.65	469.9	RV, SP
			49.8	369.9	RV, SP				56.65	466.7	LV, SP
			49.8	373.8	RV, SP				56.65	461.7	LV, SP

(B)						<i>O. aspinata</i>					
Zone	Subzone	Bed N.	Bed height	Geometric shell size	Shell preservation	Zone	Subzone	Bed N.	Bed height	Geometric shell size	Shell preservation
			49.8	376.1	LV, SP				56.65	464.2	LV, SP
			49.8	352.5	RV, SP				56.65	493.5	LV, SP
			49.8	296.6	LV, SP				56.65	448.8	LV, SP
			49.8	364.7	LV, SP				56.65	471.6	LV, SP
			49.8	395.0	LV, SP				56.65	359.4	RV, SP
			49.8	372.2	RV, SP				56.65	430.9	LV, SP
			49.8	379.8	RV, SP				56.65	393.5	RV, SP
			49.8	323.8	RV, SP				56.65	455.6	LV, SP
			49.8	286.8	RV, SP				56.65	405.9	RV, SP
			49.8	324.5	RV, SP				56.65	465.5	LV, SP
			49.8	371.6	LV, SP				56.65	477.1	LV, SP
			49.8	279.0	RV, SP				56.65	441.6	LV, SP
			49.8	366.7	RV, SP				56.65	460.4	LV, SP
			49.8	377.0	LV, SP				56.65	403.9	RV, SP
			49.8	320.4	LV, SP				56.65	454.6	LV, SP
			49.8	296.4	LV, SP				56.65	410.8	RV, SP
			49.8	342.9	RV, SP				56.65	369.4	RV, SP
			49.8	473.3	RV, SP				56.65	479.4	LV, SP
			49.8	358.7	RV, SP				56.65	380.9	LV, SP
			49.8	359.8	LV, SP				56.65	453.1	LV, SP
			49.8	379.1	RV, SP				56.65	481.2	LV, SP
			49.8	330.6	LV, SP				56.65	445.0	LV, SP
			49.8	322.3	RV, SP				56.65	350.0	RV, SP
			49.8	336.2	RV, SP				56.65	374.7	RV, SB
			49.8	287.9	RV, SP				56.65	401.0	RV, SP
			49.8	252.2	LV, SP				56.65	307.5	LV, SP
			49.8	405.1	LV, SP				56.65	282.6	LV, SP
			49.8	342.4	RV, SP				56.65	384.7	RV, SP
			49.8	279.6	LV, SP				56.65	364.0	RV, SP
			49.8	399.0	RV, SP				56.65	258.5	RV, SP
			49.8	369.5	RV, SP				56.65	361.8	SB
			49.8	398.6	RV, SP				56.65	275.7	RV, SP
			49.8	345.8	RV, SP				56.65	279.1	RV, SP
			49.8	381.3	RV, SP				56.65	376.2	LV, SP
			49.8	362.1	RV, SP				56.65	310.7	RV, SP
			49.8	320.6	RV, SP				56.65	330.9	RV, SP
			49.8	369.2	RV, SP				56.65	314.9	RV, SP
			49.8	394.5	RV, SP				56.65	352.1	LV, SP
			49.8	254.1	RV, SP				56.65	381.0	RV, SP

(B)						<i>O. aspinata</i>					
Zone	Subzone	Bed N.	Bed height	Geometric shell size	Shell preservation	Zone	Subzone	Bed N.	Bed height	Geometric shell size	Shell preservation
			49.8	323.5	RV, SP				56.65	364.2	RV, SP
			49.8	356.9	LV, SP				56.65	376.3	RV, SP
			49.8	373.9	LV, SP				56.65	326.0	RV, SP
			49.8	405.1	LV, SP				56.65	297.5	RV, SP
			49.8	343.7	LV, SP				56.65	370.2	RV, SP
			49.8	362.8	RV, SP				56.65	393.5	LV, SP
			49.8	358.6	LV, SP				56.65	304.4	RV, SP
			49.8	288.4	RV, SP				56.65	286.6	LV, SP
			49.8	385.8	RV, SP				56.65	342.6	RV, SP
			49.8	314.8	RV, SP				56.65	385.3	RV, SP
			49.8	365.1	RV, SP				56.65	373.9	RV, SP
			49.8	325.7	RV, SP				56.65	331.0	RV, SP
			49.8	362.1	LV, SP				56.65	367.9	SB
			49.8	321.6	RV, SP				56.65	368.5	RV, SP
			49.8	323.0	RV, SP				56.65	381.8	RV, SP
			49.8	354.7	RV, SP				56.65	369.4	RV, SP
			49.8	297.9	LV, SP				56.65	372.1	RV, SP
			49.8	263.8	RV, SP				56.65	383.1	RV, SP
			49.8	372.3	RV, SP				56.65	330.4	RV, SP
			49.8	365.6	RV, SP				56.65	411.1	RV, SP
			49.8	308.8	RV, SP				56.65	355.3	RV, SP
			49.8	303.9	RV, SP				56.65	313.2	RV, SP
			49.8	353.6	RV, SP				56.65	366.0	RV, SP
			49.8	318.2	RV, SP				56.65	290.2	RV, SP
			49.8	248.9	RV, SP				56.65	328.8	RV, SP
			49.8	258.4	RV, SP				56.65	382.7	RV, SP
			49.8	271.4	LV, SP				56.65	240.3	RV, SP
			49.8	227.3	RV, SP				56.65	312.3	RV, SP
			49.8	197.0	RV, SP				56.65	279.7	RV, SP
			49.8	261.6	RV, SP				56.65	384.5	RV, SB
			49.8	289.9	RV, SP				56.65	374.0	RV, SP
			49.8	255.6	RV, SP				56.65	282.9	LV, SP
			49.8	268.1	RV, SP				56.65	371.0	SB
			49.8	262.1	RV, SP				56.65	268.3	RV, SP
			49.8	223.6	LV, SP				56.65	330.6	LV, SP
			49.8	278.4	RV, SP				56.65	365.5	RV, SP
			49.8	287.6	RV, SP				56.65	297.5	SB
			49.8	231.6	RV, SP				56.65	387.7	LV, SP
			49.8	244.7	RV, SP				56.65	363.0	RV, SP

(B)						<i>O. aspinata</i>					
Zone	Subzone	Bed N.	Bed height	Geometric shell size	Shell preservation	Zone	Subzone	Bed N.	Bed height	Geometric shell size	Shell preservation
			49.8	285.0	RV, SP				56.65	390.3	RV, SP
			49.8	216.5	LV, SP				56.65	367.0	RV, SP
			49.8	212.1	RV, SP				56.65	288.9	RV, SP
			49.8	244.9	RV, SP				56.65	269.1	RV, SP
			49.8	241.6	RV, SP				56.65	366.0	SB
			49.8	278.9	RV, SP				56.65	367.1	RV, SP
			49.8	349.0	RV, SP				56.65	331.3	LV, SP
			49.8	247.8	RV, SP				56.65	269.5	LV, SP
			49.8	245.1	LV, SP				56.65	308.1	RV, SP
			49.8	214.6	LV, SP				56.65	321.7	LV, SP
									56.65	340.4	RV, SP
									56.65	187.7	LV, SP
									56.65	261.4	RV, SP
									56.65	209.0	RV, SP
									56.65	276.8	RV, SP
									56.65	261.1	RV, SB
									56.65	257.6	RV, SP
									56.65	230.7	RV, SP

(C)																	
<i>O. aspinata</i>																	
Zone	Subzone	Bed N.	Bed H.	Geometric shell size	Shell pres.	Zone	Subzone	Bed N.	Bed H.	Geometric shell size	Shell pres.	Zone	Subzone	Bed N.	Bed H.	Geometric shell size	Shell pres.
liasicus Zone	Alsatites laqueus subzone	SAB 86	56.95	418.5	RV, SP	liasicus Zone	Alsatites laqueus subzone	SAB 90	57.3	386.7	LV, SP	angulata Zone	Schlotheimia angulata subzone	SAB 94	59.85	430.7	RV, SP
			56.95	393.1	LV, SP				57.3	437.2	LV, SP				59.85	403.3	RV, SP
			56.95	500.0	RV, SP				57.3	531.8	RV, SP				59.85	449.9	LV, SP
			56.95	407.6	RV, SP				57.3	420.5	RV, SP				59.85	434.6	LV, SP
			56.95	482.2	LV, SP				57.3	530.2	LV, SP				59.85	489.2	RV, SP
			56.95	482.5	LV, SP				57.3	538.4	RV, SP				59.85	505.2	RV, SP
			56.95	480.8	LV, SP				57.3	523.7	RV, SP				59.85	528.6	LV, SP
			56.95	481.6	LV, SP				57.3	394.7	RV, SP				59.85	389.1	RV, SP
			56.95	431.1	RV, SP				57.3	384.8	LV, SP				59.85	469.4	RV, SP
			56.95	465.8	LV, SP				57.3	442.7	LV, SP				59.85	378.4	LV, SP
			56.95	555.7	LV, SP				57.3	375.2	LV, SP				59.85	474.8	RV, SP
			56.95	390.2	LV, SP				57.3	454.1	RV, SP				59.85	471.9	LV, SP
			56.95	471.6	RV, SP				57.3	422.4	LV, SP				59.85	486.0	RV, SP
			56.95	364.5	RV, SB				57.3	374.3	RV, SP				59.85	433.9	RV, SP
			56.95	432.9	RV, SP				57.3	424.2	LV, SP				59.85	391.2	LV, SP

(C)						<i>O. aspinata</i>											
Zone	Subzone	Bed N.	Bed H.	Geometric shell size	Shell pres.	Zone	Subzone	Bed N.	Bed H.	Geometric shell size	Shell pres.	Zone	Subzone	Bed N.	Bed H.	Geometric shell size	Shell pres.
			56.95	407.6	RV, SP				57.3	392.1	RV, SP				59.85	444.1	LV, SP
			56.95	399.5	SB				57.3	441.7	RV, SP				59.85	381.4	LV, SP
			56.95	401.1	RV, SP				57.3	380.0	RV, SP				59.85	484.4	LV, SP
			56.95	384.9	RV, SP				57.3	475.1	RV, SP				59.85	428.8	RV, SP
			56.95	401.3	RV, SP				57.3	441.1	RV, SP				59.85	419.1	LV, SP
			56.95	408.2	RV, SP				57.3	461.4	RV, SP				59.85	500.5	LV, SP
			56.95	400.7	LV, SP				57.3	365.2	RV, SP				59.85	448.5	LV, SP
			56.95	380.4	RV, SP				57.3	425.3	LV, SP				59.85	449.9	LV, SP
			56.95	468.5	RV, SP				57.3	399.5	RV, SP				59.85	378.1	RV, SP
			56.95	401.6	RV, SP				57.3	451.2	RV, SP				59.85	431.1	LV, SP
			56.95	413.1	RV, SP				57.3	474.4	LV, SP				59.85	495.2	LV, SP
			56.95	420.8	RV, SP				57.3	376.1	RV, SP				59.85	388.5	RV, SP
			56.95	503.4	LV, SP				57.3	532.1	RV, SP				59.85	410.2	RV, SP
			56.95	415.0	RV, SP				57.3	444.7	RV, SP				59.85	535.5	RV, SP
			56.95	397.8	LV, SP				57.3	549.8	RV, SP				59.85	450.6	LV, SP
			56.95	488.8	LV, SP				57.3	382.7	LV, SP				59.85	559.3	RV, SP
			56.95	430.5	RV, SP				57.3	411.0	RV, SP				59.85	425.1	SB
			56.95	388.6	LV, SP				57.3	486.4	RV, SP				59.85	392.4	RV, SP
			56.95	412.0	RV, SP				57.3	379.4	RV, SP				59.85	375.6	LV, SP
			56.95	382.8	LV, SP				57.3	435.9	LV, SP				59.85	494.9	LV, SP
			56.95	420.8	RV, SP				57.3	382.2	RV, SP				59.85	384.8	RV, SP
			56.95	436.5	LV, SP				57.3	548.6	RV, SP				59.85	407.6	RV, SP
			56.95	406.7	LV, SP				57.3	554.4	RV, SP				59.85	545.9	LV, SP
			56.95	425.5	RV, SP				57.3	427.0	RV, SP				59.85	464.1	LV, SP
			56.95	406.3	RV, SP				57.3	499.5	LV, SP				59.85	433.4	LV, SP
			56.95	375.0	RV, SP				57.3	442.3	LV, SP				59.85	413.4	LV, SP
			56.95	404.8	RV, SP				57.3	555.2	RV, SP				59.85	465.7	RV, SP
			56.95	404.3	RV, SP				57.3	456.9	LV, SP				59.85	435.4	LV, SP
			56.95	435.7	LV, SP				57.3	451.5	LV, SP				59.85	496.9	LV, SP
			56.95	419.3	LV, SP				57.3	490.7	RV, SP				59.85	425.9	LV, SP
			56.95	485.8	LV, SP				57.3	428.8	LV, SP				59.85	616.2	RV, SP
			56.95	395.8	RV, SP				57.3	505.6	LV, SP				59.85	572.8	RV, SP
			56.95	398.4	LV, SP				57.3	489.9	LV, SP				59.85	443.6	LV, SP
			56.95	393.5	LV, SP				57.3	366.8	RV, SP				59.85	386.0	RV, SP
			56.95	486.7	LV, SP				57.3	504.8	RV, SP				59.85	549.6	RV, SP
			56.95	415.9	RV, SP				57.3	405.0	RV, SP				59.85	383.1	RV, SP
			56.95	419.9	RV, SP				57.3	394.4	LV, SP				59.85	385.7	LV, SP
			56.95	428.3	RV, SP				57.3	377.6	RV, SP				59.85	495.9	LV, SP
			56.95	429.7	LV, SP				57.3	455.0	LV, SP				59.85	469.2	RV, SP

(C)						<i>O. aspinata</i>											
Zone	Subzone	Bed N.	Bed H.	Geometric shell size	Shell pres.	Zone	Subzone	Bed N.	Bed H.	Geometric shell size	Shell pres.	Zone	Subzone	Bed N.	Bed H.	Geometric shell size	Shell pres.
			56.95	473.4	LV, SP				57.3	475.2	LV, SP				59.85	388.4	RV, SP
			56.95	486.0	SB				57.3	458.6	RV, SP				59.85	557.6	RV, SP
			56.95	432.6	LV, SP				57.3	383.7	RV, SP				59.85	516.8	RV, SP
			56.95	497.9	LV, SP				57.3	442.1	RV, SP				59.85	429.0	RV, SP
			56.95	405.2	LV, SP				57.3	454.1	RV, SP				59.85	384.0	RV, SP
			56.95	470.1	LV, SP				57.3	442.5	LV, SP				59.85	439.8	RV, SP
			56.95	405.4	RV, SP				57.3	520.8	LV, SP				59.85	386.6	RV, SP
			56.95	401.1	RV, SP				57.3	524.7	RV, SP				59.85	479.6	RV, SP
			56.95	423.7	LV, SP				57.3	454.8	LV, SP				59.85	442.9	RV, SP
			56.95	506.4	LV, SP				57.3	378.5	RV, SP				59.85	523.8	RV, SP
			56.95	386.8	RV, SP				57.3	390.7	RV, SP				59.85	424.8	RV, SP
			56.95	418.2	LV, SP				57.3	438.2	LV, SP				59.85	435.9	LV, SP
			56.95	462.2	RV, SP				57.3	434.8	LV, SP				59.85	463.7	LV, SP
			56.95	430.0	RV, SP				57.3	499.4	LV, SP				59.85	532.5	RV, SP
			56.95	484.7	LV, SP				57.3	488.2	LV, SP				59.85	372.9	LV, SP
			56.95	483.8	RV, SP				57.3	358.3	LV, SP				59.85	386.6	RV, SP
			56.95	379.5	LV, SP				57.3	420.0	LV, SP				59.85	438.2	LV, SP
			56.95	480.4	LV, SP				57.3	379.2	LV, SP				59.85	407.0	RV, SP
			56.95	400.5	LV, SP				57.3	390.5	RV, SP				59.85	565.0	LV, SP
			56.95	472.3	LV, SP				57.3	548.6	RV, SP				59.85	379.8	RV, SP
			56.95	468.9	LV, SP				57.3	425.6	RV, SP				59.85	523.4	RV, SP
			56.95	393.7	RV, SP				57.3	507.6	RV, SP				59.85	454.5	RV, SP
			56.95	475.3	LV, SP				57.3	459.7	RV, SP				59.85	386.9	RV, SP
			56.95	399.7	LV, SP				57.3	463.1	LV, SP				59.85	447.0	LV, SP
			56.95	452.4	RV, SP				57.3	450.3	RV, SP				59.85	489.1	LV, SP
			56.95	433.8	RV, SP				57.3	494.3	LV, SP				59.85	402.7	RV, SP
			56.95	406.1	RV, SP				57.3	395.1	RV, SP				59.85	506.0	LV, SP
			56.95	463.2	LV, SP				57.3	422.2	RV, SP				59.85	472.4	RV, SP
			56.95	392.6	LV, SP				57.3	444.8	LV, SP				59.85	506.2	LV, SP
			56.95	370.7	RV, SP				57.3	404.2	RV, SP				59.85	357.8	RV, SP
			56.95	354.3	RV, SP				57.3	437.8	LV, SP				59.85	547.7	RV, SP
			56.95	468.9	LV, SP				57.3	484.0	LV, SP				59.85	460.3	RV, SP
			56.95	420.4	RV, SP				57.3	373.3	LV, SP				59.85	509.6	LV, SP
			56.95	396.1	RV, SP				57.3	520.3	RV, SP				59.85	453.1	RV, SP
			56.95	438.1	RV, SP				57.3	389.7	RV, SP				59.85	373.3	RV, SP
			56.95	496.6	RV, SP				57.3	378.4	RV, SP				59.85	472.2	RV, SP
			56.95	350.8	RV, SP				57.3	450.5	RV, SP				59.85	442.4	LV, SP
			56.95	389.5	LV, SP				57.3	453.9	LV, SP				59.85	436.6	LV, SP
			56.95	407.9	SB				57.3	526.9	RV, SP				59.85	393.5	RV, SP

(C)						<i>O. aspinata</i>											
Zone	Subzone	Bed N.	Bed H.	Geometric shell size	Shell pres.	Zone	Subzone	Bed N.	Bed H.	Geometric shell size	Shell pres.	Zone	Subzone	Bed N.	Bed H.	Geometric shell size	Shell pres.
			56.95	389.5	RV, SP				57.3	436.4	RV, SP				59.85	452.1	RV, SP
			56.95	385.1	RV, SP				57.3	449.9	LV, SP				59.85	359.7	RV, SP
			56.95	405.2	LV, SP				57.3	355.8	LV, SP				59.85	395.2	RV, SP
			56.95	400.8	RV, SP				57.3	378.9	RV, SP				59.85	517.9	LV, SP
			56.95	394.0	RV, SP				57.3	448.7	RV, SP				59.85	511.0	LV, SP
			56.95	399.8	RV, SP				57.3	411.7	LV, SP				59.85	493.3	LV, SP
			56.95	419.4	LV, SP				57.3	434.7	RV, SP				59.85	378.4	RV, SP
			56.95	316.3	RV, SP				57.3	368.3	LV, SP				59.85	375.6	RV, SP
			56.95	329.4	RV, SP				57.3	482.8	LV, SP				59.85	400.2	RV, SP
			56.95	318.9	RV, SP				57.3	503.0	RV, SP				59.85	431.8	LV, SP
			56.95	369.0	RV, SP				57.3	437.0	LV, SP				59.85	434.7	RV, SP
			56.95	283.5	RV, SP				57.3	436.4	RV, SP				59.85	533.7	RV, SP
			56.95	255.6	LV, SP				57.3	472.0	RV, SP				59.85	524.4	RV, SP
			56.95	287.6	LV, SP				57.3	554.9	RV, SP				59.85	457.6	RV, SP
			56.95	315.6	LV, SP				57.3	377.6	LV, SP				59.85	494.0	LV, SP
			56.95	375.2	RV, SP				57.3	468.2	LV, SP				59.85	451.5	RV, SP
			56.95	323.0	RV, SP				57.3	370.2	LV, SP				59.85	504.3	LV, SP
			56.95	287.1	RV, SP				57.3	442.3	RV, SP				59.85	481.4	LV, SP
			56.95	353.8	LV, SP				57.3	394.0	LV, SP				59.85	558.3	LV, SP
			56.95	334.5	RV, SP				57.3	390.8	RV, SP				59.85	407.9	LV, SP
			56.95	369.8	RV, SP				57.3	412.5	LV, SP				59.85	384.9	RV, SP
			56.95	369.1	RV, SP				57.3	466.8	LV, SP				59.85	434.8	LV, SP
			56.95	346.1	RV, SP				57.3	466.2	LV, SP				59.85	399.8	RV, SP
			56.95	331.0	RV, SP				57.3	368.1	LV, SP				59.85	508.7	LV, SP
			56.95	327.8	RV, SP				57.3	453.1	RV, SP				59.85	490.0	RV, SP
			56.95	309.9	RV, SP				57.3	467.5	LV, SP				59.85	454.6	LV, SP
			56.95	390.6	RV, SP				57.3	372.4	LV, SP				59.85	479.8	RV, SP
			56.95	306.6	RV, SP				57.3	397.4	RV, SP				59.85	419.5	LV, SP
			56.95	291.9	RV, SP				57.3	398.2	RV, SP				59.85	391.4	LV, SP
			56.95	307.8	LV, SP				57.3	446.0	LV, SP				59.85	550.5	RV, SP
			56.95	335.1	RV, SP				57.3	345.2	RV, SP				59.85	261.2	RV, SP
			56.95	367.2	RV, SP				57.3	472.6	LV, SP				59.85	396.8	RV, SP
			56.95	308.2	RV, SP				57.3	468.3	RV, SP				59.85	329.2	LV, SP
			56.95	322.2	RV, SP				57.3	426.9	RV, SP				59.85	519.6	LV, SP
			56.95	368.6	RV, SP				57.3	438.2	RV, SP				59.85	428.0	LV, SP
			56.95	325.4	RV, SP				57.3	364.9	RV, SP				59.85	452.2	LV, SP
			56.95	271.9	RV, SP				57.3	470.0	LV, SP				59.85	440.5	LV, SP
			56.95	319.1	RV, SP				57.3	463.5	RV, SP				59.85	431.0	RV, SP
			56.95	314.7	RV, SP				57.3	523.2	LV, SP				59.85	368.5	LV, SP

(C)						<i>O. aspinata</i>											
Zone	Subzone	Bed N.	Bed H.	Geometric shell size	Shell pres.	Zone	Subzone	Bed N.	Bed H.	Geometric shell size	Shell pres.	Zone	Subzone	Bed N.	Bed H.	Geometric shell size	Shell pres.
			56.95	329.2	RV, SP				57.3	371.1	LV, SP				59.85	444.0	LV, SP
			56.95	286.7	RV, SP				57.3	392.0	RV, SP				59.85	542.5	RV, SP
			56.95	270.9	RV, SP				57.3	459.3	LV, SP				59.85	432.3	LV, SP
			56.95	250.6	RV, SP				57.3	472.0	RV, SP				59.85	382.8	RV, SP
			56.95	374.1	RV, SP				57.3	461.7	RV, SP				59.85	466.7	RV, SP
			56.95	318.8	LV, SP				57.3	449.6	LV, SP				59.85	498.5	LV, SP
			56.95	312.6	LV, SP				57.3	550.9	RV, SP				59.85	393.4	RV, SP
			56.95	325.9	RV, SP				57.3	450.4	RV, SP				59.85	436.4	RV, SP
			56.95	343.1	RV, SP				57.3	464.7	LV, SP				59.85	440.7	LV, SP
			56.95	308.9	RV, SP				57.3	362.9	RV, SP				59.85	469.6	RV, SP
			56.95	335.1	LV, SP				57.3	378.9	RV, SP				59.85	511.7	RV, SP
			56.95	356.1	LV, SP				57.3	365.2	LV, SP				59.85	406.4	SB
			56.95	321.2	LV, SP				57.3	423.8	RV, SP				59.85	390.6	RV, SP
			56.95	299.1	RV, SP				57.3	393.9	RV, SP				59.85	451.6	LV, SP
			56.95	294.7	RV, SP				57.3	510.6	RV, SP				59.85	454.6	RV, SP
			56.95	287.9	RV, SP				57.3	385.7	RV, SP				59.85	372.7	LV, SP
			56.95	307.5	RV, SP				57.3	429.2	RV, SP				59.85	508.1	LV, SP
			56.95	275.3	LV, SP				57.3	441.1	LV, SP				59.85	420.1	LV, SP
			56.95	282.5	LV, SP				57.3	436.0	RV, SP				59.85	387.3	RV, SP
			56.95	281.8	SB				57.3	429.2	LV, SP				59.85	479.4	RV, SP
			56.95	271.5	SB				57.3	480.5	LV, SP				59.85	554.6	RV, SP
			56.95	331.7	RV, SP				57.3	459.5	LV, SP				59.85	362.3	LV, SP
			56.95	365.9	RV, SP				57.3	448.2	LV, SP				59.85	316.9	RV, SP
			56.95	319.4	LV, SP				57.3	462.3	RV, SP				59.85	312.6	LV, SP
			56.95	317.6	RV, SP				57.3	422.2	LV, SP				59.85	321.9	RV, SP
			56.95	282.4	RV, SP				57.3	370.6	LV, SP				59.85	258.3	LV, SP
			56.95	274.6	RV, SP				57.3	386.0	LV, SP				59.85	328.4	LV, SP
			56.95	316.0	RV, SP				57.3	395.6	RV, SP				59.85	314.1	LV, SP
			56.95	259.2	SB				57.3	389.6	LV, SP				59.85	328.5	LV, SP
			56.95	257.9	RV, SP				57.3	429.7	RV, SP				59.85	365.1	LV, SP
			56.95	320.3	RV, SP				57.3	363.8	LV, SP				59.85	283.5	LV, SP
			56.95	299.4	RV, SP				57.3	459.0	LV, SP				59.85	319.5	RV, SP
			56.95	268.2	LV, SP				57.3	400.6	RV, SP				59.85	315.4	RV, SP
			56.95	348.3	RV, SP				57.3	391.5	RV, SP				59.85	371.4	RV, SP
			56.95	328.8	LV, SP				57.3	443.3	LV, SP				59.85	381.1	LV, SP
			56.95	303.5	LV, SP				57.3	467.1	LV, SP				59.85	272.0	LV, SP
			56.95	286.5	LV, SP				57.3	511.5	RV, SP				59.85	304.9	LV, SP
			56.95	277.0	LV, SP				57.3	556.0	RV, SP				59.85	270.2	RV, SP
			56.95	298.3	SB				57.3	453.0	RV, SP				59.85	267.6	RV, SP

(C)						<i>O. aspinata</i>											
Zone	Subzone	Bed N.	Bed H.	Geometric shell size	Shell pres.	Zone	Subzone	Bed N.	Bed H.	Geometric shell size	Shell pres.	Zone	Subzone	Bed N.	Bed H.	Geometric shell size	Shell pres.
			56.95	351.9	RV, SP				57.3	431.5	RV, SP				59.85	260.1	LV, SP
			56.95	265.2	RV, SP				57.3	486.7	RV, SP				59.85	316.5	LV, SP
			56.95	335.9	RV, SP				57.3	491.9	RV, SP				59.85	315.5	LV, SP
			56.95	285.8	RV, SP				57.3	478.0	RV, SP				59.85	316.0	RV, SP
			56.95	375.9	RV, SP				57.3	552.1	RV, SP				59.85	303.4	LV, SP
			56.95	298.4	RV, SP				57.3	426.4	LV, SP				59.85	315.3	RV, SP
			56.95	213.3	LV, SP				57.3	385.6	RV, SP				59.85	379.4	LV, SP
			56.95	200.6	RV, SP				57.3	447.5	RV, SP				59.85	290.1	LV, SP
			56.95	175.0	LV, SP				57.3	381.1	LV, SP				59.85	306.9	LV, SP
			57.2	460.0	LV, SP				57.3	532.5	LV, SP				59.85	273.0	RV, SP
			57.2	383.8	RV, SP				57.3	424.8	LV, SP				59.85	358.8	RV, SP
			57.2	453.8	LV, SP				57.3	447.8	RV, SP				59.85	265.8	LV, SP
			57.2	444.0	LV, SP				57.3	367.2	RV, SP				59.85	269.9	LV, SP
			57.2	377.4	RV, SP				57.3	386.8	RV, SP				59.85	319.6	RV, SP
			57.2	470.5	RV, SP				57.3	543.8	RV, SP				59.85	337.2	RV, SP
			57.2	470.4	LV, SP				57.3	418.7	RV, SP				59.85	293.5	RV, SP
			57.2	386.6	RV, SP				57.3	437.5	LV, SP				59.85	323.8	RV, SP
			57.2	504.6	LV, SP				57.3	461.6	RV, SP				59.85	313.8	LV, SP
			57.2	445.8	RV, SP				57.3	494.6	RV, SP				59.85	272.7	RV, SP
			57.2	395.4	RV, SP				57.3	371.9	LV, SP				59.85	313.8	RV, SP
			57.2	367.5	RV, SP				57.3	428.5	RV, SP				59.85	266.6	RV, SP
			57.2	401.3	RV, SP				57.3	371.4	RV, SP				59.85	279.9	RV, SP
			57.2	391.0	RV, SP				57.3	364.8	RV, SP				59.85	380.9	RV, SP
		SAB8	57.2	400.2	RV, SP				57.3	242.0	RV, SP				59.85	266.5	LV, SP
		8	57.2	405.0	RV, SP				57.3	309.2	LV, SP				59.85	388.7	RV, SP
			57.2	398.0	RV, SP				57.3	347.5	RV, SP				59.85	270.0	LV, SP
			57.2	403.5	RV, SP				57.3	319.5	LV, SP				59.85	278.9	LV, SB
			57.2	461.5	LV, SP				57.3	272.6	LV, SP				59.85	374.4	LV, SP
			57.2	462.9	LV, SP				57.3	249.8	LV, SP				59.85	373.7	LV, SP
			57.2	430.1	RV, SP				57.3	255.6	LV, SP				59.85	345.0	RV, SP
			57.2	483.7	LV, SP				57.3	330.3	LV, SP				59.85	318.6	RV, SP
			57.2	396.3	RV, SP				57.3	370.7	RV, SP				59.85	293.0	LV, SP
			57.2	409.6	RV, SP				57.3	307.8	LV, SP				59.85	278.7	RV, SP
			57.2	455.5	LV, SP				57.3	306.8	LV, SP				59.85	329.1	RV, SP
			57.2	390.5	RV, SP				57.3	293.8	LV, SP				59.85	268.1	LV, SP
			57.2	396.5	RV, SP				57.3	302.7	LV, SP				59.85	267.0	LV, SP
			57.2	430.3	RV, SP				57.3	319.2	RV, SP				59.85	273.9	RV, SP
			57.2	389.8	RV, SP				57.3	356.1	LV, SP				59.85	313.2	LV, SP
			57.2	384.4	RV, SP				57.3	257.3	RV, SP				59.85	389.2	RV, SP

(C)						<i>O. aspinata</i>											
Zone	Subzone	Bed N.	Bed H.	Geometric shell size	Shell pres.	Zone	Subzone	Bed N.	Bed H.	Geometric shell size	Shell pres.	Zone	Subzone	Bed N.	Bed H.	Geometric shell size	Shell pres.
			57.2	456.2	LV, SP				57.3	356.4	RV, SP				59.85	280.0	RV, SP
			57.2	386.6	RV, SP				57.3	364.4	LV, SP				59.85	268.3	LV, SP
			57.2	476.6	LV, SP				57.3	306.0	RV, SP				59.85	308.7	LV, SP
			57.2	386.7	RV, SP				57.3	347.3	LV, SP				59.85	286.0	LV, SP
			57.2	386.7	RV, SP				57.3	369.4	RV, SP				59.85	277.4	RV, SP
			57.2	460.9	RV, SP				57.3	315.5	LV, SP				59.85	310.2	LV, SP
			57.2	461.9	LV, SP				57.3	375.4	RV, SP				59.85	313.4	RV, SP
			57.2	395.5	LV, SP				57.3	319.7	RV, SP				59.85	270.7	RV, SP
			57.2	389.7	RV, SP				57.3	353.8	RV, SP				59.85	275.0	LV, SP
			57.2	462.1	LV, SP				57.3	275.9	RV, SP				59.85	277.3	RV, SP
			57.2	389.1	RV, SP				57.3	267.3	RV, SP				59.85	376.2	RV, SP
			57.2	367.0	LV, SP				57.3	314.6	LV, SP				59.85	293.4	RV, SP
			57.2	421.5	SB				57.3	320.6	RV, SP				59.85	311.4	LV, SP
			57.2	385.2	RV, SP				57.3	365.4	RV, SP				59.85	309.8	LV, SP
			57.2	393.9	RV, SP				57.3	269.7	LV, SP				59.85	280.3	RV, SP
			57.2	372.7	LV, SP				57.3	257.6	LV, SP				59.85	279.4	RV, SP
			57.2	404.4	RV, SP				57.3	318.9	LV, SP				59.85	284.1	RV, SP
			57.2	384.7	RV, SP				57.3	308.0	RV, SP				59.85	276.3	RV, SP
			57.2	396.8	RV, SP				57.3	305.5	LV, SP				59.85	378.5	LV, SP
			57.2	461.4	LV, SP				57.3	400.9	LV, SP				59.85	306.0	RV, SP
			57.2	472.4	LV, SP				57.3	297.1	RV, SP				59.85	376.3	LV, SP
			57.2	396.2	RV, SP				57.3	251.3	LV, SP				59.85	280.9	RV, SP
			57.2	407.3	RV, SP				57.3	251.0	LV, SP				59.85	323.8	RV, SP
			57.2	388.3	RV, SP				57.3	312.8	LV, SP				59.85	263.1	RV, SP
			57.2	458.7	LV, SP				57.3	373.1	LV, SP				59.85	322.6	LV, SP
			57.2	386.9	RV, SP				57.3	354.5	RV, SP				59.85	252.0	LV, SP
			57.2	463.2	LV, SP				57.3	362.7	RV, SP				59.85	274.0	RV, SP
			57.2	391.8	LV, SP				57.3	328.0	RV, SP				59.85	323.4	RV, SP
			57.2	457.6	LV, SP				57.3	336.3	LV, SP				59.85	280.9	LV, SP
			57.2	452.3	LV, SP				57.3	314.8	RV, SP				59.85	308.7	LV, SP
			57.2	274.8	LV, SP				57.3	300.4	LV, SP				59.85	319.2	LV, SP
			57.2	283.3	LV, SP				57.3	305.9	RV, SP				59.85	279.2	RV, SP
			57.2	320.9	SB				57.3	267.6	RV, SP				59.85	331.2	RV, SP
			57.2	331.9	RV, SP				57.3	322.3	LV, SP				59.85	284.3	RV, SP
			57.2	301.2	RV, SP				57.3	365.1	LV, SP				59.85	261.4	LV, SP
			57.2	388.3	RV, SP				57.3	267.2	LV, SP				59.85	265.9	LV, SP
			57.2	371.2	RV, SP				57.3	282.9	LV, SP				59.85	300.8	LV, SP
			57.2	384.5	LV, SP				57.3	294.6	LV, SP				59.85	273.6	RV, SP
			57.2	348.8	LV, SP				57.3	322.5	LV, SP				59.85	316.0	RV, SP

(C)						<i>O. aspinata</i>											
Zone	Subzone	Bed N.	Bed H.	Geometric shell size	Shell pres.	Zone	Subzone	Bed N.	Bed H.	Geometric shell size	Shell pres.	Zone	Subzone	Bed N.	Bed H.	Geometric shell size	Shell pres.
			57.2	310.5	LV, SP				57.3	310.9	RV, SP				59.85	258.9	LV, SP
			57.2	381.1	RV, SP				57.3	356.2	LV, SP				59.85	338.2	LV, SP
			57.2	308.7	LV, SP				57.3	324.0	LV, SP				59.85	449.9	RV, SP
			57.2	258.3	RV, SP				57.3	382.5	RV, SP				59.85	370.0	RV, SP
			57.2	372.9	RV, SP				57.3	324.1	RV, SP				59.85	296.1	LV, SP
			57.2	264.0	LV, SP				57.3	302.4	LV, SP				59.85	309.1	LV, SP
			57.2	373.2	LV, SP				57.3	396.2	RV, SP				59.85	325.6	RV, SP
			57.2	394.6	LV, SP				57.3	258.6	LV, SP				59.85	373.3	LV, SP
			57.2	364.7	RV, SP				57.3	272.4	RV, SP				59.85	269.9	RV, SP
			57.2	349.2	RV, SP				57.3	266.5	LV, SP				59.85	253.1	LV, SP
			57.2	365.4	RV, SP				57.3	310.9	RV, SP				59.85	322.7	RV, SP
			57.2	362.0	RV, SP				57.3	362.4	LV, SP				59.85	382.3	RV, SP
			57.2	319.1	RV, SP				57.3	241.5	LV, SP				59.85	249.5	LV, SP
			57.2	313.6	RV, SP				57.3	186.6	RV, SP				59.85	332.7	LV, SP
			57.2	275.4	LV, SP				57.3	250.1	LV, SP				59.85	276.3	RV, SP
			57.2	266.8	LV, SP				57.3	193.7	RV, SP				59.85	308.2	RV, SP
			57.2	328.1	RV, SP				57.3	194.0	RV, SP				59.85	274.6	RV, SP
			57.2	289.8	LV, SP				57.3	205.2	RV, SP				59.85	283.7	RV, SP
			57.2	322.0	SB				57.3	196.4	RV, SP				59.85	333.5	RV, SP
			57.2	370.5	RV, SP				57.3	265.5	RV, SP				59.85	272.6	RV, SP
			57.2	374.6	RV, SP				57.3	220.7	RV, SP				59.85	270.6	LV, SP
			57.2	351.1	RV, SP				57.3	257.9	LV, SP				59.85	363.4	LV, SP
			57.2	288.2	RV, SP				57.3	182.5	RV, SP				59.85	276.1	RV, SP
			57.2	284.9	RV, SP				57.3	181.8	LV, SP				59.85	207.5	RV, SP
			57.2	317.9	LV, SP				57.3	224.2	RV, SP				59.85	304.1	LV, SP
			57.2	329.3	RV, SP				57.3	222.1	LV, SP				59.85	373.5	LV, SP
			57.2	271.3	LV, SP				57.3	229.5	RV, SP				59.85	325.1	RV, SP
			57.2	357.9	RV, SP				57.3	197.6	RV, SP				59.85	265.8	RV, SP
			57.2	255.1	RV, SP				57.3	217.1	RV, SP				59.85	336.6	RV, SP
			57.2	451.0	LV, SP				57.3	220.4	LV, SP				59.85	325.4	RV, SP
									57.3	218.5	LV, SP				59.85	340.5	RV, SP
									57.3	224.4	RV, SP				59.85	277.5	LV, SP
									57.3	221.9	RV, SP				59.85	322.8	LV, SP
									57.3	233.6	RV, SP				59.85	319.6	LV, SP
									57.3	233.7	LV, SP				59.85	257.2	LV, SP
									57.3	179.9	RV, SP				59.85	336.1	RV, SP
									57.3	229.5	LV, SP				59.85	300.2	RV, SP
									57.3	232.1	RV, SP				59.85	204.3	RV, SP
									57.3	229.5	LV, SP				59.85	199.1	LV, SP

(C)						<i>O. aspinata</i>											
Zone	Subzone	Bed N.	Bed H.	Geometric shell size	Shell pres.	Zone	Subzone	Bed N.	Bed H.	Geometric shell size	Shell pres.	Zone	Subzone	Bed N.	Bed H.	Geometric shell size	Shell pres.
									57.3	233.9	RV, SP				59.85	187.5	LV, SP
									57.3	216.1	LV, SP				59.85	198.0	LV, SP
															59.85	217.7	LV, SP
															59.85	229.7	RV, SP
															59.85	185.7	LV, SP
															59.85	225.6	LV, SP
															59.85	232.0	RV, SP
															59.85	198.6	RV, SP
															59.85	240.1	RV, SP
															59.85	253.2	LV, SP
															59.85	227.2	LV, SP
															59.85	237.9	RV, SP
															59.85	203.1	RV, SP
															59.85	196.5	LV, SP
															59.85	200.5	LV, SP
															59.85	235.6	RV, SP
															59.85	233.6	LV, SP
															59.85	182.3	RV, SP
															59.85	221.4	LV, SP
															59.85	187.7	LV, SP
															59.85	194.4	RV, SP
															59.85	215.7	RV, SP
															59.85	202.2	RV, SP
															59.85	238.6	RV, SP
															59.85	259.0	LV, SP
															59.85	233.7	LV, SP
															59.85	189.4	LV, SP
															59.85	186.2	LV, SP
															59.85	237.4	LV, SP
															59.85	228.5	RV, SP
															59.85	216.2	RV, SP
															59.85	235.8	RV, SP
															59.85	285.8	RV, SP
															61.8	441.3	RV, SP
															61.8	507.6	LV, SP
															61.8	404.4	RV, SP
															61.8	438.1	RV, SP
															61.8	441.7	RV, SP
															61.8	423.0	LV, SP

(C)	<i>O. aspinata</i>																	
Zone	Subzone	Bed N.	Bed H.	Geometric shell size	Shell pres.	Zone	Subzone	Bed N.	Bed H.	Geometric shell size	Shell pres.	Zone	Subzone	Bed N.	Bed H.	Geometric shell size	Shell pres.	
																61.8	420.3	LV, SP
																61.8	482.9	LV, SP
																61.8	488.1	LV, SP
																61.8	481.9	LV, SP
																61.8	400.8	RV, SP
																61.8	372.5	RV, SP
																61.8	498.5	RV, SP
																61.8	411.2	LV, SP
																61.8	476.9	LV, SP
																61.8	390.2	RV, SP
																61.8	272.0	LV, SP
																61.8	326.4	RV, SP
																61.8	275.7	SB
																61.8	442.9	SB
																61.8	306.0	RV, SP
																61.8	278.0	RV, SP
																61.8	382.5	RV, SP
																61.8	296.2	RV, SP
																61.8	312.7	SB
																61.8	320.0	LV, SP
																62.5	419.4	RV, SP
																62.5	398.6	RV, SP
																62.5	346.4	LV, SP
																62.5	304.1	RV, SP
																62.5	269.7	RV, SP
																62.5	282.8	RV, SP
																62.5	331.0	RV, SP
																62.5	322.5	RV, SP
																62.5	291.0	RV, SP
																62.5	324.6	RV, SP
																62.5	340.2	RV, SP
																62.5	274.9	LV, SP
																62.5	283.1	LV, SP
																62.5	283.8	RV, SP
																62.5	331.2	LV, SP
																62.5	284.3	SB

Table A4.24 A-B: *O. aspinata* shell thickness data from every individual per bed in St Audrie's Bay with the corresponding stratigraphic zones, subzones and bed height (Presented in Section 3.5.5) (measured in μm).

(A)		<i>O. aspinata</i>															
Zone	Subzone	Bed N.	Bed H.	Shell thickness	Shell pres.	Zone	Subzone	Bed N.	Bed H.	Shell thickness	Shell pres.	Zone	Subzone	Bed N.	Bed H.	Shell thickness	Shell pres.
Lilstock F.	Langport Member	SAB8	12.2	17.8	RV, SP	liasicus Zone	W. portlocki subzone	SAB 60	40.7	24.6	LV, SP	liasicus Zone	Alsatites laqueus subzone	SAB 76	53.6	57.4	LV, SP
			12.2	21.2	RV, SP				40.7	38.6	LV, SP				53.6	41.7	RV, SP
			12.2	23.0	LV, SP				40.7	34.4	LV, SP				53.6	36.8	RV, SP
			12.2	26.5	LV, SP				40.7	19.2	LV, SP				53.6	21.1	LV, SP
			12.2	26.3	LV, SP				40.7	32.2	RV, SP				53.6	35.4	RV, SP
			12.2	21.2	LV, SP				40.7	28.7	SB				53.6	38.6	RV, SP
			12.2	24.7	LV, SP				40.7	26.8	LV, SP				53.6	22.4	RV, SP
			12.2	20.9	RV, SP				40.7	23.1	LV, SP				53.6	41.4	RV, SP
			12.2	39.3	LV, SP				40.7	11.6	LV, SP				53.6	21.3	LV, SP
			12.2	31.5	LV, SP				40.7	33.2	LV, SP				53.6	29.1	LV, SP
			12.2	29.2	LV, SP				40.7	33.2	RV, SP				53.6	27.0	LV, SP
			12.2	21.7	LV, SP				40.7	27.6	RV, SP				53.6	44.8	LV, SP
			12.2	16.9	LV, SP				40.7	18.4	RV, SP				53.6	22.3	RV, SP
			12.2	29.8	LV, SP				40.7	24.2	RV, SP				53.6	13.9	LV, SP
			12.2	50.1	RV, SP				40.7	11.9	LV, SP				53.6	15.2	RV, SP
			12.2	12.8	RV, SP				40.7	10.4	SB				53.6	21.9	RV, SP
			12.2	15.7	SB				40.7	13.0	RV, SP				53.6	21.6	RV, SP
			12.2	21.0	LV, SP				40.7	14.2	LV, SP				53.6	13.3	SB
			12.2	18.0	RV, SP				40.7	17.6	RV, SP				53.6	22.1	RV, SP
			12.2	29.9	RV, SP				40.7	37.2	LV, SP				53.6	18.9	RV, SP
		12.2	29.3	RV, SP	40.7		30.2	RV, SP	53.6	19.0	RV, SP						
		12.2	27.4	RV, SP	40.7		21.8	LV, SP	53.6	15.5	RV, SP						
		12.2	16.7	RV, SP	47		34.6	RV, SP	53.6	28.7	RV, SP						
		12.2	12.6	LV, SP	47		26.1	RV, SP	53.6	22.1	RV, SP						
		SAB11	12.5	25.9	LV, SP		47	30.8	RV, SP	53.6	19.7			RV, SP			
			12.5	34.7	SB		47	23.9	LV, SP	55.5	46.3			LV, SP			
			12.5	34.7	RV, SP		47	16.8	RV, SP	55.5	19.5			RV, SP			
			12.5	32.0	LV, SP		47	13.0	RV, SP	55.5	24.7			RV, SP			
			12.5	43.5	RV, SP		47	25.2	LV, SP	55.5	39.5			RV, SP			
			12.5	35.3	LV, SP		47	36.8	LV, SP	55.5	37.1			LV, SP			
			12.5	39.6	RV, SP		47	22.0	RV, SP	55.5	28.1			RV, SP			
			12.5	39.6	LV, SP		47	20.6	LV, SP	55.5	37.6			LV, SP			
			12.5	36.6	LV, SP		47	19.9	RV, SP	55.5	21.4			SB			
			12.5	34.7	RV, SP		47	14.4	LV, SP	55.5	24.6			RV, SP			
				12.5	39.9		RV, SP			47	30.2			RV, SP	55.5	33.2	LV, SP

(A)						<i>O. aspinata</i>														
Zone	Subzone	Bed N.	Bed H.	Shell thickness	Shell pres.	Zone	Subzone	Bed N.	Bed H.	Shell thickness	Shell pres.	Zone	Subzone	Bed N.	Bed H.	Shell thickness	Shell pres.			
			12.5	36.9	LV, SP				47	22.9	RV, SP				55.5	29.6	SB			
			12.5	39.7	LV, SP				47	15.5	RV, SP				55.5	39.4	LV, SP			
			12.5	33.0	RV, SP				47	16.2	LV, SP				55.5	22.4	LV, SP			
			12.5	32.6	LV, SP				47	18.1	LV, SP				55.5	43.8	LV, SP			
			12.5	34.8	LV, SP				47	16.3	RV, SP				55.5	20.3	RV, SP			
			12.5	30.9	RV, SP				47	19.1	LV, SP				55.5	24.0	LV, SP			
			12.5	35.4	RV, SP				47	31.6	RV, SP				55.5	27.7	RV, SP			
			12.5	23.9	SB				47	14.3	RV, SP				55.5	23.1	LV, SP			
			12.5	12.7	RV, SP				47	15.4	LV, SP				55.5	19.1	RV, SP			
			12.5	31.7	RV, SP				47	20.6	LV, SP				55.5	32.1	SB			
Pre-planorbis		SAB17	15	26.1	LV, SP				48.9	20.6	LV, SP				55.5	26.0	RV, SP			
			15	25.0	RV, SP				48.9	31.4	LV, SP				55.5	30.4	RV, SP			
			15	44.1	LV, SP				48.9	28.6	LV, SP				55.5	37.3	RV, SP			
		SAB26 A	17.4	21.5	LV, SP				48.9	29.2	LV, SP				55.5	25.3	SB			
			17.4	26.7	RV, SP				48.9	13.2	RV, SP				55.5	44.5	SB			
			17.4	32.2	LV, SP				48.9	18.0	RV, SP				55.7	31.0	LV, SP			
			17.4	49.9	RV, SP				48.9	21.0	LV, SP				55.7	28.2	LV, SP			
			17.4	25.4	RV, SP				48.9	18.9	RV, SP				55.7	33.8	LV, SP			
			17.4	22.1	RV, SP				48.9	22.0	SB				55.7	27.3	RV, SP			
			17.4	36.4	RV, SP				48.9	29.7	RV, SP				55.7	31.0	LV, SP			
			17.4	29.1	RV, SP				48.9	40.9	RV, SP				55.7	34.9	SB			
			17.4	19.5	LV, SP				48.9	22.9	LV, SP				55.7	29.1	LV, SP			
			17.4	49.0	RV, SP				48.9	19.0	LV, SB				55.7	30.5	RV, SP			
			17.4	18.1	RV, SP				48.9	23.3	LV, SB				55.7	19.1	RV, SP			
			17.4	24.3	RV, SP				48.9	14.3	RV, SP				55.7	46.3	RV, SP			
			17.4	34.5	LV, SP				48.9	16.2	LV, SP				55.7	34.3	LV, SP			
			17.4	29.5	RV, SP				48.9	16.7	LV, SP				55.7	40.1	RV, SP			
			17.4	46.5	RV, SP				48.9	22.3	RV, SP				55.7	30.4	LV, SP			
			17.4	44.3	RV, SP				48.9	18.9	RV, SP				55.7	36.2	RV, SP			
			17.4	49.3	LV, SP				48.9	12.8	LV, SP				55.7	23.9	LV, SP			
			17.4	30.3	SB				48.9	16.7	RV, SP				55.7	36.2	RV, SP			
			17.4	33.6	RV, SP				48.9	9.8	SB				55.7	23.9	RV, SP			
			17.4	20.1	LV, SP				49.3	18.9	RV, SP				55.7	32.9	RV, SP			
			17.4	19.2	RV, SP				49.3	31.8	RV, SP				55.7	23.9	RV, SP			
			17.4	18.3	SB				49.3	19.2	RV, SP				55.7	45.2	RV, SP			
			SAB28	17.9	21.2				RV, SP	49.3	19.2				RV, SP	55.7	10.7	LV, SP		
				17.9	27.0				LV, SP	49.3	41.9				RV, SP	55.7	36.0	LV, SP		
			planorbis	Ps.	SAB30				18.7	47.8	LV, SP				SAB6 6	49.3	27.9	RV, SP	55.7	13.5
											49.3					28.7	LV, SP	55.7	25.7	SB
															49.3	23.9	LV, SP	55.7	37.5	LV, SP
															49.3	39.9	RV, SP	55.7	20.7	SB
															49.3	28.4	RV, SP			

(A)						<i>O. aspinata</i>												
Zone	Subzone	Bed N.	Bed H.	Shell thickness	Shell pres.	Zone	Subzone	Bed N.	Bed H.	Shell thickness	Shell pres.	Zone	Subzone	Bed N.	Bed H.	Shell thickness	Shell pres.	
Zone	planorbis subzone	A	18.7	20.6	LV, SP				49.3	32.8	RV, SP				55.7	16.0	RV, SP	
			18.7	25.4	LV, SP				49.3	34.8	LV, SP				56.65	45.6	RV, SP	
			18.7	23.1	LV, SP				49.3	31.6	LV, SP				56.65	34.3	LV, SP	
			18.7	16.9	SB				49.3	14.1	LV, SP				56.65	32.3	RV, SP	
			18.7	26.2	LV, SP				49.3	38.6	LV, SP				56.65	21.3	RV, SP	
			18.7	26.9	LV, SP				49.3	20.8	SB				56.65	32.9	RV, SP	
			18.7	17.1	SB				49.3	31.0	RV, SP				56.65	32.7	RV, SP	
			18.7	18.6	SB				49.3	25.6	LV, SP				56.65	31.8	LV, SP	
			18.7	28.3	RV, SP				49.3	20.1	LV, SP				56.65	31.4	LV, SP	
			18.7	22.4	LV, SP				49.3	13.6	RV, SP				56.65	51.0	RV, SP	
			18.7	36.9	LV, SP				49.3	14.7	RV, SP				56.65	36.1	RV, SP	
			18.7	11.7	SB				49.3	22.2	RV, SP				56.65	40.5	LV, SP	
			18.7	24.7	LV, SP				49.3	21.4	RV, SP				56.65	46.8	RV, SP	
			18.7	15.2	LV, SP				49.3	22.8	RV, SP				56.65	43.9	RV, SP	
			18.7	20.3	RV, SP				49.3	11.5	RV, SP				56.65	41.6	SB	
			18.7	18.6	LV, SP				49.44	34.0	SB				56.65	36.2	RV, SP	
			18.7	15.6	RV, SP				49.44	28.3	RV, SP				56.65	13.8	SB	
			18.7	11.6	LV, SP				49.44	21.1	LV, SP				56.65	48.7	SB	
			18.7	25.7	RV, SP				49.44	14.5	RV, SP				56.65	33.4	LV, SB	
			18.7	11.3	LV, SP				49.44	37.2	LV, SP				56.65	23.7	SB	
			SAB34	19.8	28.0				LV, SP	49.44	34.9				RV, SP	56.65	47.3	SB
				19.8	25.7				RV, SP	49.44	25.1				SB	56.65	15.7	RV, SB
				19.8	29.4				LV, SP	49.44	57.0				LV, SP	56.65	16.3	LV, SP
				19.8	16.8				LV, SP	49.44	35.8				RV, SP	56.65	15.7	RV, SP
		19.8		24.5	LV, SP			49.44	27.4	LV, SP	56.95			21.7	LV, SP			
		19.8		29.2	RV, SP			49.44	31.9	LV, SP	56.95			26.9	SB			
		19.8		12.4	SB			49.44	23.0	LV, SP	56.95			24.4	LV, SP			
		19.8		16.7	RV, SP			49.44	39.9	LV, SP	56.95			30.1	RV, SP			
		19.8		19.2	SB			49.44	27.4	SB	56.95			20.1	RV, SP			
		19.8		9.8	RV, SP			49.44	29.5	RV, SP	56.95			43.5	LV, SP			
		19.8		20.5	RV, SP			49.44	10.7	RV, SP	56.95			36.7	SB			
		19.8		27.0	LV, SP			49.44	18.3	RV, SP	56.95			42.7	LV, SP			
		19.8		21.4	RV, SP			49.44	11.7	LV, SP	56.95			37.5	LV, SP			
		19.8		12.8	RV, SP			49.44	23.9	RV, SP	56.95			34.5	LV, SP			
		19.8		16.0	RV, SP			49.44	27.8	RV, SP	56.95			40.7	RV, SP			
		19.8		13.5	RV, SP			49.44	18.1	RV, SP	56.95			45.0	LV, SP			
		19.8		12.3	RV, SP			49.44	28.0	LV, SP	56.95			59.5	LV, SP			
		19.8		9.9	RV, SP			49.44	21.0	LV, SP	56.95			15.7	RV, SP			
		19.8		21.8	LV, SP			49.44	21.0	RV, SP	56.95			20.0	RV, SP			

(A)						<i>O. aspinata</i>											
Zone	Subzone	Bed N.	Bed H.	Shell thickness	Shell pres.	Zone	Subzone	Bed N.	Bed H.	Shell thickness	Shell pres.	Zone	Subzone	Bed N.	Bed H.	Shell thickness	Shell pres.
	C. johnstoni subzone	SAB40	19.8	19.2	SB			SAB7 OV.B	49.8	35.2	LV, SP			SAB88	56.95	38.8	SB
			23.2	44.7	RV, SP				49.8	40.0	RV, SP				56.95	18.2	LV, SP
			23.2	37.6	RV, SP				49.8	32.8	RV, SP				56.95	20.1	LV, SP
			23.2	38.8	RV, SP				49.8	38.5	LV, SP				56.95	43.8	SB
			23.2	14.3	LV, SP				49.8	34.7	LV, SP				56.95	19.1	SB
			23.2	40.1	RV, SP				49.8	31.7	LV, SP				56.95	27.5	SB
			23.2	19.1	RV, SP				49.8	18.5	RV, SP				56.95	46.6	LV, SP
			23.2	46.1	LV, SP				49.8	40.1	RV, SP				56.95	33.6	RV, SP
			23.2	36.2	LV, SP				49.8	31.9	RV, SP				57.2	40.6	LV, SP
			23.2	33.6	RV, SP				49.8	16.7	LV, SP				57.2	35.7	RV, SP
			23.2	37.4	SB				49.8	35.1	RV, SP				57.2	42.0	LV, SP
			23.2	35.4	LV, SP				49.8	14.9	RV, SP				57.2	32.4	LV, SP
			23.2	43.8	LV, SP				49.8	31.3	RV, SP				57.2	46.1	RV, SP
			23.2	50.3	SB				49.8	15.9	SB				57.2	42.0	RV, SP
			23.2	38.5	LV, SP				49.8	18.2	RV, SP				57.2	44.2	SB
			23.2	26.5	RV, SP				49.8	33.5	LV, SP				57.2	40.9	LV, SP
			23.2	27.0	RV, SP				49.8	36.6	RV, SP				57.2	44.6	RV, SP
			23.2	22.3	RV, SP				49.8	22.6	RV, SP				57.2	30.9	LV, SP
			23.2	24.8	RV, SP				49.8	17.4	RV, SP				57.2	40.0	RV, SP
			23.2	18.0	RV, SP				49.8	15.3	RV, SP				57.2	18.1	RV, SP
		23.2	36.2	RV, SP	49.8			13.0	RV, SP	57.2	17.6			RV, SP			
		23.2	24.7	LV, SP	49.8			13.5	RV, SP	57.2	27.8			LV, SP			
		23.2	22.9	RV, SP	49.8			13.0	LV, SP	57.2	18.3			LV, SP			
		23.2	21.9	LV, SP	50.6			32.2	RV, SP	57.2	27.1			SB			
		23.8	24.8	LV, SP	50.6			35.8	LV, SP	57.2	32.2			LV, SP			
		23.8	14.2	LV, SP	50.6			38.1	RV, SP	57.2	30.3			SB			
		23.8	27.7	RV, SP	50.6			36.7	RV, SP	57.2	37.5			SB			
		23.8	23.3	RV, SP	50.6			43.9	RV, SP	57.2	27.5			RV, SP			
		23.8	25.9	RV, SP	50.6			29.6	RV, SP	57.2	16.1			RV, SP			
		23.8	35.4	RV, SP	50.6			35.6	RV, SP	57.2	27.9			RV, SP			
		23.8	44.2	SB	50.6			38.6	LV, SP	57.2	14.5			RV, SP			
		23.8	34.0	RV, SP	50.6			23.1	LV, SP	SAB90	57.3			23.0	LV, SP		
		23.8	32.6	SB	50.6			26.5	LV, SP		57.3			27.0	LV, SP		
		23.8	37.7	LV, SP	50.6			29.8	LV, SP		57.3			44.9	RV, SP		
		23.8	40.7	RV, SP	50.6			26.0	LV, SP		57.3			31.7	RV, SP		
		23.8	33.8	LV, SP	50.6			23.6	LV, SP		57.3			44.1	LV, SP		
		23.8	35.9	LV, SP	50.6			24.1	RV, SP		57.3			32.1	SB		
		23.8	18.8	RV, SP	50.6			29.6	LV, SP		57.3			40.2	RV, SP		
		23.8	18.8	RV, SP	50.6			26.8	LV, SP		57.3			50.9	RV, SP		

(B)		<i>O. aspinata</i>			
Zone	Subzone	Bed N.	Bed height	Shell thickness	Shell preservation
angulata Zone	Schlotheimia angulata subzone	SAB94	59.85	40.1	RV, SP
			59.85	36.6	RV, SP
			59.85	38.0	LV, SP
			59.85	23.4	LV, SP
			59.85	26.8	RV, SP
			59.85	48.7	RV, SP
			59.85	41.7	LV, SP
			59.85	47.6	RV, SP
			59.85	28.7	RV, SP
			59.85	32.8	LV, SP
			59.85	32.3	RV, SP
			59.85	25.6	LV, SP
			59.85	22.5	SB
			59.85	30.6	SB
			59.85	22.9	SB
			59.85	17.2	RV, SP
			59.85	43.5	LV, SP
			59.85	23.6	RV, SP
			59.85	13.0	LV, SP
			59.85	29.5	LV, SP
		59.85	14.3	LV, SP	
		59.85	14.2	RV, SP	
		SAB96	61.8	36.0	RV, SP
			61.8	33.5	LV, SP
			61.8	36.4	RV, SP
			61.8	38.3	RV, SP
			61.8	31.3	RV, SP
			61.8	28.3	LV, SP
			61.8	43.4	LV, SP
			61.8	39.1	LV, SP
			61.8	18.9	LV, SP
			61.8	11.7	LV, SP
			61.8	14.4	RV, SP
			61.8	43.1	RV, SP
			61.8	19.6	RV, SP
			61.8	28.3	RV, SP
			61.8	17.5	LV, SP
			61.8	11.9	RV, SP
			61.8	12.1	SB
			61.8	27.4	SB
			61.8	16.9	RV, SP
			61.8	35.5	RV, SP
		61.8	23.5	RV, SP	
		61.8	27.8	SB	
		61.8	20.4	LV, SP	
		SAB98	62.5	31.3	RV, SP
			62.5	29.7	RV, SP
			62.5	19.0	LV, SP
			62.5	14.3	RV, SP
			62.5	23.3	RV, SP
			62.5	14.3	SB
			62.5	14.1	SB
			62.5	16.0	SB
			62.5	16.9	SB
62.5	22.6		SB		
62.5	25.8		SB		
62.5	21.4		RV, SP		
62.5	16.2		RV, SP		
62.5	15.2		SB		
62.5	17.6		RV, SP		
62.5	26.0		RV, SP		
62.5	20.9		SB		
62.5	27.3		SB		
62.5	16.2		RV, SP		
62.5	16.7		SB		
62.5	36.6	LV, SP			
62.5	33.3	SB			
62.5	20.3	SB			
62.5	11.8	SN			

A4.2.2: Relationships between the fossil size recorded and the number of individuals measured at St Audrie's Bay.

Table A4.25: *L. hisingeri* geometric shell size results from the statistical analysis when determining any relationship between the mean, min, max and range and the number of individuals measured in St Audrie's Bay (Presented in Section 3.5.1).

Correlation question	Number of individuals	R ² value
Minimum geometric <i>L. hisingeri</i> shell size against the number of individuals measured on each bed	20	0.266
Maximum geometric <i>L. hisingeri</i> shell size against the number of individuals measured on each bed	20	0.0058
Mean geometric <i>L. hisingeri</i> shell size against the number of individuals measured on each bed	20	0.1825
Range geometric <i>L. hisingeri</i> shell size against the number of individuals measured on each bed	20	0.5908
Minimum geometric <i>L. hisingeri</i> shell size against the number of individuals measured on each bed in the Pre-planorbis Zone	13	0.2605
Maximum geometric <i>L. hisingeri</i> shell size against the number of individuals measured on each bed in the Pre-planorbis Zone	13	0.1778
Mean geometric <i>L. hisingeri</i> shell size against the number of individuals measured on each bed in the Pre-planorbis Zone	13	0.000002
Range geometric <i>L. hisingeri</i> shell size against the number of individuals measured on each bed in the Pre-planorbis Zone	13	0.5176
Minimum geometric <i>L. hisingeri</i> shell size against the number of individuals measured on each bed in the Planorbis Zone	5	0.6982
Maximum geometric <i>L. hisingeri</i> shell size against the number of individuals measured on each bed in the Planorbis Zone	5	0.0105
Mean geometric <i>L. hisingeri</i> shell size against the number of individuals measured on each bed in the Planorbis Zone	5	0.3682
Range geometric <i>L. hisingeri</i> shell size against the number of individuals measured on each bed in the Planorbis Zone	5	0.7598
Minimum geometric <i>L. hisingeri</i> shell size against the number of individuals measured on each bed in the liasicus Zone	2	1
Maximum geometric <i>L. hisingeri</i> shell size against the number of individuals measured on each bed in the liasicus Zone	2	1
Mean geometric <i>L. hisingeri</i> shell size against the number of individuals measured on each bed in the liasicus Zone	2	1
Range geometric <i>L. hisingeri</i> shell size against the number of individuals measured on each bed in the liasicus Zone	2	1
Minimum geometric <i>L. hisingeri</i> shell size against the number of individuals measured in each zone	3	0.1607
Maximum geometric <i>L. hisingeri</i> shell size against the number of individuals measured in each zone	3	0.7382
Mean geometric <i>L. hisingeri</i> shell size against the number of individuals measured in each zone	3	0.9544
Range geometric <i>L. hisingeri</i> shell size against the number of individuals measured in each zone	3	0.807

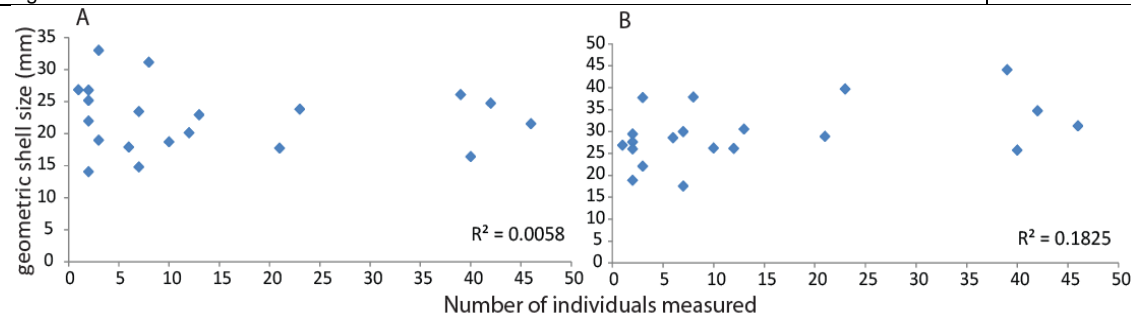


Figure A4.13: St Audrie's Bay, *L. hisingeri* (A) mean and (B) maximum geometric sizes on each bed versus the corresponding number of individuals measured in each bed (Presented in Section 3.5.1).

Relationships between *Liostrea* geometric shell size and the number of individuals measured on each zone

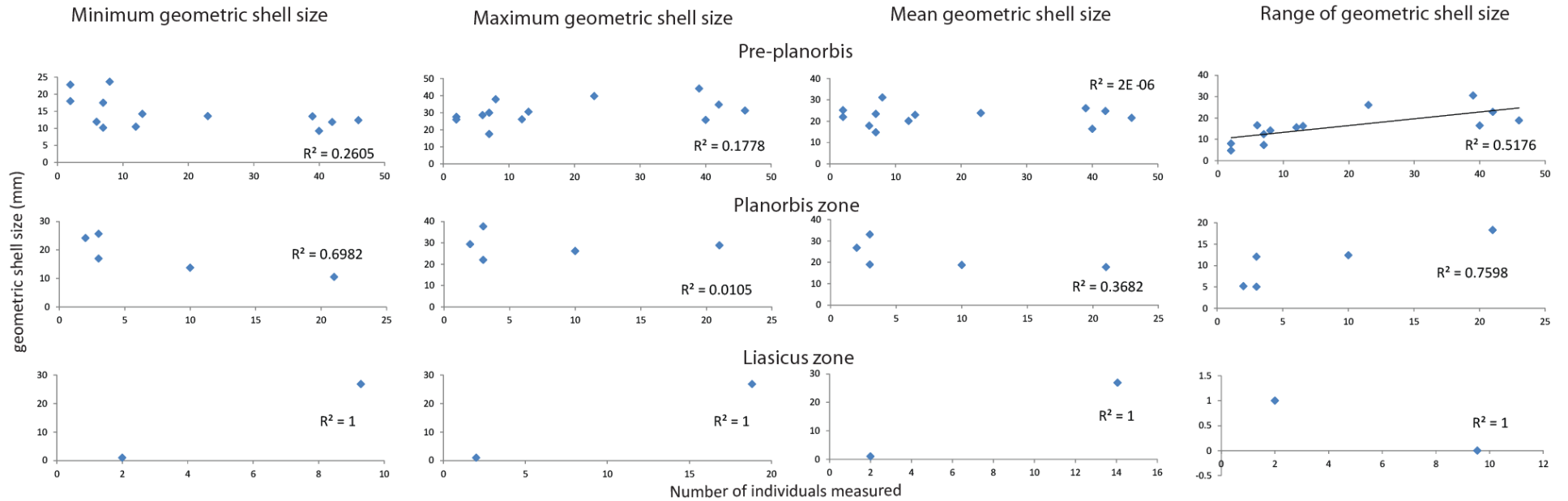


Figure A4.14: *L. hisingeri* geometric shell size data (the mean, minimum, maximum and range of geometric shell size verses the number of individuals measured from each bed in each Pre-planorbis Zone, Planorbis Zone, liasicus Zone) from St Audrie's Bay (Presented in Section 3.5.1).

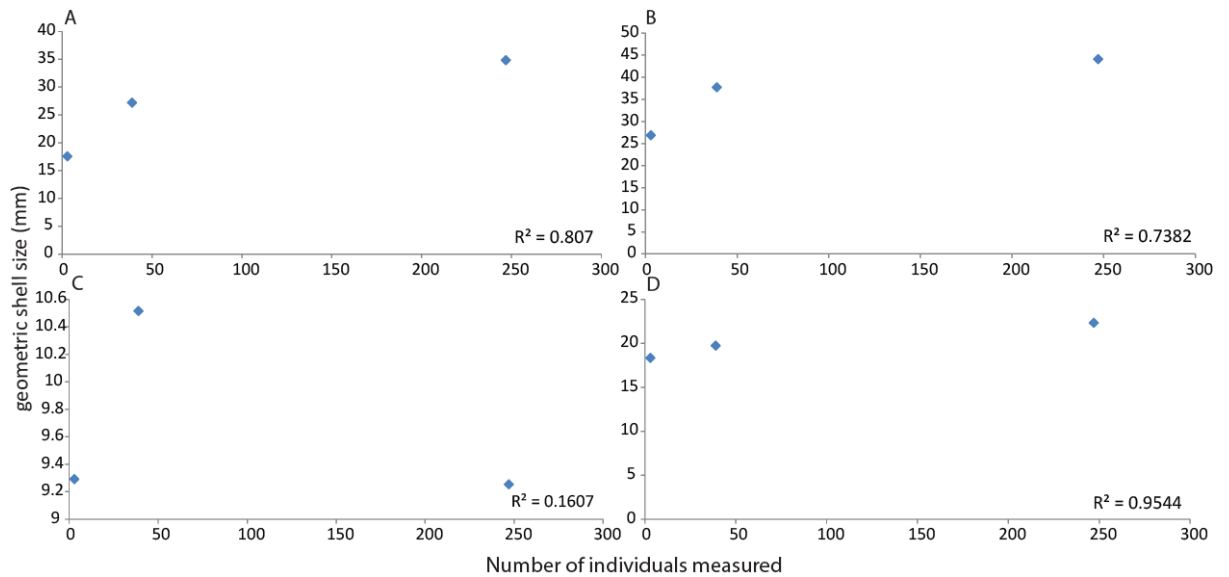


Figure A4.15: *L. hisingeri* geometric shell size data (D) mean, (C) minimum, (B) maximum and (A) range of geometric shell size versus the number of individuals measured in each zone from St Audrie's Bay (Presented in Section 3.5.1).

Table A4.26: *O. aspinata* geometric shell size results from the statistical analysis when determining any relationship between the mean, min, max and range and the number of individuals measured in St Audrie's Bay (Presented in Section 3.5.1).

Correlation question	Number of individuals	R ² value
Minimum geometric <i>O. aspinata</i> shell size against the number of individuals measured on each bed	30	0.6827
Maximum geometric <i>O. aspinata</i> shell size against the number of individuals measured on each bed	30	0.0669
Mean geometric <i>O. aspinata</i> shell size against the number of individuals measured on each bed	30	0.3259
Range geometric <i>O. aspinata</i> shell size against the number of individuals measured on each bed	30	0.4334
Minimum geometric <i>O. aspinata</i> shell size against the number of individuals measured on each bed in the Lilstock formation	2	1
Maximum geometric <i>O. aspinata</i> shell size against the number of individuals measured on each bed in the Lilstock formation	2	1
Mean geometric <i>O. aspinata</i> shell size against the number of individuals measured on each bed in the Lilstock formation	2	1
Range geometric <i>O. aspinata</i> shell size against the number of individuals measured on each bed in the Lilstock formation	2	1
Minimum geometric <i>O. aspinata</i> shell size against the number of individuals measured on each bed in the Pre-planorbis Zone	3	0.0415
Maximum geometric <i>O. aspinata</i> shell size against the number of individuals measured on each bed in the Pre-planorbis Zone	3	0.2602
Mean geometric <i>O. aspinata</i> shell size against the number of individuals measured on each bed in the Pre-planorbis Zone	3	0.0847
Range geometric <i>O. aspinata</i> shell size against the number of individuals measured on each bed in the Pre-planorbis Zone	3	0.9292
Minimum geometric <i>O. aspinata</i> shell size against the number of individuals measured on each bed in the Planorbis Zone	7	0.5608
Maximum geometric <i>O. aspinata</i> shell size against the number of individuals measured on each bed in the Planorbis Zone	7	0.5357
Mean geometric <i>O. aspinata</i> shell size against the number of individuals measured on each bed in the Planorbis Zone	7	0.0017
Range geometric <i>O. aspinata</i> shell size against the number of individuals measured on each bed in the Planorbis Zone	7	0.7639
Minimum geometric <i>O. aspinata</i> shell size against the number of individuals measured on each bed in the Iiasicus Zone	15	0.3469
Maximum geometric <i>O. aspinata</i> shell size against the number of individuals measured on each bed in the Iiasicus Zone	15	0.1131
Mean geometric <i>O. aspinata</i> shell size against the number of individuals measured on each bed in the Iiasicus Zone	15	0.0006

Correlation question	Number of individuals	R ² value
measured on each bed in the liasicus Zone		
Range geometric <i>O. aspinata</i> shell size against the number of individuals measured on each bed in the liasicus Zone	15	0.3325
Minimum geometric <i>O. aspinata</i> shell size against the number of individuals measured on each bed in the angulata Zone	3	0.9974
Maximum geometric <i>O. aspinata</i> shell size against the number of individuals measured on each bed in the angulata Zone	3	0.8227
Mean geometric <i>O. aspinata</i> shell size against the number of individuals measured on each bed in the angulata Zone	3	0.0228
Range geometric <i>O. aspinata</i> shell size against the number of individuals measured on each bed in the angulata Zone	3	0.9287
Minimum geometric <i>O. aspinata</i> shell size against the number of individuals measured in each zone	5	0.1091
Maximum geometric <i>O. aspinata</i> shell size against the number of individuals measured in each zone	5	0.0841
Mean geometric <i>O. aspinata</i> shell size against the number of individuals measured in each zone	5	0.0247
Range geometric <i>O. aspinata</i> shell size against the number of individuals measured in each zone	5	0.1866

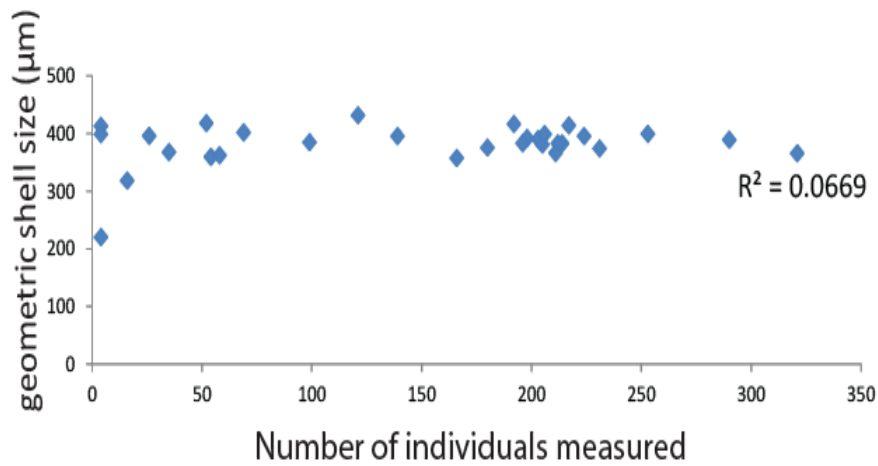


Figure A4.16: St Audrie's Bay, *O. aspinata* mean geometric sizes on each bed versus the corresponding number of individuals measured in each bed (Presented in Section 3.5.1).

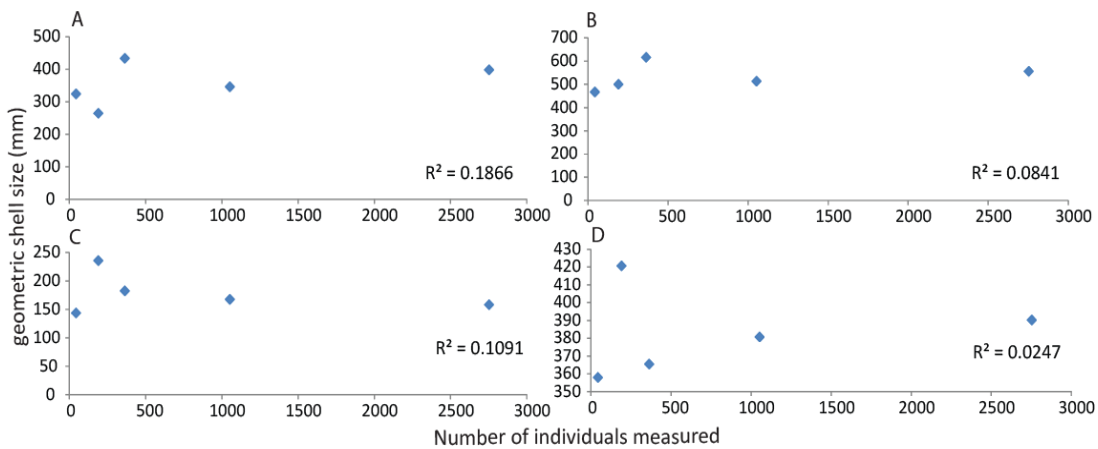
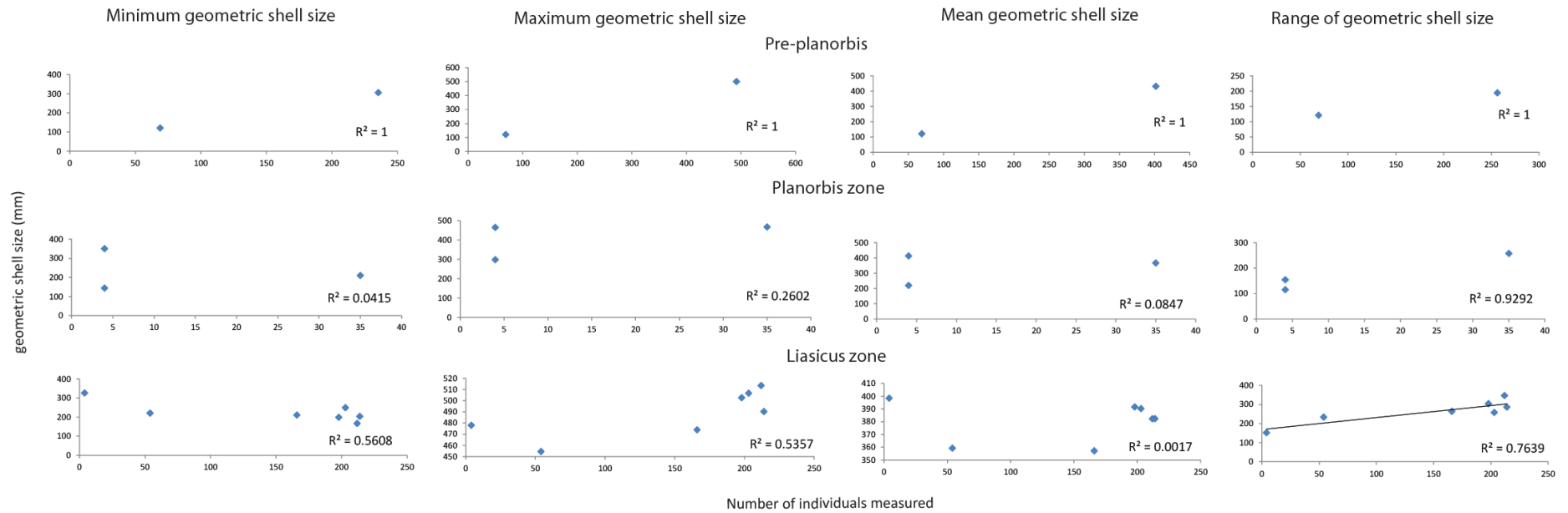
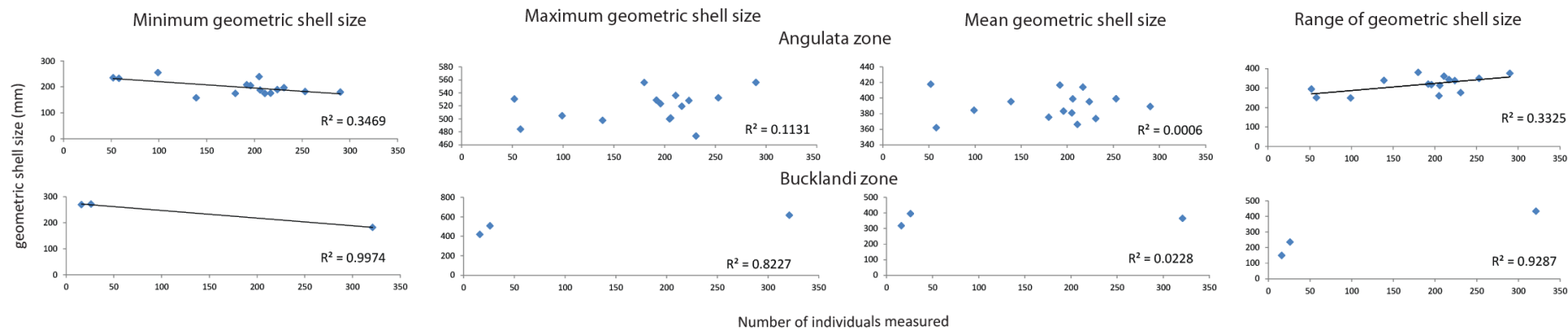


Figure A4.17: *O. aspinata* geometric shell size data (D) mean, (C) minimum, (B) maximum and (A) range of geometric shell size versus the number of individuals measured within each zone from St Audrie's Bay (Presented in Section 3.5.1).

Relationships between *Ogmoconchella* geometric shell size and the number of individuals measured on each zoneFigure A4.18A: *O. aspinata* geometric shell size data (the mean, minimum, maximum and range of geometric shell size versus the number of individuals measured from each bed in each Pre-planorbis Zone, Planorbis Zone, liasicus Zone) from St Audrie's Bay (Presented in Section 3.5.1).

Relationships between *Ogmoconchella* geometric shell size and the number of individuals measured on each zoneFigure A4.18B: *O. aspinata* geometric shell size data (the mean, minimum, maximum and range of geometric shell size versus the number of individuals measured from each bed in each angulata Zone and bucklandi Zone) from St Audrie's Bay (Presented in Section 3.5.1).Table A4.27: *O. aspinata* shell thickness results from the statistical analysis when determining any relationship between the mean, min, max and range and the number of individuals measured in St Audrie's Bay (Presented in Section 3.5.1).

Correlation question	Number of individuals	R ² value
Minimum <i>O. aspinata</i> shell thickness against the number of individuals measured on each bed	29	0.6242
Maximum <i>O. aspinata</i> shell thickness against the number of individuals measured on each bed	29	0.0954
Mean <i>O. aspinata</i> shell thickness against the number of individuals measured on each bed	29	0.0374
Range <i>O. aspinata</i> shell thickness against the number of individuals measured on each bed	29	0.5021
Minimum <i>O. aspinata</i> shell thickness against the number of individuals measured on each bed in the Lilstock Formation	2	1
Maximum <i>O. aspinata</i> shell thickness against the number of individuals measured on each bed in the Lilstock Formation	2	1
Mean <i>O. aspinata</i> shell thickness against the number of individuals measured on each bed in the Lilstock Formation	2	1
Range <i>O. aspinata</i> shell thickness against the number of individuals measured on each bed in the Lilstock Formation	2	1
Minimum <i>O. aspinata</i> shell thickness against the number of individuals measured on each bed in the Pre-planorbis Zone	3	0.6573
Maximum <i>O. aspinata</i> shell thickness against the number of individuals measured on each bed in the Pre-planorbis Zone	3	0.5286
Mean <i>O. aspinata</i> shell thickness against the number of individuals measured on each bed in the Pre-planorbis Zone	3	0.2027
Range <i>O. aspinata</i> shell thickness against the number of individuals measured on each bed in the Pre-planorbis Zone	3	0.7765
Minimum <i>O. aspinata</i> shell thickness against the number of individuals measured on each bed in the Planorbis Zone	6	0.8763
Maximum <i>O. aspinata</i> shell thickness against the number of individuals measured on each bed in the Planorbis Zone	6	0.0557

Correlation question	Number of individuals	R ² value
Mean <i>O. aspinata</i> shell thickness against the number of individuals measured on each bed in the Planorbis Zone	6	0.4095
Range <i>O. aspinata</i> shell thickness against the number of individuals measured on each bed in the Planorbis Zone	6	0.3938
Minimum <i>O. aspinata</i> shell thickness against the number of individuals measured on each bed in the liasicus Zone	15	0.1155
Maximum <i>O. aspinata</i> shell thickness against the number of individuals measured on each bed in the liasicus Zone	15	0.2053
Mean <i>O. aspinata</i> shell thickness against the number of individuals measured on each bed in the liasicus Zone	15	0.2235
Range <i>O. aspinata</i> shell thickness against the number of individuals measured on each bed in the liasicus Zone	15	0.1227
Minimum <i>O. aspinata</i> shell thickness against the number of individuals measured on each bed in the angulata Zone	3	0.7382
Maximum <i>O. aspinata</i> shell thickness against the number of individuals measured on each bed in the angulata Zone	3	0.9944
Mean <i>O. aspinata</i> shell thickness against the number of individuals measured on each bed in the angulata Zone	3	0.9682
Range <i>O. aspinata</i> shell thickness against the number of individuals measured on each bed in the angulata Zone	3	0.9771
Minimum <i>O. aspinata</i> shell thickness against the number of individuals measured in each zone	5	0.2987
Maximum <i>O. aspinata</i> shell thickness against the number of individuals measured in each zone	5	0.9135
Mean <i>O. aspinata</i> shell thickness against the number of individuals measured in each zone	5	0.0014
Range <i>O. aspinata</i> shell thickness against the number of individuals measured in each zone	5	

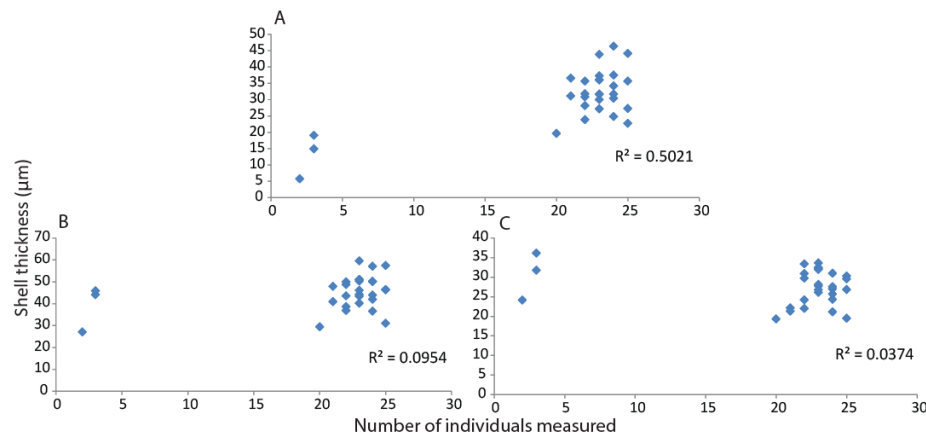


Figure A4.19: St Audrie's Bay, *O. aspinata* maximum, mean and range of shell thickness on each bed versus the corresponding number of individuals measured in each bed (Presented in Section 3.5.1).

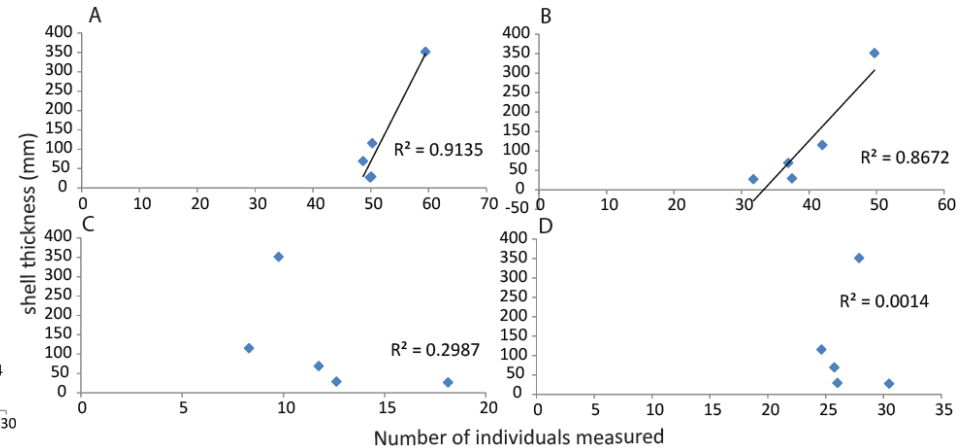
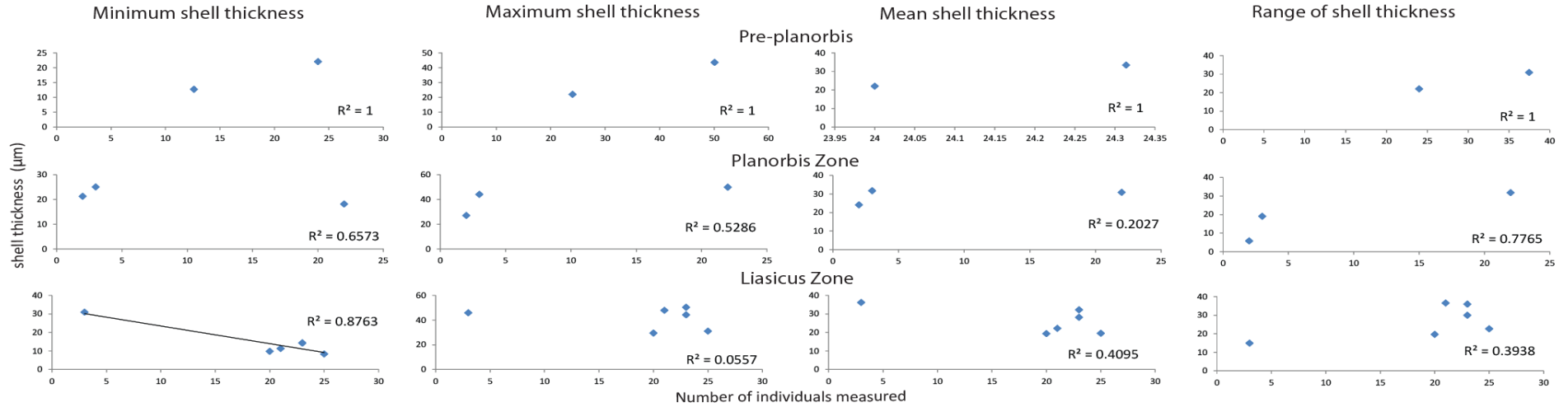
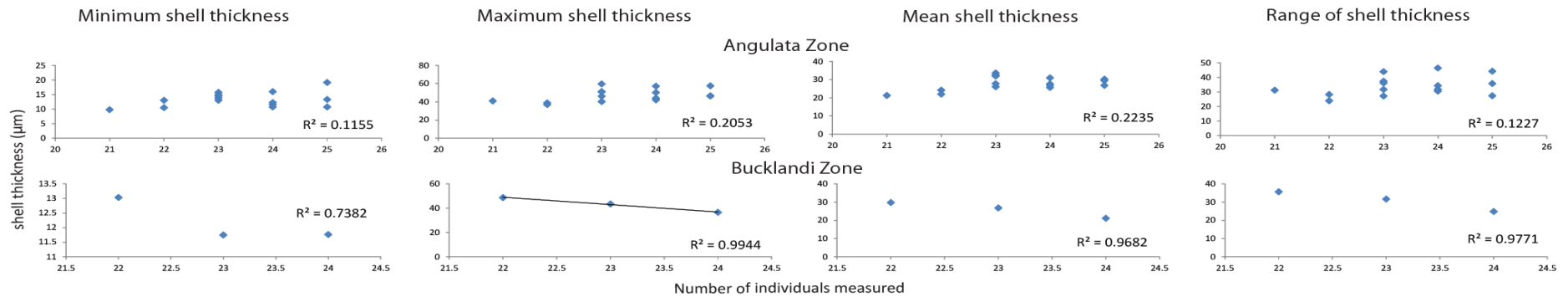


Figure A4.20: *O. aspinata* shell thickness data (D) mean, (C) minimum, (A) maximum and (B) range of geometric shell size versus the number of individuals measured within each zone from St Audrie's Bay (Presented in Section 3.5.1).

Relationships between *Ogmoconchella* shell thickness and the number of individuals measured on each zoneFigure A4.21A: *O. aspinata* shell thickness data (the mean, minimum, maximum and range of geometric shell size verses the number of individuals measured from each bed in each Pre-planorbis Zone, Planorbis Zone, liassic Zone) from St Audrie's Bay (Presented in Section 3.5.1).Relationships between *Ogmoconchella* shell thickness and the number of individuals measured on each zoneFigure A4.21B: *O. aspinata* shell thickness data (the mean, minimum, maximum and range of geometric shell size verses the number of individuals measured from each bed in each angulata Zone and bucklandi Zone) from St Audrie's Bay (Presented in Section 3.5.1).

A4.2.3: Statistical analysis results for fossil data from St Audrie's Bay.

Table A4.28A: *L. hisingeri* statistical results from the geometric shell size from every bed within the Pre-planorbis Zone from St Audrie's Bay using the Kruskal-Wallis and the Mann Whitney tests (Presented in Section 3.5.3).

Pre-planorbis Zone												
H (chi ²)	81.02	Hc (tie corrected)	81.02	p(same)	2.64 x 10 ⁻¹²							
	SAB16	SAB18	SAB18A	SAB19A	SAB19	SAB20	SAB21	SAB22	SAB23	SAB24	SAB25	SAB26
SAB12	0.2888	0.01212	0.0000633	0.02677	0.000000548	0.0000000212	0.001068	0.1479	0.732	0.000000116	0.0000116	0.0000790
SAB16		0.009945	0.001998	0.05704	0.0003359	0.000193	0.002165	0.05704	0.5203	0.000858	0.00146	0.01078
SAB18			0.1495	0.1709	0.4716	0.005836	0.1391	0.9273	0.3254	0.03395	0.000596	0.1306
SAB18A				0.4447	0.2685	0.1686	1	0.7989	0.07218	0.2203	0.003357	0.7171
SAB19A					0.1883	0.9326	0.6605	0.6985	0.2433	0.9759	0.151	0.8023
SAB19						0.001105	0.2874	0.8974	0.06065	0.01067	0.0000841	0.2441
SAB20							0.432	0.4469	0.02195	0.4524	0.004445	0.5785
SAB21								0.8836	0.07415	0.4265	0.01767	0.9219
SAB22									0.4047	0.4864	0.08965	0.7259
SAB23										0.02219	0.008132	0.0899
SAB24											0.08171	0.2618
SAB25												0.02007

Table A4.28B-C: *L. hisingeri* statistical results from the geometric shell size from every bed within the (B) Planorbis Zone and (C) liasicus Zone from St Audrie's Bay using the Kruskal-Wallis and the Mann Whitney tests (Presented in Section 3.5.3).

(B) Planorbis Zone					
H (chi ²)	11.3	Hc (tie corrected)	11.3	p(same)	0.02336
	SAB35	SAB36	SAB41	SAB43	
SAB29	0.01136	0.3865	0.02249	0.08086	
SAB35		0.05621	0.5973	0.485	
SAB36			0.06784	0.1489	
SAB41				0.7998	

(C) liasicus Zone	
H (chi ²)	1.5
Hc (tie corrected)	1.5
p(same)	0.2207
	SAB71
SAB63	0.5403

Table A4.29: Kruskal-Wallis and Mann Whitney results for the compiled *L. hisingeri* geometric zone data in St Audrie's Bays (Presented in Section 3.5.3).

H (chi ²)	6.662	planorbis Zone	liasicus Zone
Hc (tie corrected)	6.662	Pre-planorbis Zone	0.01294
p(same)	0.03575	planorbis Zone	0.9222

Table A4.30: Kruskal-Wallis and Mann Whitney results for the compiled *L. hisingeri* geometric subzone data in St Audrie's Bays (Presented in Section 3.5.3).

H (chi ²)		7.024		
Hc (tie corrected)		7.024	p(same)	0.07113
	Ps. planorbis		johnstoni	Alsatites laqueus
Pre-planorbis Zone		0.08598	0.04293	0.4312
Ps. planorbis			0.8001	0.8579
johnstoni				1

Table A4.31A-C: *O. aspinata* statistical results from the geometric shell size from every bed within the (A) Lilstock Formation, (B) Pre-planorbis Zone and (C) Planorbis Zone from St Audrie's Bay using the Kruskal-Wallis and the Mann Whitney tests (Presented in Section 3.5.5).

(A) Lilstock Formation		(B) Pre-planorbis Zone			(C) Planorbis Zone							
H (chi ²)	10.94	H (chi ²)	9.572		H (chi ²)	58.31	Hc (tie corrected)	58.31	p(same)	9.91 x 10 ⁻¹¹		
Hc (tie corrected)	10.94	Hc (tie corrected)	9.572			SAB30A	SAB34	SAB40	SAB42	SAB44	SAB52	
p(same)	0.0009433	p(same)	0.008344		SAB30	0.001	0.008108	0.2127	0.02945	0.6745	0.5174	
	SAB11		SAB26A	SAB28	SAB30A		0.7056	0.0000000129	0.000000147	0.2116	0.000000344	
SAB8	0.0009479		SAB17	0.203	0.03038	SAB34		0.0005768	0.0003527	0.2374	0.003051	
			SAB26A		0.005882	SAB40				0.1932	0.8241	0.5184
						SAB42				0.9621	0.02845	
						SAB44					0.757	

Table A4.31D: *O. aspinata* statistical results from the geometric shell size from every bed within the liasicus Zone from St Audrie's Bay using the Kruskal-Wallis and the Mann Whitney tests (Presented in Section 3.5.5).

liasicus Zone														
H (chi ²)	143.1	Hc (tie corrected)	143.1	p(same)	1.74 x 10 ⁻²³									
	SAB62	SAB64	SAB66	SAB68	SAB70V.B	SAB70V.T	SAB74	SAB76	SAB80	SAB82	SAB84	SAB86	SAB88	SAB90
SAB60	0.0000693	0.0008269	0.4442	0.02336	0.1478	0.05424	0.0000000407	0.000000611	0.0000152	0.0004973	0.000137	0.2182	0.04527	0.009091
SAB62		0.9102	0.0000164	0.001873	0.0000117	0.0002075	0.001489	0.005655	0.02262	0.9038	0.6242	0.000179	0.009867	0.3396
SAB64			0.0001401	0.01984	0.0005677	0.006165	0.01522	0.01407	0.05355	0.8141	0.8151	0.003991	0.05069	0.5679
SAB66				0.03768	0.4524	0.1582	1.18 x 10 ⁻¹²	0.00000000218	0.00000329	0.0000247	0.0000289	0.5448	0.1273	0.000983
SAB68					0.1803	0.5598	0.00000000852	0.00000376	0.0001192	0.01268	0.001022	0.2609	0.783	0.1509
SAB70 V.B						0.5469	5.27 x 10 ⁻¹²	0.00000000337	0.00000735	0.0001481	0.0000125	0.8339	0.362	0.006536
SAB70 V.T							0.000000000925	0.000000183	0.0000393	0.002747	0.000281	0.4817	0.59	0.06165
SAB74								0.9936	0.6715	0.002198	0.01951	0.00000000278	0.00000738	0.001052

SAB76									0.6431	0.003669	0.02223	0.00000002 66	0.0001229	0.004545
SAB80										0.03146	0.07186	0.0000882	0.0005484	0.02715
SAB82											0.6041	0.001928	0.04882	0.5967
SAB84												0.000749	0.01387	0.2407
SAB86													0.5603	0.03669

Table A4.31E: *O. aspinata* statistical results from the geometric shell size from every bed within the angulata Zone from St Audrie's Bay using the Kruskal-Wallis and the Mann Whitney tests (Presented in Section 3.5.5).

Angulate Zone		
	H (chi ²)	6.638
	Hc (tie corrected)	6.638
	p(same)	0.0362
	SAB96	SAB98
SAB94	0.08495	0.08577
SAB96		0.002549

Table A4.32: Kruskal-Wallis and Mann Whitney results for the compiled *O. aspinata* geometric zone data in St Audrie's Bay (Presented in Section 3.5.5).

H (chi ²)	110.5	Hc (tie corrected)	110.5	p(same)	5.76 x 10 ⁻²³
	Pre-planorbis Zone	planorbis Zone	liasicus Zone	angulata Zone	
Lilstock Formation	0.000000213	4.37 x 10 ⁻²⁰	0.00000000239	7.84 x 10 ⁻¹³	
Pre-planorbis Zone		0.1248	0.01005	0.8668	
planorbis Zone			0.000000192	0.000665	
liasicus Zone				0.000000490	

Table A4.33: Kruskal-Wallis and Mann Whitney results for the compiled *O. aspinata* geometric subzone data in St Audrie's Bays (Presented in Section 3.5.5).

H (chi ²)	146.7	Hc (tie corrected)	146.7	p(same)	3.78 x 10 ⁻²⁹	
	Pre-planorbis Zone	Ps. planorbis	C. johnstoni	W. portlocki	Alsatites laqueus	Schlotheimia angulata
Lilstock Formation	0.000000213	1.30 x 10 ⁻²⁵	9.28 x 10 ⁻¹³	0.00000000130	0.00000000550	7.84 x 10 ⁻¹³
Pre-planorbis Zone		0.7041	0.02118	0.9425	0.008505	0.8668
Ps. planorbis			0.000000105	0.4701	1.29 x 10 ⁻¹³	0.1949
johnstoni				0.002961	0.1186	0.0000135
W. portlocki					0.0009004	0.9384
Alsatites laqueus						0.000000255

Table A4.34A-C: *O. aspinata* statistical results for the shell thickness from every bed within the (A) Lilstock Formation, (B) Pre-planorbis Zone and (C) Planorbis Zone from St Audrie's Bay using the Kruskal-Wallis and the Mann Whitney tests (Presented in Section 3.5.5).

(A) Lilstock Formation		(B) Pre-planorbis Zone			(C) Planorbis Zone					
H (chi ²)	15.32	H (chi ²)	0.5551		H (chi ²)	32.07	Hc (tie corrected)	32.07	p(same)	0.00000575
Hc (tie corrected)	15.32	Hc (tie corrected)	0.5551			SAB34	SAB40	SAB42	SAB44	SAB52
p(same)	0.001	p(same)	0.7576		SAB30A	0.4416	0.002254	0.0182	0.02324	0.3659
	SAB11		SAB26A	SAB28	SAB34		0.0001137	0.001615	0.007082	0.9363
SAB8	0.001	SAB17	0.9666	0.7728	SAB40			0.1352	0.6301	0.0001045
		SAB26A		0.4972	SAB42				0.2612	0.001832
					SAB44					0.007495

Table A4.34D: *O. aspinata* statistical results for the shell thickness from every bed within the liasicus Zone from St Audrie's Bay using the Kruskal-Wallis and the Mann Whitney tests (Presented in Section 3.5.5).

liasicus Zone														
H (chi ²)	42.37	Hc (tie corrected)	42.37	p(same)	0.000108									
	SAB62	SAB64	SAB66	SAB68	SAB70V.B	SAB70V.T	SAB74	SAB76	SAB80	SAB82	SAB84	SAB86	SAB88	SAB90
SAB60	0.4317	0.2386	0.6285	0.4748	0.4334	0.2668	0.02867	0.5867	0.04174	0.05637	0.006218	0.01766	0.01291	0.4072
SAB62		0.7246	0.132	0.06009	0.2076	0.01704	0.001727	0.1626	0.0009155	0.004277	0.0008798	0.001538	0.001034	0.0357
SAB64			0.07411	0.0395	0.1729	0.008038	0.001285	0.09591	0.000418	0.001874	0.0004634	0.001513	0.001286	0.02001
SAB66				0.7966	0.8732	0.4394	0.0592	0.992	0.09103	0.1362	0.009135	0.05682	0.04212	0.5584
SAB68					0.9576	0.628	0.1349	0.8181	0.177	0.2041	0.02916	0.1178	0.06259	0.9406
SAB70V.B						0.6021	0.1081	0.6647	0.1373	0.4091	0.03494	0.03309	0.06185	0.6604
SAB70V.T							0.244	0.3843	0.3628	0.332	0.04432	0.1699	0.08284	0.7902
SAB74								0.1031	0.8808	0.6818	0.4248	0.6938	0.617	0.2549
SAB76									0.06529	0.1744	0.04104	0.09874	0.083	0.4329
SAB80										0.9845	0.2313	0.7257	0.4575	0.2878
SAB82											0.1267	0.4701	0.4209	0.2651
SAB84												0.7088	0.4958	0.05885
SAB86													0.9125	0.1663
SAB88														0.104

Table A4.34E: *O. aspinata* statistical results for the shell thickness from every bed within the angulata Zone from St Audrie's Bay using the Kruskal-Wallis and the Mann Whitney tests (Presented in Section 3.5.5).

angulata Zone		
H (chi ²)	8.437	
Hc (tie corrected)	8.437	
p(same)	0.01472	
	SAB96	SAB98
SAB94	0.382	0.005407
SAB96	0	0.04901

Table A4.35: Kruskal-Wallis and Mann Whitney results for the compiled *O. aspinata* shell thickness zone data in St Audrie's Bay (Presented in Section 3.5.5).

H (chi ²)	14.36	Hc (tie corrected)	14.36	p(same)	0.006226
	Pre-planorbis Zone	planorbis Zone	liasicus Zone	angulata Zone	
Lilstock Formation	0.7533	0.01198	0.5049	0.07917	
Pre-planorbis Zone		0.01354	0.268	0.04861	
planorbis Zone			0.002826	0.4774	
liasicus Zone				0.09089	

Table A4.36: Kruskal-Wallis and Mann Whitney results for the compiled *O. aspinata* shell thickness subzone data in St Audrie's Bay (Presented in Section 3.5.5).

H (chi ²)	27.95	Hc (tie corrected)	27.95	p(same)	0.0000962	
	Pre-planorbis Zone	Ps. planorbis	C. johnstoni	W. portlocki	Alsatites laqueus	Schlotheimia angulata
Lilstock Formation	0.7533	0.0000321	0.3259	0.08011	0.6072	0.07917
Pre-planorbis Zone		0.0001132	0.2014	0.07525	0.3146	0.04861
Ps. planorbis			0.001648	0.1018	0.00000480	0.009593
johnstoni				0.3354	0.3856	0.4922
W. portlocki					0.1069	0.6134
Alsatites laqueus						0.06329

Table A4.37: Geometric shell size data from both species compared against each other to determine any relationships in growth in St Audrie's Bay (Presented in Section 3.7).

Correlation question	Number of individuals	R ² value
mean <i>L. hisingeri</i> verses mean <i>O. aspinata</i> geometric size	4	0.9654
95th percentile range <i>L. hisingeri</i> verses the 95th percentile range <i>O. aspinata</i> geometric size	4	0.0271
95th percentile minimum <i>L. hisingeri</i> verses the 95th percentile minimum <i>O. aspinata</i> geometric size	4	0.0008
95th percentile maximum <i>L. hisingeri</i> verses the 95th percentile maximum <i>O. aspinata</i> geometric size	4	0.8364

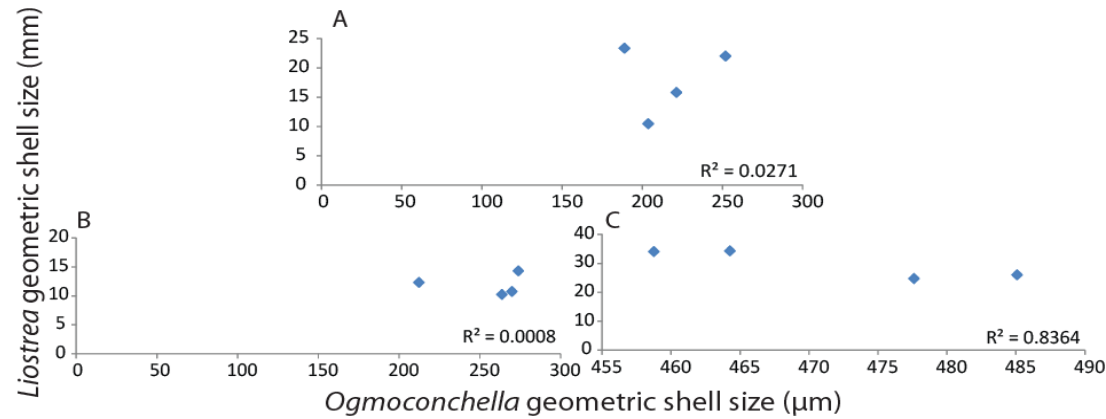


Figure A4.22: The (A) 95th percentile range, (B) 95th percentile minimum and (C) 95th percentile maximum for *L. hisingeri* and *O. aspinata* geometric size for each subzone, correlated against each other to determine any statistical correlation between the three species growth patterns at St Audrie's Bay (Presented in Section 3.5.5).

A4.3: Comparisons of fossil data between both locations

Table A4.38: Shows the mean, 95th percentile range, 95th percentile minimum and 95th percentile maximum geometric size for each subzone used in the linear regression models for *L. hisingeri* (Presented in Section 3.8.1).

<i>L. hisingeri</i> geometric size data collated into subzones										
	St Audrie's Bay	Lyme Regis	St Audrie's Bay	Lyme Regis	St Audrie's Bay	Lyme Regis	St Audrie's Bay	Lyme Regis	St Audrie's Bay	Lyme Regis
	Number of individuals		mean		95th percentile range		95th percentile min		95th percentile max	
Pre-planorbis Zone	247	132	22.31699	20.86932	21.98216	19.22775	12.32827	11.64113	34.31043	30.86888
Ps. planorbis	26	42	20.18873	19.61308	23.33341	18.99353	10.74482	10.49724	34.07822	29.49077
Johnstoni	13	96	18.78099	20.65216	10.43582	21.00375	14.30826	13.60115	24.74408	34.6049
Alsatites laqueus	3	143	18.31924	25.33606	15.79332	15.79167	10.24402	17.94497	26.03733	33.73664

Table A4.39: Shows the mean, 95th percentile range, 95th percentile minimum and 95th percentile maximum geometric size for each subzone used in the linear regression models for *O. aspinata* (Presented in Section 3.8.2).

<i>O. aspinata</i> geometric size data collated into subzones										
	St Audrie's Bay	Lyme Regis	St Audrie's Bay	Lyme Regis	St Audrie's Bay	Lyme Regis	St Audrie's Bay	Lyme Regis	St Audrie's Bay	Lyme Regis
	Number of individuals		mean		95th percentile range		95th percentile min		95th percentile max	
Pre-planorbis Zone	43	80	357.809	386.6178	251.9282	148.3244	212.3404	310.6749	464.2686	458.9993
Ps. planorbis	434	175	369.9164	369.152	188.8599	168.5198	269.9022	286.3071	458.762	454.8269
Johnstoni	619	438	388.0643	385.154	203.7103	182.1834	273.9014	274.6255	477.6117	456.8089
Portlocki	58	397	361.8209	390.1863	201.3239	202.7659	260.4051	272.4887	461.729	475.2546
Alsatites laqueus	2695	1085	390.7637	407.9975	221.3252	208.9942	263.7591	283.5985	485.0843	492.5926
Schlotheimia	363	1015	365.3365	397.3602	304.9524	268.7948	218.049	266.631	523.0014	535.4258

Table A4.40: Shows the mean, 95th percentile range, 95th percentile minimum and 95th percentile maximum shell thickness for each subzone used in the linear regression models for *O. aspinata* (Presented in Section 3.8.2).

<i>O. aspinata</i> shell thickness data collated into subzones										
	Lyme Regis	St Audrie's Bay	Lyme Regis	St Audrie's Bay	Lyme Regis	St Audrie's Bay	Lyme Regis	St Audrie's Bay	Lyme Regis	St Audrie's Bay
	Number of individuals		mean		95th percentile range		95th percentile min		95th percentile max	
Pre-planorbis Zone	47	27	31.79628	30.48463	32.05275	30.66425	16.20275	18.5395	48.2555	49.20375
Ps. planorbis	67	41	30.89179	20.75323	28.73725	18.125	15.92225	11.27	44.6595	29.395
Johnstoni	65	74	27.50038	26.78632	28.5625	33.59113	14.3365	10.77525	42.899	44.36638
Portlocki	63	22	31.15881	24.18455	32.17675	25.39988	14.766	11.65238	46.94275	37.05225
Alsatites laqueus	193	329	31.28409	28.13803	36.3185	30.8795	13.9905	13.9635	50.309	44.843
Schlotheimia	149	69	27.63281	25.74065	28.9865	30.806	13.9965	12.484	42.983	43.29

Table A4.41: Results using the Kruskal and Wallis statistical method to determine any significant difference between *L. hisingeri* geometric data from both locations (Presented in Section 3.8.1).

H (chi ²)	2.851		
Hc (tie corrected)	2.851		St Audrie's Bay
p(same)	0.0913	Lyme Regis	0.09133

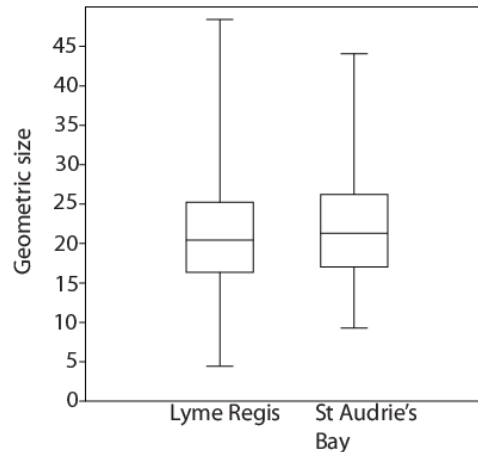


Figure A4.22: *L. hisingeri* geometric data from both locations displayed in a box plot (Presented in Section 3.8.1).

Table A4.42: Results using the Kruskal and Wallis statistical method to determine any significant difference between the zones of collated *L. hisingeri* geometric data for each location (Presented in Section 3.8.1).

Pre-planorbis Zone			
H (chi ²)	4.078		St Audrie's Bay
Hc (tie corrected)	4.078	Lyme Regis	0.04349
p(same)	0.04344		

Planorbis Zone			
H (chi ²)	0.2781		St Audrie's Bay
Hc (tie corrected)	0.2781	Lyme Regis	0.599
p(same)	0.598		

Table A4.43: Results using the Kruskal and Wallis statistical method to determine any significant difference between *L. hisingeri* geometric data for each location from the liasicus Zone (Presented in Section 3.8.1).

H (chi ²)	0.405		
Hc (tie corrected)	0.405		St Audrie's Bay
p(same)	0.5245	Lyme Regis	0.5276

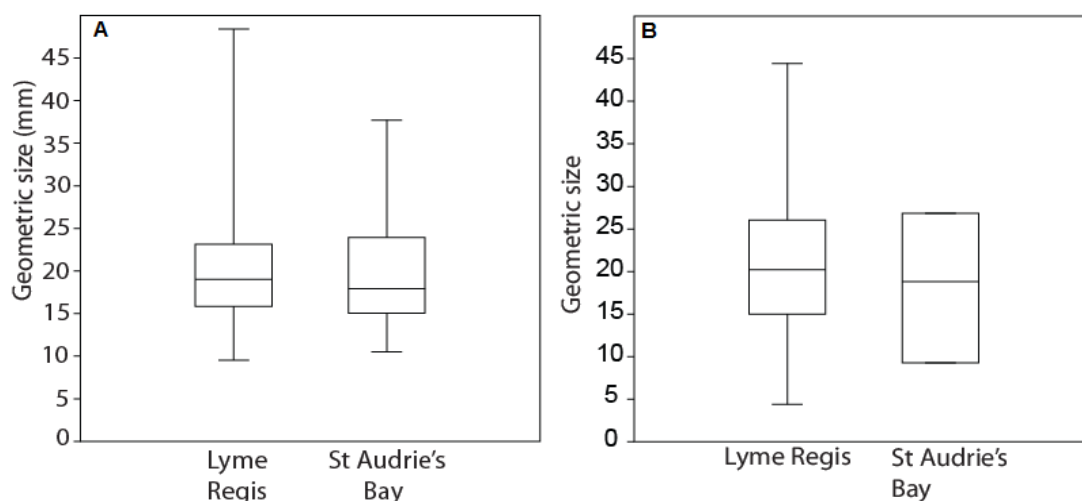


Figure A4.23: *L. hisingeri* geometric data for each location from the Planorbis Zone and liasicus Zone displayed in a box plot (Presented in Section 3.8.1).

Table A4.44: Results using the Kruskal and Wallis statistical method to determine any significant difference between *O. aspinata* geometric data from both locations (Presented in Section 3.8.2).

H (chi ²)	1.388		
Hc (tie corrected)	1.388		St Audrie's Bay
p(same)	0.2388	Lyme Regis	0.2388

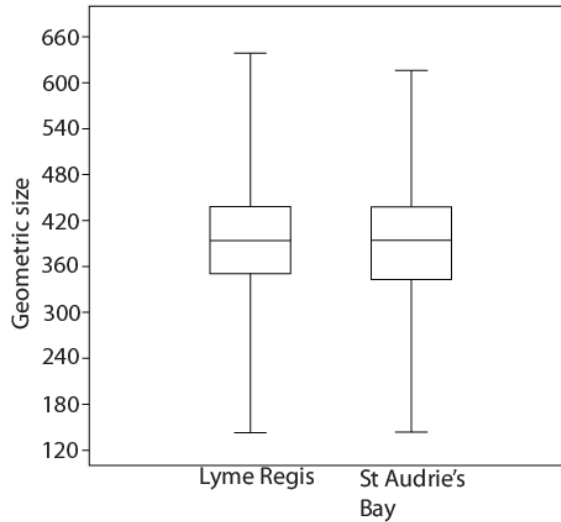


Figure A4.24: *O. aspinata* geometric data from both locations displayed in a box plot (Presented in Section 3.8.2).

Table A4.45: Results using the Kruskal and Wallis statistical method to determine any significant difference between the zones of collated *O. aspinata* geometric data for each location (Presented in Section 3.8.2).

lasicus Zone			
H (chi ²)	34.42		
Hc (tie corrected)	34.42		St Audrie's Bay
p(same)	0.0000000444	Lyme Regis	0.0000000444

angulata Zone			
H (chi ²)	32.45		
Hc (tie corrected)	32.45		St Audrie's Bay
p(same)	0.000000122	Lyme Regis	0.000000122

Table A4.46: Results using the Kruskal and Wallis statistical method to determine any significant difference between the *O. aspinata* geometric data for each location from the Pre-planorbis Zone and Planorbis Zone (Presented in Section 3.8.2).

Pre-planorbis Zone			
H (chi ²)	2.721		
Hc (tie corrected)	2.721		St Audrie's Bay
p(same)	0.09904	Lyme Regis	0.09958

Planorbis Zone			
H (chi ²)	0.03765		
Hc (tie corrected)	0.03765		St Audrie's Bay
p(same)	0.8461	Lyme Regis	0.8462

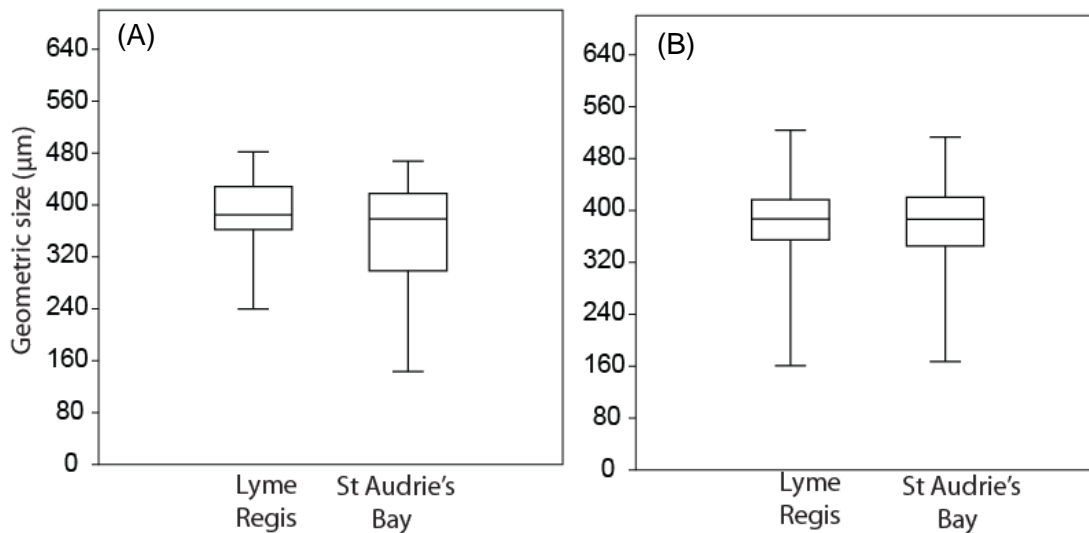


Figure A4.25: *O. aspinata* geometric data for each location from the (A) Pre-planorbis Zone and (B) Planorbis Zone displayed in box plots (Presented in Section 3.8.2).

Table A4.47: Results using the Kruskal and Wallis statistical method to determine any significant difference between the collated *O. aspinata* shell thickness data for each location (Presented in Section 3.8.2).

H (chi ²)	15.45		
Hc (tie corrected)	15.45		St Audrie's Bay
p(same)	0.0000846	Lyme Regis	0.0000846

Table A4.48: Results using the Kruskal and Wallis statistical method to determine any significant difference between the zones of collated *O. aspinata* shell thickness data for each location (Presented in Section 3.8.2).

Planorbis Zone			
H (chi ²)	14.87		
Hc (tie corrected)	14.87		St Audrie's Bay
p(same)	0.0001155	Lyme Regis	0.000116

liasicus Zone			
H (chi ²)	14.84		
Hc (tie corrected)	14.84		St Audrie's Bay
p(same)	0.000117	Lyme Regis	0.0001171

Table A4.49: Results using the Kruskal and Wallis statistical method to determine any significant difference between the zones of collated *O. aspinata* shell thickness data for each location (Presented in Section 3.8.2).

Pre-planorbis Zone			
H (chi ²)	0.4025		
Hc (tie corrected)	0.4025		St Audrie's Bay
p(same)	0.5258	Lyme Regis	0.5295

angulata Zone			
H (chi ²)	1.989		
Hc (tie corrected)	1.989		St Audrie's Bay
p(same)	0.1584	Lyme Regis	0.1588

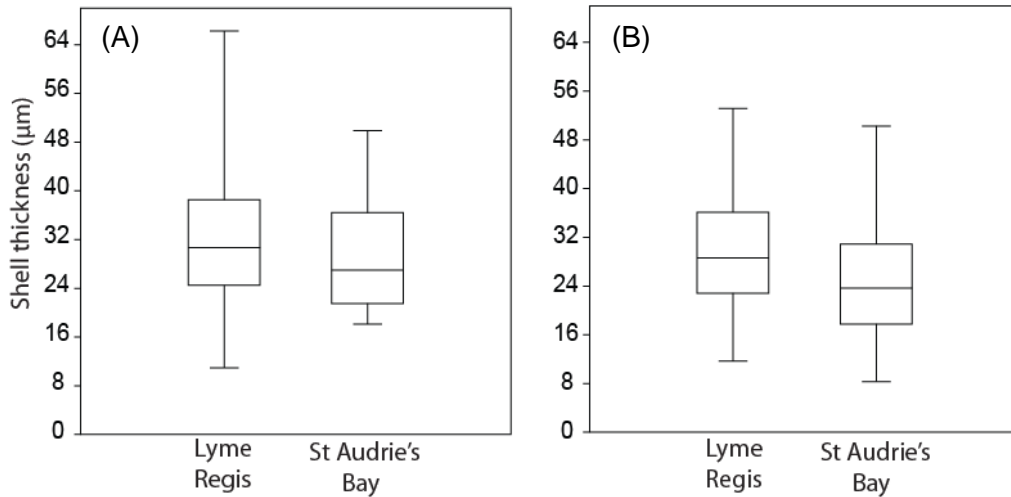


Figure A4.26: *O. aspinata* shell thickness data for each location from the (A) Pre-planorbis Zone and (B) angulata Zone displayed in box plots (Presented in Section 3.8.2).

Table A4.50: Results from a general linear model determining if the location or the age of the rocks is an important factor in the geometric size of *L. hisingeri* found (Presented in Section 3.8.1).

Tests of Between-Subjects Effects
Dependent Variable: *L. hisingeri*

Source	Type III Sum of Squares	df	Mean Square	F	Sig.
Corrected Model	538.196 ^a	5	107.639	2.417	.035
Intercept	39306.280	1	39306.280	882.522	.000
location	9.761	1	9.761	.219	.640
zones	245.601	2	122.800	2.757	.064
location * zones	134.612	2	67.306	1.511	.221
Error	33849.322	760	44.539		
Total	379610.131	766			
Corrected Total	34387.518	765			

Table A4.51: Results from a general linear model determining if the location or the age of the rocks is an important factor in the geometric size of *O. aspinata* found (Presented in Section 3.8.2).

Tests of Between-Subjects Effects
Dependent Variable: *O. aspinata*

Source	Type III Sum of Squares	df	Mean Square	F	Sig.
Corrected Model	728065.555 ^a	7	104009.365	22.378	.000
Intercept	217415750.468	1	217415750.468	46778.380	0.000
location2	126686.946	1	126686.946	27.258	.000
zones2	425290.947	3	141763.649	30.501	.000
location2 * zones2	169033.641	3	56344.547	12.123	.000
Error	34365706.232	7394	4647.783		
Total	1161876173.202	7402			
Corrected Total	35093771.787	7401			

Table A4.52: Results from a general linear model determining if the location or the age of the rocks is an important factor in the shell thickness of *O. aspinata* found (Presented in Section 3.8.2).

Tests of Between-Subjects Effects
Dependent Variable: *O. aspinata* shell thickness

Source	Type III Sum of Squares	df	Mean Square	F	Sig.
Corrected Model	5129.946 ^a	7	732.849	7.352	.000
Intercept	509259.058	1	509259.058	5108.615	0.000
location3	1211.161	1	1211.161	12.150	.001
zone3	2356.760	3	785.587	7.881	.000
location3 * zone3	292.953	3	97.651	.980	.402
Error	113143.990	1135	99.686		
Total	1048056.644	1143			
Corrected Total	118273.936	1142			

Table A4.53: Geometric shell size data from both species and both locations compared against each other to determine any relationships in growth between locations (Presented in Section 3.8).

Correlation question	Number of individuals	R ² value
Lyme Regis 95th percentile range of <i>L. hisingeri</i> geometric size data for each subzone verses the St Audrie's Bay 95th percentile range of <i>L. hisingeri</i> geometric size data for each subzone	4	0.0357
Lyme Regis 95th percentile minimum of <i>L. hisingeri</i> geometric size data for each subzone verses the St Audrie's Bay 95th percentile minimum of <i>L. hisingeri</i> geometric size data for each subzone	4	0.0609
Lyme Regis 95th percentile maximum of <i>L. hisingeri</i> geometric size data for each subzone verses the St Audrie's Bay 95th percentile maximum of <i>L. hisingeri</i> geometric size data for each subzone	4	0.9339
Lyme Regis mean of <i>L. hisingeri</i> geometric size data for each subzone verses the St Audrie's Bay mean of <i>L. hisingeri</i> geometric size data for each subzone	4	0.2759
Lyme Regis 95th percentile range of <i>O. aspinata</i> geometric size data for each subzone verses the St Audrie's Bay 95th percentile range of <i>O. aspinata</i> geometric size data for each subzone	6	0.3837
Lyme Regis 95th percentile minimum of <i>O. aspinata</i> geometric size data for each subzone verses the St Audrie's Bay 95th percentile minimum of <i>O. aspinata</i> geometric size data for each subzone	6	0.126
Lyme Regis 95th percentile maximum of <i>O. aspinata</i> geometric size data for each subzone verses the St Audrie's Bay 95th percentile maximum of <i>O. aspinata</i> geometric size data for each subzone	6	0.8427
Lyme Regis mean of <i>O. aspinata</i> geometric size data for each subzone verses the St Audrie's Bay mean of <i>O. aspinata</i> geometric size data for each subzone	6	0.1115
Lyme Regis 95th percentile minimum of <i>O. aspinata</i> shell thickness data for each subzone verses the St Audrie's Bay 95th percentile minimum of <i>O. aspinata</i> shell thickness data for each subzone	6	0.078
Lyme Regis 95th percentile range of <i>O. aspinata</i> shell thickness data for each subzone verses the St Audrie's Bay 95th percentile range of <i>O. aspinata</i> shell thickness data for each subzone	6	0.0443
Lyme Regis mean of <i>O. aspinata</i> shell thickness data for each subzone verses the St Audrie's Bay mean of <i>O. aspinata</i> shell thickness data for each subzone	6	0.0067
Lyme Regis 95th percentile minimum of <i>O. aspinata</i> shell thickness data for each subzone verses the St Audrie's Bay 95th percentile minimum of <i>O. aspinata</i> shell thickness data for each subzone	6	0.2151

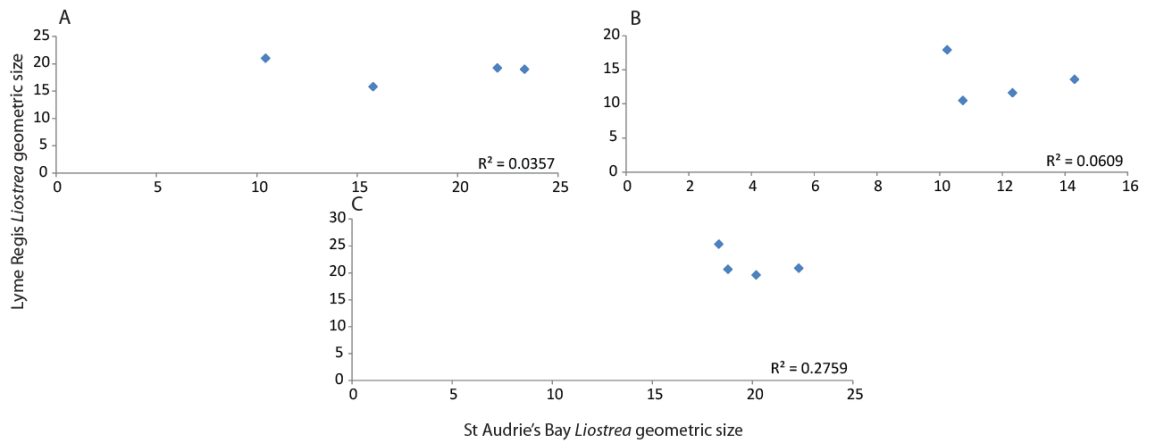


Figure A4.27: Shows if there was any correlation between locations for the *L. hisingeri*, (A) 95th percentile range, (B) 95th percentile minimum and (C) 95th percentile mean geometric size for each subzone (Presented in Section 3.8.1).

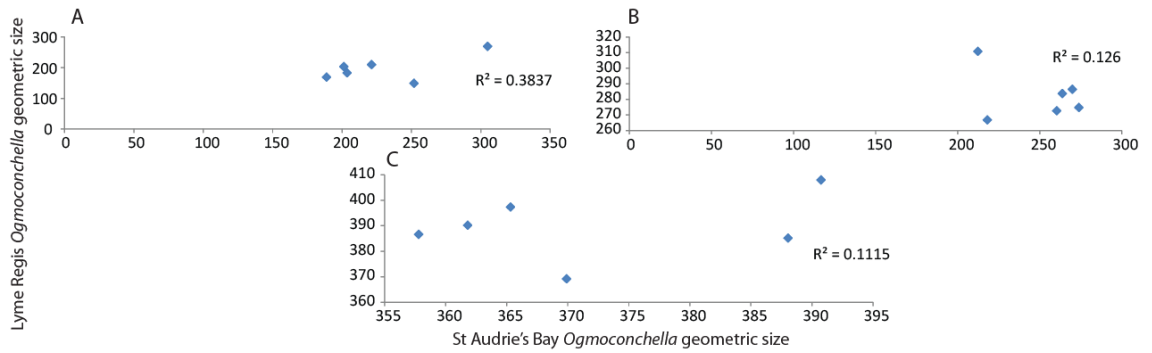


Figure A4.28: Shows if there was any correlation between locations for the *O. aspinata*, (A) 95th percentile range, (B) 95th percentile minimum and (C) 95th percentile mean geometric size for each subzone (Presented in Section 3.8.2).

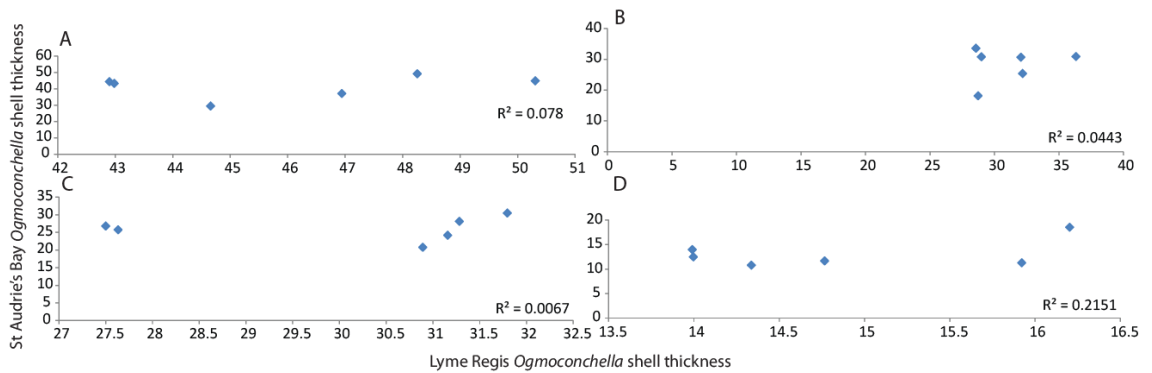


Figure A4.29: Shows if there was any correlation between locations for the *O. aspinata* (C) mean, (B) 95th percentile range, (D) 95th percentile minimum and (A) 95th percentile maximum shell thickness for each subzone (Presented in Section 3.8.2).

Appendix 5 – Raw isotope data collected from both locations and the corresponding analysis of the isotope results and $p\text{CO}_2$ data with the fossil size data (relates to Chapter 4)

A5.1: Raw isotope data from both locations

Table A5.1: Lyme Regis $\delta^{13}\text{C}$ and $\delta^{18}\text{O}$ results for *L. hisingeri*, *P. gigantea* and *O. aspinata* with corresponding bed heights (Presented in Section 4.3.2).

Lyme Regis				
Sample label	$\delta^{13}\text{C}$	Bed height for this study's logs (m)	$\delta^{18}\text{O}$	Bed height for this study's logs (m)
<i>O. aspinata</i>				
LRBLB33_05.raw	-0.50	12.85	-3.30	12.85
LRBLB37_05.raw	-0.61	13.37	-3.66	13.37
LRBLB39_05.raw	1.07	13.70	-3.06	13.70
LRBLB47_05.raw	0.73	15.30	-3.55	15.30
LRBLB51_05.raw	-0.63	16.80	-3.83	16.80
LRBLB53_05.raw	0.32	17.50	-3.33	17.50
LRBLB55_05.raw	-0.45	18.20	-4.71	18.20
LRBLB61_05.raw	1.35	19.60	-1.11	19.60
LRBLB69_05.raw	0.52	21.15	-3.17	21.15
LRBLB74A_05.raw	0.93	21.75	-2.75	21.75
LRBLB75A_05.raw	0.34	21.95	-2.94	21.95
LRBLB76A_05.raw	0.07	22.15	-3.44	22.15
LRBLB77A_05.raw	0.16	22.35	-2.58	22.35
LRBLB89_05.raw	-1.71	24.30	-3.64	24.30
LRBLB93_05.raw	0.21	25.25	-3.47	25.25
<i>P. gigantea</i>				
LRBLB23_P.raw	1.54	10.60	-1.74	10.60
LRBLB37_P.raw	1.09	13.37	-2.11	13.37
LRBLB49_P.raw	1.20	14.80	-1.89	14.80
LRBLB59_P.raw	1.27	19.35	-2.29	19.35
LRBLB61_P.raw	-1.99	19.60	-0.56	19.60
LRBLB63_P.raw	1.63	19.87	-2.66	19.87
LRBLB67_P.raw	-1.03	20.95	0.70	20.95
LRBLB69_P.raw	1.36	21.15	-2.12	21.15
LRBLB74A_P.raw	1.54	21.75	-1.74	21.75
LRBLB75A_P.raw	-0.06	21.95	0.43	21.95
LRBLB77A_P.raw	1.15	22.35	-1.49	22.35
LRBLB93_P.raw	0.84	25.25	-2.63	25.25
LRBLB95_P.raw	-0.94	25.64	-3.42	25.64
<i>L. hisingeri</i>				
LRBLB23_L.raw	0.90	10.60	-2.84	10.60
LRBLB37_L.raw	0.59	13.37	-2.76	13.37
LRBLB49_L.raw	1.63	14.80	-2.66	14.80
LRBLB55_L.raw	1.09	18.20	-2.11	18.20
LRBLB59_L.raw	1.87	19.35	-2.41	19.35
LRBLB61_L.raw	1.20	19.60	-1.89	19.60
LRBLB63_L.raw	1.21	19.87	-2.64	19.87
LRBLB67_L.raw	-2.76	20.95	0.00	20.95
LRBLB73_L.raw	0.95	21.55	-2.08	21.55
LRBLB74A_L.raw	0.75	21.75	-3.32	21.75
LRBLB76A_L.raw	0.99	22.15	-3.25	22.15
LRBLB95_L.raw	0.66	25.64	-2.51	25.64
LRBLB99_L.raw	0.90	26.75	-2.84	26.75
Bulk rock				
LRBLB1.raw	3.29	8.05	-3.30	8.05
LRBLB3.raw	1.56	8.50	-4.81	8.50
LRBLB11.raw	1.28	9.16	-4.01	9.16
LRBLB13.raw	1.57	9.48	-4.16	9.48
LRWLB14.raw	3.25	9.59	-3.76	9.59
LRBLB15.raw	1.48	9.60	-3.88	9.60

LRBLB17.raw	0.99	9.72	-3.69	9.72
LRBLB21.raw	0.29	10.30	-5.07	10.30
LRBLB23.raw	0.81	10.60	-4.87	10.60
LRBLB25.raw	0.95	10.70	-4.69	10.70
LRBLB27.raw	0.63	11.30	-4.78	11.30
LRBLB27T.raw	-0.09	11.50	-4.75	11.50
LRBLB29.raw	-0.58	12.05	-3.01	12.05
LRBLB31.raw	-0.52	12.30	-3.49	12.30
LRBLB33.raw	-0.45	12.85	-4.16	12.85
LRBLB35.raw	-0.42	13.05	-2.52	13.05
LRBLB37.raw	-0.56	13.37	-3.36	13.37
LRBLB39.raw	-0.87	13.70	-5.23	13.70
LRBLB49.raw	-0.68	14.80	-5.77	14.80
LRBLB49.raw	-0.21	14.80	-5.40	14.80
LRBLB51B.raw	-1.20	16.80	-5.19	16.80
LRBLB51.raw	-1.78	16.80	-4.77	16.80
LRBLB53.raw	-0.87	17.50	-4.96	17.50
LRBLB61.raw	-1.08	19.60	-5.18	19.60
LRBLB67.raw	-1.19	20.95	-4.28	20.95
LRBLB69.raw	-0.94	21.15	-3.42	21.15
LRBLB74A.raw	-0.90	21.75	-4.31	21.75
LRBLB75A.raw	-0.94	21.95	-4.11	21.95
LRBLB76A.raw	-1.47	22.15	-4.52	22.15
LRBLB76A.raw	0.59	22.15	-2.76	22.15
LRBLB77A.raw	-1.14	22.35	-4.35	22.35
LRBLB93.raw	-1.05	25.25	-4.32	25.25
LRBLB95.raw	-0.65	25.64	-3.82	25.64
LRBLB97.raw	-0.70	26.15	-3.89	26.15
LRBLB99.raw	-0.89	26.75	-4.63	26.75

Table A5.2: St Audrie's Bay $\delta^{13}\text{C}$ and $\delta^{18}\text{O}$ results for *L. hisingeri*, *P. gigantea* and *O. aspinata* with corresponding bed heights (Presented in Section 4.3.2).

St Audrie's Bay				
	$\delta^{13}\text{C}$	Bed height for this study's logs (m)	$\delta^{18}\text{O}$	Bed height for this study's logs (m)
<i>O. aspinata</i>				
SAB 11_05.raw	-2.74	12.50	-6.62	12.50
SAB30 05.raw	-2.42	18.70	-6.62	18.70
SAB64 05.raw	-0.04	48.90	-4.73	48.90
SAB70V B 05.raw	-0.14	49.80	-5.27	49.80
SAB70V T 05.raw	-0.29	50.60	-5.00	50.60
SAB74 05.raw	0.14	53.05	-5.53	53.05
SAB76 05.raw	0.16	53.60	-4.48	53.60
SAB80 05.raw	0.51	55.50	-4.34	55.50
SAB82 05.raw	0.11	55.70	-4.62	55.70
SAB90 05.raw	0.39	57.30	-3.56	57.30
<i>P. gigantea</i>				
SAB 40_P.raw	0.60	23.20	-2.59	23.20
SAB 47_P.raw	2.26	24.85	-1.59	24.85
SAB 52_P.raw	0.84	26.50	-2.63	26.50
SAB 53_P.raw	0.88	26.58	-1.37	26.58
SAB 62_P.raw	0.32	47.00	-8.57	47.00
SAB 64_P.raw	1.11	48.90	-2.50	48.90
SAB 66_P.raw	0.90	49.30	-2.28	49.30
SAB 68_P.raw	1.33	49.44	-1.98	49.44
SAB 70V_B_P.raw	0.75	49.80	-3.32	49.80
SAB 70V_T_P.raw	1.25	50.60	-2.55	50.60
SAB 74_P.raw	1.17	53.05	-2.62	53.05
SAB 76_P.raw	1.21	53.60	-2.64	53.60
SAB 80_P.raw	0.90	55.50	-3.38	55.50
SAB 84_P.raw	0.87	56.65	-2.55	56.65
SAB 98_P.raw	1.45	62.50	-2.73	62.50
<i>L. hisingeri</i>				
SAB 40_L.raw	-1.07	23.20	-6.65	23.20
SAB 47_L.raw	1.29	24.85	-3.08	24.85
SAB 62_L.raw	0.31	47.00	-5.77	47.00
SAB 64_L.raw	0.39	48.90	-3.40	48.90

SAB 66_L.raw	0.23	49.30	-4.24	49.30
SAB 68_L.raw	0.99	49.44	-3.25	49.44
SAB 74_L.raw	0.36	53.05	-5.22	53.05
SAB 84_L.raw	0.76	56.65	-3.38	56.65
SAB 94_L.raw	0.66	59.85	-2.51	59.85
Bulk rock				
SABWM1.raw	-3.11	0.10	1.13	0.10
SAB WM2.raw	-1.03	0.30	0.70	0.30
SAB WM3.raw	-1.99	0.60	-0.56	0.60
SAB WM4.raw	-0.06	0.70	0.43	0.70
SAB WM5.raw	-2.76	1.00	0.00	1.00
SABWM7.raw	-9.37	1.40	-2.45	1.40
SABCM1.raw	-4.05	10.20	-4.12	10.20
SABCM2.raw	-3.90	10.60	-7.24	10.60
SAB6.raw	-2.81	12.00	-3.32	12.00
SAB8.raw	-0.47	12.20	-2.51	12.20
SAB13.raw	-2.33	13.80	-4.35	13.80
SAB15.raw	0.47	14.30	-4.28	14.30
SAB17_12CM.raw	-2.16	15.00	-7.37	15.00
SAB17_30CM.raw	0.24	15.30	-6.34	15.30
SAB18A_5CM.raw	-1.75	15.45	-6.07	15.45
SAB20.raw	-0.01	15.80	-4.02	15.80
SAB22.raw	1.10	16.30	-5.36	16.30
SAB 23.raw	2.26	16.50	-1.59	16.50
SAB 25.raw	1.29	16.90	-3.08	16.90
SAB 26.raw	1.87	17.40	-2.41	17.40
SAB30.raw	-1.94	18.70	-6.61	18.70
SAB34.raw	-0.85	19.80	-5.64	19.80
SAB 40.raw	-2.74	23.20	-5.79	23.20
SAB 42.raw	1.36	23.80	-2.12	23.80
SAB 44.raw	-1.91	24.30	-5.00	24.30
SAB 47.raw	-1.56	24.85	-5.20	24.85
SAB 48.raw	1.11	24.92	-2.50	24.92
SAB 52.raw	1.45	26.50	-2.73	26.50
SAB 53.raw	1.23	26.58	-2.43	26.58
SAB 62.raw	-1.15	47.00	-5.39	47.00
SAB 66.raw	-1.12	49.30	-5.27	49.30
SAB 68.raw	0.32	49.44	-8.57	49.44
SAB 69.raw	-1.01	49.50	-4.96	49.50
SAB 70V_B.raw	1.15	49.80	-1.49	49.80
SAB 72.raw	0.95	52.30	-2.08	52.30
SAB74.raw	-0.69	53.05	-5.98	53.05
SAB 76.raw	-0.57	53.60	-4.95	53.60
SAB 80.raw	-0.77	55.50	-4.68	55.50
SAB 82.raw	0.31	55.70	-5.77	55.70
SAB 84.raw	-0.80	56.65	-4.54	56.65
SAB 86.raw	-1.04	56.95	-4.35	56.95
SAB 88.raw	1.27	57.20	-2.29	57.20
SAB 90.raw	-1.25	57.30	-4.51	57.30
SAB 94.raw	-1.97	59.85	-5.15	59.85
SAB 96.raw	-2.01	61.80	-5.05	61.80
SAB 98.raw	-0.69	62.50	-5.05	62.50

A5.2: Raw mineralogical results from both locations

Table A5.3: St Audrie's Bay mineralogical results for *L. hisingeri*, *P. gigantea* and *O. aspinata* with corresponding bed heights (Presented in Section 4.3.3).

Bed height (m)	Mass (mg)	Volume of solution (mL)	Mg/Ca (nmol/mol)	Fe ($\mu\text{g g}^{-1}$)	Mn ($\mu\text{g g}^{-1}$)
St Audrie's Bay					
<i>O. aspinata</i>					
12.2	0.3	2.0	19.7	135.4	598.7
12.5	0.4	2.0	22.6	132.9	112.3
18.7	0.2	2.0	15.2	91.9	107.4
18.7	0.2	2.0	15.7	167.5	100.2
23.2	0.5	2.0	17.9	148.3	113.1

Bed height (m)	Mass (mg)	Volume of solution (mL)	Mg/Ca (nmol/mol)	Fe ($\mu\text{g g}^{-1}$)	Mn ($\mu\text{g g}^{-1}$)
23.8	0.4	2.0	28.8	169.2	109.9
26.5	0.3	2.0	40.0	214.5	113.2
47.0	0.4	2.0	38.1	153.2	211.5
48.9	0.6	2.0	33.9	178.7	111.9
49.3	0.3	2.0	32.8	172.9	212.2
49.4	0.2	2.0	28.5	172.7	224.8
49.8	0.3	2.0	28.7	176.3	82.8
50.6	0.5	2.0	32.1	217.5	92.4
53.1	0.3	2.0	26.4	197.0	79.6
53.6	0.4	2.0	24.6	287.8	99.7
55.5	0.2	2.0	37.2	431.7	149.9
55.7	0.4	2.0	21.6	140.0	105.4
56.7	0.3	2.0	36.1	172.3	116.3
57.0	0.3	2.0	37.7	148.3	213.3
57.2	0.2	2.0	31.7	167.6	113.9
57.3	0.3	2.0	25.5	240.5	81.6
59.9	0.3	2.0	20.3	130.8	209.6
<i>L. hisingeri</i>					
24.9	0.7	10.0	9.4	161.9	105.2
26.6	1.9	10.0	8.5	121.5	206.8
47.0	0.7	10.0	23.2	104.4	93.5
48.9	1.5	10.0	22.6	114.9	97.4
49.4	0.7	10.0	18.1	135.8	51.5
56.7	1.1	10.0	18.8	89.0	122.7
59.9	0.7	10.0	11.4	144.9	120.0
<i>P. gigantea</i>					
24.9	1.0	10.0	11.5	116.4	296.8
26.5	0.8	10.0	14.7	178.4	273.1
26.6	1.5	10.0	10.8	233.0	53.6
47.0	1.7	10.0	15.3	139.8	414.1
48.9	1.2	10.0	13.9	161.0	378.2
49.3	1.0	10.0	14.6	237.3	120.4
49.4	1.7	10.0	11.9	224.4	107.3
50.6	2.6	10.0	10.6	344.6	74.2
53.1	1.0	10.0	15.6	143.0	95.9
53.6	1.5	10.0	9.8	469.6	69.1
56.7	0.6	10.0	14.2	150.7	97.5
62.5	0.2	10.0	9.2	148.9	105.8

Table A5.4: Lyme Regis mineralogical results for *L. hisingeri*, *P. gigantea* and *O. aspinata* with corresponding bed heights (Presented in Section 4.3.3).

Bed height (m)	Mass (mg)	Volume of solution (mL)	Mg/Ca (nmol/mol)	Fe ($\mu\text{g g}^{-1}$)	Mn ($\mu\text{g g}^{-1}$)
Lyme Regis					
<i>O. aspinata</i>					
10.6	0.1	2.0	20.6	222.6	118.1
12.9	0.2	2.0	28.0	142.6	289.3
13.4	0.2	2.0	19.5	155.6	461.5
13.7	0.1	2.0	16.9	132.3	375.9
15.3	0.5	2.0	17.6	252.1	107.2
16.8	0.2	2.0	17.1	783.5	88.9
17.5	0.1	2.0	16.2	171.4	57.4
18.2	0.2	2.0	16.1	253.6	43.2
19.6	0.3	2.0	16.7	149.5	48.0
21.0	0.1	2.0	19.4	195.0	111.0
21.2	0.1	2.0	24.3	197.8	42.9
21.8	0.1	2.0	19.7	167.9	60.4
22.0	0.1	2.0	18.4	176.0	90.8
22.2	0.1	2.0	287.0	218.1	37.9
22.4	0.2	2.0	20.9	167.8	578.7
24.3	0.3	2.0	17.7	221.3	81.6
25.3	0.3	2.0	28.8	141.5	535.2
<i>L. hisingeri</i>					
10.6	1.1	10.0	10.2	158.7	61.9
13.4	1.9	10.0	10.9	218.7	87.3

Bed height (m)	Mass (mg)	Volume of solution (mL)	Mg/Ca (nmol/mol)	Fe ($\mu\text{g g}^{-1}$)	Mn ($\mu\text{g g}^{-1}$)
14.8	1.5	10.0	7.1	116.0	154.0
18.2	1.6	10.0	6.6	111.2	97.4
19.4	0.8	10.0	6.7	431.9	70.4
19.6	1.0	10.0	7.5	117.2	88.5
19.9	1.2	10.0	6.3	219.1	98.1
21.0	1.0	10.0	8.0	230.6	87.5
21.6	1.2	10.0	9.2	220.1	96.9
21.8	1.2	10.0	10.5	98.8	144.8
22.2	1.2	10.0	9.9	117.3	98.2
22.4	1.1	10.0	14.7	125.9	204.5
25.3	1.3	10.0	7.2	115.4	132.7
25.6	1.1	10.0	9.8	122.2	202.3
<i>P. gigantea</i>					
10.6	0.7	10.0	10.1	315.5	228.5
13.4	1.4	10.0	13.3	130.1	49.0
14.8	0.9	10.0	7.4	222.0	85.0
19.4	1.3	10.0	9.8	232.3	78.4
19.6	1.6	10.0	9.2	124.6	73.6
19.9	1.3	10.0	8.0	135.6	86.3
21.0	1.4	10.0	7.9	328.7	200.2
21.2	1.6	10.0	9.7	131.9	74.8
21.6	1.5	10.0	7.1	118.3	138.9
21.8	1.4	10.0	10.6	116.7	93.5
22.2	1.3	10.0	11.0	115.7	223.0
22.4	1.6	10.0	9.7	231.9	84.3
25.3	1.4	10.0	10.7	339.6	69.7
25.6	1.2	10.0	9.0	132.4	326.2

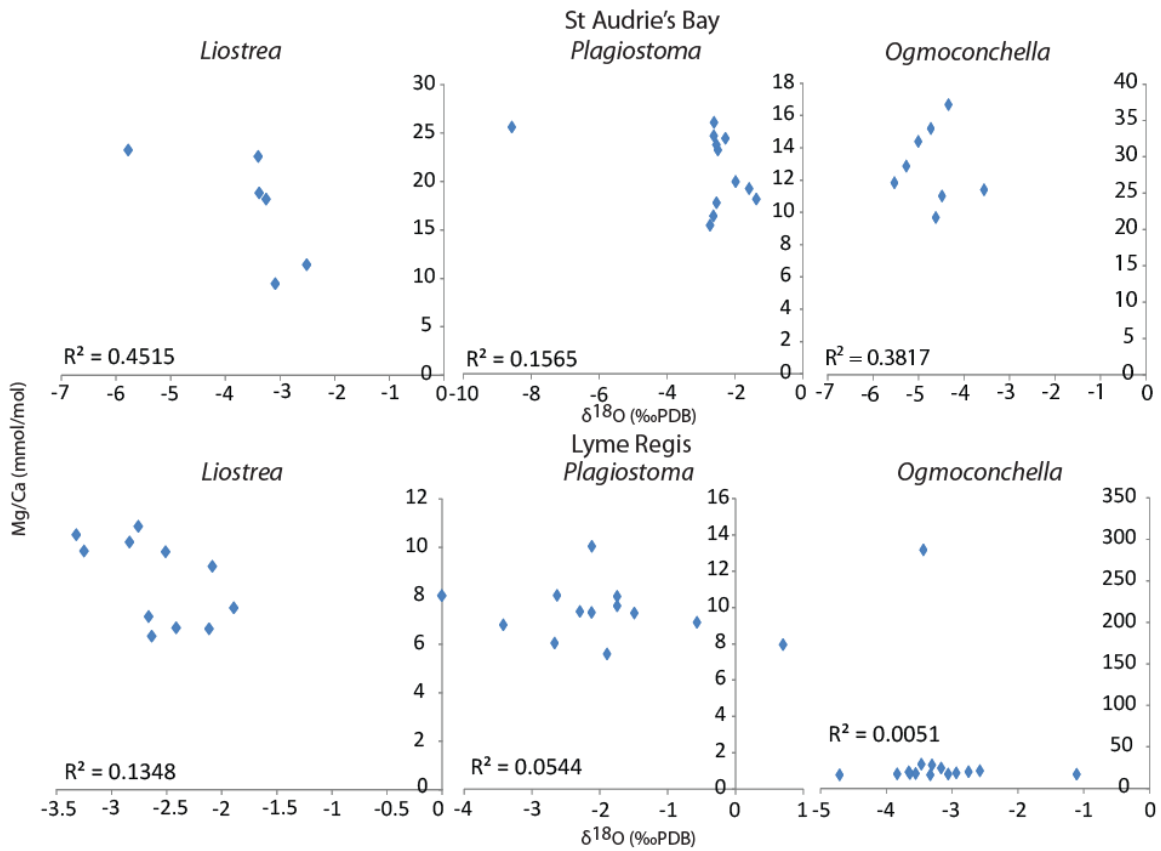


Figure A5.1a: Cross-plots of the Mg/Ca concentrations and $\delta^{18}\text{O}$ data for Lyme Regis and St Audrie's Bay showing no significant relationships (Presented in Section 4.3.7).

A5.3: Tables of the temperature data from Lyme Regis or St Audrie's Bay that corresponds with the available $p\text{CO}_2$ results.

Table A5.5: The McElwain *et al.* (1999) $p\text{CO}_2$ results and corresponding St Audrie's Bay temperature data from this study as well as previously published data. These corresponding data points are used in the linear regression models to determine any relationships between the $p\text{CO}_2$ results and temperature results (Presented in Section 4.5).

McElwain <i>et al.</i> (1999)				Temperature data from this study						Van de Schootbrugge <i>et al.</i> (2007) oyster		Korte <i>et al.</i> (2009) oysters	
				<i>L. hisingeri</i>		<i>P. gigantea</i>		Bulk rock					
St Audrie's Bay Bed Height (m)	Greenland $p\text{CO}_2$ ppm			temp value (°C)	St Audrie's Bay Bed Height (m)	temp value (°C)	St Audrie's Bay Bed Height (m)	temp value (°C)	St Audrie's Bay Bed Height (m)	temp value (°C)	St Audrie's Bay Bed Height (m)	temp value (°C)	St Audrie's Bay Bed Height (m)
	max	min	mean										
16	2058	1544	1801					35.5	16.3	12.2	16.1	16	16.8
43	1014	761	887	37.7	47								
St Audrie's Bay Bed Height (m)	Sweden $p\text{CO}_2$ ppm			temp value (°C)	St Audrie's Bay Bed Height (m)	temp value (°C)	St Audrie's Bay Bed Height (m)	temp value (°C)	St Audrie's Bay Bed Height (m)	temp value (°C)	St Audrie's Bay Bed Height (m)	temp value (°C)	St Audrie's Bay Bed Height (m)
	max	min	mean										
10.7	1386	1040	1213					45.7	10.6			11.9	11.7
23.8	2334	1751	2042	24.3	24.85	22	23.2	19.9	23.8			14.7	24.3
29.6	1980	1485	1733									18.9	28.2
31.6	678	509	593									18.6	32.8

Table A5.6: The McElwain *et al.* (1999) $p\text{CO}_2$ results and corresponding Lyme Regis temperature data from this study as well as previously published data. These corresponding data points are used in the linear regression models to determine any relationships between the $p\text{CO}_2$ results and temperature results (Presented in Section 4.5).

McElwain <i>et al.</i> (1999)				Temperature data from this study					
				<i>O. aspinata</i>		<i>P. gigantea</i>		<i>L. hisingeri</i>	
Lyme Regis Bed Height (m)	Greenland $p\text{CO}_2$ ppm			temp value (°C)	Lyme Regis Bed Height (m)	temp value (°C)	Lyme Regis Bed Height (m)	temp value (°C)	Lyme Regis Bed Height (m)
	mean	min	max						
0	698	599	798						
9.72	1801	1544	2058			18.3	10.6	23.1	10.6
15.3	1559	1337	1782	26.5	15.3	18.9	14.8	22.3	14.8
16	887	761	1014	27.8	16.8				
Lyme Regis Bed	Sweden $p\text{CO}_2$ ppm								

McElwain <i>et al.</i> (1999)				Temperature data from this study					
				Greenland $p\text{CO}_2$ ppm		<i>O. aspinata</i>		<i>P. gigantea</i>	
Lyme Regis Bed Height (m)	mean	min	max	temp value (°C)	Lyme Regis Bed Height (m)	temp value (°C)	Lyme Regis Bed Height (m)	temp value (°C)	Lyme Regis Bed Height (m)
0	1213	1040	1386						
12.6	2042	1751	2334	25.3	12.85	19.9	13.37	22.8	13.37
15	1733	1485	1980			18.9	14.8	22.3	14.8
15.22	593	509	678	26.5	15.3				

Table A5.7: The Schaller *et al.* (2011) $p\text{CO}_2$ results and corresponding St Audrie's Bay temperature data from this study as well as previously published data. These corresponding data points are used in the linear regression models to determine any relationships between the $p\text{CO}_2$ results and temperature results (Presented in Section 4.5).

Schaller <i>et al.</i> (2011)				Temperature data from this study								Van de Schootbrugge <i>et al.</i> (2007) oyster		Korte <i>et al.</i> (2009) oysters	
				Newark Basin			<i>L. hisingeri</i>		<i>P. gigantea</i>		<i>O. aspinata</i>		Bulk rock		temp value (°C)
St Audrie's Bay bed height	mean	min	max	temp value (°C)	St Audrie's Bay Bed Height (m)	temp value (°C)	St Audrie's Bay Bed Height (m)	temp value (°C)	St Audrie's Bay Bed Height (m)	temp value (°C)	St Audrie's Bay Bed Height (m)	temp value (°C)	St Audrie's Bay Bed Height (m)	temp value (°C)	St Audrie's Bay Bed Height (m)
10.5	4228.0	2818.8	5637.2							45.7	10.6			12.7	11.7
13.6	3584.0	2389.5	4778.5							30.3	13.8			15.3	13.6
18.0	3577.0	2384.8	4769.2							21.2	17.4	14.5	17.7	18.5	17.1
18.3	3453.0	2302.1	4603.9							42.2	18.7			13.9	17.2
Preakness Basalt															
19.3	4070.0	2713.5	5426.5									13.9	19.6		
19.3	4234.0	2822.8	5645.2									13.8	19.6		
19.8	3657.0	2438.1	4875.9							37.0	19.8	14.7	19.7	15.5	19.8
19.8	4015.0	2676.8	5353.2							37.0	19.8	14.7	19.7	15.4	19.8
20.0	3014.0	2009.4	4018.6											18.3	20.0
22.0	3460.0	2306.8	4613.2											17.1	22.4
23.7	2642.0	1761.4	3522.6			22.0	23.2			19.9	23.8			14.7	24.3
25.3	3708.0	2472.1	4943.9	24.3	24.9	22.2	26.5			21.6	24.9			16.9	25.3
27.7	2356.0	1570.7	3141.3			16.7	26.6			21.3	26.6			18.5	27.8
Hook Mountain Basalt															
31.3	5273.0	3515.5	7030.5											19.3	32.0
31.3	4941.0	3290.2	6591.8											19.3	32.0
48.0	3131.0	2087.4	4174.6	25.7	48.9	21.6	48.9	32.2	48.9	35.6	47.0				
53.0	2496.0	1664.1	3327.9	34.7	53.1	22.1	53.1	36.4	53.1	38.7	53.1				

Steinthorsdottir <i>et al.</i> (2011)							Temperature data from this study					Van de Schootbrugge <i>et al.</i> (2007) oyster		Korte <i>et al.</i> (2009) oysters	
							<i>L. hisingeri</i>		<i>P. gigantea</i>		Bulk rock				
St Audrie's Bay Bed Height (m)	Larne $p\text{CO}_2$ ppm carboniferous standard			Larne $p\text{CO}_2$ ppm modern standard											
	max	min	mean	max	Min	mean									
11.4	2116	1616	1866	1375	1051	1213			45.7	10.6			12.7	11.7	
13.6	2675	1471	2073	1738	956	1347			30.3	13.8			13.8	13.6	
15.5	2429	1903	2166	1579	1237	1408			39.3	15.45	16.6	15.1	12.9	15.5	
17	2010	1318	1664	1307	857	1082			24.3	16.9	16.5	17.2	18.5	17.1	
22	1874	1062	1468	1218	690	954		22	23.2	37.7	23.2	14.7	19.68	15.7	22.4

Table A5.10: The Steinthorsdottir *et al.* (2011) $p\text{CO}_2$ results and corresponding Lyme Regis temperature data from this study and previously published data. These corresponding data points are used in the linear regression models to determine any relationships between the $p\text{CO}_2$ results and temperature results (Presented in Section 4.5).

Steinthorsdottir <i>et al.</i> (2011)							Temperature data from this study					
							<i>O. aspinata</i>		<i>P. gigantea</i>		<i>L. hisingeri</i>	
Lyme Regis Bed Height (m)	Astartekloft $p\text{CO}_2$ ppm carboniferous standard			Astartekloft $p\text{CO}_2$ ppm modern standard			temp value (°C)	Lyme Regis Bed Height (m)	temp value (°C)	Lyme Regis Bed Height (m)	temp value (°C)	Lyme Regis Bed Height (m)
	mean	min	max	Mean	min	max						
0	932	625	1239	606	406	806						
9.72	1673	1422	1924	1087	924	1250			18.3	10.6	23.1	10.6
15.3	2184	1955	2413	1420	1271	1569	26.5	15.3	18.9	14.8	22.3	14.8
16	1354	1092	1616	880	710	1050	27.8	16.8				
Lyme Regis Bed Height (m)	Larne $p\text{CO}_2$ ppm carboniferous standard			Larne $p\text{CO}_2$ ppm modern standard								
	max	min	mean	Max	min	mean						
8.2	2073	1471	2675	1347	956	1738						
9.4	2166	1903	2429	1408	1237	1579						
10	1664	1318	2010	1082	857	1307			18.3	10.6	23.1	10.6
12.3	1468	1062	1874	954	690	1218	25.3	12.85	19.9	13.37	22.8	13.37

A5.3.2: Linear regression models demonstrating there were no significant relationships between the temperature data from Lyme Regis or St Audrie's Bay and the available corresponding $p\text{CO}_2$ results.

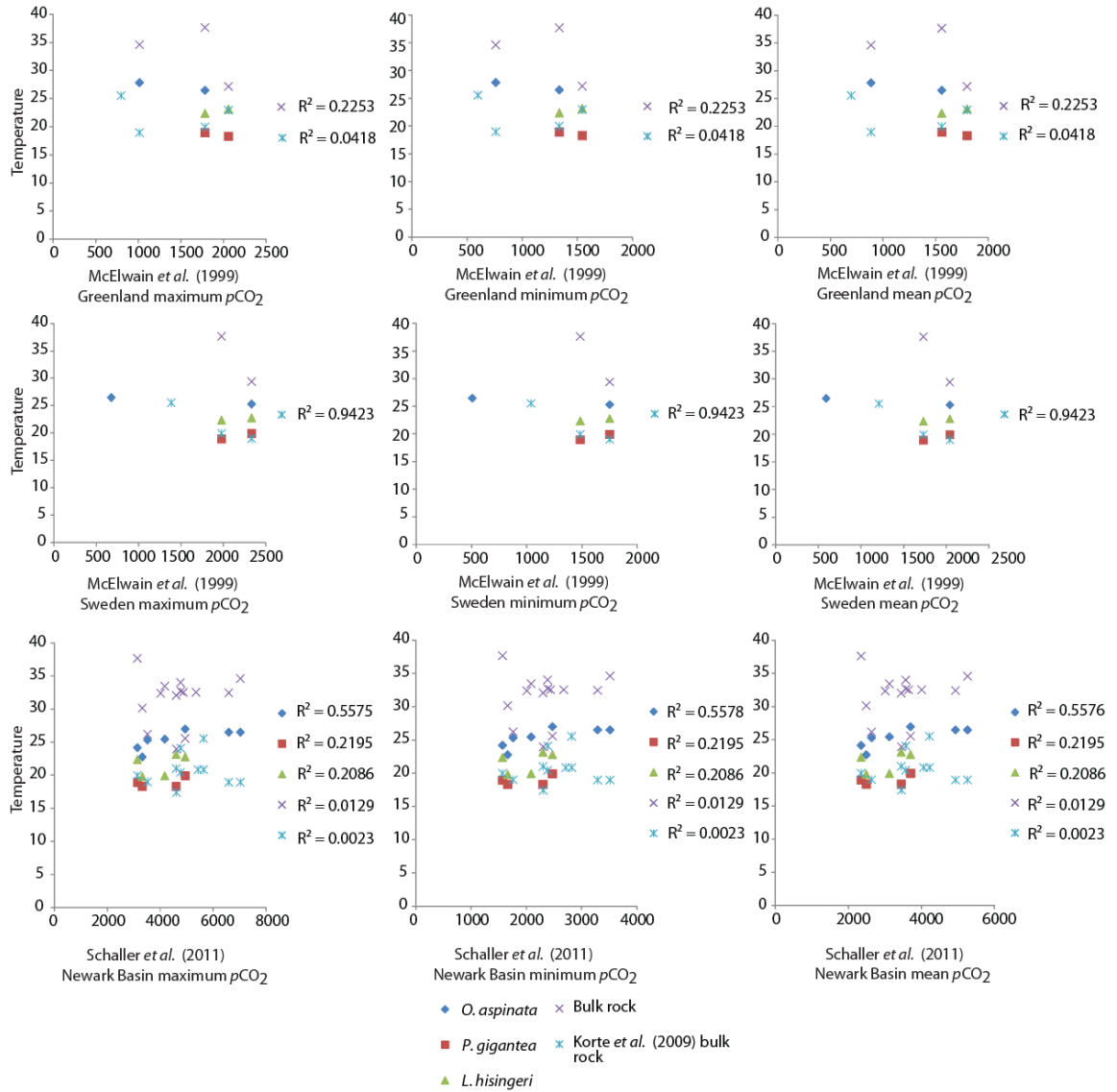


Figure A5.1: Linear regression models showing no significant relationships between the McElwain *et al.* (1999) or Schaller *et al.* (2011) $p\text{CO}_2$ results and corresponding Lyme Regis temperature data from this study as well as previously published data (Presented in Section 4.5).

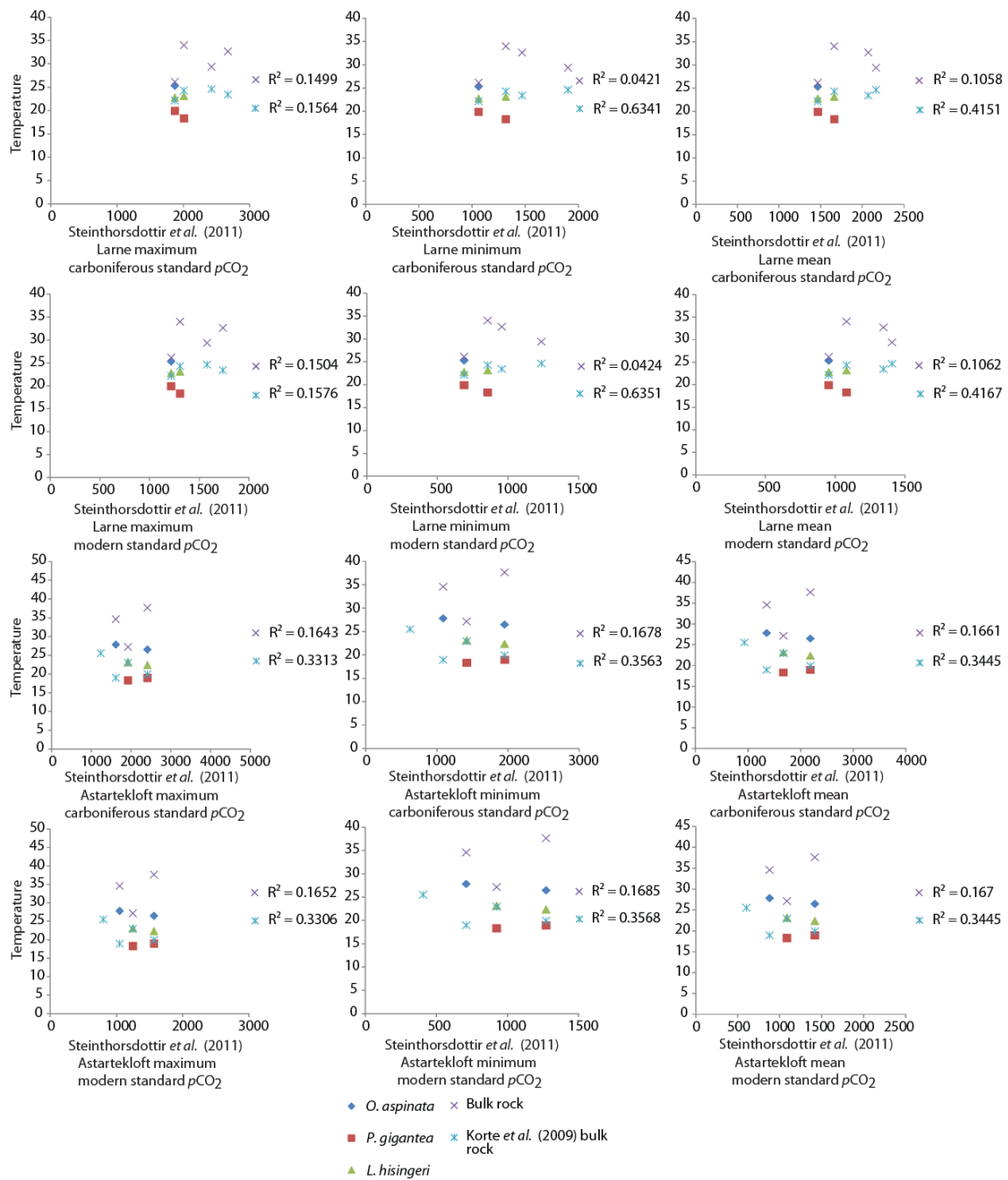


Figure A5.2: Linear regression models showing no significant relationships between the Steinthorsdottir *et al.* (2011) pCO₂ results and corresponding Lyme Regis temperature data from this study as well as previously published data (Presented in Section 4.5).

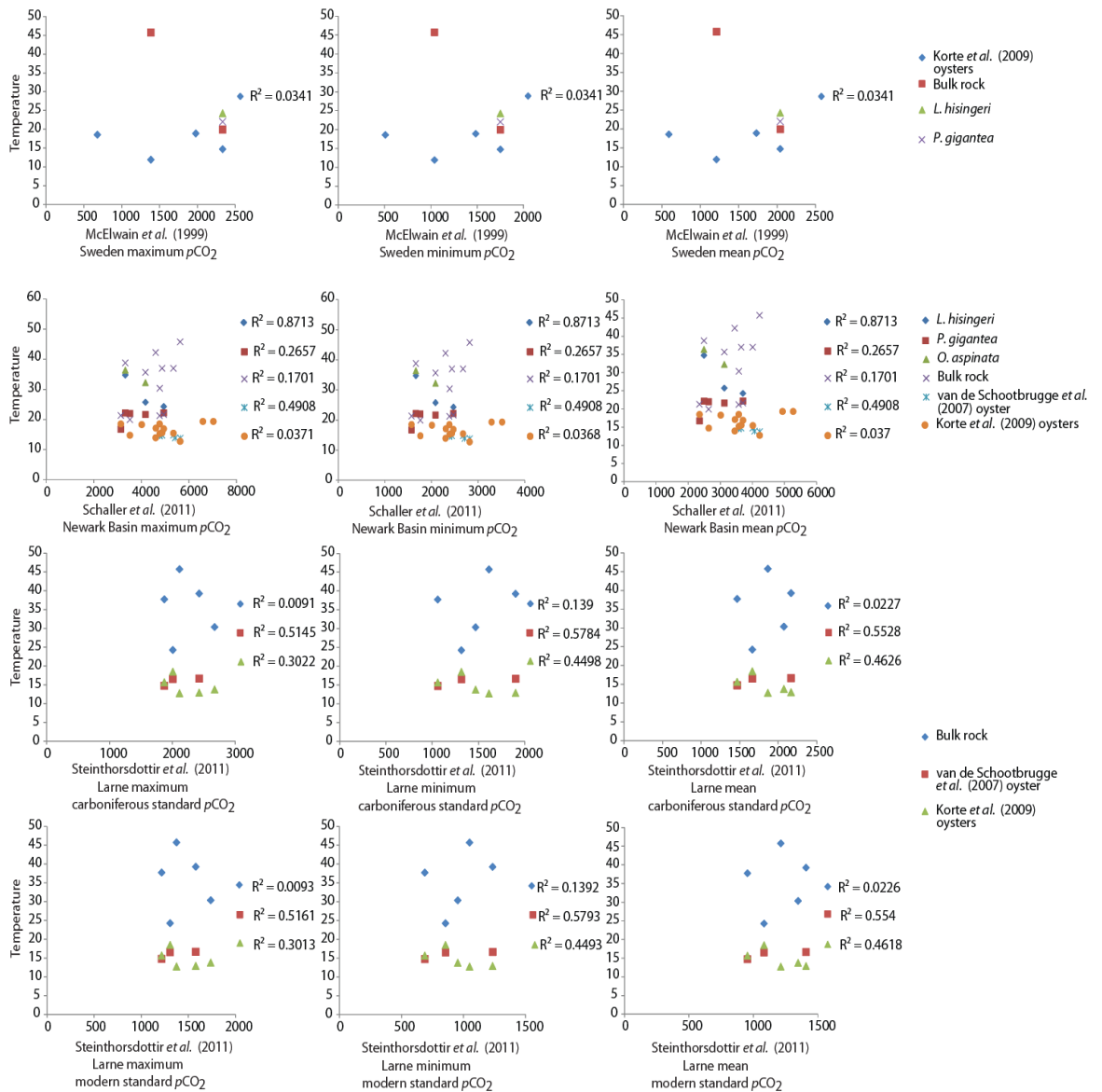


Figure A5.3: Linear regression models showing no significant relationships between the McElwain *et al.* (1999), Steinthorsdottir *et al.* (2011) or Schaller *et al.* (2011) pCO₂ results and corresponding St Audrie's Bay temperature data from this study as well as previously published data (Presented in Section 4.5).

A5.4: Tables of the available $p\text{CO}_2$ results that corresponds with the Lyme Regis or St Audrie's Bay fossil size data from this study.

Table A5.11: The Steinhorsdottir *et al.* (2011) Larne $p\text{CO}_2$ results and corresponding St Audrie's Bay *L. hisingeri* geometric shell size data. These corresponding data points are used in the linear regression models to determine any relationships between these two factors (Presented in Section 4.6).

Steinhorsdottir <i>et al.</i> (2011)							<i>L. hisingeri</i> geometric size data				
St Audrie's Bay Bed Height (m)	Larne $p\text{CO}_2$ ppm carboniferous standard min	Larne $p\text{CO}_2$ ppm carboniferous standard max	Larne $p\text{CO}_2$ ppm carboniferous standard mean	Larne $p\text{CO}_2$ ppm modern standard min	Larne $p\text{CO}_2$ ppm modern standard max	Larne $p\text{CO}_2$ ppm modern standard mean	St Audrie's Bay Bed Height (m)	Mean	95th percentile minimum	95th percentile maximum	95th percentile range
11.4	1616	2116	1866	1051	1375	1213	12.55	16.4	10.8	22.0	11.3
13.6	1471	2675	2073	956	1738	1347	14.6	14.8	10.4	17.4	7.0
15.5	1903	2429	2166	1237	1579	1408	15.5	23.0	16.1	28.8	12.7
17	1318	2010	1664	857	1307	1082	17.15	23.8	13.9	35.0	21.1
22	1062	1874	1468	690	1218	954	23.45	18.7	14.2	25.1	10.9

Table A5.12: The Steinhorsdottir *et al.* (2011) Larne $p\text{CO}_2$ results and corresponding Lyme Regis *L. hisingeri* geometric shell size data. These corresponding data points are used in the linear regression models to determine any relationships between these two factors (Presented in Section 4.6).

Steinhorsdottir <i>et al.</i> (2011)							<i>L. hisingeri</i> geometric size data				
Lyme Regis Bed Height (m)	Larne $p\text{CO}_2$ ppm carboniferous standard min	Larne $p\text{CO}_2$ ppm carboniferous standard max	Larne $p\text{CO}_2$ ppm carboniferous standard mean	Larne $p\text{CO}_2$ ppm modern standard min	Larne $p\text{CO}_2$ ppm modern standard max	Larne $p\text{CO}_2$ ppm modern standard mean	Lyme Regis Bed Height (m)	Mean	95th percentile minimum	95th percentile maximum	95th percentile range
8.2	1471	2675	2073	956	1738	1347	8.05	10.7	8.7	12.0	3.3
9.4	1903	2429	2166	1237	1579	1408	9.59	23.0	19.9	28.3	8.4
10	1318	2010	1664	857	1307	1082	10.2	26.3	15.7	41.0	25.3
12.3	1062	1874	1468	690	1218	954	12.3	22.0	14.7	35.3	20.6

Table A5.13: The Steinthorsdottir *et al.* (2011) Astartekloft $p\text{CO}_2$ results and corresponding St Audrie's Bay *L. hisingeri* geometric shell size data. These corresponding data points are used in the linear regression models to determine any relationships between these two factors (Presented in Section 4.6).

Steinthorsdottir <i>et al.</i> (2011)							<i>L. hisingeri</i> geometric size data				
St Audrie's Bay Bed Height (m)	Astartekloft $p\text{CO}_2$ ppm carboniferous standard min	Astartekloft $p\text{CO}_2$ ppm carboniferous standard max	Astartekloft $p\text{CO}_2$ ppm carboniferous standard mean	Astartekloft $p\text{CO}_2$ ppm modern standard min	Astartekloft $p\text{CO}_2$ ppm modern standard max	Astartekloft $p\text{CO}_2$ ppm modern standard mean	St Audrie's Bay Bed Height (m)	Mean	95th percentile minimum	95th percentile maximum	95th percentile range
16	1422	1924	1673	924	1250	1087	16.07	23.4	18.3	29.1	10.7

Table A5.14: The Steinthorsdottir *et al.* (2011) Astartekloft $p\text{CO}_2$ results and corresponding Lyme Regis *L. hisingeri* geometric shell size data. These corresponding data points are used in the linear regression models to determine any relationships between these two factors (Presented in Section 4.6).

Steinthorsdottir <i>et al.</i> (2011)							<i>L. hisingeri</i> geometric size data				
Lyme Regis Bed Height (m)	Astartekloft $p\text{CO}_2$ ppm carboniferous standard min	Astartekloft $p\text{CO}_2$ ppm carboniferous standard max	Astartekloft $p\text{CO}_2$ ppm carboniferous standard mean	Astartekloft $p\text{CO}_2$ ppm modern standard min	Astartekloft $p\text{CO}_2$ ppm modern standard max	Astartekloft $p\text{CO}_2$ ppm modern standard mean	Lyme Regis Bed Height (m)	Mean	95th percentile minimum	95th percentile maximum	95th percentile range
9.72	1422	1924	1673	924	1250	1087	9.72	19.7	19.7	19.7	
15.3	1955	2413	2184	1271	1569	1420	15.2	18.7	12.1	30.1	18.0
15.85	1982	3960	2971	1288	2574	1931	15.55	22.2	12.4	32.9	20.5
16	1092	1616	1354	710	1050	880	16.1	15.7	7.9	24.9	17.0

Table A5.15: The McElwain *et al.* (1999) Greenland and Sweden $p\text{CO}_2$ results and corresponding St Audrie's Bay *L. hisingeri* geometric shell size data. These corresponding data points are used in the linear regression models to determine any relationships between these two factors (Presented in Section 4.6).

McElwain <i>et al.</i> (1999)							<i>L. hisingeri</i> geometric size data				
St Audrie's Bay Bed Height (m)	Greenland $p\text{CO}_2$ ppm minimum value	Greenland $p\text{CO}_2$ ppm maximum value	Greenland $p\text{CO}_2$ ppm mean value	Sweden $p\text{CO}_2$ ppm minimum value	Sweden $p\text{CO}_2$ ppm maximum value	Sweden $p\text{CO}_2$ ppm mean level	St Audrie's Bay Bed Height (m)	Mean	95th percentile minimum	95th percentile maximum	95th percentile range
10.7				1040	1386	1213	12.55	16.4	10.8	22.0	11.3
16	1544	2058	1801				16.07	23.4	18.3	29.1	10.7
23.8				1751	2334	2042	23.45	18.7	14.2	25.1	10.9

Table A5.16: The McElwain *et al.* (1999) Greenland and Sweden pCO_2 results and corresponding Lyme Regis *L. hisingeri* geometric shell size data. These corresponding data points are used in the linear regression models to determine any relationships between these two factors (Presented in Section 4.6).

Bed Height (m)	McElwain <i>et al.</i> (1999)						<i>L. hisingeri</i> geometric size data				
Lyme Regis Bed Height (m)	Greenland pCO_2 ppm minimum value	Greenland pCO_2 ppm maximum value	Greenland pCO_2 ppm mean value	Sweden pCO_2 ppm minimum value	Sweden pCO_2 ppm maximum value	Sweden pCO_2 ppm mean level	Lyme Regis Bed Height (m)	Mean	95th percentile minimum	95th percentile maximum	95th percentile range
9.72	1544	2058	1801				9.72	19.7	19.7	19.7	
12.6				1751	2334	2042	12.75	24.5	14.0	32.9	18.9
15				1485	1980	1733	14.85	22.8	20.4	25.3	4.9
15.22	1337	1782	1559	509	678	593	15.2	18.7	12.1	30.1	18.0
15.85	1553	2070	1811				15.55	22.2	12.4	32.9	20.5
16	761	1014	887				16.1	15.7	7.9	24.9	17.0

Table A5.17: The Schaller *et al.* (2011) Newark Basin pCO_2 results and corresponding St Audrie's Bay *L. hisingeri* geometric shell size data. These corresponding data points are used in the linear regression models to determine any relationships between these two factors (Presented in Section 4.6).

Schaller <i>et al.</i> (2011)				<i>L. hisingeri</i> geometric size data				
St Audrie's Bay Bed Height (m)	Newark Basin pCO_2 ppm minimum value	Newark Basin pCO_2 ppm maximum value	Newark Basin pCO_2 ppm mean value	St Audrie's Bay Bed Height (m)	Mean	95th percentile minimum	95th percentile maximum	95th percentile range
10.5	2819	5637	4228	12.55	16.4	10.8	22.0	11.3
13.6	2389	4779	3584	14.6	14.8	10.4	17.4	7.0
18	2385	4769	3577	18.1	33.0	26.7	37.5	10.9
20	2009	4019	3014	20.4	17.7	10.6	25.8	15.1
22	2307	4613	3460	20.8	26.8	24.5	29.1	4.7
23.7	1761	3523	2642	23.45	18.7	14.2	25.1	10.9
25.3	2472	4944	3708	24.11	19.0	17.1	21.6	4.5
48	2087	4175	3131	48.65	14.1	9.8	18.4	8.6
53	1664	3328	2496	51.3	26.8	26.8	26.8	

Table A5.18: The Schaller *et al.* (2011) Newark Basin $p\text{CO}_2$ results and corresponding Lyme Regis *L. hisingeri* geometric shell size data. These corresponding data points are used in the linear regression models to determine any relationships between these two factors (Presented in Section 4.6).

Schaller <i>et al.</i> (2011)				<i>L. hisingeri</i> geometric size data				
Lyme Regis Bed Height (m)	Newark Basin $p\text{CO}_2$ ppm minimum value	Newark Basin $p\text{CO}_2$ ppm maximum value	Newark Basin $p\text{CO}_2$ ppm mean value	Lyme Regis Bed Height (m)	Mean	95th percentile minimum	95th percentile maximum	95th percentile range
7.9	2389	4779	3584	8.05	10.7	8.7	12.0	3.3
10.4	2385	4769	3577	10.2	26.3	15.7	41.0	25.3
10.7	2302	4604	3453	10.5	20.3	17.2	23.5	6.3
11	2823	5645	4234	10.9	19.6	10.5	29.5	19.0
12.5	1761	3523	2642	12.3	22.0	14.7	35.3	20.6
13.4	2472	4944	3708	13.3	19.7	13.2	30.5	17.3
14.4	1571	3141	2356	14.5	21.2	15.0	29.7	14.7
15.2	1299	2599	1949	15.2	18.7	12.1	30.1	18.0
15.3	3290	6592	4941	15.55	22.2	12.4	32.9	20.5
17.5	2087	4175	3131	17.5	20.0	7.6	34.2	26.7
21.5	1664	3328	2496	21.5	34.4	34.4	34.4	

Table A5.19: The McElwain *et al.* (1999) Greenland and Sweden $p\text{CO}_2$ results and corresponding Lyme Regis *P. gigantea* geometric shell size data. These corresponding data points are used in the linear regression models to determine any relationships between these two factors (Presented in Section 4.6).

McElwain <i>et al.</i> (1999)							<i>P. gigantea</i> geometric size data				
Lyme Regis Bed Height (m)	Greenland $p\text{CO}_2$ ppm minimum value	Greenland $p\text{CO}_2$ ppm maximum value	Greenland $p\text{CO}_2$ ppm mean value	Sweden $p\text{CO}_2$ ppm minimum value	Sweden $p\text{CO}_2$ ppm maximum value	Sweden $p\text{CO}_2$ ppm mean level	Lyme Regis Bed Height (m)	Mean	95th percentile minimum	95th percentile maximum	95th percentile range
9.72	1543.5	2058	1800.75				9.56	48.4	48.4	48.4	
12.6				1750.5	2334	2042.25	12.6	53.8	53.8	53.8	
15				1485	1980	1732.5	14.85	47.8	47.8	47.8	
15.22	1336.5	1782	1559.25	508.5	678	593.25	15.2	50.1	29.3	72.3	43.0
15.85	1552.5	2070	1811.25				15.55	42.5	15.0	68.6	53.7
16	760.5	1014	887.25				16.1	48.7	25.2	67.4	42.2

Table A5.20: The Steinhorsdottir *et al.* (2011) Astartekloft $p\text{CO}_2$ results and corresponding Lyme Regis *P. gigantea* geometric shell size data. These corresponding data points are used in the linear regression models to determine any relationships between these two factors (Presented in Section 4.6).

Steinhorsdottir <i>et al.</i> (2011)							<i>P. gigantea</i> geometric size data				
Lyme Regis Bed Height (m)	Astartekloft $p\text{CO}_2$ ppm carboniferous standard min	Astartekloft $p\text{CO}_2$ ppm carboniferous standard max	Astartekloft $p\text{CO}_2$ ppm carboniferous standard mean	Astartekloft $p\text{CO}_2$ ppm modern standard min	Astartekloft $p\text{CO}_2$ ppm modern standard max	Astartekloft $p\text{CO}_2$ ppm modern standard mean	Lyme Regis Bed Height (m)	Mean	95th percentile minimum	95th percentile maximum	95th percentile range
9.72	1422	1924	1673	924	1250	1087	9.56	48.4	48.4	48.4	
15.3	1955	2413	2184	1271	1569	1420	15.2	50.1	29.3	72.3	43.0
15.85	1982	3960	2971	1288	2574	1931	15.55	42.5	15.0	68.6	53.7
16	1092	1616	1354	710	1050	880	16.1	48.7	25.2	67.4	42.2

Table A5.21: The Steinhorsdottir *et al.* (2011) Larne $p\text{CO}_2$ results and corresponding Lyme Regis *P. gigantea* geometric shell size data. These corresponding data points are used in the linear regression models to determine any relationships between these two factors (Presented in Section 4.6).

Steinhorsdottir <i>et al.</i> (2011)							<i>P. gigantea</i> geometric size data				
Lyme Regis Bed Height (m)	Larne $p\text{CO}_2$ ppm carboniferous standard min	Larne $p\text{CO}_2$ ppm carboniferous standard max	Larne $p\text{CO}_2$ ppm carboniferous standard mean	Larne $p\text{CO}_2$ ppm modern standard min	Larne $p\text{CO}_2$ ppm modern standard max	Larne $p\text{CO}_2$ ppm modern standard mean	Lyme Regis Bed Height (m)	Mean	95th percentile minimum	95th percentile maximum	95th percentile range
8.2	1471	2675	2073	956	1738	1347	8.7	33.9	33.9	33.9	
9.4	1903	2429	2166	1237	1579	1408	9.56	48.4	48.4	48.4	
10	1318	2010	1664	857	1307	1082	10.5	38.6	38.6	38.6	
12.3	1062	1874	1468	690	1218	954	12.3	35.2	21.9	49.6	27.6

Table A5.22: The Schaller *et al.* (2011) Newark Basin $p\text{CO}_2$ results and corresponding Lyme Regis *P. gigantea* geometric shell size data. These corresponding data points are used in the linear regression models to determine any relationships between these two factors (Presented in Section 4.6).

Schaller <i>et al.</i> (2011)				<i>P. gigantea</i> geometric size data				
Lyme Regis Bed Height (m)	Newark Basin $p\text{CO}_2$ ppm minimum value	Newark Basin $p\text{CO}_2$ ppm maximum value	Newark Basin $p\text{CO}_2$ ppm mean value	Lyme Regis Bed Height (m)	Mean	95th percentile minimum	95th percentile maximum	95th percentile range
7.9	2389.453	4778.547	3584	8.7	33.9	33.9	33.9	
10.4	2384.786	4769.214	3577	10.5	38.6	38.6	38.6	
10.7	2302.115	4603.885	3453	10.7	59.3	46.4	72.1	25.7
11	2822.808	5645.192	4234	10.9	33.8	30.0	37.5	7.4
11.7	2306.782	4613.218	3460	12.3	35.2	21.9	49.6	27.6
12.5	1761.421	3522.579	2642	12.6	53.8	53.8	53.8	
13.4	2472.124	4943.876	3708	13.3	25.0	16.3	35.3	19.0
14.4	1570.745	3141.255	2356	14.2	44.2	33.8	53.9	20.1

Schaller <i>et al.</i> (2011)				<i>P. gigantea</i> geometric size data				
Lyme Regis Bed Height (m)	Newark Basin $p\text{CO}_2$ ppm minimum value	Newark Basin $p\text{CO}_2$ ppm maximum value	Newark Basin $p\text{CO}_2$ ppm mean value	Lyme Regis Bed Height (m)	Mean	95th percentile minimum	95th percentile maximum	95th percentile range
15.2	1299.398	2598.602	1949	15.2	50.1	29.3	72.3	43.0
15.3	3290.165	6591.835	4941	15.55	42.5	15.0	68.6	53.7
17.5	2087.438	4174.562	3131	17.5	44.7	26.1	64.6	38.5
21.5	1664.083	3327.917	2496	21.5	93.4	78.0	111.7	33.7

Table A5.23: The McElwain *et al.* (1999) and Schaller *et al.* (2011) Newark Basin $p\text{CO}_2$ results and corresponding St Audrie's Bay *L. hisingeri* Ca and Mg levels. These corresponding data points are used in the linear regression models to determine any relationships between these two factors (Presented in Section 4.6).

McElwain <i>et al.</i> (1999)				Geometric <i>L. hisingeri</i> Ca & Mg		
St Audrie's Bay Bed Height (m)	Sweden $p\text{CO}_2$ ppm minimum	Sweden $p\text{CO}_2$ ppm maximum	Sweden $p\text{CO}_2$ ppm mean	St Audrie's Bay Bed Height (m)	Ca	Mg
23.8	1750.5	2334	2042.25	24.85	62.85	0.36
Schaller <i>et al.</i> (2011)				Geometric <i>L. hisingeri</i> Ca & Mg		
St Audrie's Bay Bed Height (m)	Newark Basin $p\text{CO}_2$ ppm minimum	Newark Basin $p\text{CO}_2$ ppm maximum	Newark Basin $p\text{CO}_2$ ppm mean	St Audrie's Bay Bed Height (m)	Ca	Mg
23.7	1761.421	3522.579	2642	24.85	62.85	0.36
25.3	2472.124	4943.876	3708	26.58	78.98	0.41
48	2087.438	4174.562	3131	48.9	49.28	0.67

Table A5.24: The McElwain *et al.* (1999) Greenland and Sweden $p\text{CO}_2$ results and corresponding Lyme Regis *L. hisingeri* Ca and Mg levels. These corresponding data points are used in the linear regression models to determine any relationships between these two factors (Presented in Section 4.6).

McElwain <i>et al.</i> (1999)						Geometric <i>L. hisingeri</i> Ca & Mg			
Lyme Regis Bed Height (m)	Greenland $p\text{CO}_2$ ppm minimum value	Greenland $p\text{CO}_2$ ppm maximum value	Greenland $p\text{CO}_2$ ppm mean value	Sweden $p\text{CO}_2$ ppm minimum value	Sweden $p\text{CO}_2$ ppm maximum value	Sweden $p\text{CO}_2$ ppm mean level	Lyme Regis Bed Height (m)	Ca	Mg
9.72	1544	2058	1801				10.6	43.41	0.27
12.6				1751	2334	2042	13.37	36.55	0.24
15	1337	1782	1559	1485	1980	1733	14.8	59.71	0.26
16	761	1014	887				18.2	59.48	0.24

Table A5.25: The Schaller *et al.* (2011) Newark Basin $p\text{CO}_2$ results and corresponding Lyme Regis *L. hisingeri* Ca and Mg levels. These corresponding data points are used in the linear regression models to determine any relationships between these two factors (Presented in Section 4.6).

Schaller <i>et al.</i> (2011)				Geometric <i>L. hisingeri</i> Ca & Mg		
Lyme Regis Bed Height (m)	Newark Basin $p\text{CO}_2$ ppm minimum value	Newark Basin $p\text{CO}_2$ ppm maximum value	Newark Basin $p\text{CO}_2$ ppm mean value	Lyme Regis Bed Height (m)	Ca	Mg
10.7	2302	4604	3453	10.6	43.41	0.27
13.4	2472	4944	3708	13.37	36.55	0.24
14.4	1571	3141	2356	14.8	59.71	0.26
17.5	2087	4175	3131	18.2	59.48	0.24
21.5	1664	3328	2496	21.55	48.74	0.27

Table A5.26: The Schaller *et al.* (2011) Newark Basin $p\text{CO}_2$ results and corresponding Lyme Regis *P. gigantea* Ca and Mg levels. These corresponding data points are used in the linear regression models to determine any relationships between these two factors (Presented in Section 4.6).

Schaller <i>et al.</i> (2011)				Geometric <i>P. gigantea</i> Ca & Mg		
Lyme Regis Bed Height (m)	Newark Basin $p\text{CO}_2$ ppm minimum value	Newark Basin $p\text{CO}_2$ ppm maximum value	Newark Basin $p\text{CO}_2$ ppm mean value	Lyme Regis Bed Height (m)	Ca	Mg
10.7	2302.115	4603.885	3453	10.6	29.13	0.18
13.4	2472.124	4943.876	3708	13.37	55.2	0.45
14.4	1570.745	3141.255	2356	14.8	35.78	0.16
17.5	2087.438	4174.562	3131	19.35	51.41	0.31
21.5	1664.083	3327.917	2496	21.55	52.95	0.23

Table A5.27: The Steinthorsdottir *et al.* (2011) Astartekloft and Larné $p\text{CO}_2$ results and corresponding Lyme Regis *L. hisingeri* Ca and Mg levels. These corresponding data points are used in the linear regression models to determine any relationships between these two factors (Presented in Section 4.6).

Steinthorsdottir <i>et al.</i> (2011)							Geometric <i>L. hisingeri</i> Ca & Mg		
Lyme Regis Bed Height (m)	Astartekloft $p\text{CO}_2$ ppm carboniferous standard min	Astartekloft $p\text{CO}_2$ ppm carboniferous standard max	Astartekloft $p\text{CO}_2$ ppm carboniferous standard mean	Astartekloft $p\text{CO}_2$ ppm modern standard min	Astartekloft $p\text{CO}_2$ ppm modern standard max	Astartekloft $p\text{CO}_2$ ppm modern standard mean	Lyme Regis Bed Height (m)	Ca	Mg
9.72	1422	1924	1673	924	1250	1087	13.37	36.55	0.24
15.3	1955	2413	2184	1271	1569	1420	18.2	59.48	0.24
16	1092	1616	1354	710	1050	880	19.35	39.72	0.16
Steinthorsdottir <i>et al.</i> (2011)							Geometric <i>L. hisingeri</i> Ca & Mg		
Lyme Regis Bed Height (m)	Larne $p\text{CO}_2$ ppm carboniferous standard min	Larne $p\text{CO}_2$ ppm carboniferous standard max	Larne $p\text{CO}_2$ ppm carboniferous standard mean	Larne $p\text{CO}_2$ ppm modern standard min	Larne $p\text{CO}_2$ ppm modern standard max	Larne $p\text{CO}_2$ ppm modern standard mean	Lyme Regis Bed Height (m)	Ca	Mg
10	1318	2010	1664	857	1307	1082	13.37	36.55	0.24
12.3	1062	1874	1468	690	1218	954	14.8	59.71	0.26

Table A5.28: The Steinhorsdottir *et al.* (2011) Astartekloft and Larne $p\text{CO}_2$ results as well as McElwain *et al.*, (1999) Greenland and Sweden $p\text{CO}_2$ results and corresponding Lyme Regis *P. gigantea* Ca and Mg levels. These corresponding data points are used in the linear regression models to determine any relationships between these two factors (Presented in Section 4.6).

Steinhorsdottir <i>et al.</i> (2011)							Geometric <i>P. gigantea</i> Ca & Mg		
Lyme Regis Bed Height (m)	Astartekloft $p\text{CO}_2$ ppm carboniferous standard min	Astartekloft $p\text{CO}_2$ ppm carboniferous standard max	Astartekloft $p\text{CO}_2$ ppm carboniferous standard mean	Astartekloft $p\text{CO}_2$ ppm modern standard min	Astartekloft $p\text{CO}_2$ ppm modern standard max	Astartekloft $p\text{CO}_2$ ppm modern standard mean	Lyme Regis Bed Height (m)	Ca	Mg
9.72	1422	1924	1673	924	1250	1087	10.6	29.13	0.18
15.3	1955	2413	2184	1271	1569	1420	14.8	35.78	0.16
Steinhorsdottir <i>et al.</i> (2011)							Geometric <i>P. gigantea</i> Ca & Mg		
Lyme Regis Bed Height (m)	Larne $p\text{CO}_2$ ppm carboniferous standard min	Larne $p\text{CO}_2$ ppm carboniferous standard max	Larne $p\text{CO}_2$ ppm carboniferous standard mean	Larne $p\text{CO}_2$ ppm modern standard min	Larne $p\text{CO}_2$ ppm modern standard max	Larne $p\text{CO}_2$ ppm modern standard mean	Lyme Regis Bed Height (m)	Ca	Mg
10	1318	2010	1664	857	1307	1082	10.6	29.13	0.18
12.3	1062	1874	1468	690	1218	954	13.37	55.2	0.45
McElwain <i>et al.</i> (1999)							Geometric <i>P. gigantea</i> Ca & Mg		
Lyme Regis Bed Height (m)	Greenland $p\text{CO}_2$ ppm minimum value	Greenland $p\text{CO}_2$ ppm maximum value	Greenland $p\text{CO}_2$ ppm mean value	Sweden $p\text{CO}_2$ ppm minimum value	Sweden $p\text{CO}_2$ ppm maximum value	Sweden $p\text{CO}_2$ ppm mean level	Lyme Regis Bed Height (m)	Ca	Mg
9.72	1543.5	2058	1800.75				10.6	29.13	0.18
12.6				1750.5	2334	2042.25	13.37	55.2	0.45
15	1336.5	1782	1559.25	1485	1980	1732.5	14.8	35.78	0.16

Table A5.29: The Schaller *et al.* (2011) Newark Basin $p\text{CO}_2$ results and corresponding St Audrie's Bay *O. aspinata* Ca and Mg levels or geometric shell size. These corresponding data points are used in the linear regression models to determine any relationships between these two factors (Presented in Section 4.6).

Schaller <i>et al.</i> (2011)				Geometric <i>O. aspinata</i> Ca & Mg			<i>O. aspinata</i> geometric size data				
St Audrie's Bay Bed Height (m)	Newark Basin $p\text{CO}_2$ ppm minimum value	Newark Basin $p\text{CO}_2$ ppm maximum value	Newark Basin $p\text{CO}_2$ ppm mean value	St Audrie's Bay Bed Height (m)	Ca	Mg	St Audrie's Bay Bed height	Mean	95th percentile min	95th percentile max	95th percentile range
10.5	2818	5637	4228	12.2	59.49	0.71	12.2	401.7	302.7	475.0	172.2
13.6	2389	4778	3584	12.5	93.45	1.28	12.5	431.4	369.1	485.2	116.1
18	2384	4769	3577	17.9			17.9	220.0	147.0	293.8	146.7
18.3	2302	4603	3453	18.4			18.4	382.5	283.7	466.6	182.8
19.3	2822	5645	4234	18.7	37.94	0.35	18.7	357.2	264.5	452.5	188.1
19.8	2676	5353	4015	19.8			19.8	359.2	261.6	445.7	184.1
22	2306	4613	3460	23.2	95.51	1.04	23.2	390.3	293.3	473.4	180.0
23.7	1761	3522	2642	23.8	59.8	1.05	23.8	391.6	256.7	486.0	229.4
25.3	2472	4943	3708	24.3			24.3	398.5	332.9	469.1	136.2
27.7	1570	3141	2356	26.5	38.87	0.95	26.5	382.4	263.6	453.9	190.3
48	2087	4174	3131	48.9	75.88	1.56	48.9	395.3	272.7	479.4	206.6
53	1664	3327	2496	53.05	56.99	0.91	53.05	416.4	324.1	486.4	162.4

Table A5.30: The Schaller *et al.* (2011) Newark Basin $p\text{CO}_2$ results and corresponding Lyme Regis *O. aspinata* Ca and Mg levels or geometric shell size. These corresponding data points are used in the linear regression models to determine any relationships between these two factors (Presented in Section 4.6).

Schaller <i>et al.</i> (2011)				Geometric <i>O. aspinata</i> Ca & Mg			<i>O. aspinata</i> geometric size data				
Lyme Regis Bed Height (m)	Newark Basin $p\text{CO}_2$ ppm minimum value	Newark Basin $p\text{CO}_2$ ppm maximum value	Newark Basin $p\text{CO}_2$ ppm mean value	Lyme Regis Bed Height (m)	Ca	Mg	Lyme Regis Bed Height (m)	Mean	95th percentile min	95th percentile max	95th percentile range
7.9	2389	4778	3584	8.8			8.8	383.8	374.0	393.6	19.7
10.4	2384	4769	3577	10.3			10.3	386.1	312.5	456.8	144.3
10.7	2302	4603	3453	10.7			10.7	355.5	287.7	427.6	139.8
11.3	2676	5353	4015	11.3			11.3	383.5	289.1	458.0	168.9
12.5	1761	3522	2642	12.85	40.50	0.69	12.85	397.7	313.5	464.9	151.4
13.4	2472	4943	3708	13.37	47.72	0.56	13.37	369.0	226.2	453.2	227.0
15.3	3290	6591	4941	15.3	76.25	0.81	15.3	390.3	274.1	469.8	195.8
17.5	2087	4174	3131	17.5	27.95	0.27	17.5	402.9	308.4	481.5	173.1
21.5	1664	3327	2496	21.55			21.55	383.7	259.5	529.0	269.5

Table A5.31: The McElwain *et al.* (1999) Greenland or Sweden $p\text{CO}_2$ results and corresponding St Audrie's Bay *O. aspinata* Ca and Mg levels or geometric shell size. These corresponding data points are used in the linear regression models to determine any relationships between these two factors (Presented in Section 4.6).

McElwain <i>et al.</i> (1999)							Geometric <i>O. aspinata</i> Ca & Mg			<i>O. aspinata</i> geometric size data				
St Audrie's Bay Bed Height (m)	Greenland $p\text{CO}_2$ ppm minimum value	Greenland $p\text{CO}_2$ ppm maximum value	Greenland $p\text{CO}_2$ ppm mean value	Sweden $p\text{CO}_2$ ppm minimum value	Sweden $p\text{CO}_2$ ppm maximum value	Sweden $p\text{CO}_2$ ppm mean level	St Audrie's Bay Bed Height (m)	Ca	Mg	St Audrie's Bay Bed Height (m)	Mean	95th percentile min	95th percentile max	95th percentile range
10.7				1039.5	1386	1212.75	12.2	59.49	0.71	12.2	401.7	302.7	475.0	172.2
16	1543.5	2058	1800.75				15			15	412.9	357.8	460.3	102.5
23.8				1750.5	2334	2042.25	23.8	59.8	1.05	23.8	391.6	256.7	486.0	229.4
41.3	877.5	1170	1023.8				40.7			40.7	361.8	260.4	461.7	201.3

Table A5.32: The McElwain *et al.* (1999) Greenland or Sweden $p\text{CO}_2$ results and corresponding Lyme Regis *O. aspinata* Ca and Mg levels or geometric shell size. These corresponding data points are used in the linear regression models to determine any relationships between these two factors (Presented in Section 4.6).

McElwain <i>et al.</i> (1999)							Geometric <i>O. aspinata</i> Ca & Mg			<i>O. aspinata</i> geometric size data				
Lyme Regis Bed Height (m)	Greenland $p\text{CO}_2$ ppm minimum value	Greenland $p\text{CO}_2$ ppm maximum value	Greenland $p\text{CO}_2$ ppm mean value	Sweden $p\text{CO}_2$ ppm minimum value	Sweden $p\text{CO}_2$ ppm maximum value	Sweden $p\text{CO}_2$ ppm mean level	Lyme Regis Bed Height (m)	Ca	Mg	Lyme Regis Bed Height (m)	Mean	95th percentile min	95th percentile max	95th percentile range
9.72	1543.5	2058	1800.75				9.72			9.72	393.6	306.4	471.5	165.1
12.6				1750.5	2334	2042.3	12.85	40.50	0.69	12.85	397.7	313.5	464.9	151.4
15.3	1336.5	1782	1559.3	508.5	678	593.25	15.3	76.25	0.81	15.3	390.3	274.1	469.8	195.8
15.87	1552.5	2070	1811.3				15.8			15.8	390.1	271.7	477.4	205.7
16	760.5	1014	887.25				16.8	55.52	0.58	16.8	396.7	251.1	487.6	236.5

Table A5.33: The Steinthorsdottir *et al.* (2011) Astartekloft $p\text{CO}_2$ results and corresponding St Audrie's Bay *O. aspinata* geometric shell size. These corresponding data points are used in the linear regression models to determine any relationships between these two factors (Presented in Section 4.6).

Steinthorsdottir <i>et al.</i> (2011)							<i>O. aspinata</i> geometric size data				
St Audrie's Bay Bed Height (m)	Astartekloft $p\text{CO}_2$ ppm carboniferous standard min	Astartekloft $p\text{CO}_2$ ppm carboniferous standard max	Astartekloft $p\text{CO}_2$ ppm carboniferous standard mean	Astartekloft $p\text{CO}_2$ ppm modern standard min	Astartekloft $p\text{CO}_2$ ppm modern standard max	Astartekloft $p\text{CO}_2$ ppm modern standard mean	St Audrie's Bay Bed Height (m)	Mean	95th percentile min	95th percentile max	95th percentile range
16	1422	1924	1673	924	1250	1087	15	412.9	357.8	460.3	102.5
41.3	1092	1354	1223	710	880	795	40.7	361.8	260.4	461.7	201.3

Table A5.34: The Steinhorsdottir *et al.* (2011) Astartekloft $p\text{CO}_2$ results and corresponding Lyme Regis *O. aspinata* Ca and Mg levels or geometric shell size. These corresponding data points are used in the linear regression models to determine any relationships between these two factors (Presented in Section 4.6).

Steinhorsdottir <i>et al.</i> (2011)							Geometric <i>O. aspinata</i> Ca & Mg			<i>O. aspinata</i> geometric size data				
Lyme Regis Bed Height (m)	Astartekloft $p\text{CO}_2$ ppm carboniferous standard min	Astartekloft $p\text{CO}_2$ ppm carboniferous standard max	Astartekloft $p\text{CO}_2$ ppm carboniferous standard mean	Astartekloft $p\text{CO}_2$ ppm modern standard min	Astartekloft $p\text{CO}_2$ ppm modern standard max	Astartekloft $p\text{CO}_2$ ppm modern standard mean	Lyme Regis Bed Height (m)	Ca	Mg	Lyme Regis Bed Height (m)	Mean	95th percentile min	95th percentile max	95th percentile range
9.72	1422	1924	1673	924	1250	1087	9.72			9.72	393.6	306.4	471.5	165.1
15.3	1955	2413	2184	1271	1569	1420	15.3	76.25	0.81	15.3	390.3	274.1	469.8	195.8
15.85	1982	3960	2971	1288	2574	1931	15.8			15.8	390.1	271.7	477.4	205.7
16	1092	1616	1354	710	1050	880	16.8	55.52	0.58	16.8	396.7	251.1	487.6	236.5

Table A5.35: The Steinhorsdottir *et al.* (2011) Larne $p\text{CO}_2$ results and corresponding St Audrie's Bay *O. aspinata* Ca and Mg levels or geometric shell size. These corresponding data points are used in the linear regression models to determine any relationships between these two factors (Presented in Section 4.6).

Steinhorsdottir <i>et al.</i> (2011)							Geometric <i>O. aspinata</i> Ca & Mg			<i>O. aspinata</i> geometric size data				
St Audrie's Bay Bed Height (m)	Larne $p\text{CO}_2$ ppm carboniferous standard min	Larne $p\text{CO}_2$ ppm carboniferous standard max	Larne $p\text{CO}_2$ ppm carboniferous standard mean	Larne $p\text{CO}_2$ ppm modern standard min	Larne $p\text{CO}_2$ ppm modern standard max	Larne $p\text{CO}_2$ ppm modern standard mean	St Audrie's Bay Bed Height (m)	Ca	Mg	St Audrie's Bay Bed Height (m)	Mean	95th percentile min	95th percentile max	95th percentile range
11.4	1616	2116	1866	1051	1375	1213	12.2	59.48	0.71	12.2	401.7	302.7	475.0	172.2
13.6	1471	2675	2073	956	1738	1347	12.5	93.45	1.28	12.5	431.4	369.1	485.2	116.1
15.5	1903	2429	2166	1237	1579	1408	15			15	412.9	357.8	460.3	102.5
17	1318	2010	1664	857	1307	1082	17.4			17.4	367.3	255.6	461.5	206.0
22	1062	1874	1468	690	1218	954	23.2	95.51	1.04	23.2	390.3	293.3	473.4	180.0

Table A5.36: The Steinhorsdottir *et al.* (2011) Larne $p\text{CO}_2$ results and corresponding Lyme Regis *O. aspinata* Ca and Mg levels or geometric shell size. These corresponding data points are used in the linear regression models to determine any relationships between these two factors (Presented in Section 4.6).

Steinhorsdottir <i>et al.</i> (2011)							Geometric <i>O. aspinata</i> Ca & Mg			<i>O. aspinata</i> geometric size data				
Lyme Regis Bed Height (m)	Larne $p\text{CO}_2$ ppm carboniferous standard min	Larne $p\text{CO}_2$ ppm carboniferous standard max	Larne $p\text{CO}_2$ ppm carboniferous standard mean	Larne $p\text{CO}_2$ ppm modern standard min	Larne $p\text{CO}_2$ ppm modern standard max	Larne $p\text{CO}_2$ ppm modern standard mean	Lyme Regis Bed Height (m)	Ca	Mg	Lyme Regis Bed Height (m)	Mean	95th percentile min	95th percentile max	95th percentile range
8.2	1471	2675	2073	956	1738	1347	8.8			8.8	383.8	374.0	393.6	19.7
9.4	1903	2429	2166	1237	1579	1408	9.6			9.6	372.6	311.8	451.7	140.0
10	1318	2010	1664	857	1307	1082	10.3			10.3	386.1	312.5	456.8	144.3
12.3	1062	1874	1468	690	1218	954	12.85	40.50	0.69	12.85	397.7	313.5	464.9	151.4

Table A5.37: The Schaller *et al.* (2011) Newark Basin $p\text{CO}_2$ results and corresponding St Audrie's Bay *O. aspinata* shell thickness. These corresponding data points are used in the linear regression models to determine any relationships between these two factors (Presented in Section 4.6).

Schaller <i>et al.</i> (2011)				<i>O. aspinata</i> shell thickness				
St Audrie's Bay Bed Height (m)	Newark Basin $p\text{CO}_2$ ppm minimum value	Newark Basin $p\text{CO}_2$ ppm maximum value	Newark Basin $p\text{CO}_2$ ppm mean value	St Audrie's Bay Bed height	Mean	95th percentile min	95th percentile max	95th percentile range
10.5	2818	5637	4228	12.2	24.3	13.2	38.1	24.9
13.6	2389	4778	3584	12.5	33.4	23.9	39.9	15.9
18	2384	4769	3577	17.9	24.1	21.5	26.7	5.2
19.3	2822	5645	4234	18.7	22.1	11.6	36.9	25.3
19.8	2676	5353	4015	19.8	19.3	9.9	29.2	19.3
22	2306	4613	3460	23.2	32.2	18.1	46.0	27.8
23.7	1761	3522	2642	23.8	28.1	17.8	40.4	22.6
25.3	2472	4943	3708	24.3	36.1	31.0	44.4	13.4
27.7	1570	3141	2356	26.5	19.5	9.8	30.5	20.8
48	2087	4174	3131	48.9	21.3	12.8	31.4	18.6
53	1664	3327	2496	53.05	31.0	16.4	43.6	27.2

Table A5.38: The Schaller *et al.* (2011) Newark Basin $p\text{CO}_2$ results and corresponding Lyme Regis *O. aspinata* shell thickness. These corresponding data points are used in the linear regression models to determine any relationships between these two factors (Presented in Section 4.6).

Schaller <i>et al.</i> (2011)				<i>O. aspinata</i> shell thickness				
Lyme Regis Bed Height (m)	Newark Basin $p\text{CO}_2$ ppm minimum value	Newark Basin $p\text{CO}_2$ ppm maximum value	Newark Basin $p\text{CO}_2$ ppm mean value	Lyme Regis Bed Height (m)	Mean	95th percentile min	95th percentile max	95th percentile range
7.9	2389	4778	3584	8.8	29.5	21.3	40.3	18.9
10.4	2384	4769	3577	10.3	31.7	17.0	47.0	30.0
10.7	2302	4603	3453	10.7	30.6	19.0	44.5	25.6
11.3	2676	5353	4015	11.3	27.5	15.2	41.4	26.1
12.5	1761	3522	2642	12.85	31.7	19.9	43.2	23.3
13.4	2472	4943	3708	13.37	21.6	12.9	36.2	23.3
14.4	1570	3141	2356	13.7	30.0	20.5	40.5	20.0
15.3	3290	6591	4941	15.3	29.2	14.8	45.5	30.7
17.5	2087	4174	3131	17.5	34.1	18.8	52.6	33.8
21.5	1664	3327	2496	21.55	24.8	15.2	36.3	21.1

Table A5.39: The McElwain *et al.* (1999) Greenland and Sweden $p\text{CO}_2$ results and corresponding St Audrie's Bay *O. aspinata* shell thickness. These corresponding data points are used in the linear regression models to determine any relationships between these two factors (Presented in Section 4.6).

McElwain <i>et al.</i> (1999)							<i>O. aspinata</i> shell thickness				
St Audrie's Bay Bed Height (m)	Greenland $p\text{CO}_2$ ppm minimum value	Greenland $p\text{CO}_2$ ppm maximum value	Greenland $p\text{CO}_2$ ppm mean value	Sweden $p\text{CO}_2$ ppm minimum value	Sweden $p\text{CO}_2$ ppm maximum value	Sweden $p\text{CO}_2$ ppm mean level	St Audrie's Bay Bed Height (m)	Mean	95th percentile min	95th percentile max	95th percentile range
10.7				1039	1386	1212	12.2	24.3	13.2	38.1	24.9
16	1543	2058	1800				15	31.7	25.1	42.3	17.1
23.8				1750	2334	2042	23.8	28.1	17.8	40.4	22.6
41.3	877	1170	1023				40.7	24.2	11.7	37.1	25.4

Table A5.40: The McElwain *et al.* (1999) Greenland and Sweden pCO_2 results and corresponding Lyme Regis *O. aspinata* shell thickness. These corresponding data points are used in the linear regression models to determine any relationships between these two factors (Presented in Section 4.6).

McElwain <i>et al.</i> (1999)							<i>O. aspinata</i> shell thickness				
Lyme Regis Bed Height (m)	Greenland pCO_2 ppm minimum value	Greenland pCO_2 ppm maximum value	Greenland pCO_2 ppm mean value	Sweden pCO_2 ppm minimum value	Sweden pCO_2 ppm maximum value	Sweden pCO_2 ppm mean level	Lyme Regis Bed Height (m)	Mean	95th percentile min	95th percentile max	95th percentile range
9.72	1543	2058	1800				9.72	30.6	12.1	49.2	37.2
12				1750	2334	2042	12.85	31.7	19.9	43.2	23.3
15.3	1336	1782	1559	508	678	593	15.3	29.2	14.8	45.5	30.7
15.87	1552	2070	1811				15.8	30.9	14.9	45.1	30.3
15.87	1552	2070	1811				15.8	33.2	16.4	49.6	33.3
16	760	1014	887				16.8	25.1	11.5	42.1	30.7
16	760	1014	887				16.8	30.3	20.4	42.1	21.7

Table A5.41: The Steinhorsdottir *et al.* (2011) Astartekloft pCO_2 results and corresponding St Audrie's Bay *O. aspinata* shell thickness. These corresponding data points are used in the linear regression models to determine any relationships between these two factors (Presented in Section 4.6).

Steinhorsdottir <i>et al.</i> (2011)							<i>O. aspinata</i> shell thickness				
St Audrie's Bay Bed Height (m)	Astartekloft pCO_2 ppm carboniferous standard min	Astartekloft pCO_2 ppm carboniferous standard max	Astartekloft pCO_2 ppm carboniferous standard mean	Astartekloft pCO_2 ppm modern standard min	Astartekloft pCO_2 ppm modern standard max	Astartekloft pCO_2 ppm modern standard mean	St Audrie's Bay Bed Height (m)	Mean	95th percentile min	95th percentile max	95th percentile range
16	1422	1924	1673	924	1250	1087	15	31.7	25.1	42.3	17.1
41.3	1092	1354	1223	710	880	795	40.7	24.2	11.7	37.1	25.4

Table A5.42: The Steinhorsdottir *et al.* (2011) Astartekloft pCO_2 results and corresponding Lyme Regis *O. aspinata* shell thickness. These corresponding data points are used in the linear regression models to determine any relationships between these two factors (Presented in Section 4.6).

Steinhorsdottir <i>et al.</i> (2011)							<i>O. aspinata</i> shell thickness				
Lyme Regis Bed Height (m)	Astartekloft pCO_2 ppm carboniferous standard min	Astartekloft pCO_2 ppm carboniferous standard max	Astartekloft pCO_2 ppm carboniferous standard mean	Astartekloft pCO_2 ppm modern standard min	Astartekloft pCO_2 ppm modern standard max	Astartekloft pCO_2 ppm modern standard mean	Lyme Regis Bed Height (m)	Mean	95th percentile min	95th percentile max	95th percentile range
9.72	1422	1924	1673	924	1250	1087	9.72	30.6	12.1	49.2	37.2
15.3	1955	2413	2184	1271	1569	1420	15.3	29.2	14.8	45.5	30.7

Steinthorsdottir <i>et al.</i> (2011)							<i>O. aspinata</i> shell thickness				
Lyme Regis Bed Height (m)	Astartekloft $p\text{CO}_2$ ppm carboniferous standard min	Astartekloft $p\text{CO}_2$ ppm carboniferous standard max	Astartekloft $p\text{CO}_2$ ppm carboniferous standard mean	Astartekloft $p\text{CO}_2$ ppm modern standard min	Astartekloft $p\text{CO}_2$ ppm modern standard max	Astartekloft $p\text{CO}_2$ ppm modern standard mean	Lyme Regis Bed Height (m)	Mean	95th percentile min	95th percentile max	95th percentile range
15.85	1982	3960	2971	1288	2574	1931	15.8	30.9	14.9	45.1	30.3
15.85	1982	3960	2971	1288	2574	1931	15.8	33.2	16.4	49.6	33.3
16	1092	1616	1354	710	1050	880	16.8	25.1	11.5	42.1	30.7
16	1092	1616	1354	710	1050	880	16.8	30.3	20.4	42.1	21.7

Table A5.43: The Steinthorsdottir *et al.* (2011) Larne $p\text{CO}_2$ results and corresponding St Audrie's Bay *O. aspinata* shell thickness. These corresponding data points are used in the linear regression models to determine any relationships between these two factors (Presented in Section 4.6).

Steinthorsdottir <i>et al.</i> (2011)							<i>O. aspinata</i> shell thickness				
St Audrie's Bay Bed Height (m)	Larne $p\text{CO}_2$ ppm carboniferous standard min	Larne $p\text{CO}_2$ ppm carboniferous standard max	Larne $p\text{CO}_2$ ppm carboniferous standard mean	Larne $p\text{CO}_2$ ppm modern standard min	Larne $p\text{CO}_2$ ppm modern standard max	Larne $p\text{CO}_2$ ppm modern standard mean	St Audrie's Bay Bed Height (m)	Mean	95th percentile min	95th percentile max	95th percentile range
11.4	1616	2116	1866	1051	1375	1213	12.2	24.3	13.2	38.1	24.9
13.6	1471	2675	2073	956	1738	1347	12.5	33.4	23.9	39.9	15.9
15.5	1903	2429	2166	1237	1579	1408	15	31.7	25.1	42.3	17.1
17	1318	2010	1664	857	1307	1082	17.4	30.9	18.3	49.3	31.0
22	1062	1874	1468	690	1218	954	23.2	32.2	18.1	46.0	27.8

Table A5.44: The Steinthorsdottir *et al.* (2011) Larne $p\text{CO}_2$ results and corresponding Lyme Regis *O. aspinata* shell thickness. These corresponding data points are used in the linear regression models to determine any relationships between these two factors (Presented in Section 4.6).

Steinthorsdottir <i>et al.</i> (2011)							<i>O. aspinata</i> shell thickness				
Lyme Regis Bed Height (m)	Larne $p\text{CO}_2$ ppm carboniferous standard min	Larne $p\text{CO}_2$ ppm carboniferous standard max	Larne $p\text{CO}_2$ ppm carboniferous standard mean	Larne $p\text{CO}_2$ ppm modern standard min	Larne $p\text{CO}_2$ ppm modern standard max	Larne $p\text{CO}_2$ ppm modern standard mean	Lyme Regis Bed Height (m)	Mean	95th percentile min	95th percentile max	95th percentile range
8.2	1471	956	2675	1738	2073	1347	8.5	40.8	40.8	40.8	
9.4	1903	1237	2429	1579	2166	1408	9.6	36.9	26.6	52.0	25.3
10	1318	857	2010	1307	1664	1082	10.3	31.7	17.0	47.0	30.0
12.3	1062	690	1874	1218	1468	954	12.85	31.7	19.9	43.2	23.3

A5.4.2: Linear regression models indicating no significant relationships between the available $p\text{CO}_2$ results that correspond with the fossil size data from Lyme Regis or St Audrie's Bay.

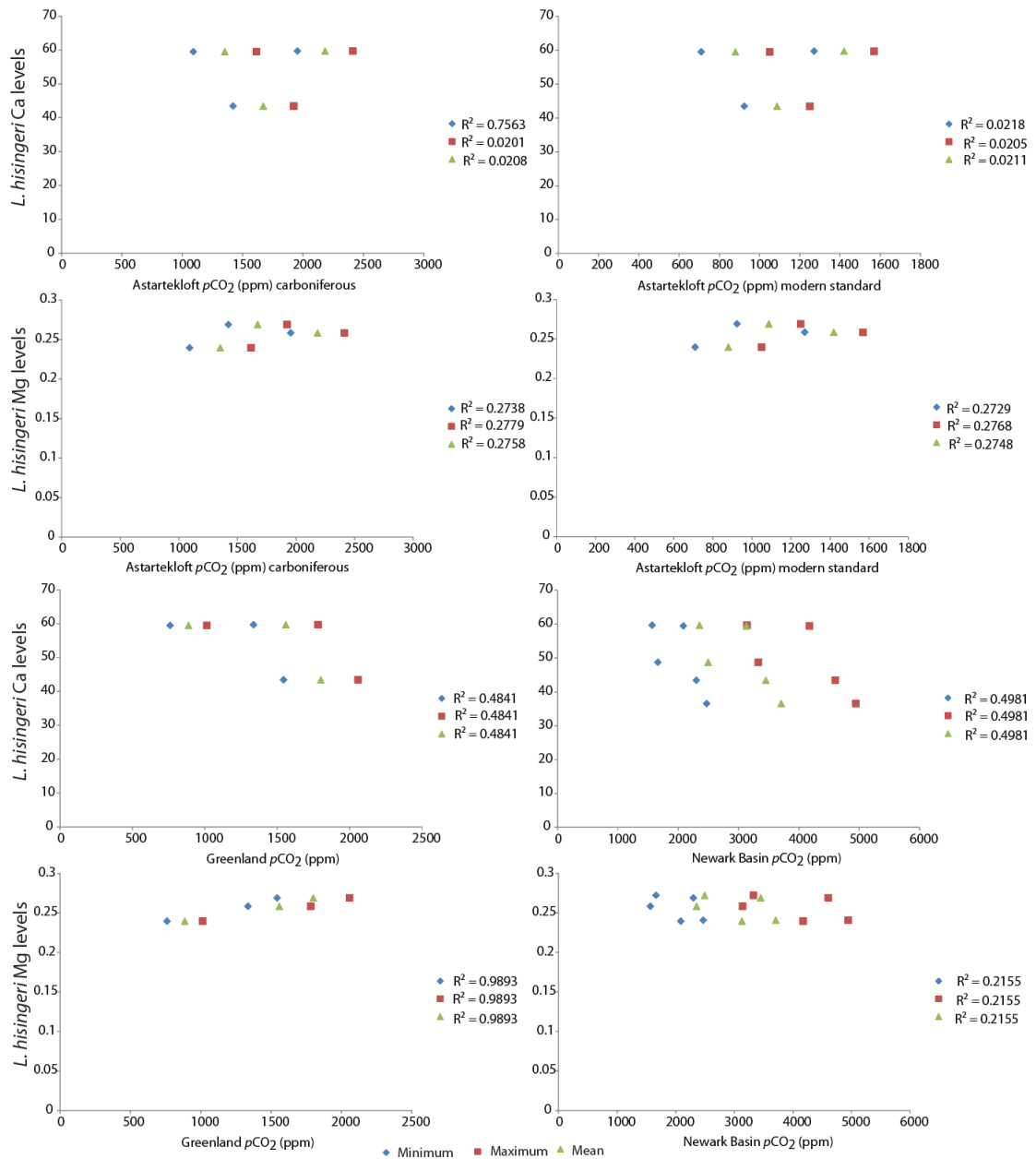


Figure A5.4: Linear regression models showing no significant relationships between the various different $p\text{CO}_2$ curves and corresponding Lyme Regis *L. hisingeri* Ca and Mg levels (Presented in Section 4.6).

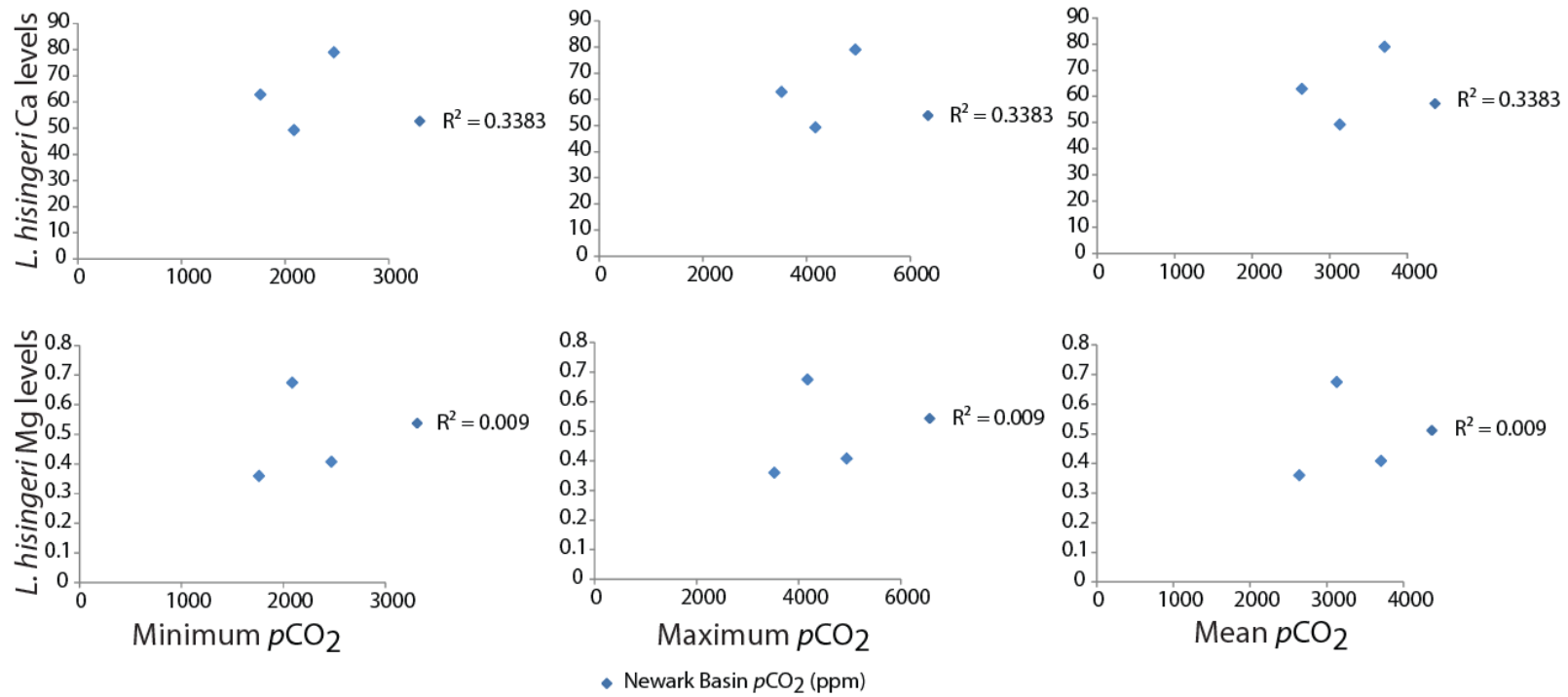


Figure A5.5: Linear regression models showing no significant relationships between the various different $p\text{CO}_2$ curves and corresponding St Audrie's Bay *L. hisingeri* Ca and Mg levels (mg/L) (Presented in Section 4.6).

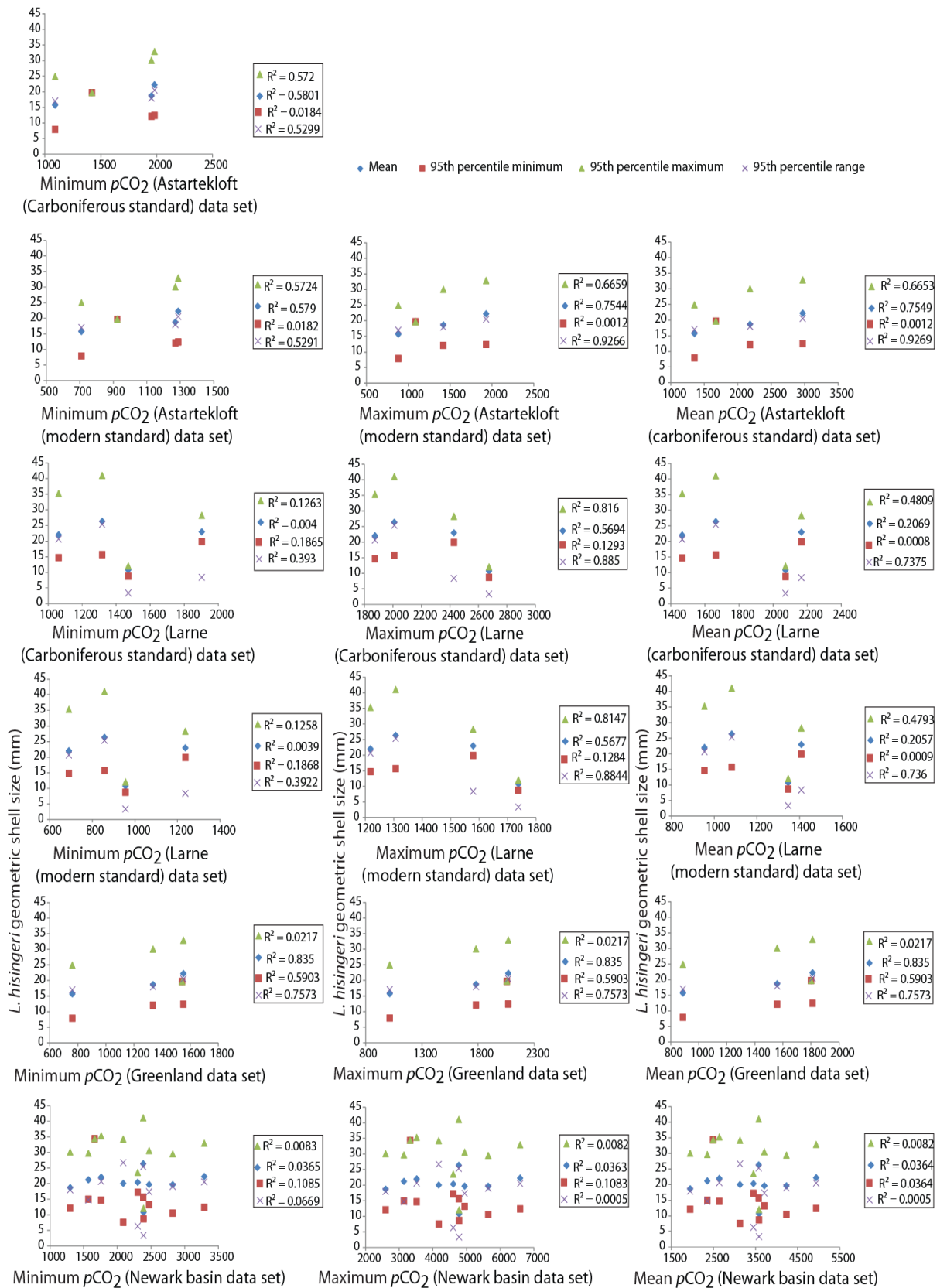


Figure A5.6: Linear regression models showing no significant relationships between the various different $p\text{CO}_2$ curves and corresponding Lyme Regis *L. hisingeri* geometric shell size (Presented in Section 4.6).

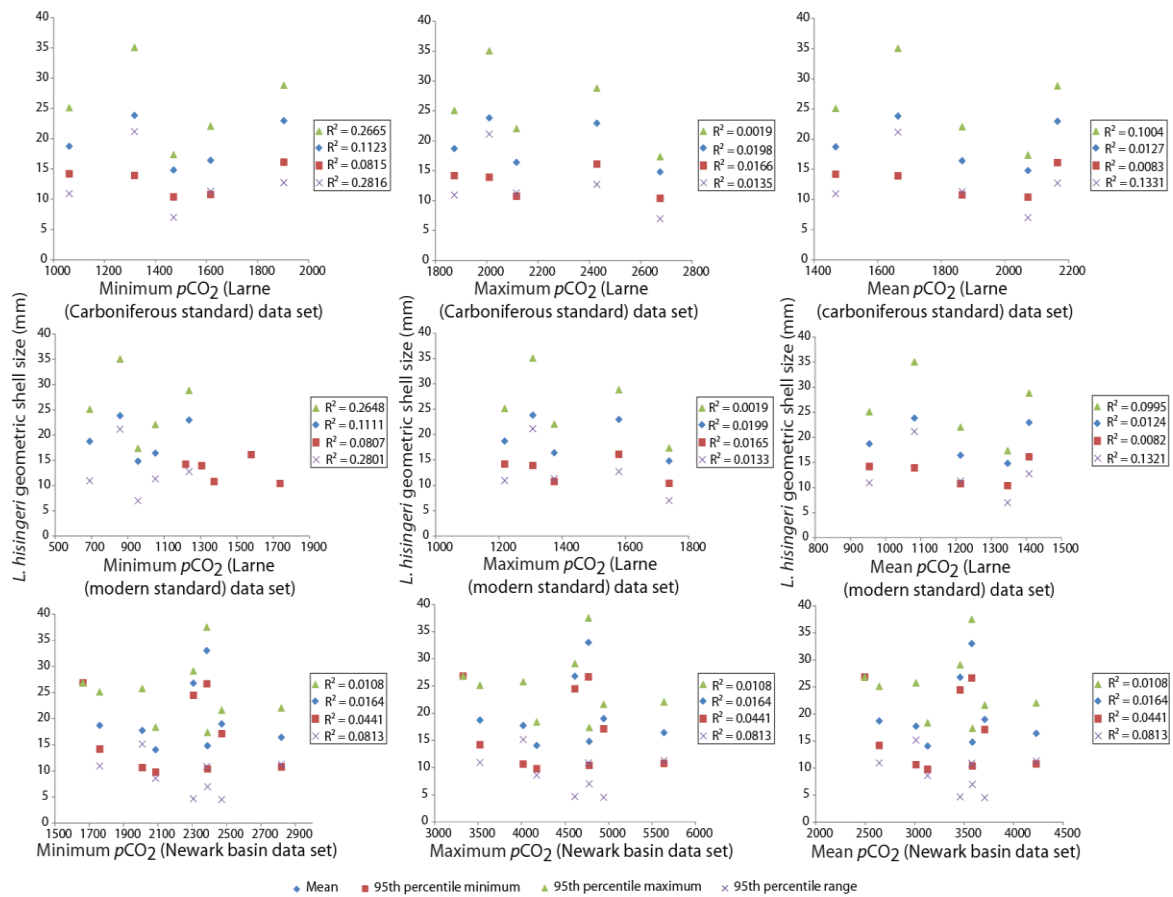


Figure A5.7: Linear regression models showing no significant relationships between the various different pCO₂ curves and corresponding St Audrie's Bay *L. hisingeri* geometric shell size (Presented in Section 4.6).

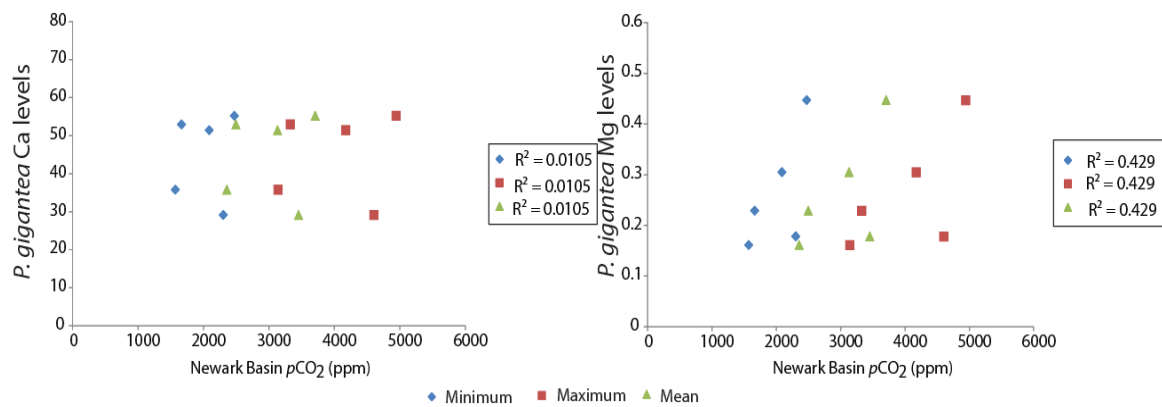


Figure A5.8: Linear regression models showing no significant relationships between the various different pCO₂ curves and corresponding Lyme Regis *P. gigantea* Ca and Mg levels (Presented in Section 4.6).

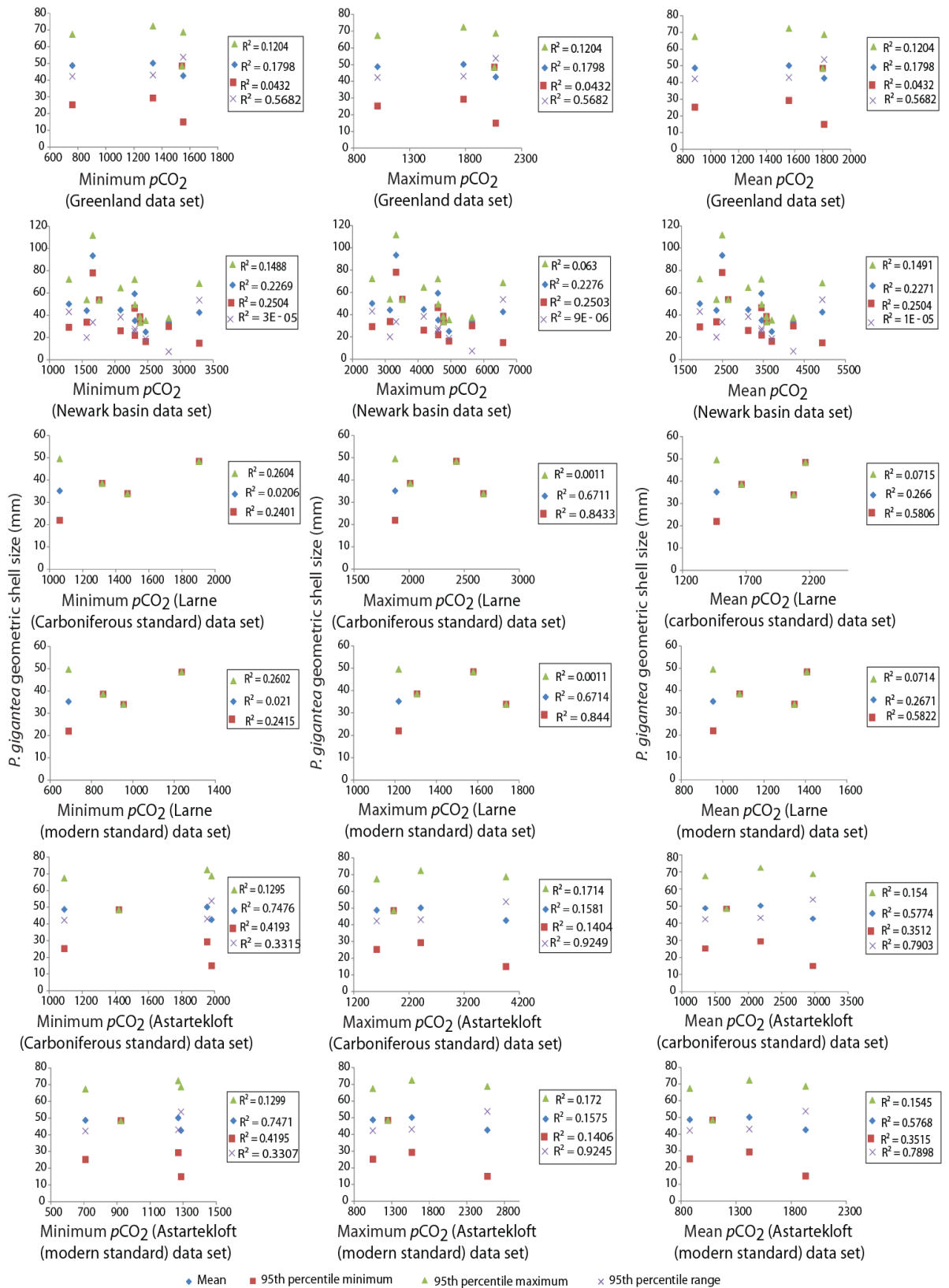


Figure A5.9: Linear regression models showing no significant relationships between the various different $p\text{CO}_2$ curves and corresponding Lyme Regis *P. gigantea* geometric shell size (Presented in Section 4.6).

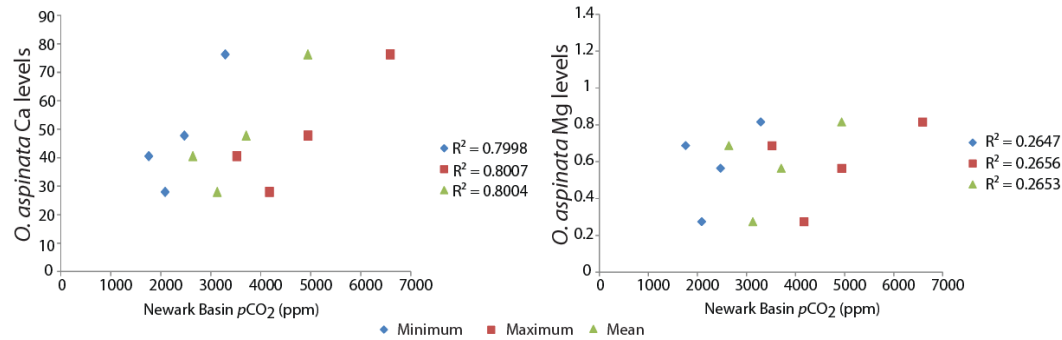


Figure A5.10: Linear regression models showing no significant relationships between the various different pCO_2 curves and corresponding Lyme Regis *O. aspinata* Ca and Mg levels (Presented in Section 4.6).

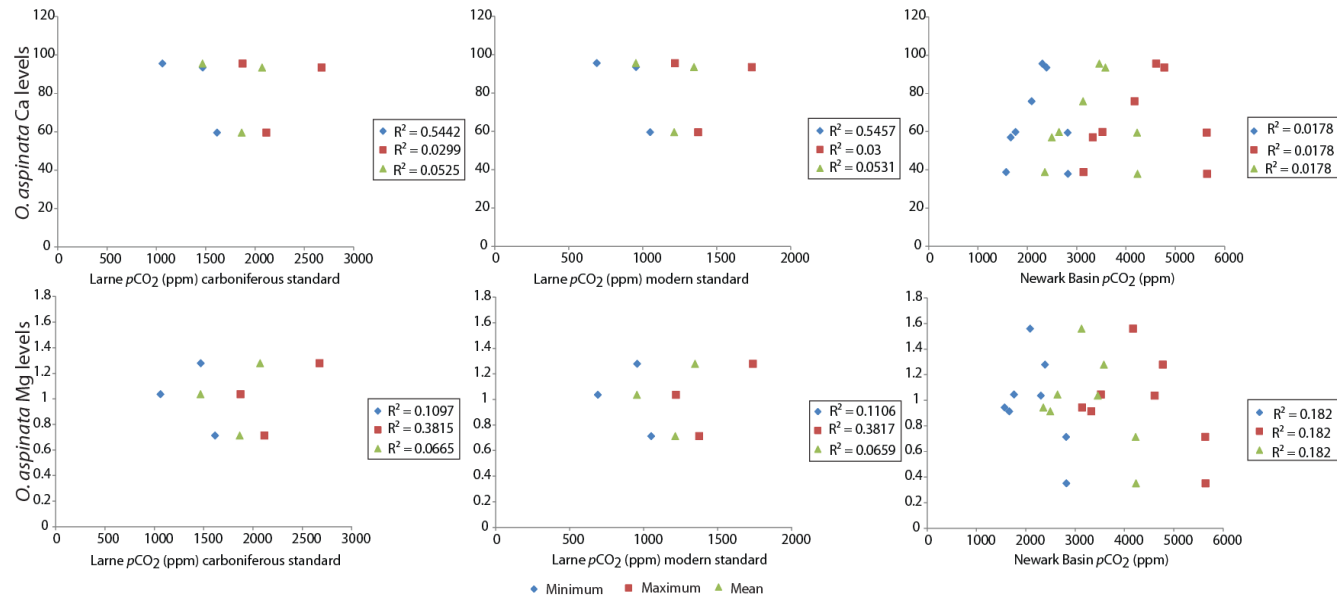


Figure A5.11: Linear regression models showing no significant relationships between the various different pCO_2 curves and corresponding St Audrie's Bay *O. aspinata* Ca and Mg levels (Presented in Section 4.6).

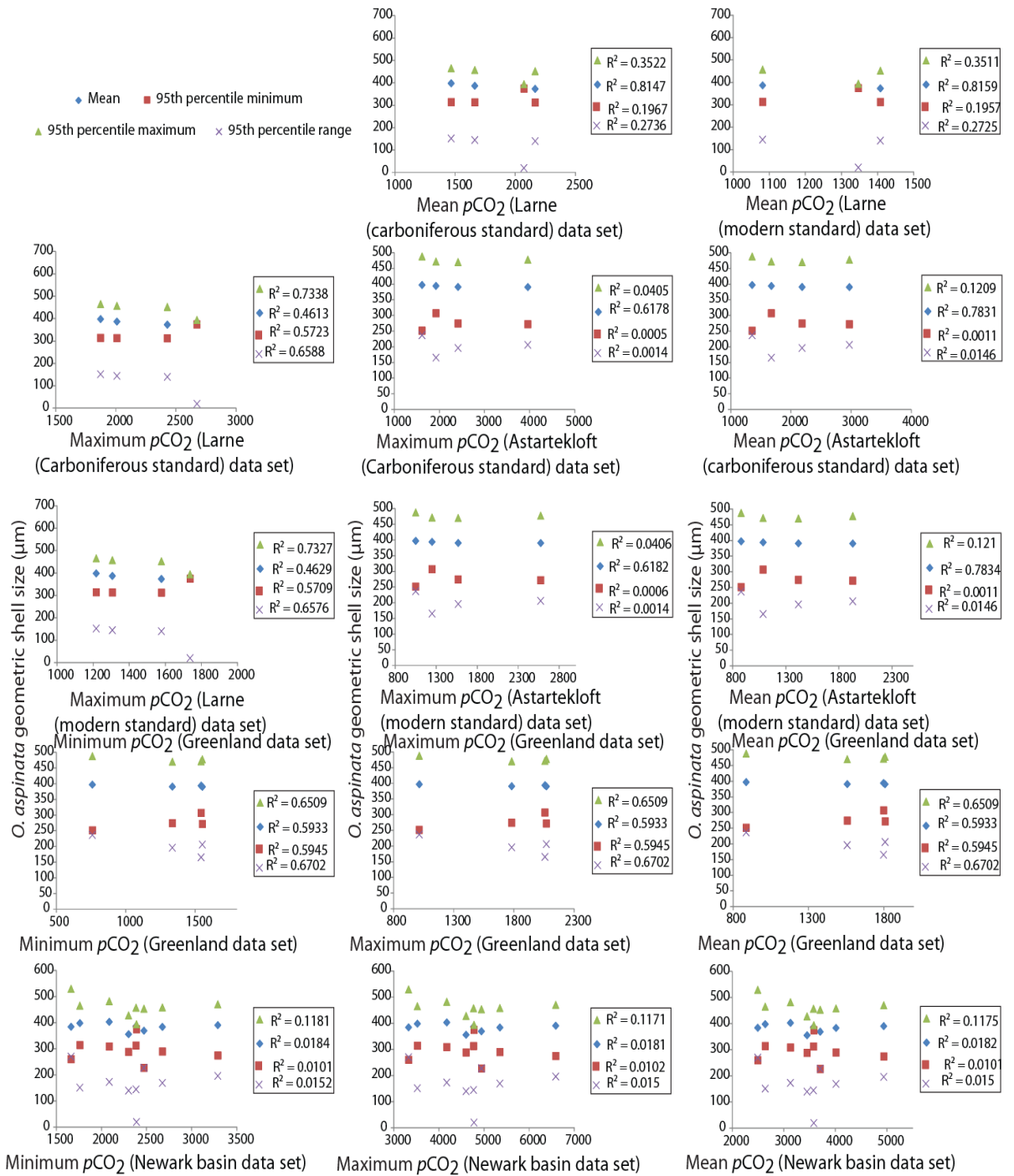


Figure A5.12: Linear regression models showing no significant relationships between the various different $p\text{CO}_2$ curves and corresponding Lyme Regis *O. aspinata* geometric shell size (Presented in Section 4.6).

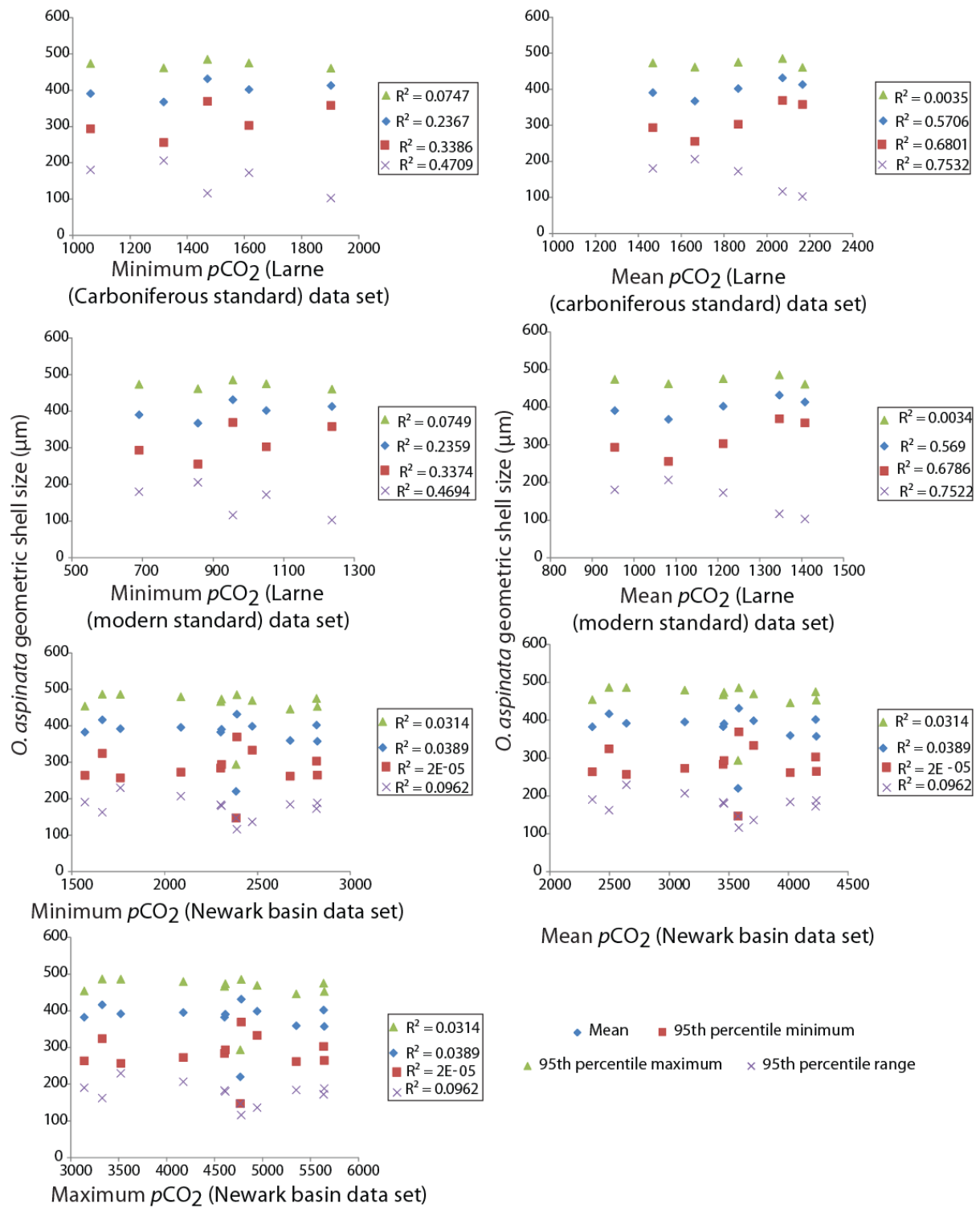


Figure A5.13: Linear regression models showing no significant relationships between the various different pCO₂ curves and corresponding St Audrie's Bay *O. aspinata* geometric shell size (Presented in Section 4.6).

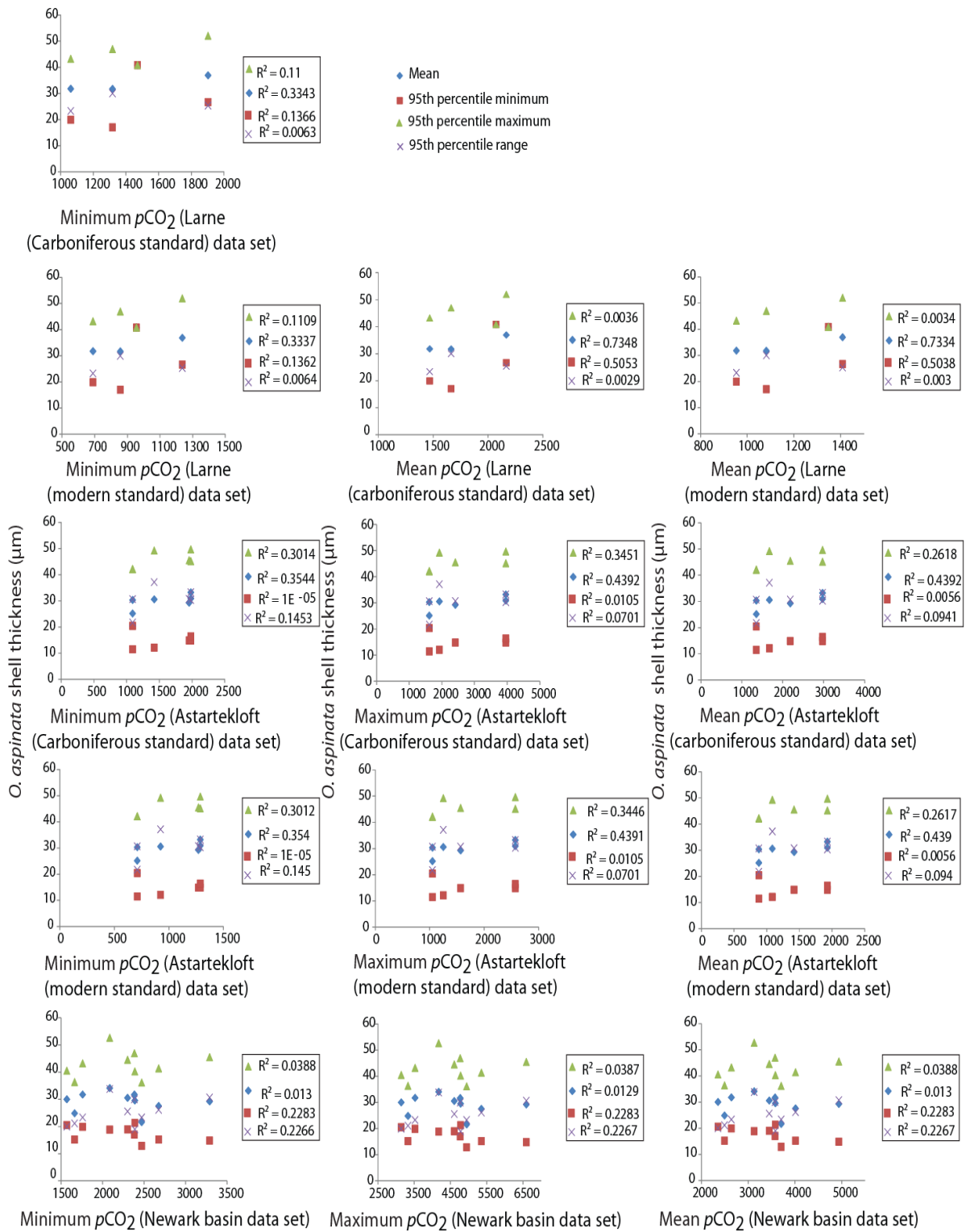


Figure A5.14: Linear regression models showing no significant relationships between the various different $p\text{CO}_2$ curves and corresponding Lyme Regis *O. aspinata* shell thickness (Presented in Section 4.6).

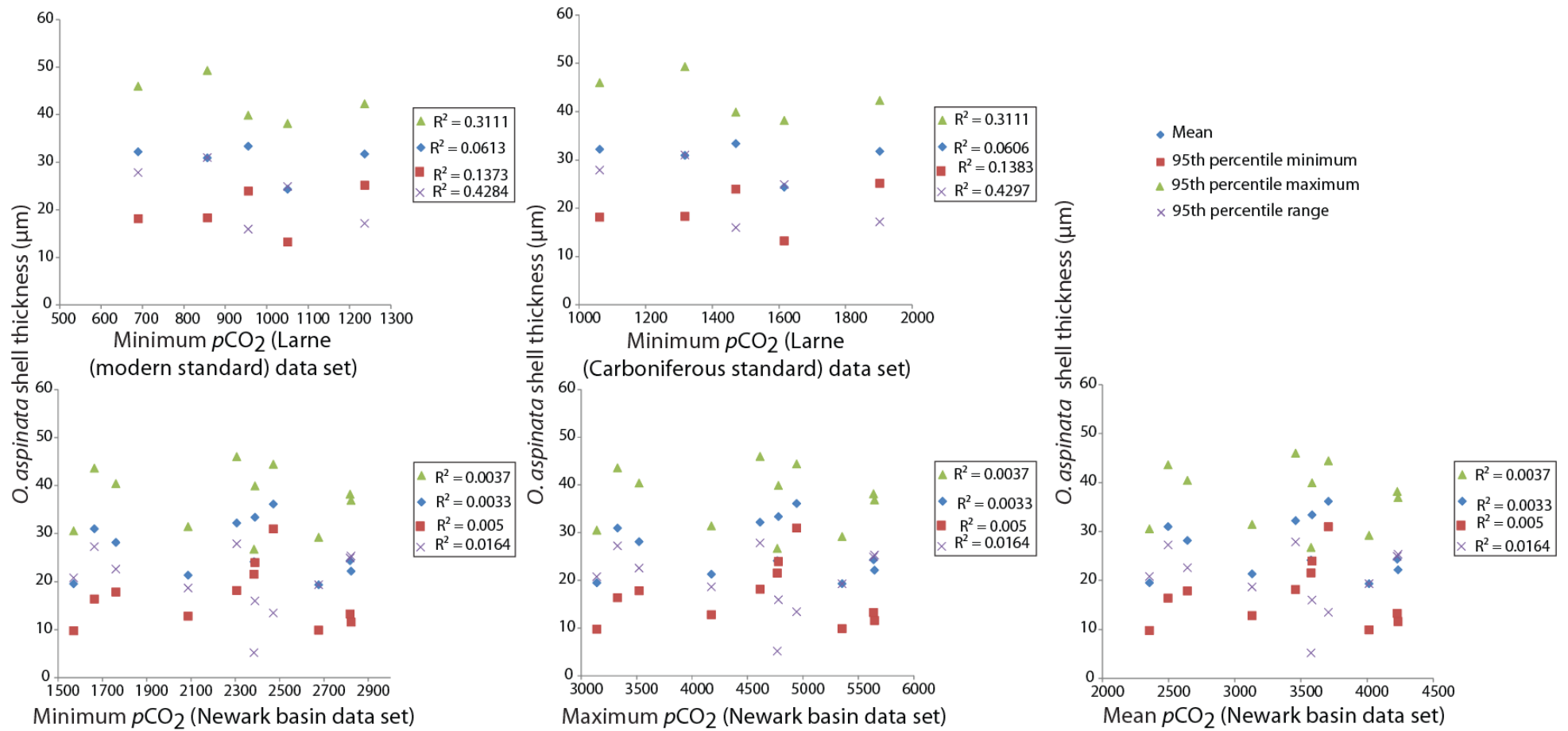


Figure A5.15: Linear regression models showing no significant relationships between the various different $p\text{CO}_2$ curves and corresponding St Audrie's Bay *O. aspinata* shell thickness (Presented in Section 4.6).

A5.5: Tables of the available temperature results that corresponds with the Lyme Regis or St Audrie's Bay fossil size data from this study.

Table A5.45: The *L. hisingeri* $\delta^{13}\text{C}$ and temperature results from this study and corresponding Lyme Regis *L. hisingeri* Ca and Mg levels or geometric shell size. These corresponding data points are used in the linear regression models to determine any relationships between these two factors (Presented in Section 4.7).

<i>L. hisingeri</i> from this study			<i>L. hisingeri</i> geometric size data				
Lyme Regis Bed Height (m)	$\delta^{13}\text{C}$	Temperature ($^{\circ}\text{C}$)	Lyme Regis Bed Height (m)	Mean	95th percentile min	95th percentile max	95th percentile range
10.6	0.9	23.1	10.5	20.3	17.2	23.5	6.3
13.37	0.6	22.8	13.3	19.7	13.2	30.5	17.3
14.8	1.6	22.3	14.85	22.8	20.4	25.3	4.9
18.2	1.1	19.9	17.75	24.0	14.1	38.6	24.5
19.35	1.9	21.2	19.55	22.0	13.9	32.9	19.0
19.6	1.2	18.9	19.75	28.4	21.7	32.3	10.7
21.55	0.9	19.8	21.5	34.4	34.4	34.4	
22.15	1.0	25.0	23.9	27.0	19.5	32.9	13.4
25.64	0.7	21.6	25.2	19.0	19.0	19.0	
26.75	0.9	23.1	27.64	23.9	20.0	27.1	7.2
			Lyme Regis Bed Height (m)	Ca	Mg		
	0.9	23.1	10.6	43.4	0.3		
	0.6	22.8	13.37	36.6	0.2		
	1.6	22.3	14.8	59.7	0.3		
	1.1	19.9	18.2	59.5	0.2		
	1.9	21.2	19.35	39.7	0.2		
	1.2	18.9	19.6	37.3	0.2		
	1.2	22.2	19.87	34.3	0.1		
	0.9	19.8	21.55	48.7	0.3		
	0.8	25.4	21.75	43.6	0.3		
	1.0	25.0	22.15	43.0	0.3		
	0.7	21.6	25.64	47.5	0.3		

Table A5.46: The *P. gigantea* $\delta^{13}\text{C}$ and temperature results from this study and corresponding Lyme Regis *L. hisingeri* Ca and Mg levels or geometric shell size. These corresponding data points are used in the linear regression models to determine any relationships between these two factors (Presented in Section 4.7).

<i>P. gigantea</i> from this study			<i>L. hisingeri</i> geometric size data				
Lyme Regis Bed Height (m)	$\delta^{13}\text{C}$	Temperature ($^{\circ}\text{C}$)	Lyme Regis Bed Height (m)	Mean	95th percentile min	95th percentile max	95th percentile range
10.6	1.5	18.3	10.5	20.3	17.2	23.5	6.3
13.37	1.1	19.9	13.3	19.7	13.2	30.5	17.3
14.8	1.2	18.9	14.85	22.8	20.4	25.3	4.9
19.35	1.3	20.7	19.55	22.0	13.9	32.9	19.0
19.87	1.6	22.3	19.75	28.4	21.7	32.3	10.7
21.15	1.4	19.9	21.5	34.4	34.4	34.4	
22.35	1.1	17.2	23.9	27.0	19.5	32.9	13.4
25.25	0.8	22.2	25.2	19.0	19.0	19.0	
			Lyme Regis Bed Height (m)	Ca	Mg		
10.6	1.5	18.3	10.6	43.4	0.3		
13.37	1.1	19.9	13.37	36.6	0.2		
14.8	1.2	18.9	14.8	59.7	0.3		
19.35	1.3	20.7	19.35	39.7	0.2		
19.87	1.6	22.3	19.87	34.3	0.1		
21.15	1.4	19.9	21.55	48.7	0.3		
21.75	1.5	18.3	21.75	43.6	0.3		
22.35	1.1	17.2	22.35	24.8	0.2		
25.25	0.8	22.2	25.25	54.0	0.2		

Table A5.47: The *O. aspinata* $\delta^{13}\text{C}$ and temperature results from this study and corresponding Lyme Regis *L. hisingeri* Ca and Mg levels or geometric shell size. These corresponding data points are used in the linear regression models to determine any relationships between these two factors (Presented in Section 4.7).

<i>O. aspinata</i> from this study			<i>L. hisingeri</i> geometric size data				
Lyme Regis Bed Height (m)	$\delta^{13}\text{C}$	Temperature ($^{\circ}\text{C}$)	Lyme Regis Bed Height (m)	Mean	95th percentile min	95th percentile max	95th percentile range
12.85	-0.5	25.3	12.75	24.5	14.0	32.9	18.9
13.37	-0.6	27.0	13.3	19.7	13.2	30.5	17.3
13.7	1.1	24.1	14.2	19.6	14.9	24.7	9.8
15.3	0.7	26.5	15.2	18.7	12.1	30.1	18.0
16.8	-0.6	27.8	16.1	15.7	7.9	24.9	17.0

<i>O. aspinata</i> from this study			<i>L. hisingeri</i> geometric size data					
17.5	0.3	25.4	17.5	20.0	7.6	34.2	26.7	
18.2	-0.5	32.1	18.9	23.0	13.9	29.6	15.7	
21.15	0.5	24.6	19.55	22.0	13.9	32.9	19.0	
21.75	0.9	22.7	21.5	34.4	34.4	34.4		
22.35	0.2	22.0	23.9	27.0	19.5	32.9	13.4	
25.25	0.2	26.0	25.2	19.0	19.0	19.0		
			Lyme Regis Bed Height (m)	Ca	Mg			
12.85	-0.5	25.3	10.6	43.4	0.3			
13.37	-0.6	27.0	13.37	36.6	0.2			
13.7	1.1	24.1	14.8	59.7	0.3			
18.2	-0.5	32.1	18.2	59.5	0.2			
21.15	0.5	24.6	21.55	48.7	0.3			
21.75	0.9	22.7	21.75	43.6	0.3			
22.15	0.1	25.9	22.15	43.0	0.3			
22.35	0.2	22.0	22.35	24.8	0.2			
25.25	0.2	26.0	25.25	54.0	0.2			

Table A5.48: The *P. gigantea* $\delta^{13}\text{C}$ and temperature results from this study and corresponding Lyme Regis *P. gigantea* Ca and Mg levels or geometric shell size. These corresponding data points are used in the linear regression models to determine any relationships between these two factors (Presented in Section 4.7).

<i>P. gigantea</i> from this study			<i>P. gigantea</i> geometric size data				
Lyme Regis Bed Height (m)	$\delta^{13}\text{C}$	Temperature ($^{\circ}\text{C}$)	Lyme Regis Bed Height (m)	Mean	95th percentile min	95th percentile max	95th percentile range
10.6	1.5	18.3	10.5	38.6	38.6	38.6	
13.37	1.1	19.9	13.3	25.0	16.3	35.3	19.0
14.8	1.2	18.9	14.85	47.8	47.8	47.8	
19.35	1.3	20.7	19.55	57.1	57.1	57.1	
21.75	1.5	18.3	21.5	93.4	78.0	111.7	33.7
22.35	1.1	17.2	22	106.2	106.2	106.2	
25.25	0.8	22.2	25.55	108.8	52.5	158.4	105.8
Lyme Regis Bed Height (m)	$\delta^{13}\text{C}$	Temperature ($^{\circ}\text{C}$)	Lyme Regis Bed Height (m)	Ca	Mg		
10.6	1.5	18.3	10.6	29.1	0.2		
13.37	1.1	19.9	13.37	55.2	0.4		
14.8	1.2	18.9	14.8	35.8	0.2		

<i>P. gigantea</i> from this study			<i>P. gigantea</i> geometric size data				
Lyme Regis Bed Height (m)	$\delta^{13}\text{C}$	Temperature ($^{\circ}\text{C}$)	Lyme Regis Bed Height (m)	Mean	95th percentile min	95th percentile max	95th percentile range
19.35	1.3	20.7	19.35	51.4	0.3		
19.87	1.6	22.3	19.87	48.7	0.2		
21.15	1.4	19.9	21.15	61.6	0.4		
21.75	1.5	18.3	21.75	51.1	0.3		
22.35	1.1	17.2	22.35	50.5	0.3		
25.25	0.8	22.2	25.25	48.3	0.3		

Table A5.49: The *L. hisingeri* $\delta^{13}\text{C}$ and temperature results from this study and corresponding Lyme Regis *P. gigantea* Ca and Mg levels or geometric shell size. These corresponding data points are used in the linear regression models to determine any relationships between these two factors (Presented in Section 4.7).

<i>L. hisingeri</i> from this study			<i>P. gigantea</i> geometric size data				
Lyme Regis Bed Height (m)	$\delta^{13}\text{C}$	Temperature ($^{\circ}\text{C}$)	Lyme Regis Bed Height (m)	Mean	95th percentile min	95th percentile max	95th percentile range
10.6	0.9	23.1	10.5	38.6	38.6	38.6	
13.37	0.6	22.8	13.3	25.0	16.3	35.3	18.95084
14.8	1.6	22.3	14.85	47.8	47.8	47.8	
18.2	1.1	19.9	18.9	87.0	80.5	93.6	13.06805
19.35	1.9	21.2	19.55	57.1	57.11	57.1	
21.55	0.9	19.8	21.5	93.4	78.0	111.7	33.67233
22.15	1.0	25.0	22	106.2	106.2	106.2	
25.64	0.7	21.6	25.55	108.8	52.6	158.4	105.8471
26.75	0.9	23.1	26	129.7	129.7	129.7	
Lyme Regis Bed Height (m)	$\delta^{13}\text{C}$	Temperature ($^{\circ}\text{C}$)	Lyme Regis Bed Height (m)	Ca	Mg		
10.6	0.9	23.1	10.6	29.1	0.2		
13.37	0.6	22.8	13.37	55.2	0.4		
14.8	1.6	22.3	14.8	35.8	0.2		
19.35	1.9	21.2	19.35	51.4	0.3		
19.6	1.2	18.9	19.6	51.4	0.3		
19.87	1.2	22.2	19.87	48.7	0.2		
21.55	0.9	19.8	21.55	52.9	0.2		
21.75	0.8	25.4	21.75	51.1	0.3		
22.15	1.0	25.0	22.15	74.8	0.5		
25.64	0.7	21.6	25.64	44.5	0.2		

Table A5.50: The *O. aspinata* $\delta^{13}\text{C}$ and temperature results from this study and corresponding Lyme Regis *P. gigantea* Ca and Mg levels or geometric shell size. These corresponding data points are used in the linear regression models to determine any relationships between these two factors (Presented in Section 4.7).

<i>O. aspinata</i> from this study			<i>P. gigantea</i> geometric size data				
Lyme Regis Bed Height (m)	$\delta^{13}\text{C}$	Temperature ($^{\circ}\text{C}$)	Lyme Regis Bed Height (m)	Mean	95th percentile min	95th percentile max	95th percentile range
12.85	-0.5	25.3	12.75	57.7	57.7	57.7	
13.37	-0.6	27.0	13.3	25.0	16.3	35.3	19.0
13.7	1.1	24.1	14.2	44.2	33.8	53.9	20.1
15.3	0.7	26.5	15.2	50.1	29.3	72.3	43.0
16.8	-0.6	27.8	16.1	48.7	25.2	67.4	42.2
17.5	0.3	25.4	17.5	44.7	26.1	64.6	38.5
18.2	-0.5	32.1	18.9	87.0	80.5	93.6	13.1
21.15	0.5	24.6	19.55	57.1	57.1	57.1	
21.75	0.9	22.7	21.5	93.4	78.0	111.7	33.7
22.15	0.1	25.9	22	106.2	106.2	106.2	
22.35	0.2	22.0	23.9	105.2	75.2	135.2	60.0
25.25	0.2	26.0	25.55	108.8	52.5	158.4	105.8
Lyme Regis Bed Height (m)	$\delta^{13}\text{C}$	Temperature ($^{\circ}\text{C}$)	Lyme Regis Bed Height (m)	Ca	Mg		
13.37	-0.6	27.0	13.37	55.2	0.4		
15.3	0.7	26.5	14.8	35.8	0.2		
18.2	-0.5	32.1	19.35	51.4	0.3		
21.15	0.5	24.6	21.15	61.6	0.4		
21.75	0.9	22.7	21.75	51.1	0.3		
22.15	0.1	25.9	22.15	74.8	0.5		
22.35	0.2	22.0	22.35	50.5	0.3		
25.25	0.2	26.0	25.25	48.3	0.3		

Table A5.51: The *O. aspinata* $\delta^{13}\text{C}$ and temperature results from this study and corresponding St Audrie's Bay *L. hisingeri* geometric shell size. These corresponding data points are used in the linear regression models to determine any relationships between these two factors (Presented in Section 4.7).

<i>O. aspinata</i> from this study			<i>L. hisingeri</i> geometric size data				
St Audrie's Bay Bed Height (m)	$\delta^{13}\text{C}$	Temperature ($^{\circ}\text{C}$)	St Audrie's Bay Bed Height (m)	Mean	95th percentile min	95th percentile max	95th percentile range
48.9	0.0	32.2	48.65	14.1	9.8	18.4	8.6
50.6	-0.3	33.6	51.3	26.8	26.8	26.8	

St Audrie's Bay Bed Height (m)	$\delta^{13}\text{C}$	Temperature ($^{\circ}\text{C}$)	St Audrie's Bay Bed Height (m)	Ca	Mg
48.9	0.0	32.2	48.9	49.3	0.7
49.8	-0.1	35.0	49.44	30.7	0.3
55.7	0.1	31.7	56.65	44.9	0.5

Table A5.52: The van de Schootbrugge *et al.* (2007) $\delta^{13}\text{C}$ and temperature results and corresponding St Audrie's Bay *L. hisingeri* geometric shell size. These corresponding data points are used in the linear regression models to determine any relationships between these two factors (Presented in Section 4.7).

van de Schootbrugge <i>et al.</i> (2007) oyster samples			<i>L. hisingeri</i> geometric size data				
St Audrie's Bay Bed Height (m)	$\delta^{13}\text{C}$	Temperature ($^{\circ}\text{C}$)	St Audrie's Bay Bed Height (m)	Mean	95th percentile min	95th percentile max	95th percentile range
15.1	3.4	15.8	15.45	20.1	12.8	25.6	12.9
15.95	3.7	18.9	15.8	24.8	12.8	33.0	20.2
16.1	3.5	11.6	16.07	23.4	18.3	29.1	10.7
16.12	3.4	14.2	16.3	22.0	18.4	25.6	7.2
17.2	2.8	16.5	17.15	23.8	13.9	35.0	21.1
17.7	1.6	14.5	18.1	33.0	26.7	37.5	10.9
19.68	1.9	14.7	20.4	17.7	10.6	25.8	15.1

Table A5.53: The Korte *et al.* (2009) $\delta^{13}\text{C}$ and temperature results and corresponding St Audrie's Bay *L. hisingeri* Ca and Mg levels or geometric shell size. These corresponding data points are used in the linear regression models to determine any relationships between these two factors (Presented in Section 4.7).

Korte <i>et al.</i> (2009) oysters			<i>L. hisingeri</i> geometric size data				
St Audrie's Bay Bed Height (m)	$\delta^{13}\text{C}$	Temperature ($^{\circ}\text{C}$)	St Audrie's Bay Bed Height (m)	Mean	95th percentile min	95th percentile max	95th percentile range
12.2	3.5	10.5	12.55	16.4	10.8	22.0	11.3
14.6	3.0	14.9	14.6	14.8	10.4	17.4	7.0
15.35	4.0	14.4	15.45	20.1	12.8	25.6	12.9
15.5	2.5	12.9	15.5	23.0	16.1	28.8	12.7
15.7	2.8	13.0	15.67	25.2	23.0	27.3	4.3
15.6	3.5	12.3	15.57	21.6	16.2	27.7	11.5
15.7	3.0	13.3	15.8	24.8	12.8	33.0	20.2
16.8	2.9	16.0	16.7	26.1	15.0	36.7	21.7
17.1	2.2	18.5	17.15	23.8	13.9	35.0	21.1
17.2	2.5	13.9	18.1	33.0	26.7	37.5	10.9

20	2.0	18.3	20.4	17.7	10.6	25.8	15.1
20.6	1.7	15.1	20.8	26.8	24.5	29.1	4.7
22.4	1.7	15.7	23.45	18.7	14.2	25.1	10.9
24.3	2.0	14.7	24.11	19.0	17.1	21.6	4.5
St Audrie's Bay Bed Height (m)	$\delta^{13}\text{C}$	Temperature ($^{\circ}\text{C}$)	St Audrie's Bay Bed Height (m)	Ca	Mg		
22.4	1.7	15.7	24.85	62.9	0.4		
25.9	2.3	19.6	26.58	79.0	0.4		

Table A5.54: The *L. hisingeri* $\delta^{13}\text{C}$ and temperature results from this study and corresponding St Audrie's Bay *L. hisingeri* Ca and Mg levels or geometric shell size. These corresponding data points are used in the linear regression models to determine any relationships between these two factors (Presented in Section 4.7).

<i>L. hisingeri</i> from this study			<i>L. hisingeri</i> geometric size data				
St Audrie's Bay Bed Height (m)	$\delta^{13}\text{C}$	Temperature ($^{\circ}\text{C}$)	St Audrie's Bay Bed Height (m)	Mean	95th percentile min	95th percentile max	95th percentile range
24.85	1.3	24.3	24.11	19.0	17.1	21.6	4.5
48.9	0.4	25.7	48.65	14.1	9.8	18.4	8.6
49.44	1.0	25.0	51.3	26.8	26.8	26.8	
St Audrie's Bay Bed Height (m)	$\delta^{13}\text{C}$	Temperature ($^{\circ}\text{C}$)	St Audrie's Bay Bed Height (m)	Ca	Mg		
24.85	1.3	24.3	24.85	62.9	0.4		
47	0.3	37.7	47	26.8	0.4		
48.9	0.4	25.7	48.9	49.3	0.7		
49.44	1.0	25.0	49.44	30.7	0.3		
56.65	0.8	25.6	56.65	44.9	0.5		
59.85	0.7	21.6	59.85	22.2	0.2		

Table A5.55: The *P. gigantea* $\delta^{13}\text{C}$ and temperature results from this study and corresponding St Audrie's Bay *L. hisingeri* Ca and Mg levels or geometric shell size. These corresponding data points are used in the linear regression models to determine any relationships between these two factors (Presented in Section 4.7).

<i>P. gigantea</i> from this study			<i>L. hisingeri</i> geometric size data				
St Audrie's Bay Bed Height (m)	$\delta^{13}\text{C}$	Temperature ($^{\circ}\text{C}$)	St Audrie's Bay Bed Height (m)	Mean	95th percentile min	95th percentile max	95th percentile range
23.2	0.6	22.0	23.45	18.7	14.2	25.1	10.9
26.5	0.8	22.2	24.11	19.0	17.1	21.6	4.5
48.9	1.1	21.6	48.65	14.1	9.8	18.4	8.6
50.6	1.2	21.8	51.3	26.8	26.8	26.8	
St Audrie's Bay Bed Height (m)	$\delta^{13}\text{C}$	Temperature ($^{\circ}\text{C}$)	St Audrie's Bay Bed Height (m)	Ca	Mg		

23.2	0.6	22.0	24.85	62.9	0.4
26.58	0.9	16.7	26.58	79.0	0.4
48.9	1.1	21.6	48.9	49.3	0.7
49.44	1.3	19.3	49.44	30.7	0.3
56.65	0.9	21.8	56.65	44.9	0.5

Table A5.56: The *O. aspinata* $\delta^{13}\text{C}$ and temperature results from this study and corresponding St Audrie's Bay *O. aspinata* Ca and Mg levels or geometric shell size or shell thickness. These corresponding data points are used in the linear regression models to determine any relationships between these two factors (Presented in Section 4.7).

<i>O. aspinata</i> from this study			<i>O. aspinata</i> geometric size data					<i>O. aspinata</i> shell thickness				
St Audrie's Bay Bed Height (m)	$\delta^{13}\text{C}$	Temperature (°C)	St Audrie's Bay Bed Height (m)	Mean	95th percentile min	95th percentile max	95th percentile range	St Audrie's Bay Bed Height (m)	Mean	95th percentile min	95th percentile max	95th percentile range
48.9	0.0	32.2	48.9	395.3	272.7	479.4	206.6	48.9	21.3	12.8	31.4	18.6
49.8	-0.1	35.0	49.8	373.6	246.5	450.2	203.8	49.8	26.1	13.1	39.8	26.7
50.6	-0.3	33.6	50.6	380.8	266.9	463.8	196.8	50.6	27.6	16.2	38.5	22.3
53.05	0.1	36.4	53.05	416.4	324.1	486.4	162.4	53.05	31.0	16.4	43.6	27.2
53.6	0.2	31.0	53.6	413.9	302.2	506.1	203.9	53.6	26.8	14.1	44.2	30.1
55.5	0.5	30.3	55.5	417.7	268.9	505.1	236.2	55.5	30.3	19.7	44.4	24.7
55.7	0.1	31.7	55.7	395.2	278.9	478.7	199.8	55.7	29.5	14.0	44.1	30.1
57.3	0.4	26.5	57.3	389.0	222.0	528.7	306.7	57.3	27.7	16.4	44.8	28.3
St Audrie's Bay Bed Height (m)	$\delta^{13}\text{C}$	Temperature (°C)	St Audrie's Bay Bed Height (m)	Ca	Mg							
48.9	0.0	32.2	48.9	75.9	1.6							
49.8	-0.1	35.0	49.8	47.5	0.8							
50.6	-0.3	33.6	50.6	79.4	1.5							
53.05	0.1	36.4	53.05	57.0	0.9							
53.6	0.2	31.0	53.6	64.9	1.0							
55.5	0.5	30.3	55.5	31.8	0.7							
55.7	0.1	31.7	55.7	71.6	0.9							
57.3	0.4	26.5	57.3	70.7	1.1							

Table A5.57: The *L. hisingeri* $\delta^{13}\text{C}$ and temperature results from this study and corresponding St Audrie's Bay *O. aspinata* Ca and Mg levels or geometric shell size or shell thickness. These corresponding data points are used in the linear regression models to determine any relationships between these two factors (Presented in Section 4.7).

<i>L. hisingeri</i> from this study			<i>O. aspinata</i> geometric size data				<i>O. aspinata</i> shell thickness					
St Audrie's Bay Bed Height (m)	$\delta^{13}\text{C}$	Temperature (°C)	St Audrie's Bay Bed Height (m)	Mean	95th percentile min	95th percentile max	95th percentile range	St Audrie's Bay Bed Height (m)	Mean	95th percentile min	95th percentile max	95th percentile range
24.85	1.3	24.3	24.3	398.5	332.9	469.1	136.2	24.3	36.1	31.0	44.4	13.4
47	0.3	37.7	47	398.9	281.6	473.9	192.3	47	22.0	14.3	34.4	20.1
48.9	0.4	25.7	48.9	395.3	272.7	479.4	206.6	48.9	21.3	12.8	31.4	18.6
49.3	0.2	29.8	49.3	366.0	224.9	450.5	225.5	49.3	25.7	13.7	39.7	26.0
49.44	1.0	25.0	49.44	383.0	269.7	453.7	184.0	49.44	27.0	12.1	39.5	27.4
53.05	0.4	34.7	53.05	416.4	324.1	486.4	162.4	53.05	31.0	16.4	43.6	27.2
56.65	0.8	25.6	56.65	398.8	271.1	481.6	210.6	56.65	33.6	15.7	48.6	32.9
59.85	0.7	21.6	59.85	365.2	215.7	524.4	308.7	59.85	29.7	14.2	47.4	33.2

St Audrie's Bay Bed Height (m)	$\delta^{13}\text{C}$	Temperature (°C)	St Audrie's Bay Bed Height (m)	Ca	Mg
24.85	1.3	24.3	23.8	59.8	1.0
47	0.3	37.7	47	47.9	1.1
48.9	0.4	25.7	48.9	75.9	1.6
49.3	0.2	29.8	49.3	44.7	0.9
49.44	1.0	25.0	49.44	42.0	0.7
53.05	0.4	34.7	53.05	57.0	0.9
56.65	0.8	25.6	56.65	51.7	1.1
59.85	0.7	21.6	59.85	43.5	0.5

Table A5.58: The *P. gigantea* $\delta^{13}\text{C}$ and temperature results from this study and corresponding St Audrie's Bay *O. aspinata* Ca and Mg levels or geometric shell size or shell thickness. These corresponding data points are used in the linear regression models to determine any relationships between these two factors (Presented in Section 4.7).

<i>P. gigantea</i> from this study			<i>O. aspinata</i> geometric size data					<i>O. aspinata</i> shell thickness				
St Audrie's Bay Bed Height (m)	$\delta^{13}\text{C}$	Temperature (°C)	St Audrie's Bay Bed Height (m)	Mean	95th percentile min	95th percentile max	95th percentile range	St Audrie's Bay Bed Height (m)	Mean	95th percentile min	95th percentile max	95th percentile range
23.2	0.6	22.0	23.2	390.3	293.3	473.4	180.0	23.2	32.2	18.1	46.0	27.8
26.5	0.8	22.2	26.5	382.4	263.6	453.9	190.3	26.5	19.5	9.8	30.5	20.8
48.9	1.1	21.6	48.9	395.3	272.7	479.4	206.6	48.9	21.3	12.8	31.4	18.6
49.3	0.9	20.6	49.3	366.0	224.9	450.5	225.5	49.3	25.7	13.7	39.7	26.0
49.44	1.3	19.3	49.44	383.0	269.7	453.7	184.0	49.44	27.0	12.1	39.5	27.4
49.8	0.8	25.4	49.8	373.6	246.5	450.2	203.8	49.8	26.1	13.1	39.8	26.7
50.6	1.2	21.8	50.6	380.8	266.9	463.8	196.8	50.6	27.6	16.2	38.5	22.3
53.05	1.2	22.1	53.05	416.4	324.1	486.4	162.4	53.05	31.0	16.4	43.6	27.2
53.6	1.2	22.2	53.6	413.9	302.2	506.1	203.9	53.6	26.8	14.1	44.2	30.1
55.5	0.9	25.6	55.5	417.7	268.9	505.1	236.2	55.5	30.3	19.7	44.4	24.7
56.65	0.9	21.8	56.65	398.8	271.1	481.6	210.6	56.65	33.6	15.7	48.6	32.9
62.5	1.4	22.7	62.5	318.0	273.6	403.8	130.2	62.5	21.1	14.1	33.0	18.9
St Audrie's Bay Bed Height (m)	$\delta^{13}\text{C}$	Temperature (°C)	St Audrie's Bay Bed Height (m)	Ca	Mg							
23.2	0.6	22.0	23.2	95.5	1.0							
26.5	0.8	22.2	26.5	38.9	0.9							
48.9	1.1	21.6	48.9	75.9	1.6							
49.3	0.9	20.6	49.3	44.7	0.9							
49.44	1.3	19.3	49.44	42.0	0.7							
49.8	0.8	25.4	49.8	47.5	0.8							
50.6	1.2	21.8	50.6	79.4	1.5							
53.05	1.2	22.1	53.05	57.0	0.9							
53.6	1.2	22.2	53.6	64.9	1.0							
55.5	0.9	25.6	55.5	31.8	0.7							
56.65	0.9	21.8	56.65	51.7	1.1							

Table A5.59: The van de Schootbrugge *et al.* (2007) $\delta^{13}\text{C}$ and temperature results and corresponding St Audrie's Bay *O. aspinata* Ca and Mg levels or geometric shell size or shell thickness. These corresponding data points are used in the linear regression models to determine any relationships between these two factors (Presented in Section 4.7).

van de Schootbrugge <i>et al.</i> (2007) oyster			<i>O. aspinata</i> geometric size data					<i>O. aspinata</i> shell thickness				
St Audrie's Bay Bed Height (m)	$\delta^{13}\text{C}$	Temperature (°C)	St Audrie's Bay Bed Height (m)	Mean	95th percentile min	95th percentile max	95th percentile range	St Audrie's Bay Bed Height (m)	Mean	95th percentile min	95th percentile max	95th percentile range
15.1	3.4	15.8	15	412.9	357.8	460.3	102.5	15	31.7	25.1	42.3	17.1
17.4	2.5	14.3	17.4	367.3	255.6	461.5	206.0	17.4	30.9	18.3	49.3	31.0
17.7	1.6	14.5	17.9	220.0	147.0	293.8	146.7	17.9	24.1	21.5	26.7	5.2
19.6	2.3	13.9	18.7	357.2	264.5	452.5	188.1	18.7	22.1	11.6	36.9	25.3
19.68	1.9	14.7	19.8	359.2	261.6	445.7	184.1	19.8	19.3	9.9	29.2	19.3
St Audrie's Bay Bed Height (m)	$\delta^{13}\text{C}$	Temperature (°C)	St Audrie's Bay Bed Height (m)	Ca	Mg							
17.7	1.6	14.5	18.7	37.9	0.4							

Table A5.60: The Korte *et al.* (2009) $\delta^{13}\text{C}$ and temperature results and corresponding St Audrie's Bay *O. aspinata* Ca and Mg levels or geometric shell size or shell thickness. These corresponding data points are used in the linear regression models to determine any relationships between these two factors (Presented in Section 4.7).

Korte <i>et al.</i> (2009) oysters			<i>O. aspinata</i> geometric size data					<i>O. aspinata</i> shell thickness				
St Audrie's Bay Bed Height (m)	$\delta^{13}\text{C}$	Temperature (°C)	St Audrie's Bay Bed Height (m)	Mean	95th percentile min	95th percentile max	95th percentile range	St Audrie's Bay Bed Height (m)	Mean	95th percentile min	95th percentile max	95th percentile range
12.2	3.5	10.5	12.2	401.7	302.7	475.0	172.2	12.2	24.3	13.2	38.1	24.9
12.8	3.6	13.1	12.5	431.4	369.1	485.2	116.1	12.5	33.4	23.9	39.9	15.9
14.95	3.2	16.2	15	412.9	357.8	460.3	102.5	15	31.7	25.1	42.3	17.1
17.2	2.5	13.9	17.4	367.3	255.6	461.5	206.0	17.4	30.9	18.3	49.3	31.0
19.8	2.2	15.5	19.8	359.2	261.6	445.7	184.1	19.8	19.3	9.9	29.2	19.3
22.4	2.5	15.1	23.2	390.3	293.3	473.4	180.0	23.2	32.2	18.1	46.0	27.8
24.3	2.0	14.7	24.3	398.5	332.9	469.1	136.2	24.3	36.1	31.0	44.4	13.4
25.9	2.3	19.6	26.5	382.4	263.6	453.9	190.3	26.5	19.5	9.8	30.5	20.8
St Audrie's Bay Bed Height (m)	$\delta^{13}\text{C}$	Temperature (°C)	St Audrie's Bay Bed Height (m)	Ca	Mg							
12.2	3.6	11.7	12.2	59.5	0.7							
12.8	3.6	13.1	12.5	93.5	1.3							
19.8	2.2	15.5	18.7	37.9	0.4							
22.4	1.7	15.7	23.2	95.5	1.0							
24.3	2.0	14.7	23.8	59.8	1.0							
25.9	2.3	19.6	26.5	38.9	0.9							

A5.5.2: Linear regression models demonstrating there were no significant relationships between the available temperature results that correspond with the Lyme Regis or St Audrie's Bay fossil size data from this study.

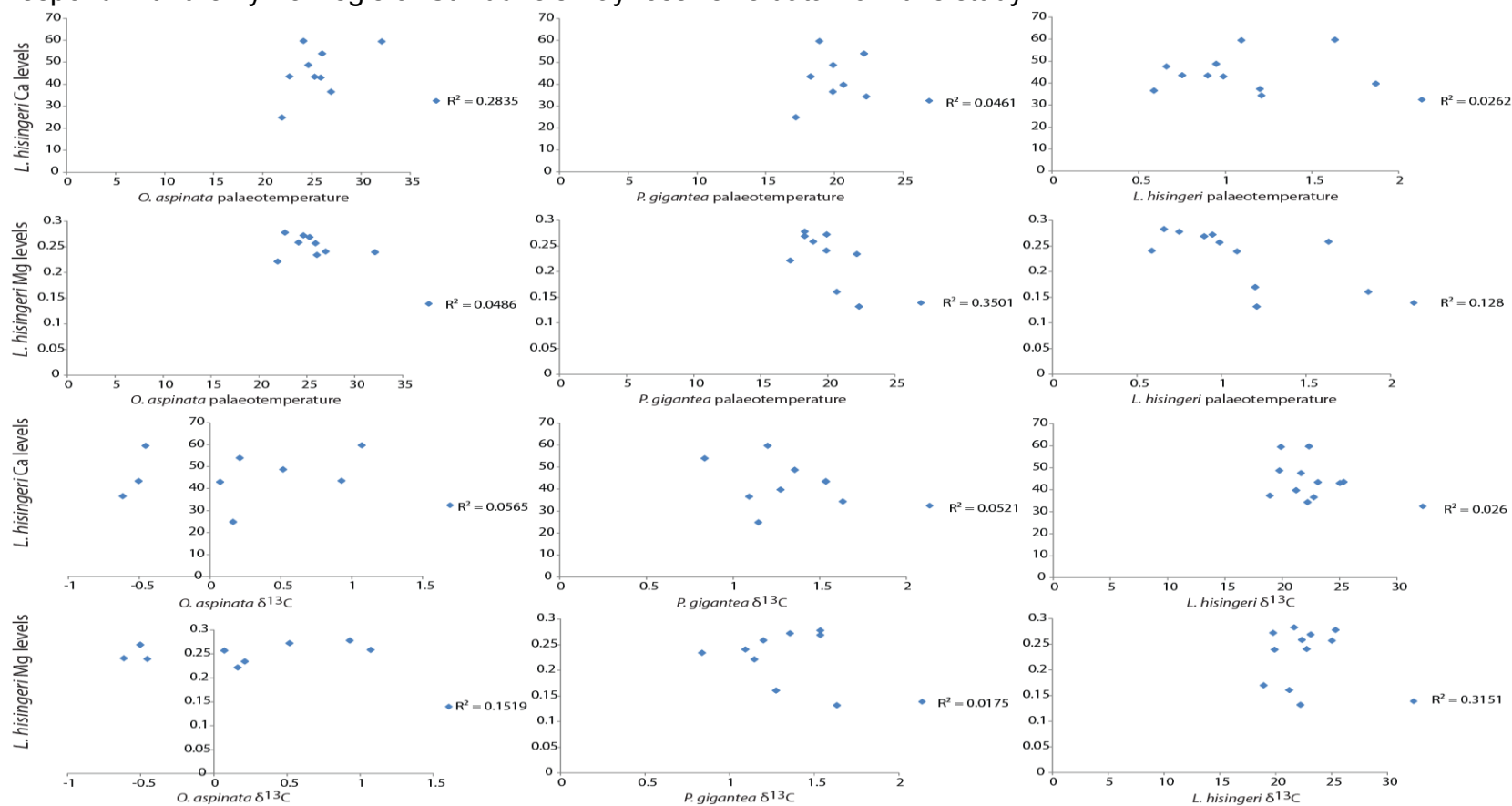


Figure A5.16: Linear regression models showing no significant relationships between the various different $\delta^{13}C$ and temperature curves (both from this study and those previously published) and corresponding Lyme Regis *L. hisingeri* Ca and Mg levels (Presented in Section 4.7).

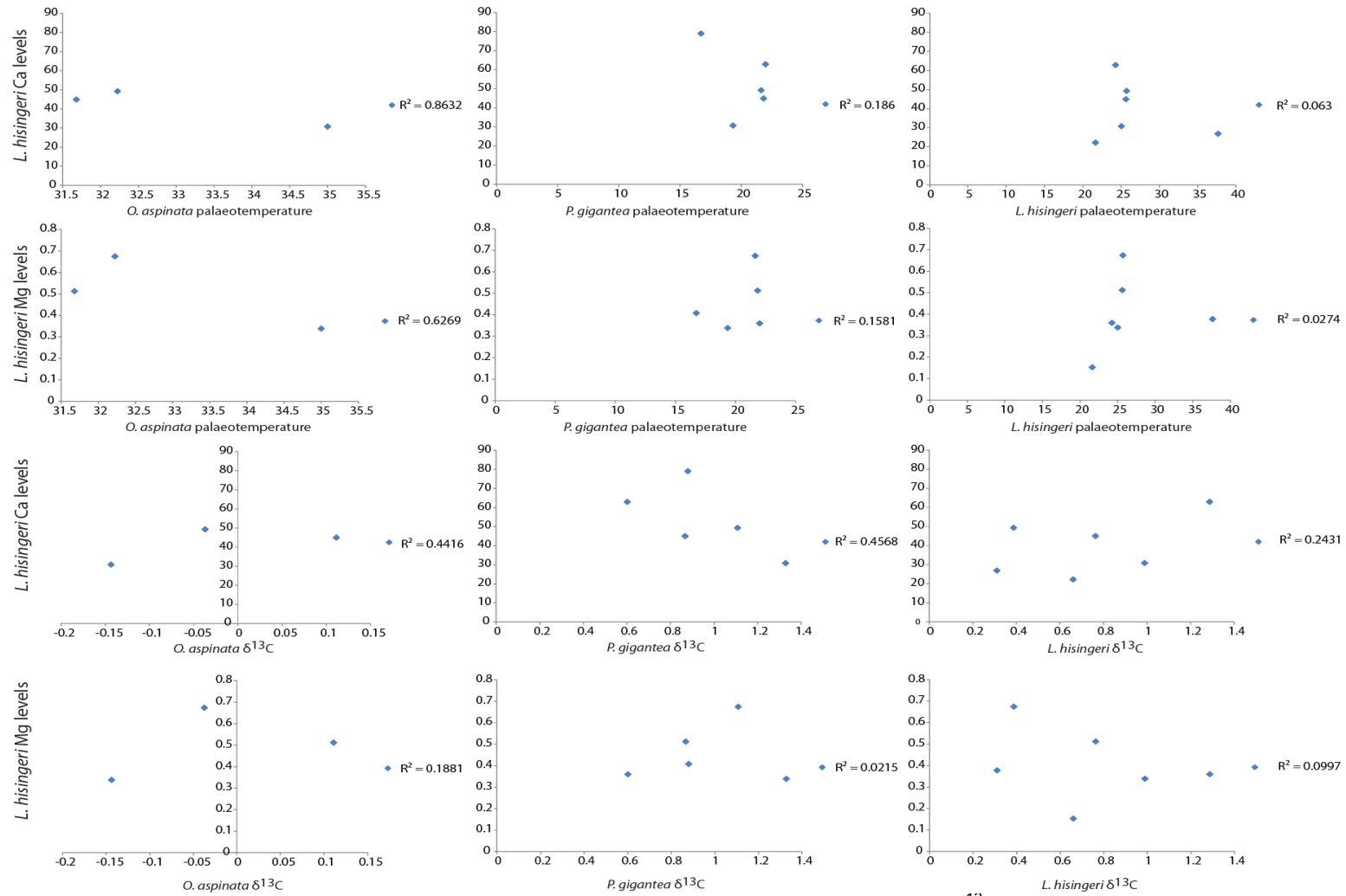


Figure A5.17: Linear regression models showing no significant relationships between the various different $\delta^{13}\text{C}$ and temperature curves (both from this study and those previously published) and corresponding St Audrie's Bay *L. hisingeri* Ca and Mg levels (Presented in Section 4.7).

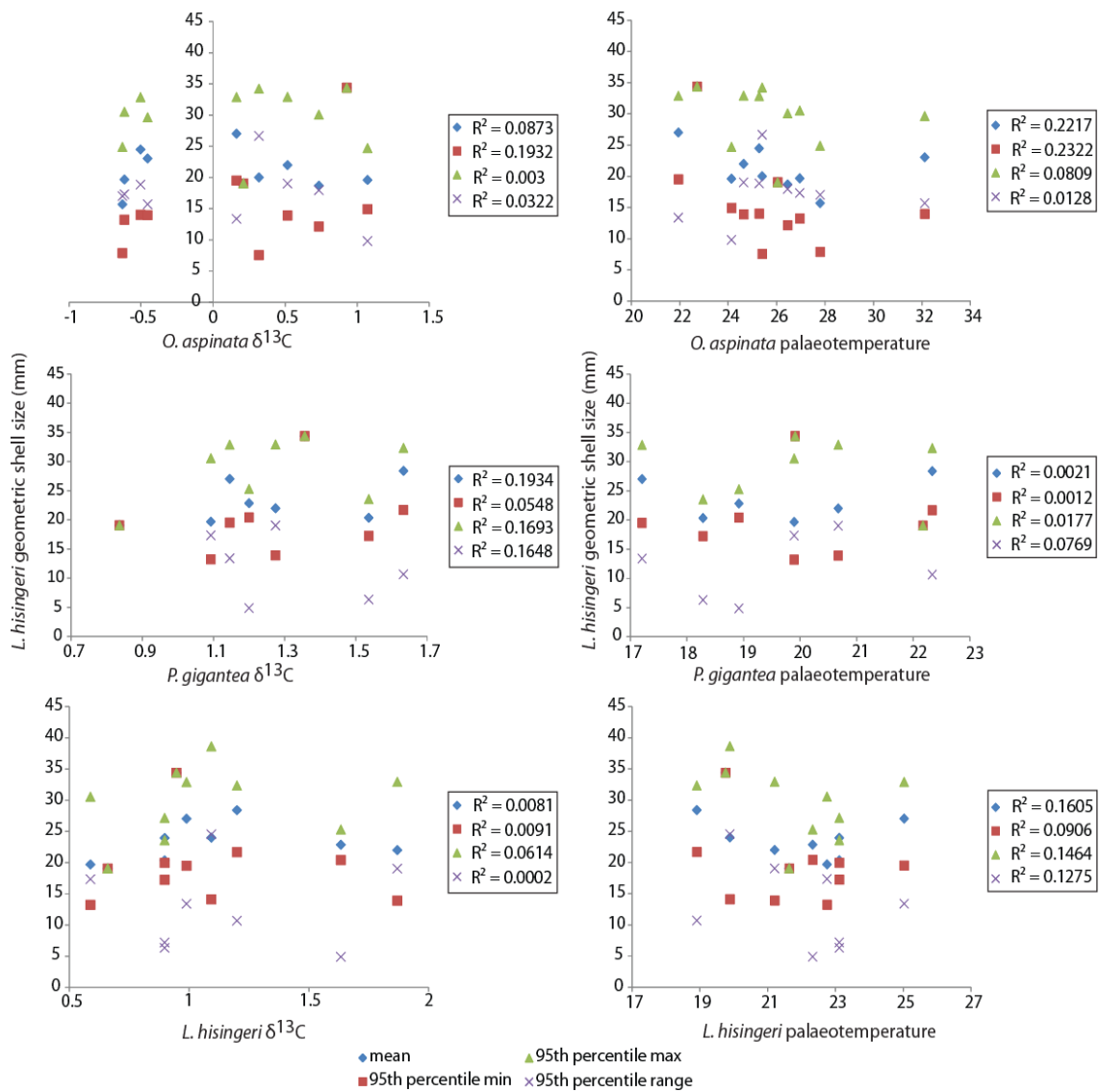


Figure A5.18: Linear regression models showing no significant relationships between the various different $\delta^{13}\text{C}$ and temperature curves (both from this study and those previously published) and corresponding Lyme Regis *L. hisingeri* geometric shell size (Presented in Section 4.7).

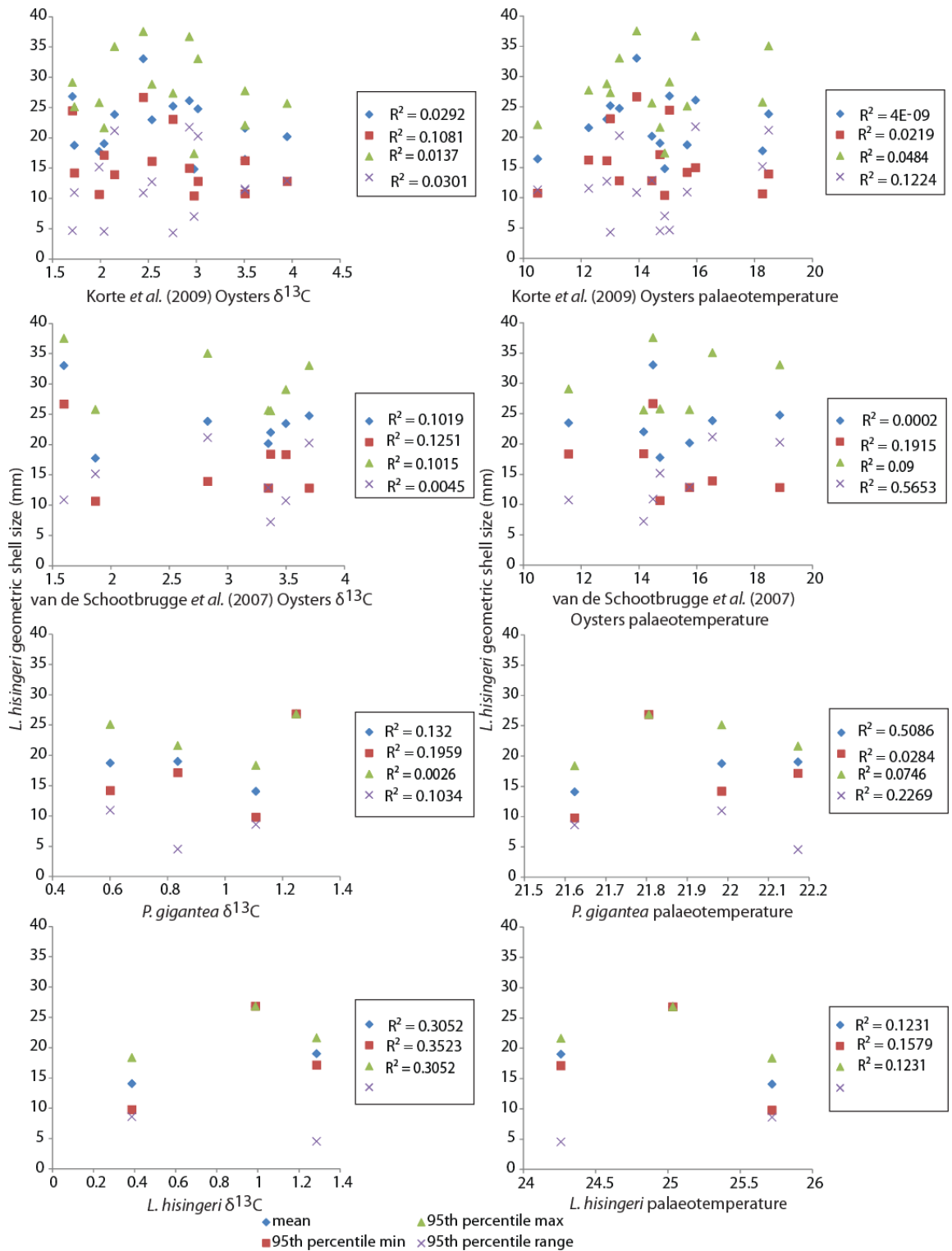


Figure A5.19: Linear regression models showing no significant relationships between the various different $\delta^{13}\text{C}$ and temperature curves (both from this study and those previously published) and corresponding St Audrie's Bay *L. hisingeri* geometric shell size (Presented in Section 4.7).

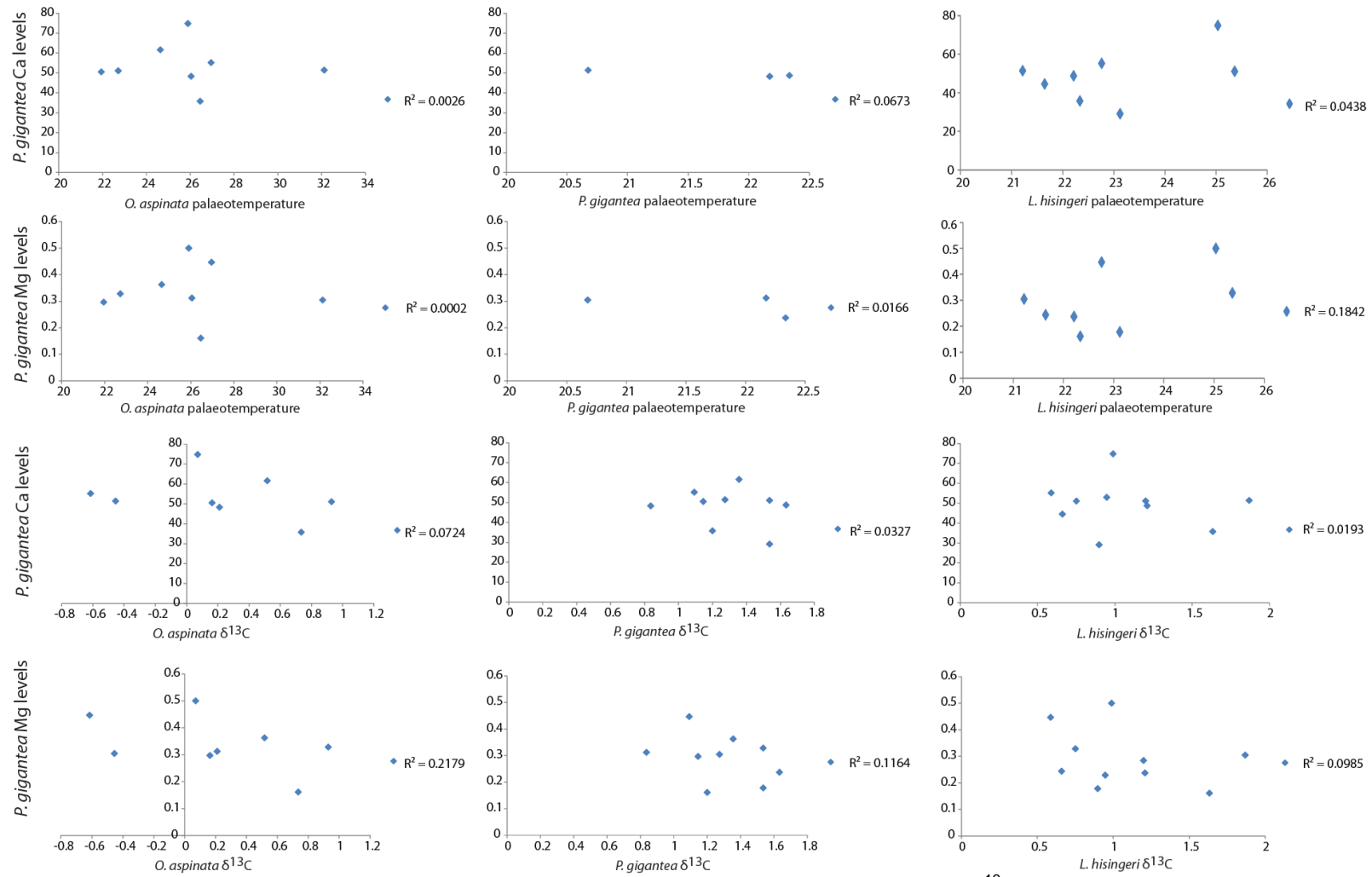


Figure A5.20: Linear regression models showing no significant relationships between the various different $\delta^{13}\text{C}$ and temperature curves (both from this study and those previously published) and corresponding Lyme Regis *P. gigantea* Ca and Mg levels (Presented in Section 4.7).

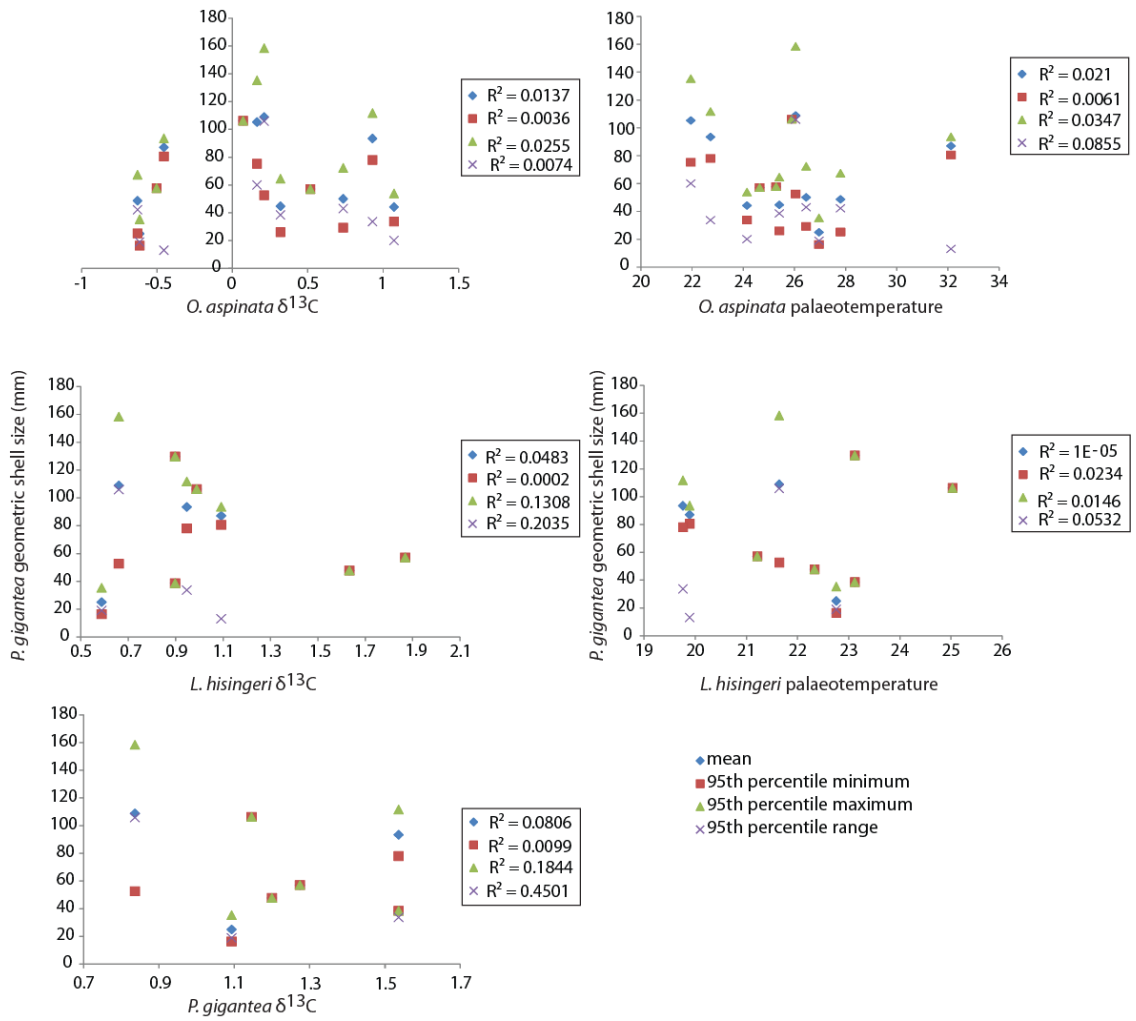


Figure A5.21: Linear regression models showing no significant relationships between the various different $\delta^{13}\text{C}$ and temperature curves (both from this study and those previously published) and corresponding Lyme Regis *P. gigantea* geometric shell size (Presented in Section 4.7).

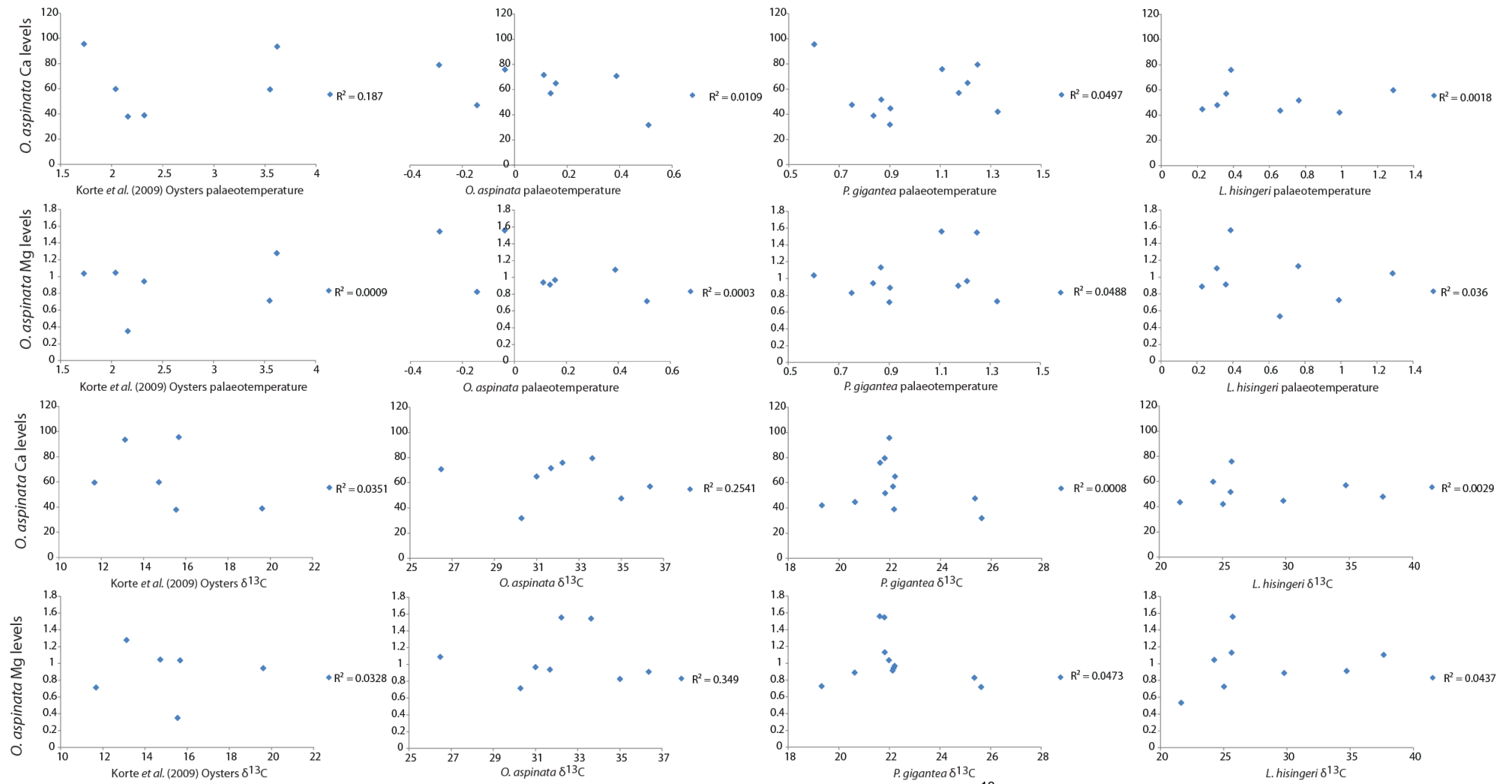


Figure A5.22: Linear regression models showing no significant relationships between the various different $\delta^{13}\text{C}$ and temperature curves (both from this study and those previously published) and corresponding St Audrie's Bay *O. aspinata* Ca and Mg levels (Presented in Section 4.7).

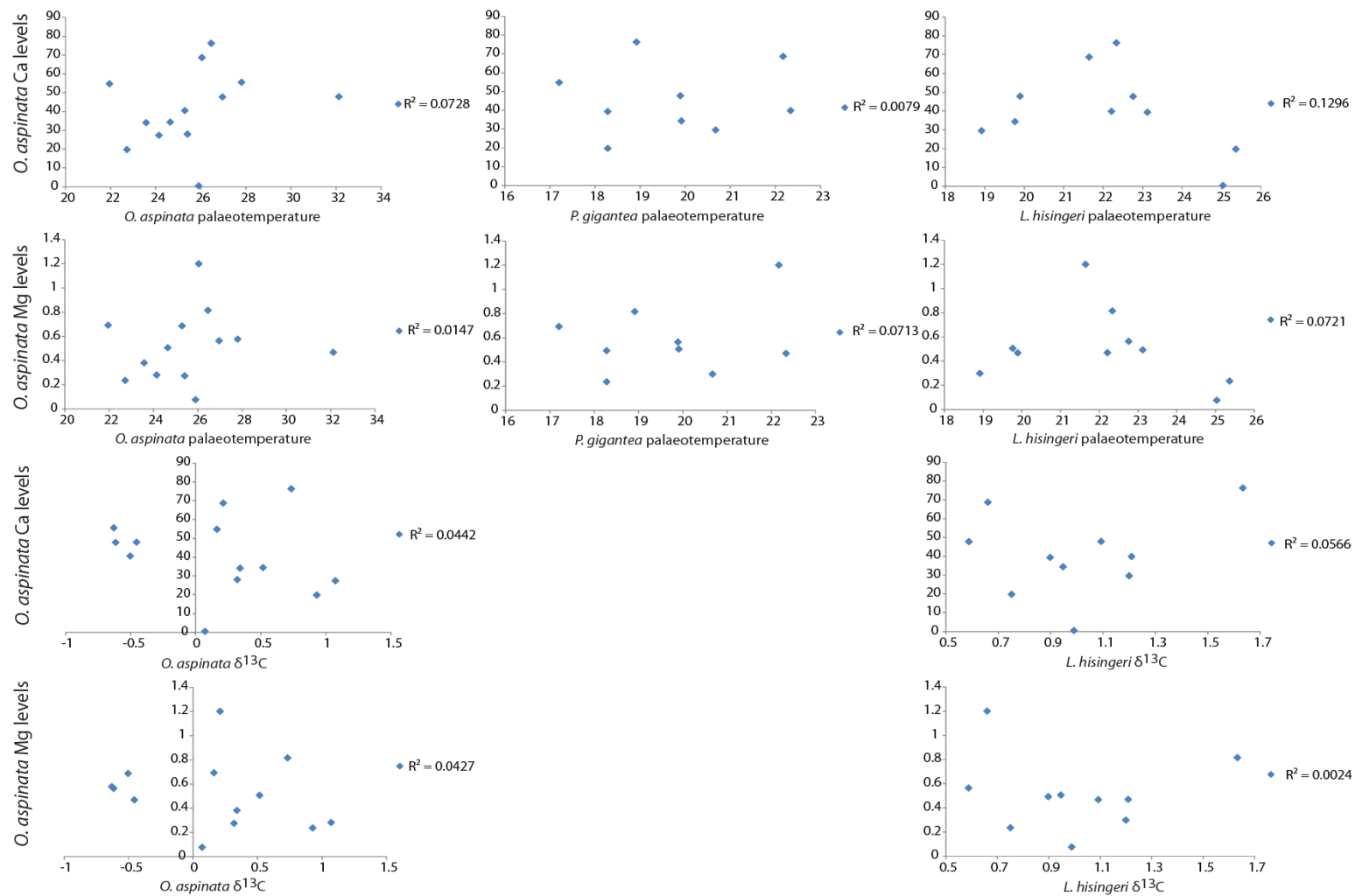


Figure A5.23: Linear regression models showing no significant relationships between the various different $\delta^{13}\text{C}$ and temperature curves (both from this study and those previously published) and corresponding Lyme Regis *O. aspinata* Ca and Mg levels (Presented in Section 4.7).

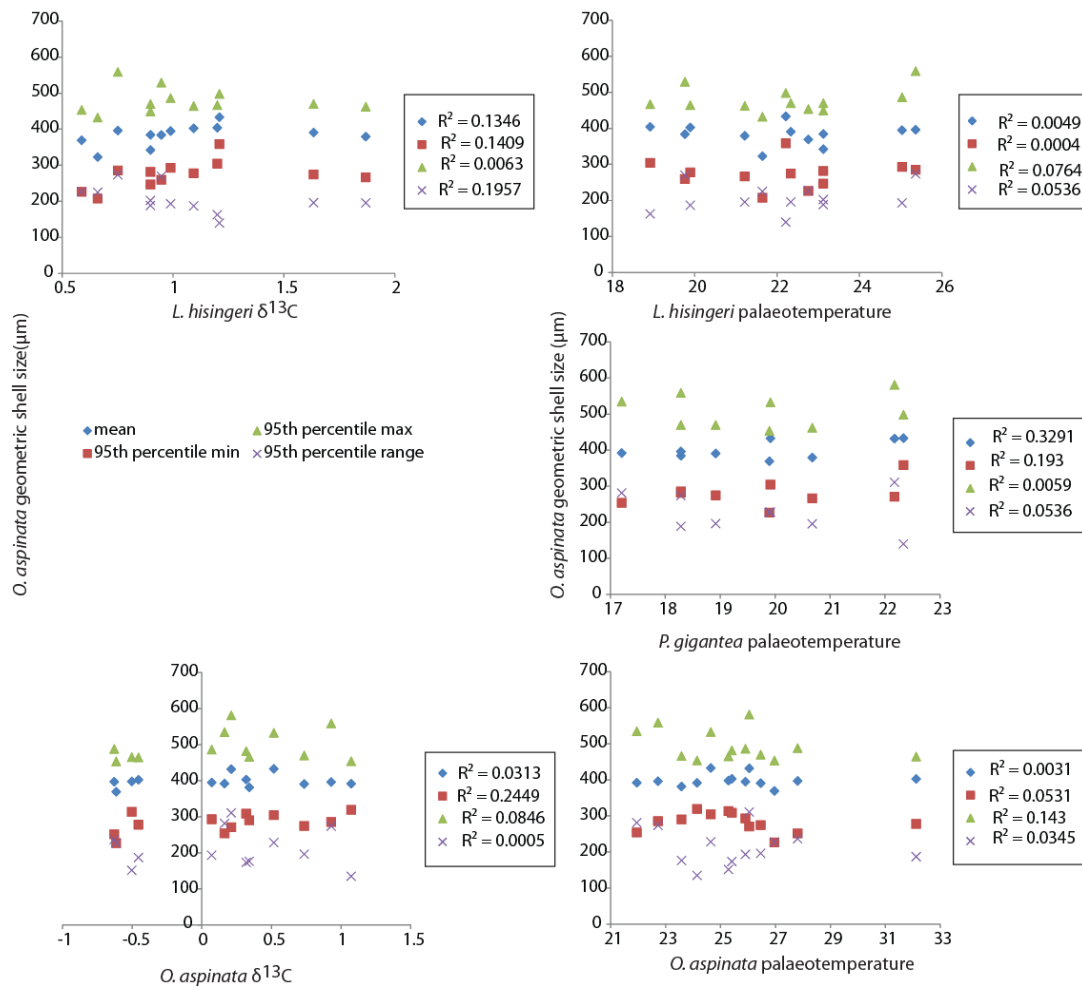


Figure A5.24: Linear regression models showing no significant relationships between the various different $\delta^{13}\text{C}$ and temperature curves (both from this study and those previously published) and corresponding Lyme Regis *O. aspinata* geometric shell size (Presented in Section 4.7).

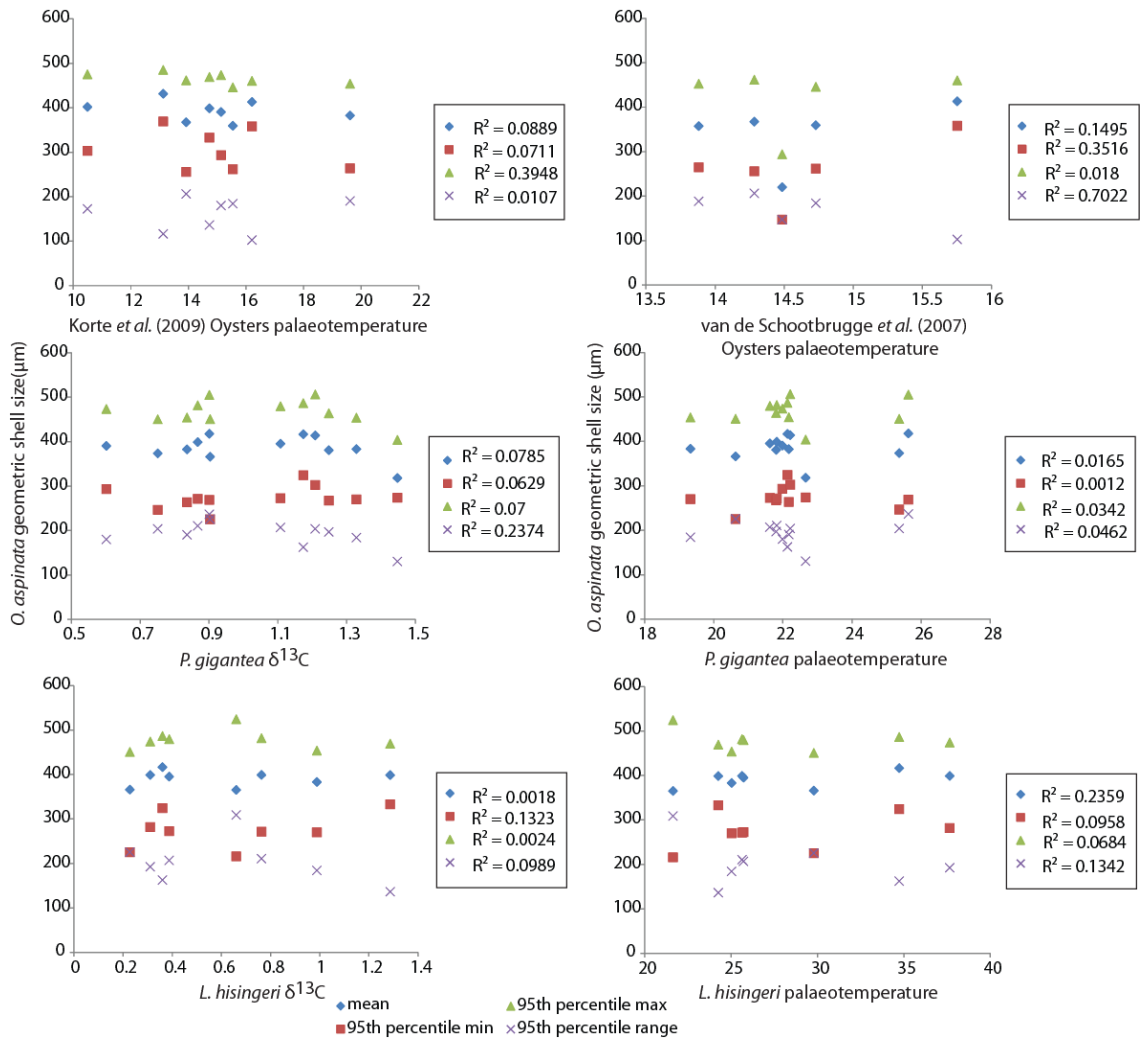


Figure A5.25: Linear regression models showing no significant relationships between the various different $\delta^{13}C$ and temperature curves (both from this study and those previously published) and corresponding St Audrie's Bay *O. aspinata* geometric shell size (Presented in Section 4.7).

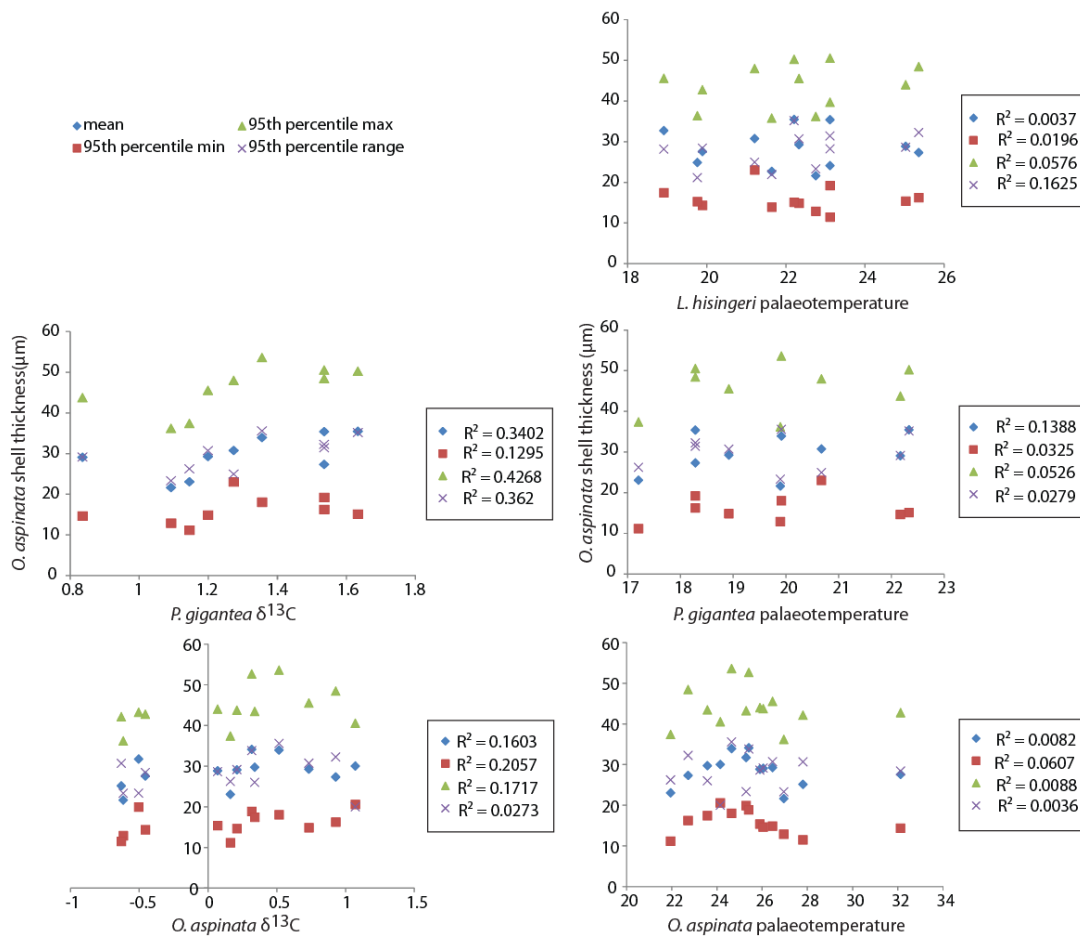


Figure A5.26: Linear regression models showing no significant relationships between the various different $\delta^{13}\text{C}$ and temperature curves (both from this study and those previously published) and corresponding Lyme Regis *O. aspinata* shell thickness (Presented in Section 4.7).

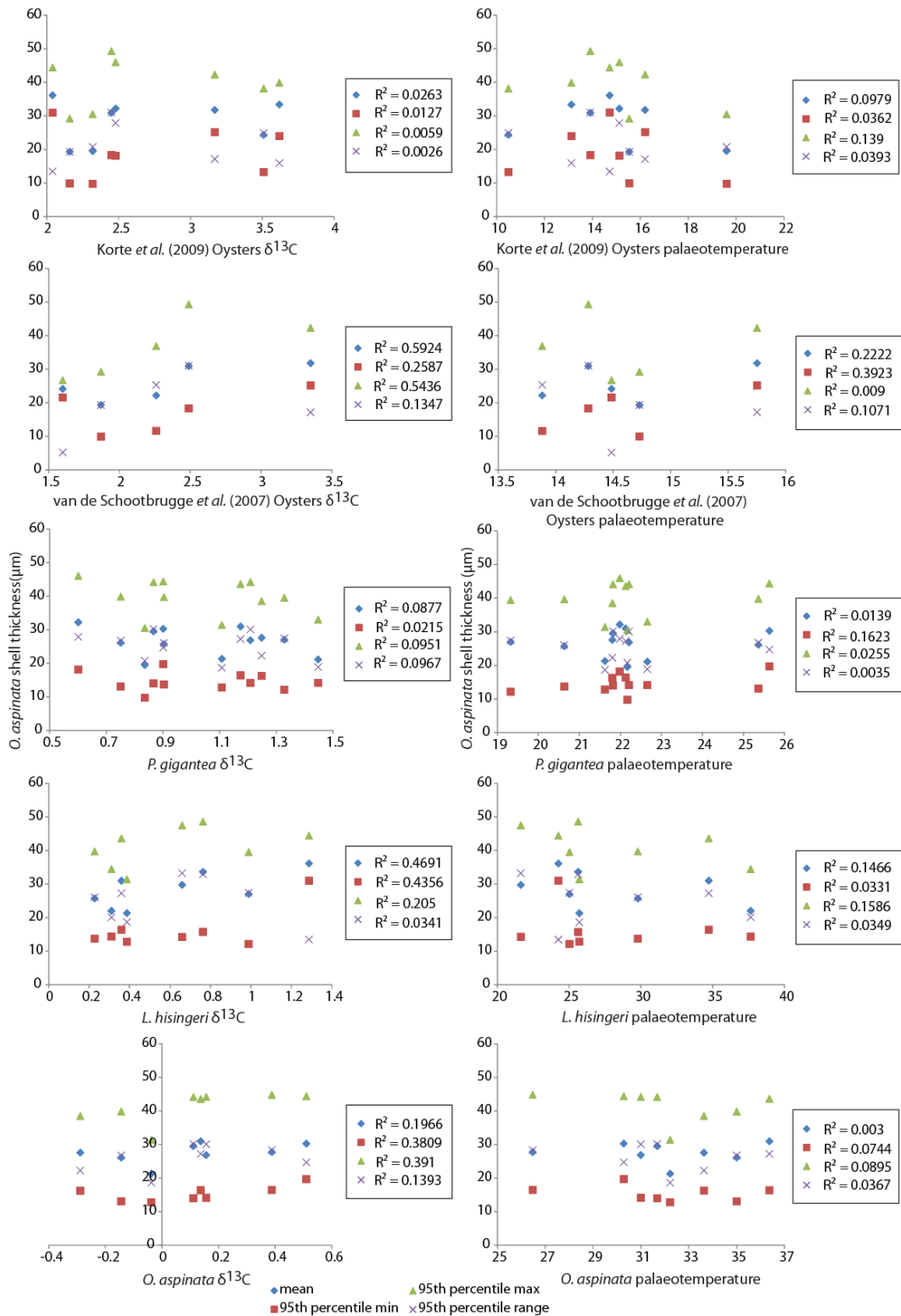


Figure A5.27: Linear regression models showing no significant relationships between the various different δ¹³C and temperature curves (both from this study and those previously published) and corresponding St Audrie's Bay *O. aspinata* shell thickness (Presented in Section 4.7).

Appendix 6 – Raw ostracod data and its statistical analysis (relates to Chapter 5)

A6.1: TA and ICPOES results collected during the experiment

Table A6.1: pH, salinity, oxygen and Total Alkalinity data collected during the experiment and run through the CO₂sys program (Presented in Section 5.3.4) (measured in mg/L).

Treatment	Sal				Tinp			
ID2	Mean	Min	Max	Standard deviation	Mean	Min	Max	Standard deviation
15 Control	33.02	31.00	34.00	0.75	15.60	14.20	16.70	0.59
15 Acid	33.02	31.00	34.00	0.75	15.67	14.30	16.80	0.60
19 Control	33.23	32.00	35.00	0.91	19.50	17.70	20.20	0.57
19 Acid	33.23	32.00	35.00	0.91	19.41	18.00	20.10	0.54
	TA				pHinp			
ID2	Mean	Min	Max	Standard deviation	Mean	Min	Max	Standard deviation
15 Control	2203.98	2117.00	2511.00	51.13	8.05	7.94	8.18	0.06
15 Acid	2201.00	2120.90	2332.80	41.98	7.85	7.67	7.97	0.07
19 Control	2244.35	2100.50	2336.20	62.58	8.09	7.99	8.18	0.04
19 Acid	2241.06	2099.50	2333.80	60.72	7.89	7.79	8.03	0.07
	TC				pCO ₂ inp			
ID2	Mean	Min	Max	Standard deviation	Mean	Min	Max	Standard deviation
15 Control	2046.32	1947.10	2387.10	62.17	530.80	374.90	784.50	87.65
15 Acid	2115.28	2017.80	2246.50	47.97	882.57	658.30	1377.10	155.53
19 Control	2045.07	1916.20	2166.80	62.98	497.22	390.30	632.00	59.65
19 Acid	2124.20	1971.30	2231.90	69.52	844.47	570.10	1087.20	152.30
	OmegaCainp				OmegaArip			
ID2	Mean	Min	Max	Standard deviation	Mean	Min	Max	Standard deviation
15 Control	2.90	2.24	3.74	0.36	1.86	1.43	2.39	0.23
15 Acid	1.93	1.30	2.47	0.26	1.24	0.83	1.58	0.17
19 Control	3.57	2.91	4.37	0.36	2.31	1.88	2.83	0.23
19 Acid	2.40	1.88	3.38	0.37	1.55	1.21	2.20	0.24
	HCO ₃ inp				CO ₃ inp			
ID2	Mean	Min	Max	Standard deviation	Mean	Min	Max	Standard deviation
15 Control	1906.69	1785.90	2249.70	68.16	119.93	92.70	154.70	14.67
15 Acid	2002.53	1904.00	2128.70	48.83	80.05	54.30	102.30	10.71
19 Control	1880.97	1765.70	2016.90	64.71	147.63	119.50	181.40	15.08
19 Acid	1997.04	1845.50	2108.10	72.92	99.13	77.50	141.30	15.36

Table A6.2: Mineral concentrations determined from field collected samples when using the ICPOES, each value is the value from the machine as each sample (made up of 5 individuals) was only tested once (Presented in Section 5.3.8) (measured in mg/kg).

				Element content of ostracods in mg/kg								
Sample Labels	N. used in each test	Vol. (ml)	Weight (g)	Al 396.152	Ba 455.403	Ca 317.933	Ca 393.366	Ca 422.673	Cr 267.716	Cu 327.395	Fe 234.350	Fe 238.204
<i>Leptocythere</i> sp.	5	10	0.0001	1699.20	25.90	228179.0 0	241338.0 0	238501.0 0	8.50	16.50	10000.60	9675.20
<i>L. castanea</i>	5	10	0.00015	2751.47	46.27	125615.3 3	137901.3 3	132564.0 0	32.53	335.27	8053.400	8271.13
<i>L. lacertosa</i>	5	10	0.00003	4259.67	3685.67	341040.0 0	375100.0 0	359646.6 7	-389.67	219.00	20965.00 0	22824.67
food		10	0.807	40.58	0.2	50.83	55.05	54.14	0.12	0.95	76.225	77.54
Sample Labels		Vol. (ml)	Weight (g)	K 766.491	Mg 280.270	Mn 257.610	Na 589.592	Si 251.432	Si 251.611	Sr 407.771	Ti 336.122	Zn 213.857
<i>Leptocythere</i> sp.	5	10	0.0001	37329.9 0	6477.00	1899.50	31564.20	3035.40	1426.90	1553.30	-623.300	1685.30
<i>L. castanea</i>	5	10	0.00015	11306.1 3	3639.47	90.80	12050.60	2984.73	2565.00	854.80	-434.533	1366.53
<i>L. lacertosa</i>	5	10	0.00003	13484.3 3	12632.0 0	181.33	54443.33	3326.67	3469.00	2463.67	-	5611.33
food		10	0.807	12.18	21.25	0.62	19.12	51.56	49.86	0.43	0.908	1.78

A6.2: *Leptocythere* sp. raw data sets

Table A6.3a: *Leptocythere* sp.: the raw data sets (Geometric shell size used in the Kruskal-Wallis, Mann-Whitney pairwise comparison tests, linear regression models, Spearman's rank and general linear model (Presented in Sections 5.5/5.6) (measured in μm).

Geometric shell size								
field collected	21 day 15°C control alive	434.37	21 day 15°C acid alive	451.86	21 day 19°C control alive	440.84	21 day 19°C acid dead	415.10
445.84		379.07		417.25		423.88		404.04
445.40		466.15		442.36		427.61		427.11
465.26		449.07		437.72	21 day 19°C control dead	484.49		444.78
469.41	21 day 15°C control dead	436.01	21 day 15°C acid dead	413.29		416.89		410.14
443.23		430.11		416.71		453.59		434.85
453.15		405.12		407.57		423.62		440.44
428.27		438.50		428.11		424.88	95 day 19°C acid dead	435.17
454.07		426.15		441.32		398.15		416.04
412.58		425.94		434.04		420.12		423.62
436.38		435.88		403.39		410.68		347.36
408.95		442.73		465.65	95 day 19°C control dead	412.22		394.56
414.36		411.07		450.72		418.88		402.56
431.19		442.79		424.55		432.21		397.39
432.42		410.61	95 day 15°C acid dead	419.73		381.10		444.67
416.33		426.18		452.98		393.03		428.14
401.55		421.47		396.21		449.83		411.24
434.08		402.02		419.98		406.18		447.20
473.08		464.39		362.66		383.31		415.82
428.20	95 day 15°C control dead	410.47		437.45		398.02		379.98
428.85		430.40		401.99		407.58		421.58
447.73		430.23				411.33		434.70
420.50		409.66				425.05		422.23
434.52		442.72				423.11		
428.30		411.79				429.97		
402.15		412.53						
416.08		340.03						
455.05		432.66						
425.12		428.85						
418.54		425.29						
420.35		411.03						
465.88		414.83						
412.74		408.54						
428.45		415.11						
416.94		407.54						
429.20		432.48						
422.27		407.18						
452.94		416.79						
435.88		434.80						
447.15		445.17						
425.81		452.55						

Table A6.3b: *Leptocythere* sp.: the raw data sets (Mean shell thickness used in the Kruskal-Wallis, Mann-Whitney pairwise comparison tests, linear regression models, Spearman's rank and general linear model (Presented in Sections 5.5/5.6) (measured in μm).

Mean shell thickness								
field collected	21 day 15°C control alive	8.66	21 day 15°C acid alive	11.63	21 day 19°C control alive	14.13	21 day 19°C acid dead	13.53
13.48		9.89		14.00	21 day 19°C control dead	12.45		8.87
10.20	21 day 15°C control dead	13.90	21 day 15°C acid dead	11.24		13.07		12.50
9.80		9.64		13.13		14.20		11.10
12.22		12.65		11.50		12.13		15.00
13.85		13.75		14.45		13.16	95 day 19°C acid dead	8.07
12.63		13.53		9.46		13.40		9.96
9.44		13.78		10.60	95 day 19°C control dead	10.88		11.13
12.71		14.20		14.60		12.48		10.71
10.59		9.40		10.77		11.35		10.22
12.82		12.30	95 day 15°C acid dead	9.58		12.65		8.22
12.30		13.98		10.48		9.28		15.45
11.55		14.13		12.10		11.95		12.70
12.65		7.38		12.30		11.72		11.75
14.33		7.45		8.89		11.74		11.90
15.18	95 day 15°C control dead	10.05				13.45		10.58
11.63		12.08				11.30		11.78
12.17		14.30				10.84		13.75
13.45		13.93						12.95
11.85		8.18						10.39
11.70		13.50						
14.23		14.03						
13.05		11.66						
11.66		10.43						
11.18		13.20						
13.08		11.75						
13.73		8.06						
13.40		15.05						
14.70		13.90						
13.28		13.78						
14.18		15.55						
		13.80						
		16.15						

Table A6.3c: *Leptocythere* sp.: the raw data sets (Average Mg used in the Kruskal-Wallis, Mann-Whitney pairwise comparison tests, linear regression models, Spearman's rank and general linear model (Presented in Sections 5.5/5.6) (measured in %).

Average Mg								
field collected	21 day 15°C control alive	0.87	21 day 15°C acid alive	0.78	21 day 19°C control alive	0.61	21 day 19°C acid dead	0.77
0.69		0.83	21 day 15 acid dead	0.55	21 day 19°C control dead	0.73		0.59
0.95	21 day 15°C control dead	0.76		0.59		0.72		0.71
0.94		0.9		0.76		0.84		0.92
0.85		0.94		0.75		0.83		0.67
0.81		0.93		0.77		0.59	95 day 19°C acid dead	2.5
0.87		0.56		0.67		0.65		1.47
1.09		0.75		0.68	95 day 19°C control dead	0.8		2.05
0.83		0.94	95 day 15°C acid dead	0.78		0.47		2.05
0.76		1.36		0.69		0.71		2.03
0.81		0.93		0.54		0.6		2.03
0.82		0.79		0.78		0.69		2.22
0.66		0.53				0.69		2.48
0.94		1.05				0.66		2.03
0.82		0.66				0.75		1.77
1.03	95 day 15°C control dead	0.7				0.95		2.18
0.83		0.58						1.65
0.81		0.71						1.66
0.78		0.57						1.6
0.64		0.86						2
0.8		0.8						
0.58		0.69						
0.94		0.59						
0.73		0.67						
1.08		0.87						
0.82		0.77						
0.72		0.66						
0.98		0.73						
0.67		0.74						
0.72		0.84						
0.82		0.6						
1.06		0.65						
		0.67						

Table A6.3d: *Leptocythere* sp.: the raw data sets (Average Ca used in the Kruskal-Wallis, Mann-Whitney pairwise comparison tests, linear regression models, Spearman's rank and general linear model (Presented in Sections 5.5/5.6) (measured in %).

Average Ca								
field collected	21 day 15°C control alive	68.95	21 day 15°C acid alive	50.99	21 day 19°C control alive	52.37	21 day 19°C acid dead	61.35
49.87		56.32		48.83	21 day 19°C control dead	51.22		50.33
50.95	21 day 15°C control dead	54.84	21 day 15°C acid dead	61.47		47.03		47.96
55.23		48.4		49.37		46.7		46.22
49.98		55.54		49.27		53.3		54.66
54.99		48.39		47.9		47.18	95 day 19°C acid dead	42.94
46.44		60.69		50.22		62.44		50.26
57.65		66.38		47.96	95 day 19°C control dead	49.81		48.64
57.62		46.9		50.92		46.44		43.73
51.63		63.31	95 day 15°C acid dead	49.66		47.11		45.57
47.97		47.38		49.77		48.28		48.8
48.16		54.12		52.09		47.66		48.31
52.4		68.25		50.6		49.83		48.09
46.32		44.67		47.43		47.36		49.68
51.49		49.03				53.02		49.54
58.09	95 day 15°C control dead	48.97				50.93		51.12
47.66		56.94				48.5		46.83
48.43		50.81				54.27		49.52
68.35		52.55				50.22		45.84
58.47		46.97				42.1		44.43
47.5		48.66						
69.22		50.3						
55.25		47.75						
67.76		51.23						
49.97		50.73						
57.31		50.23						
54.9		51.03						
47.94		48.07						
62.44		52.01						
51.82		48.12						
65.74		48.93						
46.37		46.18						
		53.67						
		48.75						
		50.68						

A6.2.2: *Leptocythere* sp. analysis of raw data

Geometric shell size

Between-Subjects Factors				Tests of Between-Subjects Effects					
	Value	Label	N	Dependent Variable: data21dayalive					
ph	2.00	ph control	7	Source	Type III Sum of Squares	df	Mean Square	F	Sig.
	3.00	ph acid	4	Corrected Model	86.762 ^a	2	43.381	.069	.934
temperature	2.00	15	8	Intercept	1819975.128	1	1819975.128	2875.454	.000
	3.00	19	3	ph	52.694	1	52.694	.083	.780
				temperature	3.289	1	3.289	.005	.944
				ph *					
				temperature	0.000	0			
				Error	5063.480	8	632.935		
				Total	2073756.331	11			
				Corrected Total	5150.242	10			

a. R Squared = .017 (Adjusted R Squared = -.229)

Between-Subjects Factors				Tests of Between-Subjects Effects					
	Value	Label	N	Dependent Variable: data21dayalivevsdead					
temperature3	2.00	15	33	Source	Type III Sum of Squares	df	Mean Square	F	Sig.
	3.00	19	18	Corrected Model	444.485 ^a	6	74.081	.170	.983
ph3	2.00	ph control	30	Intercept	5783481.928	1	5783481.928	13281.247	.000
	3.00	ph acid	21	temperature3	19.722	1	19.722	.045	.832
alive_dead	1.00	alive	11	ph3	3.124	1	3.124	.007	.933
	2.00	dead	40	alive_dead	179.033	1	179.033	.411	.525
				temperature3	45.512	1	45.512	.105	.748
				temperature3 * ph3	8.097	1	8.097	.019	.892
				temperature3 * alive_dead					
				ph3 *					
				alive_dead	30.782	1	30.782	.071	.792
				temperature3	0.000	0			
				temperature3 * ph3 *					
				alive_dead					
				Error	19160.340	44	435.462		
				Total	9409469.615	51			
				Corrected Total	19604.825	50			

a. R Squared = .023 (Adjusted R Squared = -.111)

Figure A6.1a: *Leptocythere* sp.: geometric shell size (μm) results from the general linear model analysis (Presented in Sections 5.5/5.6).

Geometric shell size

Between-Subjects Factors				Tests of Between-Subjects Effects					
	Value	Label	N	Dependent Variable: data21daydead					
temperature2	2.00	15	25	Source	Type III Sum of Squares	df	Mean Square	F	Sig.
	3.00	19	15	Corrected Model	65.201 ^a	3	21.734	.056	.983
ph2	2.00	ph control	23	Intercept	6735166.960	1	6735166.960	17200.001	.000
	3.00	ph acid	17	temperature2	11.209	1	11.209	.029	.867
				ph2	24.178	1	24.178	.062	.805
				temperature2	45.512	1	45.512	.116	.735
				* ph2					
				Error	14096.860	36	391.579		
				Total	7335713.284	40			
				Corrected Total	14162.061	39			

a. R Squared = .005 (Adjusted R Squared = -.078)

Between-Subjects Factors				Tests of Between-Subjects Effects					
	Value	Label	N	Dependent Variable: data95daysdead					
temperature4	2.00	15	29	Source	Type III Sum of Squares	df	Mean Square	F	Sig.
	3.00	19	30	Corrected Model	517.857 ^a	3	172.619	.314	.815
ph4	2.00	control	36	Intercept	8533719.061	1	8533719.061	15537.707	.000
	3.00	acid	23	temperature4	110.013	1	110.013	.200	.656
				ph4	62.880	1	62.880	.114	.736
				temperature4	185.863	1	185.863	.338	.563
				* ph4					
				Error	30207.452	55	549.226		
				Total	10209213.337	59			
				Corrected Total	30725.309	58			

a. R Squared = .017 (Adjusted R Squared = -.037)

Between-Subjects Factors				Tests of Between-Subjects Effects					
	Value	Label	N	Dependent Variable: data21daydeadvs95daydead					
temperature5	2.00	15	54	Source	Type III Sum of Squares	df	Mean Square	F	Sig.
	3.00	19	45	Corrected Model	4295.280 ^a	7	613.611	1.260	.279
ph5	2.00	control	59	Intercept	14998394.682	1	14998394.682	30806.345	.000
	3.00	ph acid	40	temperature5	88.009	1	88.009	.181	.672
experiment_length	1.00	21	40	ph5	79.218	1	79.218	.163	.688
	2.00	95	59	experiment_length	3634.307	1	3634.307	7.465	.008
				temperature5	14.320	1	14.320	.029	.864
				* ph5					
				temperature5	18.553	1	18.553	.038	.846
				*					
				experiment_length					
				ph5 *	2.098	1	2.098	.004	.948
				experiment_length					
				temperature5	196.231	1	196.231	.403	.527
				* ph5 *					
				experiment_length					
				Error	44304.312	91	486.861		
				Total	17544926.621	99			
				Corrected Total	48599.592	98			

a. R Squared = .088 (Adjusted R Squared = .018)

Figure A6.1b: *Leptocythere* sp.: geometric shell size (µm) results from the general linear model analysis (Presented in Sections 5.5/5.6).

Mean shell thickness

Between-Subjects Factors				Tests of Between-Subjects Effects					
	Value	Label	N	Dependent Variable: data21dayalive					
				Source	Type III Sum of Squares	df	Mean Square	F	Sig.
temperature1	2.00	15	4	Corrected Model	20.121 ^a	2	10.060	5.654	.150
	3.00	19	1	Intercept	613.624	1	613.624	344.852	.003
ph1	2.00	control	3	temperature1	15.682	1	15.682	8.813	.097
	3.00	acid	2	ph1	12.532	1	12.532	7.043	.117
				temperature1 * ph1	0.000	0			
				Error	3.559	2	1.779		
				Total	703.574	5			
				Corrected Total	23.679	4			

a. R Squared = .850 (Adjusted R Squared = .699)

Between-Subjects Factors				Tests of Between-Subjects Effects					
	Value	Label	N	Dependent Variable: data21dayalivevsdead					
				Source	Type III Sum of Squares	df	Mean Square	F	Sig.
temperature3	2.00	15	25	Corrected Model	26.906 ^a	6	4.484	1.008	.438
	3.00	19	12	Intercept	2196.360	1	2196.360	493.880	.000
ph3	2.00	control	22	temperature3	16.683	1	16.683	3.751	.062
	3.00	acid	15	ph3	4.964	1	4.964	1.116	.299
alivevsdead	2.00	alive	5	alivevsdead	.150	1	.150	.034	.855
	3.00	dead	32	temperature3 * ph3	1.222	1	1.222	.275	.604
				temperature3 * alivevsdead	8.230	1	8.230	1.851	.184
				ph3 * alivevsdead	10.640	1	10.640	2.392	.132
				temperature3 * ph3 * alivevsdead	0.000	0			
				Error	133.415	30	4.447		
				Total	5621.199	37			
				Corrected Total	160.321	36			

a. R Squared = .168 (Adjusted R Squared = .001)

Figure A6.2a: *Leptocythere* sp.: mean shell thickness (μm) results from the general linear model analysis (Presented in Sections 5.5/5.6).

Mean shell thickness

Between-Subjects Factors				Tests of Between-Subjects Effects					
	Value	Label	N	Dependent Variable: data21daydead					
				Source	Type III Sum of Squares	df	Mean Square	F	Sig.
temperature2	2.00	15	21	Corrected	5.410 ^a	3	1.803	.389	.762
	3.00	19	11	Model					
ph2	2.00	control	19	Intercept	4263.714	1	4263.714	919.358	.000
	3.00	acid	13	temperature2	2.927	1	2.927	.631	.434
				ph2	1.443	1	1.443	.311	.581
				temperature2	1.222	1	1.222	.264	.612
				* ph2					
				Error	129.856	28	4.638		
				Total	4917.625	32			
				Corrected Total	135.266	31			

a. R Squared = .040 (Adjusted R Squared = -.063)

Between-Subjects Factors				Tests of Between-Subjects Effects					
	Value	Label	N	Dependent Variable: data95daydead					
				Source	Type III Sum of Squares	df	Mean Square	F	Sig.
temperature4	2.00	15	23	Corrected	26.475 ^a	3	8.825	2.376	.083
	3.00	19	26	Model					
ph4	2.00	control	29	Intercept	5192.654	1	5192.654	1397.989	.000
	3.00	acid	20	temperature4	.624	1	.624	.168	.684
				ph4	13.628	1	13.628	3.669	.062
				temperature4	7.615	1	7.615	2.050	.159
				* ph4					
				Error	167.147	45	3.714		
				Total	7056.029	49			
				Corrected Total	193.622	48			

a. R Squared = .137 (Adjusted R Squared = .079)

Between-Subjects Factors				Tests of Between-Subjects Effects					
	Value	Label	N	Dependent Variable: data21daydeadvs95daydead					
				Source	Type III Sum of Squares	df	Mean Square	F	Sig.
temperature5	2.00	15	44	Corrected	34.840 ^a	7	4.977	1.223	.301
	3.00	19	37	Model					
ph5	2.00	control	48	Intercept	9300.581	1	9300.581	2285.980	.000
	3.00	acid	33	temperature5	.624	1	.624	.153	.697
experiment length	2.00	alive	32	ph5	10.949	1	10.949	2.691	.105
	3.00	dead	49	experiment length	8.688	1	8.688	2.135	.148
				temperature5	.900	1	.900	.221	.639
				* ph5					
				temperature5 *	3.292	1	3.292	.809	.371
				experiment length					
				ph5 * experiment length	2.192	1	2.192	.539	.465
				temperature5 * ph5 * experiment length	6.925	1	6.925	1.702	.196
				Error	297.003	73	4.069		
				Total	11973.653	81			
				Corrected Total	331.843	80			

a. R Squared = .105 (Adjusted R Squared = .019)

Figure A6.2b: *Leptocythere* sp.: mean shell thickness (μm) results from the general linear model analysis (Presented in Sections 5.5/5.6).

Average Mg

Between-Subjects Factors				Tests of Between-Subjects Effects					
	Value	Label	N	Dependent Variable: data21dayalive					
temperature2	2.00	15	3	Source	Type III Sum of Squares	df	Mean Square	F	Sig.
	3.00	19	1	Corrected	.038 ^a	2	.019	24.047	.143
ph2	2.00	control	3	Model					
	3.00	acid	1	Intercept	1.550	1	1.550	1937.779	.014
				temperature2	.038	1	.038	48.000	.091
				ph2	.003	1	.003	4.083	.293
				temperature2	0.000	0			
				* ph2					
				Error	.001	1	.001		
				Total	2.426	4			
				Corrected Total	.039	3			

a. R Squared = .980 (Adjusted R Squared = .939)

Between-Subjects Factors				Tests of Between-Subjects Effects					
	Value	Label	N	Dependent Variable: data21dayalivesdead					
temperature4	2.00	15	23	Source	Type III Sum of Squares	df	Mean Square	F	Sig.
	3.00	19	12	Corrected	.203 ^a	6	.034	1.299	.290
ph4	2.00	control	22	Model					
	3.00	acid	13	Intercept	6.192	1	6.192	237.366	.000
alivesdead	2.00	alive	4	temperature4	.034	1	.034	1.289	.266
	3.00	dead	31	ph4	.012	1	.012	.454	.506
				alivesdead	.000	1	.000	.006	.937
				temperature4	.054	1	.054	2.065	.162
				* ph4					
				temperature4	.007	1	.007	.280	.601
				* alivesdead					
				ph4 *	.006	1	.006	.234	.632
				alivesdead					
				temperature4	0.000	0			
				* ph4 *					
				alivesdead					
				Error	.730	28	.026		
				Total	21.731	35			
				Corrected Total	.934	34			

a. R Squared = .218 (Adjusted R Squared = .050)

Figure A6.3a: *Leptocythere* sp.: average Mg (%) data results from the general linear model analysis (Presented in Sections 5.5/5.6).

Average Mg

Between-Subjects Factors				Tests of Between-Subjects Effects					
	Value	Label	N	Dependent Variable: data21daydead					
temperature3	2.00	15	20	Source	Type III Sum of Squares	df	Mean Square	F	Sig.
	3.00	19	11	Corrected Model	.165 ^a	3	.055	2.033	.133
ph3	2.00	control	19	Intercept	15.285	1	15.285	565.631	.000
	3.00	acid	12	temperature3	.010	1	.010	.370	.548
				ph3	.048	1	.048	1.762	.196
				temperature3	.054	1	.054	1.994	.169
				* ph3					
				Error	.730	27	.027		
				Total	19.305	31			
				Corrected Total	.894	30			

a. R Squared = .184 (Adjusted R Squared = .094)

Between-Subjects Factors				Tests of Between-Subjects Effects					
	Value	Label	N	Dependent Variable: data95daydead					
temperature5	2.00	15	22	Source	Type III Sum of Squares	df	Mean Square	F	Sig.
	3.00	19	24	Corrected Model	16.505 ^a	3	5.502	142.263	.000
ph5	2.00	control	27	Intercept	34.553	1	34.553	893.463	.000
	3.00	acid	19	temperature5	3.392	1	3.392	87.722	.000
				ph5	3.343	1	3.343	86.433	.000
				temperature5	3.428	1	3.428	88.638	.000
				* ph5					
				Error	1.624	42	.039		
				Total	75.854	46			
				Corrected Total	18.129	45			

a. R Squared = .910 (Adjusted R Squared = .904)

Between-Subjects Factors				Tests of Between-Subjects Effects					
	Value	Label	N	Dependent Variable: data21daydeadvs95daydead					
temperature6	2.00	15	42	Source	Type III Sum of Squares	df	Mean Square	F	Sig.
	3.00	19	35	Corrected Model	18.933 ^a	7	2.705	79.285	.000
ph6	2.00	control	46	Intercept	46.864	1	46.864	1373.754	.000
	3.00	acid	31	temperature6	1.355	1	1.355	39.715	.000
experiment length	2.00	alive	31	ph6	1.139	1	1.139	33.396	.000
	3.00	dead	46	experiment length	1.116	1	1.116	32.715	.000
				temperature6	2.006	1	2.006	58.803	.000
				* ph6					
				temperature6	1.722	1	1.722	50.467	.000
				* experiment length					
				ph6 * experiment length	1.933	1	1.933	56.673	.000
				temperature6 * ph6 * experiment length	1.151	1	1.151	33.726	.000
				Error	2.354	69	.034		
				Total	95.159	77			
				Corrected Total	21.287	76			

a. R Squared = .889 (Adjusted R Squared = .878)

Figure A6.3b: *Leptocythere* sp.: average Mg (%) data results from the general linear model analysis (Presented in Sections 5.5/5.6).

Average Ca

Between-Subjects Factors				Tests of Between-Subjects Effects					
	Value	Label	N	Dependent Variable: data21dayalive					
temperature2	2.00	15	4	Source	Type III Sum of Squares	df	Mean Square	F	Sig.
	3.00	19		Corrected Model	174.109 ^a	2	87.055	2.121	.320
ph2	2.00	control	3	Intercept	10983.564	1	10983.564	267.594	.004
	3.00	acid	2	temperature2	70.247	1	70.247	1.711	.321
				ph2	161.926	1	161.926	3.945	.185
				temperature2 * ph2	0.000	0			
				Error	82.091	2	41.046		
				Total	15653.011	5			
				Corrected Total	256.200	4			

a. R Squared = .680 (Adjusted R Squared = .359)

Between-Subjects Factors				Tests of Between-Subjects Effects					
	Value	Label	N	Dependent Variable: data21dayalivevsdead					
temperature4	2.00	15	24	Source	Type III Sum of Squares	df	Mean Square	F	Sig.
	3.00	19		Corrected Model	281.089 ^a	6	46.848	1.041	.420
ph4	2.00	control	22	Intercept	39637.334	1	39637.334	880.660	.000
	3.00	acid	14	temperature4	60.678	1	60.678	1.348	.255
alivevsdead	2.00	alive	5	ph4	131.098	1	131.098	2.913	.099
	3.00	dead		31	alivevsdead	8.367	1	8.367	.186
				temperature4 * ph4	30.517	1	30.517	.678	.417
				temperature4 * alivevsdead	29.098	1	29.098	.646	.428
				ph4 * alivevsdead	70.706	1	70.706	1.571	.220
				temperature4 * ph4 * alivevsdead	0.000	0			
				Error	1305.251	29	45.009		
				Total	103013.727	36			
				Corrected Total	1586.340	35			

a. R Squared = .177 (Adjusted R Squared = .007)

Figure A6.4a: *Leptocythere* sp.: Average Ca (%) data results from the general linear model analysis (Presented in Sections 5.5/5.6).

Average Ca

Between-Subjects Factors			Tests of Between-Subjects Effects						
	Value	Label	N	Dependent Variable: data21daydead					
temperature3	2.00	15	20	Source	Type III Sum of Squares	df	Mean Square	F	Sig.
	3.00	19	11	Corrected Model	73.183 ^a	3	24.394	.538	.660
ph3	2.00	control	19	Intercept	74402.370	1	74402.370	1642.356	.000
	3.00	acid	12	temperature3	7.193	1	7.193	.159	.693
				ph3	11.937	1	11.937	.263	.612
				temperature3 * ph3	30.517	1	30.517	.674	.419
				Error	1223.160	27	45.302		
				Total	87360.716	31			
				Corrected Total	1296.343	30			

a. R Squared = .056 (Adjusted R Squared = -.048)

Between-Subjects Factors			Tests of Between-Subjects Effects						
	Value	Label	N	Dependent Variable: data95daydead					
temperature5	2.00	15	25	Source	Type III Sum of Squares	df	Mean Square	F	Sig.
	3.00	19	28	Corrected Model	60.896 ^a	3	20.299	2.999	.039
ph5	2.00	control	33	Intercept	98082.074	1	98082.074	14490.224	.000
	3.00	acid	20	temperature5	32.905	1	32.905	4.861	.032
				ph5	6.124	1	6.124	.905	.346
				temperature5 * ph5	3.156	1	3.156	.466	.498
				Error	331.673	49	6.769		
				Total	128033.946	53			
				Corrected Total	392.570	52			

a. R Squared = .155 (Adjusted R Squared = .103)

Between-Subjects Factors			Tests of Between-Subjects Effects						
	Value	Label	N	Dependent Variable: data21daydeadvs95daydead					
temperature6	2.00	15	45	Source	Type III Sum of Squares	df	Mean Square	F	Sig.
	3.00	19	39	Corrected Model	389.774 ^a	7	55.682	2.722	.014
ph6	2.00	control	52	Intercept	167667.574	1	167667.574	8195.563	.000
	3.00	acid	32	temperature6	32.603	1	32.603	1.594	.211
experiment length	2.00	alive	31	ph6	17.986	1	17.986	.879	.351
	3.00	dead	53	experiment length	157.043	1	157.043	7.676	.007
				temperature6 * ph6	9.906	1	9.906	.484	.489
				temperature6 * experiment length	2.435	1	2.435	.119	.731
				ph6 * experiment length	1.219	1	1.219	.060	.808
				temperature6 * ph6 * experiment length	29.152	1	29.152	1.425	.236
				Error	1554.833	76	20.458		
				Total	215394.662	84			
				Corrected Total	1944.607	83			

a. R Squared = .200 (Adjusted R Squared = .127)

Figure A6.4b: *Leptocythere* sp.: Average Ca (%) data results from the general linear model analysis (Presented in Sections 5.5/5.6).

Shell preservation

Between-Subjects Factors				Tests of Between-Subjects Effects					
	Value	Label	N	Dependent Variable: data21dayalive					
				Source	Type III Sum of Squares	df	Mean Square	F	Sig.
temperature2	2.00	15	8	Corrected Model	.879 ^a	2	.439	.620	.562
	3.00	19	3	Intercept	22.753	1	22.753	32.121	.000
ph2	2.00	control	7	temperature2	.762	1	.762	1.076	.330
	3.00	acid	4	ph2	.500	1	.500	.706	.425
				temperature2 * ph2	0.000	0			
				Error	5.667	8	.708		
				Total	36.000	11			
				Corrected Total	6.545	10			

a. R Squared = .134 (Adjusted R Squared = -.082)

Between-Subjects Factors				Tests of Between-Subjects Effects					
	Value	Label	N	Dependent Variable: data21dayalivevsdead					
				Source	Type III Sum of Squares	df	Mean Square	F	Sig.
temperature4	2.00	15	33	Corrected Model	42.206 ^a	6	7.034	8.480	.000
	3.00	19	18	Intercept	168.899	1	168.899	203.604	.000
ph4	2.00	control	30	temperature4	1.717	1	1.717	2.070	.157
	3.00	acid	21	ph4	.214	1	.214	.259	.614
alivevsdead	2.00	alive	11	alivevsdead	3.068	1	3.068	3.698	.061
	3.00	dead	40	temperature4 * ph4	26.865	1	26.865	32.386	.000
				temperature4 * alivevsdead	.158	1	.158	.191	.665
				ph4 * alivevsdead	2.042	1	2.042	2.461	.124
				temperature4 * ph4 * alivevsdead	0.000	0			
				Error	36.500	44	.830		
				Total	405.000	51			
				Corrected Total	78.706	50			

a. R Squared = .536 (Adjusted R Squared = .473)

Figure A6.5a: *Leptocythere* sp.: shell preservation (rank) data results from the general linear model analysis (Presented in Sections 5.5/5.6).

Shell preservation

Between-Subjects Factors				Tests of Between-Subjects Effects					
	Value	Label	N	Dependent Variable: data21daydead					
				Source	Type III Sum of Squares	df	Mean Square	F	Sig.
temperature3	2.00	15	25	Corrected	30.142 ^a	3	10.047	11.731	.000
	3.00	19	15	Model					
ph3	2.00	control	23	Intercept	284.404	1	284.404	332.061	.000
	3.00	acid	17	temperature3	4.404	1	4.404	5.142	.029
				ph3	.016	1	.016	.019	.892
				temperature3	26.865	1	26.865	31.367	.000
				* ph3					
				Error	30.833	36	.856		
				Total	369.000	40			
				Corrected Total	60.975	39			

a. R Squared = .494 (Adjusted R Squared = .452)

Between-Subjects Factors				Tests of Between-Subjects Effects					
	Value	Label	N	Dependent Variable: data95daydead					
				Source	Type III Sum of Squares	df	Mean Square	F	Sig.
temperature5	2.00	15	31	Corrected	133.285 ^a	3	44.428	29.639	.000
	3.00	19	37	Model					
ph5	2.00	control	39	Intercept	2395.817	1	2395.817	1598.284	.000
	3.00	acid	29	temperature5	47.268	1	47.268	31.533	.000
				ph5	35.140	1	35.140	23.442	.000
				temperature5	4.868	1	4.868	3.248	.076
				* ph5					
				Error	95.936	64	1.499		
				Total	2961.000	68			
				Corrected Total	229.221	67			

a. R Squared = .581 (Adjusted R Squared = .562)

Between-Subjects Factors				Tests of Between-Subjects Effects					
	Value	Label	N	Dependent Variable: data95daydeadvs21daydead					
				Source	Type III Sum of Squares	df	Mean Square	F	Sig.
temperature6	2.00	15	56	Corrected	483.194 ^a	7	69.028	54.452	.000
	3.00	19	52	Model					
ph6	2.00	control	62	Intercept	1914.760	1	1914.760	1510.433	.000
	3.00	acid	46	temperature6	35.229	1	35.229	27.790	.000
experiment length	2.00	alive	40	ph6	14.469	1	14.469	11.414	.001
	3.00	dead	68	experiment length	303.793	1	303.793	239.643	.000
				temperature6	7.112	1	7.112	5.610	.020
				* ph6					
				temperature6	7.071	1	7.071	5.578	.020
				*					
				experiment length					
				ph6 *	13.007	1	13.007	10.260	.002
				experiment length					
				temperature6	29.431	1	29.431	23.216	.000
				* ph6 *					
				experiment length					
				Error	126.769	100	1.268		
				Total	3330.000	108			
				Corrected Total	609.963	107			

a. R Squared = .792 (Adjusted R Squared = .778)

Figure A6.5b: *Leptocythere* sp.: shell preservation (rank) data results from the general linear model analysis (Presented in Sections 5.5/5.6).

Geometric shell size statistics (Alive)			
H (chi ²)	0.8038	Hc (tie corrected)	0.8038
p(same)	0.8485		
field collected	21 day 15°C control alive	21 day 15°C acid alive	21 day 19°C control alive
field collected	0.5815	0.5539	0.8301
	21 day 15°C control alive	0.8852	0.5959
		21 day 15°C acid alive	0.5959

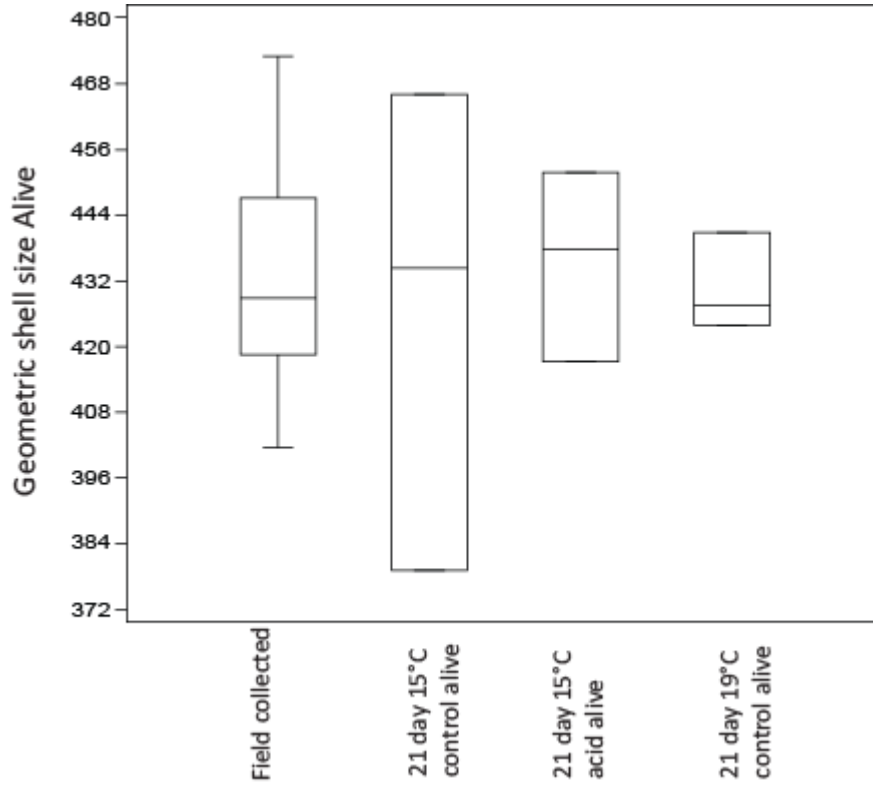


Figure A6.6: *Leptocythere* sp.: The table shows the data analysed using Kruskal-Wallis and Mann-Whitney pairwise comparison test for any significant difference in alive Geometric shell size with the numbers in red highlighting those numbers that show a significant difference. The box plot shows the minimum, maximum, median and first and third quartile of the data set (Presented in Sections 5.5/5.6).

Mean shell thickness statistics (Alive)			
H (chi ²)	6.072	Hc (tie corrected)	6.072
p(same)	0.1082		
field collected	21 day 15°C control alive	21 day 15°C acid alive	21 day 19°C control alive
field collected	0.03228	0.907	0.2882
	21 day 15°C control alive	0.2453	0.5403
		21 day 15°C acid alive	0.5403

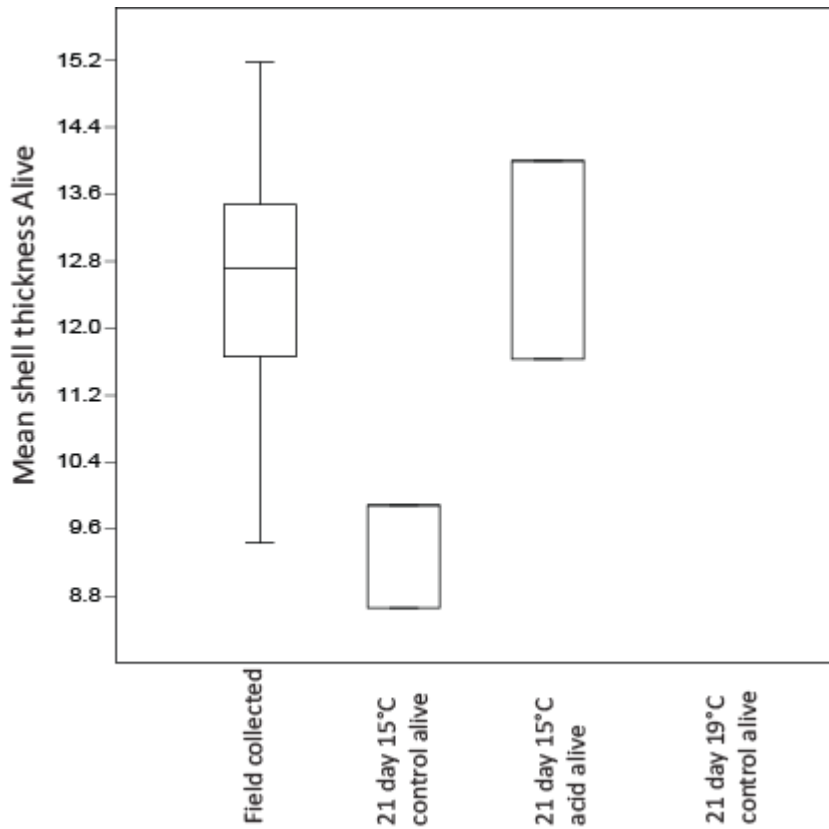


Figure A6.7: *Leptocythere* sp.: The table shows the data analysed using Kruskal-Wallis and Mann-Whitney pairwise comparison test for any significant difference in alive Mean shell thickness with the numbers in red highlighting those numbers that show a significant difference. The box plot illustrates the original data showing the minimum, maximum, median and first and third quartile of the data set (Presented in Sections 5.5/5.6).

Shell Mg level statistics (Alive)			
H (chi ²)	3.507	Hc (tie corrected)	3.52
p(same)	0.3182		
field collected	21 day 15°C control alive	21 day 15°C acid alive	21 day 19°C control alive
field collected	0.4962	0.5506	0.1287
	21 day 15°C control alive	0.5403	0.5403
		21 day 15°C acid alive	1

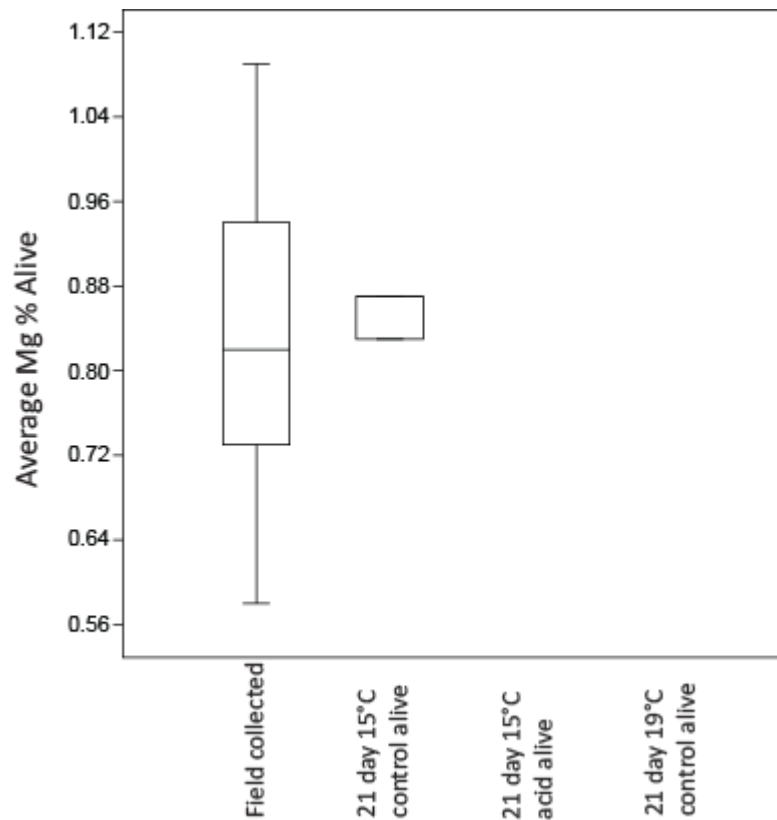


Figure A6.8: *Leptocythere* sp.: The table shows the data analysed using Kruskal-Wallis and Mann-Whitney pairwise comparison test for any significant difference in average alive level of Mg % with the numbers in red highlighting those numbers that show a significant difference. The box plot illustrates the original data showing the minimum, maximum, median and first and third quartile of the data set (Presented in Sections 5.5/5.6).

Shells Ca level statistics (Alive)			
H (chi ²)	3.072	Hc (tie corrected)	3.072
p(same)	0.3806		
field collected	21 day 15°C control alive	21 day 15°C acid alive	21 day 19°C control alive
field collected	0.1412	0.5213	1
	21 day 15°C control alive	0.2453	0.5403
		21 day 15°C acid alive	0.5403

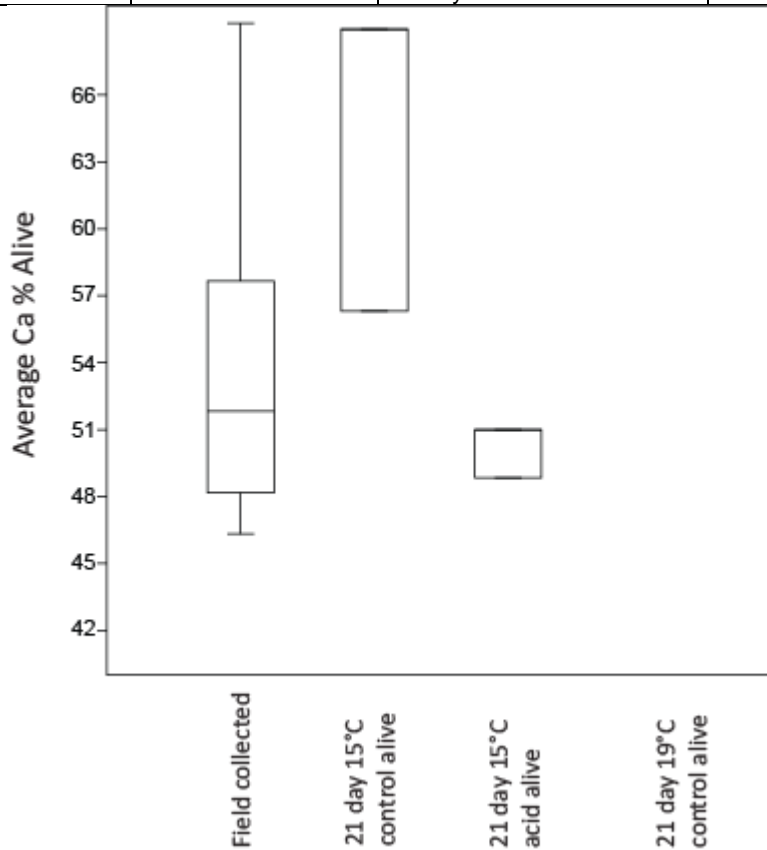


Figure A6.9: *Leptocythere* sp.: The table shows the data analysed using Kruskal-Wallis and Mann-Whitney pairwise comparison test for any significant difference in average alive level of Ca % with the numbers in red highlighting those numbers that show a significant difference. The box plot illustrates the original data showing the minimum, maximum, median and first and third quartile of the data set (Presented in Sections 5.5/5.6).

Table A6.4: *Leptocythere* sp.: The table shows the data analysed using Kruskal-Wallis and Mann-Whitney pairwise comparison test for any significant difference in live shell preservation with the numbers in red highlighting those numbers that show a significant difference (Presented in Sections 5.5/5.6).

Shell preservation statistics (Alive)			
H (chi ²)	5.478	Hc (tie corrected)	20.59
p(same)	0.0001282		
field collected	21 day 15°C control alive	21 day 15°C acid alive	21 day 19°C control alive
field collected	0.000007877	0.000007877	0.00037
	21 day 15°C control alive	0.64	0.5541
		21 day 15°C acid alive	0.8383

Table A6.5: *Leptocythere* sp.: The table shows the data analysed using Kruskal-Wallis and Mann-Whitney pairwise comparison test for any significant difference in dead shell preservation with the numbers in red highlighting those numbers that show a significant difference (Presented in Sections 5.5/5.6).

Shell preservation statistics (Dead)								
H (chi ²)	131.1	Hc (tie corrected)	135.8	p(same)	1.75 x 10 ⁻²⁵			
field collected	21 day 15°C control dead	21 day 15°C acid dead	21 day 19°C control dead	21 day 19°C acid dead	95 day 15°C control dead	95 day 15°C acid dead	95 day 19°C control dead	95 day 19°C acid dead
field collected	5.07 x 10 ⁻¹³	0.000000263	0.00000000313	1.64 x 10 ⁻¹¹	1.81 x 10 ⁻¹⁴	1.03 x 10 ⁻¹¹	3.19 x 10 ⁻¹³	4.60 x 10 ⁻¹⁴
	21 day 15°C control dead	0.0003027	0.0305	0.2384	0.00278	0.000129	0.00000168	0.00000307
		21 day 15°C acid dead	0.05346	0.00049	0.00000268	0.0003	0.0000177	0.00000585
			21 day 19°C control dead	0.00801	0.000025	0.00075	0.000069	0.0000280
				21 day 19°C acid dead	0.360	0.004973	0.000327	0.0000653
					95 day 15°C control dead	0.000182	0.00000126	0.00000102
						95 day 15°C acid dead	0.3572	0.00639
							95 day 19°C control dead	0.00314

Table A6.6: *Leptocythere* sp.: The table shows the data analysed using Kruskal-Wallis and Mann-Whitney pairwise comparison test for any significant difference in dead Geometric shell size with the numbers in red highlighting those numbers that show a significant difference (Presented in Sections 5.5/5.6).

Geometric shell size statistics (Dead)								
H (chi ²)	16.67	Hc (tie corrected)	16.67	P(same)	0.03379			
field collected	21 day 15°C control dead	21 day 15°C acid dead	21 day 19°C control dead	21 day 19°C acid dead	95 day 15°C control dead	95 day 15°C acid dead	95 day 19°C control dead	95 day 19°C acid dead
field collected	0.411	0.3892	0.2868	0.3168	0.01551	0.08046	0.00176	0.01028
	21 day 15°C control dead	0.9779	0.5397	0.8879	0.3001	0.1805	0.03817	0.1383
		21 day 15°C acid dead	0.894	0.8836	0.452	0.3055	0.08411	0.2155
			21 day 19°C control dead	0.9539	0.6224	0.3253	0.2067	0.4084
				21 day 19°C acid dead	0.6283	0.4433	0.1675	0.4036
					95 day 15°C control dead	0.6649	0.1581	0.6681
						95 day 15°C acid dead	0.852	0.9202

Geometric shell size statistics (Dead)								
H (chi ²)	16.67	Hc (tie corrected)	16.67	P(same)	0.03379			
field collected	21 day 15°C control dead	21 day 15°C acid dead	21 day 19°C control dead	21 day 19°C acid dead	95 day 15°C control dead	95 day 15°C acid dead	95 day 19°C control dead	95 day 19°C acid dead
							95 day 19°C control dead	0.6625

Table A6.7: *Leptocythere* sp.: The table shows the data analysed using Kruskal-Wallis and Mann-Whitney pairwise comparison test for any significant difference in average dead level of Mg % with the numbers in red highlighting those numbers that show a significant difference (Presented in Sections 5.5/5.6).

Shells Mg level statistics (Dead)								
H (chi ²)	52.84	Hc (tie corrected)	52.88	p(same)	0.000000114			
field collected	21 day 15°C control dead	21 day 15°C acid dead	21 day 19°C control dead	21 day 19°C acid dead	95 day 15°C control dead	95 day 15°C acid dead	95 day 19°C control dead	95 day 19°C acid dead
field collected	1	0.005273	0.1268	0.09455	0.00155	0.04842	0.01196	0.000000531
	21 day 15°C control dead	0.06795	0.1475	0.2364	0.03057	0.1921	0.1085	0.00000773
		21 day 15°C acid dead	0.5672	0.5677	0.7389	0.5074	0.791	0.00024
			21 day 19°C control dead	1	0.7136	0.7484	0.6797	0.00052
			21 day 19°C acid dead		0.6542	0.9021	0.8411	0.00121
					95 day 15°C control dead	1	0.9795	0.00000114
						95 day 15°C acid dead	0.9381	0.0031
							95 day 19°C control dead	0.0000633

Table A6.8: *Leptocythere* sp.: The table shows the data analysed using Kruskal-Wallis and Mann-Whitney pairwise comparison test for any significant difference in average dead level of Ca % with the numbers in red highlighting those numbers that show a significant difference (Presented in Sections 5.5/5.6).

Shells Ca level statistics (Dead)								
H (chi ²)	17.26	Hc (tie corrected)	17.26	p(same)	0.02748			
field collected	21 day 15°C control dead	21 day 15°C acid dead	21 day 19°C control dead	21 day 19°C acid dead	95 day 15°C control dead	95 day 15°C acid dead	95 day 19°C control dead	95 day 19°C acid dead
field collected	0.8977	0.2748	0.2659	0.4642	0.06828	0.2003	0.01453	0.00074
	21 day 15°C control dead	0.6919	0.3132	0.6221	0.2937	0.6221	0.1119	0.02703
		21 day 15°C acid dead	0.8303	0.9352	0.89	0.871	0.4052	0.1388
			21 day 19°C control dead	0.9273	0.9273	0.9273	0.7589	0.199
				21 day 19°C acid dead	0.8121	0.8345	0.375	0.1378
					95 day 15°C control dead	0.9188	0.2037	0.01185
						95 day 15°C acid dead	0.5542	0.05482
							95 day 19°C control dead	0.2894

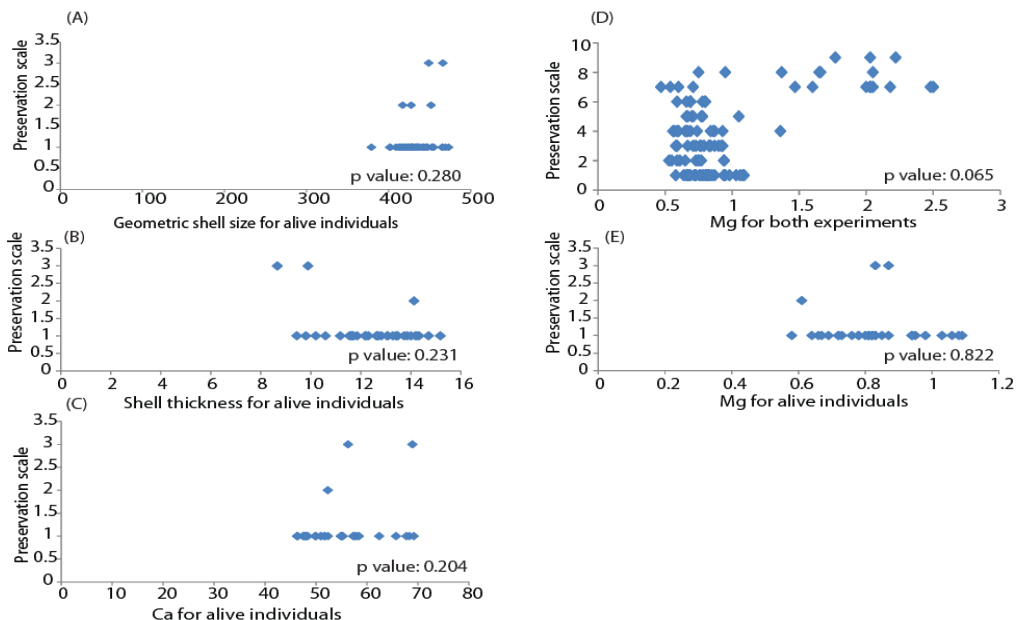


Figure A6.10: *Leptocythere* sp.: Linear regression models and Spearman's rank results (p-values) from comparing all the different) data sets (Geometric shell size (µm), Mean shell thickness (µm), Average Mg % and Ca %) against the relevant preservation rank to determine if there are any correlations and trends between the different data sets and preservation. Trend lines on the linear regression models indicate that the data shows a significant correlation (Presented in Sections 5.5/5.6).

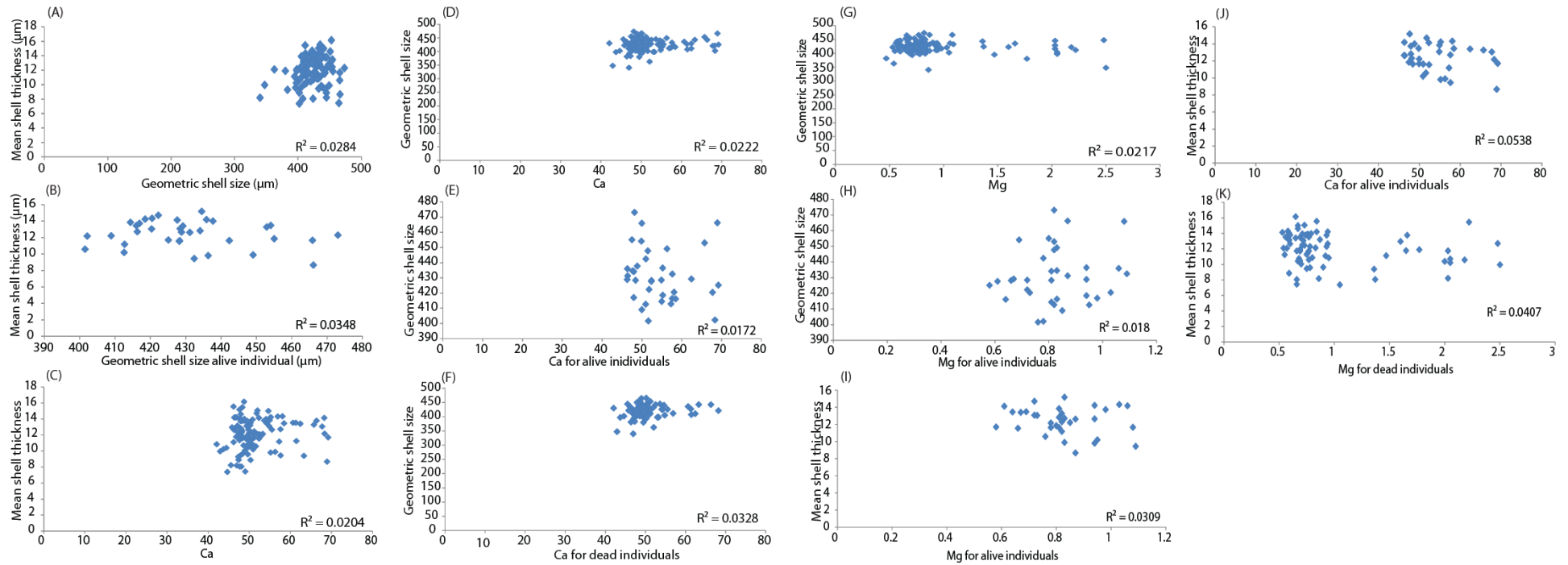


Figure A6.11: *Leptocythere* sp.: Linear regression models comparing all the data against each other to determine if there are any correlations and trends between the different data sets (Geometric shell size (μm), Mean shell thickness (μm), Average Mg % and Ca %). Trend lines on the linear regression models indicate that the data shows a significant correlation (Presented in Sections 5.5/5.6).

Table A6.9: *Leptocythere* sp.: results from the statistical analysis when determining any correlations between the different data sets (Presented in Section 5.7).

Leptocythere sp.		
Correlation question	Number of individuals	R ² value
Preservation against geometric shell size for both experiments	150	0.1203
Preservation against geometric shell size for alive individuals	51	0.0484
Preservation against geometric shell size for dead individuals	99	0.0806
Preservation against shell thickness for both experiments	116	0.0776
Preservation against shell thickness for alive individuals	35	0.1673
Preservation against shell thickness for dead individuals	81	0.0812
Preservation against average Mg for both experiments	112	0.2956
Preservation against average Mg for alive individuals	34	0.0033
Preservation against average Mg for dead individuals	78	0.3687
Preservation against average Ca for both experiments	119	0.1701
Preservation against average Ca for alive individuals	34	0.0681
Preservation against average Ca for dead individuals	85	0.1534
Correlation question	Number of individuals	R ² value
Geometric shell size against shell thickness for both experiments	113	0.0284
Geometric shell size against shell thickness for alive individuals	35	0.0348
Geometric shell size against shell thickness for dead individuals	78	0.0573
Geometric shell size against average Mg for both experiments	112	0.0217
Geometric shell size against average Mg for alive individuals	35	0.018
Geometric shell size against average Mg for dead individuals	77	0.0216
Shell thickness against average Mg for both experiments	107	0.041
Shell thickness against average Mg for alive individuals	34	0.0309
Shell thickness against average Mg for dead individuals	73	0.0407
Geometric shell size against average Ca for both experiments	119	0.0222
Geometric shell size against average Ca for alive individuals	36	0.0172
Geometric shell size against average Ca for dead individuals	83	0.0328
Shell thickness against average Ca for both experiments	115	0.0204
Shell thickness against average Ca for alive individuals	35	0.0538
Shell thickness against average Ca for dead individuals	80	0.0811

A6.3: *L. castanea* raw data sets

Table A6.10a: *L. castanea*: the raw data sets (Geometric shell size (µm) used in the Kruskal-Wallis, Mann-Whitney pairwise comparison tests, linear regression models, Spearman's rank and general linear model (Presented in Sections 5.5/5.6).

Geometric shell size																
field collected	21 day 15°C control alive	445.75	21 day 15°C acid alive	438.97	21 day 19°C control alive	393.66	21 day 19°C acid alive	437.92	95 day 15°C control dead	438.47	95 day 15°C acid dead	406.31	95 day 19°C control dead	424.58	95 day 19°C acid dead	386.16
461.55		451.75		449.54		421.21		433.44		435.65		377.24		413.48		410.51
438.07		451.63		456.31	21 day 19°C control dead	431.47		427.54		431.58		402.19		443.31		436.43
414.04		413.31		383.47		441.95		440.66		428.02		388.83		442.17		432.30
416.16		380.64		446.90		434.02		444.88		395.69		420.47		426.82		445.53
432.87		417.91		398.01		439.04		448.11		433.61		419.11		405.82		452.98
432.68		432.66	21 day 15°C acid dead	420.23		426.73	21 day 19°C acid dead	437.64		422.18		432.06		413.30		390.90
411.37		425.61		440.82		426.42		411.37		451.35		333.28		442.97		444.63
437.03		435.87		393.44		433.41		409.40		406.96		399.17		393.70		431.13
441.45	21 day 15°C control dead	445.27		406.39		366.98		418.13		387.89		420.25		432.86		435.31
441.13		413.03		432.01		416.37		434.99		460.34		386.11		403.61		408.57
456.43		427.85		432.12		398.56		446.84		420.23		474.98		408.48		420.19
457.66		396.39		441.40		443.42		469.06		420.05		334.75		428.30		388.53
422.07		446.85		427.95		416.57		405.80		407.19		246.20		406.97		404.16
448.54		410.85		435.68		408.77		443.46		432.65				419.13		440.68
457.17		435.60		424.81		446.30		399.52		436.67				410.26		436.68
438.82		396.67		430.79		417.17		432.42		409.73				389.18		389.93
430.00		412.51		416.50		421.53		414.11		391.09				423.60		430.02
431.47		431.68		414.00		359.45		474.77		413.30				406.20		395.51
430.72		432.07		405.60		353.41		378.92		366.70				438.08		395.61
457.85		443.31		434.11		353.40		440.71		408.89				441.15		403.43
438.46		447.76		439.63		432.12		428.56		410.13				407.22		403.17
462.43		418.74		432.81		419.90		411.37		436.14				424.16		408.38

Geometric shell size															
422.19		359.39						420.06		422.38				430.33	403.28
442.97		417.75						422.05		452.23				429.85	365.74
440.46		393.54						414.29		380.44				419.78	418.04
438.99		350.39						442.26		409.58				411.02	399.82
441.58		412.64						454.29		409.97					429.05
436.57		358.65								401.59					419.48
444.44		432.42								410.05					414.36
457.06		400.70								434.82					417.02
439.98										411.66					374.12
486.62										431.85					433.61
440.97										437.63					442.24
418.15										397.02					451.93
446.32															
442.03															
451.73															
430.82															
435.15															
433.14															
454.93															
415.35															
444.26															
469.76															
425.38															

Table A6.10b: *L. castanea*: the raw data sets (Mean shell thickness (μm) used in the Kruskal-Wallis, Mann-Whitney pairwise comparison tests, linear regression models, Spearman's rank and general linear model (Presented in Sections 5.5/5.6).

Mean shell thickness																
field collected	21 day 15°C control alive	11.10	21 day 15°C acid alive	8.20	21 day 19°C control alive	13.13	21 day 19°C acid alive	13.45	95 day 15°C control dead	9.68	95 day 15°C acid dead	11.20	95 day 19°C control dead	12.98	95 day 19°C acid dead	11.07
12.68	8.80		5.54		21 day 19°C control dead	7.80		10.14		13.40		16.70		9.62		11.85
15.43	6.39		13.85			8.19		11.93		14.35		13.72		12.88		9.64
11.41	6.74		5.74			12.43		6.96		10.75		12.53		10.22		12.21
9.75	11.80	21 day	10.43			10.63	21 day	15.15		10.28		10.07		15.30		12.23

Table A6.10c: *L. castanea*: the raw data sets (Average Mg (%)) used in the Kruskal-Wallis, Mann-Whitney pairwise comparison tests, linear regression models, Spearman's rank and general linear model (Presented in Sections 5.5/5.6).

Average Mg																
field collected	21 day 15°C control alive	0.6	21 day 15°C acid alive	0.87	21 day 19°C control alive	0.91	21 day 19°C acid alive	0.82	95 day 15°C control dead	0.77	95 day 15°C acid dead	0.75	95 day 19°C control dead	0.67	95 day 19°C acid dead	1.87
1.02		1.41		1.95	21 day 19°C control dead	1.46		0.86		0.78		0.66		0.86		1.59
0.71		1.16		0.82		1.02		0.87		0.71		0.58		0.62		1.39
0.72		1.46		0.69		0.99		0.96		1.1		0.64		0.51		1.41
0.8		0.71	21 day 15°C acid dead	0.74		1	21 day 19°C acid dead	1.41		0.82		0.64		0.65		1.51
0.77		0.66		0.95		0.75		1.24		0.57		0.73		0.69		1.71
1.33		0.76		0.96		1.12		0.97		0.67		0.82		1.13		1.56
0.79	21 day 15°C control dead	0.82		0.87		0.56		1.21		0.7				0.58		1.7
0.55		0.91		0.93		0.66		0.82		0.78				0.62		2.21
0.43		0.77		0.67		1.08		1.1		0.55				0.56		2.06
0.9		1.03		0.69		0.7		1.04		1.12				0.64		1.65
0.67		0.85		0.63		0.72		1.17		0.6				0.85		1.73
0.97		0.87		0.52		0.84		1.06		0.61				0.75		1.68
0.96		0.71		0.82		0.85		1.5		0.69				0.66		1.25
0.59		0.8		0.83				0.85		0.67				0.61		2.06
1.11		0.76		0.75				0.71		0.72				0.68		1.72
0.96		2.03		0.63				1.96		0.85				0.71		1.92
0.75		1.36		0.81				0.8		0.67				0.68		2.42
0.8		1.01						0.7		0.81				0.68		2.9
0.99		0.77						0.79		0.67				0.96		1.2
0.7		0.87						0.7		0.62				0.59		1.91
0.84		0.6						1.02		0.45						1.52
0.77		1.1						1.23		0.7						3.28
0.72		0.79						1.44		0.67						2.53
0.73		1								0.96						1.81
0.57										0.63						1.59
0.6										0.64						1.98
0.93										0.74						1.78
0.86										1.24						1.91
0.97										0.76						2.26
0.71																2.26

Average Mg															
															2.57
															2.78
															1.75
															1.72
															0.92

Table A6.10d: *L. castanea*: the raw data sets (Average Ca (%)) used in the Kruskal-Wallis, Mann-Whitney pairwise comparison tests, linear regression models, Spearman's rank and general linear model (Presented in Sections 5.5/5.6).

Average Ca															
field collected	21 day 15°C control alive		21 day 15°C acid alive		21 day 19°C control alive		21 day 19°C acid alive		95 day 15°C control dead		95 day 15°C acid dead		95 day 19°C control dead		95 day 19°C acid dead
		62.74		56.36		50.65		61.22		55.61		54.45		51.97	47.28
62.54		57.98		54.69		49.79		43.88		49.24		48.96		45.5	51.92
53.53		67.71		51.48		52.04		55.69		47.56		51.55		52.87	44.35
58.13		58.19		61.26		50.27		58.34		50.47		58.66		52.05	48.61
55.32		63.84	21 day 15°C acid dead	50.53		47.35	21 day 19°C acid dead	52.79		51.61		55.97		52.91	51.17
59.17		49.66		48.76		64.62		53.58		49.14		55.21		51.2	52.37
58.79		52.71		50.22		47.1		49.37		48.64		54.13		46.91	62.06
51.89	21 day 15°C control dead	50.53		47.7		49.94		52.76		43.93		49.38		49.69	53.34
63.49		54.91		49.25		54.93		50.47		50.04		54.63		55.7	57.16
54.57		48.85		51.1		49.85		58.46		49.89		51.31		51.62	55.59
77.95		50.08		56.09		55.12		50.39		49.18				48.29	53.98
50.99		51.7		53.96		58.55		55.19		49.29				56.18	58.77
67.62		56.52		49.58		43.76		51.76		46.78				54.42	54.88
50.58		45.44		48.33		52.63		49.66		47.84				57.21	48.47
65.44		48.07		50.1		50.43		51.43		55.27				54.87	52.71
60.82		49.43		50.98		51.13		58.06		50.3				54.84	59.77
51.33		50.1		47.43		53.36		51.97		49.29				60.32	54.1
64.29		50.74		48.91		49.28		64.46		48.02				47.37	57.24
51.42		53.82		52.14		50.07		56.05		47.32				51.74	55.08

Average Ca															
50.03		55.12				53.16		49.98		52.06				55.86	52.19
50.72		53.52						49.42		51.37				50.06	51.44
62.36		50.52						66.86		52.4				70.63	48.99
53.17		47.51						49.03		50.58				48.73	43.24
50.94		52.82						51.78		54.71				42.46	53.97
61.56		58.07						47.39		50.53				51.36	44.72
50.09		50.97								48.37					44.61
67.1										49.78					47.87
47.6										54.76					50.41
47.82										62.04					45.4
61.01										60.36					51
48.38										52.69					47.62
62.37										53.39					45.91
															46.29
															50.12
															49.35
															59.33
															56.17
															67.51

Table A6.10e: *L. castanea*: the raw data sets (Shell preservation (rank) used in the Kruskal-Wallis, Mann-Whitney pairwise comparison tests, linear regression models, Spearman's rank and general linear model (Presented in Sections 5.5/5.6).

Shell Preservation																
field collected	21 day 15°C control alive	1	21 day 15°C acid alive	2	21 day 19°C control alive	2	21 day 19°C acid alive	2	95 day 15°C control dead	4	95 day 15°C acid dead	8	95 day 19°C control dead	7	95 day 19°C acid dead	8
1		1		3		2		2		5		9		7		8
1		2		5	21 day 19°C control dead	2		2		4		8		10		5
1		1		5		2		1		5		5		10		8
1		1		2		4		3		4		7		7		6
1		2		5		3		3		10		6		7		7
1		1	21 day 15°C acid dead	3		2	21 day 19°C acid dead	2		3		7		6		7
1		1		3		2		2		4		9		7		8
1		1		2		3		3		3		10		5		5
1	21 day 15°C control dead	2		2		2		4		5		10		7		5
1		2		3		2		2		4		9		7		7
1		1		2		3		2		2		6		6		7

A6.3.2: *L. castanea* analysis of raw data

Geometric shell size

Between-Subjects Factors				Tests of Between-Subjects Effects					
	Value	Label	N	Dependent Variable: data21dayalive					
				Source	Type III Sum of Squares	df	Mean Square	F	Sig.
temperature2	2.00	15	15	Corrected Model	1501.947 ^a	3	500.649	1.015	.408
	3.00	19	8	Intercept	3072267.731	1	3072267.731	6230.072	.000
ph2	2.00	control	11	temperature2	128.733	1	128.733	.261	.615
	3.00	acid	12	ph2	1073.637	1	1073.637	2.177	.156
				temperature2 * ph2	1004.599	1	1004.599	2.037	.170
				Error	9369.568	19	493.135		
				Total	4251313.210	23			
				Corrected Total	10871.515	22			

a. R Squared = .138 (Adjusted R Squared = .002)

Between-Subjects Factors				Tests of Between-Subjects Effects					
	Value	Label	N	Dependent Variable: data21dayalivesdead					
				Source	Type III Sum of Squares	df	Mean Square	F	Sig.
temperature4	2.00	15	54	Corrected Model	6919.479 ^a	7	988.497	1.645	.132
	3.00	19	51	Intercept	10022837.011	1	10022837.011	16683.333	.000
ph4	2.00	control	54	temperature4	52.434	1	52.434	.087	.768
	3.00	acid	51	ph4	2965.230	1	2965.230	4.936	.029
alivesdead1	2.00	alive	23	alivesdead1	500.485	1	500.485	.833	.364
	3.00	dead	82	temperature4 * ph4	929.832	1	929.832	1.548	.216
				temperature4 * alivesdead1	179.478	1	179.478	.299	.586
				ph4 * alivesdead1	26.491	1	26.491	.044	.834
				temperature4 * ph4 * alivesdead1	737.647	1	737.647	1.228	.271
				Error	58274.639	97	600.769		
				Total	18742993.682	105			
				Corrected Total	65194.118	104			

a. R Squared = .106 (Adjusted R Squared = .042)

Figure A6.12a: *L. castanea*: geometric shell size data results from the general linear model analysis (Presented in Sections 5.5/5.6).

Geometric shell size

Between-Subjects Factors				Tests of Between-Subjects Effects					
	Value	Label	N	Dependent Variable: data21daydead					
				Source	Type III Sum of Squares	df	Mean Square	F	Sig.
temperature3	2.00	15	39	Corrected Model	3708.773 ^a	3	1236.258	1.972	.125
	3.00	19	43	Intercept	14292849.575	1	14292849.575	22796.047	.000
ph3	2.00	control	43	temperature3	54.810	1	54.810	.087	.768
	3.00	acid	39	ph3	3516.453	1	3516.453	5.608	.020
				temperature3 * ph3	16.073	1	16.073	.026	.873
				Error	48905.070	78	626.988		
				Total	14491680.472	82			
				Corrected Total	52613.843	81			

a. R Squared = .070 (Adjusted R Squared = .035)

Between-Subjects Factors				Tests of Between-Subjects Effects					
	Value	Label	N	Dependent Variable: data95daydead					
				Source	Type III Sum of Squares	df	Mean Square	F	Sig.
temperature5	2.00	15	49	Corrected Model	10739.599 ^a	3	3579.866	4.969	.003
	3.00	19	62	Intercept	16297805.500	1	16297805.500	22623.760	.000
ph5	2.00	control	62	temperature5	5014.192	1	5014.192	6.960	.010
	3.00	acid	49	ph5	6830.510	1	6830.510	9.482	.003
				temperature5 * ph5	4042.250	1	4042.250	5.611	.020
				Error	77081.139	107	720.384		
				Total	19134693.832	111			
				Corrected Total	87820.738	110			

a. R Squared = .122 (Adjusted R Squared = .098)

Between-Subjects Factors				Tests of Between-Subjects Effects					
	Value	Label	N	Dependent Variable: data21daydeadvs95daydead					
				Source	Type III Sum of Squares	df	Mean Square	F	Sig.
temperature6	2.00	15	88	Corrected Model	15817.388 ^a	7	2259.627	3.318	.002
	3.00	19	105	Intercept	30411614.217	1	30411614.217	44656.861	.000
ph6	2.00	control	105	temperature6	2839.869	1	2839.869	4.170	.043
	3.00	acid	88	ph6	146.407	1	146.407	.215	.643
experiment length	2.00	alive	82	experiment length	3694.543	1	3694.543	5.425	.021
	3.00	dead	111	temperature6 * ph6	2107.018	1	2107.018	3.094	.080
				temperature6 * experiment length	1795.404	1	1795.404	2.636	.106
				experiment length * ph6	9910.720	1	9910.720	14.553	.000
				experiment length * temperature6 * ph6	1599.190	1	1599.190	2.348	.127
				Error	125986.209	185	681.007		
				Total	33626374.303	193			
				Corrected Total	141803.597	192			

a. R Squared = .112 (Adjusted R Squared = .078)

Figure A6.12b: *L. castanea*: geometric shell size data results from the general linear model analysis (Presented in Sections 5.5/5.6).

Mean shell thickness

Between-Subjects Factors				Tests of Between-Subjects Effects					
	Value	Label	N	Dependent Variable: data21dayalive					
				Source	Type III Sum of Squares	df	Mean Square	F	Sig.
temperature2	2.00	15	11	Corrected Model	23.261 ^a	3	7.754	.948	.448
	3.00	19	5	Intercept	1046.515	1	1046.515	127.899	.000
ph2	2.00	control	8	temperature2	22.087	1	22.087	2.699	.126
	3.00	acid	8	ph2	7.730	1	7.730	.945	.350
				temperature2 *	1.277	1	1.277	.156	.700
				ph2					
				Error	98.188	12	8.182		
				Total	1616.206	16			
				Corrected Total	121.449	15			

a. R Squared = .192 (Adjusted R Squared = -.011)

Between-Subjects Factors				Tests of Between-Subjects Effects					
	Value	Label	N	Dependent Variable: data21dayalivesdead					
				Source	Type III Sum of Squares	df	Mean Square	F	Sig.
temperature4	2.00	15	42	Corrected Model	137.828 ^a	7	19.690	2.972	.008
	3.00	19	42	Intercept	4002.553	1	4002.553	604.163	.000
ph4	2.00	control	43	temperature4	4.950	1	4.950	.747	.390
	3.00	acid	41	ph4	.005	1	.005	.001	.979
alivesdead1	2.00	alive	16	alivesdead1	8.127	1	8.127	1.227	.272
	3.00	dead	68	temperature4 *	1.488	1	1.488	.225	.637
				ph4					
				temperature4 *	42.928	1	42.928	6.480	.013
				alivesdead1					
				ph4 *	27.678	1	27.678	4.178	.044
				alivesdead1					
				temperature4 *	.793	1	.793	.120	.730
				ph4 *					
				alivesdead1					
				Error	503.496	76	6.625		
				Total	10702.808	84			
				Corrected Total	641.325	83			

a. R Squared = .215 (Adjusted R Squared = .143)

Figure A6.13a: *L. castanea*: mean shell thickness results from the general linear model analysis (Presented in Sections 5.5/5.6).

Mean shell thickness

Between-Subjects Factors			Tests of Between-Subjects Effects							
	Value	Label	N	Dependent Variable: data21daydead						
				Source	Type III Sum of Squares	df	Mean Square	F	Sig.	
temperature3	2.00	15	31	Corrected Model	82.242 ^a	3	27.414	4.329	.008	
	3.00	19	37	Intercept	8533.309	1	8533.309	1347.448	.000	
ph3	2.00	control	35	temperature3	36.548	1	36.548	5.771	.019	
	3.00	acid	33	ph3	55.446	1	55.446	8.755	.004	
				temperature3 * ph3	.212	1	.212	.033	.856	
				Error	405.308	64	6.333			
				Total	9086.602	68				
				Corrected Total	487.550	67				

a. R Squared = .169 (Adjusted R Squared = .130)

Between-Subjects Factors			Tests of Between-Subjects Effects							
	Value	Label	N	Dependent Variable: data95daydead						
				Source	Type III Sum of Squares	df	Mean Square	F	Sig.	
temperature5	2.00	15	38	Corrected Model	35.276 ^a	3	11.759	2.244	.089	
	3.00	19	54	Intercept	9152.048	1	9152.048	1746.922	.000	
ph5	2.00	control	53	temperature5	15.466	1	15.466	2.952	.089	
	3.00	acid	39	ph5	3.973	1	3.973	.758	.386	
				temperature5 * ph5	6.420	1	6.420	1.226	.271	
				Error	461.028	88	5.239			
				Total	11840.265	92				
				Corrected Total	496.304	91				

a. R Squared = .071 (Adjusted R Squared = .039)

Between-Subjects Factors			Tests of Between-Subjects Effects							
	Value	Label	N	Dependent Variable: data21daydeadvs95daydead						
				Source	Type III Sum of Squares	df	Mean Square	F	Sig.	
temperature6	2.00	15	69	Corrected Model	118.297 ^a	7	16.900	2.965	.006	
	3.00	19	91	Intercept	17657.188	1	17657.188	3097.980	.000	
ph6	2.00	control	88	temperature6	50.230	1	50.230	8.813	.003	
	3.00	acid	72	ph6	16.036	1	16.036	2.814	.096	
experiment length	2.00	alive	68	experiment length	.429	1	.429	.075	.784	
	3.00	dead	92	temperature6 * ph6	4.341	1	4.341	.762	.384	
				temperature6 * experiment length	2.729	1	2.729	.479	.490	
				ph6 * experiment length	45.691	1	45.691	8.017	.005	
				temperature6 * ph6 * experiment length	2.012	1	2.012	.353	.553	
				Error	866.336	152	5.700			
				Total	20926.867	160				
				Corrected Total	984.633	159				

a. R Squared = .120 (Adjusted R Squared = .080)

Figure A6.13b: *L. castanea*: mean shell thickness results from the general linear model analysis (Presented in Sections 5.5/5.6).

Average Mg

Between-Subjects Factors				Tests of Between-Subjects Effects					
	Value	Label	N	Dependent Variable: data21dayalive					
temperature2	2.00	15	11	Source	Type III Sum of Squares	df	Mean Square	F	Sig.
	3.00	19	5	Corrected Model	.089 ^a	3	.030	.192	.900
ph2	2.00	control	8	Intercept	8.956	1	8.956	58.231	.000
	3.00	acid	8	temperature2	.041	1	.041	.269	.613
				ph2	.004	1	.004	.028	.870
				temperature2 * ph2	.014	1	.014	.088	.772
				Error	1.846	12	.154		
				Total	16.969	16			
				Corrected Total	1.934	15			

a. R Squared = .046 (Adjusted R Squared = -.193)

Between-Subjects Factors				Tests of Between-Subjects Effects					
	Value	Label	N	Dependent Variable: data21dayalivesdead					
temperature4	2.00	15	43	Source	Type III Sum of Squares	df	Mean Square	F	Sig.
	3.00	19	38	Corrected Model	.939 ^a	7	.134	1.505	.179
ph4	2.00	control	39	Intercept	30.006	1	30.006	336.693	.000
	3.00	acid	42	temperature4	5.792E-05	1	5.792E-05	.001	.980
alivesvsdead1	2.00	alive	16	ph4	.004	1	.004	.049	.826
	3.00	dead	65	alivesvsdead1	.009	1	.009	.096	.758
				temperature4 * ph4	.023	1	.023	.258	.613
				temperature4 * alivesvsdead1	.149	1	.149	1.674	.200
				ph4 * alivesvsdead1	.003	1	.003	.036	.850
				temperature4 * ph4 * alivesvsdead1	.136	1	.136	1.522	.221
				Error	6.506	73	.089		
				Total	80.319	81			
				Corrected Total	7.444	80			

a. R Squared = .126 (Adjusted R Squared = .042)

Figure A6.14a: *L. castanea*: average Mg data results from the general linear model analysis (Presented in Sections 5.5/5.6).

Average Mg

Between-Subjects Factors				Tests of Between-Subjects Effects						
	Value	Label	N	Dependent Variable: data21daydead						
				Source	Type III Sum of Squares	df	Mean Square	F	Sig.	
temperature3	2.00	15	32	Corrected Model	.841 ^a	3	.280	3.671	.017	
	3.00	19	33	Intercept	54.165	1	54.165	708.982	.000	
ph3	2.00	control	31	temperature3	.290	1	.290	3.791	.056	
	3.00	acid	34	ph3	.000	1	.000	.002	.964	
				temperature3 * ph3	.505	1	.505	6.605	.013	
				Error	4.660	61	.076			
				Total	63.350	65				
				Corrected Total	5.502	64				

a. R Squared = .153 (Adjusted R Squared = .111)

Between-Subjects Factors				Tests of Between-Subjects Effects						
	Value	Label	N	Dependent Variable: data95daydead						
				Source	Type III Sum of Squares	df	Mean Square	F	Sig.	
temperature5	2.00	15	37	Corrected Model	30.512 ^a	3	10.171	93.211	.000	
	3.00	19	57	Intercept	64.325	1	64.325	589.524	.000	
ph5	2.00	control	51	temperature5	5.358	1	5.358	49.105	.000	
	3.00	acid	43	ph5	5.149	1	5.149	47.191	.000	
				temperature5 * ph5	6.168	1	6.168	56.528	.000	
				Error	9.820	90	.109			
				Total	168.821	94				
				Corrected Total	40.332	93				

a. R Squared = .757 (Adjusted R Squared = .748)

Between-Subjects Factors				Tests of Between-Subjects Effects						
	Value	Label	N	Dependent Variable: data21daydeadvs95daydead						
				Source	Type III Sum of Squares	df	Mean Square	F	Sig.	
temperature6	2.00	15	69	Corrected Model	33.312 ^a	7	4.759	49.624	.000	
	3.00	19	90	Intercept	118.248	1	118.248	1233.068	.000	
ph6	2.00	control	82	temperature6	4.058	1	4.058	42.316	.000	
	3.00	acid	77	ph6	2.591	1	2.591	27.023	.000	
experiment length	2.00	alive	65	experiment length	.195	1	.195	2.038	.155	
	3.00	dead	94	temperature6 * ph6	5.088	1	5.088	53.052	.000	
				temperature6 * experiment length	1.566	1	1.566	16.334	.000	
				ph6 * experiment length	2.534	1	2.534	26.426	.000	
				temperature6 * ph6 * experiment length	1.559	1	1.559	16.258	.000	
				Error	14.481	151	.096			
				Total	232.171	159				
				Corrected Total	47.792	158				

a. R Squared = .697 (Adjusted R Squared = .683)

Figure A6.14b: *L. castanea*: average Mg data results from the general linear model analysis (Presented in Sections 5.5/5.6).

Average Ca

Between-Subjects Factors				Tests of Between-Subjects Effects					
	Value	Label	N	Dependent Variable: data21dayalive					
				Source	Type III Sum of Squares	df	Mean Square	F	Sig.
temperature2	2.00	15	11	Corrected Model	89.787 ^a	3	29.929	.772	.532
	3.00	19	5	Intercept	29556.216	1	29556.216	761.943	.000
ph2	2.00	control	8	temperature2	54.827	1	54.827	1.413	.257
	3.00	acid	8	ph2	.742	1	.742	.019	.892
				temperature2 * ph2	31.211	1	31.211	.805	.387
				Error	465.487	12	38.791		
				Total	51902.834	16			
				Corrected Total	555.274	15			

a. R Squared = .162 (Adjusted R Squared = -.048)

Between-Subjects Factors				Tests of Between-Subjects Effects					
	Value	Label	N	Dependent Variable: data21dayalivesdead					
				Source	Type III Sum of Squares	df	Mean Square	F	Sig.
temperature4	2.00	15	45	Corrected Model	476.326 ^a	7	68.047	3.488	.003
	3.00	19	45	Intercept	98054.337	1	98054.337	5025.756	.000
ph4	2.00	control	46	temperature4	20.705	1	20.705	1.061	.306
	3.00	acid	44	ph4	1.288	1	1.288	.066	.798
alivesdead1	2.00	alive	16	alivesdead1	96.044	1	96.044	4.923	.029
	3.00	dead	74	temperature4 * ph4	53.170	1	53.170	2.725	.103
				temperature4 * alivesdead1	87.582	1	87.582	4.489	.037
				ph4 * alivesdead1	.234	1	.234	.012	.913
				temperature4 * ph4 * alivesdead1	10.256	1	10.256	.526	.471
				Error	1599.850	82	19.510		
				Total	252184.075	90			
				Corrected Total	2076.176	89			

a. R Squared = .229 (Adjusted R Squared = .164)

Figure A6.15a: *L. castanea*: average Ca results from the general linear model analysis (Presented in Sections 5.5/5.6).

Average Ca

Between-Subjects Factors				Tests of Between-Subjects Effects					
	Value	Label	N	Dependent Variable: data21daydead					
				Source	Type III Sum of Squares	df	Mean Square	F	Sig.
temperature3	2.00	15	34	Corrected Model	85.378 ^a	3	28.459	1.756	.164
	3.00	19	40	Intercept	195133.268	1	195133.268	12041.412	.000
ph3	2.00	control	38	temperature3	49.029	1	49.029	3.025	.086
	3.00	acid	36	ph3	.900	1	.900	.056	.814
				temperature3 * ph3	35.464	1	35.464	2.188	.144
				Error	1134.363	70	16.205		
				Total	200281.241	74			
				Corrected Total	1219.740	73			

a. R Squared = .070 (Adjusted R Squared = .030)

Between-Subjects Factors				Tests of Between-Subjects Effects					
	Value	Label	N	Dependent Variable: data95daydead					
				Source	Type III Sum of Squares	df	Mean Square	F	Sig.
temperature5	2.00	15	42	Corrected Model	60.015 ^a	3	20.005	.871	.459
	3.00	19	63	Intercept	221102.733	1	221102.733	9627.060	.000
ph5	2.00	control	57	temperature5	.078	1	.078	.003	.954
	3.00	acid	48	ph5	16.284	1	16.284	.709	.402
				temperature5 * ph5	46.397	1	46.397	2.020	.158
				Error	2319.647	101	22.967		
				Total	285931.621	105			
				Corrected Total	2379.661	104			

a. R Squared = .025 (Adjusted R Squared = -.004)

Between-Subjects Factors				Tests of Between-Subjects Effects					
	Value	Label	N	Dependent Variable: data21daydeadvs95daydead					
				Source	Type III Sum of Squares	df	Mean Square	F	Sig.
temperature6	2.00	15	76	Corrected Model	145.834 ^a	7	20.833	1.031	.411
	3.00	19	103	Intercept	414857.539	1	414857.539	20538.636	.000
ph6	2.00	control	95	temperature6	27.801	1	27.801	1.376	.242
	3.00	acid	84	ph6	12.010	1	12.010	.595	.442
experiment length	2.00	alive	74	experiment length	9.800	1	9.800	.485	.487
	3.00	dead	105	temperature6 * ph6	.135	1	.135	.007	.935
				temperature6 * experiment length	23.886	1	23.886	1.183	.278
				ph6 * experiment length	4.364	1	4.364	.216	.643
				temperature6 * ph6 * experiment length	81.150	1	81.150	4.018	.047
				Error	3454.009	171	20.199		
				Total	486212.862	179			
				Corrected Total	3599.843	178			

a. R Squared = .041 (Adjusted R Squared = .001)

Figure A6.15b: *L. castanea*: average Ca results from the general linear model analysis (Presented in Sections 5.5/5.6).

Shell preservation

Between-Subjects Factors				Tests of Between-Subjects Effects					
	Value	Label	N	Dependent Variable: data21dayalive					
				Source	Type III Sum of Squares	df	Mean Square	F	Sig.
temperature2	2.00	15	15	Corrected Model	21.582 ^a	3	7.194	8.694	.001
	3.00	19	8	Intercept	86.827	1	86.827	104.928	.000
ph2	2.00	control	11	temperature2	.552	1	.552	.667	.424
	3.00	acid	12	ph2	7.219	1	7.219	8.724	.008
				temperature2 *	5.493	1	5.493	6.639	.018
				ph2					
				Error	15.722	19	.827		
				Total	146.000	23			
				Corrected Total	37.304	22			

a. R Squared = .579 (Adjusted R Squared = .512)

Between-Subjects Factors				Tests of Between-Subjects Effects					
	Value	Label	N	Dependent Variable: data21dayalivesdead					
				Source	Type III Sum of Squares	df	Mean Square	F	Sig.
temperature4	2.00	15	55	Corrected Model	32.106 ^a	7	4.587	8.074	.000
	3.00	19	53	Intercept	284.213	1	284.213	500.285	.000
ph4	2.00	control	56	temperature4	.075	1	.075	.133	.716
	3.00	acid	52	ph4	10.173	1	10.173	17.906	.000
alivesdead1	2.00	alive	23	alivesdead1	.019	1	.019	.033	.857
	3.00	dead	85	temperature4 *	9.953	1	9.953	17.520	.000
				ph4					
				temperature4 *	1.168	1	1.168	2.056	.155
				alivesdead1					
				ph4 *	2.927	1	2.927	5.153	.025
				alivesdead1					
				temperature4 *	1.254	1	1.254	2.208	.140
				ph4 *					
				alivesdead1					
				Error	56.810	100	.568		
				Total	609.000	108			
				Corrected Total	88.917	107			

a. R Squared = .361 (Adjusted R Squared = .316)

Figure A6.16a: *L. castanea*: shell preservation results from the general linear model analysis (Presented in Sections 5.5/5.6).

Shell preservation

Between-Subjects Factors				Tests of Between-Subjects Effects					
	Value	Label	N	Dependent Variable: data21daydead					
				Source	Type III Sum of Squares	df	Mean Square	F	Sig.
temperature3	2.00	15	40	Corrected Model	10.512 ^a	3	3.504	6.908	.000
	3.00	19	45	Intercept	415.169	1	415.169	818.455	.000
ph3	2.00	control	45	temperature3	.965	1	.965	1.902	.172
	3.00	acid	40	ph3	3.246	1	3.246	6.399	.013
				temperature3 * ph3	6.148	1	6.148	12.120	.001
				Error	41.088	81	.507		
				Total	463.000	85			
				Corrected Total	51.600	84			

a. R Squared = .204 (Adjusted R Squared = .174)

Between-Subjects Factors				Tests of Between-Subjects Effects					
	Value	Label	N	Dependent Variable: data95daydead					
				Source	Type III Sum of Squares	df	Mean Square	F	Sig.
temperature5	2.00	15	61	Corrected Model	179.154 ^a	3	59.718	14.908	.000
	3.00	19	81	Intercept	6232.120	1	6232.120	1555.804	.000
ph5	2.00	control	77	temperature5	17.851	1	17.851	4.456	.037
	3.00	acid	65	ph5	66.612	1	66.612	16.629	.000
				temperature5 * ph5	77.014	1	77.014	19.226	.000
				Error	552.790	138	4.006		
				Total	7358.000	142			
				Corrected Total	731.944	141			

a. R Squared = .245 (Adjusted R Squared = .228)

Between-Subjects Factors				Tests of Between-Subjects Effects					
	Value	Label	N	Dependent Variable: data21daydeadvs95daydead					
				Source	Type III Sum of Squares	df	Mean Square	F	Sig.
temperature6	2.00	15	101	Corrected Model	1329.990 ^a	7	189.999	70.064	.000
	3.00	19	126	Intercept	4308.963	1	4308.963	1588.985	.000
ph6	2.00	control	122	temperature6	11.760	1	11.760	4.337	.038
	3.00	acid	105	ph6	42.902	1	42.902	15.821	.000
experiment length	2.00	alive	85	experiment length	1158.734	1	1158.734	427.298	.000
	3.00	dead	142	temperature6 * ph6	55.702	1	55.702	20.541	.000
				temperature6 * experiment length	3.632	1	3.632	1.339	.248
				ph6 * experiment length	14.106	1	14.106	5.202	.024
				temperature6 * ph6 * experiment length	13.088	1	13.088	4.826	.029
				Error	593.878	219	2.712		
				Total	7821.000	227			
				Corrected Total	1923.868	226			

a. R Squared = .691 (Adjusted R Squared = .681)

Figure A6.16b: *L. castanea*: shell preservation results from the general linear model analysis (Presented in Sections 5.5/5.6).

Geometric shell size statistics (Alive)				
H (ch1^2)	5.774	Hc (tie corrected)	5.774	
p(same)	0.2167			
field collected	21 day 15°C control alive	21 day 15°C acid alive	21 day 19°C control alive	21 day 19°C acid alive
field collected	0.1637	0.7589	0.03736	0.8953
	21 day 15°C control alive	0.68	0.2888	0.4437
		21 day 15°C acid alive	0.4047	0.8102
			21 day 19°C control alive	0.06675

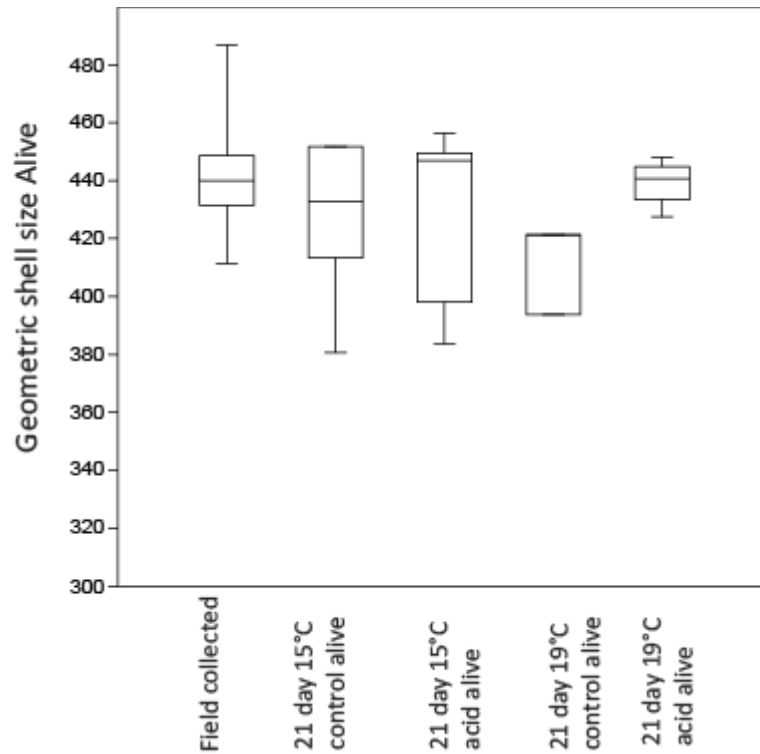


Figure A6.16: *L. castanea*: The table shows the data analysed using Kruskal-Wallis and Mann-Whitney pairwise comparison test for any significant difference in alive Geometric shell size (μm) with the numbers in red highlighting those numbers that show a significant difference. The box plot illustrates the original data showing the minimum, maximum, median and first and third quartile of the data set (Presented in Sections 5.5/5.6).

Mean shell thickness statistics (Alive)					
H (ch1^2)	9.343		Hc (tie corrected)		9.343
p(same)	0.05308				
field collected	21 day 15°C control alive	21 day 15°C acid alive	21 day 19°C control alive	21 day 19°C acid alive	
field collected	0.01438	0.07366	0.2788	0.6594	
	21 day 15°C control alive	0.3951	0.1904	0.2986	
		21 day 15°C acid alive	0.7237	0.4705	
			21 day 19°C control alive	0.7237	

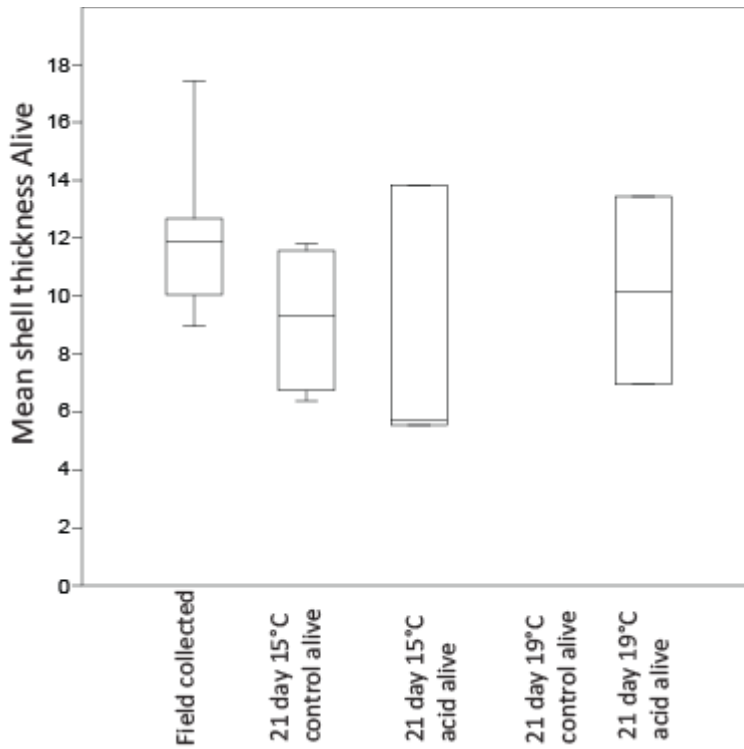


Figure A6.17: *L. castanea*: The table shows the data analysed using Kruskal-Wallis and Mann-Whitney pairwise comparison test for any significant difference in alive Mean shell thickness (μm) with the numbers in red highlighting those numbers that show a significant difference (Presented in Sections 5.5/5.6).

Shell Mg level statistics (Alive)				
H (ch1^2)	2.04	Hc (tie corrected)	2.042	
p(same)	0.7281			
field collected	21 day 15°C control alive	21 day 15°C acid alive	21 day 19°C control alive	21 day 19°C acid alive
field collected	0.587	0.4703	0.5384	0.2847
	21 day 15°C control alive	0.6366	1	0.7768
		21 day 15°C acid alive	0.7237	0.8839
			21 day 19°C control alive	0.7237

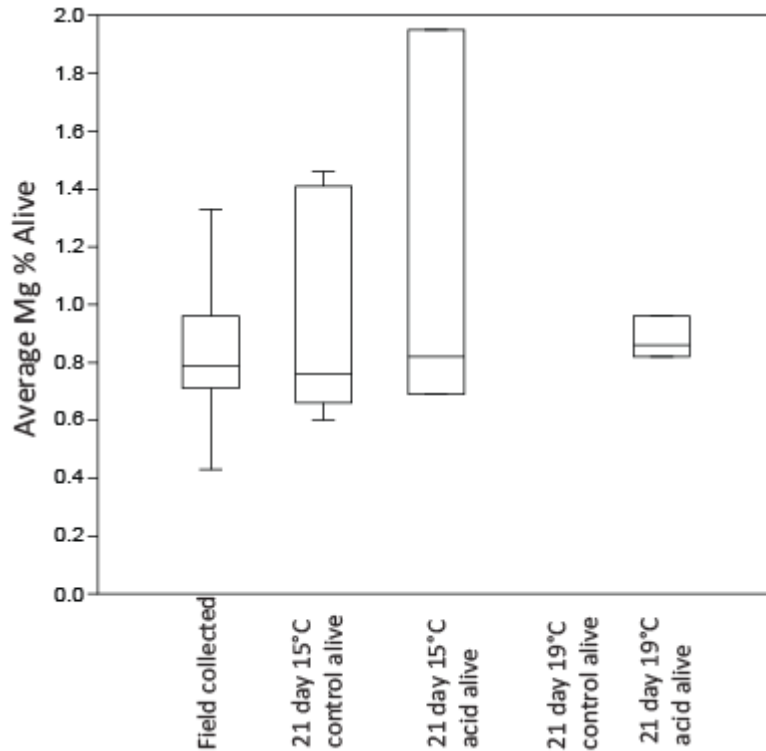


Figure A6.18: *L. castanea*: The table shows the data analysed using Kruskal-Wallis and Mann-Whitney pairwise comparison test for any significant difference in average alive level of Mg % with the numbers in red highlighting those numbers that show a significant difference. Each box plot illustrates the original data showing the minimum, maximum, median and first and third quartile of the data set (Presented in Sections 5.5/5.6).

Shell Ca level statistics (Alive)					
H (ch1^2)	2.144		Hc (tie corrected)		2.144
p(same)	0.7093				
	field collected	21 day 15°C control alive	21 day 15°C acid alive	21 day 19°C control alive	21 day 19°C acid alive
	field collected	0.4514	0.9793	0.3297	0.6974
		21 day 15°C control alive	0.3951	0.3827	0.5083
			21 day 15°C acid alive	0.2888	0.8852
				21 day 19°C control alive	0.7237

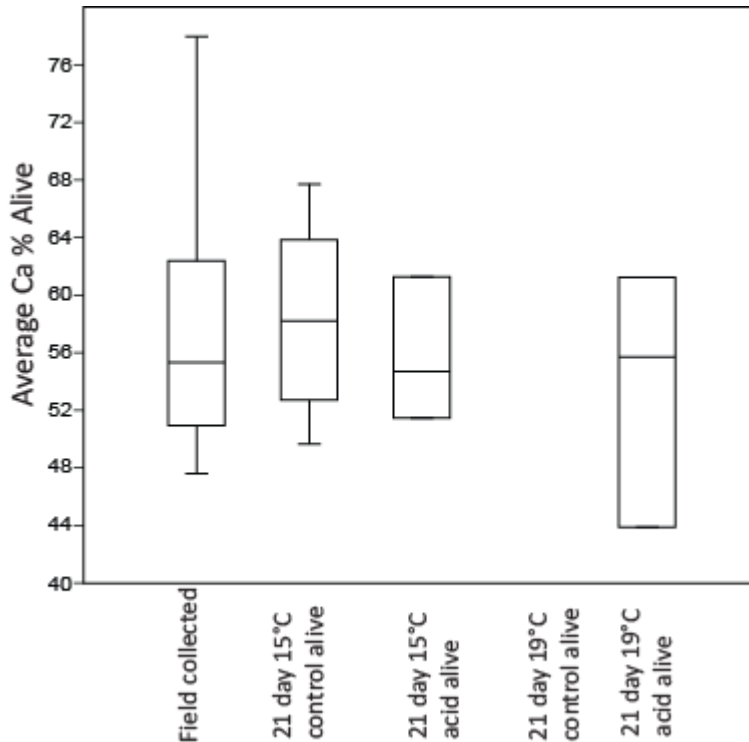


Figure A6.19: *L. castanea*: The table shows the data analysed using Kruskal-Wallis and Mann-Whitney pairwise comparison test for any significant difference in average alive level of Ca % with the numbers in red highlighting those numbers that show a significant difference. The box plot illustrates the original data showing the minimum, maximum, median and first and third quartile of the data set (Presented in Sections 5.5/5.6).

Table A6.11: *L. castanea*: The table shows the data analysed using Kruskal-Wallis and Mann-Whitney pairwise comparison test for any significant difference in alive shell preservation (rank) with the numbers in red highlighting those numbers that show a significant difference (Presented in Sections 5.5/5.6).

Shell preservation statistics (Alive)					
H (ch1^2)	28.56		Hc (tie corrected)		54.48
p(same)	4.17×10^{-11}				
	field collected	21 day 15°C control alive	21 day 15°C acid alive	21 day 19°C control alive	21 day 19°C acid alive
	field collected	0.001594	2.1×10^{-12}	2×10^{-11}	0.0000000022
		21 day 15°C control alive	0.00202	0.06708	0.0186
			21 day 15°C acid alive	0.2012	0.1092
				21 day 19°C control alive	0.8474

Table A6.12: *L. castanea*: The table shows the data analysed using Kruskal-Wallis and Mann-Whitney pairwise comparison test for any significant difference in dead shell preservation (rank) with the numbers in red highlighting those numbers that show a significant difference (Presented in Sections 5.5/5.6).

Shell preservation statistics (Dead)								
H (chi ²)	219.4	Hc (tie corrected)	224.7	p(same)	3.8 x 10⁻⁴⁴			
field collected	21 day 15°C control dead	21 day 15°C acid dead	21 day 19°C control dead	21 day 19°C acid dead	95 day 15°C control dead	95 day 15°C acid dead	95 day 19°C control dead	95 day 19°C acid dead
field collected	0.0000000302	1.39 x 10⁻¹⁴	1.4 x 10⁻¹⁵	6.6 x 10⁻¹⁶	4.6 x 10⁻¹⁸	7.51 x 10⁻¹⁵	3.13 x 10⁻¹⁷	1.21 x 10⁻¹⁸
	21 day 15°C control dead	0.00052	0.00089	0.00186	0.0000000014	0.00000000202	9.98 x 10⁻¹¹	7.98 x 10⁻¹²
		21 day 15°C acid dead	0.3769	0.1161	0.000061	0.0000000221	0.00000000449	0.000000000712
			21 day 19°C control dead	0.4624	0.0000011	0.00000000186	0.000000000173	1.63 x 10⁻¹¹
			21 day 19°C acid dead		0.00000009	0.000000000672	5.92 x 10⁻¹¹	5.65 x 10⁻¹²
					95 day 15°C control dead	0.000163	0.0000319	0.00000718
						95 day 15°C acid dead	0.1771	0.08732
							95 day 19°C control dead	0.9842

Table A6.13: *L. castanea*: The table shows the data analysed using Kruskal-Wallis and Mann-Whitney pairwise comparison test for any significant difference in dead Geometric shell size (µm) with the numbers in red highlighting those numbers that show a significant difference (Presented in Sections 5.5/5.6).

Geometric shell size statistics (Dead)								
H (chi ²)	48.39	Hc (tie corrected)	48.39	p(same)	0.0000000831			
field collected	21 day 15°C control dead	21 day 15°C acid dead	21 day 19°C control dead	21 day 19°C acid dead	95 day 15°C control dead	95 day 15°C acid dead	95 day 19°C control dead	95 day 19°C acid dead
field collected	0.0000843	0.00109	0.00021	0.01377	0.00000192	0.0000143	0.00000434	0.00000390
	21 day 15°C control dead	0.2287	0.7429	0.1361	0.7368	0.1155	0.7554	0.9673
		21 day 15°C acid dead	0.4453	0.7446	0.2418	0.005135	0.2281	0.1847
			21 day 19°C control dead	0.2689	0.973	0.06165	0.8192	0.8259
			21 day 19°C acid dead		0.1295	0.007426	0.1813	0.07805
					95 day 15°C	0.02074	0.8536	0.6135

Geometric shell size statistics (Dead)								
H (chi ²)	48.39	Hc (tie corrected)	48.39	p(same)	0.0000000831			
field collected	21 day 15°C control dead	21 day 15°C acid dead	21 day 19°C control dead	21 day 19°C acid dead	95 day 15°C control dead	95 day 15°C acid dead	95 day 19°C control dead	95 day 19°C acid dead
					control dead			
						95 day 15°C acid dead		
							0.01188	0.05557
							95 day 19°C control dead	0.5415

Table A6.14: *L. castanea*: The table shows the data analysed using Kruskal-Wallis and Mann-Whitney pairwise comparison test for any significant difference in dead Mean shell thickness (µm) with the numbers in red highlighting those numbers that show a significant difference (Presented in Sections 5.5/5.6).

Mean shell thickness statistics (Dead)								
H (chi ²)	23.8	Hc (tie corrected)	23.8	p(same)	0.00247			
field collected	21 day 15°C control dead	21 day 15°C acid dead	21 day 19°C control dead	21 day 19°C acid dead	95 day 15°C control dead	95 day 15°C acid dead	95 day 19°C control dead	95 day 19°C acid dead
field collected	0.5545	0.01213	0.01202	0.9846	0.9882	0.7955	0.285	0.005364
	21 day 15°C control dead	0.01918	0.1607	0.5886	0.562	0.537	0.8588	0.1763
		21 day 15°C acid dead	0.00195	0.05306	0.02566	0.3497	0.01091	0.000277
			21 day 19°C control dead	0.05681	0.01489	0.1611	0.07193	0.4319
			21 day 19°C acid dead	0.8948	0.832	0.5017	0.04137	
					95 day 15°C control dead	0.7313	0.2383	0.008151
						95 day 15°C acid dead	0.5578	0.1471
							95 day 19°C control dead	0.151

Table A6.15: *L. castanea*: The table shows the data analysed using Kruskal-Wallis and Mann-Whitney pairwise comparison test for any significant difference in average dead level of Mg % with the numbers in red highlighting those numbers that show a significant difference (Presented in Sections 5.5/5.6).

Shell Mg level statistics (Dead)								
H (chi ²)	108.8	Hc (tie corrected)	108.8	p(same)	6.70 x 10 ⁻²⁰			
field collected	21 day 15°C control dead	21 day 15°C acid dead	21 day 19°C control dead	21 day 19°C acid dead	95 day 15°C control dead	95 day 15°C acid dead	95 day 19°C control dead	95 day 19°C acid dead
field collected	0.07518	0.5792	0.2236	0.00128	0.06989	0.08425	0.01001	9.99 x 10 ⁻¹²
	21 day 15°C control dead	0.06253	0.7639	0.1109	0.00115	0.003645	0.000293	0.000000882
		21 day 15°C acid dead	0.1092	0.00184	0.2834	0.167	0.07689	0.000000787
			21 day 19°C control dead	0.1009	0.02801	0.0322	0.006321	0.000000415
			21 day 19°C acid dead		0.0000222	0.001325	0.00000765	0.000000126
					95 day 15°C control dead	0.5091	0.2425	5.77 x 10 ⁻¹²
					95 day 15°C acid dead		0.8943	0.0000363
							95 day 19°C control dead	0.000000005 20

Table A6.16: *L. castanea*: The table shows the data analysed using Kruskal-Wallis and Mann-Whitney pairwise comparison test for any significant difference in average dead level of Ca % with the numbers in red highlighting those numbers that show a significant difference (Presented in Sections 5.5/5.6).

Shell Ca level statistics (Dead)								
H (chi ²)	22.79	Hc (tie corrected)	22.79	p(same)	0.00365			
field collected	21 day 15°C control dead	21 day 15°C acid dead	21 day 19°C control dead	21 day 19°C acid dead	95 day 15°C control dead	95 day 15°C acid dead	95 day 19°C control dead	95 day 19°C acid dead
field collected	0.005139	0.000806	0.00656	0.06761	0.00022	0.2549	0.03349	0.005227
	21 day 15°C control dead	0.267	0.804	0.4011	0.33	0.1359	0.5071	0.8856
		21 day 15°C acid dead	0.2981	0.03419	0.698	0.01357	0.09929	0.2819
			21 day 19°C control dead	0.3571	0.465	0.1617	0.5223	0.8456
			21 day 19°C acid dead		0.04953	0.627	0.7828	0.397

Shell Ca level statistics (Dead)								
H (chi^2)	22.79	Hc (tie corrected)	22.79	p(same)	0.00365			
field collected	21 day 15°C control dead	21 day 15°C acid dead	21 day 19°C control dead	21 day 19°C acid dead	95 day 15°C control dead	95 day 15°C acid dead	95 day 19°C control dead	95 day 19°C acid dead
					95 day 15°C control dead	0.04621	0.1456	0.4612
						95 day 15°C acid dead	0.4993	0.2481
							95 day 19°C control dead	0.648

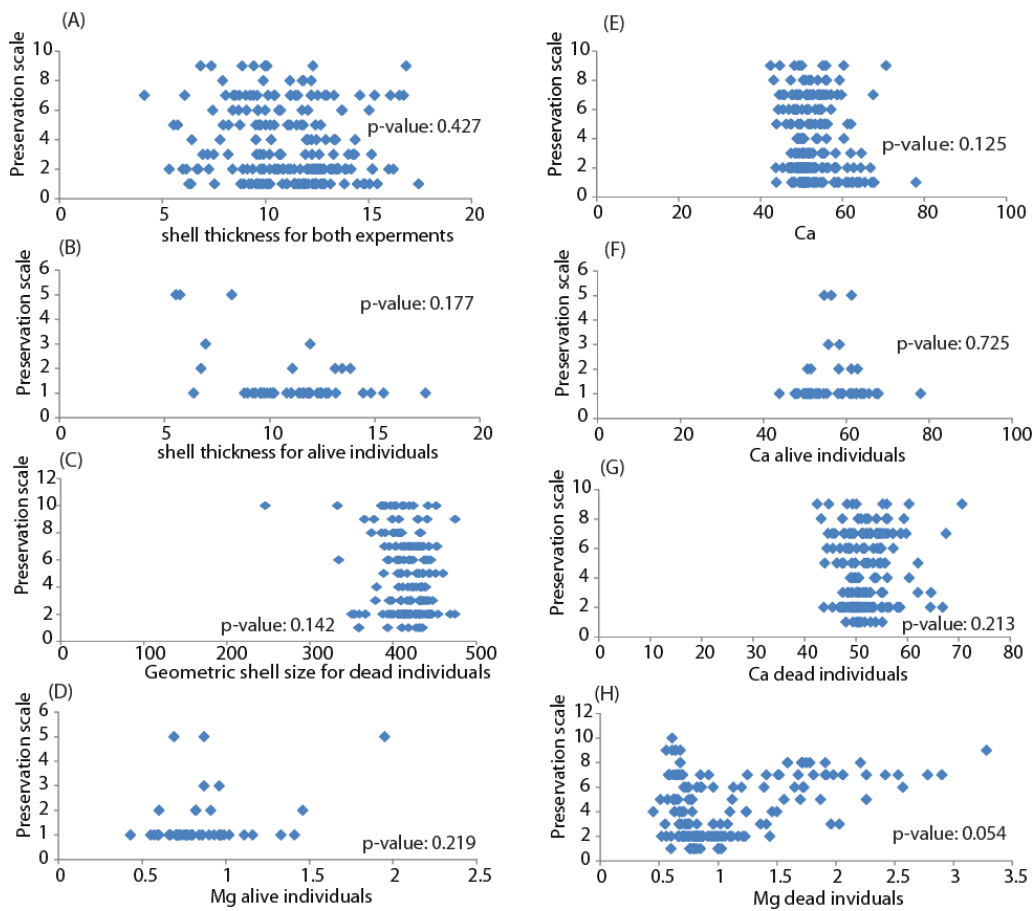


Figure A6.20: *L. castanea*: Linear regression models and Spearman's rank results (p-values) from comparing all the different data sets (Geometric shell size, Mean shell thickness, Average Mg and Ca %) against the relevant preservation rank to determine if there are any correlations and trends between the different data sets and preservation. Trend lines on the linear regression models indicate that the data shows a significant correlation (Presented in Sections 5.7).

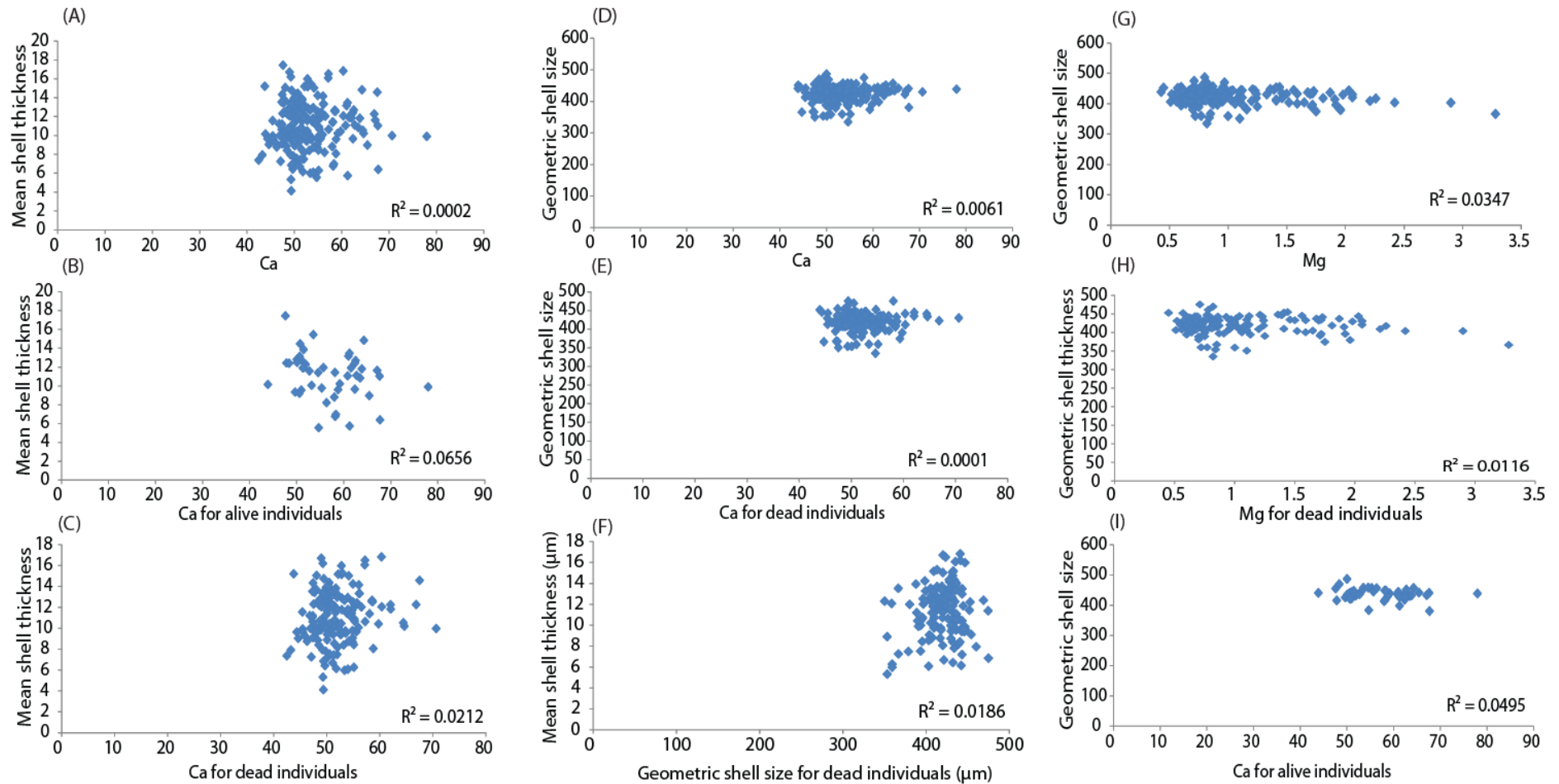


Figure A6.21: *L. castanea*: Linear regression models comparing all the data against each other to determine if there are any correlations and trends between the different data sets (Geometric shell size, Mean shell thickness, Average Mg and Ca %). Trend lines on the linear regression models indicate that the data shows a significant correlation (Presented in Sections 5.7).

Table A6.17: *L. castanea* results from the statistical analysis when determining any correlations between the different data sets (Presented in Sections 5.7).

<i>L. castanea</i>		
Correlation question	Number of individuals	R ² value
Preservation against geometric shell size for both experiments	261	0.0821
Preservation against geometric shell size for alive individuals	68	0.0595
Preservation against geometric shell size for dead individuals	193	0.0195
Preservation against shell thickness for both experiments	207	0.0168
Preservation against shell thickness for alive individuals	47	0.2345
Preservation against shell thickness for dead individuals	160	0.0148
Preservation against average Mg for both experiments	205	0.1563
Preservation against average Mg for alive individuals	46	0.1055
Preservation against average Mg for dead individuals	159	0.1316
Preservation against average Ca for both experiments	226	0.0164
Preservation against average Ca for alive individuals	47	0.0003
Preservation against average Ca for dead individuals	179	0.0067
Correlation question	Number of individuals	R ² value
Geometric shell size against shell thickness for both experiments	191	0.0406
Geometric shell size against shell thickness for alive individuals	47	0.3049
Geometric shell size against shell thickness for dead individuals	144	0.0186
Geometric shell size against average Mg for both experiments	189	0.0347
Geometric shell size against average Mg for alive individuals	46	0.171
Geometric shell size against average Mg for dead individuals	143	0.0116
Shell thickness against average Mg for both experiments	190	0.1505
Shell thickness against average Mg for alive individuals	46	0.1818
Shell thickness against average Mg for dead individuals	144	0.1657
Geometric shell size against average Ca for both experiments	207	0.0061
Geometric shell size against average Ca for alive individuals	47	0.0495
Geometric shell size against average Ca for dead individuals	160	0.0001
Shell thickness against average Ca for both experiments	207	0.0002
Shell thickness against average Ca for alive individuals	47	0.0656
Shell thickness against average Ca for dead individuals	160	0.0212

A6.4: *L. lacertosa* raw data sets

Table A6.18a: *L. lacertosa*: the raw data sets. Geometric shell size (µm) comparison tests, linear regression models, Spearman's rank and general linear model (Presented in Sections 5.5/5.6).

Geometric shell size								
field collected	21 day 15°C control alive	311.12	21 day 15°C acid alive	317.59	21 day 19°C control alive	359.05	21 day 19°C acid alive	289.56
261.21		315.00		290.56		362.94		390.73
203.65		303.79		307.82		327.42		380.38
					21 day 19°C control dead			
232.20		332.22		282.75		317.48		310.30
210.40		315.97		239.50		301.77		306.35
223.89		299.60		310.08		373.70		308.57
197.28		310.49		327.02		371.61		304.13
223.85		296.57		286.75		324.83		297.12
213.92		381.99		279.14		288.55		281.94
			21 day 15°C acid					
186.15		378.06		301.48		315.51		283.46

Geometric shell size								
			dead					
229.47		305.26		327.06		321.10	21 day 19°C acid dead	306.66
241.75	21 day 15°C control dead	301.31		332.34		282.07		299.19
221.61		302.93		305.84		296.95		304.44
275.48		305.31		277.31		299.92		309.54
211.20		294.67		311.74	95 day 19°C control dead	380.99		302.19
		314.87	95 day 15°C acid dead	285.81		310.17		324.82
		291.14		313.12		276.57		304.94
	95 day 15°C control dead	303.48		230.47		298.90	95 day 19°C acid dead	292.98
		318.69		277.96		311.16		321.69
		284.05		318.06		291.66		314.65
		303.27		296.68		297.09		288.43
		287.35		299.07		326.46		296.31
		302.92		272.57		263.56		269.45
		315.19		305.93		296.56		263.36
		306.49		305.59		309.51		287.53
		322.42		314.82		309.29		316.64
		276.36		315.19		290.97		284.76
		306.31		287.85		286.80		296.55
		308.21		304.28		292.96		272.11
		282.35		294.23		275.73		307.48
		319.33		286.86		253.86		308.90
		307.50		263.06		276.85		299.24
		305.63		310.90		298.49		286.87
		297.39		273.27		324.84		302.65
		280.58		274.15		286.42		298.07
		281.19		262.93		297.02		275.85
		304.48		291.41		310.24		294.75
		227.90		285.16		309.52		307.88
		254.68		237.70		219.97		307.62
		302.20		255.59		321.60		316.51
		270.20				312.22		310.74
		303.81						301.16
		278.29						
		279.20						
		298.68						
		304.32						
		306.24						
		310.25						
		293.69						
		297.71						
		322.35						
		284.06						
		292.85						
		314.14						

Table A6.18b: *L. lacertosa*: the raw data sets. Mean shell thickness (μm) comparison tests, linear regression models, Spearman's rank and general linear model (Presented in Sections 5.5/5.6).

Mean shell thickness								
field collected	21 day 15°C control alive	6.50	21 day 15°C acid alive	9.82	21 day 19°C control alive	10.88	21 day 19°C acid alive	5.58
10.02		8.24		9.65	21 day 19°C control dead	9.41		8.97
11.25		6.71		5.66		6.78		10.44
7.09		7.09		8.86		11.00		13.35
9.81		10.85		12.16		6.87		7.93
8.69		7.55		10.02		11.54		10.14
9.73		8.01		6.91		7.01		5.50
		8.77	21 day 15°C acid dead	9.49		7.73		7.80
		9.59		9.63		10.50	21 day 19°C acid dead	10.88
	21 day 15°C control dead	11.68		10.55	95 day 19°C control dead	5.45		10.34
		10.42	95 day 15°C acid dead	9.02		8.64		10.05
		9.84		10.55		7.89		9.47
		8.32		9.26		10.41		8.01
	95 day 15°C control dead	11.65		8.14		8.06	95 day 19°C acid dead	11.14
		10.27		10.33		8.97		10.07
		7.95		11.37		9.39		7.90
		10.49		12.03		6.24		11.21
		9.93		10.66		12.18		8.82
		8.35		4.31		7.33		4.93
		8.68		6.70		9.59		5.86
		7.26		9.66		7.95		10.03
		7.07		7.81		8.37		10.64
		7.87		8.98		6.22		6.96
		11.64		4.64		6.24		10.41
		7.34		5.07		7.27		8.69
		11.03		4.07		7.63		8.47
		11.65				6.10		7.70
		9.99				12.20		8.05
		8.77				6.86		10.17
		9.91				8.21		6.19
		7.79				6.44		7.50
		7.17				10.70		10.94
		10.65				9.82		8.45
		9.45				10.81		11.70
		9.66						10.51
		10.33						10.27
		6.54						
		8.91						
		8.72						

Table A6.18c: *L. lacertosa*: the raw data sets (Average Mg (%)) comparison tests, linear regression models, Spearman's rank and general linear model (Presented in Sections 5.5/5.6).

Average Mg								
field collected	21 day 15°C control alive	1.32	21 day 15°C acid alive	0.73	21 day 19°C control alive	0.7	21 day 19°C acid alive	0.66
0.66		0.54		0.56	21 day 19°C control dead	0.57		0.76
0.68		0.75		0.58		0.79		0.83
0.43		1.08		0.43		0.84		0.74
0.53		0.81		0.51		0.56		0.67
0.48		0.75		0.69		0.72		0.72
		0.87		0.63		0.83		0.92
		0.61	21 day 15°C acid dead	0.64		0.66		1.1
		0.7		0.76	95 day 19 control dead	0.73		1.83
	21 day 15°C control dead	0.8		0.63		0.83	21 day 19°C acid dead	0.85
		0.71		0.68		0.61		0.73
		1.09	95 day 15°C acid dead	0.55		0.62		0.7
	95 day 15°C control dead	0.55		0.58		0.62		0.73
		0.63		0.7		0.52		0.92
		0.92		0.61		0.71	95 day 19°C acid dead	2.01
		0.8		0.59		0.69		2.21
		0.7		0.6		0.55		1.29
		0.75		0.61		0.74		2.87
		0.7		0.65		0.74		2.5
		0.75		0.46		0.64		2.68
		0.69		0.66		1.07		3.14
		0.63		0.92		0.67		2.39
		0.75		0.62		0.64		2.66
		0.73		0.85		0.65		2.52
		0.63		0.54		0.73		3.21
		0.74		0.72		0.72		2.15
		0.86				0.58		1.45
		0.7				0.61		2.03
		0.63				0.74		2.02
		0.56				0.56		1.67
		0.53						2.04
		0.71						2.04
		1.08						2.86
								3.01
								1.28
								2.41
								2.08
								2.07
								2.28

Table A6.18d: *L. lacertosa*: the raw data sets (Average Ca (%)) comparison tests, linear regression models, Spearman's rank and general linear model (Presented in Sections 5.5/5.6).

Average Ca								
field collected	21 day 15°C control alive	70.05	21 day 15°C acid alive	48.08	21 day 19°C control alive	47.36	21 day 19°C acid alive	65.33
69.42		65.81		48.59	21 day 19°C	66.83		54.06

Average Ca							
					control dead		
56.84		63.73		79.26		46.19	57.96
60.7		59.32		80.22		59.38	54
68.36		52.14		68.91		56.29	50.78
75.11		51.65		72.16		62.17	63.07
69.13		54.94		65.75		50.82	64.8
			21 day 15°C acid dead				
		52.09		45.23		53.43	70.56
		51.67		50.96		65.14	54.13
				54.33	95 day 19°C control dead	53.51	21 day 19°C acid dead
	21 day 15°C control dead	49.29		52.41		48.99	44.5
			95 day 15°C acid dead				
		55.9		52.82		49.62	46.81
		53.36		53.38		49.93	48.16
		53.94		55.04		52.84	45.45
	95 day 15°C control dead						95 day 19°C acid dead
		52.66		50.07		50.15	47.65
		51.92		51.18		47.39	47.03
		50.76		51.04		47.59	50.06
		52.41		53.17		51.36	48.61
		52.6		48.81		48.6	47.78
		51.34		47.12		49.04	46.22
		48.39		52.09		51.75	59.79
		53.81		50.81		51.75	48.91
		48.49		59.91		51.15	48.39
		46.34		58.86		48.19	46.72
		48.86		49.46		49.81	50.85
		49.34		43.49		49.54	47.86
		48.82		42.71		54.54	52.32
		51.84		52.51		53.78	51.84
		56.63		46.34		52.66	50.45
		49.52				49.9	49.35
		55.09				51.35	52.11
		48.34				45.41	52.11
		51.89				53.25	44.35
		50.63				52.58	51.76
		51.98				53.04	52.35
		51.22				52.25	50.67
		49.13					52.41
		51.62					48.84
		52.73					49.61
		49.83					
		48.38					
		49.37					
		51.42					

Table A6.18e: *L. lacertosa*: the raw data sets (Shell preservation (rank) comparison tests, linear regression models, Spearman's rank and general linear model) (Presented in Sections 5.5/5.6).

Shell Preservation								
field collected	21 day 15°C control alive	1	21 day 15°C acid alive	1	21 day 19°C control alive	2	21 day 19°C acid alive	2
1		1		1		2		2
1		2		2		2		3
1		1		2	21 day 19°C control dead	3		2
1		3		5		3		2
1		1		3		2		1
1		1		2		5		1
1		2		2		2		1
1		3		3		3		3

Shell Preservation							
1		2	21 day 15°C acid dead	2		2	2
1		2		2		5	21 day 19°C acid dead
1	21 day 15°C control dead	2		5		2	3
1		2		4		2	2
1		1		2		2	2
1		2		2	95 day 19°C control dead	3	2
		2	95 day 15°C acid dead	4		3	2
		1		4		9	2
	95 day 15°C control dead	3		5		6	95 day 19°C acid dead
		3		3		5	5
		3		2		6	4
		3		5		6	6
		2		10		3	5
		2		5		4	4
		2		10		5	5
		2		3		3	7
		5		3		3	9
		3		3		5	8
		5		4		3	5
		7		6		9	5
		2		6		6	9
		2		3		4	5
		2		10		3	6
		2		10		7	5
		2		10		3	6
		2		4		3	4
		5		3		2	6
		10		7		2	7
		5		7		3	9
		2		10		3	4
		10		7		6	5
		5		10		3	5
		10		7		3	4
		10		5		5	5
		10				5	
		2					
		7					
		10					
		10					
		2					
		2					
		7					
		2					
		5					
		2					
		4					
		10					
		10					
		10					

A6.4.2: *L. lacertosa* analysis of raw data

Geometric shell size

Between-Subjects Factors				Tests of Between-Subjects Effects					
	Value	Label	N	Dependent Variable: data21dayalive					
				Source	Type III Sum of Squares	df	Mean Square	F	Sig.
temperature2	2.00	15	20	Corrected Model	8465.017 ^a	3	2821.672	2.872	.053
	3.00	19	13	Intercept	2583792.714	1	2583792.714	2630.041	.000
ph2	2.00	control	14	temperature2	3757.115	1	3757.115	3.824	.060
	3.00	acid	19	ph2	6409.720	1	6409.720	6.524	.016
				temperature2 * ph2	43.989	1	43.989	.045	.834
				Error	28490.048	29	982.415		
				Total	3310253.617	33			
				Corrected Total	36955.065	32			

a. R Squared = .229 (Adjusted R Squared = .149)

Between-S subjects Factors				Tests of Between-Subjects Effects					
	Value	Label	N	Dependent Variable: data21dayalivevsdead					
				Source	Type III Sum of Squares	df	Mean Square	F	Sig.
temperature4	2.00	15	32	Corrected Model	9886.190 ^a	7	1412.313	1.921	.084
	3.00	19	31	Intercept	5269655.865	1	5269655.865	7167.844	.000
ph4	2.00	control	31	temperature4	3284.577	1	3284.577	4.468	.039
	3.00	acid	32	ph4	3668.520	1	3668.520	4.990	.030
alivevsdead1	2.00	alive	33	alivevsdead1	1704.513	1	1704.513	2.318	.134
	3.00	dead	30	temperature4 * ph4	442.715	1	442.715	.602	.441
				temperature4 * alivevsdead1	1011.220	1	1011.220	1.375	.246
				ph4 * alivevsdead1	3116.286	1	3116.286	4.239	.044
				temperature4 * ph4 * alivevsdead1	129.927	1	129.927	.177	.676
				Error	40434.902	55	735.180		
				Total	6213276.389	63			
				Corrected Total	50321.092	62			

a. R Squared = .196 (Adjusted R Squared = .094)

Figure A6.22a: *Leptocythere lacertosa*: geometric shell size (μm) results from the general linear model analysis (Presented in Sections 5.5/5.6).

Geometric shell size

Between-Subjects Factors				Tests of Between-Subjects Effects					
	Value	Label	N	Dependent Variable: data21daydead					
				Source	Type III Sum of Squares	df	Mean Square	F	Sig.
temperature3	2.00	15	12	Corrected Model	1092.909 ^a	3	364.303	.793	.509
	3.00	19	18	Intercept	2693812.646	1	2693812.646	5863.540	.000
ph3	2.00	control	17	temperature3	345.003	1	345.003	.751	.394
	3.00	acid	13	ph3	11.933	1	11.933	.026	.873
				temperature3 * ph3	557.819	1	557.819	1.214	.281
				Error	11944.854	26	459.417		
				Total	2903022.772	30			
				Corrected Total	13037.764	29			
a. R Squared = .084 (Adjusted R Squared = -.022)									

Between-Subjects Factors				Tests of Between-Subjects Effects					
	Value	Label	N	Dependent Variable: data95daydead					
				Source	Type III Sum of Squares	df	Mean Square	F	Sig.
temperature5	2.00	15	62	Corrected Model	2052.997 ^a	3	684.332	1.399	.247
	3.00	19	52	Intercept	9613208.246	1	9613208.246	19648.173	.000
ph5	2.00	control	64	temperature5	953.269	1	953.269	1.948	.166
	3.00	acid	50	ph5	699.682	1	699.682	1.430	.234
				temperature5 * ph5	567.422	1	567.422	1.160	.284
				Error	53819.401	110	489.267		
				Total	9940156.948	114			
				Corrected Total	55872.398	113			
a. R Squared = .037 (Adjusted R Squared = .010)									

Between-Subjects Factors				Tests of Between-Subjects Effects					
	Value	Label	N	Dependent Variable: data21daydeadvs95daydead					
				Source	Type III Sum of Squares	df	Mean Square	F	Sig.
temperature6	2.00	15	74	Corrected Model	9164.847 ^a	7	1309.264	2.708	.012
	3.00	19	70	Intercept	8186098.803	1	8186098.803	16928.793	.000
ph6	2.00	control	81	temperature6	929.208	1	929.208	1.922	.168
	3.00	acid	63	ph6	224.704	1	224.704	.465	.497
experiment length	2.00	alive	30	experiment length	4921.396	1	4921.396	10.177	.002
	3.00	dead	114	temperature6 * ph6	107.526	1	107.526	.222	.638
				temperature6 * experiment length	7.237	1	7.237	.015	.903
				ph6 * experiment length	77.804	1	77.804	.161	.689
				temperature6 * ph6 * experiment length	1012.004	1	1012.004	2.093	.150
				Error	65764.255	136	483.561		
				Total	12843179.721	144			
				Corrected Total	74929.102	143			
a. R Squared = .122 (Adjusted R Squared = .077)									

Figure A6.22b: *Leptocythere lacertosa*: geometric shell size (μm) results from the general linear model analysis (Presented in Sections 5.5/5.6).

Mean shell thickness

Between-Subjects Factors				Tests of Between-Subjects Effects					
	Value	Label	N	Dependent Variable: data21dayalive					
				Source	Type III Sum of Squares	df	Mean Square	F	Sig.
temperature2	2.00	15	16	Corrected Model	8.194 ^a	3	2.731	.624	.608
	3.00	16	9	Intercept	979.204	1	979.204	223.608	.000
ph2	2.00	control	10	temperature2	4.295	1	4.295	.981	.333
	3.00	acid	15	ph2	1.220	1	1.220	.279	.603
				temperature2 * ph2	6.671	1	6.671	1.523	.231
				Error	91.961	21	4.379		
				Total	1983.021	25			
				Corrected Total	100.155	24			

a. R Squared = .082 (Adjusted R Squared = -.049)

Between-Subjects Factors				Tests of Between-Subjects Effects					
	Value	Label	N	Dependent Variable: data21dayalivevsdead					
				Source	Type III Sum of Squares	df	Mean Square	F	Sig.
temperature4	2.00	15	23	Corrected Model	20.594 ^a	7	2.942	.831	.569
	3.00	16	22	Intercept	2478.959	1	2478.959	699.871	.000
ph4	2.00	control	22	temperature4	.512	1	.512	.145	.706
	3.00	acid	23	ph4	.145	1	.145	.041	.841
alivevsdead1	2.00	alive	25	alivevsdead1	1.429	1	1.429	.403	.529
	3.00	dead	20	temperature4 * ph4	1.690	1	1.690	.477	.494
				temperature4 * alivevsdead1	6.263	1	6.263	1.768	.192
				ph4 * alivevsdead1	1.782	1	1.782	.503	.483
				temperature4 * ph4 * alivevsdead1	7.349	1	7.349	2.075	.158
				Error	131.055	37	3.542		
				Total	3822.750	45			
				Corrected Total	151.649	44			

a. R Squared = .136 (Adjusted R Squared = -.028)

Figure A6.23a: *Leptocythere lacertosa*: mean shell thickness (μm) results from the general linear model analysis (Presented in Sections 5.5/5.6).

Mean shell thickness

Between-Subjects Factors				Tests of Between-Subjects Effects						
	Value	Label	N	Dependent Variable: data21daydead						
				Source	Type III Sum of Squares	df	Mean Square	F	Sig.	
temperature3	2.00	15	7	Corrected Model	5.361 ^a	3	1.787	.731	.548	
	3.00	16	13	Intercept	1636.410	1	1636.410	669.741	.000	
ph3	2.00	control	12	temperature3	2.010	1	2.010	.822	.378	
	3.00	acid	8	ph3	.574	1	.574	.235	.634	
				temperature3	1.254	1	1.254	.513	.484	
				* ph3						
				Error	39.094	16	2.443			
				Total	1839.730	20				
				Corrected Total	44.454	19				

a. R Squared = .121 (Adjusted R Squared = -.044)

Between-Subjects Factors				Tests of Between-Subjects Effects						
	Value	Label	N	Dependent Variable: data95daydead						
				Source	Type III Sum of Squares	df	Mean Square	F	Sig.	
temperature5	2.00	15	42	Corrected Model	13.636 ^a	3	4.545	1.199	.315	
	3.00	16	48	Intercept	6572.709	1	6572.709	1733.439	.000	
ph5	2.00	control	51	temperature5	.104	1	.104	.028	.869	
	3.00	acid	39	ph5	.438	1	.438	.116	.735	
				temperature5	12.718	1	12.718	3.354	.071	
				* ph5						
				Error	326.088	86	3.792			
				Total	7223.438	90				
				Corrected Total	339.724	89				

a. R Squared = .040 (Adjusted R Squared = .007)

Between-Subjects Factors				Tests of Between-Subjects Effects						
	Value	Label	N	Dependent Variable: data21daydeadvs95daydead						
				Source	Type III Sum of Squares	df	Mean Square	F	Sig.	
temperature6	2.00	15	49	Corrected Model	27.688 ^a	7	3.955	1.105	.366	
	3.00	16	61	Intercept	4926.357	1	4926.357	1375.998	.000	
ph6	2.00	control	63	temperature6	2.031	1	2.031	.567	.453	
	3.00	acid	47	ph6	.175	1	.175	.049	.825	
experiment length	2.00	alive	20	experiment length	12.775	1	12.775	3.568	.062	
	3.00	dead	90	temperature6	6.179	1	6.179	1.726	.192	
				* ph6						
				temperature6	1.345	1	1.345	.376	.541	
				* experiment length						
				ph6 * experiment length	.927	1	.927	.259	.612	
				temperature6	.197	1	.197	.055	.815	
				* ph6 * experiment length						
				Error	365.181	102	3.580			
				Total	9063.168	110				
				Corrected Total	392.869	109				

a. R Squared = .070 (Adjusted R Squared = .007)

Figure A6.23b: *Leptocythere lacertosa*: mean shell thickness (μm) results from the general linear model analysis (Presented in Sections 5.5/5.6).

Average Mg

Between-Subjects Factors				Tests of Between-Subjects Effects					
	Value	Label	N	Dependent Variable: data21daysalive					
temperature2	2.00	15	16	Source	Type III Sum of Squares	df	Mean Square	F	Sig.
	3.00	19	10	Corrected Model	.439 ^a	3	.146	1.977	.147
ph2	2.00	control	10	Intercept	6.726	1	6.726	90.928	.000
	3.00	acid	16	temperature2	.029	1	.029	.392	.538
				ph2	.000	1	.000	.004	.948
				temperature2 * ph2	.148	1	.148	2.006	.171
				Error	1.627	22	.074		
				Total	18.214	26			
				Corrected Total	2.066	25			

a. R Squared = .212 (Adjusted R Squared = .105)

Between-Subjects Factors				Tests of Between-Subjects Effects					
	Value	Label	N	Dependent Variable: data21daysalivesdead					
temperature4	2.00	15	23	Source	Type III Sum of Squares	df	Mean Square	F	Sig.
	3.00	19	22	Corrected Model	.536 ^a	7	.077	1.544	.183
ph4	2.00	control	20	Intercept	16.081	1	16.081	324.310	.000
	3.00	acid	25	temperature4	.010	1	.010	.200	.657
alivesvsdead1	2.00	alive	26	ph4	.008	1	.008	.159	.693
	3.00	dead	19	alivesvsdead1	4.511E-05	1	4.511E-05	.001	.976
				temperature4 * ph4	.223	1	.223	4.502	.041
				temperature4 * alivesvsdead1	.027	1	.027	.537	.468
				ph4 * alivesvsdead1	.004	1	.004	.075	.786
				temperature4 * ph4 * alivesvsdead1	.015	1	.015	.301	.587
				Error	1.835	37	.050		
				Total	29.128	45			
				Corrected Total	2.371	44			

a. R Squared = .226 (Adjusted R Squared = .080)

Figure A6.24a: *Leptocythere lacertosa*: average Mg % data results from the general linear model analysis (Presented in Sections 5.5/5.6).

Average Mg

Between-Subjects Factors				Tests of Between-Subjects Effects						
	Value	Label	N	Dependent Variable: data21daysdead						
				Source	Type III Sum of Squares	df	Mean Square	F	Sig.	
temperature3	2.00	15	7	Corrected Model	.079 ^a	3	.026	1.915	.171	
	3.00	19	12	Intercept	9.979	1	9.979	721.519	.000	
ph3	2.00	control	10	temperature3	.003	1	.003	.181	.676	
	3.00	acid	9	ph3	.014	1	.014	1.000	.333	
				temperature3 * ph3	.076	1	.076	5.489	.033	
				Error	.207	15	.014			
				Total	10.915	19				
				Corrected Total	.287	18				
				a. R Squared = .277 (Adjusted R Squared = .132)						

Between-Subjects Factors				Tests of Between-Subjects Effects						
	Value	Label	N	Dependent Variable: data95daydead						
				Source	Type III Sum of Squares	df	Mean Square	F	Sig.	
temperature5	2.00	15	36	Corrected Model	44.258 ^a	3	14.753	154.904	.000	
	3.00	19	47	Intercept	93.236	1	93.236	978.987	.000	
ph5	2.00	control	43	temperature5	12.738	1	12.738	133.746	.000	
	3.00	acid	40	ph5	11.600	1	11.600	121.799	.000	
				temperature5 * ph5	13.905	1	13.905	146.001	.000	
				Error	7.524	79	.095			
				Total	164.071	83				
				Corrected Total	51.782	82				
				a. R Squared = .855 (Adjusted R Squared = .849)						

Between-Subjects Factors				Tests of Between-Subjects Effects						
	Value	Label	N	Dependent Variable: data21daydeadvs95daydead						
				Source	Type III Sum of Squares	df	Mean Square	F	Sig.	
temperature6	2.00	15	43	Corrected Model	47.003 ^a	7	6.715	81.641	.000	
	3.00	19	59	Intercept	48.054	1	48.054	584.258	.000	
ph6	2.00	control	53	temperature6	2.125	1	2.125	25.840	.000	
	3.00	acid	49	ph6	1.763	1	1.763	21.438	.000	
experiment length	2.00	alive	19	experiment length	1.444	1	1.444	17.562	.000	
	3.00	dead	83	temperature6 * ph6	3.314	1	3.314	40.295	.000	
				temperature6 * experiment length	2.398	1	2.398	29.158	.000	
				ph6 * experiment length	2.375	1	2.375	28.878	.000	
				temperature6 * ph6 * experiment length	1.744	1	1.744	21.207	.000	
				Error	7.731	94	.082			
				Total	174.985	102				
				Corrected Total	54.734	101				
				a. R Squared = .859 (Adjusted R Squared = .848)						

Figure A6.24b: *Leptocythere lacertosa*: average Mg % data results from the general linear model analysis (Presented in Sections 5.5/5.6).

Average Ca

Between-Subjects Factors				Tests of Between-Subjects Effects					
	Value	Label	N	Dependent Variable: data21dayalive					
				Source	Type III Sum of Squares	df	Mean Square	F	Sig.
temperature2	2.00	15	16	Corrected Model	463.532 ^a	3	154.511	1.875	.163
	3.00	19	10	Intercept	39036.547	1	39036.547	473.814	.000
ph2	2.00	control	10	temperature2	219.296	1	219.296	2.662	.117
	3.00	acid	16	ph2	300.550	1	300.550	3.648	.069
				temperature2 * ph2	10.829	1	10.829	.131	.720
				Error	1812.534	22	82.388		
				Total	96648.051	26			
				Corrected Total	2276.066	25			

a. R Squared = .204 (Adjusted R Squared = .095)

Between-Subjects Factors				Tests of Between-Subjects Effects					
	Value	Label	N	Dependent Variable: data21dayalivesdead					
				Source	Type III Sum of Squares	df	Mean Square	F	Sig.
temperature4	2.00	15	24	Corrected Model	1547.756 ^a	7	221.108	3.831	.003
	3.00	19	23	Intercept	87737.739	1	87737.739	1520.142	.000
ph4	2.00	control	22	temperature4	139.862	1	139.862	2.423	.128
	3.00	acid	25	ph4	19.043	1	19.043	.330	.569
alivesdead1	2.00	alive	26	alivesdead1	248.560	1	248.560	4.307	.045
	3.00	dead	21	temperature4 * ph4	12.216	1	12.216	.212	.648
				temperature4 * alivesdead1	133.549	1	133.549	2.314	.136
				ph4 * alivesdead1	529.466	1	529.466	9.174	.004
				temperature4 * ph4 * alivesdead1	75.537	1	75.537	1.309	.260
				Error	2250.955	39	57.717		
				Total	155785.493	47			
				Corrected Total	3798.711	46			

a. R Squared = .407 (Adjusted R Squared = .301)

Figure A6.25a: *Leptocythere lacertosa*: average Ca % data results from the general linear model analysis (Presented in Sections 5.5/5.6).

Average Ca

Between-Subjects Factors				Tests of Between-Subjects Effects					
	Value	Label	N	Dependent Variable: data21daydead					
				Source	Type III Sum of Squares	df	Mean Square	F	Sig.
temperature3	2.00	15	8	Corrected Model	419.137 ^a	3	139.712	5.417	.008
	3.00	19	13	Intercept	52194.550	1	52194.550	2023.869	.000
ph3	2.00	control	12	temperature3	.048	1	.048	.002	.966
	3.00	acid	9	ph3	230.744	1	230.744	8.947	.008
				temperature3	98.559	1	98.559	3.822	.067
				* ph3					
				Error	438.421	17	25.789		
				Total	59137.442	21			
				Corrected Total	857.558	20			

a. R Squared = .489 (Adjusted R Squared = .399)

Between-Subjects Factors				Tests of Between-Subjects Effects					
	Value	Label	N	Dependent Variable: data95daydead					
				Source	Type III Sum of Squares	df	Mean Square	F	Sig.
temperature5	2.00	15	47	Corrected Model	17.703 ^a	3	5.901	.672	.572
	3.00	19	52	Intercept	245631.356	1	245631.356	27955.879	.000
ph5	2.00	control	56	temperature5	9.476	1	9.476	1.078	.302
	3.00	acid	43	ph5	2.509	1	2.509	.286	.594
				temperature5	5.849	1	5.849	.666	.417
				* ph5					
				Error	834.707	95	8.786		
				Total	254609.465	99			
				Corrected Total	852.411	98			

a. R Squared = .021 (Adjusted R Squared = -.010)

Between-Subjects Factors				Tests of Between-Subjects Effects					
	Value	Label	N	Dependent Variable: data21daydeadvs95daydead					
				Source	Type III Sum of Squares	df	Mean Square	F	Sig.
temperature6	2.00	15	55	Corrected Model	509.819 ^a	7	72.831	6.407	.000
	3.00	19	65	Intercept	169517.968	1	169517.968	14912.877	.000
ph6	2.00	control	68	temperature6	2.143	1	2.143	.189	.665
	3.00	acid	52	ph6	210.318	1	210.318	18.502	.000
experiment length	2.00	alive	21	experiment length	24.494	1	24.494	2.155	.145
	3.00	dead	99	temperature6	100.916	1	100.916	8.878	.004
				* ph6					
				temperature6	1.129	1	1.129	.099	.753
				*experiment length					
				ph6 *	174.297	1	174.297	15.333	.000
				experiment length	64.975	1	64.975	5.716	.018
				* ph6 *					
				experiment length					
				Error	1273.129	112	11.367		
				Total	313746.907	120			
				Corrected Total	1782.948	119			

a. R Squared = .286 (Adjusted R Squared = .241)

Figure A6.25b: *Leptocythere lacertosa*: average Ca %data results from the general linear model analysis (Presented in Sections 5.5/5.6).

Shell preservation

Between-Subjects Factors				Tests of Between-Subjects Effects					
	Value	Label	N	Dependent Variable: data21daysalive					
				Source	Type III Sum of Squares	df	Mean Square	F	Sig.
temperature2	2.00	15	20	Corrected Model	1.888 ^a	3	.629	.791	.509
	3.00	19	13	Intercept	99.742	1	99.742	125.316	.000
ph2	2.00	control	14	temperature2	.041	1	.041	.051	.823
	3.00	acid	19	ph2	.403	1	.403	.506	.482
				temperature2 * ph2	.785	1	.785	.986	.329
				Error	23.082	29	.796		
				Total	153.000	33			
				Corrected Total	24.970	32			

a. R Squared = .076 (Adjusted R Squared = -.020)

Between-Subjects Factors				Tests of Between-Subjects Effects					
	Value	Label	N	Dependent Variable: data21daysalivesdead					
				Source	Type III Sum of Squares	df	Mean Square	F	Sig.
temperature4	2.00	15	32	Corrected Model	12.004 ^a	7	1.715	1.952	.079
	3.00	19	31	Intercept	256.569	1	256.569	292.078	.000
ph4	2.00	control	31	temperature4	.163	1	.163	.186	.668
	3.00	acid	32	ph4	1.081	1	1.081	1.231	.272
alivesvsdead	2.00	alive	33	alivesvsdead	2.246	1	2.246	2.557	.116
	3.00	dead	30	temperature4 * ph4	4.811	1	4.811	5.477	.023
				temperature4 * alivesvsdead	.486	1	.486	.553	.460
				ph4 * alivesvsdead	.014	1	.014	.016	.901
				temperature4 * ph4 * alivesvsdead	.820	1	.820	.934	.338
				Error	48.313	55	.878		
				Total	367.000	63			
				Corrected Total	60.317	62			

a. R Squared = .199 (Adjusted R Squared = .097)

Figure A6.26a: *Leptocythere lacertosa*: shell preservation (rank) data used in the general linear model analysis (Presented in Sections 5.5/5.6).

Shell preservation

Between-Subjects Factors				Tests of Between-Subjects Effects					
	Value	Label	N	Dependent Variable: data21daysdead					
				Source	Type III Sum of Squares	df	Mean Square	F	Sig.
temperature3	2.00	15	12	Corrected Model	6.235 ^a	3	2.078	2.142	.119
	3.00	19	18	Intercept	162.643	1	162.643	167.596	.000
ph3	2.00	control	17	temperature3	.643	1	.643	.663	.423
	3.00	acid	13	ph3	.709	1	.709	.731	.400
				temperature3 * ph3	5.091	1	5.091	5.246	.030
				Error	25.232	26	.970		
				Total	214.000	30			
				Corrected Total	31.467	29			

a. R Squared = .198 (Adjusted R Squared = .106)

Between-Subjects Factors				Tests of Between-Subjects Effects					
	Value	Label	N	Dependent Variable: data95daydead					
				Source	Type III Sum of Squares	df	Mean Square	F	Sig.
temperature5	2.00	15	69	Corrected Model	44.985 ^a	3	14.995	2.282	.083
	3.00	19	56	Intercept	3316.248	1	3316.248	504.646	.000
ph5	2.00	control	71	temperature5	4.809	1	4.809	.732	.394
	3.00	acid	54	ph5	41.067	1	41.067	6.249	.014
				temperature5 * ph5	.795	1	.795	.121	.729
				Error	795.143	121	6.571		
				Total	4189.000	125			
				Corrected Total	840.128	124			

a. R Squared = .054 (Adjusted R Squared = .030)

Between-Subjects Factors				Tests of Between-Subjects Effects					
	Value	Label	N	Dependent Variable: data21daydeadvs95daydead					
				Source	Type III Sum of Squares	df	Mean Square	F	Sig.
temperature6	2.00	15	81	Corrected Model	228.813 ^a	7	32.688	5.857	.000
	3.00	19	74	Intercept	1332.427	1	1332.427	238.753	.000
ph6	2.00	control	88	temperature6	.053	1	.053	.010	.922
	3.00	acid	67	ph6	12.548	1	12.548	2.248	.136
experiment length	2.00	alive	30	experiment length	183.014	1	183.014	32.794	.000
	3.00	dead	125	temperature6 * ph6	2.706	1	2.706	.485	.487
				temperature6 * experiment length	2.805	1	2.805	.503	.479
				ph6 * experiment length	4.101	1	4.101	.735	.393
				temperature6 * ph6 * experiment length	5.855	1	5.855	1.049	.307
				Error	820.374	147	5.581		
				Total	4403.000	155			
				Corrected Total	1049.187	154			

a. R Squared = .218 (Adjusted R Squared = .181)

Figure A6.26b: *Leptocythere lacertosa*: shell preservation (rank) data used in the general linear model analysis (Presented in Sections 5.5/5.6).

Table A6.19: *L. lacertosa*: The table shows the data analysed using Kruskal-Wallis and Mann-Whitney pairwise comparison test for any significant difference in alive Geometric shell size (μm) with the numbers in red highlighting those numbers that show a significant difference (Presented in Sections 5.5/5.6).

Geometric shell size statistics (Alive)				
H (chi ²)	32.25	Hc (tie corrected)	32.25	
P(same)	0.0000170			
field collected	21 day 15°C control alive	21 day 15°C acid alive	21 day 19°C control alive	21 day 19°C acid alive
field collected	0.0000281	0.00018	0.0098	0.0000471
	21 day 15°C control alive	0.05752	0.1611	0.2178
		21 day 15°C acid alive	0.01623	0.4379
			21 day 19°C control alive	0.1508

Mean shell thickness statistics (Alive)				
H (chi ²)	4.172	Hc (tie corrected)	4.172	
P(same)	0.3832			
field collected	21 day 15°C control alive	21 day 15°C acid alive	21 day 19°C control alive	21 day 19°C acid alive
field collected	0.08748	0.8303	0.4533	0.6514
	21 day 15°C control alive	0.2898	0.1637	0.7363
		21 day 15°C acid alive	0.3827	0.8622
			21 day 19°C control alive	0.3329

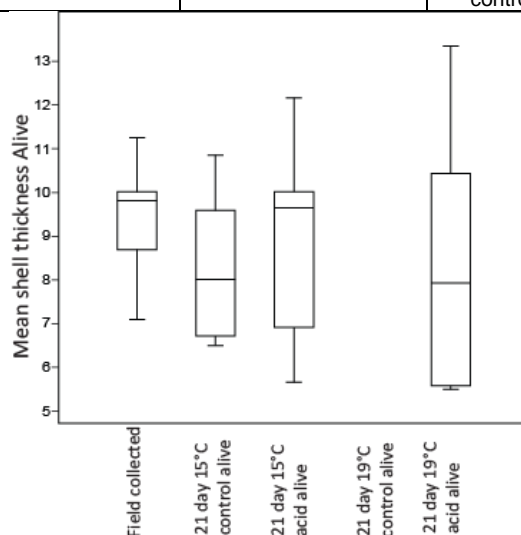


Figure A6.27: *Leptocythere lacertosa*: The table shows the data analysed using Kruskal-Wallis and Mann-Whitney pairwise comparison test for any significant difference in live Mean shell thickness (μm) with the numbers in red highlighting those numbers that show a significant difference. The box plot illustrates the original data showing the minimum, maximum, median and first and third quartile of the data set (Presented in Sections 5.5/5.6).

Table A6.20: *L. lacertosa*: The table shows the data analysed using Kruskal-Wallis and Mann-Whitney pairwise comparison test for any significant difference in average alive level of Mg % with the numbers in red highlighting those numbers that show a significant difference (Presented in Sections 5.5/5.6).

Shell Mg level statistics (Alive)				
H (chi ²)	14.64	Hc (tie corrected)	14.65	
P(same)	0.005479			
field collected	21 day 15°C control alive	21 day 15°C acid alive	21 day 19°C control alive	21 day 19°C acid alive
field collected	0.01628	0.5691	0.2416	0.00925

	21 day 15°C control alive	0.01978	0.5993	0.7238
		21 day 15°C acid alive	0.3827	0.00592
			21 day 19°C control alive	0.4862

Mean shell thickness statistics (Dead)								
H (chi^2)	7.377	Hc (tie corrected)	7.377	P(same)	0.4966			
field collected	21 day 15°C control dead	21 day 15°C acid dead	21 day 19°C control dead	21 day 19°C acid dead	95 day 15°C control dead	95 day 15°C acid dead	95 day 19°C control dead	95 day 19°C acid dead
field collected	0.4555	0.8973	0.5613	0.6481	0.828	0.4389	0.1542	0.8505
	21 day 15°C control dead	0.8597	0.3502	0.7133	0.3141	0.2375	0.08199	0.3936
		21 day 15°C acid dead	0.475	1	0.4963	0.3419	0.1374	0.5743
			21 day 19°C control dead	0.5101	0.5029	0.6906	0.5424	0.839
				21 day 19°C acid dead	0.3755	0.302	0.09503	0.5893
					95 day 15°C control dead	0.4843	0.0864	0.9441
						95 day 15°C acid dead	0.8621	0.5777
							95 day 19°C control dead	0.2081

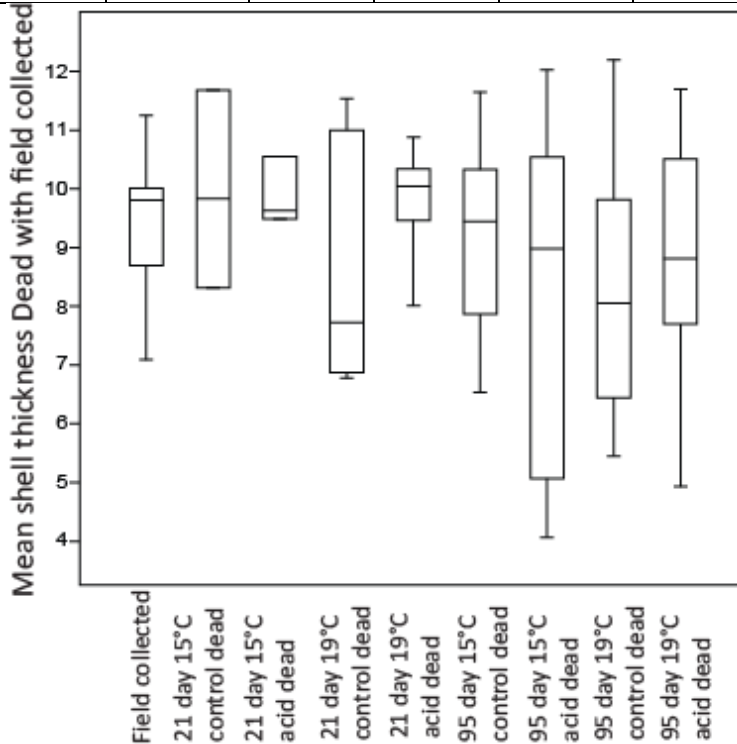


Figure A6.28: *Leptocythere lacertosa*: The table shows the data analysed using Kruskal-Wallis and Mann-Whitney pairwise comparison test for any significant difference in dead Mean shell thickness (μm) with the numbers in red highlighting those numbers that show a significant difference. The box plot illustrates the original data showing the minimum, maximum, median and first and third quartile of the data set (Presented in Sections 5.5/5.6).

Shell Ca level statistics (Alive)				
H (chi ²)	7.429		Hc (tie corrected) 7.429	
P(same)	0.1149			
field collected	21 day 15°C control alive	21 day 15°C acid alive	21 day 19°C control alive	21 day 19°C acid alive
field collected	0.05183	0.9431	0.2113	0.08748
	21 day 15°C control alive	0.2898	0.1637	0.6588
		21 day 15°C acid alive	0.1904	0.2443
			21 day 19°C control alive	0.1637

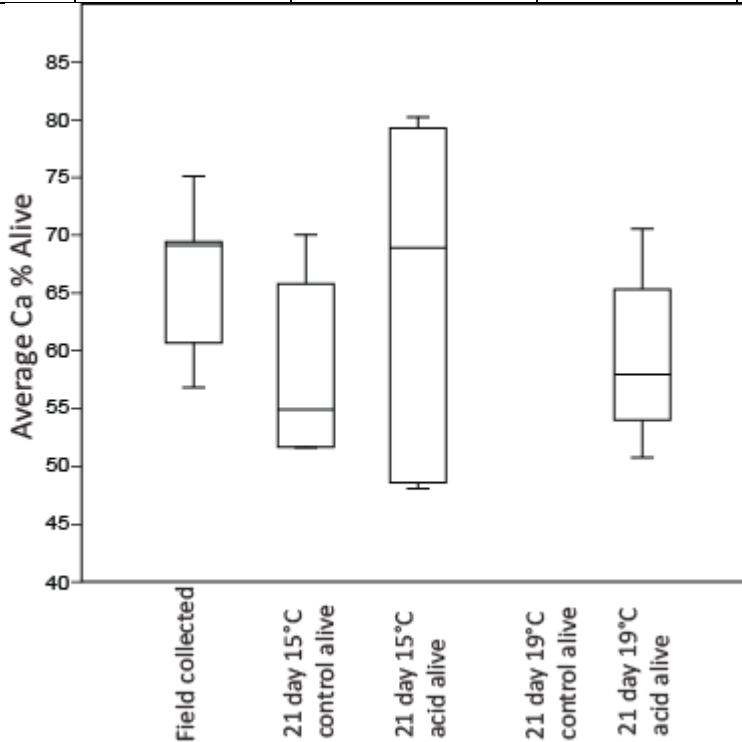


Figure A6.29: *Leptocythere lacertosa*: The table shows the data analysed using Kruskal-Wallis and Mann-Whitney pairwise comparison test for any significant difference in average alive level of Ca % with the numbers in red highlighting those numbers that show a significant difference. The box plot illustrates the original data showing the minimum, maximum, median and first and third quartile of the data set (Presented in Sections 5.5/5.6).

Table A6.21: *L. lacertosa*: The table shows the data analysed using Kruskal-Wallis and Mann-Whitney pairwise comparison test for any significant difference in alive shell preservation (rank) with the numbers in red highlighting those numbers that show a significant difference (Presented in Sections 5.5/5.6).

Shell preservation statistics (Alive)				
H (chi ²)	15.44		Hc (tie corrected) 18.7	
P(same)	0.000899			
field collected	21 day 15°C control alive	21 day 15°C acid alive	21 day 19°C control alive	21 day 19°C acid alive
field collected	0.00234	0.00017	0.000094	0.00037
	21 day 15°C control alive	0.2588	0.4944	0.5953
		21 day 15°C acid alive	0.8359	0.5111
			21 day 19°C control alive	0.8458

Table A6.22: *L. lacertosa*: The table shows the data analysed using Kruskal-Wallis and Mann-Whitney pairwise comparison test for any significant difference in dead shell preservation (rank) with the numbers in red highlighting those numbers that show a significant difference (Presented in Sections 5.5/5.6).

Shell preservation statistics (Dead)								
H (chi ²)	76.27	Hc (tie corrected)	78.17	P(same)	1.14×10^{-13}			
field collected	21 day 15°C control dead	21 day 15°C acid dead	21 day 19°C control dead	21 day 19°C acid dead	95 day 15°C control dead	95 day 15°C acid dead	95 day 19°C control dead	95 day 19°C acid dead
field collected	0.0010 77	0.000022	0.00000 32	0.000013	0.0000000 138	0.0000000 916	0.00000005 12	0.0000001
	21 day 15°C control dead	0.06959	0.02048	0.06582	0.002493	0.000197	0.000186	0.00012
		21 day 15°C acid dead	0.8651	0.662	0.1412	0.006492	0.02867	0.00129
			21 day 19°C control dead	0.4032	0.09308	0.000366	0.004062	0.000034
			21 day 19°C acid dead		0.04239	0.000272	0.000863	0.000045
					95 day 15°C control dead	0.05117	0.6305	0.0593
					95 day 15°C acid dead		0.02334	0.8672
							95 day 19°C control dead	0.00388

Table A6.23: *L. lacertosa*: The table shows the data analysed using Kruskal-Wallis and Mann-Whitney pairwise comparison test for any significant difference in dead Geometric shell size (µm) with the numbers in red highlighting those numbers that show a significant difference (Presented in Sections 5.5/5.6).

Geometric shell size statistics (Dead)								
H (chi ²)	47.11	Hc (tie corrected)	47.11	P(same)	0.000000146			
field collected	21 day 15°C control dead	21 day 15°C acid dead	21 day 19°C control dead	21 day 19°C acid dead	95 day 15°C control dead	95 day 15°C acid dead	95 day 19°C control dead	95 day 19°C acid dead
field collected	0.00062	0.00062	0.00002 81	0.0003	0.00000 0124	0.000002 62	0.0000010 6	0.00000051 4
	21 day 15°C control dead	0.298	0.3397	0.284	0.8198	0.1691	0.6575	0.5996
		21 day 15°C acid dead	0.9599	0.6171	0.1662	0.04827	0.1546	0.1273
			21 day 19°C control dead	0.8563	0.06228	0.004862	0.08219	0.03935
			21 day 19°C acid dead		0.1399	0.03216	0.233	0.1325
					95 day 15°C	0.1178	0.935	0.9657

Geometric shell size statistics (Dead)								
H (chi^2)	47.11	Hc (tie corrected)	47.11	P(same)	0.000000146			
field collected	21 day 15°C control dead	21 day 15°C acid dead	21 day 19°C control dead	21 day 19°C acid dead	95 day 15°C control dead	95 day 15°C acid dead	95 day 19°C control dead	95 day 19°C acid dead
					control dead			
						95 day 15°C acid dead	0.1585	0.1352
							95 day 19°C control dead	0.8403

Table A6.24: *L. lacertosa*: The table shows the data analysed using Kruskal-Wallis and Mann-Whitney pairwise comparison test for any significant difference in average dead level of Mg % with the numbers in red highlighting those numbers that show a significant difference (Presented in Sections 5.5/5.6).

Shell Mg level statistics (Dead)								
H (chi^2)	67.2	Hc (tie corrected)	67.25	P(same)	1.73 x 10⁻¹¹			
field collected	21 day 15°C control dead	21 day 15°C acid dead	21 day 19°C control dead	21 day 19°C acid dead	95 day 15°C control dead	95 day 15°C acid dead	95 day 19°C control dead	95 day 19°C acid dead
field collected	0.03689	0.2187	0.06136	0.01193	0.01438	0.2383	0.05664	0.00056
	21 day 15°C control dead	0.1116	0.3619	0.7642	0.1146	0.0439	0.06534	0.00598
		21 day 15°C acid dead	0.6366	0.1099	0.6819	0.2499	0.7487	0.00174
			21 day 19°C control dead	0.2548	0.8523	0.2899	0.444	0.0000730
			21 day 19°C acid dead	0.2141	0.01618	0.04869		0.00056
					95 day 15°C control dead	0.04124	0.2331	0.0000000742
						95 day 15°C acid dead	0.188	0.000000174
							95 day 19°C control dead	0.0000000480

Table A6.25: *L. lacertosa*: The table shows the data analysed using Kruskal-Wallis and Mann-Whitney pairwise comparison test for any significant difference in average dead level of Ca % with the numbers in red highlighting those numbers that show a significant difference (Presented in Sections 5.5/5.6).

Shell Ca level statistics (Dead)								
H (chi ²)	37.76	Hc (tie corrected)	37.76	P(same)	0.00000834			
field collected	21 day 15°C control dead	21 day 15°C acid dead	21 day 19°C control dead	21 day 19°C acid dead	95 day 15°C control dead	95 day 15°C acid dead	95 day 19°C control dead	95 day 19°C acid dead
field collected	0.01421	0.01421	0.03316	0.00811	0.000153	0.000596	0.000172	0.00024
	21 day 15°C control dead	0.4705	0.2696	0.01996	0.0925	0.2505	0.08213	0.03981
		21 day 15°C acid dead	0.1488	0.1779	0.7827	0.966	0.8366	0.3427
			21 day 19°C control dead	0.01041	0.01276	0.0282	0.01128	0.00764
			21 day 19°C acid dead		0.000664	0.01888	0.001545	0.00639
					95 day 15°C control dead	0.7099	0.9021	0.1247
						95 day 15°C acid dead	0.8439	0.1878
							95 day 19°C control dead	0.1239

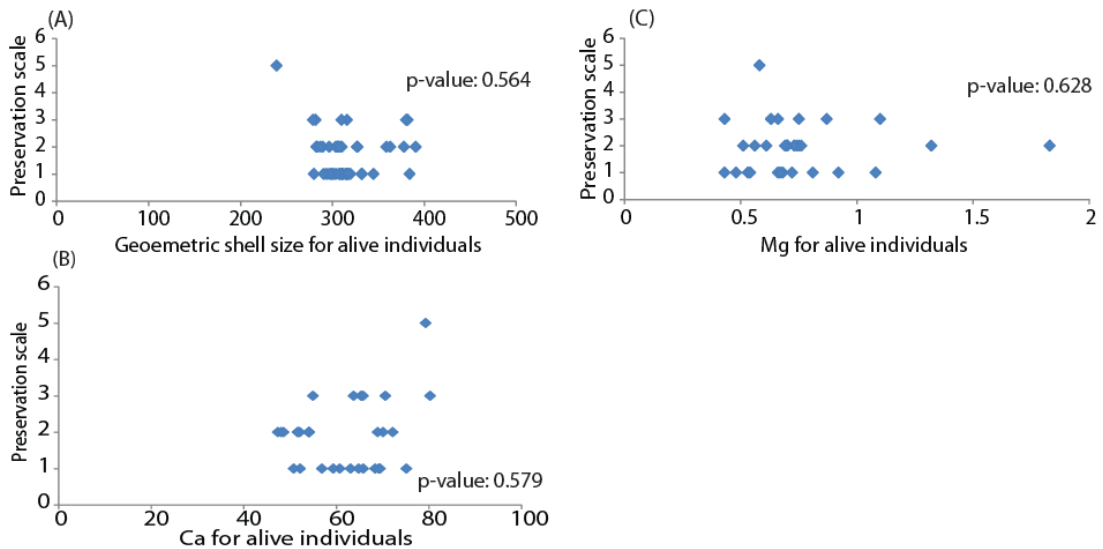


Figure A6.30: *L. lacertosa*: Linear regression models and Spearman's rank results (p-values) from comparing all the different data sets (Geometric shell size (μm), Mean shell thickness (μm), Average Mg and Ca %) against the relevant preservation rank to determine if there are any correlations and trends between the different data sets and preservation. Trend lines on the linear regression models indicate that the data shows a significant correlation (Presented in Section 5.7).

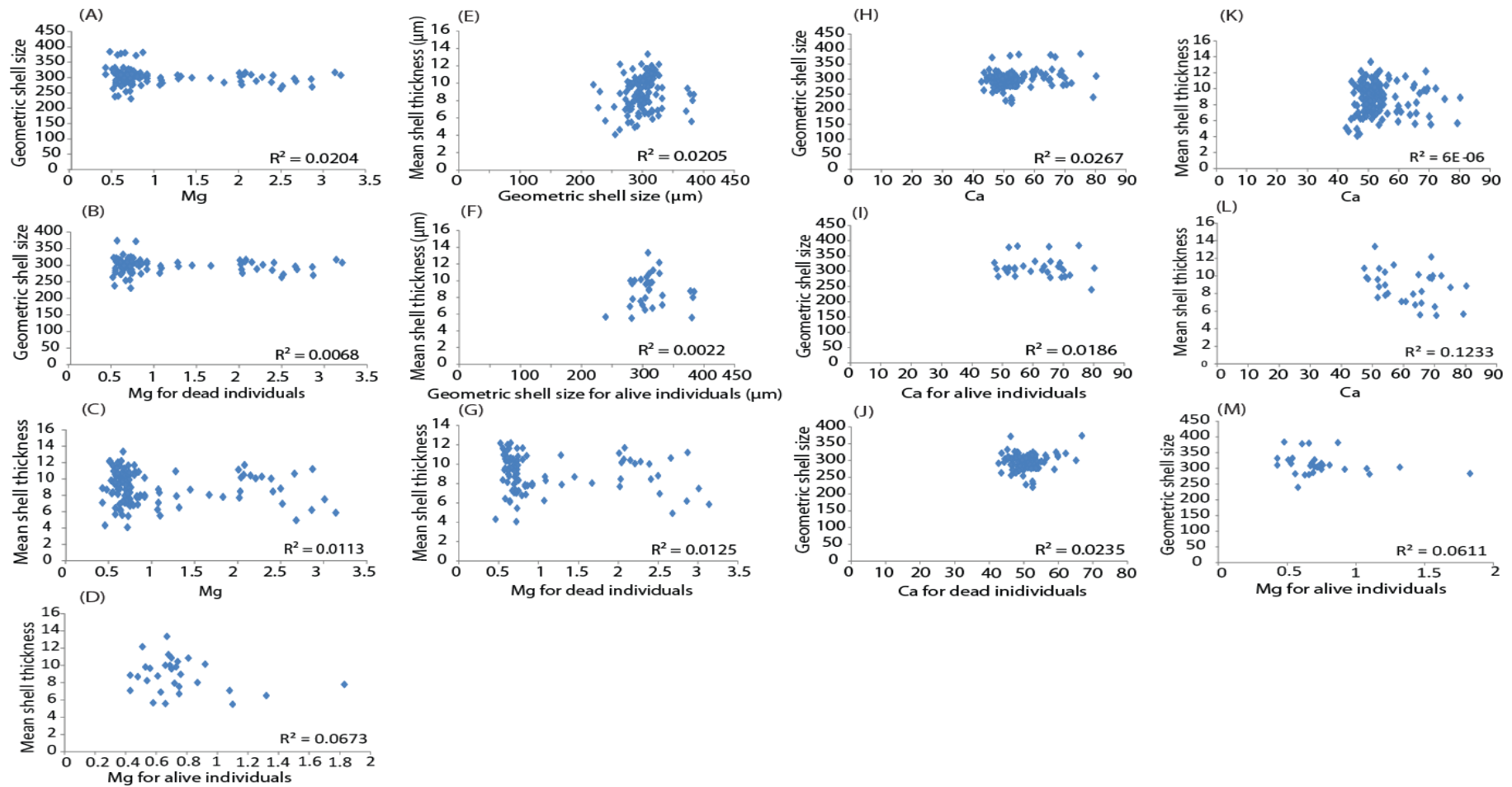


Figure A6.31: *L. lacertosa*: Linear regression models comparing all the data against each other to determine if there are any correlations and trends between the different data sets (Geometric shell size (µm), Mean shell thickness (µm), Average Mg and Ca %). Trend lines on the linear regression models indicate that the data shows a significant correlation (Presented in Section 5.7).

Table A6.26: *L. lacertosa* results from the statistical analysis when determining any correlations between the different data sets (Presented in Section 5.7).

L. lacertosa		
Correlation question	Number of individuals	R ² value
Preservation against geometric shell size for both experiments	191	0.1042
Preservation against geometric shell size for alive individuals	47	0.0093
Preservation against geometric shell size for dead individuals	144	0.0716
Preservation against shell thickness for both experiments	141	0.1006
Preservation against shell thickness for alive individuals	31	0.2824
Preservation against shell thickness for dead individuals	110	0.1247
Preservation against average Mg for both experiments	133	0.2455
Preservation against average Mg for alive individuals	30	0.0004
Preservation against average Mg for dead individuals	103	0.2377
Preservation against average Ca for both experiments	152	0.099
Preservation against average Ca for alive individuals	31	0.0636
Preservation against average Ca for dead individuals	121	0.0288
Correlation question	Number of individuals	R ² value
Geometric shell size against shell thickness for both experiments	134	0.0205
Geometric shell size against shell thickness for alive individuals	31	0.0022
Geometric shell size against shell thickness for dead individuals	103	0.0434
Geometric shell size against average Mg for both experiments	125	0.0204
Geometric shell size against average Mg for alive individuals	30	0.0611
Geometric shell size against average Mg for dead individuals	95	0.0068
Shell thickness against average Mg for both experiments	122	0.0113
Shell thickness against average Mg for alive individuals	30	0.0673
Shell thickness against average Mg for dead individuals	92	0.0125
Geometric shell size against average Ca for both experiments	144	0.0267
Geometric shell size against average Ca for alive individuals	31	0.0186
Geometric shell size against average Ca for dead individuals	113	0.0235
Shell thickness against average Ca for both experiments	141	0.00006
Shell thickness against average Ca for alive individuals	31	0.1233
Shell thickness against average Ca for dead individuals	110	0.0624

References

- Aberhan, M., Weidemeyer, S., Kiessling, W., Scasso, R.A. and Medina, F.A. 2007. Faunal evidence for reduced productivity and uncoordinated recovery in Southern Hemisphere Cretaceous–Paleogene boundary sections. *Geology*, **35**, 227–230.
- Abramovich, S. and Keller, G. 2003. Planktonic foraminiferal response to the latest Maastrichtian abrupt warm event: a case study from South Atlantic DSDP Site 525A. *Marine Micropaleontology*, **48**, 225–249.
- Ager, D.V. and Smith, W.E. 1973. The Coast of South Devon and Dorset. *In*: Capewell, J.G. (2nd ed.) Geologist's Association Guides No. 23 between Branscombe and Burton Bradstock. *The Geologist's Association, Benham and Company Ltd, Colchester*.
- Al-Aasm, I. 2003. Origin and characterization of hydrothermal dolomite in the Western Canada Sedimentary Basin. *Journal of Geochemical Exploration*, **78–79**, 9–15.
- Al-Aasm, I., Lonnee, J. and Clarke, J. 2000. Multiple fluid flow events and the formation of saddle dolomite: examples from Middle Devonian carbonates of the Western Canada Sedimentary Basin. *Journal of Geochemical Exploration*, **69–70**, 11–15.
- Allen, P.A. and Allen, R.A. 2005. *Basin Analysis: Principles and Applications*. Blackwell Publishing, Oxford, 549pp.
- Alroy, J., 2010. The Shifting Balance of Diversity Among Major Marine Animal Groups. *Science*, **329**, 1191–1194.
- Alroy, J., Aberhan, M., Bottjer, D.J., Foote, M., Fürsich, F.T., Harries, P.J., Hendy, A.J.W., Holland, S.M., Ivany, L.C., Kiessling, W., Kosnik, M.A., Marshall, C.R., McGowan, A.J., Miller, A.I., Olszewski, T.D., Patzkowsky, M.E., Peters, S.E., Villier, L., Wagner, P.J., Bonuso, N., Borkow, P.S., Brenneis, B., Clapham, M.E., Fall, L.M., Ferguson, C.A., Hanson, V.L., Krug, A.Z., Layou, K.M., Leckey, E.H., Nürnberg, S., Powers, C.M., Sessa, J.A., Simpson, C., Tomašových, A. and Visaggi, C.C. 2008. Phanerozoic trends in the global diversity of marine invertebrates. *Science*, **321**, 97–100.
- Andersson, A.J., Mackenzie, F.T. and Gattuso, J.P. 2011. Effects of Ocean Acidification on Benthic Processes, Organisms, and Ecosystems. *In*: Gattuso, J.-P., Hansson, L. (eds), *Ocean Acidification*, Oxford University Press, Oxford, 122–153.
- Anderson, T.F. and Arthur, M.A. 1983. Stable isotopes of oxygen and carbon and their application to sedimentologic and paleoenvironmental problems. *In*:

Arthur, M.A. (ed.), *Stable isotopes in sedimentary geology: SEPM Short Course*, **10**, 1–151.

Anestis, A., Lazou, A., Pörtner, H.O. and Michaelidis, B. 2007. Behavioral, Metabolic, and molecular stress responses of marine bivalve *Mytilus galloprovincialis* during long-term acclimation at increasing ambient temperature. *American Journal of Physiology-Regulatory, Integrative and Comparative Physiology*, **293**, 911–921.

Anestis, A., Pörtner, H.O., Lazou, A. and Michaelidis, B. 2008. Metabolic and molecular stress responses of sublittoral bearded horse mussel *Modiolus barbatus* to warming sea water: implications for vertical zonation. *The Journal of Experimental Biology*, **211**, 2889–2898.

Armstrong, H. A. and Brasier, M. D. 2005. *Microfossils* (2nd ed.). Blackwell Publishing, Oxford, 296pp.

Arnold, K.E., Findlay, H.S., Spicer, J.I., Daniels, C.L. and Boothroyd, D. 2009. Effects of CO₂-related acidification on aspects of the larval development of the European lobster, *Homarus gammarus* (L.). *Biogeosciences*, **6**, 174–754.

Athersuch, J., Horne, D.J. and Whittaker, J.E. 1989. Marine and brackish water ostracods (Superfamilies Cypridacea and Cytheracea): keys and notes for the identification of the species. *In: Kermack, D.M., Barnes, R.S.K. (Eds.), Synopses of the British Fauna, New Series*. The Linnean Society of London and the Estuarine and Brackish-water Sciences Association, Avon, **43**, 1–345.

Bamber, R.N. 1990. The effects of acidic seawater on three species of lamellibranch mollusc. *Journal of Experimental Marine Biology and Ecology*, **143**, 181–191.

Bartolini, A., Guex, J., Spangenberg, J.E., Schoene, B., Taylor, D.G., Schaltegger, U. and Atudorei, V. 2012. Disentangling the Hettangian carbon isotope record: implications for the aftermath of the end-Triassic mass extinction. *Geochemistry, Geophysics, Geosystems*, **13**, 1–11.

Barras, C.G. and Twitchett, R.J. 2007. Response of the marine infauna to Triassic-Jurassic environmental change: Ichnological data from southern England. *Palaeogeography, Palaeoclimatology, Palaeoecology*, **244**, 223–241.

Barry, J., Seibel, B. A., Drazen, J., Tamburri, M., Lovera, C. and Brewer, P. 2002. Field experiments on direct ocean CO₂ sequestration: the response of deep-sea faunal assemblages to CO₂ injection at 3200 m off central California. *EOS Transactions of the American Geophysical Union*, **83**, OS51F-02.

- Beesley, A., Lowe, D.M., Pascoe, C.K. and Widdicombe, S. 2008. Effects of CO₂-induced seawater acidification on the health of *Mytilus edulis*. *Climate Research*, **37**, 215–225.
- Beerling, D.J. and Berner, R.A. 2002. Biogeochemical constraints on the Triassic-Jurassic boundary carbon cycle event. *Global Biogeochemical Cycles*, **16** (3), 1–13.
- Beerling, D.J. and Royer, D.L. 2002. Reading a CO₂ signal from fossil stomata. *New Phytologist*, **153**, 387–397.
- Beerling, D. J., Lomas, M. R. and Grocke, D. R. 2002. On the nature of methane gas dissociation during the Toarcian and Aptian oceanic anoxic events. *American Journal of Science*, **302**, 28–49.
- Bednaršek, N., Tarling, G.A., Bakker, D.C.E., Fielding, S., Cohen, A., Kuzirian, A., McCorkles, D., Leze, B. and Montagna, R. 2012. Description and quantification of pteropod shell dissolution: a sensitive bioindicator of ocean acidification. *Global Change Biology*, **18**, 2378–2388.
- Belcher, C. M., Mander, L., Rein, G., Jervis, F. X., Haworth, M., Hesselbo, S. P., Glasspool, I. J. and McElwain, J. C. 2010. Increased fire activity at the Triassic/Jurassic boundary in Greenland due to climate-driven floral change. *Nature Geoscience*, **3** (6), 426–429.
- Bennett, C.E., Williams, M., Leng, M.J., Siveter, D.J., Davies, S.J., Sloane, H.J. and Wilkinson, I.P. 2011. Diagenesis of fossil ostracods: Implications for stable isotope based palaeoenvironmental reconstruction. *Palaeogeography, Palaeoclimatology, Palaeoecology*, **305**, 150–161.
- Benton, M.J. 1999. The history of life: large databases in palaeontology. *In*: D. A. T. Harper (ed.), *Numerical Palaeobiology*, Wiley, Chichester, 249–283.
- Berner, R.A. 1994. GEOCARB II: A revised model of atmospheric CO₂ over Phanerozoic time. *American Journal of Science*, **294**, 56–91.
- Berner, R.A. & Beerling, D.J. 2007. Volcanic degassing necessary to produce a CaCO₃ undersaturated ocean at the Triassic–Jurassic boundary. *Palaeogeography, Palaeoclimatology, Palaeoecology*, **244** (1-4), 368–373.
- Berner, R. A. & Kothavala, Z. 2001. GEOCARB III: A revised model of atmospheric CO₂ over Phanerozoic time. *American Journal of Science*, **301**, 182–204.
- Bernasconi, S.M., Črne, A.E., Méhay, S., Keller, C.E., Hochuli, P., Erba, E. and Weissert, H. 2009. CO₂ pulses and carbonate and biotic crises in the Mesozoic. *Geochimica et Cosmochimica Acta, Supplement*, **73**, A113.

- Berge, J.A., Bjerkeng, B., Pettersen, O., Schaanning, M.T. and Øxnevad, S. 2006. Effects of increased seawater concentrations of CO₂ on growth of the bivalve *Mytilus edulis* L. *Chemosphere*, **62**, 681–687.
- Bibby, R., Cleall-Harding, P., Rundle, S., Widdicombe, S. and Spicer, J.I. 2007. Ocean acidification disrupts induced defences in the intertidal gastropod *Littorina littorea*. *Biology Letters*, **3**, 699–701.
- Bibby, R., Widdicombe, S., Parry, H., Spicer, J. and Pipe, R. 2008. Effects of ocean acidification on the immune response of the blue mussel *Mytilus edulis*. *Aquatic Biology*, **2**, 67–74.
- Bijma, J., Spero, H. J. and Lea, D. W. 1999. Reassessing foraminiferal stable isotope geochemistry: impact of the oceanic carbonate systems (experimental results). In: Fisher, G. and Wefer, G. (eds), *Use of Proxies in Paleoceanography: Examples from the South Atlantic*, Springer-Verlag, New York, 489–512.
- Bijma, J., Honisch, B. and Zeebe, R. E. 2002. Impact of the ocean carbonate chemistry on living foraminiferal shell weight: comment on Carbonate ion concentration in glacial-age deep waters of the Caribbean Sea by W. S. Broecker and E. Clark. *Geochemistry, Geophysics, Geosystems*, **3** (11), 1064. doi:10.1029/2002GC000388.
- Blakey, R. 2010. NAU Geology, for educational, non-profit, non-commercial purposes.
- Bloos, G. 1990. Sea level changes in the Upper Keuper and in the Lower Lias of Central Europe. *Cahiers de l'Institut Catholique, Lyon, Serie Scientifique*, **3**, 5–16.
- Bloos, G. and Page, K.N. 2000. The basal Jurassic Ammonite Succession in the North-West European province – Review and new results. *GeoResearch Forum*, **6**, 27–40.
- Boomer, I. and Ainsworth, N.R. 2009. Lower Jurassic (Hettangian–Toarcian) In: Whittaker, J.E. and Hart, M.B. (eds), *Ostracods in British Stratigraphy*, The Micropalaeontological Society, Special Publications, London, 175–197.
- Bonis, N.R. 2010. *Palaeoenvironmental changes and vegetation history during the Triassic–Jurassic transition*. PhD thesis, Universiteit Utrecht.
- Bonis, N.R., Kurschner, W.M. and Krystyn, L. 2009. A detailed palynological study of the Triassic-Jurassic transition in key sections of the Eiberg Basin (Northern Calcareous Alps, Austria). *Review of Palaeobotany and Palynology*, **156**, 376–400.

- Bonis, N.R., Ruhl, M. and Kurschner, W.M. 2010a. Climate change driven black shale deposition during the end-Triassic in the western Tethys. *Palaeogeography, Palaeoclimatology, Palaeoecology*, **290**, 151–159.
- Bonis, N.R., Ruhl, M. and Kürschner, W.M. 2010b. Milankovitch-scale palynological turnover across the Triassic–Jurassic transition at St. Audrie's Bay, SW UK. *Journal of the Geological Society, London*, **167**, 877–888.
- Bralower, T.J., 2002. Evidence of surface water oligotrophy during the PETM: nanofossil assemblage data from Ocean Drilling Program Site 690, Maud Rise, Weddell Sea. *Paleoceanography*, **17** (2), 13-1–13-12.
- Brand, U. 1989. Biogeochemistry of late Paleozoic North American brachiopods and secular variation of seawater composition. *Biogeochemistry*, **7**, 159–193.
- Brand, U., Logan, A., Hiller, N. and Richardson, J. 2003. Geochemistry of modern brachiopods: applications and implications for oceanography and paleoceanography. *Chemical Geology*, **198**, 305–334.
- Brand, U. and Veizer, J. 1980. Chemical diagenesis of a multicomponent carbonate system — I: trace elements. *Journal of Sediment Petrology*, **50**, 1219–1236.
- Breecker, D. O., Sharp, Z. D. and McFadden, L. D. 2010. Atmospheric CO₂ concentrations during ancient greenhouse climates were similar to those predicted for A. D. 2100. *Proceeding of National Academy of Sciences, USA*, **107**, 576–580.
- Bullen, S.B. and Sibley, D.F. 1984. Dolomite selectivity and mimic replacement. *Geology*, **12**, 655–658.
- Carter, J.G., Barrera, E. and Tevesz, M.J.S. 1998. Thermal potentiation and mineralogical evolution in the Bivalvia (Mollusca). *Journal of Paleontology*, **72** (6), 991–1010.
- Chivas, A.R., De Deckker, P. and Shelley, J.M.G. 1983. Magnesium, strontium, and barium partitioning in nonmarine ostracod shells and their use in paleoenvironmental reconstructions—a preliminary study. *In: Maddocks, R.F. (ed.), Applications of Ostracoda*, University of Houston Geoscience, Houston, 238–249.
- Clapham, M.E. and Payne, J.L. 2011. Acidification, anoxia, and extinction: A multiple logistic regression analysis of extinction selectivity during the Middle and Late Permian. *Geology*, **39** (11), 1059–1062.
- Clémence, M.-E., Bartolini, A., Gardin, S., Paris, G., Beaumont, V. and Page, K.N. 2010. Early Hettangian benthic–planktonic coupling at Doniford (SW

England) Palaeoenvironmental implications for the aftermath of the end-Triassic crisis. *Palaeogeography, Palaeoclimatology, Palaeoecology*, **295**, 102–115.

Clémence, M.E. and Hart, M.B. 2013. Proliferation of Oberhauserellidae during the recovery following the late Triassic Extinction: paleoecological implications. *Journal of Paleontology*, **87** (6), 1004–1015.

Cohen, A.S. and Coe, A.L. 2002. New geochemical evidence for the onset of volcanism in the Central Atlantic magmatic province and environmental change at the Triassic-Jurassic boundary. *Geology*, **30**, 267–270.

Črne, A.E., Weissert, H., Goričan, Š. and Bernasconi, S.M. 2011. A biocalcification crisis at the Triassic-Jurassic boundary recorded in the Budva Basin (Dinarides, Montenegro). *Geological Society of America, Bulletin*, **123** (1/2), 40–50.

Cusack, M., Parkinson, D., Freer, A., Perez-Huerta, A., Fallick, A.E. and Curry, G.B. 2008. Oxygen isotope composition in *Modiolus modiolus* aragonite in the context of biological and crystallographic control. *Mineralogical Magazine*, **72** (2), 569–577.

Dahl, T. W., Hammarlund, E.U., Anbar, A.D., Bond, D.P.G., Gill, B.C., Gordon, G.W., Knoll, A.H., Nielsen, A.T., Schovsbo, N.H. and Canfield, D.E. 2010. Devonian rise in atmospheric oxygen correlated to the radiations of terrestrial plants and large predatory fish. *Proceedings of the National Academy of Sciences, USA*, **107** (42), 17911–17915.

Decrouy, L., Vennemann, T. W. and Ariztegui, D. 2011. Controls on ostracod valve geochemistry, Part 1: Variations of environmental parameters in ostracod (micro-) habitats. *Geochimica et Cosmochimica Acta*, **75**, 7364–7379.

Decrouy, L., Vennemann, T. W. and Ariztegui, D. 2011. Controls on ostracod valve geochemistry: Part 2. Carbon and oxygen isotope compositions. *Geochimica et Cosmochimica Acta*, **75**, 7380–7399.

Deenen, M.H.L., Ruhl, M., Bonis, N.R., Krijgsman, W., Kuerschner, W.M., Reitsma, M. and van Bergen, M.J. 2010. A new chronology for the end-Triassic mass extinction. *Earth and Planetary Science Letters*, **291** (1–4), 113–125.

De Deckker, P., Chivas, A.R. and Shelley, J.M.G. 1999. The uptake of magnesium and strontium in the euryhaline ostracod *Cyprideis* determined from in vitro experiments. *Palaeogeography, Palaeoclimatology, Palaeoecology*, **148** (1–3), 105–116.

- Demaison, G.J. and Moore, G.T. 1980. Anoxic environments and oil source bed genesis. *Bulletin American Association of Petroleum Geologists*, **64**, 1178–1209.
- Dickens, G.R., O’Neil, J.R., Rea, D.K. and Owen, R.M. 1995. Dissociation of oceanic methane hydrate as a cause of the carbon isotope excursion at the end of the Paleocene. *Paleoceanography*, **10**, 965–971.
- Doney, S.C., Balch, W.M., Fabry, V.J. and Feely, R.A. 2009. Ocean Acidification: A critical emerging problem for the ocean sciences. *Oceanography*, **22** (4), 16–25.
- Douvillé, H., 1904. Paléontologie mollusques fossiles *In: J. de Morgan, Mission scientifique en Perse, Vol. 3, Pt 4, E. Leroux, Paris, 191–380.*
- Drexler, E., 1958. Foraminiferen und Ostracoden aus dem Lias von Siebeldingen Pfalz. *Geologisches Jahrbuch*, **75**, 475–554.
- Dupont, S. and Thorndyke, M. 2008. Ocean acidification and its impact on the early life-history stages of marine animals. *In: Briand F, (ed.), Impacts of Acidification on Biological, Chemical and Physical Systems in the Mediterranean and Black Seas. CIESM Workshop Monograph 36, Monaco.*
- Edel, J.B. and Düringer, P.H. 1997. The apparent polar wander path of the European plate in Upper Triassic–Lower Jurassic times and the Liassic intraplate fracturing of Pangea: new palaeomagnetic constraints from NE France and SW Germany. *Geophysical Journal International*, **128**, 331–344.
- Fabry, V.J., Seibel, B.A., Feely, R.A. and Orr, J.C. 2008. Impacts of ocean acidification on marine fauna and ecosystem processes. *ICES Journal of Marine Science: Journal du Conseil*, **65** (3), 414–432.
- Feely, R.A., Sabine, C.L., Lee, K., Berelson, W., Kleypas, J., Fabry, V.J. and Millero, F.J. 2004. Impact of anthropogenic CO₂ on the CaCO₃ system in the oceans. *Science*, **305**, 362–366.
- Findlay, H.S., Kendall, M.A., Spicer, J.I., Turley, C. and Widdicombe, S. 2008. Novel microcosm system for investigating the effects of elevated carbon dioxide and temperature on intertidal organisms. *Aquatic Biology*, **3**, 51–62.
- Findlay, H.S., Wood, H.L., Kendall, M.A., Spicer, J.I., Twitchett, R.J. and Widdicombe, S. 2009. Calcification, a physiological process to be considered in the context of the whole organism. *Biogeosciences Discussions*, **6**, 2267–2284.
- Findlay, H.S., Wood, H.L., Kendall, M.A., Spicer, J.I., Twitchett, R.J. and Widdicombe, S. 2011. Comparing the impact of high CO₂ on calcium

- carbonate structures in different marine organisms. *Marine Biology Research*, **7** (6), 565–575.
- Fine, M. & Tchernov, D. 2007. Scleractinian coral species survive and recover from decalcification. *Science*, **315**, 1811.
- Finkel, Z.V., Katz, M.E., Wright, J.D., Schofield, O.M.E & Falkowski, P.G. 2005. Climatically driven macroevolutionary patterns in the size of marine diatoms over the Cenozoic. *Proceedings of the National Academy of Sciences, USA*, **102** (25), 8927–8932.
- Fletcher, B. J., Brentnall, S. J., Anderson, C. W., Berner, R. A. & Beerling, D. J. 2008. Atmospheric carbon dioxide linked with Mesozoic and early Cenozoic climate change. *Nature Geoscience*, **1**, 43–48.
- Flügel, E. and Munnecke, A. 2010. *Microfacies of carbonate rocks: analysis, interpretation and application* (2nd Edition). Springer, Berlin, 984pp.
- Fowell, S.J., Cornet, B. and Olsen, P.E. 1994. Geologically rapid Late Triassic extinctions: palynological evidence from the Newark Supergroup. In: Klein, G.D. (ed.), *Pangea: Paleoclimate, Tectonics and Sedimentation During Accretion, Zenith, and Breakup of a Supercontinent*, Geological Society of America, *Special Paper*, **332**, 49–57.
- Fraiser, M.L., Twitchett, R.J. and Bottjer, D.J. 2005. Unique microgastropod biofacies in the Early Triassic: Indicator of long-term biotic stress and the pattern of biotic recovery after the end-Permian mass extinction. *Comptes Rendus Palevol*, **4** (6–7), 543–552.
- Feely, R.A., Sabine, C.L., Lee, K., Berelson, W., Kleypas, J., Fabry, V.J. and Millero, F.J. 2004. Impact of anthropogenic CO₂ on the CaCO₃ system in the oceans. *Science*, **305**, 362–366.
- Freitas, P.S., Clarke, L.J., Kennedy, H., Richardson, C.A. and Abrantes, F. 2006. Environmental and biological controls on elemental (Mg/Ca, Sr/Ca and Mn/Ca) ratios in shells of the king scallop *Pecten maximus*. *Geochimica et Cosmochimica Acta*, **70**, 5119–5133.
- Frenzel, P. and Boomer, I. 2005. The use of ostracods from marginal marine, brackish waters as bio indicators of modern and Quaternary environmental change *Palaeogeography, Palaeoclimatology, Palaeoecology*, **225**, 68–92.
- Gallet, Y., Krystyn, L., Marcoux, J. and Besse, J. 2007. New constraints on the End-Triassic (Upper Norian-Rhaetian) magnetostratigraphy. *Earth and Planetary Science Letters*, **255** (3–4), 458–470.
- Galli, M.T., Jadoul, F., Bernasconi, S.M. and Weissert, H. 2005. Anomalies in global carbon cycling at the Triassic/Jurassic boundary: evidence from a

marine C-isotope record. *Palaeogeography, Palaeoclimatology, Palaeoecology*, **216**, 203–214.

Galli, M.T., Jadoul, F., Bernasconi, S.M., Cirilli, S. and Weissert, H. 2007. Stratigraphy and palaeoenvironmental analysis of the Triassic–Jurassic transition in the western Southern Alps. *Palaeogeography, Palaeoclimatology, Palaeoecology*, **244**, 52–70.

Gallois, R.W. 2007. The stratigraphy of the Penarth Group (Later Triassic) of the East Devon coast. *Proceedings of the Ussher Society*, **11**, 287–297.

Gallois, R.W. 2009. The lithostratigraphy of the Penarth Group (late Triassic) of the Severn Estuary area. *Geoscience in South-West England*, **12**, 71–84.

Gallois, R.W. and Paul, C.R.C. 2009. Lateral variations in the topmost part of the Blue Lias and basal Charmouth Mudstone Formations (Lower Jurassic) on the Devon and Dorset coast. *Proceedings of the Ussher Society*, **12**, 125–133.

Gazeau, F., Quiblier, C., Jansen, J.M., Gattuso, J.P., Middelburg, J.J. and Heip, C.H.R. 2007. Impact of elevated CO₂ on shellfish calcification. *Geophysical Research Letters*, **34**, 1–5.

Gibbs, S. J., Stoll, H. M., Bown, P. R. and Bralower, T. J. 2010. Ocean acidification and surface water carbonate production across the Paleocene–Eocene thermal maximum. *Earth Planetary Science Letters*, **295**, 583–592.

Gröcke, D.R., Price, D.G., Ruffell, A.H., Mutterlose, J. and Baraboshkin, E. 2003. Isotopic evidence for Late Jurassic–Early Cretaceous climate change. *Palaeogeography, Palaeoclimatology, Palaeoecology*, **202**, 97–118.

Golonka, J. 2007. Late Triassic and Early Jurassic palaeogeography of the world. *Palaeogeography, Palaeoclimatology, Palaeoecology*, **244**, 297–307.

Gómez, J.J. and Arias, C. 2010. Rapid warming and ostracods mass extinction at the Lower Toarcian (Jurassic) of central Spain. *Marine Micropaleontology*, **74**, 119–135.

Gómez, J.J., Canales, M.L., Ureta, S. and Goy, A. 2009. Palaeoclimatic and biotic changes during the Aalenian (Middle Jurassic) at the southern Laurasian Seaway (Basque– Cantabrian Basin, northern Spain). *Palaeogeography, Palaeoclimatology, Palaeoecology*, **275**, 14–27.

Google Earth 2013. http://www.google.co.uk/intl/en_uk/earth/

Green, M.A., Jones, M.E., Boudreau, C.L., Moore, R.L. and Westman, B.A. 2004. Dissolution mortality of juvenile bivalves in coastal marine deposits. *Limnology and Oceanography*, **49** (3), 727–734.

- Greene, S.E., Martindale, R.C., Ritterbush, K.A., Bottjer, D.J., Corsetti, F.A. and Berelson, W.M. 2012. Recognising ocean acidification in deep time: An evaluation of the evidence for acidification across the Triassic-Jurassic boundary. *Earth Science Reviews*, **113**, 72–93.
- Gregg, J.M., Shelton, K.L., Johnson, A.W., Somerville, I.D. and Wright, W.R. 2001. Dolomitization of the Waulsortian Limestone (Lower Carboniferous) in the Irish Midlands. *Sedimentology*, **48**, 745–766.
- Guex, F., Bartolini, A., Atudorei, V. and Taylor, D. 2004. High-resolution ammonite and carbon isotope stratigraphy across the Triassic-Jurassic boundary at New York Canyon (Nevada). *Earth and Planetary Science Letters*, **225**, 29–41.
- Guinotte, J.M. and Fabray, V.J. 2008. Ocean Acidification and its Potential Effects on Marine Ecosystems. *Annals New York Academy of Sciences*, **1134**, 320–342.
- Hallam, A. 1960. A sedimentary and faunal analysis of the Blue Lias of Dorset and Glamorgan. *Philosophical Transactions of the Royal Society, London, Series B*, **243**, 1–44.
- Hallam, A. 1975. Evolutionary size increase and longevity in Jurassic bivalves and ammonites. *Nature*, **258**, 493–496.
- Hallam, A. 1989. The case for sea-level change as a dominant causal factor in mass extinction of marine invertebrates. *Philosophical Transactions of the Royal Society of London, Series B*, **325**, 437–455.
- Hallam, A. 1995. Major bio-events in the Triassic and Jurassic. In: Walliser, O.H. (ed.) *Global events and event stratigraphy*, Springer-Verlag, Berlin, 265–283.
- Hallam, A. 1997. Estimates of the amount and rate of Sea-Level change across the Rhaetian Hettangian and Pliensbachian Toarcian boundaries (latest Triassic to early Jurassic). *Journal of the Geological Society, London*, **154**, 773–779.
- Hallam, A. 2002. How catastrophic was the end-Triassic mass extinction? *Lethaia*, **35** (2), 147–157.
- Hallam, A. and Wignall, P.B. 1997. *Mass Extinctions and their aftermath*. Oxford University Press, Oxford, 320pp.
- Hallam, A. and Wignall, P. B. 1999. Mass extinctions and sea-level changes. *Earth Science Reviews*, **48** (4), 217–250.

- Hammer, Ø., Harper, D.A.T. and Ryan, P.D. 2001. PAST: Paleontological Statistics Software Packages for Education and Data Analysis. *Palaeontologia Electronica*, **4**, 1. Article 4.
- Hansen, H.J. 2006. Stable isotopes of carbon from basaltic rocks and their possible relation to atmospheric isotope excursions. *Lithos*, **92**, 105–116.
- Hart, M.B. 1982. The Marine Rocks of the Mesozoic. *In*: Durrance, E.M. and Laming, D.J.C. (eds), *The Geology of Devon*. University of Exeter Press, Exeter, 179-203.
- Hart, M.B. 1987. Orbitally induced cycles in the Mesozoic sediments of S.W. England. *Proceedings of the Ussher Society*, **6**, 483–490.
- Hart, M.B. and FitzPatrick, M.E.J. 1995. Kimmeridgian palaeoenvironments; a micropalaeontological perspective. *Proceedings of the Ussher Society*, **8**, 433–436.
- Hart, M.B. and Hylton, M.D. 1999. Hettangian to Sinemurian ostracod faunas from east quantoxhead, west somerset. *Geoscience in South-West England*, **9**, 289–296.
- Harris, J.O., Maguire, G.B., Edwards, S.J. and Johns, D.R. 1999. Low dissolved oxygen reduces growth rate and oxygen consumption rate of juvenile greenlip abalone. *Haliotis laevigata* Donovan. *Aquaculture*, **174** (3–4), 265–278.
- Hauton, C., Tyrrell, T. and Williams, J. 2009. The subtle effects of sea water acidification on the amphipod *Gammarus locusta*. *Biogeosciences*, **6**, 1479–1489.
- Hautmann, M. 2004. Effect of end-Triassic CO₂ maximum on carbonate sedimentation and marine mass extinction. *Facies*, **50**, 257–261.
- Hautmann, M. 2006. Shell mineralogical trends in epifaunal Mesozoic bivalves and their relationship to seawater chemistry and atmospheric carbon dioxide concentration. *Facies*, **52**, 417–433.
- Hautmann, M., Benton, M.J. and Tomašových, A. 2008. Catastrophic ocean acidification at the Triassic-Jurassic boundary. *Neues Jahrbuch für Geologie und Paläontologie, Abhandlungen*, **249** (1), 119–127.
- Hayes, J.M., Strauss, H. and Kaufman, A.J. 1999. The abundance of $\delta^{13}\text{C}$ in marine organic matter and isotopic fractionation in the global biogeochemical cycle of carbon during the past 800 Ma. *Chemical Geology*, **161**, 103–125.
- Hemleben, C. and Bijma, J. 1994. Foraminiferal Population Dynamics and Stable Carbon Isotopes. *In*: Zahn, R., Pedersen, T.F., Kaminski, M.A. and

Labeyrie, L. *Carbon Cycling in the Glacial Ocean: Constraints on the Oceans Role in Global Change*, Elsevier, New York, 145–166.

Hendriks, I.E., Duarte, C.M. and Alvarez, M. 2010. Vulnerability of marine biodiversity to ocean acidification: A meta-analysis. *Estuarine, Coastal and Shelf Science*, **86** (2), 157–164.

Hesselbo, S.P., Gröcke, D.R., Jenkyns, H.C., Bjerrum, C.J., Farrimond, P., Morgans Bell, H.S. and Green, O.R. 2000. Massive dissociation of gas hydrates during a Jurassic oceanic anoxic event. *Nature*, **406**, 392–395.

Hesselbo, S.P., Robinson, S.A., Surlyk, F. and Piasecki, S. 2002. Terrestrial and marine extinction at the Triassic-Jurassic boundary synchronized with major carbon-cycle perturbation: a link to initiation of massive volcanism? *Geology*, **30** (3), 251–254.

Hesselbo, S.P., Robinson, S.A. and Surlyk, F. 2004. Sea-level change and facies development across potential Triassic-Jurassic boundary horizons, SW Britain. *Journal of the Geological Society, London*, **161**, 365–379.

Hiebenthal, C., Philipp, E.E.R. Eisenhauer, A. and Wahl, M. 2012. Effects of seawater $p\text{CO}_2$ and temperature on shell growth, shell stability, condition and cellular stress of Western Baltic Sea *Mytilus edulis* (L.) and *Arctica islandica* (L.). *Marine Biology*, **160** (8), 2073–2087.

Hirschmann, N. 1912. Beitrag zur Ostracodenfauna des Finnischen Meerbusens. *Acta Societatis pro Fauna et Flora Fennica*, **36** (2), 1–64.

Hoegh-Guldberg, O., Mumby, P.J., Hooten, A.J., Steneck, R.S., Greenfield, P., Gomez, E.D., Harvell, C.D., Sale, P.F., Edwards, A.J., Caldeira, K., Knowlton, N., Eakin, C.M., Iglesias-Prieto, R., Muthiga, N., Bradbury, R.H., Dubi, A. and Hatziolos, M.E. 2007. Coral Reefs Under Rapid Climate Change and Ocean Acidification. *Science*, **318**, 1737–1742.

Hönisch, B., Ridgwell, A., Schmidt, D.N., Thomas, E., Gibbs, S.J., Sluijs, A., Zeebe, R., Kump, L., Martindale, R.C., Greene, S.E., Kiessling, W., Ries, J., Zachos, J.C., Royer, D.L., Barker, S., Marchitto Jr., T.M., Moyer, R., Pelejero, C., Ziveri, P., Foster, G.L. and Williams, B. 2012. The Geological Record of Ocean Acidification. *Science*, **335**, 1058–1063.

Hounslow, M.W., Posen, P.E., Andrews, J.E. and Warrington, G. 2002. Magnetostratigraphic correlation of marine (UK) and non-marine (eastern USA) Triassic/Jurassic boundary successions. *Geophysical Research Abstracts*, **4**, EGS02-A- 01800, 27th European Geophysical Society, General Assembly, Nice.

Hounslow, M.W., Posen, P.E. and Warrington, G. 2004. Magnetostratigraphy and biostratigraphy of the Upper Triassic and lowermost Jurassic succession, St. Audrie's Bay, UK. *Palaeogeography, Palaeoclimatology, Palaeoecology*, **213**, 331–358.

Houghton, J. T., Ding, Y., Griggs, D.J., Noguer, M., van der Linden, P.J., Dai, X., Maskell, K. and Johnson, C.A. (eds) 2001. Climate change 2001: the scientific basis. Contribution of Working Group I to the Third Assessment Report of the International Panel on Climate Change. *Cambridge University Press: Cambridge, UK and New York, USA*.

Huynh, T.T. and Poulsen, C.J. 2005. Rising atmospheric CO₂ as a possible trigger for the end-Triassic mass extinction. *Palaeogeography, Palaeoclimatology, Palaeoecology*, **217**, 223–242.

Hunt, G. and Roy, K. 2006. Climate change, body size evolution, and Cope's Rule in deep-sea ostracods. *Proceedings of the National Academy of Sciences, USA*, **103** (5), 1347–1352.

International Commission on Stratigraphy. Website:
<http://www.stratigraphy.org/> 2012-2013

Intergovernmental Panel on Climate Change (IPCC), 2007. Climate Change 2007: the scientific basis. *In: Solomon, S., Qin, D., Manning, M., Chen, Z., Marquis, M., Averyt, K.B., Tignor, M. and Miller, H.L. (eds), Contribution of Working Group I to the Fourth Assessment Report of the Intergovernmental Panel on Climate Change*, Cambridge Univ. Press, New York.

Jablonski, D. 1996. Body size and macroevolution. *In: Jablonski, D., Erwin, D.H & Lipps, J.H. (eds), Evolutionary Paleobiology*, University of Chicago Press, Chicago, **2**, 256–289.

Jablonski, D. and Raup, D.M. 1995. Selectivity of end-Cretaceous marine bivalve extinctions. *Science*, **268**, 389–391.

Janz, H. and Vennemann, T. W. 2005. Isotopic composition (O, C, Sr, and Nd) and trace element ratios (Sr / Ca, Mg/ Ca) of Miocene marine and brackish ostracods from North Alpine Foreland deposits (Germany and Austria) as indicators for palaeoclimate. *Palaeogeography, Palaeoclimatology, Palaeoecology*, **225**, 216–247.

Jaraula, C.M.B., Grice, K., Twitchett, R.J., Bottcher, M.E., LeMetayer, P., Dastidar, A.G. and Opazo, L.F. 2013. Elevated pCO₂ leading to Late Triassic extinction, persistent photic zone euxinia, and rising sea levels. *Geology*, **41** (9), 955–958.

- Jenkyns, H.C. 1996. Relative sea-level change and carbon isotopes: data from the Upper Jurassic (Oxfordian) of central and Southern Europe. *Terra Nova*, **8**, 75–85.
- Jokie, P.L., Rodgers, K.S., Kuffner, I.B., Andersson, A.J., Cox, E.F. & Mackenzie, F.T. 2008. Ocean acidification and calcifying reef organisms: a mesocosm investigation. *Coral Reefs Report*, **27**, 473–483.
- Kennett, J.P., Cannariato, K.G., Hendy, I.L. and Behl, R.J. 2000. Carbon isotope evidence for methane hydrate instability during Quaternary interstadials. *Science*, **288**, 128–133.
- Kent, D. V. and Clemmensen, L. B. 1996. Paleomagnetism and cycle stratigraphy of the Triassic Fleming Fjord and Gipsdalen Formations of East Greenland. *Bulletin of the Geological Society of Denmark*, **42**, 121–136.
- Kent, D.V., Olsen, P.E. and Witte, W.K. 1995. Late Triassic–earliest Jurassic geomagnetic polarity sequence and palaeolatitudes from drill cores in Newark Rift basin, eastern North America. *Journal of Geophysical Research*, **100**, 14965–14970.
- Kent, D.V. and Olsen, P.E. 1999. Astronomically tuned geomagnetic polarity time scale for the Late Triassic. *Journal of Geophysical Research*, **104**, 12831–12841.
- Kearsey, T., Twitchett, R.J., Price, G.D. and Grimes, S.T. 2009. Isotope excursions and palaeotemperature estimates from the Permian/Triassic boundary in the Southern Alps (Italy). *Palaeogeography, Palaeoclimatology, Palaeoecology*, **279**, 29–40.
- Keyser, D. 1982. Development of the sieve pores in *Hirschmannia viridis* (O. F. Müller, 1785). In: Bate, R. E., Robinson, E. and Sheppard, L. M. (eds), *Fossil and Recent Ostracods*, Ellis Horwood Limited, Chichester, 51–60.
- Kidder, D.L. and Worsley, D.R. 2003. Causes and consequences of extreme Permo–Triassic warming to globally equable climate and relation to the Permo–Triassic extinction and recovery. *Palaeogeography, Palaeoclimatology, Palaeoecology*, **203**, 207–237.
- Kiessling, W. and Aberhan, M. 2007. Environmental determinants of marine benthic biodiversity dynamics through Triassic–Jurassic time. *Paleobiology*, **33** (3), 414–434.
- Kiessling, W., Aberhan, M., Brenneis, B. and Wagner, P.J. 2007. Extinction trajectories of benthic organisms across the Triassic–Jurassic boundary. *Palaeogeography, Palaeoclimatology, Palaeoecology*, **244**, 201–222.

- Kiessling, W. and Simpson, C. 2011. On the potential for ocean acidification to be a general cause of ancient reef crises. *Global Change Biology*, **17**, 56–67.
- Klein, R.T., Lohmann, K.C. and Thayer, C.W. 1996. Bivalve skeletons record sea-surface temperature and $\delta^{18}\text{O}$ via Mg/Ca and $\delta^{18}\text{O}/\delta^{16}\text{O}$ ratios. *Geology*, **24**, 415–418.
- Knoll, A.H., Bambach, R.K., Canfield, D.E. and Grotzinger, J.P. 1996. Comparative Earth History and Late Permian Mass Extinction. *Science*, **273**, 452–457.
- Knoll, A.H., Bambach, R.K., Payne, J.L., Pruss, S. and Fischer, W.W. 2007. Paleophysiology and end-Permian mass extinction. *Earth and Planetary Science Letters*, **256** (3–4), 295–313.
- Knoll, A.H. and W.W. Fischer. 2011. Skeletons and ocean chemistry: the long view. In: J.P. Gattuso and L. Hansson, (eds), *Ocean Acidification*, Oxford University Press, Oxford, 67–82.
- Korte, C., Hesselbo, S.P., Jenkyns, H.C., Rickaby, R.E.M. and Spötl, C. 2009. Palaeoenvironmental significance of carbon-and oxygen-isotope stratigraphy of marine Triassic Jurassic boundary sections in the SW Britain. *Journal of the Geological Society, London*, **166**, 431–445.
- Korte, C., Kozur, H.W. and Veizer, J. 2005. $\delta^{13}\text{C}$ and $\delta^{18}\text{O}$ values of Triassic brachiopods and carbonate rocks as proxies for coeval seawater and palaeotemperature. *Palaeogeography, Palaeoclimatology, Palaeoecology*, **226**, 287–306.
- Kornicker, L.S. and Sohn, I.G. 1971. Viability of ostracode eggs ingested by fish and effect of digestive fluids on ostracode shells: ecologic and paleoecologic implications In: H. J. Oertli (ed.), *Paléoécologie des Ostracodes*. Bulletin Centre Recherche Pau-SNPA, 5 (Supplement), 125–135.
- Kroeker, K.J., Kordas, R.L., Crim, R.N. and Singh, G.G. 2010. Meta-analysis reveals negative yet variable effects of ocean acidification on marine organisms. *Ecology Letters*, **13** (11), 1419–1434.
- Kühl, C. 1980. Die Variabilität von *Leptocythere psammophila* Guillaume, 1976: Schalenabmessungen und Schalenstrukturen (Crust.: Ostracoda: Cytheridae). *Verhandlungen des Naturwissenschaftlichen Vereins in Hamburg, NF*. **23**, 275–301.
- Kump, L. R. 2000. What Drives Climate? *Nature*, **408**, 651–652.

- Kump, L.R. and Arthur, M.A. 1999. Interpreting carbon-isotope excursions: Carbonates and organic matter. *Chemical Geology*, **161**, 181–198.
- Kurihara, H., Asai, T., Kato, S. and Ishimatsu, A. 2008. Effects of elevated $p\text{CO}_2$ on early development in the mussel *Mytilus galloprovincialis*. *Aquatic Biology*, **4**, 225–233.
- Kurihara, H., Kato, S. and Ishimatsu, A. 2007. Effects in increased seawater $p\text{CO}_2$ on early development of the oyster *Crassostrea gigas*. *Aquatic Biology*, **1**, 91–98
- Iannace, A., Capuano, M. and Galluccio, L. 2011. “Dolomites and dolomites” in Mesozoic platform carbonates of the Southern Apennines: Geometric distribution, petrography and geochemistry. *Palaeogeography, Palaeoclimatology, Palaeoecology*, **310**, 324–339.
- Lang, W.D. 1924. The Blue Lias of the Devon and Dorset Coasts. *Proceedings of the Geologists' Association, London*, **35** (3), 169–185.
- Lea, D.W., Mashiotta, T.A. and Spero, H.J. 1999. Controls on magnesium and strontium uptake in planktonic foraminifera determined by live culturing. *Geochimica et Cosmochimica Acta*, **63**, 2369–2379.
- Lear, C.H., Rosenthal, Y. and Slowey, N. 2002. Benthic foraminiferal Mg/Ca paleothermometry: a revised core-top calibration. *Geochimica et Cosmochimica Acta*, **66**, 3375–3387.
- Leonard, S.R. 1983. *Some aspects of the biology of three species of littoral teleosts*. Final honours research report, University of Newcastle. (Unpublished).
- Lewis, D.E. and Cerrato, R.M. 1997. Growth uncoupling and the relationship between shell growth and metabolism in the soft shell clam *Mya arenaria*. *Marine Ecology Progress Series*, **158**, 177–189.
- Lord, A.R. 1971. Revision of some Lower Lias Ostracoda from Yorkshire. *Palaeontology*, **14**, 624–665.
- Lord, A.R. and Davis, P.G. 2010. Fossils from the Lower Lias of the Dorset Coast. *The Palaeontological Association, London*, 436 pp.
- Lucas, S.G., Taylor, D.G., Guex, J., Tanner, L.H. and Krainer, K. 2007. Updated proposal for Global Stratotype Section and Point for the base of the Jurassic System in the New York Canyon area, Nevada, USA. *International Subcommission on Jurassic Stratigraphy, Newsletter*, **34**, 34–42.

- Lund, J.J. 1977. Rhaetic to Lower Liassic palynology of the onshore south-eastern North Sea Basin. *Geological Survey of Denmark Bulletin*, **2**, (109), 1–129.
- Maier, C., Hegeman, J., Weinbauer, M.G. and Gattuso, J.P. 2009. Calcification of the cold-water coral *Lophelia pertusa* under ambient and reduced pH. *Biogeosciences*, **6**, 167–180.
- Machel, H.G. and Lonnee, J. 2002. Hydrothermal dolomite—a product of poor definition and imagination. *Sedimentary Geology*, **152**, 163–171.
- Malchus, N. and Steuber, T. 2002. Stable isotope records (O, C) of Jurassic aragonitic shells from England and NW Poland: palaeoecologic and environmental implications. *Geobios*, **35**, 29–39.
- Mander, L., Kurschner, W.M. and McElwain, J.C. 2013. Palynostratigraphy and vegetation history of the Triassic-Jurassic transition in East Greenland. *Journal of the Geological Society, London*, **170**, 37–46.
- Mander, L. and Twitchett, R.J. 2008. Quality of the Triassic-Jurassic Bivalve Fossil Record in Northwest Europe. *Palaeontology*, **51** (6), 1213–1223.
- Mander, L., Twitchett, R.J. and Benton, M.J. 2008. Palaeoecology of the Late Triassic extinction event in the SW UK. *Journal of the Geological Society, London*, **165**, 319–332.
- Marco-Barba, J., Carbonell, E. and Mesquita-Joanes, F. 2012. Empirical calibration of shell chemistry of *Cyprideis torosa* (Jones, 1850) (Crustacea: Ostracoda). *Geochimica et Cosmochimica Acta*, **93**, 143–163.
- Martin, K.D. 2004. A re-evaluation of the relationship between trace fossils and dysoxia. In: McIlroy, D. (Ed.), *The Application of Ichnology to Palaeoenvironmental and Stratigraphic Analysis*. Geological Society, London, Special Publications, **228**, 145–166.
- Martindale, R.C., Berelson, W.M., Corsetti, F.A., Bottjer, D.J. and West, A.J. 2012. Constraining carbonate chemistry at a potential ocean acidification event (the Triassic–Jurassic boundary) using the presence of corals and coral reefs in the fossil record. *Palaeogeography, Palaeoclimatology, Palaeoecology*, **350–352**, 114–123.
- Marzoli, A., Bertrand, H., Knight, K.B., Cirilli, S., Burratti, N., Verati, C., Nomade, S., Renne, P.R., Youbi, N., Martini, R., Allenbach, K., Neuwerth, R., Rapaille, C., Zaninetti, L. & Bellieni, G. 2004. Synchrony of the Central Atlantic Magmatic Province and the Triassic-Jurassic boundary climatic and biotic crisis. *Geology*, **32** (11), 973–976.

- Marzoli, A., Renne, P., Piccirillo, E.N., Ernesto, M., Bellieni, G. & De Min, A. 1999. Extensive 200-Million-Year-Old continental flood basalts of the Central Atlantic Magmatic Province. *Science*, **284**, 616–618.
- Mayall, M.J. 1983. An earthquake origin for synsedimentary deformation in a late Triassic lagoonal sequence, southwest Britain. *Geological Magazine*, **120**, 613–622.
- Mayor, D.J., Matthews, C., Cook, K., Zuur, A.F. and Hay, S. 2007. CO₂-induced acidification affects hatching success in *Calanus finmarchicus*. *Marine Ecology Progress Series*, **350**, 91–97.
- McClintock, J.B., Angus, R.A., McDonald, M.R., Amsler, C.D., Catledge, S.A. and Vohra, Y.K. 2009. Rapid dissolution of shells of weakly calcified Antarctic benthic macro-organisms indicates high vulnerability to ocean acidification. *Antarctic Science*, **21** (5), 449–456.
- McDonald, M.R., McClintock, J.B., Amsler, C.D., Rittschof, D., Angus, R.A. and Orihuela, B. 2009. Effects of ocean acidification over the life history of the barnacle *Amphibalanus amphitrite*. *Marine Ecology Progress Series*, **385**, 179–187.
- McElwain, J. C. 1998. Do fossil plants signal palaeoatmospheric CO₂ concentration in the geological past? *Philosophical Transactions of The Royal Society, London*, **B353**, 83–96.
- McElwain, J.C. and Chaloner, W.G. 1995. Stomatal Density and Index of Fossil Plants Track Atmospheric Carbon Dioxide in the Palaeozoic. *Annals of Botany*, **76**, 389–395.
- McElwain, J.C., Beerling, D.J. and Woodward, F.I. 1999. Fossil Plants and Global Warming at the Triassic-Jurassic Boundary. *Science*, **285**, 1386–1390.
- McElwain, J.C., Murphy, J.W. and Hesselbo, S.P. 2005. Changes in carbon dioxide during an oceanic anoxic event linked to intrusion of Gondwana coals. *Nature*, **435**, 479–483.
- McElwain, J.C., Popa, M.E., Hesselbo, S.P., Haworth, M. and Surlyk, F. 2007. Macroecological responses of terrestrial vegetation to climatic and atmospheric change across the Triassic/Jurassic boundary in East Greenland. *Paleobiology*, **33** (4), 547–573.
- McElwain, J.C., Wagner, P.J. and Hesselbo, S.P. 2009. Fossil Plant Relative Abundances Indicate Sudden Loss of Late Triassic Biodiversity in East Greenland. *Science*, **324**, 1554–1556.
- McGhee, G.R., Sheehan, P.M., Bottjer, D.J. and Droser, M.L. 2004. Ecological ranking of Phanerozoic biodiversity crises: ecological and

- taxonomic severities are decoupled. *Palaeogeography, Palaeoclimatology, Palaeoecology*, **211**, 289–297.
- McHone, J.G. 2000. Non-plume magmatism and rifting during the opening of the central Atlantic Ocean. *Tectonophysics*, **316** (3-4), 287–296.
- McRoberts, C.A., Furrer, H. and Jones, D.S. 1997. Palaeoenvironmental interpretation of a Triassic–Jurassic boundary section from Western Austria based on palaeoecological and geochemical data. *Palaeogeography, Palaeoclimatology, Palaeoecology*, **136**, 79–95.
- McRoberts, C.A., Krystyn, L. and Hautmann, M. 2012. Macrofaunal response to the end-Triassic mass extinction in the west-tethyan kossen basin, Austria. *Palaios*, **27**, 607–616.
- McRoberts, C.A. and Newton, C.R. 1995. Selective extinction among end-Triassic European bivalves. *Geology*, **23**, 102–104.
- McRoberts, C.A., Ward, P.D. and Hesselbo, S. 2007. A proposal for the base Hettangian stage (=base Jurassic System) GSSP at New York Canyon, Nevada, USA using carbon isotopes. *International Subcommission on Jurassic Stratigraphy, Newsletter*, **34**, 43–49.
- Metcalfe, B., Twitchett, R. J. and Price-Lloyd, N. 2011. Changes in size and growth rate of 'Lilliput' animals in the earliest Triassic. *Palaeogeography, Palaeoclimatology, Palaeoecology*, **308** (1-2), 171–180.
- Michaelidis, B., Ouzounis, C., Paleras, A. and Pörtner, H.O. 2005. Effects of long-term moderate hypercapnia on acid-base balanced and growth rate in marine mussels *Mytilus galloprovincialis*. *Marine Ecology Progress Series*, **293**, 109–118.
- Mizuta, D., Junior, N.S. and Lemos, C.E.F. 2012. Interannual variation in commercial oyster (*Crassostrea gigas*) farming in the sea (Florianópolis, Brazil, 27°44' S; 48°33' W) in relation to temperature, chlorophyll and associated oceanographic conditions. *Aquaculture*, **366–367**, 105–114.
- Moghadam, H.V. and Paul, C.R.C. 2000. Trace Fossils of the Jurassic, Blue Lias, Lyme Regis, Southern England. *Ichnos*, **7** (4), 283–306.
- Morettini, E., Santantonio, M., Bartolini, A., Cecca, F., Baumgartner, P.O. and Hunziker, J.C. 2002. Carbon isotope stratigraphy and carbonate production during the Early-Middle Jurassic: examples from the Umbria-Marche-Sabina Apennines (central Italy). *Palaeogeography, Palaeoclimatology, Palaeoecology*, **184**, 251–273.
- Morrison, J.O. and Brand, U. 1986. Paleocene geochemistry of recent marine invertebrates. *Geoscience Canada*, **13**, 237–254.

- Neale, J.W. 1983. The Ostracoda and uniformitarianism. 1. The later record: Recent, Pleistocene and Tertiary. *Proceedings of the Yorkshire Geological Society*, **44**, 305–326.
- Nienhuis, S., Palmer, A.R. and Harley, C.D.G. 2010. Elevated CO₂ affects shell dissolution rate but not calcification rate in a marine snail. *Proceedings of the Royal Society, London*, **B277**, 2553–2558.
- Nunn, E.V. and Price, G.D. 2010. Late Jurassic (Kimmeridgian–Tithonian) stable isotopes ($\delta^{18}\text{O}$, $\delta^{13}\text{C}$) and Mg/Ca ratios: New palaeoclimate data from Helmsdale, northeast Scotland. *Palaeogeography, Palaeoclimatology, Palaeoecology*, **292**, 325–335.
- Oertli, H.J. 1985. Ostrakoden aus der Oligozanen und Mioanen Molasse der Schweiz. *Abhandlungen der Schweizerischen paläontologischen Gesellschaft*, **73**, 1–120.
- Olsen, P.E., 1999. Giant lava flows, mass extinctions, and mantle plumes. *Science*, **284**, 604–605.
- Orr, J.C., Fabry, V.J., Aumont, O., Bopp, L., Doney, S.C., Feely, R.A., Gnanadesikan, A., Gruber, N., Ishida, A., Joos, F., Key, R.M., Lindsay, K., Maier-Reimer, E., Matear, R., Monfray, P., Mouchet, A., Najjar, R.G., Plattner, G.K., Rodgers, K.P., Sabine, C.L., Sarmiento, J.L., Schlitzer, R., Slater, R.D., Totterdell, I.J., Weirig, M.F., Yamanaka, Y. and Yool, A. 2005. Anthropogenic ocean acidification over the twenty-first century and its impact on calcifying organisms. *Nature*, **437**, 691–686.
- Opazo, L.F. 2012. *Extinction and recovery dynamics of Triassic-Jurassic Macro-Invertebrate communities*. Unpublished PhD thesis, Plymouth University.
- Orbell, G. 1973. Palynology of the British Rhaeto-Liassic. *Bulletin of the Geological Survey of Great Britain*, **44**, 1–44.
- Page, K.N. 2001. Golden spiked! – The UK's first Global Stratotype Section and Point for a Jurassic stage boundary, in Somerset. *Geoscience in south-west England*, **10**, 177–182.
- Page, K. N. 2004. Biostratigraphy of invertebrate macrofossils and microfossils: Macrofossils – Ammonites. In: Simms, M.J., Chidlaw, N., Morton, N. and Page, K.N. (eds), *British Lower Jurassic Stratigraphy*, Joint Nature Conservation Committee, Peterborough, 28–31.
- Page, K.N. 2005. The Hettangian ammonite faunas of the west Somerset coast (Southwest England) and their significance for the correlation of the candidate GSSP (Global Stratotype and Point) for the base of the Jurassic

System at St. Audrie's Bay. *Colloque L'Hettangien à Hettange de la science au patrimoine, Hettange (Moselle, France), Université Henri Poincaré*, 15–19.

Page, K. N. 2010. Stratigraphical framework. *In*: Lord, A. and Davis, P. (eds). *Fossils from the Lower Lias of the Dorset Coast*, The Palaeontological Association, London, 33–53.

Page, K.N. and Bloos, G. 1995. The base of the Jurassic system in west Somerset, South-west England – New observations on the succession of ammonite faunas of the Lowest Hettangian stage. *Proceedings of the Ussher Society*, **9**, 231–235.

Palfy, J. 2005. Correlated environmental change and extinction at the Triassic-Jurassic boundary. *In*: Hanzo, M. (ed.), *The Hettangian in Hettange; from Science to Geological Heritage*, Univ. Henri Poincaré, Nancy, 5–8.

Palfy, J., Demény, A., Haas, J., Heténi, M., Orchard, M. and Vető, I. 2001. Carbon isotope anomaly and other geochemical changes at the Triassic-Jurassic boundary from a marine section in Hungary. *Geology*, **29**, 1047–1050.

Palfy, J., Demény, A., Haas, J., Carter, E.S., Görög, A., Halász, D., Oravecz-Scheffer, A., Hetényi, M., Márton, E., Orchard, M.J., Ozsvárt, P., Vető, I. and Zajzon, N. 2007. Triassic-Jurassic boundary events inferred from integrated stratigraphy of the Csővár section, Hungary. *Palaeogeography, Palaeoclimatology, Palaeoecology*, **244**, 11–33.

Palfy, J., Mortensen, J.K., Carter, E.S., Smith, P.L., Friedman, R.M. and Tipper, H.W. 2000. Timing the end-Triassic mass extinction: first on land, then in the sea? *Geology*, **28**, 39-42.

Palmer, C. P. 1972. Lower Lias (Lower Jurassic) between Watchet and Lillstock in North Somerset (UK). *Newsletters on Stratigraphy*, **2** (1), 1–30.

<http://paleobiodb.org/#/>

Passlow, V. 1997. Quaternary ostracods as palaeoceanographic indicators: a case study off southern Australia. *Palaeogeography, Palaeoclimatology, Palaeoecology*, **131** (3–4), 315–325.

Patzkowsky, M.E. and Holland, S.M. 2012. *Stratigraphic Paleobiology: Understanding the distribution of fossil taxa in time and space*. University of Chicago Press Ltd, Chicago, 256pp.

Paul, C.R.C., Allison, P.A. and Brett, C.E. 2008. The occurrence and preservation of ammonites in the Blue Lias Formation (lower Jurassic) of Devon and Dorset, England and their palaeoecological, sedimentological and

diagenetic significance. *Palaeogeography, Palaeoclimatology, Palaeoecology*, **270**, 258–272.

Payne, J.L. 2005. Evolutionary dynamics of gastropod size across the end-Permian extinction and through the Triassic recovery interval. *Paleobiology*, **31**, 269–290.

Pelejero, C., Calvo, E. and Hoegh-Guldberg, O. 2010. Paleo-perspectives on ocean acidification. *Trends in Ecology and Evolution*, **25** (6), 332–344.

Peng, Y., Shi, G.R., Gao, Y., He, W. and Shen, S. 2007. How and why did the Lingulidae (Brachiopoda) not only survive the end-Permian mass extinction but also thrive in its aftermath? *Palaeogeography, Palaeoclimatology, Palaeoecology*, **252**, 118–131.

Petes, L.E., Menge, B.A. and Murphy, G.D. 2007. Environmental stress decreased survival growth and reproduction in New Zealand mussels. *Journal of Experimental Marine Biology and Ecology*, **351**, 83–91.

Popp, B.N., Anderson, T.F. and Sandberg, P.A. 1986. Brachiopods as indicators of original isotopic compositions in some Paleozoic limestones. *Geological Society America, Bulletin*, **97**, 1262–1269.

Pörtner, H.O. 2008. Ecosystem effects of ocean acidification in times of ocean warming: a physiologist's view. *Marine Ecology Progress Series*, **373**, 203–217.

Pörtner, H.O. and Farrell, A.P. 2008. Physiology and climate change. *Science*, **322**, 690–692.

Posenato, R. 2009. Survival patterns of macrobenthic marine assemblages during the end-Permian mass extinction in the western Tethys (Dolomites, Italy). *Palaeogeography, Palaeoclimatology, Palaeoecology*, **280** (1–2), 150–167.

Price, G.D. 2010. Carbon-isotope stratigraphy and temperature change during the Early–Middle Jurassic (Toarcian–Aalenian), Raasay, Scotland, UK. *Palaeogeography, Palaeoclimatology, Palaeoecology*, **285**, 255–263.

Price, G.D. and Gröcke, D.R. 2002. Strontium-isotope stratigraphy and oxygen- and carbon-isotope variation during the Middle Jurassic–Early Cretaceous of the Falkland Plateau, South Atlantic. *Palaeogeography, Palaeoclimatology, Palaeoecology*, **183**, 209–222.

Price, G.D. and Page, K.N. 2008. A carbon and oxygen isotopic analysis of molluscan faunas from the Callovian–Oxfordian boundary at Redcliff Point, Weymouth, Dorset: implications for belemnite behaviour. *Proceedings of the Geologists' Association, London*, **119** (2), 153–160.

- Price, G.D., Twitchett, R.J., Wheeley, J.R. and Buono, G. 2013. Isotopic evidence for long term warmth in the Mesozoic. *Scientific Reports*, **3**, 1438. DOI: 10.1038/srep01438
- Radley, J.D. 2002. The late Triassic and early Jurassic succession at Southam Cement Works, Warwickshire. *Mercian Geologist*, **15**, 171–174.
- Railsback, L.B., Anderson, T.F., Ackerly, S.C. and Cisne, J.L. 1989. Paleooceanographic modelling of temperature-salinity profiles from stable isotopic data. *Paleoceanography*, **4** (5), 585–591.
- Rampino, M.R. 2010. Mass extinctions of life and catastrophic flood basalt volcanism. *Proceedings of the National Academy of Sciences, USA*, **107**, 6555–6556.
- Range, P., Pilo, D., Ben-Hamadou, R., Chicharo, M.A., Matias, D., Joaquim, S., Oliveira, A.P. and Chicharo, L. 2012. Seawater acidification by CO₂ in a coastal lagoon environment: Effects on life history traits of juvenile mussels *Mytilus galloprovincialis*. *Journal of Experimental Marine Biology and Ecology*, **424–425**, 89–98.
- Rayssac, N., Pernet, F., Lacasse, O. and Tremblay, R. 2010. Temperature effect on survival, growth, and triacylglycerol content during the early ontogeny of *Mytilus edulis* and *M. trossulus*. *Marine Ecology Progress Series*, **417**, 183–191.
- Retallack, G.J. 2001. A 300-million-year record of atmospheric carbon dioxide from fossil plant cuticles. *Nature*, **411**, 287–290.
- Retallack, G. 2002. Carbon dioxide and Climate over the past 300 Myr. *Philosophical Transactions of the Royal Society, London*, **A360**, 659–673.
- Retallack, G.J., Sheldon, N.D., Carr, P.F., Fanning, M., Thompson, C.A., Williams, M.L., Jones, B.G. and Hutton, A. 2011. Multiple Early Triassic greenhouse crises impeded recovery from Late Permian mass extinction. *Palaeogeography, Palaeoclimatology, Palaeoecology*, **308**, 233–251.
- Reyment, R.A. 1966. Preliminary observations of gastropod predation in the western Niger Delta. *Palaeogeography, Palaeoclimatology, Palaeoecology*, **2**, 81–102.
- Rhoads, D. L. and Morse, J. W. 1971. Evolutionary and Ecologic Significance of Oxygen-deficient Marine Basins. *Lethaia*, **4**, 413–428.
- Rico-Villa, B., Pouvreau, S. and Robert, R. 2009. Influence of food density and temperature on ingestion, growth and settlement of Pacific oyster larvae *Crassostrea gigas*. *Aquaculture*, **287**, 395–401.

- Riebesell, U., Fabry, V.J. and Gattuso J.P. (eds), 2010. Guide for Best Practices in Ocean Acidification Research and Data Reporting. Available online at: [http://www.epoca-project.eu/index.php/ Home/Guide-to-OA-Research/](http://www.epoca-project.eu/index.php/Home/Guide-to-OA-Research/) (accessed 2009-2013).
- Ries, J.B., Cohen, A.L. and McCorkle, D.C. 2009. Marine calcifiers exhibit mixed responses to CO₂-induced ocean acidification. *Geological Society of America, Bulletin*, **37** (12), 1131–1134.
- Roca, J.R. and Danielopol, D.L. 1991. Exploration of interstitial habitats by the phytophilous Ostracod *Cypridopsis vidua* (O.F. Millier): experimental evidence. *Annales de Limnologie*, **27**, 243–252.
- Rosenfeld, A. 1982. The secretion process of the Ostracod carapace. *In*: Bate, R.H., Robinson, E. and Sheppard, L.M. (eds), *Fossil and Recent Ostracods*, British Micropalaeontological Society Series: Ellis Horwood Limited, Chichester, 12–24.
- Rosenthal, Y., Boyle, E.A. and Slowey, N. 1997. Temperature control on the incorporation of magnesium, strontium, fluorine, and cadmium into benthic foraminiferal shells from Little Bahama Bank: prospects for thermocline paleoceanography. *Geochimica et Cosmochimica Acta*, **61**, 3633–3643.
- Royer, D.L. 2001. Stomatal density and stomatal index as indicators of paleoatmospheric CO₂ concentrations. *Review of Palaeobotany and Palynology*, **114**, 1–28.
- Royer, D.L. 2006. CO₂-forced climate thresholds during the Phanerozoic. *Geochimica et Cosmochimica Acta*, **70**, 5665–5675.
- Royer, D. L., Berner, R. A., Montañez, I. P., Tabor, N. J. and Beerling, D. J. 2004. CO₂ as a primary driver of Phanerozoic climate. *GSA Today*, **14**, 4–10.
- Ruhl, M. and Kürschner, W.M. 2011. Multiple phases of carbon cycle disturbance from large igneous province formation at the Triassic-Jurassic transition. *Geology*, **39** (5), 431–434.
- Ruhl, M., Kürschner, W.M. and Krystyn, L. 2009. Triassic-Jurassic organic carbon isotope stratigraphy of key sections in the western Tethys realm (Austria). *Earth and Planetary Science Letters*, **281**, 169–187.
- Ruhl, M., Veld, H. and Kürschner, W.M. 2010. Sedimentary organic matter characterization of the Triassic-Jurassic boundary GSSP at Kuhjoch (Austria). *Earth and Planetary Science Letters*, **292**, 17–26.
- Sars, G.O. 1866. Oversigt af Norges marine Ostracoder. *In*: Fordhandlinger i Videnskabs-Selskabet i Christiania, **1864-1865**, 1–130.

- Schaller, M.F., Wright, J.D. and Kent, D.V. 2011. Atmospheric $p\text{CO}_2$ Perturbations Associated with the Central Atlantic Magmatic Province. *Science*, **331**, 1404–1409.
- Schubert, J.K. and Bottjer, D.J. 1995. Aftermath of the Permian–Triassic mass extinction event: palaeoecology of Lower Triassic carbonates in the Western USA. *Palaeogeography, Palaeoclimatology, Palaeoecology*, **116**, 1–39.
- Sepkoski, J.J. 1996. Patterns of Phanerozoic extinction: a perspective from global data bases. *In: Walliser, O.H. (ed.), Global events and event stratigraphy*, Springer, Berlin, 35–52.
- Shackleton, N.J. and Kennett, J.P. 1975. Palaeotemperature history of the Cenozoic and the initiation of Antarctic glaciation: oxygen and carbon isotope analysis in DSDP sites 277, 279 and 281. *In: Kennett, J.P. (ed.), Initial reports of the Deep Sea Drilling Project*. United States Government Printing Office, **29**, 743–755.
- Shaviv, N. J. & Veizer, J. 2003. Celestial driver of Phanerozoic climate? *GSA Today*, **13**, 4–10.
- Shiryama, Y. and Thorton, H. 2005. Effect of increased atmospheric CO_2 on shallow water marine benthos. *Journal of Geophysical Research*, **110**, C09S08.doi: 10.1029/2004JC002618.
- Simms, M.J. 2003. Uniquely extensive seismite from the latest Triassic of the United Kingdom: evidence for bolide impact? *Geology*, **31**, 557–560.
- Simms, M.J. 2004. The Wessex Basin (Dorset and central Somerset). *In: Simms, M.J., Chidlaw, N., Morton, N. and Page, K.N. (eds), British Lower Jurassic Stratigraphy*, Geological Conservation Review Series, No. **30**, Joint Nature Conservation Committee, Peterborough, 53–110.
- Simms, M.J. 2007. Uniquely extensive soft sediment deformation in the Rhaetian of the UK: evidence for earthquake or impact? *Palaeogeography, Palaeoclimatology, Palaeoecology*, **244**, 407–423.
- Simms, M.J. and Jeram, A.J. 2007. Waterloo Bay, Larne, Northern Ireland: a candidate Global Stratotype section and Point for the base of the Hettangian Stage and Jurassic System. *In: Bown, P., Morton, N & Lees, J. 2007. International Subcommission of Jurassic Stratigraphy, Newsletter*, **34**, 50–68.
- Song, H.J., Tong, J.A. and Chen, Z.Q. 2011. Evolutionary dynamics of the Permian-Triassic foraminifer size: Evidence for Lilliput effect in the end-Permian mass extinction and its aftermath. *Palaeogeography, Palaeoclimatology, Palaeoecology*, **308** (1–2), 98–110.

Sowerby, J. 1814. Nos. IX and X in the mineral conchology of Great Britain; or colored figures and descriptions of those remains of testaceous animals or shells, which have been preserved at various times and depths in the Earth. *The Mineral Conchology of Great Britain*, **1** (9–10), 98–178.

Spero, H. J., Bijma, J., Lea, D. W. and Bemis, B. E. 1997. Effect of seawater carbonate concentration on foraminiferal carbon and oxygen isotopes. *Nature*, **390**, 497–500.

Spero, H. J., Bijma, J. and Lea, D. W. 1998. Re-evaluation of the oxygen isotopic composition of planktonic foraminifera: Experimental results and revised paleotemperature equations. *Paleoceanography*, **13** (2), 150–160.

Stanley, G.D.J. 2003. The evolution of modern corals and their early history. *Earth-Science Reviews*, **60** (3–4), 195–225.

Steinhorsdottir, M., Jeram, A.J. and McElwain, J.C. 2011. Extremely elevated CO₂ concentrations at the Triassic/Jurassic boundary. *Palaeogeography, Palaeoclimatology, Palaeoecology*, **308**, 418–432.

Swift, A. 1999. Stratigraphy (including biostratigraphy). In: Swift, A. & Martill, D.M. (eds) *Fossils of the Rhaetian Penarth Group*. The Palaeontological Association, London, 15–30.

Swift, A. and Martill, D.M. (eds), 1999. *Fossils of the Rhaetian Penarth Group*. The Palaeontological Association, London, 312pp.

The Royal Society, 2005. Ocean acidification due to increasing atmospheric carbon dioxide. *Policy Document*, 12/05, 1–60.

Talmage, S.C. and Gobler, C.J. 2009. The effects of elevated carbon dioxide concentrations on the metamorphosis, size, and survival of larval hard clams (*Mercenaria mercenaria*), bay scallops (*Argopecten irradians*), and eastern oysters (*Crassostrea virginica*). *Limnology and Oceanography*, **54** (6), 2072–2080.

Tanner, L.H., Hubert, J.F., Coffey, B.P. and McInerney, D.P. 2001. Stability of atmospheric CO₂ levels across the Triassic/Jurassic boundary. *Nature*, **411**, 675–677.

Tanner, L.H., Lucas, S.G. and Chapman, M.G. 2004. Assessing the record and causes of Late Triassic extinctions. *Earth-Science Reviews*, **65**, 103–139.

Theisen, B.F. 1966. The Life History of Seven Species of Ostracods from a Danish Brackish-Water Locality. *Meddelelser frå Danmarks Fiskeri-og Havundersøgelser, N. S.*, **4** (8), 215–270.

- Tomašových, A. and Siblik, M. 2007. Evaluating compositional turnover of brachiopod communities during the end-Triassic mass extinction (Northern Calcareous Alps): Removal of dominant groups, recovery and community reassembly. *Palaeogeography, Palaeoclimatology, Palaeoecology*, **244**, 170–200.
- Tucker, M.E. and Wright, V.P. 1990. *Carbonate Sedimentology*. Blackwell Scientific Publications, Oxford, 482pp.
- Tunncliffe, V., Davies, K.T.A., Butterfield, D.A., Embley, R.W., Rose, J.M. and Chadwick, W.W. 2009. Survival of mussels in extremely acidic waters on a submarine volcano. *Nature Geoscience*, **2** (5), 344–348.
- Twitchett, R.J. 2001. Incompleteness of the Permian–Triassic fossil record: a consequence of productivity decline? *Geological Journal*, **36**, 341–353.
- Twitchett, R.J. 2006. The Palaeoclimatology, palaeoecology and palaeoenvironmental analysis of mass extinction events. *Palaeogeography, Palaeoclimatology, Palaeoecology*, **232**, 190–213.
- Twitchett, R.J. 2007. The Lilliput effect in the aftermath of the end-Permian extinction event. *Palaeogeography, Palaeoclimatology, Palaeoecology*, **252**, 132–144.
- Twitchett, R.J., Krystyn, L., Baud, A., Wheeley, J.R. and Richoz, S. 2004. Rapid marine recovery after the end-Permian mass extinction in the absence of marine anoxia. *Geology*, **32**, 805–808.
- Urbanek, A. 1993. Biotic crises in the history of Upper Silurian graptoloids: a palaeobiological model. *Historical Biology*, **7**, 29–50.
- van de Schootbrugge, B., Tremolada, F., Rosenthal, Y., Bailey, T.R., Feist-Burkhardt, S., Brinkhuis, H., Pross, J., Kent, D.V. and Falkowski, P.G. 2007. End-Triassic calcification crisis and blooms of organic-walled ‘disaster species’. *Palaeogeography, Palaeoclimatology, Palaeoecology*, **244**, 126–141.
- van de Schootbrugge, B., Payne, J.L., Tomašových, A., Pross, J., Fiebig, J., Benbrahim, M., Föllmi, K.B. and Quan, T.M. 2008. Carbon cycle perturbation and stabilization in the wake of the Triassic-Jurassic boundary mass-extinction event. *Geochemistry, Geophysics, Geosystems*, **9** (4), Q04028, doi:10.1029/2007GC001914.
- Van der Putten, E., Dehairs, F., Keppens, E. and Baeyens, W. 2000. High resolution distribution of trace elements in the calcite shell layer of modern *Mytilus edulis*: environmental and biological controls. *Geochimica et Cosmochimica Acta*, **64**, 997–1011.

- Vannier, J., Abe, K. and Ikuta, K. 1998. Feeding in myodocopid ostracods: functional morphology and laboratory observations from videos. *Marine Biology*, **132**, 391–408.
- Veizer, J., Godderis, Y. & François, L. M. 2000. Evidence for decoupling of atmospheric CO₂ and global climate during the Phanerozoic eon. *Nature*, **408**, 698–701.
- Veron, J.E.N. 2008. Mass extinctions and ocean acidification: biological constraints on geological dilemmas. *Coral Reefs*, **27** (3), 459–472.
- Von Hillebrandt, A., Krystyn, L. and Kuerschner, W.M. 2007. A candidate GSSP for the base of the Jurassic in the Northern Calcareous Alps (Kuhjoch section, Karwendel Mountains, Tyrol, Austria. *In*: Bown, P., Morton, N & Lees, J. 2007. *International Subcommission of Jurassic Stratigraphy, Newsletter*, **34** (1), 2–22.
- Von Hillebrandt, A., Krystyn, L., Kürschner, W.M., Bonis, N.R., Ruhl, M., Richoz, S., Schobben, M.A.N., Urlichs, M., Bown, P.R., Kment, K., McRoberts, C.A., Simms, M. and Tomášových, A. 2013. The Global Stratotype Sections and Point (GSSP) for the base of the Jurassic System at Kuhjoch (Karwendel Mountains, Northern Calcareous Alps, Tyrol, Austria). *Episodes*, **36** (3), 162–198.
- Wall-Palmer, D., Jones, M.T., Hart, M.B., Fisher, J.K., Smart, C.W., Hembury, D.J., Palmer, M.R. and Fones, G.R. 2011. Explosive volcanism as a cause for mass mortality of pteropods. *Marine Geology*, **282** (3–4), 231–239.
- Wanamaker, A.D., Kreutz, K.J., Borns, H.W., Introne, D.S., Feindel, S., Funder, S., Rawson, P.D. and Barber, B.J. 2007. Experimental determination of salinity, temperature, growth, and metabolic effects on shell isotope chemistry of *Mytilus edulis* collected from Maine and Greenland. *Paleoceanography*, **22**, 1–12.
- Ward, P.D., Garrison, G.H., Haggart, J.W., Kring, D.A. and Beattie, M.J. 2004. Isotopic evidence bearing on Late Triassic extinction events, Queen Charlotte Islands, British Columbia, and implications for the Duration and cause of the Triassic/Jurassic mass extinction. *Earth and Planetary Science Letters*, **224**, 589–600.
- Ward, P.D., Haggart, J.W., Carter, E.S., Wilbur, D., Tipper, H.W. and Evans, T. 2001. Sudden productivity collapse associated with the Triassic-Jurassic boundary mass extinction. *Science*, **292**, 1148–1151.
- Warrington, G., Audley-Charles, M.G., Elliott, R.E., Evans, W.B., Ivimey-Cook, H.C., Kent, P.E., Robinson, P.L., Shotton, F.W. and Taylor, F.M. 1980.

A correlation of Triassic rocks in the British Isles. *Geological Society of London, Special Report*, **13**, 78pp.

Warrington, G., Cope, J.C.W. and Ivimey-Cook, H.C. 2008. The St Audrie's Bay- Doniford Bay section, Somerset, England: updated proposal for a candidate Global Stratotype Section and Point for the base of the Hettangian Stage and of the Jurassic System. *In: Morton, N. and Hesselbo, S. (eds), International Subcommission of Jurassic Stratigraphy, Newsletter*, **35** (1), 2–66.

Warrington, G., Ivimey-Cook, H.C. and Cope, J.C.W. 1994. St Audrie's Bay, Somerset, England: a candidate Global Stratotype Section and Point for the base of the Jurassic System. *Geological Magazine*, **131** (2), 191–200.

Warrington, G., Whittaker, A. and Scrivener, R.C. 1986. The late Triassic succession in central and eastern Somerset. *Proceedings of the Ussher Society*, **6** (3), 368–374.

Weedon, G.P. 1985. Hemipelagic shelf sedimentation and climatic cycles: the basal Jurassic (Blue Lias) of south Britain. *Earth and Planetary Science Letters*, **76**, 321–335.

Weedon, G.P., Jenkyns, H.C., Coe, A.L. and Hesselbo, S.P. 1999. Astronomical calibration of the Jurassic time-scale from cyclostratigraphy in British mudrock formations. *Philosophical Transactions of the Royal Society, London*, **A357**, 1787–1813.

Whiteley, N.M., 2011. Physiological and ecological responses of crustaceans to ocean acidification. *Marine Ecology Progress Series*, **430**, 257–271

Whiteside, J.H., Olsen, P.E., Kent, D.V., Fowell, S.J. Et-Touhami, M. 2007. Synchrony between the CAMP and the Triassic-Jurassic mass-extinction event? *Palaeogeography, Palaeoclimatology, Palaeoecology*, **244**, 345–367.

Whiteside, J.H., Olsen, P.E., Eglinton, T., Brookfield, M.E. and Sambrotto, R.N. 2010. Compound-specific carbon isotopes from Earth's largest flood basalt eruptions directly linked to the end-Triassic mass extinction. *Proceedings of the National Academy of Sciences, USA*, **107**, 6721–6725.

Whittaker, A. and Green, G. W. 1983. *Geology of the Country around Weston-Super-Mare*. Memoirs of the Geological Survey of Great Britain. HMSO, London.

Wickins, J.F. 1984. The effect of hypercapnic seawater on growth and mineralization in penaeid prawns. *Aquaculture*, **41**, 37–48.

- Widdicombe, S. and Spicer, J.I. 2008. Predicting the impact of ocean acidification on benthic biodiversity: What can animal physiology tell us? *Journal of Experimental Marine Biology and Ecology*, **366**, 187–197.
- Wierzbowski, H. 2004. Carbon and oxygen isotope composition of Oxfordian–Early Kimmeridgian belemnite rostra: palaeoenvironmental implications for Late Jurassic seas. *Palaeogeography, Palaeoclimatology, Palaeoecology*, **203** (1–2), 153–168.
- Wignall, P.B. 1994. *Black Shales*. Oxford Monographs on Geology and Geophysics No. 30, Oxford Scientific Publications, Oxford, U.K., 127pp.
- Wignall, P.B. 2001. Sedimentology of the Triassic-Jurassic boundary beds in Pinhay Bay (Devon, SW England). *Proceedings of the Geologists' Association, London*, **112**, 349–360.
- Wignall, P.B. 2005. The Link between Large Igneous Province Eruptions and Mass Extinctions. *Elements*, **1** (5), 293–297.
- Wignall, P.B. and Bond, D.P.G. 2008. The end-Triassic and Early Jurassic mass extinction records in the British Isles. *Proceedings of the Geologists' Association, London*, **119**, 73–84.
- Wignall, P.B. and Twitchett, R.J. 1996. Oceanic anoxia and the end Permian mass extinction. *Science*, **272**, 1155–1158.
- Williams, C.J., Hesselbo, S.P., Jenkyns, H.C. and Morgans-Bell, H.S. 2001. Quartz silt in mudrocks as a key to sequence stratigraphy (Kimmeridge Clay Formation, Late Jurassic, Wessex Basin, UK). *Terra Nova*, **13**, 449–455.
- Wilson, M.A. and Palmer, T.J. 1992. "Hardgrounds and hardground faunas". *University of Wales, Aberystwyth, Institute of Earth Studies Publications*, **9**, 1–131.
- Wood, H.L., Spicer, J.I. and Widdicombe, S. 2008. Ocean acidification may increase calcification rates, but at a cost. *Proceedings of the Royal Society of London*, **B275**, 1767–1773.
- Wright, P.V., Cherns, L. and Hodges, P. 2003. Missing molluscs: Field testing taphonomic loss in the Mesozoic through early large-scale aragonite dissolution. *Geology*, **31**, 211–214.
- Yamada, Y. and Ikeda, T. 1999. Acute toxicity of lowered pH to some oceanic zooplankton. *Plankton Biology and Ecology*, **46** (1), 62–67.
- Yin, J. and McRoberts, C.A. 2006. Latest Triassic–earliest Jurassic bivalves of the germig formation from Ianongla (Tibet, China). *Journal of Paleontology*, **80** (1), 104–120.

Zachos, J.C., Pagani, M., Sloan, L., Thomas, E. and Billups, K. 2001. Trends, rhythms, and aberrations in global climate 65 Ma to present. *Science*, **292**, 686–693. doi:10.1126/ science.1059412.

Zachos, J.C., Röhl, U., Schellenberg, S.A., Sluijs, A., Hodell, D.A., Kelly, D.C., Thomas, E., Nicolo, M., Raffi, I., Lourens, L.J., McCarren, H. and Kroon, D. 2005. Rapid Acidification of the Ocean during the Paleocene-Eocene Thermal Maximum. *Science*, **308**, 1611–1615.

Zachos, J.C., Wara, M.W., Bohaty, S.M., Delaney, M.L., Petrizzo, M.R., Brill, A., Bralower, T.J. and Premoli-Silva, I. 2003. A transient rise in tropical sea surface temperature during the Paleocene–Eocene Thermal Maximum. *Science*, **302**, 1551–1554.

Zeebe, R.E. 2012. History of Seawater Carbonate Chemistry, Atmospheric CO₂ and Ocean Acidification. *Annual Review of Earth and Planetary Sciences*, **40**, 141–165.